TITLE PAGE

A Geologic Play Book for Trenton-Black River Appalachian Basin Exploration

Final Report

Reporting Period Start Date: October 1, 2003
Reporting Period End Date: March 30, 2006

Principal Authors:

Douglas G. Patchen, John B. Hickman, David C. Harris, James A. Drahovzal, Paul D. Lake, Langhorne B. Smith, Richard Nyahay, Rose Schulze, Ronald A. Riley, Mark T. Baranoski, Larry H. Wickstrom, Christopher D. Laughrey, Jaime Kostelnik, John A. Harper, Katharine Lee Avary, John Bocan, Michael Ed. Hohn and Ronald McDowell

June 28, 2006

DOE Award Number: DE-FC26-03NT41856

West Virginia University Research Corporation
P.O. Box 6845, Morgantown, WV 26506-6845

University of Kentucky Research Foundation
109 Kinkead Hall, Lexington, KY 40506-0057

New York State Museum Institute
Room 3140 CEC, Albany, NY 12230

Ohio Division of Geological Survey
4383 Fountain Square, Columbus, OH 43224

Pennsylvania Geological & Topographic Survey
400 Waterfront Drive, Pittsburgh, PA 15222-4745

West Virginia Geological & Economic Survey
1 Mont Chateau Road, Morgantown, WV 26508-8079

DISCLAIMER

“This report was prepared as an account of work sponsored by an agency of the United States Government. Neither the United States Government nor any agency thereof, nor any of their employees, makes any warranty, express or implied, or assumes any legal liability or responsibility for the accuracy, completeness, or usefulness of any information, apparatus, product, or process disclosed, or represents that its use would not infringe privately owned rights. Reference herein to any specific commercial product, process, or service by trade name, trademark, manufacturer, or otherwise does not necessarily constitute or imply its endorsement, recommendation, or favoring by the United States Government or any agency thereof. The views and opinions of authors expressed herein do not necessarily state or reflect those of the United States Government or any agency thereof.”

ABSTRACT

Appalachian basin architecture during Middle Ordovician time was dominated by a Black River ramp to the northwest flanked by the central Appalachian basin along its southeast margin, with the deeper Sevier basin still farther to the east and southeast. The ramp margin, which marked the western edge of the central Appalachian basin, was in the approximate location of the western edge of the Rome trough. Black River carbonate rocks were deposited on this broad, stable, shallow-water ramp as epeiric seas transgressed much of what is now the Appalachian region, while thick, shaley carbonates were being deposited within the trough-influenced foredeep and clastic sediments were being deposited in the Sevier basin. The elongate, north-northeast-trending depocenter that developed during early Black River time would continue to exist and even expand throughout the remainder of the Ordovician Period.

Trenton time was marked by the appearance of the Trenton platform in the north, extending from what is now Indiana to New York State, and the Lexington platform to the south, centered in what is now eastern Kentucky, southwestern West Virginia and western Virginia. These two platforms were separated by a shallow, interplatform sub-basin that covered much of what is now Ohio. During early Trenton time low-relief carbonate buildups developed on the Trenton and Lexington platforms that surrounded the interplatform Utica Shale/Point Pleasant sub-basin. Craton-wide transgression continued, and platform carbonate deposition kept pace with increased water depth producing extensive, relatively clean carbonates on the Trenton platform while more argillaceous carbonates were deposited on the Lexington platform and in the central Appalachian basin. At a later time, clastic muds poured into the basin from the east, interfingering with Trenton carbonate beds and producing shales like the Logana Shale Member of the Lexington Formation on the Lexington platform. Ultimately, interbedded limestones and calcareous shales and black shales of the Point Pleasant Formation were deposited within the interplatform sub-basin, followed by more widespread deposition of the Utica Shale.

Trenton-Black River production in the Appalachian basin can be separated into older, “historic” production in the shallower portions of the basin, especially in the Lima-Indiana trend in Indiana and northwestern Ohio, and the current gas play that began in New York and subsequently has been extended to northern Pennsylvania and southwestern West Virginia. Oil and gas production in northwest Ohio is closely associated with the Ordovician-aged margin that developed between the edge of the carbonate platform and the adjacent interplatform shale basin. This margin was interpreted from thickness and facies maps of the Trenton Limestone and may have been created by a series of faults that were reactivated during Trenton time, causing higher subsidence rates in the shale basin relative to the carbonate platform. There may be exploration potential along the entire edge of the platform, from Indiana to northern Pennsylvania, especially where the platform margin is associated with a clean carbonate facies. Hydrothermal dolomite reservoirs in the historic Lima-Indiana trend and in more recent Ontario fields were developed in clean grainstones and packstones that developed on skeletal shoals along the platform margin. Current production from hydrothermal

dolomite reservoirs in New York also is associated with clean carbonate facies, although these are largely restricted to Black River Group carbonates. Gas production in West Virginia, however, is associated with fractured limestones in the Trenton and Black River. No dolomite has been encountered to date in either the Black River or Trenton in the deeper, West Virginia portion of the basin.

The reactivation of basement faults played an important role in the creation of Trenton-Black River fractured limestone and hydrothermal dolomite reservoirs in the Appalachian basin. Throughout most of the basin, there are a number of long, normal faults parallel or subparallel to regional strike that are offset by a second set of northwest-trending faults. However, only the northwest-trending fault system may have been reactivated during Late Ordovician compression from the southeast to become conduits for basement-derived hydrothermal fluids. These fluids rose to the level of the Black River and Trenton to dolomitize limestone beds in those units. The resulting hydrothermal dolomite features have subtle seismic signatures, complicating seismic interpretation and pointing out the need for high-resolution seismic data and 3-D data to locate and develop gas fields.

Petrographic data from thin section and core descriptions are useful to document the distribution of porous and permeable carbonate rock facies in the Trenton Limestone and Black River Group, as well as the spatial distribution of reservoir seals, compartmentalization and diagenetically-controlled pore geometry in producing fields. Petrographic results support, in part, conclusions from the stratigraphic study, i.e., that porous hydrothermal dolomite reservoirs in northwest Ohio formed in what were originally clean grainstones and packstones. However, there are distinctive pore textures in Trenton and Black River dolowackestones and dolomudstones as well. In these reservoirs, macroporosity (vugs and fractures) is not fabric selective, whereas mesoporosity (moldic and intercrystalline voids) is fabric selective. Microporosity is both inter- and intracrystalline. Porosity developed through a combination of fracturing, selective dissolution of allochems (usually crinoids) and dissolution of both calcite and dolomite. Dolowackestones and dolomudstones actually are the most productive reservoirs in the Trenton and Black River in the Appalachian basin. The best reservoirs occur when fractures provide interconnections between large dissolution voids yielding collapse breccias and adjacent zebra fabrics.

Fluid inclusion and geochemistry data and resulting interpretations support a hydrothermal origin for all of the dolomite types that occur in the Trenton and Black River across the study area. Fluid inclusion homogenization temperatures suggest that the dolomite formed at temperatures between 85 and 170 degrees celsius, with generally higher temperatures in New York and Ohio, and lower temperatures in Kentucky. The fluids that formed the dolomites were saline brines, as evidenced by the range in salinity values for the fluid inclusions, from 14.5wt% in New York to 20wt% in Ohio. These values are 4 to 6 times the salinity of normal sea water. The dolomites are enriched in iron and manganese, trace elements that are virtually absent in sea water but common in subsurface brines. The dolomites also commonly have radiogenetic strontium isotope values, which suggest that the saline fluids passed through basement or deep, immature

siliciclastic rocks prior to forming the dolomites. All of these geochemical analyses support a hot, subsurface origin for the dolomites.

Further evidence suggests that the dolomites are of a hydrothermal, not a geothermal, origin. Maximum depth of burial extrapolated from conodont alteration index (CAI) data suggests that the rocks were not buried to sufficient depths to reach temperatures as high as those indicated by the fluid inclusion data. Data from cores in Kentucky and northwest Ohio is unequivocal: there is no way that these dolomites could be of geothermal origin, because the rocks were never buried to sufficient depths. The same is true for Trenton and Black River dolomites in Ontario and Michigan. However, in New York, CAI values suggest that the Black River was buried to depths where the temperature equaled or exceeded the fluid inclusion homogenization temperature. But, if dolomitization occurred during early burial, the dolomite still would be hydrothermal in origin, and evidence such as the timing of faulting and the relatively low salinity of the fluid inclusions suggests that dolomitization occurred very early in the burial history of the host rocks.

Although still speculative, a fault-related hydrothermal alteration model is supported by all of the known facts at this time. The preferred style of faulting is a negative flower structure, but the same general principles would apply to faults along the margins of the interplatform sub-basin in Ohio and the Jeptha Knob structure in Kentucky. Black River Group carbonates were deposited on a relatively stable platform prior to a major collision between North America and a volcanic island arc that began in earliest Trenton time and continued through the Ordovician into the Silurian. These collisions reactivated older faults and created new faults oriented subparallel to the orogenic belt. High-temperature, high-pressure saline fluids flowed up active basement-rooted strike-slip and transtensional faults during the time of Trenton Limestone and Utica Shale deposition, until they encountered low-permeable beds in the base of the Trenton in New York and the Utica in Ohio. At that point, the fluids flowed laterally into more permeable Black River and Trenton beds. As the fluids cooled, they leached the host limestone beds, producing vugs in a migrating front that moved away from the fault zone. Permeability behind this front was enhanced by fracturing and continued leaching. Subsequently, these higher-permeability beds were invaded by warmer, dolomite-supersaturated fluids, precipitating dolomite, initially in a halo of matrix dolomite, particularly on the downthrown sides of negative flower structures. Matrix dolomitization was followed by further fracturing, brecciation and vug development as tectonic activity continued. Fractures and vugs were lined with saddle dolomite soon after they were formed. As time passed, a range of other minerals, including quartz, bitumen, sulfides and calcite were precipitated.

Natural gases produced from Trenton and Black River reservoirs in Kentucky and Ohio are thermogenetic, cracked from kerogens in organic-rich source rocks and from reservoir oils at higher maturation temperatures. Evidence from carbon isotope distributions indicates that the gas in the Homer field in Kentucky is compartmentalized, probably due to faulting, with two groups of gases produced from different wells. The two types of gases are thermogenic gas associated with oil, and thermogenic gas that

formed in the transition zone between oil-associated gas and postmature gas. Potential source rocks for the Kentucky gases include shales in the Upper Ordovician Utica Shale and Point Pleasant Formation; dolomitic mudstones in the Middle Ordovician Trenton Formation; the Middle Ordovician Wells Creek Formation; and rocks within the Cambrian Rome Formation.

Natural gases produced from fractured limestones in Cottontree field, West Virginia are postmature and can be interpreted as either mixed thermogenetic gases generated in source rocks in the Utica Shale, Point Pleasant Formation, Trenton Formation, Wells Creek Formation, or the Rome Formation, as in Kentucky; or as abiogenic gases of deep crustal origin.

Natural gases produced from the York field in northeastern Ohio are thermogenic gases associated with condensate. The Utica Shale is the most probable source rock for these gases, with migration occurring from a deeper portion of the basin northeast of the gas field.

Natural gases produced from dolomitized Black River rocks in south central New York and north central Pennsylvania are unique. These gases consistently exhibit low wetness, heavy $\delta 13C_1$ values, and unusual methane δ^2H that become isotopically lighter as the $\delta 13C_1$ becomes heavier. In addition to the strong negative correlation between methane $\delta^{13}C$ and δ^2H, the gases show notable carbon isotopic reversals among the C_1 through C_3 hydrocarbons, particularly when compared to the normal carbon isotope distributions exhibited by Trenton and Black River thermogenic gases produced in Kentucky and Ohio. $\delta^{15}N$ of nitrogen produced in the New York and Pennsylvania gases has a mean value of –6.7 permil, and may have originated through devolatilization reactions associated with kimberlite intrusions. High nitrogen concentrations in some wells may have a negative impact on economic reserves in portions of the play. Noble gas geochemistry indicates highly variable flux of both mantle and radiogenic crustal gases. These data reflect high heat flow coupled with deep-seated faulting and fracturing, and hydrothermal fluid migration. The noble gas data also indicate some gas leakage from the reservoirs, and highly variable residence times for natural gases in the different New York and Pennsylvania fields.

The hydrocarbons produced from Black River reservoirs in New York and Pennsylvania might be the first documented occurrence of a commercial abiogenic natural gas accumulation. The data are compelling, but further confirmation will be necessary to fully support this interpretation. If correct, this interpretation of the gases will have a direct bearing on the interpreted mechanisms, processes and timing of hydrothermal dolomitization in the region. However, if the abiogenic hydrocarbon hypothesis is incorrect, then Black River gases produced in New York and Pennsylvania are a mixture of isotopically heavy, postmature gas generated from an unidentified, deep-basin source rock, and residual, isotopically-light ethane and propane. It is important to consider that the magnitude of the observed $\delta^{13}C$ enrichment and simultaneous $\delta^{13}C$ depletion in the ethane and propane are difficult to explain in a thermogenic gas accumulation.

Hydrogen sulfide poses a potential problem with deeper Black River gas production in Pennsylvania, and perhaps West Virginia. In Pennsylvania, the $\delta^{34}S$ of sulfur in the produced H_2S suggests that thermochemical sulfate reduction is responsible for the generation of gas in the reservoir.

It is difficult to collect and analyze production data for the Trenton-Black River gas play. Production data for most of the "historical" wells drilled in older fields do not exist in the public record, and wells that have been drilled and completed in the current play are so new that production records, although complete, are of short duration. The data that do exist, however, indicate a high degree of variability in reservoir performance within the hydrothermal play area of south-central New York. Recent horizontal drilling technology has proven to be quite successful in this area and offers good potential in the future as the play continues to develop.

All of the stratigraphic, structural, petrographic, geochemical, gas analyses and production data collected and generated for and during this project were assembled by a small resource assessment team that was charged with developing a model to assess the undiscovered gas resource of this play. To accomplish this, the team modified a model that has been used by the U.S. Geological Survey in its resource assessments. The team took into account the thickness, distribution and richness of potential source rocks; the approximate locations of the gas-, gas-and-oil, and oil-generating areas, based on thermal maturity interpreted from conodont alteration data; the maximum and minimum play areas to assess, based on current production data, gas shows and "favorable" geologic parameters developed elsewhere by project geologists; the timing of maturity and fluid migration; and the size and number of fields that might be discovered in the first 30 years of this play development.

The maximum assessment area was divided into two plays, a hydrothermal dolomite play area in the shallower part of the basin, extending from south-central New York and north-central Pennsylvania through Ontario and Ohio into eastern Kentucky; and a fractured limestone play in the deeper portion of the basin in Pennsylvania and West Virginia. Small areas of historic production in Kentucky and near the eastern end of Lake Ontario in New York have been attributed to the presence of bioclastic limestone reservoirs. However, these areas were included with the area of hydrothermal dolomite for assessment purposes and were not assessed separately.

A basic assumption was that high-pressure fluids migrating upward from the basement ultimately would reach a maximum height, even if unrestricted by fault seals, and would then descend. Thus, hydrothermal dolomite would only be formed in the Trenton and Black River in areas where fluids were capable of reaching these limestone units. In areas of the basement where the rock interval between the basement and the Black River was too great for these units to be reached by high-temperature, high-pressure fluids, if dolomitization of host limestones did occur, it would occur in deeper Cambrian carbonates, and production from the Trenton and Black River would be confined to fractured, but non-dolomitized zones.

Undiscovered gas resources were estimated through a Monte-Carlo simulation method developed by the USGS. This procedure required the team to estimate the number of undiscovered fields and the size of those fields. Thus, values for the minimum, median and maximum number of fields that might be discovered, and the minimum, median and maximum sizes of those fields, were entered into the program. For each play, gas resource numbers were generated at the 90%, 50% and 10% probability (confidence) levels. The final resource numbers for the entire assessment area are as follows: there is a 90% probability that at least 2.7 Tcf will be discovered; a 50% probability that at least 6.0 Tcf will be discovered; and a 10% probability that at least 11.0 Tcf will be discovered. Most of this gas is predicted to be found in the HTD play area.

TABLE OF CONTENTS

	Page
Title page	i
Disclaimer	ii
Abstract	iii
Table of Contents	ix
Executive Summary	1
Research Results	4
Regional Stratigraphy of the Trenton-Black River Interval	4
Geologic Structure and Seismic Analysis	39
Petrography of the Trenton Limestone and Black River Group Carbonate Rocks in the Appalachian Basin	64
Geochemical and Fluid Inclusion Analyses of Trenton-Black River Limestones and Dolomites	101
Geochemistry of Natural Gases from Trenton Limestone and Black River Group Carbonate Reservoirs, Appalachian Basin	162
Trenton-Black River Production History and Analysis	212
Exploration Fairways and Undiscovered Gas Assessment Model	229
Trenton-Black River Key Field and Play Descriptions	255
Summary and Conclusions	337
References	346
Appendices	370
A. Description of Project Website, Database and GIS-IMS	371
B. Details and Results of the Bentonite Correlation Study for the Trenton-Black River Consortium and the New York State Museum	395
C. Samples of Supposed Deicke and Millbrig K-bentonite	397
D. Origin and Reservoir Characteristics of Upper Ordovician Trenton-Black River Hydrothermal Dolomite Reservoirs in New York	399
E. Petrology of the Trenton Limestone and Black River Group	442
1. Non-skeletal grains and skeletal components	
2. Diagenesis	
3. Dolomite textures	
4. Base metal sulfide mineralization	
5. Dolomite porosity	
F. Page-sized plates from the Stratigraphy chapter	544
G. Page-sized plates from the Seismic and Structure chapter	572

LIST OF ILLUSTRATIONS

List of Figures

Chapter 1: Regional Stratigraphy of the Trenton-Black River Interval

Figure 1-1. Correlation chart for Precambrian through Ordovician rocks in the central Appalachian basin and surrounding areas
Figure 1-2. Map showing major tectonic features and paleogeography during Early Cambrian time
Figure 1-3. Generalized schematic cross section illustrating the relationships of the mapped Cambrian basal sandstones to other geologic units and structure
Figure 1-4A. Map showing basin architecture during Precambrian to Middle Cambrian Mount Simon Sandstone/Conasauga Formation time;
B. Map showing basin architecture during Late Cambrian/Early Ordovician time
Figure 1-5. Facies map of late Black River time
Figure 1-6. Facies map of Trenton/Point Pleasant time
Figure 1-7A. Map showing basin architecture during Middle Ordovician Trenton to Late Ordovician "Kope" or equivalent time;
B. Map showing basin architecture during Late Ordovician "Kope" or equivalent time to top of Ordovician time
Figure 1-8. Representative well on the clean carbonate Trenton Platform; Ohio Geological Survey, Stone Company
Figure 1-9. Representative well from the argillaceous carbonate Trenton Platform; Belden and Blake, 1 Huber
Figure 1-10. Representative well of the Utica/Point Pleasant sub-basin; Chevron, 1-A Prudential
Figure 1-11. Representative well of the Utica/Point Pleasant sub-basin; Ohio Geological Survey, American Aggregates
Figure 1-12. Representative well on the Lexington Platform; Signal Oil and Gas, Henry Stratton
Figure 1-13. Representative well of a clean Trenton carbonate in the deeper basinal area; United Fuel Gas, 1 Sponaugle

Chapter 2: Geologic Structure and Seismic Analysis

Figure 2-1. Map showing the seismic data available to the consortium for interpretation
Figure 2-2. Interval velocity, acoustic impedance and synthetic seismogram for a well in eastern Ohio
Figure 2-3. Precambrian provinces in the study area
Figure 2-4. Seismic section across the Rockcastle River fault zone in the western Rome trough of eastern Kentucky

Figure 2-5. Seismic section across the Irvine-Paint Creek fault zone in the Rome trough of eastern Kentucky
Figure 2-6. Composite seismic section through central Kentucky across the deepest portion of the basin
Figure 2-7. Composite seismic section through eastern Kentucky across the deepest portion of the basin
Figure 2-8. Composite seismic section through southwestern West Virginia across the deepest portion of the basin
Figure 2-9. Composite seismic section through northern West Virginia across deepest portion of the basin
Figure 2-10. Composite seismic section from south central New York to central Pennsylvania
Figure 2-11. Schematic model of fault-related hydrothermal alteration for Trenton-Black River reservoirs

Chapter 3: Petrography of the Trenton Limestone and Black River Group Carbonates

Figure 3-1. Carbonate matrix in the Trenton Limestone and Black River Group, Union Furnace, Pennsylvania:
A. Skeletal wackestone or packed biomicrite from the Black River, Union Furnace, Pennsylvania;
B. Dark organic-rich matrix in a skeletal wackestone or packed biomicrite from the Trenton, Union Furnace, Pennsylvania
Figure 3-2. Limestone tempesites or turbidites interbedded with siliciclastic shales in the Trenton Formation at Union Furnace, Pennsylvania
Figure 3-3. Very fine-grained quartz arenite from a very thin sandstone bed in the Black River, Union Furnace, Pennsylvania:
A. Low magnification view;
B. Higher magnification view, same sandstone
Figure 3-4. K-bentonites in the Trenton Limestone and Black River Group:
A. Deicke K-bentonite at Union Furnace, Pennsylvania;
B. Millbrig K-bentonite from core near Union Furnace outcrop;
C. Millbrig K-bentonite in the Chevron 1A Prudential core, Marion County, Ohio
Figure 3-5. Completely micritized ooids in the Black River Group
Figure 3-6. Micrite envelope on echinoid grain and peloidal cement:
A. Large echinoid fragment exhibits a bored rim and well-developed micrite envelope;
B. Same photomicrograph in cross-polarization;
C. High magnification view of the peloidal cement that fills both the bored edge of the echinoid grain and the void space immediately below it
Figure 3-7. Peloidal cement fabric in the Black River Group:
A. Core sample of apparent burrowed and bioturbated wackestone or sparse biomicrite, Gray #1 well, Steuben County, New York;
B. Thin section photomicrograph of the same sample;
C. Higher magnification view of the same sample;

D. Progressively higher magnification view of the same sample;
E. Another thin section view of peloidal cement in the same sample;
F. Peloidal cement fills a void formed earlier through dissolution of part of a bryozoan fragment;
G. Peloidal cement that once filled all of the zooecia of a bryozoan grain now mimics the original fossil structure

Figure 3-8. Hardgrounds and peloidal cements:
A. Stacked, amalgamated hardground in the Trenton Formation exposed southeast of Lexington, central Kentucky;
B. Plan view of bryozoans encrusting the top of a hardground, Trenton Formation, central Kentucky;
C. Thin section photomicrograph of the hardground surface in 3-8A;
D. A planar and undercut hardground in the Black River Group exposed at Union Furnace, Pennsylvania;
E. Thin section photomicrograph of the hardground shown in 3-8D;
F. Thin section photomicrograph of the hardground shown in 3-8D

Figure 3-9. High magnification view of chalcedony replacing nonplanar dolomite that mimically replaces a crinoid grain:
A. View under crossed polars showing typical radiating habit of chalcedony;
B. Same view, but with the gypsum plate inserted

Figure 3-10. Macropores and mesopores in the Black River Group, Whiteman #1 well, Chemung County, New York

Chapter 4: Geochemical and Fluid Inclusion Analysis

Figure 4-1. Distribution of Trenton-Black River dolomitized reservoirs
Figure 4-2. Field map and core locations for south central New York
Figure 4-3. Dolomites from the Gray and Whiteman cores in south central New York
Figure 4-4. Locations of wells studied and various dolomite types in NW Ohio
Figure 4-5. Facies dolomite core from NW Ohio with coarse, porous matrix dolomite
Figure 4-6. Breccia with saddle dolomite matrix dolomite and pyrite
Figure 4-7. Locations of cores studied for geochemistry in southern Ohio, Kentucky and West Virginia
Figure 4-8. Map and cross section of Jeptha Knob, Kentucky
Figure 4-9. Porous dolomite from the Lexington (Trenton) and High Bridge (Black River) in core JK-1 at Jeptha Knob
Figure 4-10. Photograph of primary fluid inclusion from Whiteman well in New York
Figure 4-11. Secondary petroleum inclusions formed along micro-crack
Figure 4-12. Results of fluid inclusion analysis for New York dolomites
Figure 4-13. Results of fluid inclusion analysis for Ohio dolomites
Figure 4-14. Results of Jeptha Knob dolomite fluid inclusion analysis
Figure 4-15. Results of all fluid inclusion analyses to date
Figure 4-16. Stable isotope data from New York
Figure 4-17. Stable isotope data from Ohio dolomites
Figure 4-18. Stable isotope values from Kentucky Jeptha Knob dolomites and limestones

Figure 4-19. Stable isotope data from West Virginia Sand Hill core
Figure 4-20. Chart used to determine fluid composition by plotting homogenization temperature and d18O values for same sample
Figure 4-21. Data from New York, Ohio and Kentucky plotted on previous
Figure 4-22. Trace element data from New York
Figure 4-23. Trace element data from Ohio samples
Figure 4-24. Strontium isotope ratio curve for seawater through time
Figure 4-25. Strontium isotope ratios for saddle dolomite in Ohio samples
Figure 4-26. Strontium isotope ratios for matrix dolomite in Ohio samples
Figure 4-27. Strontium isotope ratios for Jeptha Knob dolomite in Kentucky
Figure 4-28. Variations in salinity with depth in sedimentary basins
Figure 4-29. Variations in salinity with depth in crystalline basement rocks of the Canadian Shield
Figure 4-30. Temperature ranges for CAI values
Figure 4-31. Map of maximum burial temperatures based on CAI
Figure 4-32. Maximum burial temperatures and fluid inclusion homogenization temperatures from saddle and matrix dolomites in Trenton-Black River reservoirs
Figure 4-33. Idealized permeability evolution of a fault zone
Figure 4-34. Vertically exaggerated line over three Black River fields in New York
Figure 4-35. Schematic model for development of Trenton-Black River hydrothermal dolomite reservoirs
Figure 4-36A. Paleogeographic map for Trenton Limestone with oil and gas fields; B. Closeup of producing area
Figure 4-37. Paleogeographic map of Ladyfern and other Devonian Slave Point hydrothermal dolomite and leached limestone reservoirs
Figure 4-38. Map showing locations of cores used for OH-KY-WV cross section
Figure 4-39. Cross section of gamma ray logs and ^{13}C data from Ohio, Kentucky and West Virginia
Figure 4-40. Map of locations in New York ^{13}C cuttings-based cross section
Figure 4-41. Cross section of ^{13}C based on cuttings from four wells form northwestern New York
Figure 4-42. Line of section for NY-WV cross section
Figure 4-43. Cross section with ^{13}C data from northern New York through Wilson Hollow Field to Sand Hill well, West Virginia

Chapter 5: Geochemistry of Natural Gases from Trenton and Black River Reservoirs

Figure 5-1. Regional map of the study area showing Trenton and Black River gas fields and well locations for the natural gas samples discussed in this report
Figure 5-2. Map showing locations of the wells sampled for gas geochemistry in Cottontree field, West Virginia and Homer and Colin Fork fields, Kentucky
Figure 5-3. Methane isotopic composition of natural gases from Homer and Colin Fork fields, Kentucky
Figure 5-4. Distribution of $\delta^{13}C$ in methane through isobutane in natural gases from Homer and Colin Fork fields, Kentucky

Figure 5-5. Chung plot showing the isotopic composition of individual hydrocarbons in natural gases from Homer and Colin Fork fields, Kentucky as a function of the number of carbon atoms (C_n) in the hydrocarbon
Figure 5-6. Methane isotopic composition of natural gases from Cottontree field, West Virginia
Figure 5-7. Distribution of $\delta^{13}C$ in methane and ethane in natural gases from Cottontree field, West Virginia
Figure 5-8. Chung plot showing the isotopic composition of individual hydrocarbons in natural gases from Cottontree field, West Virginia
Figure 5-9. Map showing locations of the wells sampled for gas geochemistry in the York field, Ashtabula County, Ohio
Figure 5-10. Methane isotopic composition of natural gases from York field, Ohio
Figure 5-11. Distribution of $\delta^{13}C$ in methane through isobutane in natural gases from York field, Ohio
Figure 5-12. Chung plot showing the isotopic composition of individual hydrocarbons in natural gases from York field, Ohio
Figure 5-13. Map showing the locations of the wells sampled for gas geochemistry in the Black River gas fields of New York and Pennsylvania
Figure 5-14. $\delta^{15}N$ versus nitrogen concentration in the Black River gases produced in New York and Pennsylvania
Figure 5-15. $\delta^{13}CO_2$ versus carbon dioxide concentration in the Black River gases produced in New York and Pennsylvania
Figure 5-16. *Ra* versus ^{4}He in the Black River gases produced in New York and Pennsylvania
Figure 5-17. *Ra* versus $^{40}Ar/^{36}Ar$ in the Black River gases produced in New York and Pennsylvania
Figure 5-18. *Ra* versus $^{40}Ar^*$ versus $^{40}Ar_o$ in the Black River gases produced in New York and Pennsylvania
Figure 5-19. $^{20}Ne/^{36}Ar$ versus ^{4}He in the Black River gases produced in New York and Pennsylvania
Figure 5-20. Bitumen coating hydrothermal dolomites in the Black River reservoir rocks on New York: A) Backscattered SEM photomicrograph of bitumen coating a crystal of delafossite, Gray #1 well, Steuben County, New York; B) Back-scattered SEM photomicrograph of bitumen coatings on nonplanar-c hydrothermal (saddle) dolomite, Whitman #1 well, Chemung County, New York
Figure 5-21. Methane isotopic composition of Black River natural gases from New York and Pennsylvania fields
Figure 5-22. Methane isotopic composition of all Black River natural gases in the Appalachian basin sampled and analyzed for this report
Figure 5-23. Distribution of $\delta^{13}C$ in methane through propane in natural gases from the New York Black River fields
Figure 5-24. Chung plot showing the isotopic composition of individual hydrocarbons in natural gases from the New York Black River fields
Figure 5-25. Distribution of $\delta^{13}C$ in methane through propane in natural gases from the Pennsylvania Black River fields

Figure 5-26. Chung plot showing the isotopic composition of individual hydrocarbons in natural gases from the Pennsylvania Black River fields
Figure 5-27. Plot of $\delta^{13}C$ values of individual hydrocarbon gases (n-alkanes, C_1 through iC_4) against carbon number for all Trenton/Black River gases sampled and analyzed during this study
Figure 5-28. Nitrogen concentration versus helium concentration in all Trenton/Black River natural gases sampled and analyzed for this study: A) N_2 versus He plot with field locations of the gases noted; B) Same plot with best-fit line calculated from linear regression showing moderate correlation between helium and nitrogen in the gases
Figure 5-29. $\delta^{13}C$ of methane versus $\delta^{13}C$ of ethane for all Trenton/Black River natural gases sampled and analyzed during this study
Figure 5-30. $\delta^{13}C$ of methane versus $\delta^{13}C$ of propane for all Trenton/Black River natural gases sampled and analyzed during this study

Chapter 6: Trenton-Black River Production History and Analysis

Figure 6-1. Map showing location of selected HTD and FLS gas fields
Figure 6-2. Map showing location of Quackenbush Hill field, Steuben and Chemung counties, New York
Figure 6-3. Graph of annual production and number of wells contributing to annual production for Quackenbush Hill field
Figure 6-4. Map showing the location of the York field, Ashtabula County, Ohio
Figure 6-5. Graph of annual production for York field and number of wells contributing to annual production for York field
Figure 6-6. Map showing the location of County Line field, Chemung, Schyler and Steuben counties, New York
Figure 6-7. Graph of annual production for County Line field and number of wells contributing to annual production for County Line field
Figure 6-8. Map showing the location of the Cottontree field, Roane County, West Virginia
Figure 6-9. Graph of annual production for Cottontree field and number of wells contributing to annual production for Cottontree field
Figure 6-10. Map showing the locations of the Trixie and Trixie Consolidated fields, Clay County, Kentucky
Figure 6-11. Map showing the location of Honey Creek and Albany Consolidated fields
Figure 6-12. Map showing the location of Honey Creek field, Marion County, Ohio
Figure 6-13. Map showing the location of Albany Consolidated field, Clinton County, Kentucky
Figure 6-14. Map of wells in western New York with year 2 production indicated by relative size of circle
Figure 6-15. Map of wells in central West Virginia with year 2 production indicated by relative size of circle

Chapter 7: Exploration Fairways and Undiscovered Gas Assessment Model

Figure 7-1. Regional assessment area
Figure 7-2. Isolith map of potential shale source rocks
Figure 7-3. Map of maximum TOC values for potential shale source rocks
Figure 7-4. Map of minimum TOC values for potential shale source rocks
Figure 7-5. Map of average TOC values for potential shale source rocks
Figure 7-6. Map of minimum CAI values in the assessment area
Figure 7-7. Map of maximum CAI values in the assessment area
Figure 7-8. Map of oil and gas generating windows, immature and over mature areas
Figure 7-9. Isopach map of the interval between the basement and Black River Group
Figure 7-10. Map of Trenton-Black River play areas

Chapter 8: Trenton-Black River Key Field and Play Descriptions

Figure 8-1. Black River wells of south-central New York
Figure 8-2. Trenton-Black River regional cross section
Figure 8-3. Well log from Auburn geothermal field
Figure 8-4. Well logs from the Ballyhack Creek field
Figure 8-5. Well logs from the Beans Station field
Figure 8-6. Well log from the Caton field
Figure 8-7. Well log from the Cooper Hill field
Figure 8-8. Well logs from the County Line field
Figure 8-9. Well log from the Cutler Creek field
Figure 8-10. Well logs from the Glodes Corners Road field
Figure 8-11. Well log from the Guyanoga Valley field
Figure 8-12. Well logs from the Langdon Hill field
Figure 8-13. Well logs from the Muck Farm field
Figure 8-14. Well logs from the Pine Hill field
Figure 8-15. Well logs from the Quackenbush Hill field
Figure 8-16. Horizontal well logs and directional surveys in Quackenbush Hill field.
A. Reed #1 well
B. Hakes #1 well
C. Andrews #1 well
Figure 8-17. Well log from the Riverside field
Figure 8-18. Well log from the Seeley Creek field
Figure 8-19. Well log from the Sexton Hollow field
Figure 8-20. Well log from the South Corning field
Figure 8-21. Well logs from the Terry Hill South field
Figure 8-22. Well log from the West River field
Figure 8-23. Well log from the Whiskey Creek field
Figure 8-24. Well logs from the Wilson Hollow field
Figure 8-25. Well log from the Zimmer Hill field
Figure 8-26. Cross section from York field, NE Ohio
Figure 8-27. Time-structure map on top Trenton, York field

List of Plates

Chapter 1: Regional Stratigraphy of the Trenton-Black River Interval

Plate 1-1. Map showing location of cross-section lines and Trenton-Black River cores, dolomitized zones and outcrops in project area
Plate 1-2. Regional stratigraphic cross section Dip A-A'
Plate 1-3. Regional stratigraphic cross section Dip B-B'
Plate 1-4. Regional stratigraphic cross section Dip C-C'
Plate 1-5. Regional stratigraphic cross section Dip D-D'
Plate 1-6. Regional stratigraphic cross section Dip E-E'
Plate 1-7. Regional stratigraphic cross section Dip F-F'
Plate 1-8. Regional stratigraphic cross section Dip G-G'
Plate 1-9. Regional stratigraphic cross section Dip H-H'
Plate 1-10. Regional stratigraphic cross section Dip I-I'
Plate 1-11. Regional stratigraphic cross section Dip J-J'
Plate 1-12. Regional stratigraphic cross section Dip K-K'
Plate 1-13. Regional stratigraphic cross section Dip L-L'
Plate 1-14. Regional stratigraphic cross section Strike A-A'
Plate 1-15. Regional stratigraphic cross section Strike B-B'
Plate 1-16. Regional stratigraphic cross section Strike C-C'
Plate 1-17. Regional stratigraphic cross section Strike D-D'
Plate 1-18. Regional stratigraphic cross section Strike E-E'
Plate 1-19. Regional stratigraphic cross section Strike F-F'
Plate 1-20. Interval-thickness map of the Cambrian pre-Knox (top of Precambrian to base of Cambrian Knox and equivalents)
Plate 1-21. Interval-thickness map of the basal Cambrian sandstones (includes the Cambrian Mt. Simon, unnamed Conasauga sandstone, Potsdam and older Rome Trough basal sandstone); inset map illustrates the boundaries for these respective mapped units
Plate 1-22. Interval-thickness map of the Cambrian-Ordovician Knox (base of Knox to top of Knox)
Plate 1-23. Interval-thickness map of the Cambrian Rose Run sandstone (top of the Copper Ridge to top of Rose Run; includes the Upper Sandy Member of the Gatesburg Formation in Pennsylvania and the Theresa Formation sandstone equivalent in New York)
Plate 1-24. Interval-thickness map of the Black River and "Wells Creek" (top of Knox to top of Black River)
Plate 1-25. Interval-thickness map of the Black River (top of "Wells Creek" to top of Black River
Plate 1-26. Interval-thickness map of the Trenton/Curdsville (top of Black River to top of Trenton/Curdsville); extent of the Logana also shown
Plate 1-27. Interval-thickness map of the Trenton/Lexington (top of Black River to top of the Trenton/Lexington Limestone)

Plate 1-28. Interval-thickness map of the "Utica" (top of Trenton to top of "Utica"; includes the "Point Pleasant" and the Antes Shale); extent of the "Utica" and the "Point Pleasant" also shown
Plate 1-29. Interval-thickness map of the "Kope," (top of the Trenton/Lexington to the top of the "Kope;" includes the partial equivalents of the Reedsville and Martinsburg in West Virginia, Pennsylvania and New York, and the Blue Mountain/Georgian Bay in Ontario; also includes the "Utica" and "Point Pleasant")
Plate 1-30. Interval-thickness map of the upper Ordovician undifferentiated (top of the "Kope" and equivalents to the top of the Ordovician undifferentiated)

Chapter 2: Geologic Structure and Seismic Analysis

Plate 2-1. Structural features map of region
Plate 2-2. Structure of the Top of the Precambrian section
Plate 2-3. Structure of the Base of the Knox Supergroup
Plate 2-4. Structure of the Top of the Knox Supergroup
Plate 2-5. Structure of the Top of the Black River Limestone
Plate 2-6. Structure of the Top of the Trenton Limestone
Plate 2-7. Structure of the Top of the Ordovician section
Plate 2-8. Structure of the Base of the Devonian Shale section

List of Tables

Chapter 2: Geologic Structure and Seismic Analysis

Table 2-1. Seismic data contributors for the Trenton-Black River Consortium
Table 2-2. List of included plates

Chapter 3: Petrography of the Trenton Limestone and Black River Group Carbonates

Table 3-1. Core and outcrop samples of Trenton Limestone and Black River Group, Appalachian Basin

Chapter 4: Geochemical and Fluid Inclusion Analysis

Table 4-1. Ohio cores sampled for dolomite
Table 4-2. Sample of results of fluid inclusion analysis
Table 4-3. Abundance of iron and manganese in seawater and subsurface brines

Chapter 5: Geochemistry of Natural Gases from Trenton and Black River Reservoirs

Table 5-1. Trenton-Black River gas geochemistry data
Table 5-2. Trenton-Black River noble gas data
Table 5-3. Trenton-Black River He isotopes gas analysis

Chapter 6: Trenton-Black River Production History and Analysis

Table 6-1. Summary gas production by field
Table 6-2. Summary oil production by field
Table 6-3 New York Horizontal Wells

Chapter 8: Trenton-Black River Key Field and Play Descriptions

Table 8-1. Reservoir data for 25 Trenton-Black River fields in New York
Table 8-2. Directional wells in New York
Table 8-3. Well from the Auburn geothermal field
Table 8-4. Wells from the Ballyhack Creek field
Table 8-5. Wells from the Beans Station field
Table 8-6. Well from the Caton field
Table 8-7. Well from the Cooper Hill field
Table 8-8. Wells from the County Line field
Table 8-9. Wells from the Cutler Creek field
Table 8-10. Wells from the Glodes Corners Road field
Table 8-11. Well from the Guyanoga Valley field
Table 8-12. Wells from the Langdon Hill field
Table 8-13. Wells from the Muck Farm field
Table 8-14. Wells from the Pine Hill field
Table 8-15. Wells from the Quackenbush Hill field
Table 8-16. Horizontal wells from Quackenbush Hill field
Table 8-17. Well from the Riverside field
Table 8-18. Well from the Seeley Creek field
Table 8-19. Well from the Sexton Hollow field
Table 8-20. Well from the South Corning field
Table 8-21. Wells from the Terry Hill South field
Table 8-22. Well from the West River field
Table 8-23. Well from the Whiskey Creek field
Table 8-24. Wells from the Wilson Hollow field
Table 8-25. Well from the Zimmer Hill field

EXECUTIVE SUMMARY

This "Geologic Play Book of Trenton–Black River Exploration" in the Appalachian basin incorporates and integrates regional stratigraphic relationships and facies trends; structural geology and seismic interpretations; carbonate petrology; isotope and fluid inclusion analyses; natural gas geochemistry; and an evaluation of production history and trends to produce an integrated stratigraphic-structural-diagenetic model for the development of hydrothermal dolomite reservoirs in these carbonate units and a model for the assessment of undiscovered natural gas resources in two Trenton-Black River gas plays. These two plays are defined as a hydrothermal dolomite gas play on the western side of the basin, extending from New York and Ontario southward through Ohio into northern Kentucky; and a fractured limestone gas play on the eastern side of the basin, extending from north central Pennsylvania southward through West Virginia into eastern Kentucky. Through much of the basin, the boundary between the two plays approximates the western edge of the Rome trough.

The play book is the result of a contract awarded to the West Virginia University Research Corporation (Research Corporation) by the U.S. Department of Energy through the National Energy Technology Laboratory. The Research Corporation assigned the contract to the Appalachian Oil and Natural Gas Research Consortium (AONGRC), a program at the National Research Center for Coal and Energy at West Virginia University. The AONGRC organized a Trenton-Black River Research Team, consisting of recognized experts at the State geological surveys in Kentucky, Ohio, Pennsylvania and West Virginia, and the New York State Museum Institute, an agency in the New York State Education Department.

The Research Corporation, working with the AONGRC, created an industry-government-academic partnership, the "Trenton-Black River Appalachian Basin Exploration Consortium" (the Consortium), to co-fund and assist the research effort. Seventeen gas exploration companies joined the Consortium, contributing cost share through a two-year membership fee.

This project had three main objectives, all of which were met: to develop an integrated structural-stratigraphic-diagenetic model for the origin of Trenton-Black River hydrothermal dolomite reservoirs; to define possible fairways within which to conduct more detailed studies leading to further development of the gas resource in these reservoirs; and to develop an integrated, multi-faceted, resource assessment model of Trenton-Black River reservoirs in New York, Ohio, Pennsylvania, Kentucky and West Virginia.

The Consortium achieved these goals by conducting research in eight integrated task areas: structural and seismic analysis and mapping; analysis of stratigraphic relationships and thickness trends; analysis of petrographic data and synthesis of depositional environments; analysis of isotope geochemistry and fluid inclusion data; analysis and summary of petroleum geochemistry data; analysis of production data,

histories and horizontal well technology; developing and managing a project website, database and GIS-IMS; and play book compilation and resource assessment.

Evidence from the stratigraphic, structural, petrographic and geochemical tasks clearly indicates that hydrothermal dolomites in the Black River Group and overlying Trenton Limestone are the result of fault-related hydrothermal alteration of limestones. Carbonate beds in these two units were deposited on a relatively stable platform prior to major plate collisions that began in the Late Ordovician and continued into the Early Silurian. These collisions resulted in reactivation of old faults, or activation of new, basement-deep faults. High-pressure, high-temperature fluids moved up active, basement-rooted, strike-slip and transtensional faults during late Middle and early Late Ordovician time, until they encountered a low-permeable zone at the base of the Trenton Limestone. As the hot fluids moved laterally beneath this low-permeable zone, they cooled and leached limestone beds in the upper part of the Black River, enhancing permeability in these beds. Subsequent hot fluids that moved up the fault system were able to migrate farther from the faults, precipitating dolomite in the leached limestone zone, particularly on the downthrown sides of faults in negative flower structures. Matrix dolomitization was followed by further fracturing, brecciation and vug development as tectonic activity continued. The exploration model for Trenton-Black River hydrothermal dolomite reservoirs is to look for seismic evidence of subtle, basement-rooted wrench faults and negative flower structures that cut these limestones with evidence of movement within the first kilometer of burial. Faults with minor offset that do not extend far above the target formations are typically the best candidates because these faults have not breached the seal for hydrothermal fluids and hydrocarbons that were emplaced later.

The Trenton-Black River play is an expensive, high-tech, high-risk play that requires accurate interpretation of seismic data, including 3-D data. Future seismic programs should be concentrated over more favorable fairways, including: the Rome trough in Pennsylvania, West Virginia and eastern Kentucky; areas of high-faulting associated with the current hydrothermal dolomite play in south-central New York; over an area of similar faulting in northwest Pennsylvania; and around the margin of an area interpreted from isopach and facies maps of the Trenton Limestone as the “Trenton Platform,” extending from northwest Ohio eastward into northwest Pennsylvania, and then southwestward into West Virginia and southern Ohio where it has been referred to as the “Lexington Platform.” These potential fairways help to divide the Trenton-Black River gas play into two separate plays: a hydrothermal dolomite (HTD) play on the western side of the basin; and a fractured limestone play on the eastern side of the basin.

The HTD play extends throughout the shallower portion of the basin, areas where hot fluids rising up through basement-rooted faults could reach the Black River and perhaps the lowermost limestone beds in the overlying Trenton Limestone before they either cooled or lost energy and flowed back down the faults into the basement. The HTD play area includes the area of current activity in south central New York, and the area of older Trenton-Black River production in northwest Ohio that is associated with the margin of the Trenton Platform. Clean limestones deposited around the margin of the

platform are interpreted as being more prone to dolomitization than other facies types in these carbonate units.

The boundary between the HTD play and the fractured limestone play, although chosen based on a maximum thickness of rock between the top of the Black River down to the basement through which hot, dolomitizing fluids have been shown to rise, approximates the western edge of the Rome trough in much of Pennsylvania, West Virginia and Kentucky. The Rome trough is an area of intense faulting and fracturing, and periodic reactivation of faults within the trough would fracture limestone beds in the overlying Black River and younger Trenton Limestone. Although the basement may be too deep in this area for hot fluids rising from the basement to reach and dolomitize limestones in the Trenton and Black River, it is quite probable that hot fluids have dolomitized limestones in older Cambrian limestone formations within and over the Rome trough.

Undiscovered gas resources were assessed for both of these plays employing and modifying a method used by the United States Geological Survey in their resource assessments. During this assessment, the following were considered: thickness, richness and thermal maturation of potential source rocks; regional stratigraphy and structural geology; discovery trends and sizes of current fields; and estimated ultimate recovery of existing fields. It was estimated that there is a 90% probability of finding at least an additional 2.7 Tcf of gas in these two plays; a 50% probability of finding 6.0 Tcf; and a 10% probability of discovering another 11.0 Tcf. Most of this gas is expected to be discovered in the HTD play area.

RESEARCH RESULTS

REGIONAL STRATIGRAPHY OF THE TRENTON-BLACK RIVER INTERVAL

By Ronald A. Riley, Mark T. Baranoski and Lawrence H. Wickstrom, Ohio Division of Geological Survey

The primary objectives of the regional stratigraphy task were to: 1) place the Trenton Limestone, Black River Group, Utica Shale and equivalent lithostratigraphic units within a regional framework; 2) model the depositional environment and basin architecture; and 3) integrate findings with the results of other tasks of the consortium to delineate potential areas of exploration interest. The stratigraphic framework that was developed established regionally-consistent formation/interval boundaries that were used to produce structure, isopach and facies maps. This regionally-consistent stratigraphic framework also provided a better understanding of the complexly interwoven geologic parameters controlling Trenton-Black River reservoirs. In addition, the framework allowed lateral facies changes to be separated and mapped regionally for the first time. Because deposition of these facies was tectonically influenced, their detailed mapping is critical to understand basin evolution and reservoir development. Integrating results of other tasks within the regional stratigraphic framework enabled development of a stratigraphic-structural-diagenetic model for the origin of Trenton-Black River reservoirs and delineation of potential areas of exploration interest.

Methods

To achieve the stated objectives, Ohio Division of Geological Survey (ODGS) geologists generated a network of regional stratigraphic cross sections (Plates 1-1 through 1-19); interpreted geophysical logs for regional mapping; generated regional isopach maps for selected Cambrian-Ordovician intervals (Plates 1-20 through 1-30); compiled a stratigraphic correlation chart (Figure 1-1); created generalized maps showing the major tectonic features and basin architecture during Middle Cambrian through Late Ordovician time and generalized facies maps for the Black River and Trenton/Point Pleasant equivalent strata (Figures 1-2 through 1-7); and developed type logs illustrating the major Trenton facies (Figures 1-8 through 1-13). Geophysical-log data were integrated with core and sample descriptions and with published work on Middle and Upper Ordovician outcrop and subsurface studies. Core data are from wells located primarily in the western portion of the Appalachian basin in western Ohio and central Kentucky, and are sparse for the deeper portions of the basin in New York, West Virginia and Pennsylvania (Plate 1-1). Continuous cores through the entire Trenton-Black River interval and cores with dolomitized zones were targeted for study and correlated to geophysical logs. Core examination focused on dolomitized zones, porous zones, intervals with oil shows, and marker beds (i.e., bentonite beds) to assist in refining the regional correlations and analyzing zones with reservoir potential.

A network of 18 cross sections was generated across the Appalachian basin to illustrate the regional stratigraphy of the Middle and Upper Ordovician succession of strata (Plates1-1 through 1-19). All logs for the 225 wells used in constructing these

cross sections were converted to LAS (Log ASCII Standard) format for construction of the final cross sections. Throughout the basin, geophysical logs for approximately 1,800 unique wells that penetrated the Trenton and Black River were scanned (tiff format) and approximately 500 well logs were converted to vector (LAS) format.

A depositional strike direction of approximately northeast-southwest for the Trenton interval was established using a preliminary isopach map. In so doing, it was assumed that parallel isopach-contour lines showing thick to thin areas could be used to define a regional deposition strike direction.

Six cross-section lines oriented parallel to strike, and 12 cross-section lines oriented perpendicular to strike (i.e., dip direction) were constructed (Plate 1-1). Logs of continuous Trenton/Black River cores or Precambrian penetrations were prioritized and included in many of the cross sections. Formation picks on logs used in these cross sections were correlated with described cores and digital photographs to refine the lithostratigraphic correlations. Informal unit names used for regional correlation purposes and mapping within the project are shown on the ends of all cross sections. Some of these names do not represent formal unit names recognized by all states of the consortium, but rather were assigned to ensure equivalence of units encoded in the mapping database. Therefore, where formal names are being used to represent these informal mapping units, these formal names may be placed within quotation marks.

Mapped units correlated on the geophysical-log cross sections across the entire project area and included in the database are: 1) top of the Precambrian, 2) base of the "Knox," 3) top of the "Knox," 4) top of the "Wells Creek," 5) top of the "Gull River," 6) top of the "Black River," 7) top of the "Curdsville," 8) top of the "Logana," 9) top of the "Trenton/Lexington," 10) top of the "Point Pleasant," 11) top of the "Utica," 12) top of the "Kope," and 13) top of the "Ordovician." Facies relationships for all units in the uppermost portion of the Ordovician are not shown on the cross sections, as this was not an integral part of the study. Formal stratigraphic names as used within each state are shown within the log columns of the cross sections. Equivalent units and nomenclature for the Appalachian basin, eastern Indiana, and southern Michigan are shown in the regional stratigraphic correlation chart (Figure 1-1).

ODGS geologists interpreted tops on all geophysical logs used in the cross sections, and tops on supplemental Ohio wells that were used in the creation of regional interval thickness maps. Each state geological survey within the consortium interpreted tops for geophysical logs from their respective state, and all tops were tied to the regional cross sections. A total of 2,031 wells were used for regional mapping across the project area. As with the wells used in the cross sections, interpreted geophysical-log tops used in mapping were correlated to core and sample descriptions to refine stratigraphic interpretation. Dolomitized zones from geophysical logs and cores also were noted and are displayed to help delineate potential areas of HTD (hydrothermal dolomite) and fault trends (Plate 1-1).

Regional interval-thickness maps generated for this final report are included in the following plates:

- Plate 1-20, preKnox (the top of the Precambrian to the base of the Cambrian-Ordovician Knox)
- Plate 1-21, basal Cambrian sandstone (includes the Cambrian Mt. Simon, unnamed Conasauga sandstone, Potsdam and Rome Trough basal sandstone)
- Plate 1-22, Knox (Cambrian-Ordovician base of Knox to top of Knox)
- Plate 1-23, Rose Run sandstone (top of Cambrian Copper Ridge to top of Rose Run; includes the Upper Sandy member of the Gatesburg Formation in Pennsylvania and Theresa sandstone equivalent in New York)
- Plate 1-24, Black River and Wells Creek (top of Knox to top of Black River)
- Plate 1-25, Black River (top of Ordovician "Wells Creek" to top of Black River)
- Plate 1-26, Trenton/Curdsville (top of Ordovician Black River to top of Trenton/Curdsville)
- Plate 1-27, Trenton/Lexington (top of Ordovician Black River to top of Trenton/Lexington)
- Plate 1-28, "Utica" (top of Ordovician Trenton/Lexington to top of "Utica," includes the "Point Pleasant" and Antes Shale).
- Plate 1-29, "Kope" (top of Ordovician Trenton/Lexington to top of "Kope" and equivalents; includes the "Utica" and "Point Pleasant")
- Plate 1-30, upper Ordovician undifferentiated (top of "Kope" and equivalents to top of Ordovician undifferentiated).

Interval-thickness maps for the basal Cambrian sandstone and the Rose Run sandstone were based on published maps of the Midwest Regional Carbon Sequestration Project (MRCSP) (Wickstrom, Venteris, Harper and others, 2005), and were modified by incorporating New York and Ontario data.

Digital locations of Trenton–Black River oil and gas fields were obtained from the Appalachian, Illinois and Michigan basin states (including Ontario), and a Trenton-Black River oil and gas fields map was generated to assist in relating stratigraphy to producing trends (Plate 1-1). Geographix software was used to construct the cross sections and preliminary interval-thickness maps. Final interval-thickness maps were produced using kriging algorithms available in ArcGIS Geostatistical Analyst.

The goal of the mapping portion of the stratigraphic task was to produce geological trend maps. Hence, the contour maps and grids are not formal, optimized geostatistical models. Detailed exploratory-data analysis (testing for normality), variogram modeling (anisotropy etc.), and detrending were not conducted for this project. Variograms for each map were calculated over a lag spacing of 60,000 feet for 12 lags. The variogram scale was chosen to give a compromise between modeling local details and obtaining realistic estimates over spatial gaps in the data. A circular approach, divided into four quadrants (sections), was used to obtain neighboring data for kriging estimates. A minimum of 2 points and maximum of 5 points were used per quadrant. The error in the interpolated values was evaluated by cross validation ("jackknifing"). Typical error estimates range from 30- to 60-feet RMSE (root mean square error) for

most of the interval-thickness maps. The exception is the preKnox interval-thickness map, which has a RMSE of 500 feet due to poor well control on the Precambrian surface. Interval-thickness maps were produced by contouring 5,000-foot resolution grids. Grids were produced by block kriging and smoothed with a low-pass filter to reduce noise due to data gaps and the search procedure. Initial maps were created using this procedure, checked for erroneous data points, and then remapped with erroneous points corrected or removed. The final, computer-generated contour maps occasionally violate individual well points, contrary to what a geologist would do if contouring by hand. The algorithm used for contouring is based on the best geostatisistical prediction of thickness for every portion of the map area, and not on the literal value of individual data points. A clipping boundary was used for the map extent, which was defined to the west by cross-section well control, to the south and east by the Allegheny Front, and to the north by the appropriate outcrop or subcrop boundary. The eastern boundaries of maps were clipped at the limit of well control for that respective interval if data did not extend to the Allegheny Front.

Maps showing basin architecture from Precambrian to Late Ordovician time, and facies maps illustrating late Black River time and late Trenton-Point Pleasant time, were constructed to develop a better understanding of the basin architecture and the paleogeography and facies distribution of these units (Figures 1-2 through 1-7). These maps were integrated with the regional cross sections, interval-thickness maps, core and sample descriptions, and published references. Representative geophysical well logs are presented to assist the explorationist in understanding the major Trenton and Black River facies, as defined in this report (Figures 1-8 through 1-13).

Stratigraphic Nomenclature

The primary objective of the stratigraphy task was to develop a regionally consistent stratigraphic framework for the Trenton/Black River-Utica interval and coeval units. Numerous stratigraphic names have been applied to the Ordovician succession of rocks across the Appalachian basin. The informal stratigraphic units that were adopted for use in the cross sections and maps of this report (see previous section) also are used in the following discussions of stratigraphy and stratigraphic nomenclature. Stratigraphic equivalents of these units across the basin can be seen in the regional stratigraphic correlation chart (Figure 1-1). The correlation chart, based on the formal nomenclature of each state geological survey in the consortium, was subdivided into the Laurentian craton, the Rome trough and the eastern basin. The Cambrian and Ordovician units that were mapped are discussed in ascending stratigraphic order.

Central Appalachian Basin Architecture and Geometry During Cambrian-Ordovician Deposition

Paleozoic basin architecture and geometry of the eastern U.S. are directly related to the underpinning Precambrian features of the region and indirectly to far-field stresses and crustal-loading of the lithosphere during geologic time (Quinlan, and Beaumont, 1984). The effects of the deep-seated, Precambrian and early Cambrian structures and

boundaries has been demonstrated by numerous researchers in the region (Wagner, 1976; Beardsley and Cable, 1983; Quinlan and Beaumont, 1984; Harper, 1989; Read, 1989; Drahovzal, and others, 1992; Wickstrom and others, 1992; Gao and others, 2000; Baranoski, 2002; Ettensohn and others, 2002). Precambrian provinces within this region include the Eastern Granite Rhyolite (EGR), East Continent Rift Basin (ECRB), and Grenville Province (GP) domains (Figures 1-2 and 1-3).

The Cambrian-age Rome trough (RT) is another deep, major tectonic feature within the region that had profound affects on subsequent stratigraphic and structural evolution (Figures 1-2 and 1-3).

Plate tectonic movement and resulting mountain building and rifting processes are considered the dominant control of far-field stresses, which affected sediment accumulation on and from the Laurentian craton. Regional features typically are inherent zones of crustal weakness within the Precambrian terrain and include province and domain boundaries, intrusive bodies, reactivated thrust faulting, strike-slip faulting, and rift zones. Pre-existing faults, zones of weakness, and regional topography will often determine how a local area will react to the far-field forces. The interval maps for this study, although not truly representative isochronous units, generally support the migrating flexural lithosphere model of Quinlan and Beaumont (1984). The resulting architecture and geometry of the basins evolved over time as the sedimentary sequences were deposited and compacted. The effects of paleo-climate, paleo-oceanic circulation, and variable compaction of sediments also affected depositional setting as well as basin geometry (i.e. Late Ordovician: Holland, and Patzkowsky, 1996; Pope, and Read, 1997; Brett, and others, 2004).

Platform areas and depocenter locations shifted laterally in response to tectonic/orogenic forces, thus affecting subsequent observed thickness patterns. Subsidence rates, variable sediment supply and accumulation, and eustatic sea-level variations are considered to be the dominant responses to tectonic/orogenic forces yielding the basin geometries and architecture of the region. The Taconic orogeny was the major tectonic event following early Black River time and throughout the remaining Ordovician time in the region (Ettensohn and others, 2002). The Cincinnati arch was absent prior to Silurian time (Kolata and others, 2001). The reader is referred to the structural section of this report for a more in-depth discussion on the regional features and related local structures.

Terminology for carbonate depositional facies is defined to standardize and facilitate descriptive models, depositional elements, and potential trends for hydrocarbon reservoirs. The thickness and extent of these depositional elements are essentially what defines the architecture and geometry of the mapped units. Carbonate ramps are defined to "have gentle slopes (generally <1°) on which shallow wave-agitated facies of the nearshore zone pass downslope (without marked break in slope) into deeper water, low-energy deposits" (Ahr, 1973; Wilson, 1975; Read, 1985). "Homoclinal ramps have relatively uniform, gentle slopes (1m/km, or a fraction of a degree) into the basin" (Read, 1985). This ramp model adequately describes the overall architecture of the stable

portion of the eastern Laurentian craton during Early Paleozoic time. The ramp architecture may contain additional elements including: platform, platform margin, basin and sub-basin. These terms are used descriptively to map and isolate facies changes and relative thickness variations. Boundaries of the elements were delineated qualitatively on the basis of lithologic variations from geophysical logs, and linear trends in the thickness variations of mapped units. The platform areas generally consist of relatively higher-energy, clean-carbonate buildups, which merge toward relatively lower-energy, argillaceous carbonates of the platform margin, and then into deeper, restricted, shale-dominated deposits of the basin and sub-basin. Read (1985) defines a typical carbonate platform as being a broad, flat-topped region with a relatively steep-sided seaward-facing margin where higher-energy carbonate deposition takes place. He also describes the great variability of carbonate platform facies models where some platforms may have gently sloping margins with ramp-like profiles. The Trenton facies model presented in this report represents an overall ramp-like setting with low-relief carbonate platforms rimming a deeper water sub-basin.

Early and Middle Cambrian Time

The Proto-Appalachian and the Proto-Illinois/Michigan basins developed on and adjacent to the exposed Precambrian provinces composing the Laurentian craton (Figure 1-2). The Laurentian craton was deeply eroded and parts subsided due to sediment loading relative to other portions during Early Cambrian through Middle Ordovician Wells Creek/Beekmantown time. The Rome trough became the first major Paleozoic-age regional structural feature affecting geometry and architecture of the central Appalachian basin area (Figures 1-4 A and B) (Beardsley and Cable, 1983). The Rome trough was a southwest-northeast-trending extensional basin system between the exposed Precambrian craton and the lower Paleozoic continental margin during Early and Middle Cambrian time. The Rome trough is bounded on the west by a series of en echelon normal faults and to the east by a positive magnetic anomaly interpreted to be a horst block by various researchers (Ammerman and Keller, 1968; Gao, and others, 2000).

The deposition of terriginous sediments from the exposed craton, mixed with marine sediments (e.g. lower Cambrian basal sandstone, Rome and Tomstown formations), is the earliest preserved sedimentary event to the southeast. The associated deposits are especially well represented within the deepest portions of the Rome trough. Eventually, significant volumes of exposed Precambrian Laurentian craton were eroded, deposited and preserved as the Mt. Simon Sandstone to the west in the Proto-Illinois/Michigan basins, while to the southeast these sediments mixed with continental-margin and open-marine sediments to form the Conasauga Formation, Maryville Limestone and equivalents (Figures 1-3, and 1-4A) (Read, 1989). Transgressive basal sandstones (Mt. Simon Sandstone) show major accumulation in the Proto-Illinois/Michigan basin during this time (Plate 1-20) while to the southeast a mixture of Middle Cambrian siliciclastics and carbonates was deposited, reaching great thickness within the Rome trough and relatively minor thicknesses upon the Ohio platform (Figure 1-4B). The overall shape of the depocenters for the Proto-Appalachian and Proto-Illinois/Michigan basins followed axes trending northeast-southwest and north-south respectively. The northwest boundary fault system of the Rome trough continued to be

active throughout this deposition and, in part, controlled subsidence of the Proto-Appalachian basin. The largest fault offset, and accompanying thickest deposition within the trough, represents Precambrian through Middle Cambrian Rome Formation time.

Late Cambrian/Early Ordovician Knox Time

As transgression continued, the craton was largely drowned and open-water conditions spread across the region (Plate 1-21 and Figure 1-4B). The Proto-Appalachian and Proto-Illinois/Michigan basin geometries were similar to the underlying interval as subsidence continued during Late Cambrian/Early Ordovician Knox time. Carbonate deposition dominated the region (Plate 1-22) with the exception of a notable regressive/trangressive event recording the deposition of the Rose Run sandstone (Plate 1-23). The regional Knox unconformity exposed the craton and Ohio platform, allowing extensive erosion of this area once again. This regional unconformity, which is not recognized in the eastern depocenter, accentuated the shape and extent of the adjoining proto basins. The contours for the Knox interval form a prominent, broad, south-plunging nose across Ohio (Plate 1-22). The northwest boundary fault system of the Rome trough continued to control subsidence during this time but with diminished effect on sedimentation and depositional patterns as compared to the early Cambrian.

Middle/Late Ordovician Black River Time

Middle/Late Ordovician Black River time marks an important change in basin architecture as the region transformed from a passive/extensional regime to a compressive regime with collision of the Taconic arc from the east-southeast. During this time the architecture evolved into a broad, stable, shallow-water carbonate ramp as epeiric seas transgressed much of the region (Keith, 1989). The Black River ramp dipped southeast to eastward and extended from the Michigan Basin and across the central Appalachian basin and sloped very gently to the Rome trough (Plates 1-24 and 1-25, and Figure 1-5). These carbonate mudstones are lithostratigraphically consistent across most of the region west of the fore-deep associated with the Rome trough. These relatively uniform carbonates accumulated in shallow, “tropical," warm-water seas (Keith, 1989; Holland and Patzkowsky, 1996) at a paleolatitude of approximately 20° south of the equator (Scotese and McKerrow, 1990) (Figure 1-5). Thick shaley carbonates were deposited within the Rome trough-influenced fore-deep, and further to the southeast, black and gray shales dominated the Sevier Basin. An archipelago of volcanic island arcs formed along the Laurentian craton margin (present day Virginia) in response to the subduction of the oceanic lithosphere (Figure 1-5) and provided extensive ash deposits across the carbonate ramp (Kolata, and others, 1996).

An elongate-shaped depocenter characteristic of the central Appalachian basin came into existence during Black River time (Plates 1-24 and 1-25, Figure 1-5). The overall shape of the central Appalachian basin depocenter followed a north-northeast-trending axis in West Virginia and Pennsylvania. This thick depocenter would continue and expand throughout the Ordovician and remaining Paleozoic, thus defining the thicker portion of the central Appalachian basin at the southeastern margin of the Laurentian

craton. The thickest area is flanked on the northwest by tighter northeast-trending contours, which follow the northwestern side of the Rome trough trend in eastern Kentucky, northwestern West Virginia and southwestern Pennsylvania. Keith (1989) and Ettensohn and others (2002) suggested that the Black River ramp architecture is a relatively tabular geometry indicating widespread crustal stability of the region. Examination of the Black River thickness map (Plate 1-25, Figure 1-5) indicates otherwise, showing three prominent thick and thin southeast-trending areas, which extend to the thick depocenter. One of the thick southeast-trending areas extends from the Chatham sag at the western end of Lake Erie, across all of eastern Ohio into the thick depocenter. The north-south trending western boundary of the Grenville Province and Bowling Green fault system were apparently active at this time, providing more rapid subsidence in apparent association with the Chatham sag. These sinuous trends separating the thick and thin areas provide potential fairways for exploration and demonstrate that the Laurentian craton interior is not the uniform, regionally consistent, tabular body envisioned by some previous workers (Keith, 1989; Wickstrom and others, 1992).

Late Ordovician Trenton Time

The central Appalachian basin architecture continued to evolve during Trenton time with the appearance of low-relief carbonate buildups of the Trenton and Lexington platforms surrounding the interplatform Utica/Point Pleasant sub-basin (Plate 1-27, Figure 1-6). The craton-wide marine transgression continued as overall water depth increased, while platform carbonate production kept pace. The entire platform from the Indiana/Michigan area to the central Appalachian basin forms an overall ramp-like slope typical of Read's (1985) model. Significant regional changes involved paleoclimate, and the increased volumes of temperate-marine, fossiliferous carbonates during the transgression (Keith, 1989; Holland and Patzkowsky, 1996). Paleolatitude 15° south approximately bisects the study area (Scotese and McKerrow, 1990) (Figure 1-6). The most extensive, relatively clean carbonates developed on the Trenton platform in Indiana, Ohio, Michigan, Ontario and New York. Localized clean carbonate build-ups accumulated with generally argillaceous carbonates on the Lexington platform. Kolata and others (2001) considered Trenton platform carbonates approximately time equivalent with those of Lexington platform. The appearance of dark brown and black shales marked another significant change in paleogeography during Late Ordovician time (Kolata and others, 2001). These dominantly clastic muds poured in westward from the volcanic island arcs and Taconic mountains to the east. Volcanic island-arc systems along the Laurentian craton margin, which were present during Black River time, migrated northeastward and continued to provide volcanic ash beds and clastic sediments to the extensive carbonate platform (Kolata, and others, 1996).

The Utica/Point Pleasant sub-basin has previously been termed the "Point Pleasant" basin (Wickstrom and others, 1992) and includes the narrow "Sebree Trough" feature. Schwalb (1980) first applied the name "Sebree Valley" to a northeast-southwest trending feature in western Kentucky that he described as a “trough-like, clastic filled depression." Many researchers have used the term "Sebree Trough" and extended this

feature from western Kentucky through southeastern Indiana, and into northwestern Ohio (Bergström and Mitchell, 1987; Wickstrom, 1988; 1990; Mitchell and Bergström, 1991; Wickstrom and others, 1992; Bergström and Mitchell, 1992; 1994; Keith and Wickstrom, 1993; Bergström and Mitchell, 1994; Kolata and others, 1996; Pope and Read, 1997; Hohman, 1998; Kolata and others, 2001; Ettensohn and others, 2002; Richardson and Bergström, 2003; Brett and others, 2004; Ettensohn and others , 2004; Ludvigson and others, 2004; and McLaughlin and others, 2004). The origin and regional extent of the linear area of thin Trenton is problematic and not fully understood. Therefore, we are withholding the use of the term "Sebree Trough".

The overall southeast-to-eastward-dipping Black River ramp architecture remained in place during the earliest Trenton and Curdsville deposition (Plate 1-26). As the Taconic orogeny increased in intensity, a series of bulges and downwarped areas resulted, setting up shallow-water platforms and inter-platform sub-basins (Wickstrom and others, 1992). Significant volumes of dark brown and black shales of the Logana Member of the Lexington Formation marked the disappearance of the regional ramp and the emergence of this new complex of carbonate platforms surrounding a sub-basin (Plate 1-27, Figure 1-6). As relatively clean carbonates continued to be deposited upon the shallower-water carbonate platforms, interbedded limestones and calcareous shales and brown and black shales of the Point Pleasant Formation and, subsequently, the Utica Shale were deposited within the inter-platform sub-basin. Nearer to the Taconic foreland basin (in present-day eastern Pennsylvania and central New York) subsidence, carbonate deposition and sediment influx were at a maximum as evidenced by the very thick accumulation of relatively argillaceous Trenton carbonates in this area. Carbonates of the Lexington platform display intermediate thickness and argillaceous content. Carbonates accumulating on the more distal Trenton platform of northwestern Ohio, Indiana and Michigan are thinner, but display the cleanest limestone of the platforms, being further removed from the terriginous sources. Apparently, the Trenton platform of this region did not subside concurrently with sediment accumulation, or sea level remained more constant, during this time. These complexly interwoven stratigraphic elements and their relative timing are very important to our understanding of the depositional and diagenetic history of the productive Trenton reservoirs. The platform-margin areas may provide potential fairways for exploration.

Late Ordovician Trenton/Utica Time

During deposition of the Utica Shale, the intensity of the Taconic orogeny once again increased causing a rapid rise in sea level or increased subsidence of the region resulting in the Utica Shale replacing carbonate deposition on the platforms. The resultant isopach map of the Point Pleasant and Utica formations (Plate 1-28) shows the in-fill of the sub-basin, the somewhat normal depocenter in the center of the central Appalachian basin area, and the eventual drowning of the platforms, illustrated by the thinner deposits where the carbonate platforms had been (see Plate 1-27). Also of note on Plate 1-28 is the relative thick deposition of the Point Pleasant-Utica interval within the northeast trending trough area adjacent to the northwest Ohio platform.

Late Ordovician Time

Following Utica time the intensity of the Taconic orogeny apparently lessened, and the seas covering the region returned to a more open-marine ramp environment with mixed shale and limestone deposition. The depositional pattern returned once again to that established during Black River time with the "typical" central Appalachian basin depocenter trending north-northeast through present-day West Virginia and east-central Pennsylvania. It would appear that the thick Trenton platform of central New York was the last of the carbonate platforms to be drowned as the "Kope" interval thickness map (Figure 1-7A; Plate 1-29) exhibits a thinning over its location. Interestingly, the uppermost carbonate of the New York platform was also the least argillaceous deposition of that platform (see log signatures on cross sections (e.g., Plate 1-13).

In general, the "Kope" and equivalents and upper Ordovician strata exhibit an increase in carbonate content, as the rocks get younger in the basin until, toward the end of Ordovician time, a resurgence of shale (Juniata and Queenston) is seen in the central Appalachian basin (Figure 1-7B; Plate 1-30). This interval in the western fringe of the Appalachian basin, and continuing into the Illinois and Michigan basins (see cross sections and Figure 1-1), is marked largely by carbonate deposition (Drakes and Whitewater formations).

Cambrian Sandstone Stratigraphy

Regional isopach maps of the Cambrian basal sandstones and Rose Run sandstone were generated to assist in the investigation of the hypothesis that these intervals influenced, or were necessary to provide a mechanism for, dispersal of hydrothermal fluids that dolomitized the Trenton-Black River reservoir (Plates 1-21 and 1-23). Proximity to the basement and a basal sandstone aquifer is thought to have an impact on the type of hydrothermal alteration. Two possible models of hydrothermal fluid migration are: 1) that fluid flow originated primarily in the basement and migrated quickly to the Trenton-Black River interval through active fault systems; or 2) that the fluids primarily originated within, and migrated laterally through, basal Cambrian and Rose Run sandstone and then upward via fault systems into the overlying Trenton-Black River interval. Some researchers have indicated that the presence of basal Cambrian sandstone is necessary for the formation of Trenton-Black River HTD reservoirs (Hickman and Kent, 2005). A more detailed discussion of hydrothermal alteration will be discussed in Chapter IV (Isotope Geochemistry and Fluid Inclusion Analysis).

Basal Cambrian Sandstone

The stratigraphically complex basal Cambrian sandstones lie unconformably on the Precambrian basement. The Mt. Simon Sandstone is the thickest sandstone unit in this interval. This unit has been misunderstood in the past, and many previous workers have assumed that the Mt. Simon was present as a continuous sandstone unit across much of the Appalachian Basin (Janssens, 1973; Gupta, 1993). Recent research (Baranoski, in preparation) indicates the true Mt. Simon Sandstone of the Illinois and Michigan basins

pinches out in central Ohio. East of this pinch-out, thinner, less continuous sandstones are found in the basal sandstone position. During the MRCSP study (2005), four basic units within this interval were mapped (Plate 1-21; Figure 1-3): 1) the Mt. Simon Sandstone of the Proto-Illinois/Michigan Basin area (Michigan, Indiana, western Kentucky and western Ohio); 2) the unnamed dolomitic sandstone of the Conasauga Group (eastern Ohio, northern Kentucky, western Pennsylvania and West Virginia); 3) Potsdam Sandstone (northern and north-central Pennsylvania and New York); and 4) stratigraphically older, unnamed basal Cambrian sandstone in the fault-bounded Rome trough and eastern Proto-Appalachian basin (eastern Kentucky, West Virginia and western Pennsylvania). The unnamed basal sandstone of the Rome trough may be equivalent to the Antietam Formation of eastern Pennsylvania and Maryland. The transition of the Mt. Simon Sandstone of the Illinois and Michigan basins and western Ohio to the less continuous sandstones in the east is evident on the interval thickness map (Plate 1-21).

The origins of names for the units of this interval are as follows: the Mt. Simon was first used by Walcott (1914) to designate an exposure near Eau Claire, Wisconsin (type section); the Potsdam was described by Emmons (1838) for a sandstone cropping out in Potsdam, New York; and the Conasauga Group was named for exposures in the Conasauga Valley of northwest Georgia (Hayes, 1891). Lithologically, the Mt. Simon is a white, pink or purple, fine- to coarse-grained, moderately to well-sorted, quartz arenite that can be arkosic. Thin interbeds of red, green, gray or black, sandy to silty shale also occur. Locally, thin beds of tight, silica-cemented arenite are present. The unnamed Conasauga sandstone and Potsdam Sandstone consist of interbedded, cyclical-appearing sandstones and dolostones. The sandstone is typically white to light-gray and pinkish gray, and fine- to medium-grained, and arkosic sandstones occur in the basal portions of the Potsdam in northwestern Pennsylvania and New York. The basal sandstones of the Rome trough are arkosic and interbedded with red and green shale, siltstone, sandy shale and nodular evaporites.

Thickness of the Cambrian basal sandstone interval ranges from zero over Precambrian highs to more than 300 feet in western Ohio (Plate 1-21). The interval thickness generally thins to the east and southeast, except for a thick trend in south-central New York and localized areas affected by the Rome trough. Thickness of 200 feet or more is coincident with the prolific Trenton-Black River producing areas in northwest Ohio and also in south-central New York. This seems to support the idea that basal Cambrian sandstones are beneficial for HTD reservoir development. However, there is production from clearly dolomitized Black River north of the basal Cambrian sandstone subcrop line in Ontario where no basal Cambrian sandstones are present (Terry Carter, personal comm.). The presence of Black River production clearly refutes the idea that the Trenton-Black River fields are restricted to areas underlain by basal Cambrian sandstone as proposed by Hickman and Kent (2005). However, in the absence of any basal sandstone, it has been suggested that the basal portion of the Shadow Lake Formation is sandy and porous and the Precambrian surface may have adequate porosity and permeability to have acted as pathways for hydrothermal fluid movement (Terry Carter, personal comm.).

Rose Run Sandstone or Equivalents

The Cambrian Rose Run sandstone is the only laterally persistent sandstone within the Knox Dolomite. This sandstone interval can be correlated in the subsurface from eastern Ohio, where it subcrops beneath the Knox unconformity, to eastern Kentucky, western West Virginia (upper sandstone member of the Knox), Pennsylvania (Upper Sandy Member of the Gatesburg Formation equivalent) and New York (partial equivalent of the Theresa Formation) (Plate 1-23). The Rose Run sandstone was first described and named by Freeman (1949) from the Judy and Young #1 Rose Run Iron Co. well in Bath County, Kentucky. In that well, the unit consists of about 70 feet of poorly sorted sandstone approximately 300 feet below the Knox unconformity. A detailed review of nomenclature and previous work on the Rose Run and equivalent units can be found in Riley and others (1993) and Baranoski and others (1996). Lithologically, the Rose Run interval as described in subsurface core in Ohio, consists of white- to light-gray, fine-to medium-grained, sub- to well-rounded, moderately sorted, quartz arenites to subarkoses interbedded with thin lenses of nonporous dolomite (Riley and others, 1993; Baranoski and others, 1996). Glauconite and green shale laminae occur locally. Low-angle cross-bedding is the most common sedimentary structure observed in both core and Formation Microscanner Image (FMI) logs. Ripple marks also have been noted in both core and FMI logs. Polygonal mud cracks are present in several of the cores, indicating subaerial exposure of the sandstones during low stands in sea level.

The Rose Run equivalent (Upper Sandy Member of the Gatesburg Formation) as observed in core and outcrop in Pennsylvania, contains three principal facies: 1) sandstone: 2) mixed sandstone and dolostone; and 3) dolostone (Riley and others, 1993). The sandstone facies consists of light-gray, fine-grained, well-sorted, predominantly silica-cemented quartz arenites. Cross bedding is present, including herringbone cross-stratification. The mixed sandstone and dolostone facies is dominated by sandstone that consists of fine- to medium-grained, moderately well-sorted, predominantly dolomite-cemented quartz arenites. The dolostone facies is light-gray to olive-gray and displays nodular bedding and bioturbation. Outcrops in central Pennsylvania contain “ribbon rocks” (thin-bedded, wave-rippled and burrowed dolostone), wavy dololaminites, flat-pebble conglomerates and thrombolitic algal mounds in the dolostone facies (Riley and others, 1993). Ooid grainstones are common within the dolostone facies.

The Rose Run sandstone interval thickens gradually from 0 feet at the western limit of the subcrop to about 200 feet throughout the area of eastern Ohio and northwestern Pennsylvania (Plate1-23). The irregular nature of the Rose Run isopach map in Ohio near the subcrop is a result of erosion on the Knox unconformity. Various paleotopographic features, including numerous erosional remnants, are present along the subcrop trend as a result of paleodrainage. East of this broad zone of gradual thickening, the contour lines on the isopach map become narrower in western Pennsylvania, resulting from the rapid thickening that is present in the Rome Trough. Various authors have indicated that the Rome Trough was actively subsiding during Rose Run deposition (Wagner, 1976; Harper, 1991). Approximately 470 feet of Rose Run sandstone were

encountered in the Amoco #1 Svetz well in Somerset County, Pennsylvania before drilling was stopped at 21,640 feet.

The Rose Run sandstone, or its equivalents, is clearly absent west of the subcrop line in the prolific Trenton-Black River fields of northwestern Ohio, the Scipio field of southern Michigan, and in southern Ontario. Whereas there is some Theresa sandstone (Rose Run equivalent) in the Black River producing areas of New York, we can unequivocally state that the presence of the Rose Run sandstone (or its equivalents) is not necessary to provide a pathway for Trenton-Black River HTD reservoir development for most of the producing area.

Ordovician Stratigraphy

Isopach and facies maps presented in this section represent a regional synthesis of the stratigraphy of the following Ordovician units, as discussed in ascending stratigraphic order: the Black River Group, the Trenton/Lexington Limestone (including the Lexington Undifferentiated, Curdsville and Logana members), the Point Pleasant Formation, the Utica Shale, the "Kope," and their equivalent units (Plates 1-24 through 1-30). This section of the report is focused on the broadly defined facies present during middle to late Black River and late Trenton/Point Pleasant times (Figures 1-5 and 1-6). Regional facies for the Black River and late Trenton/Point Pleasant time periods consist largely of clean carbonate mudstones, argillaceous carbonate mudstones, clean carbonate grainstones and packstones, argillaceous carbonate grainstones and packstones, calcareous shale and interbedded limestone, and shale. Regional facies patterns are important for understanding the location of the best potential reservoir rocks. Facies maps assist the explorationist in determining tectonic controls and potential areas for the best places for hydrothermal dolomite to form. Mapping the facies regionally also may help to better understand differences in seismic signature of the Trenton across the basin, which in turn may be useful as a potential exploration tool.

Black River Group

Vanuxem (1842) first applied the name "Black River Group" for rocks cropping out along the Black River in Oneida and Lewis counties, New York. Newberry (1873) was the first to use the name in Ohio. The Black River rocks are equivalent to the High Bridge Group of central and eastern Kentucky and the Stones River Group in Tennessee (Figure 1-1). The lower interval of the Black River contains a clean, and typically tight, carbonate mudstone that is referred to by Ohio drillers as the "Gull River." This lithologically uniform unit can be correlated regionally on geophysical logs across the entire project area, although it is not recognized as a formal unit. Instead, it is a partial equivalent to the lower portion of the Loysburg Formation in Pennsylvania and a partial equivalent to the lowermost portion of the Gull River Formation in southwestern Ontario.

An overview of regional Black River nomenclature can be found in Ryder (1992). The Black River directly overlies the Wells Creek Formation, or the Knox Group on paleotopographic highs where the Wells Creek is absent. As examined in core and

outcrop, this unit is lithologically consistent and uniform across the region (Figure 1-5; Plates 1-24 and 1-25). Black River facies consist of shallow subtidal to peritidal carbonates that were deposited across a very low-relief carbonate ramp (Keith, 1989; Pope and Read, 1997). It is predominantly a light-medium-brown to gray, burrow-mottled, stylolitic mudstone. Fossils are not abundant, but occur locally. Chert is present locally, especially in the upper part of the unit. Rip-up clasts also are present locally, indicating higher-energy deposition. Geophysical gamma-ray-log response typically is very low in these clean carbonates with low shale content. Basinward to the southeast, a facies change occurs where the cleaner mudstones recognized in core and on geophysical logs become more argillaceous in the deeper-water portion of the basin (Figure 1-5; Plates 1-7, 1-24 and 1-25).

Numerous volcanic ash beds, commonly referred to as potassium bentonites, or K-bentonites, are found within the Black River through Trenton-Lexington strata. Volcanic ash beds are valued as geologic time markers as they represent a widespread, instantaneous geologic event, a volcanic eruption. Within the study area, the Millbrig (mud cave of drillers; alpha of Stith, 1979), Deicke (pencil cave of drillers; beta of Stith, 1979) and Ocoonita (gamma of Stith, 1979) are the most continuous and more readily correlated of all K-bentonites found in the outcrop and subsurface. In cores in western and southern Ohio, the Millbrig occurs near the top of the Black River and marks a change from a typical Black River bioturbated mudstone lithology to the overlying highly fossiliferous, grainstone/packstone lithology typical of the Trenton.

The Black River-Trenton contact is generally a gradational zone in which Black River and Trenton lithologies are interlayered through a zone up to 10 feet thick, although Wickstrom and others (1992) noted a sharp contact in cores from Logan and Butler counties, Ohio. Hardgrounds have been observed on the Black River-Trenton contact in cores in Butler and Wyandot counties, Ohio (Wickstrom and others, 1992) and in Indiana (Keith, 1985). At the Union Furnace outcrop in central Pennsylvania, the Millbrig occurs in the Salona Formation (Trenton equivalent), approximately 40 feet above the Nealmont mudstone (Black River equivalent). On the basis of the contact in relation to the K-bentonite, the Black River-Trenton boundary appears to be diachronous. The Millbrig is used to correlate the top of the Black River in the subsurface in much of Ohio, Indiana and Kentucky because it is a reliable marker on geophysical logs. Where the Millbrig is absent, the contact is found by close correlation to neighboring geophysical logs or by tying the well's geophysical logs to cores or sample descriptions.

The source for the volcanic ash of the bentonites was to the east and southeast, originating from active island-arc volcanism associated with the Taconic orogeny (Cisne and others, 1982; Kolata and others, 1996). The foreland basin associated with this orogeny developed in two phases named the Blountian and Taconic tectophases (Rodgers, 1971). According to Ettensohn and others (2002), there was a time transgressive northeastward shift of convergence during the Blountian and Taconic tectophases of the Taconic orogeny. The earlier Blountian tectophase was strongest at the Virginia Promontory, and possibly the Alabama promontory, and created the Sevier Basin turbidite deposition in Alabama, Georgia, Tennessee and Virginia. The initial

collision during the Blountian tectophase created this portion of the island-arc system (Figure 1-5). The later Taconic tectophase generated the Martinsburg foreland basin in northern Virginia, Maryland and Pennsylvania (Ettensohn and others, 2002; Pope and Read 1997), and created the island-arc system to the northeast (not shown on this figure).

The interval thickness of the Wells Creek and Black River ranges from over 2,700 feet in the Rome trough in West Virginia to less than 50 feet on the eastern side of the mapped area, and up to 200 feet on the western side of the mapped area (Plate 1-24). Evidence of the Rome trough being active at this time is indicated by a dramatic increase in the rate of thickening in the western portion of West Virginia and eastern Kentucky. The interval thickness map of the Black River (Plate 1-25) indicates similar trends but with fewer irregularities caused by the paleogeomorphic effects of the Knox unconformity.

Trenton/Lexington Limestone

Vanuxem (1838) first applied the name "Trenton Limestone" to rocks forming Trenton Falls in Trenton Township, Oneida County, New York. The name Trenton was first introduced into Ohio nomenclature by Orton (1888). The Trenton rocks are equivalent to the Lexington Limestone of Kentucky (Campbell, 1898) as described in the type section in Lexington, Kentucky. A comparison of the nomenclature for the Trenton Limestone and equivalent rocks across the project area is shown in Figure 1-1.

We correlate the sharp contact at the top of the Trenton Limestone in the Trenton platform of northwestern Ohio and eastern Indiana to the gradational top of the Lexington Limestone in the Utica/Point Pleasant sub-basin (Figure 1-6). In the subsurface, the Lexington Limestone is subdivided, in ascending stratigraphic order, into the Curdsville Member, Logana Member and Lexington Undifferentiated Member (Figure 1-1). Both core and geophysical well logs indicate that the Logana and Lexington Undifferentiated are relatively higher in shale content than the Trenton Limestone of the platform or of the Curdsville Member.

Pope and Read (1997) subdivide the late Middle to Late Ordovician supersequence into four large third-order sequences. The Curdsville Member represents the transgressive systems tract (TST) of sequence 1 and consists of medium-gray to brownish-gray, medium-to fine-crystalline wackestone to grainstone. The Curdsville Member is a cleaner carbonate represented by a lower gamma-ray response similar to the Trenton and has a gradational contact with the overlying Logana Member. The Logana Member is thought to represent a maximum flood surface (MFS) of sequence 1 (Pope and Read, 1997). It consists of deeper water, olive-gray to black, calcareous, medium- to thin-bedded, fossiliferous (primarily thin-shelled brachiopods) shale, and thin beds of coarse-to fine-crystalline, argillaceous, fossiliferous, olive-gray limestone. The distinct lithology of the Logana Member can be identified and correlated on geophysical logs by its higher gamma and increased neutron response. Source rock analyses of Ohio wells discussed later in the resource assessment chapter shows this unit to be a potential source rock.

The limit of the Logana Member as we have correlated it on core and geophysical logs is present throughout most of Ohio in the sub-basin region, and extends into Kentucky and western West Virginia (Plate 1-26). Project work based on regional cross sections indicates that beyond the extent line, the Logana Member may be time equivalent to part of the Trenton Limestone, to the base of the Utica Shale to the southwest, and with the Salona to the east. Isotope geochemistry investigations (Chapter IV) used in correlating the Guttenberg Isotope Carbon Excursion (GICE), facilitate establishment of probable time lines.

Facies present during late Trenton/Point Pleasant time primarily consist of clean or argillaceous carbonate grainstones, packstones, and wackestones, plus shale and calcareous shale with interbedded limestone (Figure 1-6). It should be noted that this is the authors' interpretation for an approximate time marker. The Trenton Limestone top mapped for this region is a diachronous surface, and thus is not time equivalent throughout the basin. The upper portion of the thick Trenton platform development in New York, for example, is younger than the thinner Trenton platform development in northwest Ohio, southeast Michigan and eastern Indiana. Also, the relationship of the Point Pleasant Formation with the Trenton Limestone is not well understood because of a lack of good biostratigraphic time markers. The Point Pleasant Formation appears to have been deposited in part contemporaneously with the Trenton Limestone in northwestern Ohio, but also appears to have been deposited over the Trenton along portions of the platform margin to the southwest.

On the Trenton platform in northwestern Ohio, Indiana and Michigan the Trenton consists of a clean carbonate comprised primarily of a grainstone-packstone texture, and has a sharp upper contact with the overlying Utica Shale. The type well for this facies is the cored Ohio Geological Survey, Stone Company well (APINO 3417160004) in Williams County, Ohio (Figure 1-8). Approximately 230 feet of Trenton is present below the sharp upper contact with the overlying Utica Shale. The Millbrig K-bentonite marks the contact with the underlying mudstone of the Black River. In southwestern Ontario, the Trenton Group (Cobourg, Sherman Fall, and Kirkfield formations) thickens and consists primarily of grainstones and wackestones (Coniglio and others, 1994).

A facies change to a more argillaceous carbonate occurs in western Ontario (Figure 1-6) and extends into New York. Previous researchers have shown a facies change in western Ontario indicating this eastward transition from a clean carbonate to a more argillaceous carbonate (Keith, 1985; Wickstrom and others, 1992). In this facies, the Trenton consists of an argillaceous carbonate with a grainstone-packstone texture and a sharp upper contact with the overlying Utica Shale. As shown in a type well, Belden and Blake, 1 Huber (APINO 3110122859) in Steuben County, New York (Figure 1-9), the Trenton reaches a thickness of approximately 700 feet, compared to the 230 feet present in the Williams County, Ohio well. A clean carbonate, which may have exploration potential for hydrothermal dolomite reservoirs, is present within the upper 100 feet of Trenton in this New York well.

To the south of these platform carbonate facies is a deeper-water sub-basin where the Utica Shale and calcareous shales of the Point Pleasant Formation were being deposited, in part contemporaneously with the clean Trenton platform carbonates. Well-developed Trenton carbonate grainstones-packstones on the Trenton Platform margin become thin to the southeast into a sub-basin of increasing shale content. Within this sub-basin, the overlying dark Utica shales are thickest where the Trenton is the thinnest. Representative wells of this facies are illustrated by the Chevron, Prudential well (APINO 3410120196) in Marion County, Ohio (Figure 1-10) and the Ohio Geological Survey American Aggregates well (3416560005) in Warren County, Ohio (Figure 1-11). In both of these cored wells, the cores and geophysical logs indicate that the Trenton/Lexington Limestone can be subdivided into the Curdsville Member, Logana Member and Lexington Undifferentiated Member. The top of the Trenton/Lexington is an argillaceous carbonate with a gradational contact to the overlying Utica Shale and Point Pleasant Formation compared to the cleaner Trenton carbonates on the platform to the north.

On the southern margin of the Utica/Point Pleasant sub-basin, the Lexington platform is developed, where carbonate packstones, and wackestones were deposited, in part, contemporaneously with the Utica and Point Pleasant clastics of the sub-basin (Figure 1-6). The Lexington platform is a deeper water platform than the Trenton platform in northwestern Ohio as indicated by more argillaceous material and a more gradational upper contact with the overlying Point Pleasant. A representative well for this facies is the Signal Oil and Gas, Henry Stratton well (APINO 1619524577) in Pike County, Kentucky (Figure 1-12). The Trenton interval in this well is approximately 550 feet thick and has tentatively been subdivided into the Curdsville Member, Logana Member and Lexington Undifferentiated Member. A thin (20 feet) Point Pleasant was deposited above the Trenton/Lexington and grades upward into the overlying Kope Formation. Based on sample and core data, the dark-black, organic-rich shale characteristic of the Utica Shale is absent in this well.

Localized areas of clean carbonate buildups have been identified in the deeper basinal areas where the Trenton is typically an argillaceous carbonate. One of these clean carbonate buildups is illustrated by the United Fuel Gas, 1 Sponaugle well (APINO 4707100006) in Pendleton County, West Virginia (Figure 1-13). This well contains a clean Trenton carbonate in sharp contact with the overlying Utica. This upper Trenton interval is located at the top of an overthrusted and repeated Trenton section (entire interval not displayed). Clean carbonate buildups in this deeper portion of the basin have been described in outcrop work in Kentucky and Virginia by Pope and Read (1997), and also were suggested by Keith (1989) in a facies map of Shermanian time.

The interval-thickness map of the Trenton/Lexington illustrates the basin geometry during this time as defined by the Utica/Point Pleasant sub-basin and the thick carbonate platforms that developed along much of the sub-basin margin (Plate 1-27). Trenton/Lexington thickness ranges from over 200 feet on the Trenton platform in northwestern Ohio to more than 300 feet on the Lexington Platform in central Kentucky, and to over 850 feet on the Trenton platform in central New York. Within the western

portion of the Utica/Point Pleasant sub-basin, this interval thins to less than 50 feet along the northeast-southwest trending "Sebree feature," that has been discussed by various authors (Freeman, 1953; Wagner, 1966; Wickstrom, et al., 1992; Hohman, 1997; Ettensohn, et al., 2002). The areas of historic oil and gas production from the Trenton-Black River in northwestern Ohio, Indiana and south-central New York are coincident with the platform margin in these states. The authors recognize the platform margin as an important trend to explore for potential Trenton-Black River HTD reservoirs within the project area.

Point Pleasant Formation and Utica Shale

Orton (1873) first assigned the name "Point Pleasant" to strata exposed at Point Pleasant, Clermont County, Ohio. Specifically, the name was assigned to the lowest formation in the Cincinnati Group. The Point Pleasant Formation is equivalent to the Clays Ferry Formation of Kentucky, which consists of interbedded limestone and shale of nearly equal proportions. It overlies the Lexington Limestone, and underlies the Kope Formation. The Point Pleasant is not formally used outside of southern Ohio, but a correlation line based on geophysical logs, cores and sample descriptions has been extended throughout the sub-basin region for mapping purposes. In New York, the Dolgeville Formation is considered equivalent to the Point Pleasant (Taury Smith, personal comm.).

The name "Utica Shale" was first used by Emmons (1842) to refer to the black shale in the Mohawk Valley, New York that underlies the Lorraine shales and overlies the Trenton Limestone. In southwestern Ontario, the Collingwood Formation is a partial equivalent to the Utica Shale (Coniglio and others, 1994).

The facies relationships between the Trenton/Lexington and overlying Utica/Point Pleasant units are the most complex across the region. Locally, the Utica and Point Pleasant display an intertonguing relationship. The Trenton/Lexington Limestone grades laterally and upward to dominantly dark-gray to brown-to-black, platy, finely laminated, locally calcareous Utica Shale and interbedded limestone and calcareous shale of the Point Pleasant Formation. The top of the Point Pleasant is placed at the occurrence of thin, interbedded limestone in the shale interval overlying the Trenton. Based on core, sample descriptions, and geophysical logs, the Point Pleasant is limited south of a line extending from the Indiana-Kentucky border, and extends northwest through western and northern Ohio, across northern Pennsylvania, and into eastern New York (Plate 1-28). North of the line showing the limit of Point Pleasant, the Trenton is overlain by a sharp contact with the overlying Utica Shale. South of this line, the contact of the Trenton with the overlying Point Pleasant is a gradational contact.

The Utica Shale is defined as a dark-brown to black, organic-rich shale. It represents a major transgression across the eastern United States, and the shales indicate a large influx of organic material, restricted circulation, and low-energy conditions (Bergstrom and Mitchell, 1992; Ryder, 1992; Wickstrom, 1996). Based on examination of core, sample descriptions and geophysical logs, the Utica Shale is absent in south-

central Ohio, Kentucky and southern West Virginia (Plate 1-28). The Utica Shale appears partially coeval with the Trenton Limestone of the platform and entirely coeval, as well as overlapping, with the Point Pleasant Formation of the Utica/Point Pleasant Sub-basin area. The Utica Shale is absent over most of the Lexington Platform due to facies transition with overlying gray shale of the Kope Formation.

In the mapped area, the interval thickness of the "Utica" is over 350 feet in western Ohio adjacent to the platform margin, and attains a thickness of over 500 feet in eastern New York. It reaches a maximum thickness of over 700 feet in the Rome trough region of Pennsylvania (Plate 1-28). Throughout the rest of the project area, the "Utica" interval is generally less than 300 feet in thickness.

"Kope" and Equivalent Interval

The Kope was named for rocks outcropping at Kope Hollow, Brown County, Ohio by Weiss and Sweet (1964) for a predominantly shale unit. In Ohio, it is only recognized as a formal unit in the southwestern portion of the state, but a correlation line for the top of the Kope was extended throughout the project area for mapping purposes and to assist in understanding the basin architecture. For this project, the top of the "Kope" mapping unit was interpreted as a gray-to-black shale that overlies the black, organic-rich Utica Shale and underlies a unit in the "Cincinnati Undifferentiated" that contains interbedded shale and limestone. This correlation line was extended across the project area using geophysical logs. Partial equivalents to this unit throughout the project area are the Reedsville Shale in northwestern Pennsylvania and West Virginia, the Martinsburg Formation in central Pennsylvania, the Lorraine Group in west-central New York, and the Blue Mountain Formation and Georgian Bay Formation in southwestern Ontario (Figure 1-1).

The interval thickness of the "Kope" ranges from 250 feet in the western portion of the project to over 1,500 feet in the eastern portion of the project (Plate 1-29). In western Ohio, a reflection of the northeast-southwest trending "Sebree feature" of the Utica/ Point Pleasant sub-basin is still evident during this time. A thin trend is present over the thick Trenton carbonate platform in New York. Similar depositional patterns are observed on the interval-thickness map of the upper Ordovician undifferentiated (Plate 1-30). Thickness of this interval is over 500 feet in western Ohio and attains a thickness of over 2,100 feet in the eastern portion of the mapped area.

Cross Sections Illustrating Middle and Upper Ordovician Stratigraphic Relationships

A network of cross sections (Plate 1) was developed to unravel the regional stratigraphy and facies relationships, which are necessary for understanding the productive Trenton-Black River reservoirs. Cross sections are tied to open-file reports, published reports, continuous core and geophysical well logs, and Geolog sample descriptions. For all cross sections in this report, the top of the Black River Group is used for the datum.

Cross-section Dip A-A' through Dip D-D' (Plates 1-2 through 1-5) are all oriented northwest to southeast. These cross sections illustrate subsurface lithostratigraphic correlations that extend from the producing Trenton platform margin area across the Utica/Point Pleasant sub-basin area to the Lexington platform region. Well-developed Trenton carbonate grainstones and packstones on the Trenton platform margin in northwestern Ohio are over 350 feet thick, and thin to about 30 feet thick to the southeast into a sub-basin of deeper water Utica Shale and Point Pleasant calcareous shales. Within this sub-basin the overlying dark Utica shales are thickest where the Trenton is the thinnest. These dark Utica shales appear to be coeval with the Point Pleasant Formation and Lexington to the southeast. The Kope Formation overlies the Point Pleasant Formation and is partially coeval with the Utica Shale within the sub-basin. The Lexington is subdivided in ascending order into: the Curdsville Member, the Logana Member and the Lexington Undifferentiated Member. The top of the Lexington is chosen on geophysical logs using the best-developed carbonate bed at the base of the Point Pleasant Formation.

Cross sections Dip E-E' through K-K' (Plates 1-6 through 1-12) roughly parallel the previous cross sections, and extend from the Trenton platform in northwestern Ohio, Indiana, Michigan and Ontario, across the Utica/Point Pleasant sub-basin, and terminate in an area of deeper-water carbonate that is composed of more argillaceous Lexington carbonates. Similar facies relationships are evident in the previous cross sections. On the productive Trenton platform, the Trenton carbonates obtain a thickness of 480 feet and thin to approximately 80 feet in the sub-basin. The upper portion of the Trenton appears to be, in part, coeval with the Point Pleasant strata of the deeper water sub-basin. Trenton equivalent strata (Lexington Undifferentiated, Logana and Curdsville members) in the sub-basin thicken to the deeper-water carbonate where the unit reaches a maximum thickness of 640 feet. The overlying Ordovician shales and the underlying Black River both indicate basinward thickening to the east and southeast. The "Gull River" and Wells Creek Formation intervals indicate thickening over the Rome Trough feature.

Cross section Dip L-L' also trends northwest-southeast (Plate 1-13), and illustrates the Trenton Platform area from Durham Regional Municipality, Ontario to Broome County, New York. The Trenton platform carbonates reach a maximum thickness of 750 feet in Steuben County, New York, and thin to the southeast along the platform margin to approximately 230 feet. An unnamed clean carbonate facies in the upper portion of the Trenton Limestone is present in the Bonham, Radigan, McClurg, Kennedy and Huber wells in Steuben, Livingston and Schuyler counties, New York. There is currently no known Trenton production from this clean carbonate facies. It may be a viable exploration target for HTD reservoirs. The Dolgeville Formation (Point Pleasant-type rocks) is present above the Trenton at the southeastern end of this line and displays a similar relationship along the platform margin that is observed in northwestern Ohio.

Strike cross section A-A' (Plate 1-14) trends southwest-northeast and extends along the Trenton platform from northeast Indiana, across southeastern Michigan,

northwest Ohio and southern Ontario into western New York. The Trenton platform ranges in thickness from 199 feet in eastern Indiana to 556 feet in central New York. The Point Pleasant is absent throughout the platform region shown here, and the Utica Shale or equivalent unit directly overlies the Trenton Formation.

Strike cross section B-B' (Plate 1-15) trends southwest-northeast beginning in the Utica/Point Pleasant sub-basin and then onto the Trenton platform from northwestern Ohio to central New York. At the southern end of the line, the Trenton carbonates are thin (less than 28 feet thick) in the Utica/Point Pleasant sub-basin region and thicken to 670 feet in the Trenton platform in New York. The clean unnamed carbonate facies in the uppermost Trenton also is present at the northeastern end of this cross section as seen in the McClurg and Smith wells in Livingston and Cayuga counties, New York.

Strike cross sections C-C', D-D', E-E' and F-F' (Plates 1-16 through 1-19) also trend southwest-northeast and begin in the Lexington platform region, cross the Utica/Point Pleasant sub-basin, and extend onto the Trenton platform of New York. The Lexington interval is subdivided here into the Curdsville Member, Logana Member and Lexington Undifferentiated Member and attains a thickness of 350 feet in the Lexington platform region. These cross sections then cross the deeper-water, more anoxic and restricted-circulation environment of the Utica/Point Pleasant sub-basin. Here, the Lexington interval (Curdsville Member, Logana Member and Lexington Undifferentiated Member) is typically less then 150 feet thick. The Point Pleasant Formation is present in the sub-basin region and has a gradational contact with the underlying Lexington Limestone. These cross sections extend onto the Trenton platform in New York where these thick platform carbonates attain a thickness of up to 830 feet. The clean, unnamed Trenton carbonate facies of New York also is seen in cross section E-E' (Plate 1-18).

Stratigraphic Summary and Conclusions

Understanding the basin architecture and facies distribution has important implications for Trenton-Black River exploration. Preliminary isopach maps of the Trenton interval, and preliminary facies maps representing Trenton/Point Pleasant time, indicate that exploration potential exists along the entire platform margin, especially where there are clean carbonates. Vast unexplored areas are present along the platform margin underlying the Ohio and Pennsylvania portions of Lake Erie that could yield large reserves.

The best reservoir facies for hydrothermal dolomite (HTD) reservoir development might be the clean Trenton and Black River carbonate facies. Comparison of the Trenton-Black River producing fields to the type of producing reservoir supports that idea. Producing HTD reservoirs in the historic Lima-Indiana producing trend in northwest Ohio and Indiana, and in producing fields in Ontario, indicate that the best reservoirs are clean carbonates in the Trenton grainstones and packstones. The grainstones that developed on skeletal shoals along the platform margin, and that extend from Indiana, to northwest Ohio, to Ontario, and across northern Pennsylvania, appear to have high potential for hydrothermal dolomite (HTD) reservoir development. Production

in HTD reservoirs in New York, thus far, has been from the cleaner carbonate of the Black River and has not yet been found to extend up into the Trenton Limestone. Project investigators suspect that the more argillaceous nature of the Trenton carbonates may inhibit the process of HTD reservoirs to develop. There is, however, an upper, cleaner portion of the Trenton in portions of western New York which may have exploration potential for HTD reservoirs, which is, as yet, untested.

Trenton-Black River production in Kentucky and West Virginia, thus far, has been from fractured limestone reservoirs. This also seems to support the idea that the dirtier, more argillaceous carbonates in these deeper, basinal areas may not be as conducive to HTD reservoir development as the cleaner carbonates on the northern Trenton platforms. However, there does exist in this deeper portion of the basin, localized areas of cleaner carbonate buildups in the Trenton that may be more conducive to HTD reservoir development. If these localized areas of cleaner carbonates with a sharp upper contact could be imaged with seismic reflection data, it could assist in identifying potential exploration trends for Trenton-Black River production where the seismic signature can be mapped. Seismic modeling is required to lend credence to this idea.

Basal Cambrian sandstones are present throughout most of the known Trenton-Black River HTD producing areas, except for a few localized gas fields in Ontario. These basal sandstone units, when present in conjunction with fault and fracture systems, may be important in providing migration pathways for hydrothermal fluids that create the Trenton-Black River and underlying Knox HTD reservoirs. However, there are clearly Black River HTD producing areas in Ontario where there is no basal Cambrian sandstone present. Thus, other possible hydrothermal migration pathways such as the Shadow Lake Sandstone or equivalent may be important for HTD reservoir development. The Rose Run sandstone is not present over much of the historical Trenton-Black River producing trends and thus is not a necessary component for hydrothermal fluid migration pathways. A more detailed discussion of hydrothermal alteration is presented later in this report.

Acknowledgements

The authors would like to thank Joe Wells for his assistance in database management and format. Eric Venteris was responsible for generating the final isopach maps, and Donovan Powers provided the basemap and final cartographic work for the maps presented in this report. A special thanks is given to Lisa VanDoren for the cartographic work in the final presentation of the cross sections and figures. We also thank Dennis Hull for his review of the manuscript.

LAURENTIAN CRATON | ROME TROUGH | EASTERN BASIN

SYSTEM	SERIES	SOUTHEASTERN MICHIGAN	EASTERN INDIANA	NORTHERN KENTUCKY AND SOUTHWESTERN OHIO	WEST-CENTRAL OHIO	EASTERN OHIO	NORTHWESTERN PENNSYLVANIA	SOUTHWESTERN ONTARIO	WEST-CENTRAL NEW YORK	CENTRAL AND EASTERN KENTUCKY	CENTRAL WEST VIRGINIA	PENNSYLVANIA PORTION OF THE ROME TROUGH	CENTRAL PENNSYLVANIA	EASTERN WEST VIRGINIA	EASTERN TENNESSEE AND SOUTHWESTERN VIRGINIA
ORDOVICIAN	Upper (International) / Upper (North American)	Cincinnati Series	Maquoketa Gp	Drakes Fm Whitewater Fm Liberty Fm Waynesville Fm Arnheim Fm Grant Lake Fm Miamitown Sh Fairview Fm	Cincinnati gp	Queenston Sh	Queenston Fm Reedsville Sh	Queenston Fm Georgian Bay Fm	Queenston Fm Lorraine Gp	Drakes Fm Grant Lake Ls Ashlock Fm Calloway Creek Ls	Juniata Fm Reedsville Sh	Juniata Fm / Bald Eagle Fm Reedsville Sh	Juniata Fm / Bald Eagle Fm Reedsville Sh / Martinsburg Fm	Juniata Fm Oswego Ss Reedsville Fm Martinsburg Fm	Shellmound Fm Sequatchie Fm Juniata Fm Leipers Ls Nashville Gp Inman Fm Reedsville Sh Martinsburg Fm
	Upper (International) / Middle (North American)	Trenton Ls	Trenton Ls Lexington Ls	Kope Fm Point Pleasant Fm Lexington Ls Lexington Und Mbr Logana Mbr Curdsville Mbr	Kope Fm "Utica Sh" Point Pleasant Fm Lexington Ls Logana Mbr Curdsville Mbr Trenton Ls	Point Pleasant Fm Trenton Ls	Utica Sh Point Pleasant Fm Trenton Ls	Blue Mountain Fm Collingwood Fm Cobourg Fm Sherman Fall Fm Kirkfield Fm	Utica Fm Trenton Ls	Garrard Slt Clays Ferry Fm Lexington Ls	Trenton Ls	Utica Sh Trenton Ls	Antes Fm Coburn Fm Salona Fm Nealmont Fm Linden Hall Fm Snyder Fm Hatter Fm	Dolly Ridge Fm Trenton Gp Nealmont Ls Chambersburg Gp Chickamauga Ls Stones River Gp	Bays Fm Ottosee Sh Chapman Ridge Ss Holston Fm Sevier Sh
		Black River Gp Glenwood Fm	Black River Gp Ancell Gp	Black River Ls Carntown unit Black River Gp Wells Creek Fm	Black River Gp "Gull River Ls" Wells Creek Fm	Trenton Gp Black River Gp	Black River Ls Loysburg Fm Wells Creek Fm Beekmantown Fm	Coboconk Fm Gull River Fm Shadow Lake Fm	Black River Ls	High Bridge Gp Wells Creek Dol St. Peter Ss	Black River Gp	Black River Ls Loysburg Fm Beekmantown Fm	Loysburg Fm	Black River Ls St. Paul Gp Lincolnshire Ls New Market Ls Row Park Ls	Lenoir Ls
	Middle (International) / Lower	Prairie du Chien Gp	Knox Super Gp	Beekmantown Dol Rose Run Ss	Beekmantown dol Rose Run ss	Knox Dol	Beekmantown Fm Mines Mbr Upper Sandy mbr	Black River Gp	Tribes Hill Fm Little Falls Fm	Beekmantown Dol Rose Run Ss	Knox Gp unnamed dol upper ss mbr	Beekmantown Gp Mines Mbr Upper Sandy mbr	Beekmantown Gp Bellefonte Fm Axemann Fm Nittany Fm Larke Fm Stonehenge Fm	Beekmantown Gp Pinesburg Station Dol Rockdale Run Fm Stonehenge Ls Stoufferstown Mbr	Knox Gp Mascot Dol Kingsport Fm Chepultepec Dol Jonesboro Ls
	Upper	Trempealeau Fm Franconia Fm Galesville Ss Eau Clair Fm Munising Gp	Davis Fm Eau Clair Fm Munising Gp	Copper Ridge Dol Eau Claire Fm Conasauga Fm	Copper Ridge dol Eau Claire Fm Conasauga Fm	Gatesburg Fm	Middle Dolomite mbr Lower Sandy mbr Warrior Fm Potsdam Ss	Potsdam Fm	Galway Fm Theresa Fm Potsdam Fm	Copper Ridge Dol Maynardville Ls Nolichucky Sh Maryville Ls	Knox Gp Copper Ridge Dol Maynardville Ls Nolichucky Sh Maryville Ls Rogersville Sh Rutledge Ls Pumkin Valley Sh	Gatesburg Fm Middle Dolomite mbr Lower Sandy mbr Warrior Fm Pleasant Hill Fm ? not penetrated by drilling	Gatesburg Fm Conococheague Gp Mines Mbr Upper Sandy mbr Ore Hill Mbr Lower Sandy mbr Stacy Mbr Warrior Fm Pleasant Hill Fm Elbrook Fm	Conococheague Gp Elbrook Fm Catoctin Fm Swift Run Fm	Copper Ridge Dol Conoco-cheague Dol Maynardville Ls Nolichucky Sh Maryville Ls Rogersville Sh Rutledge Ls Conasauga Sh Honaker Fm Elbrook Dol
CAMBRIAN	Middle	Mount Simon Ss	Mount Simon Ss	Mount Simon Ss	Mount Simon Ss				Mount Simon Ss Rogersville Sh Rutledge Ls Pumkin Valley Sh	Conasauga Gp	Conasauga Gp	Conasauga Gp	Elbrook Fm		
	Lower								Rome Fm		Rome Fm Shady/Tomstown Dol Basal Ss		Waynesboro Fm Tomstown Fm Antietam Fm Weverton-Loudoun Fms	Waynesboro Fm Tomstown Dol ? Antietam Fm Harpers Fm Weverton-Loudoun Fms ?	Rome Fm Shady Dol
PRECAMBRIAN		Granite Rhyolte Complex	Middle Run Fm	Middle Run Fm	Granite Rhyolte Complex		Grenville Complex								

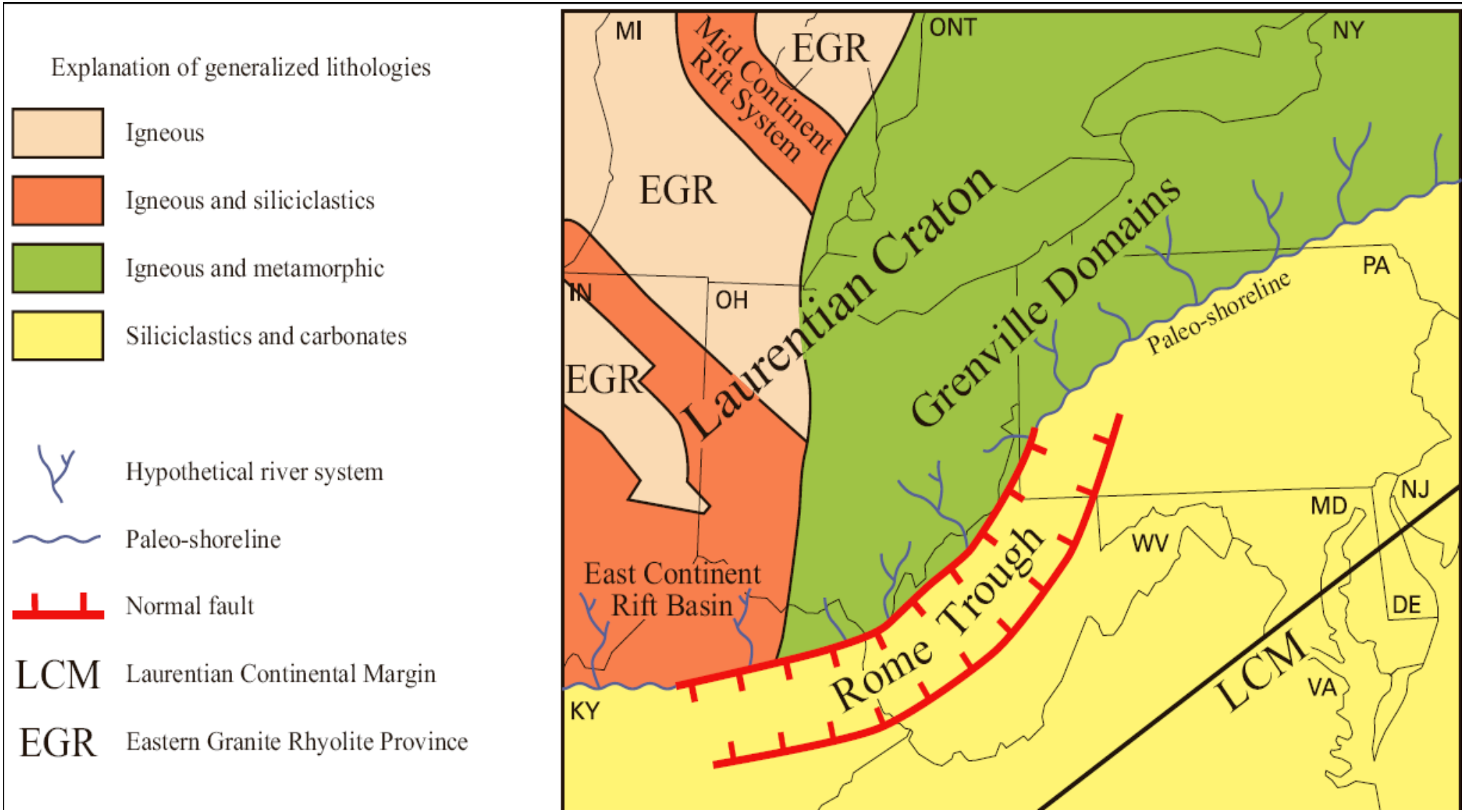

Figure 1-2. Map showing major tectonic features and paleogeography during Early Cambrian time.

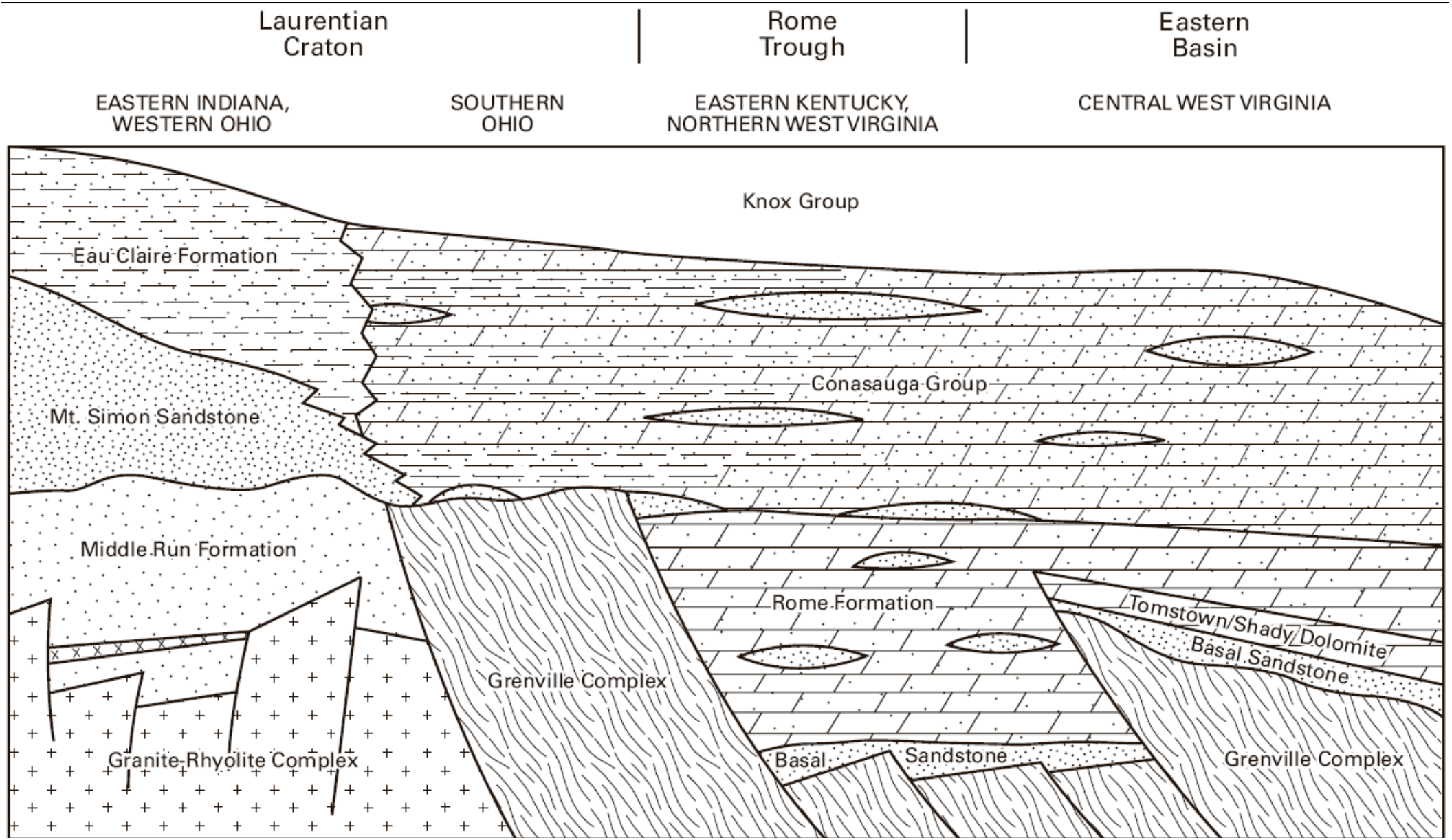

Figure 1-3. Generalized schematic cross section illustrating the relationships of the mapped Cambrian basal sandstones to other geologic units and structure (from Wickstrom, L. H., Venteris, E. R., Harper, J. A. and others, 2005).

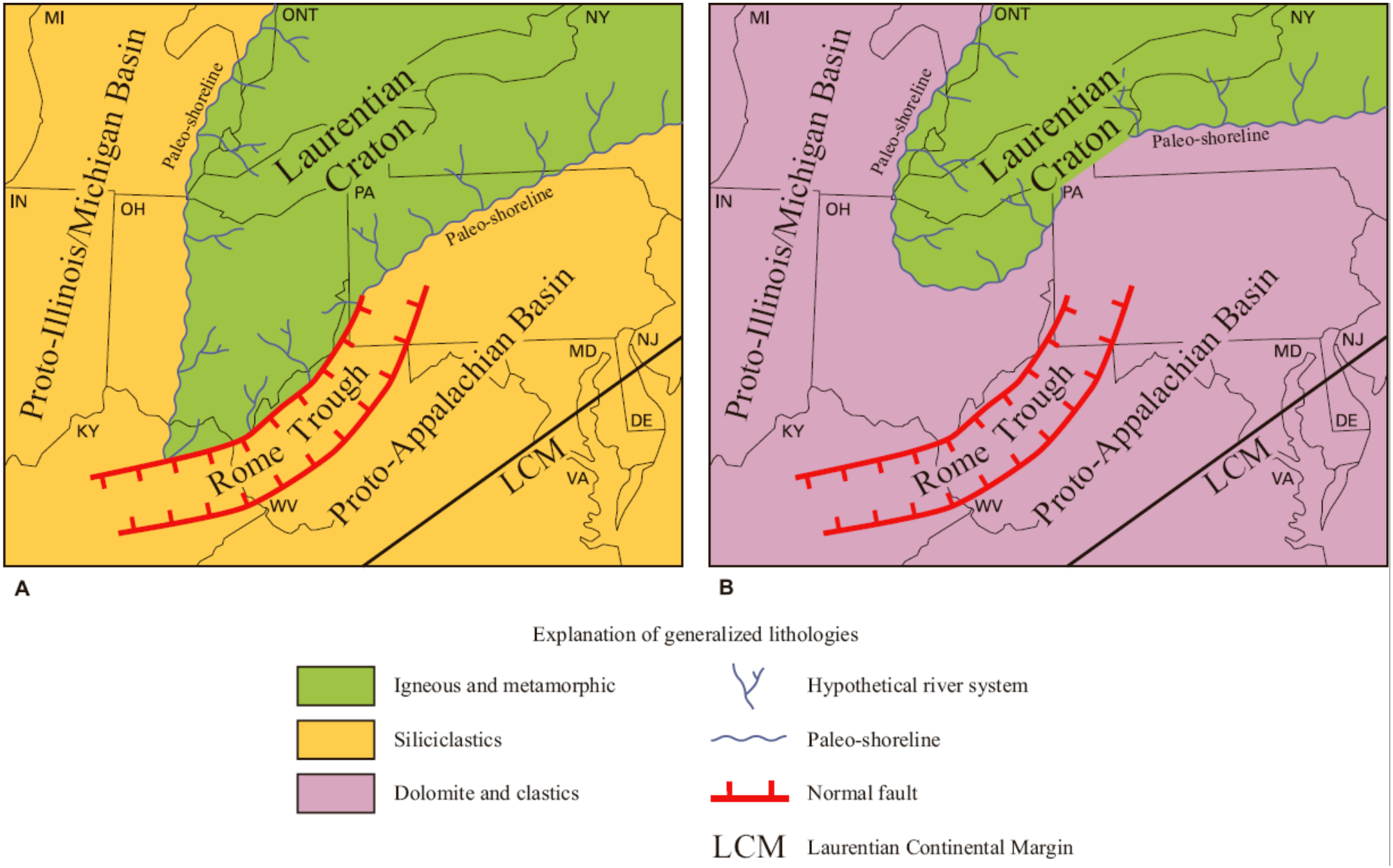

Figure 1-4A. Map showing basin architecture during Precambrian to Middle Cambrian Mount Simon Sandstone/Conasauga Formation time.

Figure 1-4B. Map showing basin architecture during Late Cambrian/Early Ordovician time.

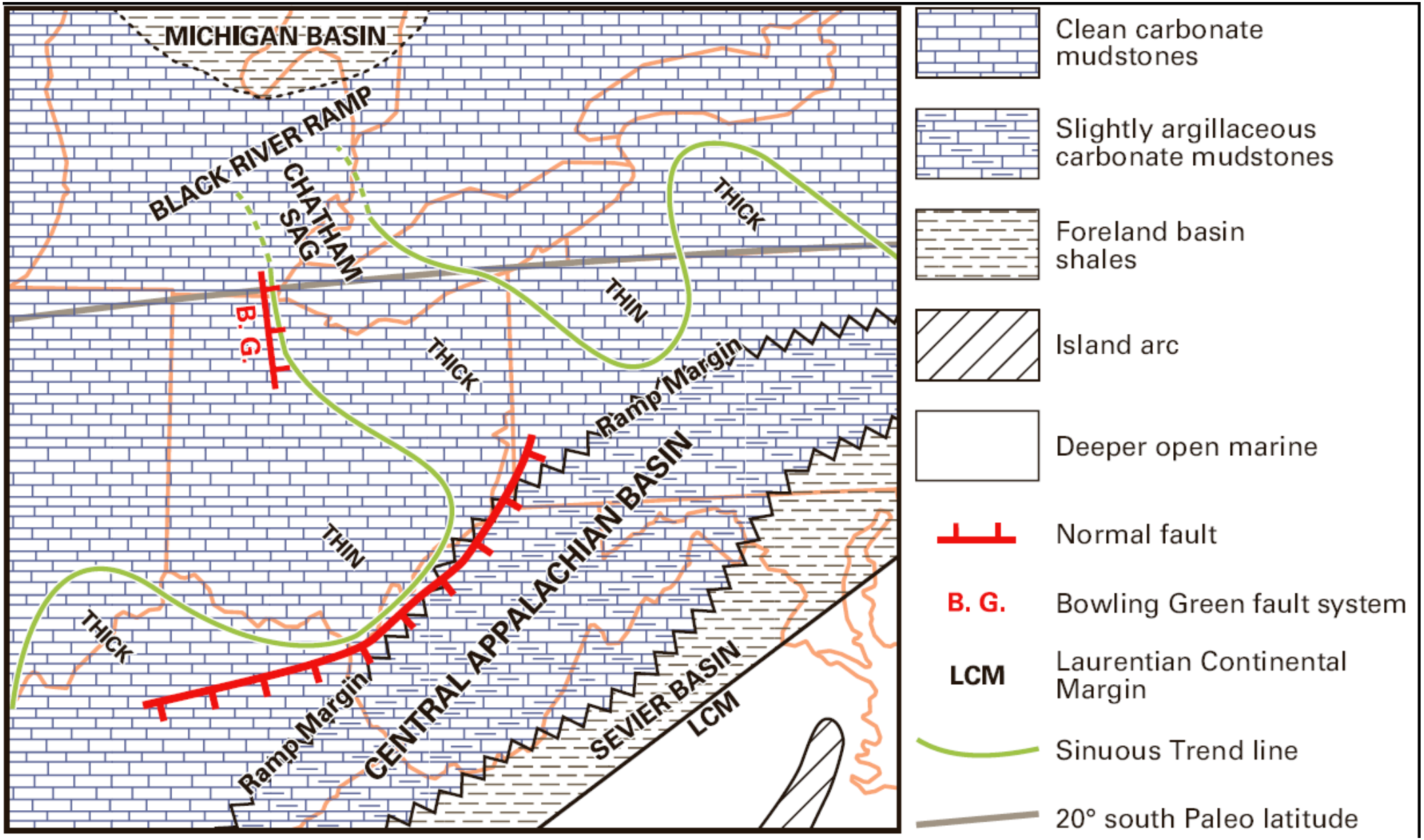

Figure 1-5. Facies map of late Black River time. Paleolatitude is from Scotese and McKerrow (1990).

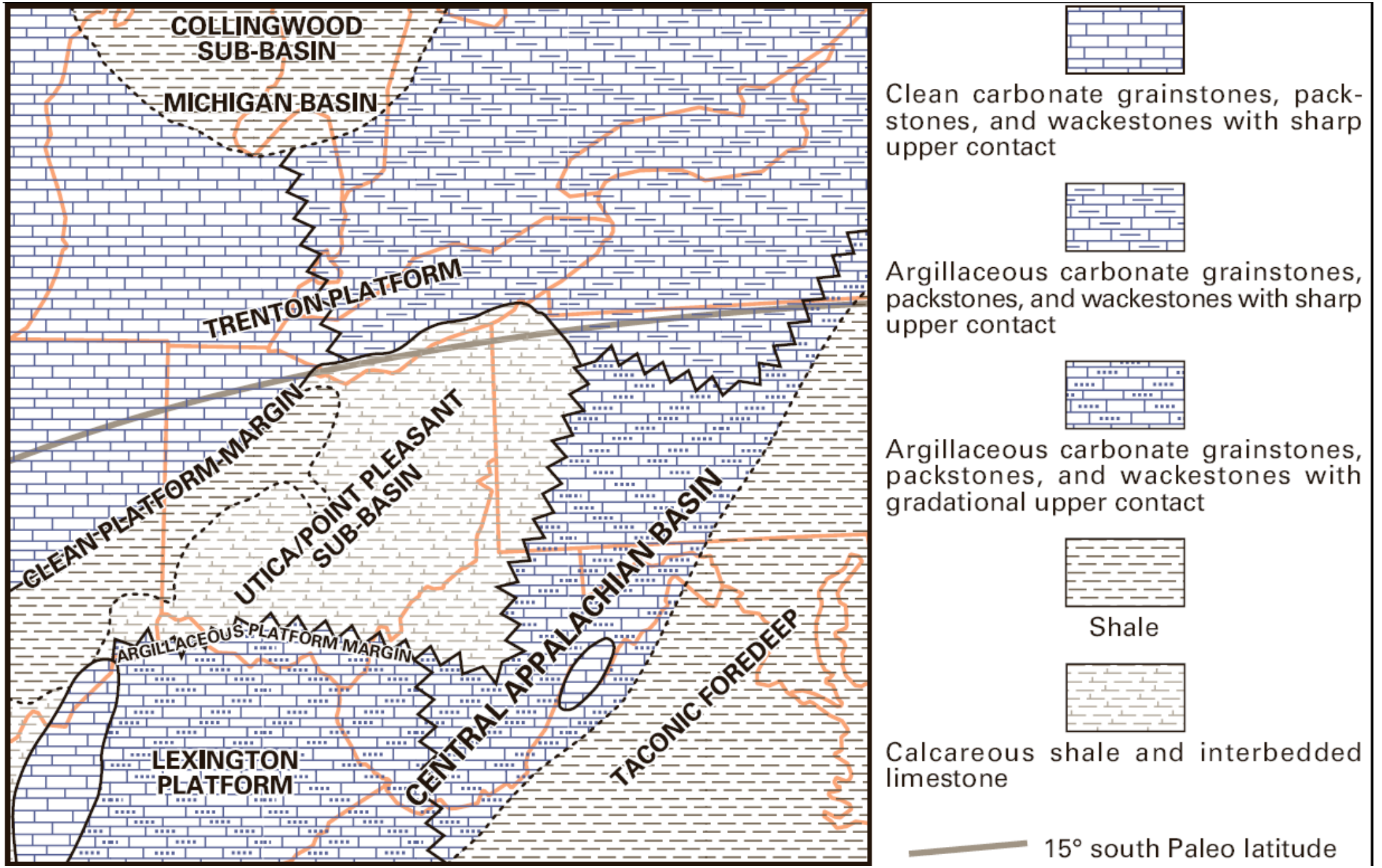

Figure 1-6. Facies map of Trenton/Point Pleasant time. Paleolatitude is from Scotese and McKerrow (1990).

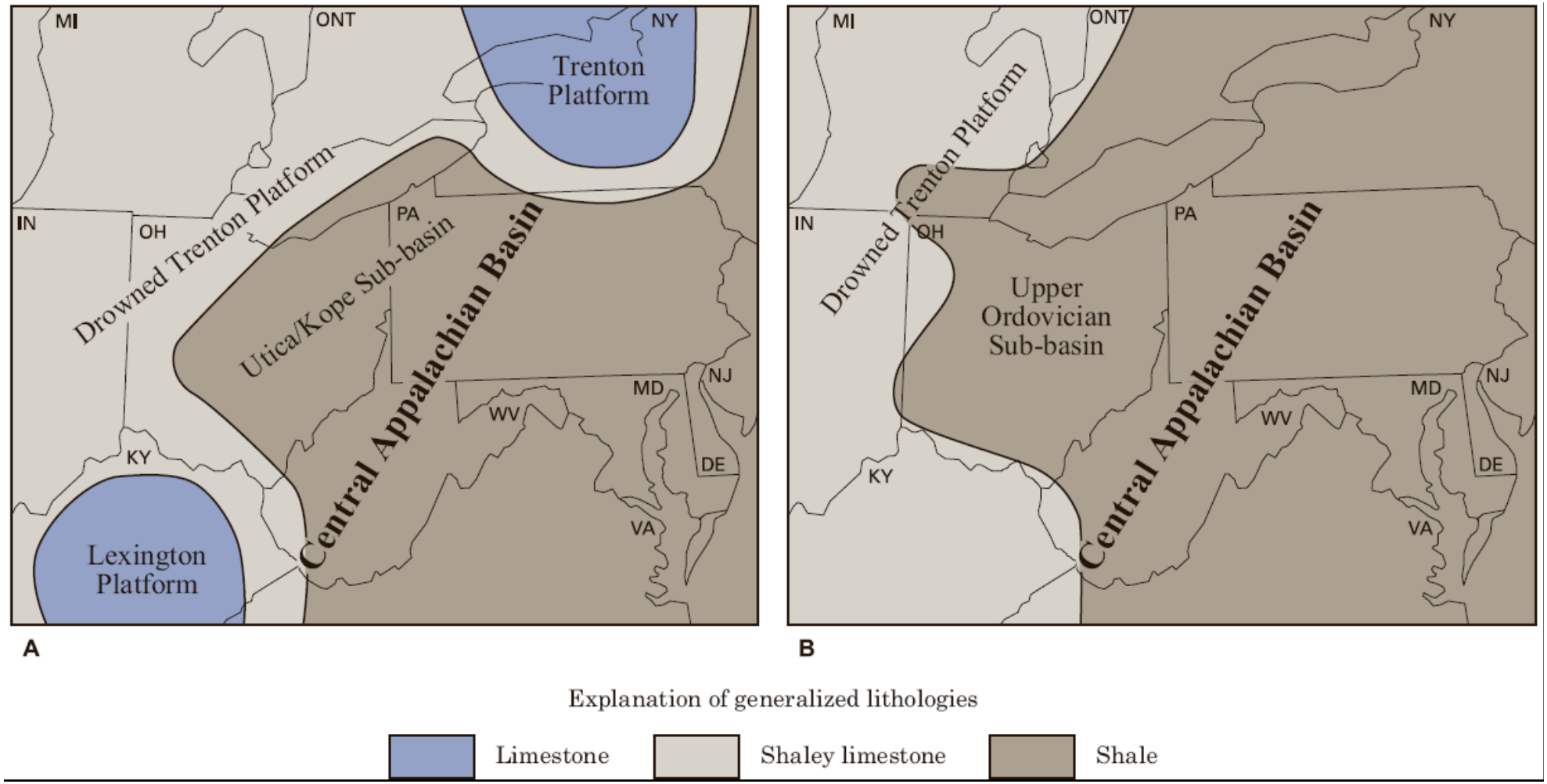

Figure 1-7A. Map showing basin architecture during Middle Ordovician Trenton to Late Ordovician “Kope” or equivalent time.

Figure 1-7B. Map showing basin architecture during Late Ordovician “Kope” or equivalent time to top of Ordovician time.

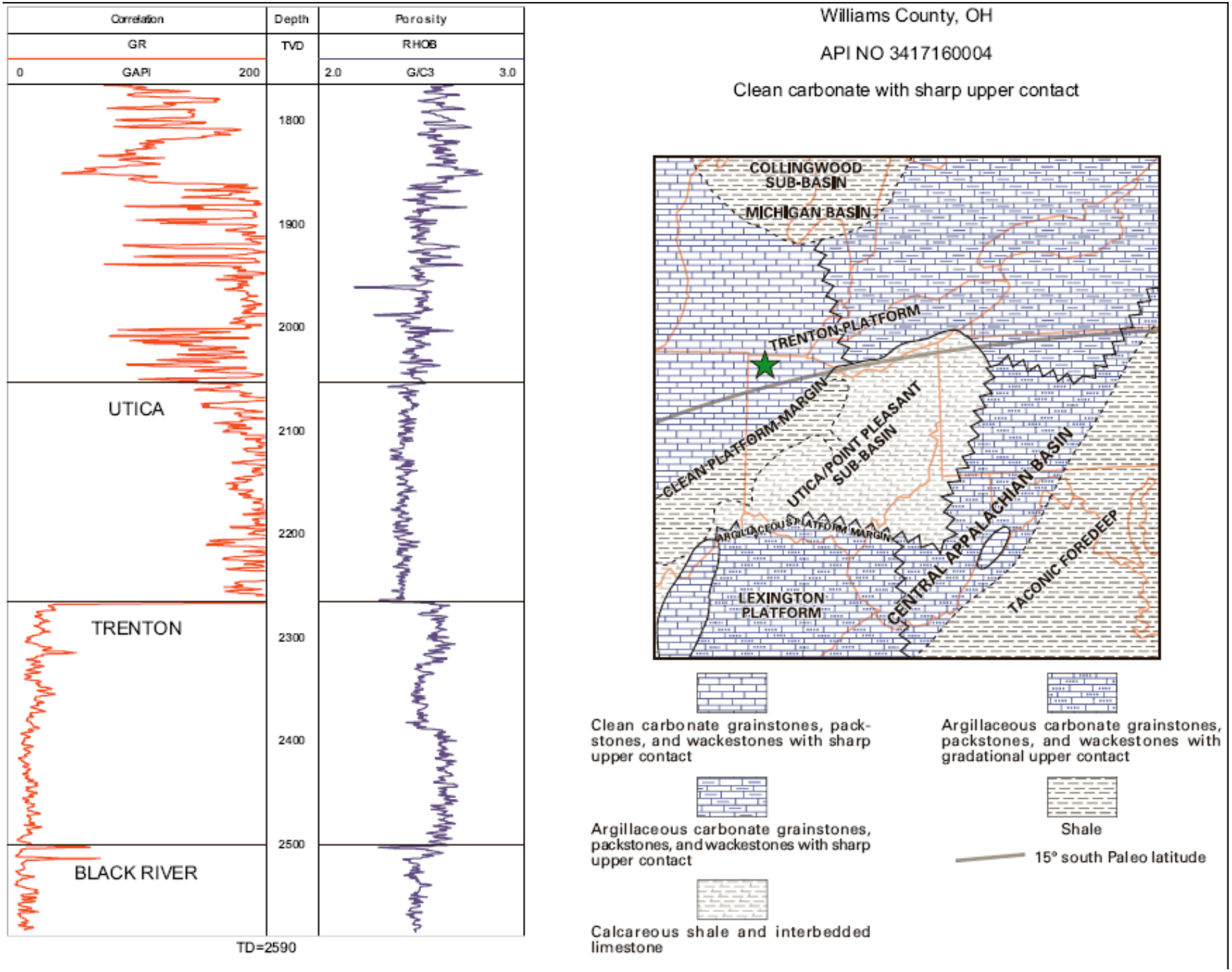

Figure 1-8. Representative well on the clean carbonate Trenton Platform; Ohio Geological Survey, Stone Company.

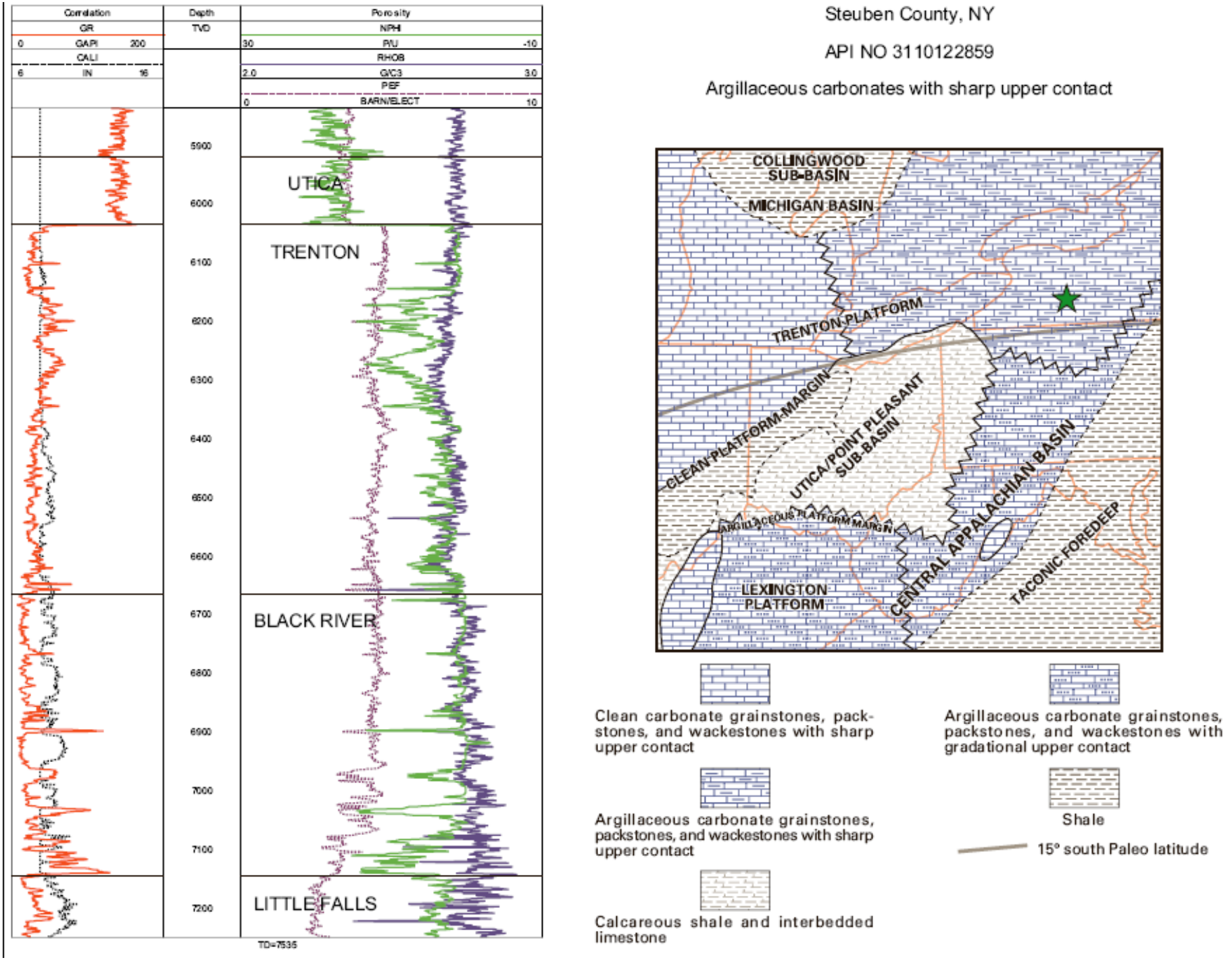

Figure 1-9. Representative well from the argillaceous carbonate Trenton Platform; Belden and Blake, 1 Huber.

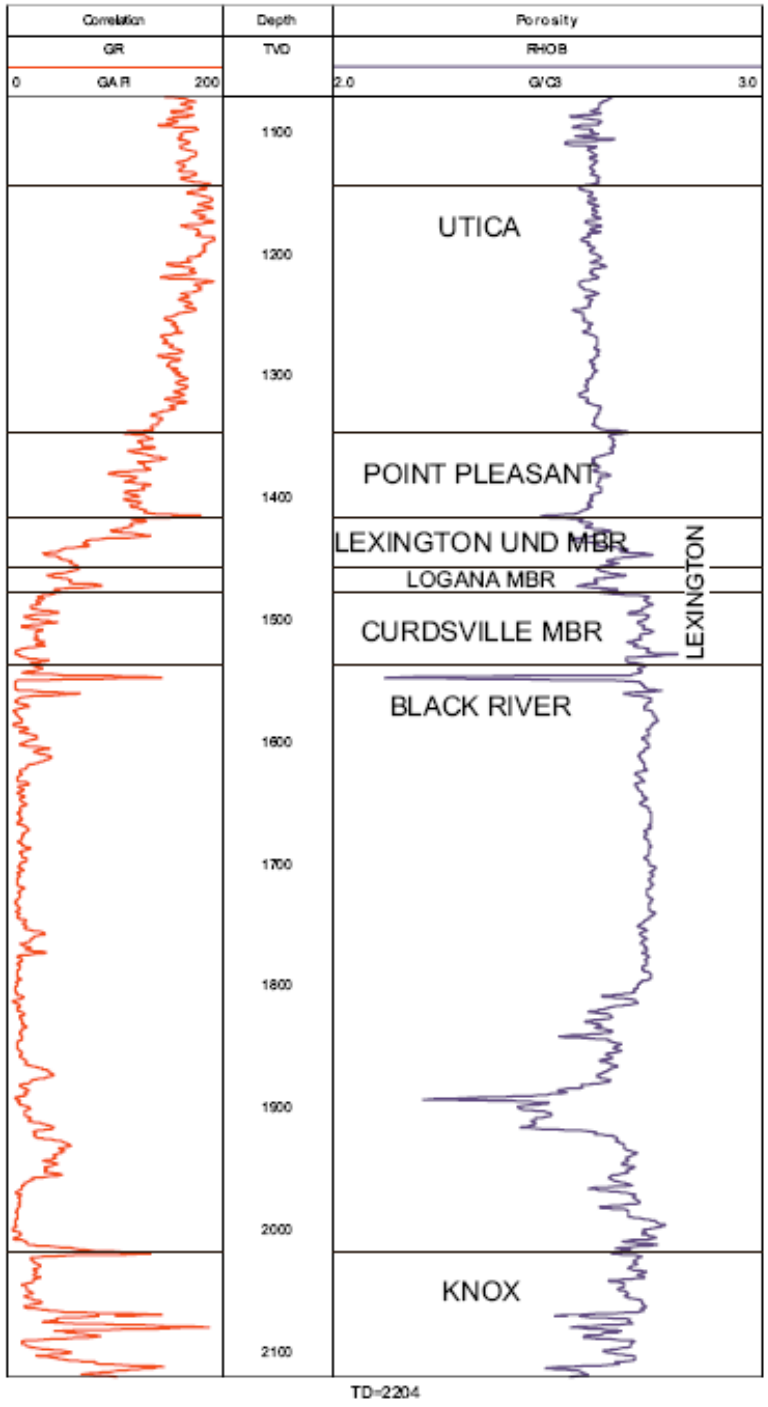

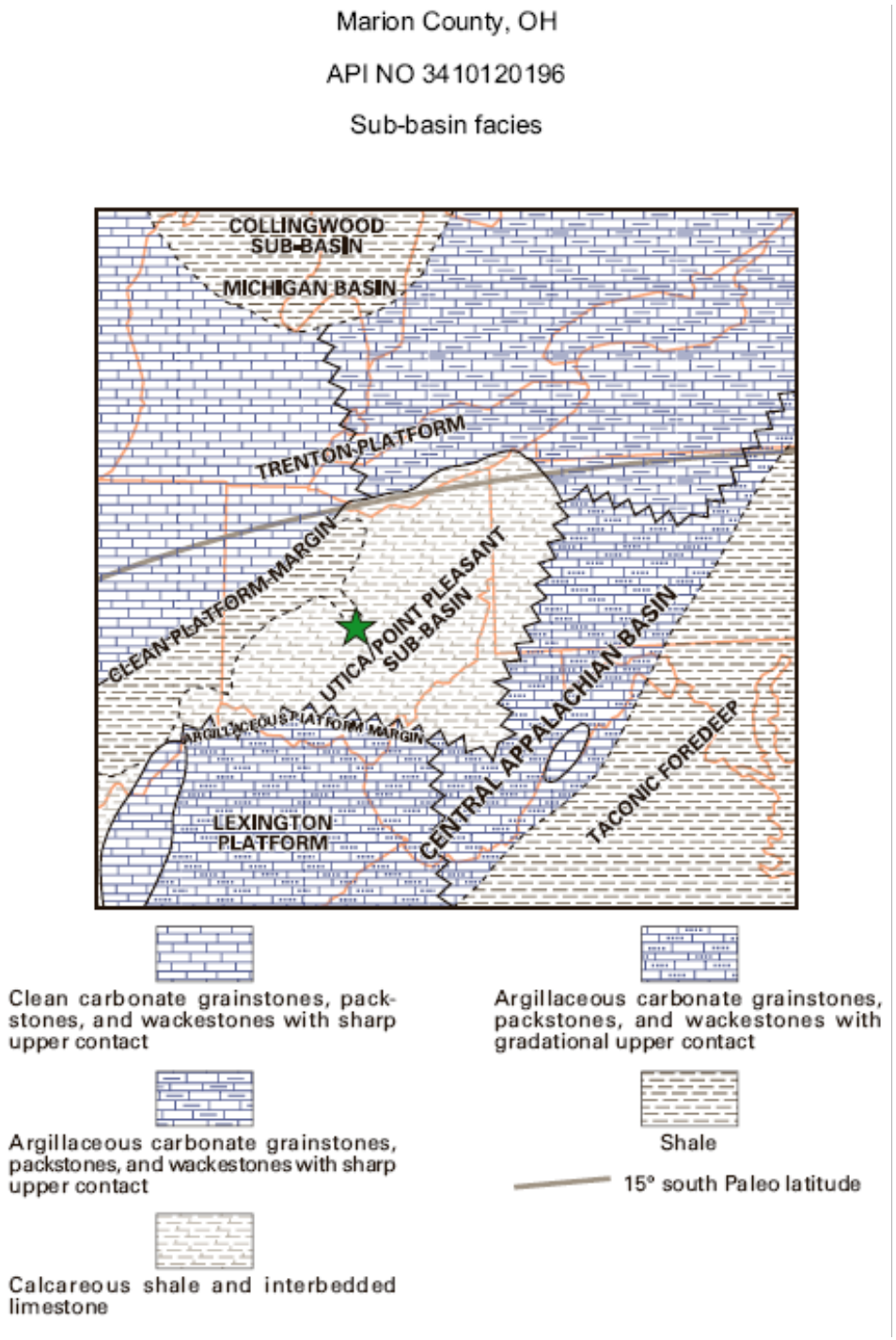

Figure 1-10. Representative well of the Utica/Point Pleasant sub-basin; Chevron, 1-A Prudential.

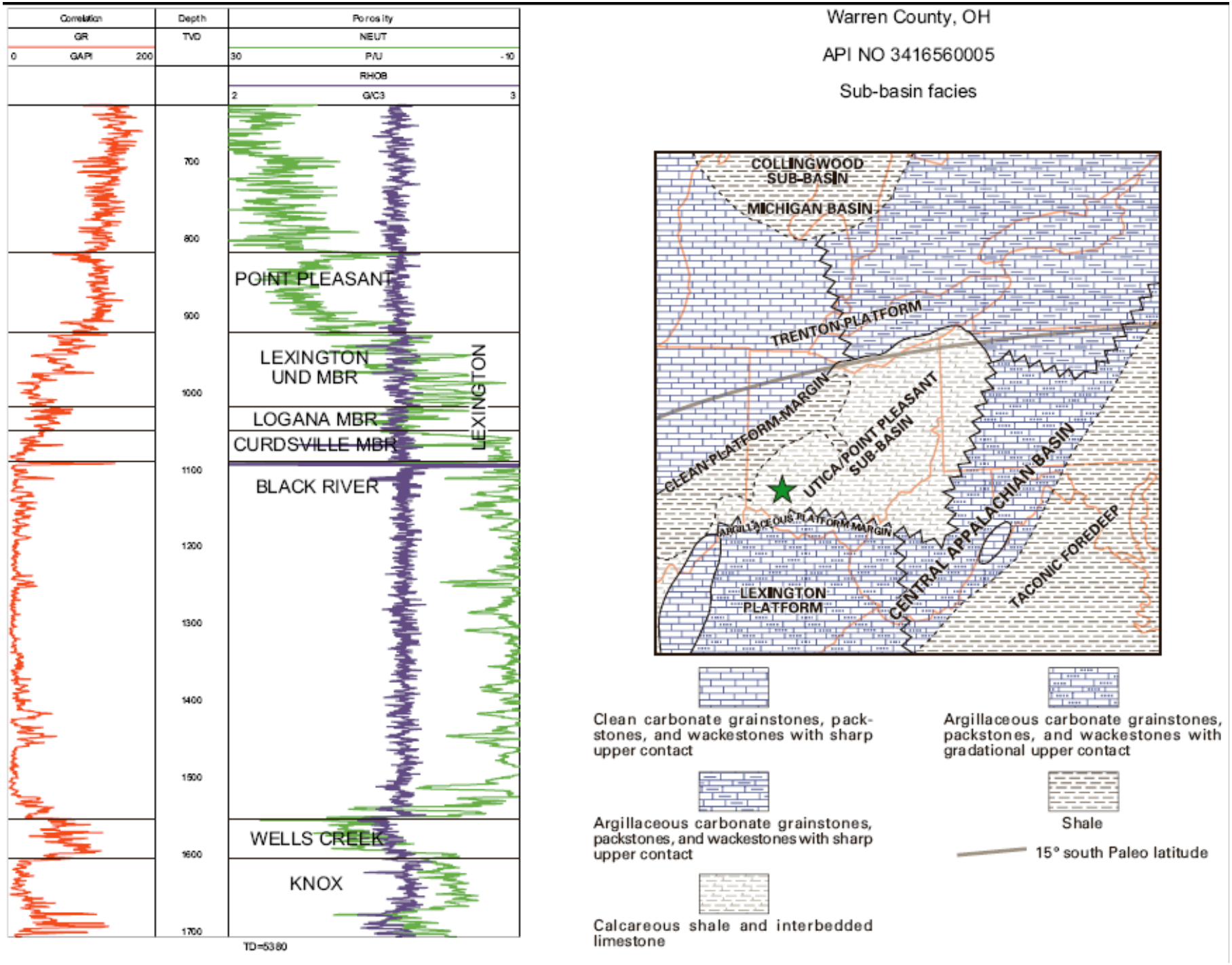

Figure 1-11. Representative well of the Utica/Point Pleasant sub-basin; Ohio Geological Survey, American Aggregates.

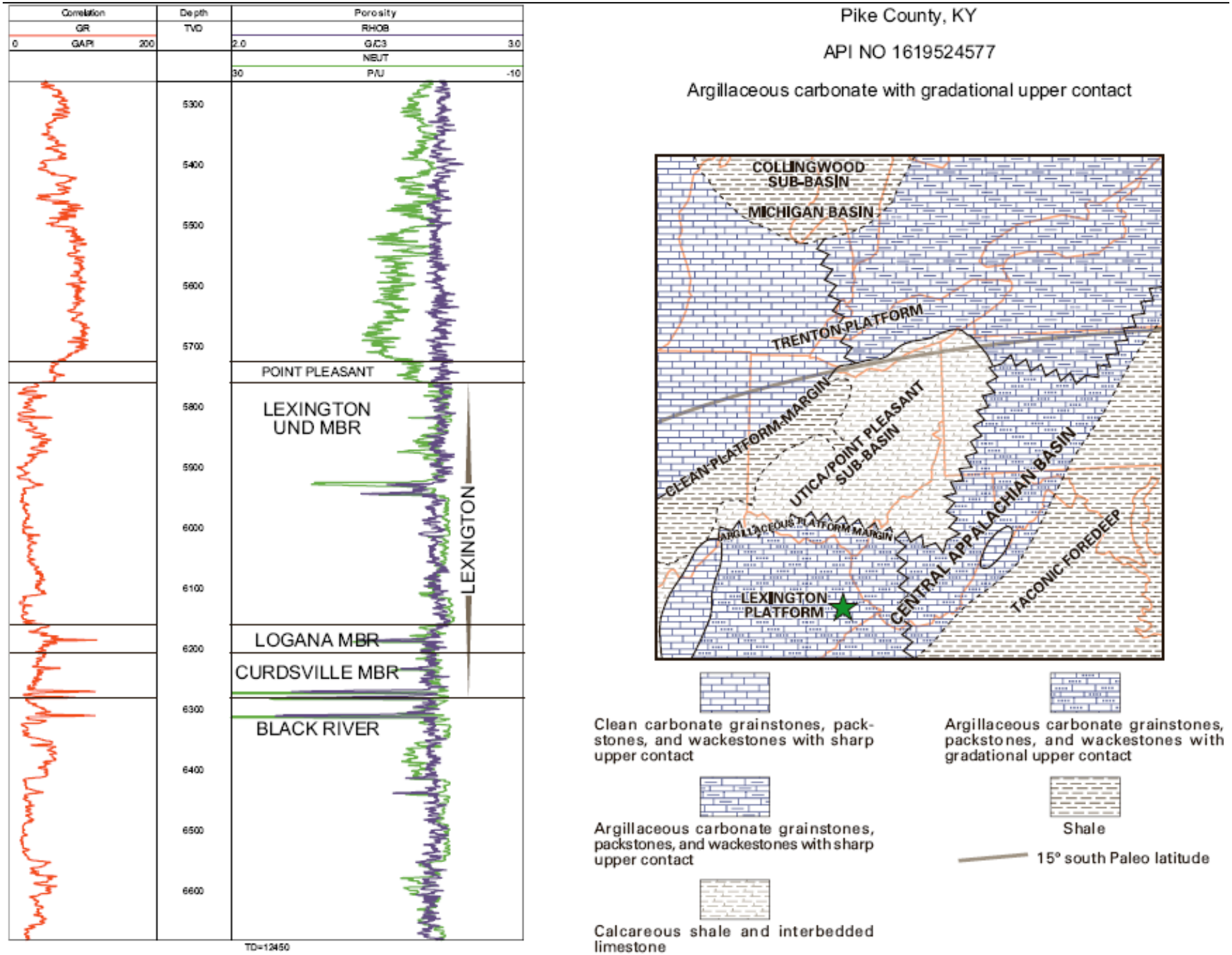

Figure 1-12. Representative well on the Lexington Platform; Signal Oil and Gas, Henry Stratton.

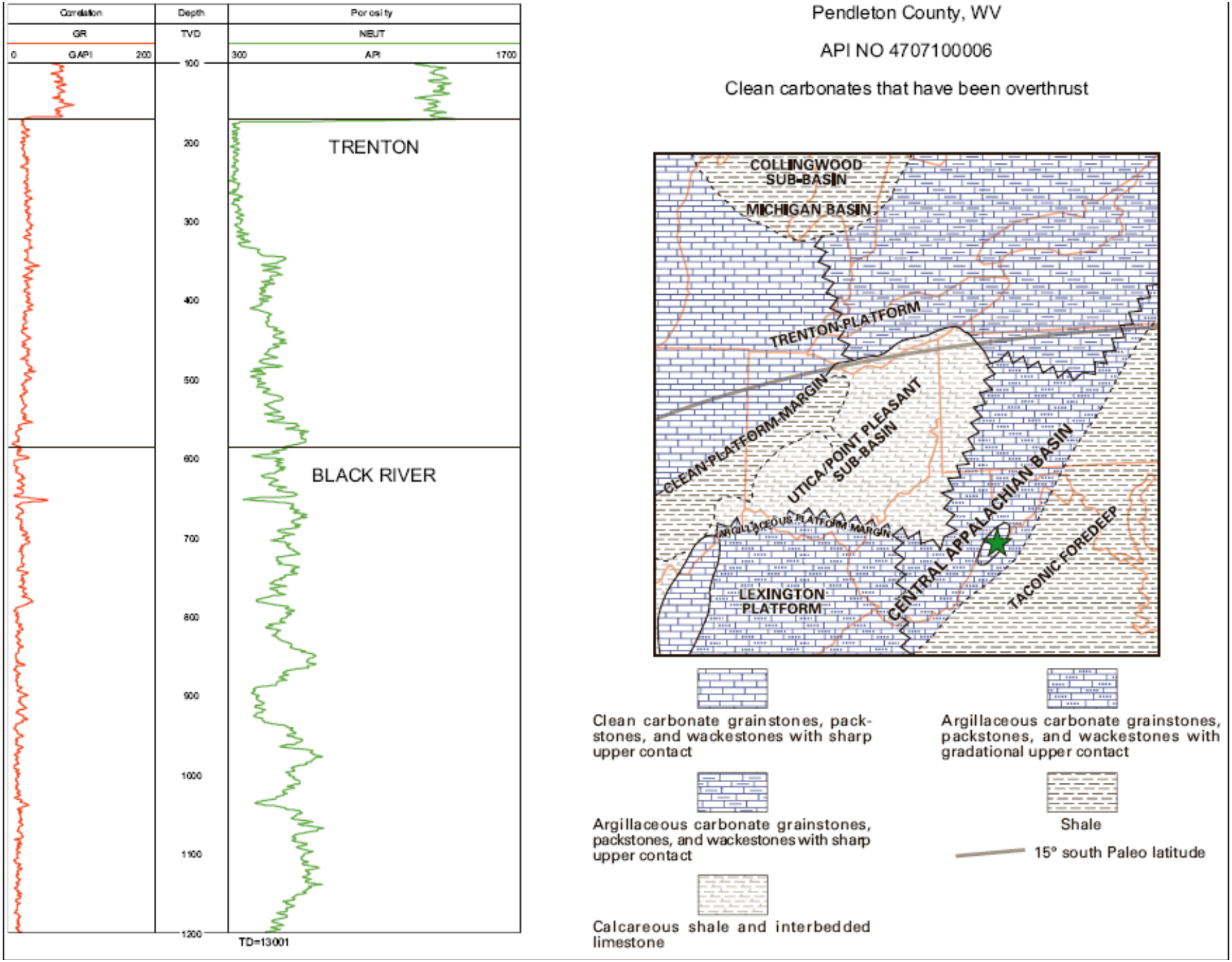

Figure 1-13. Representative well of a clean Trenton carbonate in the deeper basinal area; United Fuel Gas, 1 Sponaugle.

GEOLOGIC STRUCTURE AND SEISMIC ANALYSIS

By J.B. Hickman, D.C. Harris, J.A. Drahovzal and P.D. Lake, Kentucky Geological Survey

Introduction

Structural and seismic analyses were carried out to characterize the major geologic structures in the study area and to determine as closely as possible their timing relative to the fracturing, dolomitization and hydrocarbon charging of the Trenton-Black River interval. To accomplish this, well log tops, seismic, aeromagnetic and Bouger gravity anomaly data were used to map the structure of a series of horizons from the Precambrian unconformity to the base of the Devonian "black" shales. The interpretation also included the delineation of fault locations and major structural axes at the various horizons.

Data Compilation

Although less than originally anticipated, a considerable amount of 2-D seismic data was compiled for this project. Seismic data were solicited from the participating companies, but for a number of reasons, this was a difficult request for industry. Despite the problems with assembling the desired seismic database, more than 3,500 miles of Appalachian basin digital and paper reflection seismic data were compiled. Figure 2-1 displays the distribution of seismic data available for interpretation in the project. Table 2-1 lists the sources of this data from the geological surveys and the industrial partners.

Well data for the project were compiled from the databases of the five state geological surveys. Digitized geophysical well logs for 390 wells and stratigraphic well tops from 2064 wells were used for seismic correlation and structural analysis.

Company	**Results**
KY Geological Survey	Data covers much of Kentucky, West Virginia; some in Pennsylvania, New York; co-rights with USGS
New York State Museum	Western New York
PA Geological Survey	Western Pennsylvania
OH Geological Survey	Reprocessed COCORP lines OH-1, OH-2
Abarta	Three lines in central Kentucky
North Coast	Several lines in West Virginia
Talisman	3-D part Rochester Field, Ontario; 2-D data on New York/Pennsylvania border
Ultra	Limited data inspected in Pensylvania

Table 2-1. Seismic Data Contributors for the Trenton-Black River Consortium

The Study Area

The area of study is the broad, hydrocarbon-productive foreland Appalachian basin that lies between the Cincinnati-Ohio-Indiana Platform-Findlay-Algonquin arch complex in western Ohio, central Kentucky and central Tennessee and the structural Allegheny Front along the west edge of the Valley and Ridge Province. The Allegheny Front as defined here and by Rodgers (1970, Pl.1) extends from the Powell Valley anticline on the Pine Mountain block in southwestern Virginia, then along the St. Clair-Hunter Valley fault trend to the Willis Mountain anticline of West Virginia, Virginia, Maryland and Pennsylvania, and finally to the west side of the Nittany arch in central Pennsylvania. The basin lies south of the Canadian Shield and the Adirondack uplift in New York and Ontario. The extent of the study area as defined for this project is shown on Plate 2-1 and subsequent plates.

Approach and Methods

Data Loading

Digital seismic data (SEGY files) were loaded into Seismic-Micro Technology's Kingdom Suite software, and raster images of paper lines (TIF files) were loaded into the PetraSeis module of Geoplus Petra software platform for use in seismic interpretation. Digital geophysical logs from 390 wells were also loaded into Petra and Kingdom Suite software for use in making synthetic seismograms, calculating depth conversions, and for the identification of questionable seismic horizons.

Seismic/Acoustic Velocity Analysis

Before a basin-wide interpretation of stratigraphic horizons could be accomplished from reflection seismic data, reflectors observed within the seismic profiles have to be identified. In areas where wells with sonic logs exist within close proximity of seismic data, the creation of synthetic seismograms (capable through the use of numerous available petrophysical software programs) allows this correlation to be done fairly easily (see Figure 2-2). Unfortunately however, there are many areas within the Appalachian Basin where either no sonic logs are available, or those logs that were recorded do not cover the entire sedimentary section. To guarantee accurate horizon interpretation in these areas, a 16-layer velocity model was created in order to calculate the elevations of well tops in two-way-travel time (as opposed to feet subsea). These values were then compared to the nearby seismic data for stratigraphic correlation purposes. This additional step within the interpretation process functioned both as a quality check mechanism and to assist in the correlation of log tops to reflecting seismic horizons in areas with seismic data of poor quality.

To create this model, sonic logs from 107 wells throughout the 5-state project area were used to calculate average velocities within the numerous stratigraphic horizons. The boundaries between layers were chosen based on changes in sonic velocity across that stratigraphic top. This resulted in 16 packages of geologic units, grouped by their relative interval velocity. Analysis at a finer scale (e.g., a layer for every formation) would be of little use because a change in sonic velocity (either positive or negative) is required to produce a seismic reflection.

For each of the model layers, the average velocity within that layer was calculated from the sonic log with TerraStation™ petrophysical software at each well location that had a sonic log covering that interval.

These average sonic velocity values were taken at each well point, and then gridded into a continuous surface covering the project area. By using this gridding method, we could compensate for subtle lateral variations within the geological units. This is important for a project of this large of an area, as even the most homogenous geologic units change when viewed over 700 miles. These grids were edited as necessary in order to account for local geology or structures (unconformities, fault truncations, etc).

Once these 16 regional velocity grids were complete, the appropriate velocity values for wells without sonic logs could be determined for each layer. Using ArcGIS software, the velocity values of the grid cell that corresponded to the X/Y location for each well were sampled from the grid for 1508 wells within the project area. Then, using stratigraphic well tops and their corresponding layer velocities in a Microsoft Excel spreadsheet, a two-way-travel time was calculated for the top of each layer for each of these 1508 wells. This overall method proved quite productive, and yielded an average two-way-time error of less than 6%, based upon well data.

Seismic Interpretation and Mapping

Where possible, all of the horizons that were to be mapped (see below) were interpreted (where resolvable) on the seismic sections. Most of the other resolvable horizons were interpreted as well to aid in the basin-wide analysis.

Structure maps were created for the five-state study area for the following horizons:
Base of the Devonian “black” shales
Top of the Ordovician-aged section
Top of the Trenton Limestone
Top of the Black River Group
Top of the Knox Group
Base of the Knox Group
Top of the Precambrian igneous/metamorphic crystalline basement

Formation elevations from well data provided much of the data for these maps. However, the addition of horizon elevations interpreted from the 2-D reflection seismic profiles added not only to the overall data density, but also to information on regional dip trends, fault zone width and offset, and anticline/syncline axis magnitude and character.

Precambrian Basement Structure

The structure of the top of the Precambrian represents the configuration of the unconformable surface separating Paleozoic Cambrian rocks above from Precambrian Proterozoic rocks beneath (Plate 2-2). Despite differences in composition and age of the

Precambrian rocks below this unconformity, these rocks have been generally referred to as "basement rocks" and form the critical underpinning for the geology of the sedimentary rocks lying above (Figure 2-3).

Rocks below the Precambrian unconformity surface include metamorphic, igneous and sedimentary lithologies belonging to several different tectonic provinces. Rocks of the Grenville Province, lying east of a line extending from south-central Kentucky across western Ohio and into the easternmost part of Michigan, are composed of Middle Proterozoic metamorphic rocks with some igneous intrusions. The age of metamorphism for the Grenville Province rocks in the study area ranges from 1.1 to 0.880 Ga (Lidiak and others, 1966; Keller and others, 1983; Hoppe and others, 1983; Van Schmus and Hinze, 1985; Lucius and Von Frese, 1988; Drahovzal and others, 1992). Protolith ages of the Grenville rocks are, at least in part, much older ~ 1.457 Ga (Hoppe and others, 1983).

Grenville Province strata were thrust (from present-day east-southeast towards the west-northwest) over other Precambrian terrains during the Grenville Orogeny (Green and others, 1988; Pratt and others, 1989; Culotta and others, 1990, Drahovzal and others, 1992; Stark, 1997; Dean and Baranoski, 2002a, b). This continent-continent collision is thought to have created a large mountain chain that was mostly eroded during the following prolonged Precambrian exposure, which created the vast unconformity as mapped today. The westernmost limit of Grenville Province rocks (at the suture line with provinces to the west) is called the Grenville Front (Figure 2-3). Rocks of the East Continent Rift Basin, the Granite-Rhyolite Province, Penokean Province and the Midcontinent Rift System occur west of the Grenville Front.

The Eastern Granite-Rhyolite Province is a vast expanse of Precambrian terrain that consists of various Middle Proterozoic unmetamorphosed igneous and dominantly felsic volcanic rocks. Age-dating of rocks from this province indicate that they are of a similar age to the Grenville protoliths, ranging in age from 1.48-1.45 Ga (Lidak and Zietz, 1976; Hoppe and others, 1983; Denison and others, 1984; Bickford and other, 1986).

The East Continent Rift Basin (ECRB) is a recently defined, Middle to Late (?) Proterozoic province of rocks lying west of (and partially buried beneath) the Grenville Front. This region of the Precambrian is characterized by abundant sedimentary rocks interbedded with felsic and mafic volcanic rocks (Shrake and others, 1990; Drahovzal and others, 1992; Wickstrom and others, 1992a). The thick sedimentary and volcanic rocks of this interval that have been encountered by drilling consist primarily of lithic arenites and basalts that are thought to range in age from ≥1.5 to 0.6(?) Ga (Drahovzal and others, 1992; Drahovzal, 1997; Santos and others, 2002; Stark, 1997; Drahovzal and Harris, 2004).

East of the study area, Precambrian rocks are exposed in the Blue Ridge where Grenville and Piedmont metamorphic rocks are exposed in the westward-thrusted blocks of the Appalachian Mountains. The top of basement ranges from the surface in outcrops within the Upper Peninsula of Michigan and the Appalachian Blue Ridge to depths greater than a speculated 43,000 feet subsea in southeastern Pennsylvania, east of the Allegheny Front (Shumaker, 1996). The deepest mapped area within our study area west of the Allegheny Front

is in east-central Pennsylvania where basement is interpreted from seismic data to be up to 30,000 feet below sea level.

The shallowest basement in the study area occurs along the Cincinnati arch in west-central Ohio and north central Kentucky. Basement here lies at less than 2,000 feet below sea level. The Cincinnati arch extends from central Tennessee to west-central Ohio where it joins the Findlay/Algonquin arch, separating the Appalachian basin from the Illinois basin. At this point the arch curves northeast into Canada and separates the Appalachian basin from the Michigan basin. Throughout the subsidence of the surrounding basins, the Cincinnati-Findlay-Algonquin arch complex remained relatively stable, or subsided at a slower rate. Therefore, the structural relief of the arches is thought to be mostly the result of differential subsidence with occasional tectonic arching rather than that of overall uplift (Wickstrom and others, 1992b). However, it should be pointed out that the majority of the subsidence of the surrounding basins occurred in the Silurian and later, and that the structural surface of the top of the Precambrian as mapped (Plate 2-2) represents its present-day configuration. The major sedimentary basins, as we know them today, were not present during the Precambrian or during much of the Paleozoic Era.

Reactivated basement faults cut the Cincinnati arch, Ohio-Indiana platform, and Findlay arch complex in a few places. These include the Grenville Front fault (reactivated suture) that extends from south-central Kentucky north to eastern Michigan. In northern Ohio and southern Michigan this fault system is well documented as the north-south trending Bowling Green fault system, which is exposed at the surface. To the south in west-central Ohio, there are no faults exposed at the surface and little well control, and as a result the extent of the Paleozoic movement is unknown and the location of the basement fault is imprecise, being based largely on potential field data (Lidiak and Zietz, 1976; Mayhew and others, 1982; Denison and others, 1984; Lidiak and others, 1985). Further south, the Grenville Front is once again expressed at the surface by a major fault system, the Lexington fault system in central Kentucky. Several minor northwest-oriented faults cut the Ohio-Indiana platform in west-central Ohio.

Much of the basement configuration for Ohio is based on oil and gas well data. These data have been supplemented in this project by about 600 miles of reflection seismic data. To the east of the Cincinnati-Findlay arch in Ohio is the Appalachian basin. Several minor, northwest-trending faults cut the southeast flank of the Findlay arch in northeastern Ohio and northwestern Pennsylvania. Across much of the area in central and eastern Ohio, the basement structure is a gentle (about 1 degree) east-southeast dipping monocline that increases slightly in dip in eastern Ohio. This surface has been interrupted in places by local changes in dip that have been interpreted as basement faults like those associated with the Cambridge arch, the Cow Run anticline and the Burning Springs anticline in southeastern Ohio (Baranoski, 2002) and westrn West Virginia. Baranoski (2002) interpreted these anticlines as forming during the Alleghany orogeny.

To the east and northeast in Pennsylvania and New York, there are a number of long, normal faults that are parallel to subparallel to regional strike. These faults generally exhibit offsets of less than 500 feet, are usually down-to-the-south and are offset by northwest-oriented lineaments that have been interpreted as faults with offsets ranging from 0 to 2,500 feet

(Wickstrom and others, 2005). The results of this study, however, indicate that the vertical offset across the northwest-oriented faults range from 0 to generally less than 500 feet. This fault complex offsets a gently-dipping monocline that also is cut by down-to-southeast and a few down-to-northwest normal faults that extend along and subparallel to strike. The overall strike of the monocline rotates from southeast-dipping to south-dipping in eastern Pennsylvania and New York. The Precambrian unconformity surface ranges from 0 feet subsea in northern New York to 30,000 feet subsea in east-central Pennsylvania at the edge of the Allegheny Front. Details of the basement geology of Pennsylvania can be found in Saylor (1999) and Alexander and others (2005). The results of this study coincide fairly closely with basement configuration and depth shown by Saylor (1999).

One of the most striking features in the basement of the Appalachian basin is the Rome trough. The Rome trough is a complex graben that extends from just west of the Lexington fault system in central Kentucky to north-central Pennsylvania and possibly into southern New York (Woodward, 1961; McGuire and Howell, 1963; Harris 1975; Wagner, 1976; Cardwell, 1977; Beardsley and Cable, 1983; Shumaker, 1986, 1996; Harper, 1989; Drahovzal and Noger, 1995; Wilson, 2000, Gao and others, 2000; and Harris and others, 2004). The trough is the result of a Cambrian rifting event that down-dropped basement rocks and resulted in syntectonic sedimentation during Early to Late Cambrian time (Ryder, 1992; Harris and Drahovzal, 1996; Harris and others, 2004). The complexly-faulted nature of the Rome trough in eastern Kentucky has been interpreted from a relatively large number of basement tests that have been integrated with available seismic data, and from the surface geology. Fewer well data and surface geologic expression are present farther to the northeast across West Virginia and Pennsylvania so that graben geometry relies more on available seismic data in that region.

In Kentucky, the Rome trough is an east-northeast oriented basin with structural relief on the basement that is as much as 12,500 feet from the northern boundary just north of the Kentucky River fault zone in Elliot County, Kentucky at ~4,500 feet below sea level, down dip (13 mi SSE) to >17,000 feet below sea level in Johnson County, Kentucky. On the north and higher side, the graben is a marked by two, gently-dipping platforms that are bounded by down-to-south normal faults, including two major fault zones—the north bounding Kentucky River and the medial Irvine-Paint Creek fault zone. Bounding the trough to the south is the down-to-north Rockcastle River fault zone. Locally, in Clay County, Kentucky, basement offset along the Rockcastle River fault zone is as much as 4,000 feet. Here some of that relief was formed by later Alleghanian reverse movement that further lifted the southern block relative to the northern block (Figure 2-4). Basement is lowered as much as 4,500 feet locally across the medial Irvine-Paint Creek fault system where later reactivation by Alleghanian contraction caused local uplift and inversion (Figure 2-5). Overall, the graben generally deepens to the south and east ranging from about 5,000 to 7,500 feet below sea level along the Grenville Front to more than 17,000 feet deep near the Kentucky/West Virginia state line.

The basement faulting patterns and style of the Rome trough change from Kentucky to West Virginia. In Kentucky, the major syntectonic faulting occurs on the northern boundaries of two sub-grabens, one north and one to the south of the Irvine-Paint Creek fault system. In southern West Virginia, however, the faulting patterns change so that the majority of the vertical offset at the top of the Precambrian is to the south. As the trough extends to the northeast into

central and northern West Virginia, the offset on the northwest side of the trough (Ohio River fault) lessens to the point that it becomes what many researchers have called the "Ohio-West Virginia hinge zone" (Ryder and others, 1992; Harris and others, 2004). Along the state line, a southeast-dipping half graben with thickened Cambrian sediments to the southeast formed. The half graben is bounded on the southeast by a single, steep, down-to-the-northwest syntectonic normal fault system called the East-Margin fault (Shumaker, 1993). Smaller down-to-the southeast normal faults offset basement northwest of the boundary fault. Basement offset along the East-Margin fault in southwestern West Virginia near the Kentucky line is greater than any part of the trough, ranging from 7,000 to more than 11,500 feet based on seismic interpretations of this study and that of Wickstrom and others (2005). Top of basement is estimated to be 17,000 to 23,500 feet subsea. Along the northwest edge, the half graben shallows to 10,000 to12,000 feet subsea.

Gao and others (2000) suggest that there are three separate sections of the trough in Kentucky and West Virginia that are separated by two basement structures. These structures have been interpreted as two accommodation zones extending along the 38th Parallel and the Burning–Mann lineaments. The same general structure as in the northern segment of West Virginia appears to continue into southwestern Pennsylvania at least as far north as the Pittsburgh-Washington lineament (Lavin and others, 1982; Parrish and Lavin, 1982; Alexander and others, 2005).

North of the Pittsburgh-Washington lineament in west-central Pennsylvania, the structural character of the basement changes to a wide monocline that is bounded on the northwest by a major down-to-southeast normal growth fault and a series shorter, down-to-southeast dipping normal faults. Offsets across the lineaments are less than 500 feet, similar to that of Saylor (1999). Offsets across the down-to-southeast faults are generally less than 500 feet. The presence of the Rome trough north of the Pittsburgh-Washington lineament is equivocal, but it has been postulated by a number of workers (Harris, 1975; Wagner, 1976; Shumaker, 1986, 1996; Harper, 1989; Stark, 1997a; Jacobi and others, 2004) to extend into or nearly to New York state. Beardsley and Cable (1983, figure 5a) interpret the presence of the Rome trough in northern Pennsylvania near the New York line along a seismic profile that shows growth in the Cambrian section. Although the pre-Knox section does thicken to the southeast, no other clear growth faulting is seen in the Cambrian rocks of Pennsylvania based on the seismic available in the study. Displacements along these faults are considerably smaller that the equivalent faults in Kentucky and West Virginia, with offsets at the top of Precambrian ranging from around 500 to 1,000 feet.

Tectonic History of the Region

Extension during the Middle Cambrian (Ryder, 1992) deformed the Precambrian and Lower Cambrian rocks in the study area. The faulting associated with this lithospheric extension created the Rome trough in Kentucky, West Virginia and Pennsylvania. The trough has been interpreted as a part of a larger network of extensional systems that extend from central Pennsylvania to Oklahoma that formed during the opening of the Early Paleozoic Iapetus Ocean and the breakup of the continent of Rodinia (Thomas, 1991).

Initial sedimentation into this rift during the Early Cambrian was transgressive across a tectonically quiet area. Substantial faulting was initiated during the Middle Cambrian when syndepositional faults resulted in thicker sediments and basin-floor fans on the downthrown blocks (Ryder, 1992; Harris and Drahovzal, 1996). The mixed carbonates and clastics of the Rome Formation and Conasauga Group to the southwest, grading into the predominantly carbonate Elbrook Formation to the northeast were deposited within this rift during the Middle to earliest Late Cambrian. The uppermost members of these strata also were deposited outside of the rift, but not nearly to the same thickness as those rocks within it.

By the end of the Dresbachian Age, the tectonic extension and associated syndepositional faulting had ended. Other than some slight thickening over the trough that can be attributed to sagging from post-depositional compaction of the earlier strata, the region appears to have been tectonically stable and undeformed until near the end of the Middle Ordovician. Evidence in the sedimentary record from this period suggest that the far-field stresses from the collision of an island arc with the eastern margin (present day direction) of Laurentia were deforming the interior of the craton. This deformation is expressed in soft sediment deformation features (seismites) in and around the Jessamine Dome in central Kentucky (Ettensohn, et al., 2002). As the eastward dipping subduction/collision zone approached, vertical loading of the Laurentian plate created a foreland basin, introducing increasing amounts of deepwater clastic facies into the eastern portion of the study area. This arc collision continued through the Late Ordovician and into the Early Silurian, becoming the Taconic orogeny (Ettensohn, and Brett, 2002).

Synorogenic clastic wedges from the Taconic orogeny can be found from northern Georgia all the way to Newfoundland, Canada. Based on the thickness and distribution of these wedges, a major component of the collision appears be centered near (present day) eastern Pennsylvania and southeastern New York (Thomas, 2005; Smith, in press). Because the fault offsets observed on seismic data within producing Trenton-Black River hydrothermal dolomite/fractured limestone oil and gas fields in New York, Pennsylvania and West Virginia decrease to zero within the Upper Ordovician to Lower Silurian strata, tectonic compression from the Taconic orogeny is the most likely cause of these faults. This hypothesis is further supported by the proximity of the eastern Pennsylvania/southeastern New York collision point of the volcanic arc.

The region experienced another period of tectonic quiescence during the Late Silurian, and is characterized by abundant regional carbonate deposition. Then, during the Devonian to Early Mississippian Periods the eastern margin of the continent underwent another collisional orogeny, the Acadian. Contrary to the wide extent of the Taconic, this event affected mostly the central to northern Appalachians. This was quickly followed by the Alleghanian orogeny during the Late Mississippian to Permian Periods. The deformation associated with the Alleghanian is predominantly in the central and southern Appalachians.

In addition to the examples given above with regard to fault movement during the Appalachian orogenies, there are numerous examples in Kentucky, West Virginia and Pennsylvania of reactivated basement faults causing local inversion structures within the younger strata. The shallow folding in the Pennsylvanian rocks in figures 2-4 and 2-5 were created

during a period of contraction associated with the Alleghany orogeny (Drahovzal and White, 2002). Gao and others (2000), however, suggest that some of the similar inversion structures observed to the northeast in West Virginia may have been attributable to the Taconic and Acadian orogenies as well as the Alleghany (though no direct evidence was provided). Wilson (2000) suggested that there may have been inversion during the Late Devonian based on thinning of the interval between the Devonian Onondaga and the Mississippian Greenbrier reflectors on seismic data, but also suggested that the thinning could have been the result of detachment and thickening of the section east of the Rome trough (Shumaker and Wilson, 1996). Shumaker (1996) observed inverted structures from the Trenton Limestone up through the Devonian Huron Shale above the East-Margin fault in central West Virginia on seismic data, but did not attribute it to any particular orogenic event.

Discussion

Fault-Related Dolomitization and Hydrocarbon Production

In Kentucky, oil-stained Trenton dolostone bodies are often associated with northwest-oriented faults. The northwest-oriented, Eagle Nest fault complex (Black, 1974; Black and Haney, 1975) in the northwestern part of the Rome trough at the intersection with the Kentucky River fault zone is the location of the Ordovician Stoner Branch dolostone body (Harris, 2002; Harris and Wilcox, 2005). This fault complex and the oil-bearing dolostone body are exposed just south of the Kentucky River fault zone in Clark County. The dolostone body is equivalent to the Calloway Creek Limestone and the Garrard Siltstone. Nearby, a small dolostone body called the "light bulb structure" also is exposed just north of the Kentucky River fault zone, along northwest-oriented faults and is oil-bearing (Richard Beardsley, personal communication, 2000). This dolostone body is within the Trenton (Lexington Limestone, locally).

The Raccoon Mountain field on the Rockcastle River uplift in Laurel and Clay counties, on the south side of the Rockcastle River fault zone has produced oil and gas from the Black River/High Bridge Group. The field is adjacent to a possible northwest-oriented cross fault proposed by Drahovzal and Noger (1995), based upon younger structures at the surface. The nature of the cross fault is unknown but is speculated to have a wrench component (Drahovzal and Noger, 1995). Probable dolomite has been indicated on the porosity log in the Atlantic Gas #1 McFadden well (Harris, 2001) within this field, and produced 15 Mcfpd of gas from an open hole completion. The bounding Rockcastle River fault zone has been interpreted as a basement-rooted normal fault that was later reactivated into Alleghanian wrench fault.

To the northeast in Lee County, the Ashland #1 Combs well encountered about 5 feet of dolomite as indicated by the PE log in the Black River/High Bridge Group (Harris, 2001). The well produced 207 Mcfpd of gas and lies adjacent to a northwest-oriented basement fault near its intersection with a northeast-oriented basement fault on the Precambrian map (Plate 2-2). These faults lie just south of the Irvine-Paint Creek Fault Zone.

To the northeast in western Johnson County, the Black River/High Bridge Group is productive in the Minefork field. Here the neutron porosity log appears to indicate fractures in

the Ashland #1 Conley well, rather than dolomite. This fractured limestone reservoir produced 226 BOPD from two zones (Harris, 2001). The well lies adjacent to a major north-south fault with basement offset up to 4,500 feet that is associated with the north-south Paint Creek Uplift (shown near the center of Figure 2-7).

All of the oil- and gas-bearing Black River formations in Kentucky are associated with reactivated basement faults associated with at least some component of Alleghanian structural movement. This is in contrast to the Trenton-Black River dolostones farther north in New York and Pennsylvania that appear to be associated with Late Ordovician Taconic tectonics.

Styles and Timing of Basement Faulting

Past exploration for Trenton-Black River hydrocarbons has shown that basement faulting (often with a wrench component), structural sags and hydrothermal dolomite within the Trenton and Black River carbonates can indicate the presence of a potential reservoir. One of the major objectives of this task was to map the basement faults within the Appalachian basin.

The structure of the basement, in particular, has in many cases influenced the subsequent structural history of the overlying Paleozoic rocks. In many cases, major basement faults were reactivated by later orogenic movement to fault the younger overlying rocks. Other basement faults show little or no reactivation and exhibit no shallow expression in Paleozoic rocks. Still other faults in Paleozoic rocks apparently have no basement roots, being solely the result of shallow tectonics. Careful study is required when assessing the faulting in a region to distinguish these three types of faults and their subsequent potential influence on the emplacement of dolomitizing fluids.

Numerous basement faults exist in New York state; however, the well and reflection seismic data show very little or no evidence of Cambrian syntectonic sedimentation. In contrast, Pennsylvania has areas with basement offset and syntectonic sedimentation (Figure 2-10), although not to the same degree as seen in the Rome trough in Kentucky and West Virginia (Figures 2-6 to 2-9).

It is important to note that in Pennsylvania, basement faults seem to have played an important role in the location of the overlying salt tectonic décollement thrusts within the Silurian section (see Figure 2-10). Therefore, surface antiforms and thrusts may help locate basement faults of a certain age. How some basement faults with mostly Cambrian offsets affected the locations of later salt tectonics is not clear, especially because not all basement faults lie under Silurian or later thrusts. Analysis of seismic data and isopach maps of the stratigraphic layers help identify which of these surface structures are indeed indicative of the type of underlying reactivated basement faults associated with possible Trenton-Black River reservoirs.

As mentioned previously in this report, the producing Trenton-Black River fields in New York and northern Pennsylvania appear to be centered on reactivated basement faults that propagated up to the top of the Trenton or just into the overlying Utica Shale. Because these faults did not propagate or otherwise deform any strata younger than the Late Ordovician at these

locations, it can be inferred that these faults were reactivated during the Taconic orogeny *but not* in the later Acadian and Alleghanian orogenies.

Because all three of these events affected the region, why did these faults not get reactivated again? One possibility is that it was due to the change of dominant lithologies over time. At the time of the Taconic orogeny, the bulk of the strata in what would become the eastern Appalachian basin consisted of massive carbonates (Cambrian Elbrook Formation, Early Ordovician Knox Group, and the Middle Ordovician Black River and Trenton limestones) along with the igneous/metamorphic basement. Limestones, dolomites and these basement rocks are relatively strong, allowing large amounts of tectonic force to be transferred laterally over great distances. This rigid strength also tends to make these types of rocks deform in a brittle fashion. By the time of the Acadian and Alleghanian orogenies, the amount of clastics within the basin (especially shales and Silurian evaporites) had increased dramatically. Although there are limestones, dolomites and quartz arenite sandstone beds in the post-Silurian section, they are relatively thin and often interbedded with shales. These weaker, more ductile units are more apt to either deform in place or to form décollement zones that propagate towards the surface (as opposed to transferring the forces laterally). This would lead to more folding, thrusting and other "thin-skinned" types or regional deformation. This type of deformation is fairly dominant to the east nearer the collision zone, but dies out before reaching the central portion of New York where the Trenton-Black River production exists today.

Another probable reason that only certain basement faults were reactivated to create Trenton-Black River hydrothermal dolomite reservoirs is that only some were oriented in a favorable direction for reactivation. Although faults oriented perpendicular to the primary tectonic force (σ_1) could be reactivated, the associated compression would tend to destroy porosity and permeability. Without this "open" path for deep hydrothermal fluids (not to mention hydrocarbons) to migrate through, no reservoir would be created.

However, if the preexisting basement fault (or even just a segment along one) was oriented so that the regional tectonic forces produced local transtension, this could reactivate the fault in such a way that the permeability of the fault zone could be preserved, paving the way for hydrothermal fluid intrusion. In several cases in New York, at least, this seems to be what has happened, as evidenced by the presence of en echelon sags and "negative flower" structures on seismic over Trenton-Black River fields (Figure 2-11). A similar interpretation has been given for the structure of the Ordovician Albion-Scipio field in southern Michigan (Harding, 1974). The Lima-Indiana trend in northwest Ohio may be the exception, because it is oriented perpendicular to Taconic compression.

Determining the Source of the Dolomitizing Fluids

One of the unknowns about the development of the productive dolomitized zones within the Trenton and Black River (TBR) units of the Appalachian Basin is the source and timing of the dolomitizing fluids. Where did these magnesium-rich fluids come from, and how were they heated to "hydrothermal" levels?

Numerous lines of evidence suggest that these fluids migrated along basement-rooted faults. Because in many, if not most, cases these faults terminate in the strata just above the Trenton Limestone, these fluids probably did not migrate downward from a higher source. Instead, the high magnesium levels within the fluid that was needed to dolomitize large portions of the Ordovician limestone units must have come from a deeper source.

No evidence has been found that suggests extensive leaching of the dolomites within the Knox Group. Therefore, the likely source of magnesium is even deeper, from the igneous and metamorphic rocks of the Precambrian Grenville "basement". This also would explain the occurrence of other non-magnesium metal ions observed within the hydrothermal dolomites. Within a cored fault zone in central Kentucky, sphalerite, barite and pyrite were reported (Harris, et al., 2004) in the hydrothermal dolomites within the Upper Ordovician section. All of this suggests that the heated brines that formed the dolomite had spent a considerable time in close contact with either basement rocks, or within the relatively immaturely-weathered basal sandstones derived from the basement.

Determining the Source of the Elevated Temperatures

Stratigraphic data suggest that the Trenton was faulted and dolomitized by Late Ordovician time in the northern part of the study area. In Kentucky, however, evidence for Late Ordovician timing is less clear as many of the faults were reactivated during the Alleghanian Orogeny. At the end of the Ordovician, the depth to the Precambrian was roughly 1250m in New York, and 1600m in Kentucky. If we assume from the analysis above that the fluids came from the basement, they would have to have originated from at least this depth. Because igneous and metamorphic rocks tend to have close to 0% porosity, it is reasonable to assume that the large volume of fluid needed to create the amount of dolomite observed probably came from within the upper, weathered portion of the basement or within the overlying basal sandstones. It is unlikely that the aperture of the fault itself could contain sufficient volumes, especially with the increasing pressure at depth.

If we assume a high surface temperature of 28°C and a high geothermal gradient of 30°C/km, the expected ambient temperatures within the upper portion of the Precambrian during the Late Ordovician would be around 76°C for Kentucky and 65°C for New York. However, fluid inclusion data from TBR dolomites in central Kentucky and western New York indicate that the dolomitizing fluids were at much higher temperatures. The homogenization temperatures for these inclusions were 104°C for central Kentucky and 140°C for the New York samples. If a pressure correction is applied to these values to account for the depth of burial, these values increase even further. The values rise to 110-122°C for Kentucky, depending on whether you assume a hydrostatic or a lithostatic pressure gradient. The calculation of the pressure corrected values for the New York samples was not complete at the time of this writing.

What is the source of this extra 35-45°C for Kentucky and 75+°C (uncorrected) for New York Ordovician dolomites? Possible additional heat sources that have been suggested include deep-seated (upper mantle) fault fluids, volcanics or pluton emplacement, an anomalous "thermal pulse" from within the mantle, or co-seismic frictional heating.

If the assumption that dolomitization occurred during the Late Ordovician is correct, then excess heat from emplacement of igneous plutons is unlikely. Hydrothermal dolomites have been documented in an area that extends from eastern Tennessee to southern Ontario. The likelihood of a continent-scale volcanic event occurring over this broad area without having any igneous rocks observed above the Precambrian unconformity seems quite remote. Similar evidence of a mantle derived "thermal pulse" during this period has not been documented, either.

Using deep-seated fault fluids as both a source of excess heat and for magnesium content is an attractive option, but the ability of that type of hydrothermal system to generate the volumes of fluids needed is questionable, but not impossible.

The last hypothesis for a Late Ordovician heat source is co-seismic frictional heating. In this scenario, earthquake motions along wrench faults create frictional heat within and immediately adjacent to the fault zone. Pore fluid within this area is heated by conduction and expands, rising rapidly up newly-formed fault conduits (direction of lowest pressure). Repeated faulting episodes are needed to achieve the required fluid volume, but this scenario works well with the "fault-valve" model of Sibson and Rowland (2003). In this model, fault conduits are periodically plugged by precipitated minerals from hydrothermal fluids. After being plugged, fluid pressures and temperatures rise below the fault blockage until another earthquake ruptures the fault-sealing plug of minerals. Once this is breached, fluids expand rapidly up the fault conduit which lowers the pressure (and therefore temperature) at depth. At these lower pressures and temperatures, minerals precipitate out of the fluids until the fault is plugged once again. Repeated episodes of this type create a "pump valve" affect for the hydrothermal fluids. More work is needed to evaluate this scenario to determine if it is applicable to the TBR dolomites.

Unfortunately, data suggesting Late Ordovician HTD emplacement are somewhat circumstantial. There is evidence of fault movement during this period (from localized thickening of Upper Ordovician shales above reactivated faults from increased accommodation space), and the assumption is made that the dolomitizing fluids probably migrated at the same time. If fluid migration and dolomitization of these rocks occurred after the Ordovician Period, then other scenarios are possible. It is possible that the faulting occurred during the Taconic Orogeny, but that the dolomitizing fluids migrated to the Trenton-Black River later, during the Acadian Orogeny. With more sediments deposited on top of the Ordovician section, depth of burial of the Precambrian basement would be greater. This would in turn cause the ambient temperatures to be higher as well, reducing the need for an additional heat source. In addition, there is evidence of a Middle Devonian "thermal event" which has been interpreted from illite-based Rb/Sr data. This also may coincide with volcanic intrusives within New York, adding an additional possible heat source for the hydrothermal fluids.

Structural Conclusions

1) The reactivation of basement faults plays an integral part in the creation of Trenton-Black River fractured limestone/hydrothermal dolomite reservoirs in the Appalachian basin.

2) Primarily, only appropriately-oriented faults within the Precambrian basement were reactivated to create Trenton-Black River HTD reservoirs.

3) These features have subtle seismic signatures, which complicate interpretations and illustrate the need for high-resolution seismic data. This complexity also suggests that 3D seismic is required for appropriate exploitation of discovered fields.

4) Areas where reactivated faults breached the overlying Upper Ordovician shales may be dry due to leakage, not due to a lack of hydrocarbon charge or source-to-trap migration pathways.

See Plates 2-1 through 2-8 for additional information on the regional structures and stratigraphic depths of units studied within this project.

Plate Number	**Contents**
Plate 2-1	Structural features map of region
Plate 2-2	Structure of the Top of the Precambrian section
Plate 2-3	Structure of the Base of the Knox Supergroup
Plate 2-4	Structure of the Top of the Knox Supergroup
Plate 2-5	Structure of the Top of the Black River Limestone
Plate 2-6	Structure of the Top of the Trenton Limestone
Plate 2-7	Structure of the Top of the Ordovician section
Plate 2-8	Structure of the Base of the Devonian Shale section

Table 2-2. List of included Plates.

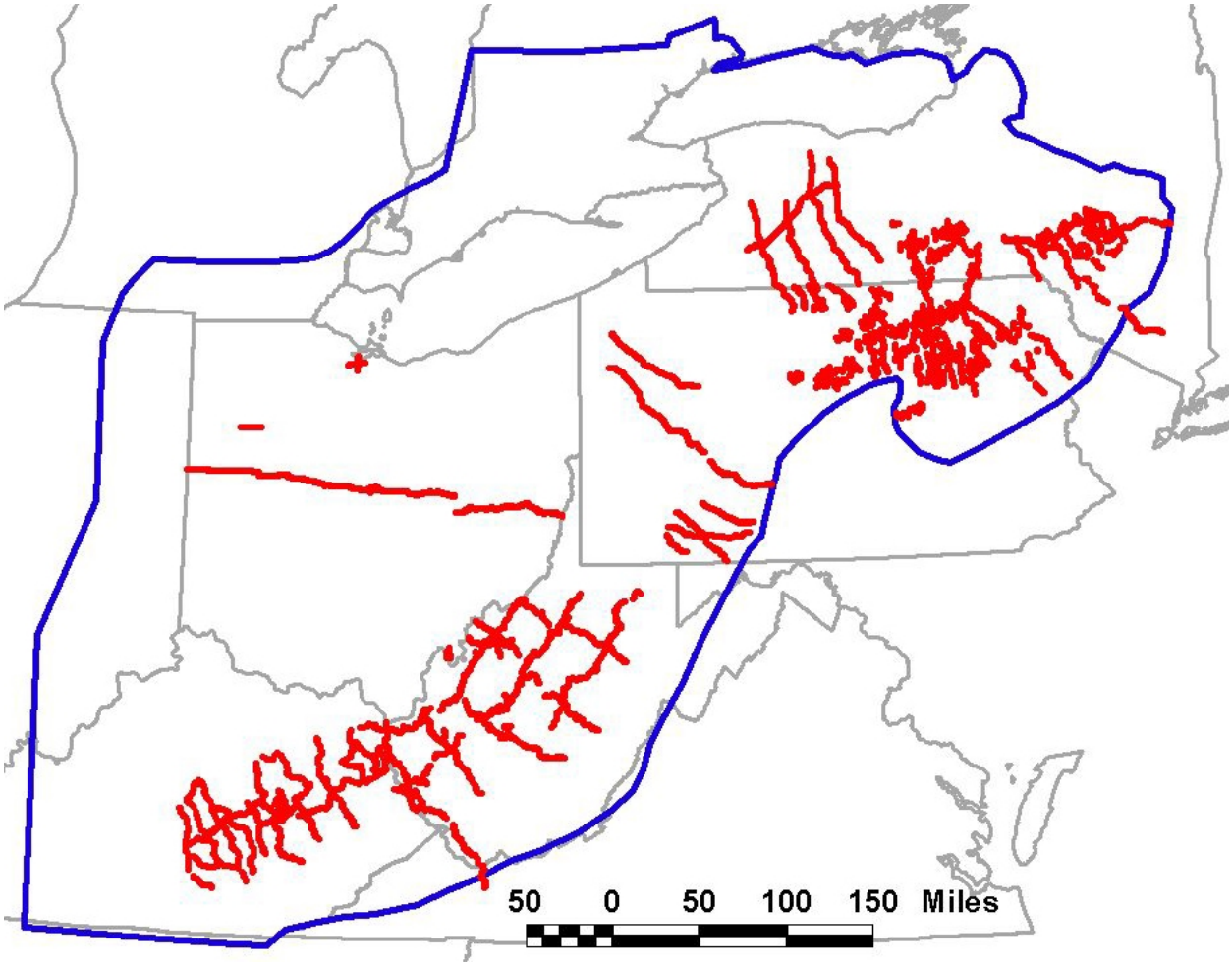

Figure 2-1. Map showing the seismic data available to the Consortium for interpretation. The blue polygon represents the project area within the Appalachian basin.

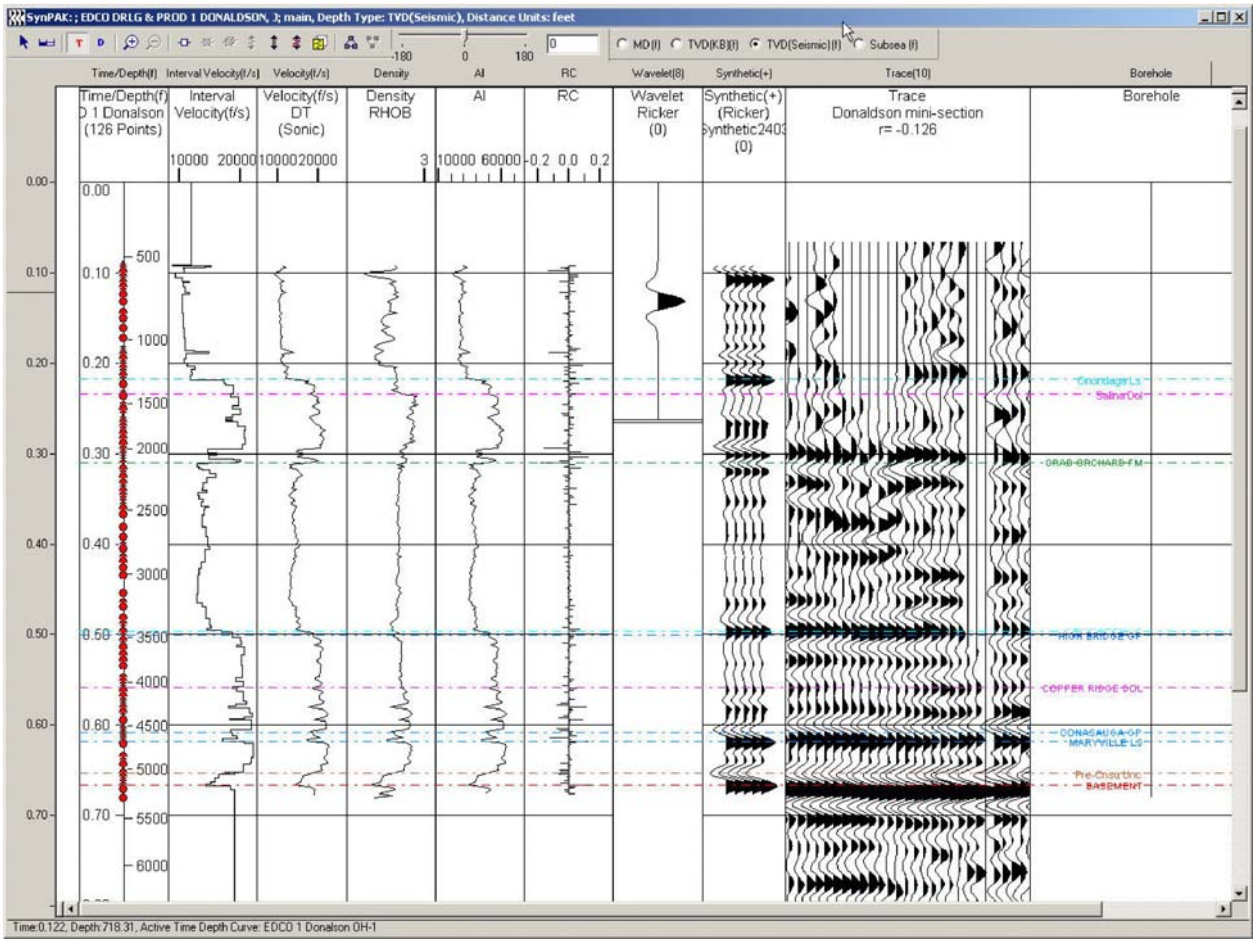

Figure 2-2. Interval velocity, acoustic impedance and synthetic seismogram for a well in eastern Ohio. The calculated waveforms matches well with the wavelet traces taken from a nearby seismic line. For reference and comparison, the Trenton-Black River reflector occurs at about 0.50 seconds and the Grenville basement reflector is around 0.67 seconds.

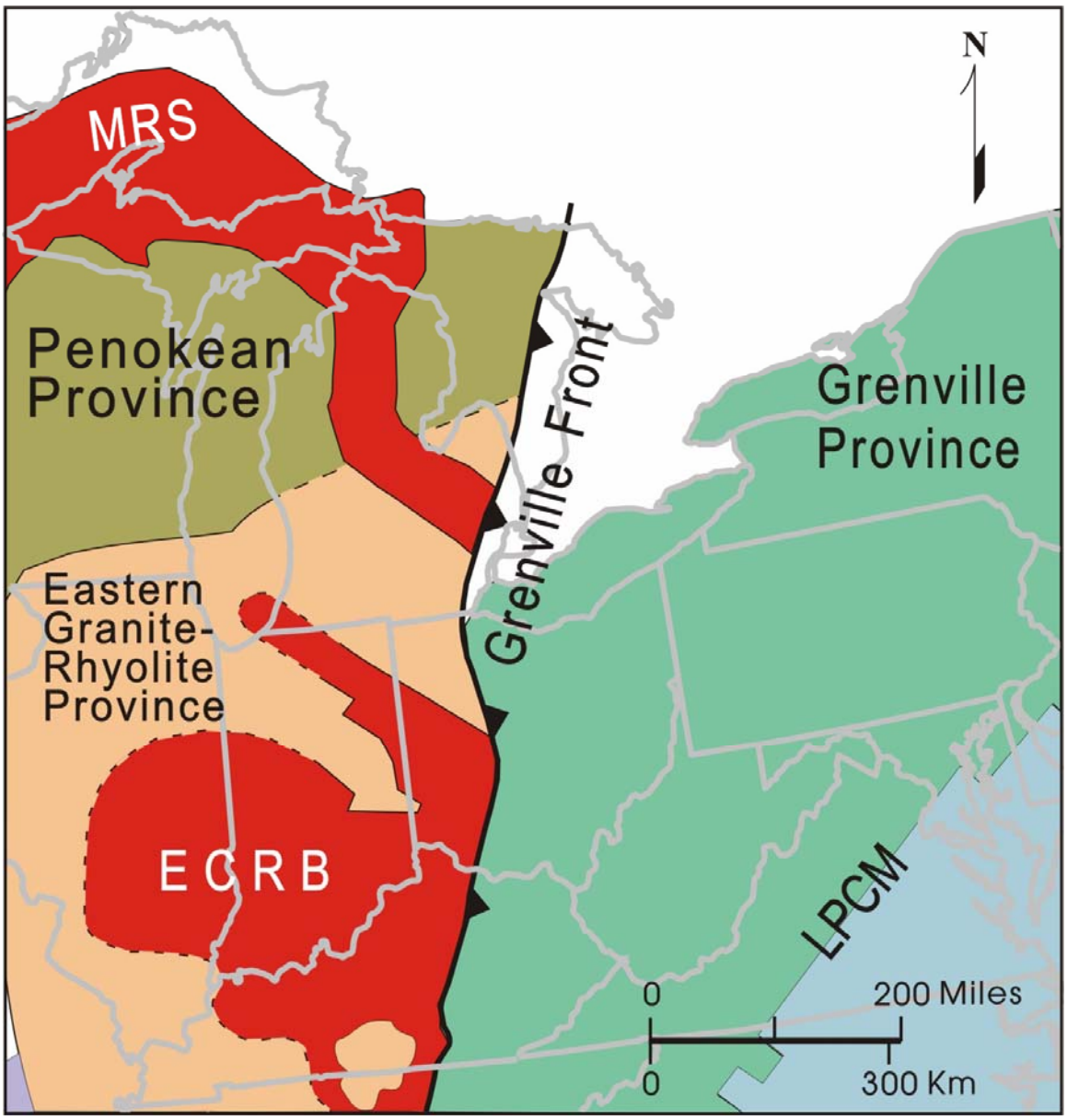

Figure 2-3. Precambrian provinces in the Consortium study area. ECRB: East Continent Rift Basin, MRS: Midcontinent Rift System, and LPCM: Late Proterozoic continental margin. Map is modified from Drahovzal and others, 1992; Drahovzal, 1997; and includes elements from Van Schmus and others, 1993; and Van Schmus and Hinze, 1993. From Wickstrom and others (2005).

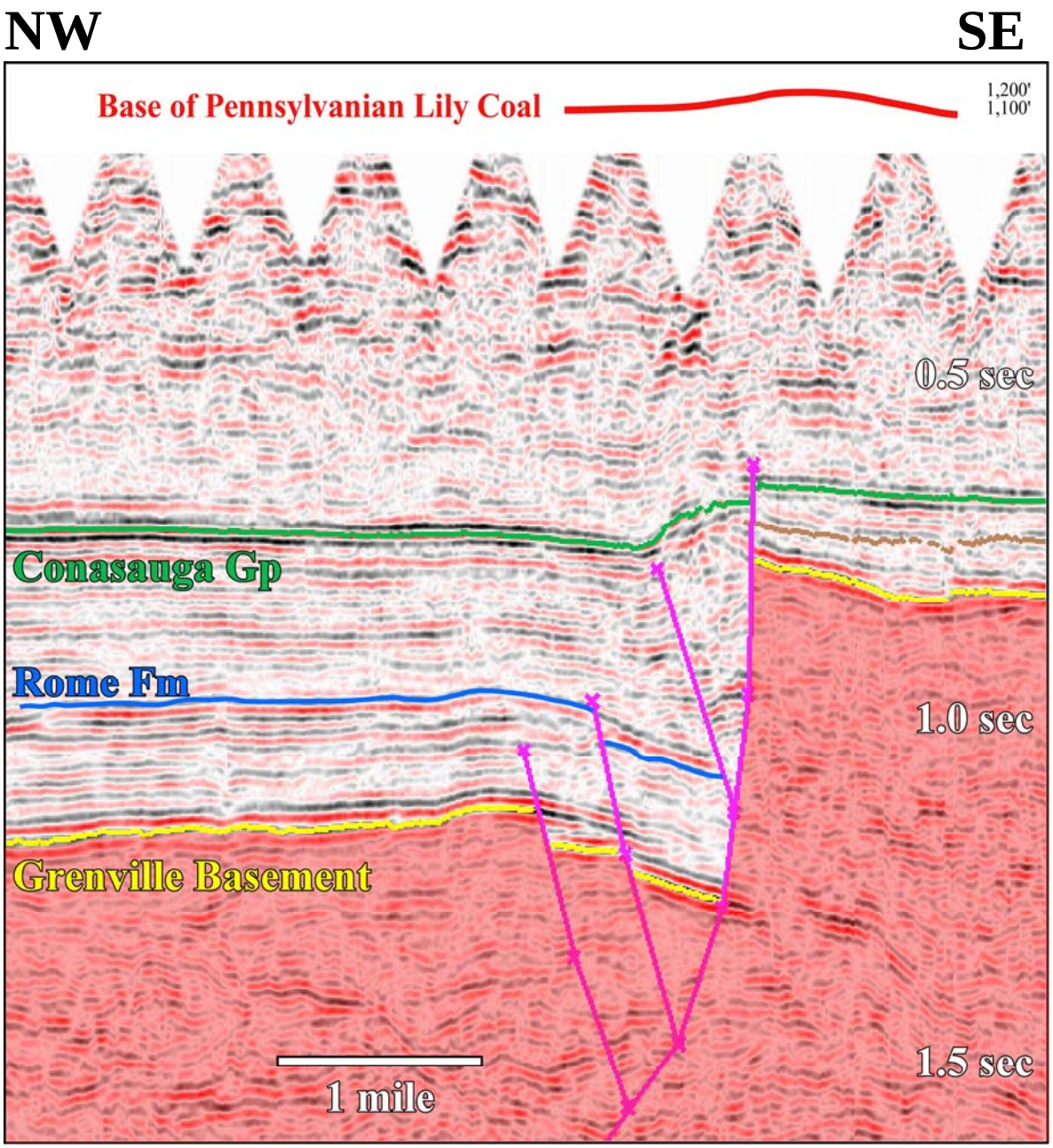

Figure 2-4. The Rockcastle River fault zone in the western Rome trough of eastern Kentucky. Note the thickening of the Rome and Conasauga sections on the northern block, indicating syntectonic deposition during the Middle Cambrian. Inversion along the deep structure resulted in the formation of a local, fault-paralleling anticlinal structure on the southern block during post-Pennsylvanian time as shown by the folding in the Lily coal (Pomerene, 1964). This later contractional event was likely associate with the Alleghany orogeny. Reflection sags in the High Bridge Group on other proprietary data not shown here could indicate the presence of dolomite in this section. This is near the Raccoon Mountain field that produced oil and gas from the High Bridge Group.

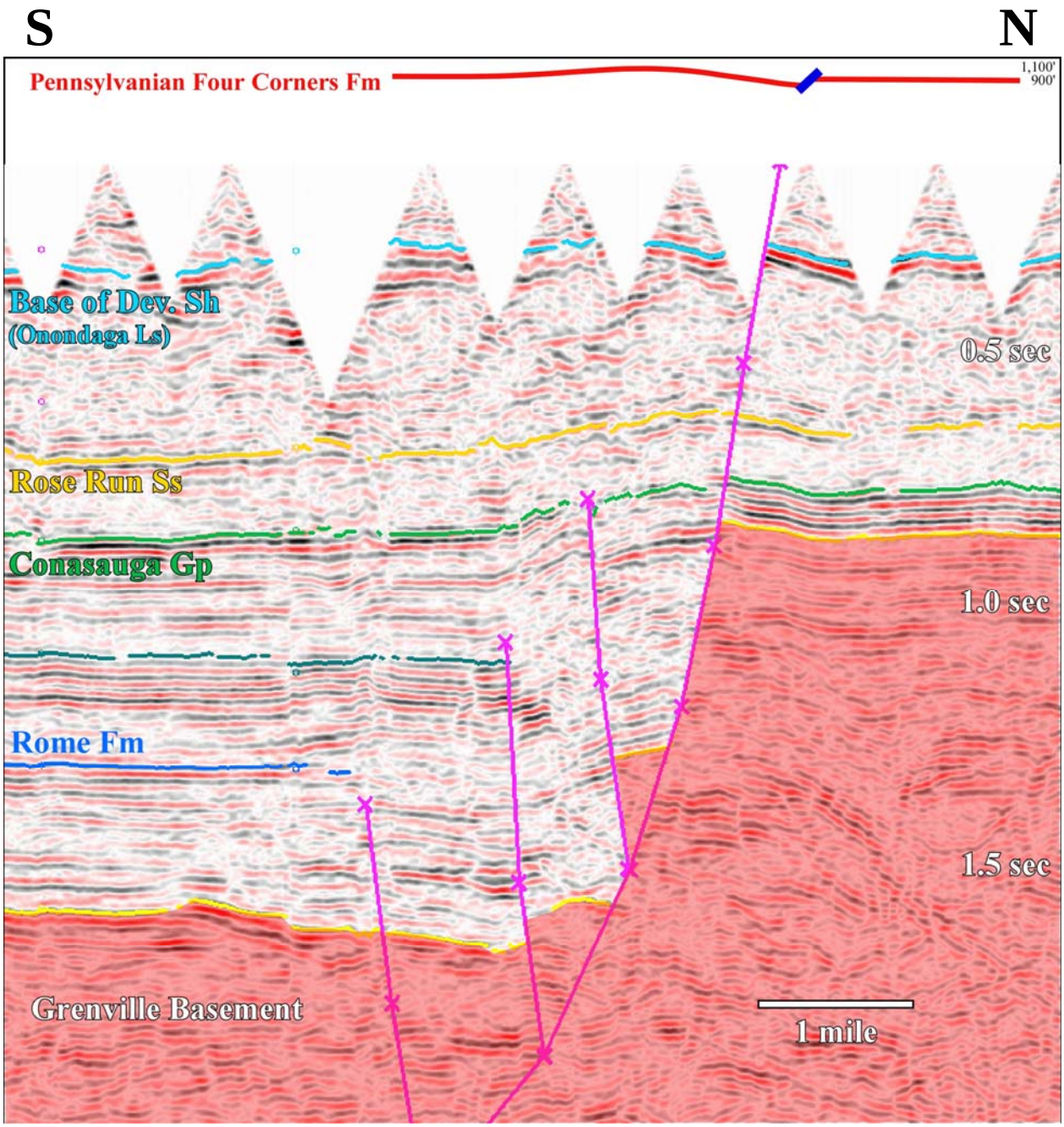

Figure 2-5. The Irvine-Paint Creek fault zone in the Rome trough of eastern Kentucky. Note the steep fault that offsets basement and the related syntectonic thickening of the Cambrian sedimentary section on the southern block. Later compression (probably from the Alleghanian orogeny) reactivated many of the basement faults, creating localized inversion structures which are responsible for the folding of the Caney anticline in the Pennsylvanian rocks above. A profile of the Magoffin Member of the Four Corners Formation mapped at the surface (Sable, 1978) illustrates this inversion structure (which is within the shallow muted zone of this seismic line). The surface-mapped profile is at the approximate scale and location with respect to this seismic line.

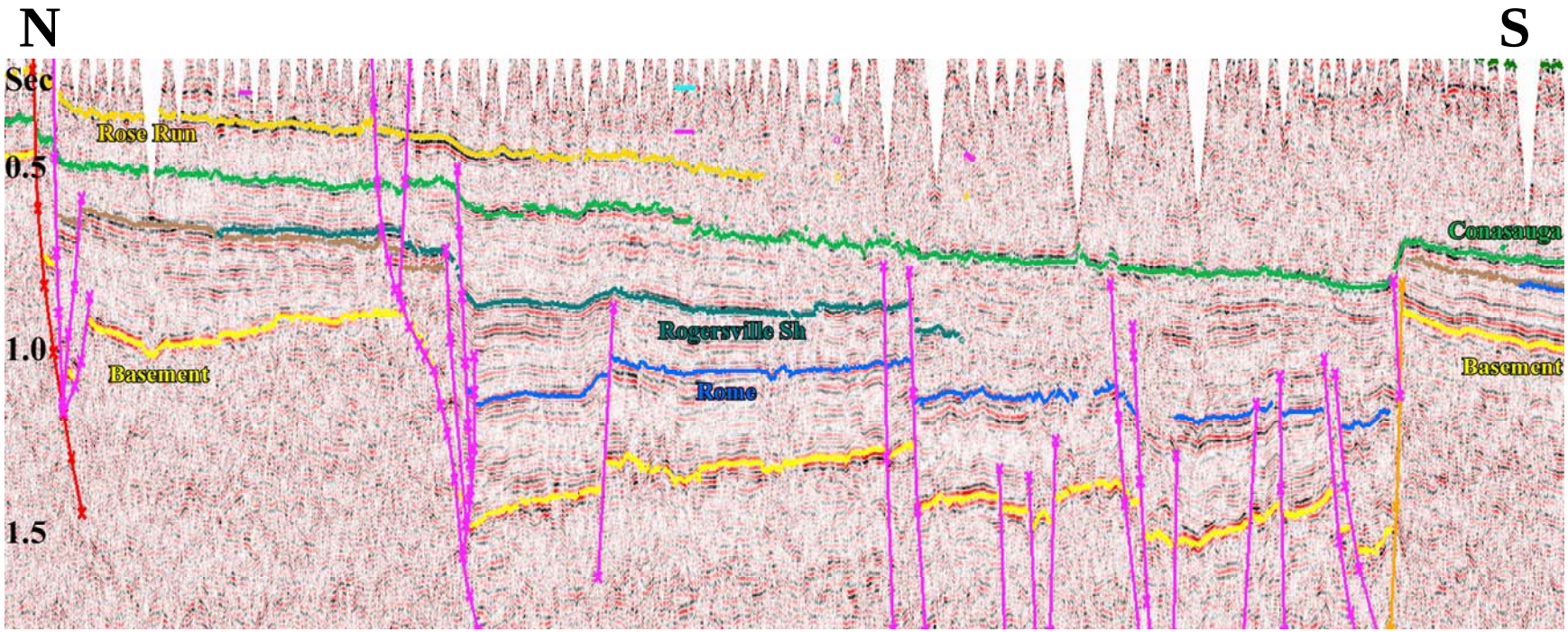

Figure 2-6. Composite seismic line through central Kentucky (Montgomery to Leslie County) across deepest portion of the basin. The approximate length of this section is 76 miles. The Kentucky River fault system is represented by the fault in red on the left, the Rockcastle River fault system is visible in orange on the right side of the section. Note the thickened Cambrian section due to extensive syndepositional faulting. The peculiar shape of the Irvine-Paint Creek fault system on this line (fault with ~ 0.5 sec of basement offset in the left-center) is due to a jog in the seismic line (was recorded along a curving road).

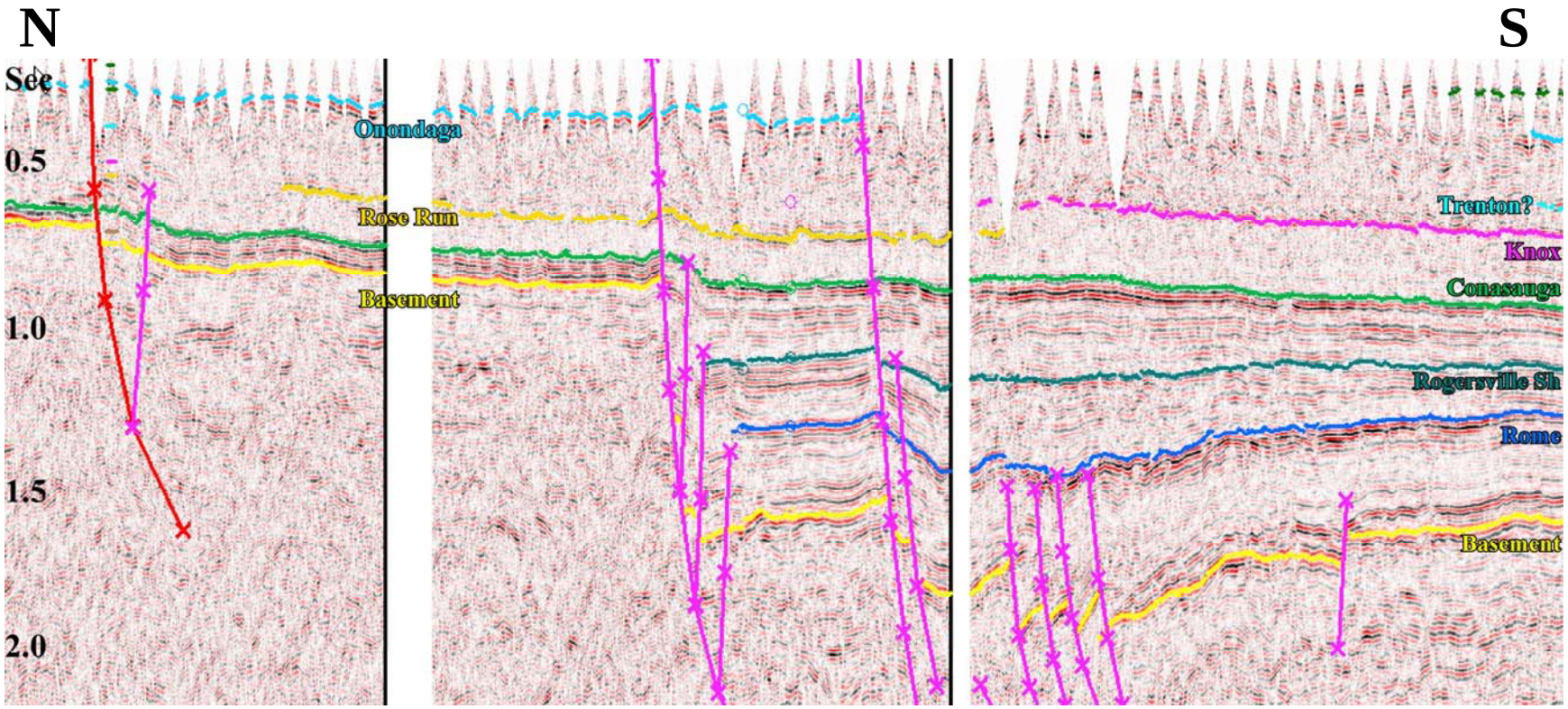

Figure 2-7. Composite seismic line through eastern Kentucky (Morgan to Magoffin County) across deepest portion of the basin. The approximate length of this section is 49 miles. Moving northeast along strike from the line shown in Figure 2-6, the offset caused by the Kentucky River fault system (red) at this location is relatively minor compared to the ~ 0.75 sec basement offset caused by the Irvine-Paint Creek fault system near the center of this figure.

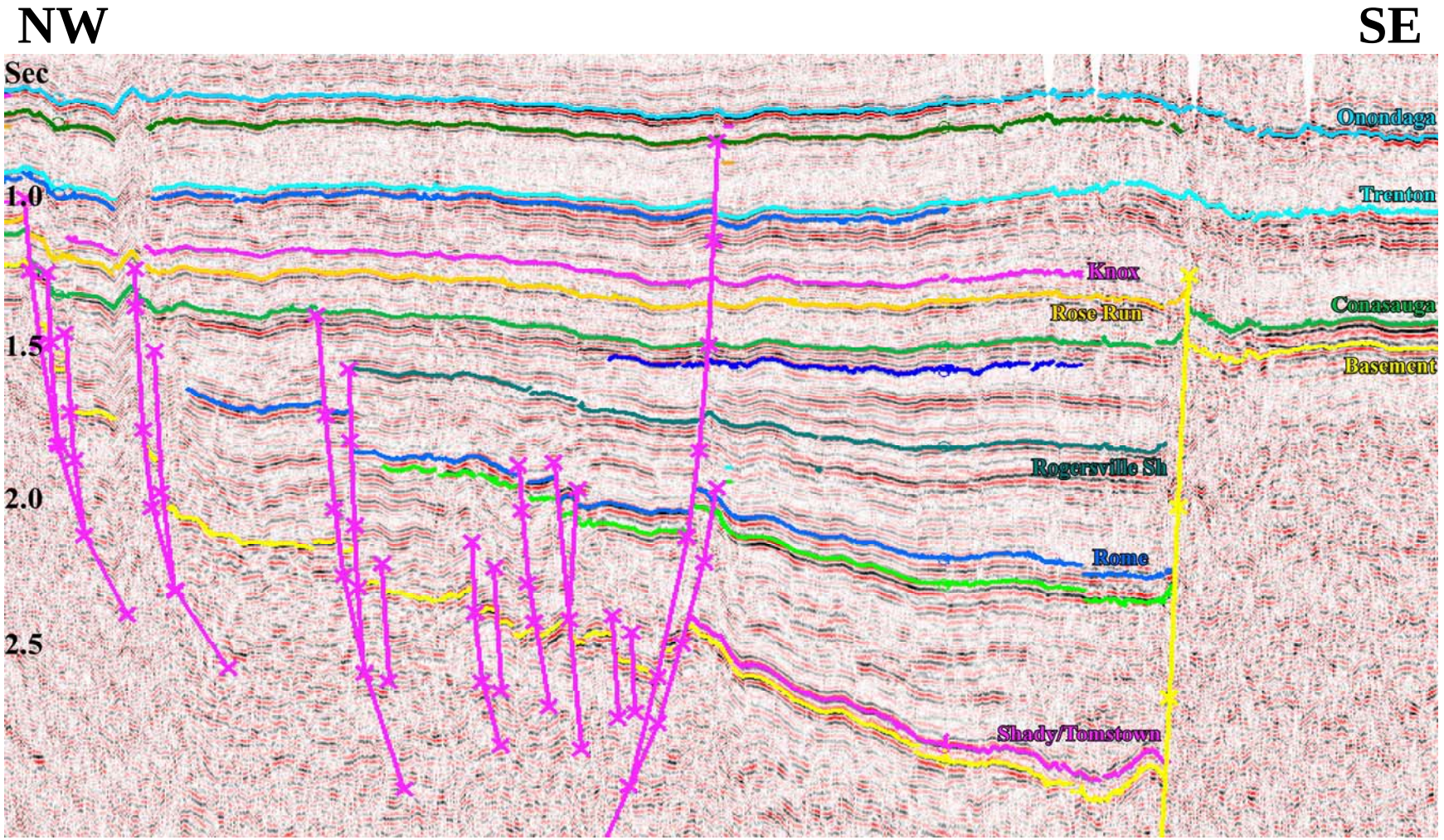

Figure 2-8. Composite seismic line through southwestern West Virginia (Cabell to Boone County) across deepest portion of the basin. The approximate length of this section is 55 miles. Moving along strike into southern West Virginia, the overall structure of the Rome trough has changed dramatically. The Irvine-Paint Creek fault system and its associated shallow northern shelf are absent here. Also of note, the Acadian and/or Alleghanian inversion structures visible along the East Margin fault (yellow) has increased dramatically compared to the Kentucky sections.

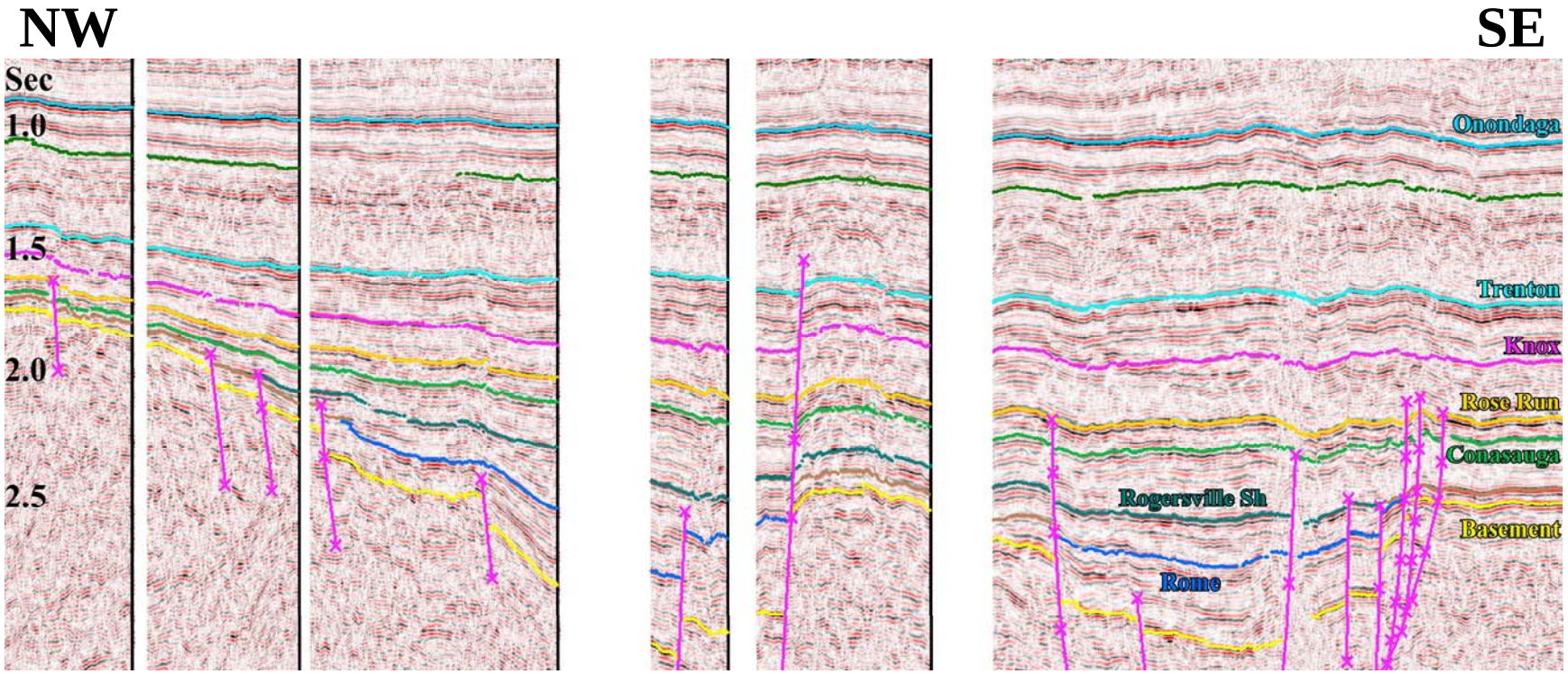

Figure 2-9. Composite seismic line through northern West Virginia (Pleasants to Randolph County) across deepest portion of the basin. The approximate length of this section is 67 miles. Here, the northwestern edge of the Rome trough has become more of a tectonic "hinge zone" as compared to the traditional graben-like structures seen to the south. The tectonic extension that created this rift system is more dissipated here, leading to a wider and shallower "trough" depression.

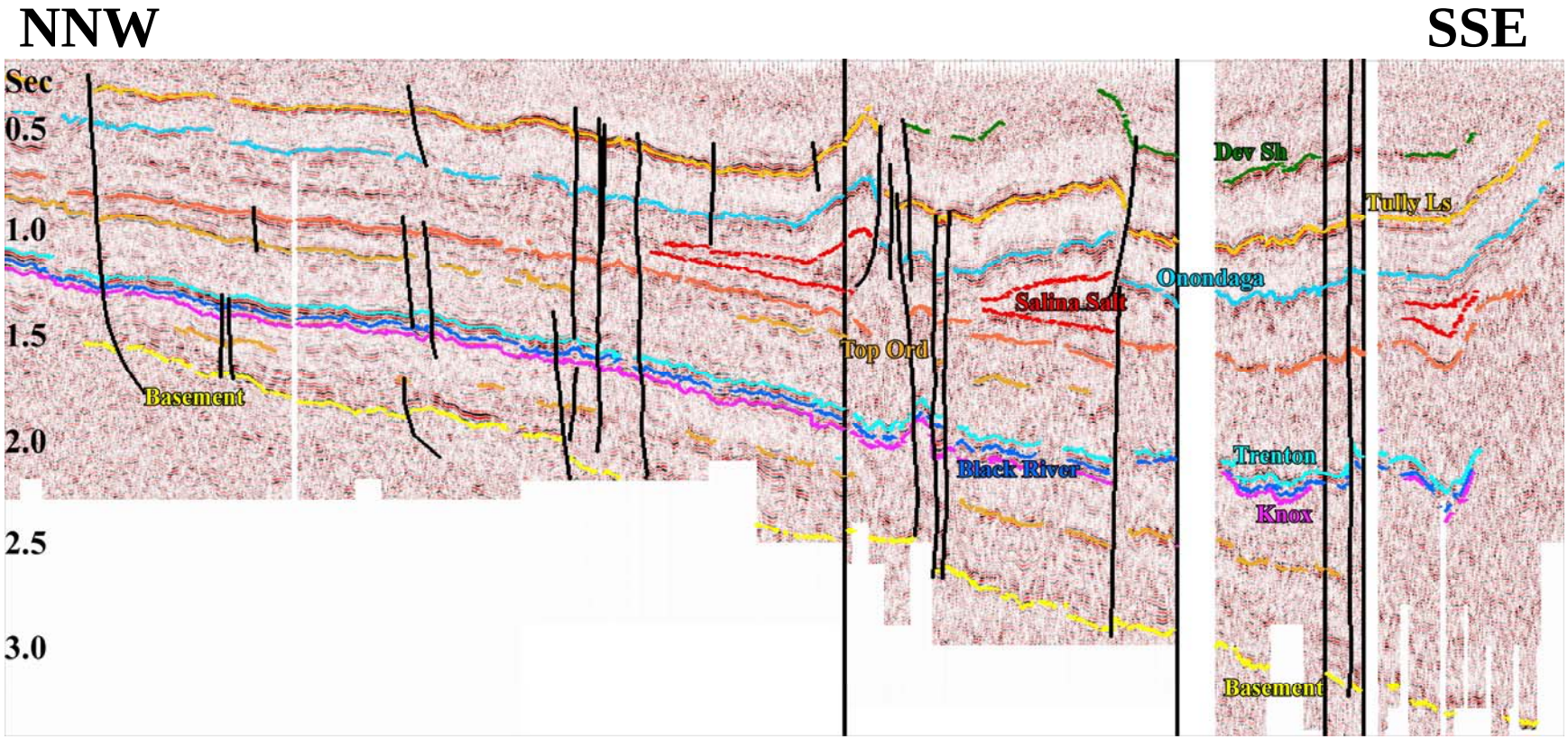

Figure 2-10. Composite seismic line from south-central New York (Schuyer County) to central Pennsylvania (Columbia County). The approximate length of this section is 87 miles. Note that much of the thickening has occurred below the Beekmantown Group and within the Rose Run Formation. Also note the connection with Alleghanian salt tectonics, basement faults and Trenton sag features. Note the Alleghanian salt tectonics that occurred because of the mobilization of evaporites in the Silurian Salina Group. Seismic resolution is poor at depth; however it is possible with the help of well control, to resolve the basement on these and other lines within the study area. There is a possible connection between the spatial distribution of the basement faults, Trenton sags, and the later salt tectonics.

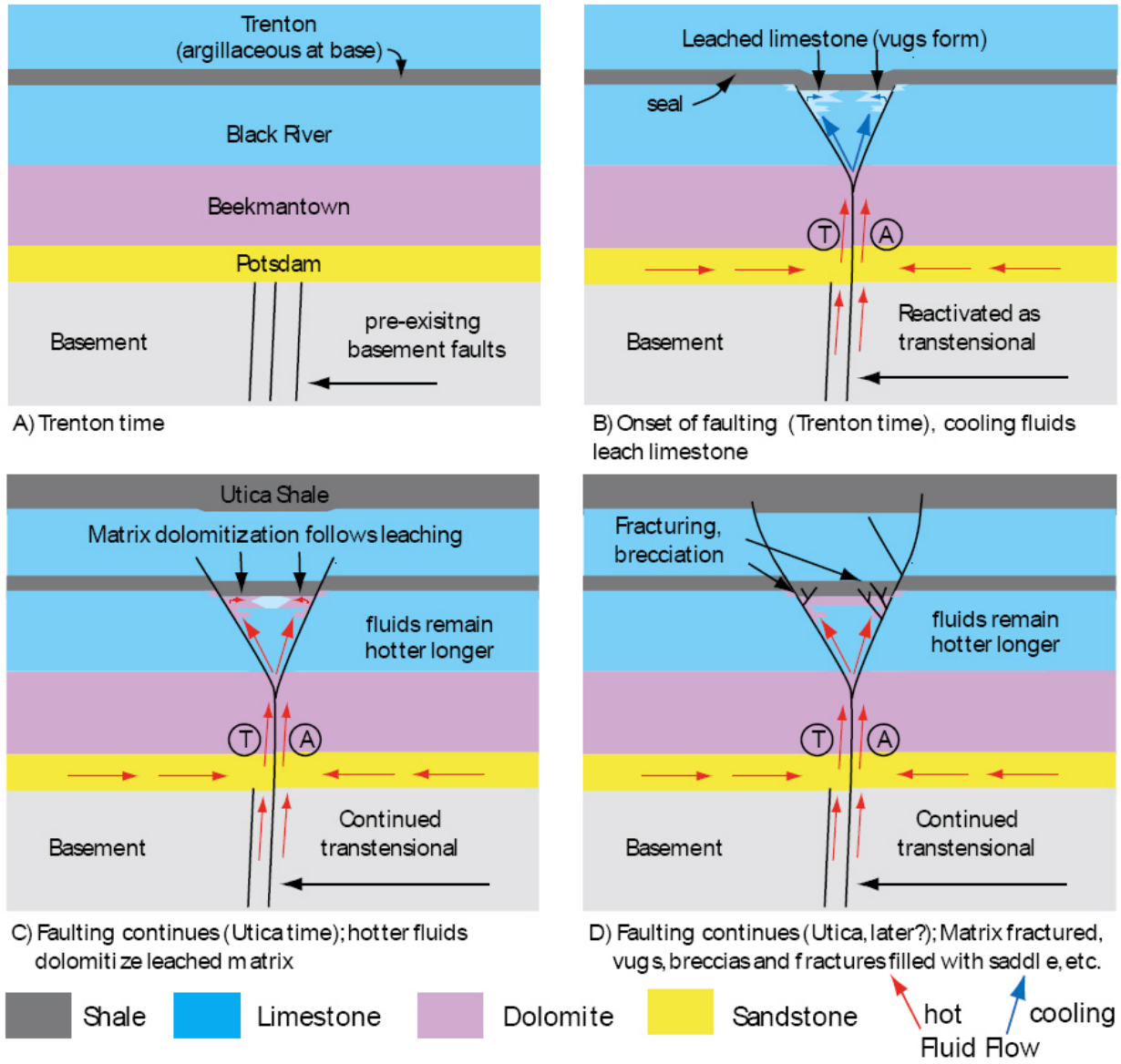

Figure 2-11. Schematic model of fault-related hydrothermal alteration for Trenton-Black River reservoirs proposed by L.B Smith (in press).

PETROGRAPHY OF THE TRENTON LIMESTONE AND BLACK RIVER GROUP CARBONATE ROCKS IN THE APPALACHIAN BASIN

By Christopher D. Laughery and Jaime Kostelnik, Pennsylvania Geological Survey

Introduction

Carbonate petrography is the study of limestones, dolostones, and associated rocks by optical and electron microscopy (Scholle and Ulmer-Scholle, 2003). Our purpose in the petrographic portion of this study is to: 1) enhance field studies and core descriptions of Trenton Limestone and Black River Group carbonate rocks in the Appalachian basin; 2) interpret the diagenetic history of these rocks, particularly with regard to its effects on porosity and permeability; and 3) provide a frame of reference for the geochemical data and interpretations presented elsewhere in this study.

Petrographic data enhance field and core descriptions of carbonate rocks through the identification of constituent grains, matrix, and depositional texture. These data enable us to develop detailed classifications of the reservoir rocks and interpret their depositional setting.

Interpretations of the diagenetic history of the Trenton and Black River carbonates provide us with a sense of the comparative timing of significant diagenetic events, such as cementation or secondary porosity development relative to the emplacement of hydrocarbons in the reservoirs. Such interpretations are particularly critical for understanding Trenton and Black River reservoirs. Cambro-Ordovician carbonate reservoirs worldwide are dominated by meter-scale, peritidal, mud-dominated cycles and thin-bedded, heterogeneous layering; the only buildups are thrombolitic or microbial, and reservoir quality is controlled by fracturing, dolomitization, and karst development beneath the top-Saulk unconformity (Markello, 2005). The Trenton Limestone and Black River Group consist of remarkably tight carbonate rocks that were completely lithified throughout the basin during marine and burial diagenesis. Reservoirs only occur where fracturing and dolomitization created adequate storage capacity for commercial hydrocarbon accumulations.

Petrography provides a frame of reference for the geochemical data we use to understand the dolomitization processes that yielded the most important petroleum reservoirs in the Trenton and Black River carbonates in the Appalachian basin. The geochemical data include stable carbon and oxygen isotopes, fluid inclusions, $^{87}Sr/^{86}Sr$ ratios, and trace element (Fe and Mn) distributions.

The petrographic data presented herein are useful on a broad scale for documenting the distribution of porous and permeable carbonate rock facies in the Trenton Limestone and Black River Group in the Appalachian basin. The data allow us to determine the spatial distribution of reservoir seals, compartmentalization, and diagenetically-controlled pore geometry in the productive gas fields.

Methods

We collected samples from 17 different cores of Trenton and/or Black River carbonate rocks recovered from wells throughout the Appalachian basin. The cores we examined and sampled are listed in Table 1. We described the cores before sampling, and these descriptions will be integrated into the pending report on stratigraphy. We also collected cuttings samples from one well in Pennsylvania for thin sections, and prepared numerous thin sections from outcrop samples in Pennsylvania and Kentucky. In all, we analyzed 740 thin sections of Trenton and Black River carbonates. Selected samples were further studied by scanning electron microscopy and energy-dispersive X-ray spectroscopy.

We used a Leica DML polarizing microscope equipped with a Leica DFC camera for all transmitted light microscopy. We examined selected unembedded and unpolished samples on a Hitachi S-2600N variable pressure scanning electron microscope (SEM) operating with a pressure of 10 Pascals using the backscattered electron detection imaging system at 20 kV and a working distance of 15 mm. The elemental composition of these samples was determined using Quartz Imaging System's Quartz XOne energy-dispersive X-ray spectroscopy (EDS) package with a Gresham Sirius 10/UTW/SEM detector having a 10 mm^2 crystal and an ultra thin polymer window. We used the same SEM operating at 20 kV and a working distance of 15 mm when conducting EDS analyses.

We classified all carbonate rock samples using the classification systems of both Dunham (1962) and Folk (1962). We found Dunham's (1962) classification useful for microfacies analysis when we could use it – it is descriptive, objective, and easy to use in the field or laboratory, and it conveys some genetic information. But the Dunham classification fell short in naming many of the Trenton and Black River limestones and dolostones significantly altered by diagenesis. In these instances the Folk (1962) classification system provided us with a useful, objective and descriptive terminology that provided for grain size, allochem composition, and diagenetic alterations. For these reasons, we use carbonate names from both systems interchangeably throughout this report. We classified all dolostones using the classification system of Wright (2001). We classified carbonate porosity using the systems of both Choquette and Pray (1970) and Luo and Machel (1995).

Constituents

Skeletal Grains

The skeletal constituents of carbonate rocks reflect the distribution of calcium carbonate-secreting organisms throughout geologic time. Many new carbonate-secreting marine organisms emerged by Middle Ordovician time, some 450 million years ago, and these are well represented in the composition of Trenton and Black River rocks. Fragments of brachiopods, bryozoans, crinoids, corals, trilobites, calcareous algae, and gastropods comprise the principal skeletal grains in the rocks. The distribution of these organisms in the carbonate depositional realm was controlled by environmental factors

such as water depth, temperature, salinity, substrate, and turbulence. Thus, the correct identification of these skeletal grain types and their depositional texture is critical for correct environmental interpretations.

The original mineralogy of the skeletal grains, i.e., aragonite, low-Mg calcite, high-Mg calcite, or a mixture of aragonite and calcite, affected the fate of the skeletal grains during diagenesis. Their susceptibility to recrystallization, dissolution, and dolomitization was particularly important to the development of Trenton and Black River carbonate reservoirs in the subsurface.

Skeletal grains are identified on the basis of their size, shape, microstructure, and original mineralogy (Tucker and Wright, 1990; Scholle and Ulmer-Scholle, 2003). Appendix I provides a comprehensive review and photographic guide of the major skeletal grains that occur in the Trenton and Black River rocks of the Appalachian basin.

Non-skeletal Grains

Non-skeletal carbonate grains in the Trenton and Black River rocks include ooids, peloids, grain aggregates and clasts. Appendix I includes a general review and photographic guide of the non-skeletal grains found in the Trenton and Black River rocks of the Appalachian basin.

Ooids are a type of coated carbonate grain, spherical to sub spherical in shape, consisting of one or more regular concentric lamellae around a nucleus. The nucleus is often a carbonate particle, but can be a non-carbonate clastic particle, too. The term ooid is restricted to grains less than 2 mm in diameter, and most ooids range from 0.2 to 0.5 mm in diameter. This is the size of fine- to medium-grained sand in the Wentworth scale. Recent marine ooids exhibit tangential, radial, or random microfabrics. Ancient marine ooids may have relic tangential microstructures or, more commonly, radial microfabrics. Many ancient ooids are micritic or display replacement with neomorphic spar. We only found ooids in portions of the Black River Group. We did not find any ooids in the Trenton Formation rocks that we examined, and we could not find any report of Trenton ooids in the literature.

While ooids are locally important, peloids are the most diverse and abundant non-skeletal grains in the limestones and dolostones that we examined, and their origins are diverse and complex. Indeed, many, if not most, of the peloids in the Trenton and Black River carbonates may not be grains at all but cements instead. The original textures of the peloidal limestones appear to have influenced dolomitization processes and subsequent dolomite fabrics and porosity distributions in the Trenton and Black River petroleum reservoirs throughout the Appalachian basin.

Peloids are a type of non-skeletal carbonate particle formed of cryptocrystalline and microcrystalline calcium carbonate, and/or carbonate microspar (Scholle and Ulmer-Scholle, 2003, p. 254). Peloids are spherical, cylindrical, or angular particles composed of aggregated carbonate mud and/or precipitated calcium carbonate. They exhibit no

internal structure. There is no defined restriction on the size or origin of peloids, thus the term allows reference to allochems composed of micritic material without implying their specific origin (McKee and Gutschick, 1969).

Peloids are polygenetic, and identifying their precise origin is often difficult in carbonate rocks (see discussions by Macintyre, 1985 and Scholle and Ulmer-Scholle, 2003). Some peloids are fecal in origin (carbonate pellets), while others are grains derived from calcareous algae, micritized allochems, and reworked mud clasts (Tucker and Wright, 1990; see the examples presented in Appendix I). Most peloidal textures in carbonate rocks, however, probably are chemical in origin, i.e., cements in which the peloids appear as clots with a flocculent fabric- the *structure grumeleuse* of Bathurst (1975, p. 511 – 513 and Figure 350). These clots are the nucleation sites of small crystals of high-magnesium calcite (Tucker and Wright, 1990). The nuclei may be organic, possibly microbial matter (Chafetz, 1986) or simply sub-microcrystalline, radial, acicular calcite crystals that grew around a small number of nuclei (Bosak and others, 2004). In either case, the peloids precipitated *in situ* as marine cement on or just below the sea floor (Tucker and Wright, 1990; Malone and others, 2001; Bosak and others, 2004). The recent work of Bosak and others (2004) recommends that abiotic mechanisms should be the null-hypothesis for peloid formation.

Peloidal textures are ubiquitous in the Trenton and Black River carbonates throughout the Appalachian basin. They occur in all carbonate rock types and their origins are quite diverse. Appendix I contains numerous examples of peloids that clearly are carbonate grains. In many instances, however, we interpreted peloidal fabrics in Trenton and Black River rocks as cement. We discuss peloidal cement textures in detail below in the section on diagenesis.

Most of the dolomitized carbonate rocks of Black River age in the subsurface of west central New York State and north central Pennsylvania exhibit a precursor peloidal fabric that dominated the limestones there. The petrophysical character of microporosity in these precursor peloidal limestones may have been critical in controlling the migration of dolomitizing fluids through the rocks adjacent to faulted and fractured strata (see Cantrell and Hagerty, 1999). These peloidal textures also are common in dolomitized limestones in western Ohio and central Kentucky.

Matrix

Fine-grained matrix in the Trenton Limestone and Black River Group consists of calcite micrite, microspar, pseudospar, and terrigenous clay minerals. Micrite is composed of small calcite crystals 1 to 4 μm in diameter. These crystals formed through the breakdown of coarser carbonate grains, such as calcareous algae, or through inorganic precipitation on the seafloor (Tucker and Wright, 1990; Scholle and Ulmer-Scholle, 2003). Figure 1 shows several examples of micrite matrix in the Trenton and Black River carbonates. Microspar consists of calcite crystals 5 to 30 μm in diameter. It forms through neomorphic recrystallization of micrite. Pseudospar also is a recrystallization product of finer calcite, but it is even coarser than microspar with crystal diameters of 30 to 50μm.

Clay mineral, predominately illite, mixed-layer illite-chlorite, and smectite, occur in some Trenton Formation samples, particularly in ramp slope carbonates intimately interbedded with terrigenous shales (Figure 2). Some of the matrix material in the Trenton Formation is organic rich (up to 3.74% total organic carbon), and might be important as a petroleum source rock.

Other Components (non-authigenic)

In addition to terrigenous clay minerals, non-carbonate sedimentary components of the Trenton Limestone and Black River Group include detritial quartz silt and very fine sand, bentonite, and rare glauconite. The quartz entered the carbonate environments as air-borne and/or water-borne sediment. Very fine quartz sand and silt dispersed throughout some of the limestones in the Black River Group (<1% of the rock) might be air-borne, but was more likely reworked from very thin, fluvial and paralic siliciclastic accumulations that were deposited on the carbonate ramp during sea level lowstands (Figure 3). The volcaniclastic k-bentonites (Figure 4) are interbedded with the carbonates, and were rapidly deposited below storm wave base by volcanism along the island arc that formed along the southeastern Laurentian continental margin during the Taconic orogeny (Thompson, 1999). Reworked fragments of these k-bentonites occur in some of the limestones.

Microfacies and Depositional Environments

All of the principal carbonate rock types occur in the Trenton Formation and Black River Group of the Appalachian basin. The depositional texture of the original limestones correlates directly to the sedimentary environments of the carbonate ramp on which the various rock types accumulated. Tidal flat and lagoonal limestones mostly consist of mudstone and wackestone, with thin packstone/grainstone deposits that collected within tidal channels. These rocks were deposited in peritidal settings as low-energy, shallowing-upward successions and thick lagoonal successions. Although less common, some grainstones and packstones accumulated as high-energy, shallowing-upward successions deposited as beach carbonates in the peritidal settings.

Subtidal deposits include boundstones, grainstones, packstones, wackestones, and mudstones deposited in both shallow and deeper carbonate ramp setting. Rocks that formed above wave base on the shallow ramp include hardground-bounded, amalgamated grainstone, and grainstone-capped high energy shoaling successions. Skeletal packstone/wackestone – mudstone successions, also bound by well-developed hardgrounds, formed on the deeper ramp below fair-weather wavebase. Graded carbonate beds – tempestites and turbidites – accumulated in slope and basin margin environments. These consist of upward-fining grainstone/packstone and wackestone/mudstone couplets separated by siliciclastic shales. The carbonate materials were introduced from the carbonate ramp, while the shales came from the Taconic highlands and volcanic arc along the southeast margin of Laurentia (Pope and Steffens, 2003).

Diagenesis

The term diagenesis refers to all of the processes that affect sediment from just after deposition up to the lowest grade of metamorphism, the greenschist facies (Pettijohn and others, 1987). It is the sum of physical, chemical, and biochemical changes occurring in a sedimentary deposit after its initial accumulation, excluding metamorphism (Friedman and Saunders, 1978). Diagenesis in the rocks of the Trenton Limestone and Black River Group included seven major processes: 1) microbial micritization; 2) cementation; 3) neomorphism; 4) replacement; 5) physical and chemical compaction; 6) dissolution; and 7) dolomitization (see, Tucker and Wright, 1990, p.314). Dolomitization is the most important diagenetic aspect of the Trenton and Black River petroleum reservoirs and is discussed separately in the next section of this report.

Note: The term diagenesis is used differently by organic geochemists, and we employ their usage in the petroleum geochemistry reports of this research. In petroleum geochemistry, diagenesis is the process involving the biological, physical, and chemical alteration of the organic debris in sediments without a pronounced effect from rising temperature (Hunt, 1996). It covers the range of temperature up to about 50°C (122°F). Readers should bear these different usages in mind when reading this report.

Microbial Micritization

Partial to complete microbial micritization of skeletal grains, ooids, and probable pellets occurs in most carbonate rock types in the Trenton Limestone and Black River Group throughout the Appalachian basin. Microbial micritization is most evident in bioclastic grainstones and packstones where micrite envelops developed on skeletal grains, and in some mixed oolitic/peloidal grainstones and packstones where the peloids show compelling evidence of carbonate grain degradation and replacement with micrite. In both cases, the micritization process may have been mediated by endolithic algae, fungi, or bacteria and associated biochemical or physiochemical processes.

The micrite envelops shown in Appendix II (Micritization Examples #1 - 4) formed around many of the bioclasts in mixed-fossil grainstones. These envelopes are essentially identical to those shown and discussed by Milliman (1974), Bathurst (1975), Tucker and Wright (1990), and Scholle and Ulmer-Scholle (2003). Bathurst (1975, p.381 – 389) suggested such envelopes formed through the filling of altered grains rather than precipitation of a new rind around the grain: algae, fungi, or bacteria bore into the grain, die, and the subsequent alteration of the organic material provides a chemical environment conducive to calcium carbonate precipitation, thus filling the voids.

Intense activity by endolithic microbes can lead to complete micritization of carbonate grains. This was relatively common during deposition of both Trenton and Black River carbonates. Figure 5 shows wholly micritized ooids in the Black River Formation in the subsurface of western New York.

The micrite envelope surrounding the echinoid fragment in Figure 6 originated in the same way as those shown Appendix II, i.e., through marine cementation within

spaces created by endolithic boring organisms. The micrite cement shown in Figure 6, however, displays a distinctive clotted or peloidal texture (Figure 6b and 6c). Higher magnification (Figure 6c) reveals that the "clots" of microcrystalline calcite in the micrite rind consist of unimodal, decimicron-size spherical clusters composed of even smaller (micron- and sub micron-size) calcite crystals. Each clot or peloid consists of a brownish, cloudy nucleus and a rim of clear, well-developed euhedral crystals. These clots grade into adjacent patches of coarser, centimicron-size microcrystalline matrix with an identical peloidal fabric or into coarser calcite spar cement. These micrite envelopes and contiguous patches of clotted microcrystalline calcite may be bacterially induced calcite precipitates, or strictly abiotic cement (Lighty, 1985; Macintyre, 1985; Chafetz, 1986; Tucker and Wright, 1990; Scholle and Ulmer-Scholle, 2003; Bosak and others, 2004).

Cementation

The precipitation of calcium carbonate cements in the Trenton and Black River limestones was a major diagenetic process during and shortly after deposition on the sea floor in Ordovician time. Burial cementation also affected the rocks. The principal calcite cements in the rocks are 1) peloidal calcite, 2) prismatic fibrous to bladed calcite rinds on allochems, 3) meniscus calcite cement, 4) syntaxial calcite overgrowths, and 5) calcite spar. Dolomite cements are important, but we discuss these later in the section on dolomite textures. Several late-stage, non-carbonate cements are associated with dolomite cements and we discuss these in the section on dolomitization.

Peloidal Cements. While microbial micrite envelopes around allochems and micrite replacement of grains are common in the Trenton and Black River carbonates of the Appalachian basin, most of the microcrystalline calcite, microspar, and pseudospar in these rocks occur as matrix in packstones, wackestones, and mudstones. As discussed above, much of this matrix originally formed *in situ* as carbonate mud derived from the breakdown of organisms, and it now exists in the rocks as neomorphic, recrystallized calcite. A great deal of the carbonate matrix in all of the limestone types, however, also formed *in situ* as peloidal cement. The clotted fabric of peloidal cement is ubiquitous in the Trenton and Black River limestones, and can usually be discerned even through most dolomite fabrics.

Figure 7 shows core and thin section photographs of Black River Group limestone recovered in the Gray #1 well core, Steuben County, NY. Figure 7a shows the macroscopic appearance of this limestone – a seeming medium gray, bioturbated and burrowed sparse biomicrite (Folk, 1962) or wackestone (Dunham, 1962). There are problems with using the Dunham (1962) classification for this sample (see discussion below) so we prefer the Folk (1962) name. Dissolution structures (solution seams) indicate moderate chemical compaction.

Thin section examination of this sample reveals that skeletal grains comprise about 20 percent of the limestone, and include crinoids, bryozoans, brachiopods, trilobites, alga, and gastropods (Figure 7b). Most allochems were altered by neomorphism, specifically recrystallization and degrading recrystallization. Authigenic

pyrite, quartz, feldspar, and anhydrite along with dolomite make up about 5.5 percent of the rock. About 75 percent of this limestone, however, consists of decimicron-size peloids that could be interpreted as either framework grains or cement (Scholle and Ulmer-Scholle, 2003; Figure 7b). If framework grains, then the peloids might have originated as 1) algal material, 2) detritial sediment, 3) pellets, or 4) a replacement of other framework grains (Tucker and Wright, 1990, p.321 and references therein). If the peloids are cement then they are *in situ* precipitates.

Careful examination of the peloids at higher magnifications (Figure 7c and 7d) reveals that they most probably are cement and not carbonate grains. Individual peloids are 50 to 100μm in diameter and consist of 1) a dark brown nucleus composed of micron-size calcite surrounded by 2) a rim of euhedral, dentate to blocky microspar. The average crystal size of the later is ~25μm. The highest magnification view (Figure 7d) shows the nuclei consist of clots of submicron-size opaque material; this material might be organic, possibly microbial matter (Chafetz, 1986) or simply submicrocrystalline, radial, acicular calcite crystals that grew around a small number of nuclei (Bosak and others, 2004). If the nuclei are organic, the peloids likely originated as *in situ* precipitates around clumps of bacteria and the microspar likely is a neomorphic recrystallization product of earlier micrite matrix (Lighty, 1985; Macintyre, 1985; Chafetz, 1986; Tucker and Wright, 1990). If the nuclei are inorganic, the opaque appearance of the peloids probably is a consequence of the small crystal grain size relative to the thickness of the thin section (Bosak and others, 2004). In this case, the peloidal nuclei are strictly abiotic in origin and formed as calcite cement from suspension and geopetal settling (Bosak and others, 2004).

The peloidal fabric in this limestone occurs as: 1) dominant groundmass or "matrix" (Figure 7a – 7d); 2) as an internal cement within the zooecia of bryozoan skeletal grains and the lumens of crinoid fragments (Figure 7e); 3) as cement filling fabric-selective pores, i.e., intraparticle voids (Figure 7f); and 4) as mimic replacement of bryozoan grains (Figure 7g).

All of the characteristics of the peloids – their uniform crystal size, restricted size range, consistent texture, monomineralogy, opaque nuclei, and euhedral outer rims-suggest that they are *in situ* precipitates which formed through cementation on or just below the sea floor (Tucker and Wright, 1990; Malone and others, 2001; Bosak and others, 2004. This peloidal fabric characterizes most of the fine-grained rocks in the Trenton and Black River carbonates that we examined.

The most compelling evidence for interpreting these peloidal textures as marine cement is the fact that this fabric is ubiquitous in Trenton Limestone and Black River Group hardgrounds throughout the basin (Figure 8). Hardgrounds are synsedimentarily lithified carbonate seafloors that become hardened *in situ* by the precipitation of carbonate cement in the primary pore space (Wilson and Palmer, 1992, p.3). They are sedimentary horizons in marine carbonates that exhibit evidence of exposure on the sea floor as lithified rock. Detailed discussions of hardgrounds in the Trenton and Black River rocks of the Appalachian basin can be found in Brett and Brookfield (1984) and

Laughrey and others (2003). All of the fine-grained or finely crystalline hardground lithologies that we examined petrographically have a peloidal fabric.

A note on classification: The Dunham (1962) classification of the sample shown in Figure 7 as a *wackestone* based on hand sample description or a *mixed-fossil/peloidal grainstone* based on thin section description is wrong because the fine calcite crystal size and peloidal fabric do not reflect the limestone's depositional texture. The Folk (1962) classification *sparse biopelmicrite* provides a better name for the rock, although one might argue for *sparse biopelsparite* instead (see Scholle and Ulmer-Scholle, 2003, p.266 – 271). We prefer the former Folk (1962) name because the peloidal nuclei volumetrically dominate the rock and their micron-size calcite crystals can be properly called micrite (see Scholle and Ulmer-Scholle, 2003, p. 266). An alternate name, from the classification scheme of Wright (1992) is *cementstone*.

Other Calcite Cements. In addition to the peloidal calcite cements just discussed, calcite cement also occurs as prismatic fibrous to bladed rinds, meniscus-type cement, syntaxial overgrowths on allochems, poikilotopic calcite spar, and void-filling spar. We interpret these various calcite cements as products of both marine and burial diagenesis.

Prismatic fibrous to bladed rinds of calcite are common on all allochems we observed in the Trenton and Black River limestones. These crystals may grow directly on the allochems, or atop micrite envelopes. Good examples are shown Appendix II (Prismatic fringe examples 1 – 3). These morphologies are typical of modern high-Mg calcite and aragonite cements (Scholle and Ulmer-Scholle, 2003), but probably precipitated as calcite in the Ordovician sea (Lowenstein and others, 2001).

We observed unique *meniscus-type cement* (Hillgartner and others, 2001) in oolitic grainstones of the Black River Formation at Union Furnace, Pennsylvania (Appendix I, nonskeletal grains, ooid example #5). Meniscus cements usually are cited as evidence for meteoric diagenesis in the vadose zone (James and Choquette, 1984; Scholle and Ulmer-Scholle, 2003), but Hillgartner and others (2001) demonstrated a marine diagenetic origin for microbially-induced meniscus cements in carbonate sands of the Bahamas and Mesozoic platform carbonates of the Swiss and French Jura Mountains. These authors cautioned that an interpretation of early vadose diagenesis should not be based on meniscus cement alone. They suggested the term *meniscus-type cement* for these unique marine cements that form in association with the calcification of microbial filaments and the trapping of percolating micrite in subtidal settings. The *meniscus-type cements* in the Black River oolitic grainstones occur along with grapestone, oolitic intraclasts, micritized grains, bladed calcite rinds, and hardgrounds all suggesting sea floor lithification.

Syntaxial calcite overgrowths are common on echinoid fragments in the Trenton and Black River rocks of the Appalachian basin (Appendix II, Syntaxial Overgrowths Examples #1 and #2). Such cements are reported from meteoric, marine, and burial diagenetic environments (Scholle and Ulmer-Scholle, 2003), ands require careful geochemical and petrographic arguments in order to be diagnostic (Tucker and Wright, 1990). We interpret the syntaxial overgrowths in the Trenton and Black River Formations

as products of marine and/or burial diagenesis because of their association with other marine cements in the rocks and the lack of any evidence for exposure to the meteoric environment (i.e., lack of grain dissolution and no evidence whatsoever of karst processes). Poikilotopic spar is likewise common (Appendix II, Poikilotopic spar Examples 1#1 and #2) and we interpret it to be of marine and/or burial diagenetic origin too.

Drusy mosaics of calcite spar fill most primary pore space in the Trenton and Black River Formations in the Appalachian basin (Appendix II, Equant Calcite Spar Examples #1 and #2, Drusy Spar Examples #1 and #2). The precipitation of this calcite spar followed chemical compaction of the limestones (Appendix II, Compaction Examples #5 and #6) indicating that these are clearly burial diagenetic environment cements (Wright and Tucker, 1990, p.352). Additional observations supporting this conclusion include broken and collapsed micrite envelopes within the spar and fractured grains cemented by the spar.

Neomorphism

A number of neomorphic fabrics occur in the Trenton and Black River rocks of the Appalachian Basin (Appendix II). Microspar and pseudospar commonly replace micrite in muddy carbonate rocks. Most of this is aggrading neomorphism (Appendix II, Neomorphism examples #1 - #3). Microspar and pseudospar also commonly replace allochems (see Appendix I, Coral Example #2 and #3).

Replacement

Numerous noncarbonate minerals replace both limestone and dolomite in the Trenton Formation and Black River Group. These include chert, chalcedony and quartz, feldspar, iron sulfides and oxides, sphalerite, fluorite, phosphate, sulfates, and chlorides. Some examples follow.

Chert and chalcedony replace both limestone and dolomite in the Trenton and Black River rocks throughout the Appalachian basin. Appendix II (silicification examples 31 - #4) and Figure 9 include examples of this replacement. Chalcedony that replaces hydrothermal dolomite is length-slow (Figure 9), possibly implying that the replacement took place in a sulfate-rich, aqueous environment (Folk and Pittman, 1971; Scholle and Ulmer-Scholle, 2003).

Compaction (including pressure solution)

Compaction fabrics in the Trenton and Black River carbonates are widespread throughout the basin. They include mechanical compaction features such as plastic deformation of soft grains and brittle fractures in grains, and chemical compaction features such as cocavo-convex and sutured contacts between grains, dissolution seams, and stylolites. Examples of these are provided in Appendix II.

Dissolution

There is very little evidence for dissolution features in the limestones of the Trenton and Black River in the basin. This is consistent with what is known of the Ordovician carbonate systems on a global scale (Markello and others, 2005), and with recent work on the local scale by Harris (2005) and Smith and others (2005). Limestone dissolution adequate for creating commercial reservoirs is restricted to processes associated with dolomitization adjacent to fractures. These are discussed below.

Dolomite Textures, Diagenesis and Porosity

Several prolific petroleum reservoirs are hosted in dolostones in the Black River Group in south central New York and north central Pennsylvania. Equally productive dolostone reservoirs in the Trenton Formation were developed in northwestern Ohio in the late 1800's and early 1900's and produced that state's only giant field (Wickstrom and others, 1992). Recent exploration in Ohio has discovered Trenton and Black River dolostone reservoirs in the north central and northeastern parts of the state. Similar dolostone reservoirs in these rocks and their equivalents produce petroleum in Kentucky, Tennessee, Michigan, Ontario and elsewhere. The petrographic and related petrophysical characteristics of the dolomite reservoir rocks are of great interest to geologists and engineers working in this play. It is clear that these petroleum reservoirs developed in hydrothermal dolomites, that these hydrothermal dolomites formed in the subsurface during the interaction of hot saline brines with the carbonate country rock, and that the hydrothermal brines migrated into the rocks they altered via faults, specifically basement-related faults with some strike-slip component (Wickstrom and others, 1992; Smith and others, 2005). It also is clear from petrographic studies that the hydrothermal fluid flux, which generated the dolomite, both created and destroyed reservoir porosity in these essentially tight rocks. The porosity and permeability distribution and evolution in the Black River and Trenton dolostone reservoirs is a direct function of 1) fractures and 2) variable reaction stoichiometry during limestone replacement and/or dolomite recrystallization as hydrothermal brines moved through these rocks via fault-related fractures.

Two basic dolomite textures exist in sedimentary rocks- planar dolomite and nonplanar dolomite (Woody and others, 1996). Planar dolomite crystals have straight boundaries, whereas nonplanar dolomite crystals have curved, lobate, serrated, indistinct, or otherwise irregular boundaries, and often have undulatory extinction (Sibley and Gregg, 1987, p. 970). Planar dolomite forms in both near-surface and burial diagenetic environments. Near-surface diagenetic environments extend to a few hundred meters of depth and are influenced by local groundwater flow systems; burial environments extend from the near surface to depths in excess of 3000 m and are influenced by intermediate to regional groundwater flow systems (Machel, 1999). Nonplanar dolomite develops at temperatures greater than 50°C in burial environments (Woody and others, 1996). Hydrothermal dolomites represent a special case of dolomitization in the burial environment where the dolomite formed at a temperature at least 5 to 10° C higher than the temperature of the surrounding strata (Machel, 2004). Geochemical data presented by

Smith and others (2005, and in the reports of this research effort) demonstrate that the reservoir dolomites of the Black River and Trenton play in the Appalachian basin satisfy this criterion. The massive, mostly nonplanar hydrothermal dolomites of the Black River and Trenton reservoirs discussed in this report formed locally around faults in burial environments (Smith and others, 2005).

For this report we chose to use the dolomite textural classification of Wright (2001). Wright's classification combines those of Sibley and Gregg (1997) and Gregg and Sibley (1994) with the recognition of a transitional texture between planar and nonplanar dolomite. The classification has two principal categories: 1) crystal size distribution – unimodal or polymodal, and 2) crystal boundary shape – planar or nonplanar. Planar crystal boundaries are further subdivided as euhedral (planar-e) or subhedral (planar-s). Planar-c dolomite is cement that lines or fills pores and planar-p dolomite is porphyrotopic. Nonplanar dolomite occurs as anhedral dolomite mosaics (nonplanar-a), saddle dolomite (nonplanar), and porphyrotopic crystals (nonplanar-p). Our complete textural description includes recognizable grains, matrix, and cement. Allochems and cements may be unreplaced, partially replaced, or completely replaced. Replacement may be mimetic or non-mimetic. Figures A3-1 through A3-9 show some of the various types of dolomite textures we observed in the Trenton and Black River rocks of the Appalachian basin.

There are two distinct types of dolomite in the Trenton and Black River rocks of the Appalachian basin- planar and nonplanar dolomites. The first type of dolomite (TYPE I) consists of micron- to centimicron-size (usually decimicron-size) planar dolomites. Most of this dolomite is matrix-selective replacement dolomite, but some planar-p and planar-e dolomites locally replace allochems too, and we observed a few examples of void filling planar-c dolomite cement (Figure A3-5). These planar dolomites are pervasively developed in thin beds of supratidal and intertidal carbonate facies (Figure A3-3B), and also occur in all subtidal facies throughout the basin as common, but intermittent lenses, laminae, and very thin beds (Figure A3-2C). The former planar dolomite probably formed in peritidal environments through reflux and/or mixing zone dolomitization; the latter formed on a local scale in buried subtidal sediments via compaction-driven fluid flow (see Machel, 2004, Figure 19). The planar dolomite textures also occur as a limestone replacement adjacent to faults; these crystals are probably hydrothermal (Smith and others, 2005; Harris, 2005), and clearly predate later nonplanar dolomite.

The second type of dolomite (TYPE II) consists of decimicron- to millimeter-size (usually centimicron-size) transitional and nonplanar dolomites. Planar-s to nonplanar (transitional) dolomite and nonplanar-a dolomite occur as an obliterative replacement of limestone (matrix and allochems) and as neomorphic recrystallization of planar dolomite. Nonplanar (saddle) dolomite occurs as pore-lining and pore-filling cement. The transitional and nonplanar dolomites occur only in association with localized, basement-related faulting and fracturing, and are most likely hydrothermal in origin (see Wickstrom and others, 1992, Harris, 2005, and Smith and others, 2005).

The iron content of both types of dolomite is highly variable throughout the basin. Harris (2005) reports that fault-related, relatively early planar dolomites in central Kentucky are nonferroan, with some iron zoning evident in the crystals, and that later nonplanar (saddle) type dolomites are iron-rich. Conversely, in northwestern Ohio, the so-called "cap dolomite" (texturally a planar type dolomite) at the top of the Trenton Formation there consists of ferroan decimicron-size planar dolomite (Keith, 1988,) while the fracture-associated nonplanar dolomites may be ferroan (Budai and Wilson, 1986), slightly ferroan (Taylor and Sibly, 1986), or nonferroan (Haefner and others, 1988). Other planar dolomites in Ohio (so-called "regional dolomite") reportedly are nonferroan (Taylor and Sibley, 1986; Keith, 1988). Smith and others (2005) report ferroan planar and nonplanar type dolomites in the subsurface of central New York State. Using EDS in conjunction with SEM microscopy, we measured iron concentrations from 2.17 to 4.26 wt. percent in nonplanar dolomites from New York. In Ohio samples, we measured iron concentrations from 0 to 1.5 wt. percent in planar dolomites (nonferroan) and 0.28 to 10.92 wt. percent in nonplanar dolomites. The highest iron concentrations occur in nonplanar (saddle) dolomite cements that line and fill pores.

Rocks recovered from most of the Trenton and Black River dolostone reservoirs in the Appalachian basin exhibit a complex combination of planar and nonplanar crystal textures. It is clear that epigenetic dolomitization and neomorphic dolomite recrystallization took place in response to exposure of the rocks to hydrothermal mineralizing fluids, and the resultant textures overprint both precedent limestone diagenetic fabrics and earlier diagenetic dolomites textures.

Association with Base-Metal Sulfide Mineralization

The formation of dolomite reservoirs in the Black River and Trenton Formations was a direct result of massive geochemical and textural alteration of their precursor carbonate mineralogy and fabric by hydrothermal, basinal saline brines (Davies, 2000; Gregg, 2004; Smith and others, 2005, and data generated during this research). These alterations included 1) dolomitization of limestone and neomorphic recrystallization of planar dolomites, 2) iterative precipitation of pore-filling nonplanar (saddle) dolomite, calcite, quartz, sulfates, halides, sulfides, and supergene metal oxides alternating with intervals of 3) carbonate dissolution. Appendices 3 and 4 and 5 include examples of all of these alterations. Geochemical evidence for the hydrothermal origin of these alterations is given elsewhere in this research by Smith, and will be presented in final form at the conclusion of this project.

This association of hydrothermal dolomitization and base-metal sulfide mineralization adjacent to faults is directly responsible for reservoir porosity and permeability in the Trenton and Black River carbonates of the Appalachian basin. These carbonates were rendered remarkably tight by limestone diagenesis, particularly marine diagenesis on and just below the sea floor, and by neomorphism during early burial. Excellent commercial porosity and permeability developed only where the hot basinal brines invaded the Trenton or Black River limestones via fault-related fractures. Dolomitization did more to reduce and destroy porosity, however, than it did to enhance

it (Figure 10). Fractured limestones in these formations are productive in West Virginia and Kentucky, but these fields do not have the same kind of reserves or sustained production as those developed in dolomite in Ohio, New York, or Pennsylvania.

All of the dolomite fabrics observed in these rocks developed before significant chemical compaction took place, an observation that constrains the timing of fracturing and hydrothermal dolomitization.

Porosity and Permeability

We use two fundamental porosity classifications in this report. The first is that of Choquette and Pray (1970), which defines the basic type of porosity present in a carbonate rock, and then provides an indication of the pore space's genesis and abundance. In this texturally descriptive scheme, the voids are fabric selective, not fabric selective, or some combination thereof. The carbonate components, crystals, or other physical structures in the rock control fabric selective pores – the voids do not cross the boundaries of these features. Pores that are not fabric selective do cross the component boundaries and are larger that the carbonate allochems or crystals that contain them. We also use the carbonate pore size classification of Luo and Machel (1995), which relates pore size to the fluid flow characteristics of the reservoir rock.

There are distinctive pore textures in Trenton and Black River dolograinstones, dolopackstones, dolowackestones, and dolomudstones. In the productive dolograinstones and dolopackstones of northwestern Ohio, the porosity development is partially related to depositional texture. This depositional texture may or may not be readily recognizable to the unaided eye. The reservoir rocks consist of planar-s to nonplanar-a and saddle dolomite. Macroporosity is not fabric selective, and consists of small to medium vugs and fractures. Mesoporosity is fabric selective, and consists of moldic and intercrystalline voids. Microporosity is both intercrystalline and intracrystalline. Porosity developed through a combination of fracturing, selective dissolution of allochems (usually crinoids), and dissolution of both calcite and dolomite. Appendix 5 includes numerous examples of these pore textures.

Dolowackestones and dolomudstones are the most productive reservoirs in the Trenton and Black River play in the Appalachian basin. The depositional texture of these rocks is readily recognizable (see Appendix 5). These rocks consist of planar-s to nonplanar-a dolomites and saddle dolomites. Macroporosity is not fabric selective, and consists of 1) voids associated with zebra and breccia fabrics, 2) small to large vugs, and 3) fractures. Mesoporosity is fabric selective, consisting of intercrystalline and moldic voids. Microporosity is both intercrystalline and intracrystalline. Porosity developed through fracturing, associated brecciation, and dissolution of both calcite and dolomite. Appendix 5 provides several examples of these pore textures.3

Petrophysical Considerations

The dominance of vuggy porosity in Trenton and Black River reservoirs, and their association with intercrystalline and fracture voids, yields a complex pore geometry. The predominance of planar-s to nonplanar dolomite textures means that we can expect bimodal to intermediate Hg capillary pressure curves with steep gradients in these rocks, reflecting poorly interconnected pore networks with large pore to throat size ratios (Woody and others, 1996). The best reservoirs occur where fractures provide interconnections between large dissolution voids yielding collapse breccias and adjacent zebra fabrics. Geologists and engineers should anticipate the fact that the Archie equation is unreliable for geophysical log evaluation of these reservoirs and use appropriate alternate techniques (Asquith, 1985).

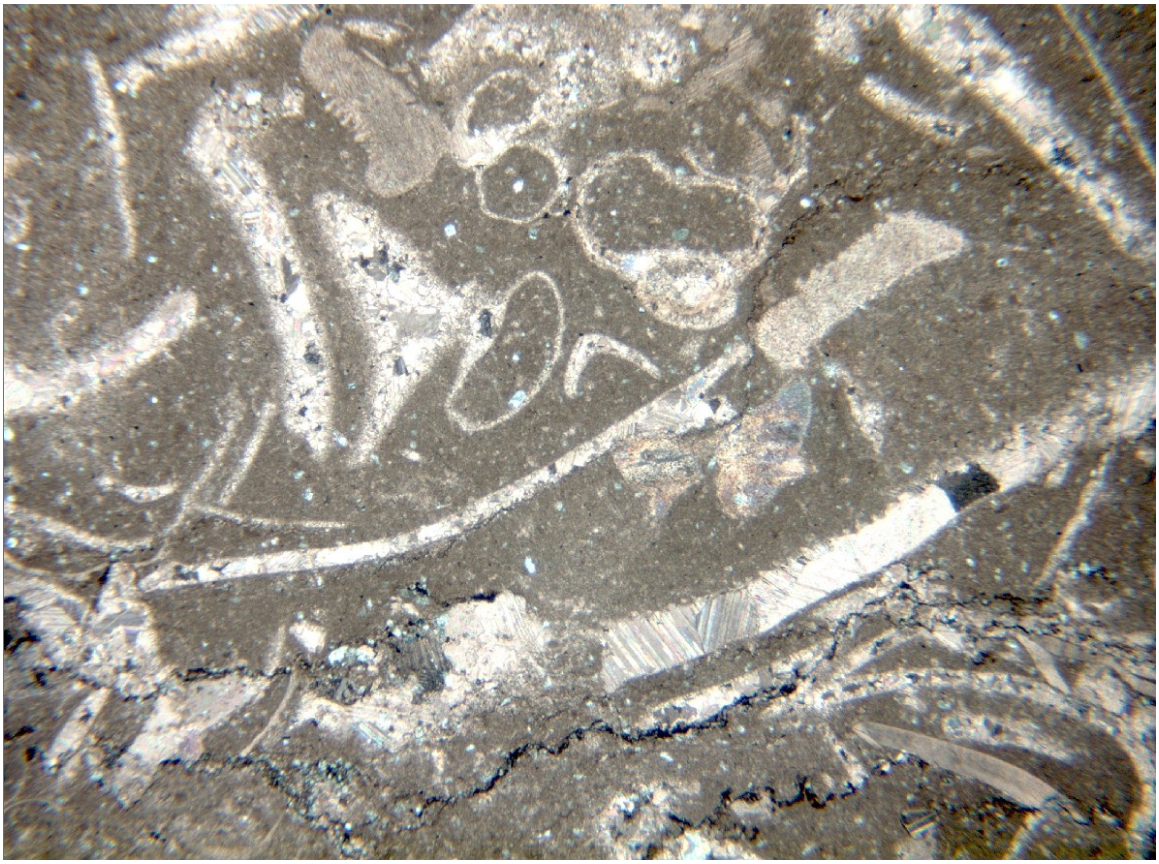

Figure 3-1A. Carbonate matrix in the Trenton Limestone and Black River Group. A. Skeletal wackestone (Dunham, 1962) or a packed biomicrite (Folk, 1962) from the Black River Group, Union Furnace, Huntingdon County, PA. The matrix consists of microcrystalline calcite, or micrite, which is presumed to have formed through the breakdown of coarser carbonate grains (Scholle and Ulmer-Scholle, 2003). Note that most of the skeletal material has undergone neomorphic recrystallization or solution followed by cavity filling with calcite cement.

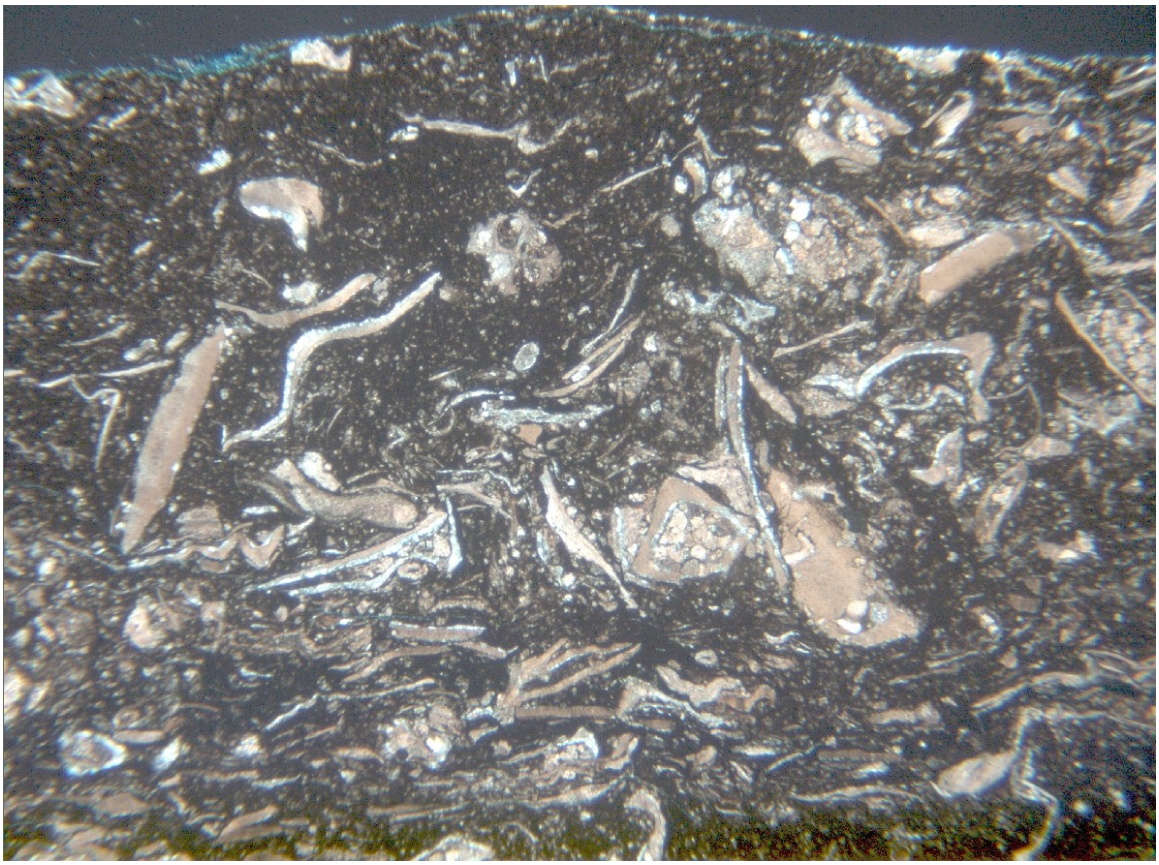

Figure 3-1B. Carbonate matrix in the Trenton Limestone and Black River Group. B. Dark organic-rich matrix in a skeletal wackestone or packed biomicrite from the Trenton Formation at Union Furnace, PA. The carbonate matrix material consists of microspar (crystals 5 - 20μm in size) presumably recrystallized from micrite. The dark, clotted organic matrix matter is kerogen.



Figure 3-2. Limestone tempesites or turbidites interbedded with siliciclastic shales in the Trenton Formation at Union Furnace, PA.

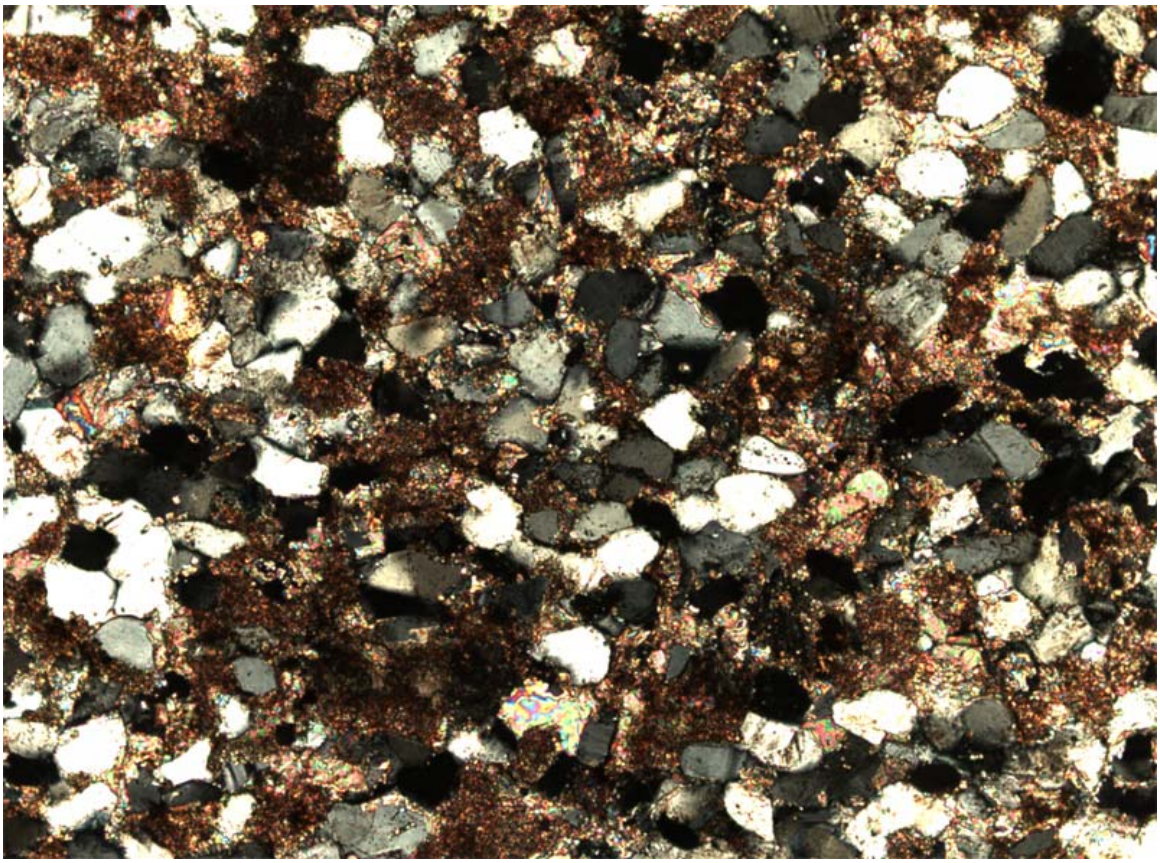

Figure 3-3A. Very fine-grained quartz arenite from a very thin sandstone bed in the Black River Group, Union Furnace, Huntington County, PA. A. Low magnification view (crossed polars) showing well sorted subrounded grains of quartz and minor feldspar cemented by calcite microspar and some anhydrite.

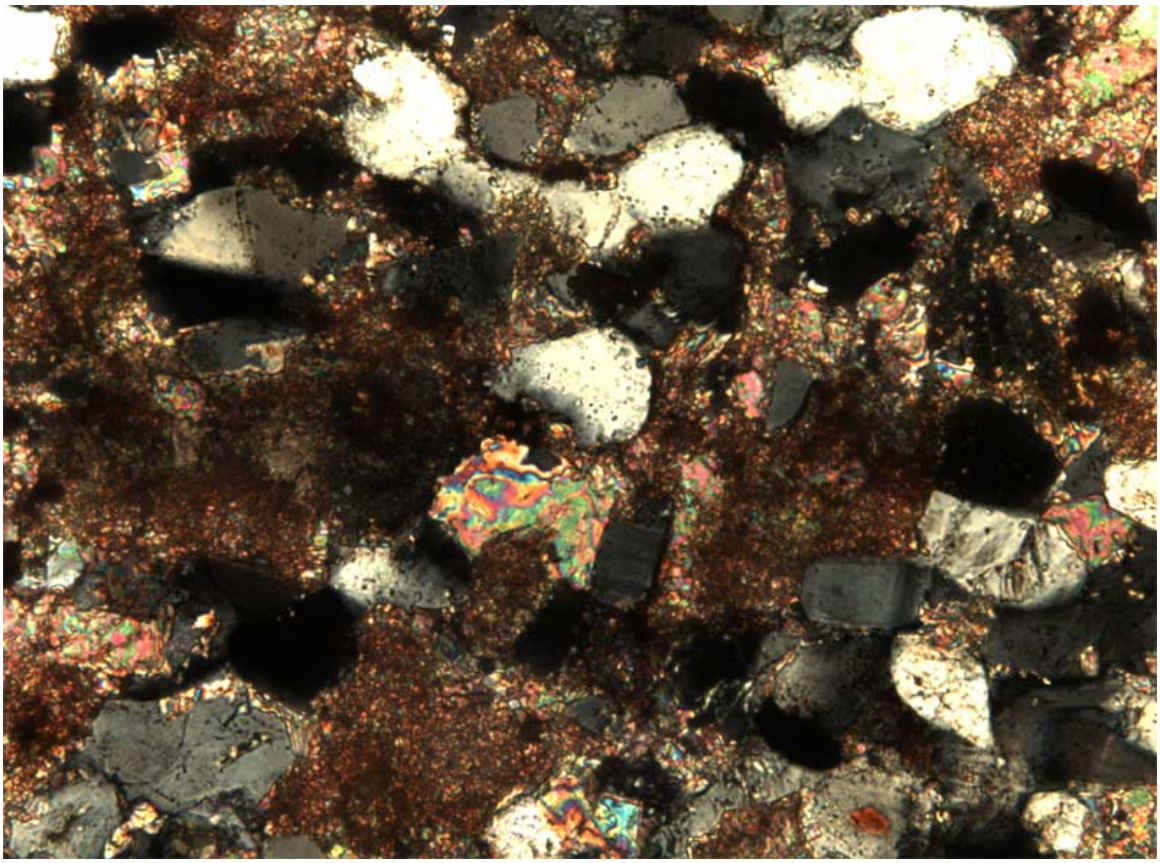

Figure 3-3B. Very fine-grained quartz arenite from a very thin sandstone bed in the Black River Group, Union Furnace, Huntington County, PA. B. Higher magnification view of sandstone shown in Figure 3A showing calcite and anhydrite cements and feldspar grains.



Figure 3-4. K-bentonites in the Trenton Limestone and Black River Group. A. Deicke k-bentonite exposed at Union Furnace, PA. B. Millbrig k-bentonite recovered in core of the Trenton Formation cut 500 ft. west of the Union Furnace outcrop. C. Millbrig k-bentonite at 1550 ft. in the Chevron 1A Prudential core, Marion County, OH.

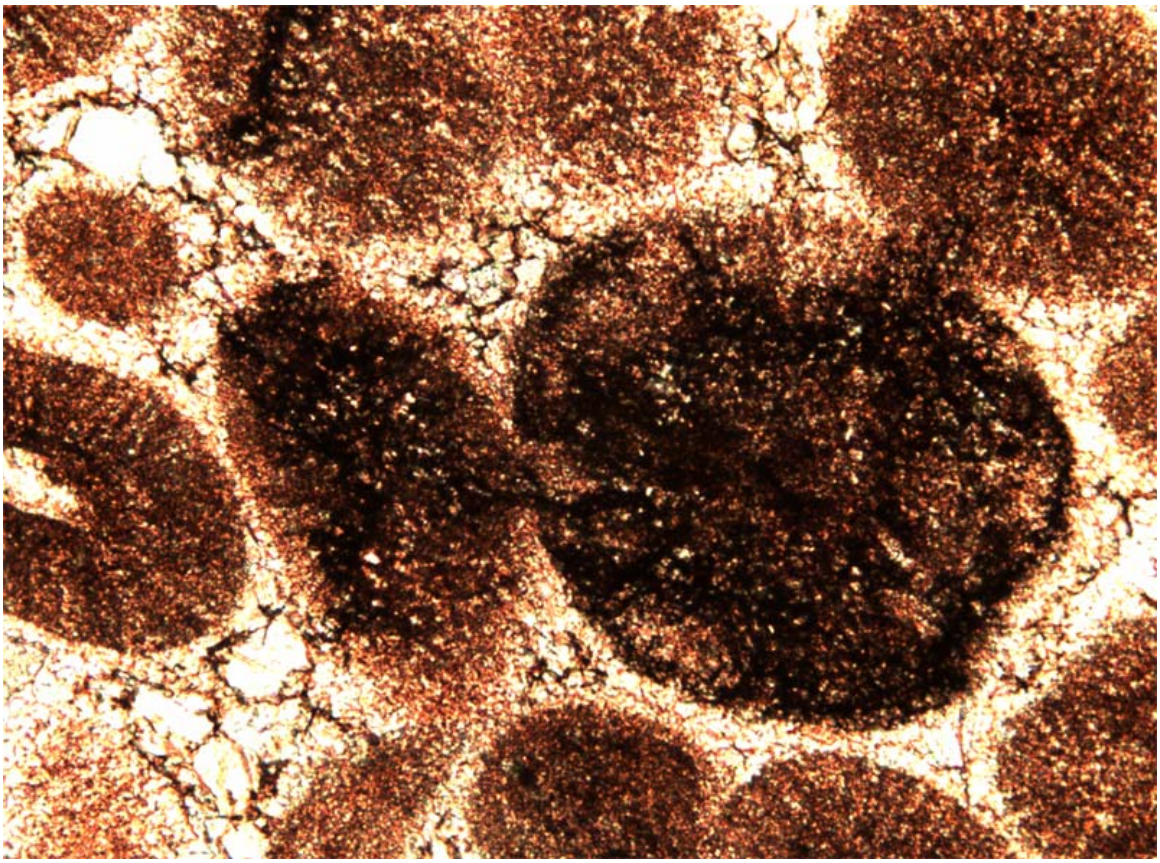

Figure 3-5. Completely micritized ooids in the Black River Group.

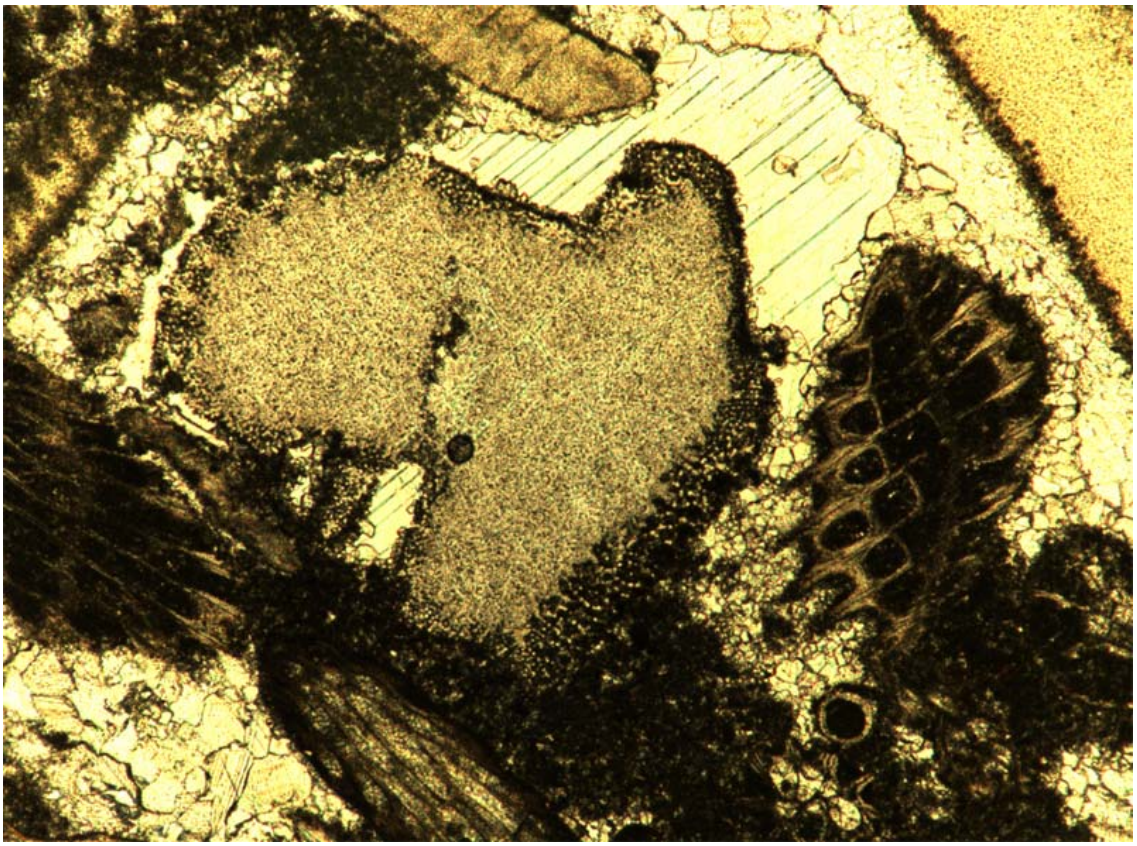

Figure 3-6A. Micrite envelope on echinoid grain and peloidal cement. A. The large echinoid fragment in the left-center of the photomicrograph exhibits a bored rim and well-developed micrite envelope

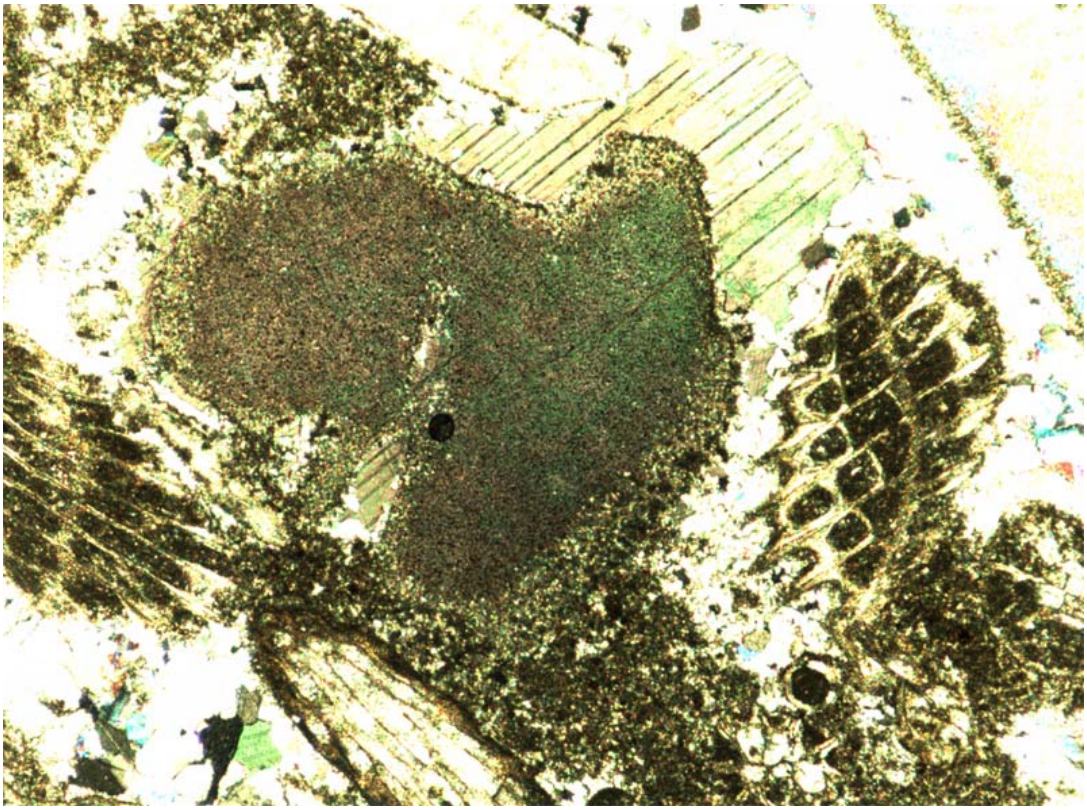

Figure 3-6B. Micrite envelope on echinoid grain and peloidal cement. B. The same photomicrograph in cross-polarized light reveals that the micrite envelope actually consists of calcite cement with a peloidal texture. Note that this peloidal cement grades into coarser peloidal cement that fills some of the pore spaces adjacent to the grain in the southeast and northwest quadrants. Identical peloidal cement fills the zooecia of bryozoan grains.

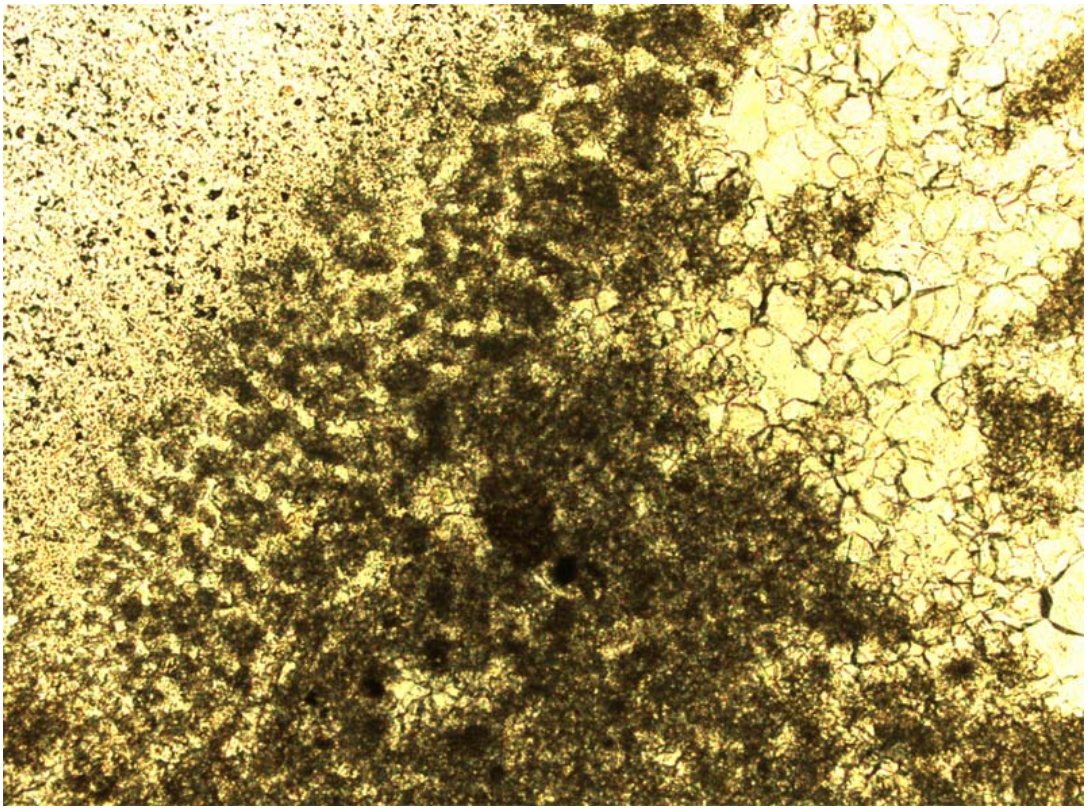

Figure 3-6C. Micrite envelope on echinoid grain and peloidal cement. C. High magnification view of the peloidal cement that fills both the bored edge of the echinoid grain and the void space immediately below it. The rest of the void space is filled with calcite spar. Montgomery #4 well, Mercer County, PA. Trenton Formation, 8495 ft.



Figure 3-7A. Peloidal cement fabric in the Black River Group. A. Core sample of apparent burrowed and bioturbated wackestone (Dunham, 1962) or sparse biomicrite (Folk, 1962). Gray #1 well, Steuben County, NY, 7823 ft.).

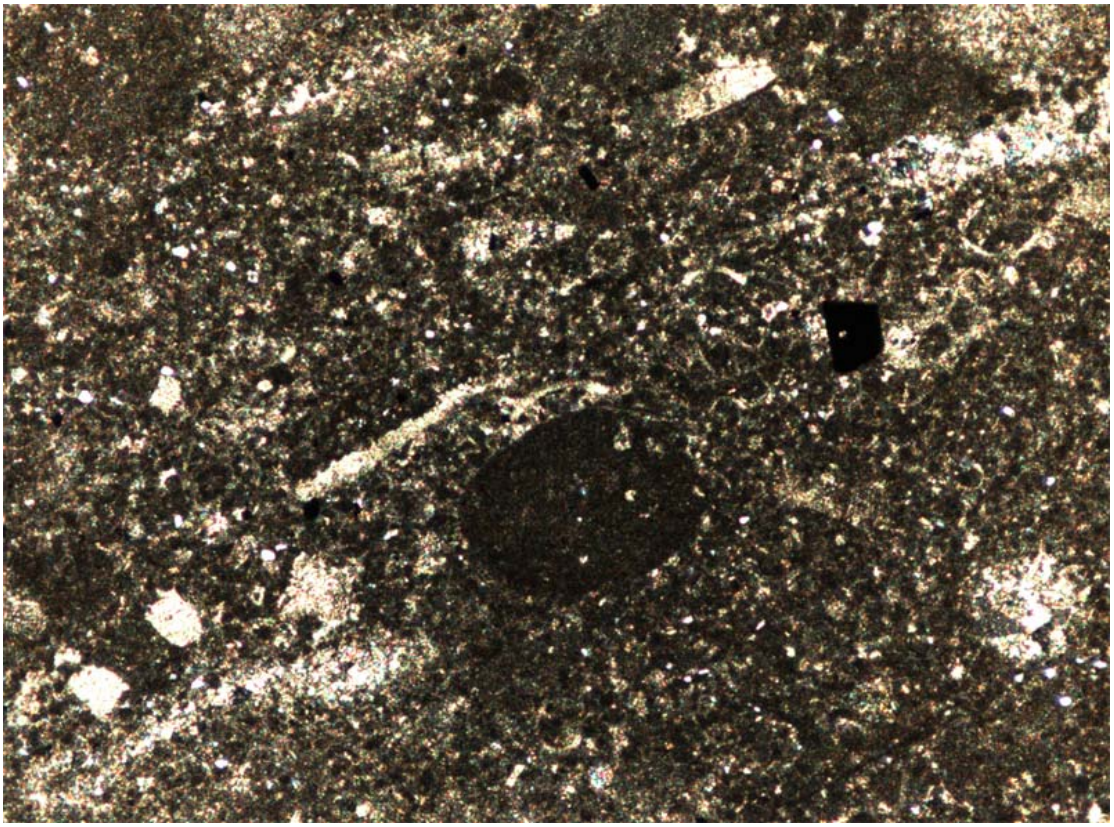

Figure 3-7B. Peloidal cement fabric in the Black River Group B. Thin section photomicrograph of the same sample. Peloids comprise 75% of the limestone. Based on this information we can modify the Folk (1962) name for this rock to a sparse biopelmicrite. Using the Dunham (1962) classification we could rename the rock a peloidal/mixed-fossil grainstone, which is erroneous because the peloids are not grains but are cement.

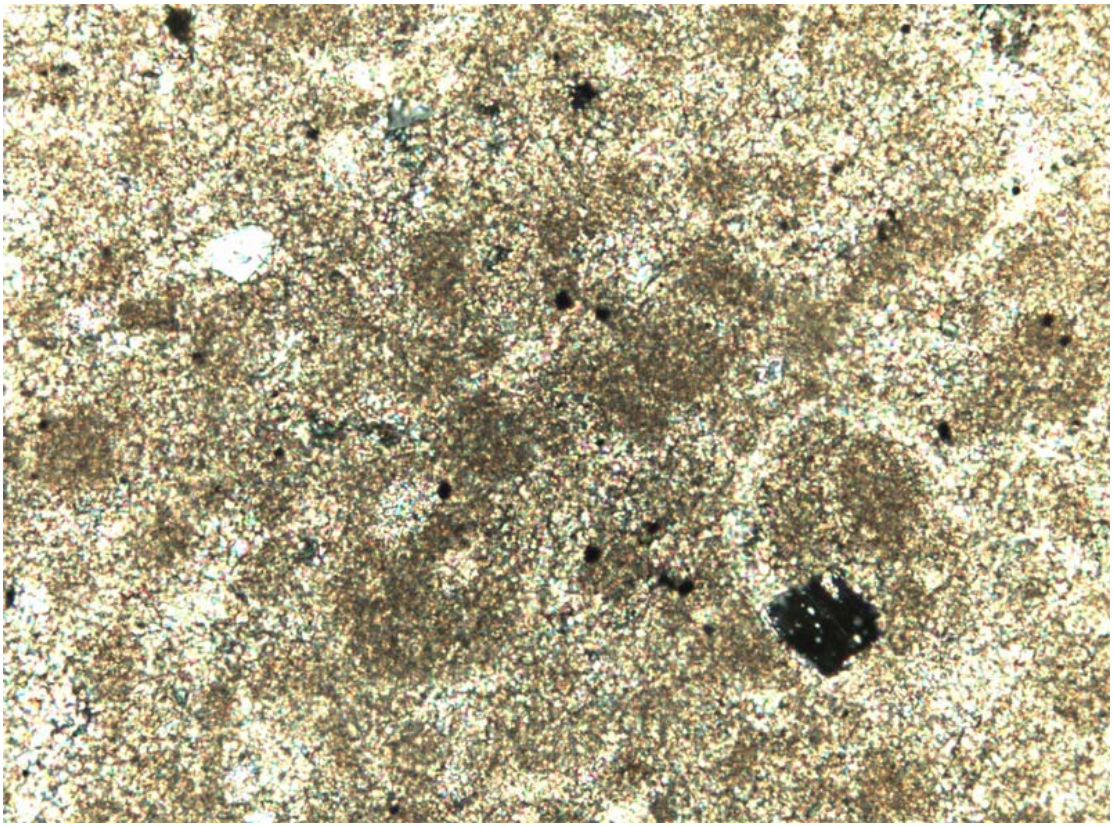

Figure 3-7C. Peloidal cement fabric in the Black River Group C and D. Progressively higher magnification views of the same sample. Note that the peloids consist of 1) a dark nucleus of micron-size calcite (opaque clots) surrounded by 2) rims of euhedral microspar.

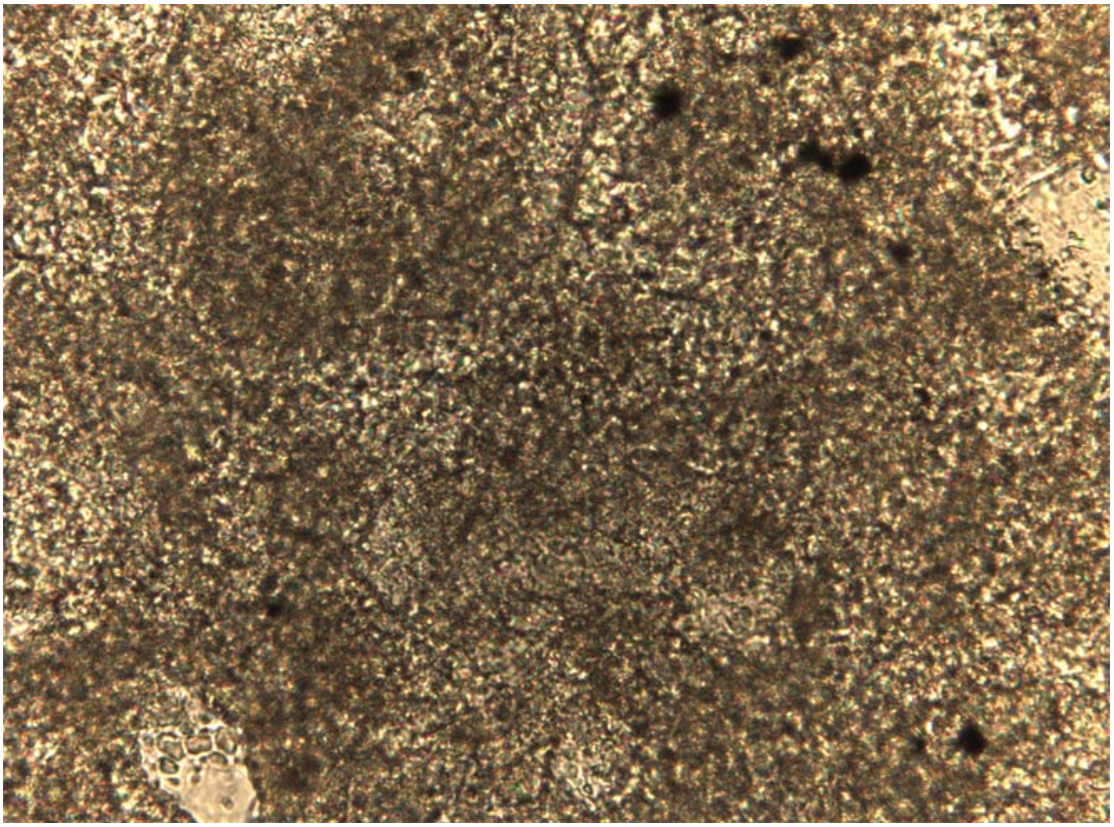

Figure 3-7D. Peloidal cement fabric in the Black River Group C and D. Progressively higher magnification views of the same sample. Note that the peloids consist of 1) a dark nucleus of micron-size calcite (opaque clots) surrounded by 2) rims of euhedral microspar.

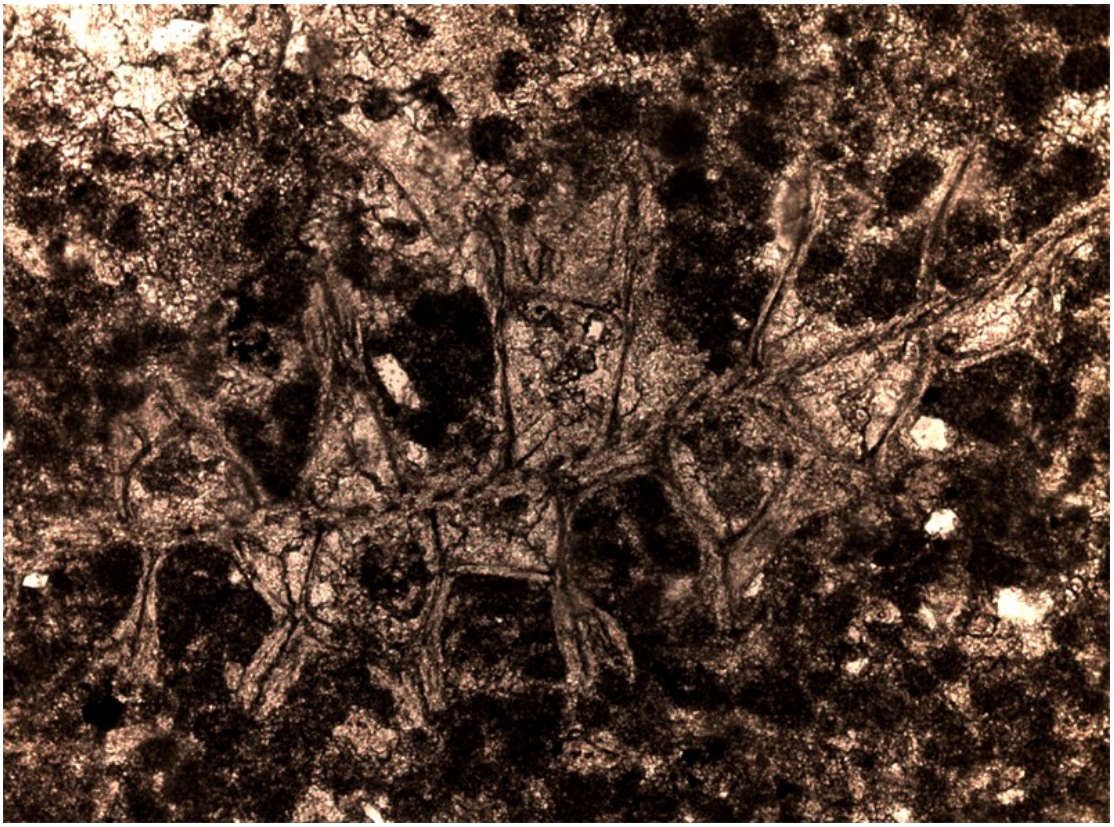

Figure 3-7E. Peloidal cement fabric in the Black River Group E. Another thin section view of peloidal cement in the same sample. Here peloidal cement fills the zooecia of a bryozoan fragment as well as lithifies the matrix.

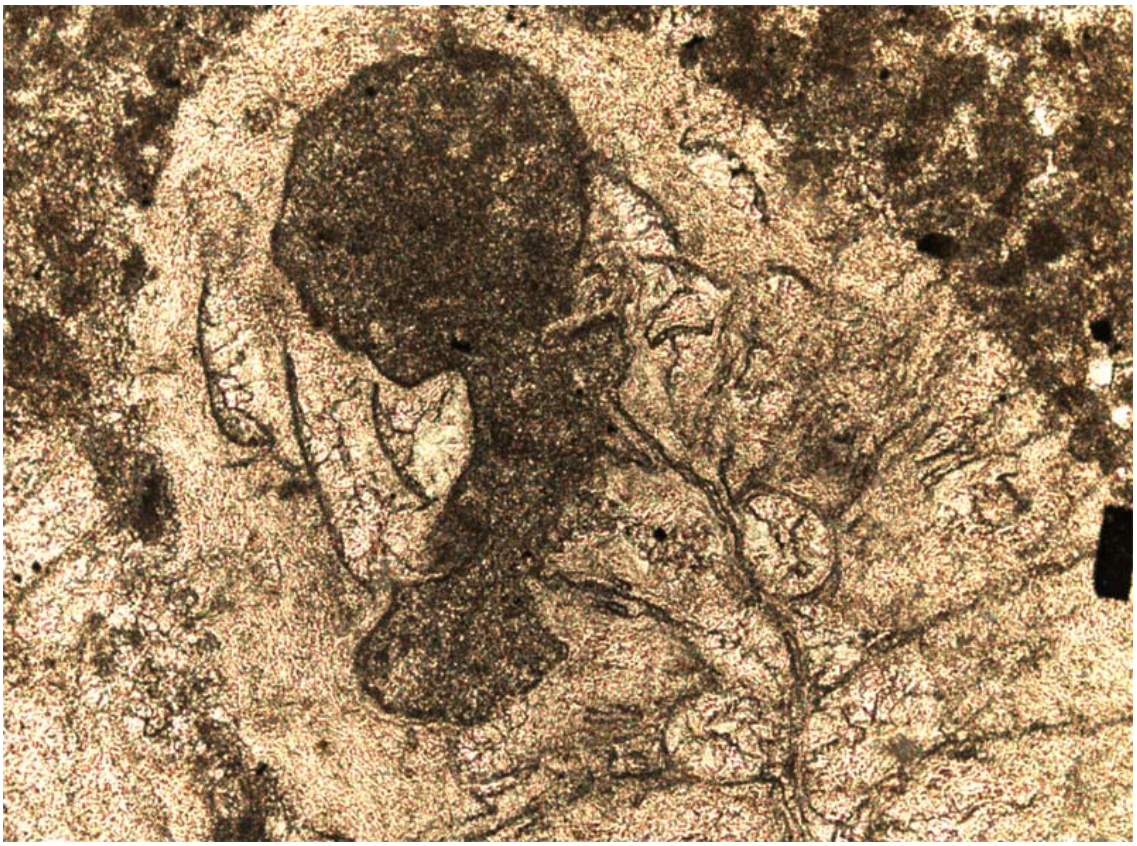

Figure 3-7F. Peloidal cement fabric in the Black River Group F. Peloidal cement fills a void formed earlier through dissolution of part of a bryozoan fragment.

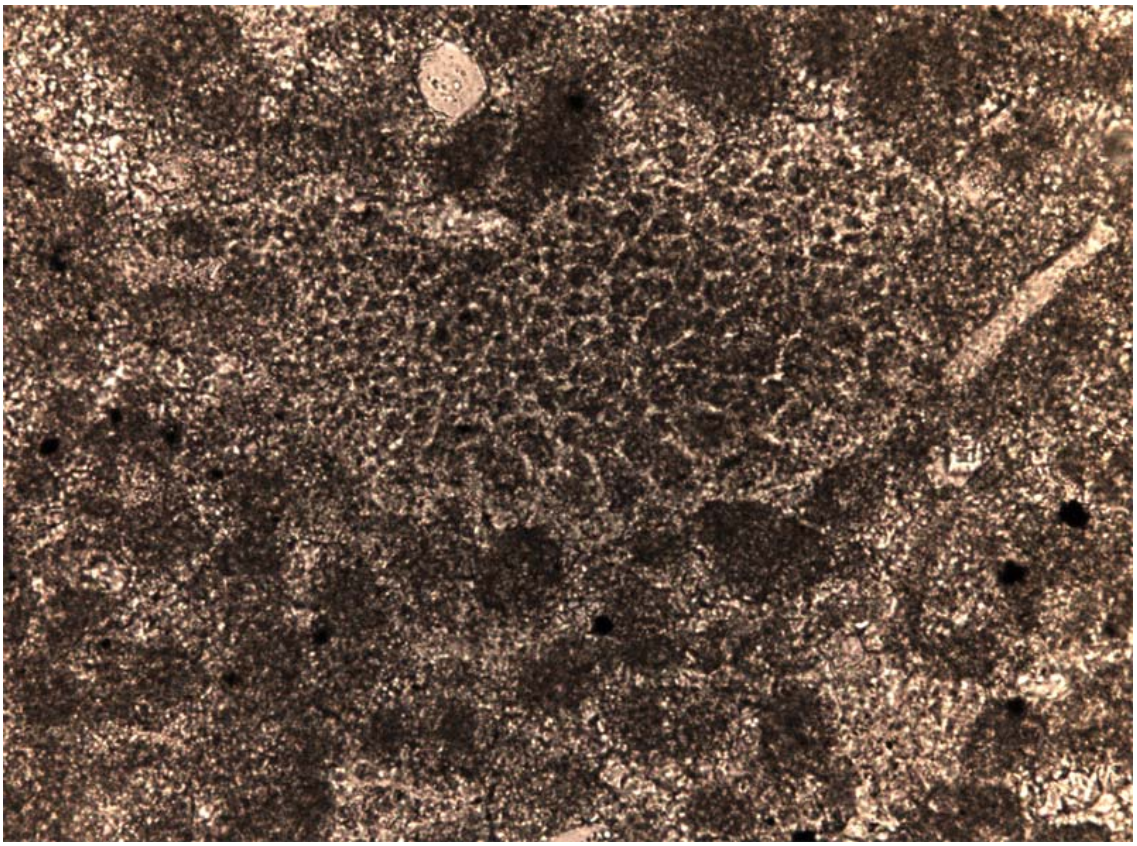

Figure 3-7G. Peloidal cement fabric in the Black River Group. G. Peloidal cement that once filled all of the zooecia of a bryozoan grain now mimics the original fossil structure.



Figure 3-8A. Hardgrounds and peloidal cements. A. Stacked, amalgamated hardground in the Trenton Formation exposed southeast of Lexington in central Kentucky. The finger points to the surface of a smooth and rolling hardground, but those beneath exhibit hummocky, undercut, pebbly, and reworked morphologies (see Brett and Brookfield, 1984, Wilson and Palmer, 1992, and Laughrey and others, 2003).



Figure 3-8B. Hardgrounds and peloidal cements. B. Plan view of bryozoans encrusting the top of a hardground, Trenton Formation, central Kentucky.

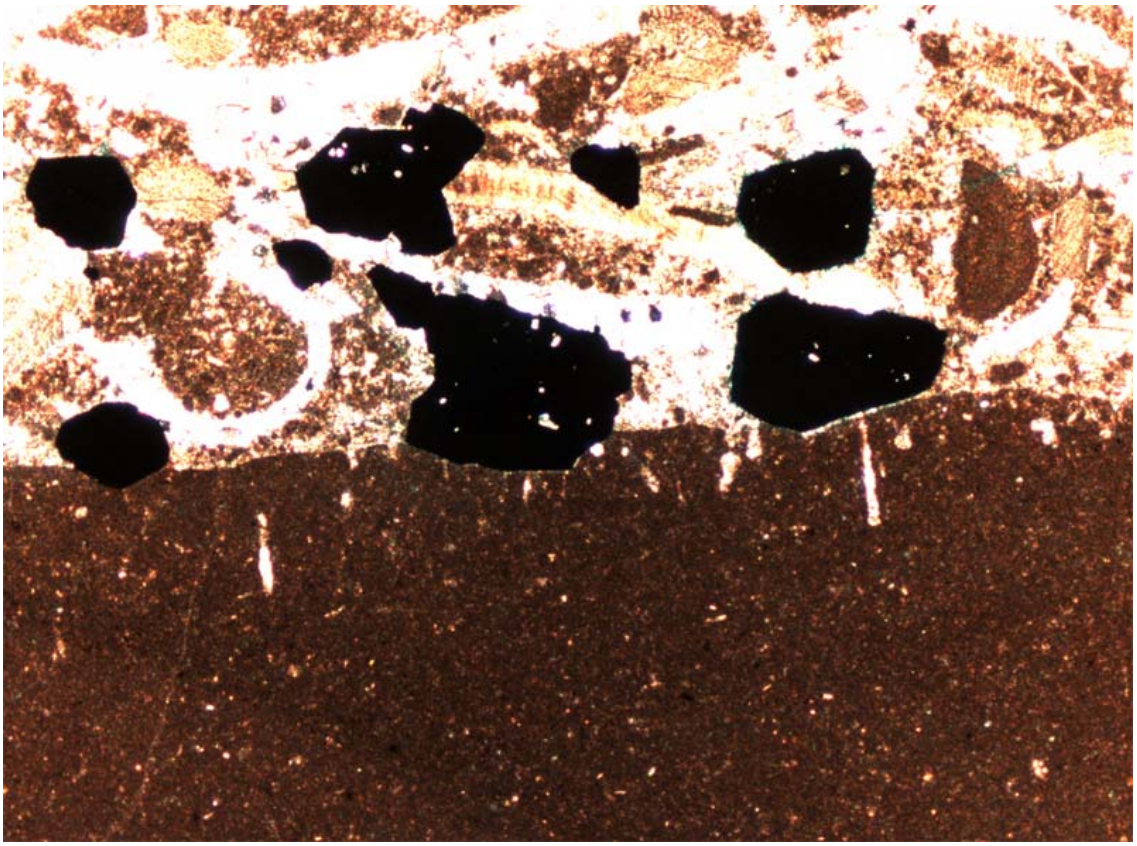

Figure 3-8C. Hardgrounds and peloidal cements. C. Thin section photomicrograph of the hardground surface that the geologist's finger points to in A. Note the peloidal cement texture of the limestone. Also note the authigenic pyrite at and just above the hardground surface.



Figure 3-8D. Hardgrounds and peloidal cements. D. A planar and undercut hardground in the Black River Group exposed at Union Furnace, Pennsylvania.

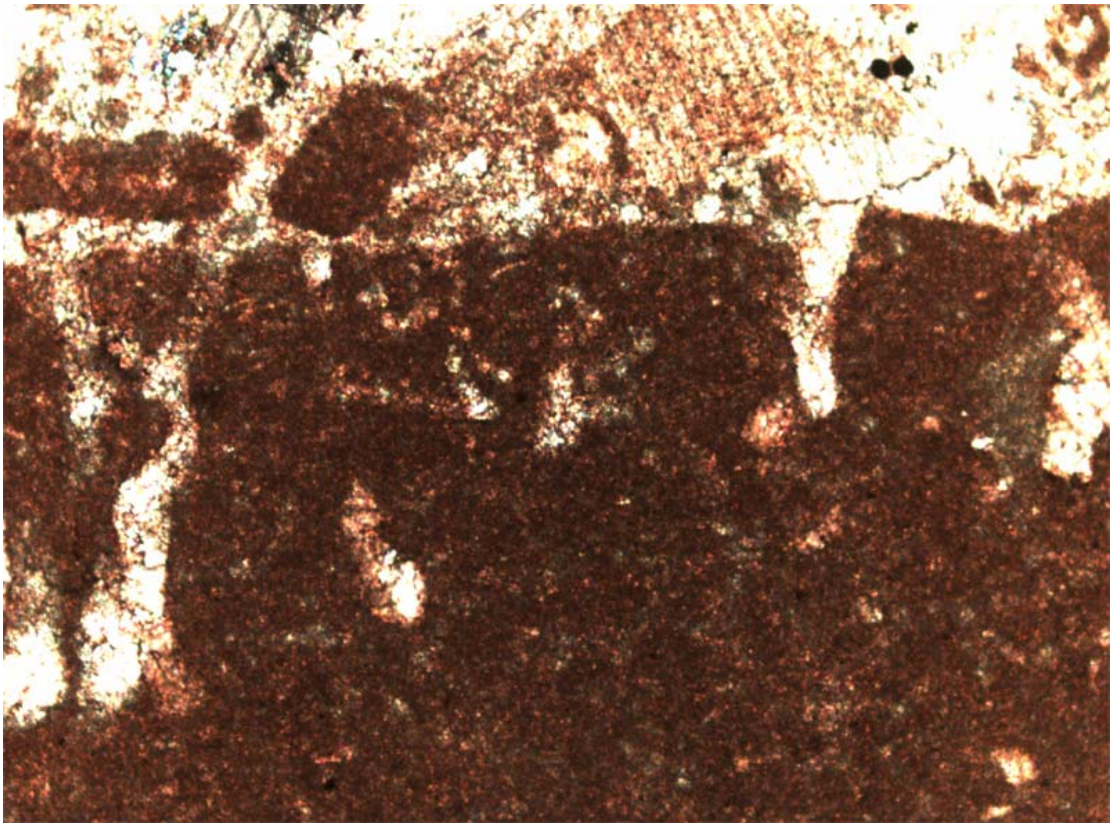

Figure 3-8E. Hardgrounds and peloidal cements. E and F. Thin section photomicrographs of the hardground shown in D. The clotted fabric characteristic of peloidal cements is evident in both photomicrographs.

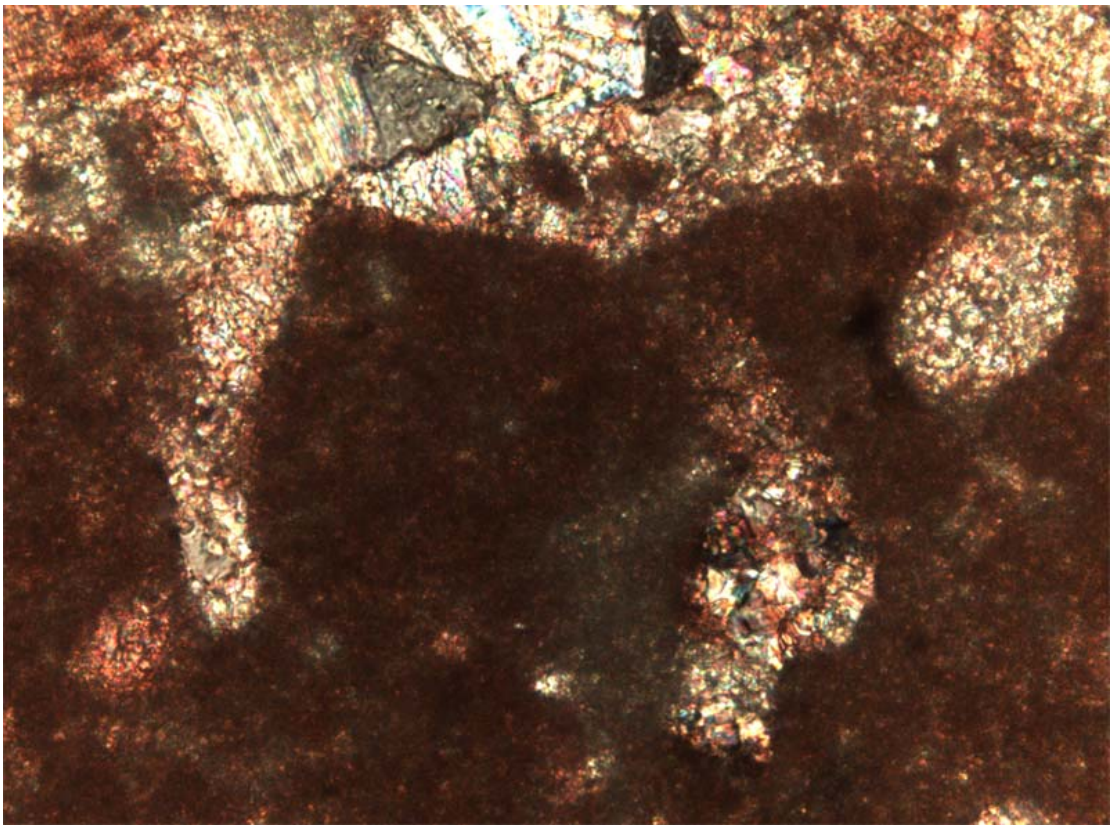

Figure 3-8F. Hardgrounds and peloidal cements. E and F. Thin section photomicrographs of the hardground shown in D. The clotted fabric characteristic of peloidal cements is evident in both photomicrographs.

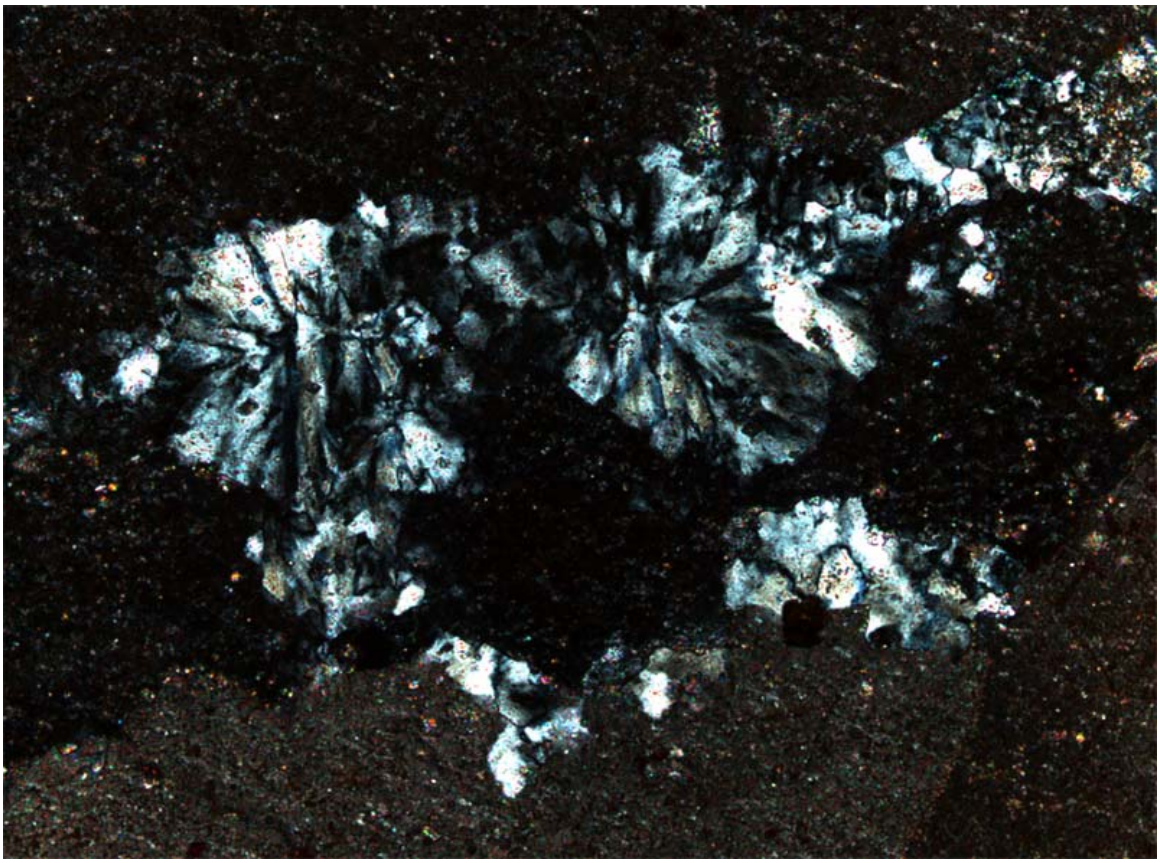

Figure 3-9A. High magnification view of chalcedony replacing nonplanar dolomite that mimically replaces a crinoid grain (see Figure A3-8 in Appendix III for additional views of this sample). A. View under crossed polars showing the typical radiating habit of chalcedony.

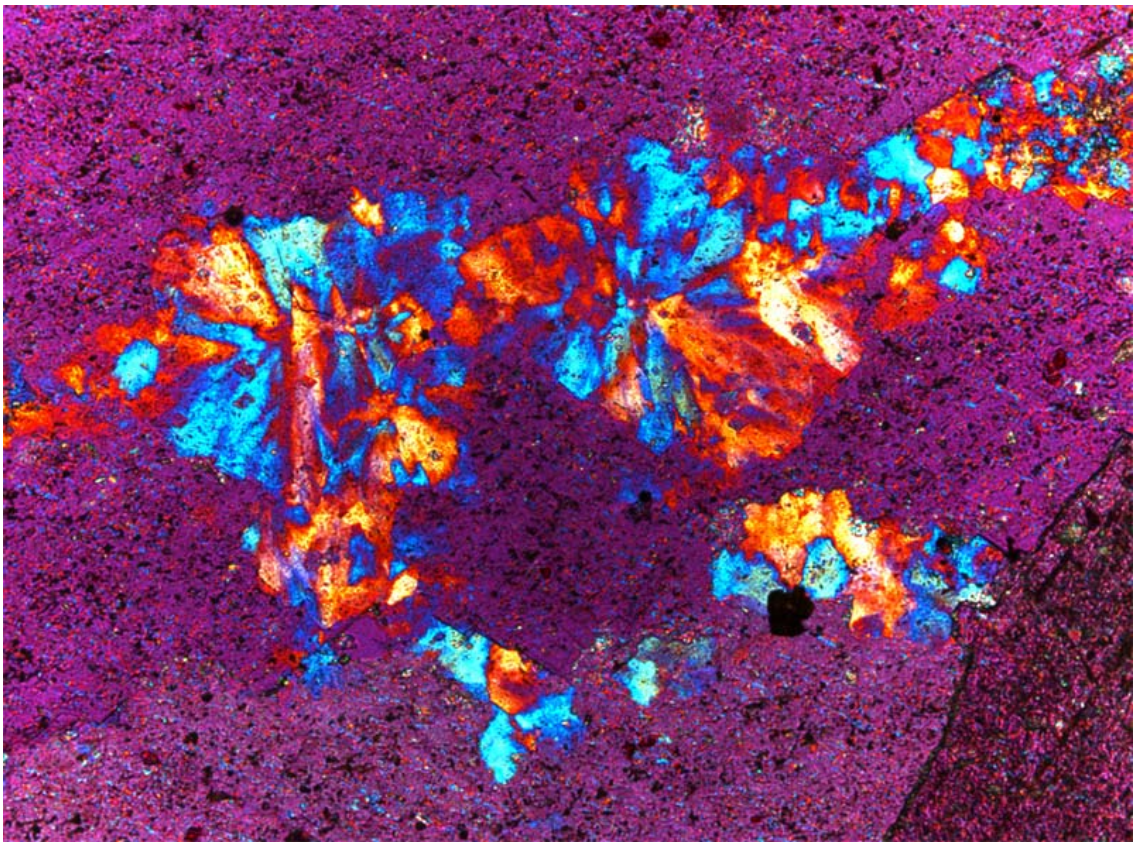

Figure 3-9B. High magnification view of chalcedony replacing nonplanar dolomite that mimically replaces a crinoid grain (see Figure A3-8 in Appendix III for additional views of this sample). B. Same view, but with the gypsum plate inserted into the microscope. The birefringence colors in the northeast and southwest quadrants increased, and the birefringence colors in the northwest and southeast quadrants decreased, indicating that the chalcedony is length-slow.

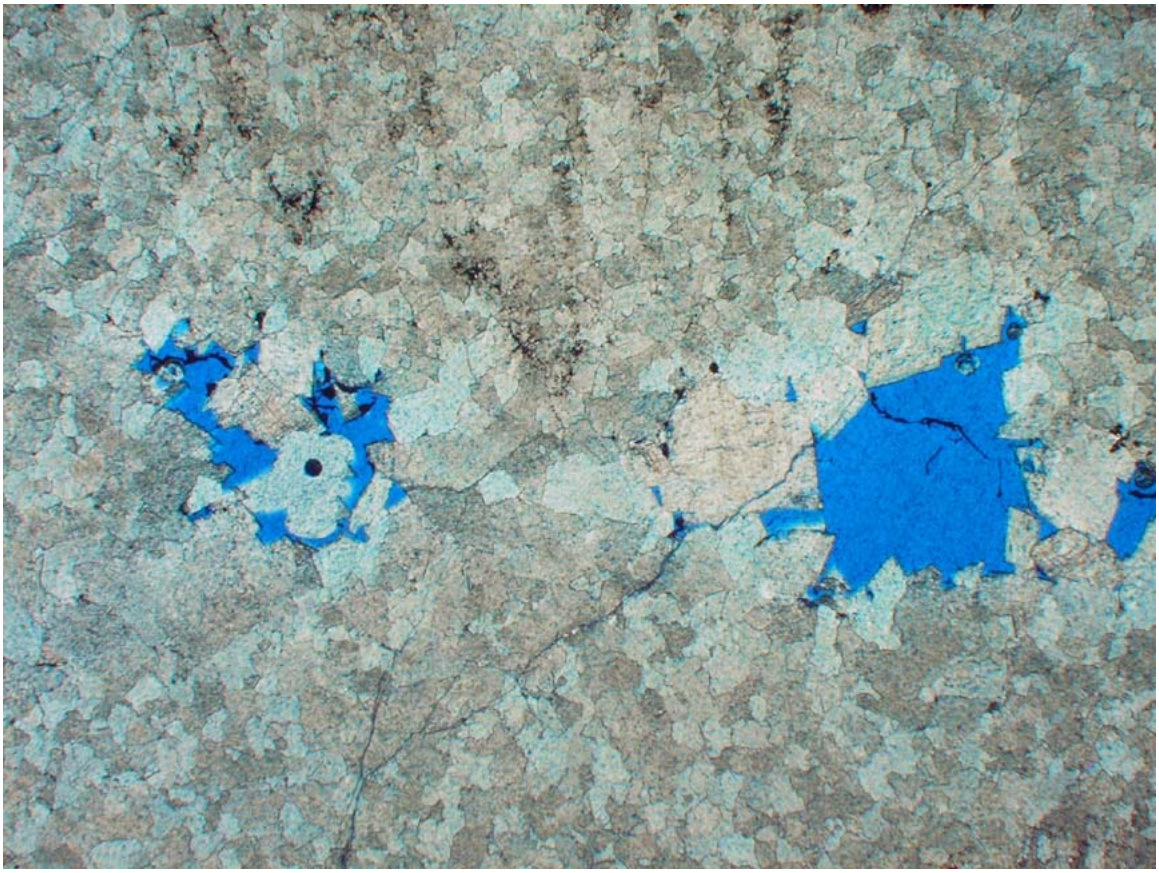

Figure 3-10. Macropores and mesopores in the Black River Group, Whiteman #1 well, Chemung County, NY, 9529 ft. Porosity consists of isolated small vugs (not fabric selective), minor intercrystalline pores (fabric selective), and fractures (not fabric selective). The rock consists of nonplanar-a dolomite, and nonplanar (saddle) dolomite cement partially fills the vugs. The vugs formed through dissolution of both calcite and dolomite. Note that dolomitization mostly obliterated porosity in this rock.

Table 3-1. Core and Outcrop Samples of Trenton Limestone and Black River Group, Appalachian Basin

New York:

- Whiteman #1 well, Chemung County. 51 thin sections (9528.5 ft. to 9557.8 ft.)
- Matejka #1 well, Chemung County. 52 thin sections (9816 ft. to 9995 ft.)
- Gray #1 well, Steuben County. 51 thin sections (7793 to 7823 ft.)

Pennsylvania:

- Bayles #1 well, Bradford County. 32 thin sections (12,415 ft. to 12,455 ft.)
- McKnight #1 well, Mercer County. 8 thin sections (6843.6 ft. to 6866.9 ft.)
- Montgomery #4 well, Mercer County. 11 thin sections (8495 ft. to 9019 ft.)
- Union Furnace outcrop, Huntingdon County, 98 thin sections

Ohio:

- Strayer #1 well, Allen County. 18 thin sections (1203.6 ft. to 1259 ft.)
- Prudential #1 well, Marion County. 38 thin sections (1481.5 ft. to 2013.5 ft.)
- Bousher #1 well, Auglaize County. 29 thin sections (1157.3 ft. to 1177.6 ft.)
- Anderson well, OH #3479, Hancock County. 32 thin sections (1321.7 ft. to 1348 ft.)
- H. Fry #1 well, Hancock County. 26 thin sections (1297 ft. to 1323.7 ft.)
- Ohio #2549 well, Wood County. 38 thin sections (1102.7 ft. to 1206.6 ft.)
- Ohio #2971 well, Wood County. 23 thin sections (1414 ft. to 1505.5 ft.)
- Ohio # 2972 well, Wood County. 6 thin sections (1463.1 ft. to 1478.3 ft.)
- Ohio #2905 well, Logan County. 7 thin sections (1508.4 to 1542.4 ft.)
- Mohring #1 well, Lucas County. 15 thin sections (1756.4 ft. to 1829 ft.)

West Virginia:

- Power Oil Company #9634 well, Wood County. 138 thin sections (9526 ft. to 10162 ft.)

Kentucky:

- Cominco American CA-35 well, Montgomery County. 67 thin sections (500.25 ft. to 1386.5 ft.)

GEOCHEMICAL AND FLUID INCLUSION ANALYSIS

By Langhorne B. Smith, New York State Museum Institute

Introduction

We have conducted a range of geochemical and fluid inclusion analyses on the Trenton and Black River limestones and dolomites in order to understand the origin of the dolomite across the study area. Understanding the origin of the dolomite helps understand where it should be located and how it should be developed. Fault-related hydrothermal dolomites should, in most cases, be played as an unconventional reservoir with a combination of structural /diagenetic traps. Hydrothermal dolomite fields commonly occur in structural lows, or sags, formed over negative flower structures. They also may form near other types of faults, including extensional margin-bounding faults or positive flower structures. Dolomites of an early origin, or those formed due to lateral fluid flow, would tend to be more widespread and traps would be more conventional four-way closures.

At the end of this Trenton-Black River play book there is a pre-print of a paper written by Langhorne Smith on the Trenton-Black River Play in New York that summarizes many of the ideas in this report in a more concise way. The purpose of this work is to present all of the data that were collected and explain how we came to our conclusions.

We conducted stable isotope, strontium isotope, trace element and fluid inclusion analyses with the goal of learning the origin of the dolomite. The combination of these analyses helps to build confidence in any interpretations. Interpretations based on each of them by themselves can be equivocal but together they can build a strong case. In general, hydrothermal dolomites have:

• Light or depleted $\delta^{18}O$ values. Oxygen stable isotope values in dolomites are directly dependent on the temperature and composition of the water. If the water has a $\delta^{18}O$ composition of +5 or +10 SMOW, even hot fluids can make heavy or isotopically enriched dolomites. Incorporation of CO_3 from the precursor limestone could also produce heavier (more positive) ^{18}O values. Because the value of the water and the rock water ratio are not known, these are the least reliable of all of the tests by themselves. When conducted in combination with other fluid inclusion analyses, however, they can be very valuable and they are also the least expensive analysis.

• Radiogenic $^{87}Sr/^{86}Sr$ ratio relative to Late Ordovician seawater. The radiogenic signature shows that fluids have flowed through continental basement rocks or feldspar rich sediments overlying the basement. Exceptions: Mafic basement rocks, resetting, incorporation of original strontium from limestone can be problems

• Higher Fe and Mn contents than the host limestones. Most of these dolomites have Mn and Fe contents that are an order of magnitude greater than the values from the limestones. Most hydrothermal fluids pick up Fe and Mn in the basement or overlying feldspar-rich sandstones. Exceptions: Some hydrothermal fluids may not interact with Fe and Mn rich rocks prior to precipitation of the dolomite.

• Fluid inclusions with homogenization temperatures >75ºC and salinities between 6 and 30 wt% (average ~20 wt % or about 6 times normal seawater).

The dolomites of the Trenton and Black River across the study area have all of these characteristics. We will demonstrate that most of these dolomites are unequivocally hydrothermal because the homogenization temperatures recorded in the fluid inclusions exceed the maximum burial temperature for most of the Trenton and Black River strata in the study area.

It is our interpretation, based on the geochemical evidence and field relations, that virtually all of the dolomite in the Trenton Limestone and Black River Group is of a hydrothermal origin. This includes the obviously fault-related dolomites in the Black River of New York, Ontario and near the Bowling Green Fault in Ohio, and the less obviously fault-related dolomite along the margin of the Sebree Trough in northwest Ohio and at the Jeptha Knob structure in Kentucky.

We also learned during the course of this project that variations in ^{13}C with depth are a powerful correlation tool for the Black River, and to a lesser extent, for the Trenton. The ^{13}C analysis creates a chronostratigraphic log, which enables correlation of same-aged strata rather than lithology. Carbon-13 is a stable isotope of carbon that is routinely analyzed when doing stable isotope analysis. These changes in ^{13}C are abrupt and can be used as a stratigraphic correlation tool when the study interval is sampled and analyzed at different sections. It is believed that these changes reflect secular variations in seawater chemistry so that changes in ^{13}C should occur in all shallow marine carbonates that are of the same age. The ^{13}C data and the bentonite stratigraphic markers show that the Trenton-Black River boundary is not a time line but actually cuts across time. This could be a very powerful tool when correlating between long distances and in places where the stratigraphic picks are not obvious.

Methods

Sampling for geochemical analysis was conducted in two ways. To obtain matrix dolomite and limestone samples a cordless drill with a masonry bit was used to make about 100 milligrams of powder. This powder was used for stable isotope analysis. The bit was cleaned after each sample was drilled and the powder was placed in small plastic vials labeled with a sample number that corresponded to the well name and depth. We also took larger samples of coarser cements and adjoining matrix dolomite using a rock saw. We powdered some of the matrix and coarse saddle dolomite and calcite cements in the laboratory and sent these powders out for stable isotope, strontium isotope and trace element analysis. We then sent the intact samples for fluid inclusions analysis. In this way we built a data set where we had all four analyses for the same samples. All tools were kept clean to avoid contamination of samples.

Fluid Inclusion Analysis

Fluid Inclusions where analyzed by Fluid Inclusion Technologies Inc, 2217 North Yellowood Avenue, Broken Arrow, OK 74012. We sent them samples of the different dolomite and cement types. The following sections on fluid inclusion analysis methods were written by Fluid Inclusion Technologies, Inc.

Sample preparation. The samples are prepared by making a standard thick, doubly polished section. A blank is cut from a blue dye impregnated sample, polished to 0.05 micron and then mounted on a slide with standard epoxy. It is then cut off to about 100 microns and polished to .05 microns. The final sample is about 70-90 microns thick. The sample is screened optically; x-y coordinates of populations we want to measure are recorded and photo-documented. Then the inclusions are circled with indelible ink and the sample is broken up into small pieces that will fit into the heating freezing stage.

Equipment. Fluid inclusion homogenization and melting temperatures are obtained on a special stage that can be heated and cooled. The heating freezing stage is a USGS type stage. It operates by passing nitrogen through a heating element and then over the sample, which sits in a special chamber designed to minimize lateral and vertical thermal gradients. The temperature is controlled with a variac. The nitrogen is either from a tank (for heating) or from a liquid nitrogen dewar (for cooling). Backpressure on a giant liquid nitrogen dewar is used to do the heating runs. The temperature is recorded by a K-type thermocouple, which sits directly on the sample chip and in fact holds it in place. It is this direct coupling that results in minimal temperature uncertainty (unlike the Linkam or Chaix Meca stages, for instance, which heat by conduction and record temperature from a more remote located PRT). Basically, you can say, the data were collected on "a USGS type heating-freezing stage manufactured by Fluid Inc. using standard techniques (Roedder, 1986, Fluid Inclusions, MSA Volume)."

Measuring homogenization temperatures (T_H). Homogenization temperatures record the temperature of the fluid at the time that it was trapped in a crystal. These can only be measured on fluid inclusions that have a vapor bubble (called two-phase inclusions). Samples are slowly heated while optically monitoring the behavior of the vapor bubble in the inclusions. Generally, the vapor bubble shrinks until it disappears (T_H to the liquid phase). Sometimes for gas-condensate inclusions, or high temperature aqueous inclusions from near-surface hydrothermal systems, the vapor will expand and the inclusion with homogenize to the vapor phase. In the T_H to liquid case, when the vapor bubble gets small we slow the heating rate to about 1-2° C/minute. When the vapor bubble looks like it is gone, a foot pedal is depressed which cuts power to the torch and immediately begins to cool the sample. If the vapor phase is truly gone, metastability prevents it from re-appearing until the inclusion is undercooled (below T_H) by 20-30 C. If the vapor phase was not truly gone, it grows back immediately when cooling begins. By cycling the temperature up and down like this, it is possible to measure T_H to within 0.1 to 0.2 C. T_H is measured to the nearest full degree, because the added accuracy is generally not warranted with natural samples, and is much more laborious. Additionally, the T_H of individual populations are typically grouped and reported to the nearest 5 C, unless individual inclusions are measured. Again, this allows us to cover a lot more ground without significantly compromising relevant accuracy.

Melting temperature (T_M). In order to determine the salinity of fluid inclusions, they are frozen to liquid nitrogen temperature (-196°C) and are slowly heated while looking for melting. First (eutectic) melting typically results in more defined appearance of individual solid crystals, because the liquid wets the surfaces between the solids. Heating rate is reduced to about 1 C/min while solids continue to melt. When it appears that the last solid has melted the inclusion is temperature cycled, as with T_H to make sure the solid does not grow back. Same principles

apply as with T_H. Here, though temperatures are measured to the nearest 0.1° C, populations are reported to the nearest 0.5° C. Temperature accuracy becomes more important at low salinities for most applications (the difference between 22 and 23 weight percent salt is not as important, interpretation wise, as the difference between 2 and 3 weight percent). The final solid to melt is not always ice. It can be hydrohalite, clathrate or some other phase. We attempt to determine this, as it has an obvious effect on the composition interpreted from phase diagrams. Usually ice is distinctive in melting behavior and clathrate generally, though not always, melts at temperatures above 0° C. Metastable ice melting can occur at temperatures above 0° C, but always does so in the absence of a vapor phase. Hydrohalite has a distinctive texture (sort of fibrous and less visible). The eutectic (first melting) temperature gives an indication of whether the system has appreciable dissolved Ca +/- Mg (visible first melting below -35°), or whether the dominant cations are Na +/- K (visible first melting above -21° or so). However, these data are in general qualitative and not very useful; so, we don't explicitly record the value unless requested to do so. Generally, high salinity inclusions in carbonate environments have a fair amount of Ca and/or Mg indicated by Te and Tm. Generally, low salinity inclusions do not.

General guidelines for interpreting microthermometric data. The following statements are provided to give the reader some general guidelines and limitations for interpreting microthermometric data. Some comments may not apply to this particular data set.

Primary vs. Secondary Inclusions

The terms primary and secondary are generally based on textural criteria. Primary inclusions occur along growth zones or are located along time-restricted portions of cements, indicating that they were trapped during growth of that portion of the crystal. Secondary inclusions generally occur along healed fractures that cut growth zones and the like, and may have formed at any time after precipitation of the enclosing (host) crystal. So-called pseudo-secondary inclusions are those that lie along a healed microfracture, but are restricted to part of the cement. In these cases it is inferred that fracturing occurred during cement formation and that cementation continued after fracturing. With many vein-fill cements, it is probable that a number of what appear to be texturally secondary inclusions are actually pseudosecondary; hence are relevant to at least a portion of the cementation history.

There are added complexities in cements with protracted burial histories, including the possibility of breaching early-formed, texturally primary inclusions and refilling them with secondary fluids (see also the section on re-equilibration, below). The resulting exploitation inclusions are often indistinguishable from true primaries, except that they give temperatures that are inconsistent with other geologic information. Most of the documented examples come from carbonate environments.

We adopt a conservative approach to interpreting inclusion origin (e.g., primary vs. secondary). When are inclusion populations given the designation pr? In the accompanying microthermometric tables it is implied that the inclusions are texturally primary, but because inclusion populations can have complex geometries, they may be cryptic secondaries. It is equally likely that some texturally secondary inclusions in fracture fill cements are actually pseudosecondaries, hence are relevant to the cementation history as discussed above.

Significance of homogenization temperature. Measured homogenization temperature (Th) is always a minimum estimate of trapping temperature (Tt). The magnitude of the correction necessary to convert Th to trapping temperature is dependent on the extent of gas undersaturation and is potentially greater at higher temperatures and greater burial depths for pure aqueous fluids with low dissolved gas content. Homogenization temperatures of petroleum inclusions are particularly subject to potentially large, upward corrections depending on the saturation state of the petroleum phase at trapping (i.e., whether it was trapped close to its bubble point or dew point, or was highly undersaturated). Experience indicates that aqueous inclusions that are co-entrapped with petroleum inclusions tend to give better estimates of petroleum inclusion formation temperature, and better absolute temperature estimates, because aqueous fluids have lower compressibility, hence steeper isochoric P-T slopes, and because they may contain dissolved gas extracted from the coeval petroleum phase. Any uninformed attempts to correct Th to Tt usually result in more uncertainty than just working with raw Th values. Our experience has been that raw Th of aqueous inclusions is typically not a bad estimate of Tt in the diagenetic realm.

Saturation state of petroleum inclusions. Comparison of coexisting aqueous and petroleum inclusion Th provides a measure of petroleum saturation state. In general, petroleum inclusion Th can vary from being nearly identical to aqueous inclusion Th in the case of petroleum inclusions trapped near bubble point or dew point, to being substantially below this value in the case of highly undersaturated petroleum fluids. Generally, it is not possible to obtain petroleum inclusions with Th above that of coeval aqueous inclusions. Petroleum inclusions trapped near bubble point may indicate the presence of a separate gas phase in the pore system or a gas leg overlying a liquid petroleum charge. However, a stronger case for a multiphase petroleum pore fluid is made if co-entrapped gas and liquid petroleum inclusions are identified in the same fracture plane or diagenetic growth zone.

Re-equilibration of inclusions. Fluid inclusions can be reset, most commonly in weak cements during continued burial after trapping of the inclusions in question. There are a number of factors that determine whether or not a given inclusion is likely to be re-equilibrated, including inclusion size, shape, host strength and fluid type. Petroleum inclusions are less commonly altered by purely mechanical disruption because their isochoric slopes are flatter in P-T space, hence they do not generate as high of internal overpressures for a given increment of overheating. They may, however, be prone to thermal alteration during overheating. Re-equilibrated inclusions are generally inferred from microthermometric analysis where Th data are highly variable, although other processes can create this distribution as well.

Research has shown that dust-rim hosted inclusions tend to re-equilibrate to near-maximum post-entrapment burial temperature, either by stretching, or through continuous refilling. Overgrowth hosted inclusions (as primaries or along fractures), on the other hand, tend to reflect cementation temperatures (possibly requiring upward corrections for undersaturation, as discussed above).

In many samples there tends to be one population of inclusions that appear to give raw Th that are close to maximum burial temperatures. These may be reset lower temperature inclusions, or could be unaltered.

API gravity. Fluorescence color has been proposed as a means of assessing API gravity and/or maturity. Empirically, inclusions that fluoresce toward the red wavelengths (e.g. those that are more orange or yellow) tend to have lower gravities and/or be lower maturity. On the other hand, more mature or higher gravity petroleum fluids tend to fluoresce toward the blue wavelengths. Experience suggests that this relationship may hold in a general sense, but can give misleading results in many cases. The cryo-optical method used in this study is a direct measure of a density-related property of the oil and, while more subjective than quantitative fluorescence measurements appears to give very good results in most cases.

Bitumen precipitates. Asphaltic bitumen precipitates within liquid petroleum fluid inclusions are generally thought to arise either through cooling and decompression of the sample during sampling from reservoir conditions or as a result of natural uplift, or by thermal alteration of early-formed liquid petroleum inclusions during continued burial. The former occurs because asphaltene solubility is temperature and pressure dependent, exhibiting minimum solubility near the bubble-point pressure of petroleum fluids for a given temperature. In general, asphaltic precipitates tend to be associated with moderate to upper-moderate gravity crudes generated from marine source rocks.

Significance of petroleum inclusion presence. Petroleum inclusions are subject to the same thermal controls on preservation as pore fluids. Consequently, if liquid petroleum fluid inclusions are found within a given sample, then the maximum temperature experienced by that sample cannot have exceeded the upper limit of thermal preservation of liquid hydrocarbons. Systems that have experienced early liquid petroleum charging followed by oil-to-gas cracking typically contain fluid inclusions that are gas-bearing with pyrobitumen dustings on the internal faces of the inclusion cavity. Inclusions also generally display evidence of having been breached. This occurs because the increase in pressure accompanying the volume increase associated with the conversion of oil to gas is sufficient to exceed the bursting strength of the inclusion cavity. Evidence of this process may be less likely in high temperature environments, or paleo-environments where burial and uplift has been geologically rapid.

Sr Isotopic Measurements on Carbonates

Strontium isotopes were measured by Mihai Ducea at the University of Arizona. The following sections are his descriptions of the methods and equipment used.

Sample preparation. About 100 mg were dissolved for each sample in 2.5M nitric acid. About 10% of that was used for trace element analyses; the remainder was taken up in 3.5M nitric acid and passed through Sr Spec chromatographic columns for rapid Sr elution. The separated Sr cut was then redissolved in 1% nitric acid. Trace elements were analyzed in this mild nitric acid using a Perkin Elmer Elan DRC-II instrument. Well-characterized USGS standards were use to calibrate the instrument (following the routine in Ducea, 2002).

High purity 14 mol l^{-1} HNO_3 and 28 mol l^{-1} HF acids purchased from Seastar Chemicals, Sydney, Canada are used. Dilute solutions of high purity acids were prepared with purified water (18 mΩ) from a Millipore system.

Separation chemistry. The separation of Sr for these samples was performed in a crown ether-based Sr Spec resin, with a particle size between 100-150 μm (available commercially from Eichrom Technologies, Darlen, IL). Column loads were 0.25 ml. The method involves passage of 1 ml sample solution in 3.5 mol l^{-1} HNO_3 medium through the extraction column, which retains Strontium. Rubidium and other matrix elements are washed from the column leaving a pure Sr fraction on the column (elution curves are available from the authors upon request). The Sr is then stripped with a small volume of diluted nitric acid (0.05 mol l^{-1} HNO_3). The highest procedural blanks measured during the course of this study were 130 pg Sr.

Isotopic determinations. Thermal ionization mass spectrometry (TIMS). Mass spectrometric analyses were carried out on a VG Sector 54 multi-collector TIMS instrument fitted with adjustable 10^{11} Ω Faraday collectors and Daly photomultipliers (Ducea et al, 2002). Concentrations of Rb and Sr were determined by isotope dilution, with isotopic compositions of Sr determined on the same spiked runs. An off-line manipulation program was used for isotope dilution calculations. Typical runs consisted of 100 Sr isotopic ratios. Ten analyses of standard SRM 987 yielded mean ratios of: $^{87}Sr/^{86}Sr = 0.710265 \pm 7$ and $^{84}Sr/^{86}Sr = 0.056316 \pm 12$.

Multiple collector ICP mass spectrometry (MC-ICPMS). Sr isotopic ratios were also measured using an IsoProbe (GV Instruments) multi-collector inductively coupled plasma mass spectrometer at the University of Arizona (Ducea et al., 2003; Ducea et al., 2006). Run parameters are given in Table 1. Samples were introduced in the mass spectrometer in 1% nitric solutions. Our standard nebulizer is a low flow (~ 100 μl/min) nebulizer from Elemental Scientific Inc.

Prior to analysis, we monitored the distribution of Krypton, which could potentially be present in the argon gas and interferes with strontium at mass 86. We noticed that the Ar gas is essentially devoid of Kr, with $^{83}Kr/^{88}Sr$ in SRM 987 solutions on the order of 10^{-7}. Overall, the Kr interference was not an issue during the course of our study. However, this interference has to be carefully monitored in any similar study, given the chances that commercially purchased Ar can contain significant amounts of Kr (Ramos et al., 2004).

The Sr isotopic data was measured statically using six Faraday cups aligned for masses 83, 84, 85, 86, 87 and 88. The cup configuration is shown in Table 2. Backgrounds were calculated either by measuring signals in the blank solution with the beam valve open at half mass distances from the peaks of interest, or by measuring backgrounds at peak positions. Data was collected in 4 blocks of 20 cycles with a period of 1 sec and a sample solution integration time of 10 sec. A blank solution for background measurement and peak centering was made over a 60 sec integration. The blank subtraction is done by on peak zero method. The signal intensities were ratioed and mass discrimination was corrected for internally using the accepted $^{86}Sr/^{88}Sr$ ratio of 0.1194, and a standard exponential correction law (Wasserburg et al., 1981). The total run time for an analysis, including blank acquisition is about 8 minutes.

We checked the ^{88}Sr peak for instrumental memory between analyses, and observed that the signal drops to zero after about 20-30 seconds after the end of an analysis. This indicates that instrumental memory is not an issue for this type of measurement.

^{85}Rb signal intensity is used to correct mass 87 = ^{87}Sr-^{87}Rb, using a $^{85}Rb/^{87}Rb$ value of 2.59265. Since Sr was chemically separated from Rb in our solutions (or in the case of the SRM 987 standard, the solution does not have Rb), the mathematical correction for Rb was insignificant in this experiment. Typical % standard errors on normalized $^{87}Sr/^{86}Sr$ were 0.001-0.002. Mass bias is determined using $^{88}Sr/^{86}Sr$ assuming no Kr (see above).

The average of 135 measurements of $^{87}Sr/^{86}Sr$ on SRM 987 during the course of this study was 0.7102284±0.000034, compared to the commonly accepted value of 0.71026 (Balcaen et al., 2005). The range of standard ratios is similar to unpublished data from GV, the maker of IsoProbe, using the same standard. The reproducibility of standard ratios is also similar to the values obtained on the TIMS instrument at UA over a six-year period (2000-2005).

Our analysis routine involves running three to five replicates of the SRM 987 standard in between five unknowns. The $^{87}Sr/^{86}Sr$ of the unknowns are then corrected using a moving average offline program that back corrects the $^{87}Sr/^{86}Sr$ of the SRM 987 to the nominal value of 0.71026.

Trace elements

Trace elements were also analyzed by Mihai Ducea at the University of Arizona. The following is his description of the methods used to determine trace element concentrations.

Trace elements were analyzed in a mild nitric acid using a Perkin Elmer Elan DRC-II instrument. Well-characterized USGS standards were use to calibrate the instrument (following the routine in Ducea, 2002). In addition, we used an internal carbonate standard (KONA1), which was analyzed several times during the course of this study, given the similar major and trace element concentrations in this standard and the unknowns.

The ICP-MS (inductively coupled plasma source mass spectrometer) consists of a quadrupole mass spectrometer with an inductively coupled argon plasma as an ion source. Liquids introduced into the plasma (7000°C) are ionized and then passed to the mass spectrometer through a two-stage ion extraction interface. The ICP-MS is capable of quantitatively determining trace elements in liquids in the range of fractions of a part per billion. Its capability for rapid multi-element analysis at high sensitivity, and relative freedom from interferences make the ICP-MS an excellent instrument for the determination of many trace elements in rocks and minerals.

Samples dissolved in nitric and/or hydrochloric acid were prepared for analysis by dilution in 1% nitric acid. Samples are introduced into the argon plasma at 1.0 ml/min using a peristaltic pump and an automatic sampler. Plasma power is 1500 watts. Under these conditions MO+/M+ (the proportion of metal ions forming oxides) is minimized. The instrument is run in "multi-element" mode averaging 10 repeats of 0.5 sec/element for a total integrated count time of 5 sec/element.

In the routine procedure practiced for this study, the following elements are analyzed (the isotopes scanned for are given in parentheses): Li(7), Na (23), Mg(24), Al (27), K(39), V (51), Cr(52), Mn (55), Fe (54), Co (59), Ni(60), Cu(63), Zn(64), Ga(69), As(75), Se(78), Rb(85), Sr(88), Ag(107), Cd(114), Sn(119), Cs(133), Ba(137), Pb(208), Bi(209), and U(238). These isotopes were chosen based on natural abundance and lack of interferences.

The reproducibility of analyses (total of sample preparation plus instrumental precision) is about 3% or less for trace elements. Major cations like Ca and Mg require additional dilution, which typically leads to lower precisions.

Sampling Strategy

In an effort to understand the origin of all of the dolomite in the Trenton and Black River, we sampled all of the different occurrences in the study area (Figure 4-1). In all states except Ohio, every known core with dolomite from the Trenton and Black River was sampled. In Ohio, ten cores were sampled from representative areas and all dolomite types.

New York Sampling Strategy

In New York (Figure 4-2), dolomite occurs around faults in the Black River and in the lowermost few feet of the Trenton. There are both matrix dolomite and saddle dolomite (Figure 4-3). Matrix dolomite is gray and replaces what was initially limestone. The matrix dolomite in New York is generally impermeable. White saddle dolomite is common, and lines vugs, fractures, zebra fabrics and breccia clasts. Both of these dolomite types are present in the dolomitized gas fields in New York. We sampled the dolomites from three cores taken from the Whiteman #1 (Short API #22839), the Gray #1 (Short API #22949) and the Matejka #1 (Short API # 10335). The samples are listed in Appendix 4-1.

Ohio Sampling Strategy

In Ohio, four different dolomite types previously have been recognized: cap dolomite, facies dolomite, and fracture-related matrix and saddle dolomite (Wickstrom et al., 1992) (Figure 4-4). The cap dolomite occurs at the top of the Trenton Formation just beneath the Utica Shale and ranges from 10-50 feet thick and is impermeable. It occurs in northwest Ohio (and in parts of Indiana, Michigan and Ontario) but is absent in the rest of the study area. The facies dolomite occurs along the margin of the Sebree Trough (Figure 4-5). This is porous matrix dolomite that can be very coarse (up to 500 microns rhombs). This dolomite is differentiated from the obvious fracture-related dolomite because it generally lacks vugs, fractures and breccias. The dolomite is laterally discontinuous and occurs along linear trends. The “fracture-related” matrix and saddle dolomite are identical to the dolomite types identified in New York (Figure 4-6).

Various models have been suggested in the past to explain these dolomite types. The fracture-related dolomites have long been interpreted to form from hot fluids migrating up faults (hydrothermal dolomite) (Harding, 1974; Hurley and Budros, 1990; Wickstrom et al., 1992). The cap dolomite has been interpreted to form due to compaction of the overlying Utica Shale and

downward expulsion of magnesium–rich fluids, which were interpreted to have dolomitized the underlying limestone (Taylor and Sibley, 1986). The facies dolomite was interpreted to have

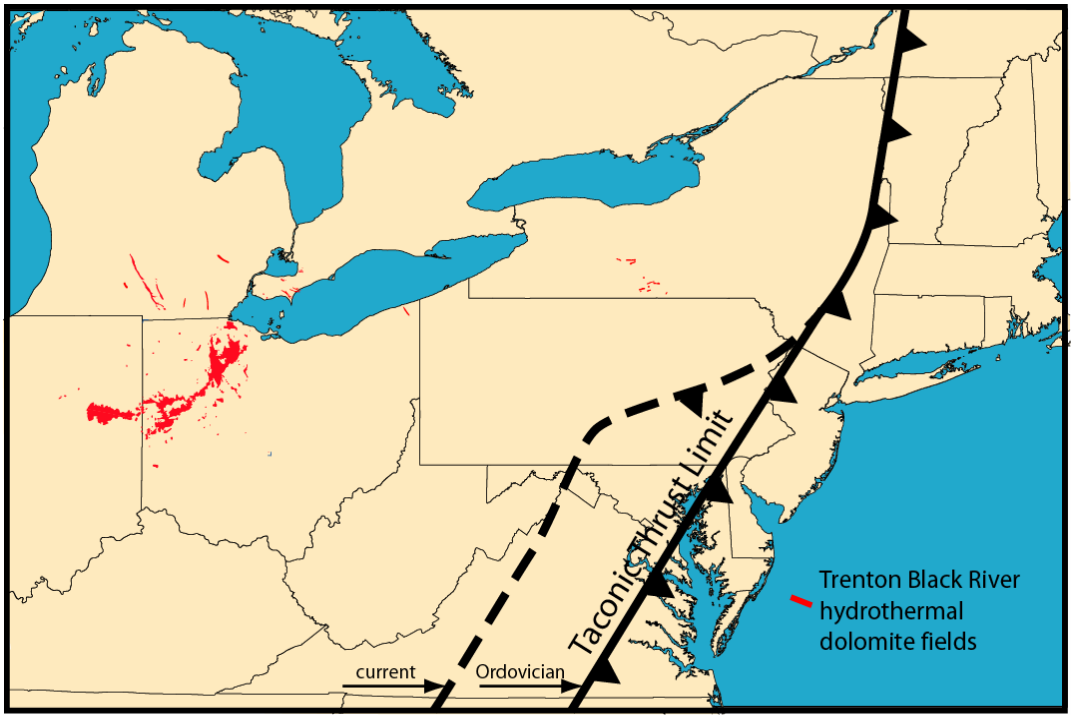

Figure 4-1. Distribution of Trenton Black River dolomitized reservoirs.

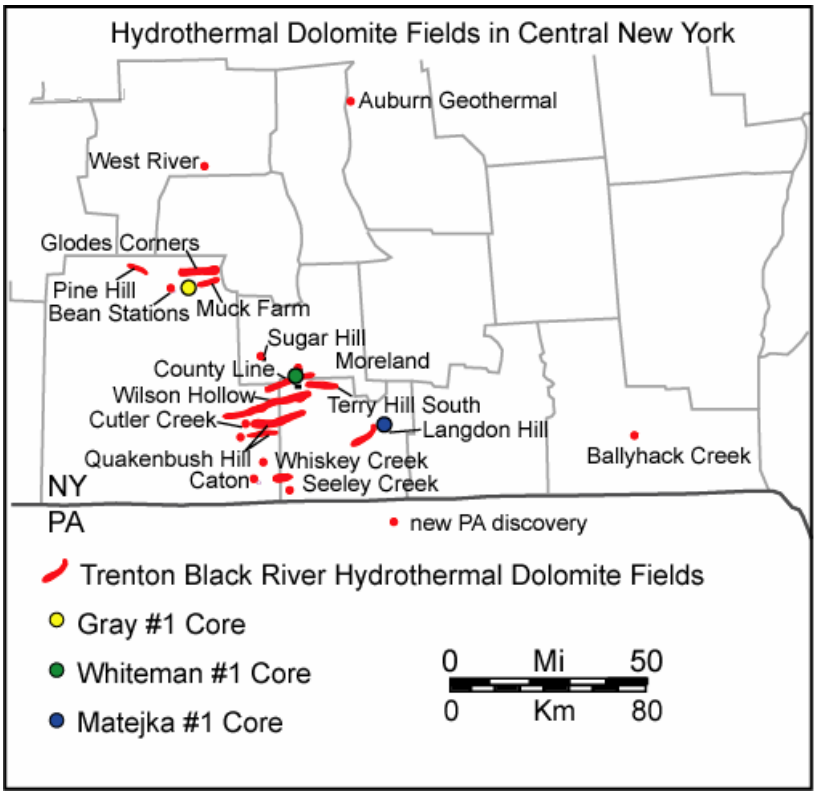

Figure 4-2. Field map and core locations for south central New York.

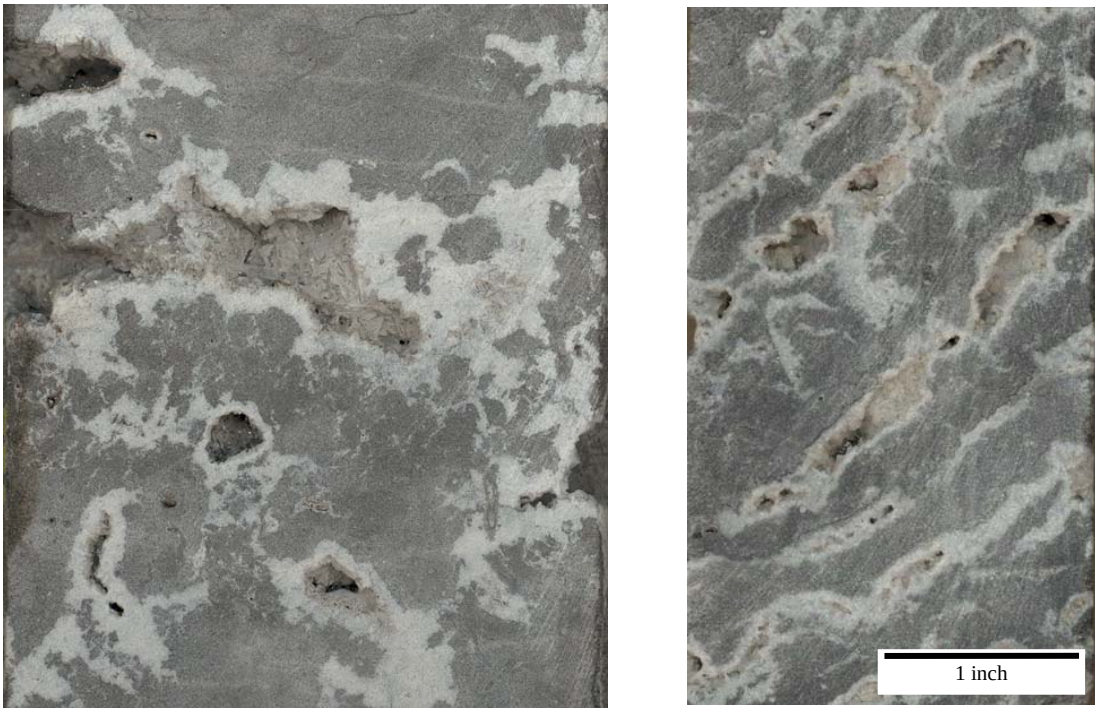

Figure 4-3. Dolomite from the Gray (left) and Whiteman (right) cores in south central New York. The gray groundmass is the matrix dolomite and the white pore-lining mineral is saddle dolomite.

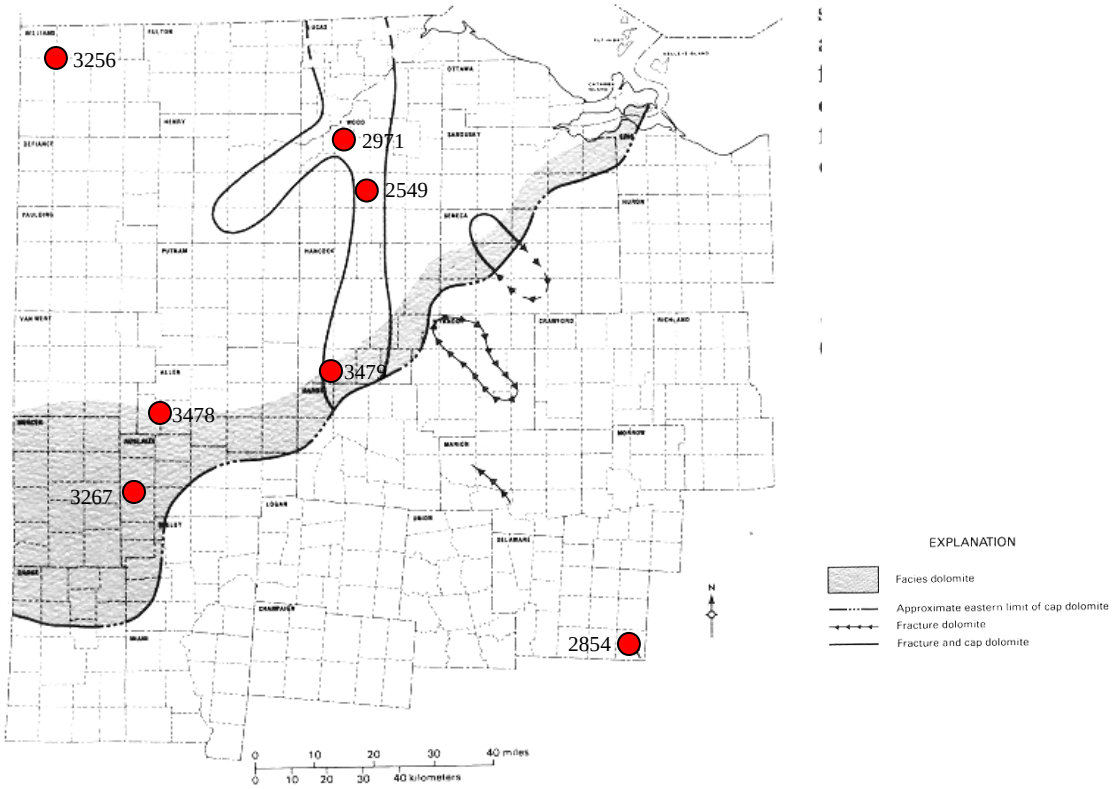

Figure 4-4. Locations of wells studied and various dolomite types in northwest Ohio (from Wickstrom et al., 1992).



Figure 4-5. Facies dolomite in core from northwest Ohio with coarse, porous matrix dolomite that was probably a grainstone prior to dolomitization. Scale is in cm.



Figure 4-6. Left: Breccia with saddle dolomite (white), matrix dolomite (brown) and pyrite (gold). Right: saddle dolomite from cores in obviously fracture-related dolomite areas in northwest Ohio (sensu Wickstrom et al., 1992).

Table 4-1. Ohio Cores Sampled for Dolomite							
Core number	Core Name	Depth	T_H (Primary)	Salinity	$\delta^{18}O$	87Sr/86/Sr	Dolomite Type
3479	Anderson	1335	115-140C	21.7-23	-8.36	0.7101	facies
3479	Anderson	1340	110-130°C	21-23	-8.47	0.7102	facies
3267	Cisco	1167	135-155°C	13-18	-7.65	0.7096	facies
2549	GB	1114	100-145°C	20.2-23	-6.63	0.7088	cap
2549	GB	1136	90-120°C	21.3	-6.8	0.7108	saddle
2549	GB	1136	95-110°C	20.2-21.7	-6.1	0.7075	frac matrix
2549	GB	1184	110-130°C	19.8-21.7	-8.25	0.7088	saddle
2549	GB	1184			-8.03	0.7086	fracture associated matrix
3372	Prudential	2015	80-90°C	21.7-23	-6.36	0.708	fracture associated matrix
2854	Piper	2938	145-155°C	22.4-23	-7.57	0.7085	saddle
2854	Piper	2938			-7.41	0.7087	fracture associated matrix
2854	Piper	2896	105-125°C	20.2-23	-8.52	0.7081	saddle
2854	Piper				-9.18	0.7122	fracture associated matrix
2791	Spitler	1496	130-140°C	21.7-22.3	-7.97	0.7132	saddle
2791	Spitler	1496			-8.68	0.7111	fracture associated matrix
2791	Spitler	1442.5	130-160°C	21-23	-8.41	0.7101	saddle
2791	Spitler	1442.5			-8.58	0.7081	fracture associated matrix
3478	Strayer	1218			-8.65	0.713	saddle
3256	Williams	2268	125-140°C	22.4-23.7	-9.49	0.7103	saddle in cap
3256	Williams	2268			-8.01	0.7149	cap
3256	Williams	2304	100-120°C	22.4-23.7	-10.15	0.7107	saddle
3256	Williams	2304			-9.58	0.7105	fracture associated matrix

formed in a similar fashion: compaction of the shale in the Sebree Trough and lateral migration of dolomitizing brine into the Trenton Formation carbonates along the margin. Wickstrom et al. (1992) suggested that perhaps all of the dolomite was of a fault-controlled hydrothermal origin. They pointed out the main problem with the shale compaction model for the other dolomite types: the Utica Shale overlies the Trenton everywhere but the upper Trenton is only locally dolomitized. In New York, for instance, there is no known dolomite at the top of the Trenton in any well. If this dolomitization model was valid, the top of the Trenton (and maybe all limestones underlying thick shale sequences) should probably be dolomitized regionally.

Sampling was done from ten cored wells listed in Table 1 and shown on the map in Figure 4-4. We tried to get representative samples of dolomites from the four dolomite types including cap dolomite, facies dolomite and fracture-related matrix and saddle dolomite.

Kentucky Sampling Strategy

In Kentucky, dolomite was analyzed from a newly acquired core from an outcrop of fault-controlled dolomite (the Allen core), and from cores in the problematic Jeptha Knob structure (Figure 4-7). Jeptha Knob is a positive, round feature in outcrop that has been interpreted to be either an impact structure or a tectonic feature. Three cores were analyzed from Jeptha Knob: two were drilled into the core of the structure and one on the flank of the structure. The two cores in the structure show that the internal structure of Jeptha Knob is heavily faulted, fractured and jumbled. From top to base, core JK-1 has a breccia of unknown affinity, an overturned, 127-foot thick dolomitized bed of High Bridge Group, an overturned dolomitized bed of Lexington Limestone, a normally-bedded Lexington Limestone section and a partially dolomitized, normally-bedded High Bridge (Black River) section overlying the Knox Dolomite. Some beds within the upper part of the core dip from 10 to 90 degrees. Core JK-3 has breccias at the top, which overlie about 800 feet of vertically-dipping, dolomitized High Bridge Group. The Trenton and Black River equivalents (Lexington and High Bridge, respectively) in the two cores in the center of the structure have abundant matrix dolomite and porosity (Figure 4-8). Some of the dolomite is coarse (up to 500 microns) and resembles the “facies” dolomite in Ohio in many respects. The off-structure core has a few beds of dolomite but is predominantly limestone. There was no obvious white saddle dolomite at Jeptha Knob. The Trenton and Black River equivalents outside of the structure are all limestone. We also include results of studies from the Allen core which was recently acquired from a stratigraphically discordant dolomite zone near the Kentucky River Fault.

Those that interpreted the feature as an impact structure suggest that the asteroid impact induced faults, caused the major disruptions of bedding and the overturned beds. Hot fluids are then interpreted to have used the impact-induced faults to flow upward and dolomitize the strata within the feature, but not in the surrounding host rock. The alternative hypothesis is that Jeptha Knob is a positive flower structure associated with underlying wrench faults. The dolomitization would have occurred as it is interpreted to have occurred in Ohio and New York – hot fluids ascending active faults and dolomitizing the strata around the faults. Black (1981) pointed out that Jeptha Knob occurs very near the major 38th parallel lineament and interpreted it to be a tectonic feature.

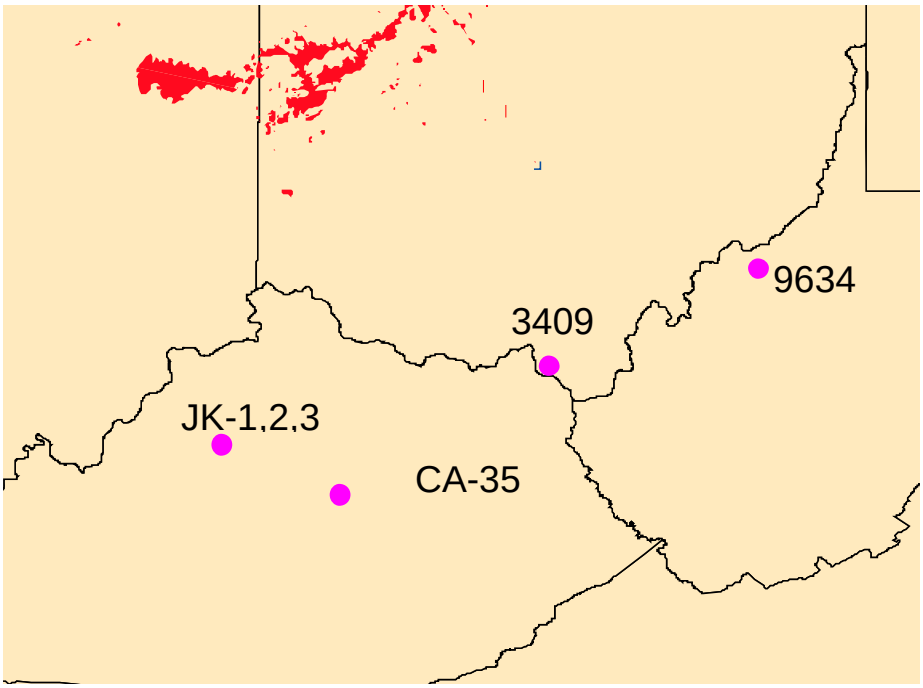

Figure 4-7. Locations of cores studied for geochemistry in southern Ohio, Kentucky and West Virginia.

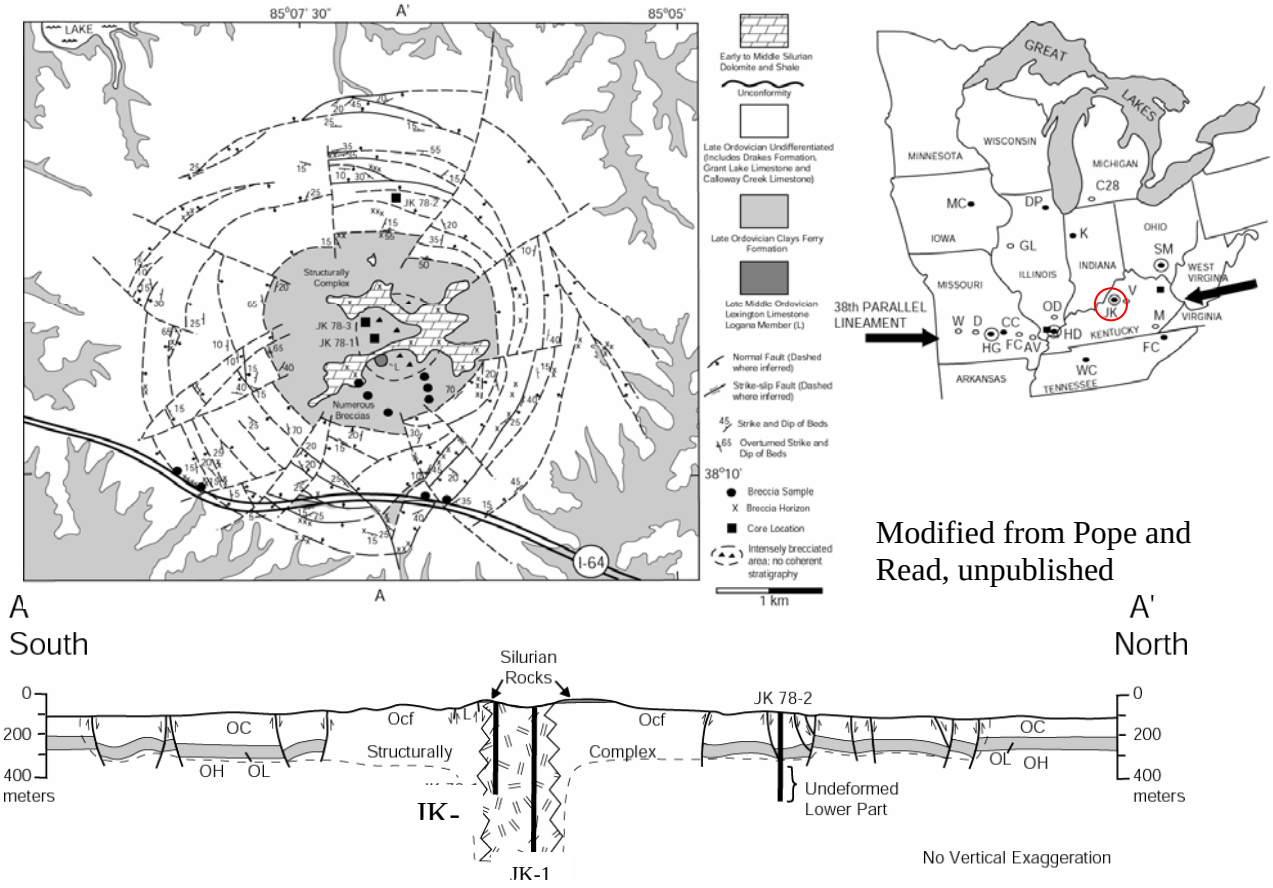

Figure 4-8. Map and cross section of Jeptha Knob, Kentucky. Jeptha Knob is west of Lexington on I-64 and is one of many circular features along the 38th parallel lineament.





Figure 4-9. Porous dolomite from the Lexington (Trenton) Limestone and High Bridge (Black River) Group in core JK-1 at Jeptha Knob in Kentucky.

It is important to understand the origin of the dolomite and the porosity at Jeptha Knob for two reasons: it is a positive feature whereas most current Trenton-Black River production is in structurally low features; and it is very porous dolomite (estimated at >25%). Positive features such as this one also may produce oil and gas, given the appropriate charge/seal scenario. If they are linked to faults and are not random impact features, this work may provide an exploration model for positive features associated with wrench faults.

West Virginia Sampling Strategy

In the Hope Natural Gas #9634 core near Sand Hill, West Virginia, there is what appears to be tight, dolomitized tidal flat facies in a formation that overlies the Knox and underlies the Black River. This is likely to be early reflux dolomite and not hydrothermal in origin. The dolomite is very fine, there are no associated fractures and there is no saddle dolomite. The fact that this facies type is one that is very commonly dolomitized by evaporation of seawater near the surface supports a low-temperature origin. This dolomite also was sampled and analyzed.

Data

Fluid Inclusions

We conducted fluid inclusion analysis on dolomite samples from New York, Ohio and Kentucky (see sample fluid inclusions in Figure 4-10 and 4-11). All of the raw data collected for this study are available on the project website.

Fluid inclusions were analyzed by Fluid Inclusion Technologies, Inc for homogenization temperature and salinity. Minerals analyzed include matrix and saddle dolomite, quartz and calcite. The raw data from Fluid Inclusion Technologies are included in Appendix 4 and a sample of that data is presented in Table 4-2.

New York Data. Primary fluid inclusions from saddle dolomite in New York wells have homogenization temperatures between 110 and 170° C with an average of 130°C (Figure 4-11). Inclusions of an equivocal primary or secondary origin from the matrix have a similar range of homogenization temperatures with a higher average of 145°C. Secondary fluid inclusions from the saddle dolomites have homogenization temperatures up to 180°C with an average of 173°C. Matrix dolomites have equivocal primary/secondary inclusions with fluid inclusion homogenization temperatures that range from 135-165°C with an average of 145°C. Post-dolomite primary and secondary quartz fluid inclusions have homogenization temperatures ranging from 155° to more than 200°C with an average of 177°C.

The salinities of the primary fluid inclusions in saddle dolomite range from 13.2 to 15.5 wt % with an average of approximately 14.4 wt % (approximately 4 times normal seawater). The salinity values of the equivocal inclusions in the matrix dolomites are similar with an average of 14.9 wt%. Secondary fluid inclusions in the post-dolomite quartz cement average 16.7 wt. % salinity.

No petroleum inclusions were found in samples from New York wells, although there were two samples that may have contained gas inclusions. The lack of secondary petroleum inclusions is significant. They are very common in Ohio samples where the Trenton and Black River produce oil, but are absent in areas of New York which produce gas. This may have implications for the timing of migration and suggests that the New York reservoirs were never charged with oil.

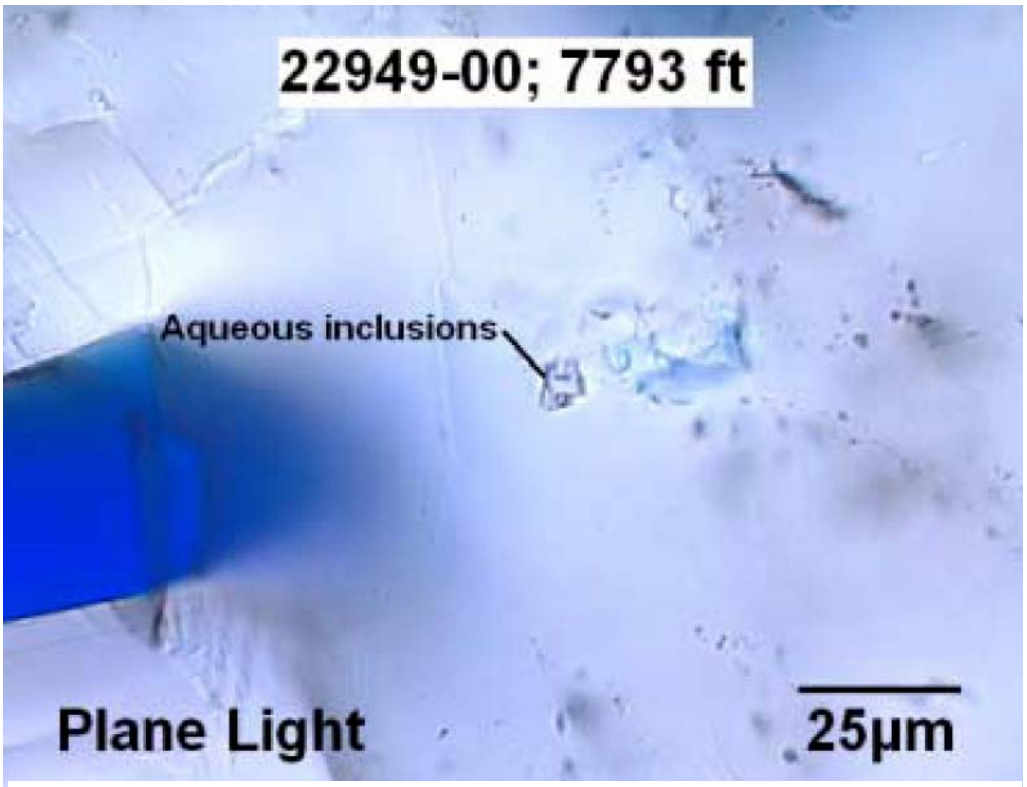

Figure 4-10. Photograph of primary fluid inclusion from Whiteman well in New York. Note vapor bubble in fluid inclusion.

Table 4-2: Cisco #1-3267;1167 ft						
Population	**Fluor Color**	**Th hc (°C)**	**API hc (°)**	**Th aq (°C)**	**Tm aq (°C)**	**Sal (wt%)**
sec; outer zoned dol A	yellow-wht	110-120 (3)	N/A			
sec; outer zoned dol B	yellow-wht	105-120 (7)	N/A			
pr; dol transect pt1 C				149 (1)	-9.3	13.2
pr; dol transect pt2 C				142 (1)	-11.5	15.5
pr; dol transect pt3 C				138 (1)	-13.2	17.1
pr; outer zoned dol D				145-155 (3)	-11.0 to -12.0	15.0-16.0
pr; outer zoned dol E				150-160 (5)	-10.0 to -11.0	14.0-15.0
pr; outer zoned dol F				135-145 (3)	-14.0 to -15.0	17.8-18.6
pr; outer zoned dol G				145-155 (4)	-13.0 to -13.5	16.9-17.3
pr; outer zoned dol H				130-140 (4)	-14.0 to -15.0	17.8-18.6

Table 4-2. Sample of results of fluid inclusion analysis.

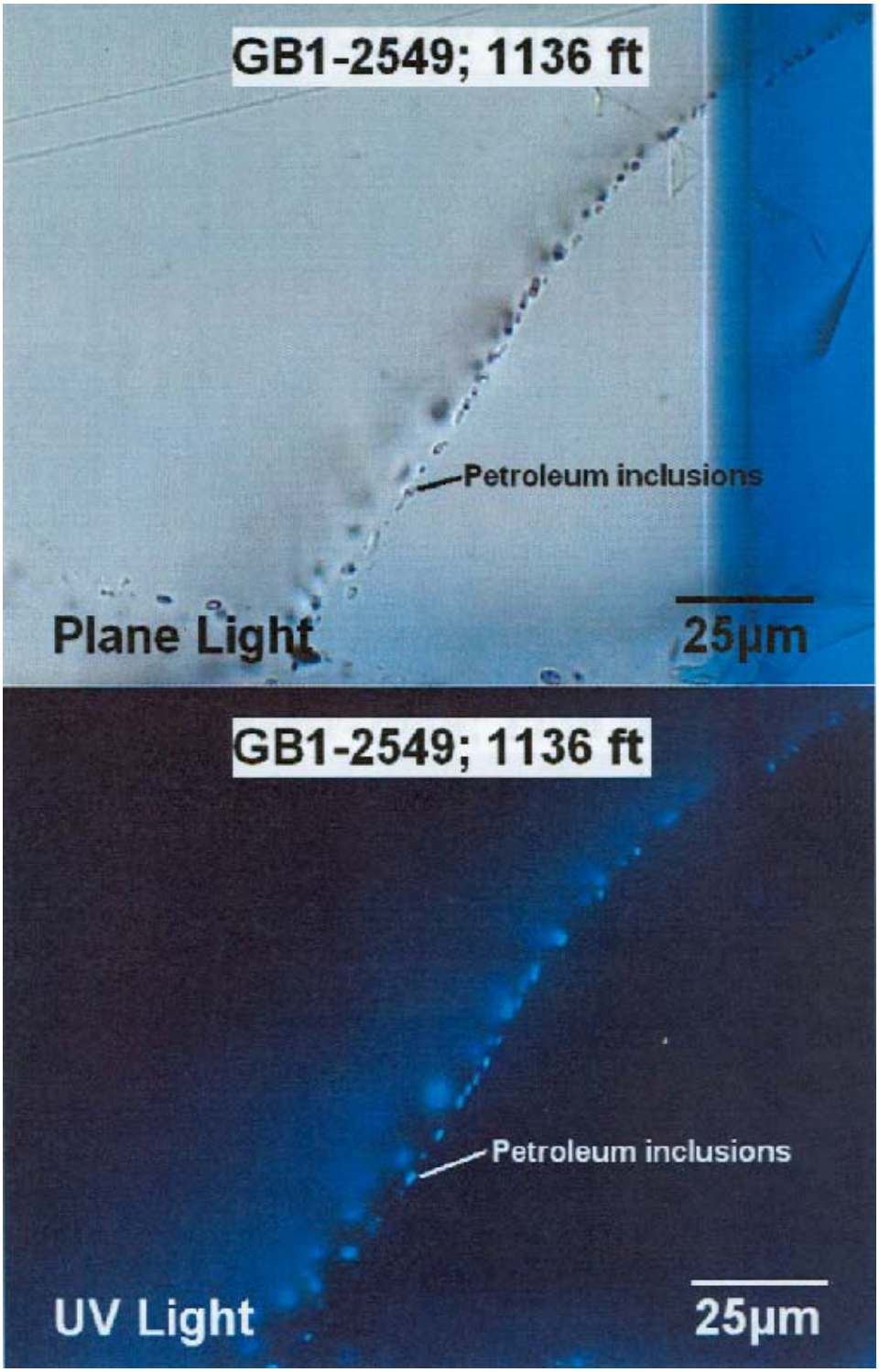

Figure 4-11 Secondary petroleum inclusions formed along micro-crack. Petroleum inclusions fluoresce in UV light.

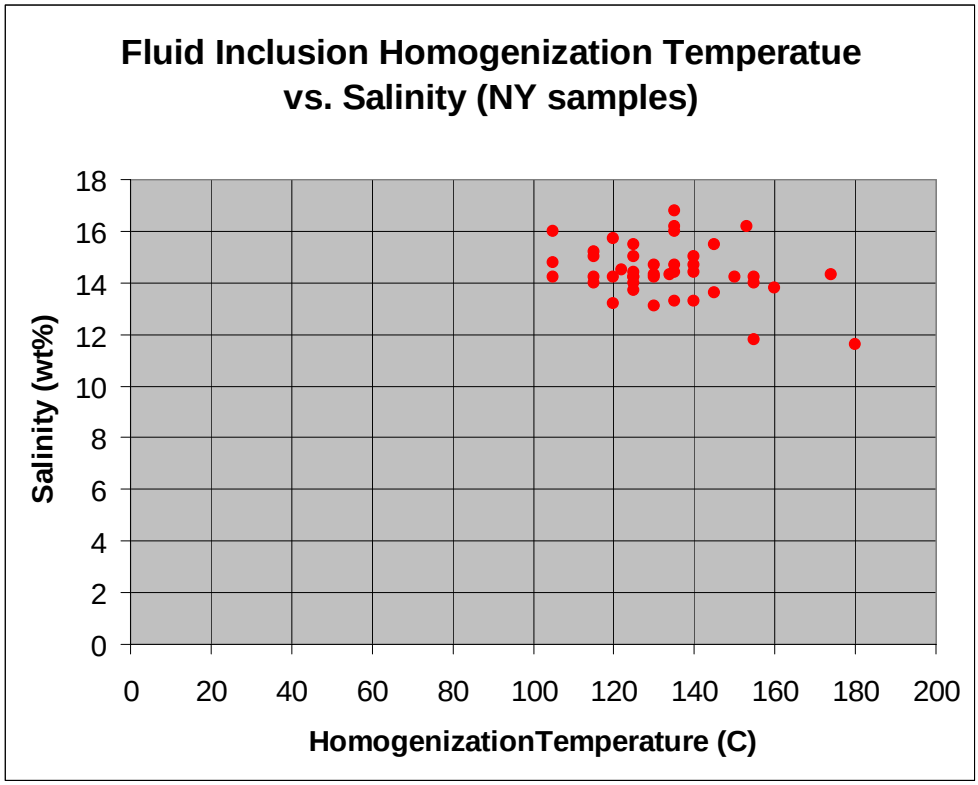

Figure 4-12. Results of fluid inclusion analysis for New York dolomites.

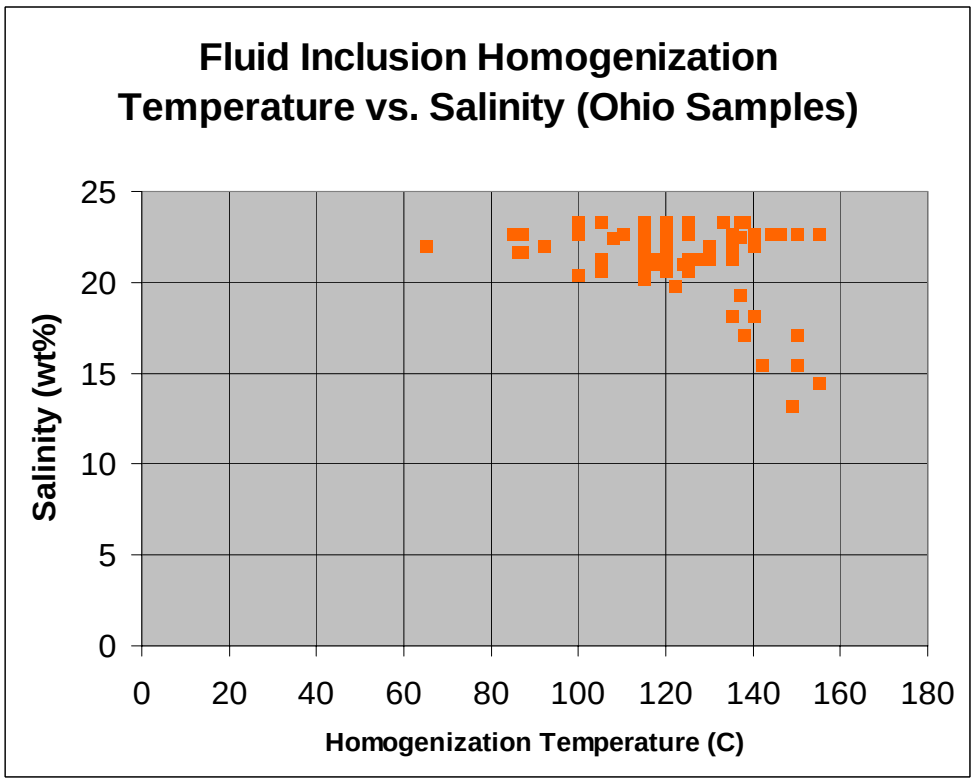

Figure 4-13. Results of fluid inclusion analysis for Ohio dolomites.

Ohio Data. Primary fluid inclusion data from Ohio samples show that all of the dolomite formed at temperatures between 85 and 160°C and that most of it formed between 110 and 160°C (Figure 4-12). This includes the facies dolomite and the cap dolomite, as well as the obviously fracture-related matrix and saddle dolomite. Almost all of the dolomite occurred in the Trenton Formation.

Two "facies dolomite" wells were sampled and analyzed for fluid inclusions - core numbers 3267 and 3479. The fluid inclusion homogenization temperatures for the dolomites from these two wells range from 120-155°C and the salinities range from 13-23 wt%. The samples were coarse matrix dolomite with no obvious fractures or vugs lined with saddle dolomite.

Several wells with cap dolomite were sampled and analyzed. Some of these were in the zone characterized by Wickstrom et al. (1992) as the fractured dolomite zone and others were in the facies dolomite area. Values were obtained for the cap dolomite in well 2549 (100-145C, 20.2-13 wt% salinity), and for the 3256 well, in which the dolomite had primary fluid inclusion homogenization temperatures between 105 and 140°C and salinities from 19-23 wt%. Dolomite in the wells with obvious fractures, zebra fabrics and other features normally associated with fault-related hydrothermal dolomites had similar values. Fluid inclusion homogenization temperatures from the saddle dolomite in these wells (nos. 2549, 2854, 2971 and 3479) had homogenization temperatures between 95 and 160°C and salinities ranging from 19-23 wt %. The average salinity for all the Ohio samples was approximately 20 wt%.

There was one well in which an interval of dolomite was encountered near the base of the Black River associated with a fault that was plugged by a very coarse veins of calcite (well 3372). This well is located in the Sebree Trough. The dolomite was fine grained and there was no saddle dolomite present. The homogenization temperatures were generally lower, ranging from 85-95°C. Salinities in the dolomite ranged from 21-23 wt%. The calcite that plugged the fault was very coarse and had common secondary inclusions that had homogenization temperatures that range from 55-75 °C and salinities ranging from 15-20 wt%. This trend of lower calcite fluid inclusions postdating hotter dolomite is similar to that found in Kentucky.

There are very common secondary petroleum inclusions in the matrix and saddle dolomite in the Ohio cores (see Table 4-1) and a few that may even be of a primary origin. Petroleum inclusions were found in wells 2854, 2549, 3256 and 2791. The homogenization temperatures of these petroleum inclusions are quite high, ranging from 80-120°C. This is in contrast to samples from New York in which there were no petroleum inclusions. The Trenton and Black River produce oil (and some gas) in Ohio, but are dry gas producers in New York.

Kentucky Data. Primary fluid inclusion data from Kentucky also suggest that the fluids that made the dolomite were hot and saline, although not as hot as the fluids in Ohio and New York. All of the dolomite fluid inclusion data comes from Jeptha Knob cores (Figure 4-13). The dolomites were all matrix dolomite, some of which were quite coarse (some crystals >500 microns). Primary fluid inclusion homogenization temperatures range from 70 to 123°C (most 85 to 115°C). Salinities ranged from 3.5 to 24 wt % with most samples between 15 and 24 wt % (average 17.4 wt%).

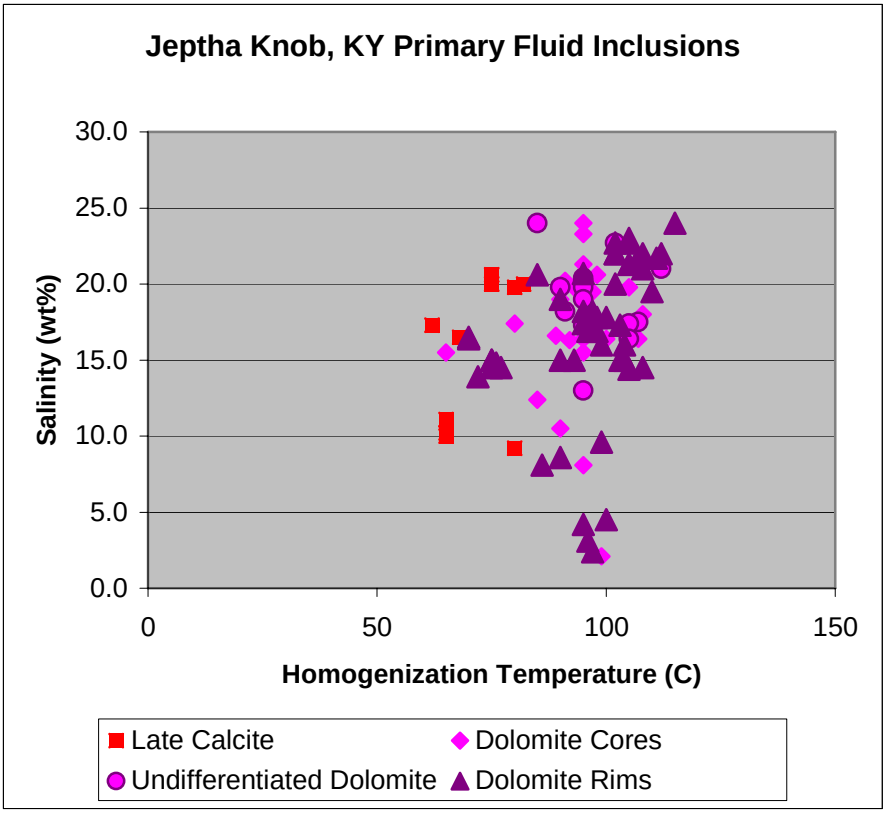

Figure 4-14. Results of Jeptha Knob dolomite fluid inclusion analysis.

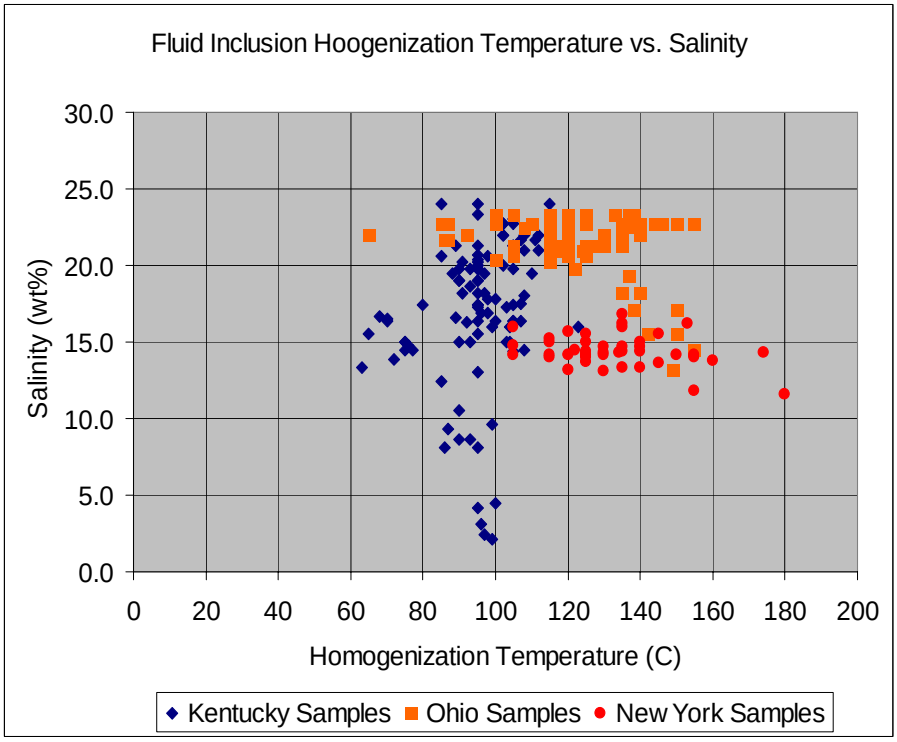

Figure 4-15. Results of all fluid inclusion analyses to date.

The fluid inclusion data suggest that all of the analyzed dolomite types formed from hot saline brines. The dolomite in New York and Ohio samples formed from fluids that were, on average, hotter than the fluids that made the dolomites in Kentucky (Figure 4-14). The facies dolomite, cap dolomite and Jeptha Knob dolomite all had values that were similar to the saddle dolomite in New York and Ohio.

Post-dolomite calcite fluid inclusions consistently have lower homogenization temperatures than the dolomites from the same samples (Figure 4-15). Primary fluid inclusions in calcite from Jeptha Knob have homogenization temperatures that range from 60-85C with an average of 73.6°C. Dolomites that predate the calcite have an average homogenization temp of 90.3°C. So the later calcite formed at cooler temperatures than the earlier dolomite.

There were two samples with secondary petroleum inclusions in quartz in the CK2 and CK8 wells in Kentucky. These wells were only studied briefly. There were no petroleum inclusions in the Jeptha Knob samples.

Stable Isotopes

Analysis of stable isotopes of carbon and oxygen is a valuable tool for learning about dolomitizing environments. Most oxygen in the world is ^{16}O meaning it has 8 neutrons and 8 protons. The most common stable isotope of oxygen is ^{18}O which has two additional neutrons. Analyses of the abundance of ^{18}O in carbonates are reported in parts per thousand (‰) versus a standard, which is the Pee Dee Belemnite (PDB). Oxygen isotopes of water are measured versus standard mean ocean water (SMOW).

Most of the carbon in the world is ^{12}C which has 6 neutrons and 6 protons. The most common stable isotope of carbon is ^{13}C, which has an additional neutron. Analyses of the abundance of ^{13}C in carbonates also are reported in parts per thousand versus the Pee Dee Belemnite (PDB). Samples that have relatively high quantities of ^{13}C or ^{18}O are said to be "enriched" or "heavy" with respect to those isotopes. Samples that have relatively low quantities of ^{13}C or ^{18}O are said to be "depleted" or "light."

More than 2000 samples have been analyzed for stable isotopes of carbon and oxygen. Steven Howe at the University of Albany and Peter Swart at the University of Miami did the analyses. Oxygen isotopes were used to help determine the origin of the dolomites. The limestones have $\delta^{18}O$ values between –4.5 and –7.5 ‰ in the Trenton Limestone and Black River Group. This is thought to be the approximate value of seawater during Trenton and Black River times. Because of the fractionation factor, dolomites that formed from the same seawater should have oxygen isotope values that are 3‰ heavier than limestones formed from the same water and in this case should have values between –1.5 and –4.5 ‰.

Increased temperature drives stable isotope values toward more negative values, and most hydrothermal dolomites have $\delta^{18}O$ values that are lighter or more negative than the associated limestones. This does not always have to be the case, however, and the samples from Jeptha Knob are a prime example. The oxygen isotope value of dolomite is directly controlled by the isotopic composition of the fluid that made the dolomite. The heavier the fluid is, the heavier the

$\delta^{18}O$ value will be at a given temperature. So it is possible that dolomites could plot in the range for expected seawater dolomites but still be hydrothermal in origin if the dolomitizing fluid was heavier (more positive) than seawater at the time the strata were deposited. It is essential to know the oxygen isotope composition of the fluid prior to making this interpretation. The method for learning the isotopic composition of the fluid will be presented later in this report.

Carbon isotopes are not very useful for determining dolomitization environments, but do have value as a stratigraphic correlation tool. This will be demonstrated in a later section.

New York Data. Stable isotopes of carbon and oxygen were analyzed on all three of the cores (Figure 4-16). The limestones in the Black River of NY have consistent $\delta^{18}O$ values around –6.5‰. Due to fractionation, dolomite that precipitated from the same water at the same temperature should have $d^{18}O$ values of around –3.5 ‰. The matrix and saddle dolomites in the Black River have $\delta^{18}O$ values between –9 and –12.5‰.

Ohio Data. Stable isotope values were analyzed for all of the dolomite types in Ohio and the data plot fairly close together (Figure 4-17). The cap dolomites had $\delta^{18}O$ values between –6.5 and –10‰; the facies dolomite had values between –7 and –9‰; the matrix dolomites associated with obvious fractures had values between –6.5 and –9‰; and the saddle dolomites had values between –8 and –9‰. These values are all significantly lighter than expected values for seawater dolomite (–1.5 to -4.5 ‰).

Kentucky Data. The Jeptha Knob dolomites have $\delta^{18}O$ values between –2 and –7 ‰ with a significant percentage of the samples in the range where one would expect seawater dolomites (-1 to –4‰) (Figure 4-18). As noted earlier, this does not necessarily rule out a higher temperature origin for the dolomites. One must first learn the isotopic composition of the fluid before interpreting the origin of the dolomite.

West Virginia Data. The only dolomite found in West Virginia was at the very bottom of the Black River in the core from the Sand Hill well. It was all very fine replacement dolomite of peritdal facies. This is very common in Lower Ordovician carbonates with no porosity or saddle dolomite and looks very different from the dolomites that produce in New York and Ohio. The data from this dolomite are presented in Figure 4-19. These dolomites were too fine to gather fluid inclusion data. This is commonly a sign that they are probably not of a hydrothermal origin. The data plot where one would expect seawater dolomites to plot on Figure 4-19. These are interpreted to be early dolomites, probably of a reflux or seawater origin.

Isotopic Composition of Dolomitizing Brines. The isotopic composition of the dolomitizing brines can be determined by plotting $\delta^{18}O$ values and fluid inclusion homogenization temperatures from the same samples on a graph developed by Friedman and O'Neil (1977) (Figure 4-20). This shows that the fluids that made the dolomites in New York averaged around +2‰; the fluids that made the dolomites in Ohio averaged around +4‰; and the brines in Kentucky averaged around +5‰ (Figure 4-21). These values are typical of subsurface brines (Figure 4-21). Because the fluid that made the dolomite at Jeptha Knob was ~10‰ heavier than Late Ordovician seawater that made the limestones, the dolomite values plotted where one would

expect seawater dolomites, even though they formed at elevated temperatures. This is an important lesson for interpreting stable isotopes.

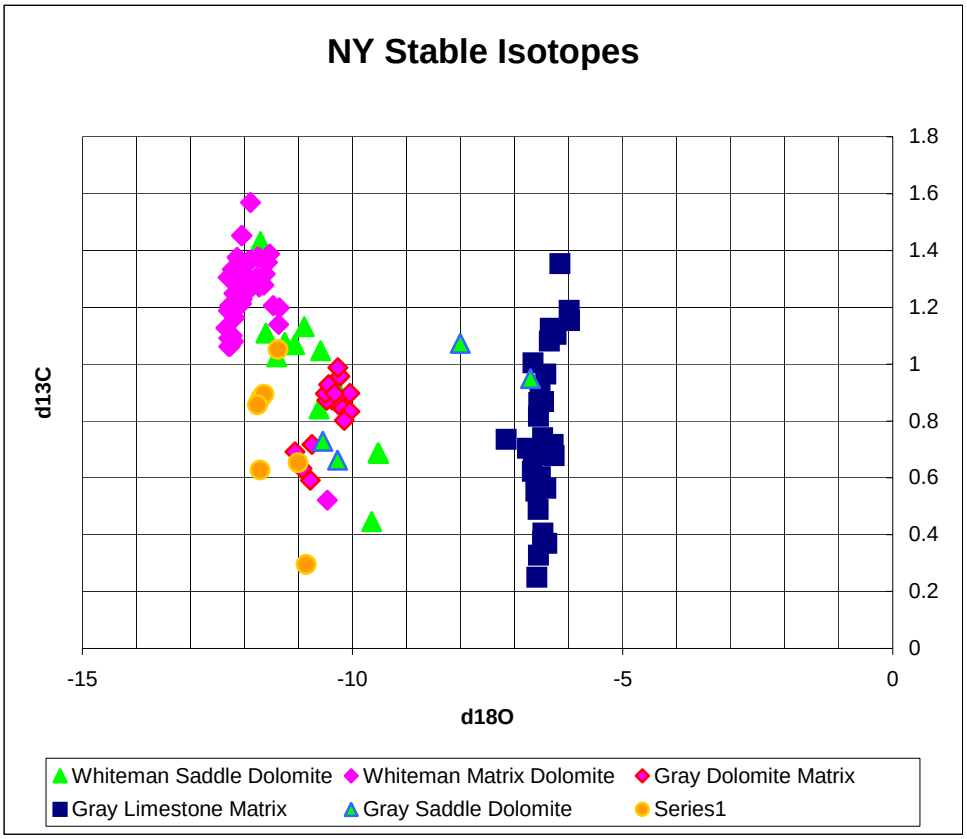

Figure 4-16. Stable isotope data from New York. Series 1 is matrix dolomite from the Matejka well.

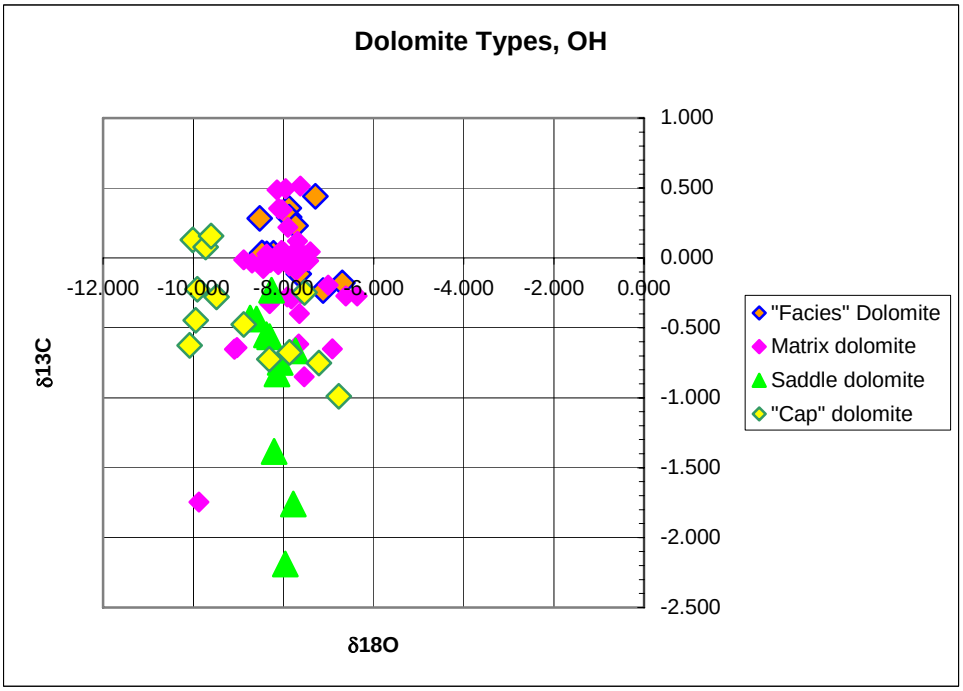

Figure 4-17. Stable isotope data from Ohio dolomites.

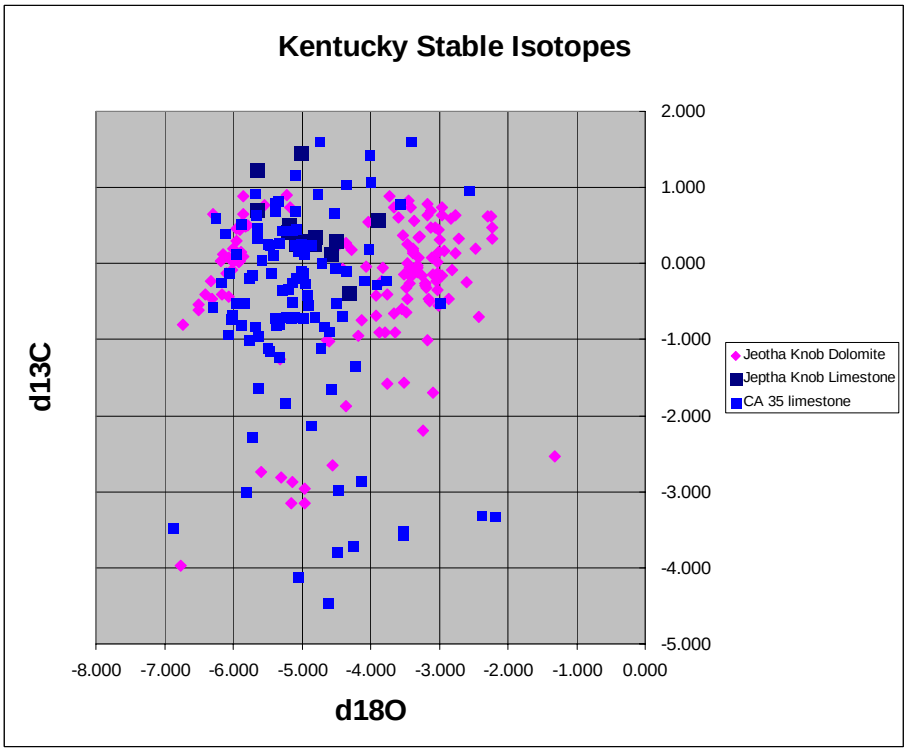

Figure 4-18. Stable isotope values from Kentucky Jeptha Knob dolomites and limestones.

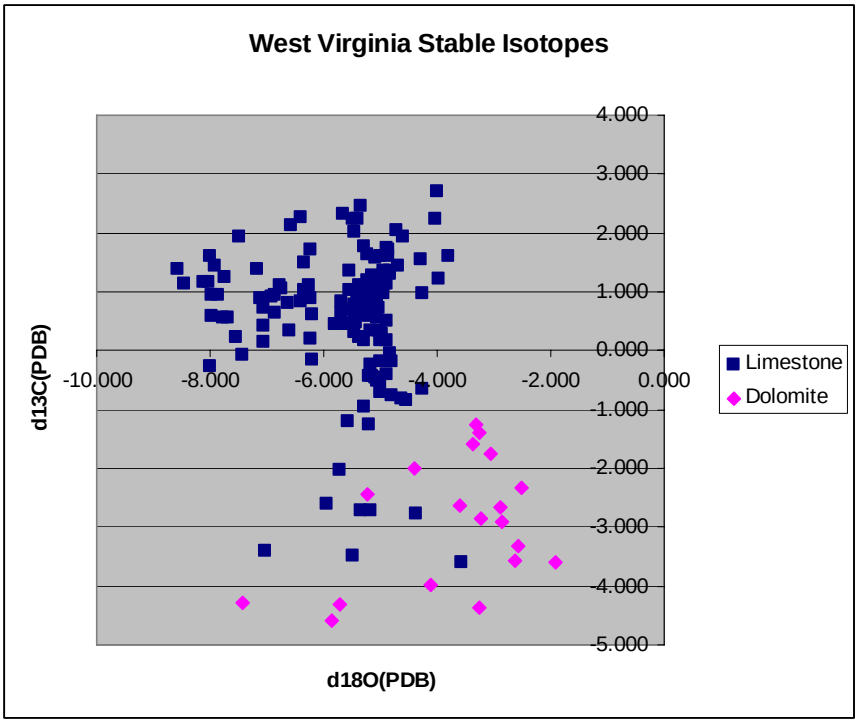

Figure 4-19. Stable isotope data from the West Virginia Sand Hill core.

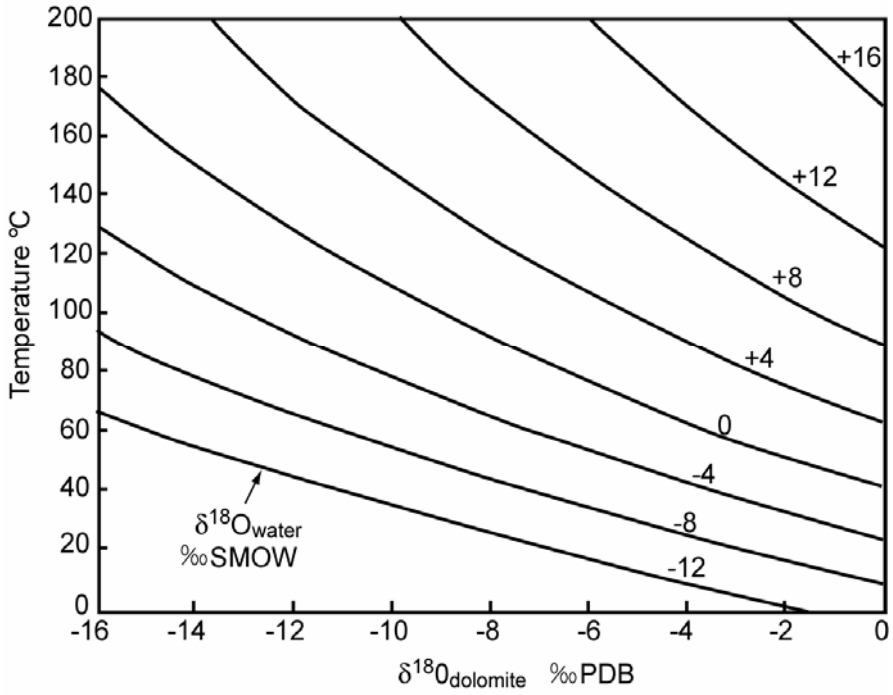

Figure 4-20. Chart used to determine fluid composition by plotting homogenization temperature and d18O values for same sample. Note how fluid composition can greatly alter d18O values of dolomites.

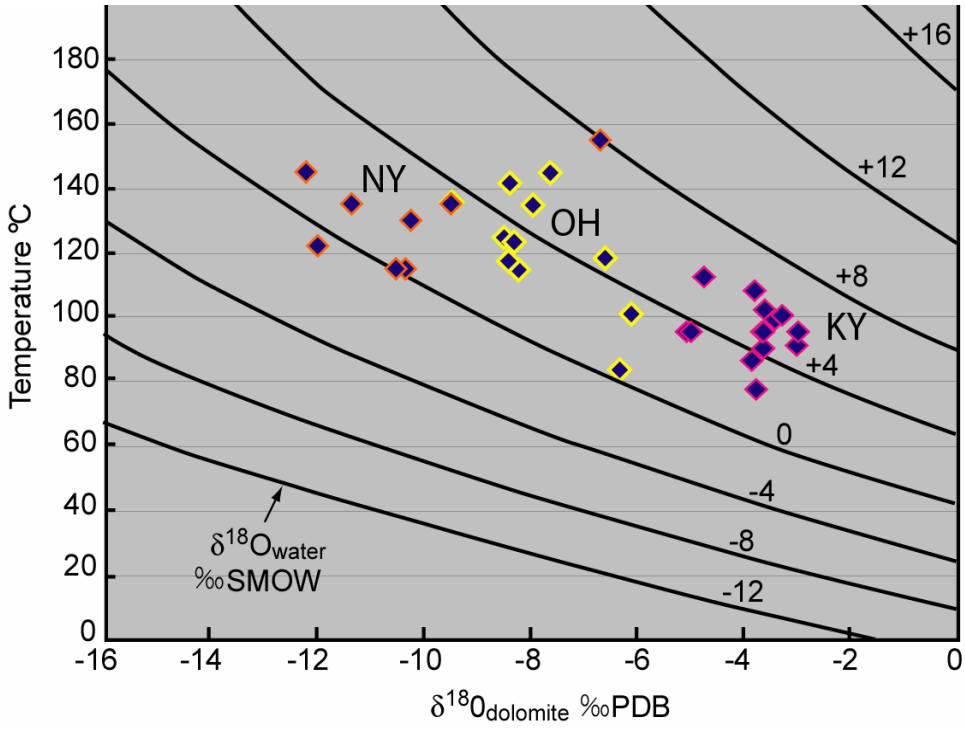

Figure 4-21. Data from New York, Ohio and Kentucky plotted on Figure 4-20. NY fluid looks like it was a bit lighter (~+2‰) than the fluid in KY and OH (around +4 or +5‰).

Trace Elements

Seawater contains very little iron or manganese. Because these elements are readily oxidized (Table 4-3), concentrations for each in seawater is below .002 ppm. Dolomites that form from seawater, therefore, should have very low Fe and Mn concentrations. Subsurface brines, on the other hand, are commonly enriched in these elements, so dolomites that form in the subsurface commonly have high Fe and Mn concentrations.

The New York dolomites have Fe concentrations averaging around 4200 ppm and Mn concentrations of around 880 ppm (Figure 4-22). The saddle dolomites in Ohio have Mn concentrations averaging 1200 ppm and Fe concentrations averaging around 8000 ppm, whereas the matrix dolomites have Mn concentrations of around 450 ppm and Fe concentrations around 8000 ppm (Figure 4-23). The Kentucky dolomites have average Fe concentrations of around 5000 ppm and Mn concentrations of around 550 ppm. The average values for the limestones are an order of magnitude lower (around 500 ppm for Fe and 50 ppm for Mn). This supports a subsurface origin for all of these dolomites.

Table 4-3. Trace Elements in Seawater and Subsurface		
Element	Seawater	Subsurface Brine
Calcium (Ca)	411 ppm	1,000-20,000
Iron (Fe)	0.002 ppm	0.01-500 ppm
Manganese (Mn)	0.0002 ppm	0.1-100 ppm
Fe/Ca	10^{-6}	10^{-3}
Mn/Ca	10^{-7}	10^{-4} or 10^{-3}

Table 4-3. Abundance of Iron and manganese in seawater and subsurface brines (from Allan and Wiggins, 1993).

Strontium Isotopes

Dolomites that formed from subsurface brines commonly (but not always) have $^{87}Sr/^{86}Sr$ ratios that are higher (more radiogenic) than seawater for the time that they formed (Allan and Wiggins, 1993). The reason for this is that continental basement rocks and feldspathic sandstones that commonly overlie the basement are enriched in radiogenic strontium (^{87}Sr). The mantle is enriched in ^{86}Sr, which is added to ocean water at spreading ridges. The ratio of $^{87}Sr/^{86}Sr$ in seawater changed with time throughout the Phanerozoic due to variations in sea-floor spreading and erosion rates. Dolomites that form in seawater should have $^{87}Sr/^{86}Sr$ ratios that are the same as seawater for that time. Hydrothermal dolomites commonly, but not always, have $^{87}Sr/^{86}Sr$ ratios that plot above seawater for the time that they were initially deposited because the fluids that make the dolomite pick up radiogenic strontium from the basement or feldspars.

The range of seawater for the time that the Trenton and Black River formed is between 0.7078 and 0.7085 (Figure 4-24). Dolomites with values higher than 0.7085 are likely to have been formed by fluids that passed through basement or immature siliciclastic rocks prior to making the dolomite. Limestones are generally more enriched in Sr than the dolomites, so some matrix dolomites may inherit seawater values for $^{87}Sr/^{86}Sr$ from the limestones they replace.

Therefore some matrix dolomites that are hydrothermal in origin may plot on seawater while saddle dolomites are almost always radiogenic.

New York Data. The strontium isotope values for the dolomites in the Black River range from 0.7085 and 0.7092 for both the matrix and saddle dolomites and are just above the range for Ordovician seawater. Although not strongly radiogenic (enriched in ^{87}Sr), the dolomites do plot above the range for seawater at the time of deposition, which suggests that the fluid that formed the dolomite passed through basement rocks or immature feldspar-rich siliciclastics prior to making the dolomite. Again, this analysis supports a subsurface origin for the dolomites where the fluid that made them flowed up from the basement or underlying immature siliciclastics.

Ohio Data. The saddle dolomites range from 0.7083 to 0.714 with all but one sample plotting above the upper limit for Trenton-Black River seawater (Figure 4-25). The matrix dolomites from Ohio have $^{87}Sr/^{86}Sr$ ratios ranging from 0.708 to 0.715 (Figure 4-26). About half of the samples have values within the range of Late Ordovician seawater. The generally lower values for the matrix dolomites suggests that they may have reused much of the strontium from the limestones while the saddle dolomites precipitated directly from the fluids flowing up the faults and more accurately reflect the composition of the dolomitizing brine.

Kentucky Values. The Jeptha Knob samples have $^{87}Sr/^{86}Sr$ ratios between 0.708 and 0.7096 with 8 of 26 measurements plotting in the seawater range and the rest above the seawater range (Figure 4-27). Again, since these dolomites are all matrix dolomites, some strontium from the limestones may have been incorporated.

The strontium isotopes suggest that the fluids that made the dolomite passed through continental basement rocks or immature feldspar rich siliciclastics prior to making the dolomite. This supports a bottom-up fluid flow path and a likely hydrothermal origin. The fact that the matrix dolomites generally have lower values suggests that they may reuse some of the strontium from the limestones they replace.

Summary of Geochemistry Results

The fluid inclusion and geochemistry results to date support a hydrothermal origin for all of the dolomite types that occur in the Trenton Limestone and Black River Group across the study area. The fluid inclusion homogenization temperatures suggest that the dolomite formed at temperatures between 85 and 170°C with generally higher temperatures in New York and Ohio and slightly lower temperatures at Jeptha Knob and at the Allen Farm in Kentucky. The fluid that made the dolomite was a saline brine. The salinity of the fluid inclusions averaged around 14.5wt % in New York, 17wt% in Kentucky and about 20wt% in Ohio. These values are 4 to 6 times the salinity of normal seawater. The oxygen isotope composition of the brine was about +2‰ in New York, and +4 ‰ in Ohio and Kentucky.

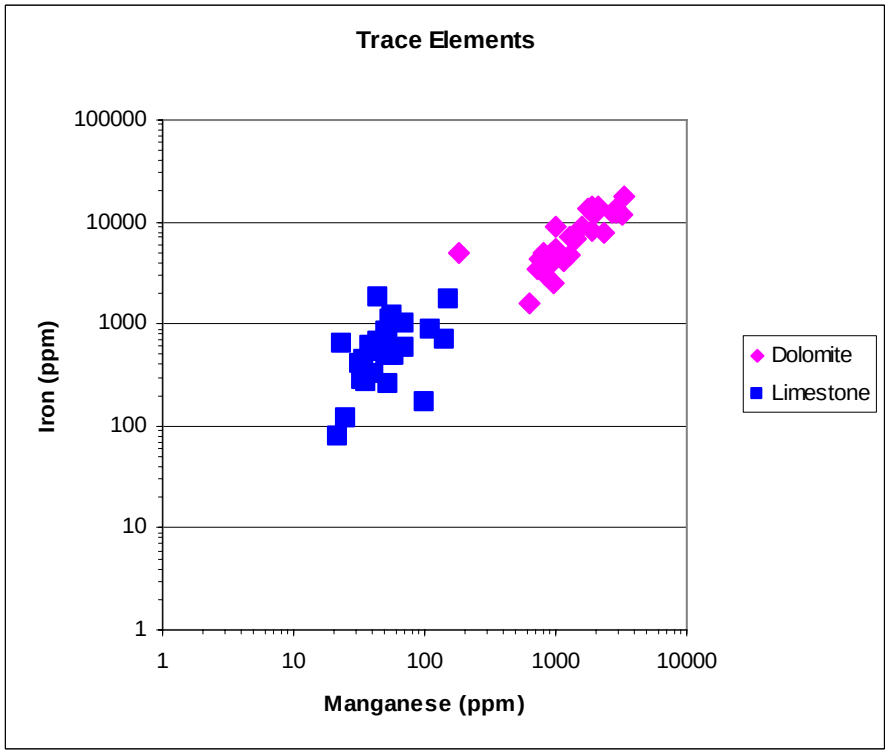

Figure 4-22. Trace element data from New York samples.

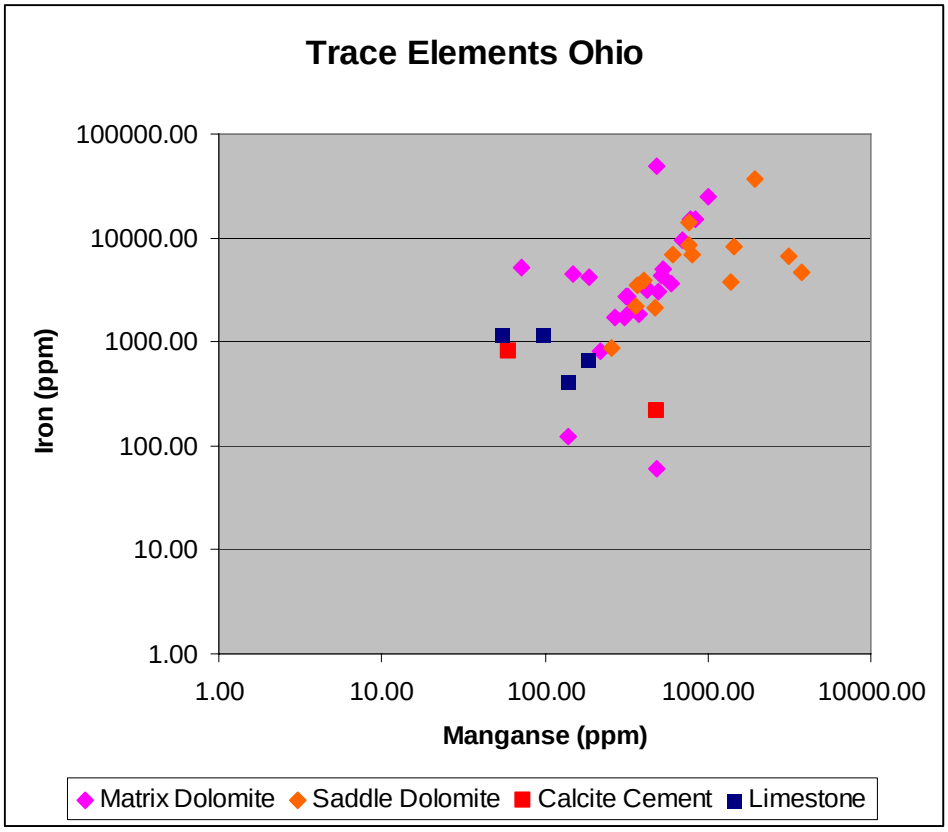

Figure 4-23. Trace element data from Ohio samples.

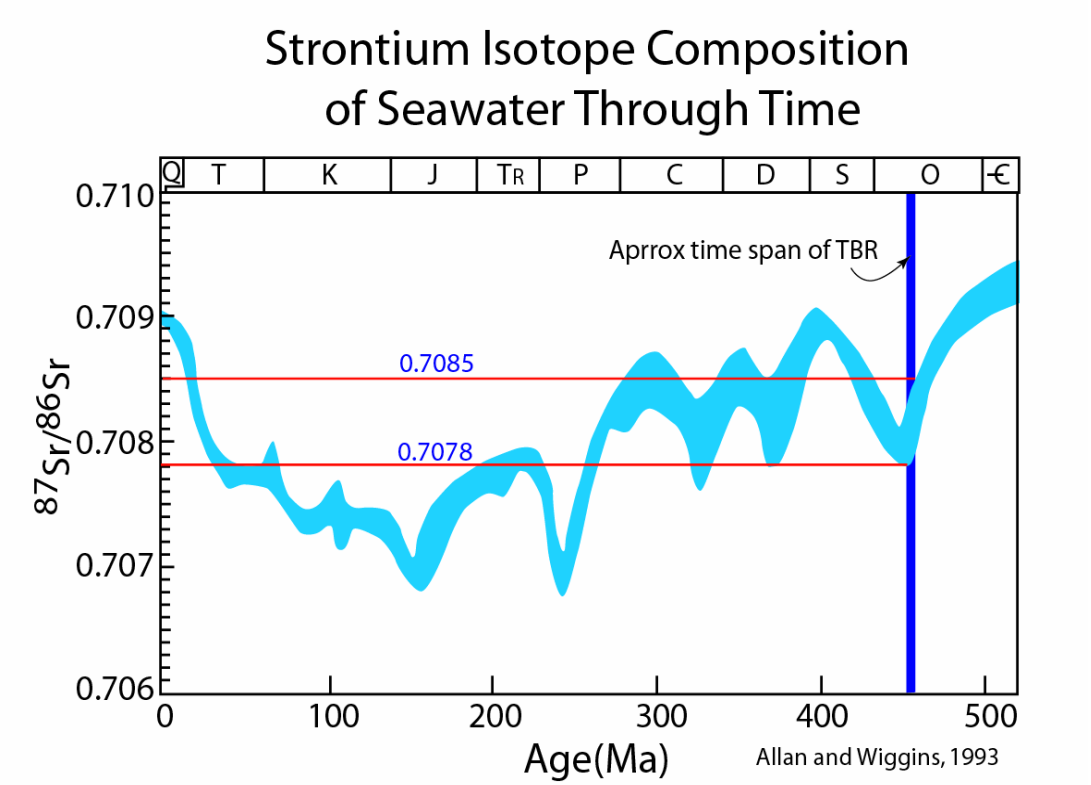

Figure 4-24. Strontium isotope ratio curve for seawater through time with range for Trenton and Black River seawater highlighted. The ratio decreased with time from the Black River to the Trenton.

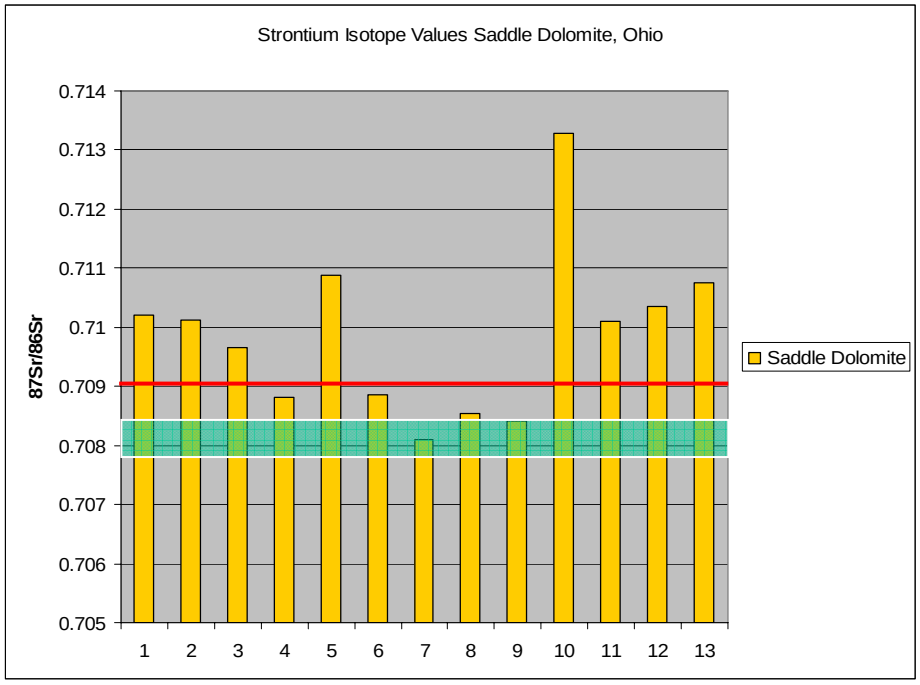

Figure 4-25. Strontium isotope ratios for saddle dolomite in Ohio samples. All but one sample exceeds the seawater ratio (shaded in green) for Trenton Black River time. Many exceed the all time maximum ratio for seawater (red line).

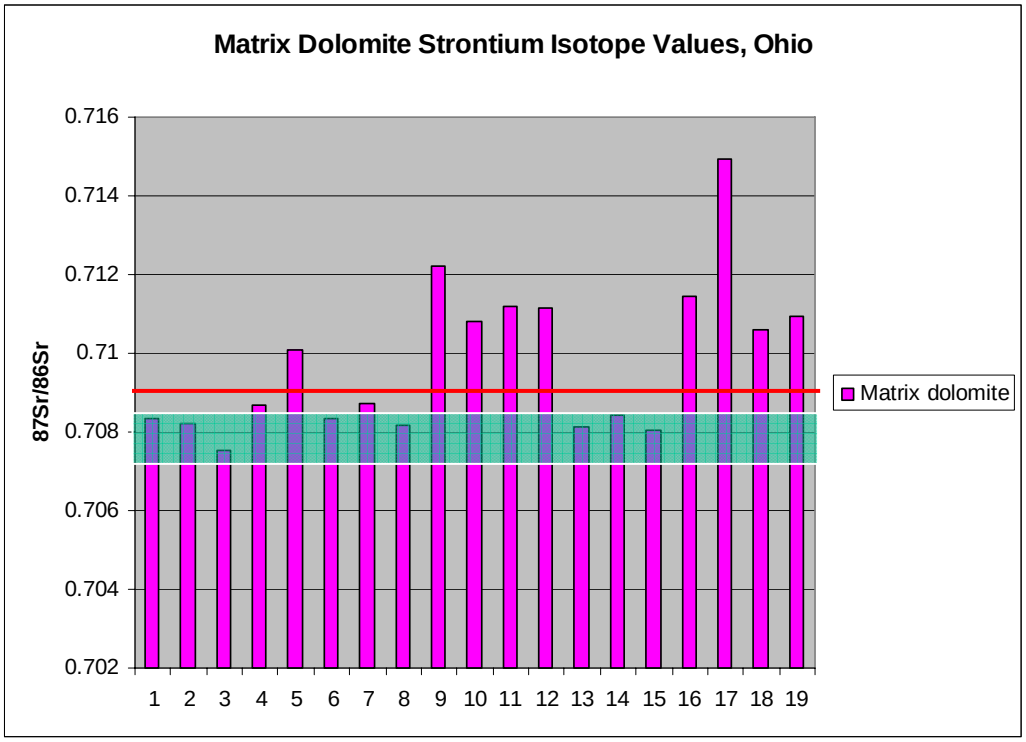

Figure 4-26. Strontium isotope ratios for matrix dolomite in Ohio samples. About half the samples fall within the seawater range and half exceed it.

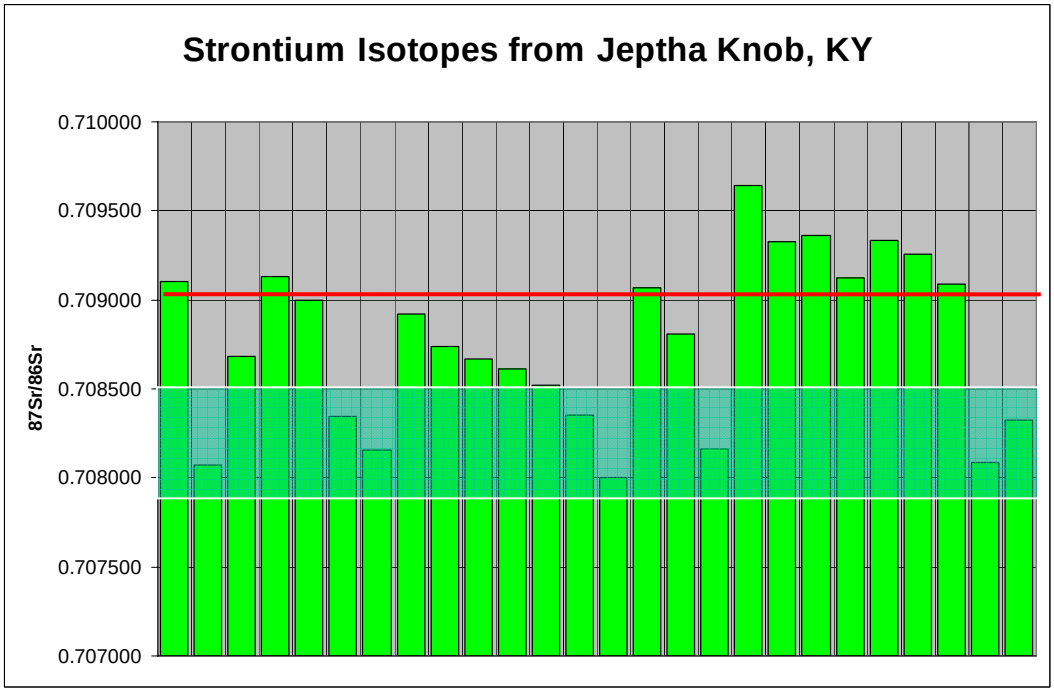

Figure 4-27. Strontium isotope ratios for Jeptha Knob dolomite in Kentucky. Eight of 26 samples occur within the seawater range and the rest are higher.

The salinity of the fluids and the $\delta^{18}O$ values track each other. In New York, the fluids are less saline and less enriched in ^{18}O. When seawater evaporates, it gets more saline and more enriched in ^{18}O. The reason for this is that the much more common ^{16}O is less dense than ^{18}O and preferentially evaporates.

We do not have a good reason for why the salinities would vary from one part of the basin to another and be greater in Ohio and Kentucky than they were in New York, but this appears to be the case. Today, the brines in all formations in New York that underlie the Silurian Salina evaporites are at or near halite saturation (~30 wt% or 300,000 ppm) which is more than double the 14.5 wt% average for the Black River dolomites.

Many previous workers have suggested that the salinity of the fluid inclusions imply that the dolomite formed after the deposition of Salina evaporites and that the saline brines that made the dolomite were sourced from the Salina evaporites. This makes intuitive sense at first, but a closer look reveals this to be unlikely. First of all, the Salina evaporites are not present across the entire study area. They are present in New York, western Pennsylvania and eastern Ohio, but are absent in northwest Ohio and in Kentucky. The salinity trend in the Trenton-Black River dolomites is the opposite of the distribution of the Salina evaporites. Average salinities in the fluid inclusions are higher in Kentucky (17 wt%) and northwest Ohio (20 wt%) where the Salina is absent and lower in New York (14.5 wt %) where the Salina is quite thick.

The fact that the salinity in the fluid inclusions in New York is half what it is today argues against a Salina source for the brines. If the Salina was the source, the brines in the fluid inclusions in New York would be much more saline and salinity would probably decrease from New York to northwest Ohio and Kentucky. This is a good argument that the Black River dolomitization probably precedes the deposition of the Salina evaporites. This begs the question, if the salinity did not come from the Salina evaporites, where did it come from? It appears that salinity increases in all sedimentary basins whether evaporites are present or not (Figure 4-28) (Hanor, 1993: Heydari, 1997). Salinity actually increases in basement rocks with depth (Figure 4-29) (Frape and Fritz, 1987). The source for the brines that made the dolomites is probably just fluids that were deeper down in the sedimentary basins or even deeper in basement. Any fluid flowing up a fault in most basins will be more saline than the fluids higher in the section.

The salinity of the fluid inclusions in Kentucky is interesting because there are a wide range of values when compared to the New York and Ohio samples (Figure 4-14). Most of the Kentucky samples are between 15 and 25 wt %, but there are a few values as low as 3.5 wt% which is a seawater value. This suggests that there may have been some mixing of fluids at Jeptha Knob. Perhaps seawater was coming down some faults and fractures as hydrothermal fluids were coming up other faults and fractures and the fluids mixed during dolomitization. A hydrothermal fluid/seawater mixture could be a powerful dolomitizing fluid because the seawater could supply magnesium and the hydrothermal fluids could provide heat, which promotes dolomitization.

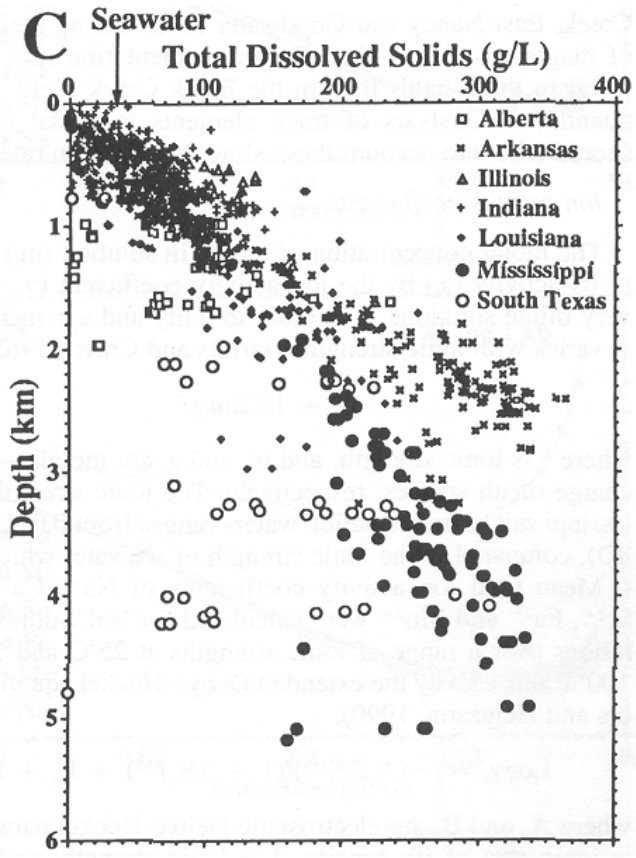

Figure 4-28. Variations in salinity with depth in sedimentary basins (from Heydari, 1997). Salinity generally increases with depth in most sedimentary basins.

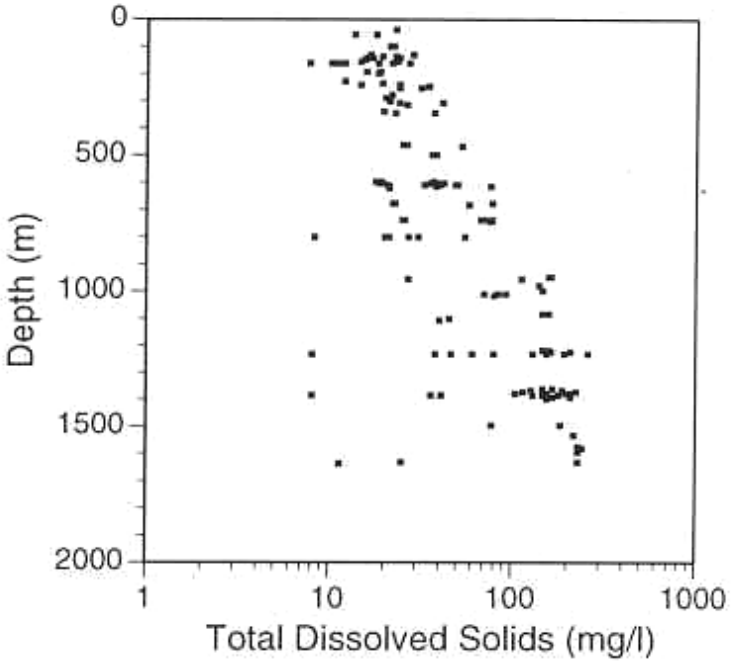

Figure 4-29. Variations in salinity with depth in crystalline basement rocks of Canadian Shield (from Frape and Fritz, 1987 by way of Deming, 1994).

The dolomite is enriched in iron and manganese, supporting a subsurface origin for the dolomitizing brine. Iron and manganese are virtually absent in seawater, but are common in subsurface brines (Table 4-3). Iron and manganese do not build up in seawater because they are easily oxidized. In reducing subsurface environments, Fe and Mn can build up to significant levels and easily get included in the dolomite matrix. The Fe and Mn are roughly an order of magnitude more common in the dolomites than they are in the limestones, which suggests that the dolomitization occurred in a subsurface environment whereas most of the limestone diagenesis occurred in a marine or possibly meteoric environment.

The dolomite also commonly has radiogenic $^{87}Sr/^{86}Sr$ values, which suggests that the fluid passed through basement rocks or immature siliciclastics prior to making the dolomite. The general trends show that the saddle dolomites are more radiogenic than the matrix dolomites. Virtually all of the saddle dolomite is radiogenic compared to Middle Ordovician seawater. Some of the matrix dolomite is radiogenic and strontium values plot on or near the range of Middle Ordovician seawater. The best explanation for this is that the saddle dolomite precipitates directly from the hydrothermal fluids whereas the matrix dolomite has a mixture of strontium from the hydrothermal fluids and strontium that was in the limestone prior to dolomitization. As dolomitization of limestone proceeds some of the elements in the limestone (including strontium) may get incorporated in the matrix dolomite. Samples with less radiogenic strontium isotope ratios may have included more strontium from the precursor limestone while those with more radiogenic values may have more of a hydrothermal fluid component.

All of these geochemical analyses support a hot subsurface origin for the dolomites. Similar values have been found in TBR dolomites in Ontario and Michigan suggesting that they too are of a hot, subsurface origin. There is no indication that any of this dolomitization is of a reflux, seawater or mixing zone origin. The next question is, are these dolomites of a hydrothermal or geothermal origin?

Hydrothermal or Geothermal?

Hydrothermal diagenesis occurs when fluids are introduced to a given formation at a temperature that exceeds the ambient temperature of that formation (*sensu* White, 1957; Davies, 2001). By this definition, there is no set temperature range in which hydrothermal alteration occurs, the water simply must be warmer than the ambient temperature of the formation, given the local geothermal gradient. For example, if a formation is buried to a depth where the ambient temperature is 50°C and a fluid is introduced that is 60°C, that fluid would there be called a hydrothermal fluid. In the absence of local igneous intrusions, the most efficient way for a hydrothermal fluid to be introduced to a formation is via rapid upward fluid flow from greater depths through high-permeability faults and fractures (Deming, 1992). Lateral and vertical unfocused fluid flow through confined formations, in the absence of faults and fractures, is in most cases too slow to generate hydrothermal conditions because fluids equilibrate with the ambient temperature as they migrate laterally through the formations (Deming, 1992).

Hydrothermal alteration is thought to occur when relatively high-pressure, high-temperature fluids flow up active faults into permeable formations that underlie sealing shales, evaporites or other low-permeability strata. Solubility of carbonates (and other minerals) is

directly affected by changes in temperature, pressure, P_{CO2}, pH and salinity, and all of these are fluctuating on short time scales in fault-related hydrothermal systems (Rimstidt, 1997). When fluids first enter the formation from the faults they may have significantly different pressure, temperature and composition than the fluids in the host rock. Because the fluids are introduced instantaneously, geologically speaking, they can overcome rock buffering and are capable of producing significant diagenesis in short periods of time. With time, the fault-derived fluids mix with fluids in the formation and eventually equilibrate with the ambient conditions. Further diagenesis is likely to occur during these periods of fluid mixing and equilibration. Hydrothermal dolomitization would most likely occur during periods of pressure drop by highly supersaturated fluids. The curved shape of saddle dolomite crystals is probably a result of rapid precipitation from *highly* supersaturated fluids (Davies, 2001; Machel, 2004). The most efficient way to introduce a fluid that is highly supersaturated with respect to dolomite into a regional limestone is via faults and fractures.

Machel and Lonee (2002) suggested that hydrothermal dolomite needs to be distinguished from "geothermal" dolomite, which is interpreted to form from fluids that are the same temperature as the surrounding rocks. Geothermal dolomite is thought to form from fluids that flow laterally or very slowly in a vertical sense.

Demonstration of a hydrothermal versus geothermal origin for dolomites and other minerals can be done in different ways. As a first pass, field relations can strongly suggest a hydrothermal origin. If dolomitization is highly localized and patchy, the patchiness can be linked to faults and the geochemistry and fluid inclusions support a high-temperature subsurface origin, the mineralization is likely to be hydrothermal in origin. This is the case with most of the Trenton and Black River dolomites in the study area. The dolomite is patchy, only occurring near faults visible on seismic and has geochemical attributes that suggest a hot, subsurface origin. This strongly suggests that fluids flowed up the faults and precipitated dolomite. Although compelling, this evidence is still viewed by some as equivocal support for a hydrothermal origin because the fluids could theoretically have flowed very slowly up the faults and dolomitized the limestone at near ambient temperatures.

The most convincing way to demonstrate a hydrothermal origin for dolomite is to determine the burial and thermal history of the formation in question and compare that to the fluid inclusion homogenization temperatures in the dolomites (Davies, 2001; Machel and Lonee, 2002). If the homogenization temperatures exceed the maximum temperatures that the formation has ever been exposed to during burial, or the known depth at the time of dolomitization, the dolomite or other minerals can be called unequivocally hydrothermal. Furthermore, if the timing of dolomitization can be constrained through crosscutting relationships and the fluid inclusion homogenization temperatures exceed the maximum burial temperature at the known time of dolomitization, these dolomites can also be said to be unequivocally hydrothermal.

Figure 4-30 is a conversion of CAI values to maximum burial temperatures determined experimentally by Hulver (1997). Hulver gives minimum and maximum temperatures for each CAI value. The minimum temperatures would be correct if the strata were buried to near their maximum burial temperatures for at least 100 million years. They would be closer to the maximum temperatures in the range if they were only buried to near their maximum temperature

for 10 million years. Figure 4-31 is a map where the CAI values for the study area have been converted to temperature ranges using Hulver's calculations. Most of the cores from KY and NW OH fall in the area where the CAI is <1.5. This suggests that the maximum burial temperature was between 30° and 52°C. The temperature would be closer to 30°C if they were at their maximum burial depth for more than 100 million years and closer to 52°C if they were buried to their maximum burial temperature for closer to 10 million years. Either way, the homogenization temperatures from the dolomites in NW Ohio and Kentucky exceed the maximum burial temperature by between 30 and 120°C. This supports a hydrothermal model where fluids that were much hotter than the ambient burial temperature flowed up faults and into shallower horizons to make the dolomite. There is no possible way that the dolomites in NW Ohio and Kentucky could be of a geothermal origin because the Trenton and Black River were never buried to a temperature equal to the homogenization temperatures in the dolomites.

The same is true for the Trenton and Black River dolomites in Ontario and Michigan. At the Hillman Field in Ontario, fluid inclusion homogenization temperatures for the dolomites ranged from 100-220°C (Coniglio et al., 1994), but CAI analysis in that area suggests that the Trenton was never buried more than a kilometer (Colquhoun, 1991). Using a geothermal gradient of 25-30°C/km and a surface temperature of 20°C, the maximum burial temperature was 45-50°C. The homogenization temperatures exceed the maximum ambient burial temperature by 50-170°C. A similar scenario occurs in Michigan where fluid inclusion homogenization temperatures from Trenton-Black River dolomites at Albion Scipio Field exceed the maximum burial temperature by 40-90°C (using fluid inclusion data from Allan and Wiggins (1993) and CAI data from Repetski et al. (2004)). In Ohio, fluid inclusion homogenization temperatures exceed the maximum burial temperature by 50-110°C.

In New York, all of the cores are located in the area where the CAI values from the overlying Utica Shale were 4.5, which suggests that the Utica was heated to between 187 and 354°C (Hulver, 1997). Therefore, in this case, the Black River was buried to a depth where the temperature was equal to, or greater than, the fluid inclusion homogenization temperatures in the dolomites (Figure 4-31). This does not mean that the dolomites in New York are not hydrothermal in origin, just that the formation was buried to a temperature that exceeded the temperature at which the dolomites formed. If the dolomitization was during early burial when the ambient temperature was still <100°C the dolomite would still be considered to be hydrothermal in origin. Other evidence, such as the timing of faulting and the relatively low salinity of the fluid inclusions, suggests that the dolomitization was very early in the burial history. The dolomitized horizons in New York are virtually identical to those in NW Ohio, Ontario and Michigan with matrix dolomitization, breccias, saddle dolomite, fractures and vugs and the clear link to faults. It is unlikely that these features would be produced in a hydrothermal setting in Ohio, Michigan, and Ontario but in a "geothermal" setting in New York.

Conodont Color Alteration Index Temperatures for Geological Heating Durations of 10-100 m.y.

CAI	Minimum Temperature (°C)†	Maximum Temperature (°C)‡	Temperature Range (°C)™	Calculated Depth of Burial (km)®
1	20±5©	20±5©	20±5	0.00±0.20
1.5	30±5	52±7	37±22	0.68±0.88
2	35±7	106±10	72±44	2.00±1.76
2-2.5*	35±7	146±6	90±62	2.80±2.48
2.5	88±9	146±6	116±36	3.82±1.46
3	127±6	160±6	144±22	4.94±0.90
3-3.5*	127±6	206±8	168±56	5.92±2.24
3.5	142±6	206±8	175±39	6.20±1.56
4	187±8	254±9	221±42	8.04±1.68
4-4.5*	187±8	354±1	267±88	9.88±3.52
4.5	236±9	354±1	291±64	10.84±2.56
5	337±1	>400	368±32	13.92±1.28

† Heating duration of 100 m.y. at maximum temperature, from Table 2.3 equations.
‡ Heating duration of 10 m.y. at maximum temperature, from Table 2.3 equations.
™ Mean of: low temperature minus its standard error, and
high temperature plus its standard error.
Total uncertainty is half their difference, considered here to be the 2 sigma equivalent.
® Geothermal gradient of 25°C/km, surface temperature of 20±5°C.
© Extremely low temperatures set to surface temperature of 20±5°C.
* Combined integer and half-integer CAI values.

Figure 4-30. Temperature ranges for CAI values from Hulver, 1997.

Fluid inclusion homogenization temperatures from the Lima-Indiana Trend in NW Ohio for matrix and saddle dolomites range from 100-160°C, but the Trenton was never buried more to a temperature of more than 52°C in this area (Figures 4-31 and 4-32). Therefore, the Trenton-Black River dolomites are unequivocally hydrothermal in Ohio, Michigan and Ontario. The Kentucky dolomites are also hydrothermal because the fluid inclusion homogenization temperatures of 60-120°C) exceed the maximum burial temperature of 52°C. If one extends the trendlines from the Rowan et al. data across the Kentucky border it appears that Jeptha Knob also was probably never buried more than a kilometer yet has fluid inclusion homogenization temperatures in excess of 100°C. The dolomites from those fields are virtually identical to those found in New York in appearance, association with wrench faults and geochemical attributes. It is unlikely that they would have formed by a different process.

It appears that all of the dolomite types in Kentucky and Ohio (including Jeptha Knob, the facies and cap dolomite types) are hydrothermal in origin. Their fluid inclusion temperatures for all those dolomite types exceed the established local maximum burial temperatures. Even though saddle dolomite is not present, these dolomites are still hydrothermal in origin. This work will have lasting scientific value because it has demonstrated that dolomite can be

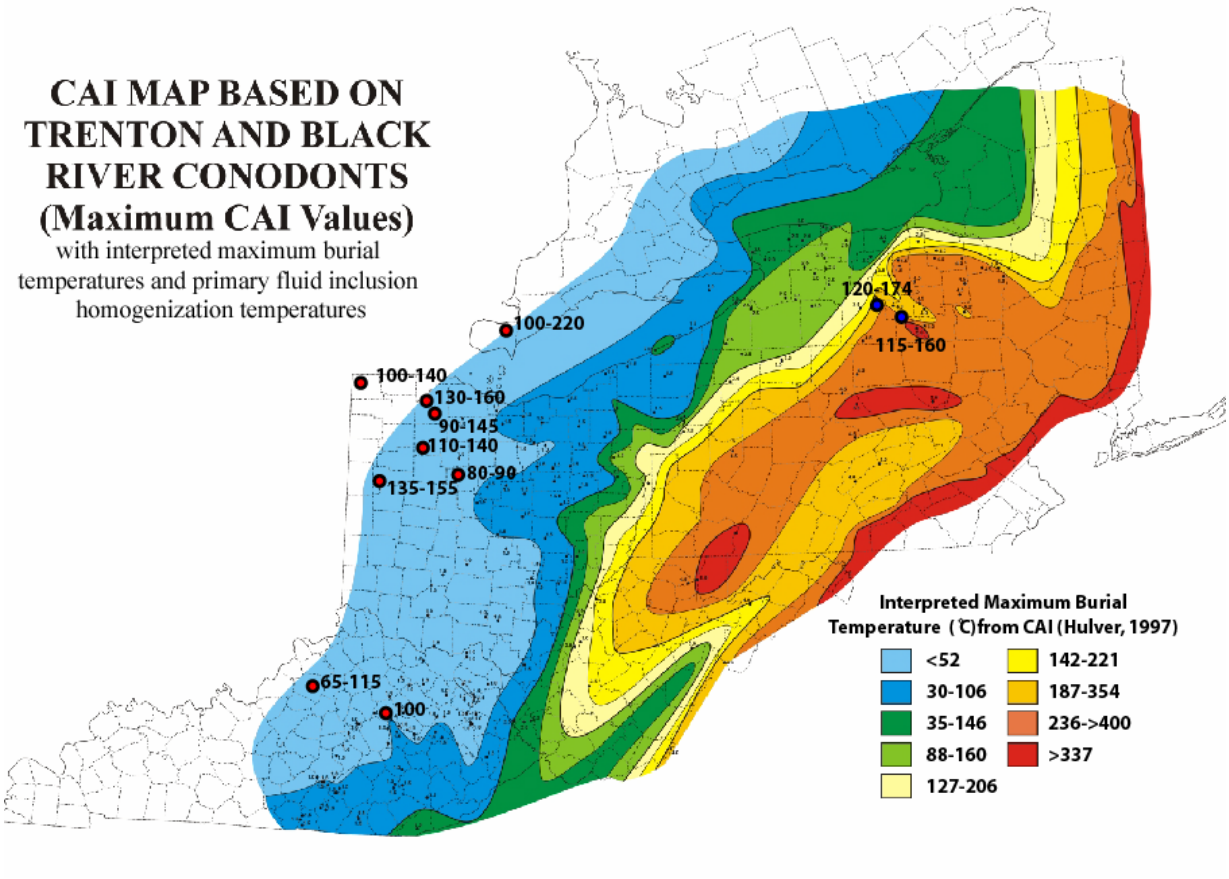

Figure 4-31. Map of maximum burial temperatures based on CAI and Hulver (1997) with range of fluid inclusions homogenization temperatures conducted for this study. Note that homogenization temperatures in Ohio and Kentucky are far higher than maximum burial temperature. New York has seen higher burial temperatures than are recorded in the fluid inclusions

hydrothermal in origin, yet have no obvious saddle dolomite or vugs. It is interpreted that the fluids are still sourced from faults, but that the matrix was more permeable at the time of dolomitization, so fluids flowed farther from the fault source, dolomitizing the limestone without significant pressure-related features, such as zebra fabrics or breccias, forming in abundance.

Other evidence that suggests a hydrothermal origin for the dolomite in these locations includes the relatively low salinity of the fluid inclusions in New York when compared to the present-day and post-Salina evaporite brines. If the dolomite had formed at great depth where the burial temperatures were equal to the 110-170°C homogenization temperatures, this would have occurred after deposition of the Salina evaporites. The composition of the subsurface brines would almost certainly have been more saline if the dolomitization post-dated Salina evaporite precipitation.

Another observation that is suggestive of hydrothermal conditions is that the late calcite has fluid inclusion values that are significantly cooler (about 17°C on average) than the earlier dolomite. This suggests that the temperature during dolomitization was higher than it was during precipitation of the calcite. This is inconsistent with steady deep burial during mineralization but consistent with hydrothermal fluid flow. Fluids that flowed up the faults were warmer during

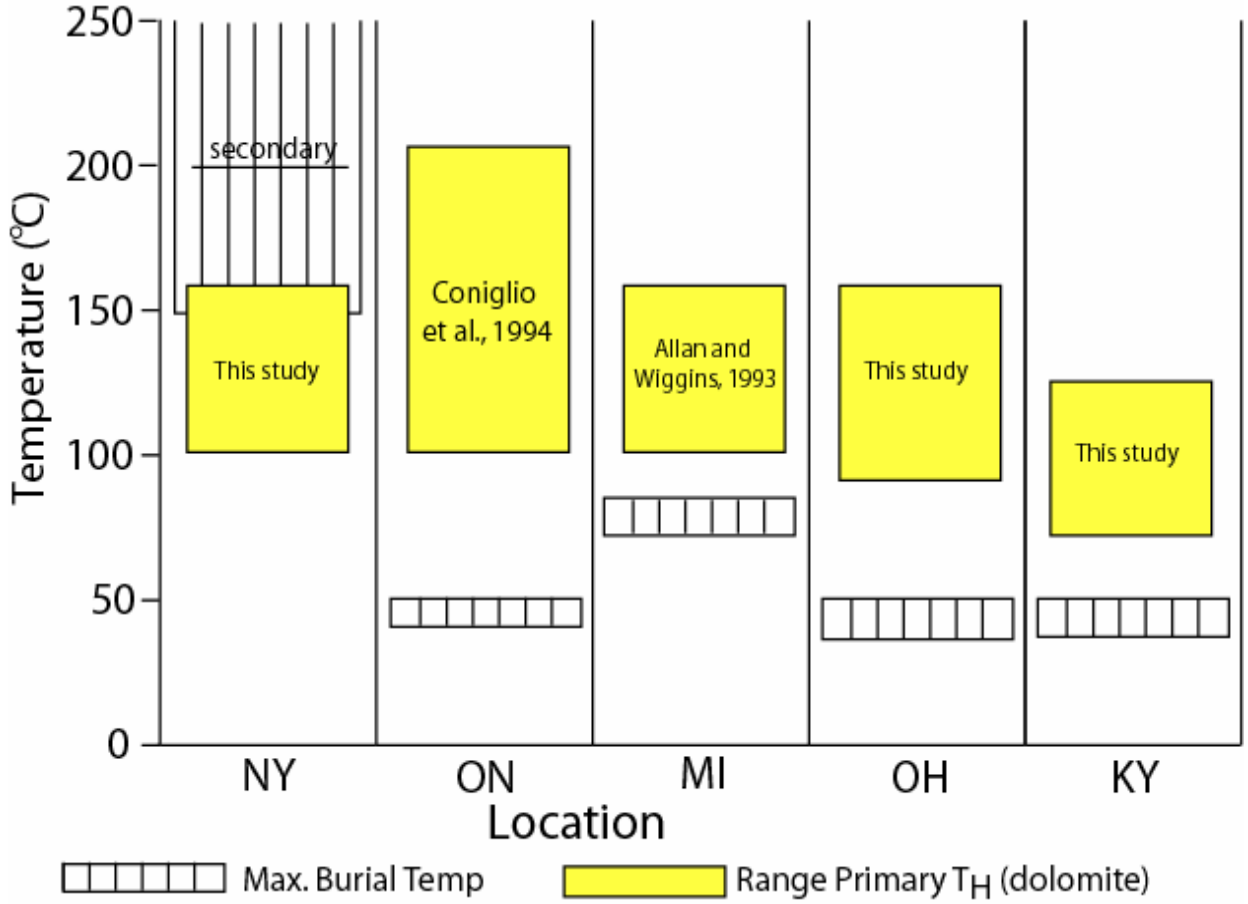

Figure 4-32. Maximum burial temperatures and fluid inclusion homogenization temperatures from saddle and matrix dolomites in Trenton-Black River reservoirs. Dolomites in Kentucky, Ohio, Michigan and Ontario are unequivocally hydrothermal, New York experienced higher burial temperatures than are recorded in the fluid inclusions.

dolomite precipitation than they were during the subsequent calcite cementation. The calcite may also be hydrothermal in origin (its homogenization temperatures also exceed the maximum ambient burial temperature) but it was just a cooler hydrothermal fluid than the fluid that precipitated the dolomite.

Timing and Depth of Burial During Alteration

Hydrothermal fluid flow is thought to be most common while faults are active and much less common during periods of tectonic quiescence (Sibson, 1990, 2000; Davies, 2001; Knipe, 1993; Muir Wood, 1994) (Figure 4-33 Knipe). If this is true, and there is good evidence to

support this contention, the timing of hydrothermal alteration is closely linked to the timing of fault movement.

Most of the faults that have associated dolomitization in New York, Ontario and Ohio appear to have been active in the Late Ordovician-Early Silurian Taconic Orogeny and mainly inactive after that time (Smith et al., 2003a, 2003b). On seismic data, most dolomitized wrench faults in New York die out in the Trenton or Utica and sags are commonly filled in during Trenton or Utica time (Figure 4-34). This suggests that most faults were active during the Taconic Orogeny but were not reactivated during subsequent mountain building events. Some fractures and faults have multiple generations of cement lining them suggesting that they were filled episodically when the faults were moving.

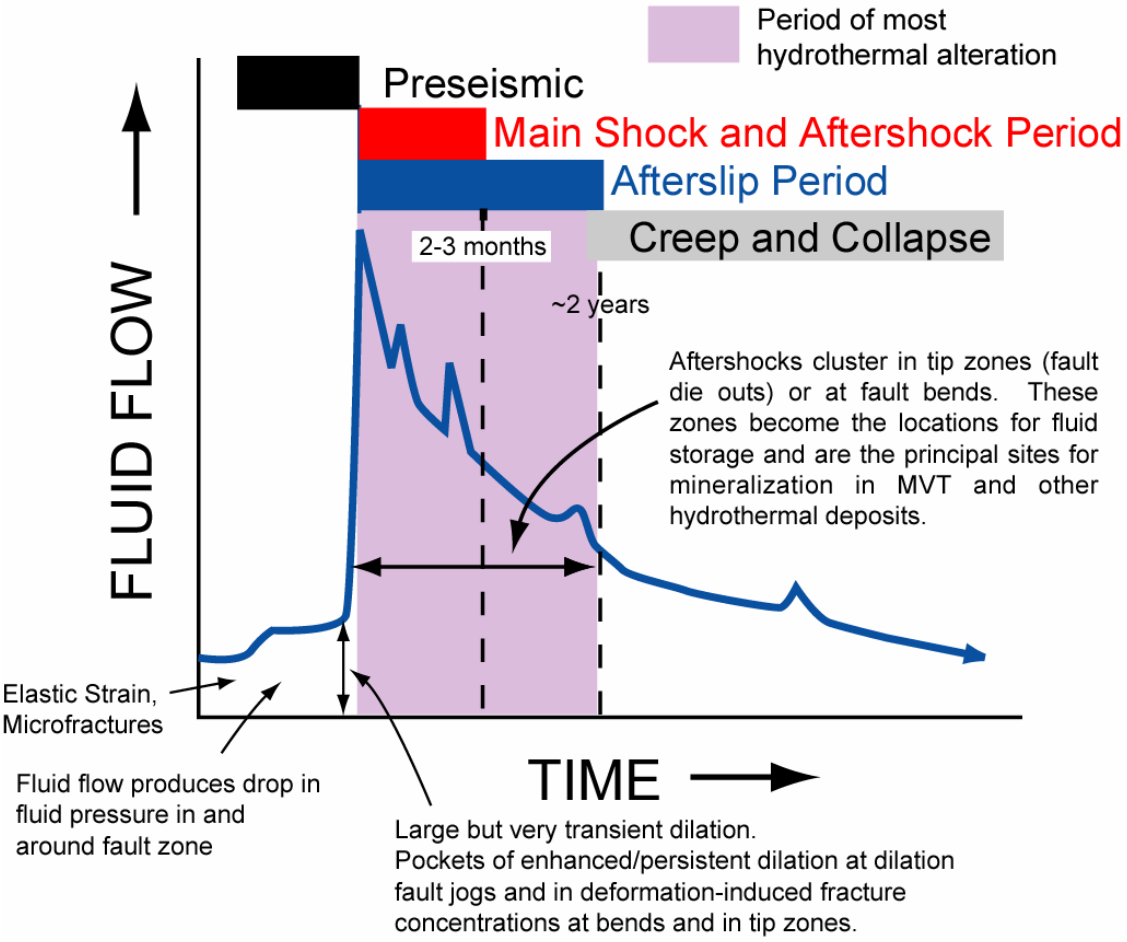

Figure 4-33. Idealized permeability evolution of a fault zone (modified from Knipe, 1993 and Davies, 2001)

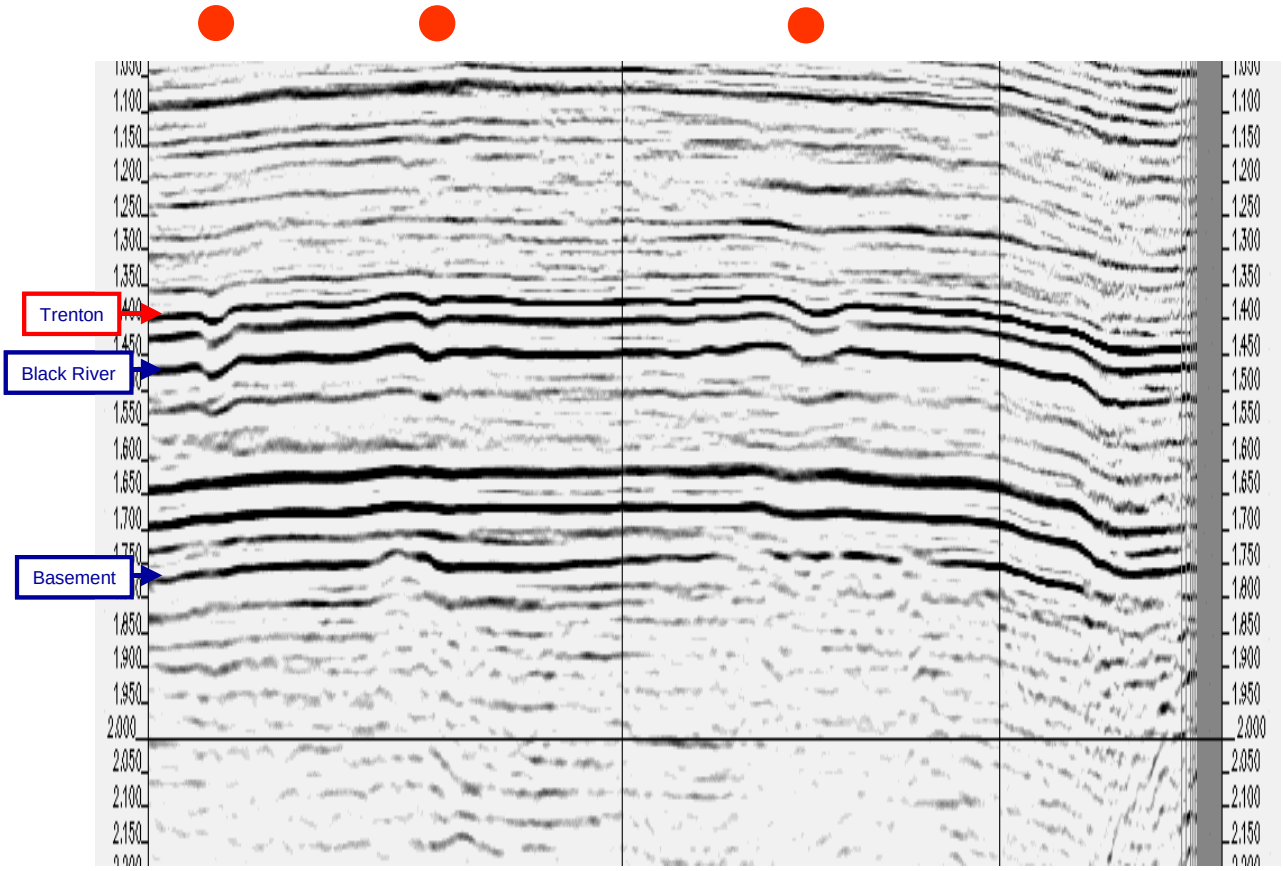

Figure 4-34. Vertically exaggerated line over three Black River fields in New York (courtesy of Talisman Energy) shows that sags in Black River are filled during Utica time.

In the Mohawk Valley, New York to the northeast of the productive area, there was widespread Trenton and Utica-aged syndepositional faulting (Bird and Dewey, 1970; Bradley and Kidd, 1991; Jacobi and Mitchell, 2002; Joy et al., 2000). These faults can have as much as 500 feet of throw in the Ordovician section, but the Silurian and Devonian strata that overlie the Ordovician section just a few kilometers to the south are not affected by the faults (Fisher, 1980). This supports an Ordovician age for the faulting as well as the concept that there was not much fault reactivation during the Devonian Acadian or Late Paleozoic Alleghenian Orogenies.

Abundant and widespread seismites (seismically disturbed beds) in outcrops of Trenton and Utica equivalents in the outcrop belt of Kentucky and Ohio (Pope et al., 1997; McLaughlin et al., 2002; Ettenshohn et al., 2002) suggest that major earthquakes and fault movements occurred far craton-ward of the collision zone to the east.

If the fault movement was primarily during the Taconic, then most of the hydrothermal alteration was probably Taconic-aged (Late Ordovician) as well. During Trenton and Utica time, when most of the faulting appears to have occurred, the Black River was buried to depths of less than 350 meters (1100 feet) in New York and the Trenton was even closer to the surface in Ohio and Kentucky. The Black River was buried to a maximum depth of about one kilometer (3200 feet) by the Early Silurian in south-central New York. If hydrothermal alteration occurred during

the period of active faulting, the Black River was buried to depths of less than a kilometer and probably less than 350 meters.

Support for a shallow burial origin come from Trenton-Black River hydrothermal dolomite reservoirs in Ohio, Ontario and Kentucky that have probably *never* been buried more than 1 kilometer yet their occurrence around faults, appearance and geochemical attributes are very similar to the dolomitized Black River reservoirs in New York. It is unlikely that virtually identical features would be produced in New York by a process different than the one that clearly occurred in Ontario, Michigan and Ohio. It is likely that the alteration occurred before the burial histories significantly diverged.

Fault-Related Hydrothermal Alteration Model

This model is speculative, but is supported by all of the known facts at this time (Figure 4-35). The fault style is a negative flower, but the same general principle would apply to the margin of the Sebree Trough and Jeptha Knob type structures. The Black River Group carbonates were deposited on relatively stable craton (Figure 4-35A). Major collision between North America and Volcanic Island Arc begins during earliest Trenton time and continues through the Late Ordovician and into the Silurian (Ettensohn and Brett, 2002). This collision led to reactivation of appropriately oriented older faults or activation of new faults. Near the thrust front, thrust loading led to normal faulting oriented subparallel to orogenic belt (Bradley and Kidd, 1991). In the more distal parts of the craton, strike-slip faulting is initiated along appropriately oriented faults.

High-pressure, high-temperature fluids flowed up active basement-rooted strike-slip and transtensional faults (particularly in dilational parts of fault zones) during the time of Trenton and Utica deposition, hit low-permeability beds at the base of the Trenton in New York and at the base of the Utica in northwest Ohio and flowed out laterally into the more permeable limestones of the Trenton and Black River. Cooling hydrothermal fluids leached the limestone and produced vugs in a migrating front moving away from the fault zone (Figure 4-35B). As permeability was enhanced by fracturing and leaching, warmer dolomite-supersaturated fluids migrated farther from fault zone precipitating dolomite (Figure 4-35C). These fluids first produced a halo of matrix dolomite, particularly on the downthrown sides of faults in negative flower structures. Because the fluids flowed up from greater depths where pressures are higher, the elevated pressure of the fluids may have led to hydro-fracturing (*sensu* Phillips, 1972), enlargement of existing fractures and further brecciation. Some dissolution vugs may have formed prior to and during matrix dolomitization. Matrix dolomitization was followed by further fracturing, brecciation and vug development as tectonic activity continued (Figure 4-35D). Fractures and vugs were lined or filled with saddle dolomite soon after their formation. This later mineralization occurred during active fracturing as is demonstrated by episodic filling of fractures as they opened.

As time passed, fluids evolved and precipitated a range of other minerals including quartz, bitumen, sulfides and calcite. Bitumen may have formed when kerogen within the altered formation and near the faults was heated by the hydrothermal fluids and small quantities of oil formed that coated some pores and fractures ("forced maturation" of Davies, 2001). If the

faulting was over by Late Ordovician or Early Silurian time (as it appears to be on many seismic lines), that would make most or all of the diagenesis Late Ordovician to Early Silurian in age. If the faulting continued or recurred during the Devonian Acadian or Pennsylvanian Alleghenian Orogenies some of the later stages of mineralization may have occurred during those times. Some calcite cementation may have occurred during later pressure solution of the adjacent limestones under normal burial conditions.

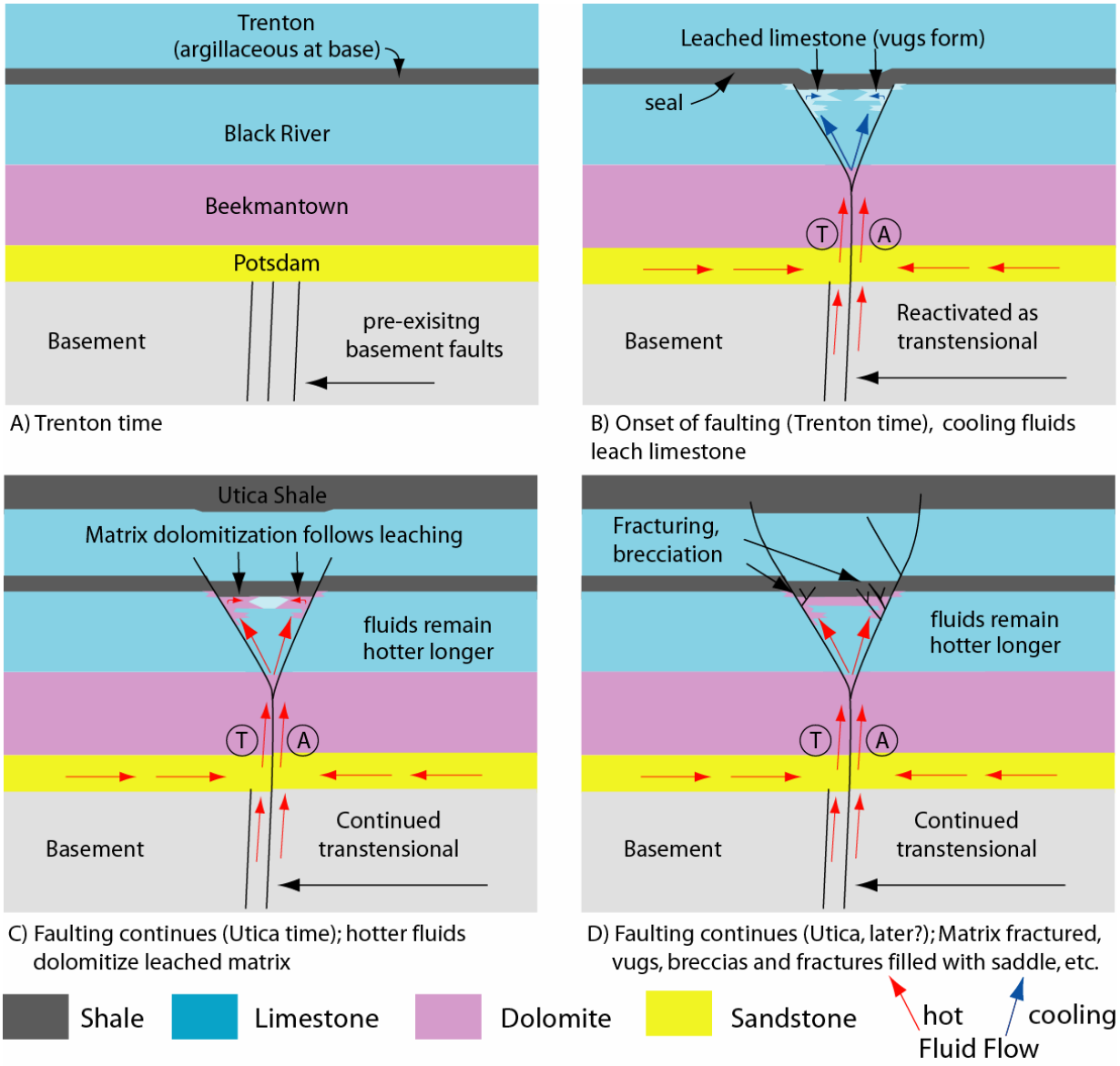

Figure 4-35. Schematic model for development of Trenton-Black River hydrothermal dolomite reservoirs.

Implications for Oil and Gas Exploration

This work shows that hydrothermal dolomite occurs in three of the five states included in the study. Outcrop observations and recent drilling success show that it occurs in Pennsylvania as well. Data limitations in West Virginia do not allow an interpretation at this time. There is good anecdotal evidence that the production in West Virginia is not from hydrothermal dolomite but is in fact from fractured limestone and interbedded shale, similar to the "limestone play" around Lake Ontario in New York. There may yet be hydrothermal dolomite fields found in West Virginia as well.

This work also suggests that hydrothermal dolomite reservoirs may be found in other structural settings besides negative flower structures or sags. The "facies" dolomite in northwest Ohio occurs along a carbonate margin likely to be controlled by a NE-SW trending normal fault that is down to the southeast. Wickstrom et al. (1990) postulated the existence of such a fault trend, but we have no seismic data over the margin with which to confirm this interpretation. The linear nature of the margin strongly suggests fault control. Jeptha Knob is a positive feature (that is also possibly related to strike-slip faulting) that has great porosity and would make an excellent reservoir given the right burial depth/charge/trap scenario.

The data presented in this report show that hydrothermal dolomitization occurs across the study area from Clinton County and the Rough Creek Graben in Kentucky to Northwest and Northeast Ohio, into Pennsylvania and on into New York. There are likely to be many new fields discovered in the study area in the coming years as there are vast amounts of acreage with no Trenton-Black River tests to date.

Link between Field Distribution and Trenton Paleogeography

As mentioned in the report on the stratigraphy (Task 1), many of the major hydrothermal dolomite oil and gas fields occur on or near the margin between the Trenton carbonate platform and time-equivalent intracratonic shale basins (Sebree Trough, Point Pleasant Basin, Taconic Foredeep?) (Figure 4-36). Figure 4-36 shows the oil and gas fields from the Trenton superimposed on a paleogeographic map for the Trenton Limestone from Keith (1986). It is here interpreted that the margins are probably set up by a series of faults that were moving during Trenton time and causing higher subsidence rates in the shale basins. Periods of active faulting are thought to be times when hydrothermal fluids flow up faults and the same faults that set up the margins may also have been conduits for hydrothermal fluids. The best locations may be at fault intersections between intraplatform faults and margin-bounding faults such as where the Bowling Green Fault Trend intersects the margin of the Sebree Trough.

There are many good fields that are not near the margin, most notably Albion Scipio, so it is not essential. There are also some fields that occur in the shale basins. One approach to exploration might be to look along mapped margins between the Trenton carbonate platform and any intracratonic shale basins, particularly where faults intersect that margin. In fact, this may be a way to explore for hydrothermal dolomites in other formations and in other parts of the

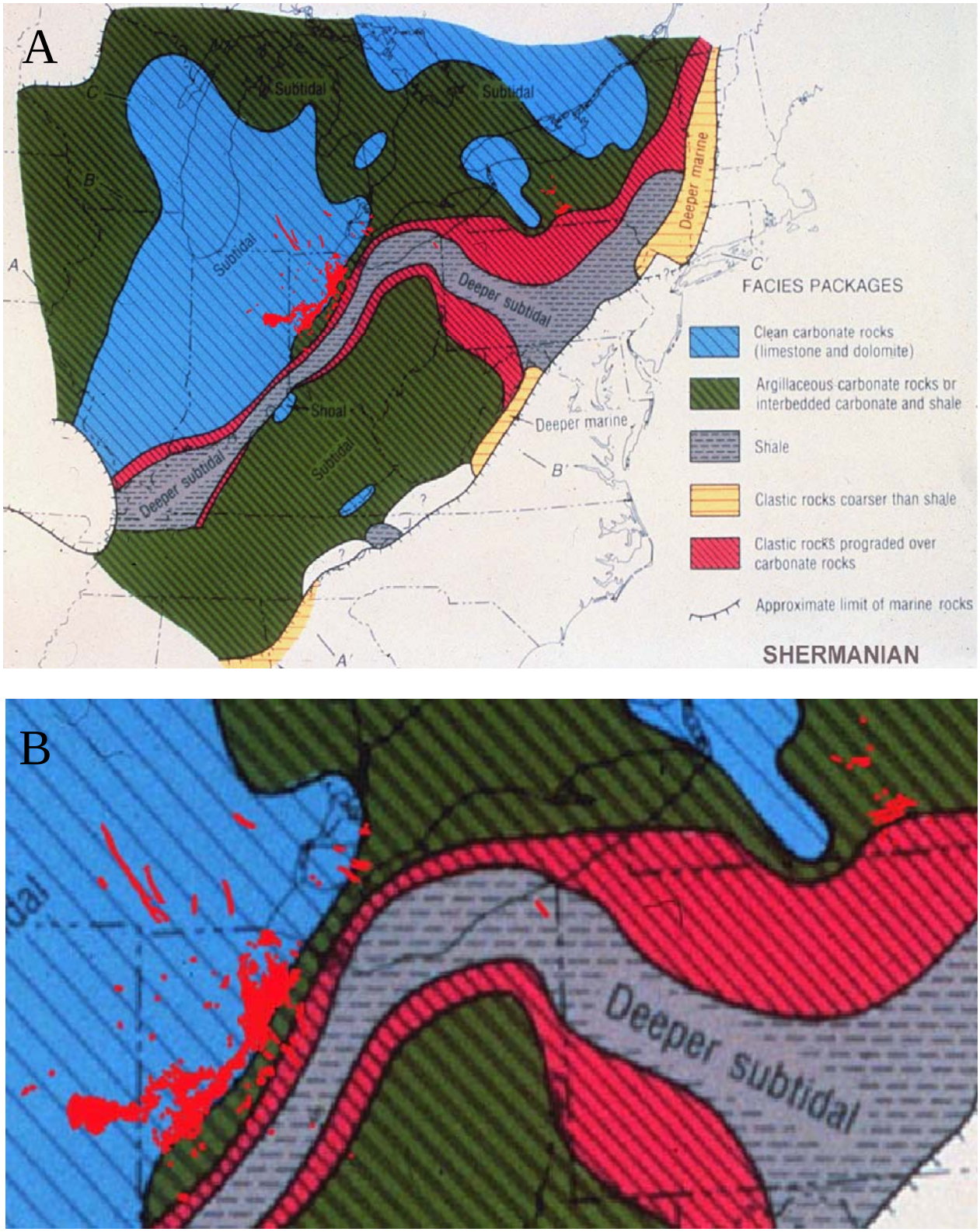

Figure 4-36. A. Paleogeographic map for Trenton Limestone from Keith (1986) with oil and gas fields in red. B. Closeup of producing area. Note close link between many fields and margin of shale basin.

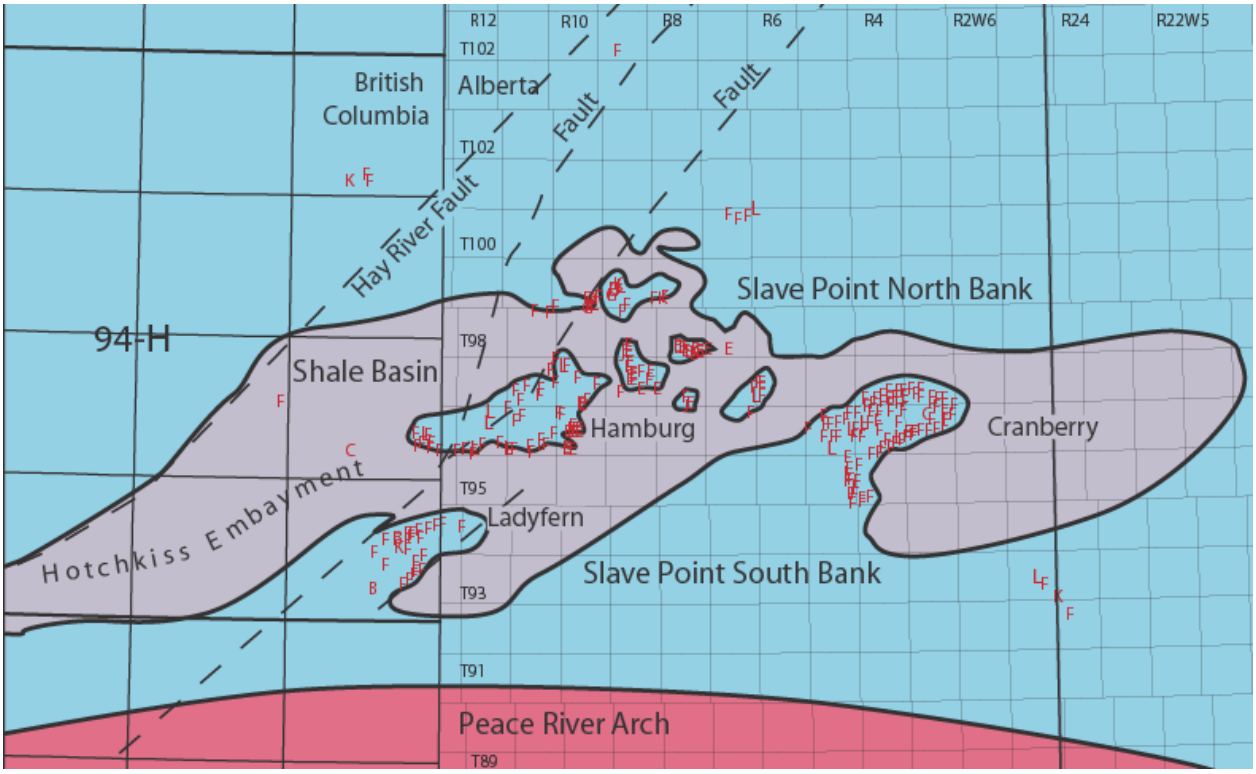

Figure 4-37. Paleogeographic map of Ladyfern and other Devonian Slave Point hydrothermal dolomite and leached limestone reservoirs (from Canadian Discovery Digest, 2002). These fields all occur on the margins of carbonate platforms with a same aged shale basin. This is virtually identical scenario to the Trenton Limestone.

world – to look for fault controlled margins between carbonate platforms and time-equivalent shale basins. One good example is the Ladyfern Field in Western Canada (~750 BCF in place), which occurs at the margin between a Devonian carbonate bank and an intracratonic shale basin (Figure 4-37). Not surprisingly, it also occurs where the Hay River Fault Zone intersects that margin.

Possible link to depth to basement

There appears to be a link between depth to basement and the occurrence of hydrothermal dolomite fields. The fields all occur where the section between the base of the Black River and the basement is less than 500 meters thick. This result is interesting and could be very important but must be viewed carefully. Graham Davies and others have long noted that dolomitization seems to be focused on basement highs and it appears that in a very broad sense that may be true in this case. There are not that many wells drilled in the areas where the base of the Black River is more than 500 meters from the basement. Vast areas of Pennsylvania and West Virginia are untested. But if there is a link between the distance to the basement and hydrothermal dolomitization, this could be a powerful tool for high-grading prospects here and elsewhere. Areas that have not been tested where the Black River is less than 500 meters from the basement

should be looked at as having greater potential than those that have thicker sections of Beekmantown and pre-Beekmantown strata. It may be that the thicker the section that underlies the Black River, the more tortuous the path for the hydrothermal fluids to reach the Trenton and Black River.

Carbon Isotope Stratigraphy

Over the past few decades, it has become clear that there are certain parts of the geological record where $\delta^{13}C$ can be used as a correlation tool (Shields, et al, 2003). Carbon isotopes are useful for correlation during times when there were major shifts in the amount of ^{13}C relative to ^{12}C in seawater that is then recorded in shallow marine limestones. In much of the geologic record, changes in $\delta^{13}C$ are so subtle and are not currently used for correlation. The method has been demonstrated to be a powerful tool in the Late Precambrian, parts of the Ordovician, the early Mississippian and Lower Cretaceous among others. This work demonstrates that there are many shifts in the upper Lower Ordovician (Trenton Black River time) that are very useful for correlation. Previous workers have spent much additional time trying to sample only certain fossils to make sure they have a pristine marine signature. This work shows that the ^{13}C signal is well-preserved and useful when well cuttings and dolomitized strata are sampled.

Carbon is included in all carbonate minerals (it's the C in CO_3). Carbon is thought to have much greater resistance to diagenetic alteration than oxygen. In other words, once a limestone is deposited, its $\delta^{13}C$ value, or the ratio of ^{13}C to ^{12}C, is in most cases not thought to change much and records the conditions of seawater at the time of deposition regardless of later diagenesis. Diagenesis can have an impact in some cases and this always needs to be considered, but this work shows that even hydrothermal dolomitization has minimal impact on the $\delta^{13}C$ values.

Assuming that the carbon isotopes have not been reset during diagenesis, the ^{13}C log is a time log. Where gamma ray and other wire-line logs are responding to lithology, the ^{13}C log is responding to changes in ocean chemistry that should occur regionally if not globally. Similar gamma ray shifts record similar changes in lithology, but they may occur at different times and the strata defined by these shifts may not correlate laterally. Like bentonites, the ^{13}C log helps us to correlate time-equivalent units. We correlate using points where shifts toward positive and negative values occur.

Bentonites also are timelines. If they can be fingerprinted to be sure that they are indeed the same bentonite from one location to another, they become a powerful tool. We supported a Masters student at Syracuse University who was working on fingerprinting and correlating bentonites using apatite phenocrysts. The results of his thesis work are included in Appendix B. His results supported our earlier picks of the Deicke and Milbrig bentonites, which occur at the top of the Black River in Ohio, West Virginia and Kentucky, and in the base of the Trenton in Pennsylvania and where they are present in New York.

Earlier work on the Trenton-Black River shows a major positive shift in stable isotope values right around the Trenton-Black River boundary just below the Milbrig bentonite. This

shift is called the Guttenburg Isotope of Carbon Excursion, or GICE (Hatch et al., 1987). The GICE has been correlated across the central and eastern United States and into Sweden and Estonia (Ludvingson et al., 1996; Patzkowsky et al., 1997; Saltzmann et al., 2000; Bergstrom et al., 2000; Simo et al., 2003; Young et al., 2003; Barta, 2004). The $\delta^{13}C$ values typically shift from 0 or +1‰ to around +3‰ at some point between the Deicke and Milbrig bentonites and then shift back to around +1‰ at some point above the Deicke. After finding this excursion in the Matejka core, we decided to see if the method had any value in correlation of the Trenton and Black River. Better regional correlations may help to answer questions about the timing of tectonic events, stratigraphic correlation, identification of periods of growth on faults and more.

Sampling for ^{13}C Stratigraphy

We completed one study of cores from Ohio, Kentucky and West Virginia, and another study using cuttings in New York, for this project. For the core study, we sampled every 5 to 10 feet using a cordless drill with a masonry bit. The cores analyzed include Ohio cores 3256, 3372 and 3409; Kentucky cores CA-35, JK-1 and Allen #1; and core number 9634 in Sand Hill, West Virginia (Figure 4-37). Most of these are long cores that go all the way from the top of the Trenton to the top of the Knox/Beekmantown. We initially sampled wells 3256, 3372 and 9634 on a 5-foot spacing and the CA-35, JK-1, and 3409 cores on a 10-foot spacing. However, we went back and sampled the cores on 5-foot spacing over the interval that included the Trenton-Black River boundary in the CA-35 and 3409 wells. The closer-spacing yields a better looking log but did not significantly change the interpretations. The raw data are in the Appendix. The CA-35 well is a mineral core that has no logs, but there are logs for a well that is about 100 feet away that correlate very nicely to the observed stratigraphy. Both the Allen core and the Jeptha Knob cores were analyzed for this study. The results fit with what we learned, but are not presented in this paper.

In New York, we sampled cuttings, spaced every 10 feet, from 5 wells. We chose wells where the Trenton-Black River contact was hard to pick in the western and northern parts of the State and hoped that the ^{13}C would help to refine our correlations. The raw data for these wells are in the Appendix.

Interpretations of ^{13}C Stratigraphy

The ^{13}C stratigraphy appears to work very well in cross sections based on well cuttings in New York and the core-based cross section for Ohio, Kentucky and West Virginia, and in a third cross section that connects the New York work to the West Virginia Sand Hill core. The curves correlate very well for the most part, but are not without their points of controversy. Points of controversy could be resolved with further sampling and analysis.

Interpretations of OH-KY-WV Cross Section. For the Ohio-Kentucky-West Virginia cross section (Figures 4-38 and 4-39), we picked points of correlation on the ^{13}C as well as the locations of the Deicke and the Millbrig bentonites and the top of the Logana Member of the Lexington Limestone and Black River and Knox Groups. In the cross section, the points of correlation are labeled on the right side and include BRC1-3, GICE and TRC1 and 2. Much was learned about the assets and liabilities of this method while constructing this cross section. This

is quite different than the version displayed previously. One of the first conclusions is that it is very difficult to correlate these logs over large distances and that it would have been much easier with more closely spaced sections. Regardless, the results are encouraging and much could be learned about the depositional and structural history of the Trenton and Black River with further study.

The cross section is hung on the Deicke bentonite, which coincides with the base of the GICE excursion in wells where both are present. Interestingly, the GICE is probably the least reliable of the excursions with which to correlate. It is obvious in the Hope Natural Gas well in West Virginia as a major excursion towards more positive values (around +3‰) but is virtually absent from the CA-35 and 3409 wells. It then occurs as more of a maximum value in the 3372 and 3256 wells than as a pronounced positive excursion.

BRC1 (short for Black River Carbon 1) is picked just above a major shift from very negative values of-3 to -5‰ to more positive values of between 0 and +1‰. The very negative values at the base of the Black River correlate between the CA-35, 3409 and Hope Natural Gas wells. Apparently, these values are more negative than seawater is ever supposed to have been during the Phanerozoic. These are either a diagenetic artifact, or they are a significant discovery of a period of very negative seawater (Matt Saltzman, pers. comm.). There is a thicker section in the Hope Natural Gas well in WV than in any other section. This makes sense because there is supposed to be very little time lost in the Knox unconformity in that location so there is some strata preserved there that is absent in the other wells. The St. Peter Sandstone is highlighted in the two wells where it occurs. Note how it occurs in lows where there was greater accommodation space.

BRC2 is picked at a negative spike that correlates from well to well across the cross section. The interval between BRC2 and BRC1 looks very similar and thins from east to west (basin to platform). The interval between BRC1 and BRC2 looks the same in all wells except the Hope Natural Gas well in WV where there is an additional excursion to more positive values. The section is much thicker in this well and the sections in the other wells that might have recorded this excursion must be thinner or absent.

BRC3 is picked at an inflection point from an overall positive trend below to a slightly negative trend above. This pick is consistent in all the wells except the 3372 well where a possible BRC3 pick would have been where the green arrow occurs on Figure 4-38. More closely spaced sections would help to refine this correlation.

As mentioned before, the GICE is not a strong pick but the bentonites are timelines and the Deicke and Millbrig picks made by the stratigraphy and petrography teams have been confirmed by the apatites studies done by Adam Carey. We will use this as a timeline in the absence of a reliable GICE pick.

There are two picks made in the Trenton: TRC1 and TRC2. TRC1 is picked at a maximum value above the GICE or Deicke pick and seems to correlate very well. The interval between the GICE and TRC1 picks shows an overall trend toward more negative values with an abrupt change back to more positive values. TRC2 only occurs in the CA-35 and 3409 wells and

is picked at the top of a similar sequence of an overall trend toward more negative values capped by an abrupt shift toward more positive values.

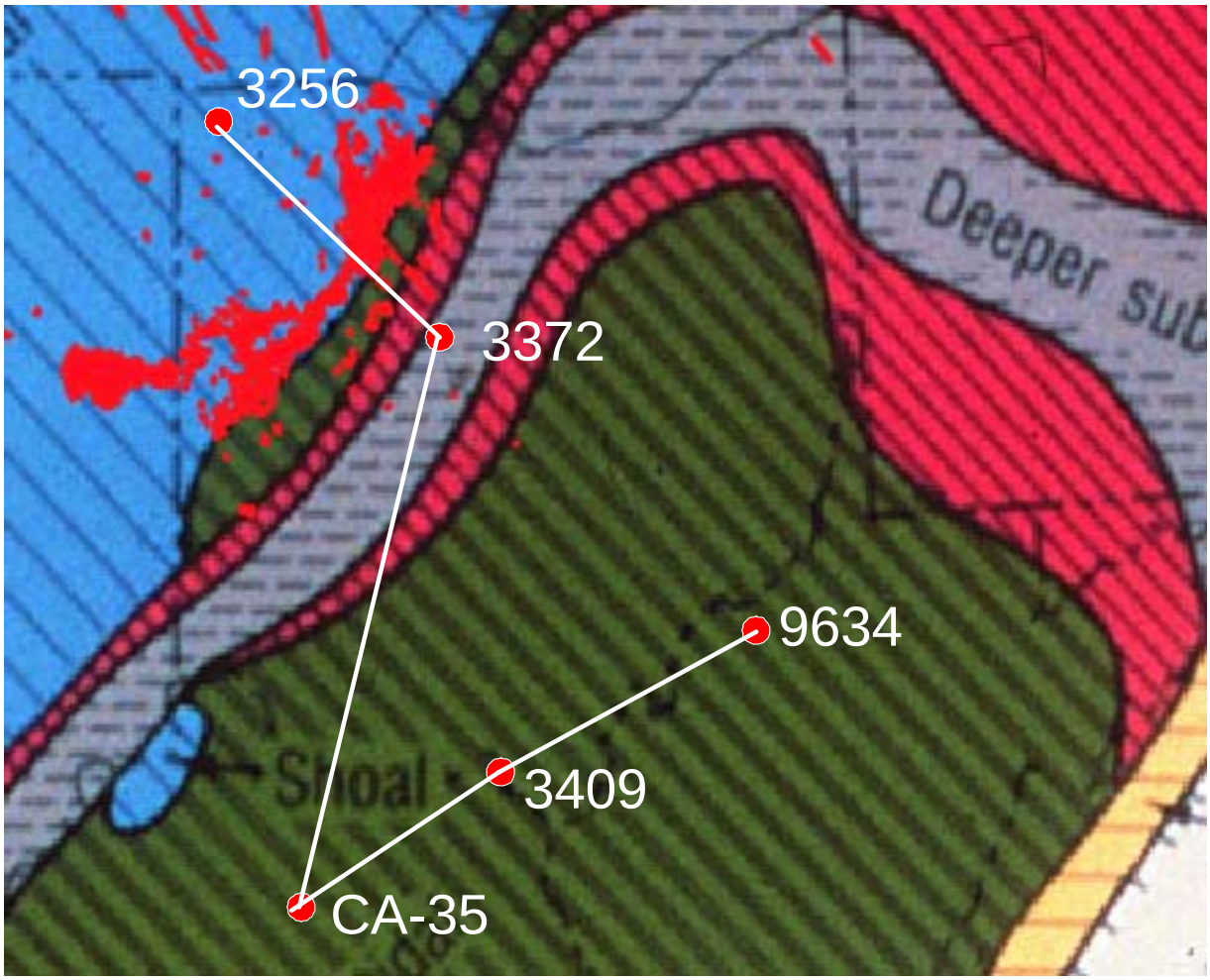

Figure 4-38. Map showing locations of cores used for OH-KY-WV cross section (over map from Keith, 1986).

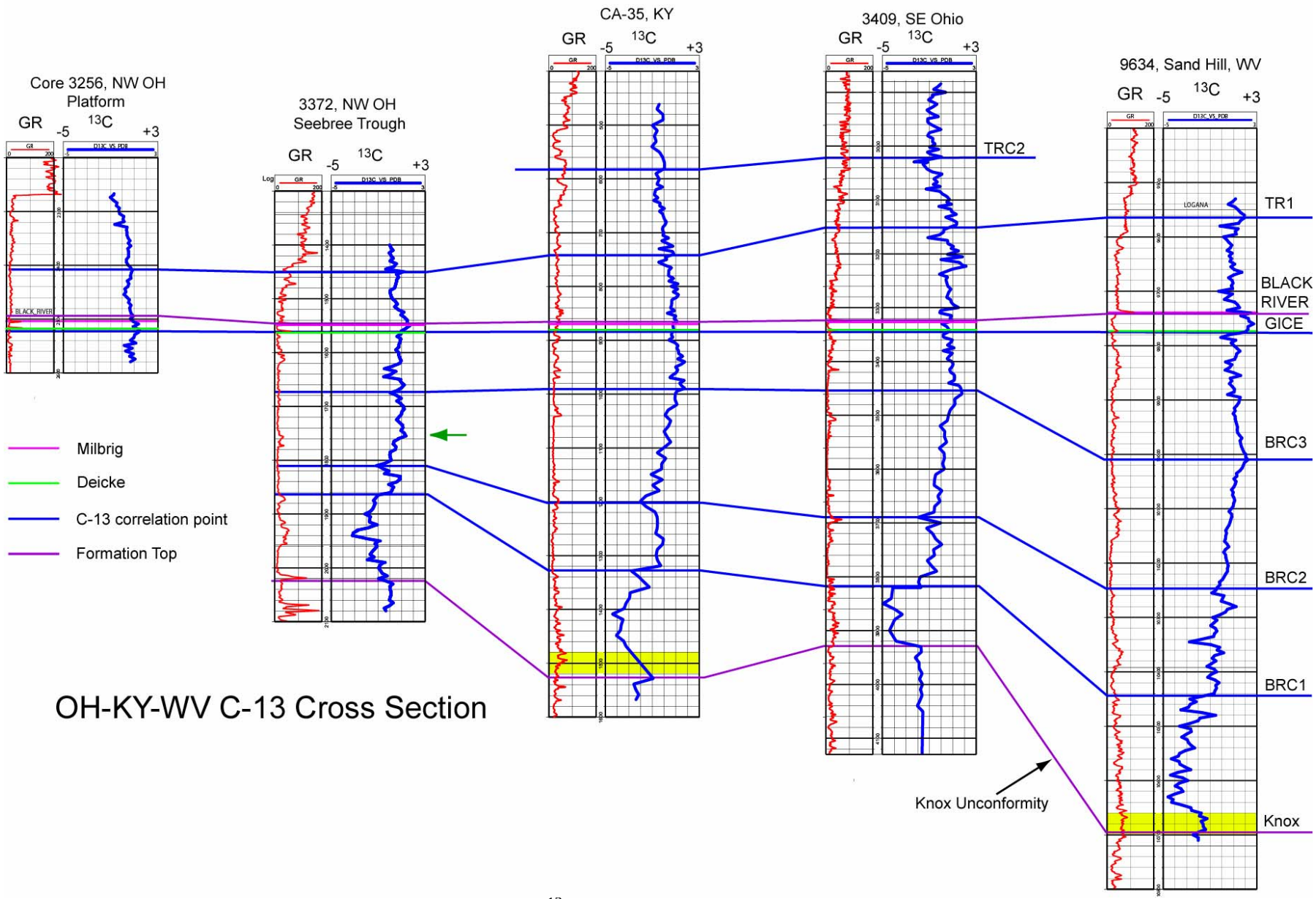

Figure 4-39. Cross section of gamma ray logs and ^{13}C data from Ohio, Kentucky and West Virginia.

This cross section is a first pass that could be refined with the addition of additional sections between these widely spaced wells. But the value of this approach is clear. Because this a chronostratigraphic cross section we can treat the intervals between the picks as time slices and the picks as time lines. We can see how subsidence rates varied from well to well by comparing the thickness of any interval between sections. During the time that the interval between BRC# and the GICE was deposited, subsidence rates were much higher at the location of the WV well than they were at the other wells. Subsidence rates were lower at the location of the 3372 well during the time that the interval between BRC1 and BRC3 was deposited and again during the time between the GICE and TRC1.

This approach also can help guide stratigraphic correlations that might otherwise be difficult or impossible. It also appears that the St. Peter Sandstone filled local lows. This work also shows that chronostratigraphic correlation of the Trenton and Black River is now possible without ever looking at any fossils which is much more time consuming and expensive. We also have a good idea of the relative ages represented by the cores and where missing section might occur.

New York Cuttings-Based Cross section. We analyzed cuttings from 4 wells for a cross section in western and north central New York (Figure 4-40). We chose wells in which it was very difficult to pick the top of the Black River and that were very different in thickness (Figure 4-41). The results are excellent and this could be a powerful tool for correlation in the Trenton and Black River in the future.

Initially, we encountered a few problems using well cuttings. The ^{13}C sections made from cuttings are a lot smoother looking than the logs from the cores – this is likely due to the coarseness of the sampling interval. One reason for coarse sampling is that the Trenton is quite shaley in these wells. Therefore, we could not obtain values for some of the samples because there was not enough carbonate in them to get a reading on the mass spec. To resolve this, we simply deleted those samples and made the curve interpolate over these depths. This made the curves less than ideal in some places and may shift correlation points by 10 or 20 feet in some cases. The curves are still very usable and give a lot of good data. A second problem was that in well 11387 it was necessary to shift the curve down about 25 feet so that it would make sense with the gamma ray log and the other wells. This is probably due to a poor sampling or a depth shift between the driller's depth and log depth. Once we made this shift, the well correlated very nicely with the other three in the cross section. These could be sources of error in any cuttings based study.

The cross section (Figure 4-41) is hung on the top of the GICE excursion. We have labeled the ^{13}C picks in a manner similar to the southern cross section with a few exceptions.

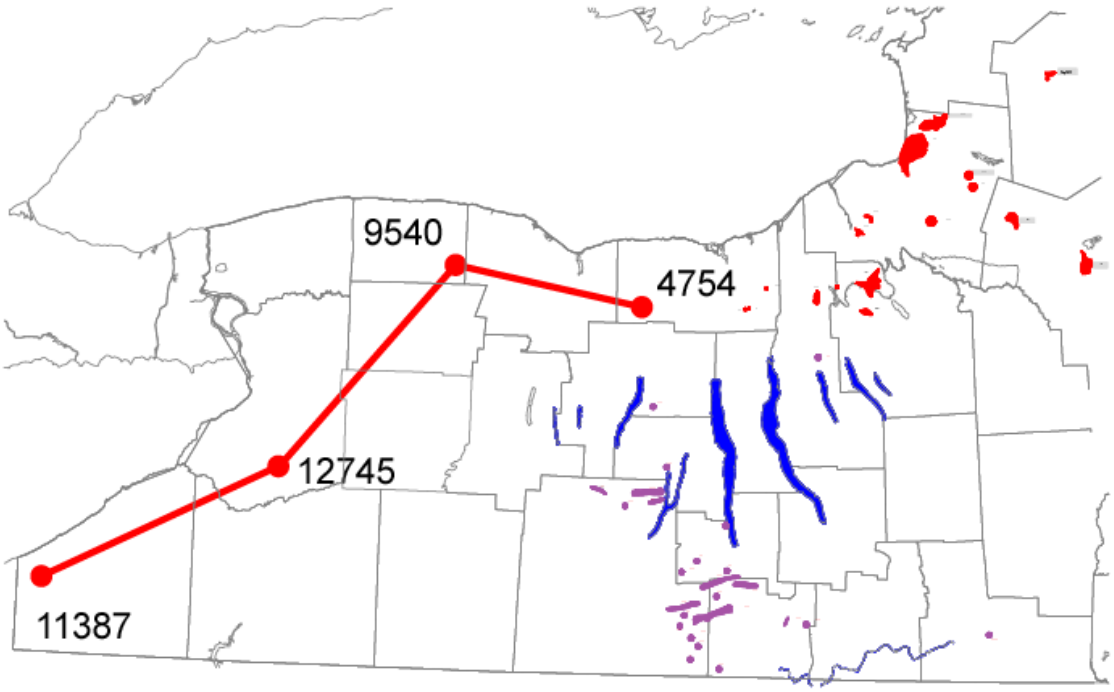

Figure 4-40. Map of locations in New York ^{13}C cuttings-based cross section.

The BRC1 and 2 picks are absent here. The ^{13}C cross sections show clearly that the basal section of the Black River found in Ohio, Kentucky and West Virginia is absent in New York. The base of the Black River in these New York wells appears to begin somewhere between picks BRC2 and BRC3 on the West Virginia cross section. This strongly suggests that the Black River onlaps to the north. The bentonites that are easily picked in the wells in the producing area of south-central New York are much harder to detect in the northwest with the exception of one spike in the blocky limestone near the top of the Trenton (picked with green line on Figure 4-41). The Deicke and the Millbrig are not obvious here.

Starting from the base, the top of the Beekmantown is picked in New York in the manner first suggested by Rickard (1973). The Black River appears to be of equal thickness in all the wells on this cross section. The ^{13}C is at its most negative value recorded in the Black River of New York at the contact (around -2‰), but it is not as negative as the values found in the lower Black River of the southern wells (as low as -5‰).

The first pick is the BRC3 pick which is the same inflection point picked in the OH-KY-WV cross section where the values change from becoming progressively more positive to trending approximately straight upward. The thickness of the interval between the top Beekmantown and BRC3 is of approximately equal thickness as is the interval between this pick and the overlying GICE pick.

The GICE is pronounced in New York. We have picked the top and the base of this positive excursion as correlation points. The GICE interval is almost 200 feet thick in the 4754 well to the northeast, but is only about 40 feet thick in the 11387 well to the southwest. This shows that much section is missing from the basal Trenton and that it gradually thins from east to

west. This thinning may explain the absence of the Deicke and Millbrig bentonites in these sections. The base of the GICE is either right on the Black River boundary or just beneath it in these wells. Most of the positive GICE excursion occurs within the Trenton. The maximum values of around +3‰ are not found in the 11387 and 12745 sections which suggests that this interval may not have been deposited and that the part of the section that is missing is the lowermost Trenton. This may imply that there is an unconformity at the Trenton Black River boundary in sections to the west.

The interval between the GICE top and the TRC1 pick is remarkably even thickness across the cross section. The TRC1 pick is quite subtle but is picked at a maximum positive value prior to a very subtle shift toward more negative values. TRC2 is also picked at a subtle maximum positive excursion prior to s shift toward slightly more negative values. This shows that subsidence somewhat variable during this time with the two wells in the middle subsiding the most and the southwestern most section (11387) subsiding the least. These are very subtle shifts that appear to be consistent from well to well. TRC3 is picked at a maximum negative value after a gradual shift toward more negative values. The interval between TRC1 and TRC 3 maintains its thickness across the cross section.

The ^{13}C helps to correlate with confidence. The correlations in the basal Trenton on this cross section would have been very difficult without the ^{13}C. Once these correlation points are on the cross section it becomes clear how to correlate the gamma ray logs. This could help as a guide when correlating reservoir intervals or mapping facies in the Trenton.

The cross section also shows subsidence increased from west to east during early Trenton time, probably due to the onset of the Taconic Orogeny. This approach helps to refine our understanding of both the stratigraphic and structural history of the basin during Trenton time. We intend to sample perhaps 30 more wells with cuttings to make high-resolution time slices through the Trenton Black River to better understand structural and stratigraphic variations throughout the State.

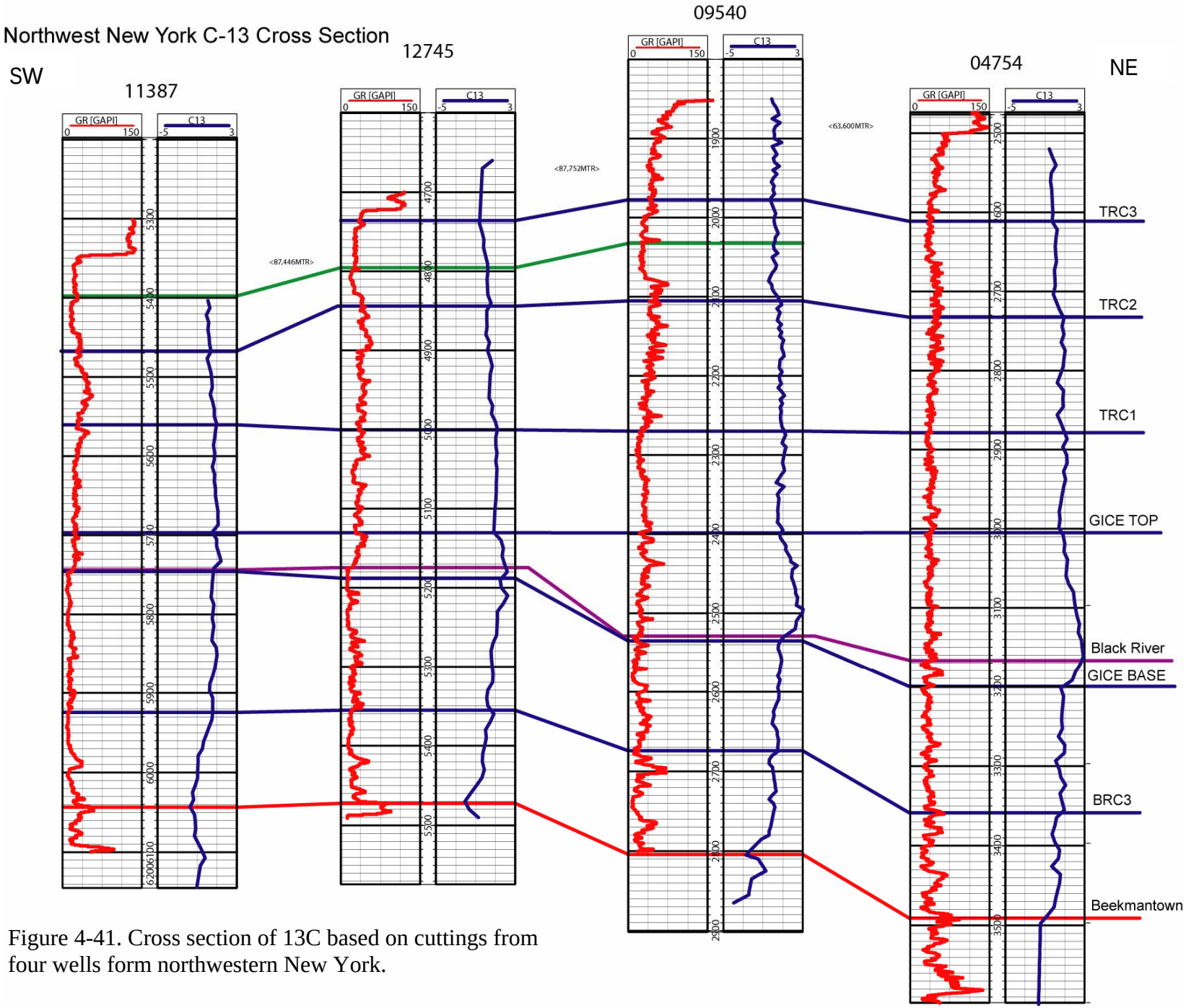

Figure 4-41. Cross section of 13C based on cuttings from four wells form northwestern New York.

North Central NY-Wilson Hollow Field-Sand Hill, WV Cross section

The purpose of this cross section (Figures 4-42 and 4-43) is to show that the picks from the New York cuttings-based cross section correlate to the New York producing area (Wilson Hollow Field) and with the wells in the OH-KY-WV cross section. The 04754 well is from the far right side of the New York cuttings-based cross-section (Figure 4-41), the 22975 well (Root #1) is from the Wilson Hollow Field in south-central New York and the Sand Hill, West Virginia well is from the far right side of the OH-KY-WV cross section (Figure 4-39). This cross section demonstrates clearly the value of the ^{13}C method in identifying stratigraphic relationships.

The pick names are all the same as in the previous cross sections. The cross section shows that the lower Black River in West Virginia onlaps the Knox Unconformity to the north. Neither the BRC1 nor the BRC2 markers are found on the ^{13}C logs in the New York wells. While these lower Black River units were being deposited in West Virginia, Kentucky and Ohio, the Beekmantown/Knox was still exposed in New York and no deposition was taking place. The Black River does thicken from the 04754 well in north central New York to the Wilson Hollow Field, but not enough to pick up either the BRC1 or BRC2 markers in the ^{13}C log.

The cross section also shows that the Trenton Black River boundary is not a timeline but in fact cuts across stratigraphy. The pick is equivocal in the 04754 well, but it is clearly about 15 feet below the base of the GICE at Wilson Hollow and about 20 feet above the base of the GICE in the Sand Hill Well. Based on this, the Deicke and the Millbrig were tentatively picked in the Wilson Hollow Field 22975 well. They occur within the basal Trenton there but in the uppermost Black River in West Virginia. This is consistent with observations at the Union Furnace outcrop in Pennsylvania where the Deicke and Millbrig also occur in the basal Trenton (Laughery and Kostelnik, 2005).

There is also a dramatic thickening of the GICE interval from Sand Hill to Wilson Hollow and from North Central NY to Wilson Hollow. The producing area in NY appears to have been subsiding faster than any other part of the basin that we have studied with ^{13}C during early Trenton time. Again, this is probably due to the inset of the Taconic Orogeny.

The Black River in the 22975 well from Wilson Hollow Field is pervasively dolomitized, but there is little impact on the ^{13}C curve, which is easily correlated to the other wells in this interval. This suggests that the carbon from the original limestone is preserved during dolomitization and increases confidence that the ^{13}C excursions are related to the original seawater composition and not later diagenesis.

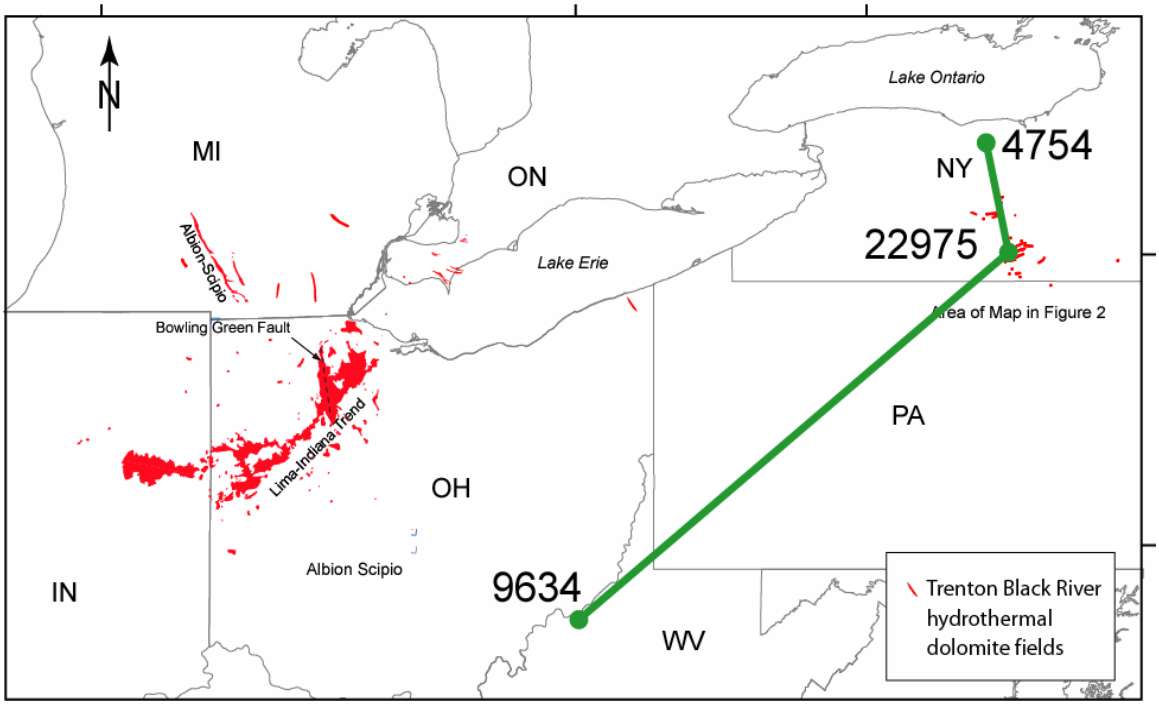

Figure 4-41. Line of section for NY-WV cross section.

Conclusions of ^{13}C study

This work has demonstrated that ^{13}C is a power correlation tool for the Trenton-Black River stratigraphic interval. Even very subtle shifts can in many cases be correlated over long distances. Several new excursions were identified and it may also be one of the first studies to successfully use cuttings. The GICE is very useful for correlation in New York, but is probably the least reliable marker in Ohio where it is largely absent. The New York State Museum plans to continue this study across New York State to make high-resolution time-slices to better understand stratigraphic relationships and timing of tectonic events in the Trenton-Black River interval.

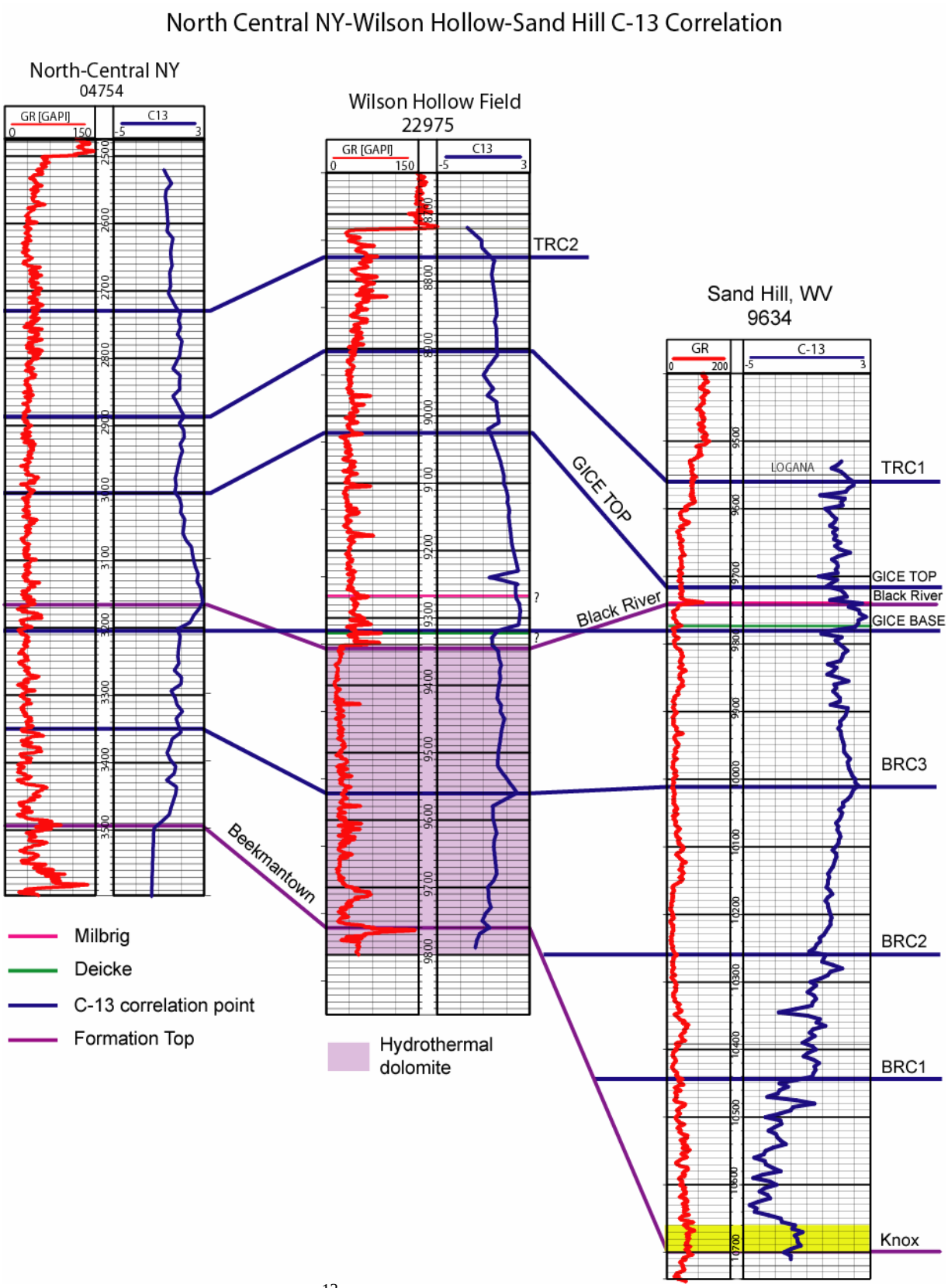

Figure 4-42. Cross section with ^{13}C data from northern New York through Wilson Hollow Field to Sand Hill West Virginia.

GEOCHEMISTRY OF NATURAL GASES FROM TRENTON AND BLACK RIVER FORMATION (MIDDLE ORDOVICIAN) CARBONATE RESERVOIRS, APPALACHIAN BASIN

By Christopher D. Laughrey and Jaime Kostelnik
Pennsylvania Geological Survey

Introduction

In this part of the Trenton-Black River play book, we discuss the occurrence and origin of thermogenic and possible abiogenic gases produced from Ordovician carbonate reservoirs in the Trenton and Black River Formations of the central Appalachian basin. We set forth the geochemical characteristics of these gases, identify their potential sources, and discuss the implications of our data for understanding petroleum generation, migration and entrapment in this important play.

Data Sources and Methodology

We collected thirty-four natural gas samples from various Trenton and Black River reservoirs throughout the Appalachian basin (Figure 5-1 and Table 5-1). Twenty-two of the samples are from the prolific producing wells of south-central New York and north-central Pennsylvania; six are from the York field in Ashtabula County in northeastern Ohio; two are from Cottontree field in West Virginia; two are from the Homer field in eastern Kentucky; and one is from the Colin Fork field in southeastern Kentucky. We collected all samples directly from the wellheads in cleaned and evacuated, double-ended, stainless steel gas cylinders.

The samples were analyzed for chemical composition, and for selected hydrocarbon and non-hydrocarbon stable isotopic composition at Isotech Laboratories in Champaign, Illinois. At Isotech Laboratories, the samples were prepared offline and then analyzed by dual-inlet isotope ratio mass spectrometer (IRMS). This work was accomplished using either a Finnigan Delta S mass spectrometer interfaced with an elemental analyzer or a Finnigan Delta Plus XL mass spectrometer. Samples with small concentrations of C_2+ hydrocarbons were prepared and analyzed online using a VG SIRA II mass spectrometer. Selected samples were shipped from Isotech Laboratories to Dr. Robert Poreda at the University of Rochester for analysis of noble gas isotopes utilizing a VG 5400 rare gas mass spectrometer fitted with a Faraday cup and Johnston electron multiplier; a Dycor quadrupole gas analyzer attached to the same vacuum lines permitted analysis of bulk gas composition as well as noble gas isotopes.

All of the data are tabulated in Tables 5-1, 5-2, and 5-3. Gas compositional data are presented in Table 5-1 as mole percent. Stable isotope results are presented in Table 5-1 using the delta (δ) notation and are reported in parts per thousand (permil). The δ-value is defined as:

$$\delta \text{ (permil)} = R_{(sample)} - R_{(standard)}/R_{(standard)} \times 1000$$

where R represents the measured isotope ratio. We measured the following stable isotope ratios in the samples:

- $^{13}C/^{12}C$ of hydrocarbon gases and carbon dioxide
- $^{2}H/^{1}H$ of hydrocarbon gases (also known as D/H)
- $^{15}N/^{14}N$ of nitrogen
- $^{34}S/^{32}S$ of hydrogen sulfide.

Refer to Hoefs (1997) for information on the specific standards used in these analyses.

The noble gas concentrations are reported as parts per million (ppm) or parts per billion (ppb), and as specific ratios in Tables 5-2 and 5-3.

The carbon and hydrogen isotope composition of hydrocarbon gases is closely controlled by the processes of petroleum generation, source rock type, burial and thermal history, migration and post-generative alteration (oxidation, leakage, etc.) (Schoell, 1983; Whiticar, 1994; Prinzhofer and Battani, 2003). The stable isotope composition of non-hydrocarbon gases such as nitrogen, carbon dioxide and hydrogen sulfide in petroleum reservoirs also provides useful information about these genetic processes (Hunt, 1996). The noble gases - helium, argon, neon and krypton - are chemically inert, and thus useful as tracers in deciphering the geologic history of a natural gas reservoir and the fluids it contains (Youngchang and others, 1996; Prinzhofer and Battani, 2003). We used all of these parameters in studying the gases produced from Trenton and Black River reservoirs in the Appalachian basin.

Petroleum geochemists recognize three principal classes of hydrocarbon gases: 1) microbial gases; 2) thermogenic gases; and 3) abiogenic gases (Wiese and Kvenvolden, 1993; Apps and van de Camp, 1993; Sherwood Lollar and others, 2002). Microbial gases are produced by bacteria in anaerobic environments through fermentation of acetate and reduction of carbon dioxide. Thermogenic gases are generated from organic matter during burial in sediments and exposure to high temperatures. Thermogenic gases are cracked from kerogen, bitumen and oil. Microbial and thermogenic gases are distinguished from one another by $\delta^{13}C$ and $\delta^{2}H$ of methane and the $C_1/(C_2 + C_3)$ ratios in the gas. Microbial gas typically has $\delta^{13}C_1 < -55$ permil, $\delta^{2}H < -150$ permil, and $C_1/(C_2 + C_3)$ ratios >100. Thermogenic gas typically has $\delta^{13}C_1 > -50$ permil, $\delta^{2}H > 250$ permil, and $C_1/(C_2 + C_3)$ ratios <100. Abiogenic gases are generated in the earth's shallow mantle, and in the deep crust via polymerization reactions such as Fischer-Tropsch reactions (Szatmari, 1989) or hydrothermal water-rock interactions, such as the serpentinization of ultramafic rocks (Sherwood Lollar and others, 2002). Abiogenic gases generated in the upper mantle exhibit three distinctive analytical criteria: (1) $\delta^{13}C_1 > -25$ permil; (2) isotopic reversals of the form $\delta^{13}C_1 > \delta^{13}C_2 > \delta^{13}C_3$; and (3) $3He/4He > 0.1Ra$ (*Ra* = atmospheric ratio) (Jenden and others, 1993). Mantle hydrocarbons probably comprise less than 200 ppm of commercial gases produced on the earth (Jenden and others, 1993). Abiogenic gases generated through water-rock interactions in the crust also exhibit isotopic reversals where $\delta^{13}C_1 > \delta^{13}C_2 > \delta^{13}C_3$, and show a distinctive inverse correlation of $\delta^{13}C_1$ and $\delta^{2}H$ between methane and ethane (Sherwood Lollar and others, 2002). Although accumulations of crustal abiogenic gas are now recognized in Precambrian rocks of Canada and South Africa, these accumulations are generally regarded as non-commercial (Apps and van de Kamp, 1993; Whiticar, 1994; Sherwood Lollar and others, 2002 and 2006). Jenden and others (1993, p. 32) however, suggest that,

> In rift or convergent margin basins, hot magmatic fluids can strip methane and other volatiles, from metamorphic basement and overlying sedimentary rocks…and commercial accumulations of this type of gas may be present…The economic value of such reserves could be impaired by dilution with carbon dioxide and nitrogen.

Gases Produced from Fractured Limestone

EASTERN KENTUCKY: COLIN FORK AND HOMER FIELDS

Gas Composition

Methane (C_1) dominates the gases produced from the Trenton Formation at Colin Fork and Homer fields (Figures 5-1 and 5-2), comprising between 81.64 to 91.38 mole percent (Table 5-1). The gases contain from 4.14 to 7.81 mole percent ethane (C_2), and from 1.49 to 3.54 mole percent propane (C_3) along with minor amounts of higher light hydrocarbons through pentane (C_5) and hexane plus (C_{6+}). Wetness ranges from 6.7 to 7.7 volume percent. Nitrogen is the only notable non-hydrocarbon gas in the samples we collected from the Kentucky fields, ranging from 2.23 to 5.17 mole percent. The gases contain trace amounts of CO_2, Ar, O_2, H_2, and He. The specific gravity of the gases ranges from 0.608 to 0.676, and the BTU values range from 1055 to 1125.

Stable Isotope Geochemistry

The $\delta^{13}C$ and $\delta^{2}H$ of methane produced from the Colin Fork and Homer fields ranges from –39.50 to –44.76 permil and –143.4 to –206.9 permil, respectively. Methane produced from the Colin Fork field and from the Lawson Heirs (T1) well at Homer field is clearly thermogenic gas associated with oil (Figure 5-3). This gas was generated along with oil from early mature to mature marine organic matter (Schoell, 1983; Whiticar, 1994), and/or from a combination of kerogen and oil cracking in the middle oil window (Tissot and Welte, 1984; Tang and others, 2000). Methane produced from the Wheeler 24 and Oliver 50 (T2) wells in the Homer field, however, is more mature: data from these gas samples plot along the border of the fields for oil-associated and postmature thermogenic gas (Schoell, 1983; Whiticar, 1994). The $\delta^{13}C$ of these methane samples is typical of gas cracked from late mature organic matter in marine petroleum source rocks (Whiticar, 1994) or from oil during catagenesis (Tissot and Welte, 1984; Tang and others, 2000).

In addition to the $\delta^{13}C$ and $\delta^{2}H$ of methane, we also measured the $\delta^{13}C$ of ethane through butane (C_4) in gas samples from Homer field. The C_1 through C_4 hydrocarbons become more enriched in ^{13}C with increasing molecular weight (i.e., become isotopically “heavier”; Figures 5-4 and 5-5), a trend that is characteristic and diagnostic of thermogenic gases (Des Marais and others, 1981; James, 1983; Chung and others, 1988; Jenden and others, 1993; Whiticar, 1994; Sherwood-Lollar and others, 2002). This trend is kinetically controlled, reflecting the lower strength of ^{12}C - ^{12}C bonds relative to ^{13}C - ^{12}C bonds in the source material (Sundberg and Bennett, 1983; Jenden and others, 1993; Tang and others, 2002). Crossplots of $\delta^{13}C_1$ versus both

$\delta^{13}C_2$ and $\delta^{13}C_3$, and of $\delta^{13}C_2$ versus $\delta^{13}C_3$ for the gas produced from the Lawson Heirs (T1) well suggest that the gases are co-genetic, and that they were generated at maturation temperatures equivalent to an $R_o \sim 0.8$. The same crossplots for the gases produced from the Oliver 50 (T2) and Wheeler 24 wells, however, suggest a mixture of different thermogenic gases generated at somewhat higher maturation temperatures ($R_o \sim 1.0$).

Reservoir Compartmentalization

The variations in $\delta^{13}C_1$ through $\delta^{13}C_4$ in the Homer field samples (Figures 5-4 and 5-5) indicate that the gases produced from the Wheeler 24 and Oliver 50 (T2) wells are almost identical, suggesting a compositionally-equilibrated reservoir (Schoell and others, 1993). The gas produced from the Lawson Heirs (T1) well, however, is isotopically distinct from the other two samples, suggesting that the reservoir penetrated in this well does not communicate with the reservoir penetrated in the other two wells (Schoell and others, 1993). This reservoir compartmentalization is most likely fault-controlled at Homer field. The isotopic compositional heterogeneity exhibited by the gases probably reflects episodic filling by petroleum that migrated from a source rock undergoing progressive burial and increasing thermal maturation, or from different source rocks altogether (Schoell and others, 1993).

Potential Source Rocks and Petroleum Migration

Potential source rocks for the gases produced from the Trenton Formation at Colin Fork and Homer fields include the Upper Ordovician shales in the Utica Shale and Point Pleasant Formation, dolomitic mudstones within the Middle Ordovician Trenton Formation, the Middle Ordovician Wells Creek Formation, strata within the Cambrian Rome Formation, and so-called deep basement potential source rocks (Swezey, 2002).

Conodont Alteration Indices (CAI) of Trenton and Black River samples from Elliott (Homer field) and Clay (Colin Fork field) counties range from 1.0 to 1.5. These values are equivalent to a vitrinite reflectance (R_o) of approximately 0.7 to 0.85 percent (Harris, 1979), which indicate early thermal maturation of organic matter in the sediments (Peters and Moldowan, 1993). We do not have any organic geochemical data from Trenton and Black River rocks in this portion of Kentucky, but Black River rocks along strike in Jackson County, WV do contain adequate organic matter to have served as petroleum source rocks (Harris, 2004, personal comm., and Rome Trough Consortium database). If some intervals within the Trenton and Black River sections in Elliott and Clay counties also contain adequate TOC, then they conceivably could have generated the gases produced from the Colin Fork field and the Lawson Heirs (T1) well in the Homer field. We also lack data from the Point Pleasant and Utica intervals in this region, but these are well-documented source rocks elsewhere in the basin and are probably of similar maturation in the Colin Fork and Homer fields. These too might have served as source rocks for the Clay County and Lawson Heirs (T1) hydrocarbons. Finally, rocks in the Cambrian Rome Formation in Garrard County, KY, west of the Colin Fork and Homer fields, contain adequate organic matter to be potential source rocks (TOC = 0.7 to 3.26 percent), and are in the early mature stage (Tmax = 444 to 446 °C).

The gases produced from the Oliver 50 (T2) and Wheeler 24 wells at Homer field, on the other hand, were generated from late mature source rocks. The CAI values of these source rocks should be ~2 (R_o equivalent of 0.9 to 1.35). Shaly intervals in the Cambrian Conasagua Group in Wayne County, WV, just east of Homer field, contain TOC of 1.2 to 4.4 percent, with Tmax values of 460 to 477 °C, and production indices (PI) of 0.51 to 0.58. Thus, these Cambrian rocks are potential source rocks in the late mature stage of thermal evolution and could be the source of the gases produced from the Oliver 50 (T2) and Wheeler 24 wells.

WEST VIRGINIA: COTTONTREE FIELD

Gas Composition

Methane is the principal gas produced at Cottontree field (Figures 5-1 and 5-2). Methane comprises almost 99 mole percent of the gas samples we collected there (Table 5-1). The gases are remarkably dry. Wetness of the two Cottontree samples is 0.74 and 0.95 volume percent. Ethane constitutes only 0.692 to 0.875 mole percent of the gas, and just traces of C_3 through C_{6+} hydrocarbons occur in the samples. There are trace amounts of He, H_2, Ar, CO_2, and N_2 in the gases. The specific gravity of the gas samples is 0.560 to 0.561, and the BTU value is 1018.

Stable Isotope Geochemistry

The $\delta^{13}C$ and $\delta^{2}H$ of methane in the gas samples from Cottontree field range from –35.12 to –35.43 permil and –133.1 to –133.8 permil, respectively (Table 5-1 and Figure 5-6). These values indicate postmature thermogenic gas generated at maturation temperatures equivalent to a R_o approaching 3.0 percent (Jenden and others, 1993; Laughrey and Baldassare, 1998). This is consistent with the Ordovician CAI values approaching 4.0 mapped in this part of Roane County, WV (Repetski and others, 2005).

The ethane in the samples collected from Cottontree field is depleted in the heavy isotope relative to the methane, with $\delta^{13}C$ values of –37.47 and –38.26 permil (Table 5-1 and Figures 5-7 and 5-8). This ethane depletion in ^{13}C with respect to methane is significant – a depletion of 2.35 to 2.83 permil. Such isotopic reversals are unusual in thermogenic gases, although they can sometimes be explained in terms of heterogeneities in the source organic matter, thermogenic gas mixing, methane oxidation, or diffusive gas leakage from the reservoir (Jenden and others, 1993; Whiticar, 1994; Prinzhofer and Huc, 1995).

Depletion in ^{13}C for ethane through butane with respect to methane is also considered diagnostic of abiogenic gases that formed through inorganic, kinetically controlled polymerization reactions (Sherwood Lollar and others, 2002). Unfortunately, we did not obtain $\delta^{13}C$ values for homologues higher than C_2 due to their minute concentrations in the samples from Cottontree field (Table 1). Confident interpretations of isotopic depletion of the higher hydrocarbons with respect to methane require comparisons to a larger range of homologues, particularly propane and butane. The nature of the ^{13}C isotopic reversals observed in the gases from Cottontree field remains enigmatic.

Potential Source Rocks and Petroleum Migration

As in Kentucky, potential source rocks for the gases produced from the Trenton Formation at Cottontree field include the Upper Ordovician shale in the Utica Shale and Point Pleasant Formation, dolomitic mudstones within the Middle Ordovician Trenton Formation, the Middle Ordovician Wells Creek Formation, strata within the Cambrian Rome Formation, and so-called deep basement potential source rocks (Swezey, 2002). As mentioned above, the CAI values in the Ordovician carbonates of the region approach 4.0. Tmax and Production Indices in the deeper potential source rocks of Cambrian age consistently exhibit values indicative of peak maturation through the postmature stage of thermal evolution. The postmature genetic signature of the gases could be correlated with the observed thermal maturation of any of these potential source rocks, thus the specific source of the Cottontree hydrocarbons is ambiguous.

Gases Produced from Deep Hydrothermal Dolomite Reservoirs

NORTHEAST OHIO: YORK FIELD

The York Field is located directly south of Lake Erie in Ashtabula County, northeast Ohio (Figures 5-1 and 5-9). The field was discovered in 1997 using 2-D seismic methods supplemented by shallow subsurface mapping (MacKenzie and Grubaugh, 2000). Of the twelve well drilled in the field, only six are productive. Gas in the productive wells is from a hydrothermal dolomite reservoir developed in the Trenton Limestone and Black River Group; non-productive wells penetrated tight limestone in these carbonate units (Minken, 2003). Porosity in the reservoir rock is not fabric selective, and consists of fractured, brecciated and vuggy dolostone that is laterally sealed by impermeable limestone and vertically sealed by tight limestone and/or the Utica Shale (Sagan and Hart, 2004). The greatest porosity in the dolomite occurs within zones of intense faulting where synthetic shear faults overlap and meet at depth to form flower structures (Sagan and Hart, 2004). Associated fracturing and rock dissolution due to hydrothermal fluid migration, base metal sulfide mineralization, and dolomitization created the storage capacity in the reservoir. Minken (2003) suggests the Mantell well, located at the southeast edge of the field (Figure 5-9) produces from a structural sag (graben) that is separate from that into which the other five productive wells penetrate (see Minken, 2003, Figure 17).

Gas Composition

Methane is the dominant hydrocarbon in the gases produced at York field, comprising between 89.42 to 90.68 mole percent (Table 1). Wetness ranges from 7.32 to 8.1 percent; the gases contain 4.45 to 5.04 mole percent ethane and 1.68 to 1.92 mole percent propane, with traces of higher light hydrocarbons through C_6+ (Table 1). Nitrogen is the only notable non-hydrocarbon in the gases, comprising 1.25 to 1.63 mole percent of the samples we analyzed. The gases contain trace amounts of helium, hydrogen, argon, oxygen, and carbon dioxide (Table 1). Specific gravity of the gas produced at York field ranges from 0.624 to 0.645 and the BTU value of the gas is 1101 to 1127.

Stable Isotope Geochemistry

The $\delta^{13}C$ and $\delta^{2}H$ of methane produced from York field samples ranges from –38.04 to –37.37 permil and –168.9 to –165.4 permil, respectively. A crossplot of these data on Schoell's (1983) interpretive genetic diagram indicates thermogenic methane associated with condensate (Figure 5-10). The respective ranges of $\delta^{13}C$ in the ethane and propane produced at York field are –34.75 to –34.36 permil and -30.83 to –30.44 permil. Crossplots of these data indicate gas generated from a single source at a maturation level equivalent to a vitrinite reflectance of Ro ~ 1.3 percent (Figures 5-11 and 5-12). The distribution of $\delta^{13}C$ values between methane and higher homologues through butane is normal, i.e., the gases become increasingly depleted in ^{12}C with increasing molecular weight (Figures 5-11 and 5-12).

Reservoir Compartmentalization

The plot of $\delta^{13}C$ versus carbon number for the York field gases shown in Figures 5-11 and 5-12 shows the nearly identical isotopic compositions of the light hydrocarbon gases produced there. Differences between the $\delta^{13}C$ values in each of the various homologues in five of the six wells in the field are only on the order of 0.06 to 0.15 permil (Table 5-1). Gases produced from the Mantell #1 well exhibit the largest observed differences in $\delta^{13}C$ of methane through butane: the $\delta^{13}C_1$ is 0.54 to 0.67 permil lighter than that measured in the other gases in the field, and the $\delta^{13}C$ of the $C_2 – C_4$ gases produced from the Mantell #1 is slightly lighter than those values in the other wells (Table 5-1 and Figures 5-11 and 5-12). With the exception of the Mantell #1 well, the distribution of $\delta^{13}C$ for the $C_1 – C_4$ hydrocarbons shown in Figures 5-11 and 5-12 suggests homogeneous gases within a laterally continuous reservoir (Schoell and others, 1993). The subtle but real differences in the isotopic compositions of the gases produced from the Mantell #1 well suggest possible reservoir compartmentalization in the field (Schoell and others, 1993). The Mantell #1 well may be producing from a separate fault block than the other wells in York field (Minken, 2003).

Potential Source Rocks and Petroleum Migration

Potential source rocks for the gases produced at York field include Upper Ordovician shales in the Utica Shale and Point Pleasant Formation, and dolomitic mudstones within the Middle Ordovician Trenton Formation (Ryder and others, 1998; Swezey, 2002). As explained above, the isotope data presented in Table 5-1 and Figures 5-10 through 5-12 indicate that the gases produced at York field are thermogenic, associated with condensate, and were gas generated from a single source at a maturation level equivalent to a vitrinite reflectance of Ro ~ 1.3. The CAI data for Trenton strata in the York field area average 1.5, with values as high as 2 observed along the Lake Erie shore just to the northeast in northwestern Pennsylvania. The Ashtabula CAI values suggest that the Trenton and Black River are somewhat less mature than the hydrocarbons produced from them; a CAI of 1.5 ~ R_o of 0.7 to 0.85 (Harris, 1979). Rock – Eval data published by Ryder and others (1998) give T_{max} = 444°C (early maturation) and PI = 0.43 (peak – late maturation) for organic matter sampled from the Utica Shale and uppermost Trenton Formation. The isotope data from the gases correlate with the PI data published by Ryder and others (1998), and with the higher CAI of 2 mapped northeast of the York field. Seismic data presented by Minkin (2003) and Sagan and Hart (2005) show that the subsurface

structure at York field is consistent with hydrocarbon migration from a the Utica Shale source northeast of the accumulation.

SOUTH CENTRAL NEW YORK AND NORTH CENTRAL PENNSYLVANIA

We measured the chemical and isotopic compositions of: 1) the non-hydrocarbon gases nitrogen, carbon dioxide and hydrogen sulfide; 2) the noble gases helium, argon, neon and krypton; and 3) the commercial hydrocarbon gases produced from the Black River Group in New York and Pennsylvania. These gases are among the most unique natural gases produced anywhere in the Appalachian basin, and their geochemistry contains numerous clues to finding deeper hydrocarbon reserves in the eastern United States and Canada. Figures 5-1 and 5-13 show the locations of the wells we sampled for the analyses.

Gas Composition

Methane is the principal component in almost all of the gases produced in New York and Pennsylvania, ranging from 92.32 to 99.14 mole percent of the total gas composition (Table 5-1). One exception is the Wolpert #1 well in Bradford County, Pennsylvania, in which methane comprises only 84.42 mole percent of the total gas composition. The methane in this sample is diluted by relatively high nitrogen (14.14 mole percent) and a minor, but significant, amount of hydrogen sulfide (0.51 mole percent). Methane, however, does dominate the hydrocarbon fraction of the gas produced from the Wolpert #1 well (99.3 mole percent) (Table 5-1). The New York and Pennsylvania gases are remarkably dry, containing only 0.362 to 0.925 mole percent ethane, 0.129 to 0.555 mole percent propane, and slight traces of C_4 through C_6+ hydrocarbon gases (Table 5-1). Wetness ranges from 0.38 to 1.08 volume percent.

Nitrogen is the dominant non-hydrocarbon gas in the New York and Pennsylvania samples, ranging from 0.10 to 14.14 mole percent. As mentioned above, it is a major component in one of the Pennsylvania gas samples (Table 5-1). Carbon dioxide ranges from 0 to 0.46 mole percent in the New York and Pennsylvania gases, and there are traces of helium, hydrogen, oxygen and argon (Table 5-1). Helium correlates moderately with nitrogen in the gases, and this observation is discussed below. One well sample from the Glodes Corners Road field of Steuben County, New York (Covert #1), contains an unusual amount of hydrogen gas, 2.27 mole percent as measured offline. Online analyses of the same samples yielded higher hydrogen volumes, as well as higher amounts of nitrogen in the Glodes Corners Road samples (Table 5-3) than did the analyses of samples prepared offline. The specific gravity of the New York and Pennsylvania gases ranges from 0.555 to 0.621, and the BTU values range from a low of 871 in the high-nitrogen Pennsylvania sample to a high of 1018 at Muck Farm field Steuben County, New York.

Non-hydrocarbon Gases

We measured the $\delta^{15}N$ of nitrogen in nine of the twenty-two gas samples collected in New York and Pennsylvania. The $\delta^{15}N$ of these samples ranges from +0.4 to –10.2 permil (Table 5-1). The mean $\delta^{15}N$ is –6.7 permil, and the standard deviation is 3.36. There is a relatively strong positive correlation (r = 0.84) between the volume of nitrogen and its $\delta^{15}N$ composition in the gases (Figure 5-14).

The origin of nitrogen and the conditions controlling its distribution in natural gases are poorly understood (see discussions in Whiticar, 1994 and Hunt, 1996). Most workers recognize three possible sources of nitrogen in natural gas reservoirs: 1) release of nitrogen-bearing functional groups from organic matter during catagenesis; 2) release of ammonia from clay minerals at elevated burial temperatures; and 3) mantle nitrogen flux (Whiticar, 1994, p. 268; Hunt, 1996, p. 230 – 231). In some instances, atmospheric nitrogen and dissolved meteoric nitrogen might contribute to the amount of this gas found in some petroleum reservoirs. Whiticar (1994, p. 276) notes that nitrogen is apparently an important component of postmature source rocks, but at the present stage of knowledge we can only recognize compositional variations and lack the systematics to interpret their occurrence. Recent work by Ballentine and others (2001), however, appears to have resolved the isotopic composition of different nitrogen sources in some mid-continent natural gases, and their approach promises to provide some of the systematics that were heretofore unavailable.

The range of $\delta^{15}N$ values in natural gases (relative to atmospheric nitrogen) reported in the literature is large, approximately from –20 permil to +30 permil (Hoefs, 1997). Organic matter and ammonia in crustal rocks typically have positive $\delta^{15}N$ values, as does nitrogen found in basalts and in diamonds with low $\delta^{13}C$ values (White, 1997). Diamonds with high $\delta^{13}C$ formed during peridotite paragenesis, however, generally contain nitrogen gas inclusions with negative $\delta^{15}N$ (average $\delta^{15}N$ of -3 permil, and a reported range of –12 permil to +5 permil). Fibrous diamonds, whose formation may be directly linked to kimberlite eruptions that transport them to the surface, exhibit uniform $\delta^{15}N$ values in their gas inclusions, with a mean of –5 permil (Boyd and others, 1994; White, 1997, p. 409). It is clearly tempting to interpret the negative $\delta^{15}N$ values observed in the Black River gases of New York and Pennsylvania as evidence of a deep crustal or even mantle origin for the nitrogen produced from the reservoirs, but caution is necessary since there can be significant isotope fractionations associated with geological processes in these environments. Recent work by Ballentine and others (2001) demonstrates that noble gas and ^{13}C ($C_1 – C_3$ hydrocarbons) data may help constrain nitrogen gas systematics, and we discuss this further below.

We measured the $\delta^{13}C$ of carbon dioxide in the same nine gas samples that we measured for $\delta^{15}N$ described above (Table 5-1). The $\delta^{13}CO_2$ of these samples ranges from –3 to –6.7 permil. The mean $\delta^{13}C$ is –5.4 permil, and the standard deviation is 1.1. A comparison of the CO_2 content of the New York and Pennsylvania samples to their carbon isotopic composition (Figure 5-15) shows only one distinct group of gases. The small range of $\delta^{13}CO_2$ values in the gases suggests a similar origin for all of the carbon dioxide in the New York and Pennsylvania fields. Although negative, these $\delta^{13}CO_2$ values all are relatively heavy, approaching that of marine carbonates (Hoefs, 1997, p. 43), and characteristic of carbon dioxide generated by the thermal destruction of carbonate rocks (Hunt, 1996, p. 221 – 225). We suggest that the CO_2 in

the Black River traps formed through high-temperature degradation of the reservoir carbonate rock, possibly in conjunction with thermochemical sulfate reduction. The latter process would oxidize reservoir hydrocarbons, and the slightly negative $\delta^{13}CO_2$ observed in the gases may reflect mixing of carbonate and hydrocarbon carbon. Further evidence for the latter process is found in the stable isotope composition of sulfur in hydrogen sulfide gas in the Wolpert #1 well in north central Bradford County, Pennsylvania (Figure 5-13 and Table 5-1).

Natural gas sampled from the Wolpert #1 well contains 0.51 mole percent (500 ppm) H_2S (Table 5-1). The $\delta^{34}S$ of this hydrogen sulfide gas is +14.7 permil (Table 5-1). Hydrogen sulfide in natural gas reservoirs has two major sources: 1) the thermal decomposition of high-sulfur crude oils during deep burial beyond the oil window; and 2) the thermochemical reduction of sulfate in pore waters (Hunt, 1996, p. 225 – 230, and p. 237). The $\delta^{34}S$ value of the H_2S produced from the Wolpert well is consistent with a sulfate source (Hoefs, 1997), and suggests the latter process was responsible for the occurrence of this dangerous gas in the reservoir.

Hydrogen sulfide is a very undesirable component in a gas resource – it dilutes the economically valuable hydrocarbon reserves, is highly toxic, and is corrosive to production equipment (Worden and others, 1995). Hydrogen sulfide generation and subsequent hydrocarbon oxidation can concentrate nitrogen in some carbonate reservoirs. Worden and others (1995) proposed that gas souring by thermochemical sulfate reduction becomes a potential problem only after a carbonate reservoir is buried to depths where it is exposed to temperatures of 140 °C and higher. Maximum bottom hole temperatures and maximum burial temperatures easily exceed this value in the Black River play of New York and Pennsylvania, yet significant H_2S has only been encountered in the Wolpert well to date (problematic levels of H_2S also occur in some Trenton wells in West Virginia). Further study of H_2S gas systematics clearly is warranted in the play.

Noble Gases

The geochemistry of noble gases coupled to stable isotope data from hydrocarbons and non-hydrocarbon gases is an emerging methodology in the study of natural gases (Jenden and others, 1993; Prinzhofer and Battani, 2003). Chinese researchers, in particular, have made a great deal of progress in this research, and much of their work may have important applications in understanding the origins of natural gas in the Trenton and Black River reservoirs of the Appalachian basin (see Yongchang and others, 1996). The chemical inertness of noble gases enables their utility as precise tracers of gas sources and the physical processes that affect a gas, such as state of the phases, migration and diffusive leakage (Prinzhofer and Battani, 2003). Furthermore, since some of the noble gas isotopes are produced by natural radioactivity (^{4}He, ^{40}Ar), they have the potential to provide information about the age of a petroleum source rock (Youngchang and others, 1996) or the residence time of hydrocarbons in a reservoir (Prinzhofer and Battani, 2003).

Tables 5-2 and 5-3 contain summaries of the noble gas data we collected for the New York and Pennsylvania Black River natural gases. These data include the relative proportions of ^{3}He and ^{4}He, ^{36}Ar and ^{40}Ar, total neon, ^{20}Ne, total krypton, and ^{84}Kr in selected gas samples.

The $^{3}He/^{4}He$ ratios fall into two distinct groups. All of the gases, from the Zimmer Hill field and on to the south and southeast, have low $^{3}He/^{4}He$ ratios between 1.48×10^{-8} and 3.08×10^{-8} (Table 2), values indicative of a crustal sedimentary origin (Hunt, 1996, p. 232). The gases from Glodes Corners Road field have higher $^{3}He/^{4}He$ ratios of 1.53×10^{-7} to 2.74×10^{-7}, values that might indicate mantle helium (Hunt, 1996, p. 232). These two groups of $^{3}He/^{4}He$ ratios are readily compared to various $^{3}He/^{4}He$ ratios reported in the literature by normalizing the $^{3}He/^{4}He$ ratios to the atmospheric ratio of 1.4×10^{-6} (*Ra*). This normalization yields *R*/*Ra* values of 0.01 to 0.19 for the New York and Pennsylvania Black River gases (Figure 5-16; Tables 5-2 and 5-3). As in the $^{3}He/^{4}He$ ratios presented in Table 5-2, *R*/*Ra* values differ significantly between the gases from Glodes Corners Road field at the northern limit of the study area and all of the other gases we sampled. The gases from Glodes Corners Road field have *R*/*Ra* values of 0.109 to 0.196, whereas all of the other New York and Pennsylvania fields have *R*/*Ra* values between 0.01 and 0.02. The ratios of $^{4}He/^{20}Ne$ in all of the gases range from 476 to 2,687.3, indicating that the variability in *R*/*Ra* values is not due to air contamination of any of the samples ($^{4}He/^{20}Ne$ of air = 0.288). With the exception of the Glodes Corners Road samples, the *R*/*Ra* values in Table 5-2 unequivocally show that most of the gases we analyzed contain helium of crustal origin (the average crustal production ratio is 0.02; see Ballentine and others, 1996). This crustal helium was generated by radioactive decay of uranium and thorium (yielding ^{4}He) and the (n, α) reaction of ^{6}Li (yielding ^{3}He) to produce characteristic crustal $^{3}He/^{4}He$ ratios <0.04 *Ra* (Jenden and others, 1993).

The *R*/*Ra* values of the Glodes Corners gases exceed 0.1, and most approach 0.2 (Figure 5-16). The mean *R*/*Ra* of the Glodes Corners Road gases is 0.17 and the standard deviation is 0.03. Whereas *R*/*Ra* values greater than 0.2 provide unambiguous identification of a mantle-derived helium component in natural gases (Poreda and others, 1986), modestly elevated values such as those in the Glodes Corners Road gases are equivocal, and may be attributed to a mantle component or to other sources such as high local lithium concentrations, cosmogenic ^{3}He implantation and release from sedimentary materials, or preferential release of ^{3}He over ^{4}He from the site of generation (Ballentine and others, 1996, p. 837). If there actually is a mantle-derived helium component in the Glodes Corners Road field yielding the elevated *R*/*Ra* in our samples, we can resolve the fraction of helium that originated in the upper mantle using the mass balance equation published by Jenden and others (1993),

$$He_{mantle}/He_{total} = (Ra_{gas} - Ra_{crust})/(Ra_{mantle} - Ra_{crust}).$$

The crustal and mantle end members are assumed to be *R*/*Ra* = 0.01 and 8, respectively (Jenden and others, 1996). This equation yields only 1.2 and 2.3 percent mantle-derived ^{4}He in the Glodes Corners gases. Thus, we can surmise that while most of the helium in the Glodes Corners gases is of crustal origin, mantle helium flux in the field is significant compared to the other Black River carbonate reservoirs in the area; this flux reflects the very deep-seated nature of basement faulting and fracturing at the northern limit of the play.

A crossplot of *Ra* versus the $^{40}Ar/^{36}Ar$ ratios of the New York and Pennsylvania gases (Figure 5-17) reveals a distribution almost identical to the plot of *Ra* versus ^{4}He shown in Figure 5-16. This consistency in the trends of noble gas composition supports the identification of a discrete gas group at Glodes Corners Road field.

The $^{40}Ar/^{36}Ar$ ratios of the New York and Pennsylvania gases vary considerably across the study area (Table 5-2). These ratios vary from 295 (approximately the atmospheric value) to 1521. The mean is 664.4, with a large standard deviation (321.4). With the exceptions of the Hakes #1 and Curren #1 wells (Tables 5-1 and 5-2), these $^{40}Ar/^{36}Ar$ values require an average ~ 55.5 percent contribution of non-atmospheric ^{40}Ar to the produced gases (the range is 22.7 to 80.6 percent non-atmospheric ^{40}Ar in the Black River gases). This excess argon is a combination of radiogenic ^{40}Ar produced in the crust and mantle-derived ^{40}Ar (Ballentine and others, 1996).

We can differentiate between primordial, mantle-derived ^{40}Ar ($^{40}Ar_o$) and radiogenic crustal ^{40}Ar ($^{40}Ar^*$) (Prinzhofer and Battani, 2003).

$$^{40}Ar_o = 295.5\ (^{36}Ar), \text{ and}$$

$$^{40}Ar^* = {}^{40}Ar - {}^{40}Ar_o.$$

Using these equations, 4.5 to 1384.1 ppm (1.5 to 80.6 %) of the measured ^{40}Ar in the samples is of crustal origin. These values indicate radically different residence times for the natural gases in the different New York and Pennsylvania fields (Prinzhofer and Battani, 2003) (Figure 5-18).

The ratios of $^{4}He/^{40}Ar$ in the samples (Table 5-2) may be used as a parameter to assess if a system is open or closed with respect to noble gases (Ozima and Podosek, 2002). Hunt (1996, p.232) notes that $^{4}He/^{40}/Ar$ ratios of 10 to 20 indicate a sedimentary origin for these particular noble gases and that ratios of 1 to 2 indicate a mantle origin. The $^{4}He/^{40}/Ar$ ratios of most natural gas pools cluster around 12 and go up to 170, indicating a sedimentary origin for most of the associated helium (Krouse, 1979; Hunt, 1996). Most of the ^{4}He and ^{40}Ar on earth are radiogenic, and their concentration in any reservoir depends on both the relative abundance of uranium, thorium, and potassium in the rocks and the epoch and duration of their accumulation (Ozima and Podosek, 2002). The $^{4}He/^{40}Ar$ ratio in any closed system reservoir is confined to a narrow range between 2 and 6 (Ozima and Podosek, 2002, p. 156.). The values reported by Hunt (1996) for sedimentary helium and argon are much in excess of the closed system ratio, suggesting differential release of ^{4}He over ^{40}Ar from the source minerals due to sediment loading in stable crustal regions – the fractionated $^{4}He/^{40}/Ar$ ratio is due to incomplete extraction (Elliot and others, 1993; Ozima and Podosek, 2002).

The $^{4}He/^{40}Ar$ ratios in the Black River gases range from 0.46 to 2.22, with a mean of 1.2 and standard deviation of 0.5 (Table 2). Two of the samples show nearly the average crustal production rate of $^{4}He/^{40}/Ar = 2.1$ (a closed system ratio), while the rest of the samples have ratios well below this value. This suggests remarkably complete extraction of both the radiogenic ^{4}He and ^{40}Ar from the Black River reservoirs due to high heat flow coupled with tectonic activity, specifically deep-seated faulting and hydrothermal fluid migration ((Ozima and Podosek, 2002). The mean $^{4}He/^{40}Ar$ of the Black River gases in New York and Pennsylvania (1.2) reflect the primordial mantle component present in the reservoirs.

Prinzhofer and Battani (2003) demonstrated that a crossplot of $^{20}Ne/^{36}Ar$ versus ^{4}He is useful for recognizing gas leakage from a reservoir. Figure 5-19 is a plot of $^{20}Ne/^{36}Ar$ versus ^{4}He for our data from Table 5-2. Since the smaller helium atoms migrate more readily than the larger noble gas isotopes, a decrease in helium concentration corresponding to an increase in the ratios of the larger noble gas atoms indicates the relative magnitude of gas leakage from the reservoir. The trend plotted in Figure 5-19 suggests such gas leakage.

Hydrocarbons

The $\delta^{13}C$ of methane ($\delta^{13}C_1$) in the gases produced from the New York and Pennsylvania Black River gas fields ranges from –32.77 to –26.02 permil (Table 5-1). The mean $\delta^{13}C_1$ is –29.7 permil, and the standard deviation is 2.13. The methane in these fields is notably heavy, i.e., depleted in the lighter ^{12}C isotope, and these values in conjunction with the low wetness values discussed above indicate distinctly postmature natural gas (Schoell, 1983 and 1988; Tissot and Welte, 1984; Jenden and others, 1993; Whiticar, 1994; Laughrey and Baldassare, 1998). Indeed, on the basis of just the $\delta^{13}C_1$ and wetness data presented in Table 5-1, we could interpret the New York and Pennsylvania Black River gases as postmature thermogenic hydrocarbons generated from a combination of oil and kerogen cracking during late catagenesis and early metagenesis (see Tissot and Welte, 1984, p. 200 – 201). Pyrobitumen in the reservoir rocks (Figure 5-20) and Rock-Eval pyrolysis data from potential source rocks of the region support such an interpretation. So do the CAI data published by Weary and others (2000): CAI values range from 4.0 to 5.0 across the study area.

The $\delta^{2}H$ of methane in these samples ranges from –156.6 to –145.1 permil (Table 5-1). The mean $\delta^{2}H$ is –150.7 permil, and the standard deviation is 3.3. Such depletion in ^{1}H is also indicative of postmature natural gas (Schoell, 1980; Wiese and Kvenvolden, 1993; Hoeffs, 1997), and a crossplot of $\delta^{13}C$ versus $\delta^{2}H$ for these methane samples supports the interpretation of the gases as late catagenetic to metagenetic (Figure 5-21). This crossplot, however, also reveals a striking anomalous trend: the $\delta^{2}H$ of the methane gases becomes isotopically lighter (more negative) as the $\delta^{13}C$ of the methane becomes heavier (more positive). Thermogenic gases worldwide exhibit a positive correlation between $\delta^{13}C$ and $\delta^{2}H$ due to increasing isotopic enrichment in both ^{13}C and ^{2}H with increasing thermal maturity (Schoell, 1983). If these gases were cracked from kerogen, bitumen, and/or oil during progressive burial and exposure to increasing subsurface temperature, both $\delta^{2}H$ and $\delta^{13}C$ of methane should become heavier with increasing maturation due to the kinetic isotope effect (KIE), a trend exhibited by all of the other Trenton/Black River gases sampled during this study (Figure 22), and indeed by all other Appalachian gases reported in the literature (Schoell, 1980 and 1983; Jenden and others, 1993; Whiticar, 1994; Hoeffs, 1997; Laughrey and Baldassare, 1998; Burruss and Ryder, 2004). It is also interesting to note that the New York and Pennsylvania Black River methane falls into an area characteristic of geothermal and hydrothermal gases, and gases found in crystalline rocks on $\delta^{2}H$ versus $\delta^{13}C$ crossplots published by Apps and van de Kamp (1993) and Whiticar (1994).

Variations in the isotopic composition of the precursor organic matter (kerogen, bitumen, or oil) offer one possible explanation for the observed negative correlation between $\delta^{2}H$ and $\delta^{13}C$ in the methane samples from New York and Pennsylvania. Burruss (2006, per. comm.) suggests that some of the scatter observed on $\delta^{13}C$ versus $\delta^{2}H$ crossplots for pre-Devonian methane in the

Appalachian basin might be due to such variation, particularly where both Types I/II marine kerogens and the unique Ordovician alga, *Gloeocapsamorpha prisca* contribute to petroleum generation in the source rocks. The negative correlation (r = -0.92) between δ^2H and $\delta^{13}C$ in the New York and Pennsylvania Black River methane is strong, however, and suggests that variations in the organic precursor material cannot adequately explain the observed trend in Figures 5-21 and 5-22.

The ^2H depletion in the Black River Group methane from New York and Pennsylvania might be due to diffusive hydrogen exchange with formation water involved in diagenetic reactions, catalytic exchange reactions mediated by metal oxides in the rocks, or methane oxidation associated with thermochemical sulfate reduction by light hydrocarbon gases in the reservoirs (Krouse and others, 1988).

Interestingly, depletion in ^2H with increasing ^{13}C in methane might be diagnostic of some abiogenic gases, particularly those generated by polymerization reactions in the earth's deep crust (Lyon and Hulston, 1984; Jenden and others, 1993; Apps and van de Kamp, 1993; Sherwood-Lollar and others, 2002 and 2006). Such abiogenic natural gases often exhibit the distinctive Shultz-Flory $\delta^{13}C$ distribution among the C_1 through C_4 alkanes in which the C_2 through C_4 hydrocarbons are progressively depleted in ^{13}C with respect to methane, a pattern opposite that shown by thermogenic gases (Des Marais and others, 1981; Chang and others, 1983; Jenden and others, 1993). Not all abiogenic gases display this isotopic reversal among the C_1 to C_4 alkanes (Horita and Berndt, 1999), but some workers consider it diagnostic of abiogenic natural gases when it is observed, particularly when the δ^2H of the same alkanes shows an inverse relationship of ^{13}C isotope depletion and ^2H isotope enrichment between homologues of increasing molecular weight (Westgate, 1998; Sherwood-Lollar and others, 2002 and 2006). Alternative explanations for carbon isotopic reversals among the C_1 through C_4 alkanes in natural gases include heterogeneities in source rock organic matter, oxidation of thermogenic gas, partial diffusive leakage of gases from a reservoir, and mixing of thermogenic gases from different sources (Jenden and others, 1993; Prinzhofer and Huc, 1995; Prinzhofer and Battani, 2003). Indeed, Jenden and others (1993) attributed the reversal of $\delta^{13}C$ values observed in Ordovician gases in New York (including one Black River field) to mixing of thermogenic hydrocarbons.

Twenty of the twenty-two gas samples that we collected from Black River dolomite reservoirs in New York and Pennsylvania exhibit $\delta^{13}C$ isotopic reversals among the C_1 to C_3 or C_1 and C_2 alkanes (Figures 5-23 to 5-26 and Table 5-1). The $\delta^{13}C$ of ethane and higher alkanes was not measured in two of the samples (the Gregory and Soderblom wells in Quackenbush field). Only nine of the gas samples had sufficient propane to obtain $\delta^{13}C$ values using online analyses; all of these nine samples display depletion in ^{13}C relative to methane through C_3. The magnitude of all these isotopic reversals is remarkable: C_2 is depleted in ^{13}C by approximately 5 to 8 permil with respect to methane, and C_3, with one exception, is depleted in ^{13}C by approximately 8 to 9 permil with respect to methane (Table 5-1 and Figures 5-23 to 5-26). The one exception is the gas produced from the Wolpert #1 well in Bradford County, Pennsylvania in which C_3 is depleted in ^{13}C by only 1.76 permil with respect to methane.

Shultz-Flory $\delta^{13}C_{1-4}$ isotopic distributions are characteristic of natural gas accumulations in pre-Devonian reservoirs throughout the Appalachian basin, particularly in Lower Silurian and Ordovician reservoirs (Jenden and others, 1993; Laughrey and Baldassare, 1998; Laughrey and Harper, 1996; Laughrey and others, 2004; Burruss and Ryder, 2004; Burruss and Laughrey, 2006). The regional gas accumulation in Lower Silurian strata of the Medina Group and Tuscarora Formation exhibits progressive enhancement of this isotopic reversal with increasing depth in the basin (Burruss and Ryder, 2004). Multivariate analyses of the molecular and isotopic data from the Appalachian basin define and end-member for this gas in the deep basin with an approximate composition of 98 mole percent methane, 1 to 2 mole percent ethane, less than 1 mole percent higher homologues, and $\delta^{13}C_1$ = -27 permil, $\delta^{13}C2$ = -40 permil, and $\delta^{13}C3$ = -41 permil (Burruss and Laughrey, 2006). This reversal is pronounced in fractured Ordovician sandstone reservoirs, and in the Black River reservoirs discussed in this report (Laughrey and Harper, 1996) (Figures 5-25 and 5-26). The chemical and isotopic composition of these gases are almost a perfect match to those hypothetical end-member proposed by Burruss and Laughrey (2006). The two most likely explanations for these carbon isotope reversals are abiogenic synthesis (Des Marais and others, 1981; Apps and van de Camp, 1993; Sherwood Lollar and others, 2002) and thermogenic gas mixing (Jenden and others, 1993).

Abiogenic Gas Interpretation

The hydrocarbon gases produced from hydrothermal dolomites in the Black River Group of New York and Pennsylvania exhibit a strong negative correlation between methane $\delta^{13}C$ and $\delta^{2}H$, and significant carbon isotopic reversals among the C_1 through C_3 hydrocarbons. The magnitude of these reversals in the Shultz-Flory $\delta^{13}C_{1-4}$ isotopic distributions is dramatic, particularly when compared to the normal carbon isotope distributions exhibited by Trenton and Black River thermogenic gases produced in Kentucky and Ohio (Figure 5-27). Some workers would clearly regard the carbon isotope distributions of these New York and Pennsylvania gases as diagnostic of abiogenic hydrocarbons, particularly when accompanied by the observed depletion in ^{2}H with increasing ^{13}C in methane (Westgate, 1998; Sherwood Lollar and others, 2002 and 2006). The carbon isotope reversals in the $C_1 - C_3$ hydrocarbons and ^{2}H depletion in the methane produced from the Black River gases are similar to those documented in abiogenic Precambrian gases from the Canadian Shield and South Africa (Sherwood Lollar and others, 2002 and 2006). Published work on the Precambrian gases suggests that the hydrocarbons were generated through Fischer-Tropsch reactions (see Szatmari, 1989) associated with serpentinization or water-rock reactions in high-grade metamorphic rocks. The $\delta^{15}N$ values of the Black River gases (mean $\delta^{15}N$ = -6.7 permil) as discussed above are consistent with nitrogen derived from devolatilization reactions associated with metamorphism. There is a moderate correlation between the nitrogen and helium contents of the New York and Pennsylvania gases (Figure 5-28). Noble gas data from these gases indicate deep crustal origins for most of the helium and argon. The observed flux of mantle-derived gases is due to high heat flow associated with deep-seated faulting and hydrothermal fluid migration. The carbon and helium isotope data indicate that the hydrocarbons are not from the mantle. The observed flux of mantle-derived noble gases, however, supports the interpretation of deep-seated faulting and vertical migration of hydrothermal fluids in the region.

The depletion in ^{2}H with increasing ^{13}C in the methane samples from New York and Pennsylvania might indeed indicate an abiogenic origin for the gases. This interpretation would be more compelling if we also observed an inverse relationship of ^{13}C isotope depletion and ^{2}H isotope enrichment in the C1 to C3 hydrocarbons (Westgate, 1998; Sherwood-Lollar and others, 2002 and 2006). Late in 2005, we resubmitted several of the same New York and Pennsylvania samples to Isotech Laboratories for further online analyses of the hydrogen isotopes in the ethane and propane. We are still awaiting the results of these analyses as of this writing.

There are some problems with an abiogenic interpretation of the gases at this time. A comparison of our data set with those published by Westgate (1998) and Sherwood Lollar and others (2002 and 2006) shows that the Precambrian gases of supposed Fischer-Tropsch synthesis differ significantly from the Black River gases produced in New York and Pennsylvania. The former gases have extremely light hydrogen isotopic compositions (methane $\delta^{2}H < -300$ permil), and are depleted in methane.

Rasmussen and others (2003) propose that the hydrocarbons produced from hydrothermal dolomites in the New York fields are abiogenic, and that their generation was associated metagenetic fluids formed by serpentinization of peridotite in intracratonic failed rifts or collisional sutures in the basement triggered by compressive, convergent orogenesis during the Acadian orogeny. They suggest that hydrothermal dolomitization of the Black River carbonates in the New York fields occurred through rock-water interactions with these fluids, and that this dolomitization was followed by CO_2 effervescence, hydrogen loss, and methane unmixing. Base metal sulfide mineralization, hydrocarbon deposition, and late stage calcite and clay mineralization followed. As unconventional as this interpretation is, the geochemistry of the gases produced from the New York and Pennsylvania Black River fields do support their model. This support could be strengthened or refuted by further work in progress by Robert Burruss at the United States Geological Survey and us. Specifically, we are looking at the isotopic composition of the hydrogen in the ethane and propane in the samples, and we will be conducting isotopic studies of: 1) the gases in fluid inclusions in the reservoir rocks; and 2) Ordovician organic matter to further constrain the possible contribution of abiogenic hydrocarbons to these reservoirs. Most workers suggest that while abiogenic hydrocarbon gases certainly exist and can be recognized using specific geochemical parameters, they do not form economically important natural gas accumulations (Sherwood Lollar and others, 2002). If the Black River gases produced from the New York and Pennsylvania fields are confirmed as abiogenic accumulations, this discovery will revolutionize petroleum exploration in the Appalachian basin and the world.

Thermogenic Gas Mixing

Jenden and others (1993) noted carbon isotopic reversals between methane and ethane in Ordovician and Silurian reservoirs in New York State, including one Black River hydrothermal dolomite field (Reading Center field) in Schuyler County, north of our study area. They attributed the observed isotopic reversals to mixing of thermogenic gases of widely different maturities. Jenden and others (1993) further postulated that a postmature gas end member was generated in a Middle Ordovician or older source rock, and that this gas migrated along the Knox unconformity until encountering vertical migration conduits associated with faults and fractures.

In this interpretation, a deep postmature methane mixes with less mature gas in the reservoir yielding the observed carbon isotopic reversals. Jenden and others (1993) utilized plots of $\delta^{13}C_1$ versus $\delta^{13}C_2$ and the carbon isotopic difference between propane and ethane versus that between ethane and methane to illustrate mixing of their hypothetical postmature gas with less mature gases from other sources. Whiticar (1996) also presented similar crossplots that show the linear relationship between of $\delta^{13}C$ for co-genetic methane versus ethane and propane, and between ethane and propane in natural gases.

We can apply such a mixing interpretation to our data by establishing the expected linear trend using the Kentucky and Ohio gases (which have normal $\delta^{13}C$ distributions between the different hydrocarbon gases) and then applying mixing estimates to the New York, Pennsylvania, and West Virginia gases that fall off of the expected trend (Figures 5-29 to 5-31). The shifts from the trend of co-genetic Kentucky and Ohio gases to the area of the plots occupied by New York, Pennsylvania, and West Virginia gases could be due to mixing of different thermogenic gases and/or to methane oxidation (Whiticar, 1996). Such a mixing interpretation requires that isotopically heavy, postmature methane, generated in a deeper undefined source bed in the basin, be mixed with residual, isotopically light ethane and propane in the Black River reservoirs. As mentioned above, the magnitude of the $\delta^{13}C_1 - \delta^{13}C_2$ and $\delta^{13}C_1 - \delta^{13}C_3$ reversals in the New York and Pennsylvania gases is uncommon, and we consider this interpretation as speculative as the abiogenic gas interpretation.

Conclusions

- Natural gases produced from Trenton and Black River reservoirs in Kentucky and Ohio are thermogenic, cracked from kerogens in organic-rich source rocks, and from reservoir oils at higher maturation temperatures.
    - Gases produced at the Homer field in Elliott County, Kentucky are compartmentalized due to faulting. The carbon isotope distributions in C_1 through C_4 gases at Homer field are useful for recognizing the compartmentalized gases.
    - Two groups of gases are produced from different wells at the Homer field:
        1. Thermogenic gas associated with oil. These gases originated from early mature to mature organic matter and/or from a combination of kerogen and oil cracking in the early to middle oil window.
        2. Thermogenic gas that formed in the transition zone between oil-associated gas and postmature gas.
    - Gas produced at Colin Fork field in Clay County, Kentucky is thermogenic gas associated with oil.

- Potential source rocks for the Kentucky gases include the Upper Ordovician Utica Shale and Point Pleasant Formation, dolomitic mudstones within the Middle Ordovician Trenton Formation, the Middle Ordovician Wells Creek Formation, and strata within the Cambrian Rome Formation.

- Natural gas produced from fractured limestones at Cottontree field in West Virginia are postmature and can be interpreted as either,

  - Mixed postmature thermogenic gases generated in the Utica and Point Pleasant shales, dolomitic mudstones within the Middle Ordovician Trenton Formation, the Middle Ordovician Wells Creek Formation or strata within the Cambrian Rome Formation, or

  - Abiogenic gases of deep crustal origin.

- Natural gases produced from the York field in northeastern Ohio are thermogenic gases associated with condensate. The Utica Shale is the probable source rock, and migration was most likely from a deeper section northeast of the field. The carbon isotope distributions in C_1 through C_4 gases at York field are useful for recognizing compartmentalization in the field.

- The natural gases produced from dolomitized Black River carbonate rocks in south central New York and north central Pennsylvania are unique.

  - The hydrocarbon gases consistently exhibit low wetness, heavy $\delta 13C_1$ values, and unusual methane δ^2H that become isotopically lighter as the $\delta 13C_1$ becomes heavier (Figure 5-22). In addition to the strong negative correlation between methane $\delta^{13}C$ and δ^2H, the gases show notable carbon isotopic reversals among the C_1 through C_3 hydrocarbons, particularly when compared to the normal carbon isotope distributions exhibited by Trenton and Black River thermogenic gases produced in Kentucky and Ohio (Figure 5-27).

  - $\delta^{15}N$ of nitrogen produced in the New York and Pennsylvania gases has a mean value of –6.7 permil, and may have originated through devolatilization reactions associated with deep-seated metamorphism. High nitrogen concentrations in some wells may have a negative impact on economic reserves in portions of the play.

  - Noble gas geochemistry indicates highly variable flux of both mantle and radiogenic crustal gases. These data reflect high heat flow coupled with deep-seated faulting and fracturing, and hydrothermal fluid migration. The noble gas data also indicate some gas leakage from the reservoirs, and highly variable residence times for natural gases in the different New York and Pennsylvania fields.

- The hydrocarbons produced from the Black River reservoirs in New York and Pennsylvania *might* actually be the first documented occurrence of a commercial abiogenic natural gas accumulation. The data are compelling, but further confirmation will be necessary to support this interpretation. If correct, this interpretation of the gases will have a direct bearing on the interpreted mechanisms, processes, and timing of hydrothermal dolomitization in the region.

- If the abiogenic hydrocarbon hypothesis is incorrect, then the Black River gases produced in New York and Pennsylvania are a mixture of isotopically heavy, postmature gas generated from an unidentified deep basin source rock, and residual isotopically light ethane and propane. It is important to consider that the magnitude of the observed $\delta^{13}C$ enrichment and simultaneous $\delta^{13}C$ depletion in the ethane and propane are difficult to explain in a thermogenic gas accumulation (Sherwood Lollar and others, 2002).

- Hydrogen sulfide poses a potential problem with deeper Black River gas production in Pennsylvania, and perhaps West Virginia. In Pennsylvania the $\delta^{34}S$ of sulfur in the produced H_2S suggests that thermochemical sulfate reduction is responsible for the generation of gas in the reservoir.

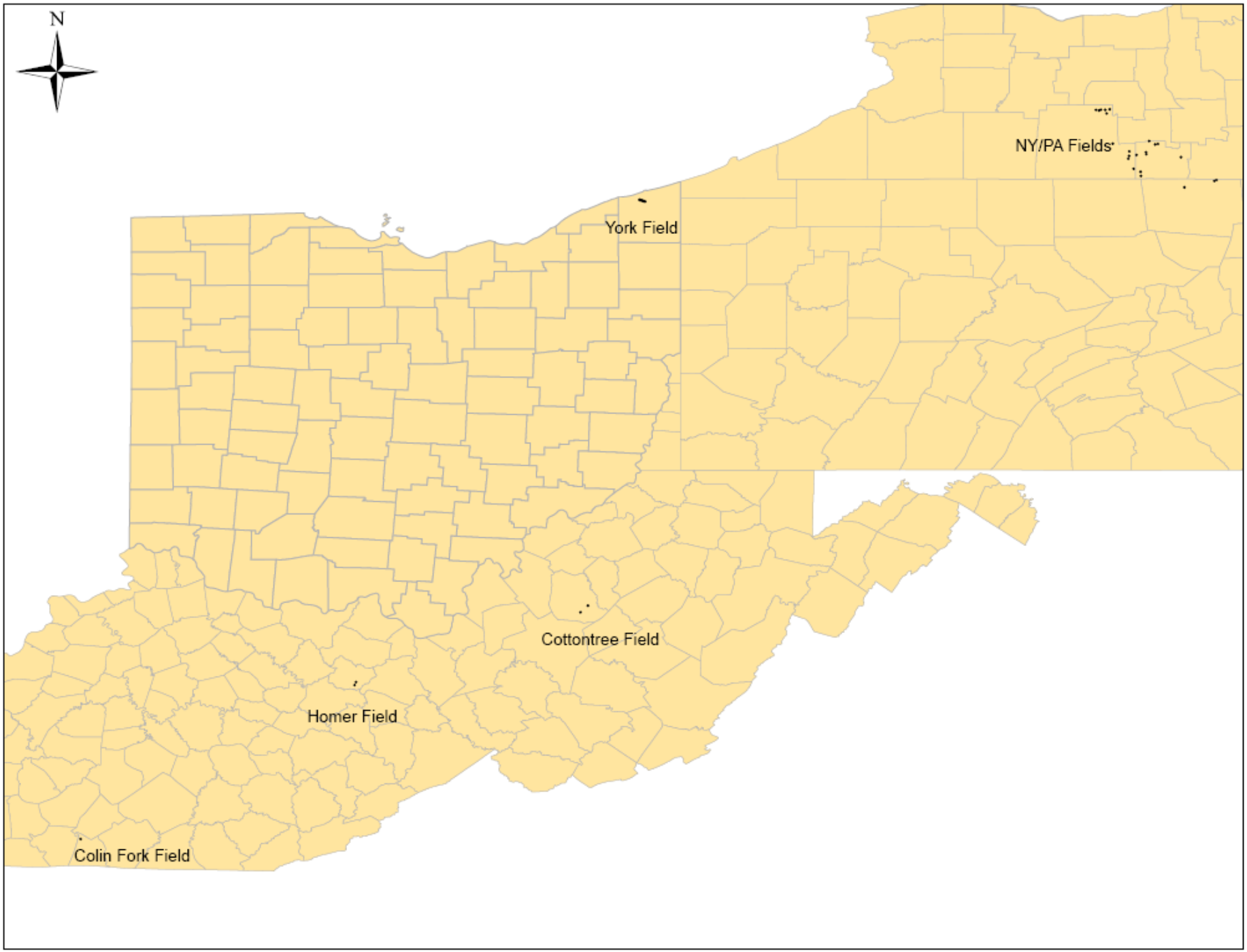

Figure 5-1. Regional map of the study area showing Trenton and Black River gas fields and well locations for the natural gas samples discussed in this report.

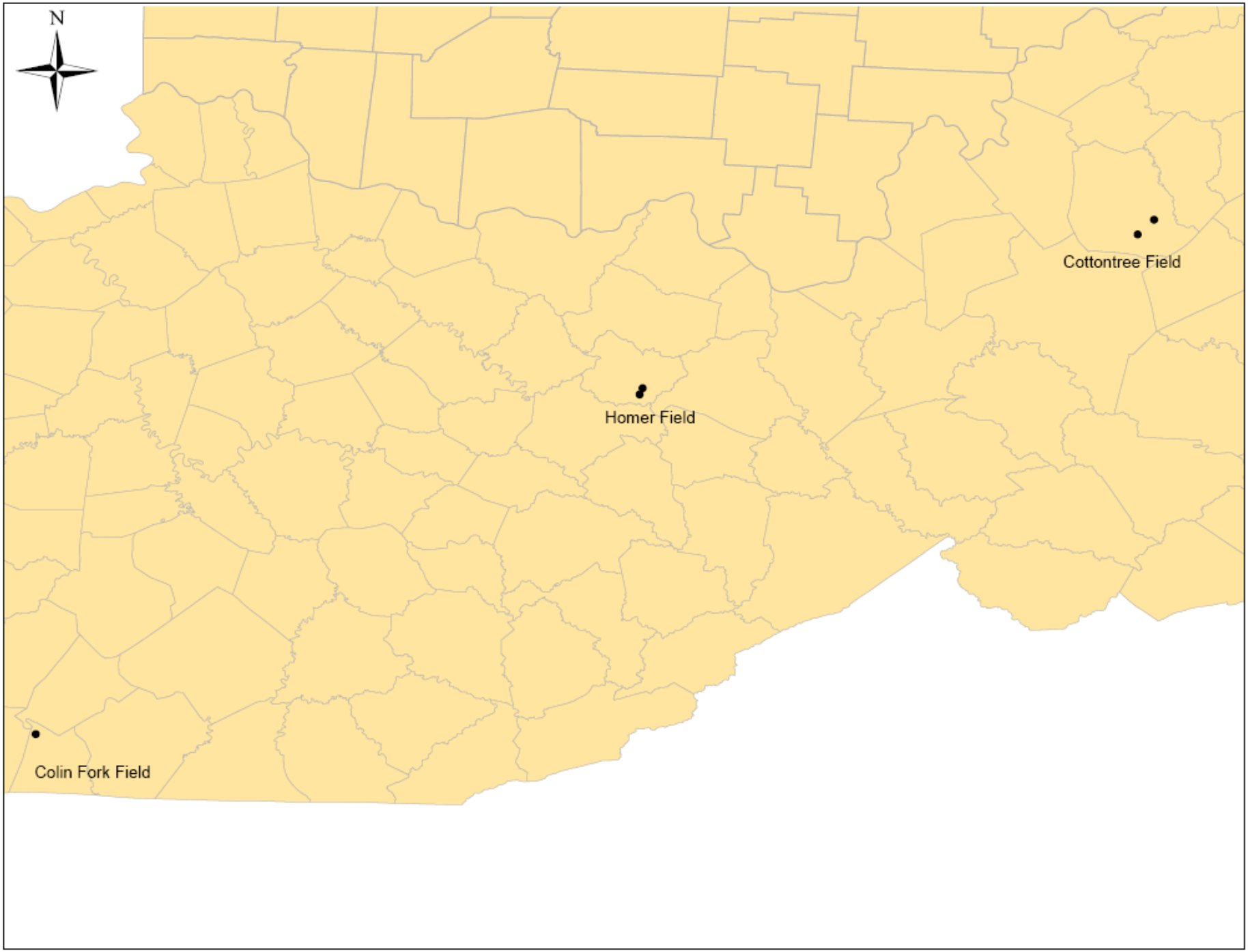

Figure 5-2. Map showing locations of the wells sampled for gas geochemistry in the Cottontree field, West Virginia, and the Homer and Colin Fork fields in Kentucky

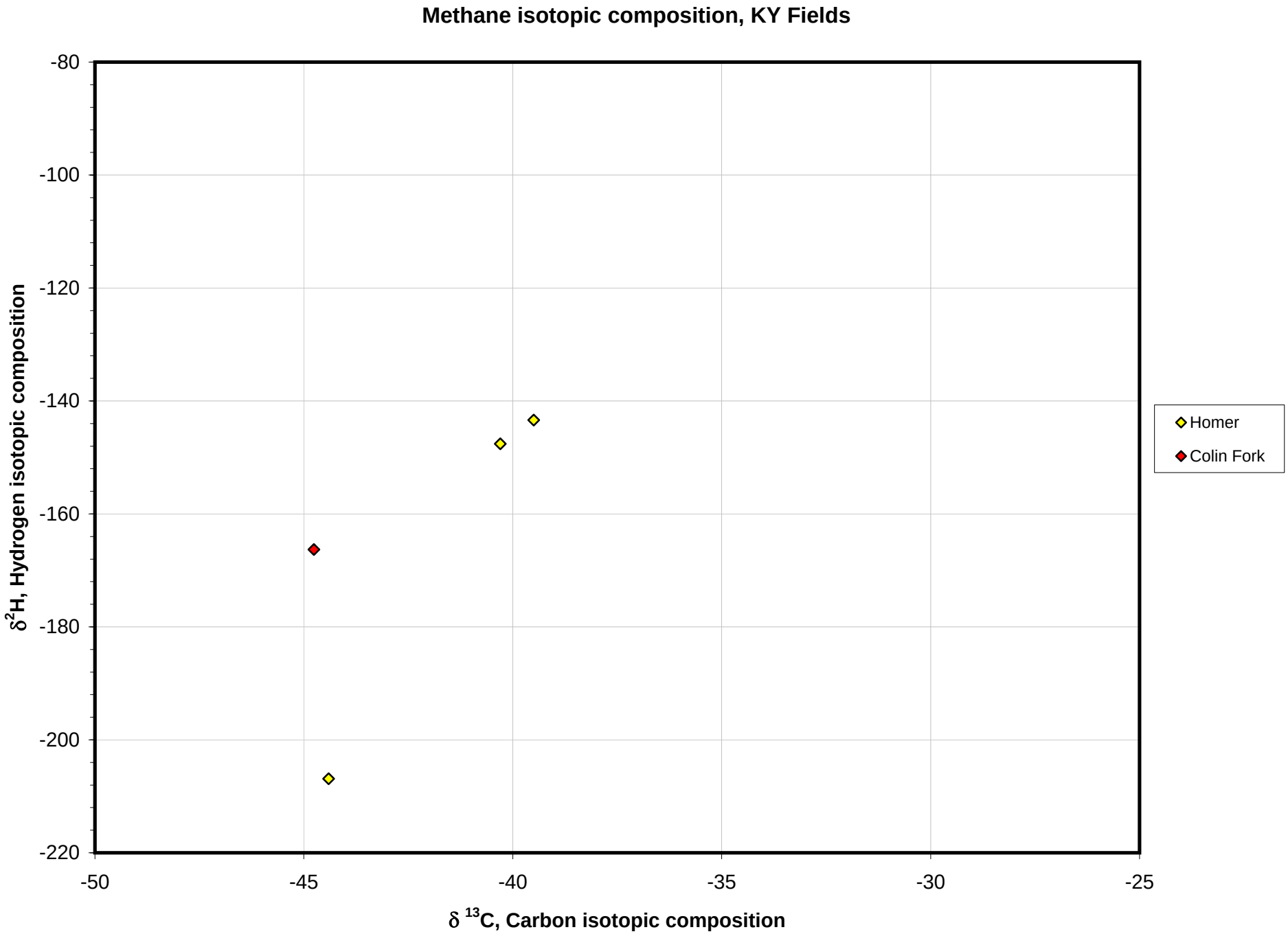

Figure 5-3. Methane isotopic composition of natural gases from Homer and Colin Fork fields, Kentucky.

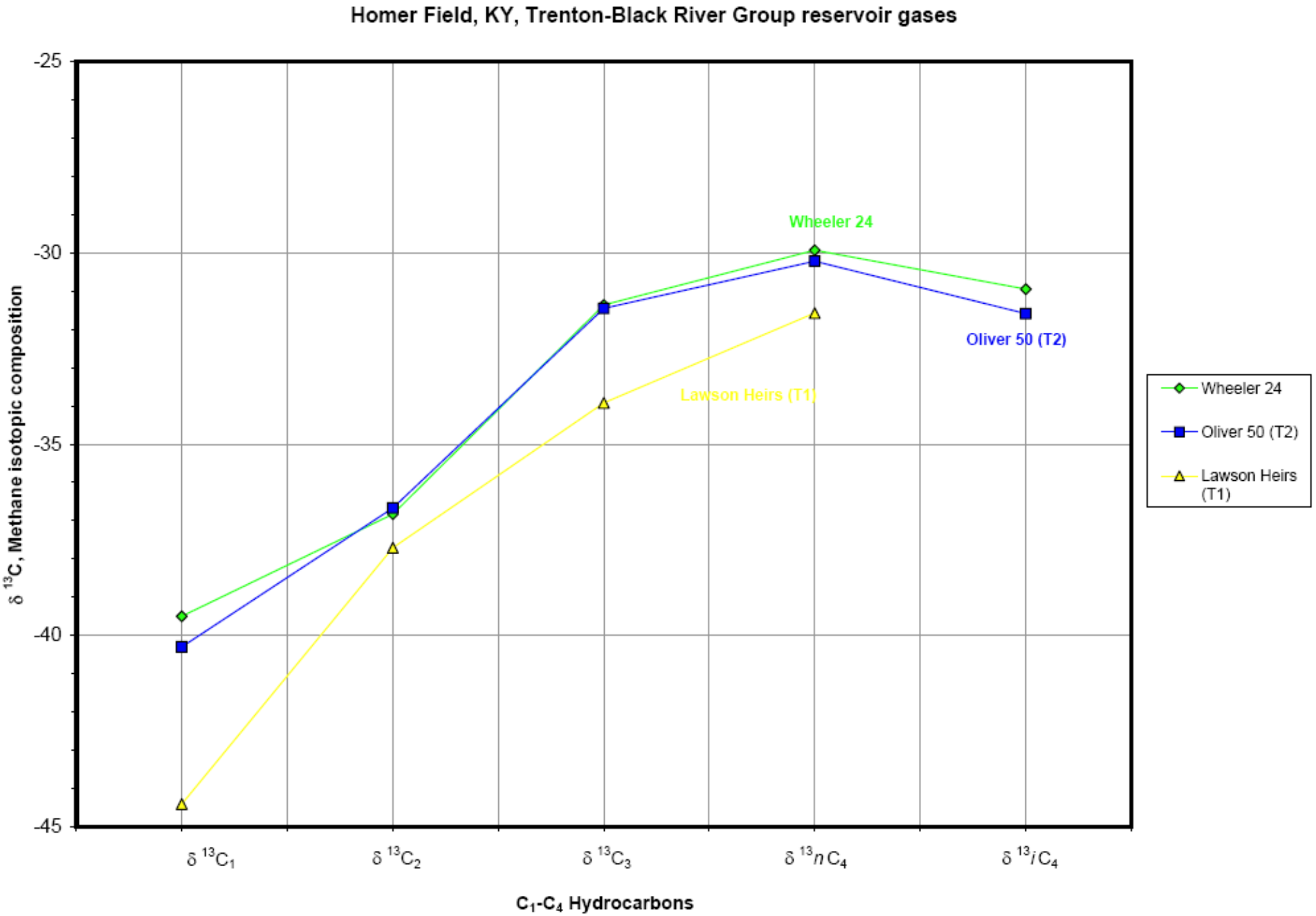

Figure 5-4. Distribution of $\delta^{13}C$ in methane through isobutane in natural gases from Homer and Colin Fork fields, Kentucky.

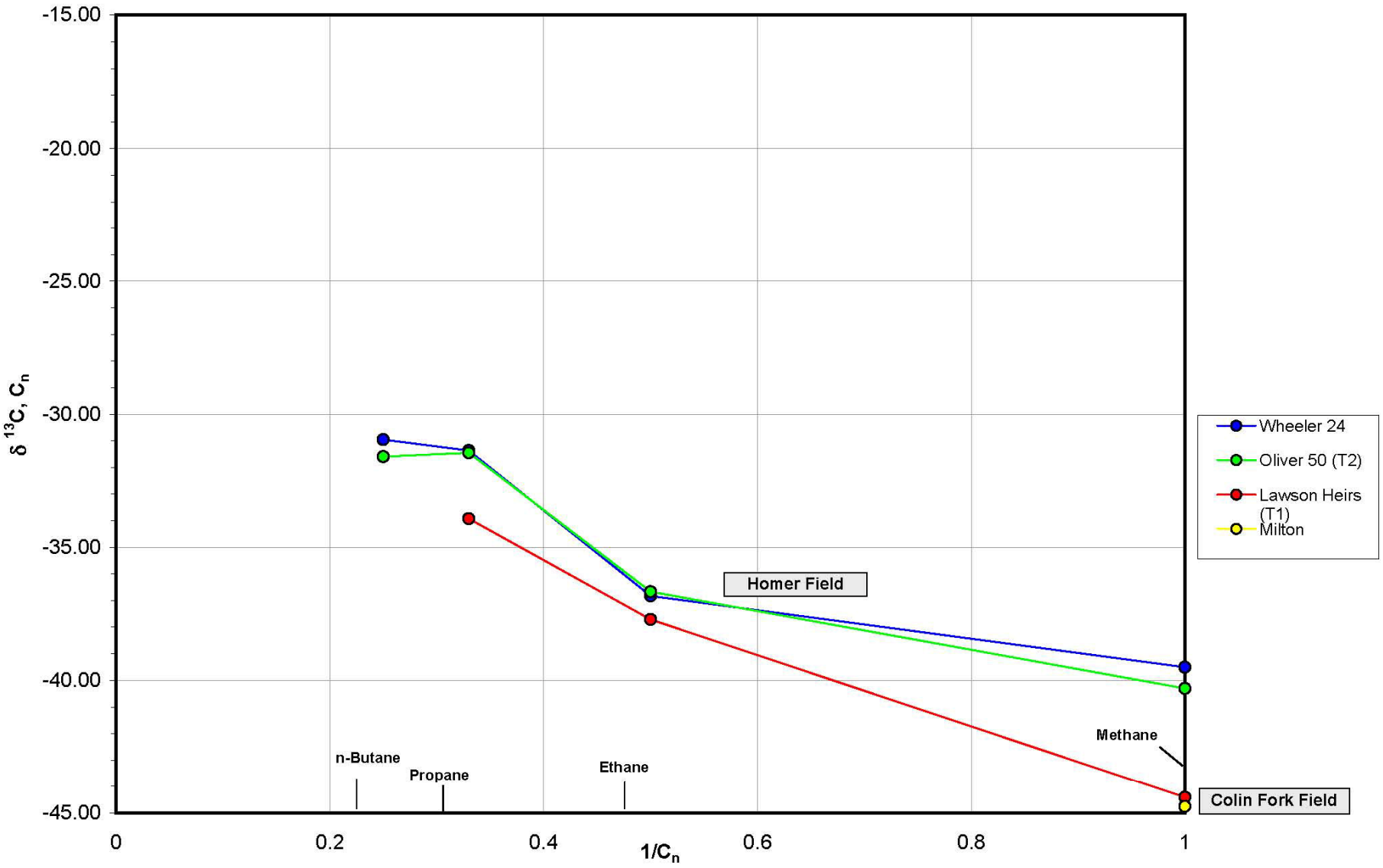

Figure 5-5. Chung plot showing the isotopic composition of individual hydrocarbons in natural gases from Homer and Colin Fork fields, Kentucky as a function of the number of carbon atoms (C_n) in the hydrocarbon (Chung and others, 1988). The kinetics of cracking alkyl side chains from high molecular weight organic matter in the source rock favors breaking ^{12}C-^{12}C bonds resulting in ^{12}C enrichment of the reservoir gases. Consequently, methane is the most ^{13}C-depleted homologue, and higher hydrocarbons exhibit increasingly heavier, or less negative, $\delta^{13}C$ values because of the increasing probability of including ^{13}C atoms in the cracking product.

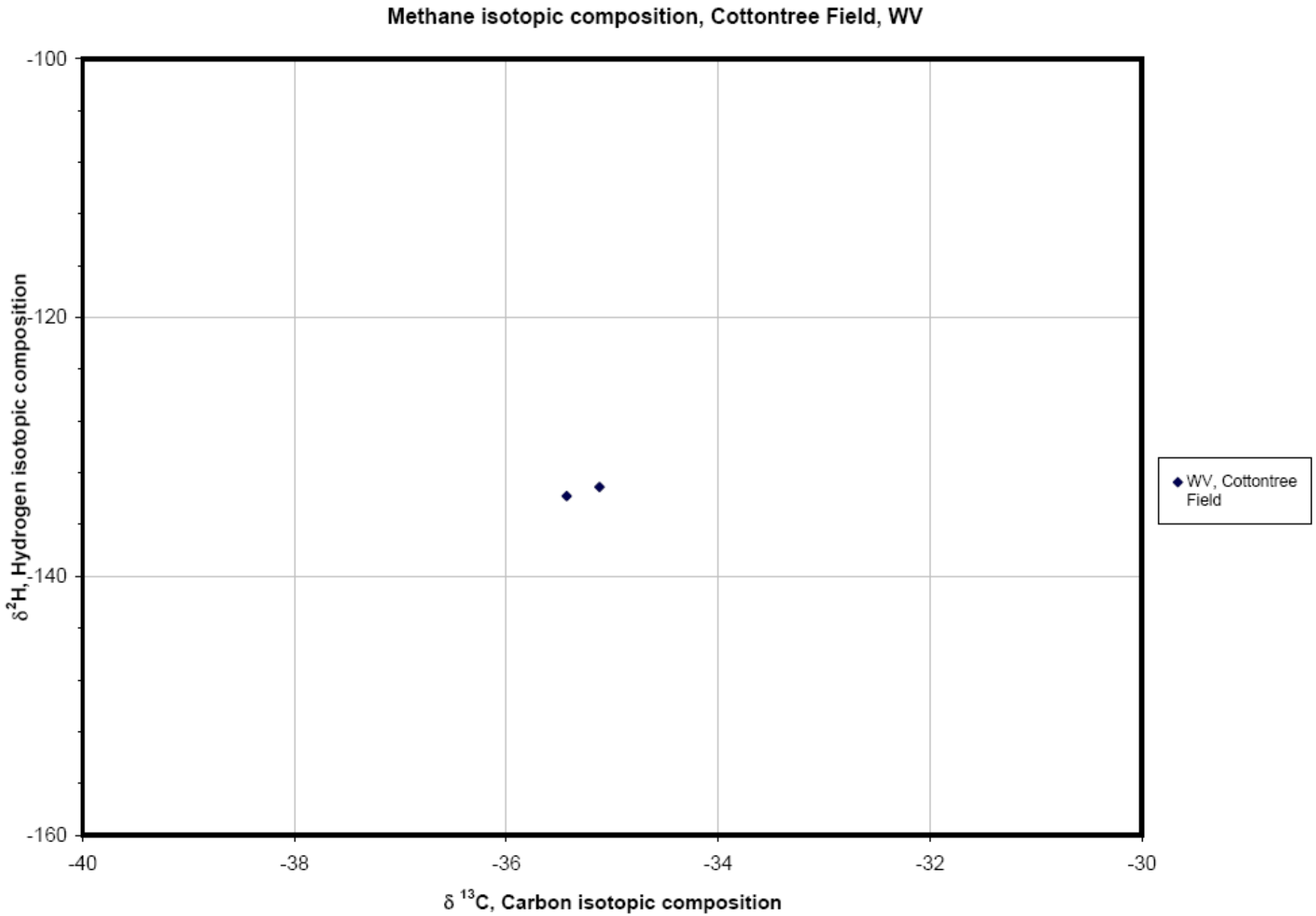

Figure 5-6. Methane isotopic composition of natural gases from Cottontree field, West Virginia.

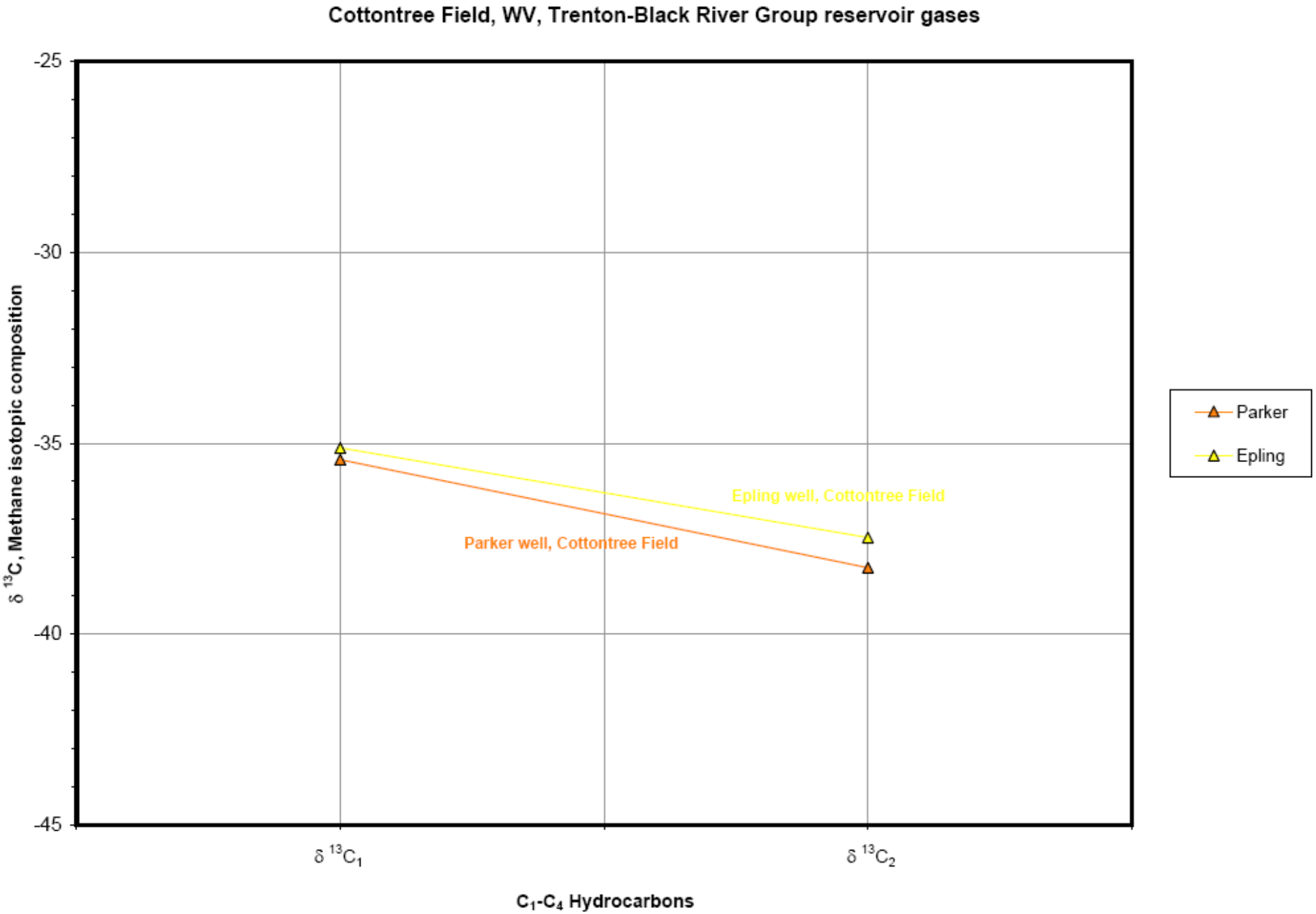

Figure 5-7. Distribution of $\delta^{13}C$ in methane and ethane in natural gases from Cottontree field, West Virginia.

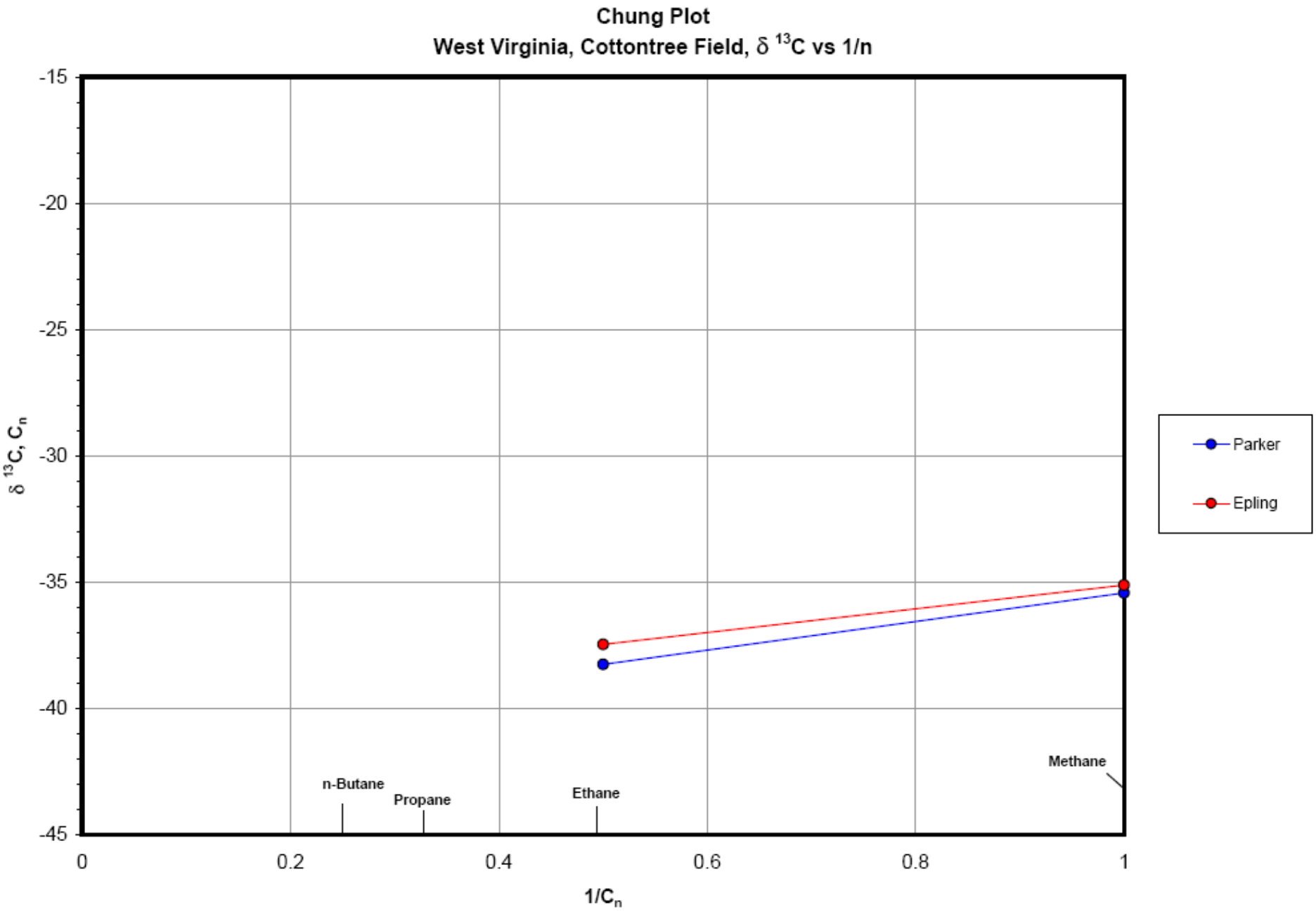

Figure 5-8. Chung plot showing the isotopic composition of individual hydrocarbons in natural gases from Cottontree field, West Virginia.

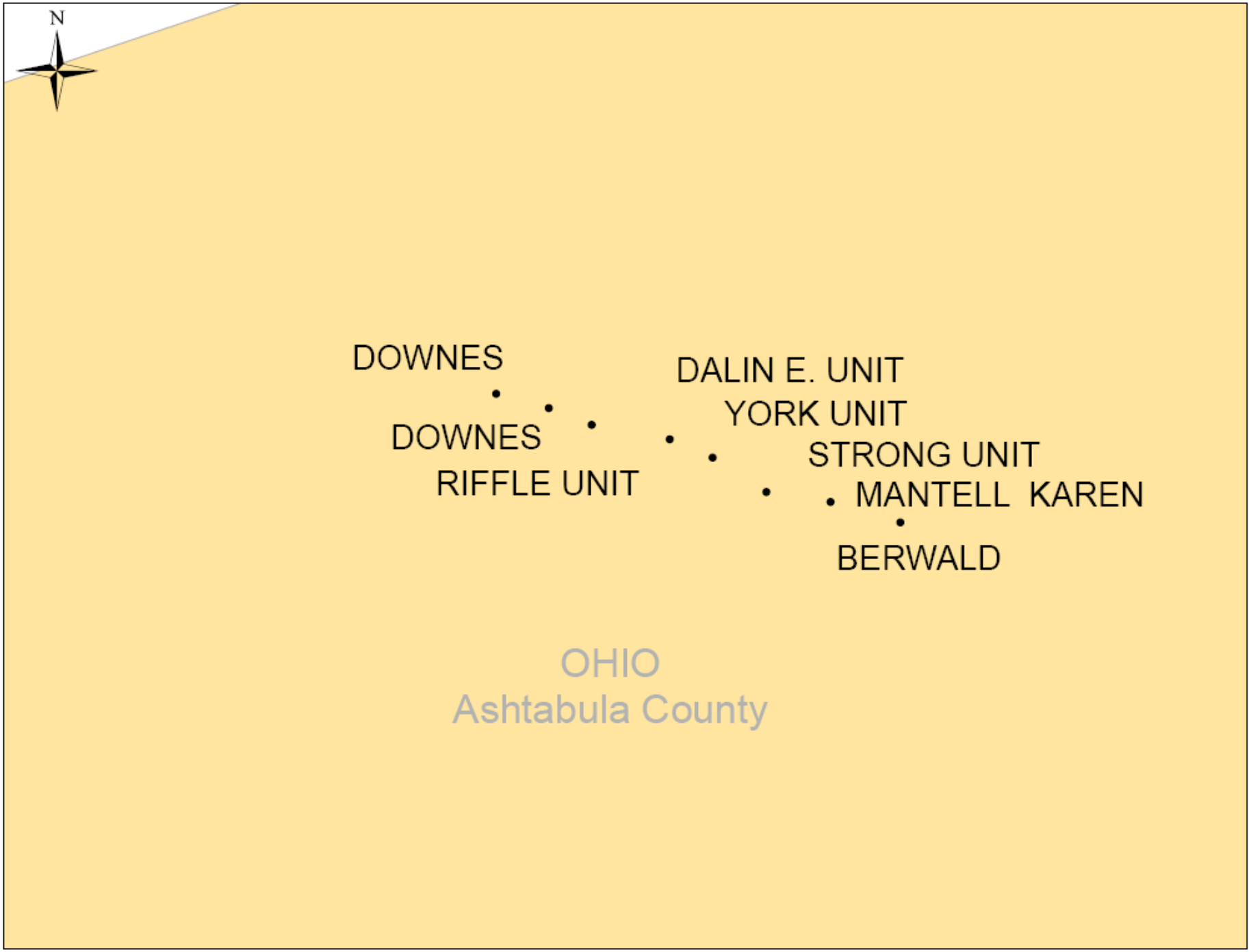

Figure 5-9. Map showing locations of the wells sampled for gas geochemistry in the York field, Ashtabula County, Ohio.

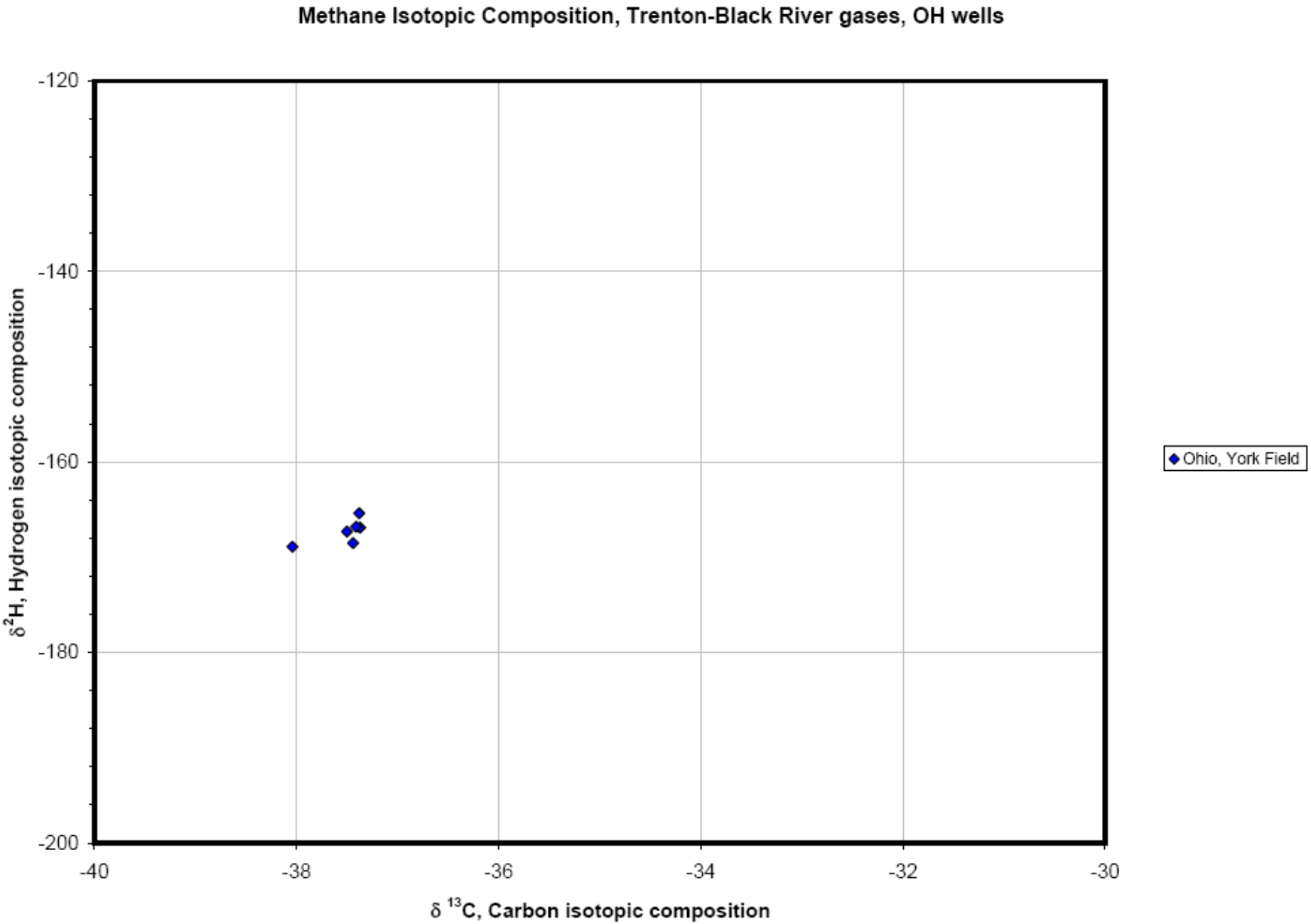

Figure 5-10. Methane isotopic composition of natural gases from York field, Ohio.

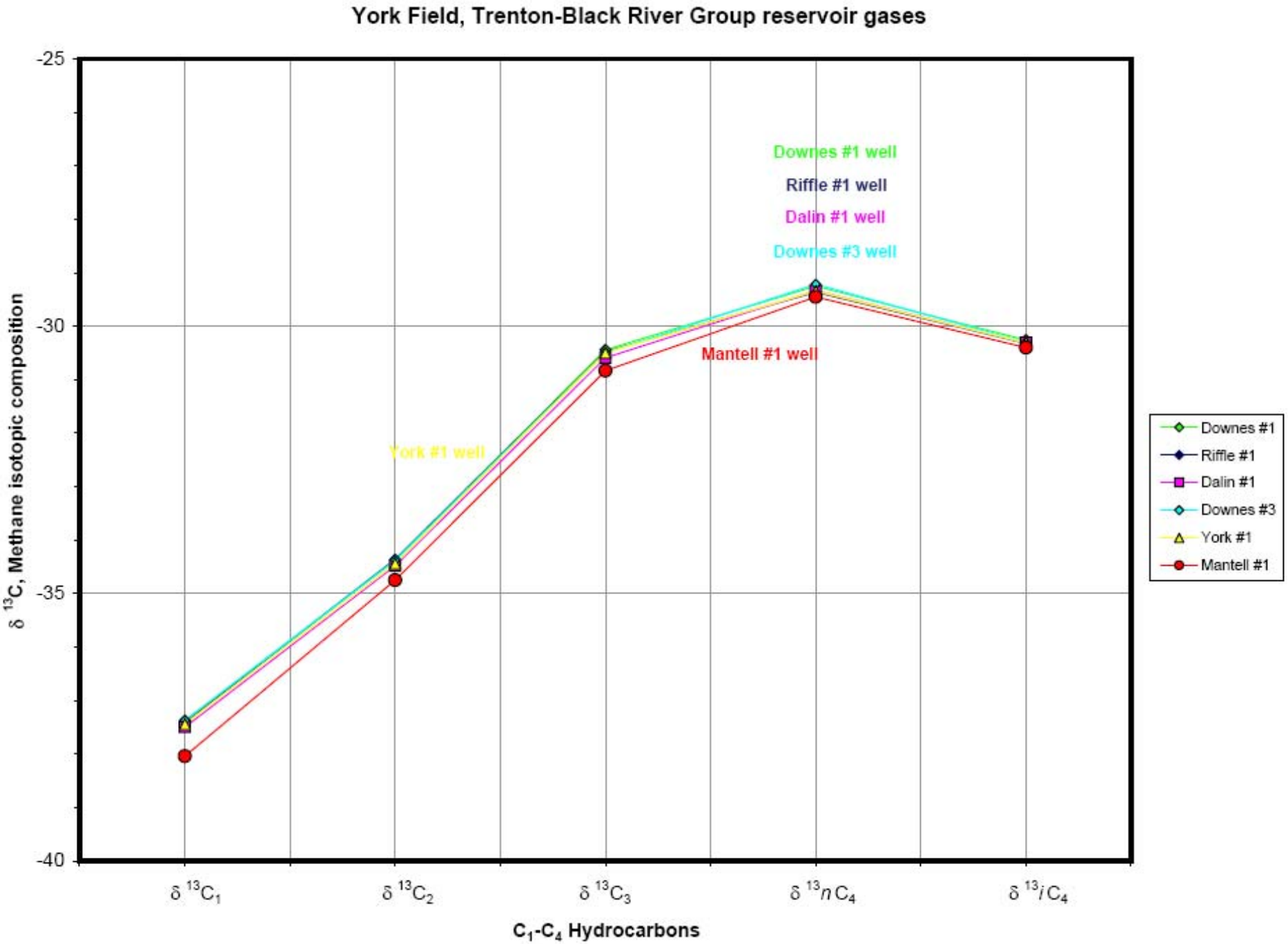

Figure 5-11. Distribution of $\delta^{13}C$ in methane through isobutane in natural gases from York field, Ohio.

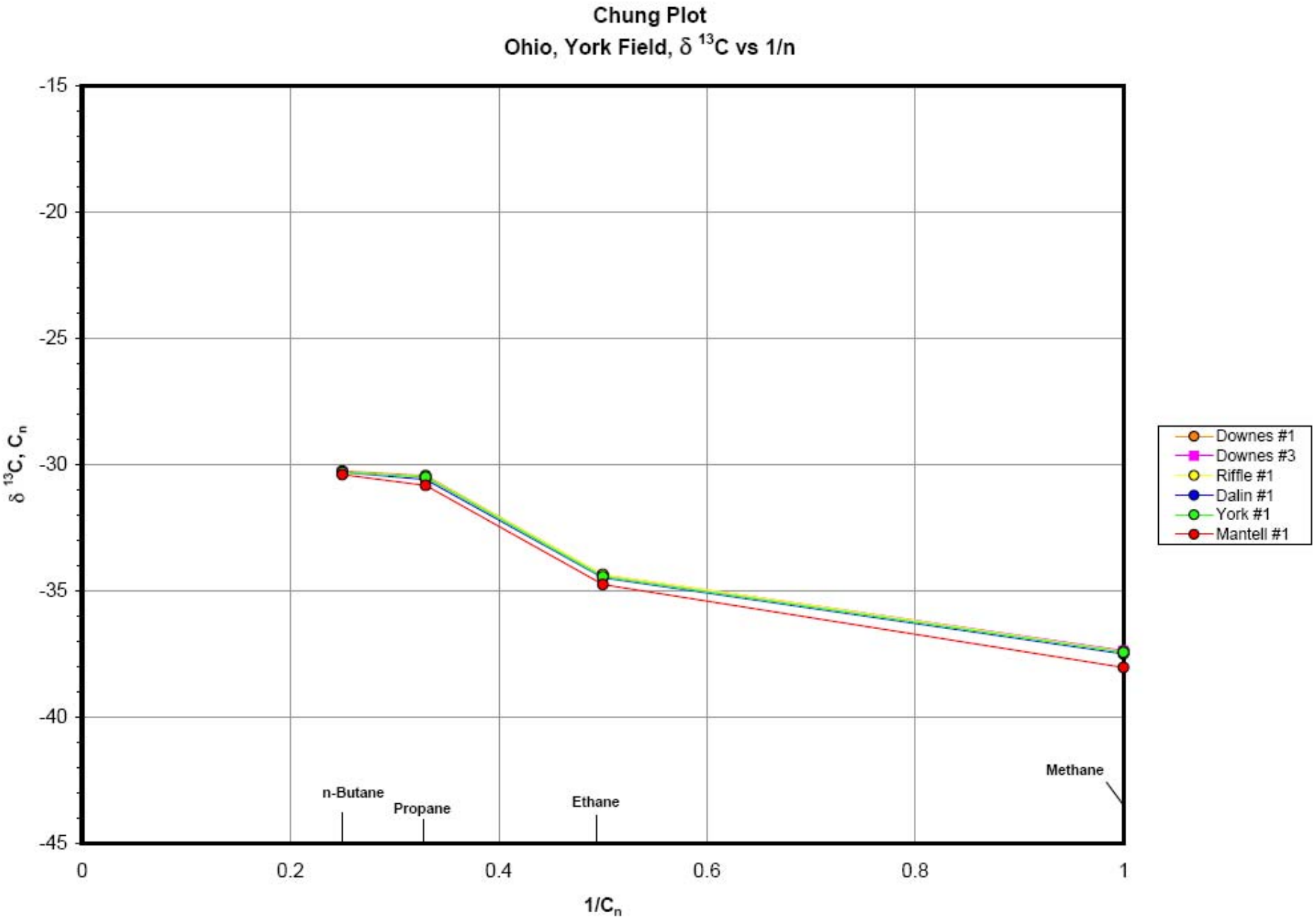

Figure 5-12. Chung plot showing the isotopic composition of individual hydrocarbons in natural gases from York field, Ohio.

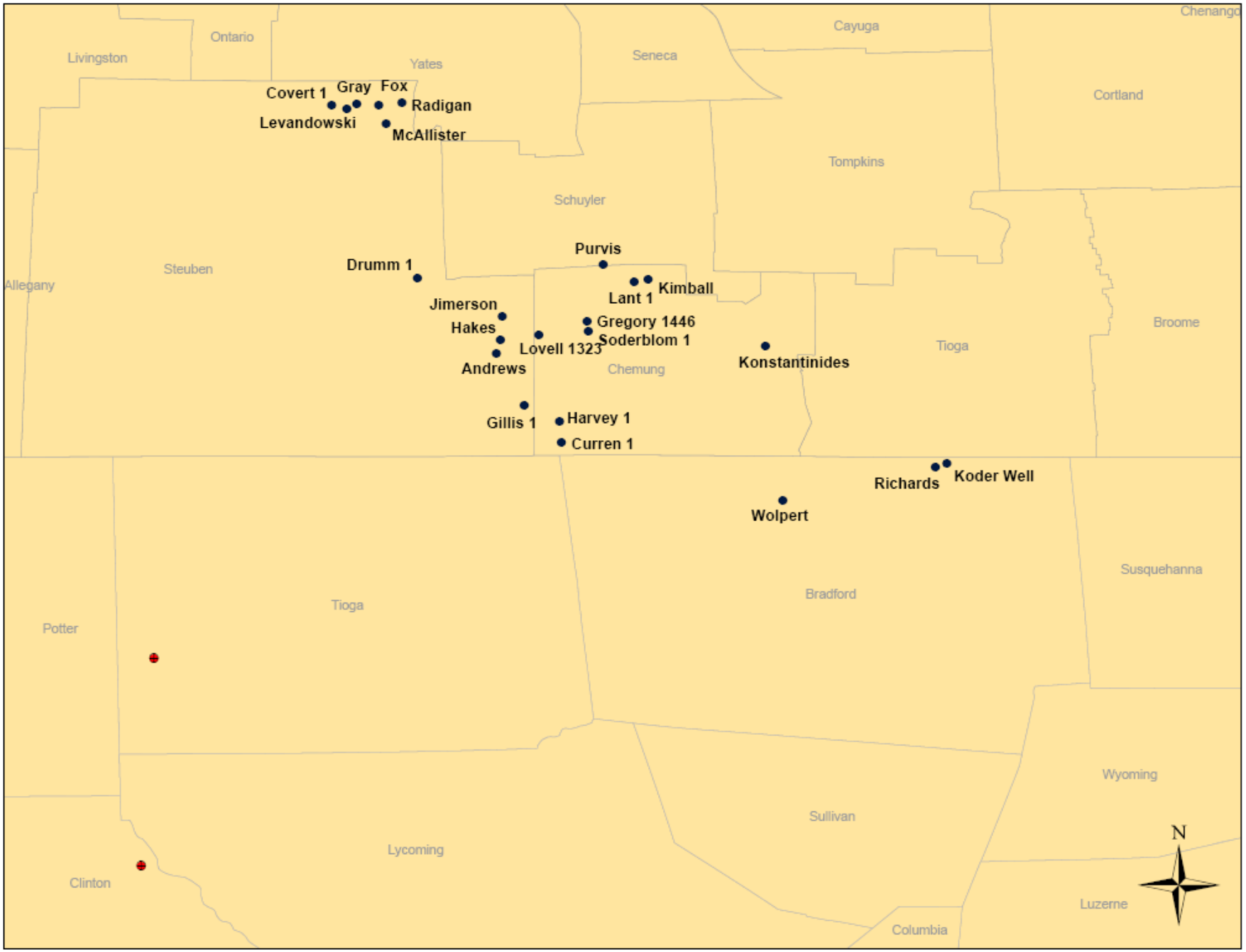

Figure 5-13. Map showing locations of the wells sampled for gas geochemistry in the productive Black River natural gas fields of New York and Pennsylvania. Three of the wells shown were not sampled during this project, but are shown because they are discussed in the text.

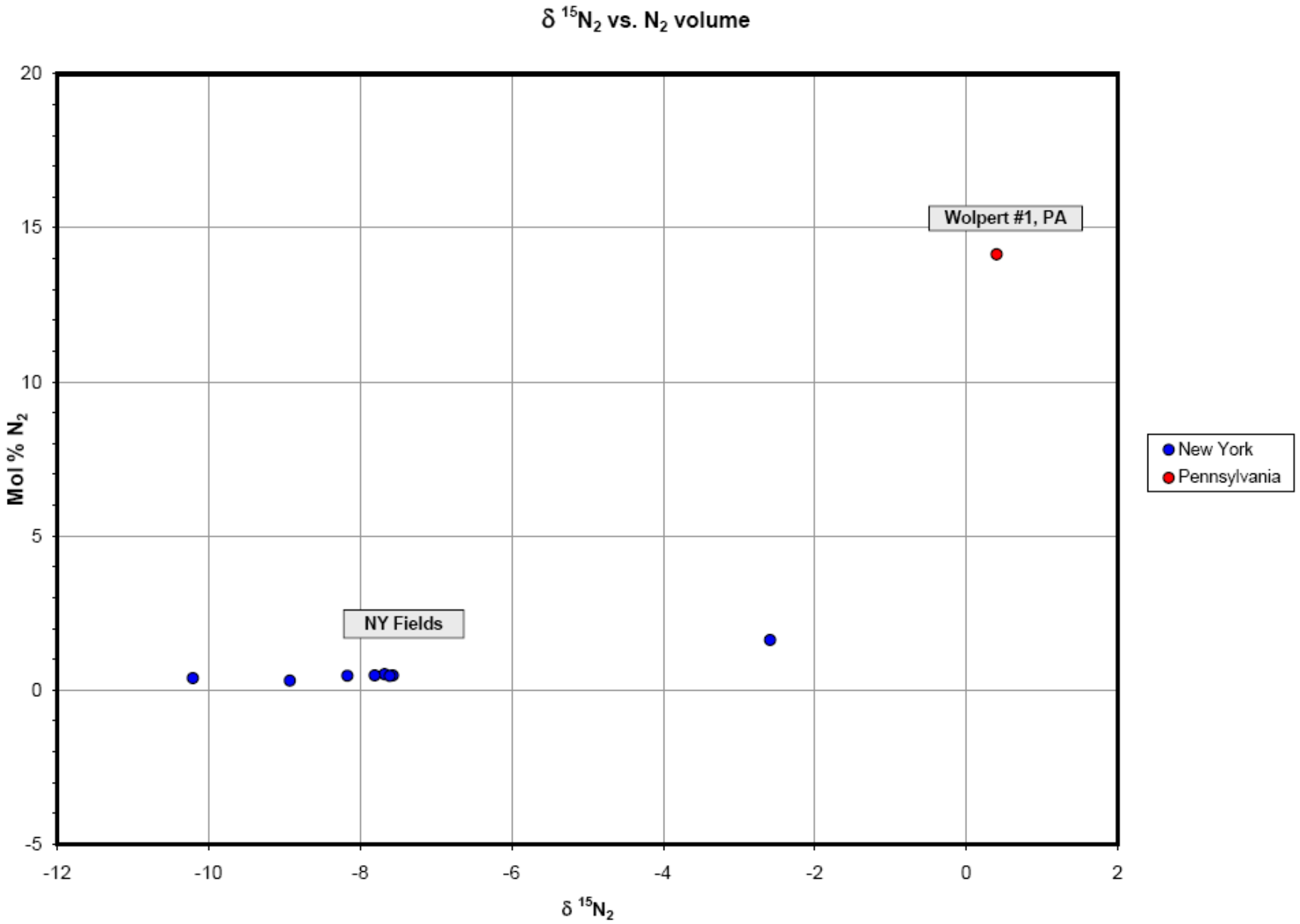

Figure 5-14. $\delta^{15}N$ versus nitrogen concentration in the Black River gases produced in New York and Pennsylvania.

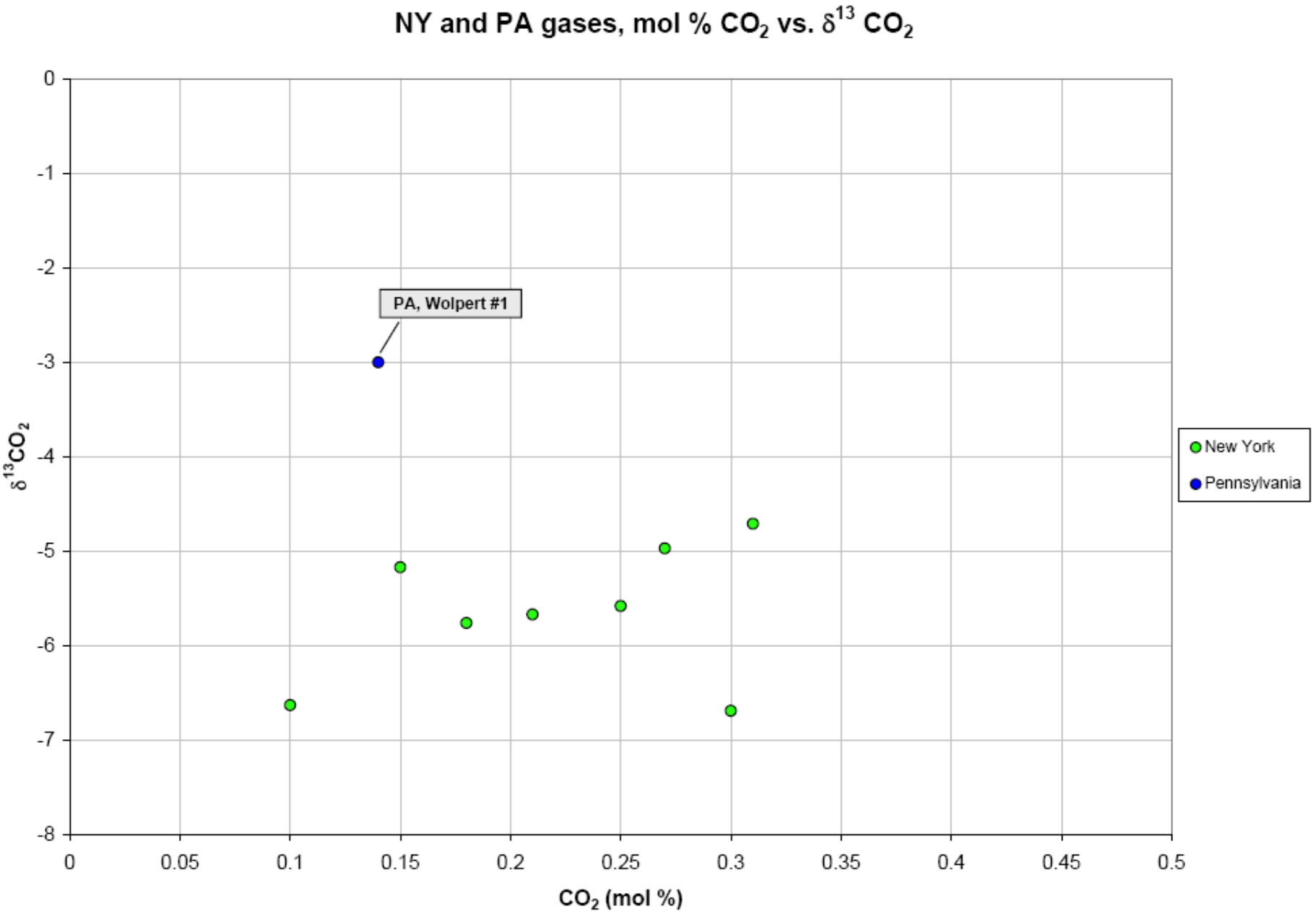

Figure 5-15. $\delta^{13}CO_2$ versus carbon dioxide concentration in the Black River gases produced in New York and Pennsylvania.

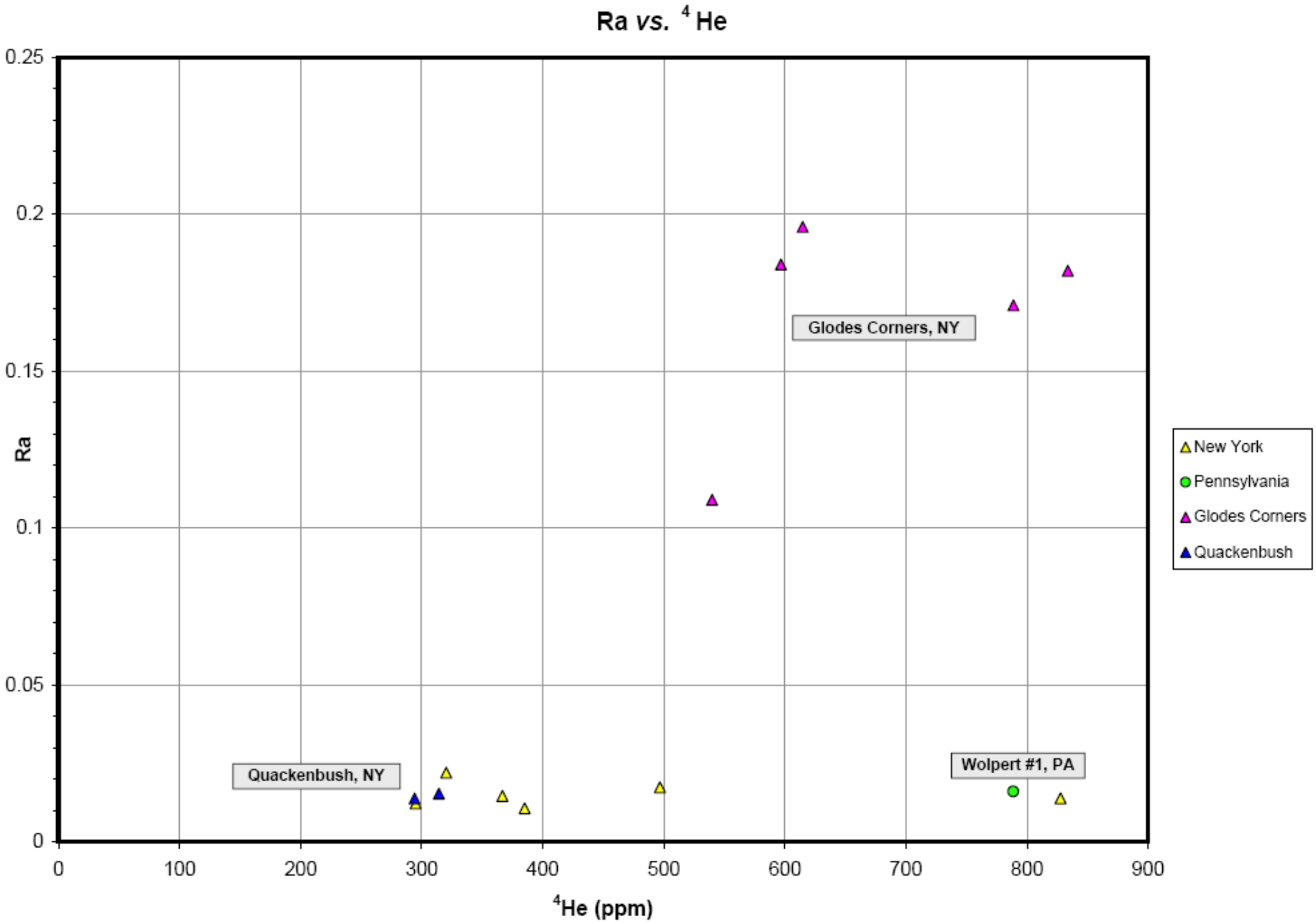

Figure 5-16. *Ra* versus ^{4}He in the Black River gases produced in New York and Pennsylvania.

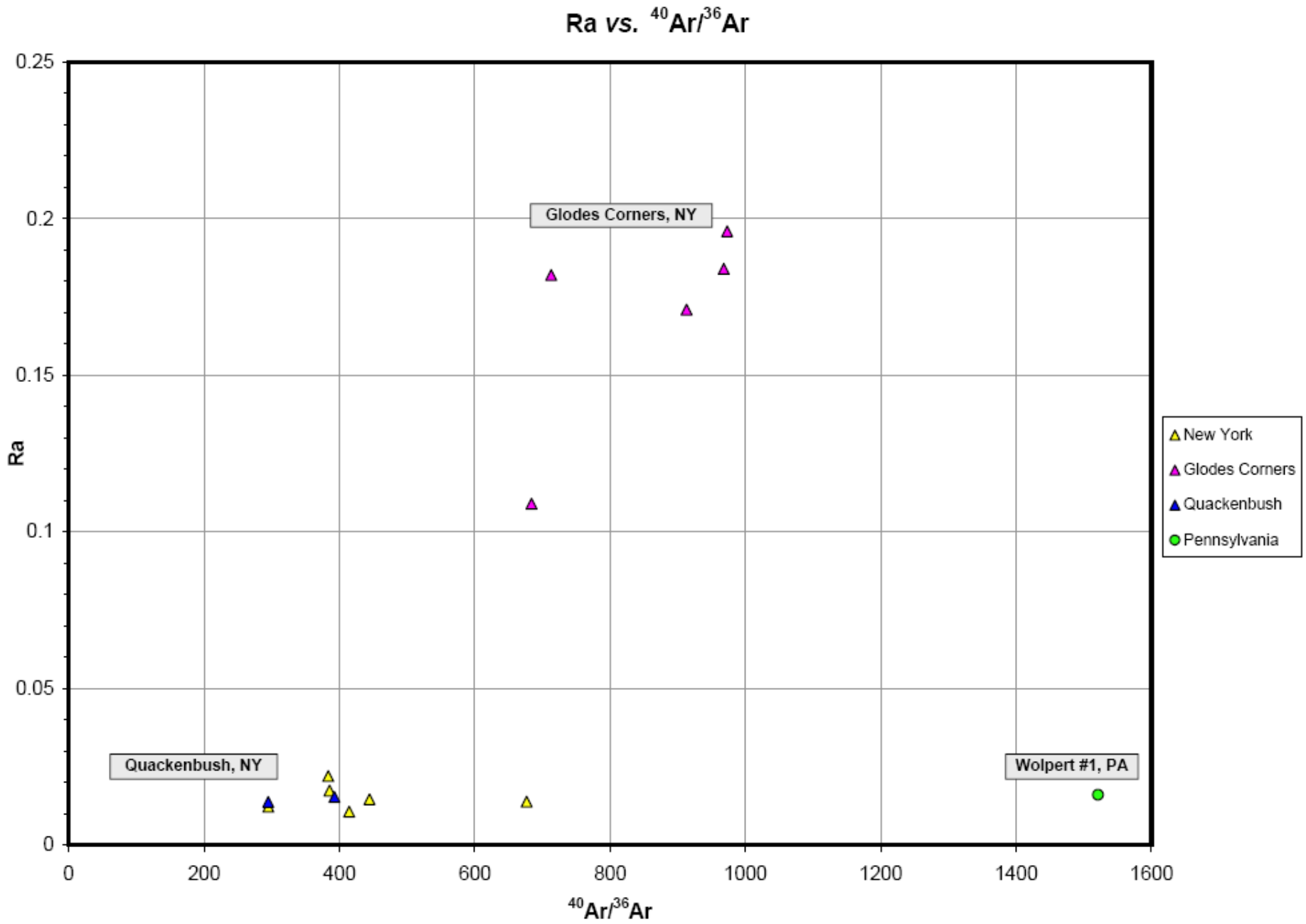

Figure 5-17. *Ra* versus $^{40}Ar/^{36}Ar$ in the Black River gases produced in New York and Pennsylvania.

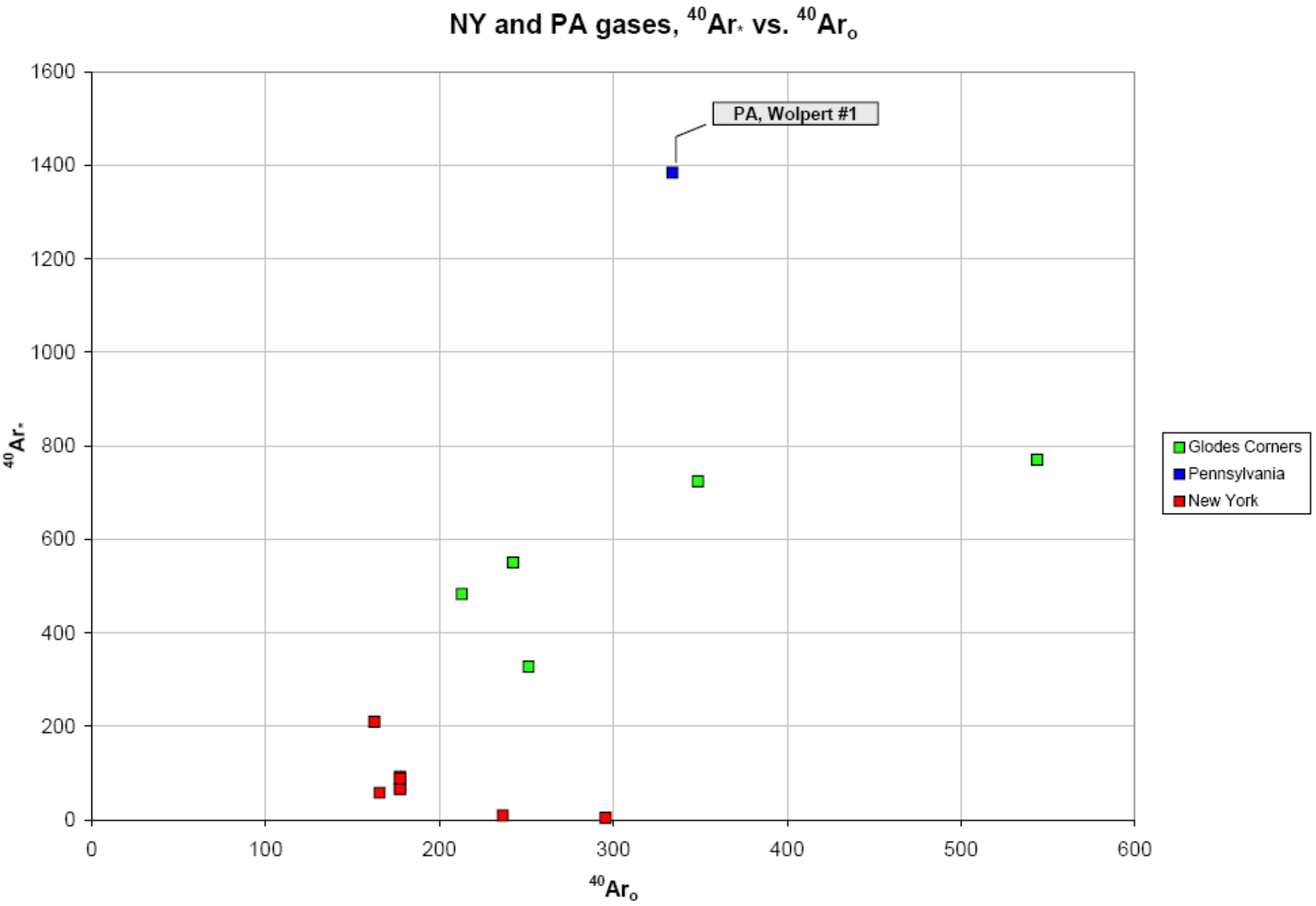

Figure 5-18. *Ra* versus $^{40}Ar^*$ versus $^{40}Ar_o$ in the Black River gases produced in New York and Pennsylvania.

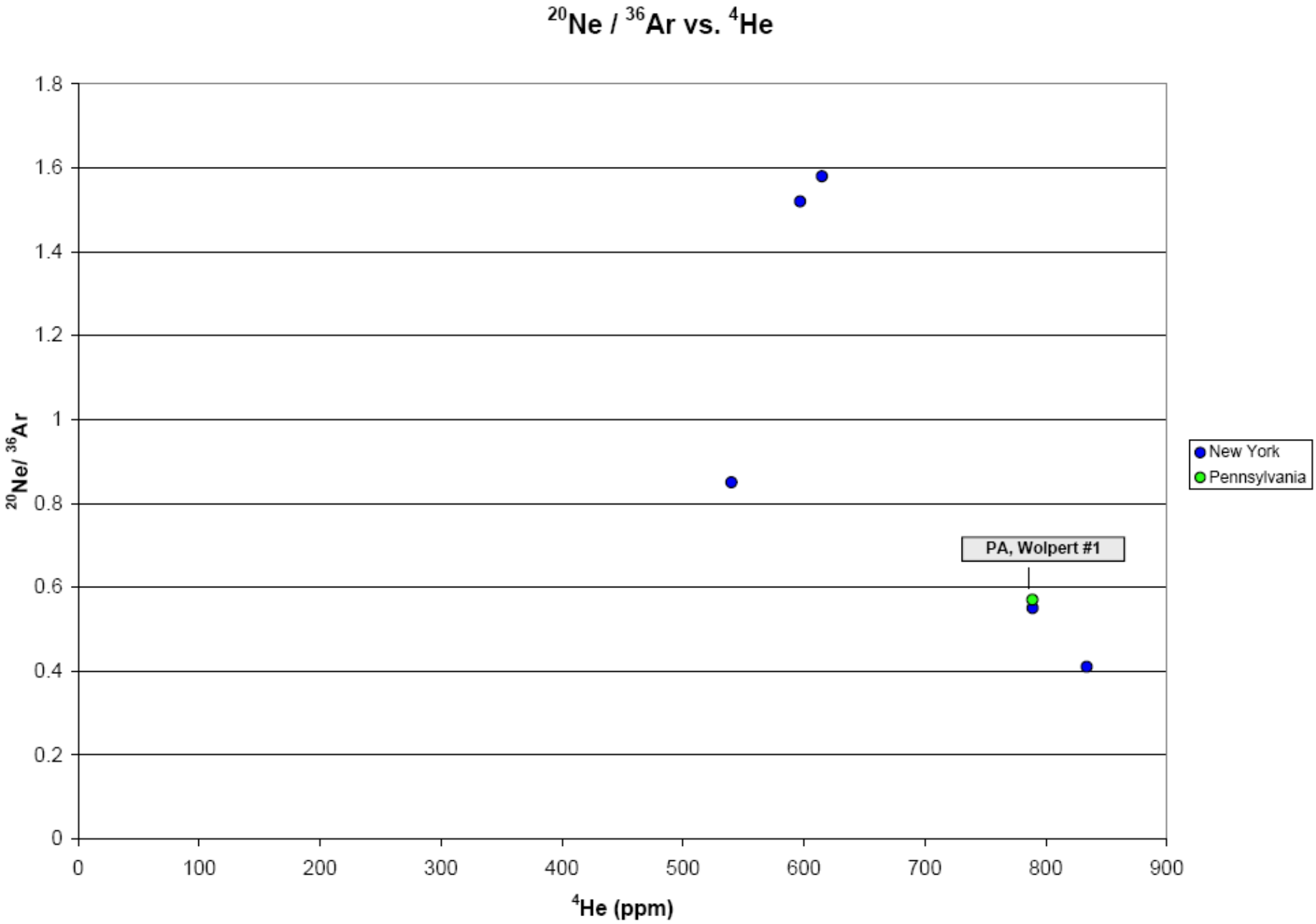

Figure 5-19. $^{20}Ne/^{36}Ar$ versus ^{4}He in the Black River gases produced in New York and Pennsylvania.



Figure 5-20. Bitumen coating hydrothermal dolomites in the Black River reservoir rocks on New York. A) Backscattered SEM photomicrograph of bitumen coating a crystal of delafossite, a copper-iron oxide, Gray #1 well, Steuben County, NY. 7799.9 ft

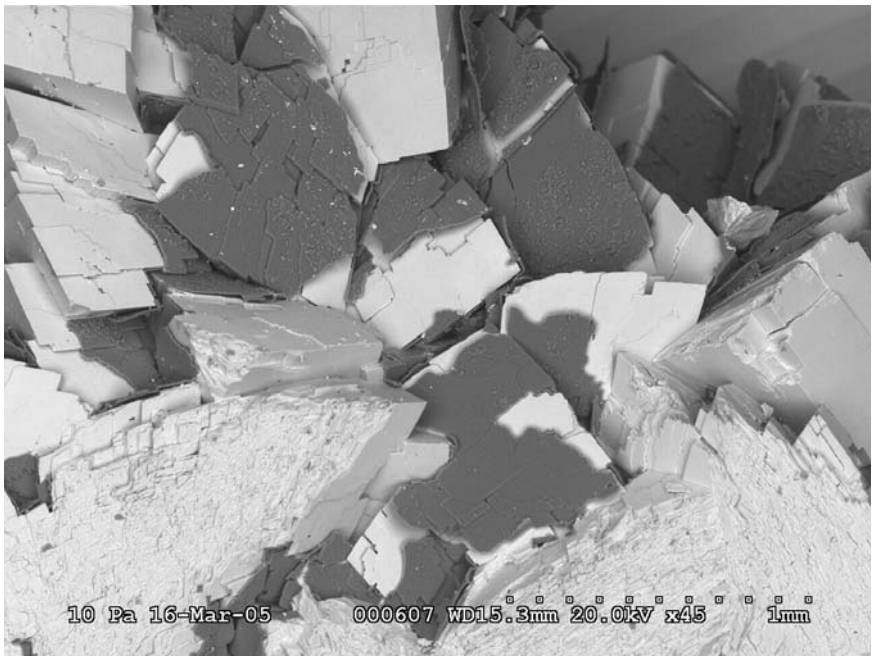

5-20B) Backscattered SEM photomicrograph of bitumen coatings on nonplanar-c hydrothermal (saddle) dolomite. Whitman #1 well, Chemung County, New York. 9531 ft.

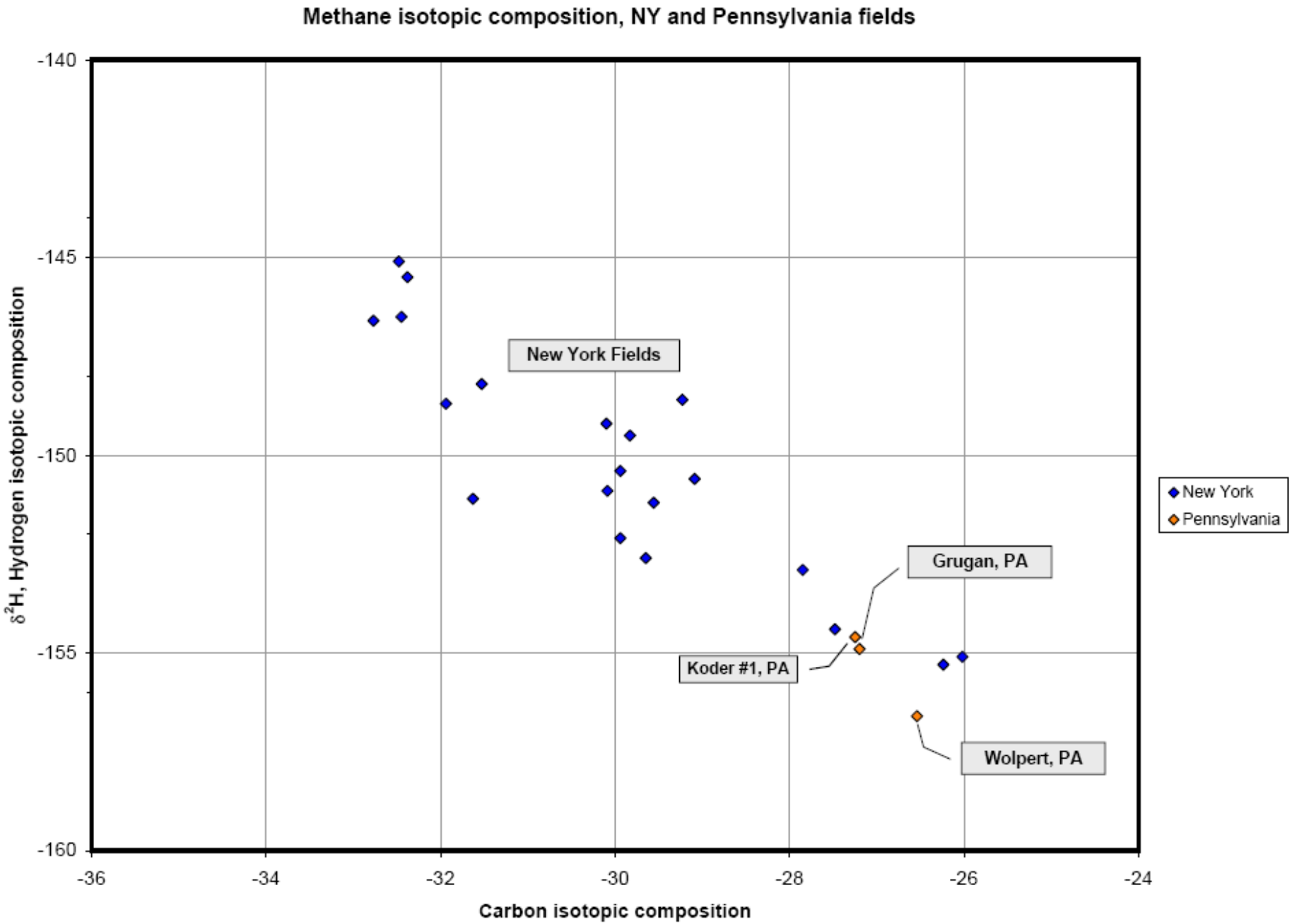

Figure 5-21. Methane isotopic composition of Black River natural gases from New York and Pennsylvania fields. The Grugan field gas sample is shown for comparison on this and most subsequent figures. See text for discussion.

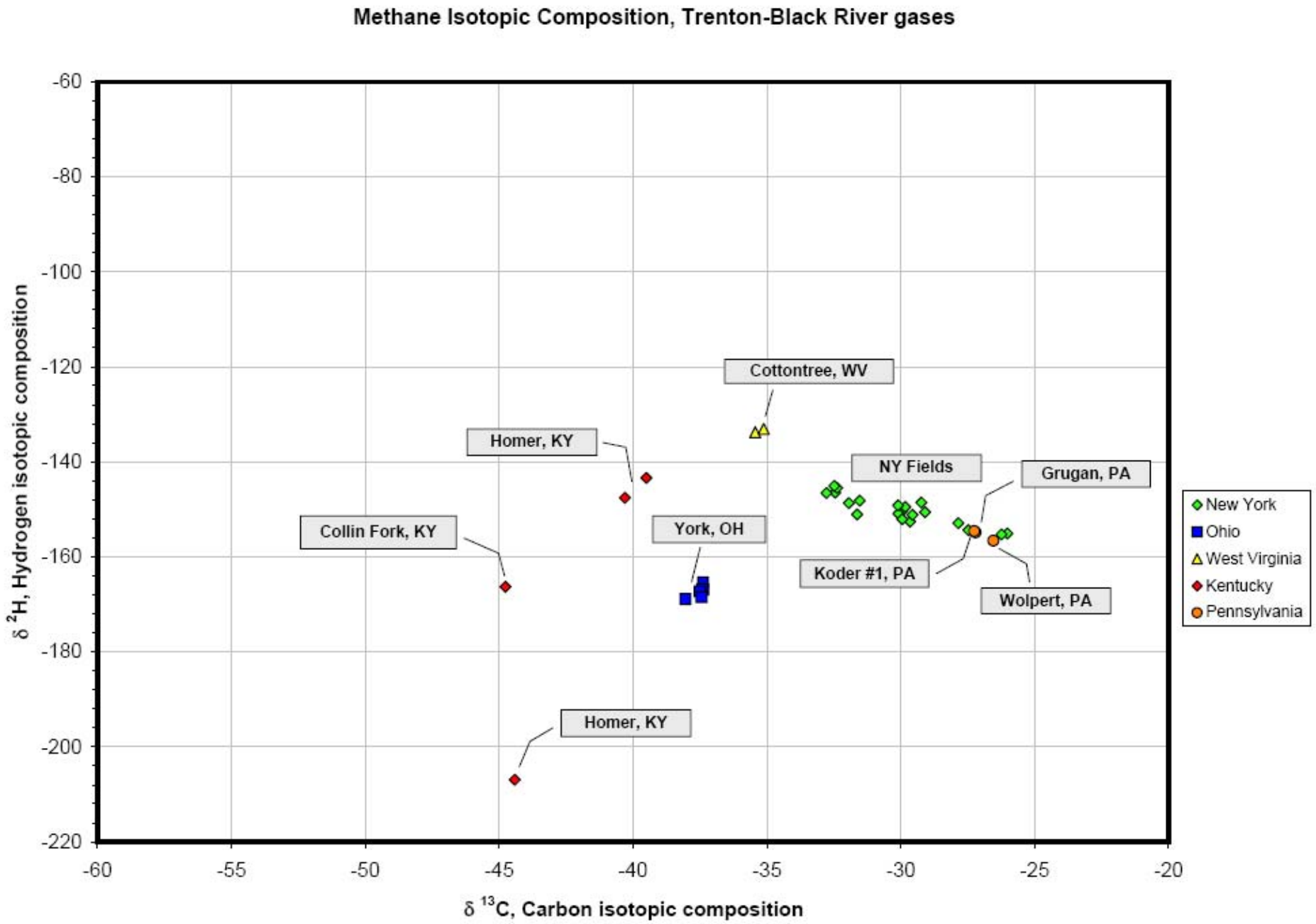

Figure 5-22. Methane isotopic composition of all Trenton and Black River natural gases in the Appalachian basin samples and analyzed for this report.

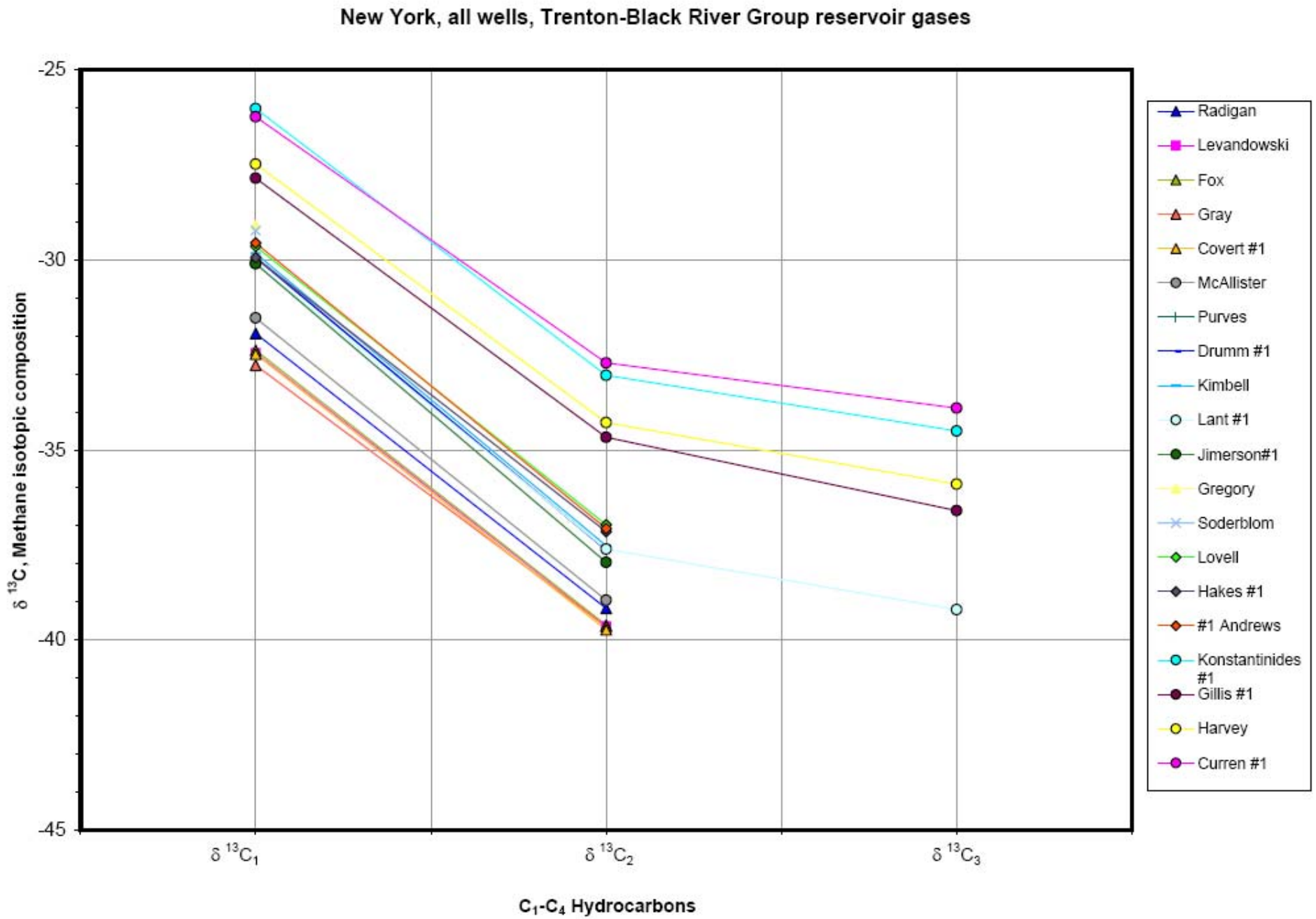

Figure 5-23. Distribution of $\delta^{13}C$ in methane through propane in natural gases from the New York Black River fields.

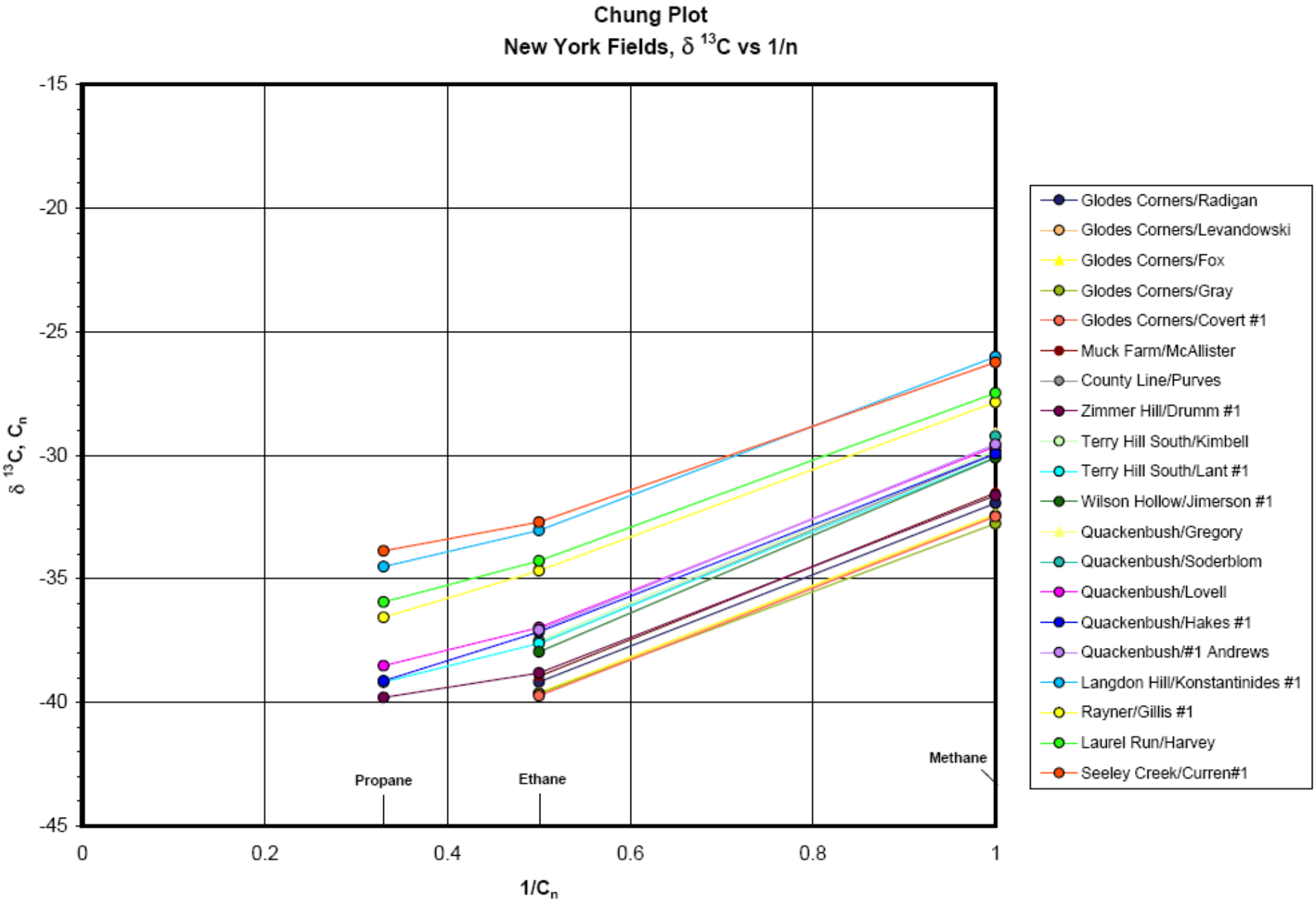

Figure 5-24. Chung plot showing the isotopic composition of individual hydrocarbons in natural gases from the New York Black River fields.

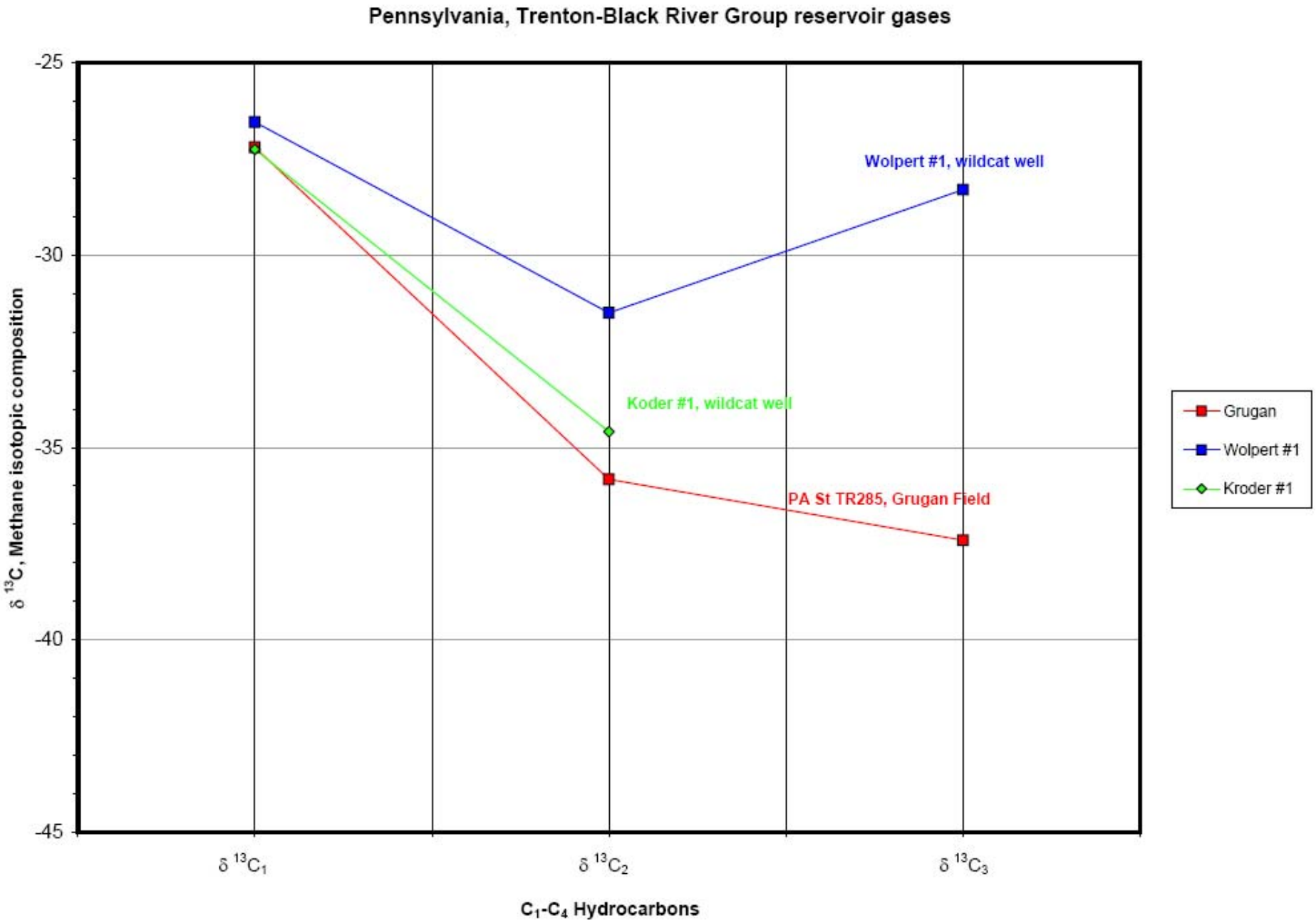

Figure 5-25. Distribution of $\delta^{13}C$ in methane through propane in natural gases from the Pennsylvania Black River fields.

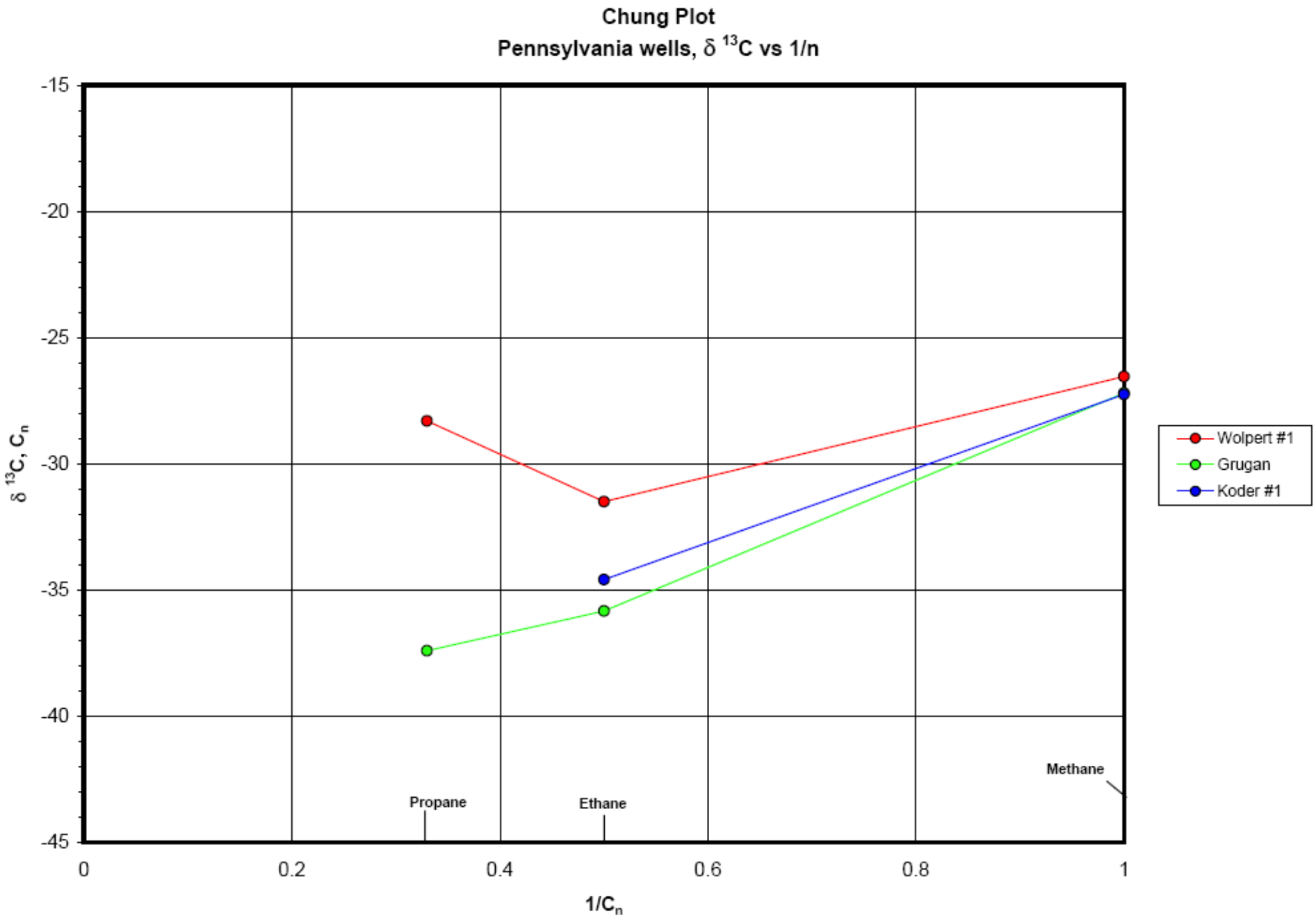

Figure 5-26. Chung plot showing the isotopic composition of individual hydrocarbons in natural gases from the Pennsylvania Black River fields.

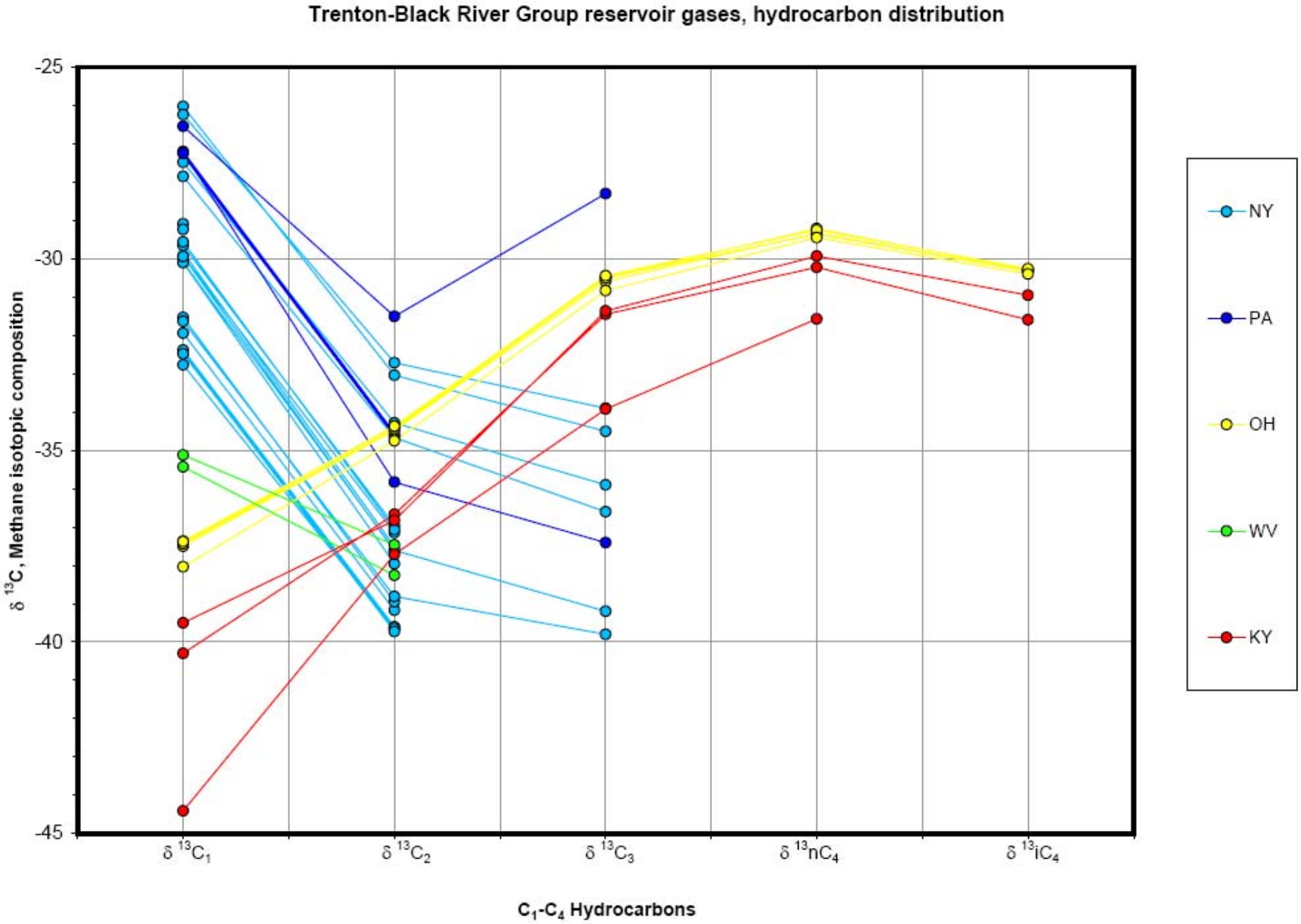

Figure 5-27. Plot of $\delta^{13}C$ values of individual hydrocarbon gases (n-alkanes, C_1 through iC_4) against carbon number for all Trenton/Black River gases sampled and analyzed during this study. All of the gases from Kentucky display a normal carbon isotope distribution that is characteristic of thermogenic natural gases. All of the gases from New York, Pennsylvania, and West Virginia how carbon isotopic reversals (Shultz-Flory distributions).

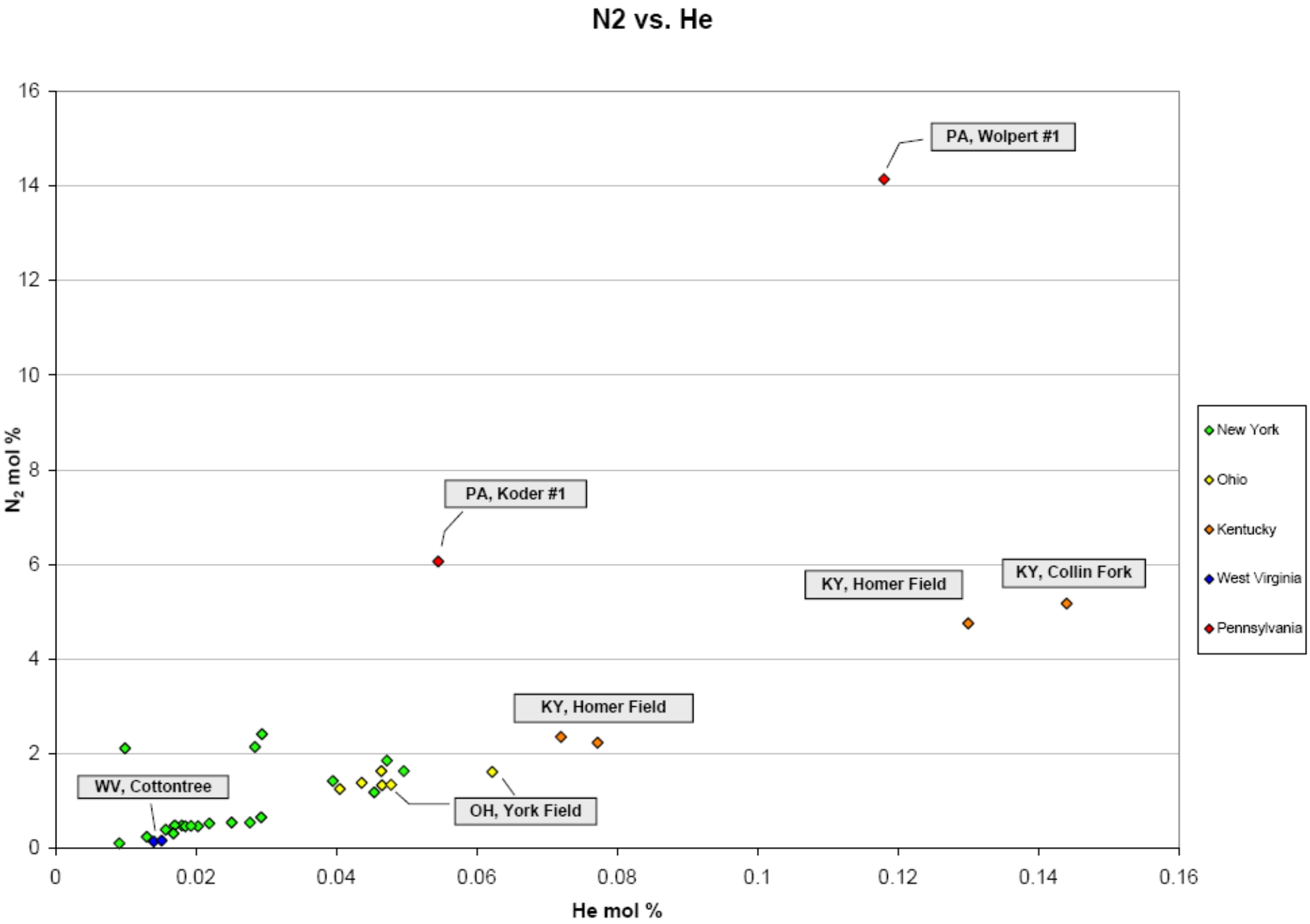

Figure 28A. Nitrogen concentration versus helium concentration in all Trenton/Black River natural gases sampled and analyzed for this study. N_2 versus He plot with field locations of the gases noted.

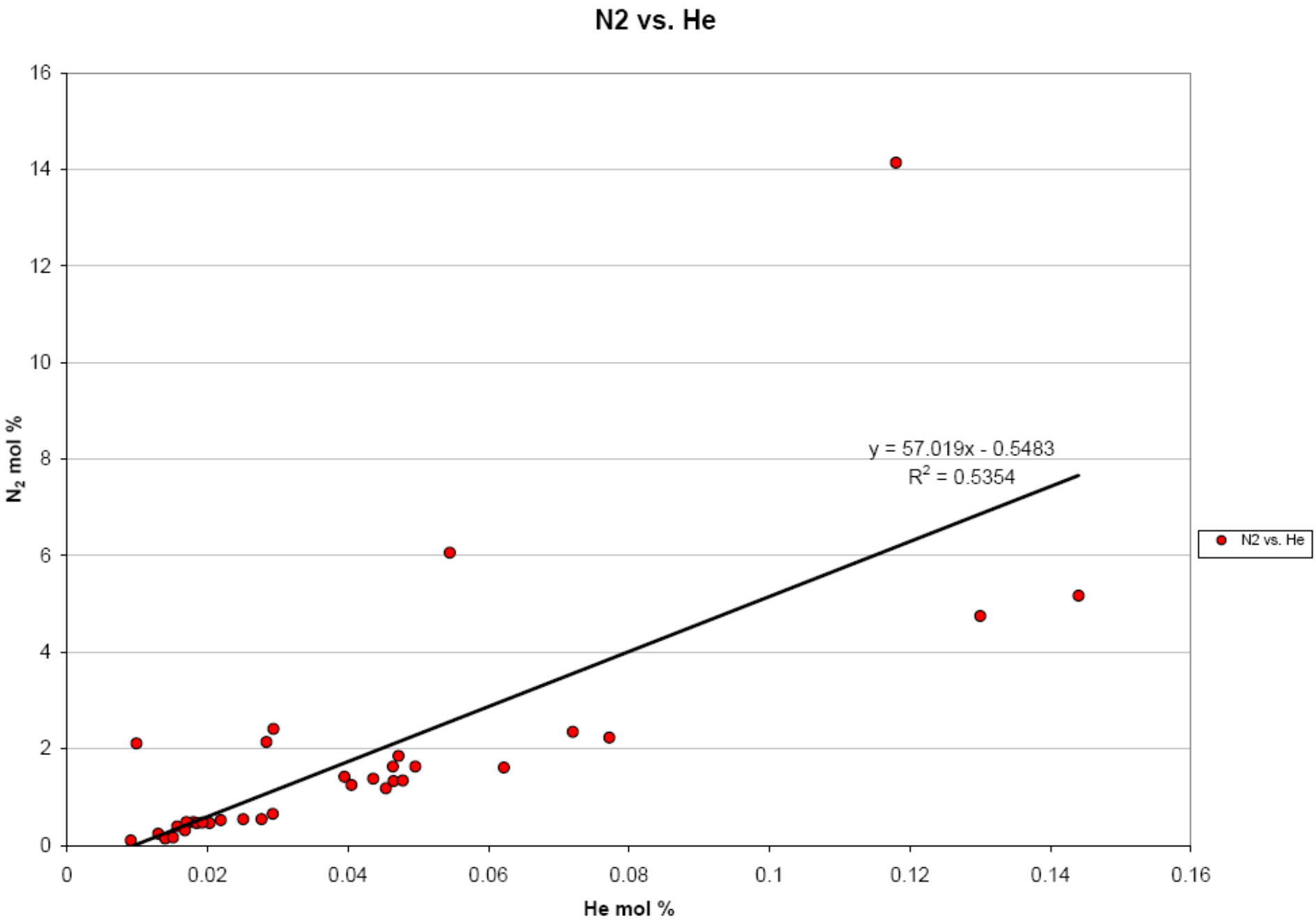

Figure 28B. Nitrogen concentration versus helium concentration in all Trenton/Black River natural gases sampled and analyzed for this study. Same plot with best-fit line calculated from linear regression showing moderate correlation between helium and nitrogen in the gases.

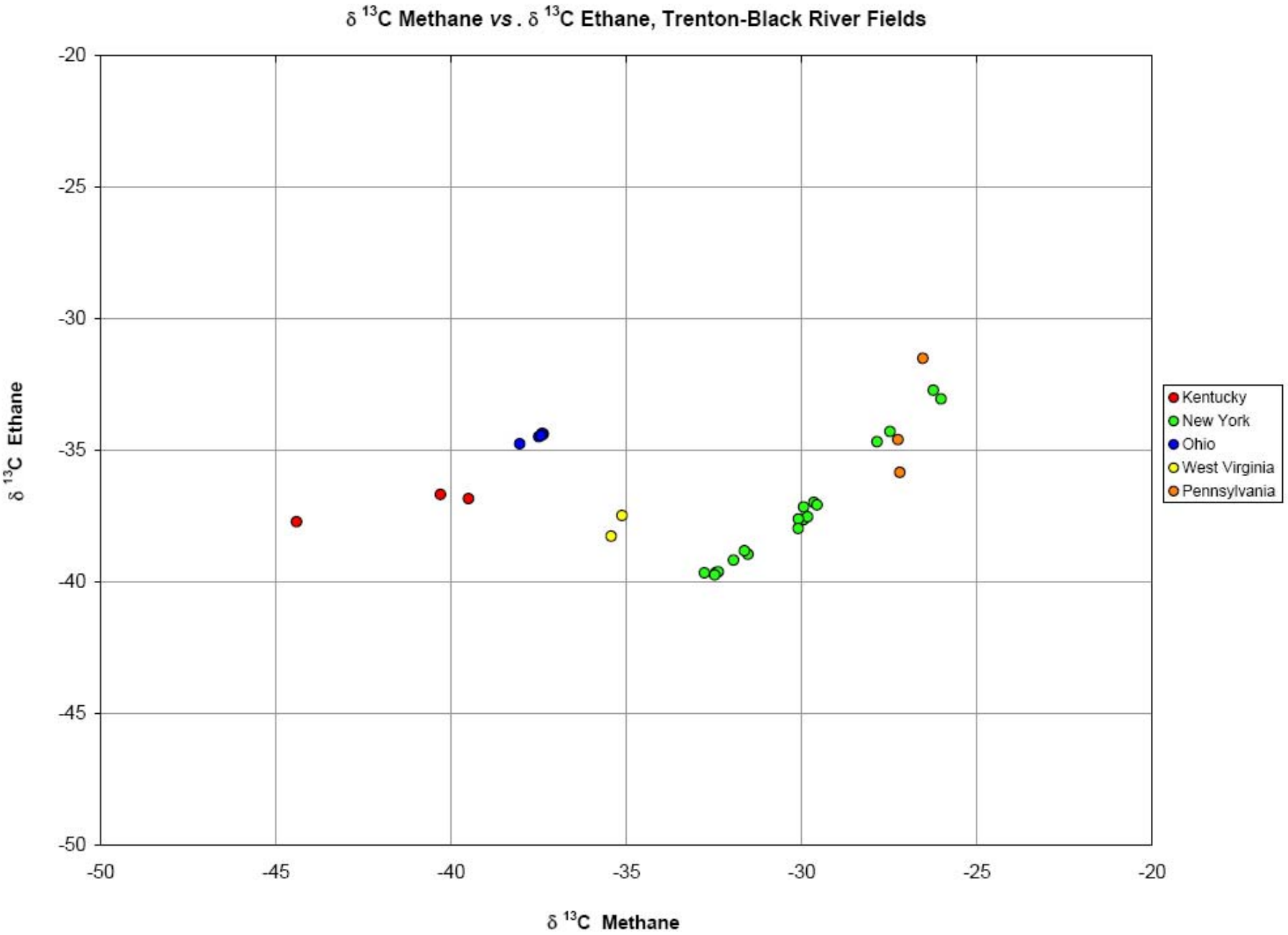

Figure 5-29. $\delta^{13}C$ of methane versus $\delta^{13}C$ of ethane for all Trenton/Black River natural gases sampled and analyzed during this study.

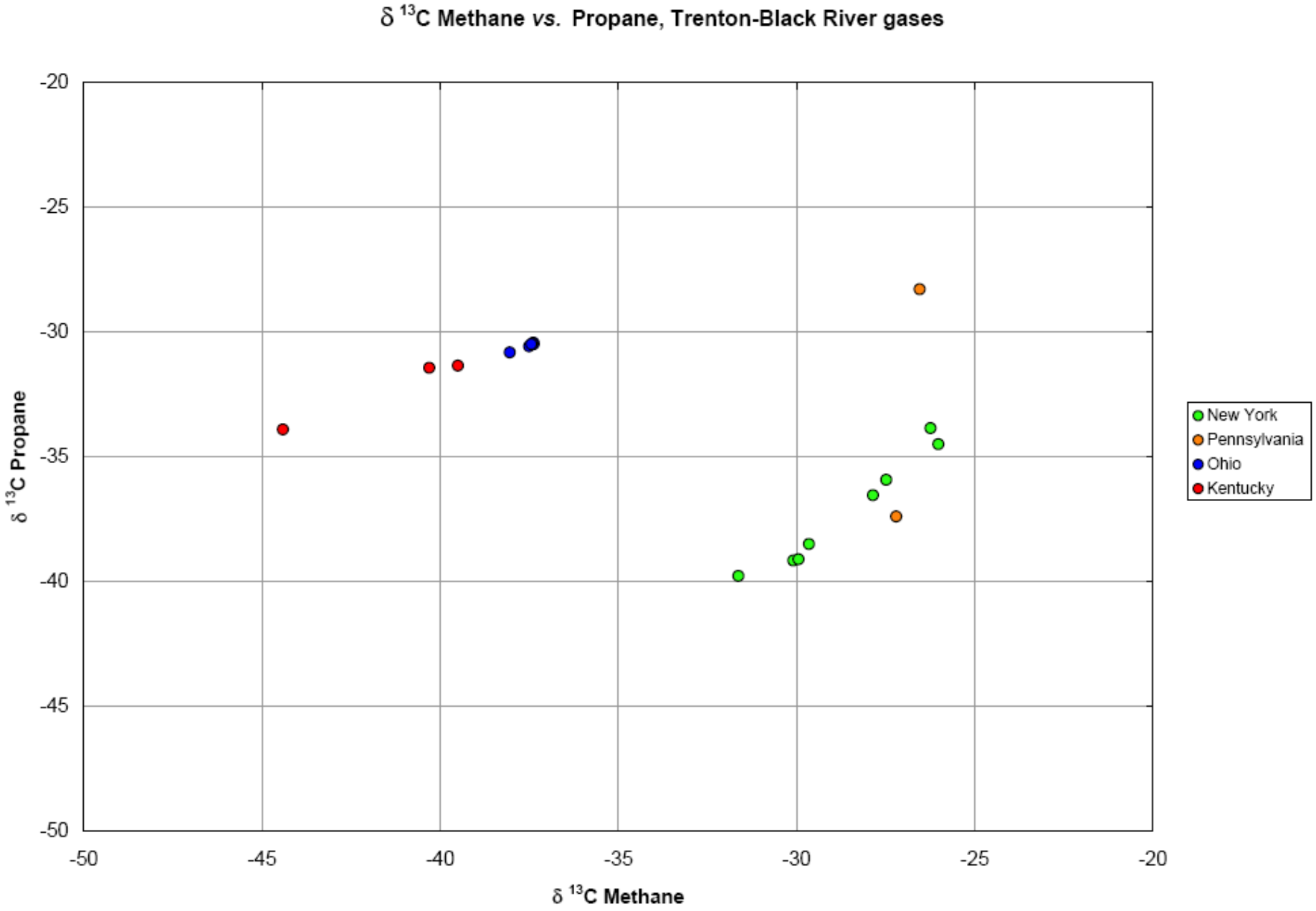

Figure 5-30. $\delta^{13}C$ of methane versus $\delta^{13}C$ of propane for all Trenton/Black River natural gases sampled and analyzed during this study.

TRENTON-BLACK RIVER PRODUCTION HISTORY AND ANALYSIS

By Katharine Lee Avary, West Virginia Geological Survey

Compilation of Production Data

There are two challenges inherent in compiling production data for the Trenton-Black River play. The older wells, many in the fractured limestone play in northern New York and Kentucky, and older, hydrothermal dolomite play wells in northwestern Ohio, do not have complete production histories available publicly. Public production data reporting for Ohio began in the 1980's and for Kentucky in the 1990's. Hence, the early years of production are unavailable for wells in these states. For the recent drilling activity which has occurred in New York in the hydrothermal dolomite fields, and in West Virginia in one of the fractured limestone fields, histories are complete, although short in duration. In addition, monthly production data are unavailable for New York, making analysis of production data on a monthly basis impossible.

The available production data (for 379 gas and 424 oil wells) were collected and summarized by well in Excel spreadsheets by well. Each well was assigned to a play (fractured limestone, FLS; or hydrothermal dolomite, HTD). Further, summaries of annual production by field for 72 gas and 45 oil fields were compiled for comparison (Table 6-1, Table 6-2).

Analysis of Production Data

Summaries of production data by field were compared and graphs of annual and cumulative production were prepared. Also, the number of wells contributing to the annual production total was graphed. Using the field summary data, three hydrothermal dolomite fields and three fractured limestone fields were selected as examples of fields with a small, medium and large amount of production relative to the fields in each play (Figure 6-1).

Hydrothermal Dolomite Gas Fields

Quackenbush Hill field (Figure 6-2, Figure 6-3) is the largest field in terms of cumulative production, with more than 43 Bcf of gas produced from 2000 to 2004. York field is a HTD field with more than 5 Bcf of gas produced from 1997 to 2004, which classifies it as having medium production. County Line is a HTD field with a relatively small amount of production, only 1.25 Bcf from 2000 to 2004.

Six horizontal wells are located in Quackenbush Hill field, Steuben and Chemung counties, NY; they were drilled beginning in 2002. The full impact of these wells will not be seen until the 2005 production data are available, as only one of these horizontal wells was on-line a full 12 months or more.

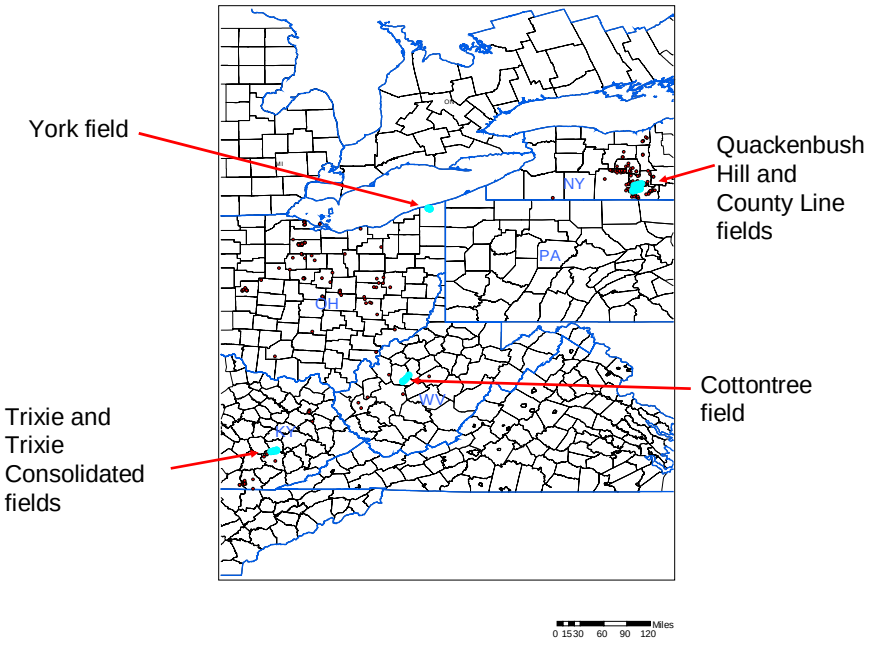

Figure 6-1. Map showing location of selected HTD and FLS gas fields

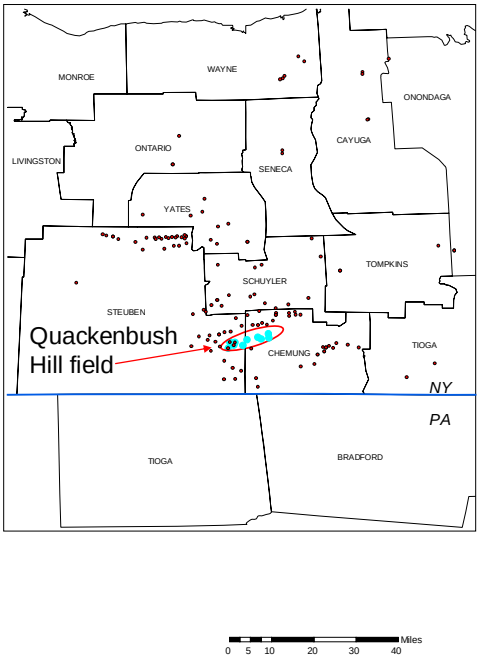

Figure 6-2. Map showing location of Quackenbush Hill field, Steuben and Chemung counties, New York.

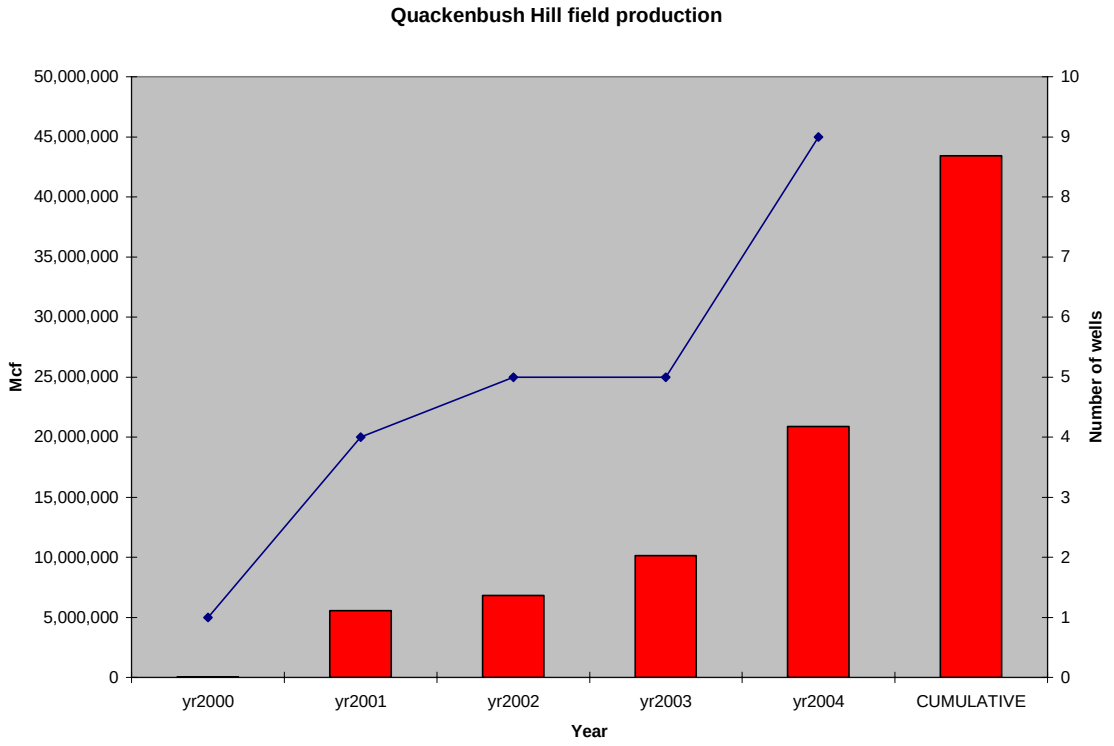

Figure 6-3. Graph of annual production and number of wells contributing to annual production for Quackenbush Hill field.

Nonetheless, this field has the largest amount of gas production of all of the HTD fields. It also has a relatively large number of producing wells (9).

York field, (Figure 6-4, Figure 6-5) located in Ashtabula County, northeastern Ohio, was discovered in 1997. Cumulative production for the field is 5.1 Bcf from 8 wells from 1998 to 2004.

County Line field, (Figure 6-6, Figure 6-7) located in Chemung, Schuyler and Steuben counties, NY, was discovered in 2000. Four wells have produced 1.3 Bcf from 2001 to 2004.

Fractured Limestone (FLS) Gas Fields

Cottontree field, Roane County, WV (Figure 6-8, Figure 6-9) is the largest of the fractured limestone fields in terms of cumulative production with more than 8 Bcf of production reported from 8 wells. Trixie is an intermediate cumulative production FLS field with 4 wells and 84 MMcf (0.08 Bcf) of gas produced from 1997 to 2003. Trixie Consolidated is a small FLS field with 3 wells and 15 MMcf (0.15 Bcf) of gas production reported from 1994 to 2003.

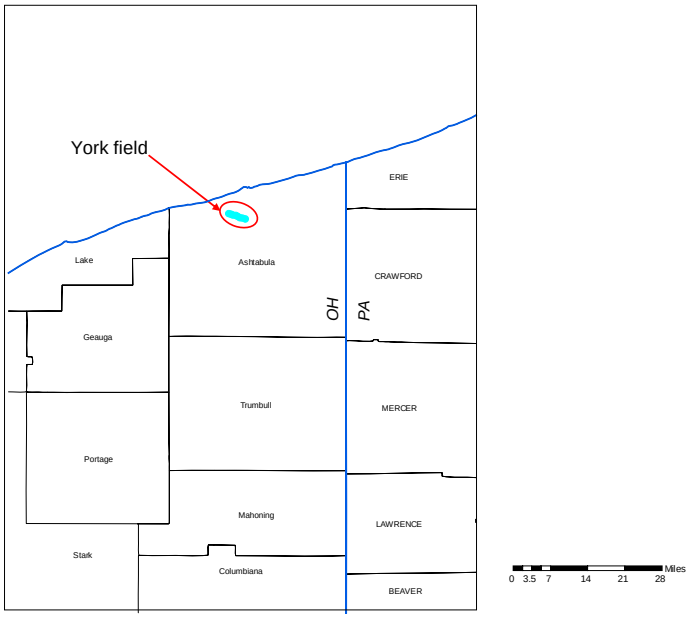

Figure 6-4. Map showing the location of the York field, Ashtabula County, Ohio.

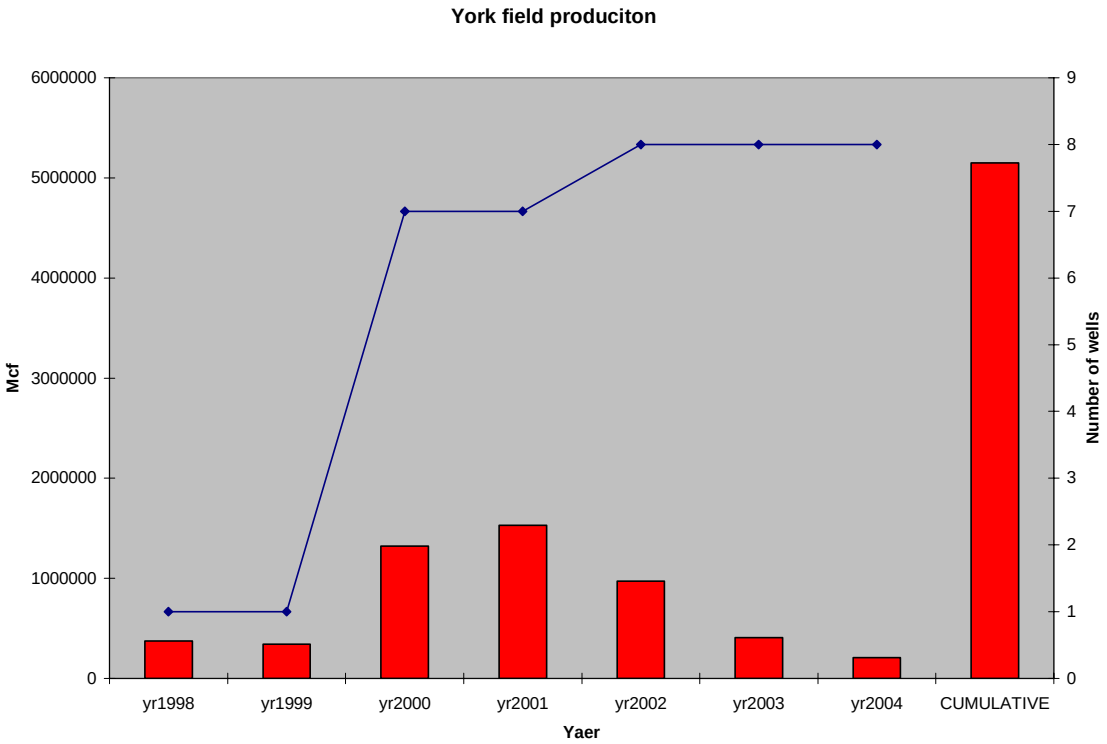

Figure 6-5 Graph of annual production for York field and number of wells contributing to annual production for York field.

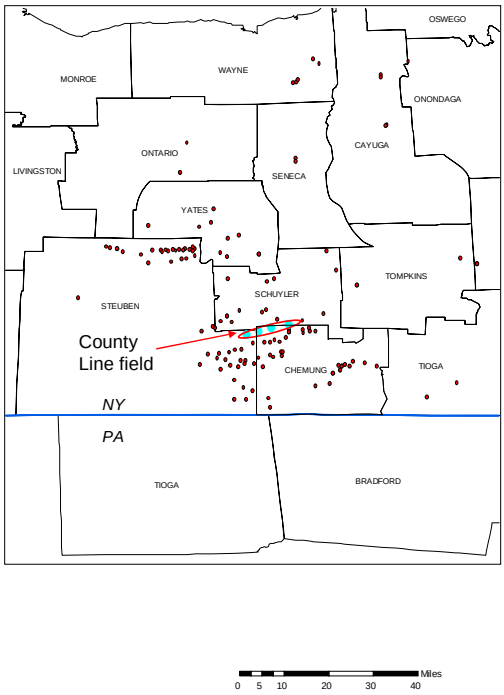

Figure 6-6. Map showing the location of County Line field, Chemung, Schyler and Steuben counties, New York.

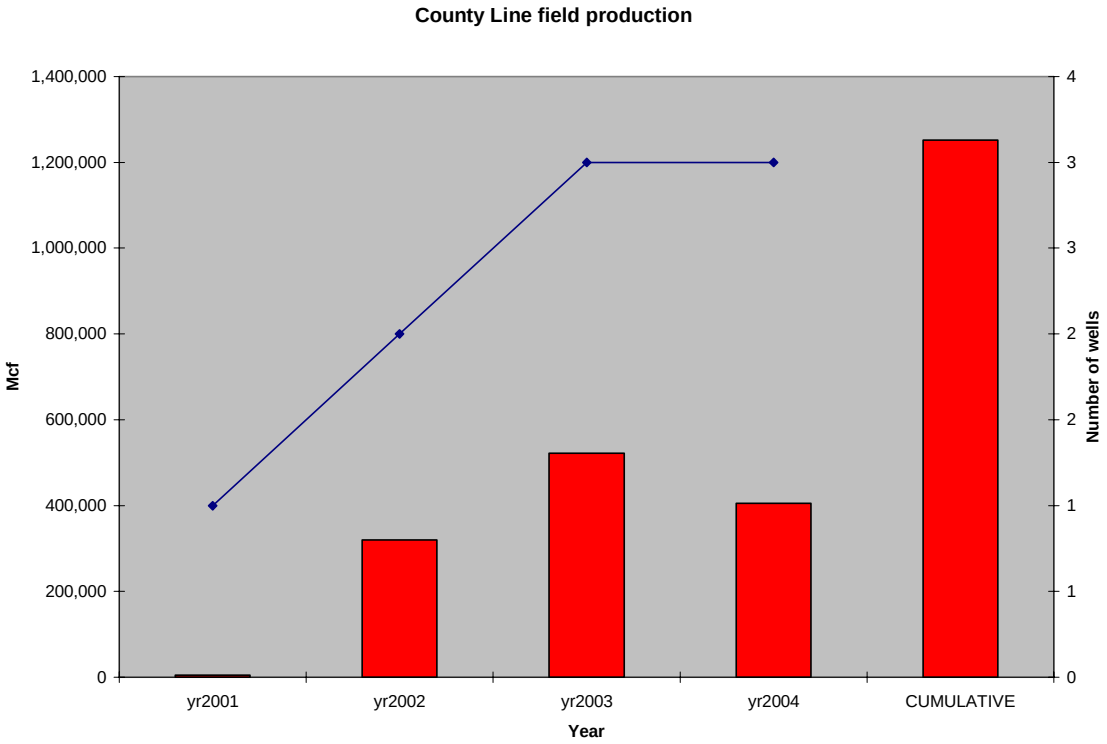

Figure 6-7 Graph of annual production for County Line field and number of wells contributing to annual production for County Line field

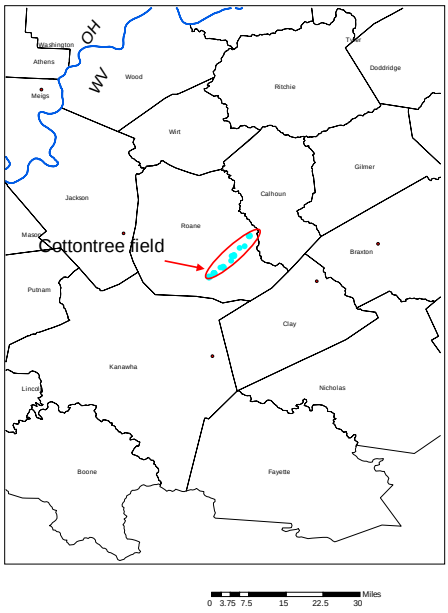

Figure 6-8. Map showing the location of the Cottontree field, Roane County, West Virginia

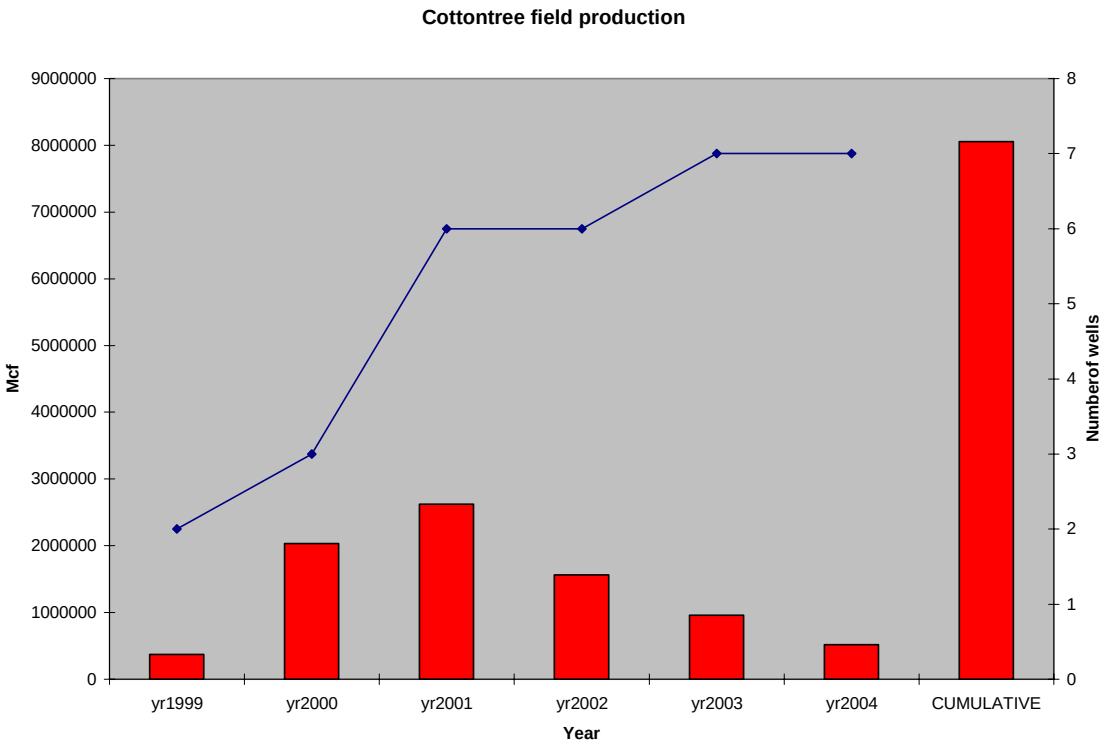

Figure 6-9 Graph of annual production for Cottontree field and number of wells contributing to annual production for Cottontree field

The discovery well for the Cottontree field, (4708704250 Parker) has produced just over 4.65 Bcf of gas, from 1999 through 2004, almost 58% of the total production from the field. The well with the next largest cumulative production (4708704261 Epling) has produced 1.1 Bcf from 2001 to 2004. The other wells in the field have all produced less than 1 Bcf, with one well (4708704253 Willa Groves) producing only 3.8 MMcf from 2003 to 2004.

Trixie and Trixie Consolidated (Figure 6-10) are two relatively small fields located in Clay County, KY. Both were discovered in 1981 and have relatively small amounts of cumulative production compared to Cottontree field. Trixie field, with 4 wells, has produced 83.7 MMcf from 1997 to 2003. The three wells in Trixie Consolidated field have produced 14.7 MMcf from 1994 to 2003 with some missing years of data. The production history is missing the first 16 years of flush production for both of these fields.

Oil Fields

Oil production data also are limited in terms of the number of wells and duration of production history. Data were summarized by field (Table 6-2) and one relatively large field from each play was selected (Figure 6-10).

Honey Creek, (Figure 6-11) an HTD field located in Marion County, Ohio was discovered in 1964; production records are available for 2 wells from 1978 to 1995. Cumulative production for this period for these 2 wells is 164,722 barrels; one well, (3410120116) has a cumulative production of 141,700 barrels, whereas the other well (3410120132) has reported production of 23,022 barrels.

Albany Consolidated, (Figure 6-13), a FLS field located in Clinton County, Kentucky, was discovered in 1961. Cumulative production of 72,689 barrels was reported from 24 wells from 1994 to 2003. One well, (1605390397) produced more than 20,000 barrels from 1999 to 2003.

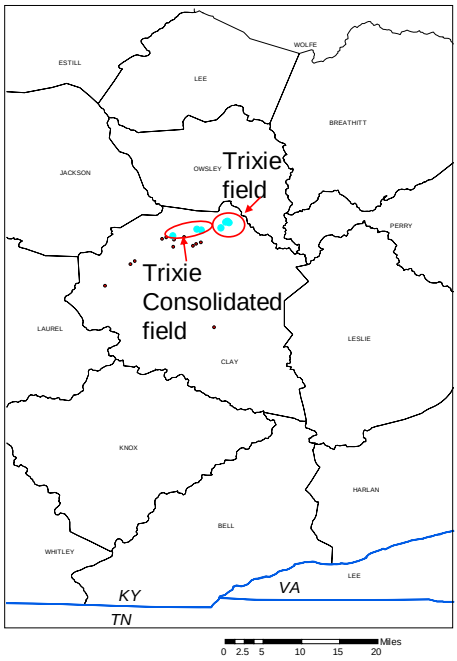

Figure 6-10. Map showing the locations of the Trixie and Trixie Consolidated fields, Clay County, Kentucky.

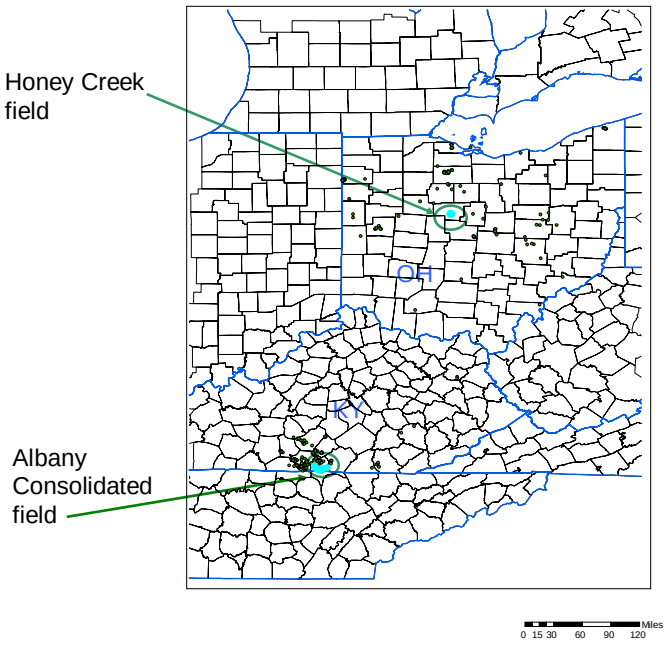

Figure 6-11. Map showing the location of Honey Creek and Albany Consolidated fields.

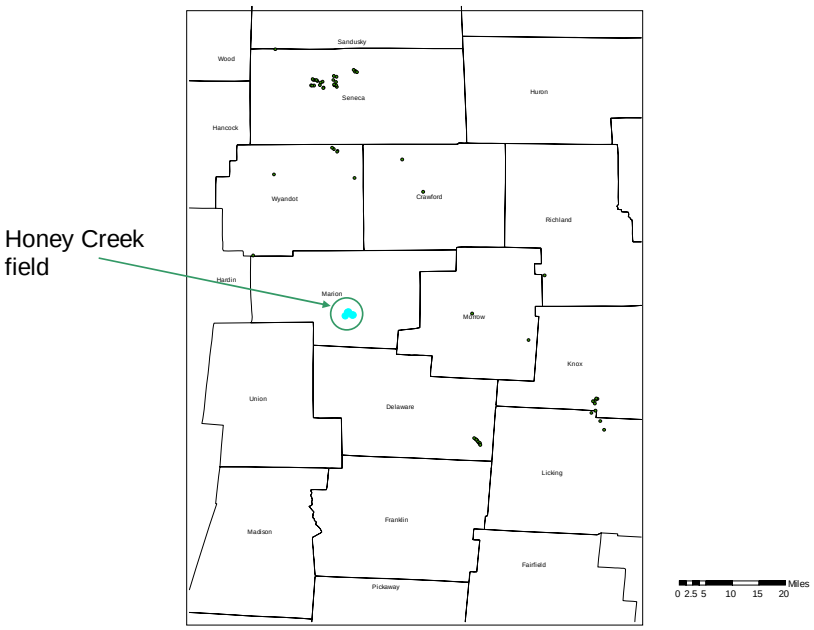

Figure 6-12. Map showing the location of Honey Creek field, Marion County, Ohio.

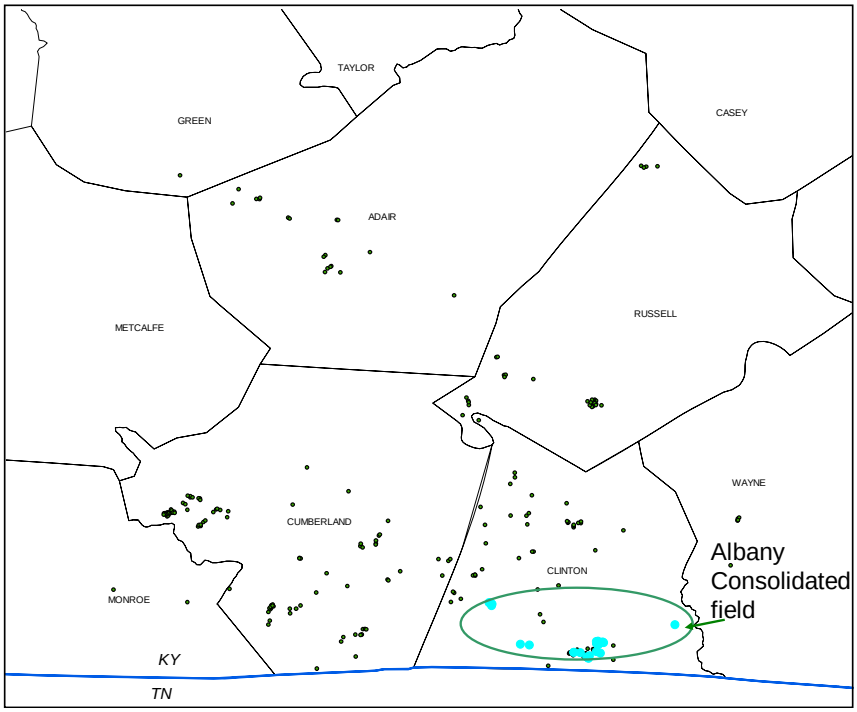

Figure 6-13. Map showing the location of the Albany Consolidated field, Clinton County, Kentucky.

Second Year Annual Gas Production

All available gas production records were evaluated and compared with completion dates to eliminate wells from evaluation that did not have complete histories. This resulted in a data set of 93 wells. Maps were created using proportional symbols to represent the volume of gas produced in the second year of the well's production history (Figure 6-14, Figure 6-15). The second year was chosen for comparison to eliminate the inconsistencies of using first year production data. The first year record may be for between 1 and 12 months, depending on when the well first was put into production.

Second year production for the FLS play ranges from 5 Mcf for a well (31117050410000) in the Butler Creek field in New York to 1,797,927 Mcf (1.8 Bcf) for a well in the Cottontree field in West Virginia (47087042500000).

Second year production for wells in the HTD play ranges from 11,740 Mcf for a well (31101229630200,) in the Caton field in New York to 1,924,767 Mcf (1.9 Bcf) for a well (31101228140100) in the Wilson Hollow field, also in New York. The Caton field well was only on line 3 months in the first production year and 6 months in the second production year.

Horizontal Well Analysis

More than 30 horizontal wells have been drilled in New York in the Trenton-Black River beginning in 2002 (Table 6-3, Figure bb). Production histories for these wells are short, but initial indications are that the horizontal wells are more productive than vertical wells. Fortuna relied upon corporate experience gained during horizontal drilling in the Black River in Ontario to drill many of these wells.

Two of the horizontal wells, both in Quackenbush Hill field, have produced more than 6 Bcf. The Henkel 1359-A well (31101228710100) has reported production of 6.287 Bcf during 2003 and 2004. This well was originally drilled in 2001 and produced 164,015 Mcf in 2001 and 2002, before being drilled horizontally.

The Reed 1 well (31101230550000) produced 6.475 Bcf in 9 months in 2004.

Two other horizontal wells in Quackenbush Hill field had reported production of more than 2 Bcf in 2004. The Andrews well (101230380000) produced 2.5 Bcf in 10 months; the Hakes 1 well (31010230540000) produced 2.9 Bcf in 8 months in 2004.

The well with the largest cumulative production of all of the New York HTD wells is a vertical well: the Lovell 1323 well (31015228310000) in the

Quackenbush Hill field, with a reported cumulative production of 15.2 Bcf from 2000 (only 1 month production) through 2004. Two other vertical wells, both in the Wilson Hollow field, have reported cumulative production in excess of 6 Bcf: The Parker 1401 (31015228910000) well has produced 6.4 Bcf from 2002 (11 months production) to 2004. The Howe 1300-A (31101228140100) well has 6.2 Bcf from 2001 to 2004.

Total production from these horizontal wells is 20.451 Bcf; total production for all the HTD wells in New York is 110 Bcf. Additional years of production data will allow further evaluation of the effectiveness of horizontal drilling in the HTD reservoirs. Initial indications are that these wells have the potential to recover significant volumes of gas.

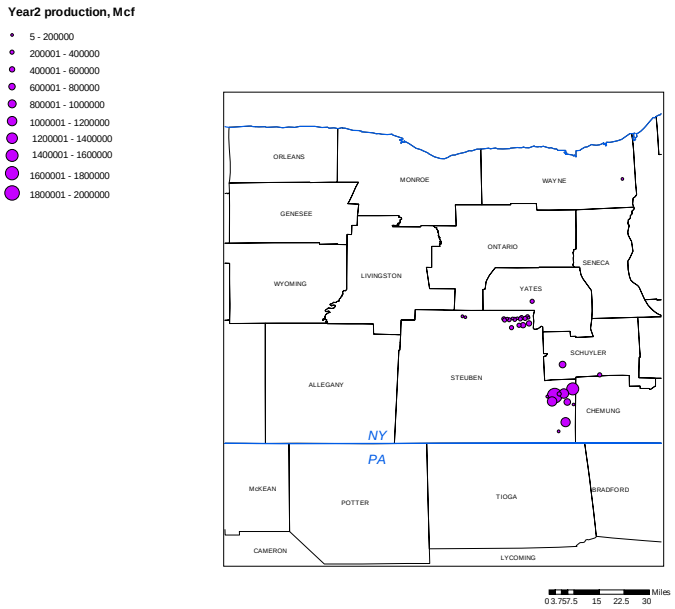

Figure 6-14. Map of wells in western New York with Year 2 production indicated by relative size of circle.

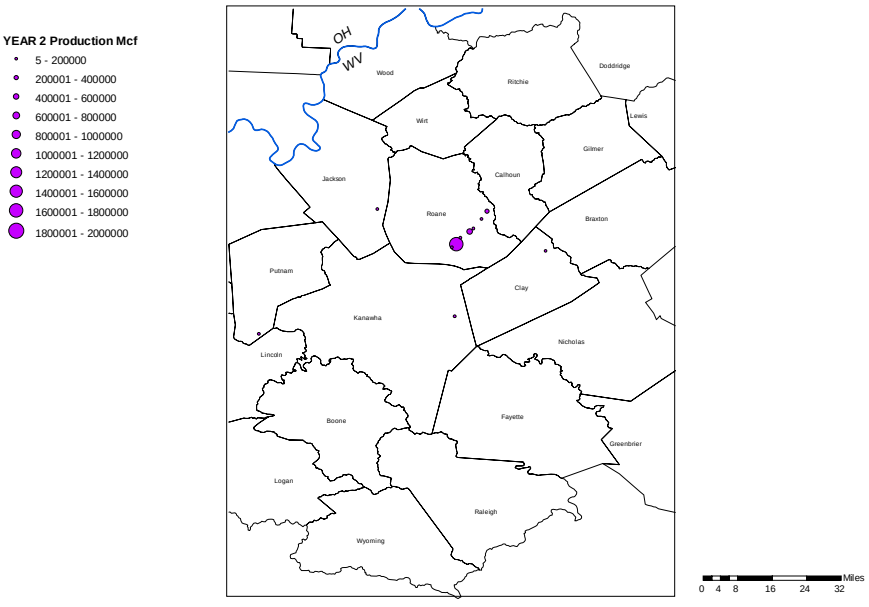

Figure 6-15. Map of wells in central West Virginia, with Year 2 production indicated by relative size of circle.

Table 6-1. Summary Gas Production by Field

FIELD_NAME	NO_ WELLS	NUMBER _YEARS	CUMULATIVE_ PROD, MCF	DISCOVERY _ DATE	COMMENTS	STATE	PLAY TYPE
Quackenbush Hill	9	5	43,432,554	2000		NY	HTD
Wilson Hollow	10	6	31,008,271	2001		NY	HTD
Glodes Corners Road	12	9	9,283,850	1985		NY	HTD
Muck Farm	4	6	7,258,442	1998		NY	HTD
Cottontree	5	6	6,912,461	1998		WV	FLS
Terry Hill South	7	4	6,847,623	2000	1 well 1 month prod 2001; 1 well 3 months prod 2001	NY	HTD
York	8	7	5,149,542	1997		OH	HTD
Cutler Creek	2	4	3,498,612	2001	1 well 1 yr prod	NY	HTD
Langdon Hill	6	3	2,182,784	2000	1 well 1 yr prod	NY	HTD
County Line	4	4	1,345,719	2000	1 well 3 mo. prod 2001; 1 well 10 mo. prod 2002 Marcellus?; 1 well 2 mo. prod 2002	NY	HTD
Sugar Hill	1	3	1,076,554	2000	2 months production 2002	NY	HTD
Whiskey Creek	1	2	1,038,558	2003	1 month 2004	NY	HTD
Seeley Creek	1	1	872,417	2003	6 months production 2004	NY	HTD
Harlem	9	6	548,183	1981		OH	HTD
Isonville Cons	2	7	488,091	1917		KY	FLS
McNutt Run	2	1	500,759	2002	3 months production 2004	NY	HTD
Sexton Hollow	1	1	459,117	2002	4 months production 2004	NY	HTD
Pine Hill	4	4	408,696	1999	474,276 cum prod est 2002 from summary reports	NY	HTD
Riverside	1	1	376,717	2001	7 months production 2004	NY	HTD
Ballyhack Creek	3	2	340,436	2002		NY	HTD
Guyanoga Valley	1	2	329,998	1999	shut in, 2002	NY	HTD
Pattons Corners	3	12	167,654	1902	formerly known as Utica field	OH	HTD
Isonville	5	7	143,838	1917		KY	FLS
Mine Fork	2	7	120,409	1919		KY	FLS
Jellico Creek	7	6	117,934	1981		KY	FLS
Trixie	4	7	83,723	1981		KY	FLS
Honey Creek	5	4	76,650	1964		OH	HTD
Burning Springs Cons	7	10	38,799	1898		KY	FLS
Auburn Geothermal	2	7	37,018	1982		NY	FLS
Caton	1	2	33,191	2003	6 months production 2004	NY	HTD
Trixie Cons	3	8	14,733	1981		KY	FLS
Cromers	11	12	14,655	1928		OH	HTD
Oak Harbor	3	6	13,566	1886		OH	HTD
Meadow Creek Cons	1	6	13,558	1960		KY	FLS
Jellico Creek North	5	6	11,158	1985		KY	FLS
Lee Chapel Cons	1	1	11,158	1975		KY	FLS
Boho	1	3	6,193	2000		KY	FLS
Fogertown	1	7	5,687	1965		KY	BLS
Ida Cons	2	2	5,666	1944		KY	BLS
Butler Creek	1	9	5,520	1996		NY	FLS
Laurel Run	1	1	4,349	2004	1 month 2004	NY	HTD
Tiffin	9	12	3,749	1896		OH	HTD
Big Branch East	1	1	3,092	1985		KY	FLS
Teges Creek	1	3	2,991	1983		KY	BLS
Marsh Creek	1	1	1,489	1998		KY	FLS
Fairview	1	8	1,112	1973		KY	FLS
Albany Cons	1	1	844	1961		KY	FLS
Oneida	1	1	822	1918		KY	FLS

Bass Lake	1	7	700	1980		NY	FLS
Pulaski	8	10	406	1891		NY	FLS
Blue Tail Rooster	1	1	7	1966		NY	FLS
Beans Station	1	0	0	2002	not very dolomitized	NY	HTD
Blanchard	1	0	0	1885	1 well; some years 1 Mcf	OH	HTD
Carey Consolidated	1	0	0	1887		OH	HTD
Catawba	1	0	0	1925		OH	HTD
Cooper Hill	1	0	0	2004		NY	HTD
Corning North	1	0	0	2004		NY	HTD
Cross Lake	1	0	0	1980		NY	FLS
Findlay Consolidated	1	0	0	1884		OH	HTD
Kasoag	1	0	0	1984		NY	FLS
Lima Consolidated	2	0	0	1885		OH	HTD
Little France	1	0	0	1981		NY	FLS
Millpond Field	1	0	0	2003		NY	FLS
Moreland	1	0	0	2003		NY	HTD
New Hampshire East	1	0	0	1962		OH	HTD
Pangburn	1	0	0	2000		NY	FLS
Rayner	1	0	0	2004		NY	HTD
South Corning	1	0	0	2004		NY	HTD
Toussaint River	3	0	0	1966		OH	HTD
West River	1	0	0	2003		NY	HTD
Zimmer Hill	1	0	0	2004		NY	HTD

Table 6-2. Summary Oil Production by Field

FIELD_NAME	NO WELLS	NUMBER_ YEARS	CUMULATIV E _PROD, BARRELS	DISCOVERY_ DATE	COMMENTS	STATE	PLAY TYPE
Honey Creek	5	18	164,722	1964	only 2 wells with volumes >0	OH	HTD
Albany Cons	24	10	72,689	1961		KY	FLS
Lee Chapel Cons	29	10	59,043	1975		KY	FLS
Concord Cons	2	7	43,424	1919		KY	BLS
Mud Camp	25	10	21,457	1986		KY	BLS
Ida Cons	14	10	18,977	1944		KY	BLS
Hayes Creek	2	7	12,560	1983		KY	FLS
Tiffin	9	20	12,240	1896		OH	HTD
Sulphur Creek Cons	7	9	11,722	1906		KY	FLS
Bliss	2	6	9,472	1970		KY	FLS
Seventy-Six Cons	7	6	8,867	1946		KY	BLS
Granville Cons	8	7	8,592	1938		KY	BLS
Salt Lick Bend Cons	12	10	6,277	1903		KY	FLS
York	8	7	6,541	1997		OH	HTD
Gradyville East Cons	7	10	6,018	1969		KY	FLS
Jellico Creek North	3	2	5,455	1985		KY	FLS
Tanbark Cons	5	10	4,763	1959		KY	FLS
Littrell Cons	4	10	3,996	1962		KY	BLS
Fogertown	1	4	3,876	1965		KY	BLS
Toussaint River	3	5	2,987	1966		OH	HTD
Bear Creek	6	6	2,918	1920		KY	FLS
Summer Shade North	17	6	2,760	1983		KY	BLS
Fanny's Creek	1	7	2,724	1906		KY	FLS
Creelsboro Cons	7	7	2,723	1861		KY	FLS
Lee Chapel	2	6	2,323	1975		KY	FLS

Big Branch East	1	1	2,160	1985		KY	FLS
Peytonsburg	1	7	2,025	1980		KY	FLS
Cromers	11	18	2,135	1928		OH	HTD
Rowena Cons	15	8	1,775	1984		KY	BLS
Creelsboro West	4	7	1,510	1981		KY	FLS
Pickett Chapel	1	5	1,470	1974		KY	BLS
Isonville	2	4	1,302	1917		KY	FLS
Sulpher Well Cons	1	5	1,263			KY	FLS
Williams Creek Cons	1	4	1,256	1945		KY	FLS
Pickett Cons	2	5	1,246	1974		KY	FLS
Findlay Consolidated	1	7	1,085	1884		OH	HTD
Union Chapel School	1	4	1,047	1984		KY	FLS
Kettle Creek Cons	12	4	1,029	1922		KY	BLS
Harlem	9	2	963	1964	only 2 wells with volumes >0	OH	HTD
Hogback	3	5	942	1961		KY	BLS
Pattons Corners	3	8	892	1902		OH	HTD
Jellico Creek	2	2	821	1981		KY	FLS
Catawba	1	7	786	1925		OH	HTD
McIver Creek	1	7	783			KY	FLS
Gradyville North	2	2	717	1970		KY	BLS

Table 6.3. New York Horizontal Wells

API_number	county	permit	field	orig_operator	subsequent_operator	lease_name	well_number	quad_ 7.5 min	latitude	longitude
3100723078	7	23078	Ballyhack Creek	B & B	CNR	Olson	1-B	Chenango Forks	42.1524300	-75.8041300
3101522911	15	22911	Langdon Hill	CNR		Schmidt	24537-A	Erin	42.1467300	-76.6930700
3101523017	15	23017	Terry Hill South	Fortuna		Hammond	1-A	Montour Falls	42.2718600	-76.8591400
3101523023	15	23023	Langdon Hill	Fortuna		Konstantinides	1	Van Etten	42.1696900	-76.6121500
3101523028	15	23028	Quackenbush Hill	Fortuna		Hepfner	1	Big Flats	42.1890800	-76.9101400
3101523104	15	23104	wildcat	CNR		Davies	24538-1A	Erin	42.1359500	-76.7152900
3101523134	15	23134	Quackenbush Hill	Fortuna		Soderblom	1	Big Flats	42.1926800	-76.8828800
3101523146	15	23146	Cooper Hill	Fortuna		Sekella	1	Van Etten	42.1602400	-76.5742700
3101523173	15	23173	unnamed	East Res		Hartman	1-B	Elmira	42.0943600	-76.7740300
3101523182	15	23182	wildcat	Fortuna		Andrews	1-A	Big Flats	42.1564100	-76.9440900
3101523186	15	23186	wildcat	East Res		Messing	1-B	Seeley Creek	42.0522600	-76.9015900
3101523203	15	23203	wildcat	Fortuna		Mallula	1	Van Etten	42.1919400	-76.5924100
3101523228	15	23228	wildcat	Fortuna		Little	1	Horseheads	42.2179700	-76.7671100
3109722829	97	22829	wildcat	Fortuna		Grand Prix	1-A	Bradford	42.3234900	-77.0607500
3109722935	97	22935	wildcat	Fortuna		Wonderview Farms	1-B	Alpine	42.3303500	-76.8736300
3109723008	97	23008	Moreland	Fortuna		Ganung	2	Beaver Dam	42.3124400	-76.8968700
3109723072	97	23072	Meads Creek	Fortuna		SRA 3	1	Bradford	42.2834400	-77.0994300
3109723086	97	23086	wildcat	Fortuna		Towner	1	Bradford	42.3033600	-77.0449600
3110122871	101	22871	Quackenbush Hill	PGE	Fortuna	Henkel	1359-A	Big Flats	42.1670800	-76.9727400
3110122978	101	22978	wildcat	Fortuna		Ballymoney	1	Rexville	42.0321000	-77.6428400
3110123038	101	23038	Quackenbush Hill	Fortuna		Andrews	1	Corning	42.1573200	-77.0235600
3110123054	101	23054	Quackenbush Hill	Fortuna		Hakes	1	Corning	42.1784900	-77.0171800
3110123055	101	23055	Quackenbush Hill	Fortuna		Reed	1	Corning	42.1676300	-77.0038800
3110123059	101	23059	Wilson Hollow	Fortuna		Apenowich	1	Corning	42.1977400	-77.1236600
3110123085	101	23085	wildcat	Fortuna		Erwin WMA	1	Campbell	42.1643300	-77.1499300
3110123100	101	23100	Cutler Creek	Fortuna		Moss	1	Corning	42.1627100	-77.0514600
3110123101	101	23101	wildcat	Fortuna		Steuben Reforestation Area 3	2	Bradford	42.2897100	-77.1068700
3110123150	101	23150	wildcat	Fortuna		TLT	1	Addison	42.0969700	-77.1399100
3110123154	101	23154	Zimmer Hill	Fortuna		Drumm	1	Savona	42.2746600	-77.1443800
3110123155	101	23155	Corning North	Fortuna		Behm	1	Corning	42.1860100	-77.0932800
3110123187	101	23187	wildcat	Fortuna		Bauer	1	Big Flats	42.1611000	-76.9920900
3110123189	101	23189	wildcat	Fortuna		Mayes	1	Savona	42.2827300	-77.1483400
3110123190	101	23190	wildcat	Fortuna		Stuart	1	Caton	42.1141200	-77.0076300
3110723185	107	23185	wildcat	Fortuna		Cotton-Hanlon	1	Van Etten	42.1601900	-76.5327400

Table 6.3. New York Horizontal Wells, cont.

API_number	comment	spud_date	date_TD	total_depth	gas_2003	gas_2004	cumulative_production	production_comments
3100723078	horizontal; directional	12/2/2004	1/29/2005	9508		0	0	
3101522911	horizontal; directional	1/2/2004	2/7/2004	10000	0	468,061	468,061	6 months production 2004
3101523017	horizontal; directional	1/18/2005	2/3/2005	11387			0	
3101523023	horizontal; gas well	3/27/2003	4/5/2003	9981	0	602,050	602,050	10 months production 2004
3101523028	horizontal	7/28/2003	11/5/2003	9853	0		0	
3101523104	horizontal; directional	5/1/2004	5/19/2004	10265		170,753	170,753	4 months production 2004
3101523134	horizontal; MD 12050	7/13/2004	10/20/2004	9695		61,247	61,247	1 month production 2004
3101523146	horizontal; 9909 TVD; MD 13115	9/13/2004	10/27/2004	9909			0	
3101523173	horizontal; directional	2/17/2005	3/16/2005	9429			0	
3101523182	directional; horizontal	4/30/2005	5/27/2005	9646			0	
3101523186	horizontal; directional; BHL 9656 FT S, 6998 FT W	9/17/2005	10/21/2005	10905				
3101523203	horizontal	5/21/2005	10/8/2005	9662				
3101523228	horizontal	7/21/2005	8/2/2005	9483				
3109722829	horizontal	4/21/2004	5/7/2004	9658	0		0	
3109722935	directional; horizontal	1/25/2004	4/13/2004				0	
3109723008	horizontal	3/3/2003	8/11/2003	13609			0	
3109723072	horizontal; 19 MMcf/ day initial test; pressure > 2000 psi; was known as McNutt Run field	12/13/2003	4/3/2004	11704		476,576	476,576	3 months production 2004
3109723086	horizontal; BHL 7900 ft S 42.20.00, 1650 ft W 77.02.30; MD 12500, TVD 8875	2/3/2004	6/17/2004	11329			0	
3110122871	horizontal; directional; first production 07/10/2001 before drld horiz	9/19/2002	12/19/2002	9975	3,520,033	2,767,277	6,287,310	
3110122878	horizontal; dry & abandoned	7/16/2002	10/4/2002	10660			0	
3110123038	gas well; horizontal	7/30/2003	1/24/2004	10117	0	2,504,129	2,504,129	10 months production 2004
3110123054	horizontal	9/18/2003	2/1/2004	13450		2,914,169	2,914,169	8 months production 2004
3110123055	horizontal	10/7/2003	9/1/2003	9881		6,474,551	6,474,551	9 months production 2004
3110123059	gas well; horizontal, BHL 6500 ft S 42.12.30, 8950 ft W 77.05.00; MD 12620, TVD 9613	9/22/2003	2/1/2004	9613			0	
3110123085	horizontal	2/5/2004		9797			0	
3110123100	horizontal; BHL14850 ft S 42.10.00, 300 ft W 77.02.30; TVD 9578; MD 12500	3/20/2004	5/27/2004	9578		467,773	467,773	3 months production 2004
3110123101	horizontal	3/25/2004	5/20/2004	13420		24,183	24,183	2 months production 2004
3110123150	horizontal; directional; BHL 9405 ft S 42.07.30, 8131 ft W 77.07.30; MD 12,000 FT	9/28/2004	12/19/2004	12000		0	0	
3110123154	horizontal;directional; 9406 ft S 42.17.30, 6566 FT W 77.07.30; MD 12000 FT	9/15/2004	1/18/2005	9405		0	0	
3110123155	horizontal; directional; BHL 11589 FT S, 2832 FT W; MD 12160	11/18/2004	3/10/2005	10071			0	
3110123187	horizontal; directional; 5083 FT S, 10,662 FT W	1/26/2005	3/19/2005	10022				
3110123189	horizontal	6/25/2005	7/26/2005	9399				
3110123190	horizontal	8/12/2005	12/15/2005	9841				
3110723185	horizontal; directional; BHL 6423 FT S, 9177 FT W	2/27/2005	4/29/2005	10230				

EXPLORATION FAIRWAYS AND UNDISCOVERED GAS ASSESSMENT MODEL

By Douglas G. Patchen, Michael Ed. Hohn, John A. Harper, Katharine Lee Avary and Ron McDowell

Objective

One of the three main objectives of the Trenton-Black River playbook project is to develop an integrated, multi-faceted, resource assessment model of the Trenton-Black River play in New York, Pennsylvania, Ohio, West Virginia and Kentucky. This objective is closely related to two additional objectives, which are to define possible fairways within which to conduct detailed studies leading to further play development; and to develop a structural-stratigraphic-diagenetic model for the origin of Trenton-Black River hydrothermal dolomite (HTD) reservoirs in the play area.

To accomplish the initial objective, the first step was to define the play outline, i.e., the maximum geographic area with Trenton-Black River potential, based on geology, gas shows and gas production. Our assessment would then estimate the gas resource within that area, again based on geology, production history and an estimate of the number and size of gas fields that we believe will be discovered within the next 30 years.

The maximum area with Trenton-Black River potential was defined as an area roughly equivalent to the Appalachian basin, extending from outcrops of these units in the east and southeast to the Cincinnati and Findlay arches that mark the western extent of the basin **(**Figure 7-1**)**. The actual area that was considered during the resource assessment, however, was somewhat smaller. Areas of the basin were removed from consideration sequentially as we considered various steps in our methodology.

Methodology

The Resource Assessment task team began by determining all potential source beds for the Trenton-Black River play, and then determining if those source beds had gone through the gas-generating window. If they had done so, it was necessary to determine when fluid migration was initiated and where and when reservoirs were created and charged by this migration.

The methodology for the final assessment included six steps. Step 1 was to identify and map source rock distribution. Initially, the distribution and thickness of each potential source rock, i.e., the Utica Shale, Logana Shale Member of the Lexington Formation and Pt. Pleasant Formation, were mapped. In addition, the total organic carbon (TOC) in each potential source rock was mapped, and then conodont alteration index (CAI) data were mapped to indicate the thermal maturity. Overlaying these maps on each other defined areas with high TOC and appropriate maturity, i.e., “pods of potential”

Regional Assessment Area

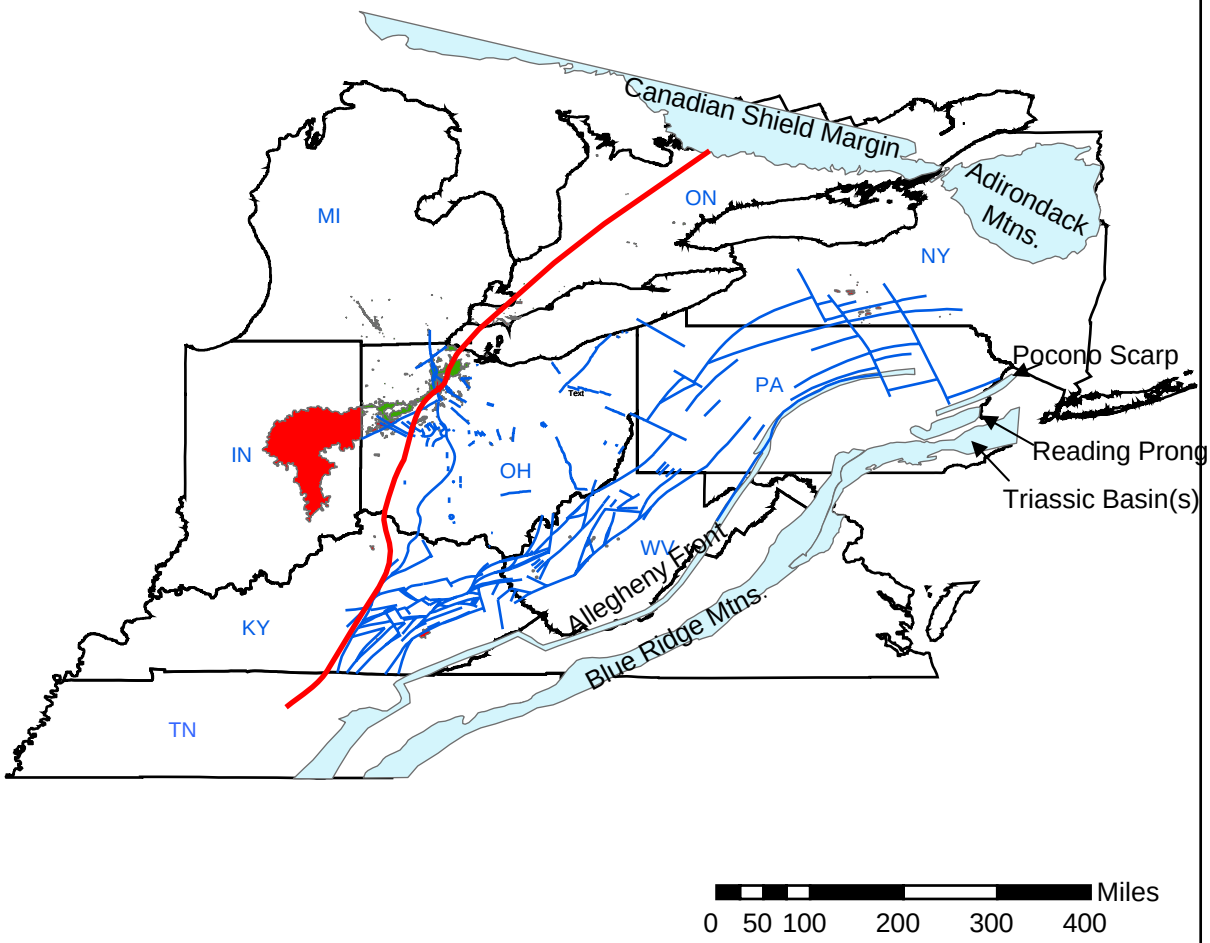

Figure 7-1.

Step 2 was to define and map the maximum and minimum play areas and the extent of different plays within the overall Trenton-Black River play area. The maximum play area is defined based on geologic observations and interpretations developed during this Trenton-Black River study. The minimum play area is restricted to those areas with current production. Therefore, it was necessary to map all wells with gas production and gas shows in the Trenton and Black River carbonates before defining, locating and mapping the extent of all Trenton-Black River plays. Three plays were defined and mapped: a hydrothermal Black River dolomite play; a fractured Trenton Limestone play; and a Trenton bioclastic limestone play. All current producing fields were assigned to one of these plays.

Although one would expect that limestone beds in the Trenton and Black River could be highly fractured over large portions of the basin, one would not expect that all of these fractured limestones have been dolomitized. To determine areas of expected hydrothermal dolomite (HTD) and fractured limestone (FLS) reservoirs we began with the assumption that the thickness of the interval between the basement and the Trenton-Black River is critical: where this interval is thin, fluids rising from the basement have a greater chance of reaching the Trenton-Black River than they do in areas where this interval is of greater thickness.

The process began with a basement structure map showing all known fault locations. Isopachs of the thickness between the basement and the base of the Black River were added to this map along with the locations of all Trenton-Black River wells. Examination of individual wells yielded the elevation of the highest known occurrence of HTD ("upwelling window"). Based on these well elevations, it was possible to extrapolate a maximum elevation of upwelling of hot fluids, projected to be the "top of expected HTD development." A corresponding thickness of approximately 4800 feet between the base of the Black River and basement marks the limit of HTD; areas with interval thicknesses greater than 4800 feet were assigned to FLS under the assumption that hydrothermal fluids rising through that much rock no longer had the ability to produce dolomitization.

Step 3 was to analyze production data for each play area, beginning with an analysis of cumulative production through time (calendar years) and well spacing, followed by a field size distribution analysis. It was decided to use second year cumulative production (add together second year production, all wells). As part of this step, it was necessary to calculate field growth, and compare anticipated growth to current field size. The current number of fields was plotted versus field size, from small to large. A gap in the curve indicates that there is some potential to find a new field of that size.

Step 4 was to determine the timing of maturity and fluid migration. Fluid inclusion data were used to determine the maximum temperature to which the rocks were exposed. Burial history diagrams were prepared for each play area, and models were run

to determine timing. This process was modified with conodont data (CAI), coal blanket effect, etc, as needed.

Step 5 was to estimate, for each play, the size of undiscovered accumulations and the number of undiscovered accumulations. Step 6 was to run a Monte Carlo simulation to generate gas resource values, using Microsoft Excel and Decisioneering Crystal Ball software. An analysis was run for each play, and the numbers were added together to arrive at a a resource estimate for the maximum play area. By convention, resource estimates were reported as 10% - 50% - 90% probabilities.

Source Rock Distribution and Total Organic Carbon Content

Isopach maps of the Utica Shale, Point Pleasant Formation and Logana Shale Member of the Lexington Formation were prepared and furnished to the resource assessment team by the stratigraphy task team. However, because the Point Pleasant Formation, an eastern facies equivalent of the lower part of the Utica Shale, only occurs in a geographically restricted area in Ohio on what has been referred to as the eastern, or Lexington Platform, and in the narrow, inter-platform area to the west, these two units were mapped together. The resulting map indicated thickness ranging from 150-350 feet in Ohio, Ontario and New York, with thicker areas (600-1000 ft) in Pennsylvania and eastern New York

The Logana Shale Member of the Lexington Formation is present in the same general area as the Point Pleasant Formation in Ohio, and it ranges in thickness from 10-50 feet. This shale member also can be mapped farther to the south, where it attains a thickness of 130 feet in southern West Virginia.

The upper part of the Lexington Limestone consists of an unnamed limestone member, generally less than 100 feet thick throughout most of Ohio, overlying the Logana Shale Member and underlying the Point Pleasant Formation. This member thickens to the south, reaching 400 feet in eastern Kentucky and southern West Virginia where the younger Point Pleasant and Utica formations are not present. Because this limestone unit is relatively thin in Ohio where younger potential source beds are present, and thickens to the south where these younger shales are not present, it was decided to combine all these units - the Utica Shale, Point Pleasant Formation, upper limestone member of the Lexington Formation and Logana Shale Member of the Lexington Formation - in a single map.

The final isolith map (Figure 7-2) includes the thickness of all organic-rich beds, shale beds and interbedded limestones from the top of the Utica Shale to the bottom of the Logana Member of the Lexington Formation in Ohio; the Logana Member in eastern Kentucky and West Virginia where the Point Pleasant and Utica are not present; and the interval from the top to the bottom of the Utica Shale where only the Utica is present in Pennsylvania, Ontario and New York. Because the shales within the Point Pleasant Formation and Logana Member of the Lexington Formation are relatively thin, and

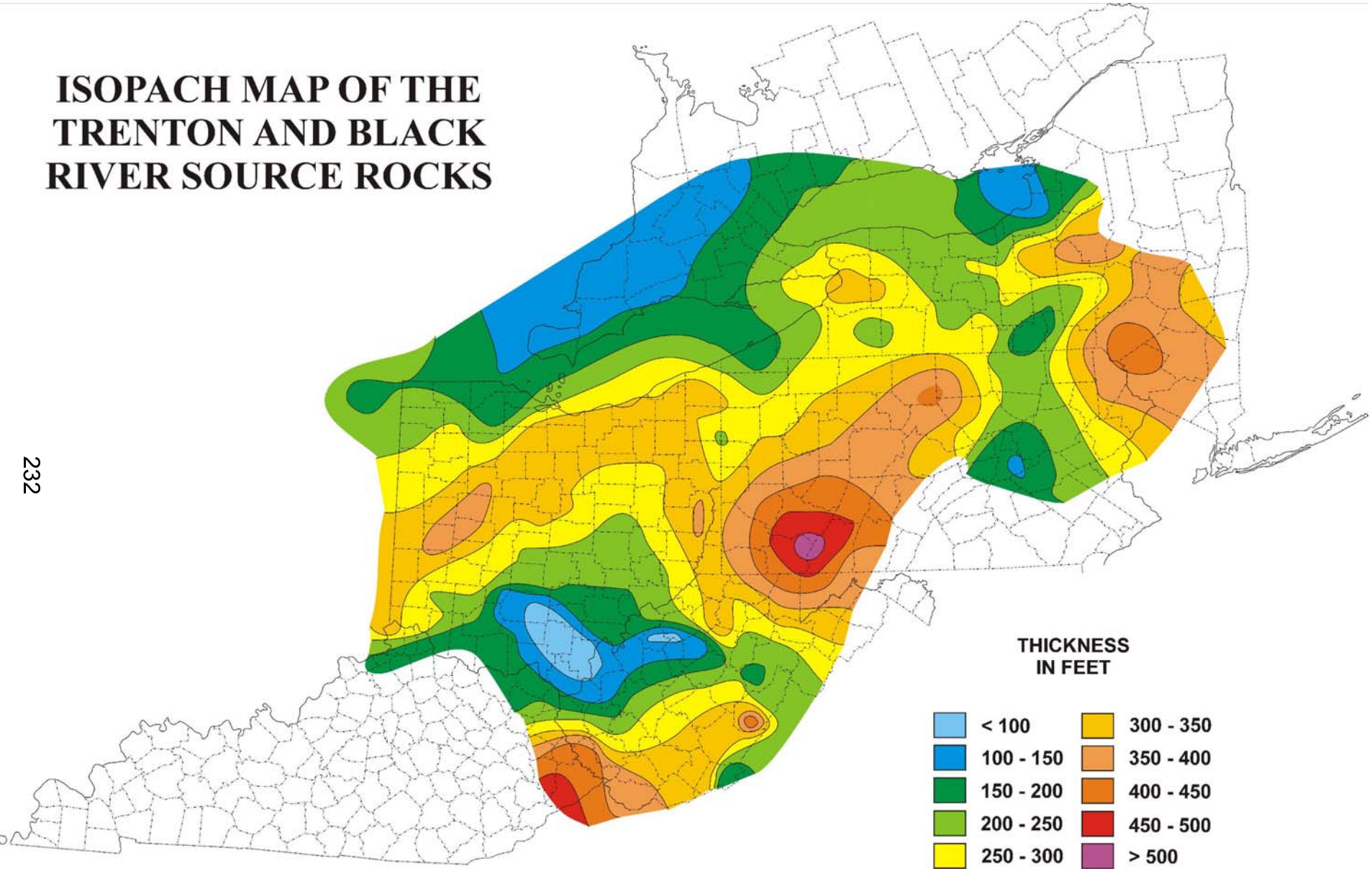
ISOPACH MAP OF THE
TRENTON AND BLACK
RIVER SOURCE ROCKS
THICKNESS
IN FEET
< 100
100 - 150
150 - 200
200 - 250
250 - 300
300 - 350
350 - 400
400 - 450
450 - 500
> 500

Figure 7-2

because total organic carbon (TOC) data were not available for the individual units, this mapping was deemed to be acceptable for our purposes.

Data for total organic carbon (TOC) were overlain on the isopach map of Ordovician shales with source rock potential and the data were contoured. For some data points (wells) both a minimum and maximum value were provided, whereas for other wells, only one value was provided. Therefore, three maps were generated: maximum TOC, average TOC, and minimum TOC, for the Utica Shale through Logana Member interval.

Adding these data defined areas of potential source rock within the larger area of shale distribution. The size of these areas varied greatly, depending on which map of TOC values was being observed. The map of maximum TOC (Figure 7-3) indicates that nearly the entire assessment area is in the good to very good range. Exceptions are thin, linear, northeast-southwest trends of fair to poor TOC values along the Ohio River between West Virginia and Ohio and smaller, parallel trends farther west in Ohio; and two northwest-southeast trends in New York, extending from Lake Ontario toward the areas of known gas production.

The map of minimum TOC values (Figure 7-4) presents a more pessimistic picture. Small areas in Ohio, Pennsylvania and New York are deemed to be very good, and occur within a much larger area of these same three states that is in the good range for TOC. However, southern Ohio and most of West Virginia is mapped as having mostly poor potential.

The TOC map that displays the most likely scenario is the map of average TOC values for the Utica through Logana interval (Figure 7-5). On this map, most of the assessment area falls within the good to very good range. Exceptions are a large area south of Lake Erie and Lake Ontario, and the parallel, southwest-northeast trends along the Ohio River and southern Ohio noted on the map of maximum TOC. A comparison of this map of average TOC with the isopach map of potential shale source beds reveals a close correlation between shale thickness and TOC. Areas of thinner shale have lower TOC values for the shale that is present, whereas areas of thicker shales have higher TOC values in those shales.

At this point, the team was prepared to superimpose maps of productive areas and potential reservoir rock on the source rock map to determine viable areas from which the gas may have been directly sourced, and areas to the west, where gas must have migrated from source beds farther to the east.

However, other data developed during the project suggest that a deeper source rock or rocks may have generated some of the gas found in Trenton and Black River reservoirs, especially in some of the New York fields (see Geochemistry Chapter). Some of these deeper beds may be shale facies in the eastern portion of the Rome Trough. Therefore, it was determined that it would be necessary to add the area of the Rome Trough to the source rock map, as an area of maximum distribution of a deeper source

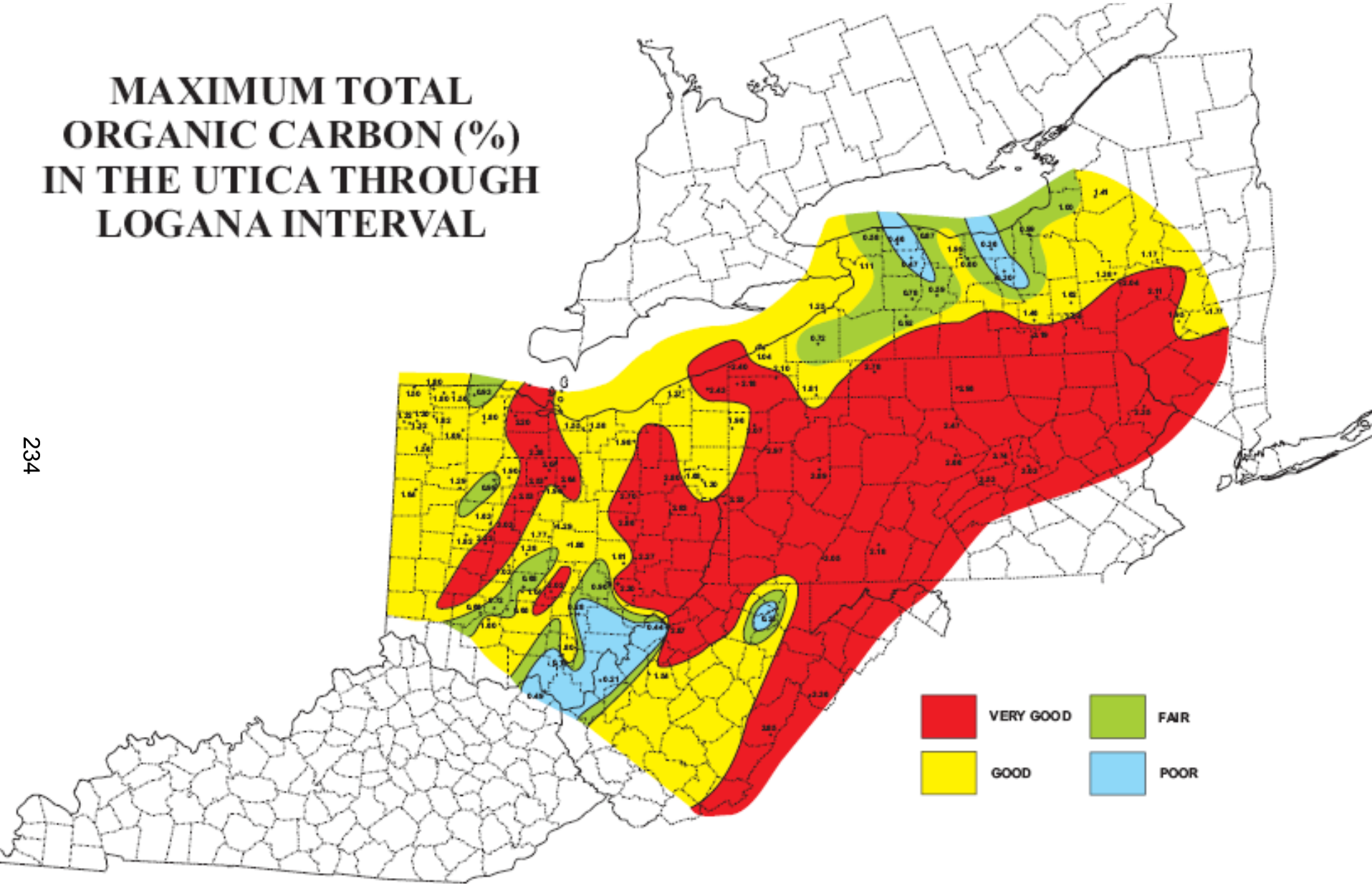
MAXIMUM TOTAL
ORGANIC CARBON (%)
IN THE UTICA THROUGH
LOGANA INTERVAL
VERY GOOD
FAIR
GOOD
POOR

Figure 7-3.

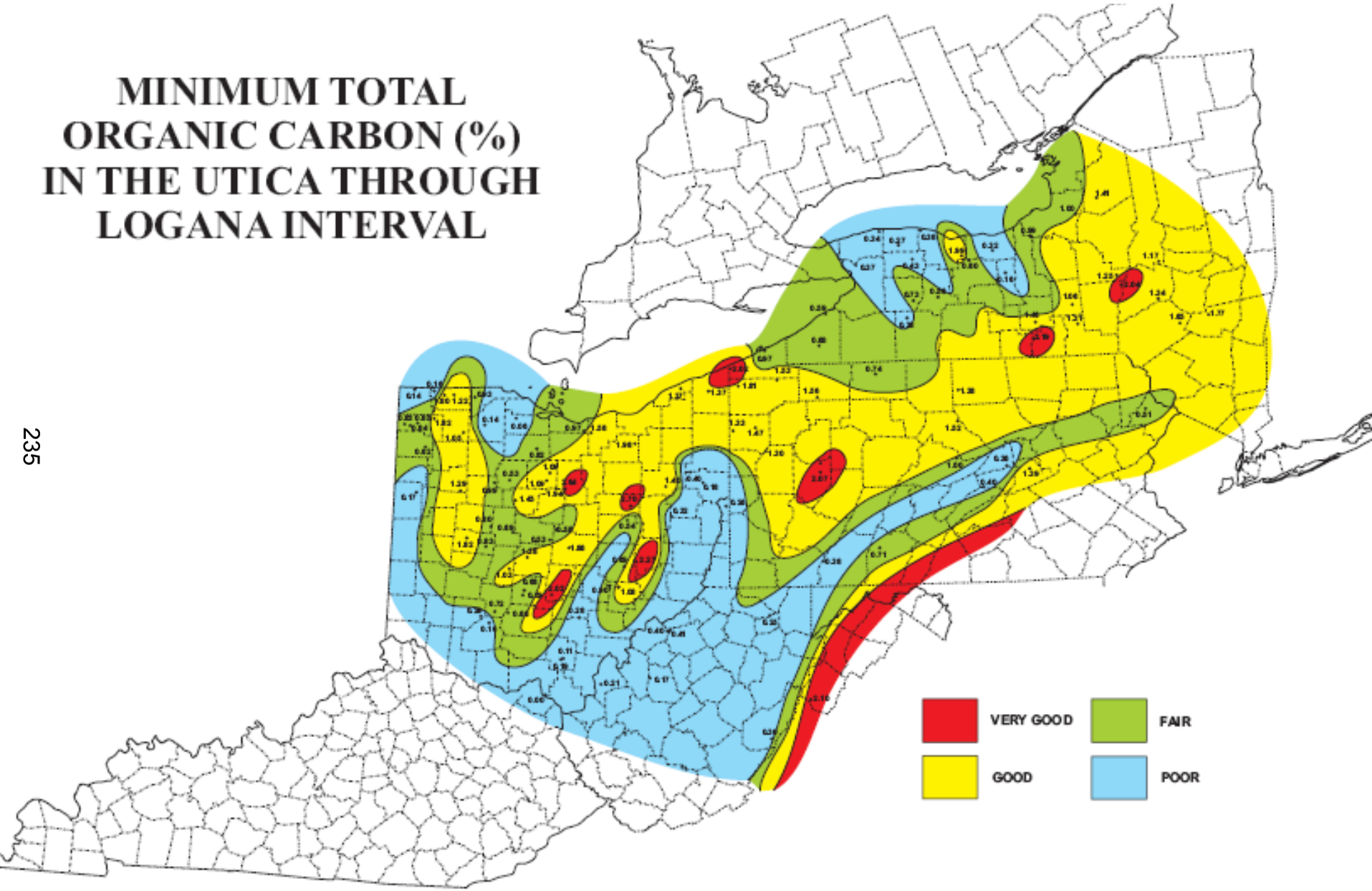
MINIMUM TOTAL
ORGANIC CARBON (%)
IN THE UTICA THROUGH
LOGANA INTERVAL
VERY GOOD
FAIR
GOOD
POOR

Figure 7-4.

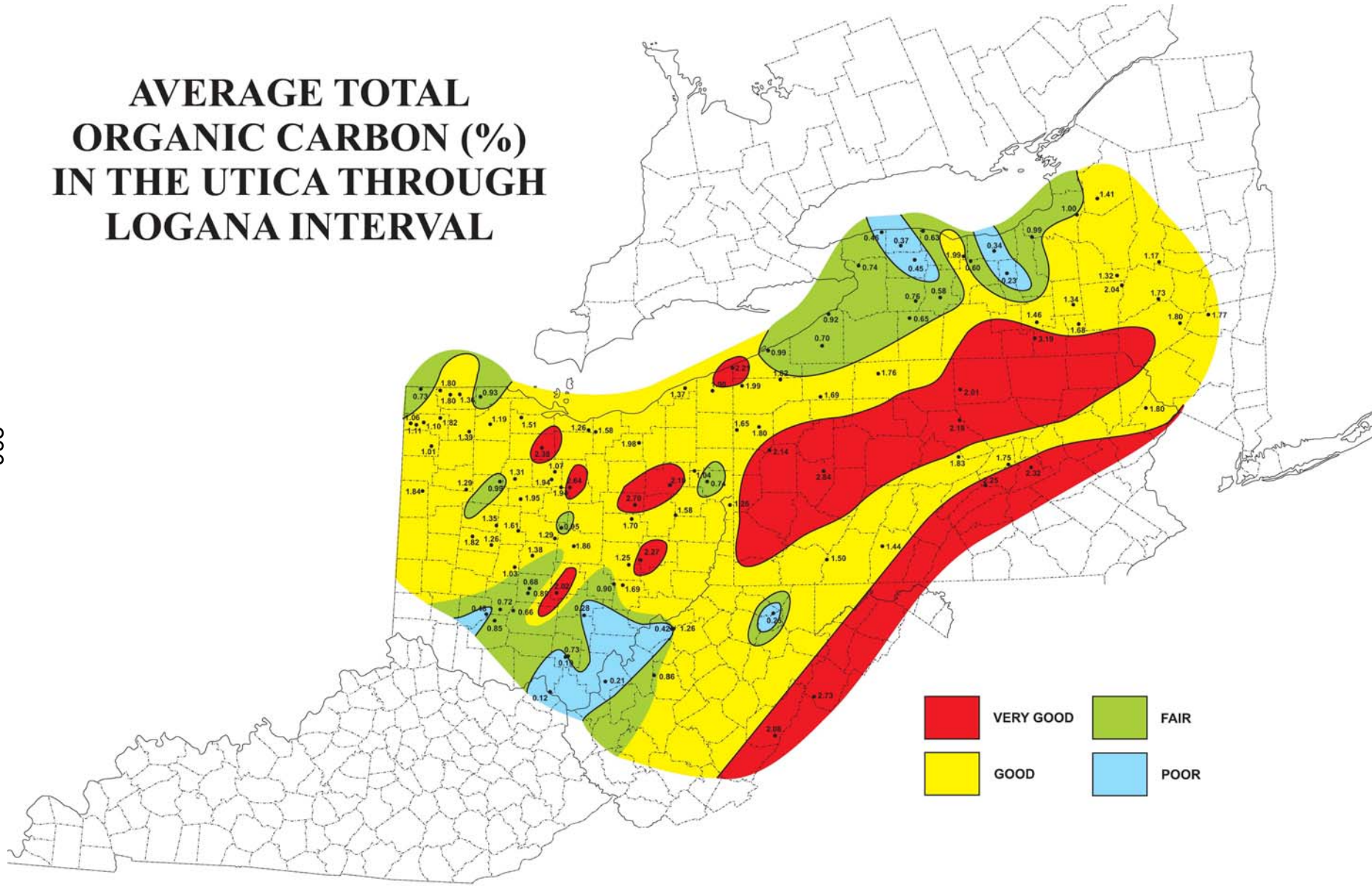
AVERAGE TOTAL
ORGANIC CARBON (%)
IN THE UTICA THROUGH
LOGANA INTERVAL
VERY GOOD
FAIR
GOOD
POOR

Figure 7-5.

rock or rocks. TOC data for deeper Cambrian rocks, such as the Rome Formation, have indicated at least a limited source rock potential in these deeper beds (see Ryder et al, 2003). TOC data from 28 deep wells in the basin indicate that in 11 of the 28 wells, TOC values were greater than 0.5% in the Beekmantown Formation and deeper formations. The highest values are 4.4% from the Rogersville Shale in a Wayne County, West Virginia deep well; 3.26% from the Rome Formation in Kentucky, 2.83% and 1.12% from the Conasauga Formation in West Virginia, and 1.17% from the Beekmantown Formation in Pennsylvania. Other TOC values range from 0.57% to 0.88% (unpublished data from the Rome Trough Consortium and the Pennsylvania Geological Survey).

Thermal Maturity (CAI)

Two maps of estimated thermal maturity were produced by contouring the minimum (Figure 7-6) and maximum (Figure 7-7) values reported by previous workers for conodont alteration index (CAI) data. If only one value was reported, that value was used as a control point on both maps. In general, the maps indicate lower CAI values (1-2) to the west in Ohio and Ontario that gradually increase eastward into New York, Pennsylvania and West Virginia. Ultimately, the CAI values exceed 5 along the eastern margin of the basin, indicating that this area is overmature. A comparison of the final maturation maps with the map of TOC data further refined the area of gas potential. The maps also show an area in central New York where the HTD fields occur that appears to indicate an almost linear thermal anomaly. Both maps suggest that the HTD trend may have been significantly hotter at one time than the surrounding area of New York and Pennsylvania, increasing CAI values to 4.5 to 5.0. Although similar linear trends shown on the TOC maps seem to confirm that this is not simply a figment of spotty data, the exact nature of the phenomenon is uncertain at this time.

Our model for field development in the Trenton-Black River play is based on vertical or nearly vertical faults extending to the basement through which hot fluids could rise to the level of the carbonate units to produce hydrothermal dolomite reservoirs. Thus, the timing of these separate events - faulting, upwelling, hydrothermal dolomite development - as well as the timing of when source beds entered the oil generating and eventually the gas generating windows, are important. Based on the work of Elizabeth Rowan (personal communication) at the U.S. Geological Survey, the potential Ordovician source rocks entered the oil window 390 million years ago during the Devonian Period, and with deeper burial, then entered the gas window 360 million years ago, still in the Devonian.

The final maps of CAI data, in conjunction with profiles of thermal maturity along cross section lines based on deep wells, were used to draw boundary lines between areas of oil generation; gas generation; overmaturation; and immature source rocks (Figure 7-8). Oil fields to the west, in the area of immature source beds, must have been charged by oil that migrated up dip from an oil-generating area. Likewise, gas fields to the west, in areas that fall into the oil window and immature areas, must have been charged by gas migrating up dip from gas-generating areas farther to the east.

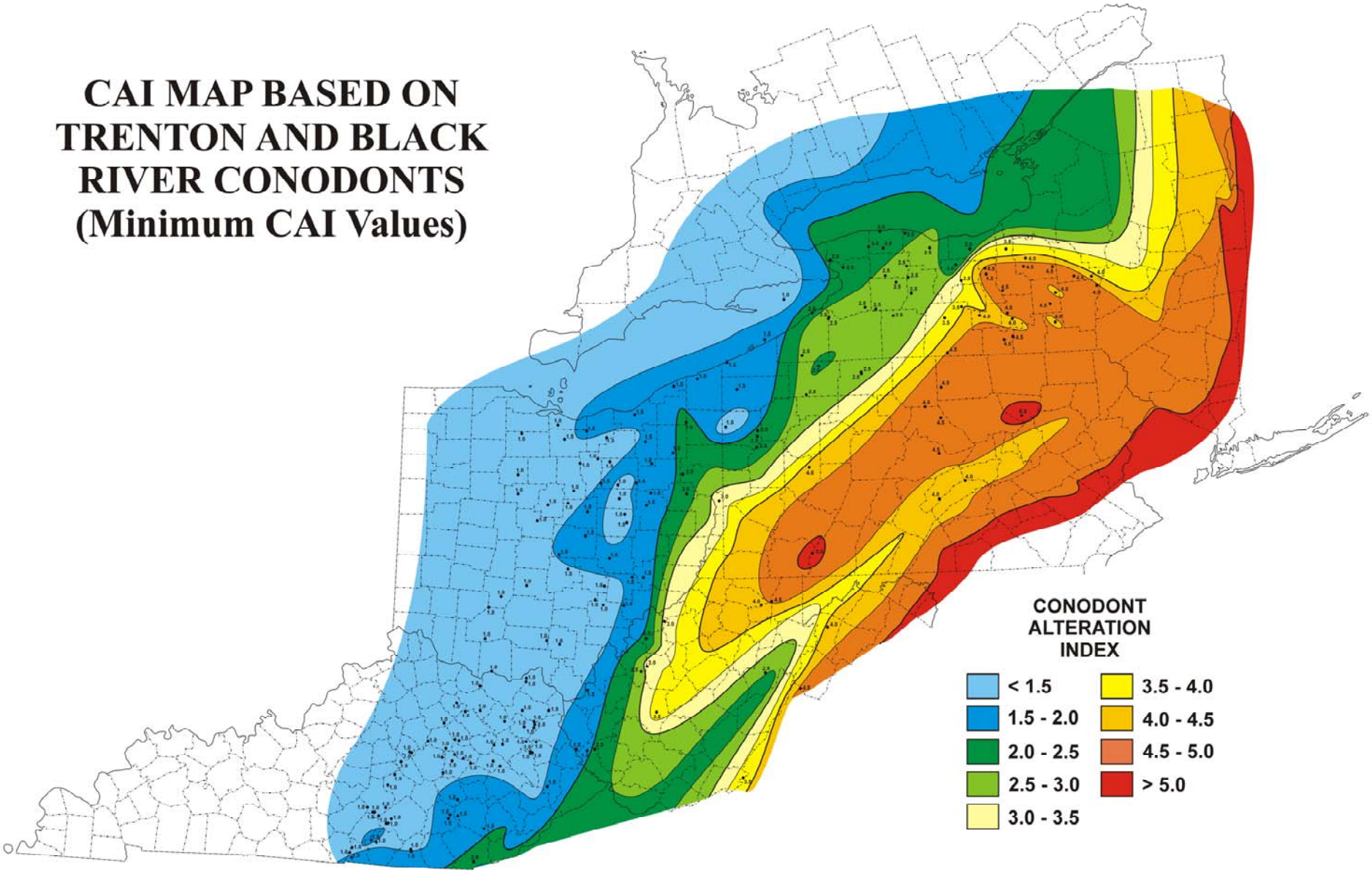
CAI MAP BASED ON
TRENTON AND BLACK
RIVER CONODONTS
(Minimum CAI Values)
CONODONT
ALTERATION
INDEX
< 1.5
1.5 - 2.0
2.0 - 2.5
2.5 - 3.0
3.0 - 3.5
3.5 - 4.0
4.0 - 4.5
4.5 - 5.0
> 5.0

Figure 7-6.

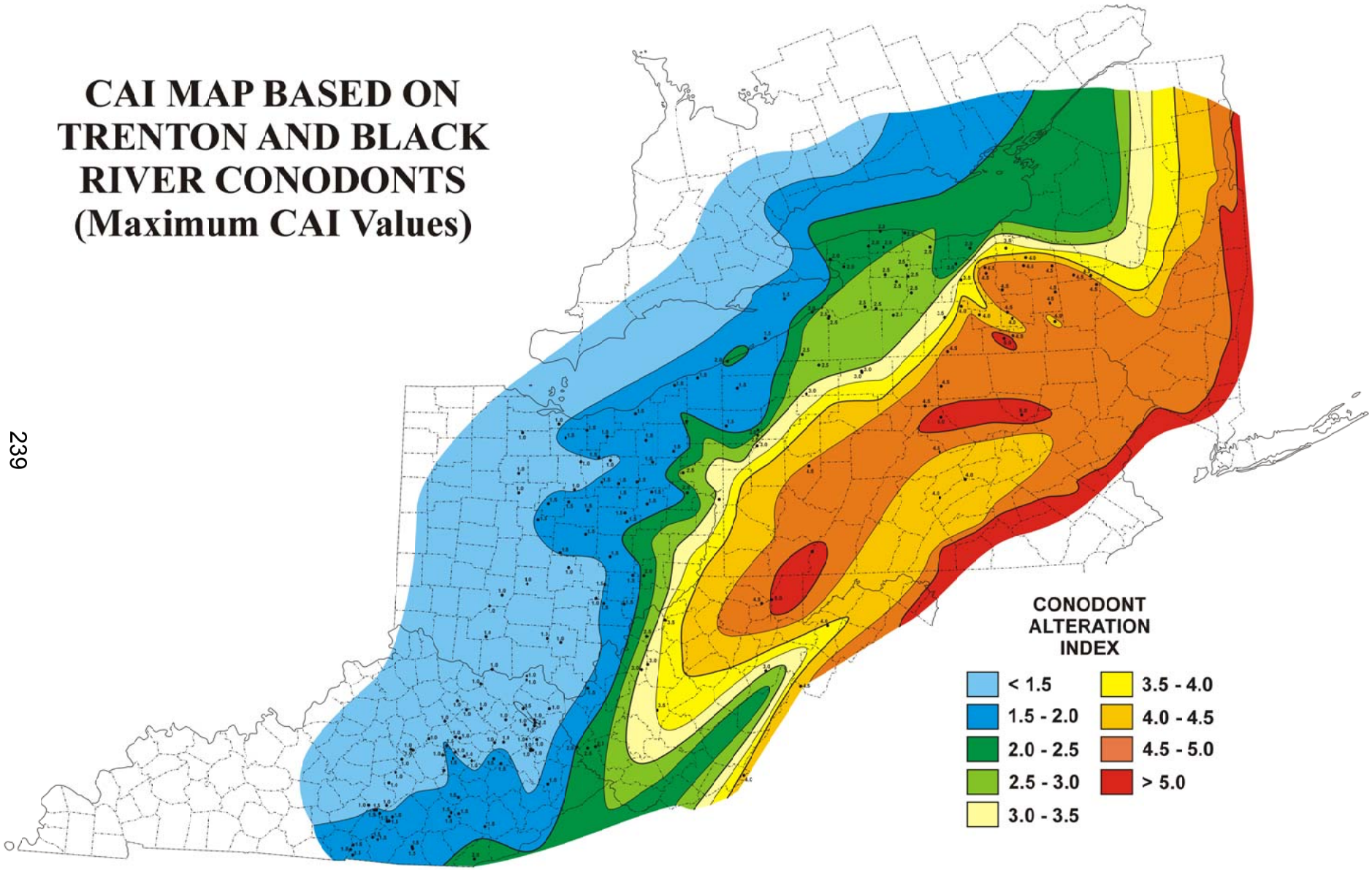
CAI MAP BASED ON
TRENTON AND BLACK
RIVER CONODONTS
(Maximum CAI Values)
CONODONT
ALTERATION
INDEX
< 1.5
1.5 - 2.0
2.0 - 2.5
2.5 - 3.0
3.0 - 3.5
3.5 - 4.0
4.0 - 4.5
4.5 - 5.0
> 5.0

Figure 7-7.

Figure 7-8

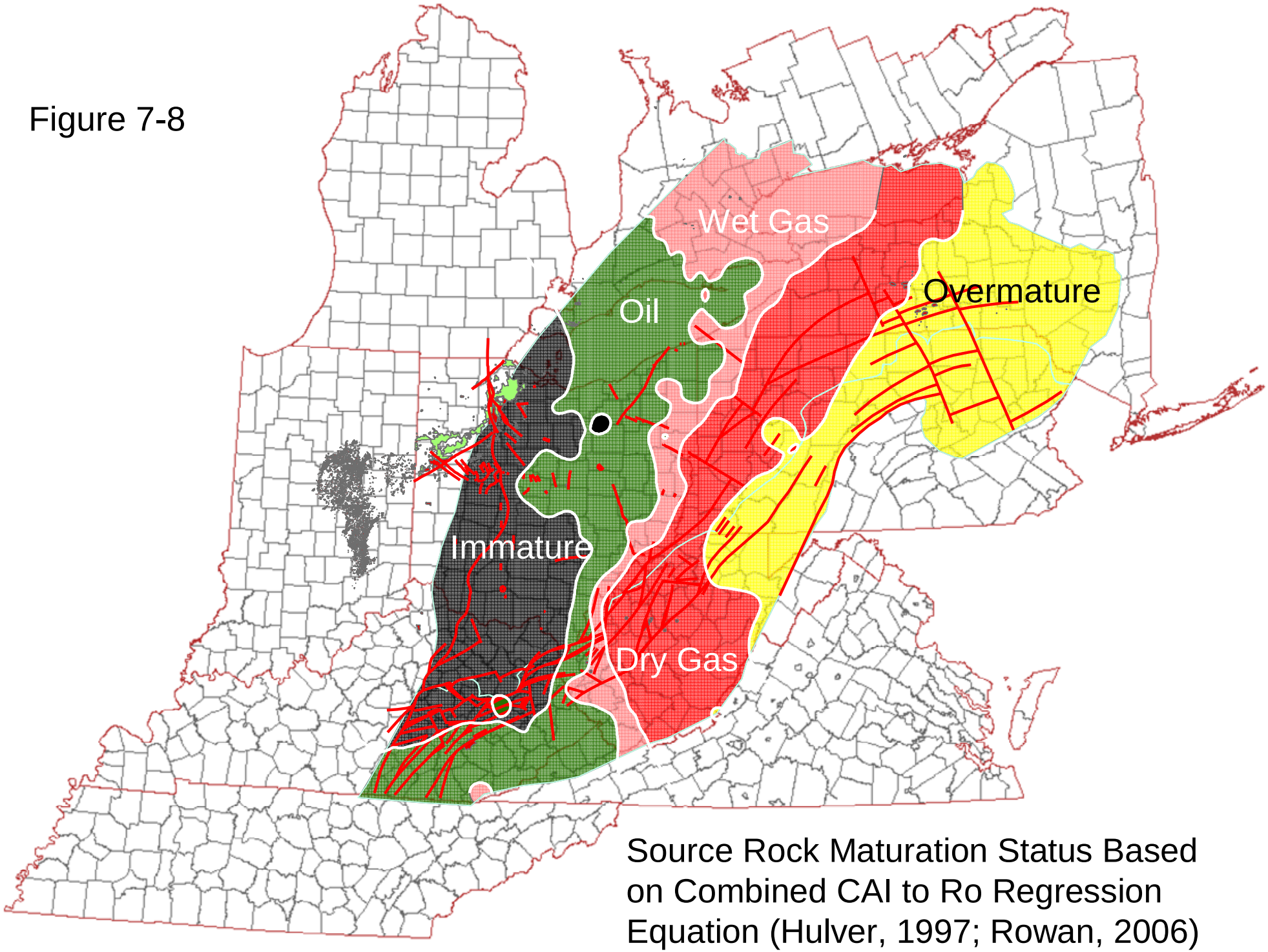

Source Rock Maturation Status Based on Combined CAI to Ro Regression Equation (Hulver, 1997; Rowan, 2006)

Play Areas

Hydrothermal dolomite reservoirs develop where hot saline fluids rise from the basement along faults or fractures to reach the host limestone beds that are then altered to dolomite. If one begins with the assumption that the energy available to cause these fluids to rise is essentially the same in different areas of Trenton and Black River deposition, then the vertical distance through which the fluids must rise becomes a significant factor. In areas where the sediment package between the top of the basement and the Trenton-Black River carbonate section is thinner, the fluids could rise to their level. However, in areas where the interval between the basement and the Trenton-Black River carbonate interval is much thicker, perhaps many thousand feet thicker, then the fluids may not have been able to rise to the level of the Trenton and Black River to alter host limestones to hydrothermal dolomite.

Thus, whereas organic-rich shales must have passed through the gas-generating window to become source beds, limestones in the Trenton and Black River must have passed through this "HTD window," i.e., have been close enough to the basement that rising fluids could reach them, in order to have HTD reservoirs developed within them.

How high did these hot dolomitizing fluids rise above the basement? This can be estimated by plotting the locations of all wells in which HTD has been encountered, and mapping the top of the HTD interval. This will yield an estimate of maximum rise of fluids at various locations, when depth to basement is taken into consideration. The resulting map will be a surface representing this maximum height of fluid movement. Then, by mapping the thickness of the sediments between the basement and the TBR interval (Figure 7-9) and comparing the two maps, we can delineate between areas where the TBR interval was within the HTD window, and areas where the fluids did not rise high enough to alter the limestones in these units. Thus, we can then estimate undrilled areas that would fall into the HTD play, and areas that would be restricted to the fractured limestone play. However, in the areas of fractured limestone at the level of the TBR, HTDs may exist at deeper levels in Beekmantown or other Cambrian carbonates, i.e., the Rome, Copper Ridge or Gatesburg.

Three TBR play areas were defined: a HTD play to the west in Kentucky, Ohio and Ontario that extends eastward into south central New York; a fractured limestone play above the Rome Trough and eastward to the edge of the assessment area; and two areas to the extreme northeast in New York and the extreme southwest in Kentucky, where gas is produced from bioclastic limestones in the Trenton Formation.

Figure 7-10 outlines the two most important play areas, the HTD and fractured limestone plays. To complete this map of TBR play areas, we added the locations of known HTD producing fields, fields that produce from fractured limestones and fields that produce from bioclastic limestones.

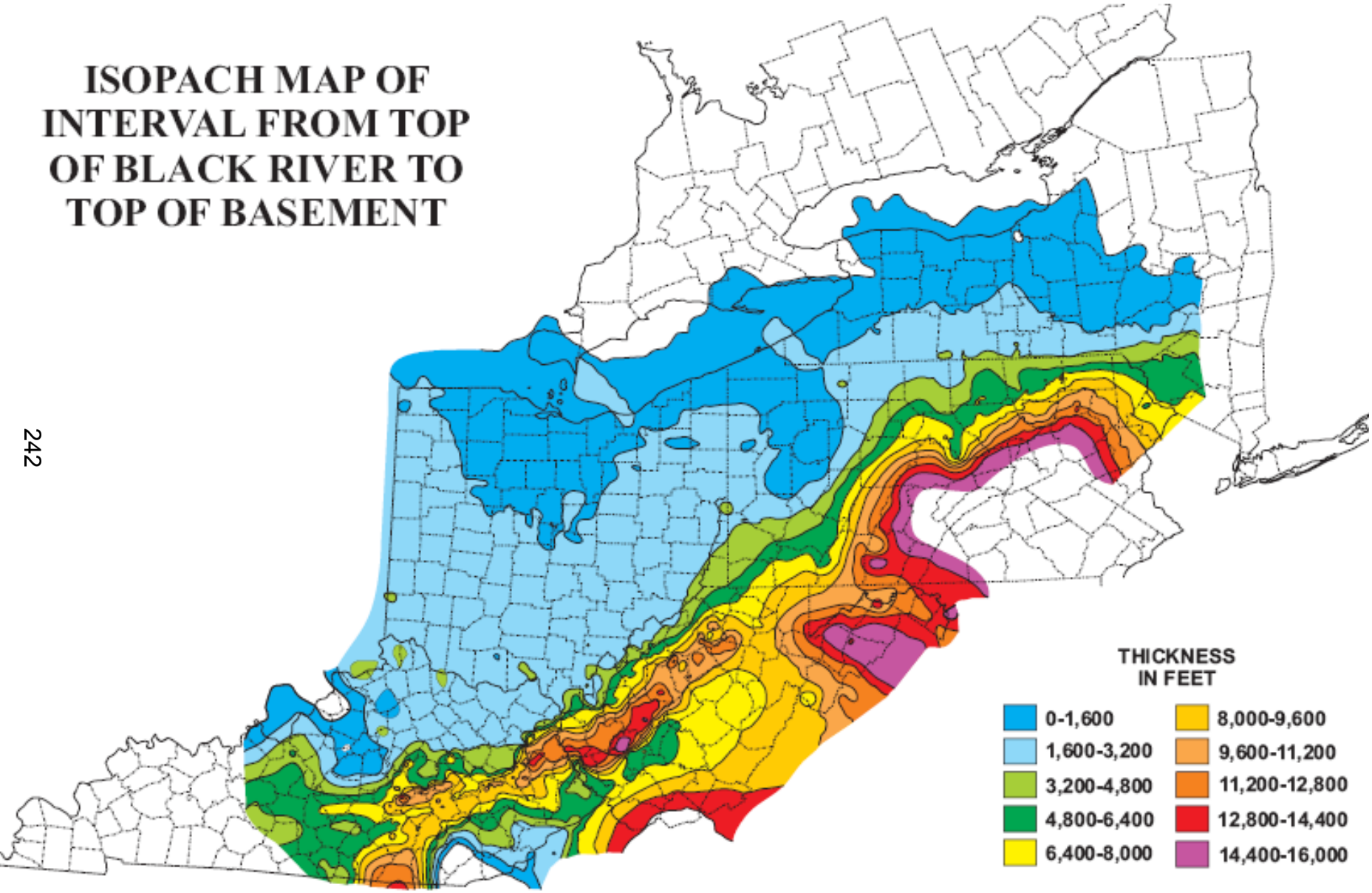
ISOPACH MAP OF
INTERVAL FROM TOP
OF BLACK RIVER TO
TOP OF BASEMENT
THICKNESS
IN FEET
0-1,600
1,600-3,200
3,200-4,800
4,800-6,400
6,400-8,000
8,000-9,600
9,600-11,200
11,200-12,800
12,800-14,400
14,400-16,000

Figure 7-9.

Play Boundaries

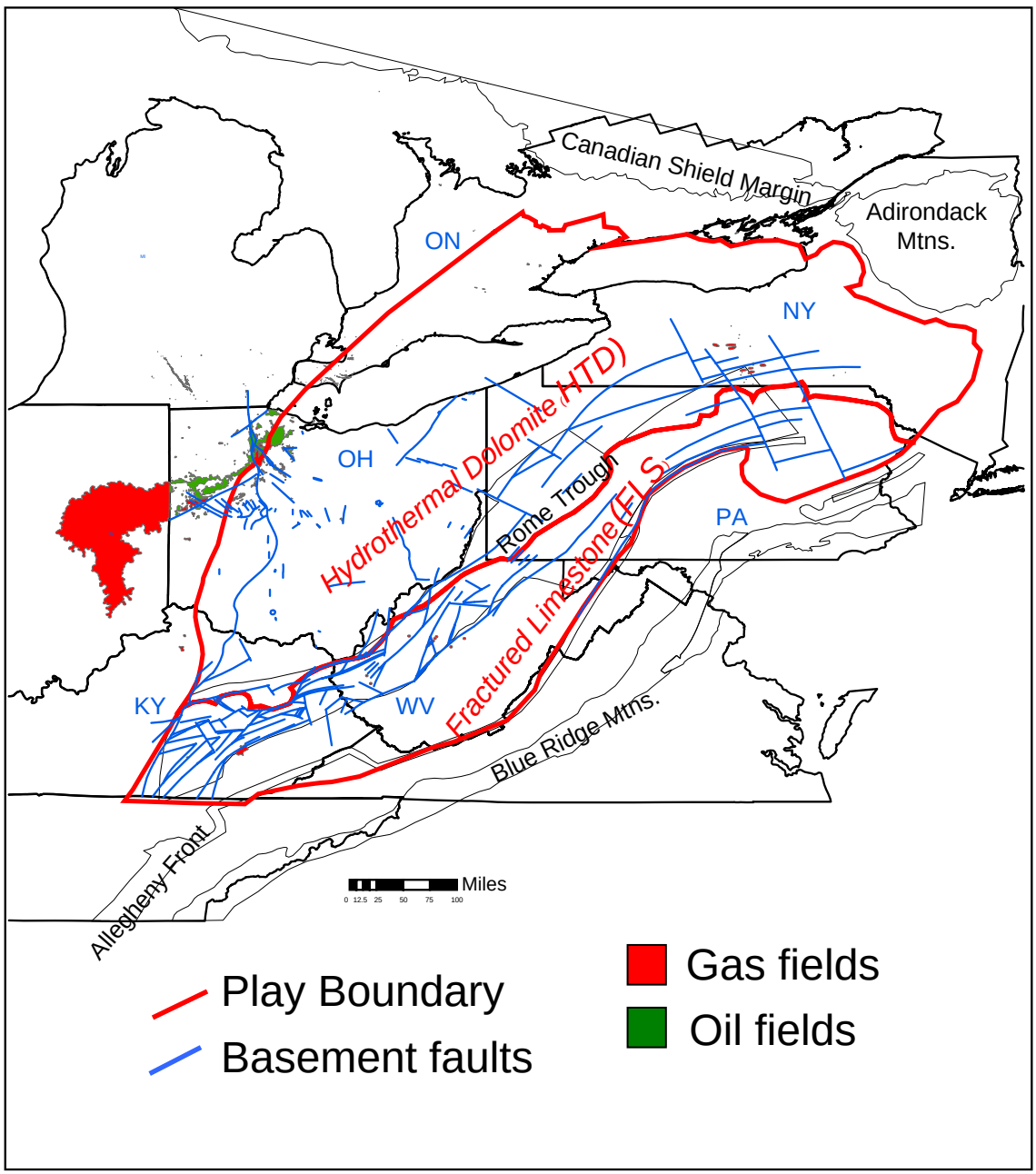

Figure 7-10.

Trenton fields in New York and Kentucky that produce from bioclastic limestones have been described in the "Atlas of Major Appalachian Gas Plays" (Roen and Walker, 1996). The two fields in Oswego County, New York were developed more than 40 years ago. According to Art Van Tyne (personal communication) an examination of cable tool sample sets from the Pulaski and Big Sandy fields did not reveal any indication of HTD or of fractures that would be necessary to develop HTD or a fractured limestone reservoir. Instead, gas entry to the well bore coincided with the occurrence of thin, "shelly" zones with good porosity. The typical well blew down quickly, from one to two million cubic feet to very low volumes in a few hours. However, though many wells held up long enough to be placed on line, their productive life was quite short. Approximately 200 wells were drilled in these two fields.

Because the area of bioclastic limestone reservoirs is quite small, the wells and fields have shown limited potential, and any data already are available through the "Atlas of Major Appalachian Gas Plays," we did not assess this play.

Assessment Areas

A viable assessment of the play areas begins with an assessment of the source rock to determine areas with the greatest potential. TOC values can be used to condemn portions of the shale source rock, as shown on isopach and isolith maps. Maturation data, from CAI data and burial history diagrams/thermal maturity profiles, enabled us to determine boundaries between immature areas and oil- generating areas; oil- and gas-generating areas; and gas-generating and overcooked areas, effectively condemning some areas and defining the limits of prospective areas in which oil and gas were generated.

Therefore, a play area, as defined earlier in the process, in combination with a viable source rock area as determined by maps of TOC and CAI, will yield an assessment area. However, we needed to add to this assessment area those areas of gas production to the west, where gas from a source closer to the center of the basin migrated up dip and pushed the play boundary toward the arches that define the western extent of the basin.

"**Sweet Spots," Play Extensions and In-fill Areas**

The final map of play assessment areas includes, at the basin scale, small areas of known production separated by much larger, undrilled areas of future potential. However, not all of the areas share the same risk. This is because the known productive and undrilled resource areas can be separated into "sweet spots" where known production is better, less productive areas, in-fill areas where future drilling can continue to develop productive areas, and play extension areas, where future drilling can extend the known play with greater certainty than completely undrilled areas farther from existing production. All of these areas can be mapped and risked, based on geology and a geologist's imagination. All three areas – "sweet spots," in-fill and extensions - affect risk analysis and allow for future play growth.

The boundary between the HTD play area to the west and the FLS play area to the east is convex westward at its northern end in New York and Pennsylvania (the Pennsylvania salient), but shifts to concave to the west in Ohio and West Virginia (Virginia recess), and then convex to the west in Kentucky (Tennessee salient). Long northwest-southeast trending faults that cross this boundary would be expected to be open in area where the arcuate boundary is convex (salients), and closed where the boundary is concave (recesses). Thus, larger, more productive HTD fields could be expected in the northeastern end of the HTD play assessment area, and smaller, less productive fields would be expected in the southwestern end of the area.

The same could be expected for fractures in the TBR that are associated with the underlying Rome Trough. In areas where the curvature of the Rome Trough is convex, the fractures would be expected to be more open than fractures in areas where the curvature is concave. Thus, along the trend of the trough, one would expect different results in different places.

A quick examination of the basement fault map would lead one to assume that all of the real potential in the fractured limestone play would be confined to the area above the Rome Trough, and that there would be little potential in the broad area to the east up to the edge of the play area. However, because gas has been encountered in the Trenton in this eastern area it must be assessed as having some potential, although probably much less than the western border of the fractured play area. During the early 1960s Cities Service Oil Company drilled deep exploratory test wells in Pocahontas and Randolph counties, WV that tested gas from the Trenton, as well as the Oswego Sandstone, Martinsburg Shale, Utica Shale and Black River Limestone. Gas flowed at rates of 1.3 MMcfpd and 3 MMcfpd from these wells, but one well blew down within a few hours, and the other within a week. A lower (Black River?) zone in the Randolph County well tested more than 4 MMcf after being perforated and acidized, but blew down to 192 Mcf in 28 hours.

The Trenton Limestone also was perforated and acidized in deep tests in Marion and Preston counties, West Virginia, but again, gas flows did not hold up. However, the presence of gas in the TBR in these four counties provides enough evidence to suggest that the fractured limestone play should be extended eastward into the area of folding adjacent to the Allegheny front.

Although a deep Cambrian test well in Armstrong County, Pennsylvania encountered several shows of gas in the Utica Shale, including one measured at 10 MMcfpd, none of the wells within the known area of the Rome Trough in Pennsylvania has ever encountered a noticeable flow or show of gas or oil from the Trenton or Black River limestones. Small shows have been encountered in the Trenton and/or Black River in wells in Juniata, Mifflin and Union counties in the Appalachian Ridge and Valley of central Pennsylvania, and in Pike County in the extreme northeastern corner of Pennsylvania, but these areas do not appear to be within the known limits of the Rome trough.

Estimating Undiscovered Field Number and Size Distribution

The most challenging step in the assessment process was to reach a group consensus on the number of fields that reasonably can be expected to be discovered in each of the TBR plays during the next 30 years, and a reasonable range in the expected size of these fields. However, before any resource values can be estimated, this process must be completed as a group dynamic.

Many factors were considered during this discussion. In addition to all of the maps described above that depict the geology of the area and annual well production data used to reconstruct the production history of the play, other data were used to allow us to make reasonable estimates. Graphs of the number of fields discovered over time and size of fields discovered versus time (see below) clearly indicated that this is an emerging frontier play that is still in its infancy. In fact, it is such a young play that adequate production histories do not exist to allow us to fully evaluate the size of fields that already have been discovered. Instead, it was necessary to "grow" the fields, based on the number of producing wells and the years of production, for fields that apparently have been fully drilled to their productive extent.

Fractured Limestone Play

Twenty two named gas fields have been discovered in the area now designated as the fractured limestone gas play. Most of these fields (20) have produced between 500 Mcf and 500 MMcf of gas; the largest has produced more than 10 Bcf. For the purposes of our resource estimate, we initially considered only including the number of undiscovered fields that would produce at least 2 Bcf of gas, although only one field currently in production has produced more than that amount. After much further discussion and examination of regional geology, drilling and discovery patterns and production histories, the group determined that the minimum size of any undiscovered field would be at least 2 Bcf, the maximum size of any undiscovered field would not exceed 100 Bcf, and the median field size would be 25 Bcf.

Twenty two (22 fields) already have been discovered in the fractured limestone play area in the last ten years. Based on this fact, the group felt comfortable in assuming that at least 5 more fields would be discovered in the first 30 years of this play development. Agreeing on an upper limit was more difficult, but eventually the group agreed that 150 was a reasonable number and that 30 is a reasonable number for the median. In reaching this agreement, the group took into consideration the facts that early discoveries often were associated with deeper Rose Run Sandstone exploration where the Trenton was not the target as it would be in the future development of the play, and that newer exploration technology already exists and will continue to be developed in the near future to accelerate field discoveries. The group also considered that there is some potential for TBR fields to be discovered in the eastern part of the play area, on each of the anticlines where gas fields have been developed in the younger Oriskany Sandstone, and where gas shows have been encountered in the Trenton and Black River.

Hydrothermal Dolomite Play

Thirty eight (38) oil and gas fields have been discovered in the HTD play area, 22 of which have been discovered in the past 30 years. Of the 38 fields, 26 are gas fields. Most of these relatively young fields (25) have produced between 50 MMcf and 50 Bcf; only one small field (more than 5 MMcf) is included in the data set. Twenty of the 26 already have produced at least 0.5 Bcf of gas, and 14 have produced at least 1 Bcf, leading us to conclude that eventually most, if not all, will reach the 2 Bcf cutoff value in cumulative production.

Our attempt to reach agreement on the upper limit of field size in this play created an interesting discussion, essentially a debate on what would, in the future, be considered to be a "field." If a number of small 8-10 well fields were discovered and developed in the same area, separated only by faults, then eventually, when the entire larger area was all drilled and developed, the final result might be something similar to the Albion-Scipio trend, a giant field with perhaps 3 Tcf potential. Eventually, several of these giant fields might be developed, each created by merging dozens of smaller fields into one giant field with hundreds of wells. However, it was equally logical to assume that these fields would be separated by large areas in which many typically small, 8-10 well fields would be found that would not merge into a giant field. So we were faced with two separate field size models for undiscovered fields: one with perhaps hundreds of relatively small fields bounded by faults that did not merge into a larger giant field; and a second model with a few giant fields and hundreds of small fields, or one Albion-Scipio for every 100 Glodes Corners Road Field.

We also considered that the HTD play area perhaps should be assessed separately in two areas and then the separate values should be added together. The northeastern end of the play, in New York and Pennsylvania, is expected to be an area of extension, where faults and fractures will be more open than the area to the southwest, where the faults and fractures are expected to be closed. Thus, it is reasonable to conclude that fields in the northeast might be both more in number and larger in size than undiscovered fields to the southwest. However, after determining separate sets of values for field number and size in each area, the group agreed to assess the entire play area as one assessment unit.

Eventually, the group determined that the least likely number of undiscovered fields would be 20, the maximum number would be 400, and the median number would be 100. As for field size, the smallest field was assumed to have 2 Bcf that would be produced, the largest 100 Bcf, and the median field size was determined to be 25 Bcf. Support for this was provided by Talisman, who estimated that Quackenbush field, the best field discovered so far in New York, will probably produce 150 Bcf. Thus, the group was speculating that there is a 10% probability that at least one more Quackenbush field to be discovered.

Production Statistics

Two types of graphs for assessing future oil and gas resources of the Trenton-Black River plays are shown below. The first set of graphs (Figures 7-11 and 7-12) shows total cumulative production by year. From the graph of annual gas production in the hydrothermal play one can conclude that there is still much gas to be found. The same graph for the limestone play suggests that much gas remains, but the large discoveries might already have been made. However, the trend is far from approaching an asymptote. Perhaps with more complete data and further technological developments leading to new field discoveries or improved production, the points representing annual production will more closely resemble the hydrothermal dolomite play.

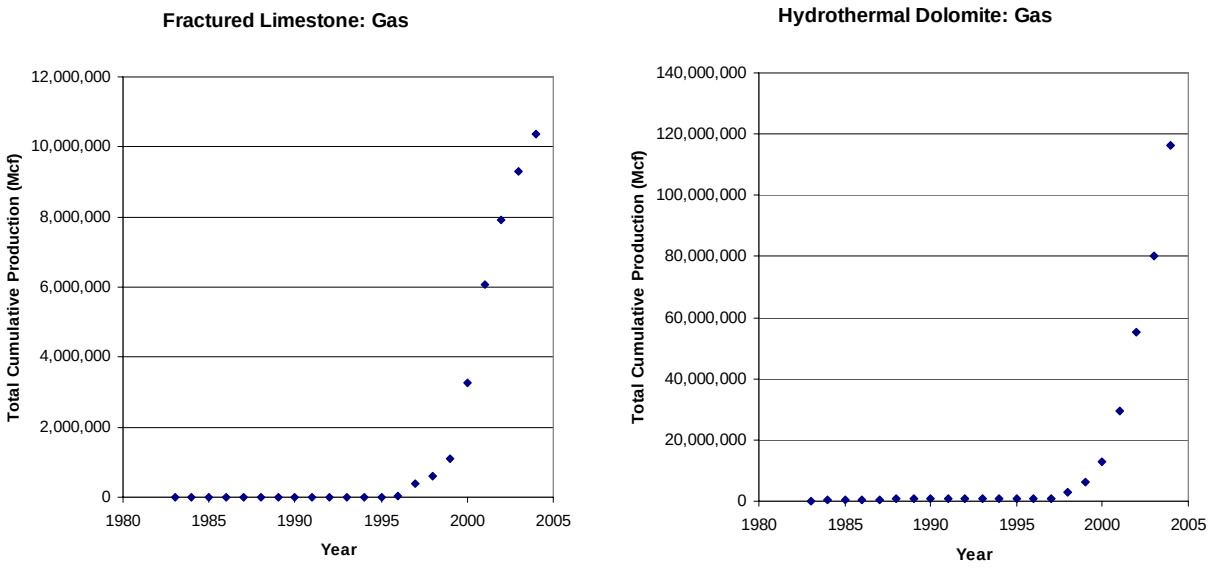

Figure 7-11.

Three oil plays in the Trenton/Black River interval provide enough data for graphing. In this case, the fractured limestone play appears to hold the greatest potential for future discovery of oil.

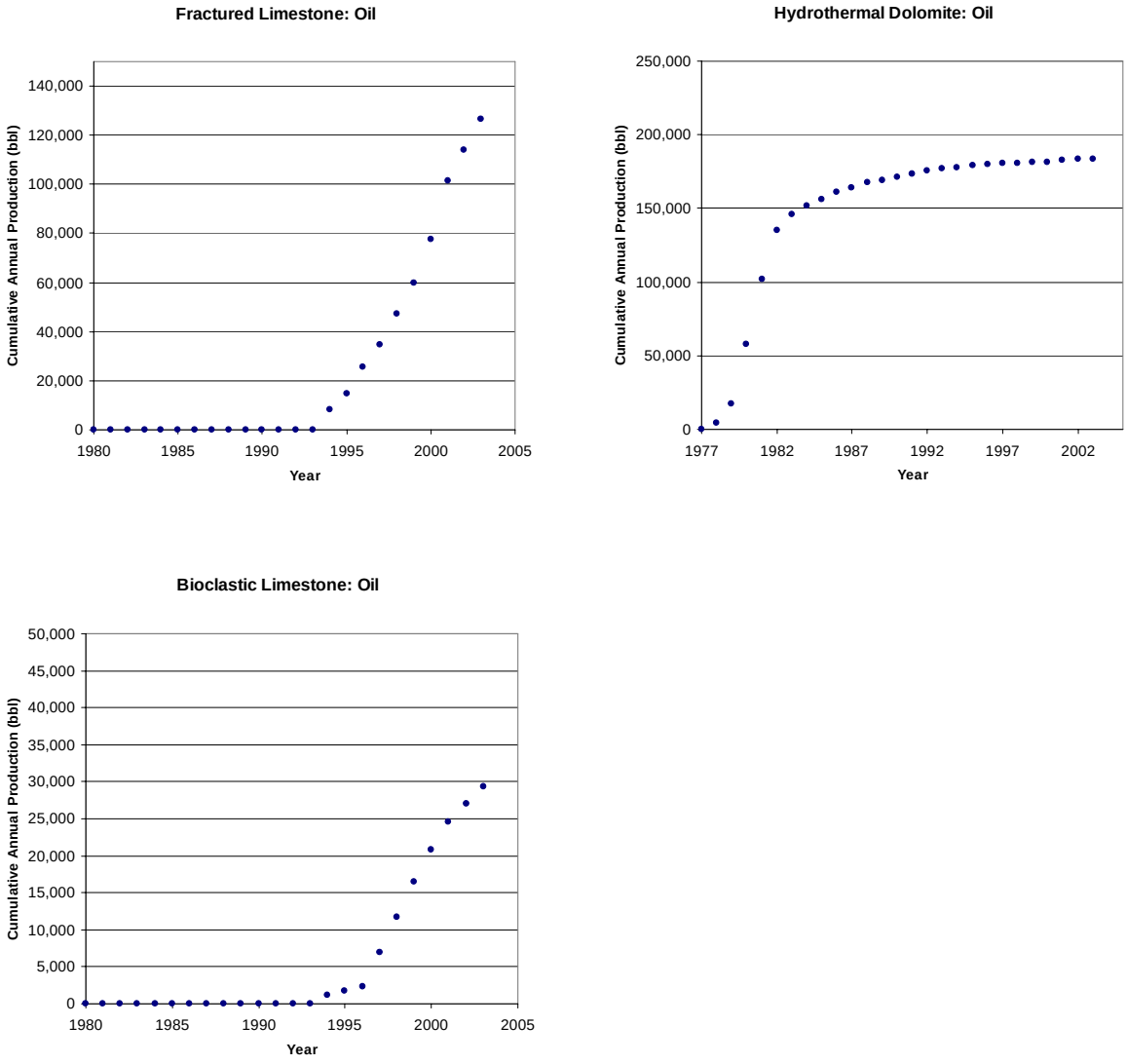

Fig. 7-12.

The second set of graphs (Figures 7-13 and 7-14) shows cumulative production by field. Histograms of total gas production by field are highly skewed, suggesting that for both plays many medium-sized fields remain to be discovered.

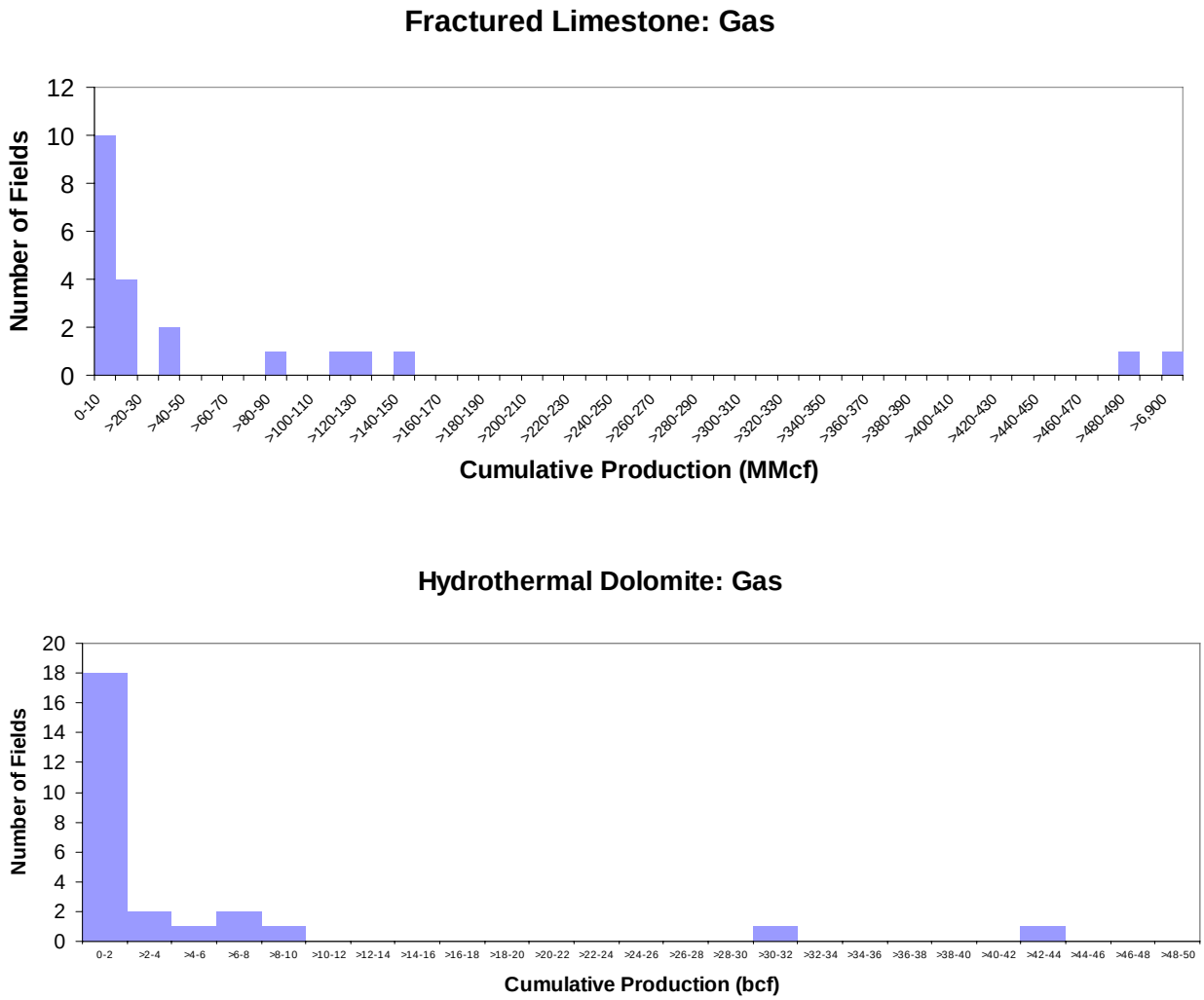

Fig. 7-13.

Histograms for oil production show a similar situation for the hydrothermal dolomite and fractured limestone plays. The results suggest that incomplete data account for the apparent fall-off in oil production from the hydrothermal dolomite play, or that oil fields of moderate size remain to be discovered in this play.

These graphs as well as geological variables cited above provided input to the resource assessment reported in the next section.

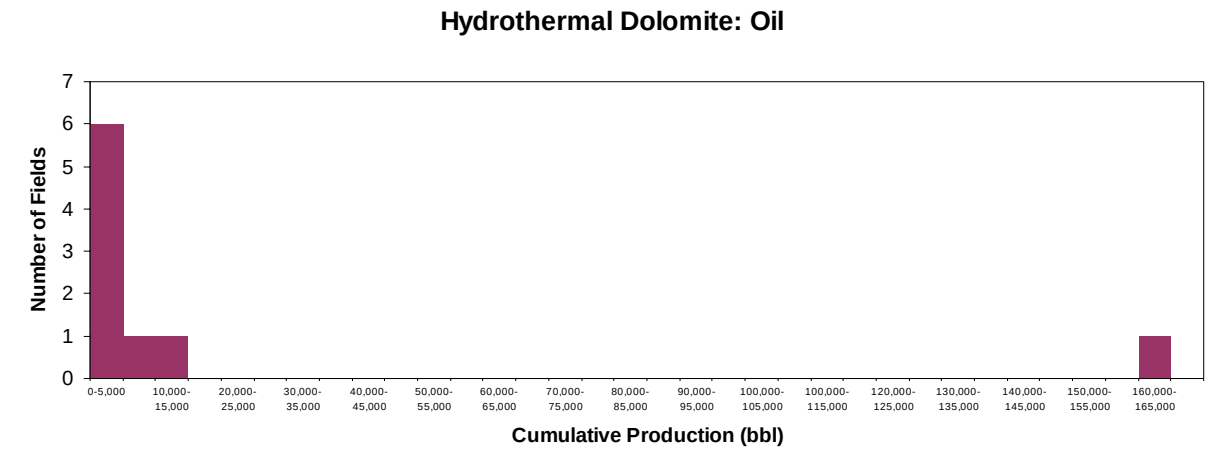
Hydrothermal Dolomite: Oil
Number of Fields
0
1
2
3
4
5
6
7
0-5,000
10,000-15,000
20,000-25,000
30,000-35,000
40,000-45,000
50,000-55,000
60,000-65,000
70,000-75,000
80,000-85,000
90,000-95,000
100,000-105,000
100,000-115,000
120,000-125,000
130,000-135,000
140,000-145,000
150,000-155,000
160,000-165,000
Cumulative Production (bbl)

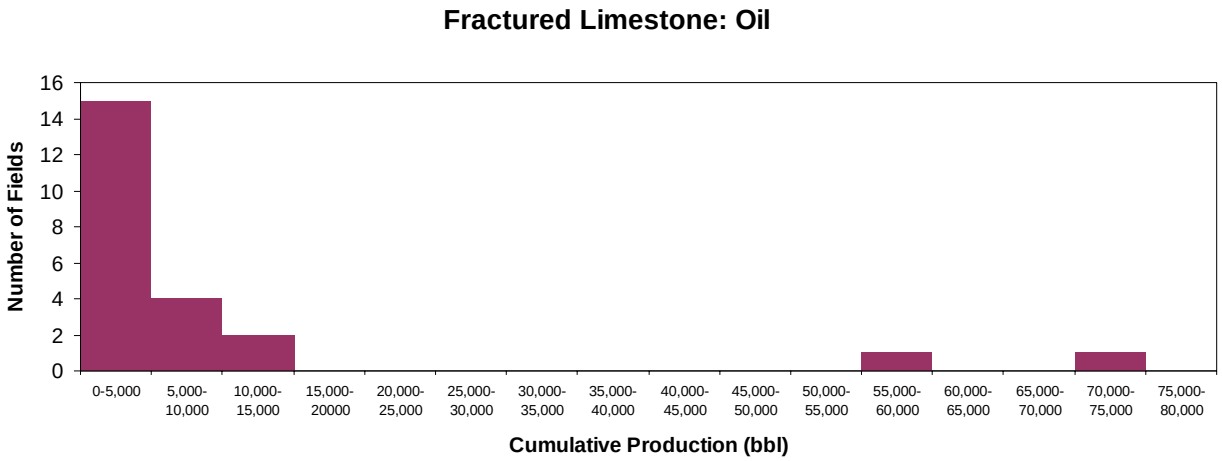
Fractured Limestone: Oil
Number of Fields
0
2
4
6
8
10
12
14
16
0-5,000
5,000-10,000
10,000-15,000
15,000-20000
20,000-25,000
25,000-30,000
30,000-35,000
35,000-40,000
40,000-45,000
45,000-50,000
50,000-55,000
55,000-60,000
60,000-65,000
65,000-70,000
70,000-75,000
75,000-80,000
Cumulative Production (bbl)

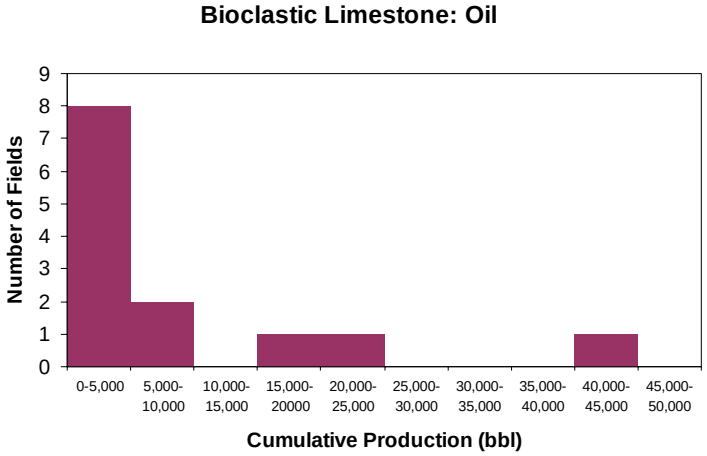
Bioclastic Limestone: Oil
Number of Fields
0
1
2
3
4
5
6
7
8
9
0-5,000
5,000-10,000
10,000-15,000
15,000-20000
20,000-25,000
25,000-30,000
30,000-35,000
35,000-40,000
40,000-45,000
45,000-50,000
Cumulative Production (bbl)

Fig. 7-14.

Monte Carlo Simulation; Determination of Resource Values

Undiscovered gas resources were estimated through a Monte-Carlo simulation method developed by the U.S. Geological Survey (Charpentier and Klett), using the Emc2 program. The procedure requires geologists to estimate the number of undiscovered fields, and the sizes of those fields. Actual input to Emc2 comprises the minimum, median, and maximum number of fields, and similarly the minimum, median, and maximum size of undiscovered gas fields (Table 1). Emc2 also allows risk-qualified estimates of resources, but this feature was not used in this study.

These graphs as well as geological variables cited above provided input to the geologists that estimated the undiscovered field numbers and sizes through discussions and development of a consensus.

Emc2 uses a triangular distribution for number of undiscovered gas fields and a lognormal distribution for size of undiscovered fields. The program samples these two distributions to obtain a probability distribution of undiscovered gas resources (Table 2).

Play	No. Undiscovered Fields			Size of Undiscovered Fields		
	Minimum	Median	Maximum	Minimum	Median	Maximum
Fractured Limestone	5	30	150	2	25	100
Hydrothermal Dolomite	20	100	400	2	25	100

Table 7-1. Input Parameters for Resource Assessment

Play	F90 (BCFG)	F50 (BCFG)	F10 (BCFG)
Fractured Limestone	652.64	1,561.11	2,988.04
Hydrothermal Dolomite	2,064.11	4,446.46	8,073.48
TOTAL	2,716.75	6,007.57	11,061.52

Table 7-2. Total Undiscovered Resources

The Appalachian basin members of the Potential Gas Committee went through a similar exercise in 2005. During that process, a small working group assessed the two Middle Ordovician carbonate play areas described in the “Atlas of Major Appalachian Gas Plays” (Roen and Walker, 1996). The PGC estimated that at a minimum, 2.5 Tcf

would be discovered in these two plays, and at a maximum, 8.5 Tcf would be discovered. The most likely volume of gas that would be discovered, according to the PGC, is 5.4 Tcf. These PGC estimates, which were not available to our working group during this process, are actually quite close to the estimates provided by the Trenton-Black River Research Consortium.

Acknowledgment

The members of the resource assessment team would like to acknowledge the assistance of Christopher Swezey, Elizabeth Rowan and Jim Coleman of the U.S. Geological Survey, who met with us on several occasions to lead us through the assessment process and facilitated the group discussion during the Monte Carlo simulation process that led up to the calculation of the final resource numbers. We also would like to acknowledge John Repetski and Robert T. Ryder of the U.S. Geological Survey who supplied us with unpublished conodont alteration index data in Kentucky and Ohio that were necessary to create the CAI isopleth maps. Without their cooperation, the maps would have been incomplete.

TRENTON-BLACK RIVER KEY FIELD AND PLAY DESCRIPTIONS

By Richard Nyahay, Rose Schulze, Langhorne B. Smith, Ron Riley and Douglas G. Patchen

Trenton-Black River Hydrothermal Dolomite Gas Play

Location and Production History

Oil and gas have been produced from laterally discontinuous dolomitized zones in the Upper Ordovician Trenton and Black River carbonates in eastern North America for more than a century. The first discoveries were made in the dolomites of the Lima-Indiana Trend of Ohio and Indiana in 1884. Most of the dolomites are demonstrably fault-related as they align with the NNW-SSE trending Bowling Green Fault and other fault zones (Wickstrom et al., 1992). More than 500 million barrels of oil and over a Tcf of gas were produced from the Lima-Indiana Trend (Wickstrom et al., 1992), making it the first giant oilfield in the world. Smaller yet still significant discoveries were subsequently made in fault-controlled dolomites at Dover Field, Ontario, and Deerfield and Northville Fields in Michigan (Hurley and Budros, 1990).

The next major discovery in Trenton-Black River laterally discontinuous dolomites was the Albion Scipio Trend in southern Michigan. Porous matrix dolomite, saddle dolomite-cemented breccias, and saddle dolomite-lined fractures and vugs, all occur in a trend of *en echelon* structural lows that is ~50 km (30 miles) long and about 1.6 km (1 mile) wide (Hurley and Budros, 1990). Albion-Scipio field has produced more than 250 MMBOE since its discovery. Several smaller fields have subsequently been discovered in Michigan and Ontario.

This summary focuses on more recent discoveries in New York and northeast Ohio. The first discovery in New York was inadvertent. A well drilled in 1982 as a geothermal test in the town of Auburn in Cayuga County found gas in what is now known to be a hydrothermal dolomite zone in the uppermost Black River. This well is still producing today. The first intentional discovery was in 1985 in laterally discontinuous dolomite in the Black River Group in the Glodes Corners Road field of south-central New York. Since then, at least twenty-five new fields have been discovered in laterally discontinuous dolomites of the Trenton-Black River (Figure 8-1 and Table 8-1). On the map, producing wells, tight dolomite, tight limestone and confidential wells are all marked with different symbols. Most of the fields are between 7000 and 10,000 feet deep. Several wells have produced at sustained rates of >10MMcf/d, and the most prolific producer (Reed #1 in Quackenbush Hill field) made 35MMcf/d for several months. As of the end of 2004, the well with the best cumulative production had produced more than 15 Bcf and is still flowing at a high rate. Overall, the trend in New York has produced 45.7 Bcf as of the end of 2004.

Things to consider as the fields are reviewed are: Where does the porous dolomite occur in each field? What makes more sense in this field, vertical or horizontal wells?

Our belief is that in New York, horizontal wells make sense in most cases because if a well is going to be a good producer it almost always has porosity in the upper 40-50 feet of the Black River. Thus, this interval is a target zone for horizontal wells. Horizontal wells help reduce the chance of hitting a tight dolomite or limestone zone within a productive feature.

In the York field in Ohio, however, porosity occurs in many different zones. It would be very difficult to choose an interval in which one would drill horizontally. Vertical wells almost certainly would be better in this setting. Exploration wells outside of areas where the dolomite occurs at known stratigraphic intervals should probably be drilled vertically or on a slanted well path. It may be that in different areas, other stratigraphic intervals are more likely to be dolomitized and once they are identified, horizontal drilling may again be preferable.

Stratigraphic and Structural Control of Reservoirs

These dolomitized fields occur in long, narrow, fault-bounded, *en echelon* structural depressions (Harding, 1974; Prouty, 1988; Hurley and Budros, 1990; Colquhoun, 1991) and along other wrench and possible normal faults (Wickstrom et al., 1992). The reservoir facies consists of matrix dolomite with saddle dolomite-cemented vugs, breccias and fractures around the faults, and the reservoirs are laterally sealed by tight, undolomitized limestone. Although some fields have a major component of cavernous porosity (Albion-Scipio is famous for its bit drops of up to ~20 meters (60 feet)), others, including those in New York, have little or no cavernous porosity. See the rest of the report and the paper by Langhorne Smith included in this report for more details on the origin of these fields.

Description of Key Fields

This report includes brief descriptions of each field along with a cross section of the wells in each field. Field data have been tabulated in Tables that are linked to the field descriptions. The cross-sections used in the figures were generated using data imported into Petra software by Geoplus from New York's ESOGIS database. These included formation tops and .las files. On the cross sections, dolomite is picked using PEF, density and neutron logs. Any strata in the Trenton or Black River that are not picked as dolomite are either composed of limestone, argillaceous limestone or bentonite. The PEF curve typically reads around 3-3.5 in dolomitized intervals whereas it is around 4.5 or 5 in limestones. Dolomite (2.86 g/cc) is denser than limestone (2.71 g/cc). When logs are plotted using a limestone density of 2.71 g/cc = 0% neutron porosity, the density log will plot to the right of the neutron log in dolomitized intervals and plot on top of the neutron in limestone intervals. This should be true in both porous and tight dolomitized intervals. Sometimes in very vuggy, high-porosity zones, it is hard to tell if the density plots to the right of the neutron, but if a zone has very high porosity in the Black River it is almost certainly dolomitized.

The cross sections include mostly vertical wells. Whenever possible, directional wells have been presented in a TVD format so that it doesn't look like the section is thickened. Where fields are mostly developed by horizontal wells, such as Quackenbush Hill Field, it is difficult to make a meaningful cross section. We plan to make map view cross sections of these fields eventually but were not able to prepare them for this study. We have only included wells that are publicly available as of April 2006. Some of these fields almost certainly already have or will have more wells drilled in them over time.

Also attached is a list of directional wells (Table 8-2) that have been drilled into the Black River reservoirs.

Auburn Geothermal Field (**Figure 8-3**). Discovered in 1982, this a one-well field **(Table 8-3)** that has produced behind pipe for more than twenty years. Thin sections made from well cuttings confirm that the productive interval is dolomitized and that there is at least a component of saddle dolomite. The dolomite interval occurs at the top of the Black River Group at depths of 4150 to 4176 feet. As of 2004, the well has officially produced 42 MMcf, but that only includes production since 1994. It is thought that the well has produced more than 200 MMcf since it was first placed on line. The older log suite confirms the dolomite interval. The density log reads higher than 2.71 and the neutron log registers porosity values between 2% and 9% through the twenty six foot interval. This is the northern-most producing field. The occurrence of gas this far north suggests that there may be many other productive fields between the main producing area and this field.

Ballyhack Creek (Figure 8-4). Discovered in 2002, this is a three-well field with only one well, the Beagell #2 **(Table 8-4),** producing from dolomitized Black River. The well has produced 340 MMcf as of 2004. Well 23078-02 only made it to the Trenton and well 23056-01 is similar to the producing well with the exception of porosities being less than 3%. The producing well is a directional well whose bottom location is to the SSE of the surface location. Surface trend of the three wells are NE – SW. The dolomitized units correlate from well-to-well suggesting that a horizontal approach may work in this area. This is the easternmost producing field, again suggesting that there may be potential between this field and the main producing area.

Beans Station (Figure 8-5). Discovered in 2002, this is a one-well field **(Table 8-5)**. The Gray # 1 well was cored and results of analysis of that core are included in this report. The original well tested a small amount of gas but was never hooked up. It has recently been sidetracked with promising results. This is a directional well whose bottom-hole position is WSW of the surface location.

Caton (Figure 8-6). Discovered in 2002, this is a one-well field **(Table 8-6)** that produced 33 MMcf as of 2004. At this time we have no logs for the producing deviated sidetrack. In the vertical well the Black River interval is all dolomite, with a strange log response. The PEF is around 2.5 which is low for dolomite and the density jumps around significantly. The neutron log shows very little porosity. There could be a significant

component of chert in this well. Quartz has a PEF response of ~2.5 and the density would be lower in a silica-rich well.

Cooper Hill (Figure 8-7). Discovered in 2005, this is a one-well field **(Table 8-7)**. This is a directional well whose bottom hole position is NW of the surface location. The field had produced no gas as of the end of 2004. The dolomite section begins approximately 60 feet below the top of the Black River interval and is 61 feet thick with porosity up to 12 %.

County Line (Figure 8-8). Discovered in 2000, this field has three producing wells **(Table 8-8)**. The trend of the field is ENE-WSW and it produced 1.34 BCF as of the end of 2004. Three of the wells are almost completely dolomitized. The best producer through the end of 2004 was the Whiteman well which was cored and studied for this report. The Whiteman #1 well was deepened and no logs are available for the deeper interval. The Youmans well has the same problem that was encountered in the vertical well at Caton Field with a neutron log showing no porosity and a density log that is highly variable. This field has a lot of tight dolomite relative to Wilson Hollow and Quackenbush Hill to the south.

Cutler Creek (Figure 8-9). Discovered in 2002, this is a two-well field **(Table 8-9)** with a deviated well and a horizontal well. The field has produced 3.5 Bcf as of the end of 2004. The Corning Game Club well is a deviated well that has produced over 3 Bcf to date. The bottom-hole location is SSW of the surface location. The Moss well, 23100-00, is a more recent horizontal well (Figure 8-9A) that trends to the northeast away from the Corning Game Club well towards Quackenbush Hill. It went through a 650 foot limestone, then through several wide dolomitized zones and then back into limestone prior to reaching Quackenbush Hill.

Glodes Corner Road (Figure 8-10). Discovered in 1985 by Columbia Natural Resources, this is the first field to be drilled in the hydrothermal dolomite play in a sag feature in New York. Currently, there are 12 producing wells, of which three are directional wells **(Table 8-10)**. The field has produced 7.5 Bcf of gas as of the end of 2004 and probably was overdrilled. Most of the wells do not go deeper than the top few feet of the Black River. The better producing wells have dolomite sections that are relatively thin, but have porosities between 5% and 12%. The best producing well, the Fox 1, 21706-00, has no log coverage. We have correlated several bentonite zones on this cross section which probably can be correlated to many of the other wells in the area.

Guyanoga Valley (Figure 8-11). Discovered in 1999, the field consists of one producing well which is a directional well **(Table 8-11)**. The well produced 330 MMcf of gas through the end of 2004. The producing interval is a relatively thin dolomite section at the top of the Black River Group in which porosity does not exceed 8%.

Langdon Hill (Figure 8-12). Discovered in 2000, this field consists of three wells **(Table 5-12)** that produced gas as of the end of 2004. This might have been the discovery field for the Black River hydrothermal dolomite play, but the Matejka #1 well

that was drilled by Shell in 1974 either did not produce economic quantities of gas or the company was looking for oil at that time. The field has produced 2.1 Bcf as of the end of 2004. Not included on this cross section (Figure 8-12) is the Konstantinides #1 horizontal well which has made 0.6 Bcf through the end of 2004.

Moreland Field. Discovered in 2003, this is a one-well field. The lone producing well is a directional well. No logs or directional surveys are available. The field has not produced to date.

Muck Farm (Figure 8-13). Discovered in 1998, this field consists of five wells **(Table 8-13)**. Four have produced, one was not completed. Wells in the field have an average completion interval of only twenty seven feet of dolomite. The field is located just south of the Glodes Corners Road field and east of the Bean Station field. The best well is the most northern one, the Snyder #1, in which the dolomite section is only 8 feet thick but has a porosity spike of 15%. The field has produced 7.25 Bcf as of the end of 2004, a volume comparable to the amount of gas produced from 12 wells in Glodes Corners Road field to the north.

Pine Hill (Figure 8-14). Discovered in 1999, this field consists of four wells **(Table 8-14)**. The field has produced 401 MMcf as of the end of 2004. Production is at the low end of the scale as compared to other fields that have more than one producing well. This is the only field that trends NW-SE. The best producing well is one where dolomite is developed at the top of the Black River and not near the bottom. There is one producing well that only has dolomite near the base of the Black River, but it has only produced 40 MMcf. All other wells that produce in this trend have porous dolomite at or near the top of the Black River.

Quackenbush Hill (Figures 8-15 and 8-16). Discovered in 2000, this field has ten producing wells **(Tables 8-15 and 8-16)**. The cross section is obviously very difficult to correlate because of the large number of deviated and horizontal wells. This field has produced 43 Bcf as of the end of 2004 and is the largest producing field in the trend. This field has the number one producing well in the trend, the Lovell #1, a vertical well that produced over 15 Bcf in four years through the end of 2004. There are several long horizontal wells in this field (Figures 8-16A, B and C). The Reed #1 well was the biggest onshore well in the U.S. in 2004 (Figure 8-16A). It has a 1650 foot lateral section, mostly in porous dolomite. The Hakes well, 23054-00 (Figure 8-16B) encountered 800 feet of limestone at the top of the Black River prior to cutting into porous, dolomitized zones. This well was drilled in a NNE direction and it looks like this limestone occurs within the middle of the field. The Andrews well, 23038-00, has a long section of porous dolomite with very little limestone (Figure 8-16C). The Henkel well, 22871-00, has a thinner dolomite section with porosities ranging from 10% to 30%. This field contains more directional wells than any other Black River field in the state. The variability of most of the producing wells gives a hint on how complex this reservoir system is to understand.

Riverside (Figure 8-17). Discovered in 2002, this is a one-well field **(Table 8-17)**. This is a directional well whose bottom-hole position is WSW of the surface location. There is a lot of chatter in the density log as there was at the Caton field. The top 140 feet and the bottom 200 feet of the Black River interval are dolomitized. The well produced 376 MMcf as of the end of 2004.

Seeley Creek (Figure 8-18). Discovered in 2004, this is a one-well field **(Table 8-18)**. This is a directional well whose bottom hole position is ESE of the surface location. The well produced 872 MMcf as of the end of 2004. Dolomite occurs in at least 5 separate beds. The bed that is second from the top appears to have the most porosity in this well. This is the southernmost producing well in the trend in NY.

Sexton Hollow (Figure 8-19). Discovered in 2000, this is another one-well field **(Table 8-19)**. The Sexton Hollow discovery well has produced 459 MMcf as of the end of 2004. There is a thick dolomite section in the upper Black River and some very high porosity spikes in the basal Trenton which may be bentonites or possibly high porosity zones.

South Corning (Figure 8-20). Discovered in 2004, this is a one-well field **(Table 8-20)**. This is a directional well whose bottom hole position is SW of the surface location. The field had not produced as of the end of 2004. Dolomite is found at the top of the Black River interval.

Sugar Hill. Discovered in 2000, this is another one-well field **(Table 8-21)**. This is a directional well whose bottom hole position is WSW of the surface location that has produced 1.07 Bcf as of the end of 2004. We do not have a good set of logs for this well.

Terry Hill South (Figure 8-21). Discovered in 2000, this field has seven producing wells **(Table 8-21).** The field has produced more than 6.4 Bcf of gas as of the end of 2004. Wells on the south side of the field have produced better than those on the northern side. The Black River is dolomitized almost everywhere it was penetrated in the five wells.

West River (Figure 8-22). Discovered in 2004, this is a one-well (22985-02) field **(Table 8-22)**. This well was sidetracked twice and the second sidetrack reportedly found gas. This is a directional well whose bottom hole position is SSW of the surface location. The well had not produced gas as of the end of 2004.

Whiskey Creek (Figure 8-23). Discovered in 2003, this is a one-well field **(Table 8-23)**. The well produced 1.03 Bcf as of the end of 2004. This is a directional well whose bottom hole position is SE of the surface location. Dolomite is not found at the top of the Black River, but the PEF response suggests that there may be some open fractures or faults in that interval. The middle part of the Black River is pervasively dolomitized.

Wilson Hollow (Figure 8-24). Discovered in 1999, the field consists of ten producing wells **(Table 8-24)**. The field has produced 30.6 Bcf as of the end of 2004 and is the second-best producing field in the trend after Quackenbush Hill which is just to the south

and parallel to Wilson Hollow field. Most wells have dolomite throughout the Black River, and all of them have dolomite in the upper 50 feet, where some of the best porosity occurs. This is an ideal field for horizontal wells because of this consistent dolomite distribution. In some wells, the basal Trenton is dolomitized. The trend of the field is ENE-WSW.

Zimmer Hill (Figure 8-25). Discovered in 2005, this is a one-well field **(Table 8-25)**. This is a horizontal well whose bottom position is NNE of the surface location. The well penetrated 360 feet of limestone, then a narrow dolomitized zone followed by another 200 feet of tight limestone before encountering a wider dolomitized zone with good porosity. Again, this well shows the lateral heterogeneity in this play and why horizontal wells are a good idea in most locations. The well did not have any production data for 2004 as it was not discovered until the following year.

York Field, Northeast Ohio (Figure 8-26). This field was discovered in 1997 and produces gas from 8 wells. Following the drilling of the York discovery well, a 3-D seismic survey was acquired. A time-structure map on top of the Trenton (Figure 8-27) revealed that the productive well occurs in a small circular sag, and subsequent wells were drilled into similar circular sags. The field has produced a total of 5.5 Bcf. Dolomite occurs at many different stratigraphic intervals in the Trenton and Black River, so horizontal wells probably would not be a good approach in this field.

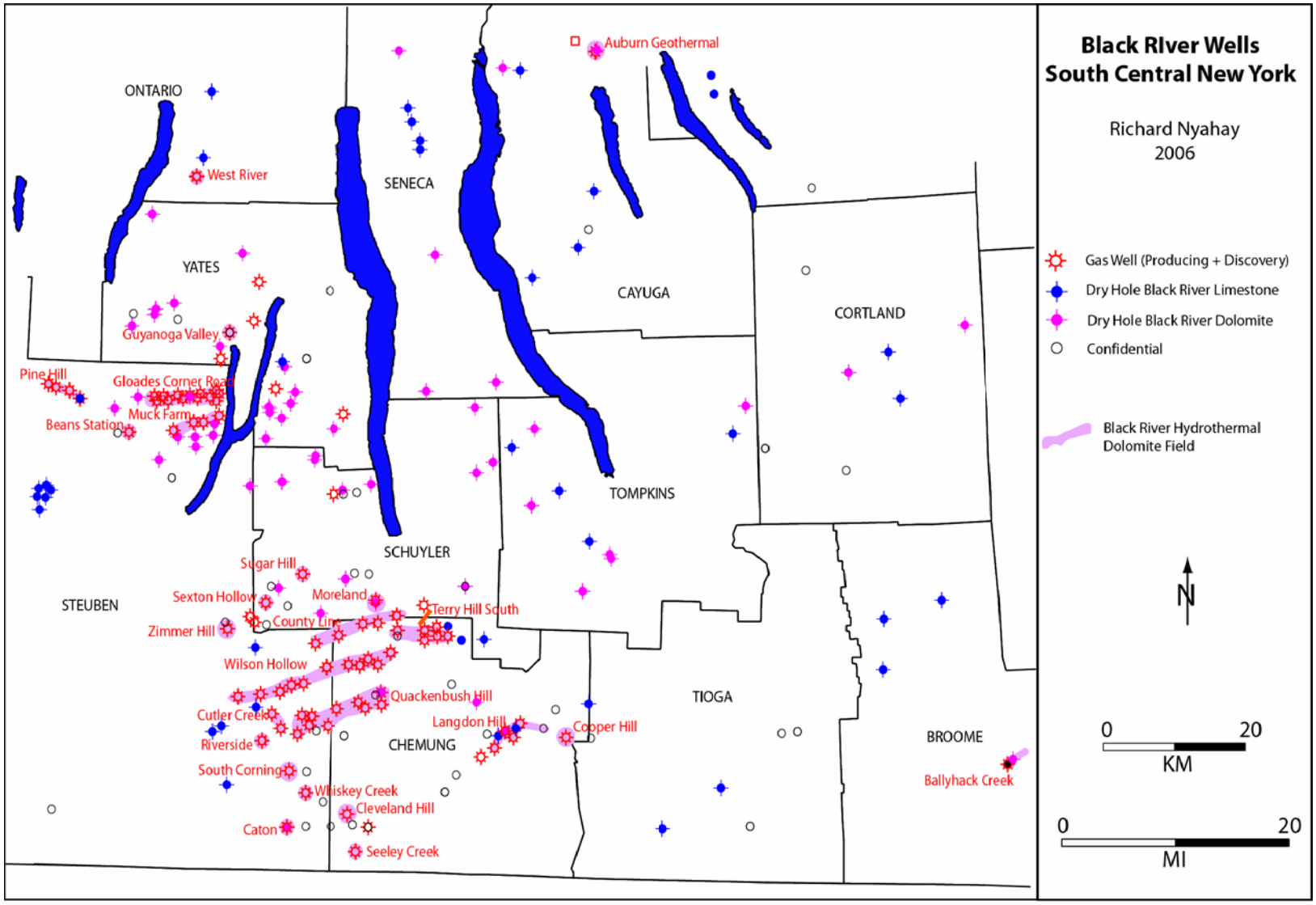

Figure 8-1. Black River Wells of South-Central New York

Field Name	Auburn Geothermal	Ballyhack Creek	Beans Station	Caton
Pool Number				
Discovered	1982	2002	2002	2002
Depth to Reservoir				
Age of Reservoir	Ordovician	Ordovician	Ordovician	Ordovician
Formation	Black River	Black River	Black River	Black River
Producing Reservoir				
Lithology	HTD	HTD (59)	HTD (191)	HTD
Trap Type				
Depositional Environment				
Discovery Well IP (Mcf)		4900	133	
Drive Mechanism				
No. Producing Wells	1	3	1	1
No. Abandoned Wells	1	1		
Area (acreage)				
Oldest Formation Penetrated				
Expected Heterogeneity Due To				
Average Thickness	8	63	115	
Average Completion Thickness		340		
Average Porosity Log (%)				
Minimum Porosity Log (%)	5	5	5	5
No. Data Points	1	1	1	1
Porosity Feet	26	9-May	110	
Reservoir Temperature (F)	120	132.7 avg	140	
Initial Reservoir Pressure		3805	2250	
Producing Interval Depths	4150-4160	9520-9545	8114 - 8229	
Present Reservoir Pressure (psi/date)				
Status				
Original Gas in Place				
Original Gas Reserves				
Production Years	8	2		2
Reported Cumulative Production	42,018	340346		33191
No. wells Reported				
Estimated Cumulative Production				
Remaining Gas In Place (Mcf/Date)				
Remaining Gas Reserves				
Recovery Factor				
Initial Open Flow Mcfpd				
Final Open Flow Mcfpd				

Table 8-1

Field Name	Cleveland Hill	Cooper Hill	County Line	Cutler Creek
Pool Number				
Discovered	2005	2005	2000	2001
Depth to Reservoir				
Age of Reservoir	Ordovician	Ordovician	Ordovician	Ordovician
Formation	Black River	Black River	Black River	Black River
Producing Reservoir				
Lithology	HTD (120)	HTD (61)	HTD (207 avg)	HTD (746 avg)
Trap Type				
Depositional Environment				
Discovery Well IP (Mcf)		4900	8000	21000
Drive Mechanism				
No. Producing Wells		1	3	1
No. Abandoned Wells			1	
Area (acreage)			2825.6	636.62
Oldest Formation Penetrated				
Expected Heterogeneity Due To				
Average Thickness			101	273
Average Completion Thickness				
Average Porosity Log (%)				
Minimum Porosity Log (%)		5	5	5
No. Data Points	1	1		2
Porosity Feet		27.75	12.25 - 108	49 - 225
Reservoir Temperature (F)	185	122	158 avg	167 avg
Initial Reservoir Pressure			3075	3390
Producing Interval Depths			8653-10182	9561-9834
Present Reservoir Pressure (psi/date)				
Status				
Original Gas in Place				
Original Gas Reserves				
Production Years			3	4
Reported Cumulative Production			1345719	3498617
No. wells Reported				
Estimated Cumulative Production				
Remaining Gas In Place (Mcf/Date)				
Remaining Gas Reserves				
Recovery Factor				
Initial Open Flow Mcfpd				
Final Open Flow Mcfpd				

Table 8-1

Field Name	Glodes Corner Road	Guyanoga Valley	Langdon Hill	Moreland
Pool Number				
Discovered	1985	1999	2000	2003
Depth to Reservoir				
Age of Reservoir	Ordovician	Ordovician	Ordovician	Ordovician
Formation	Black River	Black River	Black River	Black River
Producing Reservoir				
Lithology	HTD (89)	HTD (43.50)	HTD (66)	HTD
Trap Type				
Depositional Environment				
Discovery Well IP (Mcf)	3400	2540	4850	
Drive Mechanism				
No. Producing Wells	12	1	4	1
No. Abandoned Wells	2		1	
Area (acreage)	2640.79			
Oldest Formation Penetrated				
Expected Heterogeneity Due To				
Average Thickness	101	18	69	5195
Average Completion Thickness				
Average Porosity Log (%)				
Minimum Porosity Log (%)	5	5	5	5
No. Data Points		1	4	
Porosity Feet	.5 -118	1.5	41- 105	
Reservoir Temperature (F)	133 avg	154	170 avg	102
Initial Reservoir Pressure	2035 avg	2300	3390 avg	
Producing Interval Depths	6645-7590	5932-5950	9974-10480	7905-13100
Present Reservoir Pressure (psi/date)				
Status				
Original Gas in Place				
Original Gas Reserves				
Production Years	9	2	4	
Reported Cumulative Production	7556499	329998	2182784	
No. wells Reported				
Estimated Cumulative Production				
Remaining Gas In Place (Mcf/Date)				
Remaining Gas Reserves				
Recovery Factor				
Initial Open Flow Mcfpd				
Final Open Flow Mcfpd				

Table 8-1

Field Name	Muck Farm	Pine Hill	QuackenBush Hill	Riverside
Pool Number				
Discovered	1998	1999	2000	2002
Depth to Reservoir				
Age of Reservoir	Ordovician	Ordovician	Ordovician	Ordovician
Formation	Black River	Black River	Black River	Black River
Producing Reservoir				
Lithology	HTD 10 avg)	HTD (166)	HTD (917 avg)	HTD (294)
Trap Type				
Depositional Environment				
Discovery Well IP (Mcf)	3100	1200	26000	9715
Drive Mechanism				
No. Producing Wells	4	3	9	1
No. Abandoned Wells		1	1	
Area (acreage)	3871.68	1623.32	3176.17	
Oldest Formation Penetrated				
Expected Heterogeneity Due To				
Average Thickness	27	131	1608	273
Average Completion Thickness				
Average Porosity Log (%)				
Minimum Porosity Log (%)	5	5	5	5
No. Data Points			10	1
Porosity Feet	2.5 - 21.25	9 - 200	10.33 - 965.25	
Reservoir Temperature (F)	130.25 avg	133.5	150.6 avg	161
Initial Reservoir Pressure	2471 avg	2391	3302 avg	3605
Producing Interval Depths	6684-7342	7308-7790	9228-13230	9738-9834
Present Reservoir Pressure (psi/date)				
Status				
Original Gas in Place				
Original Gas Reserves				
Production Years	6	5	4	1
Reported Cumulative Production	7258442	401755	43069867	376717
No. wells Reported				
Estimated Cumulative Production				
Remaining Gas In Place (Mcf/Date)				
Remaining Gas Reserves				
Recovery Factor				
Initial Open Flow Mcfpd				
Final Open Flow Mcfpd				

Table 8-1

	Seeley Creek	Sexton Hollow	South Corning	Sugar Hill
Pool Number				
Discovered	2004	2000	2004	2000
Depth to Reservoir				
Age of Reservoir	Ordovician	Ordovician	Ordovician	Ordovician
Formation	Black River	Black River	Black River	Black River
Producing Reservoir				
Lithology	HTD (64.5)	HTD (145.75)	HTD (29)	HTD (No Logs)
Trap Type				
Depositional Environment				
Discovery Well IP (Mcf)	20300	940	1	30000
Drive Mechanism				
No. Producing Wells	1	1	1	1
No. Abandoned Wells				
Area (acreage)				
Oldest Formation Penetrated				
Expected Heterogeneity Due To				
Average Thickness	465	8	292	32
Average Completion Thickness				
Average Porosity Log (%)				
Minimum Porosity Log (%)	5	5	5	5
No. Data Points	1		1	
Porosity Feet	36.854	121	9.5	
Reservoir Temperature (F)	148	157	174	146
Initial Reservoir Pressure	4122	3180	1758	3800
Producing Interval Depths	11026-11491	9622-9630	9700-9992	8638-8770
Present Reservoir Pressure (psi/date)				
Status				
Original Gas in Place				
Original Gas Reserves				
Production Years	1	1		3
Reported Cumulative Production	872417	459117		31076554
No. wells Reported				
Estimated Cumulative Production				
Remaining Gas In Place (Mcf/Date)				
Remaining Gas Reserves				
Recovery Factor				
Initial Open Flow Mcfpd				
Final Open Flow Mcfpd				

Table 8-1

	Terry Hill South	West River	Whiskey Creek	Wilson Hollow	Zimmer Hill
Pool Number					
Discovered	2000	2004	2003	1999	2005
Depth to Reservoir					
Age of Reservoir	Ordovician	Ordovician	Ordovician	Ordovician	Ordovician
Formation	Black River	Black River	Black River	Black River	Black River
Producing Reservoir					
Lithology	HTD	HTD (31)	HTD (176)	HTD (180 avg)	HTD (583)
Trap Type					
Depositional Environment					
Discovery Well IP (Mcf)	17000	2248		7600	
Drive Mechanism				.	
No. Producing Wells	5	1		10	
No. Abandoned Wells	2				
Area (acreage)	4165.3			3056.13	
Oldest Formation Penetrated					
Expected Heterogeneity Due To					
Average Thickness	590	313	437	287	
Average Completion Thickness					
Average Porosity Log (%)					
Minimum Porosity Log (%)	5	5	5	5	5
No. Data Points		1	1		1
Porosity Feet	1.25 - 181	6 - 152	44	11.36 - 132	157
Reservoir Temperature (F)	154 avg	110 avg	133	164.2 avg	163
Initial Reservoir Pressure	3430 avg	1750	4122	3415 avg	3195
Producing Interval Depths	8667-11185	4784-5480	10575-11012	9496 - 10358	8928 - 12000
Present Reservoir Pressure (psi/date)					
Status					
Original Gas in Place					
Original Gas Reserves					
Production Years	4		2	5	
Reported Cumulative Production	6348401		1038558	30605887	
No. wells Reported					

Table 8-1. Black River Gas Fields, New York

Directional Wells in Black River Reservoirs of New York			
UWI (APINum)	Well Name	County	direction
31-007-22984-00-00	Merrill 1	BROOME	SW
31-007-22984-01-00	Merrill 1A	BROOME	S
31-007-22995-00-00	Beagell 2	BROOME	SSE
31-007-22995-01-00	Beagell 2-A	BROOME	S
31-007-23030-00-00	Manwaring 1	BROOME	NW
31-007-23032-00-00	Pond 1	BROOME	NNW
31-007-23056-00-00	Butkowsky #1	BROOME	WSW
31-007-23056-01-00	Butkowsky #1A	BROOME	NW
31-007-23078-00-00	Curren #1	BROOME	NNE
31-007-23078-02-00	Olson 1-B	BROOME	WNW
31-009-23456-00-00	Braymiller-Rauch #1454	CATTARAUGUS	WSW
31-009-23456-01-00	Braymiller-Rauch #1454a	CATTARAUGUS	SW
31-011-23158-00-00	Carter 1	CAYUGA	SE
31-015-22827-00-00	Bennett Family 1	CHEMUNG	N
31-015-22880-01-00	Kienzle 1-A	CHEMUNG	NNW
31-015-22889-00-00	Clauss Jr 1	CHEMUNG	SE
31-015-22899-01-00	Trimber 624536-A	CHEMUNG	NNW
31-015-22901-00-00	Roy 1	CHEMUNG	SSE
31-015-22902-01-00	Lederer 1412-A	CHEMUNG	NNW
31-015-22910-00-00	Gublo 1	CHEMUNG	NNW
31-015-22911-00-00	Schmidt 624537	CHEMUNG	NNE
31-015-22918-01-00	Gregory 1446-A	CHEMUNG	SSE
31-015-22919-01-00	Hardy 1447-A	CHEMUNG	N
31-015-22924-00-00	Johnson 1	CHEMUNG	SSE
31-015-22924-01-00	Johnson 1-A	CHEMUNG	N
31-015-22933-00-00	Usack 624684	CHEMUNG	ESE
31-015-22960-00-00	Chemung SRA 1 1459	CHEMUNG	NNE
31-015-22975-00-00	Root 1514	CHEMUNG	NNE
31-015-22979-00-00	Strope 1516	CHEMUNG	ENE
31-015-23017-00-00	Hammond 1	CHEMUNG	S
31-015-23023-00-00	Konstantinides 1	CHEMUNG	NNW
31-015-23028-00-00	Hepfner 1	CHEMUNG	NNW
31-015-23076-00-00	Curren 1	CHEMUNG	S
31-015-23097-00-00	Harvey 1	CHEMUNG	SSE
31-015-23114-00-00	Strouse 1	CHEMUNG	NW
31-015-23134-00-00	Soderblom 1	CHEMUNG	NW
31-015-23146-00-00	Sekella 1	CHEMUNG	NW
31-015-23186-01-00	Messing 1-A	CHEMUNG	SE
31-023-23035-01-00	Sega 1-A	CORTLAND	N
31-051-23003-00-00	Simpson 3	LIVINGSTON	NNW
31-067-21335-00-00	Halloran 1	ONONDAGA	ENE
31-067-22809-00-00	Bartoszewski 1-14	ONONDAGA	NE
31-067-22965-01-00	Leubner 1--A	ONONDAGA	ENE
31-067-22971-00-00	Short 1	ONONDAGA	N
31-069-22943-00-00	Stoddard 624633	ONTARIO	NNE

UWI (APINum)	Well Name	County	direction from surface location
31-069-22985-00-00	Bay 1	ONTARIO	ENE
31-069-22985-01-00	Bay 1-A	ONTARIO	SE
31-069-22985-02-00	Bay 1B	ONTARIO	SW
31-097-22829-00-00	Grand Prix 624065	SCHUYLER	SSE
31-097-22830-00-00	Grand Prix 624066	SCHUYLER	NNE
31-097-22841-00-00	SRA 2 #1	SCHUYLER	WSW
31-097-22886-02-00	Ganung 1-B	SCHUYLER	SSW
31-097-22935-00-00	Wonderview Farms 1	SCHUYLER	NNW
31-097-22935-01-00	Wonderview Farms 1-A	SCHUYLER	N
31-097-22935-02-00	Wonderview 1B	SCHUYLER	NNW
31-097-23053-00-00	WGI 1	SCHUYLER	SW
31-097-23072-00-00	SRA3 1	SCHUYLER	SW
31-097-23086-00-00	Towner 1	SCHUYLER	NNW
31-099-22909-00-00	Campion 1	SENECA	SSE
31-099-22909-01-00	Campion 1-A	SENECA	NNW
31-099-22950-01-00	Ziefle 1-A	SENECA	S
31-101-21633-00-00	Mitchell 3	STEUBEN	NNE
31-101-21712-00-00	Kozak 1	STEUBEN	WSW
31-101-22814-01-00	Howe 1300-A	STEUBEN	NNE
31-101-22844-01-00	Doyle 624125-A	STEUBEN	SW
31-101-22844-02-00	Doyle 624125-B	STEUBEN	ESE
31-101-22861-00-00	NYS GMA 2	STEUBEN	WSW
31-101-22871-00-00	Henkel 1359	STEUBEN	ENE
31-101-22871-01-00	Henkel 1359-A	STEUBEN	ESE
31-101-22884-01-00	Fratarcangelo 1371-A	STEUBEN	SW
31-101-22885-00-00	Corning Game Club 624460	STEUBEN	SSW
31-101-22892-01-00	Hartman 624546-A	STEUBEN	SE
31-101-22949-00-00	Gray 624468	STEUBEN	WSW
31-101-22958-00-00	Pace 1460	STEUBEN	WSW
31-101-22963-01-00	Maxwell 1-A	STEUBEN	N
31-101-22978-00-00	Ballymoney 1	STEUBEN	NNW
31-101-23038-00-00	Andrews 1	STEUBEN	NNW
31-101-23039-00-00	Miller 1	STEUBEN	SSE
31-101-23040-00-00	Harndon 1	STEUBEN	SE
31-101-23055-00-00	Reed #1	STEUBEN	NNW
31-101-23085-00-00	Erwin WMA 1	STEUBEN	NW
31-101-23100-00-00	Moss 1	STEUBEN	NW
31-101-23105-00-00	Eolin 1	STEUBEN	SW
31-101-23150-00-00	TLT 1	STEUBEN	NE
31-101-23154-00-00	Drumm 1	STEUBEN	NNE
31-101-23155-00-00	Behm 1	STEUBEN	N
31-107-22934-01-00	Manwaring 624470-A	TIOGA	SW
31-107-22974-00-00	TtGS Holdings	TIOGA	WNW
31-109-22997-00-00	Albanese 1	TOMPKINS	SE
31-109-22997-01-00	Albanese 1A	TOMPKINS	S
31-109-22997-02-00	Albanese 1B	TOMPKINS	VERTICAL

UWI (APINum)	Well Name	County	General direction from surface location
31-109-22998-00-00	Stevenson 1	TOMPKINS	ESE
31-109-22998-01-00	Stevenson 1-A	TOMPKINS	NNW
31-109-22998-02-00	Stevenson 1B	TOMPKINS	NNW
31-109-22998-04-00	Stevenson 1-D	TOMPKINS	SSE
31-117-23087-00-00	Hughes #2	WAYNE	ENE
31-121-23449-00-00	Jachim #3	WYOMING	WNW
31-123-22764-01-00	Costanza 1-A	YATES	SW
31-123-22764-02-00	Costanza 1-B	YATES	SW
31-123-22828-00-00	Martin 623864	YATES	SSW
31-123-22858-00-00	Mulligan 1	YATES	N
31-123-22903-00-00	Zimmerman 624466	YATES	NNW
31-123-22903-01-00	Zimmerman 624466-A	YATES	SSE
31-123-22939-01-00	Button 624469-A	YATES	SSW
31-123-22939-02-00	Button 624469-B	YATES	SSW
31-123-22940-00-00	Folts 624464	YATES	SE

Table 8-2. Directional wells in New York

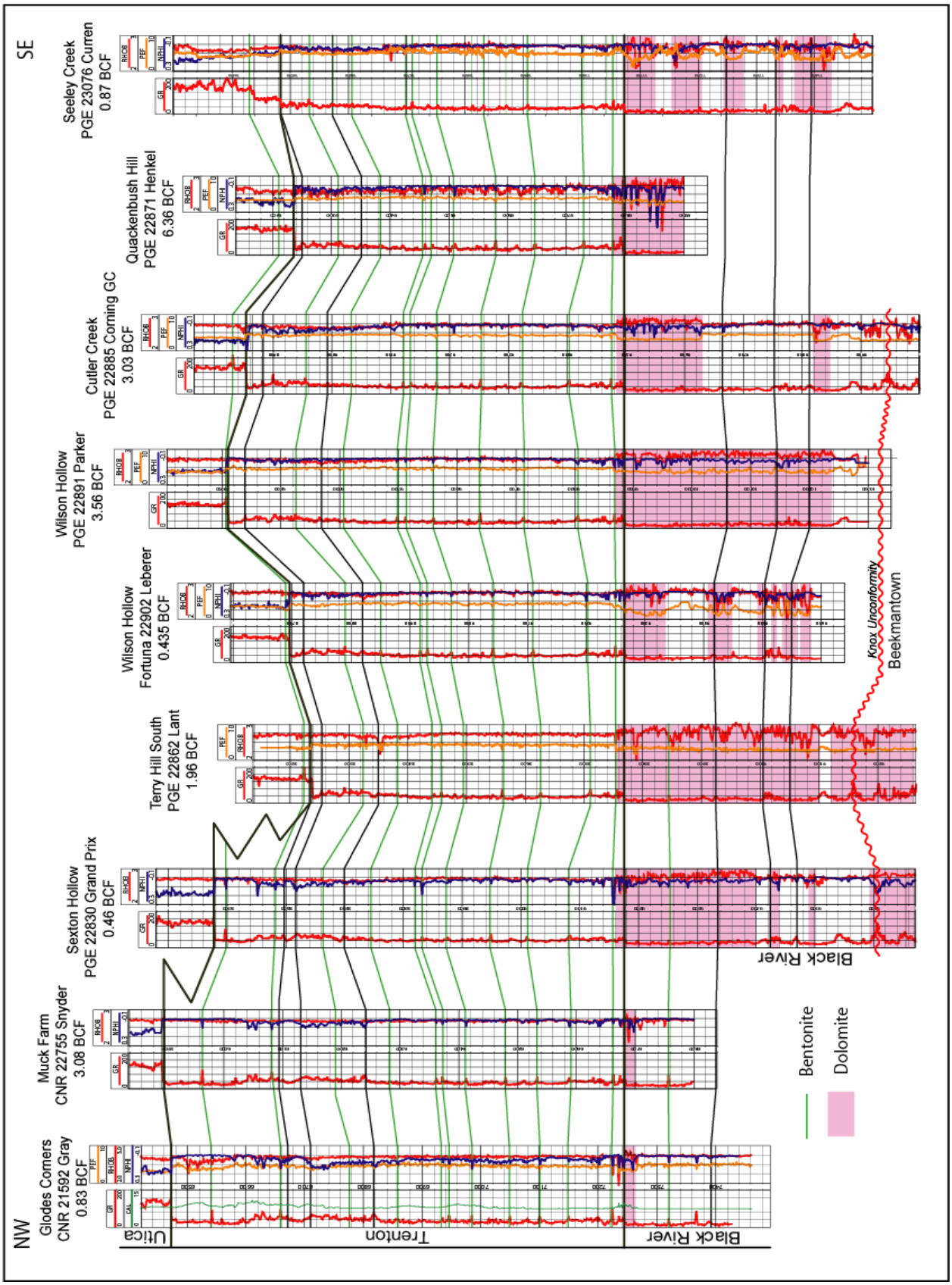

Figure 8-2 Trenton Black River regional cross section.

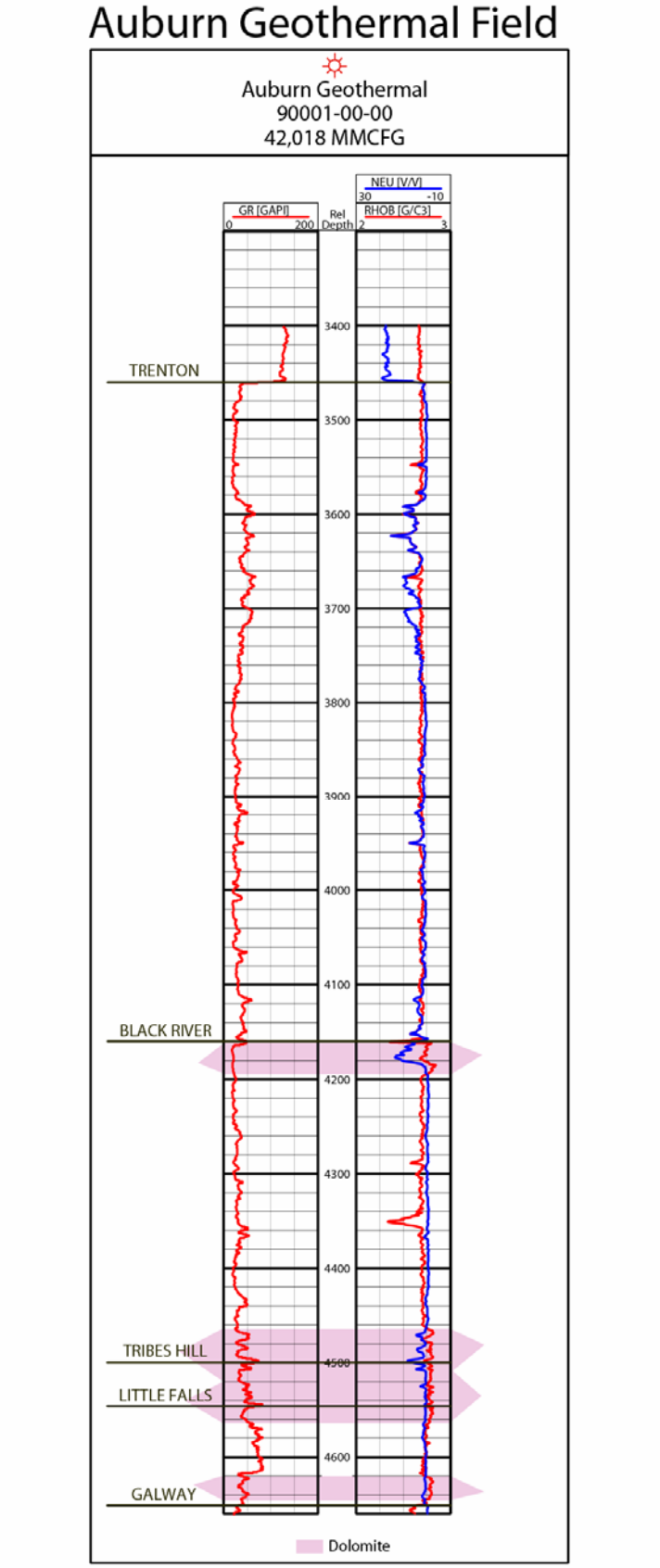

Figure 8-3 Well log from the Auburn Geothermal field.

Auburn Geothermal Field	90001-00
Pool Number	
Discovered	1982
Depth to Reservoir	
Age of Reservoir	Ordovician
Formation	Black River
Producing Reservoir	
Lithology	HTD
Trap Type	
Depositional Environment	
Discovery Well IP (Mcf)	
Drive Mechanism	
No. Producing Wells	1
No. Abandoned Wells	1
Area (acreage)	
Oldest Formation Penetrated	
Expected Heterogeneity Due To	
Average Thickness	8
Average Completion Thickness	
Average Porosity Log (%)	
Minimum Porosity Log (%)	5
No. Data Points	1
Porosity Feet	26
Reservoir Temperature (F)	120
Initial Reservoir Pressure	
Producing Interval Depths	4150-4160
Present Reservoir Pressure (psi/date)	
Status	
Original Gas in Place	
Original Gas Reserves	
Production Years	8
Reported Cumulative Production	42,018
No. wells Reported	
Estimated Cumulative Production	
Remaining Gas In Place (Mcf/Date)	
Remaining Gas Reserves	
Recovery Factor	
Initial Open Flow Mcfpd	
Final Open Flow Mcfpd	

Table 8-3. Well from the Auburn Geothermal field.

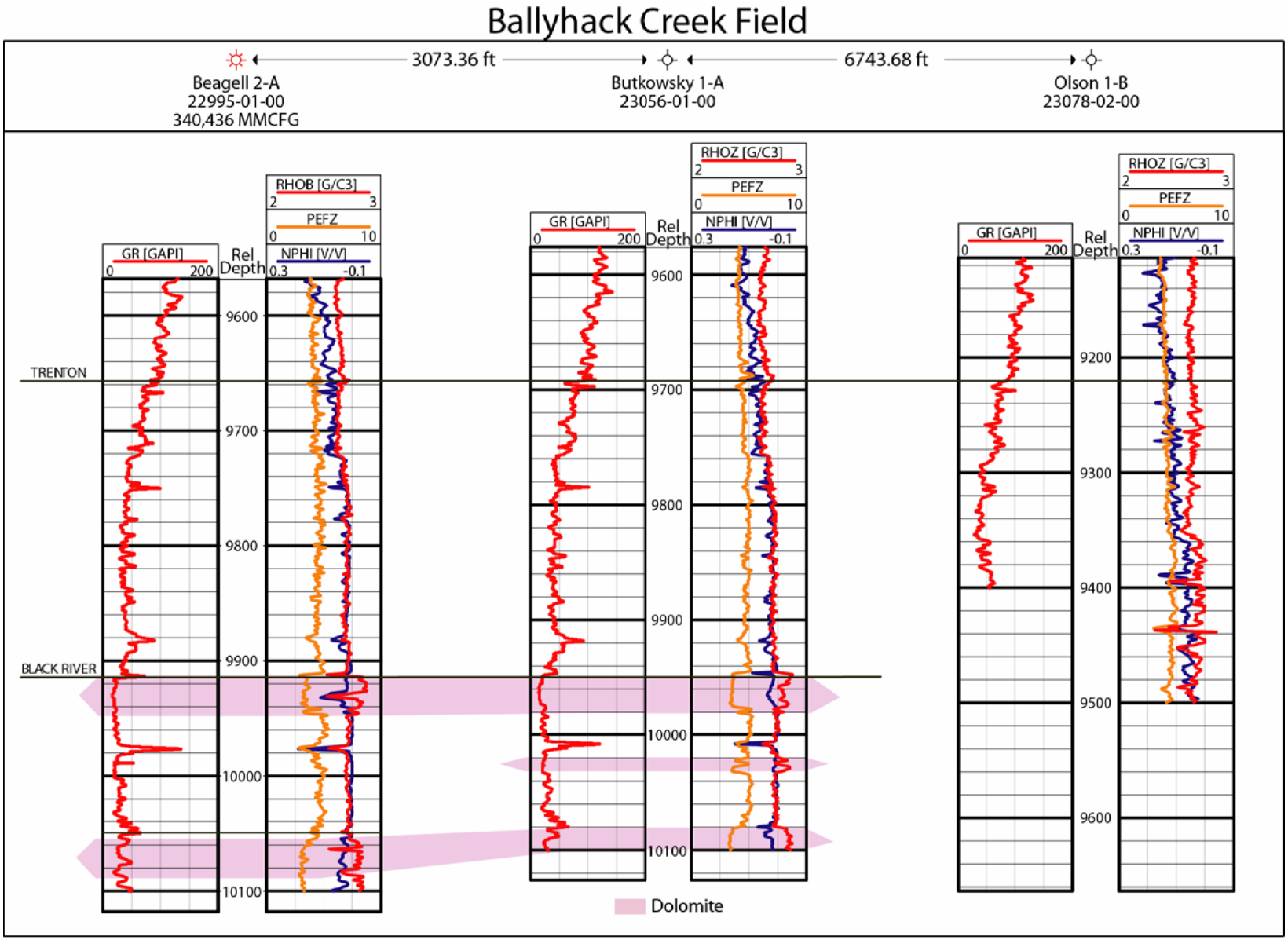

Figure 8-4 Well logs from the Ballyhack Creek field.

Ballyhack Creek Field	22995-01	23056-01	23078-02
Pool Number			
Discovered			
Depth to Reservoir			
Age of Reservoir	Ordovician	Ordovician	Ordovician
Formation	Black River	Black River	Black River
Producing Reservoir			
Lithology	HTD(53)	HTD (66)	
Trap Type			
Depositional Environment			
Discovery Well IP (Mcf)	4900		
Drive Mechanism			
No. Producing Wells			
No. Abandoned Wells			
Area (acreage)			
Oldest Formation Penetrated			
Expected Heterogeneity Due To			
Average Thickness			
Average Completion Thickness			
Average Porosity Log (%)			
Minimum Porosity Log (%)	5	5	5
No. Data Points			
Porosity Feet	9	5.3	
Reservoir Temperature (F)	136	125	137
Initial Reservoir Pressure	3805		
Producing Interval Depths	9920-10260	9520-9545	
Present Reservoir Pressure (psi/date)			
Status			
Original Gas in Place			
Original Gas Reserves			
Production Years	3		
Reported Cumulative Production	340436		
No. wells Reported			
Estimated Cumulative Production			
Remaining Gas In Place (Mcf/Date)			
Remaining Gas Reserves			
Recovery Factor			
Initial Open Flow Mcfpd			
Final Open Flow Mcfpd			
Misc. Notes	Water produced: 3609	Tested in Utica	

Table 8-4. Wells from the Ballyhack Creek field.

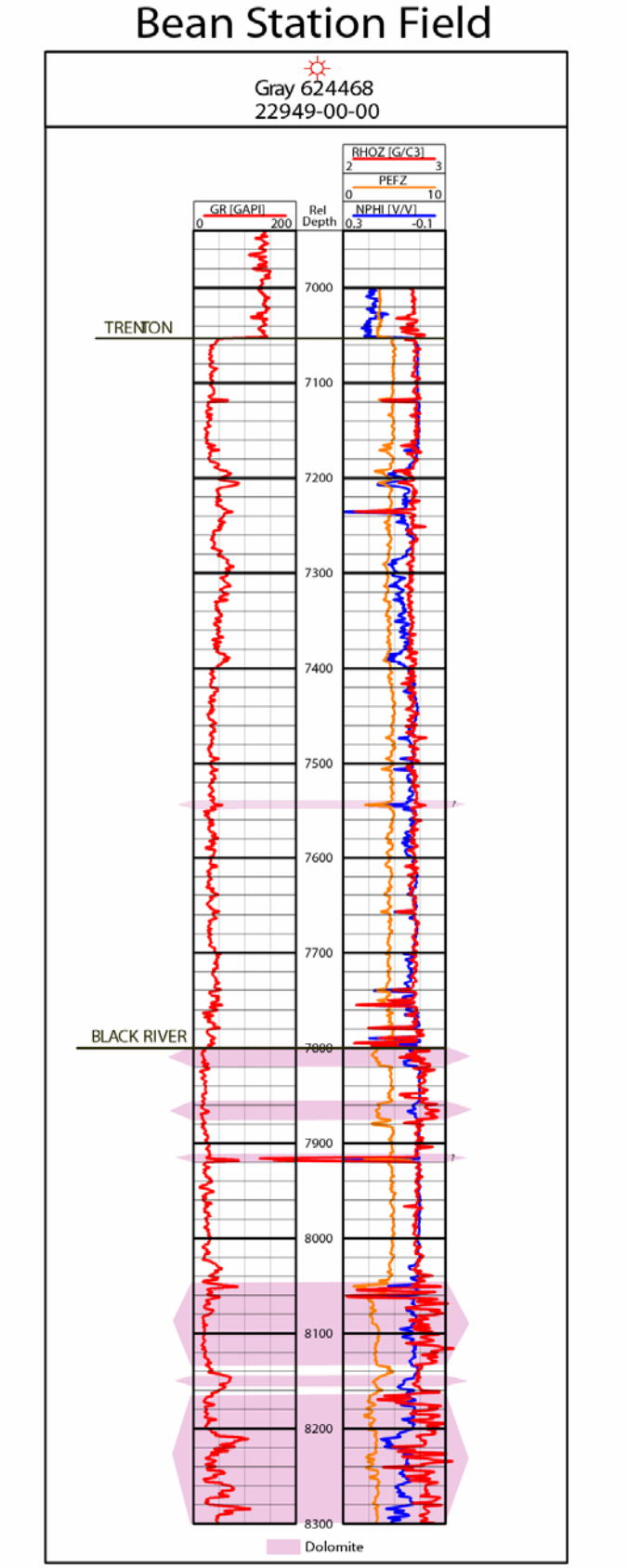

Figure 8-5 Well logs from the Bean Station field.

Beans Station Field	22949
Pool Number	
Discovered	2002
Depth to Reservoir	
Age of Reservoir	Ordovician
Formation	Black River
Producing Reservoir	
Lithology	HTD (191)
Trap Type	
Depositional Environment	
Discovery Well IP (Mcf)	133
Drive Mechanism	
No. Producing Wells	1
No. Abandoned Wells	
Area (acreage)	
Oldest Formation Penetrated	
Expected Heterogeneity Due To	
Average Thickness	
Average Completion Thickness	
Average Porosity Log (%)	
Minimum Porosity Log (%)	5
No. Data Points	1
Porosity Feet	110
Reservoir Temperature (F)	140
Initial Reservoir Pressure	2250
Producing Interval Depths	8229- 8114
Present Reservoir Pressure (psi/date)	
Status	
Original Gas in Place	
Original Gas Reserves	
Production Years	
Reported Cumulative Production	
No. wells Reported	
Estimated Cumulative Production	
Remaining Gas In Place (Mcf/Date)	
Remaining Gas Reserves	
Recovery Factor	
Initial Open Flow Mcfpd	
Final Open Flow Mcfpd	

Table 8-5. Well from the Bean Station field.

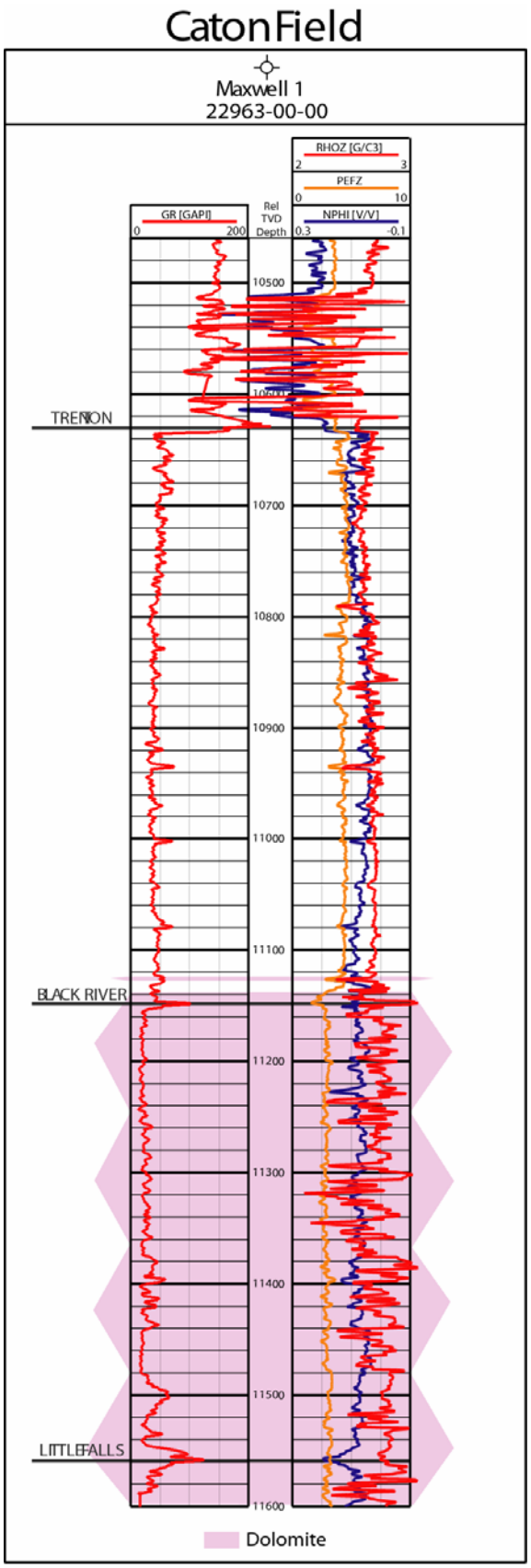

Figure 8-6 Well log from the Caton field.

Caton Field	22963-02
Pool Number	
Discovered	2002
Depth to Reservoir	
Age of Reservoir	Ordovician
Formation	Black River
Producing Reservoir	
Lithology	HTD
Trap Type	
Depositional Environment	
Discovery Well IP (Mcf)	
Drive Mechanism	
No. Producing Wells	1
No. Abandoned Wells	
Area (acreage)	
Oldest Formation Penetrated	
Expected Heterogeneity Due To	
Average Thickness	
Average Completion Thickness	
Average Porosity Log (%)	
Minimum Porosity Log (%)	
No. Data Points	1
Porosity Feet	
Reservoir Temperature (F)	
Initial Reservoir Pressure	
Producing Interval Depths	
Present Reservoir Pressure (psi/date)	
Status	
Original Gas in Place	
Original Gas Reserves	
Production Years	2
Reported Cumulative Production	33191
No. wells Reported	
Estimated Cumulative Production	
Remaining Gas In Place (Mcf/Date)	
Remaining Gas Reserves	
Recovery Factor	
Initial Open Flow Mcfpd	
Final Open Flow Mcfpd	

Table 8-6. Well from the Caton field.

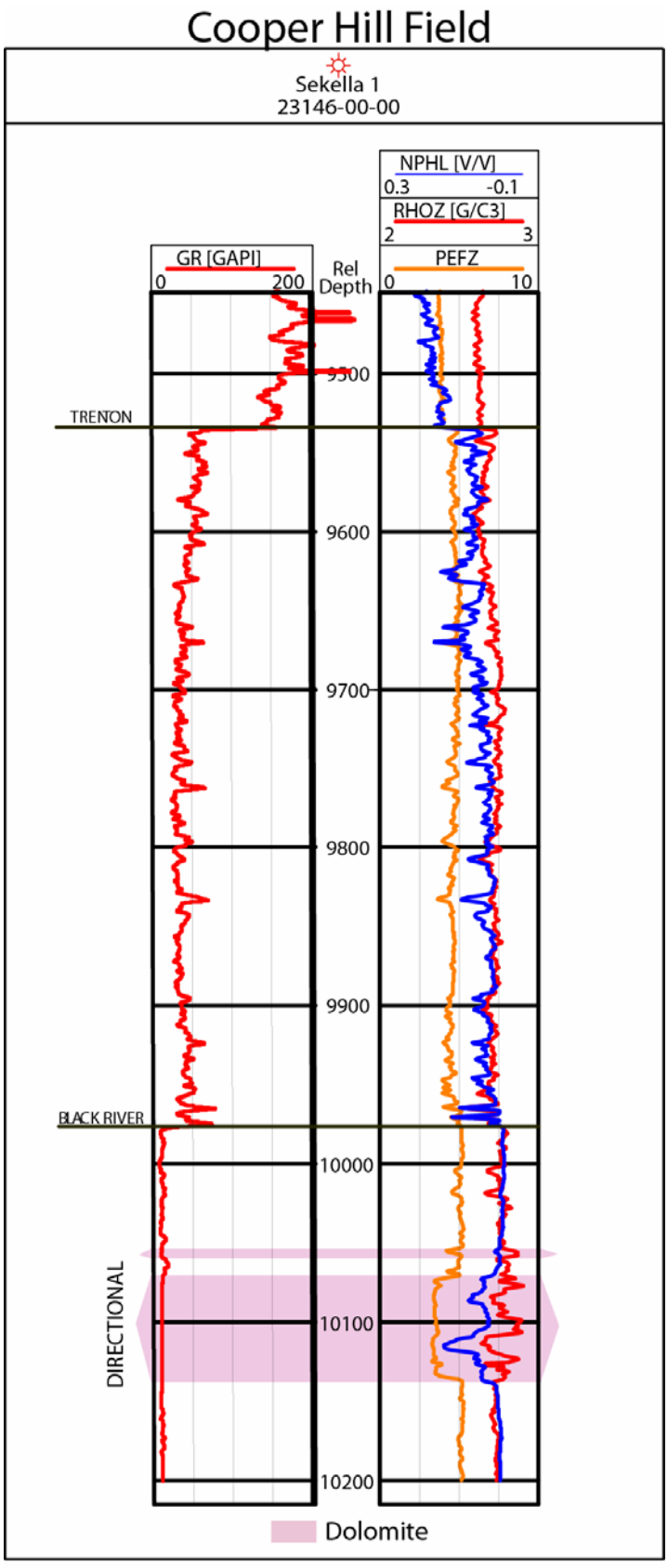

Figure 8-7 Well log from the Cooper Hill field.

Cooper Hill Field	23146-00
Pool Number	
Discovered	2005
Depth to Reservoir	
Age of Reservoir	Ordovician
Formation	Black River
Producing Reservoir	
Lithology	HTD (61)
Trap Type	
Depositional Environment	
Discovery Well IP (Mcf)	4900
Drive Mechanism	
No. Producing Wells	1
No. Abandoned Wells	
Area (acreage)	
Oldest Formation Penetrated	
Expected Heterogeneity Due To	
Average Thickness	
Average Completion Thickness	
Average Porosity Log (%)	
Minimum Porosity Log (%)	
No. Data Points	1
Porosity Feet	27
Reservoir Temperature (F)	122
Initial Reservoir Pressure	
Producing Interval Depths	
Present Reservoir Pressure (psi/date)	
Status	
Original Gas in Place	
Original Gas Reserves	
Production Years	
Reported Cumulative Production	
No. wells Reported	
Estimated Cumulative Production	
Remaining Gas In Place (Mcf/Date)	
Remaining Gas Reserves	
Recovery Factor	
Initial Open Flow Mcfpd	
Final Open Flow Mcfpd	

Table 8-7. Well from the Cooper Hill field.

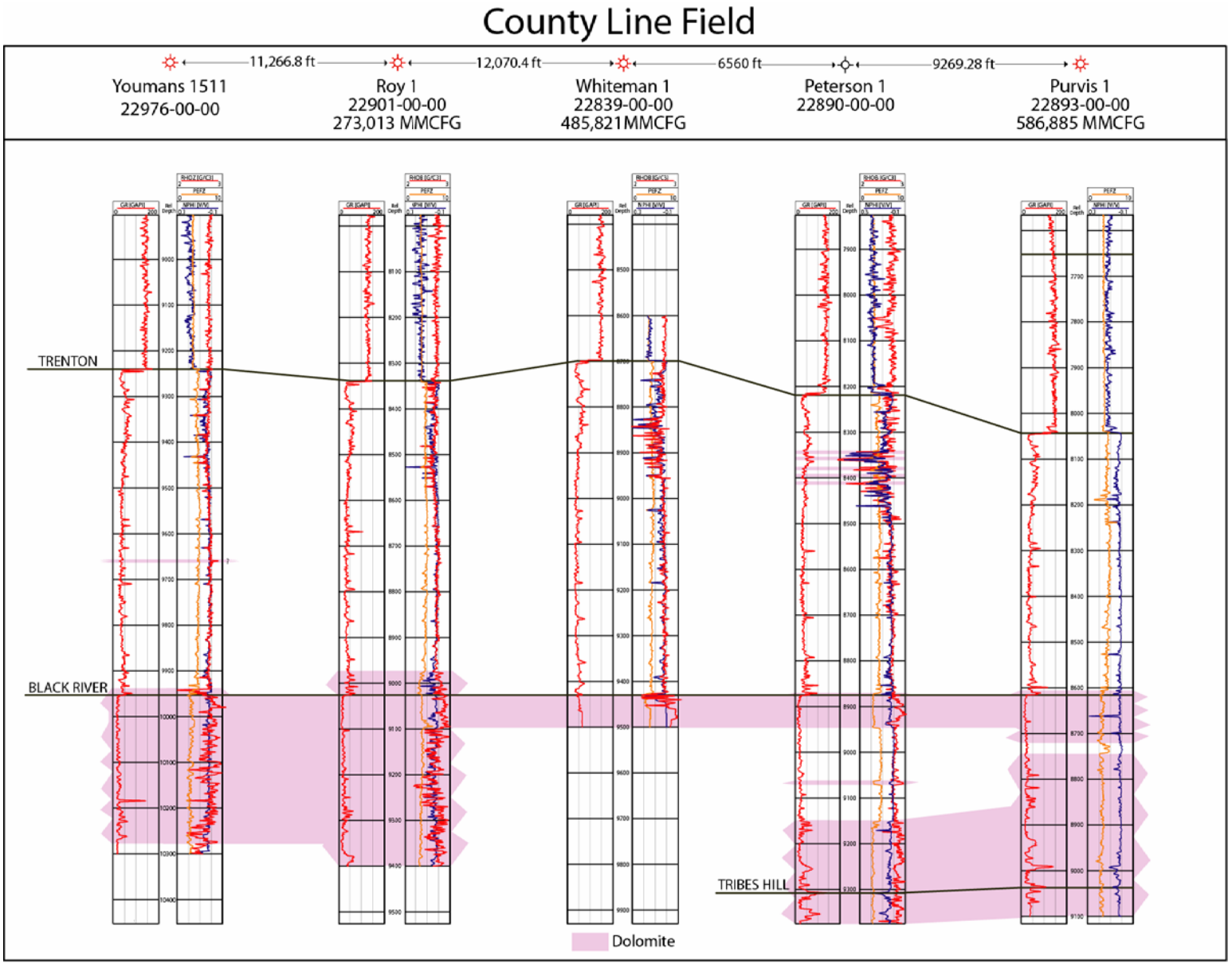

Figure 8-8 Well logs from the County Line field.

County Line Field	22839-00	22890-00	22893-00	22901-00	22976-00
Pool Number					
Discovered	2000				
Depth to Reservoir					
Age of Reservoir	Ordovician	Ordovician	Ordovician	Ordovician	Ordovician
Formation	Black River	Black River	Black River	Black River	Black River
Producing Reservoir					
Lithology	HTD(41.75)	HTD(165.91)	HTD(339.75)	HTD(314.55)	HTD(175
Trap Type					
Depositional Environment					
Discovery Well IP (Mcf)	8M	5	2M	7100	
Drive Mechanism					
No. Producing Wells	3	3	3	3	3
No. Abandoned Wells	1	1	1	1	1
Area (acreage)	235.02	31.41	32	69	178
Oldest Formation Penetrated					
Expected Heterogeneity Due To					
Average Thickness	123	6	40	95	242
Average Completion Thickness					
Average Porosity Log (%)					
Minimum Porosity Log (%)	5	5	5	5	5
No. Data Points					
Porosity Feet	12.25	70.75	24.5	108	26.25
Reservoir Temperature (F)	154	155	151	165	163
Initial Reservoir Pressure				3075	410
Producing Interval Depths	9388-9511	9034-9040	8653-8693	9063-9158	9940-10182
Present Reservoir Pressure (psi/date)					
Status					
Original Gas in Place					
Original Gas Reserves					
Production Years	3				
Reported Cumulative Production	1345719				
No. wells Reported					

Table 8-8. Wells from the County Line field.

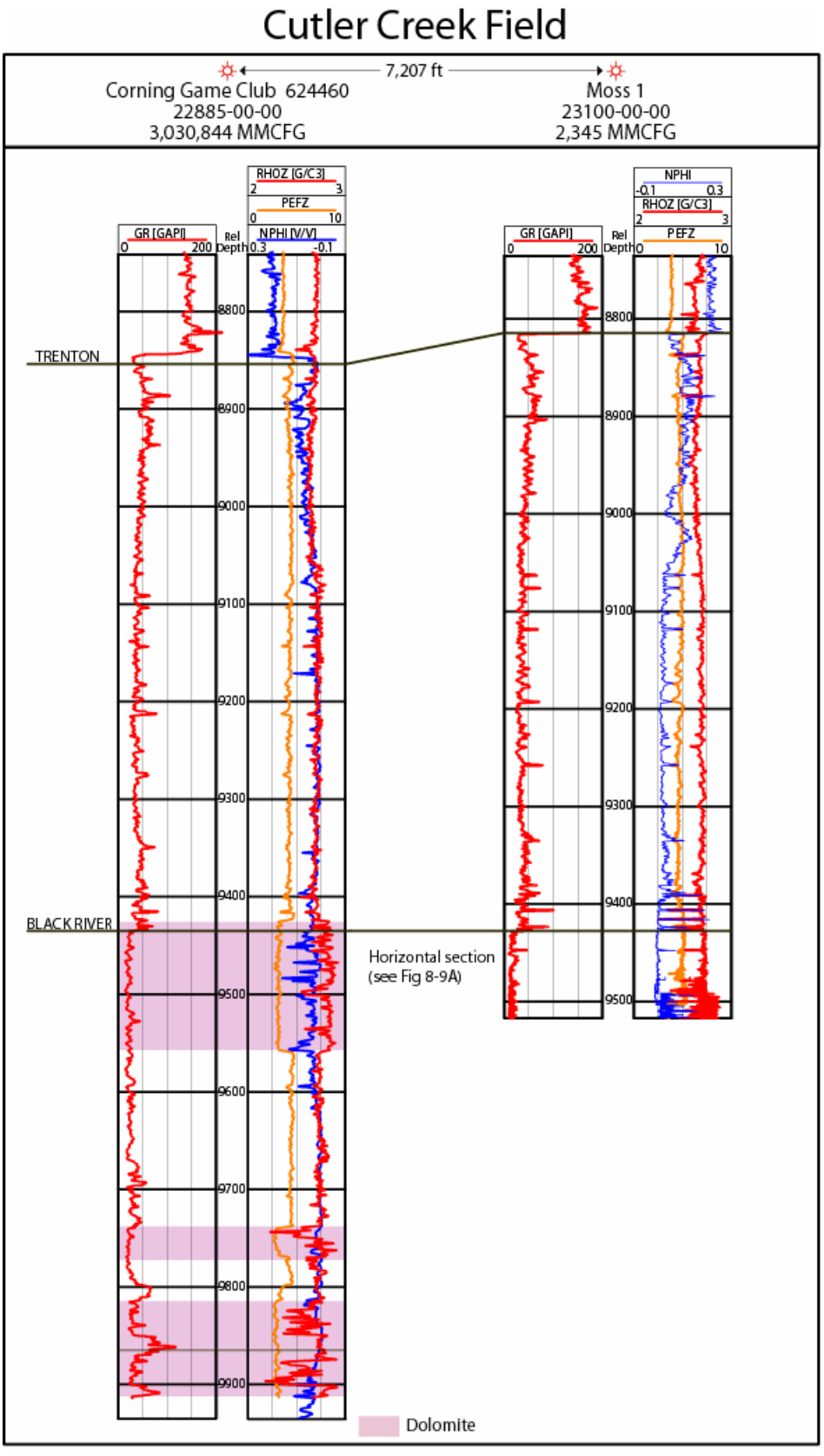

Figure 8-9 Well log from the Cutler Creek field.

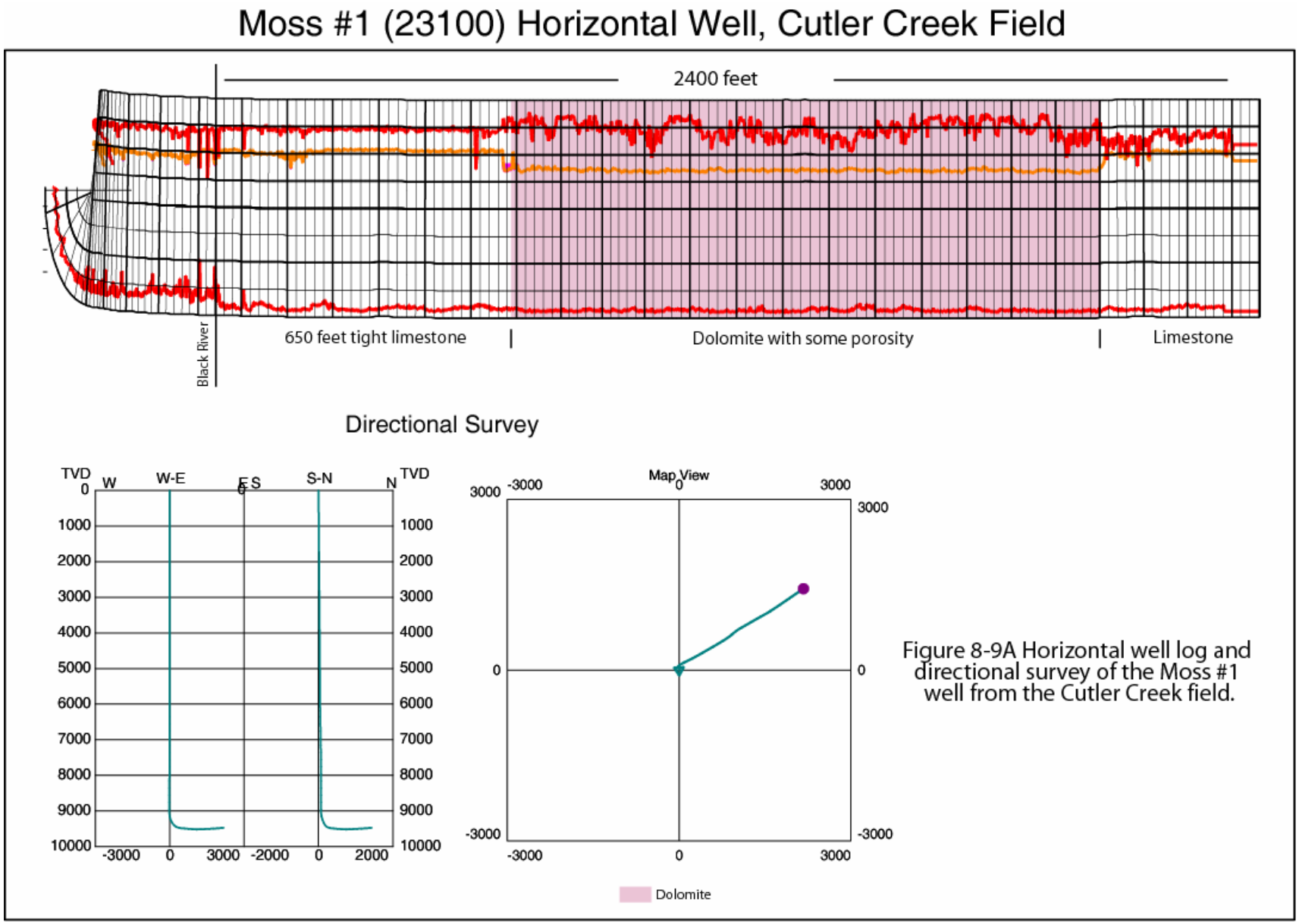

Figure 8-9A Horizontal well log and directional survey of the Moss #1 well from the Cutler Creek field.

Cutler Creek Field	22885-00	23100-00
Pool Number		
Discovered		2001
Depth to Reservoir		
Age of Reservoir	Ordovician	Ordovician
Formation	Black River	Black River
Producing Reservoir		
Lithology	HTD (163)	HTD (1330)
Trap Type		
Depositional Environment		
Discovery Well IP (Mcf)	21000	
Drive Mechanism		
No. Producing Wells	1	1
No. Abandoned Wells		
Area (acreage)	31.4	116
Oldest Formation Penetrated		
Expected Heterogeneity Due To		
Average Thickness	273	
Average Completion Thickness		
Average Porosity Log (%)		
Minimum Porosity Log (%)	5	5
No. Data Points	2	2
Porosity Feet		
Reservoir Temperature (F)	162	171
Initial Reservoir Pressure	3390	
Producing Interval Depths	9561-9834	
Present Reservoir Pressure (psi/date)		
Status		
Original Gas in Place		
Original Gas Reserves		
Production Years	4	
Reported Cumulative Production	3498617	
No. wells Reported		
Estimated Cumulative Production		
Remaining Gas In Place (Mcf/Date)		
Remaining Gas Reserves		
Recovery Factor		
Initial Open Flow Mcfpd		
Final Open Flow Mcfpd		

Table 8-9. Wells from the Cutler Creek field.

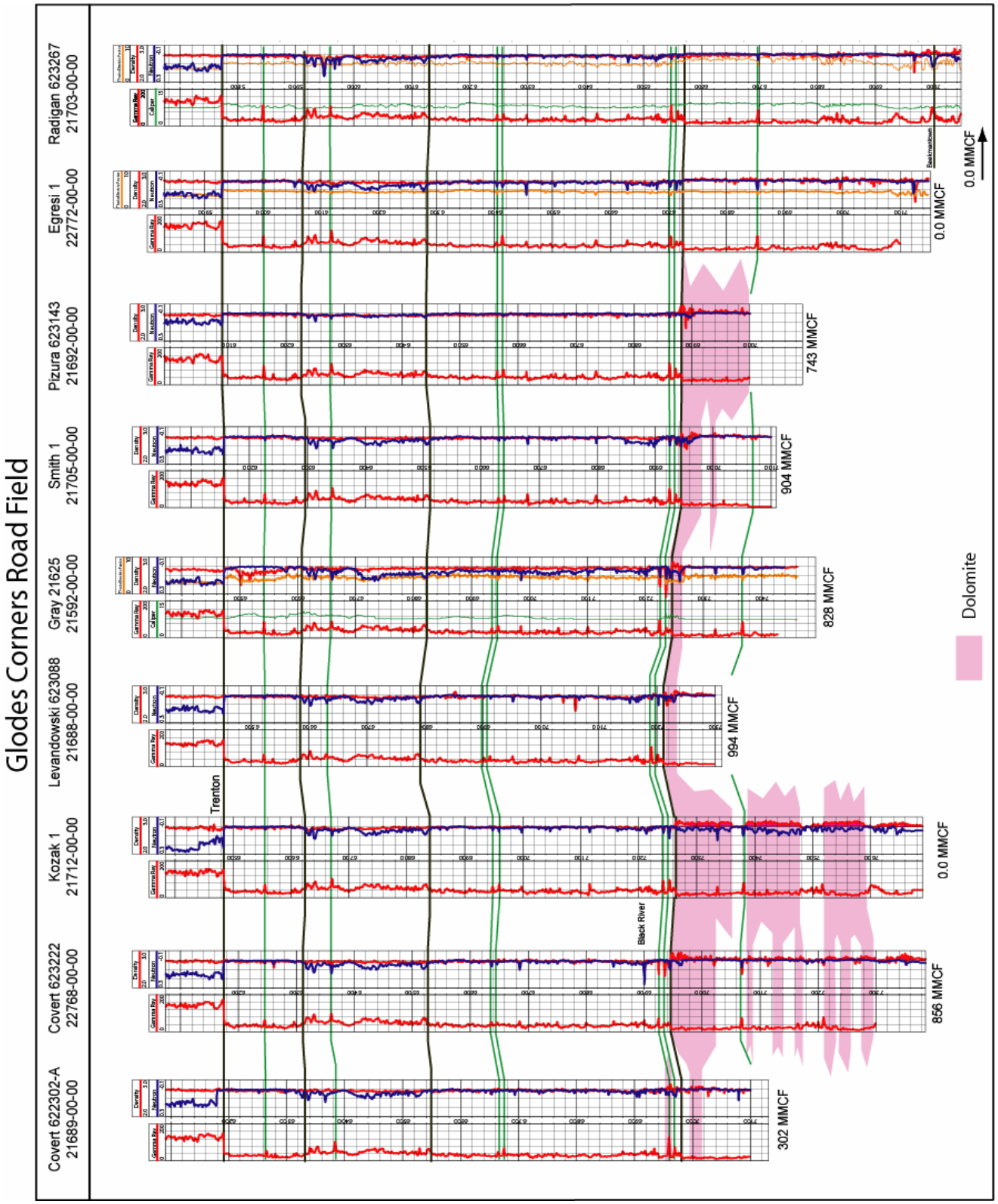

Figure 8-10. Cross Section From Glodes Corners Road Field.

Glodes Corner Road Field	19497-00	21592-00	21688-00
Pool Number			
Discovered	1986		
Depth to Reservoir			
Age of Reservoir	Ordovician	Ordovician	Ordovician
Formation	Black River	Black River	Black River
Producing Reservoir			
Lithology		HTD(23)	HTD(48.25)
Trap Type			
Depositional Environment			
Discovery Well IP (Mcf)	935	3290	2980
Drive Mechanism			
No. Producing Wells	12	12	12
No. Abandoned Wells	2	2	2
Area (acreage)	50	54.2	150
Oldest Formation Penetrated			
Expected Heterogeneity Due To			
Average Thickness	140	413	192
Average Completion Thickness			
Average Porosity Log (%)			
Minimum Porosity Log (%)	5	5	5
No. Data Points			
Porosity Feet		18.28	5.5
Reservoir Temperature (F)	133	131	129
Initial Reservoir Pressure	2404	2100	
Producing Interval Depths	7343-7483	7177-7590	7122-7314
Present Reservoir Pressure (psi/date)			
Status			
Original Gas in Place			
Original Gas Reserves			
Production Years	9		
Reported Cumulative Production	7556499		
No. wells Reported			
Estimated Cumulative Production			
Remaining Gas In Place (Mcf/Date)			
Remaining Gas Reserves			
Recovery Factor			
Initial Open Flow Mcfpd			
Final Open Flow Mcfpd			

Table 8-10. Wells from the Glodes Corner Road field

Glodes Corner Road Field	21703-00	21703-01	21705-00	21706-00	21710-00
Pool Number					
Discovered					
Depth to Reservoir					
Age of Reservoir	Ordovician	Ordovician	Ordovician	Ordovician	Ordovician
Formation	Black River	Black River	Black River	Black River	Black River
Producing Reservoir					
Lithology	HTD(62.25)		HTD(52)		
Trap Type					
Depositional Environment					
Discovery Well IP (Mcf)		6500	7000	7250	7975
Drive Mechanism					
No. Producing Wells	12	12	12	12	12
No. Abandoned Wells	2	2	2	2	2
Area (acreage)	31.4	31.4	186	31.4	31.4
Oldest Formation Penetrated					
Expected Heterogeneity Due To					
Average Thickness	2	13	23	8	46
Average Completion Thickness					
Average Porosity Log (%)					
Minimum Porosity Log (%)	5	5	5	5	5
No. Data Points					
Porosity Feet	53.25		13		
Reservoir Temperature (F)	135		130		130
Initial Reservoir Pressure		1700	2348	2058	2393
Producing Interval Depths	6968-6970	6685-6698	6935-6958	7040-7048	6645-6691
Present Reservoir Pressure (psi/date)					
Status					
Original Gas in Place					
Original Gas Reserves					
Production Years					
Reported Cumulative Production					
No. wells Reported					
Estimated Cumulative Production					
Remaining Gas In Place (Mcf/Date)					
Remaining Gas Reserves					
Recovery Factor					
Initial Open Flow Mcfpd					
Final Open Flow Mcfpd					

Table 8-10. Continued.

Glodes Corner Road Field	21712-00	22768-00	22769-00	22772-00
Pool Number				
Discovered				
Depth to Reservoir				
Age of Reservoir	Ordovician	Ordovician	Ordovician	Ordovician
Formation	Black River	Black River	Black River	Black River
Producing Reservoir				
Lithology	HTD(121.08)	HTD(231.25)		HTD(36)
Trap Type				
Depositional Environment				
Discovery Well IP (Mcf)	935	3800	5500	500
Drive Mechanism				
No. Producing Wells	12	12	12	12
No. Abandoned Wells	2	2	2	2
Area (acreage)	31.4	31.4		31.4
Oldest Formation Penetrated				
Expected Heterogeneity Due To				
Average Thickness	20	30	16	4
Average Completion Thickness				
Average Porosity Log (%)				
Minimum Porosity Log (%)	5	5	5	5
No. Data Points				
Porosity Feet	118.069	6.75		7
Reservoir Temperature (F)	139	130	141	129
Initial Reservoir Pressure	2108	1690	1500	1309
Producing Interval Depths	7552-7572	7200-7230	7250-7266	7124-7128
Present Reservoir Pressure (psi/date)				
Status				
Original Gas in Place				
Original Gas Reserves				
Production Years				
Reported Cumulative Production				
No. wells Reported				
Estimated Cumulative Production				
Remaining Gas In Place (Mcf/Date)				
Remaining Gas Reserves				
Recovery Factor				
Initial Open Flow Mcfpd				
Final Open Flow Mcfpd				

Table 8-10. Continued.

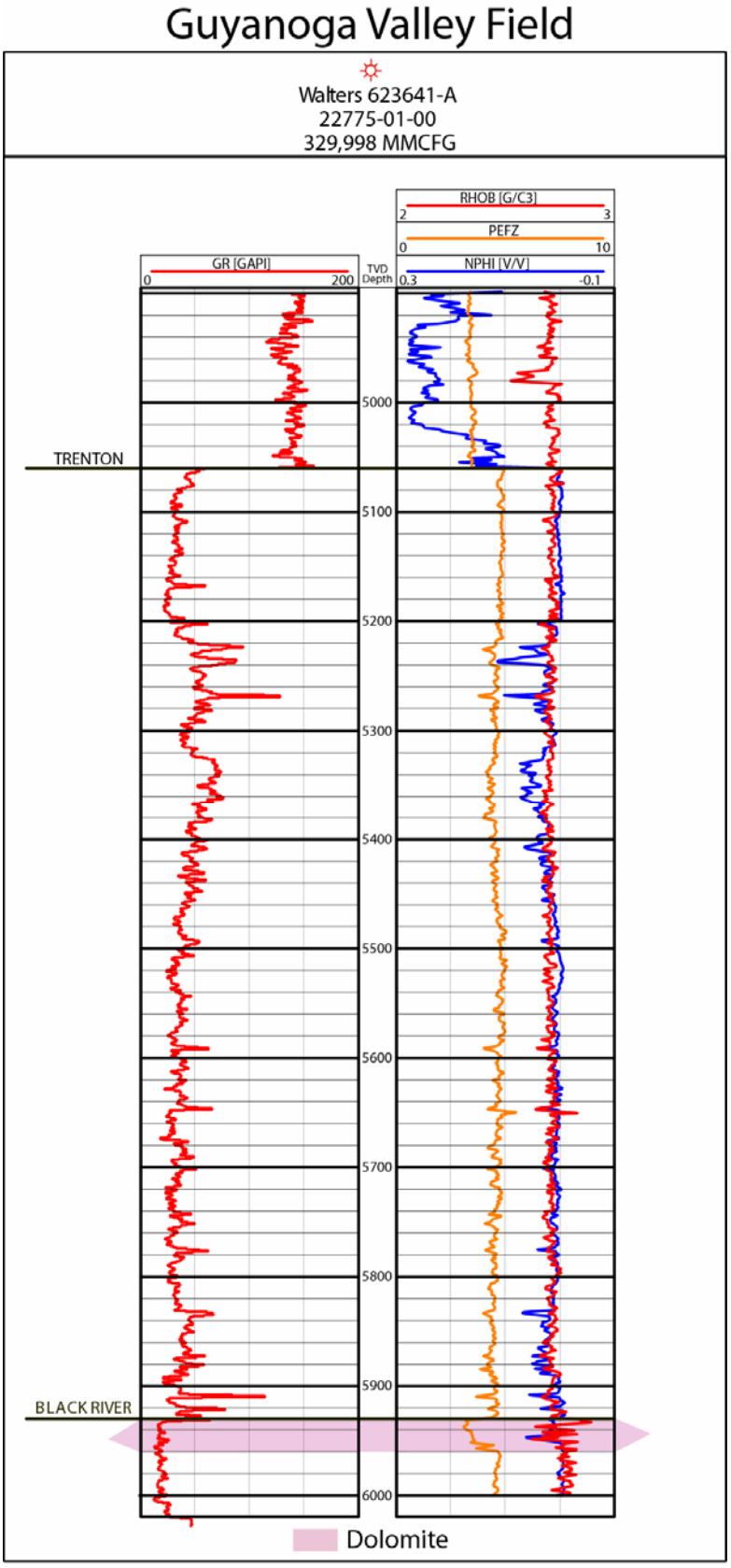

Figure 8-11 Well log from the Guyanoga Valley field.

Guyanoga Valley Field	
Pool Number	
Discovered	1999
Depth to Reservoir	
Age of Reservoir	Ordovician
Formation	Black River
Producing Reservoir	
Lithology	HTD (43.50)
Trap Type	
Depositional Environment	
Discovery Well IP (Mcf)	2540
Drive Mechanism	
No. Producing Wells	1
No. Abandoned Wells	
Area (acreage)	
Oldest Formation Penetrated	
Expected Heterogeneity Due To	
Average Thickness	
Average Completion Thickness	
Average Porosity Log (%)	
Minimum Porosity Log (%)	5
No. Data Points	1
Porosity Feet	1.5
Reservoir Temperature (F)	154
Initial Reservoir Pressure	2300
Producing Interval Depths	5932-5950
Present Reservoir Pressure (psi/date)	
Status	
Original Gas in Place	
Original Gas Reserves	
Production Years	2
Reported Cumulative Production	329998
No. wells Reported	
Estimated Cumulative Production	
Remaining Gas In Place (Mcf/Date)	
Remaining Gas Reserves	
Recovery Factor	
Initial Open Flow Mcfpd	
Final Open Flow Mcfpd	

Table 8-11. Well from the Guyanoga Valley field.

Langdon Hill Field

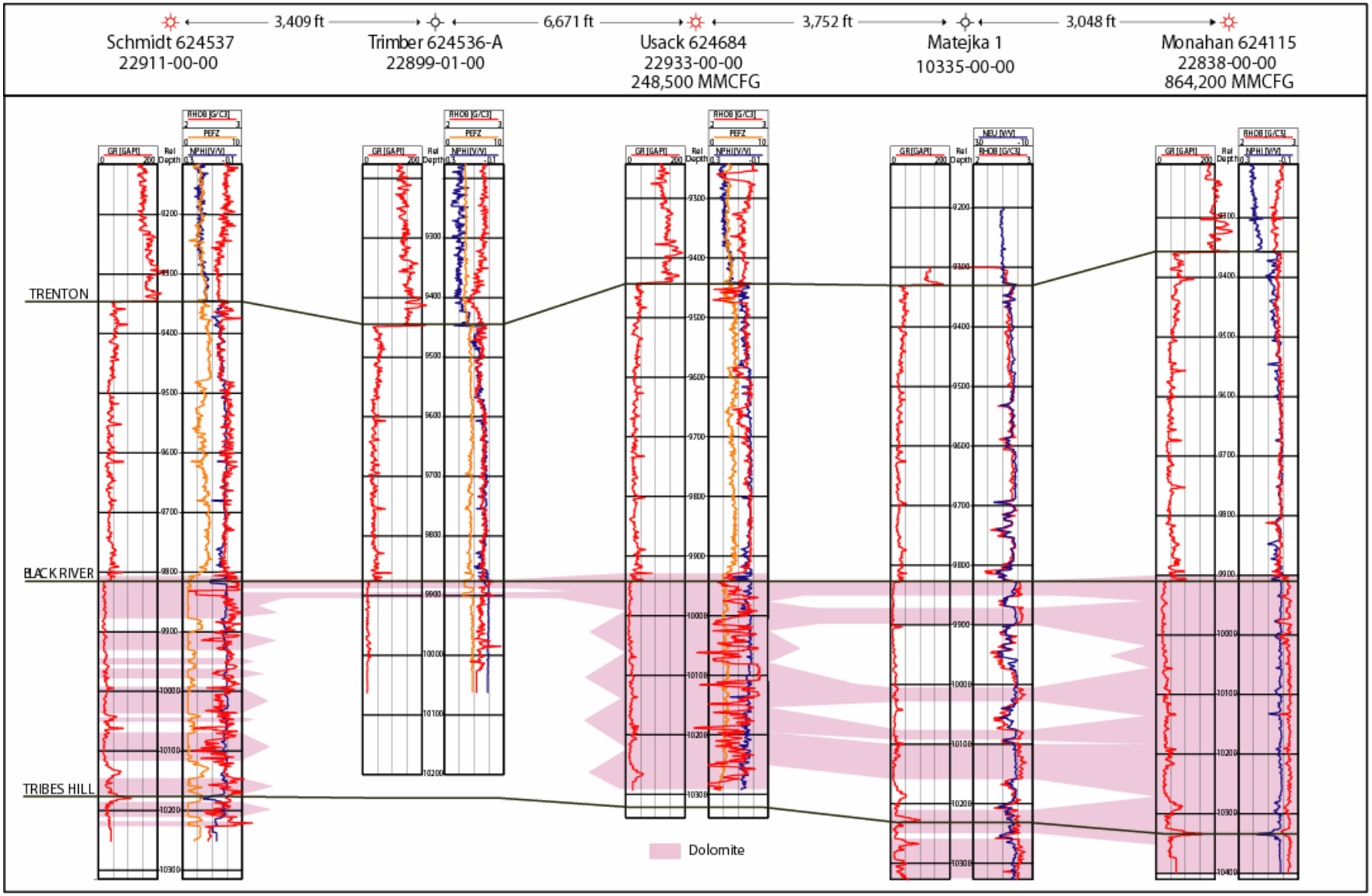

Figure 8-12 Well logs from the Langdon Hill field.

Langdon Hill	22838-00	22911-00	22933-00	23023-00	23156-00
Pool Number					
Discovered					
Depth to Reservoir					
Age of Reservoir	Ordovician	Ordovician	Ordovician	Ordovician	Ordovician
Formation	Black River	Black River	Black River	Black River	Black River
Producing Reservoir					
Lithology	HTD(29)	HTD(53.194)	HTD(89.007)		
Trap Type					
Depositional Environment					
Discovery Well IP (Mcf)	4850	940	1900		
Drive Mechanism					
No. Producing Wells					
No. Abandoned Wells					
Area (acreage)	31.4	31.4		78	
Oldest Formation Penetrated					
Expected Heterogeneity Due To					
Average Thickness	41	96	72		52.2
Average Completion Thickness					
Average Porosity Log (%)					
Minimum Porosity Log (%)					
No. Data Points	5	5	5	5	5
Porosity Feet	41.5	53.5	105		
Reservoir Temperature (F)	163	182	186	152	
Initial Reservoir Pressure	3800	2750	3620		
Producing Interval Depths	9974-10015	10384-10480	10118-10190		
Present Reservoir Pressure (psi/date)					
Status					
Original Gas in Place					
Original Gas Reserves					
Production Years	4		3	2	
Reported Cumulative Production	864169		248504	602050	
No. wells Reported					

Table 8-12 Wells from the Langdon Hill field.

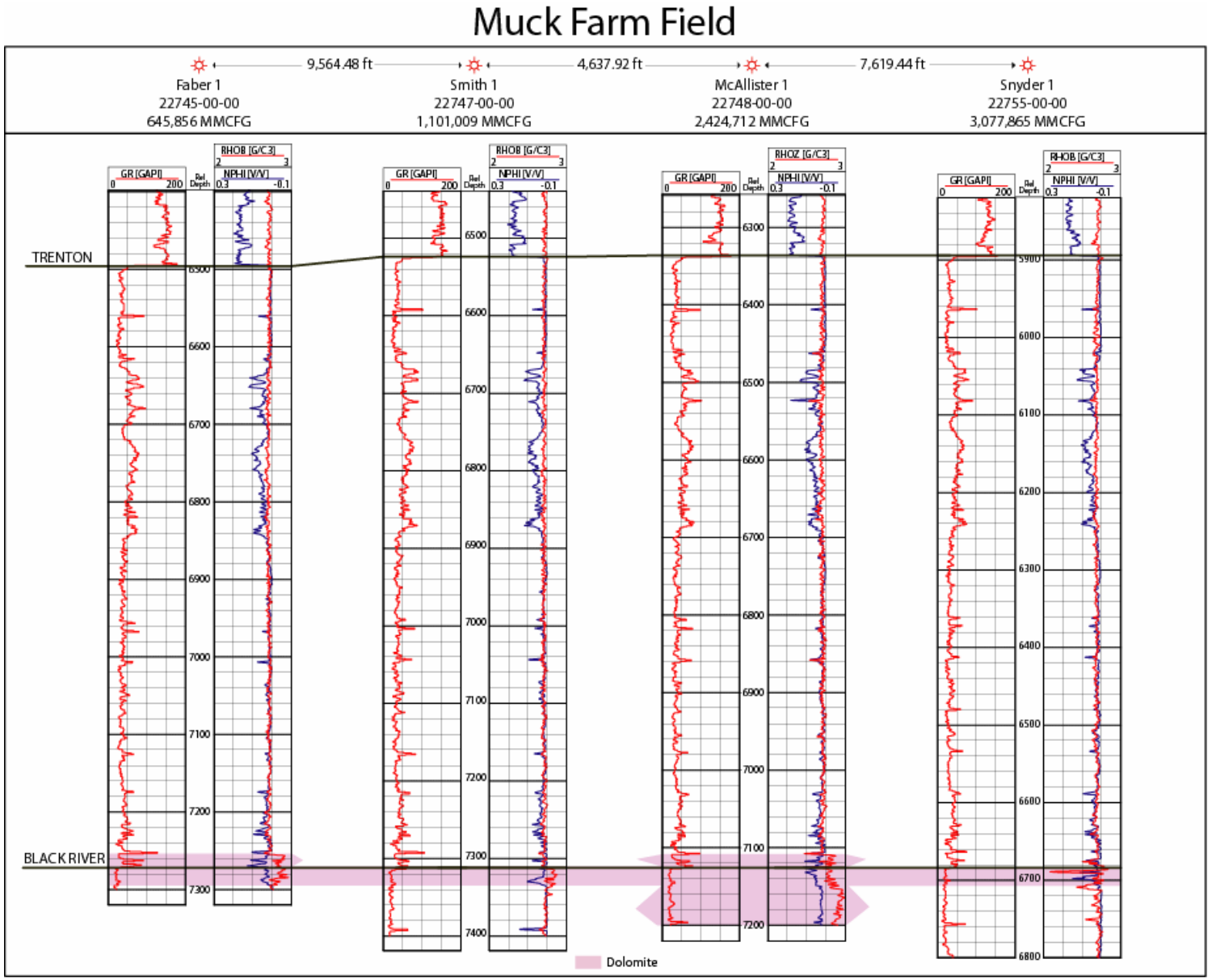

Figure 8-13 Well logs from the Muck Farm field.

Muck Farm	22745-00	22747-00	22748-00	22755-00
Pool Number				
Discovered	1998			
Depth to Reservoir				
Age of Reservoir	Ordovician	Ordovician	Ordovician	Ordovician
Formation	Black River	Black River	Black River	Black River
Producing Reservoir				
Lithology	HTD(5.5)	HTD(12.5)	HTD(14.00)	HTD(8.75)
Trap Type				
Depositional Environment				
Discovery Well IP (Mcf)	3100	2300	2100	6800
Drive Mechanism				
No. Producing Wells	4	4	4	4
No. Abandoned Wells				
Area (acreage)	31.4	31.4	31.4	31.4
Oldest Formation Penetrated				
Expected Heterogeneity Due To				
Average Thickness	29	22	27	28
Average Completion Thickness				
Average Porosity Log (%)				
Minimum Porosity Log (%)	5	5	5	5
No. Data Points				
Porosity Feet	2.5	9	21.25	7.5
Reservoir Temperature (F)	135	132	129	125
Initial Reservoir Pressure	2455	2485	2461	2485
Producing Interval Depths	7271-7300	7320-7342	7126-7153	6684-6712
Present Reservoir Pressure (psi/date)				
Status				
Original Gas in Place				
Original Gas Reserves				
Production Years	6			
Reported Cumulative Production	7258442			
No. wells Reported				
Estimated Cumulative Production				
Remaining Gas In Place (Mcf/Date)				
Remaining Gas Reserves				
Recovery Factor				
Initial Open Flow Mcfpd				
Final Open Flow Mcfpd				

Table 8-13. Wells from the Muck Farm field.

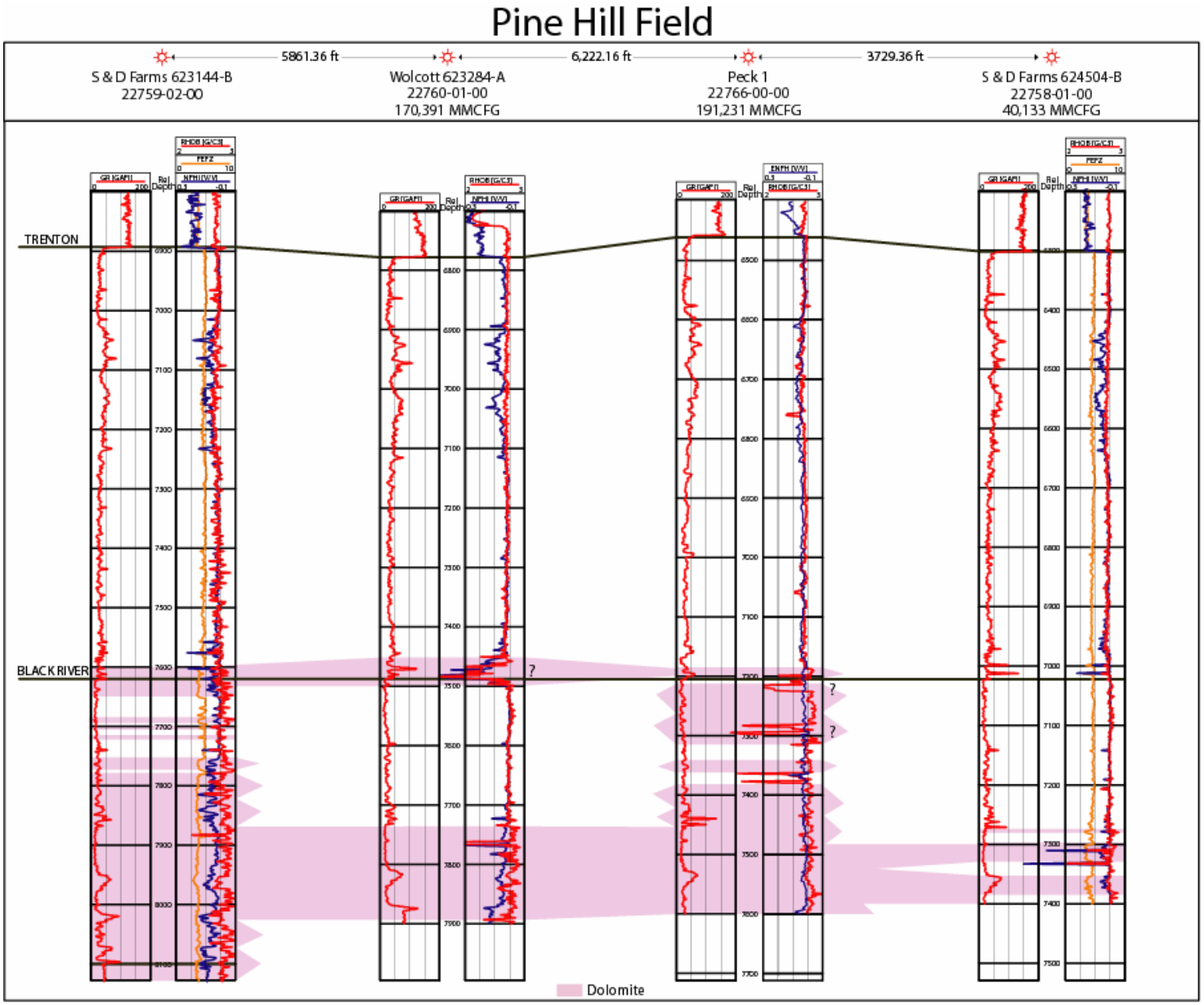

Figure 8-14 Well logs from the Pine Hill field.

Pine Hill Field	22758-01	22759-02	22760-01	22766-00
Pool Number				
Discovered	1999	1999	1999	1999
Depth to Reservoir				
Age of Reservoir	Ordovician	Ordovician	Ordovician	Ordovician
Formation	Black River	Black River	Black River	Black River
Producing Reservoir				
Lithology	HTD(61)	HTD(343)	HTD(121.75)	HTD(139.75)
Trap Type				
Depositional Environment				
Discovery Well IP (Mcf)	1200	900		
Drive Mechanism				
No. Producing Wells	3			
No. Abandoned Wells	1			
Area (acreage)	1623.32		31.4	
Oldest Formation Penetrated				
Expected Heterogeneity Due To				
Average Thickness	28	56	310	
Average Completion Thickness				
Average Porosity Log (%)				
Minimum Porosity Log (%)	5	5	5	5
No. Data Points				
Porosity Feet	21	200.5	9.1	9.75
Reservoir Temperature (F)	129	138	133	134
Initial Reservoir Pressure	2375	2375	2425	
Producing Interval Depths	7308-7336	7574-7631	7480-7790	
Present Reservoir Pressure (psi/date)				
Status				
Original Gas in Place				
Original Gas Reserves				
Production Years	5			
Reported Cumulative Production	401755			
No. wells Reported				
Estimated Cumulative Production				
Remaining Gas In Place (Mcf/Date)				
Remaining Gas Reserves				
Recovery Factor				
Initial Open Flow Mcfpd				
Final Open Flow Mcfpd				

Table 8-14. Wells from the Pine Hill field.

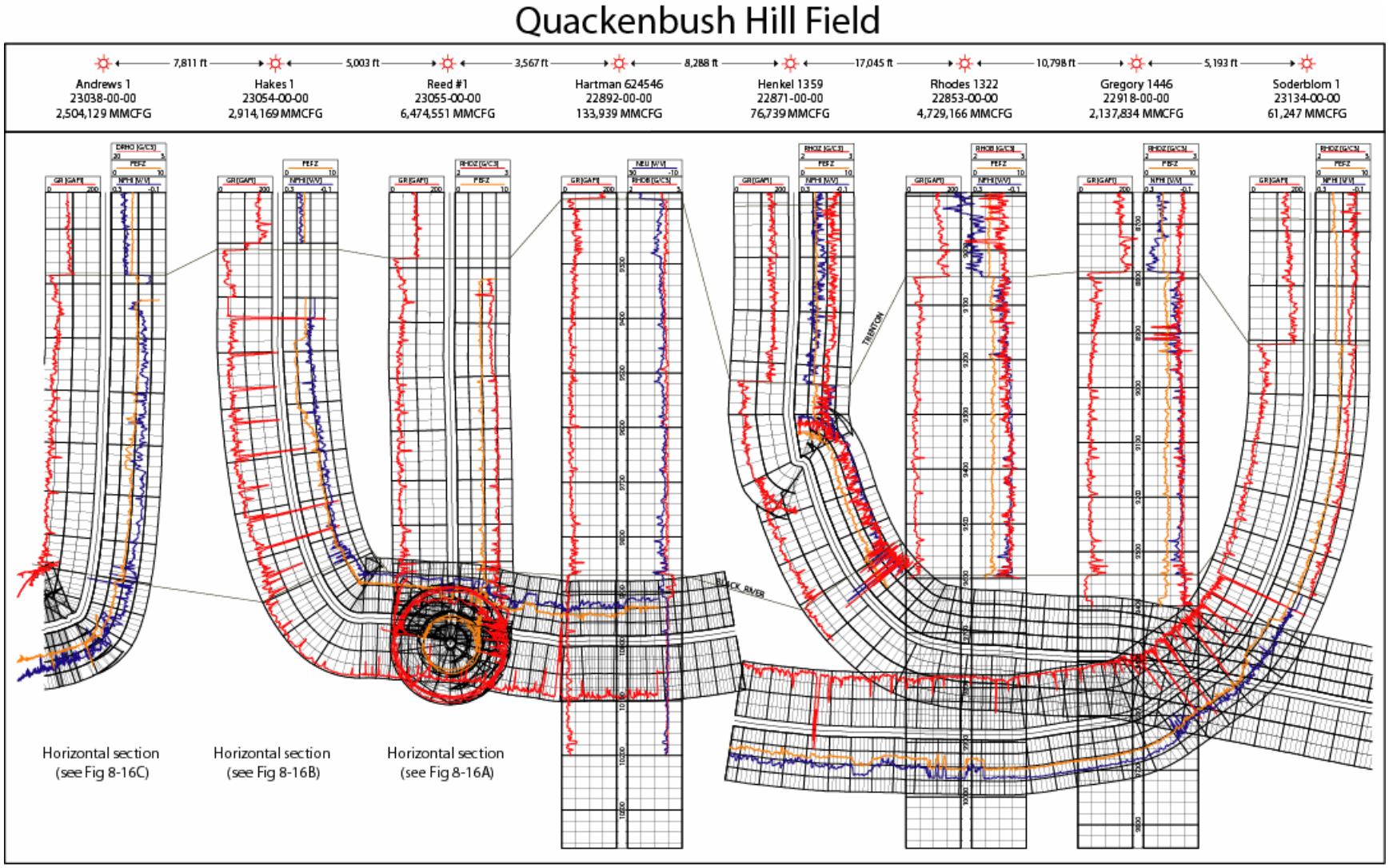

Figure 8-15 Well logs from the Quackenbush Hill field.

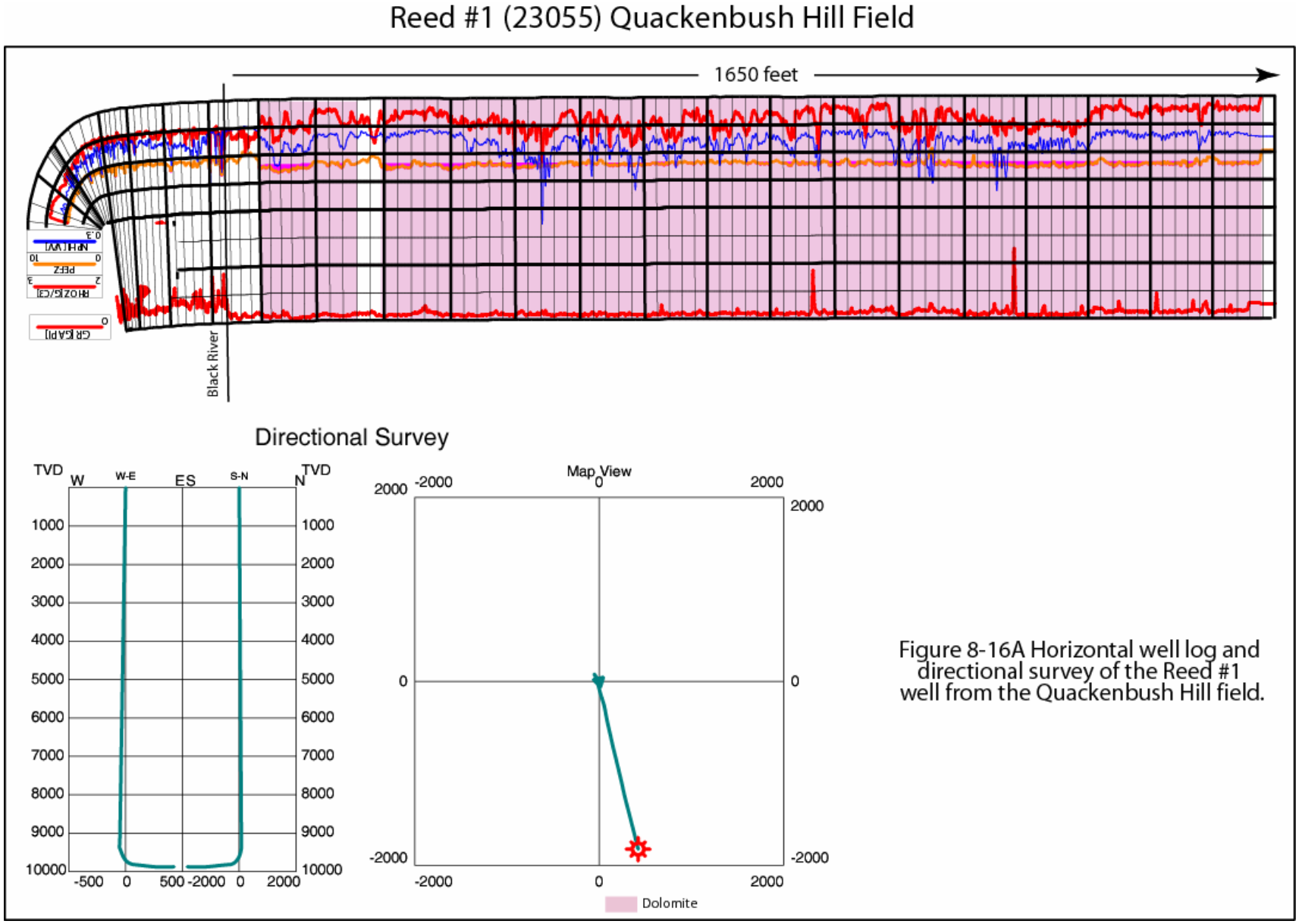

Figure 8-16A Horizontal well log and directional survey of the Reed #1 well from the Quackenbush Hill field.

Hakes #1 (23054) Quackenbush Hill Field

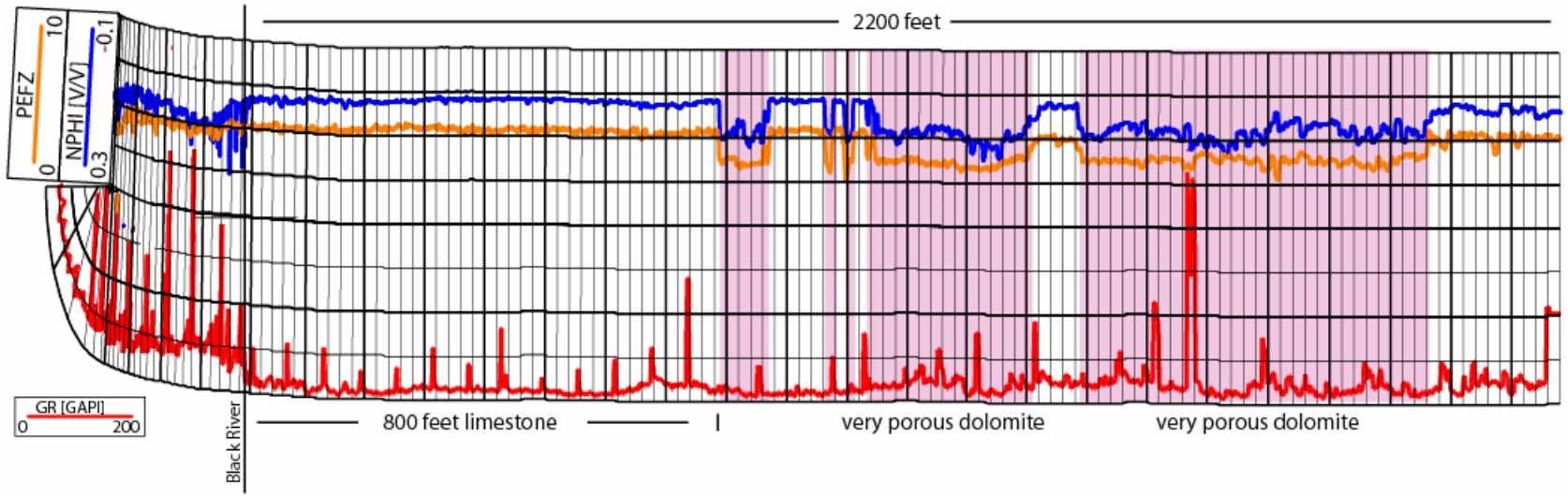

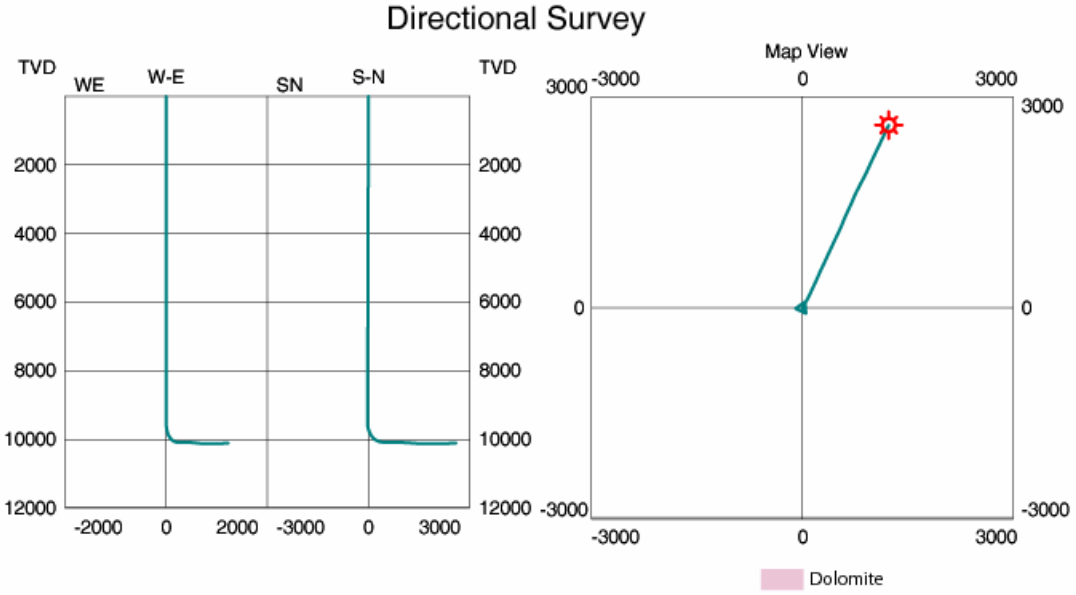

Figure 8-16B Horizontal well log and directional survey of the Hakes #1 well from the Quackenbush Hill field.

Andrews #1 (23038) Quakenbush Hill Field

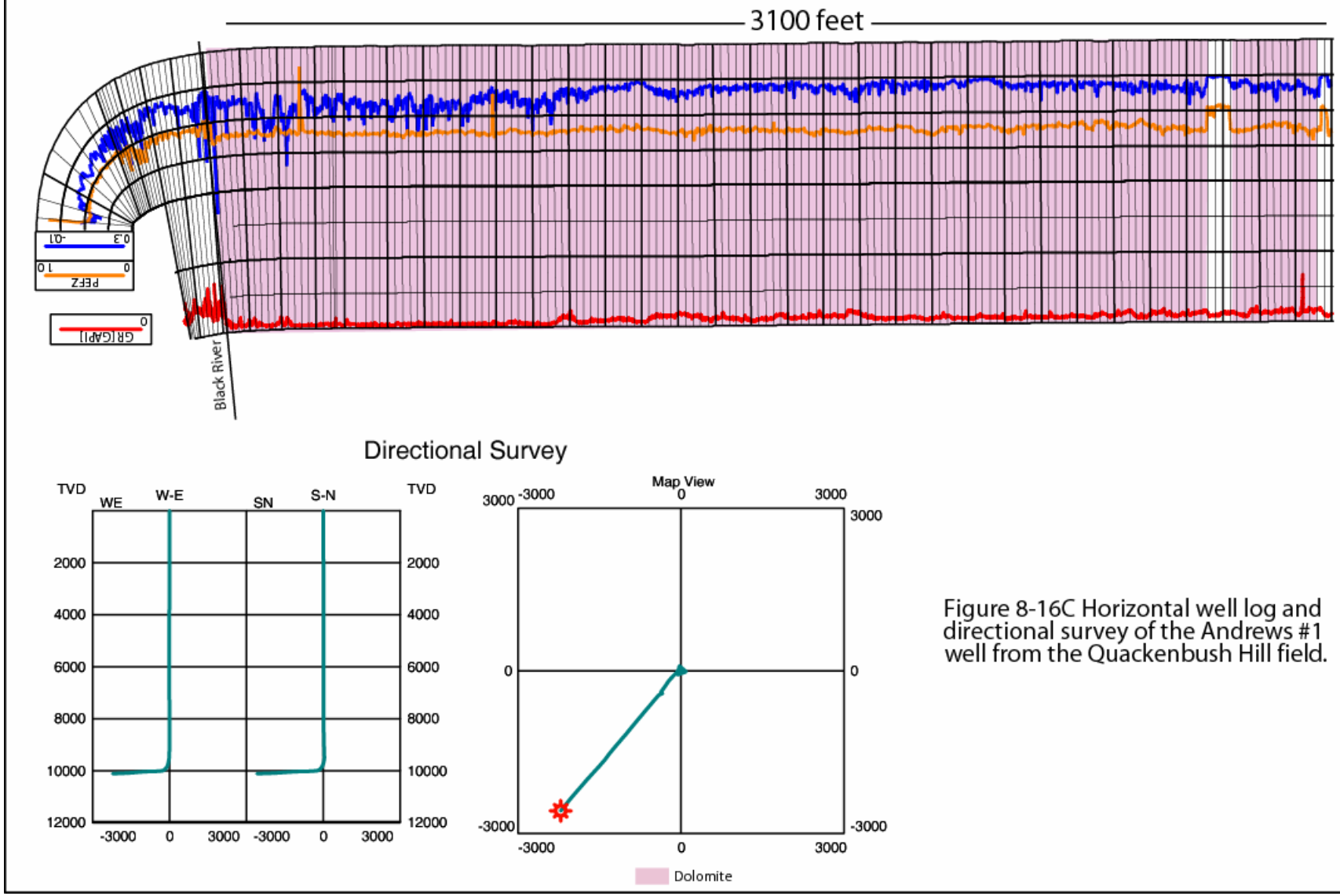

Figure 8-16C Horizontal well log and directional survey of the Andrews #1 well from the Quackenbush Hill field.

Quackenbush Hill Field	22831-00	22853-00	22871-01	22892-01
Pool Number				
Discovered	2000	2000	2000	2000
Depth to Reservoir				
Age of Reservoir	Ordovician	Ordovician	Ordovician	Ordovician
Formation	Black River	Black River	Black River	Black River
Producing Reservoir				
Lithology				HTD(120)
Trap Type				
Depositional Environment				
Discovery Well IP (Mcf)	26000	2500	15000	3400
Drive Mechanism				
No. Producing Wells	9	9	9	9
No. Abandoned Wells	1	1	1	1
Area (acreage)	38.8	75	338	34.1
Oldest Formation Penetrated				
Expected Heterogeneity Due To				
Average Thickness	137	211	2182	120
Average Completion Thickness				
Average Porosity Log (%)				
Minimum Porosity Log (%)				
No. Data Points	10			
Porosity Feet	137	211	2182	120
Reservoir Temperature (F)	125	157	145	162
Initial Reservoir Pressure	3633	3620	2820	3550
Producing Interval Depths	9687-9824	9549-9760	10143-12325	9884-9910 9974-9994
Present Reservoir Pressure (psi/date)				
Status				
Original Gas in Place				
Original Gas Reserves				
Production Years	4			
Reported Cumulative Production	43069867			
No. wells Reported				
Estimated Cumulative Production				
Remaining Gas In Place (Mcf/Date)				
Remaining Gas Reserves				
Recovery Factor				
Initial Open Flow Mcfpd				
Final Open Flow Mcfpd				

Table 8-15. Vertical wells from the Quackenbush Hill field.

Quackenbush Hill Field	22918-01	23028-00	23134-00
Pool Number			
Discovered	2000	2000	2000
Depth to Reservoir			
Age of Reservoir	Ordovician	Ordovician	Ordovician
Formation	Black River	Black River	Black River
Producing Reservoir			
Lithology	HTD(131)		
Trap Type			
Depositional Environment			
Discovery Well IP (Mcf)	3625	570	8
Drive Mechanism			
No. Producing Wells	9	9	9
No. Abandoned Wells	1	1	1
Area (acreage)	105	115.354	3176.17
Oldest Formation Penetrated			
Expected Heterogeneity Due To			
Average Thickness	108	963	2944
Average Completion Thickness			
Average Porosity Log (%)			
Minimum Porosity Log (%)			
No. Data Points			
Porosity Feet	108	936	2944
Reservoir Temperature (F)	158	140	134
Initial Reservoir Pressure	3610	2603	3614
Producing Interval Depths	9382-9404 9416-9490	11180-12116	9106-12050
Present Reservoir Pressure (psi/date)			
Status			
Original Gas in Place			
Original Gas Reserves			
Production Years			
Reported Cumulative Production			
No. wells Reported			
Estimated Cumulative Production			
Remaining Gas In Place (Mcf/Date)			
Remaining Gas Reserves			
Recovery Factor			
Initial Open Flow Mcfpd			
Final Open Flow Mcfpd			

Table 8-15. Continued.

Quackenbush Hill Field	23038-00	23054-00	23055-00
Pool Number			
Discovered	2000	2000	2000
Depth to Reservoir			
Age of Reservoir	Ordovician	Ordovician	Ordovician
Formation	Black River	Black River	Black River
Producing Reservoir			
Lithology	HTD(2563.75)	HTD(807)	HTD(964)
Trap Type			
Depositional Environment			
Discovery Well IP (Mcf)	15000	15	14
Drive Mechanism			
No. Producing Wells	9	9	9
No. Abandoned Wells	1	1	1
Area (acreage)		347	154.83
Oldest Formation Penetrated			
Expected Heterogeneity Due To			
Average Thickness	3809	3284	2357
Average Completion Thickness			
Average Porosity Log (%)			
Minimum Porosity Log (%)			
No. Data Points			
Porosity Feet	3809	3284	2357
Reservoir Temperature (F)	164	181	140
Initial Reservoir Pressure	3193		3077
Producing Interval Depths	9421-13230	9476-12760	9228-11585
Present Reservoir Pressure (psi/date)			
Status			
Original Gas in Place			
Original Gas Reserves			
Production Years			
Reported Cumulative Production			
No. wells Reported			
Estimated Cumulative Production			
Remaining Gas In Place (Mcf/Date)			
Remaining Gas Reserves			
Recovery Factor			
Initial Open Flow Mcfpd			
Final Open Flow Mcfpd			

Table 8-16. Horizontal wells from the Quackenbush Hill field.

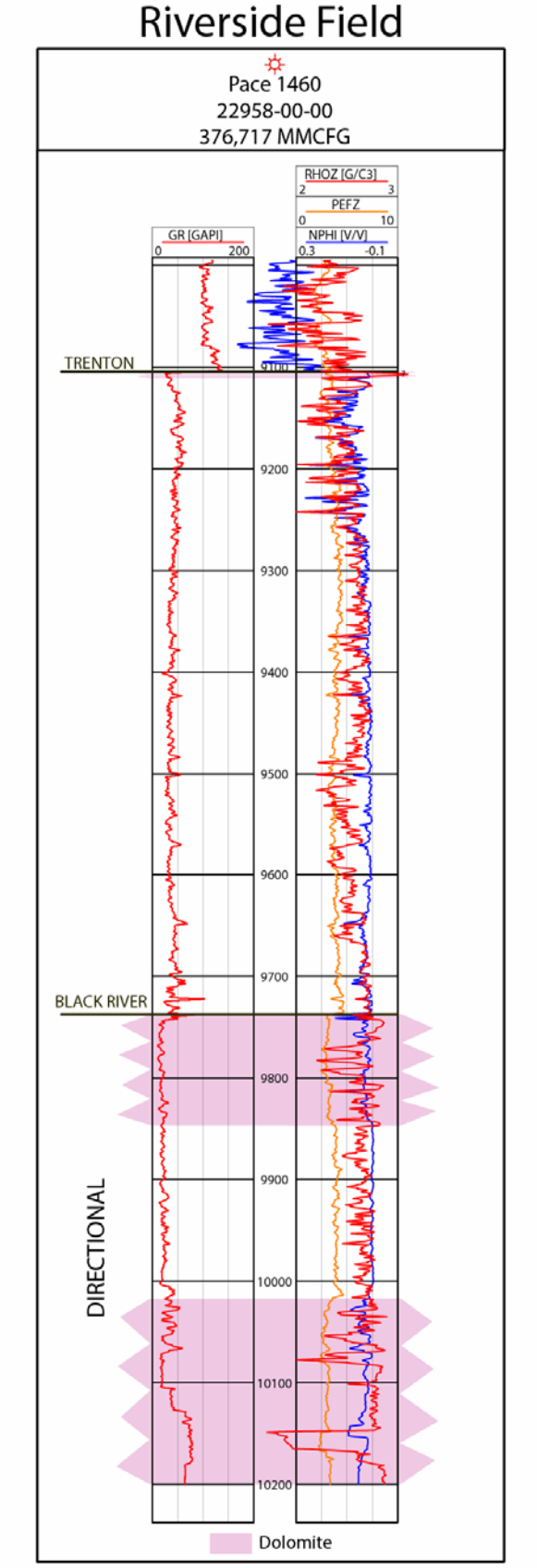

Figure 8-17 Well log from the Riverside field.

Riverside Field	22958-00
Pool Number	
Discovered	2002
Depth to Reservoir	
Age of Reservoir	Ordovician
Formation	Black River
Producing Reservoir	
Lithology	HTD (294)
Trap Type	
Depositional Environment	
Discovery Well IP (Mcf)	9715
Drive Mechanism	
No. Producing Wells	1
No. Abandoned Wells	
Area (acreage)	
Oldest Formation Penetrated	
Expected Heterogeneity Due To	
Average Thickness	
Average Completion Thickness	
Average Porosity Log (%)	
Minimum Porosity Log (%)	5
No. Data Points	1
Porosity Feet	
Reservoir Temperature (F)	161
Initial Reservoir Pressure	3605
Producing Interval Depths	9738-9834
Present Reservoir Pressure (psi/date)	
Status	
Original Gas in Place	
Original Gas Reserves	
Production Years	1
Reported Cumulative Production	376717
No. wells Reported	
Estimated Cumulative Production	
Remaining Gas In Place (Mcf/Date)	
Remaining Gas Reserves	
Recovery Factor	
Initial Open Flow Mcfpd	
Final Open Flow Mcfpd	

Table 8-17. Well from the Riverside field.

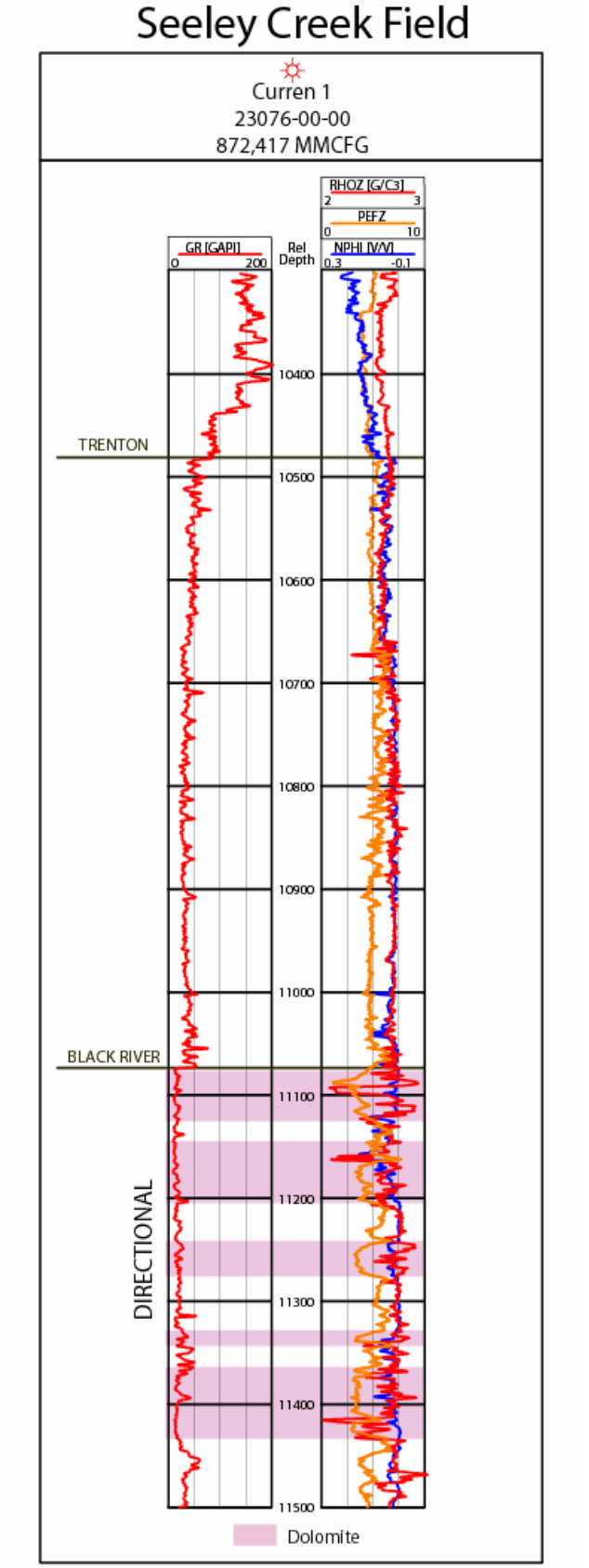

Figure 8-18 Well log from the Seeley Creek field.

Seeley Creek Field	23076-00
Pool Number	
Discovered	2004
Depth to Reservoir	
Age of Reservoir	Ordovician
Formation	Black River
Producing Reservoir	
Lithology	HTD (64.5)
Trap Type	
Depositional Environment	
Discovery Well IP (Mcf)	20300
Drive Mechanism	
No. Producing Wells	1
No. Abandoned Wells	
Area (acreage)	
Oldest Formation Penetrated	
Expected Heterogeneity Due To	
Average Thickness	
Average Completion Thickness	
Average Porosity Log (%)	
Minimum Porosity Log (%)	
No. Data Points	1
Porosity Feet	
Reservoir Temperature (F)	148
Initial Reservoir Pressure	4122
Producing Interval Depths	11026-11491
Present Reservoir Pressure (psi/date)	
Status	
Original Gas in Place	
Original Gas Reserves	
Production Years	1
Reported Cumulative Production	872417
No. wells Reported	
Estimated Cumulative Production	
Remaining Gas In Place (Mcf/Date)	
Remaining Gas Reserves	
Recovery Factor	
Initial Open Flow Mcfpd	
Final Open Flow Mcfpd	

Table 8-18. Well from the Seeley Creek field.

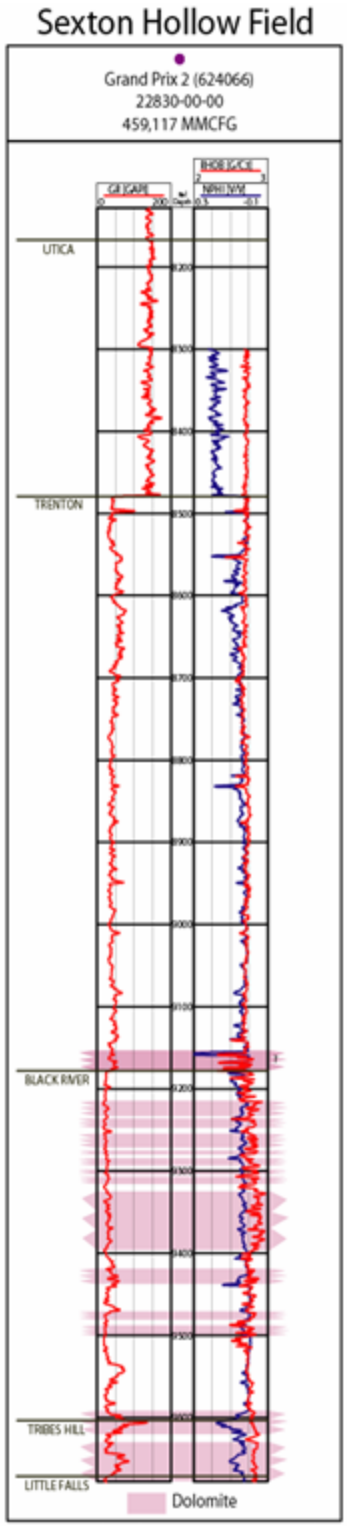

Figure 8-19 Well log from Sexton Hollow field.

Sexton Hollow Field	22830-00
Pool Number	
Discovered	2000
Depth to Reservoir	
Age of Reservoir	Ordovician
Formation	Black River
Producing Reservoir	
Lithology	HTD (145.75)
Trap Type	
Depositional Environment	
Discovery Well IP (Mcf)	940
Drive Mechanism	
No. Producing Wells	1
No. Abandoned Wells	
Area (acreage)	
Oldest Formation Penetrated	
Expected Heterogeneity Due To	
Average Thickness	
Average Completion Thickness	
Average Porosity Log (%)	
Minimum Porosity Log (%)	5
No. Data Points	
Porosity Feet	121
Reservoir Temperature (F)	157
Initial Reservoir Pressure	3180
Producing Interval Depths	9622-9630
Present Reservoir Pressure (psi/date)	
Status	
Original Gas in Place	
Original Gas Reserves	
Production Years	1
Reported Cumulative Production	459117
No. wells Reported	
Estimated Cumulative Production	
Remaining Gas In Place (Mcf/Date)	
Remaining Gas Reserves	
Recovery Factor	
Initial Open Flow Mcfpd	
Final Open Flow Mcfpd	

Table 8-19. Well from the Sexton Hollow field.

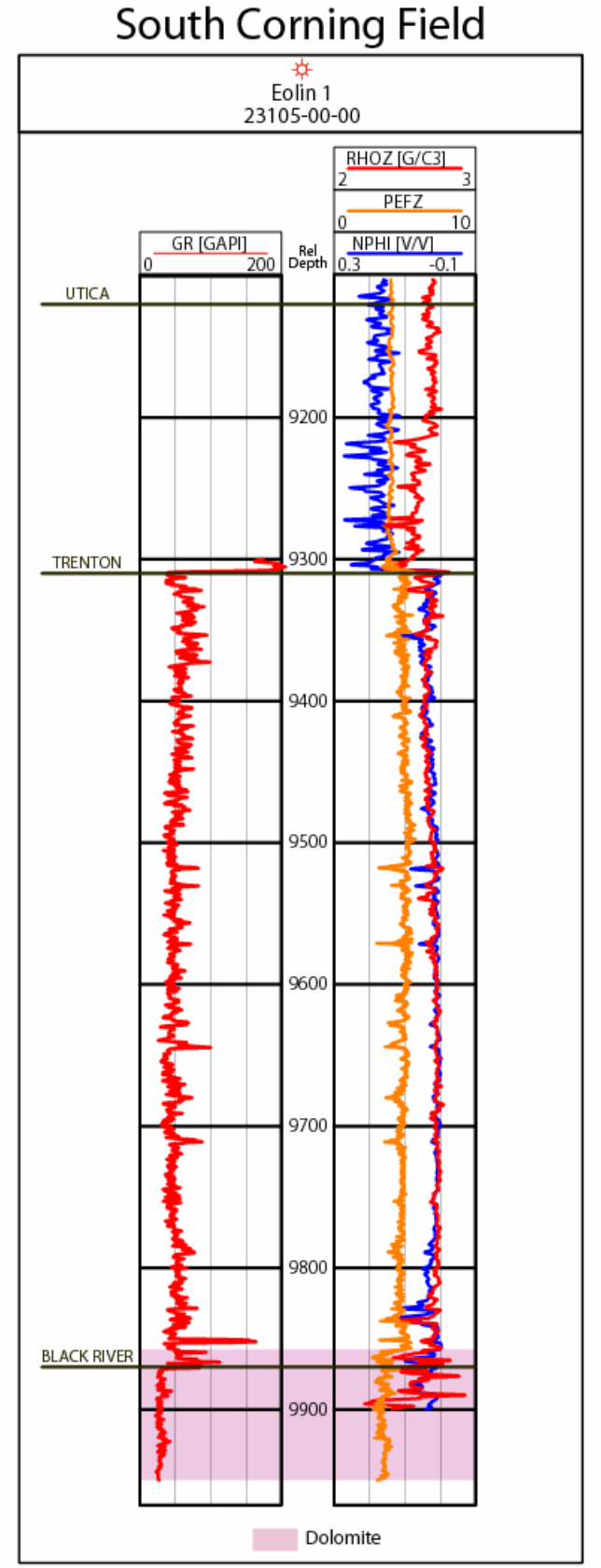

Figure 8-20 Well log from the South Corning field.

South Corning Field	23105-00
Pool Number	
Discovered	2004
Depth to Reservoir	
Age of Reservoir	Ordovician
Formation	Black River
Producing Reservoir	
Lithology	HTD (29)
Trap Type	
Depositional Environment	
Discovery Well IP (Mcf)	1
Drive Mechanism	
No. Producing Wells	1
No. Abandoned Wells	
Area (acreage)	
Oldest Formation Penetrated	
Expected Heterogeneity Due To	
Average Thickness	
Average Completion Thickness	
Average Porosity Log (%)	
Minimum Porosity Log (%)	
No. Data Points	1
Porosity Feet	
Reservoir Temperature (F)	174
Initial Reservoir Pressure	1758
Producing Interval Depths	9700-9992
Present Reservoir Pressure (psi/date)	
Status	
Original Gas in Place	
Original Gas Reserves	
Production Years	
Reported Cumulative Production	
No. wells Reported	
Estimated Cumulative Production	
Remaining Gas In Place (Mcf/Date)	
Remaining Gas Reserves	
Recovery Factor	
Initial Open Flow Mcfpd	
Final Open Flow Mcfpd	

Table 8-20. Well from the South Corning field.

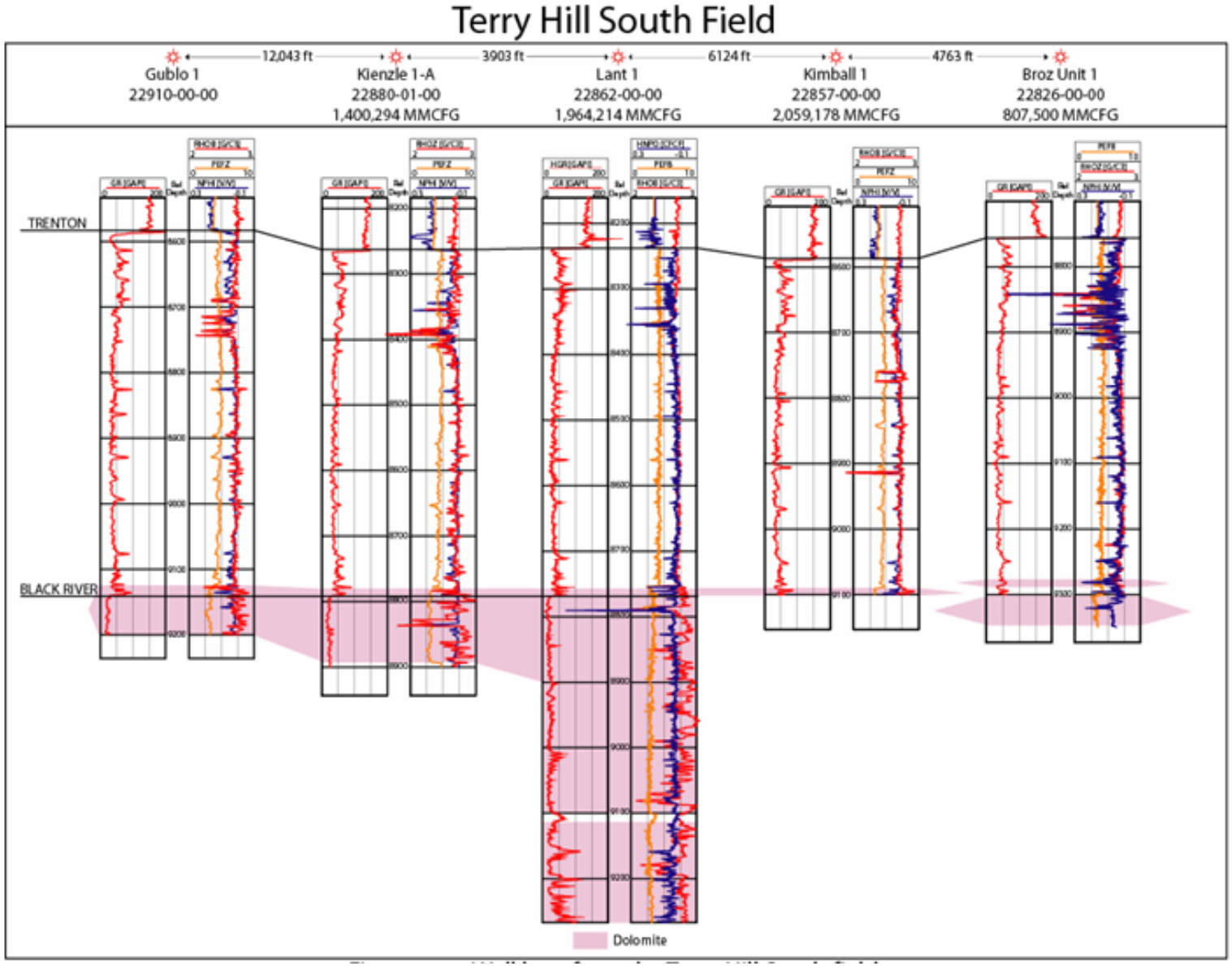

Figure 8-21 Well logs from the Terry Hill South field

Terry Hill South Field	22826-00	22857-00	22862-00	22880-01
Pool Number				
Discovered	2000			
Depth to Reservoir				
Age of Reservoir	Ordovician	Ordovician	Ordovician	Ordovician
Formation	Black River	Black River	Black River	Black River
Producing Reservoir				
Lithology			HTD(284)	HTD(48)
Trap Type				
Depositional Environment				
Discovery Well IP (Mcf)	17000	40M	15M	2098
Drive Mechanism				
No. Producing Wells	5	5	5	5
No. Abandoned Wells	2	2	2	2
Area (acreage)	555.43	62	448	57
Oldest Formation Penetrated				
Expected Heterogeneity Due To				
Average Thickness	395	136	694	255
Average Completion Thickness				
Average Porosity Log (%)				
Minimum Porosity Log (%)	5			
No. Data Points				
Porosity Feet			181	11.956
Reservoir Temperature (F)	151	169	159	150
Initial Reservoir Pressure	3200	3275	3325	3275
Producing Interval Depths	8962-9357	9030-9166	8667-9361	8787-9042
Present Reservoir Pressure (psi/date)				
Status				
Original Gas in Place				
Original Gas Reserves				
Production Years	4			
Reported Cumulative Production	6348401			
No. wells Reported				
Estimated Cumulative Production				
Remaining Gas In Place (Mcf/Date)				
Remaining Gas Reserves				
Recovery Factor				
Initial Open Flow Mcfpd				
Final Open Flow Mcfpd				

Table 8-21. Wells from the Terry Hill South field.

Terry Hill South Field	22889-01	22910-00	23017-00
Pool Number			
Discovered			
Depth to Reservoir			
Age of Reservoir	Ordovician	Ordovician	Ordovician
Formation	Black River	Black River	Black River
Producing Reservoir			
Lithology	HTD(35)	HTD(44.47)	
Trap Type			
Depositional Environment			
Discovery Well IP (Mcf)	18.5M	5	
Drive Mechanism			
No. Producing Wells	5	5	5
No. Abandoned Wells	2	2	2
Area (acreage)	32	210	50
Oldest Formation Penetrated			
Expected Heterogeneity Due To			
Average Thickness	224	77	2354
Average Completion Thickness			
Average Porosity Log (%)			
Minimum Porosity Log (%)			
No. Data Points			
Porosity Feet	1.25	4.4	
Reservoir Temperature (F)	150	165	140
Initial Reservoir Pressure	3350		4160
Producing Interval Depths	8892-9116	9154-9231	8831-11185
Present Reservoir Pressure (psi/date)			
Status			
Original Gas in Place			
Original Gas Reserves			
Production Years			
Reported Cumulative Production			
No. wells Reported			
Estimated Cumulative Production			
Remaining Gas In Place (Mcf/Date)			
Remaining Gas Reserves			
Recovery Factor			
Initial Open Flow Mcfpd			
Final Open Flow Mcfpd			

Table 8-21. Continued.

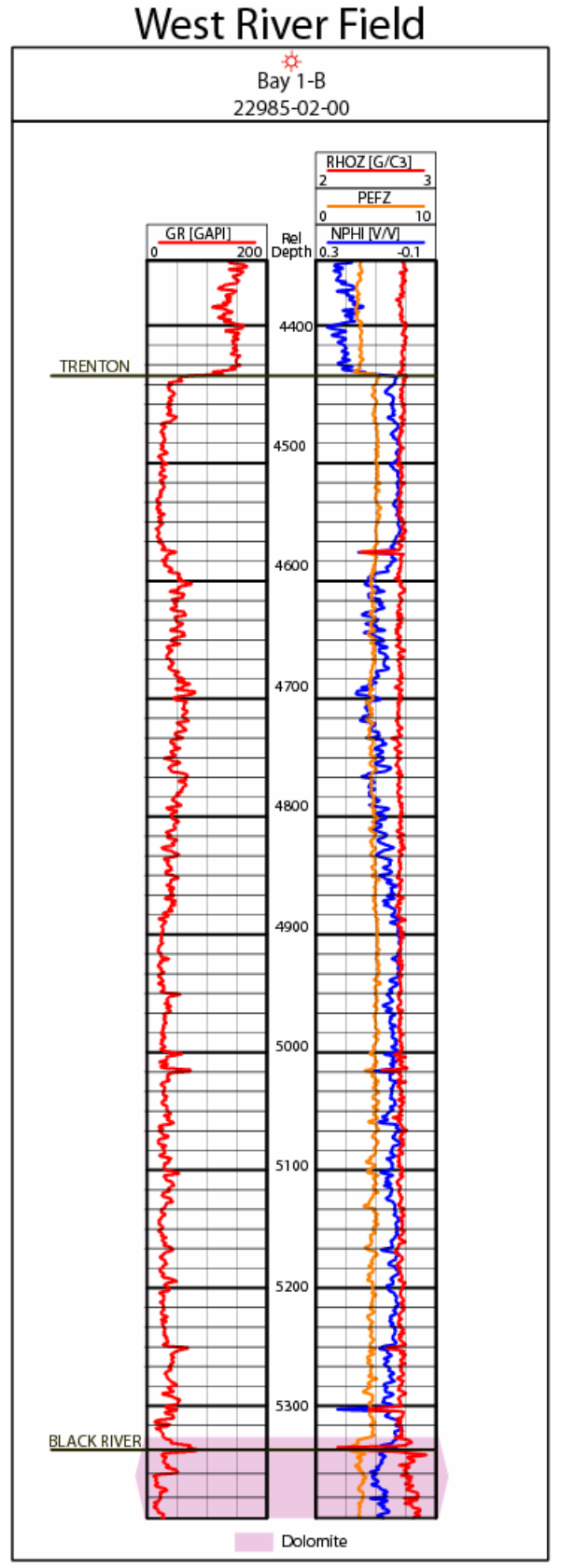

Figure 8-22 Well log from the West River field.

West River Field	22985-02	22985-01
Pool Number		
Discovered		
Depth to Reservoir		
Age of Reservoir	Ordovician	Ordovician
Formation	Black River	Black River
Producing Reservoir		
Lithology	HTD(51.71)	HTD(10.49)
Trap Type		
Depositional Environment		
Discovery Well IP (Mcf)		
Drive Mechanism		
No. Producing Wells		
No. Abandoned Wells		
Area (acreage)	285	
Oldest Formation Penetrated		
Expected Heterogeneity Due To		
Average Thickness	177	499
Average Completion Thickness		
Average Porosity Log (%)		
Minimum Porosity Log (%)	5	5
No. Data Points		
Porosity Feet	152	6
Reservoir Temperature (F)	108	113
Initial Reservoir Pressure		1750
Producing Interval Depths	5303-5480	4784-5233
Present Reservoir Pressure (psi/date)		
Status		
Original Gas in Place		
Original Gas Reserves		
Production Years		
Reported Cumulative Production		
No. wells Reported		
Estimated Cumulative Production		
Remaining Gas In Place (Mcf/Date)		
Remaining Gas Reserves		
Recovery Factor		
Initial Open Flow Mcfpd		
Final Open Flow Mcfpd		

Table 8-22. Wells from the West River field.

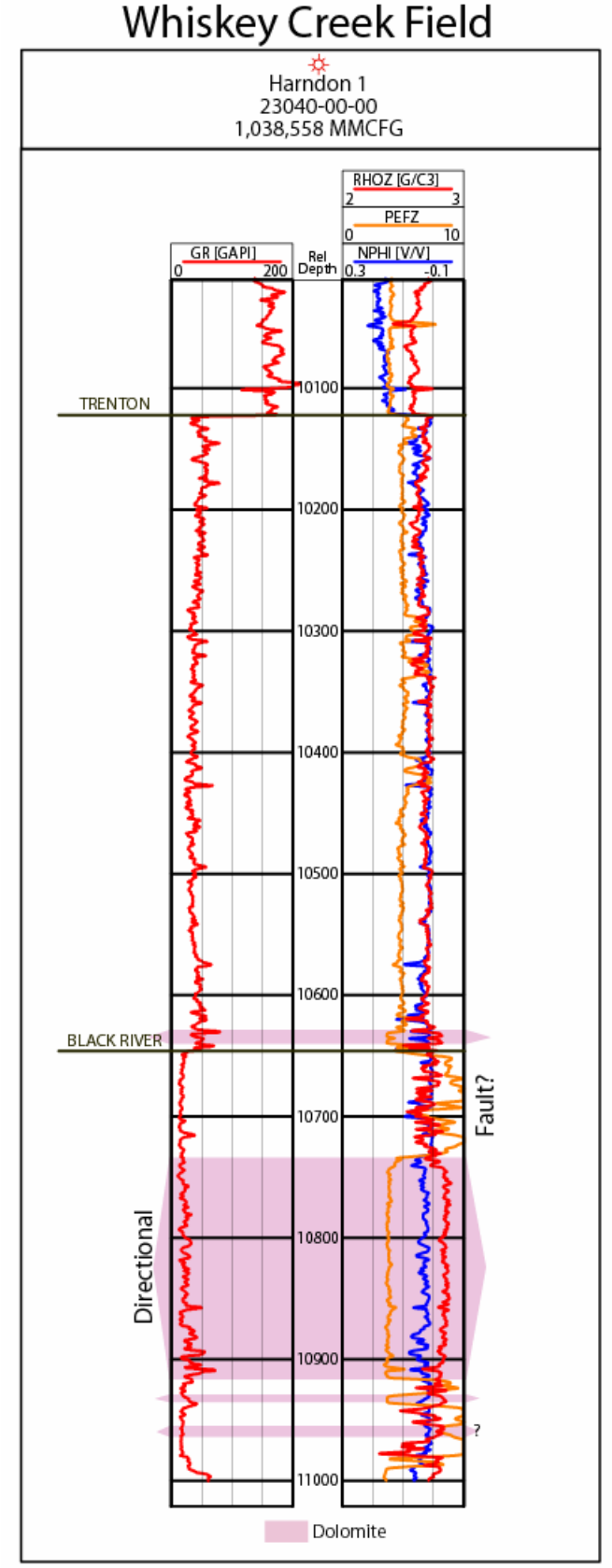

Figure 8-23 Well log from the Whiskey Creek field.

Whiskey Creek Field	23040-00
Pool Number	
Discovered	2003
Depth to Reservoir	
Age of Reservoir	Ordovician
Formation	Black River
Producing Reservoir	
Lithology	HTD (176)
Trap Type	
Depositional Environment	
Discovery Well IP (Mcf)	
Drive Mechanism	
No. Producing Wells	
No. Abandoned Wells	
Area (acreage)	
Oldest Formation Penetrated	
Expected Heterogeneity Due To	
Average Thickness	
Average Completion Thickness	437
Average Porosity Log (%)	
Minimum Porosity Log (%)	
No. Data Points	1
Porosity Feet	
Reservoir Temperature (F)	133
Initial Reservoir Pressure	4122
Producing Interval Depths	10575-11012
Present Reservoir Pressure (psi/date)	
Status	
Original Gas in Place	
Original Gas Reserves	
Production Years	2
Reported Cumulative Production	1038558
No. wells Reported	
Estimated Cumulative Production	
Remaining Gas In Place (Mcf/Date)	
Remaining Gas Reserves	
Recovery Factor	
Initial Open Flow Mcfpd	
Final Open Flow Mcfpd	

Table 8-23. Well from the Whiskey Creek field.

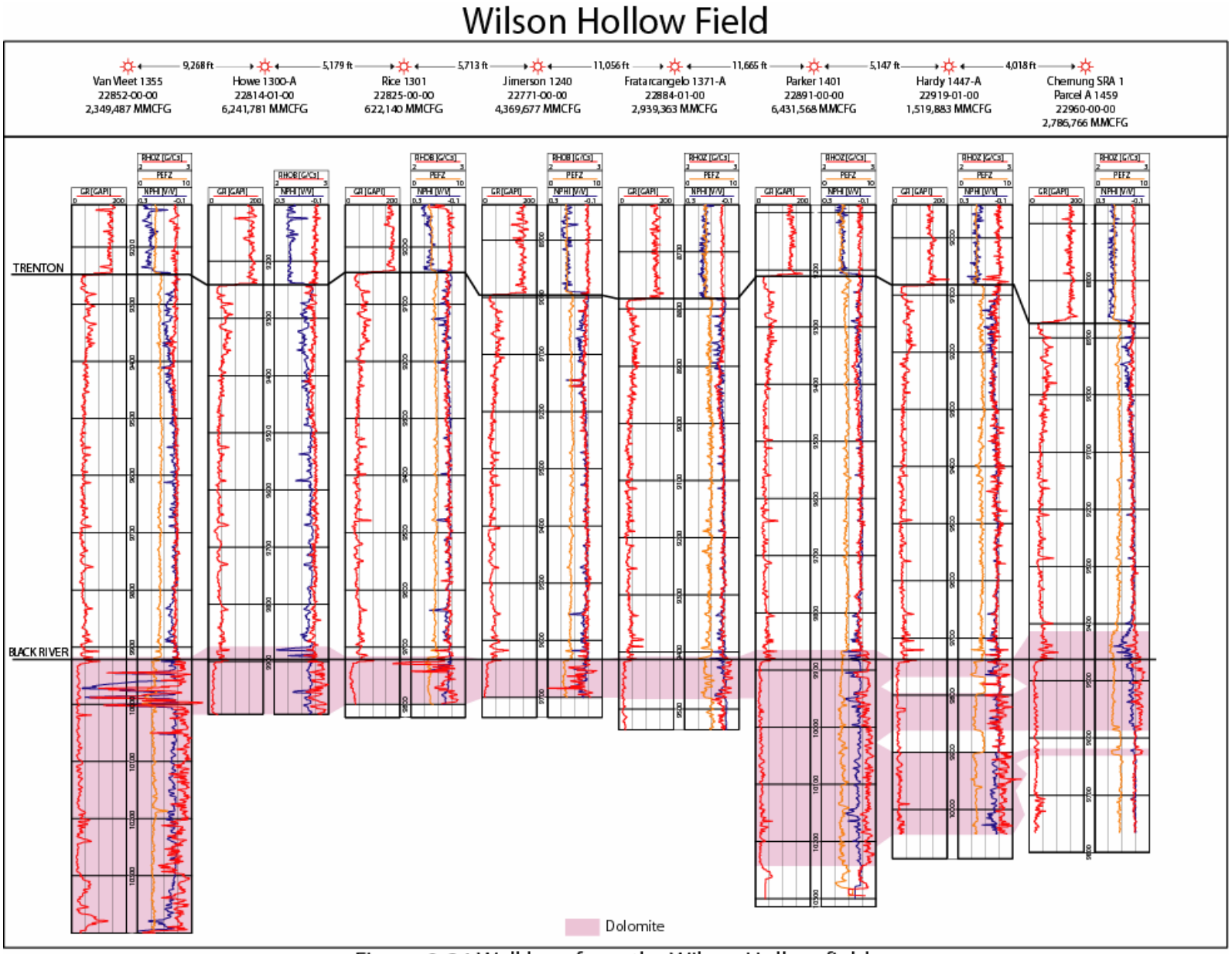

Figure 8-24 Well logs from the Wilson Hollow field.

Wilson Hollow Field	22771-00	22814-01	22825-00	22852-00
Pool Number				
Discovered	1999	1999	1999	1999
Depth to Reservoir				
Age of Reservoir	Ordovician	Ordovician	Ordovician	Ordovician
Formation	Black River	Black River	Black River	Black River
Producing Reservoir				
Lithology	HTD (41.75)	HTD (16.29)	HTD (69.50)	HTD (220)
Trap Type				
Depositional Environment				
Discovery Well IP (Mcf)	7600	8000	1486	7400
Drive Mechanism	.			
No. Producing Wells	10	10	10	10
No. Abandoned Wells				
Area (acreage)	40			
Oldest Formation Penetrated				
Expected Heterogeneity Due To				
Average Thickness	188	184	200	450
Average Completion Thickness				
Average Porosity Log (%)				
Minimum Porosity Log (%)	5	5	5	5
No. Data Points				
Porosity Feet	20	22	15	132.5
Reservoir Temperature (F)	156	169	158	161
Initial Reservoir Pressure	3625	3650	3308	3451
Producing Interval Depths	9564-9752	9930-10114	9618-9818	9970-10000
Present Reservoir Pressure (psi/date)				
Status				
Original Gas in Place				
Original Gas Reserves				
Production Years	5			
Reported Cumulative Production	30605887			
No. wells Reported				
Estimated Cumulative Production				
Remaining Gas In Place (Mcf/Date)				
Remaining Gas Reserves				
Recovery Factor				
Initial Open Flow Mcfpd				
Final Open Flow Mcfpd				

Table 8-24. Wells from the Wilson Hollow field.

Wilson Hollow Field	22884-01	22891-00	22902-01	22919-01
Pool Number				
Discovered	1999	1999	1999	1999
Depth to Reservoir				
Age of Reservoir	Ordovician	Ordovician	Ordovician	Ordovician
Formation	Black River	Black River	Black River	Black River
Producing Reservoir				
Lithology	HTD (42.55)	HTD (282.75)	HTD (355.25)	HTD (195.70)
Trap Type				
Depositional Environment				
Discovery Well IP (Mcf)	10664	22112	6588	10233
Drive Mechanism				
No. Producing Wells	10	10	10	10
No. Abandoned Wells				
Area (acreage)		100	180	180
Oldest Formation Penetrated				
Expected Heterogeneity Due To				
Average Thickness	228	338	338	408
Average Completion Thickness				
Average Porosity Log (%)				
Minimum Porosity Log (%)	5	5	5	5
No. Data Points				
Porosity Feet	6	74.25	42.994	32.72
Reservoir Temperature (F)	162	163	157	184
Initial Reservoir Pressure	3400	3360	3371	3572
Producing Interval Depths	9660-9738	9890-10228	9296-9634	9950-10358
Present Reservoir Pressure (psi/date)				
Status				
Original Gas in Place				
Original Gas Reserves				
Production Years				
Reported Cumulative Production				
No. wells Reported				
Estimated Cumulative Production				
Remaining Gas In Place (Mcf/Date)				
Remaining Gas Reserves				
Recovery Factor				
Initial Open Flow Mcfpd				
Final Open Flow Mcfpd				

Table 8-24. Continued.

Wilson Hollow Field	22960-00	22975-00
Pool Number		
Discovered	1999	1999
Depth to Reservoir		
Age of Reservoir	Ordovician	Ordovician
Formation	Black River	Black River
Producing Reservoir		
Lithology	HTD (128.75)	HTD (455.28)
Trap Type		
Depositional Environment		
Discovery Well IP (Mcf)	11837	20400
Drive Mechanism		
No. Producing Wells	10	10
No. Abandoned Wells		
Area (acreage)		23.5
Oldest Formation Penetrated		
Expected Heterogeneity Due To		
Average Thickness	96	444
Average Completion Thickness		
Average Porosity Log (%)		
Minimum Porosity Log (%)	5	5
No. Data Points		
Porosity Feet	11.36	104
Reservoir Temperature (F)	160	172
Initial Reservoir Pressure	3281	3200
Producing Interval Depths	9496-9592	9349-9691
Present Reservoir Pressure (psi/date)		
Status		
Original Gas in Place		
Original Gas Reserves		
Production Years		
Reported Cumulative Production		
No. wells Reported		
Estimated Cumulative Production		
Remaining Gas In Place (Mcf/Date)		
Remaining Gas Reserves		
Recovery Factor		
Initial Open Flow Mcfpd		
Final Open Flow Mcfpd		

Table 8-24. Continued.

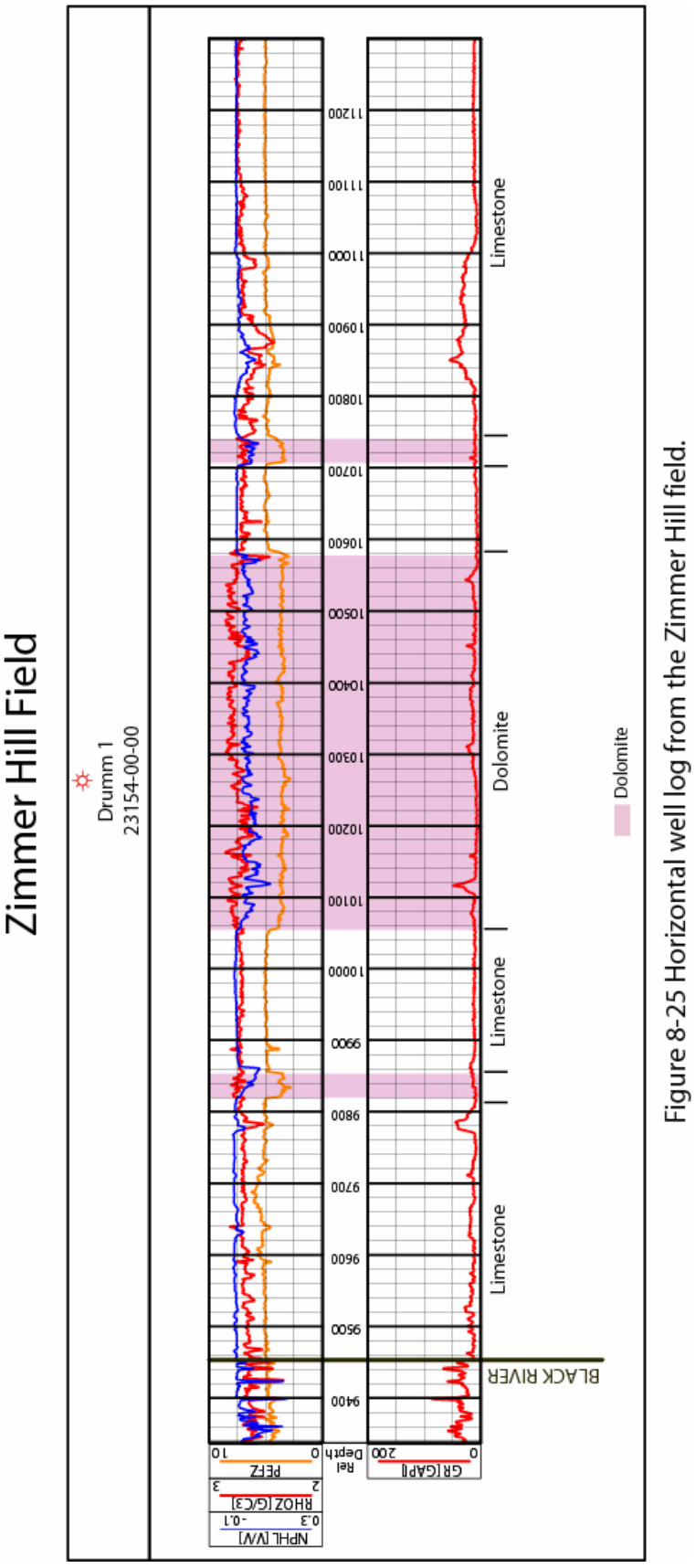

Figure 8-25 Horizontal well log from the Zimmer Hill field.

Zimmer Hill Field	23154-00
Pool Number	
Discovered	2005
Depth to Reservoir	
Age of Reservoir	Ordovician
Formation	Black River
Producing Reservoir	
Lithology	HTD (583)
Trap Type	
Depositional Environment	
Discovery Well IP (Mcf)	
Drive Mechanism	
No. Producing Wells	
No. Abandoned Wells	
Area (acreage)	
Oldest Formation Penetrated	
Expected Heterogeneity Due To	
Average Thickness	
Average Completion Thickness	
Average Porosity Log (%)	
Minimum Porosity Log (%)	5
No. Data Points	1
Porosity Feet	157
Reservoir Temperature (F)	163
Initial Reservoir Pressure	3195
Producing Interval Depths	8928 -12000
Present Reservoir Pressure (psi/date)	
Status	
Original Gas in Place	
Original Gas Reserves	
Production Years	
Reported Cumulative Production	
No. wells Reported	
Estimated Cumulative Production	
Remaining Gas In Place (Mcf/Date)	
Remaining Gas Reserves	
Recovery Factor	
Initial Open Flow Mcfpd	
Final Open Flow Mcfpd	

Table 8-25. Well from the Zimmer Hill field.

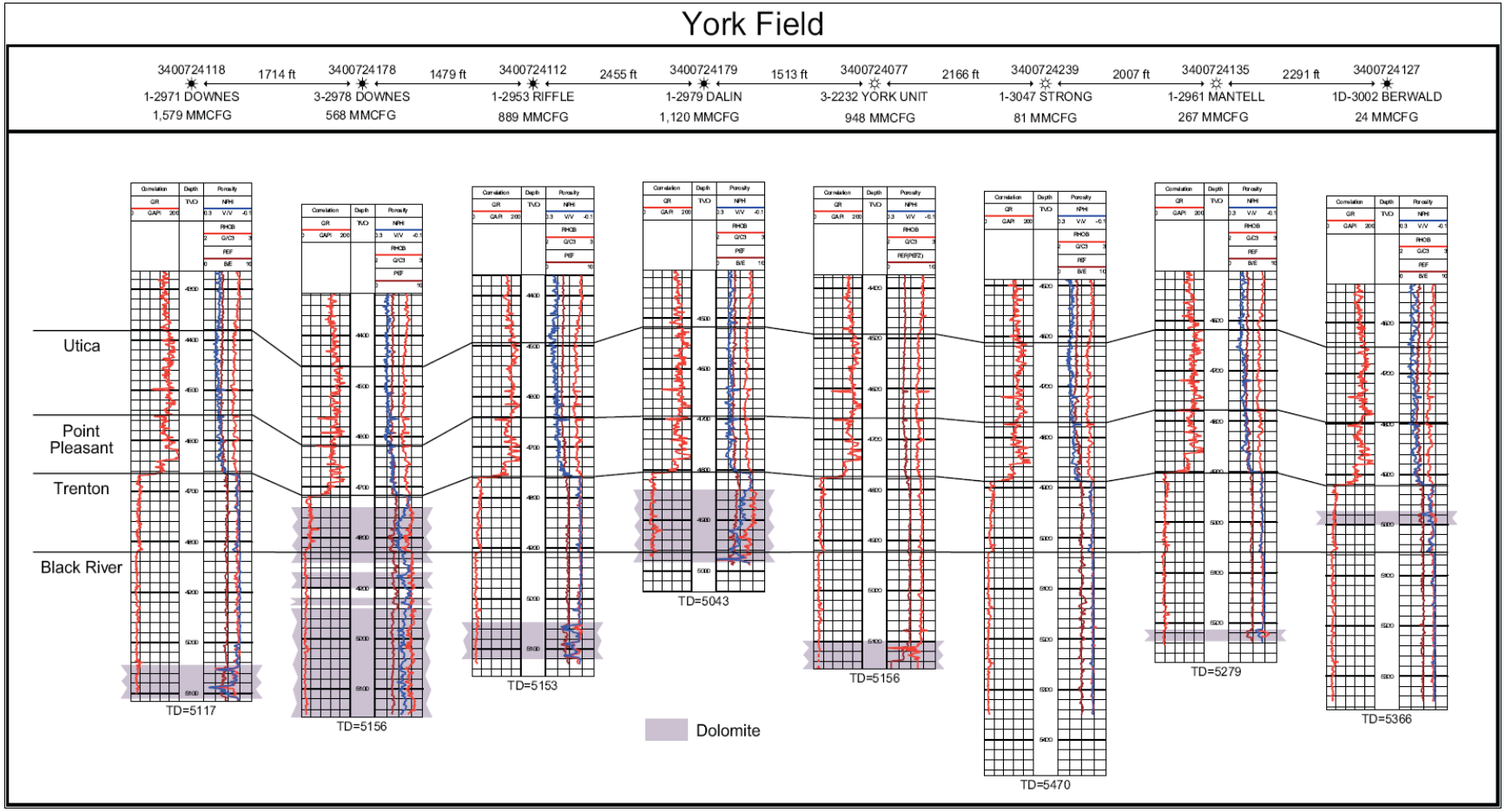

Figure 8-26. Cross section from York Field, NE Ohio (by Ron Riley).

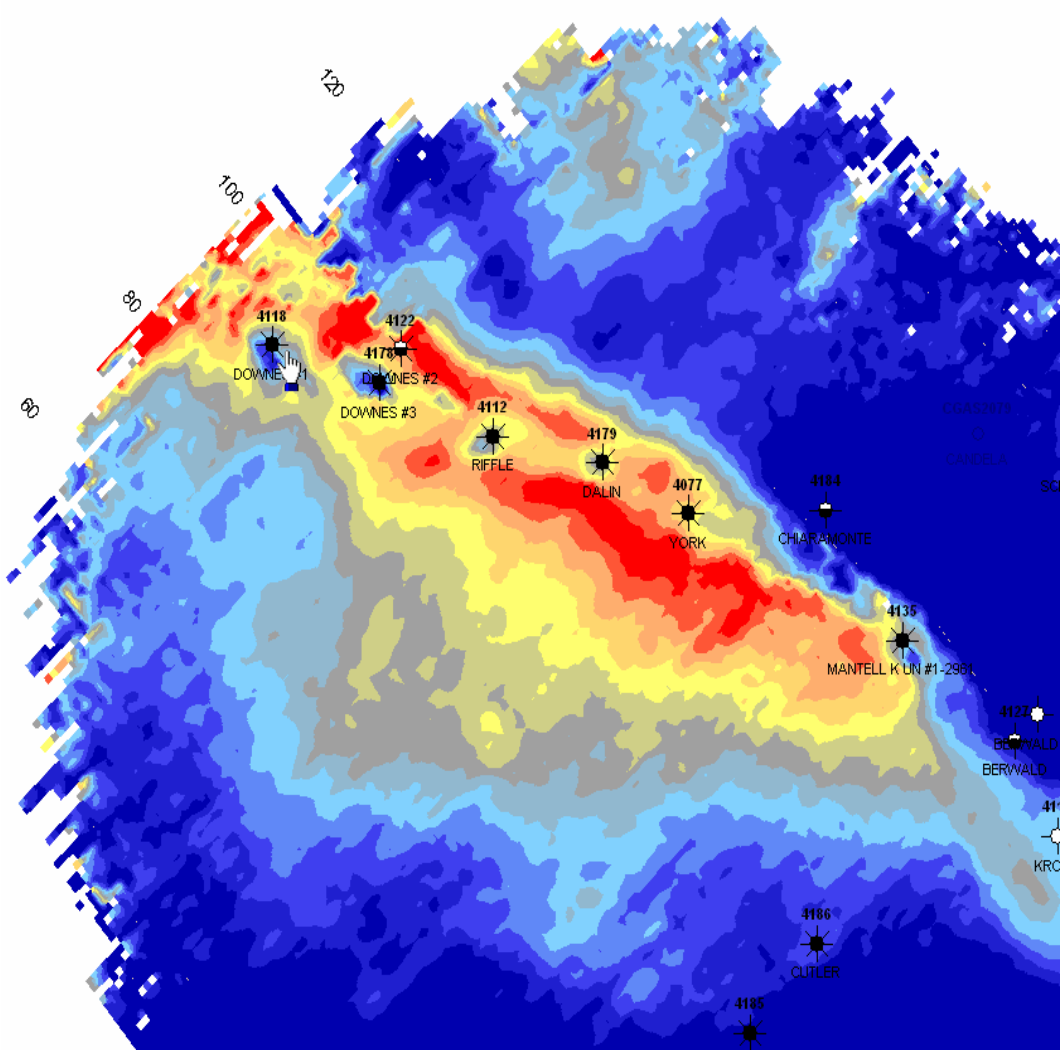

Figure 8-27. Time structure map on top Trenton, York Field, NE Ohio. Productive wells occur in circular sags.

Trenton-Black River Fractured Limestone Gas Play

Location

The fractured Trenton-Black River Limestone gas play is centered on Roane and Kanawha counties, West Virginia, an area of expected intense fracturing of Cambrian and Ordovician rocks that lie within and overlie the Rome Trough. Potentially, this play could extend to the southwest, above the Rome trough into Kentucky to the Tennessee line, and northeastward, along and above the Rome trough into Pennsylvania, nearly to the New York line. Also, the play could extend eastward all along this trend, through the high amplitude fold province and detached fold province to the Allegheny front. Although these areas are largely undrilled and under tested at present, gas shows in the 1.5 to 3.0 MMcf per day have been encountered in deep exploratory wells drilled on large anticlinal features adjacent to the structural front, indicating that this area must be assessed as having some potential.

Production History

This play was discovered in 1999 when Columbia Natural Resources successfully completed the discovery well for Cottontree field, the Frederick C. Parker 20097 well (WV permit number Roane 4250) in Roane County, West Virginia. The well was completed on June 28, 1999 at a total depth of 10,271 feet in the Black River Group. The relatively thin pay interval extended only from 10,255 to 10,271 in the Black River. Drilling was halted due to the large volume of gas encountered. The final open flow potential was 50 MMcf per day, shut in tubing pressure was 5750 psi, and the bottom hole pressure was 6600 psi, indicating that the reservoir was over pressured by approximately 2000 psi for this depth. It took several weeks to get the well shut in following the blow out and the well was not logged.

The confirmation well for the Cottontree Field, the Juanita Groves 23975 (WV permit number Roane 4255) was completed by Columbia Natural Resources (CNR) four months later (October 15, 1999) at a depth of 9,712 feet in the Trenton Limestone. The 54-ft pay interval extended from 9,658 to total depth. The final open flow potential of this well, which was drilled just to the southwest of the discovery well, was 28 MMcf per day, with a shut in tubing pressure of 4,897 psi, again indicating an over pressured reservoir. Drilling was halted in the Trenton Limestone due to the gas flow, but after the well had produced for two years, Columbia began deepening the well to the Black River Group on November 2, 2001 and reached a new total depth of 10,462 ft in the Black River on January 12, 2002. An open flow of 1,000 Mcf per day and a rock pressure of 5,147 psi were reported from the deepening episode.

Two additional Cottontree field wells were drilled in 2001, one an offset northeast of the discovery well, and the other an outpost several miles to the northeast of the discovery. The offset (Roane 4256) was sidetracked twice prior to completion, and produced only 13,597 Mcf in 2001 before being plugged and abandoned. The outpost (Roane 4259) produced 572,389 Mcf from 2001 through 2004.

The fractured limestone play was extended into Kanawha County, immediately to the south of Roane County, in 2000 when Columbia Natural Resources completed a 9,591 foot new field discovery well in the Black River Limestone. The final open flow from a depth of 9,481 feet was 15 MMcf per day, with a shut in tubing pressure of 4,575 psi. However, an analysis of the gas indicated it contained 300 ppm hydrogen sulfide. Reported production from this well for 2002-2004 is 205,905 Mcf.

During the summer and fall of 2000, CNR completed two wells in Lincoln County, southwest of previous gas wells in Roane and Kanawha counties, more directly over the center of the Rome trough. The first well (Lincoln 3097) was placed on line and produced 15,033 Mcf in 2001-02; the second well is presumed to be dry. CNR drilled a third well in Lincoln County in 2001, and this well (Lincoln 3137) produced 11,499 Mcf from 2001 through 2004.

An attempt to extend the play into Wayne County, West Virginia in 2000 failed when a 9,282 ft new field wildcat (Wayne 2037) was dry in the target formation and was plugged back to 6,509 feet.

During 2001, CNR extended the play to the west by drilling four exploratory wells in Putnam and Jackson counties, West Virginia and to the east when they completed a minor discovery well in Braxton County. The Jackson County discovery well (Jackson 2475) produced 139,934 Mcf in 2003 and 2004, and the Putnam County discovery produced 237,911 from 2001 through 2004. However, the Braxton County well (Braxton 2236) produced only 853 Mcf during 2002.

In 2002, Ardent and Cabot got involved in the play by drilling wells in Calhoun County, east of the initial Roane County discovery well. Both wells were drilled to depths greater than 12, 000 ft; both were dry, but one encountered enough gas to be transferred to the owner for farm use. The other was plugged and abandoned, but not until after it had been treated with acid and a drill stem test had been run.

Also in 2002, CNR drilled another discovery well, this time in Clay County (Clay 2644), which produced 158,647 Mcf in 2003 and another 161,768 in 2004, for a total cumulative production of 320,415 Mcf during its first two years on line. However, this well was turned over to ECA, and it has been reported that the well was plugged back from the Black River to the Newburg sandstone, and the production actually is from the Newburg. During the next two years, Eastern American Energy (EAE) drilled two additional exploratory wells in Clay County, but both wells were plugged and abandoned.

American Electric Power Company (AEP) drilled one additional deep exploratory test in July 2003 in Mason County, West Virginia. This well actually was a deep core test to ascertain the potential of Cambrian sandstones for their CO2 sequestration potential.

To summarize, during the 1999 to 2004 time interval, CNR and several other companies permitted 287 deep Trenton-Black River tests in 19 West Virginia counties, of which only 31 actually were drilled. Of these, 13 encountered enough gas to be placed on line, and at least two others encountered shows of gas in these carbonate targets. The successful gas wells were drilled in Roane, Kanawha, Clay, Jackson, Putnam and Lincoln counties; wells with gas shows were drilled in Calhoun and Braxton counties. Nearly every other permit that had been issued was canceled in 2003 or 2004. No information has been compiled to date on drilling or permitting in 2005.

Stratigraphy

The current play produces from fractured limestones in both the Trenton Limestone and the underlying Black River Group. The depocenter of the Black River Group (thickness greater than 1600 ft) is largely confined to the area of this play in West Virginia and southwestern Pennsylvania. The Black River Group thins to the southwest and northeast of the depocenter, with a noticeable area of thinning in northwestern Pennsylvania that separates two areas of thicker Black River rocks. One of these areas extends to the northwest into Ohio, the other northward into north central Pennsylvania and southern New York, to the fields that produce from hydrothermal dolomite reservoirs in New York.

The Black River Group is overlain throughout the play area by the Trenton Limestone. Bentonite beds are common in the Trenton Limestone and Black River Group, and are used to correlate the Trenton-Black River contact regionally. A regional isopach map of the Trenton Limetone reveals a prominent shelf area in most of Ohio, on which Trenton rocks are relatively thin, with thicker accumulations around this shelf area in adjacent states to the north, northeast and east. Within the area defined as the fractured limestone play, two Trenton Limestone depocenters are present, one to the southwest in eastern Kentucky and southwestern Virginia, and the other to the northeast in Pennsylvania and New York. These areas are separated by a narrow axis of thinning in north central West Virginia. The postulated edge of the Trenton shelf in Ohio would roughly coincide with the northwestern boundary of this play area in West Virginia and southwestern Pennsylvania.

In the northern half of this northeast-southwest trending play area, from north central West Virginia to the northern edge of the play near the New York-Pennsylvania border, the Trenton Limestone is overlain by the Utica Shale, a typically black, organic-rich shale with source rock potential. The contact between the Utica Shale and the Trenton Limestone is gradational, with interbeds of black shale and limestone common in a core taken in the Sand Hill well (Wood County, WV) on the Burning Springs anticline. A thickness trend in the Utica Shale coincides with the trend of this play area, with a depocenter in southwestern Pennsylvania, and another on trend in north central Pennsylvania.

The Utica Shale is not present in the southern half of this play area, from north central West Virginia to the edge of the play near the Kentucky-Tennessee border. In this

area, the Kope Formation overlies the Trenton Limestone. An area of thickening of the Kope Formation is present in southwestern West Virginia that coincides with the area in which successful gas wells have been drilled in the play.

Shows of gas were encountered in the Utica Shale, Trenton Limestone and Black River Group in older deep tests in West Virginia and Pennsylvania. These older wells were drilled in the eastern part of what is being defined as the fractured limestone play area, on large anticlinal features in the Appalachian plateau and Valley and Ridge physiographic provinces.

Structure

The western margin of the fractured limestone play area roughly coincides with the western boundary of the Rome Trough; the eastern boundary of the play is the edge of the basin at the Pre-Cambrian outcrop. Thus, the structural geology of the play area is dominated by faults and fractures associated with the Rome trough in the western part of the play area, and detached folds in the plateau and valley and ridge provinces in the eastern part of the play.

The western portion of play area is in what has been called the "low-amplitude fold province," in contrast to the so-called "high-amplitude fold province" farther east, adjacent to the Allegheny structural front. These low-amplitude folds are associated with detached thrust sheets above faults in the Upper Silurian Salina salt beds. However, fractures in older rocks below the decollement are controlled by basement structures, especially the Rome Trough, a Cambrian fault-block feature that extends from eastern Kentucky to northern Pennsylvania. This graben-trough feature is filled with Cambrian and Lower Ordovician rocks, whereas Middle Ordovician carbonates like the Black River and Trenton overlie the trough without an appreciable change in thickness in either unit that can be associated with the trough. However, both the Trenton and Black River and older carbonates are likely to have been highly fractured by later movements along trough boundary faults and faults within the trough.

The high-amplitude folds farther to the east in West Virginia and Pennsylvania were tested to some extent by deep exploratory wells drilled in the 1960s. These structures are the result of thin-skinned rather than basement-deep tectonics, with folds being developed in thrust sheets that moved westward above detachment faults in the Upper Ordovician Martinsburg Shale in the west, and in deeper Cambrian shales east of the structural front.

The width and extent of the Rome trough is evident on a regional map of basement faults compiled for this project. Nearly all of the exploratory wells that have been drilled in the West Virginia portion of the play area have been drilled in this highly-faulted trend, including all of the productive wells. The discovery well for this play, the Frederick C. Parker 20097, was drilled by Columbia Natural Resources in an area of Roane County that lies between two basement faults mapped by Shumaker (1996). The locations of all other gas wells are in close proximity to other mapped fault locations.

Reservoir

Reservoirs in the western part of the play area are developed in fractured limestones in the Trenton Limestone and Black River Group. No evidence for any hydrothermal dolomite (HTD) has been encountered, either in well cuttings or on density logs. Our current model for HTD development is that the Trenton-Black River beds in the western part of the area, above the Rome trough, are too great a distance above the basement to have been reached by hot fluids rising along basement-deep faults and fractures that perhaps dolomitized deeper Cambrian limestones, but not Middle Ordovician rocks in the area. Fractured limestone pay intervals are quite thin in wells drilled to date, only 15-50 feet, indicating perhaps that gas is flowing from a single fault zone. Reservoirs are over pressured in most wells drilled to date. The high gas volumes, longer life and over pressure in the better wells may indicate fault communication with deeper gas-bearing zones. These zones, if present, could include HTD reservoirs developed in Cambrian carbonates.

Reservoirs in the eastern part of the play area also would be expected to be formed in fractured limestones in the Trenton Limestone and Black River Group, although some minor contribution could come from overlying fractured Utica Shale beds. Reservoirs that have been encountered to date are limited in size; in wells that tested gas, the gas volume blew down from several million cubic feet a day to less than a hundred thousand cubic feet a day in only a few days to a week. This suggests that the fault and fracture networks that creates the reservoirs on the eastern anticlines are not as extensive as similar networks in fractured reservoirs to the west, above the Rome trough. The fractured reservoirs in the east also probably do not extend to greater depths, and, therefore, do not encounter deeper gas-bearing zones, especially reservoir rock with matrix porosity. Fractured limestone reservoir rock has been encountered in at least four deep wells (Finch, Walls, Tidewater's US Forest Service, Hope's WV Board of Control) on three major anticlines in the West Virginia portion of the play area (Chestnut Ridge, Deer Park, and Brown's Mountain). An additional four deep exploratory test wells drilled to the Trenton Limestone and Black River Group, or deeper units, in Pennsylvania encountered shows of gas in these carbonate units in this play area. These four wells were drilled in Armstrong, Franklin, Juniata and Union counties.

Description of Key Fields: Cottontree field, West Virginia

The only field that has been developed to date in this play is the Cottontree field in Roane County, West Virginia. Although other new field discoveries have been drilled in other counties in the play area, no fields have been developed around them.

The Cottontree discovery was drilled on a seismic prospect generated by the same team of geophysicists and geologists that picked the locations for many of the initial discoveries in the Trenton-Black River hydrothermal play area in south central New

York. In addition to their recent seismic data, this team had access to drilling records from the first deeper than Silurian test well drilled in the state (Roane County permit Roane 19), a well that encountered an unexpected flow of gas in the Trenton that was sufficient enough to burn the rig down. This well was drilled in 1932.

Although we did not have access to seismic data over this area, we can draw some conclusions regarding the position of the early Cottontree wells relative to the trend of basement faults that have been mapped in the area. In general, the trend of basement faults and the entire Rome trough feature is northeast-southwest. However, in this area of West Virginia, two long, slightly arcuate faults with a north northeast to south southwest trend have been mapped that essentially join the southwest end of a major northeast-southwest trending fault with another major fault that defines the southeastern boundary of the Rome trough in the area.

The Cottontree wells were drilled in the northern end of the roughly north-south trending lenticular area between these cross cutting faults, and the Kanawha County discovery well was drilled in the southern portion of this same north-south, lenticularly shaped area between the two wrench faults. One or both of the faults may extend to the basement. The Trenton-Beekmantown interval between the wrench faults would be confined to a narrow graben, which would show up on seismic as a sag on the top of the Trenton between the faults, similar to other prospect areas in the play.

Cottontree field lies near the western edge of the thick Black River depocenter, and the orientation of wells drilled to date parallels the regional thickness trend of the Black River. The Black River thins rapidly to the west, and increases gradually in thickness to the east. The overlying Trenton Limestone, however, is relatively thin and does not change appreciably in thickness over a wide area in this part of West Virginia. The black shale facies assigned to the Utica Shale in other parts of the basin is not present in Roane County.

The early drilling history of the Cottontree field was described above. CNR continued to drill Trenton-Black River wells in Roane County from 1999 through 2002, resulting in a total of 8 gas wells. Cumulative production, through 2004, was more than 8.6 BCF, of which 4.65 BCF came from the discovery well.

Resources and Reserves

This is a very large play area, so it is not surprising that undiscovered resources as determined by the project's resource assessment team were 0.6 Tcf at the 90% confidence level, 1.6 Tcf at the 50% confidence level, and as much as 3.0 Tcf at the 10% confidence level. Reserves in current producing wells are unknown, but probably less than 1 BCF per well in most cases. However, some exceptional wells have been, and will continued to be discovered, as evidenced by the Cottontree discovery well, which has produced more than 4 BCF to date. Unfortunately we are faced with the reality that the offset confirmation well has produced only a tenth of that volume in essentially the same

amount of time. This pattern of exceptional wells offset by wells that are marginally economic is to be expected, at least during the early years as this play is developed further.

Future Trends

The locations of wells permitted by operators in West Virginia indicate that initially these operators were interested in extending the play to the northeast and to the southwest, from the Kentucky border nearly to the Pennsylvania border, and from the eastern boundary of the Rome trough in central West Virginia westward to the Ohio River. In addition, however, several permits were issued to drill deep Trenton-Black River tests in three West Virginia counties east of the Rome trough (Braxton, Upshur, Webster) but still west of the high fold area. Unfortunately, of the nearly 300 permits issued to drill Trenton-Black River or basement deep wells in 19 West Virginia counties, only 31 were drilled, in Braxton (2), Calhoun (2), Clay (4), Jackson (2), Kanawha (1), Lincoln (3), Mason (1), Putnam (2), Roane (12), Wayne (1) and Webster (1) counties. Most of the wells that have been drilled have been to the southwest or west of the discovery well, in areas where the depth to target is shallower, rather than to the northeast, where the depth to basement increases into Pennsylvania. Thus, it is safe to assume that in the short term at least, efforts to extend this play will concentrate on the shallower ends of the trend, in southwestern West Virginia and eastern Kentucky, or in north central Pennsylvania, adjacent to the HTD play area that extends northward into south central New York. The deeper portions of the play area will be drilled later, and probably only after a certain degree of success has been obtain by drilling elsewhere in the play.

The limited reservoir capacity encountered by exploratory drilling to the east on major anticlinal structures probably will lead to reduced interest in those areas until much later in the development of this play.

SUMMARY AND CONCLUSIONS

Background: Play Development and Research Plan

Historically, areas of oil and gas production from the Trenton and Black River (Appendix D, Figure 1) had been established in Michigan (Albion-Scipio trend), Virginia (Rose Hill and Ben Hur fields) and Indiana and Ohio (Lima-Indiana trend) long before the current play began. In spite of prolific production from some of these areas, the current Trenton-Black River gas play did not begin until well after Columbia Natural Gas (CNR) drilled the discovery well for the Glodes Corners Road field in Steuben County, New York in 1985. In fact, it was not until 1995, a full decade later, that CNR drilled the confirmation well, and 1996 before the discovery and confirmation wells went on line. At this point, industry interest and gas prices instigated development and the play actually began.

The play developed rapidly in New York, attracting national interest as more discoveries were made and large open flows and annual production figures were reported. Glodes Corners Road field was developed with 12 gas wells, and only 1 dry hole, and these wells have produced in excess of 7.5 Bcf. In 1998, CNR moved slightly to the west and discovered Pine Hill field, and to the south to discover Muck Farm field (Appendix D, Figure 2). Four Muck Farm wells have produced more than 7 Bcf, and 3 wells in Pine Hill have produced more than 4 Bcf.

In 1999, a fourth field – Wilson Hollow – was discovered in New York, and the play moved into Ohio, with discovery of the York field (Figures 6-1 and 6-4), and into West Virginia when CNR drilled the discovery well for Cottontree field in Roane County (Figures 6-1 and 6-8). Wilson Hollow has proven to be one of the larger and better fields in the play. Cumulative production from 10 wells exceeded 30 Bcf in just five years.

The Cottontree discovery well came in with an initial open flow of 50 MMcf/d and a bottom hole pressure of 6600 psi from a pay interval between 10,255 and 10,271 feet, the first of several over-pressured zones in the Trenton-Black River to be encountered in West Virginia.

Following the extension of the play into West Virginia, the Appalachian Region of the Petroleum Technology Transfer Council (PTTC), in response from numerous requests for information from industry across the nation, held the first in a series of focused technology workshops on the play. The initial workshop attracted more than 100 registrants from 13 states and Canada, a testimony to the widespread interest in the play among domestic independents.

Interest continued to increase, buoyed by the discovery of 5 new fields in New York in 2000 and two more fields in 2001. A second PTTC workshop in June 2001 quickly sold out, with more than 50 hopeful registrants being turned away. Subsequent workshops in the summer and fall of 2001 and spring 2002 consistently attracted more

than 150 registrants, from 15 states and Canada, and a consistent need for more and better basinwide geologic information was expressed by these attendees.

Ultimately, PTTC hosted a Trenton-Black River Stakeholders Meeting in September 2002, which led to submittal of a successful research proposal in response to a Request for Proposals from DOE, and to the creation of the Trenton-Black River Research Consortium. The Consortium included DOE, four state geological surveys, the New York State Museum Institute, and 17 domestic gas producers.

The main goal of this research was to assemble all available basinwide information on the Trenton Limestone and Black River Group rocks and the play itself into one playbook, complete with maps, cross sections, analyses and interpretations made from a multidisciplinary, integrated study of the data. Three additional objectives were defined: to develop a resource assessment model for this complex, unconventional play; to develop a model to explain the origin of dolomite reservoirs found in the Trenton-Black River gas fields; and to define possible fairways within which industry can concentrate detailed studies leading to further exploration and discovery of gas fields.

The play continued to develop, even as the Trenton-Black River Research Consortium conducted the research that led to this playbook. At this time, 25 named fields have been discovered in New York, 13 gas wells have been drilled in six West Virginia counties, the York field was discovered in Ohio, and 3 successful wells have been drilled in Pennsylvania. Reported production from 62 wells in New York has exceeded 107 Bcf, and production from wells in Ohio and West Virginia has increased the total production from the play to more than 120 Bcf.

Research Results

The seismic and structural evidence suggests that there has been a strong structural control on this play, beginning with basin architecture and continuing through carbonate deposition and alteration of host limestone into fractured and/or dolomitic reservoirs.

Basin architecture during the Ordovician Period was determined by regional basement tectonics. These architectural features included a broad ramp that covered a vast area of what is now all or parts of Michigan, Indiana, Kentucky, Ohio, New York and Pennsylvania, a proto- or Central Appalachian basin to the southeast that extended from Kentucky to Pennsylvania, and a deeper basin still farther east that was receiving clastic sediments. The southeast edge of the ramp approximated the position of the western side of the Rome trough.

Clean Black River Group carbonate mudstones were deposited on the broad, southeast-sloping ramp, while slightly more argillaceous mudstones were being deposited in the Central Appalachian basin and fine clastics were being deposited in the Sevier basin. (Figure 1-5).

By Trenton time the architecture of the basin had been altered slightly, mainly through the development of a small, inter-platform basin, the Utica/Point Pleasant sub-basin, in what is now Ohio (Figure 1-6). A broad platform, called the Trenton platform, was present above the older Black River ramp north and west of the sub-basin, and a second platform, the Lexington platform, had developed above the older Black River ramp south of the sub-basin. The Central Appalachian basin was still present, although slightly more restricted, and gave way to the east to the Taconic foredeep.

Clean Trenton carbonate grainstones, packstones and wackestones were deposited on the western side of the Trenton platform in what is now Michigan, Indiana and northwestern Ohio. However, farther to the east and north, in Ontario and New York, carbonate grainstones, packstones and wackestones were more argillaceous, although the sharp upper contact present in the west continued through this eastern area. To the south, however, where argillaceous grainstones, packstones and wackestones were being deposited on the Lexington platform, the upper contact is more gradational. A similar depositional pattern occurred in the Central Appalachian basin, where a variety of argillaceous carbonates were being deposited, with a gradational upper contact between the Trenton and the overlying clastics interval.

The fault-controlled, southeastern edge of this platform in Indiana and Ohio (Figure 1-6) corresponds to the Lima-Indiana oil and gas trend (Appendix D, Figure 1), where reservoirs were developed along the clean carbonate margin.

Depositional patterns within this basin architecture also were controlled by regional structure. Alternating thin and thick areas of Black River carbonate deposition on the broad ramp (Figure 1-5) were controlled by the reactivation of northwest-southeast trending, basement-deep faults (Plate 1-25), and the southeastern edge of the lobes was controlled by the ramp margin, which in turn was controlled by the faults marking the western edge of the Rome trough. All of the currently known Black River productive areas in New York lie between two of these faults (Plate 1-25), with no production west or east of the fault-bounded, depositionally thin area.

Deposition of the overlying Trenton Limestone in New York illustrates an inverse thickness relationship with the underlying Black River. The thickest area of Trenton Limestone deposition in New York overlies the area of thin, but productive Black River (Plate 1-26). Deposition of slightly argillaceous Trenton carbonate rocks on the platform kept pace with subsidence of the fault-bounded area, resulting in more than 700 feet of limestone.

As stated before, most of the Trenton-Black River play fields in New York are located between the bounding faults (Plate 2-5). However, if one extends the faults to the northwest, most of the known occurrences of dolomite in well cuttings and as interpreted from well logs (Appendix D, Figure 4) fall within this fault-controlled fairway. Thus, regional fault systems have exerted some degree of control on basin architecture, depositional patterns within this architecture, the formation of dolomite and ultimately

the development of dolomitized or fractured limestone reservoirs within the Trenton and Black River limestones.

In areas of historical Trenton production in Ohio, most of the dolomitic reservoir development falls along specific trends. This suggests that Late Ordovician Taconic compression from what is now the southeast opened faults with certain orientations relative to others with a different orientation, and limestones along these fault trends were preferentially dolomitized.

Lithology also was important in dolomite development. Clean carbonates along the northeast-southwest trending Trenton shelf edge in Ohio (Figure 1-6; Figure 4-36) were preferentially dolomitized whereas more argillaceous limestones deposited on the same Trenton platform to the east in New York apparently have not been dolomitized, at least not to the extend illustrated in older models published prior to the current research.

All of the geochemical data – stable isotopes (Figures 4-16 to 4-21), fluid inclusions (Figure 4-15) and trace elements (Figures 4-22 and 4-23) – collected and developed during this research effort suggest that the dolomites encountered in the Trenton-Black River play are hydrothermal in origin. Recreating the depth of burial from conodont alteration (CAI) data (Figure 4-31) strongly indicates that the rocks were not buried to depths that would be necessary to attain the homogenization temperatures that were measured (Figure 4-32). Instead, the evidence is overwhelming that these dolomites formed from hot, saline, Fe- and Mn-rich fluids that flowed through basement rocks or immature siliciclastics prior to making the dolomite in the host limestone units.

Eventually, after considering all of the information, our research team developed a fault-controlled, hydrothermal model to explain the occurrence of dolomite developed in host limestone intervals in the Black River Group, and to a lesser extent, the Trenton Limestone in the western, shallower portions of the basin. The sequence of events leading to dolomitization and porosity development would be as follows. Shortly after deposition of the Trenton Limestone, the reactivation of pre-existing basement faults provided pathways through which hot fluids could flow upward from the basement until they reached an argillaceous barrier just above the base of the Trenton (Figures 2-11 and 4-35). As these fluids cooled, they leached the host limestone adjacent to the fault planes, forming vugs in a migrating front that moved away from the fault zone. Permeability behind this front was enhanced by continued fracturing and leaching. As faulting continued during Utica time, subsequent dolomite-supersaturated fluids that rose to the level of the leached, vugular limestone could remain hotter longer, leading to the dolomitization of the leached limestone zones. Matrix dolomitization was followed by further fracturing, brecciation and vug development as tectonic activity continued. These later-stage vugs and fractures were lined with saddle dolomite soon after they were formed.

Petrographic data support, in part, the stratigraphic model of HTD development in the cleaner, coarser-grained carbonates. However, it has been demonstrated that even the finer-grained carbonate mudstones and wackestones, as well as the coarser-grained

grainstones and boundstones, often were clay free and subsequently they, too were dolomitized. In fact, the best reservoirs are in rocks that originally were carbonate mudstones, and now would be described as dolomudstones.

There are two distinct dolomite textures – planar and transitional to nonplanar – in these fractured carbonate reservoirs. Planar dolomites consist of micron- to centimicron-sized, euhedral to subhedral crystals that selectively replace limestone matrix in all depositional facies. Less common planar-p and planar-e dolomite locally replace allochems, and rare planar-c dolomite fills pore space. Planar textures in peritidal facies might have formed during reflux and/or mixing zone diagenesis. Planar textures in subtidal facies likely formed in association with compaction-driven fluid flow in burial environments. Planar textures also occur where hydrothermal dolomite replaces limestone adjacent to fractures and faults.

Transitional to nonplanar dolomites are entirely hydrothermal. They consist of decimicron- to millimeter-sized crystals in fractured rocks adjacent to faults. Transitional and nonplanar-a dolomites occur as an obliterative replacement of allochems, matrix, and cement in limestones, and as neomorphic recrystallization of planar dolomite. Nonplanar (saddle) dolomite occurs as pore-lining and pore-filling cement.

Distinctive pore textures in Trenton and Black River reservoirs vary with carbonate rock type. Porosity is partially related to depositional texture in productive dolograinstones and dolopackstones. These rocks consist of planar-s to nonplanar-a and saddle dolomite. Mesoporosity is fabric selective, consisting of moldic and intercrystalline voids. Macroporosity is not fabric selective, and consists of small to medium vugs and fractures. Microporosity is both intercrystalline and intracrystalline. Porosity formed through a combination of fracturing, selective dissolution of allochems, and dissolution of calcite and dolomite cements.

Porosity in productive dolowackestones and dolomudstones is not fabric selective. Macroporosity consists of vugs, channels, fractures, and breccia. Vugs formed through selective dissolution of allochems followed by corrosive enlargement of the initial void. Vugs also formed through dissolution of calcite, dolomite and other cements. Channel, fracture, and breccia porosity developed in conjunction with hydraulic fracturing and brecciation by hydrothermal fluids. Some channel porosity formed through reopening stylolites.

Hydrothermal dolomitization accompanied porosity development in Trenton and Black River reservoirs, but did not provide or increase it. Porosity in all dolostones was modified by late-stage precipitation of nonplanar dolomite, calcite, quartz, feldspar, sulfides, sulfates, and oxides. Pyrobitumen lines and fills most pores.

Dolomitization may have destroyed as much or more porosity than it created. Porosity developed through a combination of fracturing, selective dissolution of allochems and dissolution of both calcite and dolomite. The best reservoirs occur in rocks in which dolomite and limestone have been dissolved, and where fractures have

provided interconnections between large dissolution voids creating collapse breccias and adjacent zebra fabrics.

Wells that encountered dolomite did not always encounter porosity within the dolomitized zones. But, the dolomitization process appears to have occurred in settings where dissolution and fracturing also occurred, so the presence of dolomite is a key indicator that porosity and commercial reservoirs may be present in the immediate area.

These fractured carbonate reservoirs in the Trenton and Black River contain significant natural gas reserves. Thermogenic gas is produced from platform and ramp limestones in eastern Kentucky and central West Virginia, and from hydrothermal dolomite (HTD) reservoirs in platform carbonates in northeast Ohio, south central New York, and north central Pennsylvania.

The distributions of stable carbon ($\delta^{13}C_1$ - $\delta^{13}C_4$) and hydrogen ($\delta^{2}H_{CH4}$) isotopes in Trenton and Black River gases from Kentucky, West Virginia and Ohio show that the hydrocarbons were generated from early- to post-mature marine source rocks in Ordovician and possibly Cambrian strata (Figures 5-3, 5-6, 5-10 and 5-22). The $\delta^{13}C_1$ - $\delta^{13}C_4$ distributions in gases produced at Homer field in Elliott County, Kentucky and at York field in Ashtabula County, Ohio indicate compartmentalization in the reservoirs Figures 5-4 and 5-11, respectively). Ethane is depleted in ^{13}C relative to methane in the West Virginia gases suggesting heterogeneities in the source organic matter, thermogenic gas mixing, methane oxidation, or diffusive gas leakage from the reservoirs (Figure 5-7).

Hydrocarbons produced from HTD reservoirs in the Black River Group of New York and Pennsylvania are unusual. Methane is depleted in ^{12}C ($\delta^{13}C_1$ = -32.7 to -26.02 permil). The C_1 to C_3 alkanes are significantly more enriched in ^{12}C with increasing molecular mass (Figures 5-17 and 5-19). These gases exhibit a strong negative correlation between $\delta^{13}C$ and $\delta^{2}H$ of methane, and some display an inverse correlation between $\delta^{13}C$ and $\delta^{2}H$ of methane and ethane (Figures 5-15 and 5-21). These isotope distributions apparently resemble those of postulated abiogenic gases. $\delta^{2}H$ values and C_1/C_{2+} ratios in our samples, however, indicate a thermogenic origin, and noble gas systematics implies a Middle Ordovician shale source rock. We attribute the unusual geochemistry of the Black River gases to a combination of fluid alteration during reservoir diagenesis, and mixing of thermogenic and deep basin hydrothermal/geothermal gas.

Non-hydrocarbons in the New York and Pennsylvania gases have multiple sources. $^{3}He/^{4}He$ and $^{40}Ar/^{36}Ar$ vary between 0.01 – 0.196 Ra and 295 – 1521, respectively, and are due to measurable contributions from the mantle and crust (Figure 5-26). Nitrogen comprises between 0.10 and 14.14 mole percent of the gases. $\delta^{15}N$ of the gases ranges from -10.2 to +0.4 permil. Combined nitrogen and noble gas systematics indicate the presence of magmatic, crustal, and atmospheric nitrogen in the gases. $\delta^{13}CO_2$ in the gases is -6.7 to -3.0 permil, indicating a carbonate source for this minor constituent. As much as 0.51 mole percent H_2S occurs in the Wolpert #1 well in Bradford County,

Pennsylvania. The $\delta^{34}S$ of this gas is +14.7 permil. Geochemical and petrographic data indicate that the H_2S formed through thermochemical sulfate reduction.

The current Trenton-Black River gas play extends from New York to West Virginia, and includes areas with recent discoveries in Pennsylvania and Ohio. Most of the fields throughout the play area are long and narrow, usually one-well wide. In New York, these linear fields have three dominant trend directions (NW-SE, W-E and SW-NE) and productivity may correlate with field orientation, to some extent.

The discovery well for the Glodes Corners Road field was located using seismic evidence of a depression on the top of the Trenton Limestone and the underlying Black River Group. It was assumed at the time that this depression was due to basement-deep faults forming fault-bounded grabens in Trenton-Black River, and that the limestone host rock along the bounding and internal faults had been dolomitized, creating a dual porosity reservoir due to dolomitization and fracturing. These early models also indicated that the faulting and dolomitization extended upward well into the Trenton Limestone. However, most of the production in New York is from dolomitized zones in the Black River. Dolomite zones do not appear to extend upward beyond the lowest Trenton bentonite (Appendix D, Figure 6).

Currently (Summer 2006) there are 25 named fields in New York, nearly half of which are one-well fields yet to be developed (Figure 8-1; Table 8-1). These fields contain 68 producing wells, although production data have been released for only 62 of them. These 62 wells have produced 107 Bcf, or 1.7 Bcf/well. More than 100 deviated wells have been drilled or planned, but the best well (15 Bcf in 4 years) is a vertical well.

Trenton-Black River wells have been drilled in more than 10 counties in West Virginia in several long, linear NE- SW trends parallel to the Ohio River and the subsurface Rome Trough (Plate 2-5). The discovery well for Cottontree field in Roane County, was near the southwest end of the longest of these drilling trends in an area bounded by two basement-deep faults. The seismic interpretation for this field is a combination of wrench faulting and a sag on the top of the Trenton and Black River. The high bottom hole pressure (6600 psi) for the discovery well clearly indicated the reservoir was over pressured for the producing depth (10,271 ft).

From 1999-2004, the West Virginia Division of Oil & Gas issued 287 permits to drill Trenton-Black River and deeper wells. Although only 31 of these were drilled, 13 wells drilled in 6 different counties encountered gas, indicating that there are several areas with potential for further development.

All 3 Pennsylvania discoveries are in Bradford County, close to the New York State line and south of the New York Trenton-Black River fields. Wells drilled to the west were unsuccessful, as were wells drilled in southwestern Pennsylvania.

Cumulative gas production from the play is approximately 120 Bcf through 2004, of which 107 Bcf was produced from New York wells. Production actually declined in

2003 relative to 2002, but increased to new high (nearly 40 Bcf) in 2004, perhaps due to horizontal drilling in New York that resulted in some high volume wells being placed on line.

Potential source rocks for the gas found in these reservoirs include shales associated with the Trenton Limestone, as well as in older Ordovician and Cambrian rocks. Total organic carbon (TOC) values for these shale are adequate throughout much of the basin (Figure 7-5). Conodont Alteration Index (CAI) data indicate relatively large oil and gas windows (Figure 7-8), but also suggest that much of the older production in Ohio must have migrated from deeper in the basin to the east. These data also suggest that potential source rocks in the eastern part of the basin are overmature.

Estimating how much gas may yet be found in the Trenton-Black River play is one of the main objectives of the playbook project. To accomplish this, team members modified a technique used by the USGS to make gas resource assessments. An initial assessment area was defined as the area that extended from the eastern outcrops westward to the Cincinnati arch, essentially the entire extent of the Appalachian basin. Project geologists then downsized this area using favorable geology and locations of known production and shows, distribution of potential source beds (Figure 7-2), and TOC and CAI data to arrive at a smaller assessment area. This assessment area was further divided into two subplays, a hydrothermal dolomite (HTD) subplay and a fractured limestone (FLS) subplay (Figure 7-10), and each subplay was assessed separately.

A key parameter in subdividing the overall play area is the thickness of rock between the basement and the Trenton-Black River carbonate section (Figure 7-9); a key assumption is that fluids rising from the basement have only enough energy to reach a certain maximum height, even when unimpeded, before descending again along fault planes. Detailed examination of well logs, cores and sample descriptions did not indicate any dolomitization in rocks that currently are more than 4800 feet above the basement. Therefore, this parameter was used to distinguish between subplay areas on an isopach map of the basement to Black River interval.

Because thickness patterns in older Cambrian and Ordovician rocks are controlled by the presence of the Rome trough, it is not surprising that the western edge of the trough approximates the dividing line between the two subplays. It also is not surprising that the subplay boundary approximates the fault-controlled edge of the Black River ramp, or that hydrothermal dolomites would preferentially be created within cleaner carbonates on the ramp and ramp edges west and north of the subplay boundary.

Limestone beds in the Black River and overlying Trenton can be expected to be more highly fractured in areas that overlie the Rome trough than in adjacent areas to the west and east. Still farther east, however, more extensive fracturing can be expected on the flanks and crests of anticlines in the high-amplitude fold province adjacent to the Allegheny front. Thus, two fairways exist in the FLS subplay area: one that coincides with the location of the Rome trough, and a second to the east that follows the trends of the larger anticlines.

Although fluids could not rise to the level of the Black River and Trenton in areas that overlie the Rome trough in the FLS play area, HTD could have formed in deeper limestone beds in the Knox and Beekmantown above and within the Rome trough area.

The method used to estimate gas resources in each subplay required that team members estimate the number and size of undiscovered fields in the assessment area, fields that can be expected to be discovered in the first 30 years of play development. The numbers and sizes of undiscovered fields were estimated at three levels of probability, 90%, 50% and 10%, for each subplay area, and these values were used to run the assessment program (see Table 7-1). The final assessment numbers (see Table 7-2), for the entire Trenton-Black River assessment area, are as follows: there is a 90% probability that at least 2.7 Tcf of gas will be discovered; a 50% probability that at least 6.0 Tcf will be discovered; and a 10% probability that at least 11.0 Tcf will be discovered. These numbers are quite comparable to estimates made by the Potential Gas Committee in 2004 of 2.5, 5.4 and 8.5 Tcf at the same levels of probability.

REFERENCES

Chapter 1: Stratigraphy

Ahr, W. M., 1973, The carbonate ramp—an alternative to the shelf model: Gulf Coast Association of Geological Societies Transactions, v. 23, p. 221-225.

Baranoski, M. T., R. A. Riley, and M. E. Wolfe, 1996, Cambrian-Ordovician Knox Group unconformity play, *in* J. B. Roen and B. J. Walker, eds., The atlas of major Appalachian basin gas plays: West Virginia Geological and Economic Survey, Publication V-25, p. 181-187.

Baranoski, M. T., 2002, Structure contour map on the Precambrian unconformity surface in Ohio and related basement features: Ohio Division of Geological Survey Map PG-23, scale 1:500,000, and 18-p. text.

Baranoski, M. T., in preparation, Subsurface Correlation and Lithostratigraphy of the Cambrian Mount Simon Sandstone, Eau Claire Formation, and Conasauga Group in Ohio: Ohio Division of Geological Survey.

Beardsley, R. W., and Cable, M. S., 1983, Overview of the evolution of the Appalachian Basin: Northeastern Geology, v. 5, p. 137-145.

Bergström, S. M., and Mitchell, C. E., 1987, Geology of Middle to Upper Ordovician Sebree Trough northwest of Cincinnati Arch, Ohio, Indiana, and Kentucky. [abs.]: American Association of Petroleum Geologists Bulletin, v. 71, p. 1101.

Bergström, S. M., and Mitchell, C. E., 1992. The Ordovician Utica shale in the eastern mid-continental region: age, lithofacies, and regional relationships, *in* Chaplin, J. R., Barrick, J. E., eds., Special Papers in Paleontology: A Special Tribute to Thomas W. Ams. Oklahoma Geological Survey Bulletin, Norman, OK, vol. 145, pp. 67–89.

Bergström, S. M., and Mitchell, C. E., 1994. Regional relationships between late Middle and early late standard successions in New York and Quebec and the Cincinnati region in Ohio, Indiana, and Kentucky, *in* Landing, E., ed., Studies in stratigraphy and paleontology in honor of Donald W. Fisher: New York State Museum Bulletin 481, p. 5-20.

Brett, C. E., McLaughlin, P. I., Baird, G. C., and Cornell, S. R., 2004, Comparative sequence stratigraphy of two classic Upper Ordovician successions, Trenton shelf (New York– Ontario) and Lexington Platform (Kentucky– Ohio): implications for eustacy and local tectonism in eastern Laurentia: Palaeogeography, Palaeoclimatology, Palaeoecology 210, 295– 329.

Campbell, M. R., 1898, Description of the Richmond quadrangle, Kentucky: U.S. Geological Survey, Geologic Atlas of the United States, Folio no. 46, 4 p.

Cisne J. L., Karis, D. E., Rabe, B. D., and Hay, B. J., 1982, Topography and tectonics of the Taconic out trench slope as revealed through gradient analysis of fossil assemblages: Lethaia, v. 15, p. 229-246.and others, 1982.

Coniglio, M., Sherlock, R., Williams-Jones, A. E., Middleton, K., and Frape, S. K., 1994, Burial and hydrothermal diagenesis of Ordovician carbonates from the Michigan Basin, Ontario, Canada: Special Publications International Association of Sedimentology, no. 21, p. 231-254.

Drahovzal, J. A., Harris, D. C., Wickstrom L. H., Walker, Dan, Baranoski, M. T., Keith, Brian, and Furer, L. C., 1992, The East Continent Rift Basin: a new discovery: Ohio Division of Geological Survey, Information Circular 57, 25 p.

Emmons, Ebenezer, 1842, Geology of New York; Part II, Survey of the second geological district: New York State Museum, 437 p.

Ettensohn, F. R., Hohman, J. C., Kulp, M. A., Rast, N., 2002, Evidence and implications of possible far-field responses to the Taconian Orogeny: Middle–Late Ordovician Lexington Platform and Sebree Trough, east– central United States: Southeastern Geology 41, 1 –36.

Ettensohn, F. R., Kasl, J. M., Stewart, A. K., 2004, Structural inversion and origin of a Late Ordovician (Trenton) carbonate buildup: evidence from the Tanglewood and Devils Hollow members, Lexington Limestone, central Kentucky (USA): Palaeogeography, Palaeoclimatology, Palaeoecology, vol. 210, p. 249–266.

Freeman, L. B., 1949, Regional aspects of Cambrian and Ordovician subsurface stratigraphy in Kentucky: American Association of Petroleum Geologists Bulletin, v. 22, p. 1655-1681.

Freeman, L. B. 1953, Regional subsurface stratigraphy of the Cambrian and Ordovician in Kentucky and vicinity: Kentucky Geological Survey Bulletin No. 12, 352 p.

Gao, D., Shumaker, R. C., Wilson, T. H., 2000. Along-axis segmentation and growth history of the Rome Trough in the central Appalachian basin: American Association of Petroleum Geologists Bulletin 84, 75–99.

Gupta, Neeraj, 1993, Geologic and fluid-density controls on the hydrodynamics of the Mt. Simon Sandstone and overlying units in Ohio and surrounding states: Ohio State University, Ph.D. dissertation, 266 p.

Harper, J. A., 1989, Effects of recurrent tectonic patterns on the occurrence and development of oil and gas resources in Western Pennsylvania: Northeastern Geology, v. 11, p. 225-245.

Harper, J. A., 1991, Preliminary assessment of the stratigraphy and structure of the Cambro-Ordovician carbonate sequence in western Pennsylvania, in Exploration strategies in the Appalachian basin: 22nd Annual Appalachian Petroleum Geology Symposium, Morgantown, WV, I. C. White Memorial Fund Pub. 3, p. 30-32.

Hayes, C. W., 1891, The overthrust faults of the southern Appalachians, with discussion by C. D. Walcott, W. M. Davis, and Bailey Willis: Geological Society of America Bulletin, v. 2, p. 143-144-148.

Hickman R. C., and Kent, W. N., 2005, Systematic exploration approach for diagenetic traps advanced: Oil and Gas Journal, p. 32-37.

Hohman, J. C., 1998, Depositional history of the upper Ordovician Trenton Limestone, Maquoketa shale and equivalent lithologic units in the Illinois Basin: an application of carbonate and mixed carbonate-siliciclastic sequence stratigraphy: PhD dissertation, University of Indiana, 186 p.

Holland, S. M., and M. E. Patzkowsky, 1996, Sequence stratigraphy and long-term paleoceanographic change in the Middle and Upper Ordovician of the eastern United States, *in* B. J. Witzke, G. A. Ludvigson, and J. Day., eds., Paleozoic sequence stratigraphy: views from the North American craton: Geological Society of America Special Paper 306, p. 117-130.

Janssens, A., 1973, Stratigraphy of the Cambrian and Lower Ordovician rocks in Ohio: Ohio Division of Geological Survey Bulletin 64, 197 p.

Keith, B. D., 1985, Facies, diagenesis, and the upper contact of the Trenton Limestone of northern Indiana, *in* Cecone, K. R., and Budai, J. W., eds., Ordovician and Silurian rocks of the Michigan Basin and its margin: Michigan Basin Geological Society Special Paper: p. 15-32.

Keith, B. D., 1989, Regional Facies of Upper Ordovician Series of eastern North America, *in* Keith, B.D., ed., Upper Ordovician rocks of eastern North America—deposition, diagenesis, and petroleum occurrence: American Association of Petroleum Geologists, Studies in Geology Series No. 29, p. 1-16.

Keith, B. D., and Wickstrom, L. H., 1993, Lima-Indiana Trend - U.S.A. Cincinnati and Findley Arches, Ohio and Indiana, *in* Beaumont, E. A., and Foster, N. H., eds., Stratigraphic Traps III: American Association of Petroleum Geologists, p. 347-367.

Kolata, D. R., Huff, W. D., Bergstrom, S. M., 1996, Ordovician K-bentonites of eastern North America: Geological Society of America, Special Paper 313, 84 p.

Kolata, D. R., Huff, W. D., Bergstrom, S.M., 2001, The Ordovician Sebree Trough: an oceanic passage to the Midcontinent United States: Geological Society of America Bulletin 113, 1067– 1078.

Ludvigson, G. A., Witzke, B. J., Gonzalez, L. A., Carpenter, S. J., Schneider, C. L., and Hasiuk, F., 2004, Late Ordovician (Turinian-Chatfieldian) carbon isotope excursions and their stratigraphic and paleoceanographic significance: Palaeogeography, Palaeoclimatology, Palaeoecology, vol. 210 p. 187–214.

McLaughlin, P. I., Brett, C. E., McLaughlin, S. L., Cornell, S. R., 2004, High-resolution sequence stratigraphy of a mixed carbonate-siliciclastic, cratonic ramp (Upper Ordovician; Kentucky–Ohio, USA): insights into the relative influence of eustasy and tectonics through analysis of facies gradients: Palaeogeography, Palaeoclimatology, Palaeoecology, vol. 210 p. 267–294.

Mitchell, C. E., Bergström, S. M., 1991, New graptolite and lithostratigraphic evidence from the Cincinnati region, U.S.A., for the definition and correlation of the base of the Cincinnatian Series (Upper Ordovician), *in* Barnes, C.R., Williams, S.H., eds., Advances in Ordovician Geology: Geological Survey of Canada, vol. 90-99, pp. 59–77.

Newberry, J. S., 1873, The geological relations of Ohio: Ohio Division of Geological Survey, V. 1, Geology and Paleontology, p. 50-88.

Orton, Edward, 1873, The Cincinnati Group, or Blue Limestone Formation: Ohio Division of Geological Survey, V. 1, Geology and Paleontology, p. 365-480.

Orton, Edward, 1888, The Trenton Limestone as a source of oil and gas in Ohio: Ohio Division of Geological Survey, V. 6, p. 101-310.

Pope, M. C., Read, J. F., 1997, High-resolution surface and subsurface sequence stratigraphy of the Middle to Late Ordovician (late Mohawkian– Cincinnatian) foreland basin rocks, Kentucky and Virginia: American Association of Petroleum Geologists Bulletin 81, 1866–1893.

Quinlan, G. M., and C. Beaumont, 1984, Appalachian thrusting, lithospheric flexure, and the Paleozoic stratigraphy of the eastern interior of North America: Canadian Journal of Earth Science, v. 21, p. 973-996.

Read, J. F., 1985, Carbonate platform facies models: American Association of Petroleum Geologists Bulletin, v. 69, no.1, p. 1-21.

Read, J. F., 1989, Controls on evolution of Cambrian-Ordovician passive margin, U.S. Appalachians, *in* P. D. Crevello, J. L. Wilson, J. F. Sarg, and J. F. Read, eds., Controls on carbonate platform and basin development: SEPM Special Publication 44, p. 147-165.

Richardson, J. G. and Bergstrom, S. M., 2003, Regional stratigraphic relations of the Trenton Limestone (Chatfieldian, Ordovician) in the eastern North American mid-continent: Northeastern Geology and Environmental Sciences, v. 18, p. 93-115.

Riley, R.A., J.A. Harper, M.T. Baranoski, C.D. Laughrey and R. W. Carlton, 1993, Measuring and predicting reservoir heterogeneity in complex deposystems: the Late Cambrian Rose Run sandstone of eastern Ohio and western Pennsylvania: prepared for U.S. Department of Energy, contract no. DE-AC22-90BC14657, 257 p.

Rodgers, John, 1971, The Taconic Orogeny: Geological Society of America Bulletin, v. 82, p. 1142-1178.

Ryder, R. T., 1992, Stratigraphic framework of Cambrian and Ordovician rocks in the central Appalachian basin from Morrow County, Ohio, to Pendleton County, West Virginia: U.S. Geological Survey Bulletin, 1839-G, p. G1-G25

Ryder, R. T., Harris, A. G., and Repetski, J. E., 1992, Stratigraphic framework of Cambrian and Ordovician rocks in the central Appalachian basin from Medina County, Ohio, through southwestern and south-central Pennsylvania to Hampshire County, West Virginia: U.S. Geological Survey Bulletin, 1839-K, p. K1-K32.

Scotese, C. R., and W. S. McKerrow, 1990, Revised world maps and introduction, *in* W. S. McKerrow and C. R. Scotese, eds., Palaeozoic palaeogeography and biogeography: Geological Society of London Memoir 12, p. 1-21.

Schwalb, H., 1980, Hydrocarbon entrapment along a Middle Ordovician disconformity, *in* Luther, M. K., ed., Proceedings of the Technical Sessions, Kentucky Oil and Gas Association, 36th and 37th annual meetings, 1972 and 1973: Kentucky Geological Survey Special Publication, p. 71.

Stith, D. A., 1979, Chemical composition, stratigraphy, and depositional environments of the Black River Group (Middle Ordovician), southwestern Ohio: Ohio Division of Geological Survey Report of Investigations 113, 36 p.

Vanuxem, Lardner, 1838, Of so much of the Geological Survey of the Third District of the State of New York as relates to objects of immediate utility: New York Geological Survey Second Annual report, p. 253-286.

_____, 1842, Survey of the third geological district, part 3 of Geology of New York: Natural History Survey of New York, 306 p.

Wagner, W.R., 1966, Stratigraphy of the Cambrian to Middle Ordovician rocks of central and western Pennsylvania: Pennsylvania Geological Survey, 4th ser., General Geology Report 49, 156 p.

Chapter 2: Structure and Seismic

Alexander, S.S., Cakir, R., Doden, A.G., Gold, D.P., and Root, S.I., 2005, Basement depth and related geospatial database for Pennsylvania: Pennsylvania Geological Survey, http://www.dcnr.state.pa.us/topogeo/openfile/basementtext.aspx

Baranoski, M.T., 2002, Structure contour map on the Precambrian unconformity surface in Ohio and related basement features: A description to accompany Division of Geological Survey Map PG-23.

Beardsley, R.W. and Cable, M.S., 1983, Overview of the evolution of the Appalachian Basin: Northeastern Geology, v. 5, nos. 3 and 4, p. 137.

Bickford, M.E., Van Schmus, W.R., and Zietz, I., 1986, Proterozoic history of the Midcontinent region of North America: Geology, v. 14, p. 492-496.

Black, D.F.B., 1974, Geologic map of the Winchester quadrangle, Clark and Madison Counties, Kentucky: U.S. Geological Survey Geologic Quadrangle Map GQ-1159.

Black, D.F.B., and Haney, D.C., 1975, Selected structural features and associated dolostone occurrences in the vicinity of the Kentucky River Fault System: Kentucky Geological Survey, Road log for Geological Society of Kentucky 1975 Field Conference, Guidebook, Ser. 10, 27 p.

Cardwell, D.H., 1977, West Virginia gas development in Tuscarora and deeper formations (with structural maps contoured on the top of Ordovician and Precambrian), West Virginia Geological and Economic Survey, Mineral Resources Series MRS-8, 34p.

Culotta, R.C., Pratt, T., and Oliver, J., 1990, A tale of two sutures: COCORP deep seismic surveys of the Grenville Province in the eastern U.S. Midcontinent: Geology, v. 18, p. 646-649.

Dean, S, and Baranoski, M, 2002a, Ohio Precambrian-1: A look at western Ohio's Precambrian tectonic setting: Oil and Gas Journal, July 22, 2002, 6p.

Dean, S, and Baranoski, M, 2002b, Ohio Precambrian-2: Deeper study of Precambrian warranted in western Ohio: Oil and Gas Journal, July 29, 2002, p. 37-40

Denison, R.E., Lidiak, E.G., Bickford., M.E., and Kisvarsanyi, E.G., 1984, Geology and geochronology of Precambrian rocks in the Central Interior Region of the United States: U. S. Geological Survey Professional Paper 1241-C, 20 p.

Drahovzal, J.A., 1997, Proterozoic sequences and their implications for Precambrian and Cambrian geologic evolution of western Kentucky: Evidence from seismic-reflection data: Seismological Research Letters, v. 68, no. 4, p. 553-566.

Drahovzal, J.A. and Harris, D.C., 2004, Potential Reservoirs for Geologic Sequestration in the East Continent Rift Basin: Kentucky Geological Survey Website, 6 p. http://www.uky.edu/KGS/emsweb/midcarb/SequesterECRB.htm

Drahovzal, J.A., Harris, D.C., Wickstrom, L.H., Walker, D., Baranoski, M.T., Keith, B.D., and Furer, L.C., 1992, The East Continent Rift Basin: A new discovery: Kentucky Geological Survey, Ser. 11, Special Publication 18, 25 p.

Drahovzal, J.A., and Noger, M.C., 1995, Preliminary map of the structure of the Precambrian surface in eastern Kentucky: Kentucky Geological Survey, Ser. 11, Map and Chart Series 8, 9 p.

Drahovzal, J.A., and White, T.M., 2002, The tectonic development of the Rome Trough: A new model and its exploration implications [abstract]: 2002 AAPG Eastern Section Meeting, Program with Abstracts, p. 14.

Ettensohn, F.R., and Brett, C.E., 2002, Stratigraphic evidence for continuation of Taconian Orogeny into Early Silurian time, *in:* Mitchell, C.E., and Jacobi, R., eds., Taconic convergence: Orogen, foreland basin, and craton: Physics and Chemistry of the Earth, v. 27, p. 279-288.

Ettensohn, F.R., Kulp, M.A., and Rast, N., 2002, Interpreting ancient marine seismites and apparent epicentral areas for paleo-earthquakes, Middle Ordovician Lexington Limestone, central Kentucky, *in:* Ettensohn, F.R., Rast, N., and Brett, C.E., eds., Ancient seismites: GSA Special Paper 359, p. 177-190.

Gao, D., Shumaker, R.C., and Wilson, T.H., 2000, Along-axis segmentation and growth history of the Rome Trough in the central Appalachian Basin: AAPG Bulletin, v. 84, p. 75-99.

Gray, J.D., Struble, R,A., Carlton, R.W., Hodges, D.A., Honeycutt, F.M., Kingsbury, R.H., Knapp, N.F., Majchszak, F.L., and Stith, D.A., 1982, An integrated study of the Devonian-age black shales in eastern Ohio: Ohio Division of Geological Survey, U.S. Department of Energy Report No. DOE/ET 1131-1399, 169p.

Green, A.G., Milkereit, B., Davidson, A., Spenser, C., Hutchinson, D.R., Cannon, W.F., Lee, M.W., Agena, W.F., Behrendt, J.C., and Hinze, W.J., 1988, Crustal structure of the Grenville front and adjacent terranes: Geology, v. 16, p. 788-792.

Harding, T.P., 1974, Petroleum traps associated with wrench faults in: AAPG Bulletin, v. 58, p.1290-1304.

Harper, J.A., 1989, Effects of recurrent tectonic patterns on the occurrence and development of oil and gas resources in western Pennsylvania: Northeastern Geology, v. 11, p. 225-245.

Harris, D.C., 2001, Trenton-Black River potential in Kentucky*, in:* Petroleum Technology Transfer Council, Appalachian Update: Trenton-Black River exploration and production: National Research Center for Coal and Energy, West Virginia University, 2p.

Harris, D.C., 2002, If this is a seismic play, why are we looking at the rocks?*, in:* Harris, D.C., Drahovzal, J.A., and White, T.M., Outcrop analogs for Trenton/Black Rive fractured dolomite reservoirs: A field trip and core workshop in central Kentucky: Appalachian Petroleum Technology Transfer Council Focused Workshop, 13p.

Harris, D.C., and Drahovzal, J.A., 1996, Cambrian hydrocarbon potential indicated in Kentucky's Rome Trough: Kentucky Geological Survey, Series XI, Information Circular 54, 11p.

Harris, D.C., Hickman, J.B., Baranoski, M.T., Drahovzal, J.A., Avery, K.L, and Nuttall, B.C., 2004, Rome Trough Consortium final report and data distribution: Kentucky Geological Survey, ser. 12, Open File Report 04-06, 1 CDROM.

Harris, D.C. and Wilcox, C.A., 2005, Outcrop analogs for fault-controlled Ordovician dolomite reservoirs, Appalachian Basin*, in:* Harris, D.C., ed., Central Kentucky outcrop analogs for Trenton/Black River Dolostone Reservoirs: Appalachian Basin Petroleum Technology Transfer Council Focused Technology Workshop, 11p.

Harris, L.D., 1975, Oil and gas data from the Lower Ordovician and Cambrian rocks of the Appalachian basin: U. S. Geological Survey Miscellaneous Investigations Series Map I-917 D.

Hoppe, W.J., Montgomery, E.W. and Van Schmus, W.R., 1983, Age and significance of Precambrian basement samples from northern Illinois and adjacent states: Journal of Geophysical Research, v. 88, p. 7270-7286.

Jacobi, R.D., Loewenstein, S., Smith, G., Fountain, J., Lugert, C., and Martin, J., 2004, Iapetan opening/Rome Trough-related faults and their reactivation history in New York State [abstract]: AAPG Eastern Section Meeting, Program with Abstracts, p. 91.

Keller, G.R., Lidiak, E.G., Hinze, W.J., and Braile, L.W., 1983, The role of rifting in the tectonic development of the Mid-continent, U.S.A.: Tectonophysics, v. 94, p. 391-412.

Kolata, D.R., Huff, W.D., and Bergstrom, S.M., 1996, Ordovician K-bentonites of eastern North America: Special Paper - Geological Society of America, Boulder, CO, Special Paper 313, 84 p.

Kolata, D.R. and Nelson, W.J., 1991 Tectonic history of the Illinois Basin*, in:* Leighton, M.W., D.R. Kolata, D.F. Oltz, and J.J. Eidel, eds., Interior cratonic basins: AAPG Memoir 51, p 263 - 285.

Lavin, P.M., Chaffin, D.L., and Davis, W.F., 1982, Major lineaments and the Lake Erie-Maryland crustal block: Tectonics, v. 1, p. 431-440.

Lidiak, E.G., Hinze, W.J., Keller, G.R., Reed, J.E., Braile, L.W. and Johnson, R.W., 1985, Geologic significance of regional gravity and magnetic anomalies in the east-central Midcontinent*, in:* Hinze, W.J., ed., The utility of regional gravity and magnetic maps: Society of Exploration Geophysicists, p. 287-307.

Lidiak, E.G., Marvin, R.F., Thomas, H.H., and Bass, M.N., 1966, Geochronology of the midcontinent region, United States, Part 4: Eastern Region: Journal of Geophysical Research, v. 71, p. 5427-5438.

Lidiak, E.G., and Zietz, I., 1976, Interpretation of aeromagnetic anomalies between latitudes 37°N and 38°N in the eastern and central United States: GSA Special Paper 167, 37 p.

Lucius, J.E., and Von Frese, R.R.B., 1988, Aeromagnetic and gravity anomaly constraints on the crustal geology of Ohio: GSA Bulletin, v. 100, p. 104-116.

McGuire, W.H., and Howell, Paul, 1963, Oil and gas possibilities of the Cambrian and Lower Ordovician in Kentucky: Lexington, Kentucky, Spindletop Research, Kentucky Dept. of Commerce, 216 p.

Mayhew, M.A., Thomas, H.H., and Wasilewski, P.J., 1982, Satellite and surface geophysical expression of anomalous crustal structure in Kentucky and Tennessee: Earth and Planetary Science Letters, v.58, p. 395-405.

Noger, M.C. and Drahovzal, J.A., 2005, Lithostratigraphy of Precambrian and Paleozoic rocks along structural cross section KY-1, Crittenden County to Lincoln County, Kentucky: Kentucky Geological Survey, Report of Investigations 13, ser. 12, 29p.

Parrish, J.B., and Lavin, P.M., 1982, Tectonic model for kimberlite emplacement in the Appalachian Plateau of Pennsylvania: Geology, v. 10, no. 7, p. 344-347.

Pomerene, J.B., 1964, Geology of the Portersburg Quadrangle Kentucky: U.S. Geological Survey Geologic Quadrangle Map GQ-359.

Pratt, T., Culotta, R., Hauser, E., Nelson, D., Brown, L., Kaufman, S., Oliver, J., and Hinze, W., 1989, Major Proterozoic basement features of the eastern Midcontinent of North America revealed by recent COCORP profiling: Geology, v. 17, p. 505-509.

Riley, R.A., Harper, J.A., Baranoski, M.T., Laughrey, C.D., and Carlton, R.W., 1993, Measuring and predicting reservoir heterogeneity in complex deposystems: the Late Cambrian Rose Run Sandstone of eastern Ohio and western Pennsylvania: Report prepared for U.S. Department of Energy, Contract No. DE-A90BC14657, 257p.

Rodgers, J., 1970, The Tectonics of the Appalachians: Wiley—Interscience, New York, 271p.

Rupp, J.A., 1991, Structure and isopach maps of the Paleozoic rocks of Indiana: Indiana Geological Survey, Special Report 48, 106p.

Ryder, R.T., 1992, Stratigraphic framework of Cambrian and Ordovician rocks in the Central Appalachian Basin from Lake County, Ohio, to Juniata County, Pennsylvania: U. S. Geological Survey Miscellaneous Investigations Series Map I-2200.

Ryder, R.T., Harris, A.G., and Repetski, J.E., 1992, Stratigraphic framework of Cambrian and Ordovician rocks in the Central Appalachian Basin from Morrow County, Ohio to Pendleton County, West Virginia: U. S. Geological Survey Bulletin 1839-K, p. K1-K32.

Sable, E.G., 1978, Geologic map of the White Oak Quadrangle, Magoffin and Morgan Counties, Kentucky: U.S. Geological Survey Geologic Quadrangle Map GQ-1480.

Santos, J.O.S., Hartman, L.A., McNaughton, N.J., Easton, R.M., Rea, R.G., and Potter, P.E., 2002, Sensitive high resolution ion microprobe (SHRIMP) detrital zircon geochronology provides new evidence for a hidden Neoproterozoic foreland basin to the Grenville Orogen in the eastern Midwest, U.S.A.: Canadian Journal of Earth Sciences, v. 39, no. 10, p. 1505-1515.

Saylor, T.E., 1999. Precambrian and lower Paleozoic metamorphic and igneous rocks in the subsurface*, in:* C.H. Shultz, ed., Chapter 3C, The geology of Pennsylvania, Pennsylvania Geological Survey and Pittsburgh Geological Society, Special Publication, no. 1, p. 51-58.

Shrake, D.L., Wolfe, P.J., Richard, B.H., Swinford, E.M., Wickstrom, L.H., Potter, P.E., and Sitler, G.W., 1990, Lithologic and geophysical description of a continuously cored hole in Warren County, Ohio, including description of the Middle Run Formation (Precambrian?) and a seismic profile across the core site: Ohio Division of Geological Survey, Information Circular No. 56.

Shumaker, R.C., 1986, Structural development of Paleozoic continental basins of eastern North America*, in:* M.J. Aldrich, Jr., and A.W. Laughlin, eds., Proceedings of the 6th International Conference on Basement Tectonics: Salt Lake City, basement Tectonics Association, p. 82-95.

Shumaker, R.C., 1993, Geology of the Warfield anticline and its significance in regional structure [abstract]: Programs with Abstracts, 24th Annual Appalachian Petroleum Geology Symposium, I.C. White Memorial Fund, Publication No. 5, p. 85-106.

Shumaker, R.C., 1996, Structural history of the Appalachian Basin*, in:* Roen, J.B. and Walker, B.J., eds. The Atlas of Major Appalachian Gas Plays, West Virginia Geological and Economic Survey, Publication V-25, Plate 1, p. 11-15.

Shumaker, R.C. and Wilson, T.H., 1996, Basement structure of the Appalachian foreland in West Virginia: its style and affect on sedimentation, *in:* van der Pluijm, B.A. and Catacosinos, P.A., eds., Basement and basins of eastern North America: Geological Society of America Special Paper 308, p. 139-155.

Sibson, R.H., and Rowland, J.V., 2003, Stress, fluid pressure and structural permeability in seismogenic crust, North Island, New Zealand: Geophysical Journal International, v. 154, n. 2, p. 584-594.

Smith, L.B., (in press), Origin and reservoir characteristics of Upper Ordovician Trenton-Black River hydrothermal dolomite reservoirs in New York, USA: AAPG Bulletin.

Stark , T.J., 1997a, The East Continent Rift Complex: Evidence and conclusions, *in:* Ojakangas, R.W., Dickas, A.B., and Green, J.C., eds., Middle Proterozoic to Cambrian Rifting, Central North America: GSA Special Paper 312, p. 253-266.

Stark, T.J., 1997b, The English Graben: A possible Precambrian rift segment of the eastern Mid-Continent, *in:* Ojakangas, R.W., Dickas, A.B., and Green, J.C., eds., Middle Proterozoic to Cambrian Rifting, Central North America: GSA Special Paper 312, p. 267-285.

Strunk, K.L., Structural relationships of the Cottage Grove and Shawneetown fault systems near Equality, Illinois, as inferred from geophysical data: unpublished thesis, Carbondale, Southern Illinois University, 72p.

Thomas, W.A., 1991, The Appalachian-Ouachita rifted margin of southeastern North America: GSA Bulletin, v. 103, p. 415-431.

Thomas, W.A., 2005, Tectonic inheritance at a continental margin: GSA Today, v. 16, n. 2, p. 4-11.

Van Schmus, W.R. and Hinze, W.J., 1985, The Midcontinent Rift System: Annual Review of Earth and Planetary Sciences, v. 13, p. 345-383.

Van Schmus, W.R., Bickford, M.E., Sims, P.K., Anderson, R.R., Shearer, C.K. and Treves, S.B., 1993, Proterozoic geology of the western Midcontinent basement, *in:* Reed, J.C., Jr and others, eds., Precambrian: Conterminous U.S.: The Geology of North America, v. C-2, Geological Society of America, p. 239-259.

Van Schmus, W.R. and Hinze, W.J., 1993, Midcontinent Rift System, *in:* Reed, J.C., Jr and others, eds., Precambrian: Conterminous U.S.: The Geology of North America, v. C-2, Geological Society of America, p. 292-303.

Wagner, W.R., 1976, Growth faults in Cambrian and Lower Ordovician rocks of western Pennsylvania: AAPG Bulletin, v. 60, no. 3, p. 414-427.

Wickstrom, L.H., Drahovzal, J.A., and Keith, B.D., 1992a, The geology and geophysics of the East Continent Rift Basin: Indiana Geological Survey Open File Report OFR 92-4, 337 p.

Wickstrom, L.H., Gray, J.D., and Stieglitz, R.D., 1992b, Stratigraphy, structure, and production history of the Trenton Limestone (Ordovician) and adjacent strata in northwestern Ohio: Ohio Division of Geological Survey, Report of Investigations No. 143, 78 p., 1 pl.

Wickstrom, L.H., Venteris, E.R., Harper, J.A., McDonald, J., Slucher, E., Carter, K.M., Greb, S.F., Wells, J.G., Harrison, W.B., III, Nuttall, B.C., Riley, R.A., Drahovzal, J.A., Rupp, J.A., Avary, K.L., Lanham, S., Barnes, D.A., Gupta, N., Baranoski, M.A., Radhakkishnan, P., Solis, M.P., Baum, G.R., Powers, D., Hohn, M.E., Parris, M.P., McCoy, K., Grammer, G.M., Pool, S., Luckhardt, C., Kish, P., 2005, Characterization of geologic sequestration opportunities in the MRCSP region: Report for DOE Cooperative Agreement No. DE-PS26-05NT42255, 152 p.

Wilson, T.H., 2000, Seismic evaluation of differential tectonic subsidence, compaction, and loading in an interior basin: AAPG Bulletin, v. 84, no. 3, p. 376-398.

Woodward, H.P., 1961, Preliminary subsurface study of southeastern Appalachian interior plateau: AAPG Bulletin, v. 45, p. 1634-1655.

Chapter 3: Petrology

Allan, J. R. and W. D. Wiggins (1993), *Dolomite reservoirs, geochemical techniques for evaluating origin and distribution*, AAPG Continuing Education Course Notes Series #36, 129 p.

Asquith, G. B. (1985), *Handbook of log evaluation techniques for carbonate reservoirs*, AAPG Methods in Exploration Series No. 5, 47 p.

Bathurst, R. G. C. (1975), *Carbonate sediments and their diagenesis*, Amsterdam, Elsevier, 658 p.

Bosak, T., V. Souaz-Egipsy, and D. K. Newman (2004), *A laboratory model of abiotic peloid formation*, Geobiology, **2**, (3), p. 189 – 198.

Brett, C. E. and M. E. Brookfield (1984), *Morphology, faunas, and genesis of Ordovician hardgrounds from southern Ontario, Canada*, Paleogeography, Paleoclimatology, and Paleoecology, **46**, p. 233 – 290.

Budai, J. M. and J. L. Wilson (1986), *Depositional patterns and diagenetic history of Trenton-Black River formations in Michigan basin* (abs.), AAPG Bulletin, **70**, p. 1063.

Cantrell, D. L. and R. M. Hagerty (1999), *Microporosity in Arab Formation carbonates, Saudi Arabia*, GeoArabia, **4** (2), Gulf PetroLink, Bahrain, p. 129 – 154.

Chafetz, H. S. (1986), *Marine peloids: a product of bacterially induced precipitation of calcite*, Journal of Sedimentary Petrology, v. 56, p. 8121 – 817.

Choquette, P. W. and L. C. Pray (1970), *Geologic nomenclature and classification of porosity in sedimentary carbonates*, AAPG Bulletin, **75**, p. 207 – 250.

Davies, G. R. (2000), *Hydrothermal dolomite reservoir facies: global and western Canada perspectives*, Course Notes, Second Edition, Graham Davies Geological Consultants LTD., Calgary, Alberta, 214 p.

Dunham, R. J. (1962), *Classification of carbonate rocks according to their depositional texture*, in W. E. Ham, ed. *Classification of carbonate rocks – a symposium*, Tulsa OK, AAPG Memoir I, p.108 – 121.

Folk, R. L. (1962), *Spectral subdivision of limestone types*, in W. E. Ham, ed. *Classification of carbonate rocks – a symposium*, Tulsa OK, AAPG Memoir I, p. 62 – 84.

Folk, R. L. and J. S. Pittman (1971), *Length-slow chalcedony: a new testament for vanished evaporites*, Journal of Sedimentary Petrology, **41**, p. 1045 – 1058.

Friedman, G. M. and J. E. Sanders (1978), *Principals of Sedimentology*, New York, John Wiley and Sons, Inc., 792 p.

Gregg, J. M. (2004), *Basin fluid flow, base-metal sulphide mineralization and the development of dolomite petroleum reservoirs*, in Braithwaite, C. J. R., G. Rizzi, and G. Darke (eds.): *The geometry and petrogenesis of dolomite hydrocarbon reservoirs*, Geological Society, London, Special Publications, 235, p. 157 – 175.

Gregg, J. M. and D. F. Sibley (1984), *Epigenetic dolomitization and the origin of xenotopic dolomite texture*, Journal of Sedimentary Petrology, **54**, p. 908 – 931.

Haefner, R. J., J. J. Mancuso, J. P. Frizado, K. L. Shelton, and J. M. Gregg (1988), *Crystallization temperature and stable isotope compositions of Mississippi Valley-Type carbonates and sulfides of the Trenton Limestone, Wyandot County, Ohio*, Economic Geology, **83**, p. 1061 – 1069.

Harris, D. C. (workshop director) (2005), *Central Kentucky outcrop analogs for Trenton/Black River dolostone reservoirs, project review and core workshop*, June 1, 2005, Lexington, KY, Petroleum Technology Transfer Council Focused Technology Workshop course notes.

Hillgartner, H. C. Dupraz, and W. Hug (2001), *Microbially induced cementation of carbonate sands: are micritic meniscus cements good indicators of vadose diagenesis?* Sedimentology, **48**, p. 117 – 131.

Hunt, J. M. (1996), *Petroleum geochemistry and geology*, New York, W. H. Freeman and Company, 743 p.

James, N. P. and P. W. Choquette (1984), Diagenesis 9, Limestones – the meteoric diagenetic environment: Geoscience Canada, **11**, p. 161 – 194.

Keith, B. D. (1988), *Reservoirs resulting from facies-independent dolomitization: case histories from Trenton and Black River carbonate rocks of the Great Lakes area*, in Keith, B. D. ed., *The Trenton Group (Upper Ordovician Series) of eastern North America, deposition, diagenesis, and petroleum*, AAPG Studies in Geology #29, p. 267 – 278.

Laughrey, C. D., J. Kostelnik, D. P. Gold, A. G. Doden, and J. A. Harper (2003), *Trenton and Black River carbonates in the Union Furnace area of Blair and Huntingdon Counties, Pennsylvania*, Field Trip Guidebook, AAPG-SPE Eastern Section Meeting, September 10, 2003, 80 p.

Lighty, R. G. (1985), *Preservation of internal reef porosity and diagenetic sealing of submerged early Holocene barrier reef, southeast Florida shelf*, in N. Schneidermann and P. M. Harris, eds, *Carbonate cements*, SEPM Special Publication No. 36, p.123 – 151.

Lowenstein, T. K., M. N. Timofeeff, S. T. Brennan, L. A. Hardie, and R. V. Demicco (2001*), Oscillations in Phanerozoic seawater chemistry: evidence from fluid inclusions*, Science, **294**, p. 1086 – 1088.

Luo, P. and H. G. Machel (1995), *Pore size and pore throat types in a heterogeneous dolostone reservoir, Devonian Grosmont Formation, western Canada sedimentary basin*, AAPG Bulletin, **79**, p. 1698 – 1720.

Machel, H. G. (1999), *Effects of groundwater flow on mineral diagenesis, with emphasis on carbonate aquifers*, Hydrogeology Journal, **7**, p. 94 – 107.

Machel, H. G. (2004), *Concepts and models of dolomitization: a critical reappraisal*, in Braithwaite, C. J. R., G. Rizzi, and G. Darke (eds.): *The geometry and petrogenesis of dolomite hydrocarbon reservoirs*, Geological Society, London, Special Publications, 235, p. 7 – 235.

Macintyre, I. G. (1985), *Submarine cements – the peloidal question*, in N. Schneidermann and P. M. Harris, eds., *Carbonate cements*, SEPM Special Publication No. 36, p.109 – 116.

Malone, M. J., N. C. Slowey, and G. M. Henderson (2001), *Early diagenesis of shallow-water periplatform carbonate sediments, leeward margin, Great Bahama Bank (Ocean Drilling Program Leg 166)*, Geological Society of America Bulletin, **33** (7), p. 881 – 894.

Markello, J. R., R. B. Koepnick, and L. E> Waite (2005), *The carbonate analogues through time (CATT) hypothesis – a systematic and predictive look at Phanerozoic carbonate reservoirs*, 2005 AAPG Annual Convention, Technical Program and Abstracts, http://aapg.confex.com/aapg/cal2005/techprogram/meeting_cal2005.htm.

McKee, E. D. and R. C. Gutschick (1969), *History of Redwall Limestone of northern Arizona*, Boulder, CO., Geological Society of America Memoir 114, 726p.

Pettijohn, F. J., P. E. Potter, and R. Siever (1987), *Sand and sandstone*, New York, Springer-Verlag, 553 p.

Pope, M. and J. B. Steffen (2003), *Widespread, prolonged late Middle to Late Ordovician upwelling in North America: a proxy record of glaciation?*, Geology, **31**, p. 63 – 66.

Scholle, P. A. and D. S. Ulmer-Scholle (2003), *A color guide to the petrography of carbonate rocks: grains, textures, porosity, diagenesis*, Tulsa, OK, American Association of Petroleum Geologists Memoir 77, 474 p.

Sibley, D. F. and J. M. Gregg (1987), *Classification of dolomite rock textures*, Journal of Sedimentary Petrology, **57**, p. 967 – 975.

Smith, L., R. Nyahay, and B. Slater (2005), *Hydrothermal dolomite core workshop and field trip*, June 7, 2005, Albany, NY, U. S. Department of Energy, Petroleum Technology and Transfer Council, Appalachian Region and NYSERDA, short course notes.

Taylor, T. R. and D. F. Sibley (1986), Petrographic and geochemical characteristics of dolomite types and the origin of ferroan dolomite in the Trenton Formation, Ordovician, Michigan basin, USA, Sedimentology, **33**, p. 61 – 86.

Thompson, A. M. (1999), *Chapter 5. Ordovician*, p.74 to 89, in Schultz, C. H., ed., *The Geology of Pennsylvania, Part II, Stratigraphy*. Pennsylvania Geological Survey, 4th Series, Special Publication 1, 888 p.

Tucker, M. E. and V. P. Wright (1990), *Carbonate sedimentology*, Oxford, UK, Blackwell Science Ltd., 482 p.

Wickstrom, L. H., J. D. Gray, and R. D. Stieglitz (1992), *Stratigraphy, structure, and production history of the Trenton Limestone (Ordovician) and adjacent strata in northwestern Ohio*, Ohio Division of Geological Survey, Report of Investigations No. 143, 78 p.

Wilson, M. A. and T. J. Palmer (1992), *Hardgrounds and hardground faunas*, University of Wales, Aberystwyth Institute of Earth Studies Publications No. 9, 131 p.

Woody, R. E., J. M. Gregg, and L. F. Koedertz (1996), *Effect of texture on petrophysical properties of dolomite: evidence from the Cambrian-Ordovician of southeastern Missouri*, AAPG Bulletin, **80**, p.119 – 132.

Wright, V. P. (1992), *A revised classification of limestones*, Sedimentary Geology, **76**, p. 177 – 185.

Wright, W. R. (2001), *Dolomitization, fluid flow, and mineralization of the Lower Carboniferous rocks of the Irish Midlands and Dublin basin*, PhD thesis, University College Dublin, Belfield, Ireland.

Chapter 4: Geochemistry of Carbonate Rocks

Allan, J. R. and W. D. Wiggins, 1993, Dolomite reservoirs: Geochemical techniques for evaluating origin and distribution, AAPG Continuing Education Course Notes No. 36, 129 p.

Balcaen, L., DeSchrijver, I., Moens, L., and Vanhaecke, F. (2005), Determination of $^{87}Sr/^{86}Sr$ isotope ratio in USGS silicate reference materials by multi-collector ICP-mass spectrometry, *International Journal of Mass Spectrometry*, *242*, 251-255.

Barta, Nathanael Calvin, 2004, Investigation of the Correlation of the Lower Chatfieldian (Upper Middle Ordovician) Strata of New York, Ontario and Pennsylvania using the Guttenberg Carbon Isotope Excursion(GICE). A thesis presented in partial fulfillment of the requirements for the degree of Master of Science in the graduate school of The Ohio State University.

Bergstrom, S. M., Huff, W. D., Kolata, D. R., and Saltzman, M. R., 2000, The Ordovician (Chatfieldian) Gutterberg carbon isotope excursion: 2, Significance for clarifying Baltoscandic and Trans-Atlantic biostratigraphic relations and the equivalence of the North American Millbrig and Baltoscandic Kinnekulle K-bentonites. Geological Society of America Abstracts with Programs, no. 4, v. 33, p. 41.

Black, D. F. B. et al., 1981, The relation of dolomite associated with faults to the stratigraphy and structure of central Kentucky. Professional Paper 1151-A. 19 p.

Colquhoun, I.M., 1991, Paragenetic history of the Ordovician Trenton Group carbonates, Southwestern Ontario [unpublished M.S. thesis], Brock University, St. Catherines, Ontario, 250p.

Coniglio, M., Sherlock, R., Williams-Jones, A.E. Middleton, K. and S.K. Frape, 1994, Burial and hydrothermal diagenesis of Ordovician carbonates from the Michigan

Basin, Ontario, Canada in B. Purser, M.Tucker and D. Zenger (eds.), Dolomites, International Association of Sedimentologists Special Publication 21, p. 231-254.

Davies, G.R., 2001, Hydrothermal (thermobaric) dolomite reservoir facies: Global and western Canadian perspectives, unpublished report, Graham Davies Geological Consultants Ltd, Calgary, 548p.

Deming, D., 1992, Catastrophic release of heat and fluid flow in the continental crust, Geology, v. 20, p. 83-86.

Ducea, M.N., Sen, G., Eiler, J., and Fimbres, J., Melt depletion and subsequent enrichment in the shallow mantle beneath Koolau volcano, Oahu (Hawaii), *Geochem. Geophys. Geosyst.* 10.1029/2001GC000184, 2002.

Ducea, M. Hacker, B., Lutkov, V., Minaev, V., Ratschbacher, L., Luffi, P., Schwab, M., Gehrels, G., McWilliams, M., Vervoort, J., and Metcalf, J., Building the Pamirs: The view from the underside, *Geology*, 31: 849-852, 2003.

Ducea, M.N., Constraints on the bulk composition and root foundering rates of continental arcs: A California arc perspective, *Journal of Geophysical Research* 107, 2001JB001643, 2002.

Frape, S. K. and Fritz, P. 1987. Saline Water and Gases in Crystalline Rocks (eds Fritz, P. and Frape, S. K.) Geological Association of Canada Special Paper. No. 33, P. 19-37.

Friedman, I. and Oneill, J. R., 1977. Composition of Stable Isotope Fractionation Factors of Geochemical Interest. US Geological Survey, Professional Paper, 440-KK.

Hanor, J.S., 1994, Origin of saline fluids in sedimentary basins: in Parnell, J., (ed.), Geofluids: Origin and migration of fluids in sedimentary basins: Geological Society of London Special Publication No. 78, p. 151-174.

Harding, T.P., 1974, Petroleum traps associated with wrench faults in: AAPG Bulletin, v. 58, p.1290-1304.

Hatch, J. R., Jacobson, S. R., Witzke, B. J., Anders, D. E., Watney, W. L., Newell, K. D. and Vuletich, A. K., 1987. Possible Late Middle Ordovician Organic carbon isotope excursion: Evidence from Ordovician Oils and Hydrocarbon Source Rocks. Mid-continent and East-Central United States. American Association Petroleum Geologists Bulletin, v. 71. p. 1343-1354.

Heydari, E., 1997, Hydrotectonic models of burial diagenesis in platform carbonates based on formation water geochemistry in North American sedimentary basins, in Montanez, I. P., Gregg, J.M., and Shelton, K. L., eds., Basin-wide diagenic patterns: integrated petrologic, geochemical, and hydrologic considerations:

Society of Economic Paleontologists and Mineralogists, Special Publication 57, p. 53-79.

Hulver, M. L., 1997, Post-orogenic evolution of the Appalachian Basin Mountain system and its foreland [unpublished Ph.D. thesis], University of Chicago, 917p.

Knipe, R.J., The influence of fault zone processes and diagenesis on fluid flow in: Horbury, A.D., and A.G. Robinson, eds., Diagenesis and basin development, AAPG Studies in Geology #26, p. 131-156.

Ludvingson, G. A., Jacobson, S. R. Witke, B. J., and Gonzalaz, L. A., 1996, Carbonate component chemostratigraphy and depositional history of the Ordovician Decorah Formation, Upper Mississippi Valley. In B. J. Witzke, G. A. Ludvigson, and J. Day (eds.), Paleozoic Sequence Stratigraphy: views from the North American Craton. Geological Society of America Special Paper, 306, p. 67-86.

Machel, H.G. and J. Lonee, 2002, Hydrothermal dolomite – a product of poor definition and imagination, Sedimentary Geology, v. 152, p. 163-171.

Nyahay, R. E., and L. B. Smith, 2003, Vertical and Lateral Distribution of Hydrothermal Dolomite in Trenton-Black River carbonates of New York [abstract], AAPG Eastern Section Program with abstracts.

Patzkowsky, M. E., Slupik, L. M., Arthur, M. A., Pancost, R. D., and Freeman, K. H., 1997, Late Middle Ordovician environmental change and extinction: Harbinger of the Late Ordovician or continuation of Cambrian patterns? Geology, v. 25, p. 911-914.

Ramos, F. C., Wolff, J.A., and Tollstrup, D.L. (2004), Measuring Sr-87/Sr-86 variations in minerals and groundmass from basalts using LA-MC-ICPMS, *Chemical Geology*, *211*, 135-158.

Repetski, J. E., Ruppert, L. F., Ryder, R. T., Weary, D. J., Rowan, E. L. and Trippi, M. H., 2004, Thermal Maturity Patterns for Ordovician, Devonian, and Pennsylvanian Rocks of the Central Appalachian Basin, Based on CAI and Vitrinite Reflectance (%Ro) [abstract], AAPG Eastern Section Meeting Program with abstracts.

Rowan, E. L., Ryder, R. T., Swezey, C. S., Repetski, J. E., Crangle, R. D., Trippi, M. H. and L. F. Ruppert., 2004, Burial and Thermal History Model of a Cross-Section through the Central Appalachian Basin, Ohio and West Virginia [abstract], AAPG Program with Abstracts.

Saltzman, M. R., Bergstrom, S. M., Huff, W. D., and Kolata, D. R.., 2000, The Ordovician (Chatfieldian) Guttenberg carbon isotope excursion; 1, New data from the eastern North American mid-continent and Baltoscandia. Geological Society of America Abstracts with Programs, no. 4, v. 33, p. 41.

Sibson, R.H., 2000, Fluid movement in normal faulting, Journal of Geodynamics, v. 29, p. 469-499.

Simo, J. A., Emerson, N. R., Byers, C. W., and Ludvigson, G. A., 2003, Anatomy of an embayment in an Ordovician epeiric sea, Upper Mississippi Valley, USA. Geology v. 31, p. 545-548.

Taylor, T.R. and D. F. Sibley, 1986, Petrographic and geochemical characteristics of dolomite types and the origin of ferroan dolomite in the Trenton Formation, Ordovician, Michigan Basin, Sedimentology, v. 33, p. 61-86.

Wasserburg, G. J., Jacobsen, S.B., DePaolo, D.J., McCulloch, M.T., and Wen, T. (1981), Precise determination of Sm/Nd ratios, Sm and Nd isotopic abundances in standard solutions, *Geochimica et Cosmochimica Acta*, *45*, 2311-2323.

Weary, D. J., Ryder, R. T., and R. E. Nyahay, 2001, Thermal maturity patterns in New York State using CAI and $\%R_O$, Northeastern Geology and Environmental Science, v. 23, p. 356-376.

Wickstrom, L.H., Gray, J.D., and R. D. Stieglitz, 1992, Stratigraphy, structure, and production history of the Trenton Limestone (Ordovician) and adjacent strata in northwestern Ohio, Ohio Geological Survey Report of Investigation 143, 78 p.

White, D. E., 1957, Thermal waters of volcanic origin, Geological Society of America Bulletin, v. 68, p. 1637-1658.

Young, S. A., Bergstrom, S. M., and Saltzman, M. R., Holmden, C. and Patterson, W. P. 2003, Paleooceanographic aspects of the Early Chatfieldian (Upper Middle Ordovician) positive δ 13 C Excursion (GICE): Abstracts with Programs-Geological Society of America, v. 35, no. 6, p. 601.

Chapter 5: Geochemistry of Gases

Apps, J. A. and P. C. van de Kamp (1993), *Energy gases of abiogenic origin in the earth's crust*, in D. G. Howell, K. Wiese, M. Fanelli, L. Zimk, and F. Cole (eds.), *The future of energy gases*, U. S. Geological Survey Professional Paper 1570, p81 – 132.

Ballentine, C. J., R. K. O'Nions, and M. L. Coleman (1996), *A Magnus opus: helium, neon, and argon isotopes in a North Sea oilfield*, Geochimica et Cosmochimica Acta **60**, p. 831 – 849.

Ballentine, C. J., A. N. Halliday, and B. Sherwood Lollar (2001*), Combined noble gas and stable isotope constraints on nitrogen gas sources within sedimentary basins*, Final Report for Period 15 March 1996 – 14 March 1999 Extended to 14 March 2000, U. S. Department of Energy Award No. DE-FGO2-96ER14615

Boyd, S. R., R. F. Pineay, and M. Javoy (1994), *Modeling the growth of natural diamonds*, Chemical Geology, **116**, p. 29 – 42.

Burruss, R. C. (2005), personal communication.

Burruss, R. C. (1993), *Stability and flux of methane in the deep crust – a review*, in D. G. Howell, K. Wiese, M. Fanelli, L. Zimk, and F. Cole (eds.), *The future of energy gases*, U. S. Geological Survey Professional Paper 1570, p. 21 – 30.

Burruss, R. C. and C. D. Laughrey (2006), *Stable isotope constraints on abiogenic hydrocarbon gas contributions to thermogenic natural gas resources in the northern Appalachian basin USA*, (abstract), American Geophysical Union Annual Meeting, Baltimore, MD, May 2006.

Chung, H. M., J. R. Gromly, and R. M. Squires (1988), *Origin of gaseous hydrocarbons in subsurface environments: theoretical considerations of carbon isotope distribution*, Chemical Geology, **71**, p. 97 – 103.

Des Marais, D. J., M. J. Stallard, N. L. Nahring, and A. H. Truesdell (1981), *Molecular carbon isotopic evidence for the origin of geothermal hydrocarbons*, Nature, **292**, p. 826 – 828.

Elliot and others (1993), Chemical Geology, **106**, p. 429 – 440.

Harris, A. G. (1979), *Conodont color alteration, an organo-mineral metamorphic index, and its application to Appalachian basin geology*, in P. A. Scholle and P. R. Schluger (eds.), *Aspects of diagenesis*, SEPM Special Publication No. 26, p. 3 – 16.

Harris, D. (2004), personal communication.

Hoefs, J. (1997), *Stable isotope geochemistry*, Berlin, Springer, 201 p.

Horita, J. and M. E. Berndt (1999), *Abiogenic methane formation and isotopic fractionation under hydrothermal conditions*, Science, **285**, p. 1055 – 1057.

Hunt, J. M. (1996), *Petroleum geochemistry and geology*, New York, Freeman, 743 p.

James, A. T. (1983), *Correlation of natural gases by use of carbon isotopic distribution between hydrocarbon components*, AAPG Bulletin, **67**, p. 1176 – 1191.

Jenden, P. D., D. J. Drozan, and I. R. Kaplin (1993), *Mixing of thermogenic natural gases in northern Appalachian basin*, AAPG Bulletin, **77**, p. 980 – 998.

Jenden, P. D., D. R. Hilton, I. R. Kaplin, and H. Craig (1993), *Abiogenic hydrocarbons and mantle helium in oil and gas fields*, in D. G. Howell, K. Wiese, M. Fanelli, L. Zimk,

and F. Cole (eds.), *The future of energy gases*, U. S. Geological Survey Professional Paper 1570, p. 233 – 252.

Krouse, H. R. (1979), *Stable isotope geochemistry of non-hydrocarbon constituents of natural gas*, in *Source prediction and separation on non-hydrocarbon constituents of natural gas,* preprint of the Tenth World Petroleum Congress, Bucharest, 1979. London: Heyden and Son.

Krouse, H. R., C. A. Vian, L. S. Eliuk, A. Ueda, and S. Halas (1988), *Chemical and isotopic evidence of thermochemical sulfate reduction by light hydrocarbon gases in deep carbonate reservoirs*, Nature, **333**, p. 415 – 419.

Laughrey, C. D. and F. J. Baldassare (1998), *Geochemistry and origin of some natural gases in the Plateau province, central Appalachian basin, Pennsylvania and Ohio*, AAPG Bulletin, **82**, p. 3217 – 335.

MacKenzie, P. and W. Grubaugh (2000), *Discovery of a new field in the Trenton-Black River interval, northeastern Ohio* (abst.), AAPG Bulletin, **84**, p. 1388.

Minkin, D. A. (2003), *A 3-D seismic case study investigating AVO, acoustic inversion, and probalistic neural networks in the Trenton-Black River interval, NE Ohio*, MS Thesis, University of Oklahoma, 148 p.

Ozima, M. and F. A. Podosek (2002), *Noble gas geochemistry*, Cambridge, Cambridge University Press, 286 p.

Peters, K. E. and J. M. Moldowan (1993), *The biomarker guide*, Englewood Cliffs, NJ, Prentice-Hall, 363 p.

Prinzhofer and Battani (2003), *Gas isotope tracing: an important tool for hydrocarbons exploration,* Oil and Gas Science Technology – Review, IFP, **58**, p. 299 – 311.

Rasmussen, J. C., S. B. Keith, M. M. Swan, D. P. Laux, and J. Caprara (2003), *Strike-slip faulting and reservoir development in New York state*, NYSERDA Report 2002-6984.

Repetski, J. E., R. T. Ryder, K. L. Avary, and M. H. Trippi (2005), *Thermal maturity patterns (CAI and %R_o) in the Ordovician and Devonian rocks of the Appalachian basin in West Virginia*, USGS Open File Report 2005-1079, 69 p.

Ryder, R. T., R. C. Burruss, and J. R. Hatch (1998), *Black shale source rocks and oil generation in the Cambrian and Ordovician of the central Appalachian basin, USA*, AAPG Bulletin, **82**, p. 412 – 441.

Sagan, J. A. and B. S. Hart (2005), *3-D seismic-based definition of fault-related porosity development Trenton-Black River interval, Saybrook, Ohio*, McGill University, Earth and Planetary Sciences, Manuscript Number: BLTN05-027, Version 2, 36 p.

Schoell, M. (1983), *Genetic characterization of natural gas*, AAPG Bulletin, **67**, p. 2225 – 2239.

Schoell, M. (1988), *Multiple origins of methane in the earth*, Chemical Geology, **71**, p. 1 – 10.

Schoell, M., P. D. Jenden, M. A. Beeunas, and D. D. Coleman (1993), *Isotope analysis of gases in gas field and gas storage operations*, SPE Gas Technology Symposium, Calgary, Alberta, Canada, 28 – 30 June, 1993, p. 337 – 343.

Sherwood Lollar, B., T. D. Westgate, J. A. Ward, G. F. Slater, and G. Lacrampe-Couloume (2002), *Abiogenic formation of alkanes in the earth's crust as a minor source for global hydrocarbon reservoirs*, Nature, **416**, p. 522 – 524.

Sherwood Lollar, B., G. Lacrampe-Couloume, G. F. Slater, J. Ward, D. P. Moser, T. M. Gihring, L.-H. Lin, and T. C. Onstott (2006), *Unraveling abiogenic and Biogenic sources of methane in the earth's deep subsurface*, Chemical Geology, **226**, p. 328 – 339.

Sundberg, K. R. and C. R. Bennett (1983), *Carbon isotope paleothermometry of natural gas*, in M. Bjoroy, P. Albrecht, C. Cornfield, and others, eds., Advances in organic geochemistry-1981, Chichester, England, John Wiley and Sons, p. 769 – 774.

Swezey, C. S. (2002), *Regional stratigraphy and petroleum systems of the Appalachian basin, North America*, USGS, Geological Investigations Series Map I-2768.

Szatmari, P. (1989), *Petroleum formation by Fischer-Tropsch synthesis in Plate Tectonics*, AAPG Bulletin, **73**, p. 989 – 998.

Tang, Y., J. K. Perry, P. D. Jenden, and M. Schoell (2000), *Mathematical modeling of stable carbon isotope ratios in natural gases*, Geochimica et Cosmochimica Acta, **64**, p. 2673 – 2687.

Tissot, B. P. and D. H. Welte (1984), *Petroleum formation and occurrence*, Berlin, Springer-Verlag, 699 p.

White, W. M. (1997), *Geochemistry*, Online Textbook: http://www.imwa.info/Geochemie/Chapters.HTML

Wiese, K. and K. A. Kvenvolden (1993), *Introduction to microbial and thermal methane*, in in D. G. Howell, K. Wiese, M. Fanelli, L. Zimk, and F. Cole (eds.), *The future of energy gases*, U. S. Geological Survey Professional Paper 1570, p. 13 – 20.

Whiticar, M. J. (1994), *Correlation of natural gases with their sources*, in L. B. Magoon and W. G Dow (eds.), *The petroleum system – from source to trap*, AAPG Memoir 60, p. 261 – 283.

Worden, R. H., P. C. Smally, and N. H. Oxtoby (1995), *Gas souring by thermochemical sulfate reduction at 140℃*, AAPG Bulletin, **79**, p. 854 – 863.

Youngchang, X., S. Ping, L. Wenhui, and T. Mingxin (1996), *Geochemistry of noble gases*, Beijing, Science Press, 275 p.

Chapter 6: Trenton-Black River Production History

Chapter 7: Exploration Fairways and Undiscovered Gas Assessment Model

Charpentier, R. R. and Klett, T. R., Monte Carlo Simulation Method *in* U.S. Geological Survey World Petroleum Assessment 2000 – Description And Results, Chapter MC. http://pubs.usgs.gov/dds/dds-060/

Roen, John B., and Walker, Brian, eds., 1996, The Atlas of Major Appalachian Gas Plays: West Virginia Geological and Economic Survey, Volume 25, 201 p.

Ryder, R.T., D.C. Harris, P. Gerome, T.J. Hainsworth, R.C. Burruss, P.G. Lillis and D.M. Jarvie, 2003, Cambrian petroleum source rocks in the Rome trough of West Virginia and Kentucky (abstract): Program and abstracts, Eastern Section, American Association of Petroleum Geologist

Chapter 8: Trenton-Black River Key Field and Play Descriptions

Colquhoun, I.M., 1991, Paragenetic history of the Ordovician Trenton Group carbonates, Southwestern Ontario [unpublished M.S. thesis], Brock University, St. Catherines, Ontario, 250p.

Harding, T.P., 1974, Petroleum traps associated with wrench faults in: AAPG Bulletin, v. 58, p.1290-1304.

Prouty, C.E., 1988, Trenton exploration and wrenching tectonics in Michigan Basin and environs in B.D. Keith, (ed.), The Trenton Group (Upper Ordovician Series) of eastern North America, A.A.P.G. Studies in Geology 29, p.207-236.

Wickstrom, L.H., Gray, J.D., and R. D. Stieglitz, 1992, Stratigraphy, structure, and production history of the Trenton Limestone (Ordovician) and adjacent strata in northwestern Ohio, Ohio Geological Survey Report of Investigation 143, 78 p.

APPENDICES

Appendix A: Description of Project Website, Database and GIS-IMS

Appendix B: Details and Results of the Bentonite Correlation Study for the Trenton/Black River Consortium and the New York State Museum

Appendix C: Samples of supposed Deicke and Millbrig K-bentonites

Appendix D: Origin and Reservoir Characteristics of Upper Ordovician Trenton-Black River Hydrothermal Dolomite Reservoirs in New York, USA

Appendix E: Petrography of the Trenton Limestone and Black River Group

1. Non-skeletal grains and skeletal components
2. Diagenesis
3. Dolomite textures
4. Base metal sulfide mineralization
5. Dolomite porosity

Appendix F: Page-sized plates from the Stratigraphy chapter

Appendix G: Page-sized plates from the Seismic and Structure chapter

APPENDIX A

DESCRIPTION OF PROJECT WEBSITE, DATABASE AND GIS-IMS

By John Bocan, West Virginia Geological Survey

Introduction

The data for the Trenton-Black River Project are served through three means via the West Virginia Geological and Economic Survey: a secure website, a database system and a geographical information system's internet map server/service (IMS).

During the life of the project, the website and thus the other services, were accessible through a user and password authentication process. As of March 22, 2006, website access had been granted to 40 industrial partner individuals and 17 survey researchers/developers. The following lists the industries and surveys represented:

Industries Represented:

- Abarta Oil & Gas
- Belden & Blake Corp.
- Cabot Oil & Gas Corp.
- CEJA Corp.
- CGAS
- Compton Petroleum
- Energy Corp of America
- EOG Resources
- Equitable Productions
- Equitable Supply
- Great Lakes Energy Partners
- North Coast Energy
- Petro Evaluation Services.
- Pioneer Nat'l Resources
- Schlumberger
- Seneca Resources
- Talisman Energy
- Texas Keystone Inc
- Ultra Petroleum Corp.
- USGS
- Vintage Petroleum

Surveys Represented:

- Kentucky Geological Survey
- New York State Museum
- Ohio Division of Geological Survey
- Pennsylvania Geological Survey
- West Virginia Geological and Economic Survey
- The United States Geological Survey - for final assessment analysis

The Website

The website has two primary functions. It serves as a repository of miscellaneous Project reports, bibliography and ancillary data. It also serves as a conduit for the database system (e.g., MS Access) and the GIS-IMS application.

The Trenton website actually consists of two websites (as shown in Figure A-1). The first one serves as a gateway with standard non-secure (http) HTML. This one directs the user to the second and proper, main and secure website (https) utilizing Active Server Pages (ASP), JavaScript, SQL and HTML. Other calls or directives to the web server are involved but are not shown for security concerns.

Below in Figure A-1 of the Project Website, all pages involve various images, scripts and code-include files. The "Default Gate" controls who has access to the site. The "Welcome Page" is what can be considered the home page to most of the other pages, but for simplicity for the graphic, only links from the login "Default Gate" and "Logout Page" are shown.

Figure A-1. The Trenton-Black River Project Website

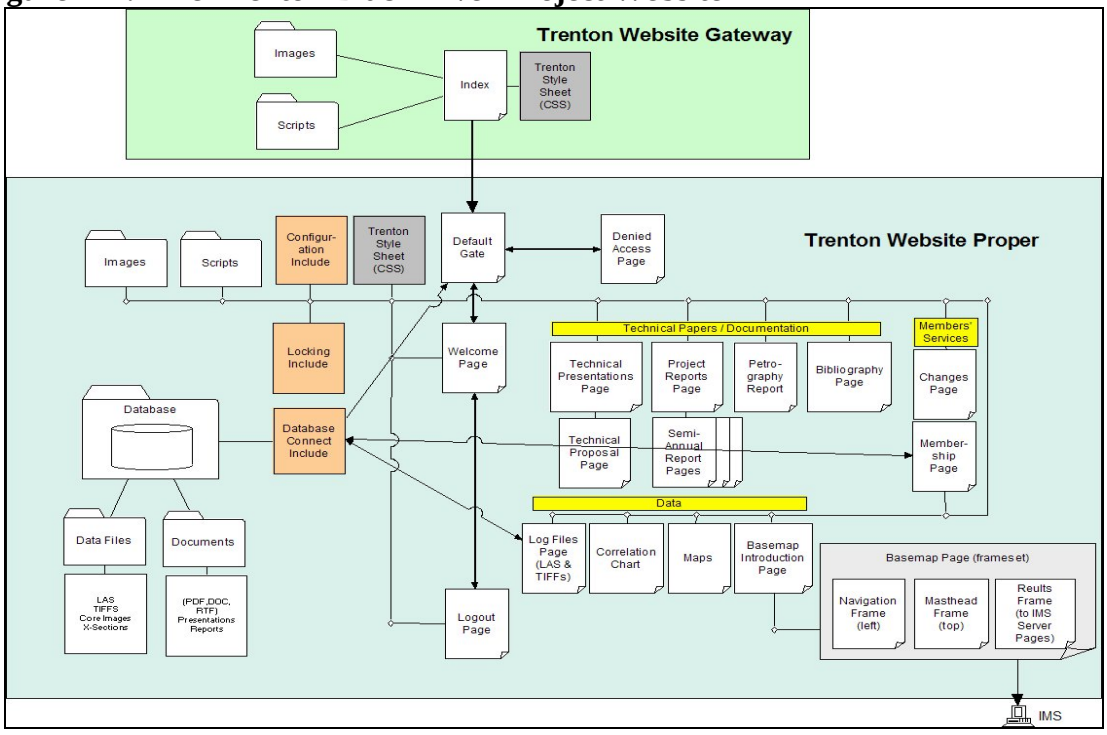

Website usage varied during the life of the project. Obviously, the opening pages such as *index.html*, *default.asp* and *welcome.asp* are the most viewed. Project reports and technical presentations were the most viewed of the substantial matter. Access to the IMS basemap application (via *basemap_intro.asp*, *basmap.asp*, *contents.asp* group) followed in rank. More specific statistics on visits, views, ranking can be found in the charts and graphs below for each year of the Project.

Visits and website usage are expected to increase substantially as the Project concludes, especially to the interactive basemap section.

Table A-1 TBR Website Visits for January to March, 2006

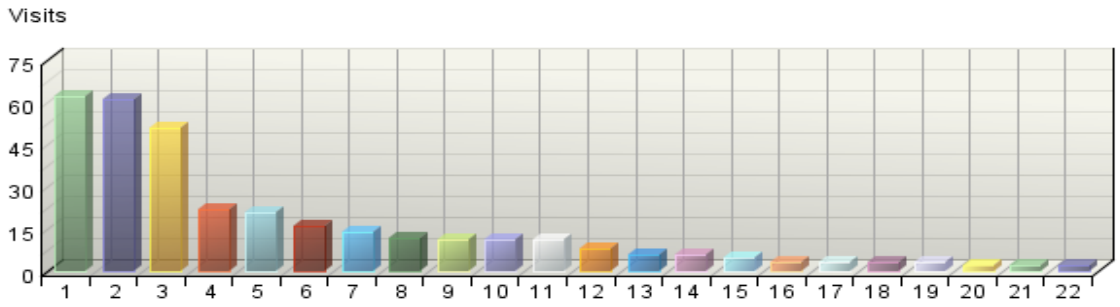

Pages: Query Results: TBR Website Visits for Jan-Mar, 2006				
	Pages	**Visits**	**Views**	**Average Time Viewed**
1.	**Welcome Page** (welcome.asp) Overall Rank: 560	62	160	00:00:27
2.	**Default Login Page** (default.asp) Overall Rank: 573	61	275	00:00:11
3.	**Trenton Gateway Page** (index.html) Overall Rank: 705	51	99	00:00:40
4.	**Default for Erroneous Login** (accessdenied.asp) Overall Rank: 813	22	28	00:00:24
5.	**Project Reports Page** (project_reports.asp) Overall Rank: 819	21	44	00:07:37
6.	**Technical Presentations Page** (technical_presentations.asp) Overall Rank: 846	16	56	00:06:18
7.	**Basemap Introduction Page** (basemapintro.asp) Overall Rank: 855	14	29	00:00:40
8.	**Logout Page** (logout.asp) Overall Rank: 868	12	13	00:00:26
9.	**Petrography Intro Page** (Petrography_Intro.asp) Overall Rank: 871	11	13	00:02:58
10.	**Basemap Page** (basemap.asp) Overall Rank: 874	11	16	00:00:00
11.	**Contents Frame for Basemap Page** (contents.asp) Overall Rank: 875	11	16	00:01:07
12.	**Correlation Chart Page** (Correlation_Chart.asp) Overall Rank: 904	8	9	00:00:07
13.	**Bibliography Page** (bibliography.asp) Overall Rank: 929	6	6	00:05:55
14.	**TBR Well Log Info Page** (TBR_well_logs.asp) Overall Rank: 931	6	59	00:00:52
15.	**Petrography Report** (as single page) (petrography.asp) Overall Rank: 940	5	7	00:04:07

Pages: Query Results: TBR Website Visits for Jan-Mar, 2006				
	Pages	**Visits**	**Views**	**Average Time Viewed**
16.	**Petrography Report–Methods Page** (Petrography_Meth.asp) Overall Rank: 977	3	4	00:00:16
17.	**Petrography Report–Figures Page** (Petrography_Figs.asp) Overall Rank: 978	3	5	00:07:19
18.	**Members' Page** (members.asp) Overall Rank: 987	3	5	00:00:39
19.	**Default Server Index Page** (index.html) Overall Rank: 990	3	3	00:00:23
20.	**Petrography Report–Diagenesis Page** (Petrography_Dia.asp) Overall Rank: 1017	2	2	00:04:11
21.	**Petrography Report–Dolomite Textures, Diagenesis, and Porosity Page** (Petrography_Dol.asp) Overall Rank: 1018	2	3	00:00:45
22.	**Petrography Report–Microfacies and Depositional Environments** (Petrography_Micro.asp) Overall Rank: 1019	2	2	00:00:11
	Subtotal for rows: 1 - 22	**-**	**854**	**-**
	Other	**-**	**17**	**-**
	Total	**-**	**871**	**-**
items 1-22 of 30 from total of 30				

Table A-2 TBR Website Visits for January to December, 2005

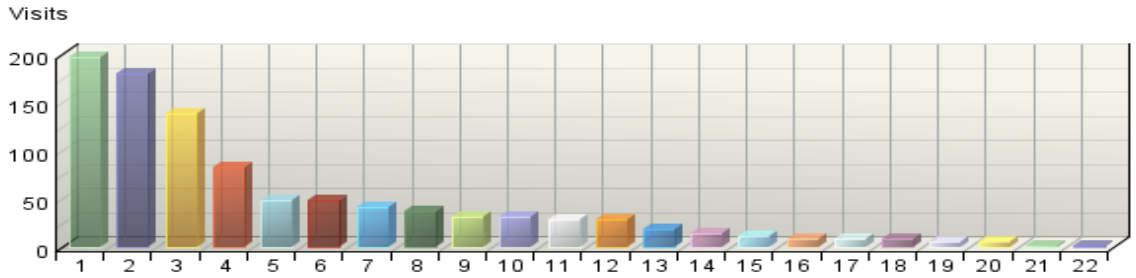

Pages: Query Results: TBR Website Visits for 2005				
	Pages	**Visits**	**Views**	**Average Time Viewed**
1.	**Default Login Page** (default.asp) Overall Rank: 474	197	904	00:00:25
2.	**Welcome Page** (welcome.asp) Overall Rank: 499	180	480	00:00:29
3.	**Trenton Gateway Page** (index.html) Overall Rank: 668	138	229	00:00:33
4.	**Technical Presentations Page** (technical_presentations.asp) Overall Rank: 792	83	195	00:03:59
5.	**Project Reports Page** (project_reports.asp) Overall Rank: 841	49	120	00:04:13
6.	**Logout Page** (logout.asp) Overall Rank: 842	48	53	00:01:23
7.	**Basemap Introduction Page** (basemapintro.asp) Overall Rank: 854	42	54	00:00:34
8.	**Default for Erroneous Login** (accessdenied.asp) Overall Rank: 862	37	40	00:00:51
9.	**TBR Well Log Info Page** (TBR_well_logs.asp) Overall Rank: 870	31	215	00:02:20
10.	**March 29th, 2005 Meeting Page** (050329meeting.asp) Overall Rank: 872	31	33	00:01:26
11.	**Contents Frame for Basemap Page** (contents.asp) Overall Rank: 875	28	38	00:02:32
12.	**Basemap Page** (basemap.asp) Overall Rank: 876	28	38	00:00:00
13.	**Members' Page** (members.asp) Overall Rank: 897	18	20	00:02:04
14.	**LAS Files Page** (las.asp) Overall Rank: 901	14	22	00:01:14
15.	**Semi-Annual Report, October 2004** (41856R02.asp) Overall Rank: 908	11	13	00:06:21
16.	**Bibliography Page** (bibliography.asp) Overall Rank: 915	9	10	00:01:58
17.	**Default Server Index Page** (index.html) Overall Rank: 918	9	10	00:00:13
18.	**Correlation Chart Page** (Correlation_Chart.asp) Overall Rank: 931	8	12	00:00:48
19.	**Semi-Annual Report, April 2004** (41856R01.asp) Overall Rank: 938	6	6	00:02:40
20.	**Trenton Technical Proposal** (technical_proposal.asp) Overall Rank: 942	6	7	00:00:28
21.	**Website Change Log Page** (changes.asp) Overall Rank: 1023	1	1	00:00:05
22.	**Trenton Gateway Section** (index.html) Overall Rank: 1035	1	2	00:00:21
	Total	-	**2,502**	-

Table A-3 TBR Website Visits for January to December, 2004

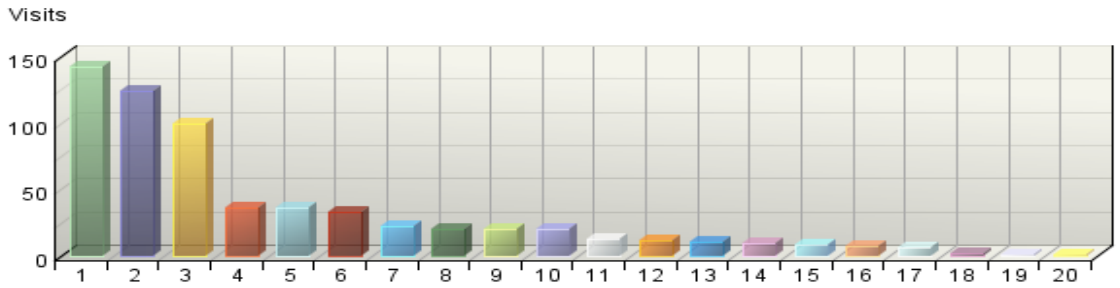

Pages: Query Results: TBR Website Visits for 2004				
	Pages	**Visits**	**Views**	**Average Time Viewed**
1.	**Trenton Gateway Page** (index.html) Overall Rank: 505	143	299	00:00:30
2.	**Default Login Page** (default.asp) Overall Rank: 575	124	715	00:00:23
3.	**Welcome Page** (welcome.asp) Overall Rank: 685	100	248	00:00:38
4.	**Logout Page** (logout.asp) Overall Rank: 800	36	39	00:04:25
5.	**Members' Page** (members.asp) Overall Rank: 801	36	39	00:03:26
6.	**Technical Presentations Page** (technical_presentations.asp) Overall Rank: 808	33	102	00:03:08
7.	**Basemap Introduction Page** (basemapintro.asp) Overall Rank: 831	23	30	00:00:36
8.	**LAS Files Page** (las.asp) Overall Rank: 843	20	26	00:01:03
9.	**Contents Frame for Basemap Page** (contents.asp) Overall Rank: 844	20	28	00:01:52
10.	**Basemap Page** (basemap.asp) Overall Rank: 845	20	29	00:00:00
11.	**Semi-Annual Report, October 2004** (41856R02.asp) Overall Rank: 868	13	16	00:11:11
12.	**Default for Erroneous Login** (accessdenied.asp) Overall Rank: 878	12	14	00:00:14
13.	**Semi-Annual Report, April 2004** (41856R01.asp) Overall Rank: 883	11	13	00:02:06
14.	**Sept. 9 2004 Meeting Page** (090904meeting.asp) Overall Rank: 888	10	10	00:02:43
15.	**Trenton Technical Proposal** (technical_proposal.asp) Overall Rank: 897	9	9	00:00:16
16.	**Bibliography Page** (bibliography.asp) Overall Rank: 904	7	7	00:01:23
17.	**Website Change Log Page** (changes.asp) Overall Rank: 910	6	6	00:00:56
18.	**Default Server Index Page** (index.html) Overall Rank: 1016	2	3	00:04:47
19.	**"Page 1" Test Page** (page1.asp) Overall Rank: 1068	1	1	00:01:18
20.	**Default Server Index Page (2nd)** (index.html) Overall Rank: 1073	1	1	00:00:06
	Total	-	**1,635**	-
items 1-20 of 20 from total of 20				

The Database

The Project database can also be divided into two facets: the various "data sets" that exist and the actual relational database management system (RDBMS). The data sets can consist of any of the miscellaneous spreadsheets, workbooks, text documents and image files as found on the Project's secure FTP site. Most of those items are working documents and files that are shared among the research team members. Most of that material, in turn, gets re-worked and then either is posted to the TBR website or transformed into shapefiles for use in the IMS application.

The RDBMS aspect did not come into fruition as expected. As data became available, more effort went into the development and population of the IMS application instead. In many regards, this change actually accommodates an optimal deployment of TBR information.

Geographic Information System – Internet Map Server/Service (GIS-IMS)

The geographical information system (GIS) and internet mapping service (IMS) provide the crux and most interactive feature of the Trenton-Black River Project. A user can view any number of geographical image layers and compare features.

These are the main layer groupings that are embodied via the ArcGIS™ shapefile structure:

- Well information
- Cross section information
- Structure fault information
- Structure contour information
- Oil and gas fields of in the Project
- Basemap information

The specifications below pertain to each specific shapefile as current at the time of this report production for Version 2 of the IMS application, March 17, 2006. Version 3 (and final version) will be slightly different from what is provided here (see "Notes About TBR IMS Map - Version 3" below Table A-4).

Notes:

- **Varchar(xxx)** denotes a string or text field. The number within the parentheses represents the number of characters in that particular text field.
- **Number(xxx)** denotes an integer field. The number within the parentheses represents the most number of digits for that particular field.
- **Number(xx,xxx)** denotes a float or decimal number. The number within the parenthesis represents the total number of digits for the field. That number after the comma is the decimal precision (e.g., "number(1,8)" would have possible values like 3.14159265 or 6.02214199).
- The bold word **(VISIBLE)** used after a layer name below denotes that particular layer is already turned on when a user first visits the TBR IMS map.

- Shapefile sets usually consist of files with the following suffixes:
  - **.dbf** – A dBASE(4) file which is much like a spreadsheet containing data.
  - **.shp** – The actual and main "shape file"; contains coordinates.
  - **.shx** – ArcView™ database index; links the .dbf and .shp files.
  - **.prj** – If a defined coordinate system is used, this file will be present.
  - **.sbn –** ArcView™ spatial index for read-write shapefiles.
  - **.xml** – An XML file containing metadata, if available.
- If provided via DVD, theses shapefiles can be loaded and viewed with ESRI's® free ArcReader™. (Look for files with the ".shp" ending).
- Shapefile sets used here have feature classes of:
  - **Points** – used for wells.
  - **Lines** – used for cross sections, contours, faults.
  - **Polygons** – used for fields, states, counties, and other "areas".
- **34** Shapefile sets are used in the TBR IMS Version 2 map.
- Unless otherwise noted, all shapefiles were created or reconfigured using ESRI® ArcGIS™ ArcMap™ 9.1 for the Trenton-Black River Project at the

  West Virginia Geological and Economic Survey
  1 Mont Chateau Road
  Morgantown, WV 26508-8079
  Phone: (304) 594-2331
  Website: http://www.wvgs.wvnet.edu
- Original TBR basemap concept and design (2004):

  ODNR-Ohio Division of Geological Survey
  2045 Morse Rd., Bldg. C-2
  Columbus, OH 43229-6693
  Phone: (614) 265-6573
  Website: http://www.ohiodnr.com/geosurvey

Table A-4 Shapefile Specifications

COORDINATE SYSTEM USED:

The TBR shapefiles with the "Albers" extension in the Layer Name use the following coordinate system and projections. The IMS map presented via the TBR website uses the Albers shapefile sets.

Projected Coordinate System: TBR_North_America_Albers_Equal_Area_Conic
Projection: Albers
False_Easting: 0.00000000
False_Northing: 0.00000000
Central_Meridian: -81.00000000
Standard_Parallel_1 : 38.50000000
Standard_Parallel_2 : 43.00000000
Latitude_Of_Origin : 40.75000000

Linear Unit: Meter
Geographic Coordinate System: GCS_North_American_1983
Datum: D_North_American_1983
Prime Meridian: 0
Angular Unit: Degree

WELL SHAPEFILES:

(1)
Layer Name: Historic Trenton Wells (PTTC)
Shapefile Set Name: ht_all_utm83_nov12_Albers; ht_all_utm83_nov12
Original Shapefile Set Name: ht_all_utm83_nov12
Shapefile Set Type: Point
Number of Records: 7,592
Shapefile Provided By: Appalachian Region PTTC
Purpose: Old Trenton wells for reference only
Fields/Attributes:

Attribute Name	Full Name/Description	Type
STATE	2 Character abbrev	varchar(254)
COUNTY	County Name	varchar(254)
CNTY_NO	3 Digit County API Number	number(254)
PERMIT_NO	Well Permit Number	number(254)
COMPANY	Company	varchar(254)
FARM_WELL_	Farm Well Name	varchar(254)
TARGET_FOR	Target Formation	varchar(254)
TARGET_DEP	Target Depth	number(14,5)
TOTAL_DEPT	Total Depth	number(14,5)
RESULTS	Results (e.g., dry, gas, shows)	varchar(254)
COMMENTS	Comments	varchar(254)
LAT	Latitude, Decimal Degrees	number(14,5)
LONG	Longitude, Decimal Degrees	number(14,5)
UTM_E	UTM Easting	number(14,5)
UTM_N	UTM Northing	number(14,5)
COUNTY_PER	County Permit (not used)	number(50)
COMP_DATE	Completion Date (mm/dd/yyyy)	number(12)

(2)
Layer Name: TBR Wells with Shows (PA, WV)
Shapefile Set Name: TBR_Shows_Albers; TBR_Shows
Original Shapefile Set Name: TBR_Shows
Shapefile Set Type: Point
Number of Records: 135
Shapefile Provided By: West Virginia Geological and Economic Survey
Purpose: Wells that show promise for production of oil or gas.
Fields/Attributes:

Attribute Name	Full Name/Description	Type
API_NO	API Number	number(12)
COUNTY	County Name	varchar(19)
TAX_DIST	Tax District (WV only)	varchar(19)
FARM_NAME	Farm Name	varchar(39)
FARM_WELL_	Farm Well Number	number(17)
UTME	UTM Easting	number(14,1)
UTMN	UTM Northing	number(14,1)
LATDD_83	Latitude, Decimal Degrees, NAD 1983	number(13,6)
LONDD_83	Longitude, Decimal Degrees, NAD 1983	number(13,6)
LATDD_27	Latitude, Decimal Degrees, NAD 1927	number(13,6)
LONDD_27	Longitude, Decimal Degrees, NAD 1927	number(13,6)
TBR_STATUS	Status within Trenton or Black River	varchar(19)
ACTIVITY	Activity (e.g., show, pay, dry, water)	varchar(10)
PRODUCT	Product (e.g., gas, oil, water)	varchar(10)
PAY_TOP_DE	Pays, Top Depth	number(16)
PAY_TOP_FM	Pays, Top Formation	varchar(16)
PAY_BTM_DE	Pays, Bottom Depth	number(18)
PAY_BTM_FM	Pays, Bottom Formation	varchar(15)
GAS_BEFORE	Gas Before	number(14)
GAS_AFTER	Gas After	number(12)
OIL_BEFORE	Oil Before	number(13)
OIL_AFTER	Oil After	number(13)
WATER_QTY	Water Quantity	number(13)
COMMENTS	Comments	varchar(108)
SOURCE	Source: Person, Survey, File	varchar(65)

(3)
Layer Name: OH_Straight_hole_well (Dol)
Shapefile Set Name: OH_Straight_hole_well_Albers; OH_Straight_hole_well
Original Shapefile Set Name: Straight_hole_well_GCS83
Shapefile Set Type: Point
Number of Records: 43
Shapefile Provided By: Ohio Division of Geological Survey
Purpose:
Fields/Attributes:

Attribute Name	Full Name/Description	Type
UniqueId	Unique ID	number(8)
Override	Override	number(12)
TypeId	Type ID	number(12)
CustomClr	Custom Clr	number(12)
WellID	Well ID (API Number)	number(31)
WellStatus	Well Status	varchar(31)
DatumEleva	Datum Elevation	number(15,4)
TotalDepth	Total Depth	number(15,4)

(4)
Layer Name: map_well_pts_Albers
Shapefile Set Name: map_well_pts_Albers; map_well_pts
Original Shapefile Set Name: map_well_pts
Shapefile Set Type: Point
Number of Records: 2,048
Shapefile Provided By: Kentucky Geological Survey
Purpose: Wells used by Project to help define map.
Fields/Attributes:

Attribute Name	Full Name/Description	Type
UWI	Universal Well Identifier (eg. API No)	number(14)
WELLNAME	Well Name	varchar(48)
LAT	Latitude, Decimal Degrees	number(13,6)
LON	Longitude, Decimal Degrees	number(13,6)
SYM	Sym	varchar(8)
ELEV_KB	Elevation KB	number(8)
B_DEVSH	Base Devonian Shale	number(10)
ODVCU	Ordovician	number(10)
TRNT_LXTN	Trenton-Lexington	number(10)
BKRV	Black River	number(10)
KNOXB_KNOX	Knox to Base of Knox	number(10)
PCMB	Precambrian	number(10)

(5)
Layer Name: TBR Wells with Cores
Shapefile Set Name: TBR_Wells_Cored_Albers; TBR_Wells_Cored
Original Shapefile Set Name: TBR_Wells_Cored
Shapefile Set Type: Point
Number of Records: 20
Shapefile Provided By: West Virginia Geological and Economic Survey
Purpose: Provide locations and ancillary data of TBR wells with cores.
Fields/Attributes:

Attribute Name	Full Name/Description	Type
API	API number of well	number(16)
STATE	2 Character abbrev. of state	varchar(7)
COUNTY	County name of well location	varchar(14)
LEASE	Lease	varchar(24)
LAT	Latitude, Decimal Degrees	number(13,6)
LON	Longitude, Decimal Degrees	number(13,6)
UTME83	UTM Easting, NAD 1983	number(12,1)
UTMN83	UTM Northing, NAD 1983	number(14,1)
CORETOP	Core top measurement	number(14)
COREBOTTOM	Core bottom measurement	number(16)
THINSECTIO	number of thin sections taken	number(12)
EXHIBIT1_D	Exhibit 1 – core descriptions (PDF if avail.)	varchar(58)
EXHIBIT2_P	Exhibit 2 – core photos (PDF if avail.)	varchar(41)

EXHIBIT3_T	Exhibit 3 – thin section (PDF if avail.)	varchar(42)
EXHIBIT4_S	Exhibit 4 – SEM data (PDF if avail.)	varchar(35)
HTML	Hyperlink to HTML page w/ links to above exhibits	varchar(30)

(6)
Layer Name: TBR OIL Producing Wells
Shapefile Set Name: TBR_Prod_Oil_060307_Albers; TBR_Prod_Oil_060307
Original Shapefile Set Name: TBR_Prod_Oil
Shapefile Set Type: Point
Number of Records: 424
Shapefile Provided By: West Virginia Geological and Economic Survey
Purpose: Shows locations and production values for TBR Oil producing wells.
Fields/Attributes:

Attribute Name	**Full Name/Description**	**Type**
API	API Number	number(19)
ALT_UWI_1	1st Alternative Universal Well Identifier	number(19)
ALT_UWI_2	2nd Alternative Universal Well Identifier	number(19)
FIELD	Oil Field Name	varchar(25)
PLAY_TYPE	Play Type (e.g., FLS, BLS)	varchar(25)
UTME83	UTM Easting, NAD 1983	number(16,3)
UTMN83	UTM Northing, NAD 1983	number(16,3)
LAT_DD_27	Latitude, Decimal Degrees, NAD 1927	number(10,6)
LON_DD_27	Longitude, Decimal Degrees, NAD 1927	number(10,6)
LAT_DD_83	Latitude, Decimal Degrees, NAD 1983	number(13,6)
LON_DD_83	Longitude, Decimal Degrees, NAD 1983	number(13,6)
XSPS83	X Value, State Plane Coord., South, NAD 1983	number(10,5)
YSPS83	Y Value, State Plane Coord., South, NAD 1983	number(10,5)
FIRSTYR	First year of production (yyyy)	number(15)
YR1947	Production for year of 1947	number(9)
YR1970	Production for year of 1970	number(9)
YR1971	Production for year of 1971	number(9)
…to…		
YR2004	Production for year of 2004	number(9)
CUMMULATIV	Cumulative production for producing life of well	number(13)
ENTERED	Initials and date (yyyy/mm/dd) info entered	varchar(15)
SOURCE	Survey, name, date (yyyy/mm/dd), orig. source	varchar(46)

(7)
Layer Name: TBR GAS Producing Wells
Shapefile Set Name: TBR_Prod_Gas_060307_Albers; TBR_Prod_Gas_060307
Original Shapefile Set Name: TBR_Prod_Gas
Shapefile Set Type: Point
Number of Records: 379
Shapefile Provided By: West Virginia Geological and Economic Survey
Purpose: Shows locations and production values for TBR Gas producing wells.
Fields/Attributes:

Attribute Name	Full Name/Description	Type
UWI	Universal Well Identifier (eg., API No.)	number(17)
ALTUWI1	1st Alternative Universal Well Identifier	number(12)
ALTUWI2	2nd Alternative Universal Well Identifier	number(19)
STATE	2 Character State Abbrev.	varchar(9)
FIELD	Oil or Gas Field Name	varchar(30)
FLDDISCYR	Field Discovery Year (yyyy)	number(18)
PLAYTYPE	Play Type (e.g., FLS, BLS)	varchar(12)
UTME83	UTM Easting, NAD 1983	number(16,3)
UTMN83	UTM Northing, NAD 1983	number(16,3)
LATDD27	Latitude, Decimal Degrees, NAD 1927	number(5,6)
LONDD27	Longitude, Decimal Degrees, NAD 1927	number(5,6)
LATDD83	Latitude, Decimal Degrees, NAD 1983	number(13,6)
LONDD83	Longitude, Decimal Degrees, NAD 1983	number(13,6)
XSPS83	X Value, State Plane Coord., South, NAD 1983	number(8,1)
YSPS83	Y Value, State Plane Coord., South, NAD 1983	number(8,1)
FIRSTYR	First year of production (yyyy)	number(9)
YR1947	Production for year of 1947	number(9)
YR1970	Production for year of 1970	number(9)
YR1971	Production for year of 1971	number(9)
…to…		
YR2004	Production for year of 2004	number(9)
CUMTV	Cumulative production for producing life of well	number(13)
ENTERED	Initials and date (yyyy/mm/dd) info entered	varchar(15)
SOURCE	Survey, name, date (yyyy/mm/dd), orig. source	varchar(46)
COMMENTS	Comments (not used)	varchar(10)

CROSS SECTION SHAPEFILES:

(8)
Layer Name: TBR Wells in Cross Sections
Shapefile Set Name: XSecPoints_Albers; XSecPoints
Original Shapefile Set Name: XSecPoints
Shapefile Set Type: Point
Number of Records: 224
Shapefile Provided By: Ohio Division of Geological Survey
Purpose: Wells used in cross section analysis.
Fields/Attributes:

Attribute Name	Full Name/Description	Type
WELL_ID	Universal Well ID (e.g., API No.)	number(254)
LONG	Longitude, Decimal Degrees	number(14,5)
LAT	Latitude, Decimal Degrees	number(14,5)
DIP	Name of Dip Line (if involved)	varchar(254)

STRIKE	Name of Stike Line (if involved)	varchar(254)

(9)
Layer Name: TBR Cross Section Lines
Shapefile Set Name: XSecLines_Albers; XSecLines
Original Shapefile Set Name: XSecLines_Albers
Shapefile Set Type: Line
Number of Records: 18
Shapefile Provided By: Ohio Division of Geological Survey
Purpose: lines to show cross section analysis
Fields/Attributes:

Attribute Name	Full Name/Description	Type
ID	ID (not used)	number(6)
DIP	Dip Line ID	varchar(4)
STRIKE	Strike Line ID	varchar(7)
XSEC_FILE	Cross Section File (PDF)	varchar(50) HYPERLINK
LINE_NAME	Name of Line	varchar(16)

FAULT SHAPEFILES: (DRAFT)

(10)
Layer Name: All Faults and Lineaments **(VISIBLE)**
Shapefile Set Name: all_flts_and_linmnts_Albers; all_flts_and_linmnts
Original Shapefile Set Name: all_flts_and_linmnts
Shapefile Set Type: Line
Number of Records: 234
Shapefile Provided By: Kentucky Geological Survey
Purpose: Combined layer showing all faults
Fields/Attributes:

Attribute Name	Full Name/Description	Type
ID	ID (not used)	number(8)
FLT_SYSTEM	Fault System	varchar(40)
DOWNTO		varchar(6)
PCOFFSET		varchar(6)
YOUNGEST_O		varchar(40)
CONFIDENCE	Confidence	number(3)
COMMENTS	Comments	varchar(40)

---

(11)
Layer Name: B Devonian Shale Faults (344)
Shapefile Set Name: 344b_devsh_flts_Albers; 344b_devsh_flts
Original Shapefile Set Name: 344b_devsh_flts

Shapefile Set Type: line
Number of Records: 52
Shapefile Provided By: Kentucky Geological Survey
Purpose: Layer for base of Devonian Shale faults.
Fields/Attributes:

Attribute Name	Full Name/Description	Type
ID	ID (not used)	number(8)
FLT_SYSTEM	Fault System	varchar(40)
DOWNTO		varchar(6)
PCOFFSET		varchar(6)
YOUNGEST_O		varchar(40)
CONFIDENCE	Confidence	number(3)
COMMENTS	Comments	varchar(40)

---

(12)
Layer Name: Ordovician Faults (361)
Shapefile Set Name: 361odvcu_flts_Albers; 361odvcu_flts
Original Shapefile Set Name: 361odvcu_flts
Shapefile Set Type: Line
Number of Records: 57
Shapefile Provided By: Kentucky Geological Survey
Purpose: Layer for base of Ordovician faults.
Fields/Attributes:

Attribute Name	Full Name/Description	Type
ID		number(8)
FLT_SYSTEM	Fault System	varchar(6)
DOWNTO		varchar(6)
PCOFFSET		varchar(6)
YOUNGEST_O		varchar(40)
CONFIDENCE	Confidence	number(3)
COMMENTS	Comments	varchar(40)

---

(13)
Layer Name: Trenton Faults (365)
Shapefile Set Name: 365trnt_flts_Albers; 365trnt_flts
Original Shapefile Set Name: 365trnt_flts
Shapefile Set Type: Line
Number of Records: 79
Shapefile Provided By: Kentucky Geological Survey
Purpose: Layer for Trenton faults.
Fields/Attributes:

Attribute Name	Full Name/Description	Type
ID	ID (not used)	number(8)
FLT_SYSTEM	Fault System	varchar(40)
DOWNTO		varchar(6)

PCOFFSET		varchar(6)
YOUNGEST_O		varchar(40)
CONFIDENCE	Confidence	number(3)
COMMENTS	Comments	varchar(40)

---

(14)
Layer Name: Black River Faults (365)
Shapefile Set Name: 365bkrv_flts_Albers; 365bkrv_flts;
Original Shapefile Set Name: 365bkrv_flts
Shapefile Set Type: Line
Number of Records: 81
Shapefile Provided By: Kentucky Geological Survey
Purpose: Layer for Black River faults.
Fields/Attributes:

Attribute Name	**Full Name/Description**	**Type**
ID	ID (not used)	number(8)
FLT_SYSTEM	Fault System	varchar(40)
DOWNTO		varchar(6)
PCOFFSET		varchar(6)
YOUNGEST_O		varchar(40)
CONFIDENCE	Confidence	number(3)
COMMENTS	Comments	varchar(40)

---

(15)
Layer Name: Knox Faults (368)
Shapefile Set Name: 375b_knox_flts_Albers; 375b_knox_flts
Original Shapefile Set Name: 375b_knox_flts
Shapefile Set Type: Line
Number of Records: 99
Shapefile Provided By: Kentucky Geological Survey
Purpose: Layer for Knox faults.
Fields/Attributes:

Attribute Name	**Full Name/Description**	**Type**
ID	ID (not used)	number(8)
FLT_SYSTEM	Fault System	varchar(40)
DOWNTO		varchar(6)
PCOFFSET		varchar(6)
YOUNGEST_O		varchar(40)
CONFIDENCE	Confidence	number(3)
COMMENTS	Comments	varchar(40)

---

(16)
Layer Name: B Knox Faults (375)

Shapefile Set Name: 375b_knox_flts_Albers; 375b_knox_flts
Original Shapefile Set Name: 375b_knox_flts
Shapefile Set Type: Line
Number of Records: 155
Shapefile Provided By: Kentucky Geological Survey
Purpose: Layer for Base of Knox faults.
Fields/Attributes:

Attribute Name	Full Name/Description	Type
ID	ID (not used)	number(8)
FLT_SYSTEM	Fault System	varchar(40)
DOWNTO		varchar(6)
PCOFFSET		varchar(6)
YOUNGEST_O		varchar(40)
CONFIDENCE	Confidence	number(3)
COMMENTS	Comments	varchar(40)

---

(17)
Layer Name: Precambrian Faults (400)
Shapefile Set Name: 400pcmb_flts_Albers; 400pcmb_flts
Original Shapefile Set Name: 400pcmb_flts
Shapefile Set Type: Line
Number of Records: 225
Shapefile Provided By: Kentucky Geological Survey
Purpose: Layer for Precambrian faults.
Fields/Attributes:

Attribute Name	Full Name/Description	Type
ID	ID (not used)	number(8)
FLT_SYSTEM	Fault System	varchar(40)
DOWNTO		varchar(6)
PCOFFSET		varchar(6)
YOUNGEST_O		varchar(40)
CONFIDENCE	Confidence	number(3)
COMMENTS	Comments	varchar(40)

STRUCTURE CONTOUR SHAPEFILES: (DRAFT)

(18)
Layer Name: B Devonian Shale Contours
Shapefile Set Name: B_DevSh_Contours_Albers; B_DevSh_Contours
Original Shapefile Set Name: B_DevSh_Contours
Shapefile Set Type: Line
Number of Records: 711

Shapefile Provided By: Kentucky Geological Survey
Purpose: Structure contours of the base of Devonian Shale.
Fields/Attributes:

Attribute Name	Full Name/Description	Type
NAME	Name (not used)	varchar(20)
AREA	Area (not used)	number(20)
VALUE	Value of line	number(20)

---

(19)
Layer Name: Ordovician Contours
Shapefile Set Name: ODVC_Contours_Albers; ODVC_Contours
Original Shapefile Set Name: ODVC_Contours
Shapefile Set Type: Line
Number of Records: 598
Shapefile Provided By: Kentucky Geological Survey
Purpose: Structure contours of the Ordovician.
Fields/Attributes:

Attribute Name	Full Name/Description	Type
NAME	Name (not used)	varchar(20)
AREA	Area (not used)	number(20)
VALUE	Value of line	number(20)

---

(20)
Layer Name: Trenton Contours
Shapefile Set Name: TRNT_Contours_Albers; TRNT_Contours
Original Shapefile Set Name: TRNT_Contours
Shapefile Set Type: Line
Number of Records: 956
Shapefile Provided By: Kentucky Geological Survey
Purpose: Structure contour lines of the Trenton.
Fields/Attributes:

Attribute Name	Full Name/Description	Type
NAME	Name (not used)	varchar(20)
AREA	Area (not used)	number(20)
VALUE	Value of line	number(20)

---

(21)
Layer Name: Black River Contours
Shapefile Set Name: BKRV_Contours_Albers; BKRV_Contours
Original Shapefile Set Name: BKRV_Contours
Shapefile Set Type: Line
Number of Records: 818
Shapefile Provided By: Kentucky Geological Survey
Purpose: Structure contour lines of the Black River.

Fields/Attributes:

Attribute Name	Full Name/Description	Type
NAME	Name (not used)	varchar(20)
AREA	Area (not used)	number(20)
VALUE	Value of line	number(20)

---

(22)
Layer Name: Knox Contours
Shapefile Set Name: KNOX_Contours_Albers; KNOX_Contours
Original Shapefile Set Name: KNOX_Contours
Shapefile Set Type: Line
Number of Records: 785
Shapefile Provided By: Kentucky Geological Survey
Purpose: Structure contour lines of the Knox
Fields/Attributes:

Attribute Name	Full Name/Description	Type
NAME	Name (not used)	varchar(20)
AREA	Area (not used)	number(20)
VALUE	Value of line	number(20)

---

(23)
Layer Name: B Knox Contours
Shapefile Set Name: B_KNOX_Contours_Albers; B_KNOX_Contours
Original Shapefile Set Name: B_KNOX_Contours
Shapefile Set Type: Line
Shapefile Provided By: Kentucky Geological Survey
Number of Records: 1,672
Purpose: Structure contour lines of the Base of Knox.
Fields/Attributes:

Attribute Name	Full Name/Description	Type
NAME	Name (not used)	varchar(20)
AREA	Area (not used)	number(20)
VALUE	Value of line	number(20)

---

(24)
Layer Name: Precambrian Contours
Shapefile Set Name: PCMB_Contours_Albers; PCMB_Contours
Original Shapefile Set Name: PCMB_Contours
Shapefile Set Type: Line
Number of Records: 2,303
Shapefile Provided By: Kentucky Geological Survey
Purpose: Structure contour lines of the Precambrian.
Fields/Attributes:

Attribute Name	Full Name/Description	Type
NAME	Name (not used)	varchar(20)
AREA	Area (not used)	number(20)
VALUE	Value of line	number(20)

OUTCROP SHAPEFILES:

(25)
Layer Name: Ordovician Outcrop (Unit 51)
Shapefile Set Name: unit51_Albers; unit51
Original Shapefile Set Name: unit51
Shapefile Set Type: Polygon
Number of Records: 66
Shapefile Provided By: Ohio Division of Geological Survey (orig., via Ontario Geological Survey)
Purpose: Location of particular outcrop.
Fields/Attributes:

Attribute Name	Full Name/Description	Type
AREA	Area of outcrop location	number(8,11)
PERIMETER	Perimeter of outcrop location	number(8,11)
BEDROCK_ID		number(10)
UNIT_NUMBE	Unit Number	number(12)
GENERALIZE		varchar(200)

(26)
Layer Name: Ordovician Outcrop
Shapefile Set Name: O_Albers; O
Original Shapefile Set Name: O
Shapefile Set Type: Polygon
Number of Records: 45
Shapefile Provided By: Ohio Division of Geological Survey (orig., via USGS King Bedrock Map)
Purpose: Location of particular outcrop.
Fields/Attributes:

Attribute Name	Full Name/Description	Type
AREA	Area	number(8.11)
PERIMETER	Perimeter	number(8,11)
KBGECOV_		number(9)
KBGECOV_ID		number(9)
ORDER_		number(3)

S1		number(1)
UNIT	(e.g., O)	varchar(5)
S2		number(1)
ROCKDESC	Rock Description (e.g., Ordovician)	varchar(50)
METAMOR		varchar(8)
ROCK	Rock (e.g., 126 O Ordovician)	varchar(60)

---

(27)
Layer Name: Ordovician Outcrop (Mohawk 02)
Shapefile Set Name: Mohawk02_Albers; Mohawk02
Original Shapefile Set Name: Mohawk02
Shapefile Set Type: Polygon
Number of Records: 85
Shapefile Provided By: Ohio Division of Geological Survey (orig., via USGS King Bedrock Map)
Purpose: Location of particular outcrop.
Fields/Attributes:

Attribute Name	**Full Name/Description**	**Type**
AREA	Area	number(8.11)
PERIMETER	Perimeter	number(8,11)
KBGECOV_		number(9)
KBGECOV_ID		number(9)
ORDER_		number(3)
S1		number(1)
UNIT	(e.g., O)	varchar(5)
S2		number(1)
ROCKDESC	Rock Description (e.g., M. Ordovician)	varchar(50)
METAMOR		varchar(8)
ROCK	Rock (e.g., 125 O2 M. Ordovician)	varchar(60)

OIL AND GAS FIELD SHAPFILES:

(28)
Layer Name: TBR Oil and Gas Fields
Shapefile Set Name: TR_merge_OilGas_allstat_Albers, TR_merge_OilGas_allstat
Original Shapefile Set Name: TR_merge_OilGas_allstat
Shapefile Set Type: polygon
Number of Records: 338
Shapefile Provided By:
Purpose: Shows oil and gas fields in the TBR study area
Fields/Attributes:

Attribute Name	**Full Name/Description**	**Type**
PROD_TYPE	Production Type (e.g., OIL or GAS)	varchar(20)

BASEMAP SHAPEFILES:

(29)
Layer Name: TBR Project Constraints **(VISIBLE)**
Shapefile Set Name: constraints_linears_Albers; constraints_linears
Original Shapefile Set Name: constraints_linears
Shapefile Set Type: Line
Number of Records: 2
Shapefile Provided By:
Purpose: Constraint lines to delineate TBR study area
Fields/Attributes:

Attribute Name	Full Name/Description	Type
Id	ID (not used)	number(6)
Name	Name of constraint line	varchar(50)

---

(30)
Layer Name: constraints_polygons_Albers (PROPOSED) **(VISIBLE)**
Shapefile Set Name: constraints_polygons_Albers; constraints_polygons
Original Shapefile Set Name: constraints_polygons
Shapefile Set Type: Polygon
Number of Records: 8
Shapefile Provided By:
Purpose: Basins, troughs, mountains for reference to help define study area. (Pocono Scarp, Allegheny Front, Reading Prong, Blue Ridge Mtns., Adirondack Mtns., Canadian Shield Margin, Triassic Basin(s), Rome Trough)
Fields/Attributes:

Attribute Name	Full Name/Description	Type
Id	ID (not used)	number(6)
Name	Name of basin, trough or mountain range	varchar()

---

(31)
Layer Name: TBR Main Study Area
Shapefile Set Name: Map_extents_GCS83_Albers; Map_extents_GCS83
Original Shapefile Set Name: Map_extents_GCS83
Shapefile Set Type: Polygon
Number of Records: 1
Shapefile Provided By:
Purpose: Shows study area within constraints
Fields/Attributes:

Attribute Name	Full Name/Description	Type
CUSTOMCLR	(not used here)	number(11)
GRIDINSIDE		number(11)
GRIDOUTSID	(not used here)	number(11)
ISPARTIAL	(not used here)	number(11)
OVERRIDE	(not used here)	number(11)
TYPEID	Type ID (1310834)	

UNIQUEID		
USEDATAIN2	(not used here)	number(11)
USEDATAINS	(not used here)	number(11)
USEDATAOUT	(not used here)	number(11)

---

(32)
Layer Name: Lakes **(VISIBLE)**
Shapefile Set Name: TBR_lakes_Albers; TBR_lakes
Original Shapefile Set Name: TBR_lakes
Shapefile Set Type: Polygon
Number of Records: 1,102
Shapefile Provided By: Ohio Division of Geological Survey
Purpose: Provides lake info; for display purposes only.
Fields/Attributes:

Attribute Name	**Full Name**	**Type**
FEATURE	Feature (lake or stream)	varchar(25)
NAME	Full name of feature	varchar(45)
STATE	State(s) in which feature is found	varchar(20)

---

(33)
Layer Name: Counties **(VISIBLE)**
Shapefile Set Name: countiesTBR_TNVA_Albers; countiesTBR_TNVA
Original Shapefile Set Name: countiesTBR_TNVA
Shapefile Set Type: Polygon
Number of Records: 865
Shapefile Provided By: Ohio Division of Geological Survey
Purpose: Provides counties base for all states that have well information.
Fields/Attributes:

Attribute Name	**Full Name/Description**	**Type**
COUNTY	County Name	varchar(30)
ST	State Abbreviation	varchar(2)

---

(34)
Layer Name: States and Province **(VISIBLE)**
Shapefile Set Name: statesTBR_TNVA_Albers; statesTBR_TNVA
Original Shapefile Set Name: statesTBR_TNVA
Shapefile Set Type: Polygon
Number of Records: 8
Shapefile Provided By: Ohio Division of Geological Survey
Purpose: Provides states base involved in the project:
KY, NY, OH, PA, WV
and for those contiguous states and province for the basemap:
MI, ON, TN, VA

Fields/Attributes:

Attribute Name	Full Name/Description	Type
ST	Two letter state abbreviation	varchar(7)
CNT_ST	Number of Counties in a State	number(9)
ST_NAME	State Name	varchar(25)

Notes About TBR IMS Map - Version 3 (due by March 30, 2006)

This version will be the Final Version for the Trenton Black River Project. It will have the following revisions and updates:

1. Revised faults and contours shapefiles.
2. New earthquake layer.
3. Updated Oil and Gas Fields shapefile.
4. Addition of the Lexington outcrop.
5. Additional material (referenced PDFs) for the Well Cores layer.
6. Improved maneuverability with combined layer/legend with expandable folders.
7. "Fine tuning".

The Final Product – Post Project

The website and IMS application are expected to exist, remain active and become fully public-accessible after the Project life. No further material will be added to the website or IMS after March 30, 2006. Current thought may place these applications under the Appalachian Region-PTTC in the future; however, this idea is not yet conclusive, but highly probable.

If time permits (as of this writing), DVDs may be created which have the aforementioned shapefiles and most of the materials found on the TBR website. These in turn will be distributed to Project researchers and industrial partners.

APPENDIX B

DETAILS AND RESULTS OF THE BENTONITE CORRELATION STUDY FOR THE TRENTON-BLACK RIVER CONSORTIUM AND THE NEW YORK STATE MUSEUM

By Adam Carey (Syracuse University)
February 2006

The correlation of suspect Millbrig and Deicke samples is achieved by the extraction and microprobe analysis of apatite phenocrysts. Included with this report is a spreadsheet to assist in the understanding of which samples were provided, and the stratigraphic details of those samples.

The microprobe analysis of the apatite phenocrysts involved a two-tiered approach. Specifically, this involved a 10 nano amp (nA) analysis and a 60 nA analysis on 3 positions of each phenocryst. Because elements such as Mg, Mn, Fe, and Sr occur as minor and trace elements in apatite a 60nA analysis is necessary to induce detectable counts. Longer count times for minor and trace elements were necessary. The elements Ca, P, F, and Cl require a 10 nA beam current to induce appropriate counts. For each analysis point a specific count time was used depending on the expected concentration of a particular element. The count times (on peak and on background) were as follows:

2 seconds: Ca
10 seconds: Cl
12 seconds: P, F, Si
40 seconds: Mg, Mn, Fe, Sr

Each phenocryst was probed in 3 spots to resolve heterogeneities in the phenocrysts. The data generated from the 3 spots were then averaged, to give a phenocryst average.

The work of Emerson et al., 2004 demonstrated that Mg and Mn are excellent discriminating elements for which to assign a chemical finger print to a bentonite sample. While my data show discrimination of samples based on elements other than Mg and Mn (e.g. Cl, Fe), Mg and Mn are the best discriminators for my data set as well.

The attached spreadsheet demonstrates which sample (core or outcrop) has been positively identified as either the Deicke or Millbrig.

Note that in some cases a sample provided did not always yield apatite phenocrysts. Those samples are given an “NA” label.

The confirmed Millbrig samples include the 3256 and 2626 Millbrig core samples, as well as the Hagan (VA) and Shakertown (KY) Millbrig outcrop samples.

The confirmed Deicke samples include the Hagan, and Union Furnace (PA) outcrop Deicke samples, as well as the 2626 core and CA-35 core Deicke samples. The 3409 Millbrig suspect is clearly Deicke, despite its initial label as a Millbrig prospect. The plotted phenocryst averages for the 3409 Millbrig suspect form a tight cluster of points with the other Deicke samples.

The 3409 core Deicke suspect is more difficult to distinguish than all other samples. Some data points of the 3409 Deicke suspect do plot with the other Deicke points; however there are 4-5 phenocryst data points that plot far outside of the well defined Deicke cluster. For this reason the 3409 Deicke prospect will retain the label of indistinguishable. Strontium isotope data from apatite phenocrysts is forthcoming from the mass spectrometer at Syracuse University. In the future these data will be presented as part of my thesis. Samson et al., 1995 demonstrated the usefulness of Sr isotopes measured on a mass spectrometer to distinguish bentonites. The issue of the indistinguishable 3409 Deicke suspect must be resolvable based on Sr isotopes.

One sample from the entire suite demonstrates a resemblance to the Dickeyville and Elkport bentonites presented by Emerson et al., 2004. That sample is named the Dolly Ridge Deicke suspect. The Mn and Mg data clearly show that the Dolly Ridge Deicke prospect is neither Deicke nor Millbrig. The sample is best associated with Dickeyville or Elkport, though the data are not conclusive.

The full suite of data and charts from all samples will be published in my thesis.

Please see the attached sheet below, from Greg Schumacher (Ohio Division of Natural Resources).

APPENDIX C

SAMPLES OF SUPPOSED DEICKE AND MILLBRIG K-BENTONITES
Collected by: Dr. Stig Bergström and Gregory Schumacher

Date: April 11 & 12, 2005. (Each sample fills 1 gallon Ziploc bag)

Shakertown, Kentucky: Millbrig thickness ~70 cm

1. Millbrig- 0-5 cm above bed base
2. Millbrig- 0-10 cm above base
3. Millbrig- 0-10 cm above base

Shakertown, Kentucky- Outcrop on U.S. 68, 1.6 km southwest of intersection with Ky. State Route 33 at entrance to Shakertown as discussed in Kolata et al. (1996, p. 27 and 71), GSA Special Paper 313. Harrodsburg 7 ½ minute Quadrangle, Tyrone Limestone

Hagan, Virginia: Deicke thickness 92 cm, Millbrig thickness 130 cm (Check Haynes)

1. Deicke- 0-10 cm above bed base
2. Deicke- (2 samples) 5-10 cm above base
3. Middle Millbrig- 40-50 cm below top of bed
4. Middle Millbrig- 50-60 cm below top
5. Middle Millbrig- 60-70 cm below top

Hagan, Virginia- See Haynes (1992, p. 50 of Virginia Div. of Mineral Resources Publication 126) Rose Hill 7 ½ minute Quadrangle and Kolata et al. (1996, p. 33 and 71), GSA Special Paper 313. Hardy Creek Limestone, Eggleston, and Trenton Formations. Deicke and Millbrig = K-bentonite beds R7 and R10 as discussed in Miller and Fuller (1954).

Dolly Ridge, West Virginia: Deicke thickness 34 cm, Millbrig not found after extensive search.

1. Deicke- 0-5 cm above bed base
2. Diecke- 5-10 cm above base
3. Diecke- 10-15 cm above base

Dolly Ridge, West Virginia: See Perry, W. J. 1972, The Trenton Group of the Nittany Anticlinorium, Eastern West Virginia. West Virginia Geological and Economic Survey Circular 13, 30 p.

Ohio Division of Geological Survey and Kentucky Geological Survey core samples collected by Adam Carey, Bryan Sell (Syracuse Univ.) and Gregory A. Schumacher on April 19, 2005 from Black River Group

1. DGS 2580 (Seneca Co.): 1,654.71-1,654.56= 0.15 foot (Deicke)
2. DGS 3256 (Williams Co.): 2,504.4 to 2,504.6= 0.2 foot (Millbrig)
3. DGS 3256 (Williams Co.): 2,515.38 to 2,515.7= 0.32 foot (Diecke)
4. DGS 2626 (Highland Co.): 1,243.0 to 1, 244.9= 1.9 feet (Millbrig)
5. DGS 2626 (Highland Co.): 1,262.3 to 1.262.9= 0.6 foot (Deicke)

6. DGS 3409 (Scioto Co.): 3,320.35 to 3,321.05= 0.7 foot (Millbrig)
7. DGS 3409 (Scioto Co.): 3,337.65 to 3,338.0= 0.35 Foot (Deicke)

8. CA-35 (Montgomery Co., KY) 890.5 to 891.0= 0.5 foot (Deicke) sampled by Dave Harris of the Kentucky Geological Survey on April 18, 2005. Tyrone Limestone

Location	Town	Confirmed Deicke	Confirmed Millbrig	Possible Elkport/Dickeyville	Core Num.	Core Depth	Formation
Outcrop Samples							
Shakertown, North Central KY	*Skakertown*						Tyrone Ls
Millbrig Suspect (70 cm thick)							
0-10 cm above base			x				
Hagan, "Pan Handle" of VA	*Hagan*						Hardy Creek Limestone, Eggleston, and Trenton Formations
Millbrig Suspect (130 cm thick)							
60-70 cm below top			x				
Deicke Suspect (92 cm thick)							
0-10 cm above base		x					
Union Furnace, Central PA	*Union Furnace*						Lower Salona
Millbrig Suspect B-15		NA					
Millbrig Suspect B-14 (duplicated)		NA					
Deicke Suspect B-12		x					
Dolly Ridge, Eastern WV	*Circleville*						Lower Trenton
Deicke Suspect							
5-10 cm above base				x			
Core Samples							
DGS 2580 (Seneca Co., North Central OH)					DGS 2580		Upper Black River
Deicke Suspect		NA				1654.71 - 1654.56 ft	
DGS 2626 (Highland Co., SW OH)					DGS 2626		Upper Black River
Millbrig Suspect			x			1243.0 - 1244.9 ft	
Deicke Suspect		x				1262.3 - 1262.9 ft	
DGS 3409 (Scioto Co., Southern OH)					DGS 3409		Upper Black River
Millbrig Suspect		x				3320.35 - 3321.05 ft	
Deicke Suspect		indistinguishable				3337.65 - 3338.0 ft	
DGS 3256 (Williams Co., NW OH)					DGS 3256		Upper Black River
Millbrig Suspect		x				2504.4 - 2504.6 ft	
Deicke Suspect		NA				2515.38 - 2515.7 ft	
Montgomery Co., North-Central KY					CA-35		Tyrone Fm
Deicke Suspect		x				890.5 - 891.0 ft	

APPENDIX D

Origin and Reservoir Characteristics of Upper Ordovician Trenton-Black River Hydrothermal Dolomite Reservoirs in New York, USA

By Langhorne B. Smith Jr., New York State Museum, Room 3140 CEC, Albany NY 12230

ACKNOWLEDGEMENTS

I would first like to thank Richard Nyahay for his help and support throughout the research and writing of this paper as well as the rest of the staff of the Reservoir Characterization Group at the New York State Museum. I would like to thank Denis Lavoie and Robert Bonnar for their excellent reviews of this paper. I would also like to thank Graham Davies, Ron Budros, Dick Beardsley and many other scientists whose input has been critical to unraveling the origins of these complex reservoirs.

ABSTRACT

In the past decade, more than twenty new natural gas fields have been discovered in laterally discontinuous dolomites of the Upper Ordovician Black River Group in south-central New York. The dolomites form around basement-rooted wrench faults that are detectable on seismic data. Most fields occur in and around elongate fault-bounded structural lows interpreted to be negative flower structures. Away from these faults, the formation is composed of impermeable limestone and forms the lateral seal for the reservoirs. In most cases the faults die out within the overlying Trenton Limestone and Utica Shale. Most porosity occurs in saddle dolomite coated vugs, breccias and fractured zones. Matrix porosity is rare in the Black River cores described for this study.

The patchy distribution around basement-rooted faults and geochemical and fluid inclusion analyses support a fault-related hydrothermal origin for the saddle and matrix dolomites. This play went for many years without detection because of its unconventional structural setting (i.e. structural lows versus highs). Using the appropriate integrated structural-stratigraphic-diagenetic model, more hydrothermal dolomite natural gas reservoirs are likely to be discovered in the Black River of New York and in carbonates around the world.

BACKGROUND

Oil and gas have been produced from laterally discontinuous dolomitized zones in the Upper Ordovician Trenton and Black River carbonates in eastern North America for more than a century. The first discoveries were made in the dolomites of the Lima-Indiana Trend of Ohio and Indiana (Figure 1) in 1884. Most of the dolomites are demonstrably fault-related as they align with the NNW-SSE trending Bowling Green Fault and other fault zones (Wickstrom et al., 1992). More than 500 million barrels of oil and over a TCF of gas were produced from the Lima-Indiana Trend (Wickstrom et al., 1992), making it the first giant oilfield in the world. Smaller yet still significant discoveries were subsequently made in fault-controlled dolomites at Dover Field, Ontario, and Deerfield and Northville Fields in Michigan (Hurley and Budros, 1990).

The next major discovery in Trenton-Black River laterally discontinuous dolomites was the Albion Scipio Trend in southern Michigan (Figure 1). Porous matrix dolomite, saddle dolomite-cemented breccias, saddle dolomite-lined fractures and vugs, occur in a trend of *en echelon* structural lows that is ~50 km long (30 miles) long and about 1.6 km (1 mile) wide (Hurley and Budros, 1990). Albion-Scipio Field has produced more than 250 MMBOE since its discovery. Several smaller fields have subsequently been discovered in Michigan and Ontario.

Natural gas was discovered in laterally discontinuous dolomite in the Black River Group of south-central New York in 1986. Since then, at least twenty new fields have been discovered in laterally discontinuous dolomites of the Trenton-Black River (Figure 2). Most of the fields are between 7000 and 10,000 feet deep. Several wells have produced at sustainable rates of > 10MMCF/D, and the best well produced in excess of 35MMCF/D for several months. As of the end of 2004, the well with the best cumulative production had produced more than 15 BCF and is still flowing at a high rate.

These dolomitized fields occur in long, narrow, fault-bounded *en echelon* structural depressions (Harding, 1974; Prouty, 1988; Hurley and Budros, 1990; Colquhoun, 1991) and along other wrench and possible normal faults (Wickstrom et al., 1992). The reservoir facies consists of matrix dolomite with saddle dolomite cemented vugs, breccias and fractures around the faults, and the reservoirs are laterally sealed by tight, undolomitized limestone. Although some fields have a major component of cavernous porosity (Albion-Scipio is famous for its bit drops of up to ~20 meters (60 feet)), others, including those in New York, have little or no cavernous porosity. Loucks (1999, 2003a, 2003b) recently suggested that the brecciation occurred when the Trenton and Black River collapsed into meteoric caves in the underlying Cambro-Ordovician Beekmantown carbonates. Later, deep-burial fluids then were interpreted to be responsible for the dolomitization and mineralization (Loucks 1999, 2003a, 2003b).

Most workers agree that the patchy dolomite formed from fluids flowing up basement-rooted faults and associated fractures (Harding, 1974; Prouty, 1988; Gregg and Sibley, 1984; Taylor and Sibley, 1988; Hurley and Budros, 1990; Colquhoun, 1991; Wickstrom et al., 1992; Coniglio et al., 1994; Davies, 2001; Smith et al., 2003) and has

nothing to do with meteoric karst. Prouty (1988) and Hurley and Budros (1990) suggested that the elongate Albion-Scipio Field in southern Michigan formed over a left-lateral strike-slip fault system and that hot fluids flowed up the faults and fractures and dolomitized the adjacent limestone. The structural sags were interpreted to have formed by transtensional faulting and the development of negative flower structures (Harding, 1974; Hurley and Budros, 1990). Wickstrom et al. (1992) suggested a similar origin for dolomite around the NW-SE trending Bowling Green Fault Zone in Northwestern Ohio

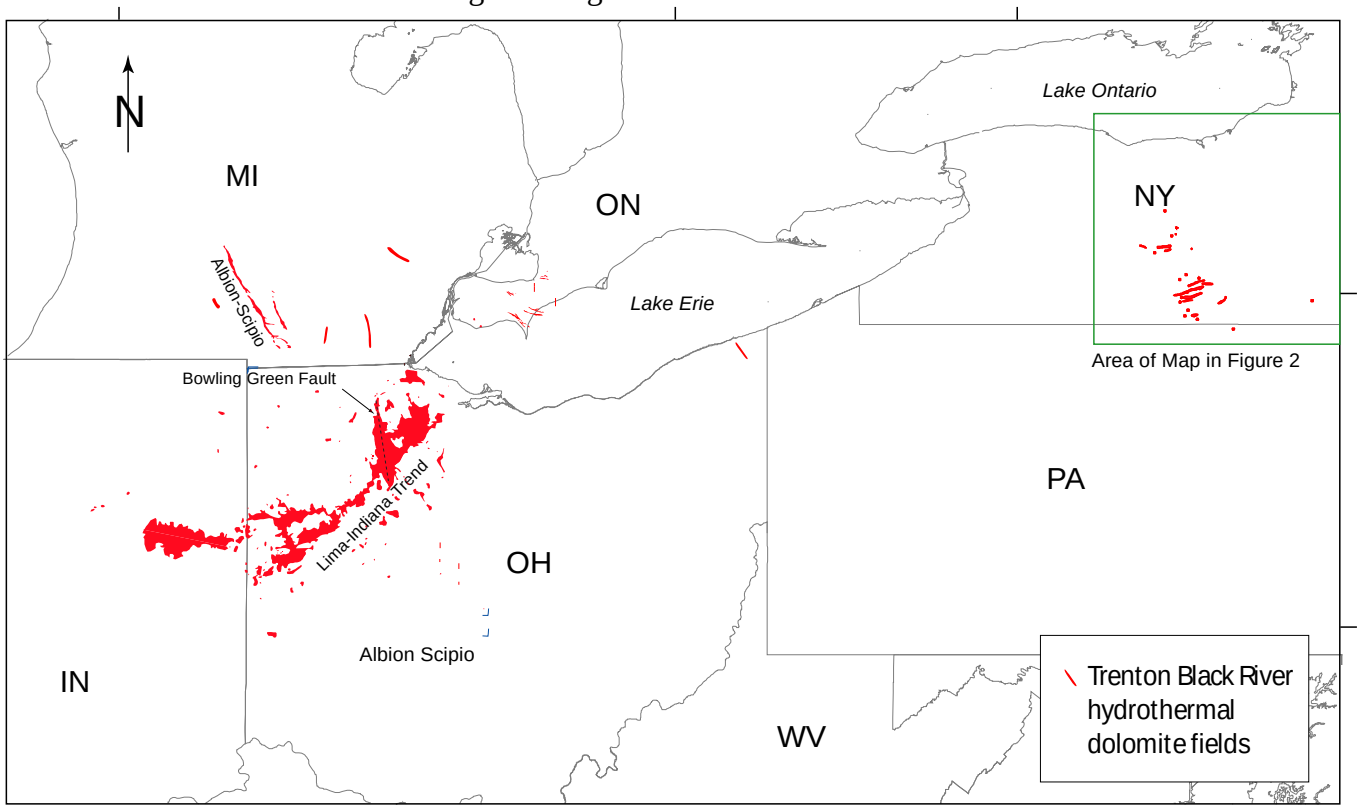

Figure 1. Map of Trenton and Black River hydrothermal dolomite fields in eastern North America.

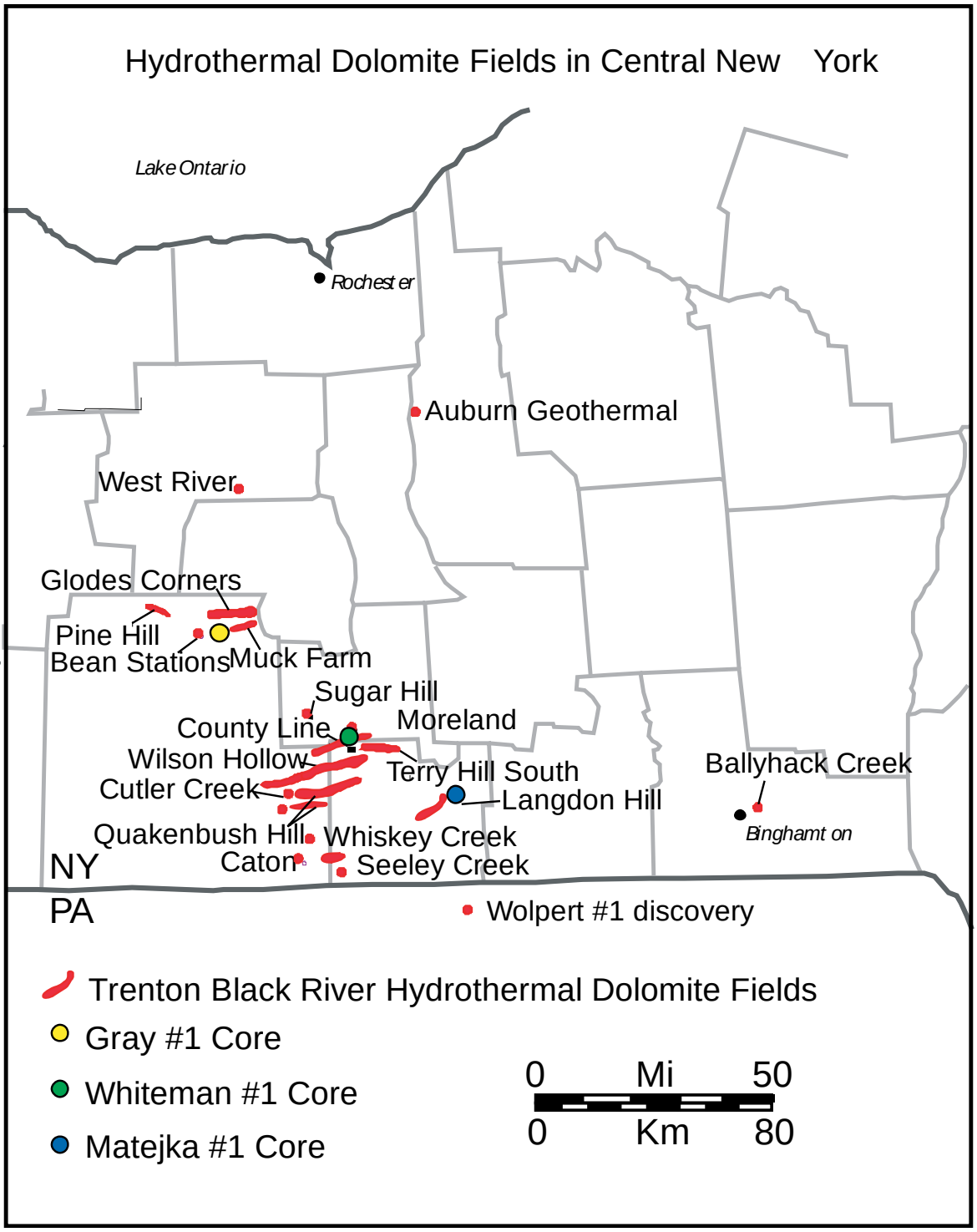

Figure 2. Map of producing dolomite fields in Black River Group of New York with locations of three cores discussed in the paper.

and Colquhoun (1991) made similar interpretations about the Hillman Field in southern Ontario.

The recently discovered natural gas fields in New York are similar to the Trenton-Black River Fields in Ohio, Michigan and Ontario. Saddle dolomite-lined vugs, fractures and breccias, and matrix dolomitization occur around subtle basement-rooted faults that are visible on seismic data. Away from the faults, the Black River is unaltered limestone.

The purpose of this paper is to present structural, stratigraphic, petrographic and geochemical data from newly discovered dolomite fields in New York that together demonstrate that they formed due to wrench faulting and bottom-up hydrothermal fluid flow and to show the similarity between the fields in New York with those in Ohio, Ontario and Michigan. The timing and depth of alteration is an ongoing controversy and data will be presented that demonstrates that the dolomitization and other hydrothermal alteration mainly occurred in the Late Ordovician, soon after deposition when the Trenton and Black River strata were buried less than a kilometer.

GEOLOGIC SETTING

The Grenville Basement, which underlies New York State and much of the Eastern United States, has been subjected to numerous tectonic events that produced numerous fault and fracture trends. The Grenville Orogeny occurred approximately 1.1 billion years ago (Moore, 1986) and during this event, thrust faults and associated tear faults formed. After the Grenville Orogeny, North America was part of a supercontinent that underwent a long-lasting episode of rifting in the Late Precambrian (620-550 ma: van Stahl, 2005). There were numerous failed rift zones such as the Rome Trough, Reelfoot Rift and many other features (Burke and Dewey, 1973; Thomas, 1991), some of which extend into New York. Along with the extensional faults there were associated strike-slip transfer faults (Thomas, 1991). The faults formed during these earlier events were likely reactivated during subsequent tectonic events.

After the Late Precambrian rifting of the supercontinent, New York was situated on a passive margin developed over the New York Promontory (Thomas, 1991). The Middle Cambrian Potsdam Sandstone (0-100 feet thick) rests unconformably on the rifted basement and is overlain by the Cambro-Ordovican Beekmantown Group carbonates and siliciclastics (Figure 3). In New York, the Beekmantown is composed of the Cambrian Little Falls Dolomite, which has common vugs, breccias and fractures partially filled with saddle dolomite, “Herkimer Diamond” quartz crystals and anthraxolite, a carbonate mineral with solid hydrocarbon in the matrix. The upper part of the Beekmantown consists of the Tribes Hill Formation, which is dolomitized near faults and mostly limestone away from faults where it outcrops in the Mohawk Valley of New York (Landing et al., 1996; Smith et al., 2004b). The Beekmantown and its equivalents across North America (Knox, Ellenburger, Arbuckle, St. George and Romaine) commonly host Mississippi Valley Type Lead-Zinc sulfide deposits and dolomitized oil and gas reservoirs. The global Lower Ordovician Knox Unconformity overlies the Beekmantown.

The overlying Black River Group is primarily composed of muddy and fine-grained shallow marine carbonates. The Black River is overlain by the Trenton Group, which is composed of deeper water argillaceous limestones and calcareous shales and high-energy shallow marine grainstones and packstones (Brett and Baird, 2002). The Trenton and Black River thin toward eastern New York, where they are absent in some places, and thicken into the south-central part of the state where most of the recent production occurs (Rickard, 1973). The Trenton is overlain by the deeper-water Utica Shale, which is a black shale that blankets much of the eastern North America. This contact is diachronous as the Trenton Limestone grades laterally into the Utica Shale to the south and east. The Utica Shale grades up into the Ordovician Lorraine Siltstone and Queenston Sandstone, which are siliciclastics that prograded from the Taconic Mountains across most of New York in the Late Ordovician.

The Taconic Orogeny began in the Late Ordovician when an island arc collided with proto-North America to the present day east of New York and continued throughout the Late Ordovician and into the Early Silurian (Ettensohn and Brett, 2002). Both the Black River and Trenton Groups have bentonite (volcanic ash) beds in them, some of which can be correlated for great distances (Kolata et al., 1996). Further evidence for tectonic activity at this time includes development of a foreland basin to the east, Late Ordovician extensional faulting in the foreland area of the Mohawk Valley (Bradley and Kidd, 1991), spatial and temporal variations in differential subsidence in the Trenton Group and the occurrence of seismites in the outcrops of Trenton and Utica-aged rocks in New York, Kentucky and Ohio (Pope et al., 1997; McLaughlin et al., 2002; Ettenshohn et al., 2002).

METHODS

Logs were analyzed and maps were constructed using *Petra* Software and then imported into *Adobe Illustrator* where they were manipulated for presentation. Cores were described using slabs and thin sections. Sampling for geochemistry was done in the laboratory at the New York State Museum. Samples of matrix dolomite, saddle dolomite, calcite and quartz were collected separately for each set of analyses. In some cases, samples were split four ways so that we could get fluid inclusion, stable isotope, trace element and strontium isotope date for the same samples.

Fluid inclusions were analyzed by Fluid Inclusion Technologies, Inc using commonly accepted techniques and equipment. Polished slabs of rock material were prepared and studied optically with a petrographic microscope. Samples were placed into a gas-flow temperature stage (manufactured by Fluid Inc.) and individual inclusions in aqueous inclusion populations were viewed optically during heating and cooling (-196°C to +200°C or higher). Phase equilibria within the trapped fluids reflect their composition and bulk density, which, in turn, is a function of trapping temperature, pressure and fluid composition for each inclusion.

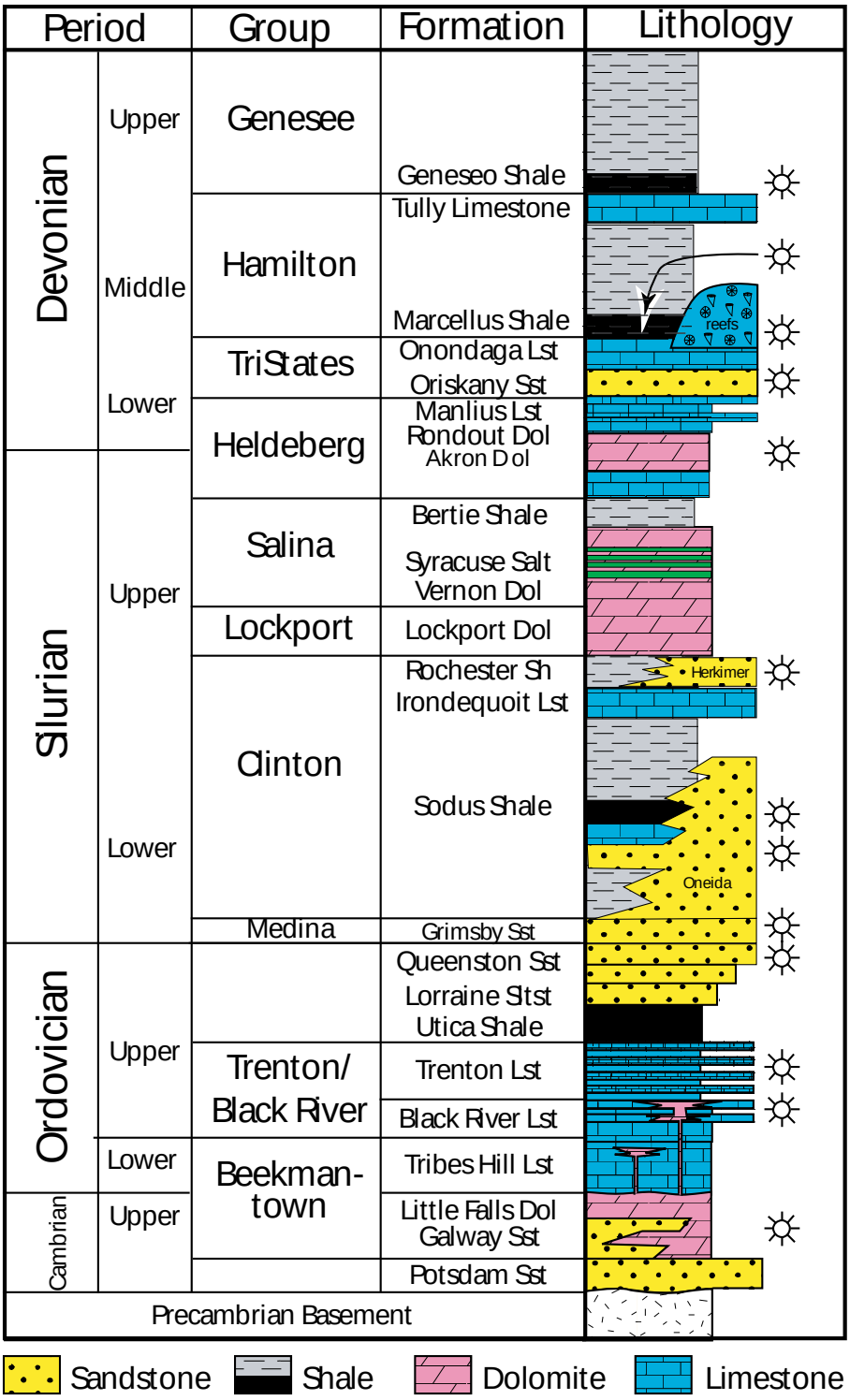

Figure 3. Generalized stratigraphic column for central New York. The Black River Group is earliest Late Ordovician in age.

Stable isotopes values were measured by Peter Swart at the University of Miami. Samples were reacted for 10 minutes using the common acid bath method at 90°C and the CO2 produced analyzed using a Finnigan MAT-251. Standard isobaric corrections were applied. Data for both C and O isotopes are reported relative to the Vienna Pee Dee Belemnite (V-PDB) using the conventional notation.

Trace elements and Strontium isotopes were analyzed by Mihai Ducea at the University of Arizona. About 100 mg were dissolved for each sample in 2.5M nitric acid. About 10% of that was used for trace element analyses; the remainder was taken up in 3.5M nitric acid and passed through Sr Spec chromatographic columns for rapid Sr elution. The separated Sr cut was then redissolved in 1% nitric acid.

Trace elements were analyzed in a mild nitric acid using a Perkin Elmer Elan DRC-II instrument. Strontium isotopes were analyzed on a VG Sector 54 instrument. During the period of our analysis, the measured $^{87}Sr/^{86}Sr$ ratios were 0.71025±1 for standard NBS 987.

DATA

Maps and Cross-Section

Figure 2 shows the distribution of Trenton-Black River producing hydrothermal dolomite fields and discoveries in New York. Many of these fields are in the process of being drilled and extended and this map is likely to look quite different when all drilling is completed.

The distribution of dolomite in the Trenton and Black River Groups helps to understand its origin. The Trenton Group carbonates are primarily limestone and argillaceous limestone throughout most of New York and are only rarely dolomitized. This is in contrast to Ohio, Michigan and Ontario where the Trenton is commonly dolomitized and produces more hydrocarbons than the underlying Black River. Furthermore, there is no “cap” dolomite in New York (*sensu* Wickstrom et al., 1992), which is a tight regional dolomite in the uppermost Trenton between 10 and 50 feet thick that blankets much of northwestern Ohio and southwestern Michigan.

Most of the dolomitization in New York occurs in the Black River Group and is laterally discontinuous. Where there are enough wells to map out dolomite bodies, the dolomite occurs in sub-linear trends that are up to 25 km long and 1 km wide (Figure 2). Undolomitized wells occur within short distances of wells with significant quantities (tens of feet) of dolomite in the same stratigraphic interval (Figure 4). All productive wells have at least some porous dolomite in the upper half of the Black River Group and almost all wells have dolomite in the top 20 feet. Figure 4 shows the distribution of wells with at least 2 feet of dolomite in the upper half of the Black River along with wells that are entirely composed of limestone in that interval. Dolomite thickness within the Black River ranges from a few feet to several hundred feet. Analysis of cuttings thin sections from dolomitized wells outside the producing area confirms the presence of both matrix

and saddle dolomite (Nyahay and Smith, 2003). As of 2003, 345 wells with logs have been drilled to the Black River. Of these, 175 wells have encountered at least some dolomite in the upper half of the Black River and 48 wells have produced at least some gas. It should be noted that since 1996, almost all wells that were drilled to the Black River were drilled into structures looking for dolomite while prior to that date they were mainly drilled with other targets in mind and were less likely to encounter dolomite.

Figure 5 is a cross section of wells in and near the Glodes Corners Road Field (the discovery field for the New York trend). The field is about 10 km long and 0.7 km wide and has produced about 8 BCF. Within the Black River, the cross-section includes several dolomitized producing wells, two tight dolomite wells and a tight limestone well. Dolomite is picked using the PEF curve or where that is absent, in zones where the density log reads greater than 2.75 g/cc or where the density log (on a limestone scale) reads about 5% less porosity than the neutron log. When the Black River is productive, it is almost always dolomitized in the uppermost 15 meters (50 feet) under the argillaceous limestones at the base of the Trenton (Figure 5). The thickening and thinning and laterally discontinuous nature of the dolomite suggests that the source of the dolomitizing fluids was highly localized.

Figure 6 is a cross section of some of the better wells in some of the major producing fields. The cross section trends from Glodes Corners Road in the Northwest to Seeley Creek Field in the southeast. In many cases, once gas was discovered, operators would stop drilling and hook the wells up so some logs do not go all the way through the Black River. Note the variable dolomitization from just a few feet in Glodes Corners Road and Muck Farms to near pervasive dolomitization in the Lant #1 (Terry Hill South Field) and Parker #1 (Wilson Hollow Field) to the more interbedded dolomitization in several other wells. This variability in dolomitization demonstrates again that the dolomitization was not regional but highly localized. The porosity distribution also varies from well to well, but the zone that is most consistently porous is in the top 50 feet (15 meters) of the Black River.

Seismic Data

Black River hydrothermal dolomite fields are discovered using seismic data. The dolomitized zones occur primarily in and around *en echelon* fault-bounded structural lows (Prouty, 1983; Hurley and Budros, 1990; Davies, 2004). These features are commonly called “grabens” or “sags.” Figure 7 is a time structure contour map of the top of the Trenton from a producing hydrothermal dolomite oil field in Ontario that shows *en echelon* sags. Oil was produced from fractured, vuggy dolomite located within the structural lows and most of the Trenton and Black River strata outside the sags are impermeable limestone (Horvath et al, 2004). The *en echelon* sags are interpreted to be negative flower structures formed as a result of transtensional (strike-slip and extensional) faulting (*c.f.* Hurley and Budros, 1990).

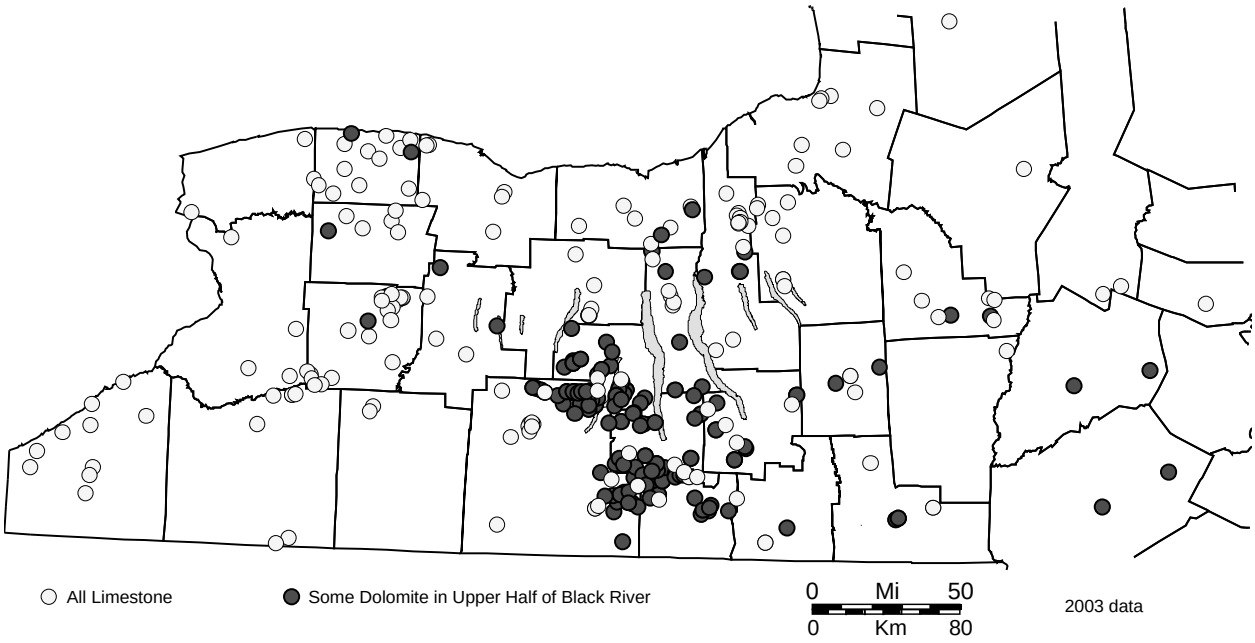

Figure 4. Map of central and western New York with locations of wells with at least two feet of dolomite in the upper half of the Black River and wells that are all limestone in this interval.

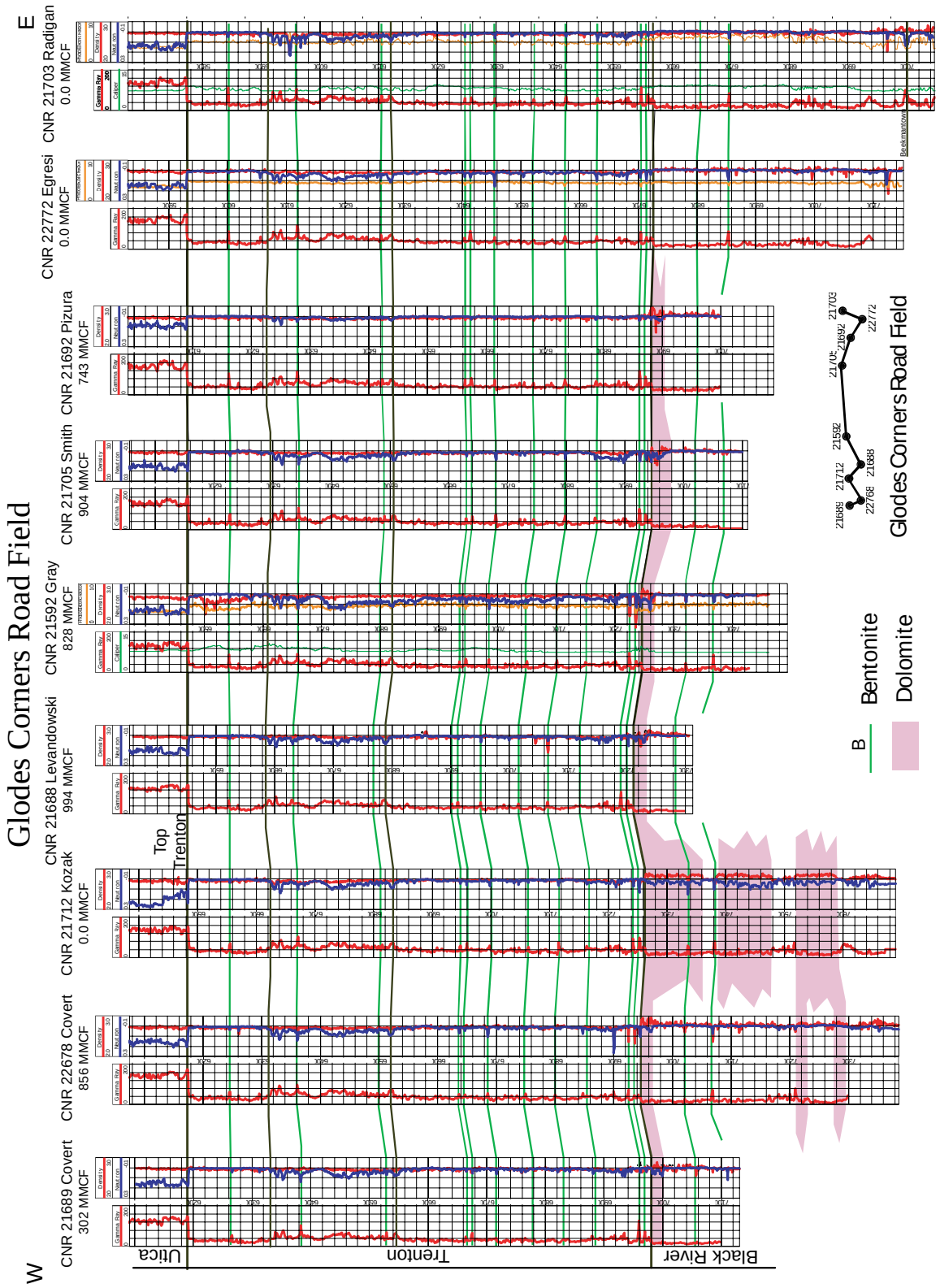

Figure 5. Cross section of Trenton Limestone and Black River Group at Glodes Corners Road Field, New York. Dolomite is highlighted in pink. The rest of the

Trenton and Black River Group are composed of limestone. Well labels include the operator (Columbia Natural Resources or CNR), the shortened API number, lease name and cumulative production as of 2003.

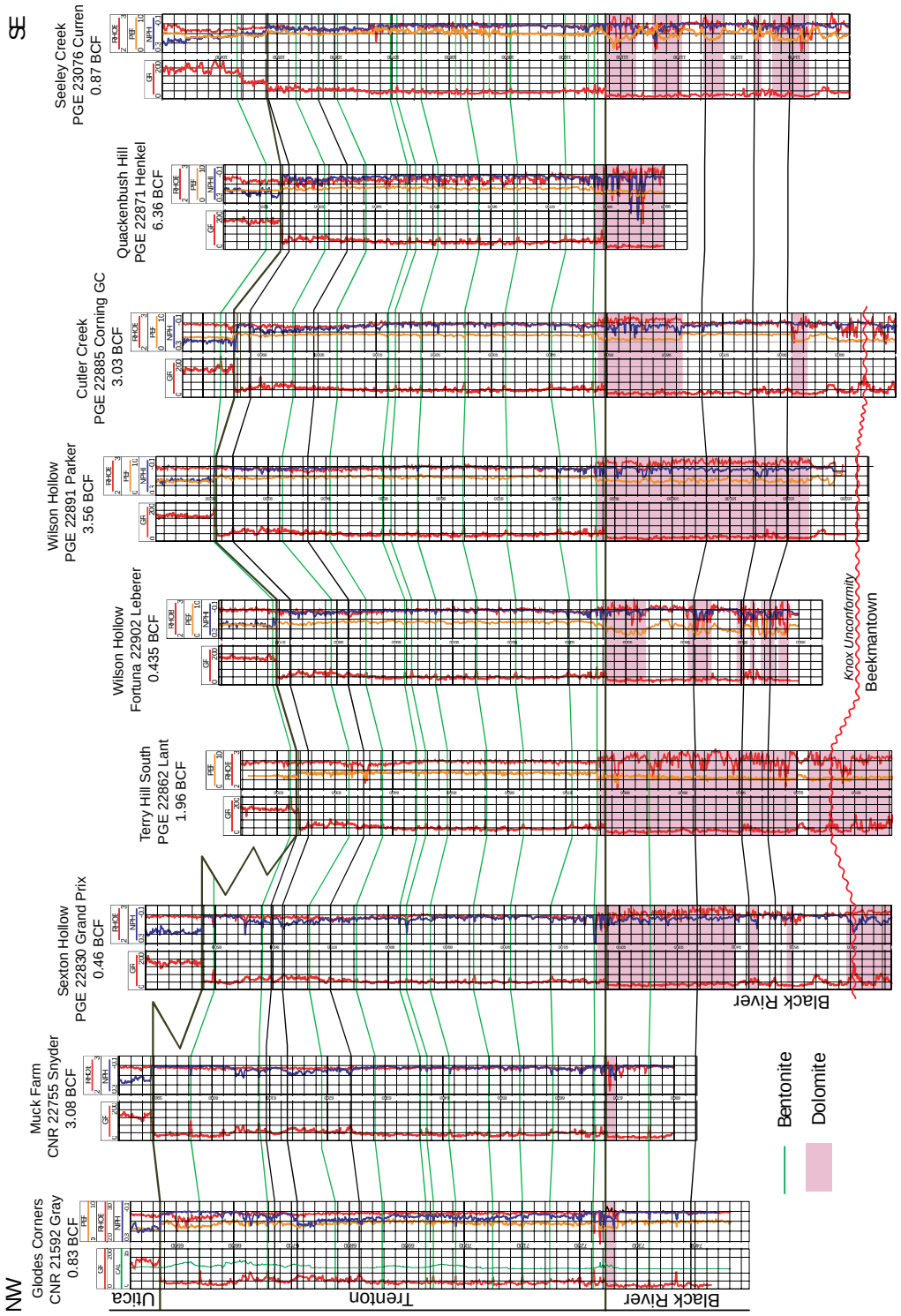

Figure 6. Cross section of Trenton and Black River Groups from NW to SE through eight of the producing fields in the trend. Note variable dolomitization and porosity development. Well labels include Field name, operator, shortened API number, lease name and production as of December 2004. The wells have produced for varying amounts of time and all continue to produce.

Figure 8 shows the seismic signature of two different productive Black River hydrothermal dolomite fields in New York, Muck Farms Field (Figures 8A, B and C) and Wilson Hollow Field (Figures 8D, E and F). The dolomite occurs in the Black River, typically within the structural lows. The fault picks in the basement (Figures 8B and 8E) are equivocal, but reflectors are demonstrably offset and faulted. Typical of some negative flower structures, reflectors immediately overlying the basement are not as obviously offset vertically by the faults while those higher in the section have clear vertical displacement (see cross sections in Dooley and McClay, 1997 for examples of how these might form). Note that the productive dolomitized structures look very different in the two cases. This is typical of wrench-faulted zones, which significantly change in character along strike. Most of the vertical offset of the seismic traces occurs within the Black River with little offset in the overlying Trenton or underlying Beekmantown. Most of the faults with associated dolomitization die out in the Trenton or overlying Utica Shale. Note that on the Muck Farm line where the Beekmantown reflector can be picked (Figure 8B), there is no collapse into the Beekmantown. Also note on the Wilson Hollow line that much of the structural sag affecting the lower Trenton and Black River is filled in by earliest Utica time (Figure 8E).

Cores

There are three publicly available cores from the Black River hydrothermal dolomite play in New York. Each of them has features that are important to understanding of the sedimentology, stratigraphy and diagenesis of this play. The locations of the cores are presented in Figure 2.

Rock Types and Stratigraphy

The Black River Group carbonates were deposited on a shallow low-relief tropical carbonate ramp. Rock types include mudstone (sometimes with fenestrae and clay drapes), fine-to coarse-grained skeletal wackestone, and very fine-to-fine peloidal packstone and grainstone (See Cornell, 2000 for more detailed facies analysis). All of these rock types can be dolomitized, but dolomitization of the peloidal grainstones and packstones may be more common. The clay drapes superficially resemble stylolites but are unrelated to pressure solution. Burrowing is common in most rock types. The Black River Group carbonates are remarkably consistent in rock type across much of eastern North America. None of these rock types is a reservoir facies in the absence of dolomitization.

The Trenton has grainstones and packstones that are coarser and more fossiliferous than those in the underlying Black River and also has common dark gray to black shale (Brett and Baird, 2002). Deeper water rock types include black or dark gray shale, fossiliferous shale and skeletal wackestone. Shallower water facies occur in some locations and they include coarse-grained skeletal grainstone and packstone. The Trenton in central New York is generally more argillaceous than it is in Ohio, Michigan and Ontario. This may be the primary reason that the Trenton is rarely dolomitized in central New York. There is virtually no porosity in the limestone facies of both the Trenton and

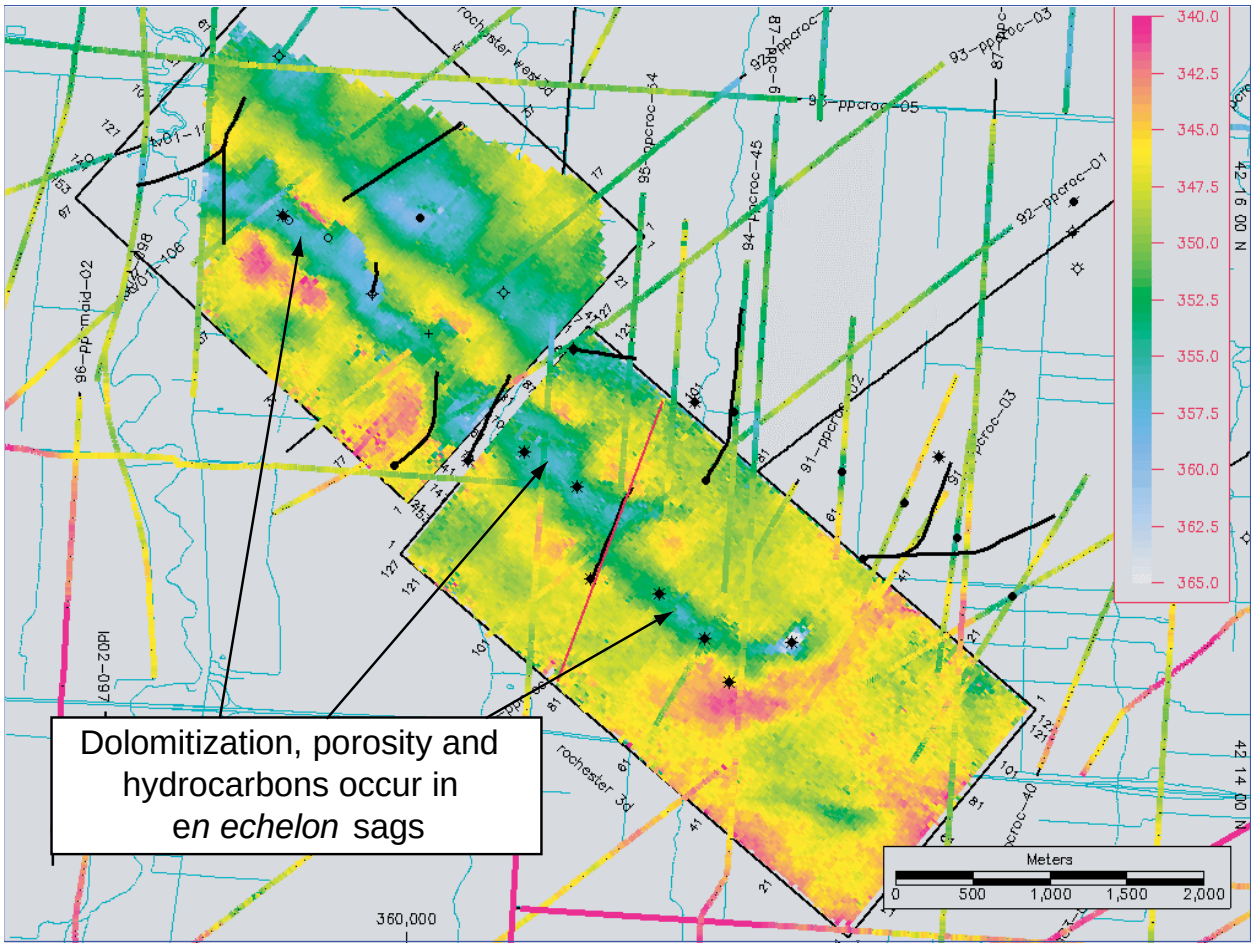

Figure 7. Time-structure map of the top of the Trenton Group, Rochester Field, Ontario from 3D seismic (courtesy Talisman Energy). Note *en echelon* sags where dolomitization, porosity and oil occur. Color bar scale is in meters below sea level.

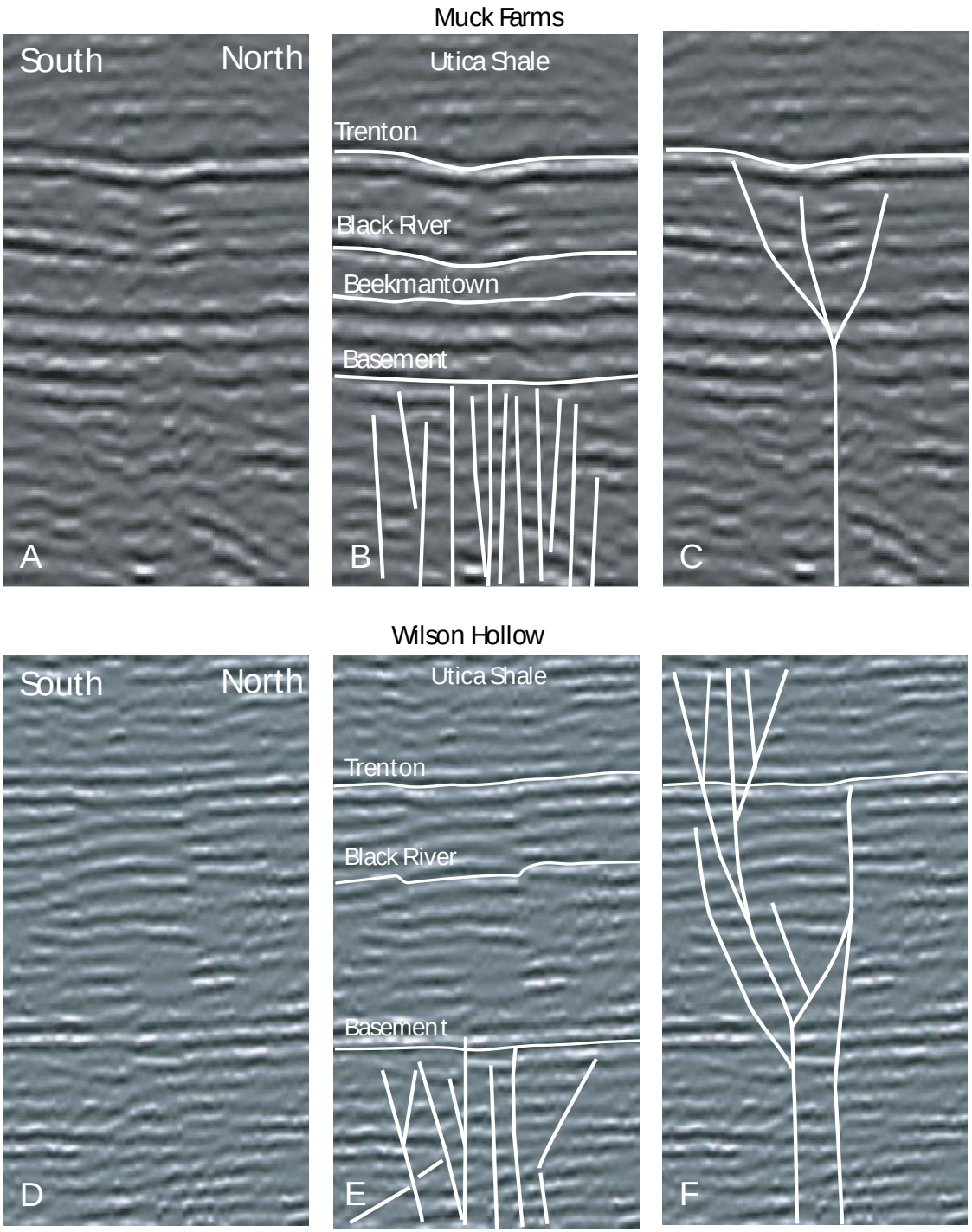

Figure 8. Seismic lines from Muck Farm and Wilson Hollow Fields, New York. A) Uninterrupted line over Muck Farm Field. B) Formation picks and possible faults in basement. Note sag at top of Trenton and lack of sag in Beekmantown. C) Interpreted flower structure with faults bounding structural sag. D) Uninterrupted line over Wilson Hollow Field. E) Formation and possible basement fault picks. Note that sag is accommodated in Trenton and lower Utica. F) Possible basement-rooted flower structure with faults bounding sag in Trenton and Black River.

Black River facies and these impermeable limestones are thought to form a vertical and lateral seal on the hydrocarbon reservoirs.

Matrix Dolomite Description

The reservoir rock types in the Trenton-Black River are hosted in laterally discontinuous dolomites. There is both matrix dolomitization and void filling saddle dolomite. Analysis of stained, impregnated thin sections from the cores shows that more than 95% of the dolomite is medium to coarse (50-400 micron) matrix-replacive dolomite. The matrix dolomite has little or no porosity in the cores studied from New York. Matrix porosity may occur in other wells, but was not present in the cores studied. This lack of matrix porosity is in contrast to Trenton-Black River dolomitized reservoirs in Ontario and Ohio where matrix porosity is more common and makes up a significant part of the reservoir (Wickstrom et al., 1992; Colquhoun, 1991).

Much of the matrix dolomitization is fabric-destructive, anhedral and nonplanar (*sensu* Sibley and Gregg, 1986). Finer dolomites are here interpreted to have been mudstones and mud-dominated wackestones and the coarser dolomites are interpreted to have been peloidal or pelletal grainstones and packstones (c.f. Lucia, 1995).

Even though this play has significant structural and diagenetic aspects, stratigraphy is still important. Strata with higher porosity and permeability remaining at the time of dolomitization were probably more likely to have been dolomitized and to have had some porosity preserved after dolomitization. As more core data are collected, a major emphasis will be placed on learning what each of the dolomitized rock types were prior to dolomitization and what the impact of original facies is on reservoir quality.

Reservoir Facies Description

Most of the open pores in the Black River dolomites occur in saddle dolomite-lined fractures, vugs, zebra fabrics, boxwork fabrics and between clasts in breccias (Figures 10 and 11). Some vugs are sub-spherical and several cm in diameter. Other vugs are elongate (a few mm wide and several cm long) and may be solution-enlarged fractures. Some of these elongate vugs are horizontal while others are inclined. Porous zebra fabrics and boxwork fabrics are both present (Figure 11). Breccias are common but not abundant and consist of mm-to cm-scale angular to corroded clasts cemented with saddle dolomite.

The Matejka #1 core (Figure 9) is in Chemung County (Figure 2) and was drilled in 1975, eleven years before the first official discovery. It encountered dolomite in the Black River and heavily fractured limestone in the overlying Trenton Group. There is some porosity in fractures in the basal Trenton limestone that are mostly cemented with coarse calcite cement (Figure 9A). The dolomite in the Black River has no porosity (Figures 9B and 9C) and no open vugs, fractures or breccias. Saddle dolomite and calcite plug fractures within the dolomitized interval. The well was plugged as a dry hole, but it

is located within a few hundred meters of a producing dolomitized well and may well have produced from the fractures in the basal Trenton limestone.

The Gray #1 core (Figure 10) was drilled to the West of Muck Farm Field and did not produce economic quantities of gas. The matrix in the upper half of the core is dolomitized and the lower half is predominantly limestone. Saddle dolomite-lined vugs occur in the dolomitized interval (Figure 10) but there are no open fractures or breccias. This well tested a very small amount of gas but not enough to justify facility costs and may be sidetracked.

The Whiteman #1 core (Figure 11) is pervasively dolomitized and has common saddle dolomite-lined vugs, zebra fabrics, breccias and fractures. Porosity primarily occurs in vugs and fractures, and there is little or no matrix porosity. The well has produced approximately 0.5 BCF in three years as of the end of 2004 and is still producing today.

Paragenetic Sequence

The paragenetic sequence of the Black River dolomitized reservoirs is presented in Figure 12 and supported with photographs in Figure 13. Prior to dolomitization, some early marine and shallow burial calcite cementation and compaction occurred along with some minor grain suturing. This early diagenesis was followed by matrix dolomitization (Figure 13A), faulting, fracturing and brecciation (Figure 11), and then saddle dolomite (Figure 13A), quartz (Figure 13B), rare authigenic feldspar (Figure 13C), pyrite, bitumen and calcite precipitation (Figure 13D). In some cases, the late calcite and/or saddle dolomite are leached by a later event (Figure 13E). Figure 13E shows bitumen in a pore that apparently was precipitated between dolomite rhombs that were later leached. Major stylolitization follows all mineralization (Figure 13F). There are no dolomite filled fractures that cut across major stylolites and matrix and saddle dolomite rhombs are clearly consumed at stylolites. All these are postdated by hydrocarbon migration, which likely occurred in the Late Paleozoic. The bitumen found lining many pores and fractures is not thought to represent a full-scale migration event.

The timing of the development of the vugs is equivocal. It may be that most vugs formed before the matrix dolomitization (the preferred interpretation) during a period of pre-dolomitization leaching. Or it may be that they formed after matrix dolomitization but before saddle dolomite was precipitated through matrix dolomite dissolution. There is no evidence of significant dolomite dissolution such as corroded rhombs lining the vugs. In some cases, vugs appear to be enlarged fractures (Figure 11), which would make their development syn- or post-fracturing.

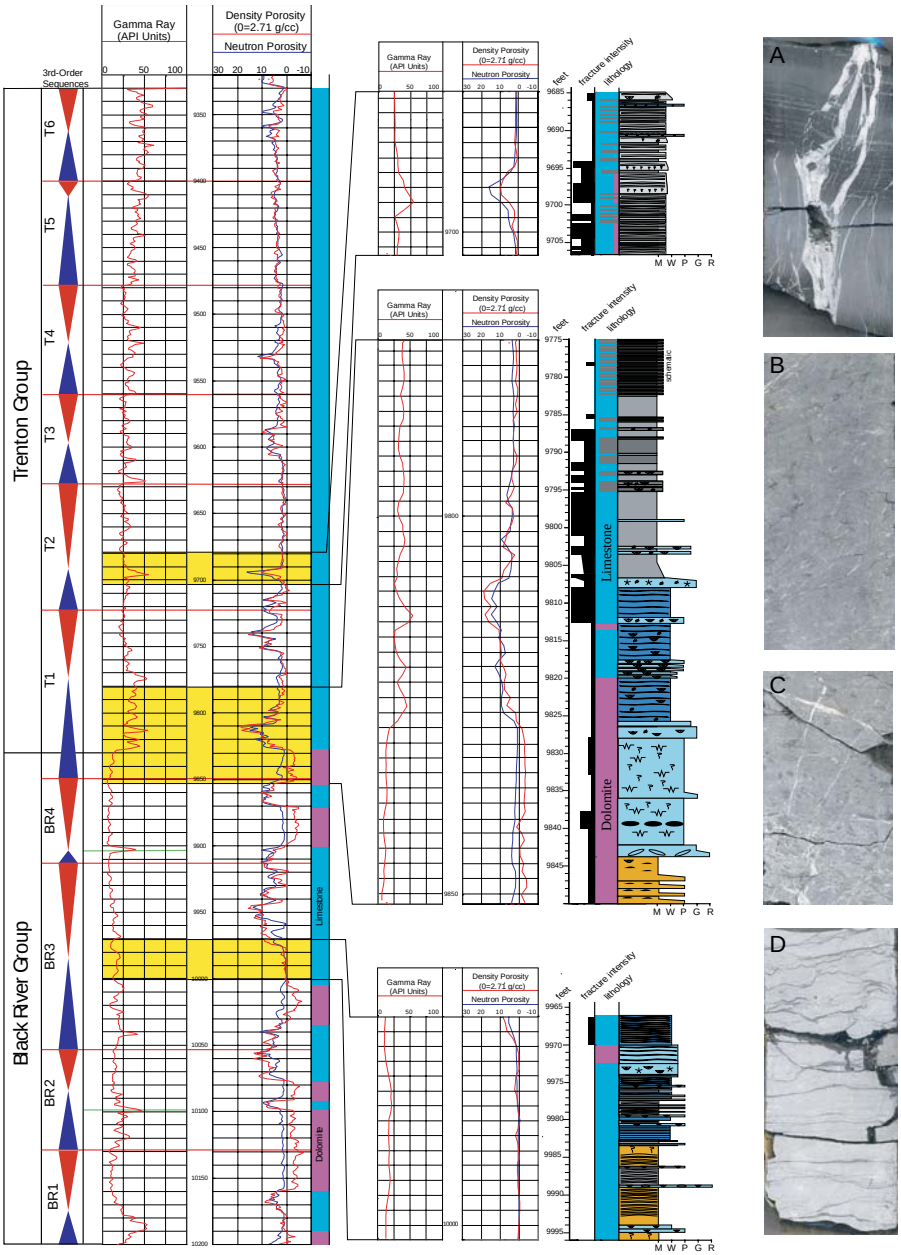

Figure 9. Core description with logs and photos from Matejka # 1 well, Chemung County, New York. Dolomitized intervals in core match with intervals where density log reads 5% less porosity than neutron log. Color code for core description: grays are deeper water mudstone, wackestone and shale, dark blue is mid ramp skeletal wackestone, light blue is shallow marine peloidal and skeletal grainstone (interpreted in dolomitized interval), tan is shallow marine argillaceous mudstone and wackestone. (M = mudstone; W = wackestone; P = packstone; G = grainstone) Photographs are lettered: A) Lower Trenton Group interbedded fossiliferous shale and mudstone is faulted and cemented with calcite. This sample is from 9787' and has some porosity in the fracture. B) Uppermost Black River dolomite with relict clay fills, minor fractures and tight, gray matrix dolomite. C) Dolomitized conglomerate from upper Black River Group with calcite cemented fractures and no porosity. D)

Typical Black River Limestone from lower core is shallow marine mudstone with clay laminae.

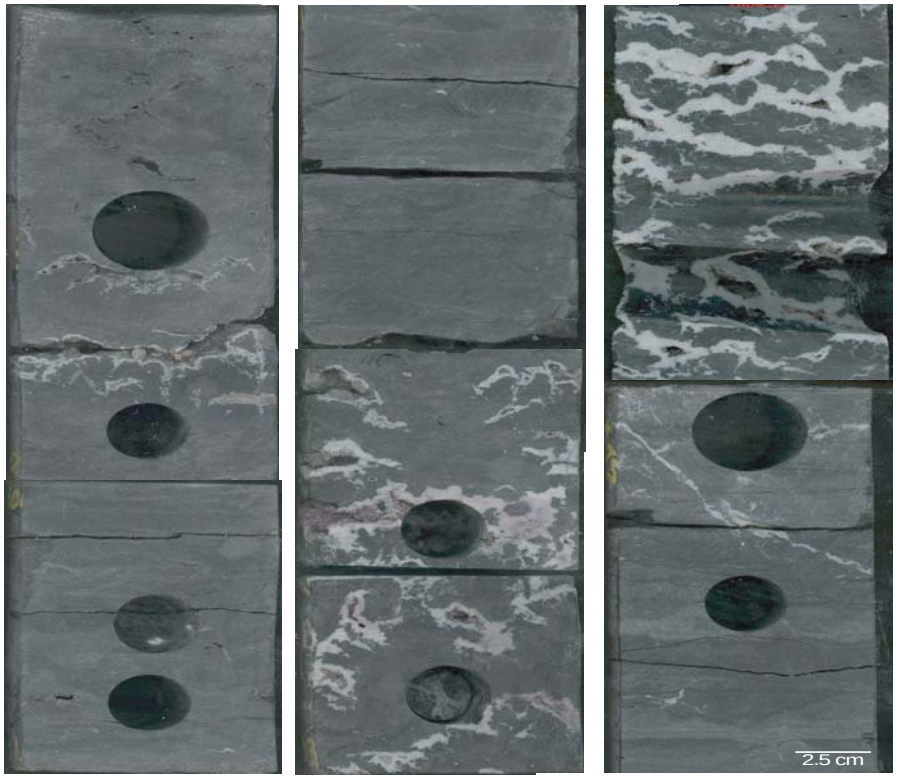

Figure 10. Core photographs from Gray #1 well, Steuben County, NY. Gray matrix dolomite with vugs lined with white saddle dolomite. Core is 9 cm (3.7 inches) wide.



Figure 11. Core photographs from Whiteman #1 well, Chemung County, NY. This core has common fractures, vugs, zebra fabrics (ZF), boxwork fabric (BF) and an overall brecciated appearance. White saddle dolomite lines vugs and fractures in gray matrix dolomite. Core is 5cm (2 inches) wide.

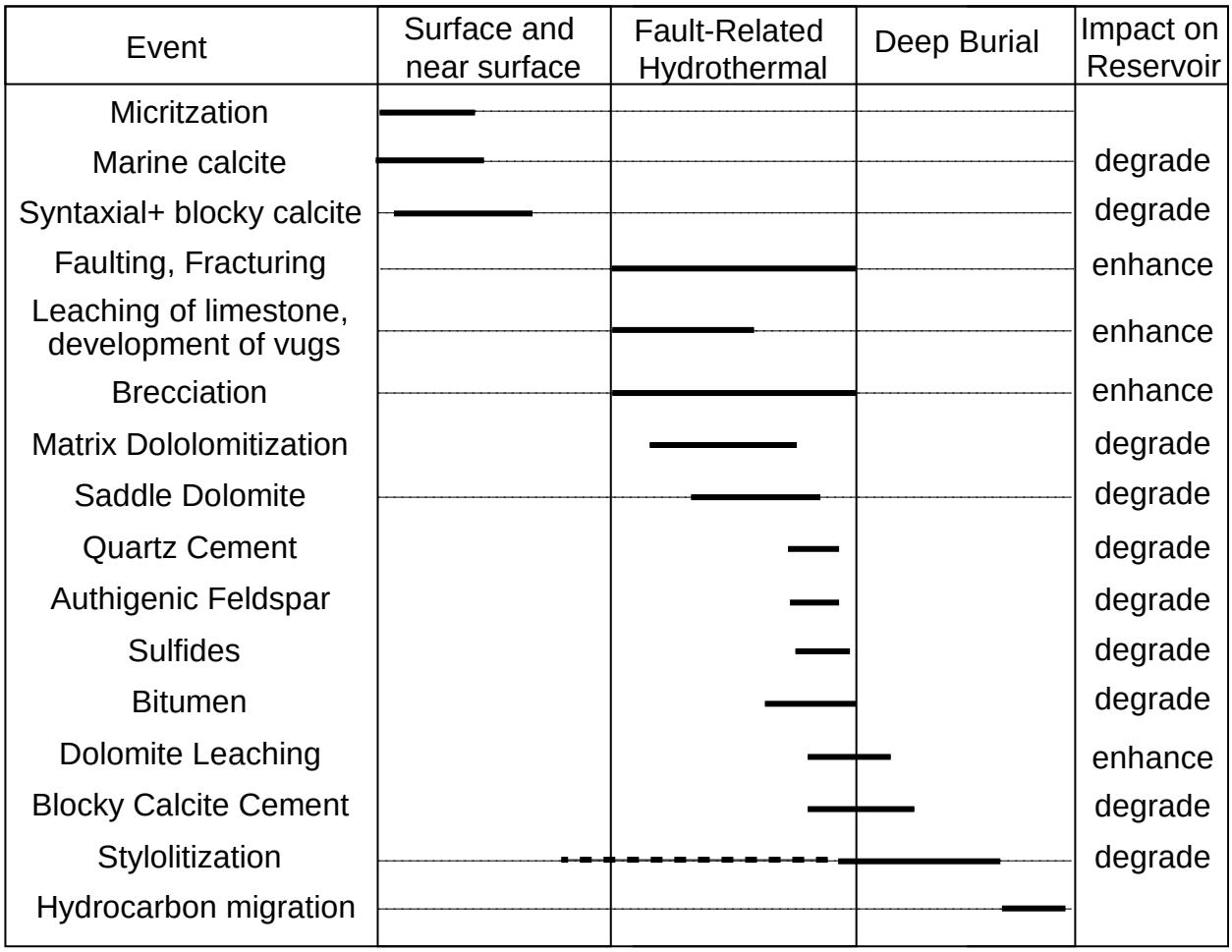

Figure 12. Paragenetic sequence of events in dolomitized cores from Black River Group of New York.

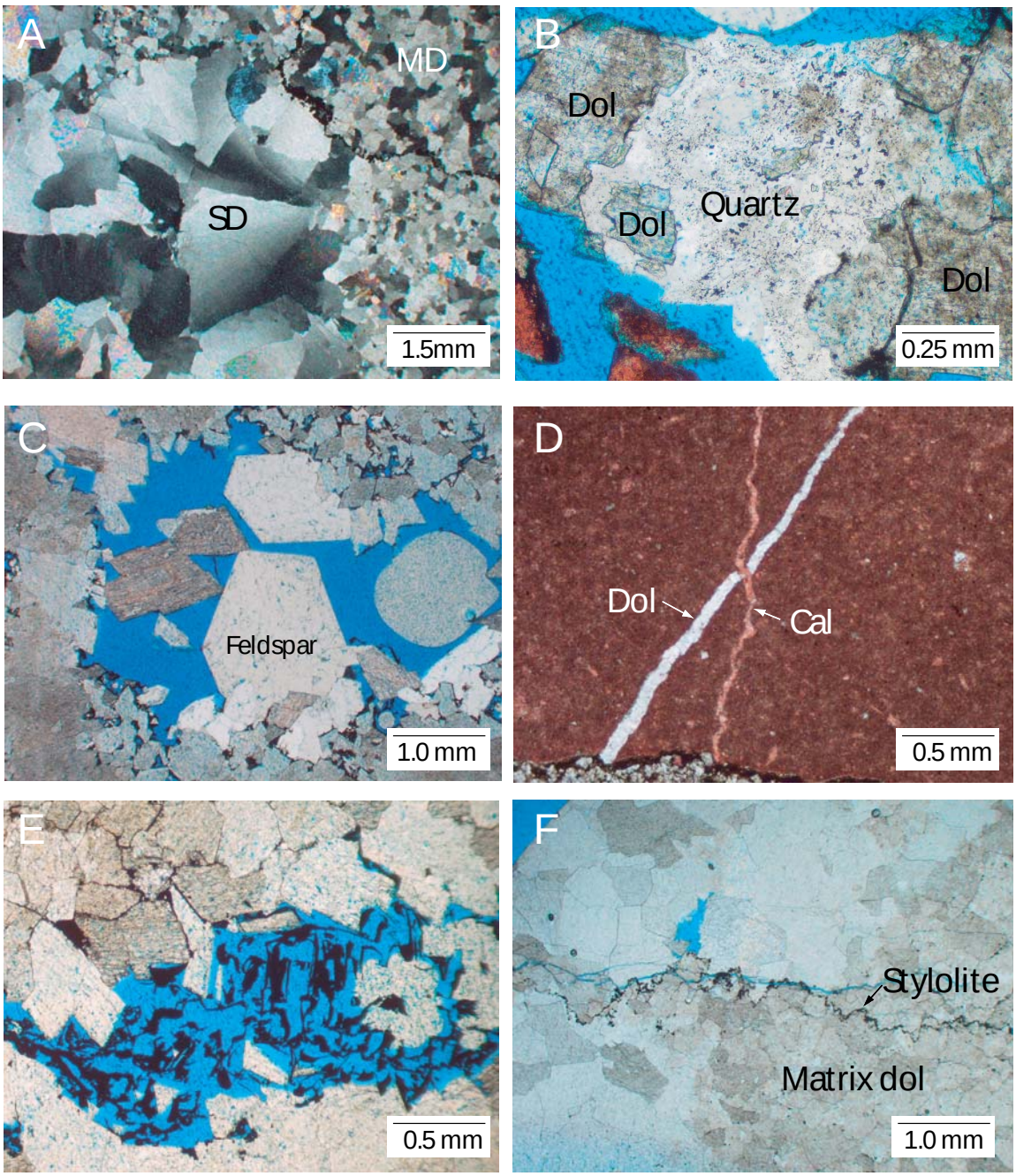

Figure 13. Thin section photographs from Black River Group, New York. A) Saddle (SD) and matrix (MD) dolomite. Gray #1 core, 7802 feet. B) Quartz cement in fractured ferroan dolomite. Auburn geothermal well cuttings, Onondaga County, NY, 4150 ft. C) Authigenic feldspar in vug. Whiteman #1 core, 9528.5 ft. D) Calcite-filled fracture clearly postdates dolomite-filled fracture. Late calcite commonly plugs porosity in Black River reservoirs. Gray #1 core, 7816 ft. E) Bitumen distribution in vug suggests that dolomite may have been leached after bitumen was precipitated. Whiteman #1 core, 9535 ft. F) Stylolite clearly postdates dolomitization. No dolomite grows across stylolites, all rhombs are consumed at stylolites. Gray #1, core 7803 ft.

Geochemistry and Fluid Inclusions

Geochemical and fluid inclusion analysis of the dolomites helps to understand their origin (Allan and Wiggins, 1993). We have conducted stable isotope, strontium isotope, trace element of the saddle dolomite, blocky calcite, matrix dolomite and matrix limestone and fluid inclusion analysis of the saddle and matrix dolomite and blocky calcite.

Fluid inclusions

Primary fluid inclusions from the saddle dolomite in the New York wells have homogenization temperatures between 110 and 170° C with an average of 130°C (Figure 14). Inclusions of an equivocal primary or secondary origin from the matrix have a similar range of homogenization temperatures with a higher average of 145°C. Secondary fluid inclusions from the saddle dolomites have homogenization temperatures up to 180°C with an average of 173°C. Matrix dolomites have equivocal primary/secondary inclusions with fluid inclusion homogenization temperatures that range from 135-165°C with an average of 145°C. Post-dolomite primary and secondary quartz fluid inclusions have homogenization temperatures ranging from 155° to more than 200°C with an average of 177°C. No petroleum inclusions were found in any mineral.

The salinities of the primary fluid inclusions in both the saddle dolomite range from 13.2 to 15.5 wt % with an average of approximately 14.4 wt % (approximately 4 times normal seawater). The salinity values of the equivocal inclusions in the matrix dolomites are similar with an average of 14.9 wt%. The secondary fluid inclusions in the post-dolomite quartz cement average 16.7 wt. %. These values show that the fluid that made the dolomites and quartz were saline brines. The values for the New York dolomites are not as saline as many brines thought to have precipitated hydrothermal dolomite in the Trenton-Black River in Ontario, Ohio and Michigan and elsewhere in the world, which average closer to 20 wt.% (Allan and Wiggins, 1993; Coniglio et al., 1994).

Stable Isotopes

Stable isotopes of carbon and oxygen were analyzed from matrix dolomite, saddle dolomite and limestone where present (Figure 15). The limestones in the Black River of NY have consistent $\delta^{18}O$ values around –6.5‰. Due to fractionation, dolomite that precipitated from the same water at the same temperature should have $\delta^{18}O$ values of around –3.5 ‰ (Friedman and O'Neil, 1977). The matrix and saddle dolomites in the Black River have $\delta^{18}O$ values between –9 and –12.5 ‰. Increased temperature and mixing of fresh water both can drive $\delta^{18}O$ values toward more negative values. The salinity of the primary fluid inclusions in the dolomites averages 4 times greater than seawater, which eliminates fresh water as a source of lighter (more negative) $\delta^{18}O$ values.

Increased temperature is then the likely source for the depletion of $\delta^{18}O$. The actual temperature of formation cannot be determined without first plotting the $\delta^{18}O$ values vs. fluid inclusion homogenization temperatures from the same samples and

backing out the oxygen isotope composition of the fluid. Figure 16 shows the $\delta^{18}O$ values and fluid inclusion homogenization temperatures for the matrix and saddle dolomites in the TBR in New York. The homogenization temperatures from each sample were averaged and plotted with $\delta^{18}O$. It suggests that the fluid was somewhere between 0 and +4 with an average of +2 ‰. Note that this is considerably heavier (more positive) than the calculated composition of Late Ordovician seawater (around –6 ‰ based on limestone values). If one assumes that the fluid composition did not vary much from around +2 ‰, the temperature of formation can be estimated with some degree of precision from stable isotope values alone using the graph in Figure 16.

Trace Elements

The trace element data show that the Trenton-Black River dolomites are enriched in iron and manganese relative to the limestones (Figure 17). The dolomites are enriched in iron and manganese relative to those that might have formed in normal seawater. The iron content of the dolomites ranges from 1600 to 13,804 ppm and has a median value of ~4250 ppm. In contrast to the dolomites, the limestones from the same cores have a median value of ~550 ppm Fe. The dolomites are also enriched in manganese and have a median value of 880 ppm Mn while the median value for the limestones is only 52 ppm. The relatively high Mn and Fe values of the dolomites support a subsurface origin for the dolomites (*c.f.* Montanez, 1994).

Strontium isotopes

Dolomites that formed from subsurface brines commonly (but not always) have $^{87}Sr/^{86}Sr$ ratios that are higher (more radiogenic) than seawater for the time that they formed (Allan and Wiggins, 1993). The range of $^{87}Sr/^{86}Sr$ ratios of seawater for Trenton and Black River time is between 0.7078 and 0.7085 (Burke et al., 1982). The strontium isotope values for the dolomites in the Black River range from 0.7085 and 0.7092 for both the matrix and saddle dolomites and are just above the range for this time interval. While not strongly radiogenic (enriched in ^{87}Sr), the dolomites do plot above the range for seawater at the time of deposition, which suggests that the fluid that formed the dolomite passed through basement rocks or immature feldspar-rich siliciclastics prior to precipitating the dolomite.

Summary of Geochemistry

The geochemical and fluid inclusion data suggest that the dolomites formed from a hot (110-200°C), saline (3-6 times normal seawater), iron- and manganese-rich, fluid that passed through basement rocks or immature siliciclastics prior to making the dolomite.

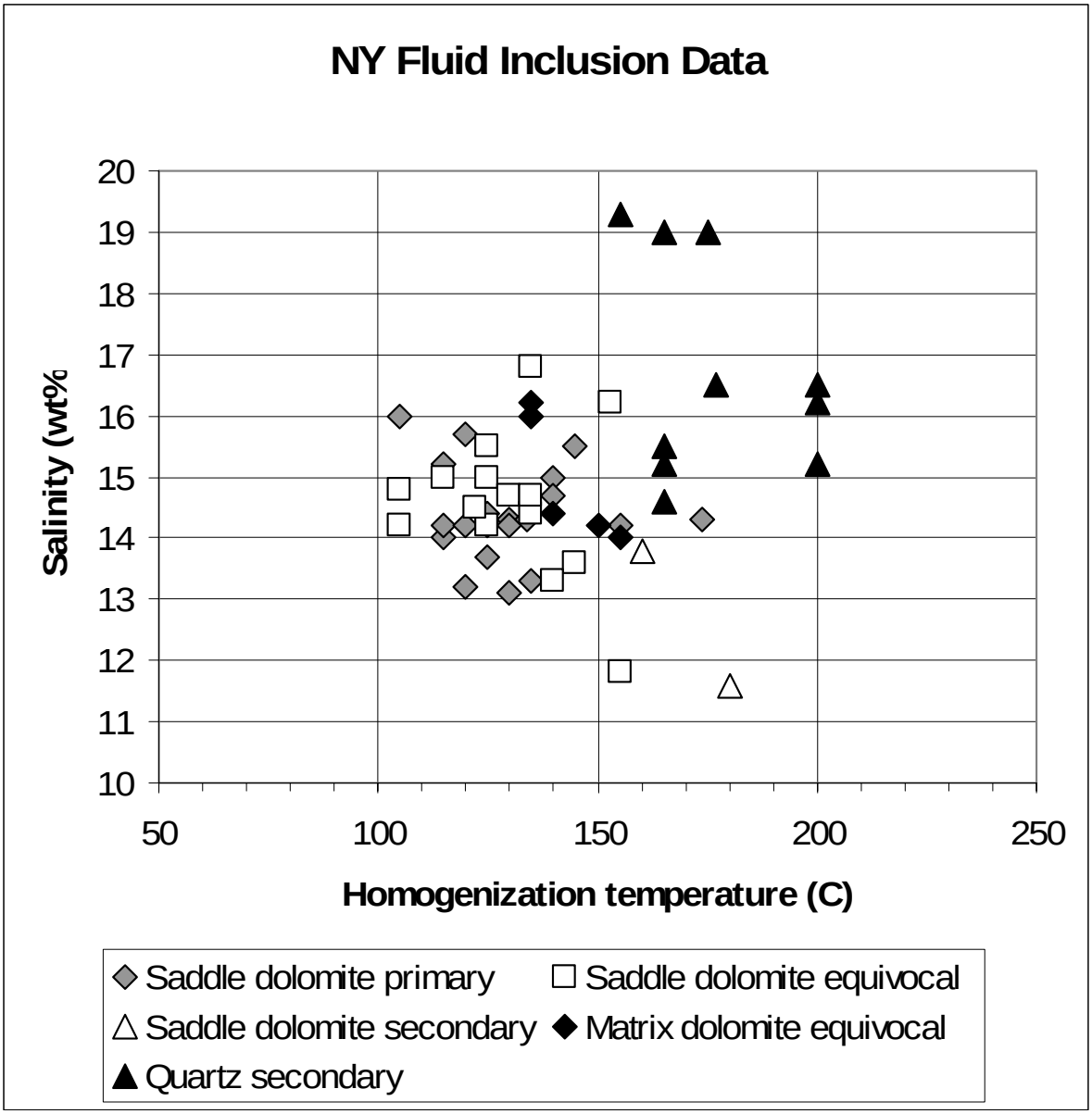

Figure 14. Fluid inclusion homogenization temperatures vs. salinity for samples from the Whiteman #1 and Gray #1 cores.

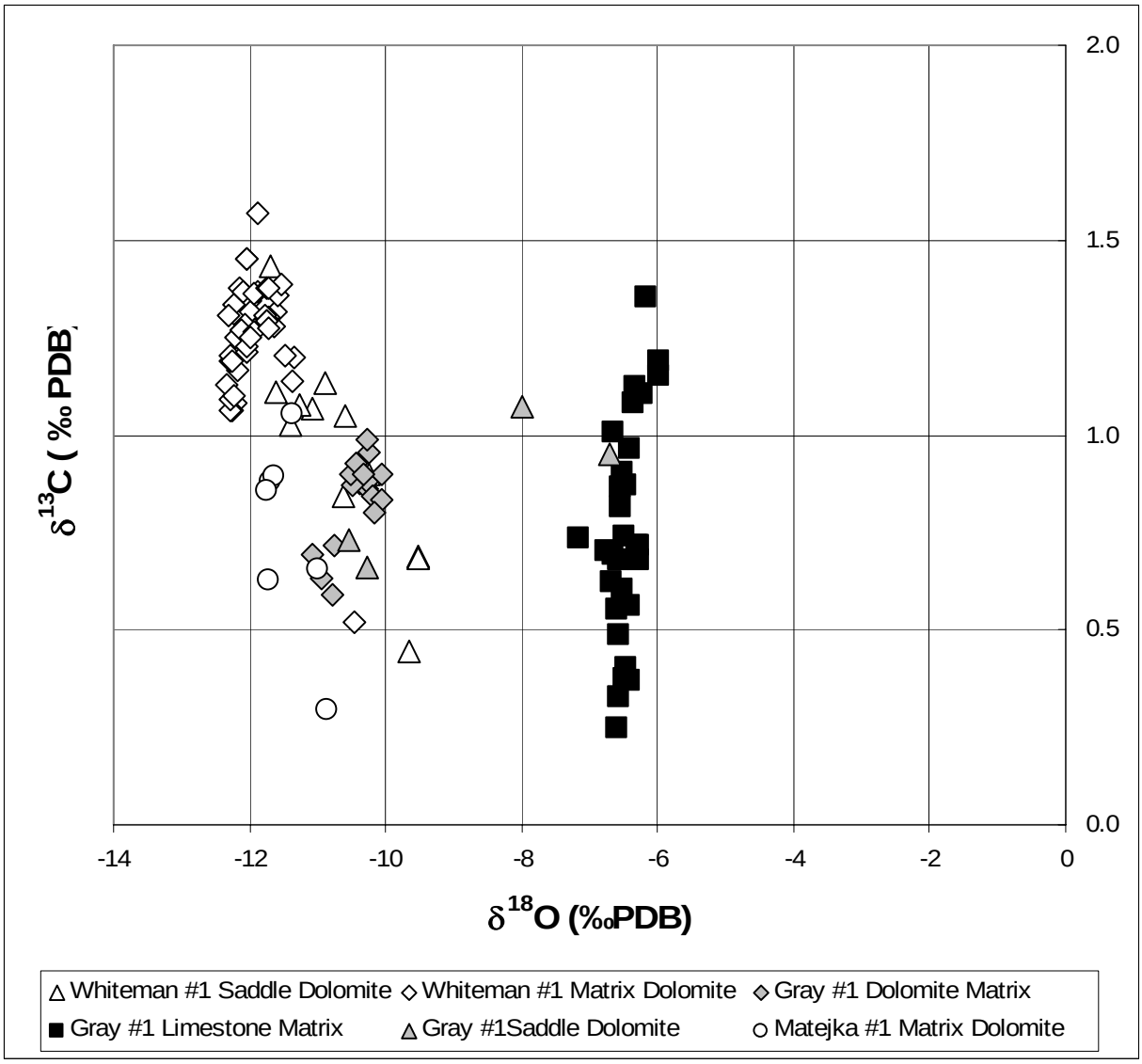

Figure 15. Stable isotope values for samples from the Whiteman #1, Gray #1 and Matejka #1 cores. Values reported versus PeeDee Belemnite standard (PDB).

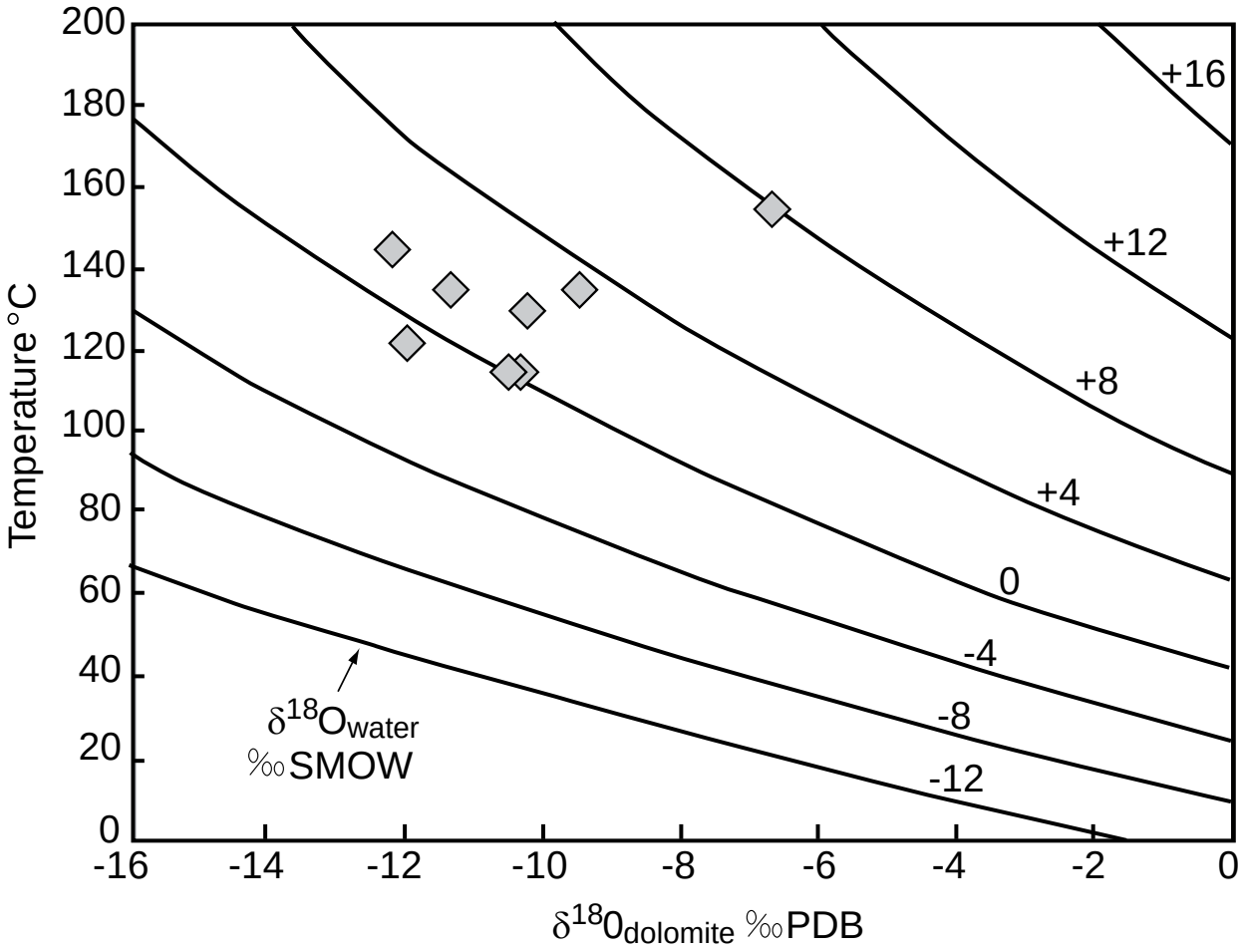

Figure 16. Average fluid inclusion homogenization temperature vs. $\delta^{18}O$ for selected samples in Gray #1 and Whiteman #1 wells. Water values measured versus standard mean ocean water (SMOW).

DISCUSSION

Hydrothermal diagenesis occurs when fluids are introduced to a given formation at a temperature that exceeds the ambient temperature of that formation (*sensu* White, 1957; Davies, 2004). By this definition, there is not a set temperature range at which hydrothermal alteration occurs, the water simply must be warmer than the ambient temperature of the formation due to the local geothermal gradient. For example, if a formation is buried to a depth where the ambient temperature is 50°C and a fluid is introduced that is 60°C, that fluid would here be called a hydrothermal fluid. In the absence of local igneous intrusions, the most likely way for a hydrothermal fluid to be introduced to a formation is via rapid upward fluid flow from greater depths through high-permeability faults and fractures (Deming, 1992). Lateral and vertical unfocused fluid flow through porous and permeable formations, in the absence of faults and fractures, is in most cases too slow to generate hydrothermal conditions because fluids equilibrate with the ambient temperature as they migrate laterally through the formation (Deming, 1994).

Solubility of carbonates (and other minerals) is directly affected by changes in temperature, pressure, partial pressure of CO_2 (P_{CO2}), pH, and salinity and all of these are fluctuating on short time scales in fault-related hydrothermal systems (Rimstidt, 1997). Subsurface fluids flowing rapidly up faults and fractures can maintain their most of their physical and chemical attributes until they are introduced to the formation and where they are then capable of producing significant diagenesis in short periods of time.

Hydrothermal alteration is in this case thought to occur when relatively high-pressure, high-temperature magnesium-rich fluids flow up active transtensional faults and into permeable formations that underlie sealing shales or other low permeability strata. The main diagenetic features produced by the hydrothermal fluids in this case are leaching and dolomitization along with less abundant quartz, bitumen and feldspar mineralization.

Timing and Depth of Burial During Alteration

Hydrothermal fluid flow is thought to be most common while faults are active and much less common during periods of tectonic quiescence (Sibson, 1990, 2000; Davies, 2001; Knipe, 1993; Muir Wood, 1994; Davies and Smith, this volume). The timing of hydrothermal alteration is closely linked to the timing of fault movement.

Most of the faults that have associated dolomitization in New York appear to have been active during Trenton and Utica time (during the Late Ordovician Taconic Orogeny) and largely inactive after that time (Smith et al., 2003a, 2003b). On seismic data, most dolomitized wrench faults in New York die out in the Trenton and Utica and sags are commonly filled in during Trenton or Utica time (see Figure 8). This suggests that most

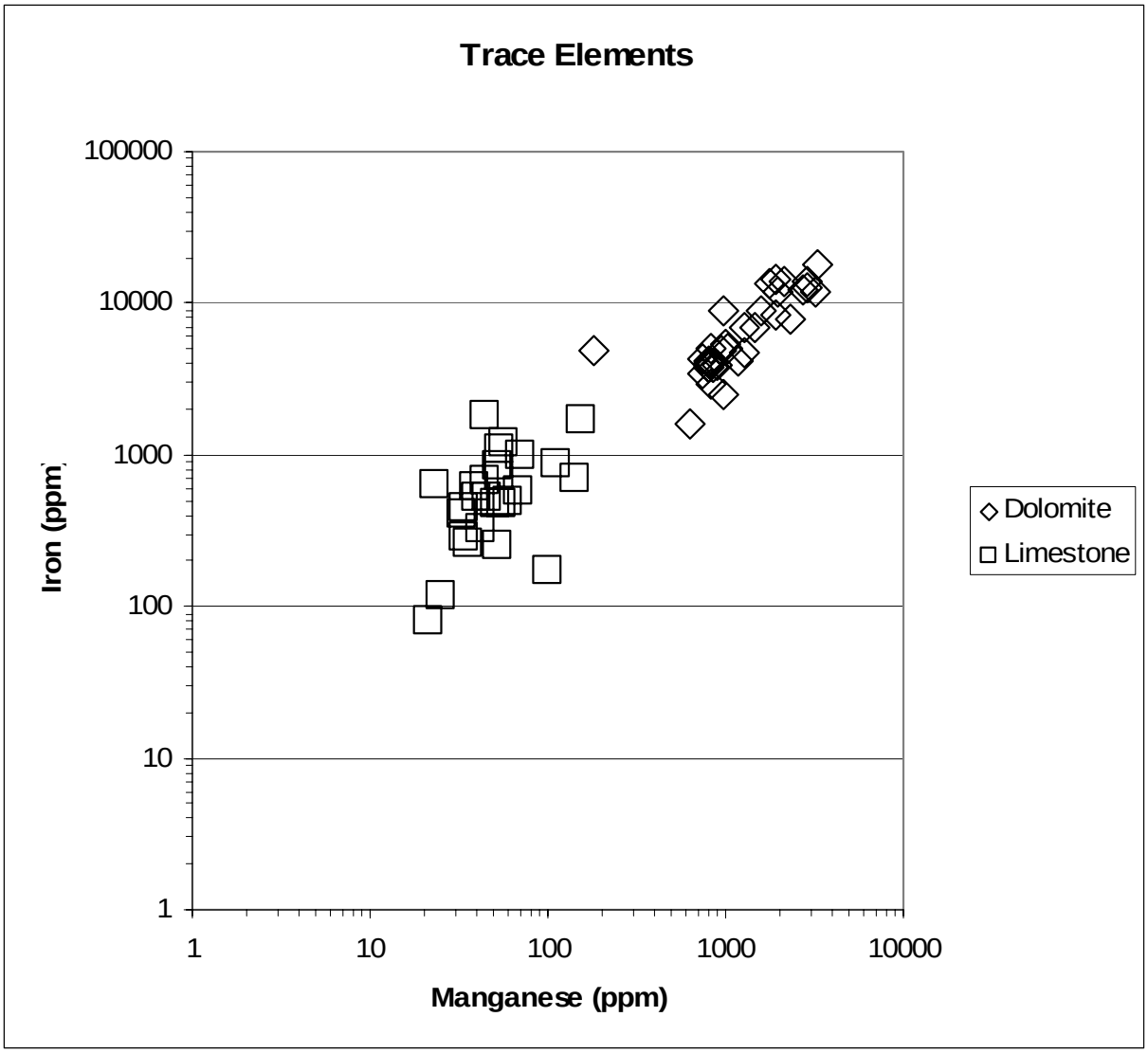

Figure 17. Trace element composition of limestones and dolomites in Gray #1 and Whiteman #1 wells. Dolomites strongly enriched in Mn and Fe relative to limestones.

of these faults were active during the Taconic Orogeny but were not reactivated during subsequent mountain building events.

Further support for significant Trenton and Utica-aged faulting comes from the Mohawk Valley to the northeast of the producing area where normal growth faults with up to 500 feet of throw were active during Trenton and Utica time (Bird and Dewey, 1970; Bradley and Kidd, 1991; Jacobi and Mitchell, 2002; Joy et al., 2000) and from seismites in the Trenton and Utica and equivalents in New York (Baird et al., 1992), Kentucky and Ohio (Pope et al., 1997; McLaughlin et al., 2002; Ettenshohn et al., 2002).

During Trenton and Utica time, when most of the faulting appears to have occurred, the Black River was buried to depths of less than 350 meters (1100 feet) in New York. If hydrothermal alteration occurred during the period of active faulting, the Black River was buried to depths of less than 350 meters.

Demonstration of a Hydrothermal Origin

As a first pass, if dolomitization is highly localized and patchy, the patchiness can be linked to faults and the geochemistry and fluid inclusions support a high-temperature subsurface origin, the mineralization is likely to be hydrothermal in origin. This is the case with the Black River dolomites in New York. The dolomite is patchy, occurs near faults visible on seismic and has geochemical attributes that suggest a hot, subsurface origin. This strongly suggests that fluids flowed up the faults and precipitated dolomite. The sags associated with the faults were filled in during Trenton and Utica time when the Black River was only buried to a depth of a few hundred meters. If fluid flow up faults is most likely to occur when the faults are active, as has been suggested by many who study this process (Knipe, 1993; Sibson, 2000; Muir Wood and King, 1993), dolomitization of the Black River is likely to have occurred as a result of fault-related hydrothermal fluid flow during the first few hundred meters of burial.

The field relations between the faults and dolomitization and the hot subsurface origin of the dolomite strongly suggest a fault-controlled hydrothermal origin it can be argued that this is a strong enough case to approach these as hydrothermal dolomite reservoirs. Some workers require more rigorous proof (Machel and Lonee, 2002), insisting that some dolomites with the same characteristics might have formed due to slow lateral or vertical flow within a deeply buried formation.

A more rigorous method to demonstrate a hydrothermal origin for dolomite is to determine when the dolomitization during the burial and thermal history of the formation in question and compare that to the fluid inclusion homogenization temperatures in the dolomites (Davies, 2001; Machel and Lonee, 2002). If the homogenization temperatures exceed the maximum temperatures that the formation has ever been exposed to during burial, or the known depth and ambient burial temperature at the time of dolomitization, the dolomite or other minerals can be called unequivocally hydrothermal (Machel and Lonee, 2002).

Weary et al. (2001) showed that the area where the dolomite fields are located in New York has experienced very high burial temperatures using conodont alteration indices (CAI) from the overlying Utica Shale. All of the cores examined for this study are located in the area where the CAI values from the overlying Utica Shale are 4.5, which suggests that the Utica was heated to between 187-354°C (Hulver, 1997) or 150-300°C (Harris, 1979). Therefore, in this case, the Black River was buried to a depth where the temperature was equal to or greater than the fluid inclusion homogenization temperatures in the dolomites (Figure 18). This does not mean that the dolomites in New York are not hydrothermal in origin, just that the formation was at some point in time buried to a temperature that exceeded the temperature at which the dolomites formed. If the dolomitization was during early burial, when the ambient temperature was still <100°C (which it appears to have been based on the timing of fault movement and interpreted fluid flow) the dolomite would still be considered to be hydrothermal in origin.

Confirmation of hydrothermal origin for similar Trenton-Black River dolomites comes from Ontario, Michigan and northwest Ohio (Figure 18). In most respects, the dolomitized horizons look the same with matrix dolomitization, breccias, saddle dolomite, fractures and vugs and the clear link to faults. At the Hillman Field in Ontario, fluid inclusion homogenization temperatures for the dolomites ranged from 100-220°C (Coniglio et al., 1994), but CAI analysis in that area suggests that the Trenton Group was never buried more than a kilometer in that area (Colquhoun, 1991). Using a geothermal gradient of 25-30°C/km and a surface temperature of 20°C, the maximum burial temperature was 45-50°C and the homogenization temperatures in the dolomites exceed the maximum ambient burial temperature by 50-170°C. A similar scenario occurs in Michigan where fluid inclusion homogenization temperatures from Trenton-Black River dolomites at Albion Scipio Field exceed the maximum burial temperature by 40-90°C (using fluid inclusion data from Allan and Wiggins (1993) and CAI data from Repetski et al. (2004)). Fluid inclusion homogenization temperatures from the Lima-Indiana Trend in NW Ohio for matrix and saddle dolomites range from 100-160°C, but the Trenton was never buried more than 800-1000 meters in this area (Fluid inclusions analyzed for this report from core in Bowling Green Fault Trend and CAI data from Rowan et al., 2004). Therefore, the Trenton-Black River dolomites are hydrothermal beyond a reasonable doubt in Ohio, Michigan and Ontario.

The dolomites from the fields in Ohio, Michigan and Ontario are virtually identical to those found in New York in appearance, association with wrench faults and geochemicalattributes. It is unlikely that they would have formed by a different process.

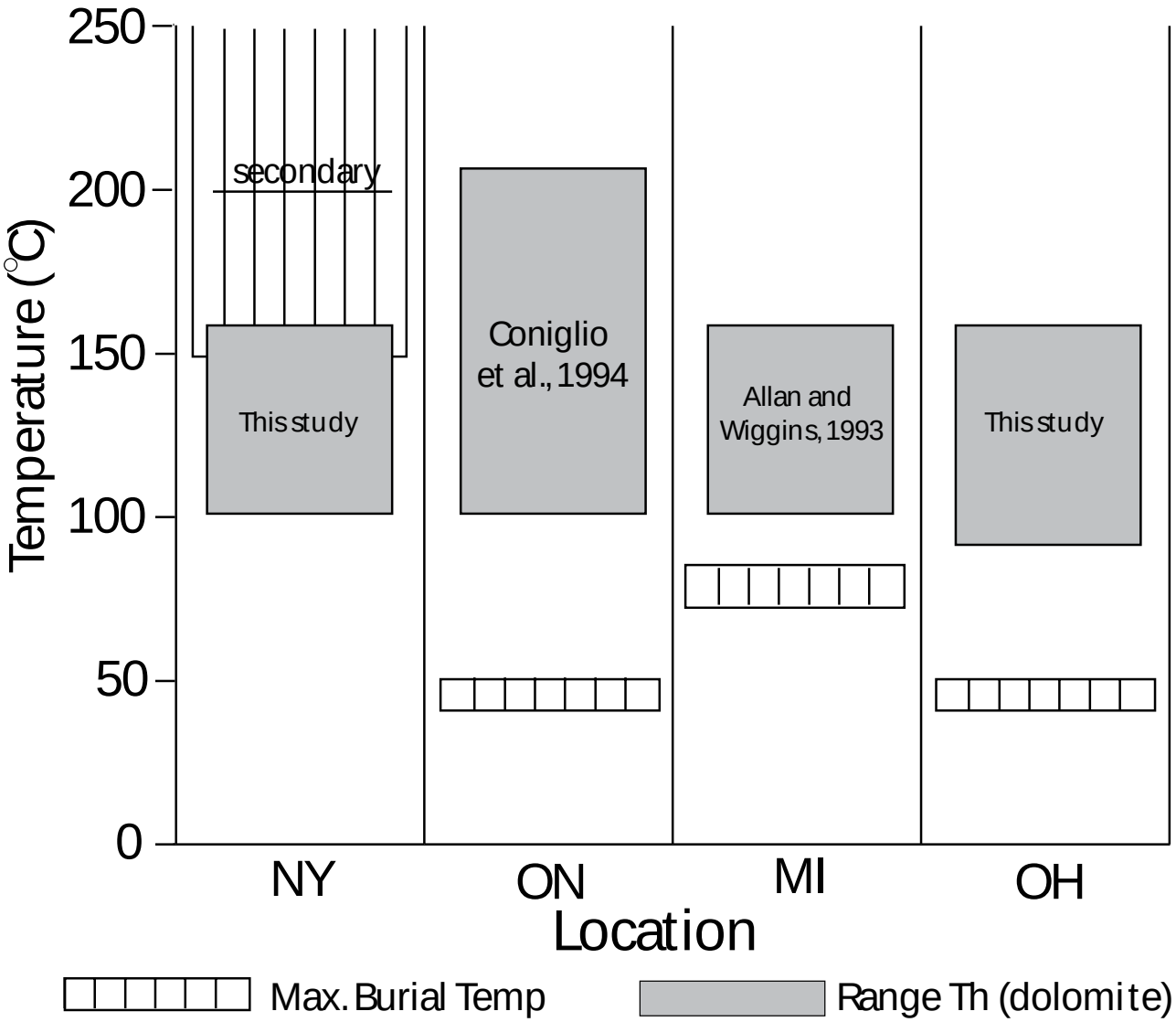

Figure 18. Fluid inclusion homogenization temperature vs. maximum burial depth. Ohio CAI data from Rowan et al., 2004. Ontario fluid inclusion data from Coniglio et al., 1994 and CAI data from Colquhoun, 1991. Michigan fluid inclusion data from Allan and Wiggins, 1993 and CAI data from Repetski et al., 2004.

Origin of Sags

The structural sags could form as a result of the combination of the development of negative flower structures, dissolution of limestone or dolomite and/or the volume reduction associated with the dolomitization of limestone. Negative flower structures form in transtensional parts of strike-slip fault zones. Negative flower structures can show an apparent volume loss because strata are displaced laterally as well as vertically (Dooley and McClay, 1997; many others). It has been convincingly demonstrated that many Trenton-Black River Fields form in structural sags associated with strike-slip faults and negative flower structures (Prouty, 1988; Hurley and Budros, 1990; Davies, 2001; others). This model can explain all of the sag development in the Trenton-Black River reservoirs.

Some relatively minor part of the sags could have been produced by dissolution or by volume reduction during dolomitization. The occurrence of vuggy porosity in most or all Trenton-Black River hydrothermal dolomite fields shows that there has been significant dissolution of limestone, dolomite or both during hydrothermal diagenesis. If the dissolved carbonate was carried away by fluids exiting the altered zone, or was precipitated in tight matrix dolomite and limestone outside of the sag, it is possible that some volume loss may have occurred due to dissolution. Mole-for mole replacement of limestone with dolomite results in a volume loss of 12-13% because dolomite molecules are smaller than calcite molecules (Weyl, 1960). This would have a minor impact on sag development, if any. In many wells, only 10 meters (33 feet) of section are dolomitized, but they still occur in sags visible on seismic. If 10 meters of dolomite were left after dolomitization of 11.3 meters of limestone, this minor volume loss (1.3 meters) would not be detectable on a seismic line.

There is no evidence that the Black River has collapsed into underlying caves in the Beekmantown as was suggested by Loucks (2003a, 2003b). This model is not supported by the seismic (Figure 8B) and can be discarded based on field relations in Ontario where the Black River Group carbonates directly overlie Cambrian siliciclastics which sit directly on the basement and the Beekmantown and equivalents are absent. If there is no Beekmantown, there can be no caves in the Beekmantown in which the overlying Black River might collapse. The sags, breccias and mineralization in the Trenton and Black River in Ontario (such as Rochester Field – Figure 7) are virtually identical to those in New York, Michigan and Ohio (Colquhoun, 1991; Coniglio et al., 1996; Bonnar, 2001). Furthermore, there is little or no offset on the top of the Beekmantown underlying many of the sags in the Black River play in New York (see Figure 8).

Fault Style

The *en echelon* sags in Figure 7 are interpreted to have formed as a result of oblique divergent slip (Smith and Nyahay, 2005) as initially proposed by Harding (1974) for similar en echelon sags at Albion Scipio Field. The main component of fault

movement is thought to be strike-slip, but with a very important extensional component. The individual sags are thought to be negative flower structures that formed over synthetic shear faults that tie back to a master transtensional fault at depth. The extensional component would tend to open the synthetic fractures and make them conduits for upward flowing hydrothermal fluids (Harding, 1974). This might occur at a dilational jog on a longer strike-slip fault or on a pre-existing fault that is reactivated in a transtensional sense rather than pure strike-slip because it is slightly misaligned with respect to the principle compressive stress.

It appears that there are many variations on this theme in the Trenton Black River Play. There may be both right-lateral and left-lateral fault movement (Smith et al., 2003) on different faults and in different parts of the basin associated with the same tectonic event. Fault intersections are common locations for sag development and hydrothermal alteration because they commonly set up quadrants of transtension and transpression. Again, zones of transtension are the most likely to be affected by hydrothermal fluid flow.

Fault-Related Hydrothermal Alteration Model

This model is speculative, but is supported by all of the known facts at this time (Figure 19). Black River Group carbonates were deposited on relatively stable craton (Figure 19A). Major collision between North America and Volcanic Island Arc begins during earliest Trenton time and continues through the Late Ordovician and into the Silurian (Ettensohn and Brett, 2002). This collision led to reactivation of appropriately oriented older faults or activation of new faults. Near the thrust front, thrust loading led to normal faulting oriented subparallel to orogenic belt (Bradley and Kidd, 1991). In the more distal parts of the craton, strike-slip faulting is initiated along appropriately oriented faults.

High-pressure, high-temperature fluids flowed up active basement-rooted strike-slip and transtensional faults (particularly in dilational parts of fault zones) during the time of Trenton and Utica deposition, hit low permeability beds at the base of the Trenton and flowed out laterally into the more permeable limestones of the Black River. Cooling hydrothermal fluids leached the limestone and produced vugs in a migrating front moving away from the fault zone (Figure 19B). As permeability was enhanced by fracturing and leaching, warmer dolomite-supersaturated fluids migrated farther from fault zone precipitating dolomite (Figure 19C). These fluids first produced a halo of matrix dolomite, particularly on the downthrown sides of faults in negative flower structures. Because the fluids flowed up from greater depths where pressures are higher, the elevated pressure of the fluids may have led to hydro-fracturing (*sensu* Phillips, 1972), enlargement of existing fractures and further brecciation. Some dissolution vugs may have formed prior to and during matrix dolomitization. Matrix dolomitization was followed by further fracturing, brecciation and vug development as tectonic activity continued (Figure 19D). Fractures and vugs were lined or filled with saddle dolomite soon after their formation. This later mineralization occurred during active fracturing as is demonstrated by episodic filling of fractures as they opened.

As time passed, fluids evolved and precipitated a range of other minerals including quartz, bitumen, sulfides and calcite. Bitumen may have formed when kerogen within the altered formation and near the faults was heated by the hydrothermal fluids and small quantities of oil formed that coated some pores and fractures ("forced maturation" of Davies, 2001). If the faulting was over by Late Ordovician or Early Silurian time (as it appears to be on many seismic lines), that would make most or all of the diagenesis Late Ordovician to Early Silurian in age. If the faulting continued or recurred during the Devonian Acadian or Pennsylvanian Alleghenian Orogenies some of the later stages of mineralization may have occurred during those times.
Some calcite cementation may have occurred during later pressure solution of the adjacent limestones under normal burial conditions.

Reservoir heterogeneity

All producing wells in the Black River produce from dolomitized intervals, but not all wells with dolomite are porous and/or productive. Some exploration wells are "geological" successes but economic failures because they find dolomite but no effective porosity or they flow water instead of gas. Out of 175 wells that have encountered dolomite in the Black River, only 48 have produced gas (27%). Understanding why some dolomite wells are tight and non-productive while others are porous and produce at higher rates is one of the main challenges in characterization of the Black River play. Some wells could be tight because they are too close to faults and were completely cemented, while others could be too far from faults and do not penetrate enough open faults and fractures. It also is possible that only a certain rock type ends up with matrix porosity after dolomitization and that this rock type is absent in the tight dolomite wells.

The Matejka #1 core (Figure 10) and the Gray #1 core (Figure 11) presented in this paper are both considered "tight" dolomite wells in that they have significant quantities of dolomite, but very low permeability. Most of the dolomite in these wells is matrix dolomite with little or no porosity. The Matejka well has tens of feet of dolomite but no vugs and few open fractures. The Gray #1 core (Figure 11) does have numerous open vugs, but they are isolated because there are few fractures and the matrix dolomite between them has little or no permeability. In many cases, bitumen, quartz or other minerals occur between the dolomite rhombs and may plug what would otherwise be effective porosity.

The Whiteman #1 core has high permeability in several beds that have vuggy and fracture porosity (Figure 11) and the well has been a good producer. This suggests that penetration of at least some open fractures may be essential to drilling a productive well in the Black River dolomite play in New York. The abundance of fractures and saddle dolomite suggest that the Whiteman core may be closer to a fault than the Matejka #1 and Gray #1 wells.

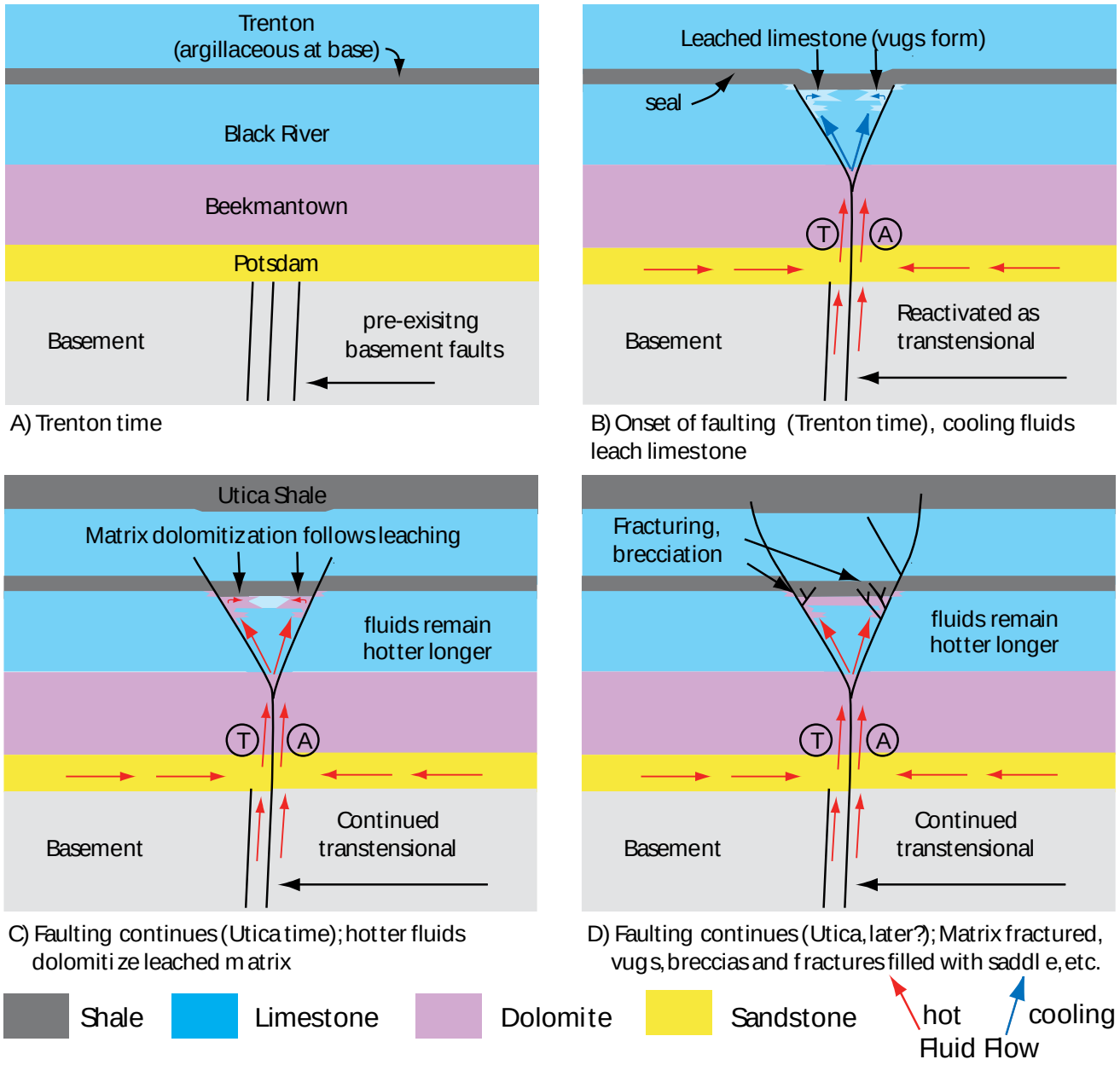

Figure 19. Schematic fault-related hydrothermal alteration model for Black River Group dolomite reservoirs, New York.

The cores studied for this paper suggest that penetrating open faults, fractures and breccias and vugs connected by fractures may be the key to drilling a successful well in this play. Most of the early wells in the trend were vertical wells that were commonly sidetracked once or twice after encountering tight dolomite or limestone. The probability of success on a vertical development well was about 35% (Bob Bonnar, Talisman Energy, pers. comm). This may be because the wells were less likely to penetrate faults and fractures. More recently, a series of horizontal wells have been drilled that have a more consistent level of success (about 60%) along with much higher initial production rates and greater cumulative production (Bob Bonnar, pers. comm.). Because horizontal wells cut across the fault and fracture zones and penetrate the formation at a range of distances from the faults, they have a much higher probability of success. It may also be the case that some successful producers have good matrix porosity, but that no cores have been acquired from these wells. Further research is required in order to fully understand all potential sources of heterogeneity.

Exploration Model

Hydrothermal dolomite (and associated leached limestone) reservoirs represent one of the most significant remaining resources in North America and other mature regions of the world. These reservoirs are likely to have been bypassed in many cases because of their common occurrence in structural lows, which are unlikely to have been drilled during earlier exploration phases. The exploration model for Trenton and Black River hydrothermal dolomite reservoirs is to look for subtle basement-rooted wrench faults and negative flower structures that cut the regional limestone with evidence for movement in the first kilometer of burial. Faults with relatively minor offset that do not extend far above the target formation are typically the best candidates because the faults have not breached the seal for the hydrothermal fluids or the hydrocarbons.

Most documented hydrothermal dolomite reservoirs occur in regional limestones, but that does not mean that hydrothermal alteration is restricted to this scenario. The effects of the hydrothermal alteration may be less obvious where entire formations are dolomitized regionally, but saddle dolomite cemented breccias, fractures and vugs and sulfide ore deposits are very common in regional dolomites and in most cases are probably fault-related hydrothermal in origin (Smith, 2004a). Hydrothermal leached limestone reservoirs may be as common or more common than hydrothermal dolomite. Although leached limestone is not a common component of the Trenton-Black River Play, it does occur in many other settings and similar exploration strategies may lead to success in leached limestone plays as well (Davies and Smith, this volume; Wierzbicki et al, this volume).

CONCLUSIONS

1. Newly discovered natural gas reservoirs in the Black River Group carbonates of New York occur in laterally discontinuous, linear, fractured, vuggy dolomite bodies that occur in structural lows associated with wrench faults.
2. Both matrix and saddle dolomite formed from hot (110-170°C), saline (14.5 wt.%), Fe- and Mn-rich brines with radiogenic strontium isotope values. All of these support a subsurface origin for the dolomite.
3. In Ohio and Michigan, fluid inclusions from similar fault-related dolomitized bodies in the Trenton and Black River have homogenization temperatures that exceed the maximum ambient burial temperature by 40-120°C. That makes the dolomite there unequivocally hydrothermal in origin. In New York, the Black River was buried to a temperature equal to or greater than the homogenization temperatures in the dolomites so the origin of the dolomite is equivocal in that sense. However, the New York dolomites are similar in their link to wrench faults, appearance and geochemical attributes to those in Ohio and Michigan and are here interpreted to have formed in the same way and at roughly the same time.
4. The dolomite, vugs breccias and fractures are interpreted to have formed when high-pressure high-temperature fluids flowed up dilational portions of strike-slip faults when the faults were active, hit a seal at the base of the Trenton and flowed laterally, altering the formation. Vugs formed when limestone was leached by a front of cooling hydrothermal fluids and dolomitization and other mineralization followed soon afterward. Alteration is thought to have occurred during the Late Ordovician Taconic Orogeny when the Formation was buried to a depth of less than 500 meters.
5. Because these reservoirs occur in structural lows, they have been bypassed for many years. More of these reservoirs (and associated leached limestone reservoirs) can and will be found in the Trenton and Black River Groups and in carbonates around the world using the appropriate integrated structural-stratigraphic diagenetic model.

REFERENCES

Allan, J.R. and W.D. Wiggins, 1993, Dolomite reservoirs: Geochemical techniques for evaluating origin and distribution, AAPG Continuing Education Course Notes No. 36, 129 p.

Baird, G.C., Brett, C.E., and D. Lehmann, 1992, The Trenton - Utica Problem Revisited: new Observations and Ideas Regarding Middle - Late Ordovician Stratigraphy and Depositional Environments in Central New York: New York State Geological Association Guidebook, p.1-40.

Bird, J. M., and J. F. Dewey, 1970, Lithosphere Plate-Continental Margin Tectonics and the Evolution of the Appalachian Orogeny. Geological Society of America Bulletin, 81:1031-1060

Bonnar, B., 2001, Talisman Energy Inc. and the Ontario Oil Patch: Does the Shoe Fit? *in:* Ontario Petroleum Institute (OPI) 2001 Annual Meeting Program.

Bradley, D.C., and Kidd, W.S.F., 1991, Flexural Extension of the Upper Continental Crust in Collisional Foredeeps: Geological Society of America Bulletin, v.103, p. 1416–1438.

Brett C. E., and G. C. Baird, 2002, Revised stratigraphy of the Trenton Group in the type area, central New York State: sedimentology, and tectonics of a Middle Ordovician shelf-to-basin succession, p. 231-263. *in:* C. E . Mitchell and R. Jacobi (eds.), Taconic Convergence: Orogen, Foreland Basin and Craton. Physics and Chemistry of the Earth, v. 27.

Burke K., and J. F. Dewey, 1973, Plume-generated triple junctions: key indicators of applying plate tectonics to old rocks: Journal of Geology, v. 81, p. 406-433.

Burke, W. H., Denison, R. E., Hetherington, E. A., Koepnick, R. B., Nelson, H. F. and J. B. Otto, 1982, Variation of seawater $^{87}Sr/^{86}Sr$ throughout Phanerozoic time *in:* Geology, v. 10, p. 516-519.

Colquhoun, I.M., 1991, Paragenetic history of the Ordovician Trenton Group carbonates, Southwestern Ontario [unpublished M.S. thesis], Brock University, St. Catherines, Ontario, 250p.

Coniglio, M., Sherlock, R., Williams-Jones, A.E. Middleton, K. and S.K. Frape, 1994, Burial and hydrothermal diagenesis of Ordovician carbonates from the Michigan Basin, Ontario, Canada in B. Purser, M.Tucker and D. Zenger (eds.), Dolomites, International Association of Sedimentologists Special Publication 21, p. 231-254.

Cornell, S. R. 2001. Sequence Stratigraphy and Event Correlations of upper Black River and lower Trenton Group Carbonates of northern New York State and southern Ontario, Canada, unpublished M.S. Thesis, University of Cincinnati, Cincinnati, Ohio.

Cornell, S. R., and C. E. Brett. 2000. K-Bentonite and sequence correlations of Upper Black River and lower Trenton Limestones from Lake Simcoe, southern Ontario Canada to Watertown, northern New York State. American Association for Petroleum Geologists Bulletin, vol. 84(9):1381.

Davies, G.R., 2001, Hydrothermal (thermobaric) dolomite reservoir facies: Global and western Canadian perspectives, unpublished report, Graham Davies Geological Consultants Ltd, Calgary, 548p.

Davies, G.R., 2004, Hydrothermal (thermobaric) dolomite and leached limestone reservoirs: general principles, genetic connections and economic significance in Canada. American Association of Petroleum Geologists, Annual Convention, Dallas, Abstracts Vol., p. A32.

Davies, G. R. and L. B. Smith, 2006,

Deming, D., 1992, Catastrophic release of heat and fluid flow in the continental crust, Geology, v. 20, p. 83-86.

Dooley, T. and K. McClay, 1997, Analog modeling of pull-apart basins, AAPG Bulletin, v. 81, p. 1804-1826.

Ettensohn, F.R., Kulp, M.A., and Rast, N., 2002, Interpreting ancient marine seismites and apparent epicentral areas for paleo-earthquakes, Middle Ordovician Lexington Limestone, central Kentucky, in Ettensohn, F.R., Rast, N., and Brett, C.E., eds., Ancient seismites: Geological Society of America Special Paper 359, p. 177-190.

Ettensohn, F.R., and Brett, C.E., 2002, Stratigraphic evidence for continuation of Taconian Orogeny into Early Silurian time: in Mitchell, C.E., and Jacobi, R., eds., Taconic convergence: Orogen, foreland basin, and craton: Physics and Chemistry of the Earth, v. 27, p. 279-288.

Gregg, J.M. and D.F Sibley, 1984, Epigenetic dolomitization and the origin of xenotopic dolomite texture, Journal of Sedimentary Petrology, v. 54, p.908-931.

Gonzalez, L.A., Carpenter, S.J. and K.C. Lohmann, 1992, Inorganic calcite morphology: the role of fluid chemistry and fluid flow, Journal of Sedimentary Petrology, v. 62, p. 382-399.

Harding, T.P., 1974, Petroleum traps associated with wrench faults in: AAPG Bulletin, v. 58, p.1290-1304.

Horvath, E., Davies, L. and M. Molgat, 2004, Example of a Trenton-Black River reservoir: a case study of the Rochester Pools, Ontario [abstract], Ontario Petroleum Institute Annual Meeting Program with abstracts.

Hulver, M. L., 1997, Post-orogenic evolution of the Appalachian Basin Mountain system and its foreland [unpublished Ph.D. thesis], University of Chicago, 917p.

Hurley, N.F. and R. Budros, 1990;Albion-Scipio and Stoney Point Fields-USA Michigan Basin in: E.A. Beaumont and N.H. Foster (eds.), Stratigraphic Traps I, Treatise of Petroleum Geology, Atlas of Oil and Gas Fields, A.A.P.G., p. 1-37.

Jacobi, R. D., and Mitchell, C. E., 2002, Geodynamical interpretation of a major unconformity in the Taconic Foredeep: slide scar or onlap unconformity?, Physics and Chemistry of the Earth, v. 27, p. 169-201.

Joy, M.P., Mitchell, C.E., and Adhya, S., 2000, Evidence of a tectonically driven sequence succession in the Middle Ordovician Taconic Foredeep *in:* Geology, v. 28, p. 727-730.

Knipe, R.J., The influence of fault zone processes and diagenesis on fluid flow in: Horbury, A.D., and A.G. Robinson, eds., Diagenesis and basin development, AAPG Studies in Geology #26, p. 131-156.

Landing, E. Westrop, S.R., and Knox, L.A., 1996, Conodonts, stratigraphy and relative sea-level changes of the Tribes Hill Formation (Lower Ordovician, east-central New York) *in*: Journal of Paleontology, v. 70, p. 656-680.

Lavoie, D., 1994. Diachronic collapse of the Ordovician continental margin, eastern Canada: comparison between the Québec Reentrant and the St. Lawrence Promontory. Canadian Journal of Earth Sciences, 31: 1309-1319.

Loucks, R.G., 2003a, Origin of Lower Ordovician Ellenburger Group Brecciated and Fractured Reservoirs in West Texas: paleocave, thermobaric, tectonic or all of the above? [abstract]: AAPG National Meeting Program with Abstracts.

Loucks, R. G., 2003b, Understanding the development of breccias and fractures in Ordovician carbonate reservoirs, in Hunt, T. J., and Lufholm, P. H., The Permian Basin: back to basics: West Texas Geological Society Fall Symposium: West Texas Geological Society Publication #03-112, p. 231–252.

Loucks, R. G., 1999, Paleocave carbonate reservoirs: origins, burial-depth modifications, spatial complexity, and reservoir implications: American Association of Petroleum Geologists Bulletin, v. 83, p. 1795–1834.

Lucia, F.J., 1995, Rock-Fabric/Petrophysical Classification of Carbonate Pore Space for Reservoir Characterization: Bulletin of the American Association of Petroleum Geologists, v. 79, p. 1275-1300.

Machel, H. G., and J. Lonee, 2002, Hydrothermal dolomite- a product of poor definition and imagination, Sedimentary Geology, v. 152, p. 163-171

Machel, H.G., 2004, Concepts and models of dolomitization: a critical reappraisal in: Braithwaite, C. J. R.,Rizzi, G. and Darke, G., eds., The Geometry and Petrogenesis of Dolomite Hydrocarbon Reservoirs. Geological Society, London, Special Publications, no. 235, p. 7–63.

McLaughlin, P.I., Brett, C.E., 2002. Upper Ordovician seismites of Kentucky: a sedimentological and sequence stratigraphic approach, Abstracts with Programs - Geological Society of America v.36, p. 102.

Moore, J.M., 1986, Introduction: the 'Grenville Problem' Then and Now in: Moore, J. M., Davidson, A., and A.J. Baer, eds., The Grenville Province, Geological association of Canada Special Paper 31, p. 1-12.

Nyahay, R. E., and L. B. Smith, 2003, Vertical and Lateral Distribution of Hydrothermal Dolomite in Trenton-Black River carbonates of New York [abstract], AAPG Eastern Section Program with abstracts

Pope, M.C., Read, J.F., Bambach, R.K., Hofmann, H.J., 1997. Late Middle to Late Ordovician seismites of Kentucky, southwest Ohio and Virginia: sedimentary recorders of earthquakes in the Appalachian basin. Geological Society of America Bulletin v. 109, p. 489– 503.

Prouty, C.E., 1988, Trenton exploration and wrenching tectonics in Michigan Basin and environs in B.D. Keith, (ed.), The Trenton Group (Upper Ordovician Series) of eastern North America, A.A.P.G. Studies in Geology 29, p.207-236.

Repetski, J. E., Ruppert, L. F., Ryder, R. T., Weary, D. J., Rowan, E. L. and Trippi, M. H., 2004, Thermal Maturity Patterns for Ordovician, Devonian, and Pennsylvanian Rocks of the Central Appalachian Basin, Based on CAI and Vitrinite Reflectance (%Ro)[abstract], AAPG Eastern Section Meeting Program with abstracts.

Rickard, L.V., 1973, Stratigraphy and Structure of the Subsurface Cambrian and Ordovician Carbonates of New York: New York State Museum Map & Chart No. 18, 77p.

Rowan, E. L., Ryder, R. T., Swezey, C. S., Repetski, J. E., Crangle, R. D., Trippi, M. H. and L. F. Ruppert., 2004, Burial and Thermal History Model of a Cross-Section through the Central Appalachian Basin, Ohio and West Virginia [abstract], AAPG Program with Abstracts

Rimstidt, J.D., 1997, Gangue mineral transport and deposition *in:* H.L. Barnes, ed., Geochemistry of Hydrothermal Ore Deposits, John Wiley and Sons, New York, p. 487-516.

Sibson, R.H., 1990, Faulting and fluid flow *in:* B.E. Nesbitt, ed., Fluids in tectonically active regimes of the continental crust, Mineralogical Association of Canada, Short Course Handbook, v. 18, p. 93-132.

Sibson, R.H., 2000, Fluid movement in normal faulting, Journal of Geodynamics, v. 29, p. 469-499.

Smith, L.B. and R.E. Nyahay, 2005, Wrench fault architecture of Trenton Black River Hydrothermal Dolomite Reservoirs, in AAPG Eastern Section Meeting Program with Abstracts

Smith, L.B., 2004a, Hydrothermal Alteration of Carbonate Reservoirs: How Common is it? *in:* AAPG National Meeting Program with Abstracts, p. A130.

Smith, L.B. Nyahay, R.E. and B. Slater, 2004b, Outcrop Analogs for Hydrothermal Dolomite Reservoirs, Mohawk Valley, New York, *in* Program with Abstracts, AAPG Eastern Section Meeting

Smith, L. B., Lugert, C. M., and R . E. Nyahay, 2003a, Integrated Characterization of Hydrothermal Dolomite Reservoirs in Trenton-Black River Carbonates of New York (abstract): AAPG National Meeting Program with Abstracts.

Smith L.B. and R.E. Nyahay, 2003b, Trenton-Black River Hydrothermal Dolomite Reservoirs: An Integrated Structural Stratigraphic Diagenetic Play in AAPG Eastern Section Program with Abstracts

Taylor, T.R. and D. F. Sibley, 1986, Petrographic and geochemical characteristics of dolomite types and the origin of ferroan dolomite in the Trenton Formation, Ordovician, Michigan Basin, Sedimentology, v. 33, p. 61-86.

Thomas, W. A., 1991, The Appalachian-Ouachita rifted margin of southeastern North America, Geological Society of America Bulletin, v. 103 p. 415-431.

van Staal, C.R., 2005. The Northern Appalachians. In: Encyclopedia of Geology. R.C. Selley, L. Robin, M. Cocks and I.R. Plimer (Editors). Elsevier, Oxford, Vol. 4: 81-91.

Weyl, P.K.1960, Porosity through dolomitization: conservation of mass requirements: Journal of Sedimentary Petrology, v. 30, p.85-90.

Weary, D. J., Ryder, R. T., and R. E. Nyahay, 2001, Thermal maturity patterns in New York State using CAI and $\%R_O$, Northeastern Geology and Environmental Science, v. 23, p. 356-376.

White, D. E., Thermal waters of volcanic origin, Geological Society of America Bulletin, v. 68, p. 1637-1658.

Wickstrom, L.H., Gray, J.D., and R. D. Stieglitz, 1992, Stratigraphy, structure, and production history of the Trenton Limestone (Ordovician) and adjacent strata in northwestern Ohio, Ohio Geological Survey Report of Investigation 143, 78 p.

Wierzbicki, R., Dravis, J.J., Al Aasm, I. And N. Harland, in review, Dolomitization and porosity evolution of Upper Jurassic Abenaki platform carbonates, Deep Panuke Reservoir, Nova Scotia: Hydrothermal or Deep Burial diagenetic processes or both?, submitted to AAPG Bulletin

APPENDIX E

Appendix E-1 – Non-skeletal grains and skeletal components of the Trenton-Black River

Non-skeletal grains

Ooids

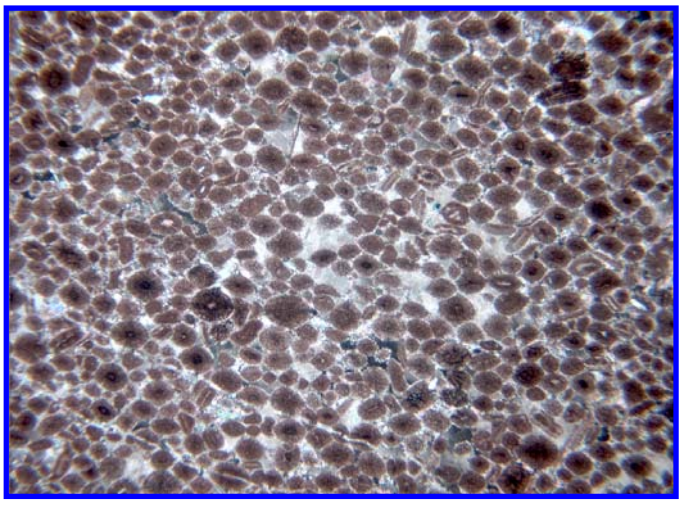

Ooids, Example #1
Pennsylvania, Union Furnace outcrop
Black River Group

This oolitic grainstone occurs in the Black River Formation of Pennsylvania. The ooids in this thin section have not been extensively micritized and the original radial fabric has been preserved.

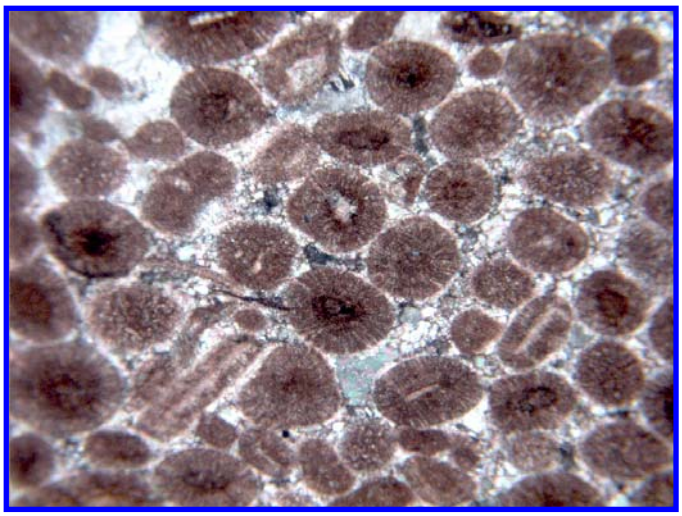

Ooids, Example #2
Pennsylvania, Union Furnace outcrop
Black River Group

This photograph is the ooid grainstone shown above at higher magnification. The radial fabric and concentric laminations of the ooid structure is more obvious in this photograph. Notice the elongate ooids that are coating elongate skeletal grains. Sparry calcite cement is the only intergranular material present.

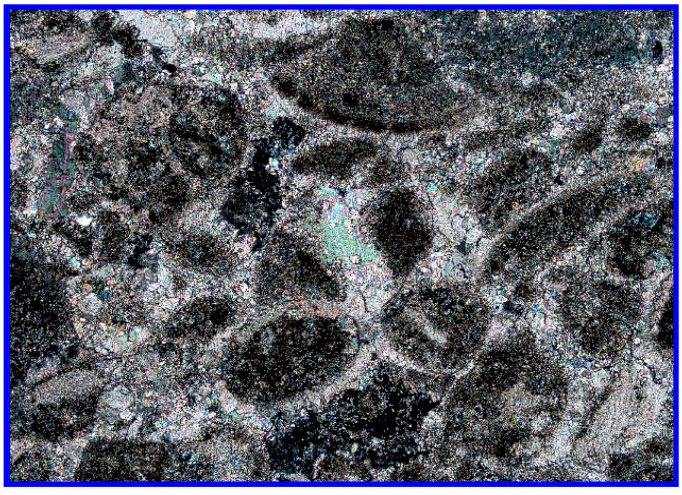

Ooids, Example #3
West Virginia, Wood County
Black River Group, 10,103 ft

Unlike the ooids above the ooids in this grainstone have been highly micritized and the outer structure has been replaced with calcite. The relic radial fabric is still recognizable. Ooids are not nearly as common in this grainstone as above. This photograph was taken under crossed polars.

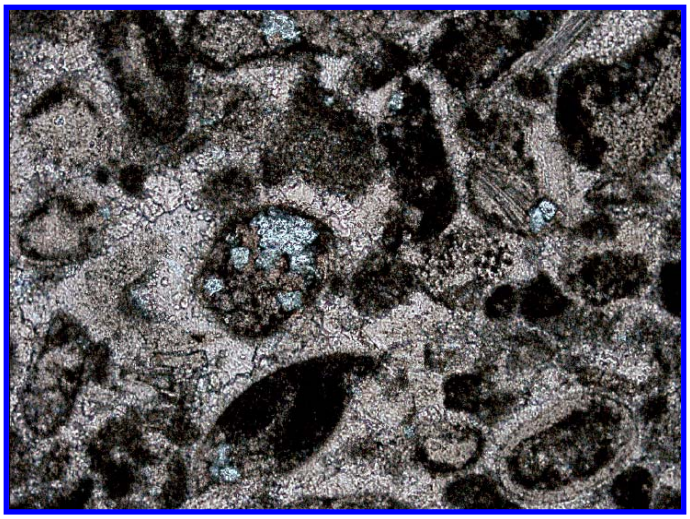

Ooids, Example #4
West Virginia, Wood County
Black River Group, 10,103 ft

This is another view of the ooid in the grainstone shown above. In this photograph, taken in plane light, the core of the ooid is highly micritized and the outer laminae replaced with calcite spar.

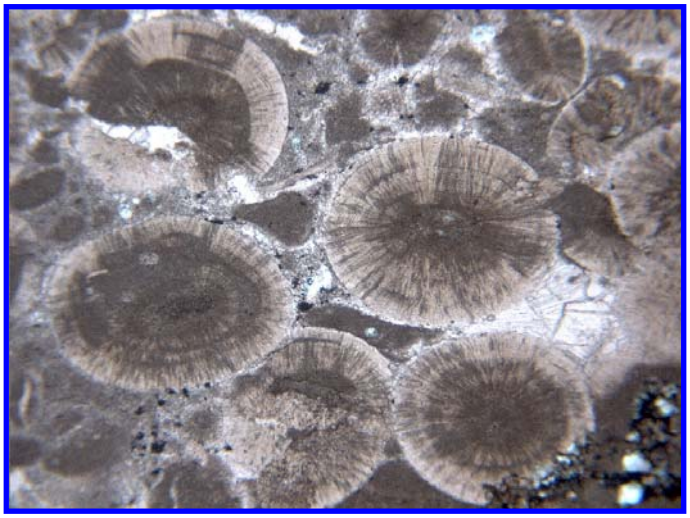

Ooids, Example #5
Pennsylvania, Union Furnace outcrop
Black River Group

The radial fabric and concentric laminations of the ooids are very evident in this photomicrograph. These ooids have been partially dissolved as a result of pressure solution. The intergranular material is both micritic matrix and sparry calcite cement. There also appear to be some meniscus type cements between the individual ooids. These cements were not precipitated in the vadose zone, but are microbially induced marine cements.

Peloids

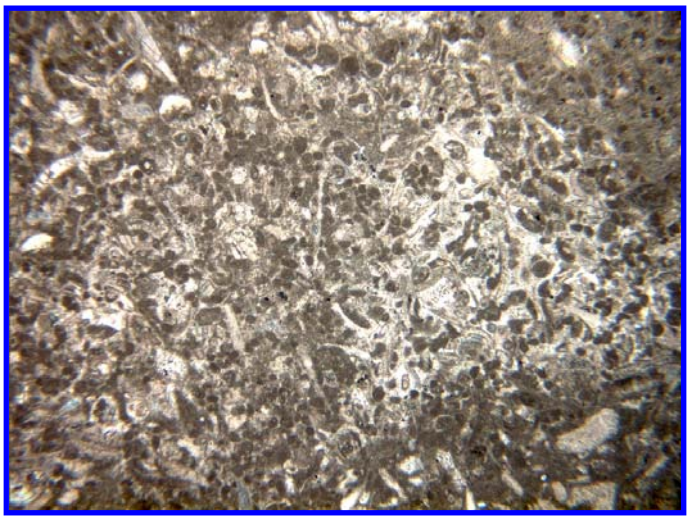

Peloids, Example #1
Pennsylvania, Union Furnace outcrop
Black River Group

The peloids in this peloidal/skeletal grainstone from Pennsylvania are small and irregularly shaped. The irregular/elongate shape of the small peloids grains may suggest that they are micritized skeletal grains.

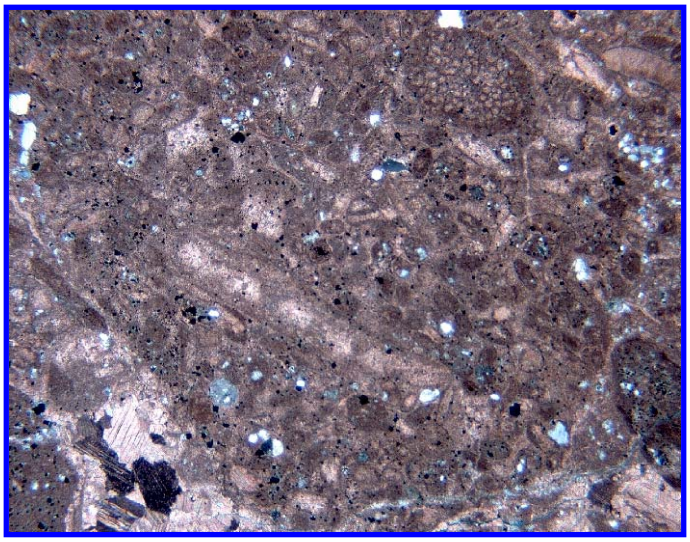

Peloids, Example #2
Pennsylvania, Union Furnace outcrop
Black River Group

The peloids in this packstone from Pennsylvania are larger than those shown above and not as abundant. Some of the peloids near the lower portion of the section have a visible core grain suggesting that the peloids in this slide are micritized ooids.

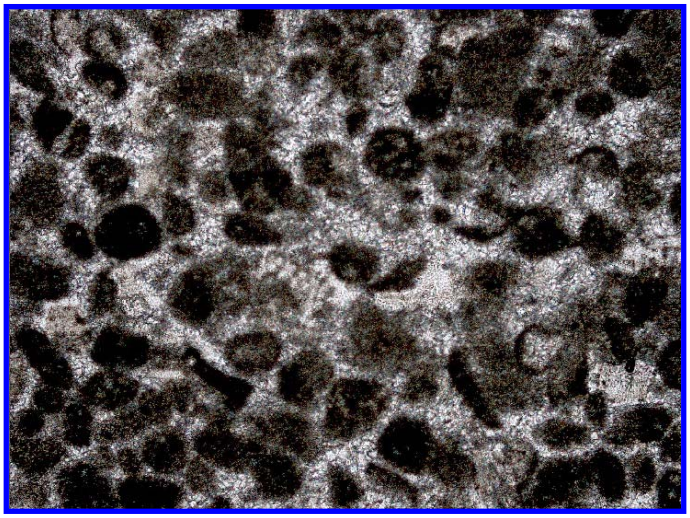

Peloids, Example #3
West Virginia, Wood County
Black River Group, 10,048 ft

The peloids in this grainstone are typical of those observed in the West Virginia core. Notice the distinct grain boundaries of the peloids in the photograph; this is very different from the 'fuzzy' boundaries observed in peloidal cements.

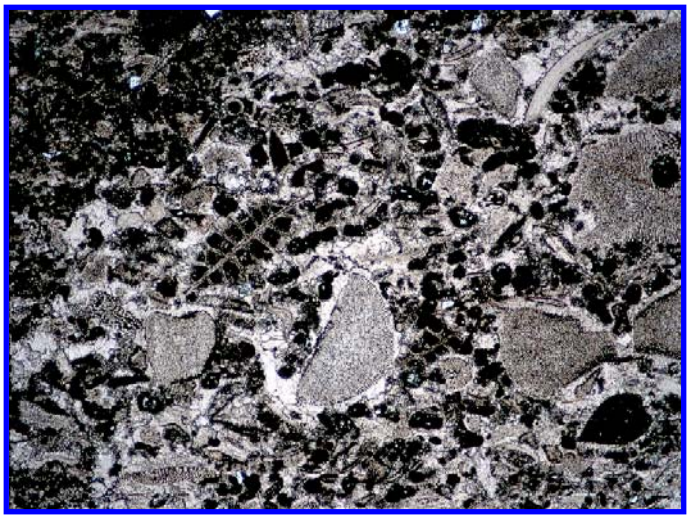

Peloids, Example #4
West Virginia, Wood County
Black River Group, 10,100 ft

The peloids in this skeletal grainstone are clearly micritized skeletal grains. Evidence for the micritization is obvious in the bivalve grain that has been completely micritized in the lower right corner of the section. The grain is clearly identified by its distinct shape.

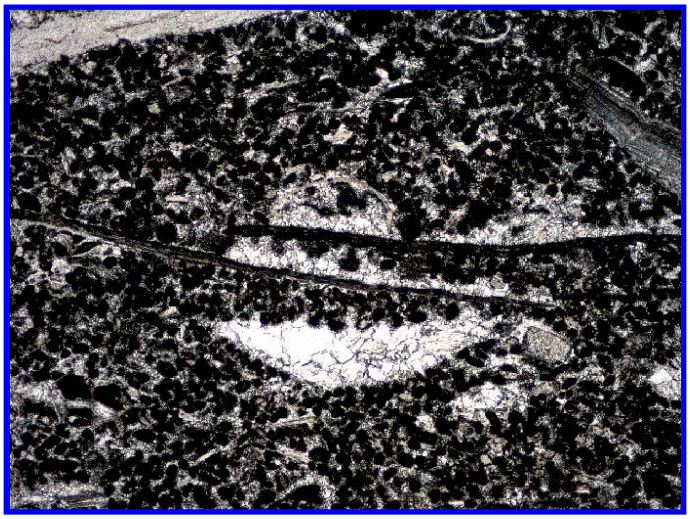

Peloids, Example #5
West Virginia, Wood County
Black River Group, 10,048 ft

The origin of the peloids is hard to determine in this thin sections. The peloids are much smaller than any of the skeletal grains present and all the peloids are about the same size and shape.

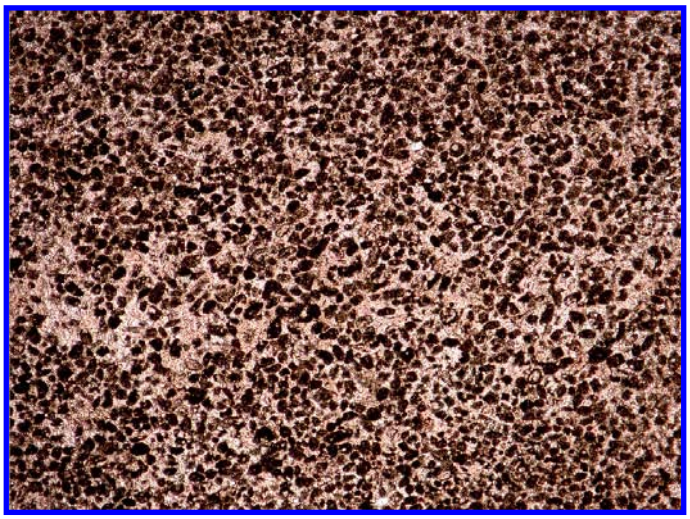

Peloids, Example #6
West Virginia, Wood County
Trenton Formation, 9796 ft

Peloids are the only grains observed in this peloidal grainstone from West Virginia. The peloids are very well sorted.

Intraclasts

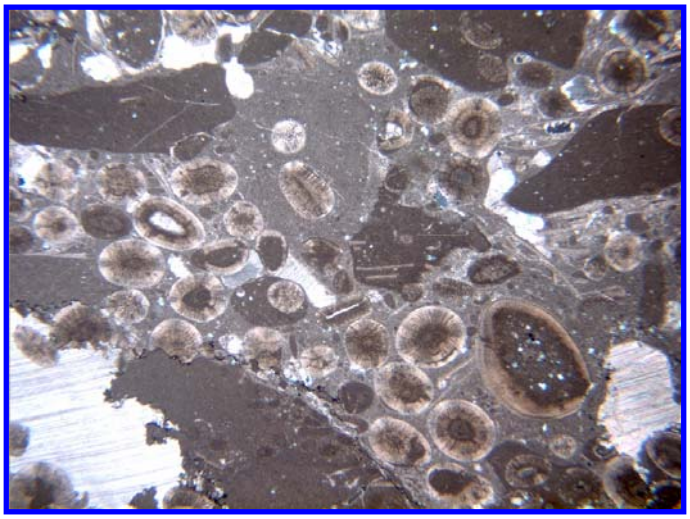

Intraclasts, Example #1
Pennsylvania, Union Furnace outcrop
Black River Group

There are two types of rip up clasts observed in this Pennsylvania, Black River thin section: mudstones and ooid wackestones. The mudstone intraclasts are dark in color and irregularly shaped. The ooids have very good preserved microstructures. The matrix in the ooid wackestones is lighter in color than that observed in the mudstone rip ups.

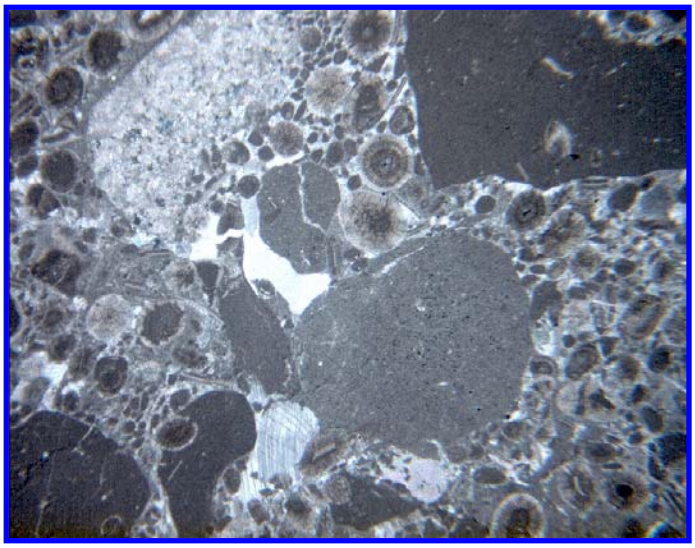

Intraclasts, Example #2
Pennsylvania, Union Furnace outcrop
Black River Group

The individual intraclasts in this mixed oolitic/mudstone intraclastic wackestone are hard to identify. It appears that you have mudstone intraclasts and oolitic wackestone intraclasts, but in some cases ooids are incorporated into the mudstone clasts.

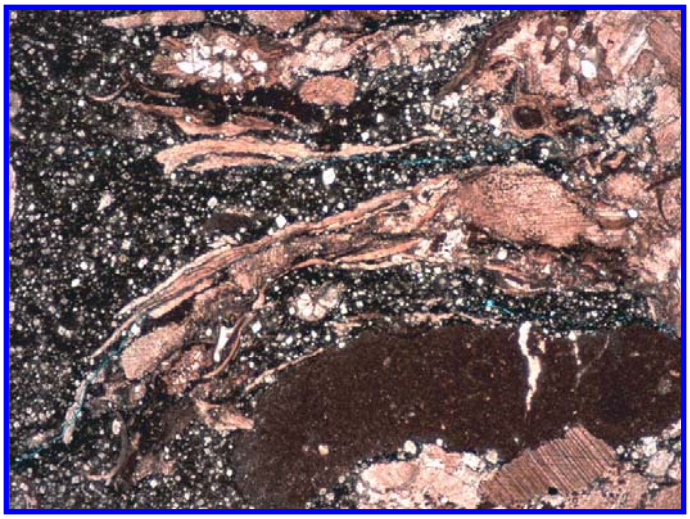

Intraclasts, Example #3
Pennsylvania, Union Furnace outcrop
Black River Group

The subrounded muddy intraclast at the bottom of the section contain some calcite filled fractures. These fractures are clearly early because they have not affected the rest of the rock.

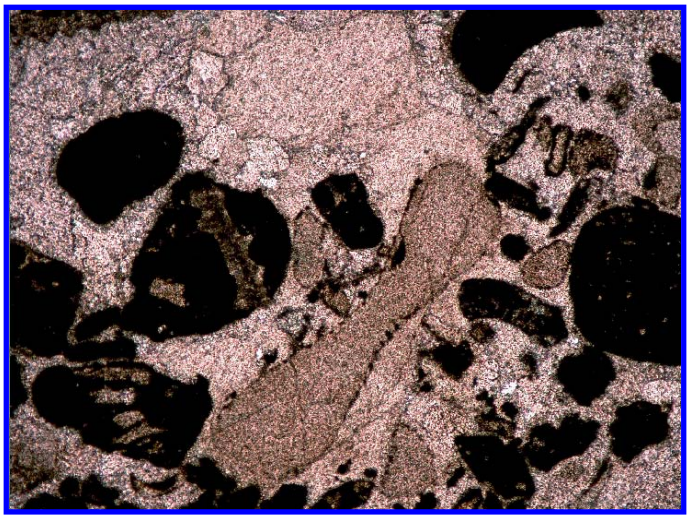

Intraclasts, Example #4
West Virginia, Wood County
Trenton Formation, 9798 ft

The rounded intraclasts in this thin section are poorly sorted showing a range of sizes and shapes. Notice that most of the intraclasts do not contain recognizable grains, but skeletal grains are observed in some of the larger ones indicating that these rocks were originally skeletal wackestones.

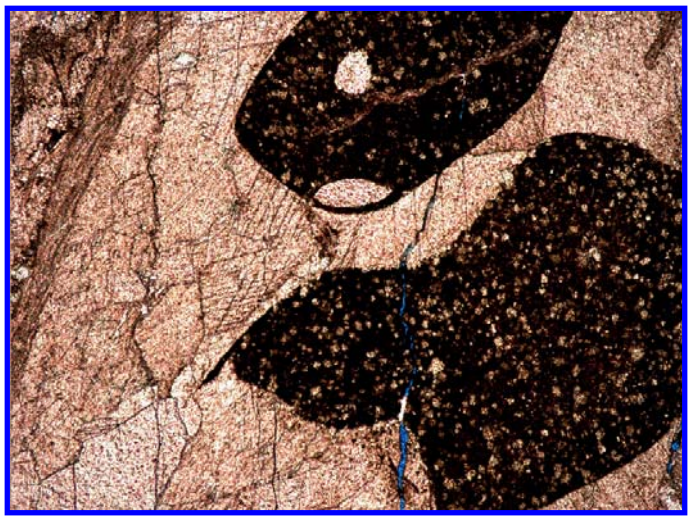

Intraclasts, Example #5
West Virginia, Wood County
Trenton Formation, 9630 ft

The intraclasts and the calcite spar are both large in this intraclastic/skeletal grainstone. The intraclasts are irregularly shaped and contains some skeletal material as well as a dolomitic matrix.

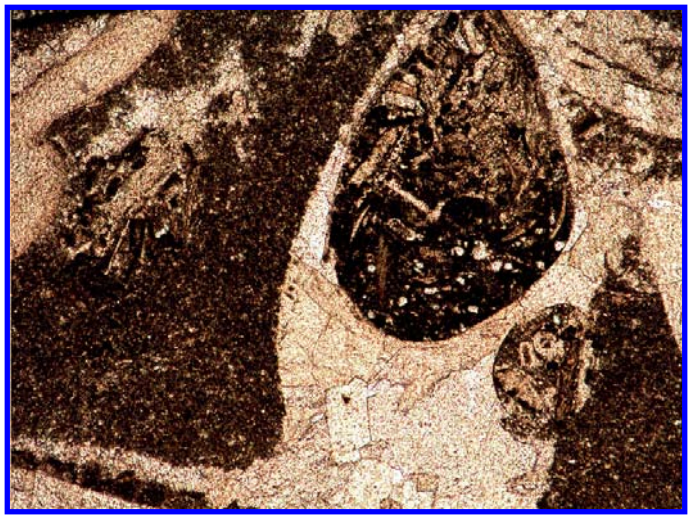

Intraclasts, Example #6
West Virginia, Wood County
Trenton Formation, 9647 ft

This intraclastic grainstone is very similar to above, but the irregular shaped intraclasts clearly contain recognizable skeletal grains.



Intraclasts, Example #7
West Virginia, Wood County
Black River Group, 9951 ft

The intraclasts in this grainstone are composed of a peloidal wackestone. The original peloids are still discernible in this thin section. Notice the variety of cements in this photo including drusy, prismatic and intragranular spar.

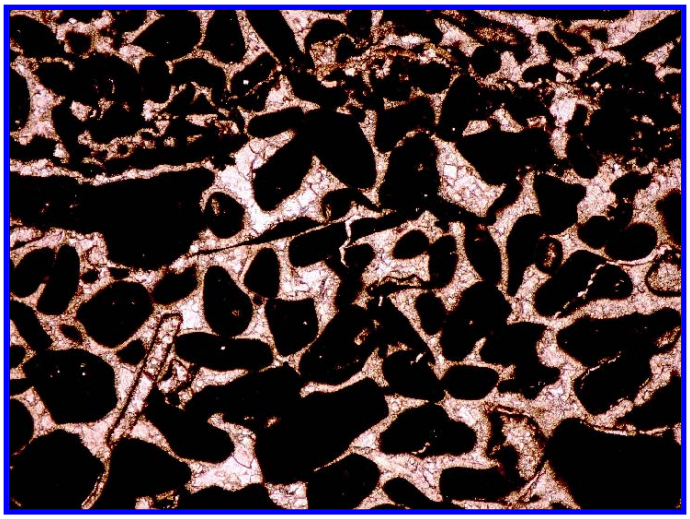

Intraclasts, Example #8
West Virginia, Wood County
Trenton Formation, 9655 ft

The intraclastic grainstone in this photograph contains a variety of irregularly shaped intraclasts. The grain shapes suggest that some are micritized skeletal grains. There is a mollusk grain in the lower left portion of the slide with a very well developed micritic envelope.

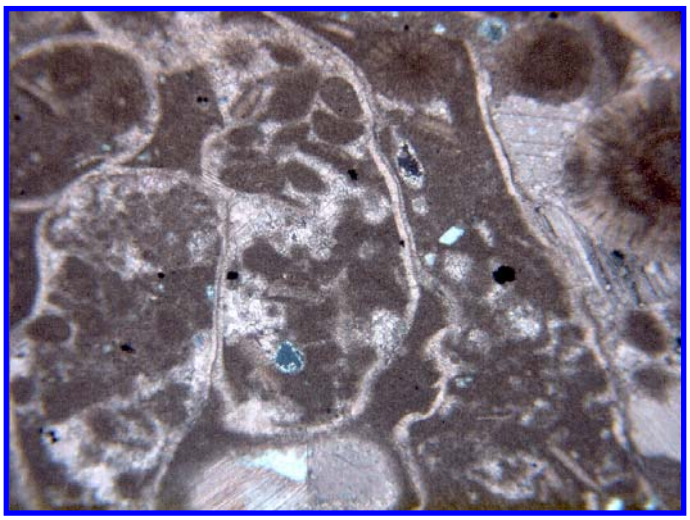

Aggregates, Example #1
Pennsylvania, Union Furnace outcrop
Black River Group

The aggregates in this thin section are comprised of peloids. Notice that the peloids are bound by sparry calcite cement. The aggregate gains also contain a thin, superficial, oolitic coating.

Non-Carbonate Grains

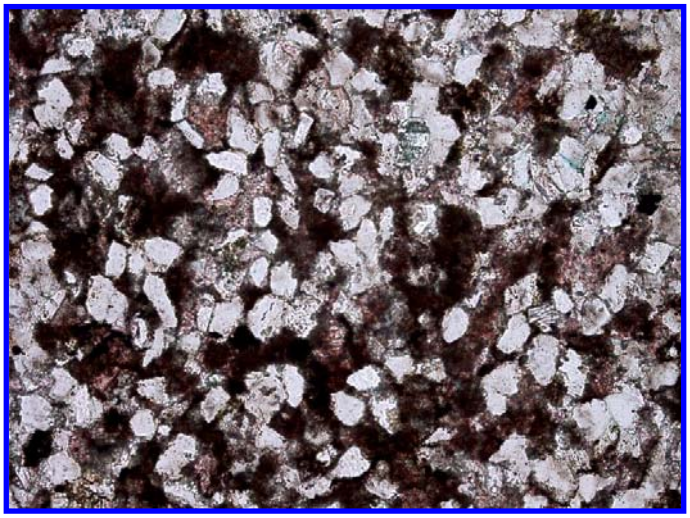

Quartz, Example #1
Pennsylvania, Union Furnace outcrop
Black River Group

The quartz grains in this rock from the Black River Group in Pennsylvania are the dominant grains present. The grains are rounded to subrounded.

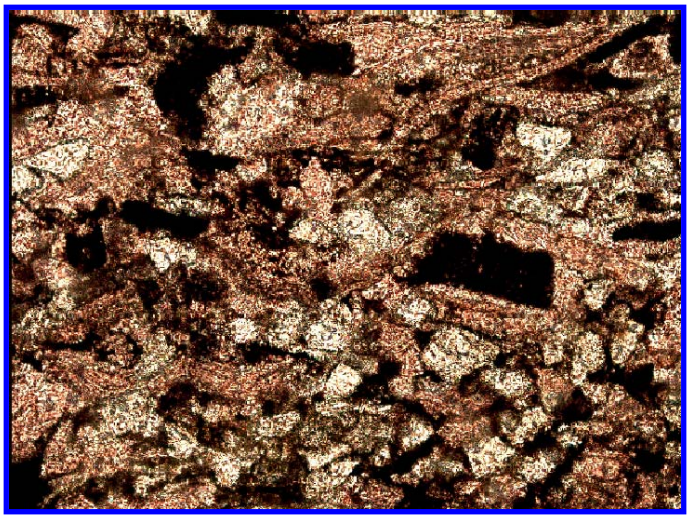

Quartz, Example #2
West Virginia, Wood County
Trenton Formation, 9662 ft

There are quartz grains found in the Trenton Formation in West Virginia. Notice the pyramidal terminations of the colorless quartz grains in this thin section. This crystal shape is characteristic of quartz.

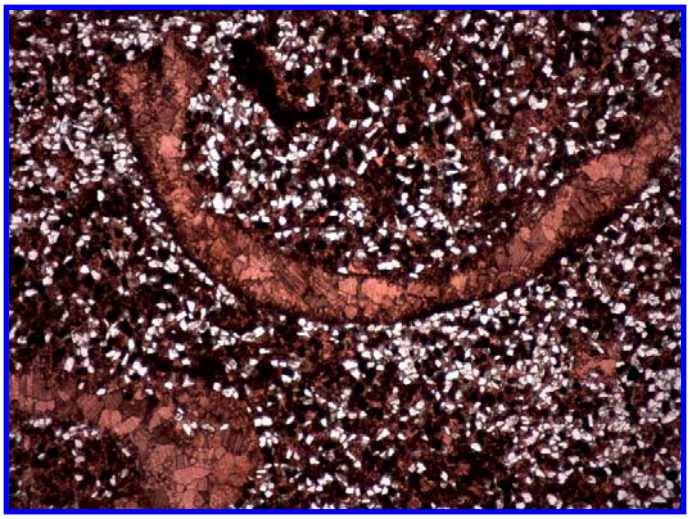

Quartz, Example #3
Pennsylvania, Union Furnace outcrop
Black River Group

Quartz is an important component in this skeletal/peloidal packstone. This quartz rich zone likely represents a time of sea level low when terrigenous sediment was transported into this lagoonal environment.

Algae

Both red and green calcareous algae are found in the Trenton and Black River Groups. These grains are much less common than the other skeletal grains observed in the formations.

Red Algae

Red algae (Rhodophyta) belonging to the Family Solenoporaceae are observed in the Trenton-Black River. The red algae are composed of high-Mg calcite and the grains are generally cm-sized. The original internal and external structures of the red algae are

often preserved because of their high-Mg calcite composition (Scholle and Ulmer-Scholle, 2003, p.22).

The red algae are identified by their very fine-scale reticulate, cellular or latticework internal structure. Solenoporoids are characterized by radiating tubular or filamentous structures and are often found as encrusting, rounded, or nodular masses (Scholle and Ulmer-Scholle, 2003, p.22).

Green Algae

Green algae (Chlorophyta) also contribute to the sediment comprising the rocks of the Trenton and Black River Groups. The abundance of green algae is much less than that of other skeletal grains present, but is similar to the abundance of red algae.

The two important green algae groups important in the Middle Ordovician are the Codiaceae and the Dasycladaceae. We have identified Codiacian variety green algae in the Trenton and Black River rocks. The codiacean algae include *Halimeda* and *Penicillus*, which are common contributors to reefs and lagoons in modern carbonate environments. In thin section *Halimeda* occurs as rounded, sand-sized grains with a swiss cheese texture; Penicillus disintegrates to lime mud or micrite and is not discernible in thin section (Tucker, 1991).

Red Algae, Example #1
West Virginia, Wood County, Trenton Formation, 9838 ft

This large red algae grain shows the characteristic simple elongate cellular or tubular fabric of the Solenopora sp. This fragment occurs in a poorly sorted skeletal wackestone near the base of the Trenton Formation.

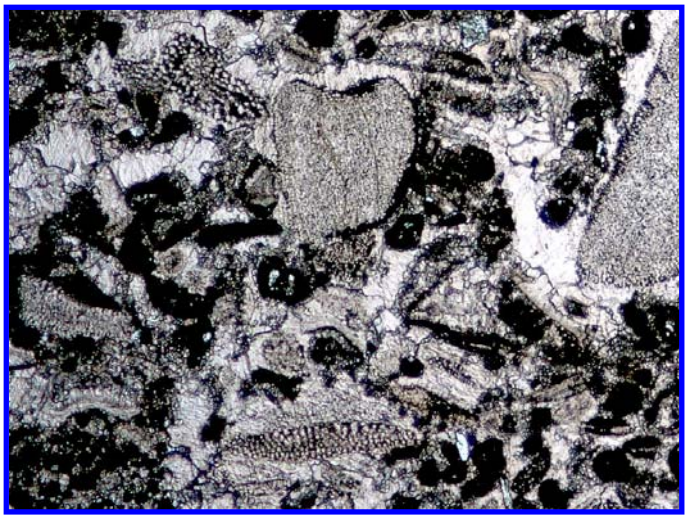

Green Algae, Example #2
West Virginia, Wood County, Trenton Formation, 10,100 ft

There a few elongate codiacian green algae present in this skeletal grainstone of the Trenton Formation.

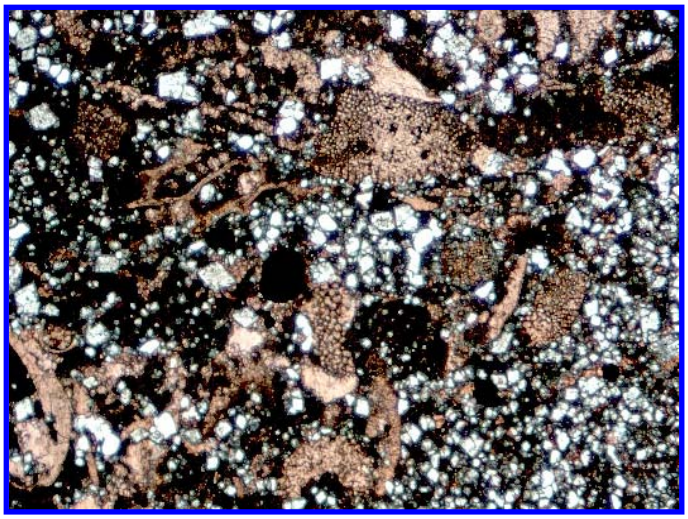

Green Algae, Example #3
West Virginia, Wood County, Trenton Formation, 10,423 ft

There are numerous irregularly shaped codiacian green algae present in this dolomitized skeletal wackestone.

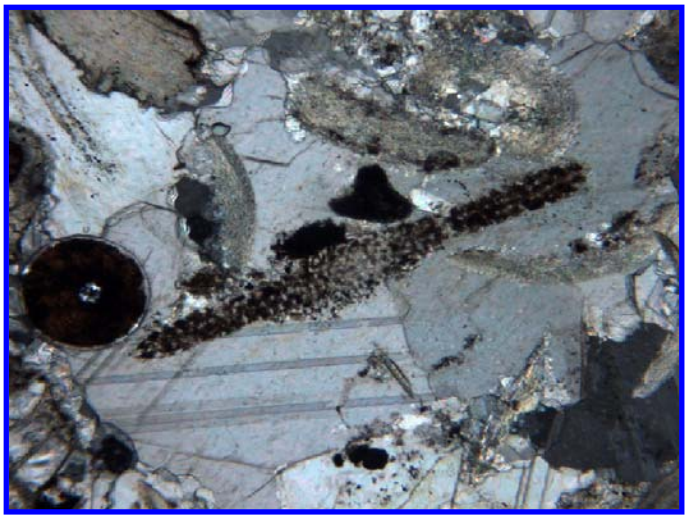

Green Algae, Example #4
Pennsylvania

This example of calcareous green algae is from the Trenton-Black River of Pennsylvania. The elongate grain is like the codiacian variety of green algae.

Brachiopods

Brachiopods were common in shallow Paleozoic seas and are common constituents of the faunal assemblages observed in the Trenton and Black River rocks of the study area. Brachiopods are bilaterally symmetrical with two valves or shells of unequal size. The shells range from smooth to corrugated or spiny. Brachiopods cannot be distinguished from bivalves in thin section without paying careful attention to the defining features of the shell microstructure (Scholle and Ulmer-Scholle, 2003).

The low-Mg calcite composition of most brachiopods shells often result in preservation of the shell microstructure. The common structure of a brachiopod shell consists of two layers. The thin outer or primary layer is comprised of fine calcite fibers oriented perpendicular to the brachiopod shell. The thin outer layer is not always preserved. The inner or secondary layer is thicker with calcite fibers inclined obliquely to the surface of the shell. The microstructure of the shell is most commonly fibrous, but can also be prismatic (Scholle and Ulmer-Scholle, 2003).

Modifications to the microstructure of the brachiopod result in distinct structures that can aid in brachiopod identification (Scholle and Ulmer-Scholle, 2003). These microstructures are:

- **Laminated** – interlaminated sheets of phosphate and chitin, not common in limestones
- **Impunctate** – primary and secondary layers lack perforations
- **Punctate** – shells have small holes that perforate the shell wall and are oriented perpendicular ot the shell surface, punctate are often filled with micrite
- **Pseudopunctate** – stacked, conical plications giving the shell a wavy appearance, unique to brachiopods, but found in only a few groups

Most of the features listed above are recognized in the brachiopods identified in thin sections of the Trenton Formation and Black River Group of the study area. Examples of these structures are shown below.



Brachiopod Example #1, Laminated
Pennsylvania, Union Furnace Outcrop, Trenton Formation, Coburn Formation

This laminated brachiopod shell occurs in a dolostone and is the only original skeletal material preserved. The grain is phosphatic which is typical of laminated brachiopod shells composed of alternating sheets of phosphate and chitin. These grains are not very common in limestones.

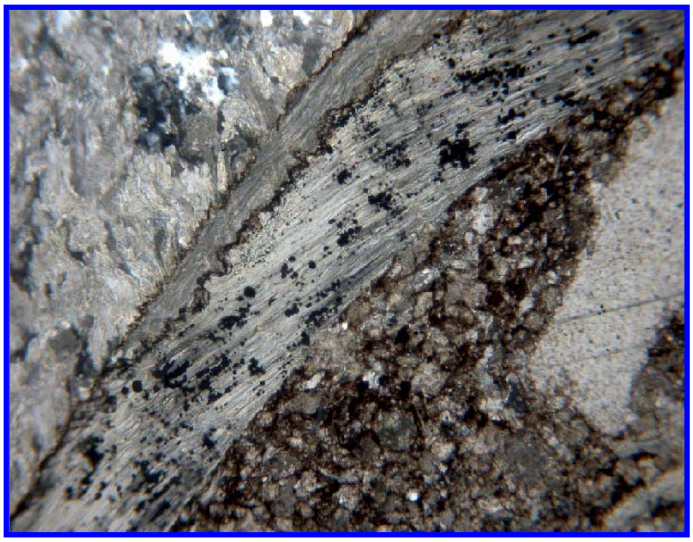

Brachiopod Example #2, Impunctate
Pennsylvania

This example of an impunctate shell also illustrates a 2 layer fibrous microstructure. The outer has been alterated or micritized and the perpendicular orientation of the calcite fibers is no longer obvious. The oblique angle of the calcite fibers comprising the inner, secondary layer is very obvious in this photo. This grain has been partially pyritized.

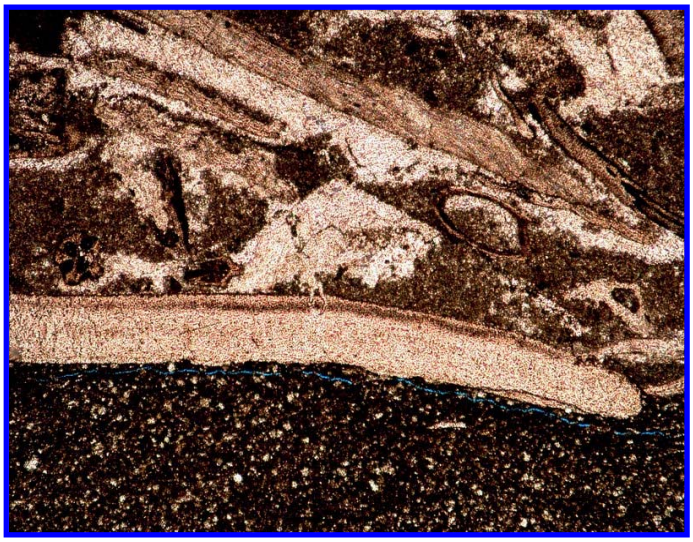

Brachiopod Example #3, Impunctate
West Virginia, Wood County, Trenton Formation, 9636 ft

There are three brachiopod fragments present in this photograph of a skeletal wackestone of the Trenton Formation. The two larger fragments are impunctate. The upper grain is a good example of the fibrous microstructure. The lower grain shows two distinct layers in the brachiopod grain. A cross-sectional view of a brachiopod spine is also present

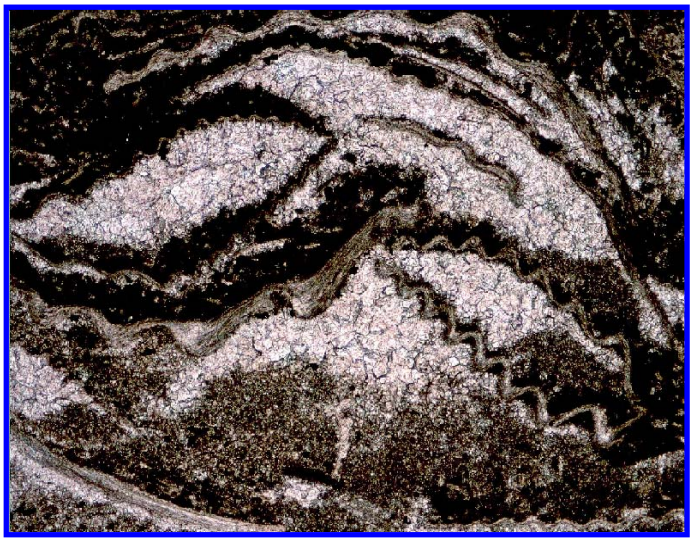

Brachiopod Example #4, Impunctate
West Virginia, Wood County, Sandhill Well, Trenton Formation, 9834 ft

The elongate brachiopod grains in this skeletal wackestone have a very distinct crenulated structure. Crenulations are common in the brachiopod grains observed in the Trenton and Black River.

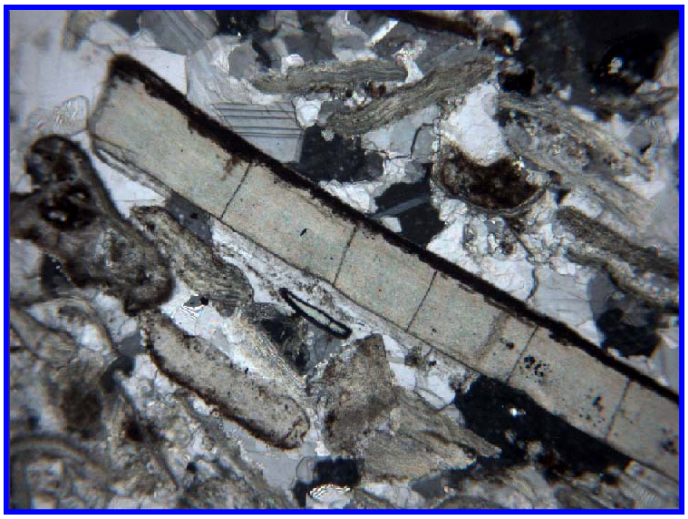

Brachiopod Example #5, Punctate
Pennsylvania, Union Furnace Outcrop

This large brachiopod grain does not have a distinct fibrous structure like that observed above, but punctate are present in this grain. The punctate are perpendicular to the surface of the shell and are dark in color because they are filled with micrite. There is also a micritic coating on the top edge of the grain.



Brachiopod Example #6, Punctate
West Virginia, Wood County, Sandhill Well, Trenton Formation, 9602 ft

Micrite filled punctate are very obvious in this large brachopod grain from the Trenton Formation. The fibrous microstructure is maintained where it has not been penetrated by the punctate.

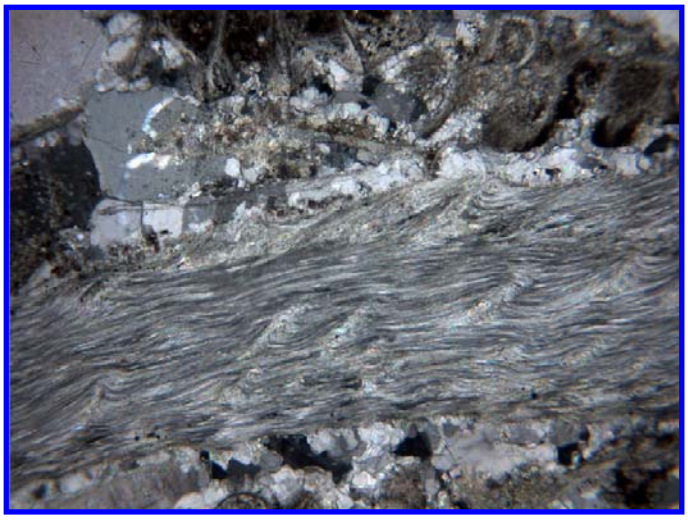

Brachiopod Example #7, Pseudopunctate
Pennsylvania, Union Furnace Outcrop

This detailed view of a brachiopod shell shows the fibrous microstructure and preserved pseudopunctate. The wavy appearance of the grain in this thin section is typical of brachiopod shell fragments throughout the Trenton and Black River.

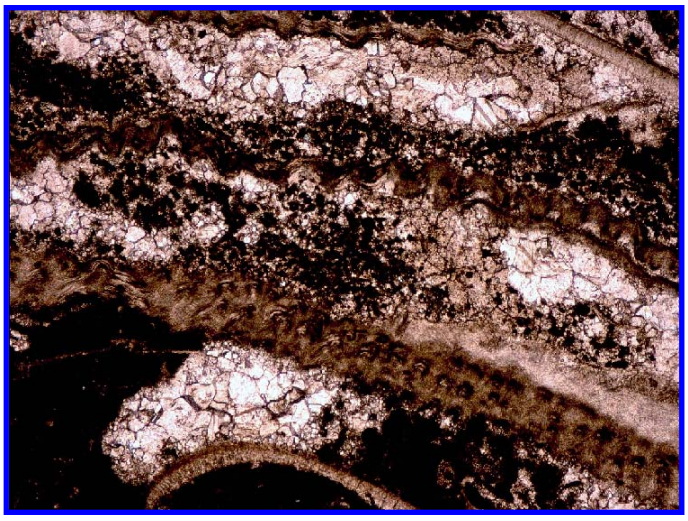

Brachiopod Example #8, Pseudopunctate

West Virginia, Wood County, Sandhill Well, Black River Group, 9912 ft

These brachiopod fragments occur in a skeletal packstone/grainstone of the Black River Group. There are two different microstructures illustrated in this photograph. The upper brachiopod fragment has a fibrous crenulated shell. The lower fragment also has a fibrous microstructure, but the small round structures on the shell are pseudopunctate. This rounded or elliptical appearance results from an oblique, nearly transverse cut through the brachiopod shell. Note that the microstructure of the fragments has been preserved, but the surrounding skeletal grains have been replaced with sparry calcite.

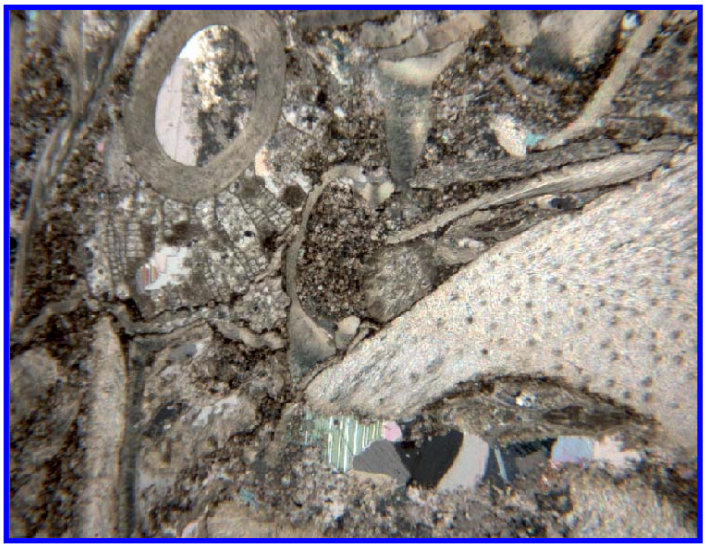

Brachiopod Example #9, Spine

Pennsylvania

The brachiopod spine in this photograph has a concentric, parallel, fibrous inner layer. The central canal of the spine has been filled with sparry calcite cement.



Brachiopod Example #10, Spine

West Virginia, Wood County, Sandhill Well, Black River Group, 10,146 ft

Most of the long spines present on certain groups of brachiopods are broken off during transport and deposition of the shells. In this example from the Black River Group the spine has not been detached. The fibrous microstructure of this grain is evident.

Bryozoans

Bryozoans are colonial organisms with skeletons composed of both aragonite and calcite (Tucker, 1991). Bryozoans are very common in the Trenton and Black River rocks and often occur as large fragments in thin section. The morphology of the bryozoan fragments depends on the orientation of the grains in thin section and the species of bryozoan observed (Scholle and Ulmer-Scholle, 2003, p.124). Bryozoan skeletons consist of foliated calcite with round holes (zooecia) filled with sparite. The most common bryozoans of the Paleozoic are of the fenestrate variety (Tucker, 1991).

Bryozoans of the Trenton and Black River occur in all rock types ranging form mudstones to grainstones. The bryozoan fragments are typically large, but some smaller fragments are also present. The zooecia of the bryozan colonies are commonly filled with sparry calcite cement and in some cases fine micritic cement (Scholle and Ulmer-Scholle, 2003, p.124). The three most common orders of byrozoans observed in the Trenton and Black River are the Trepostomida, Fenestrida, and Cryptostomida. Examples of the three orders are shown below.

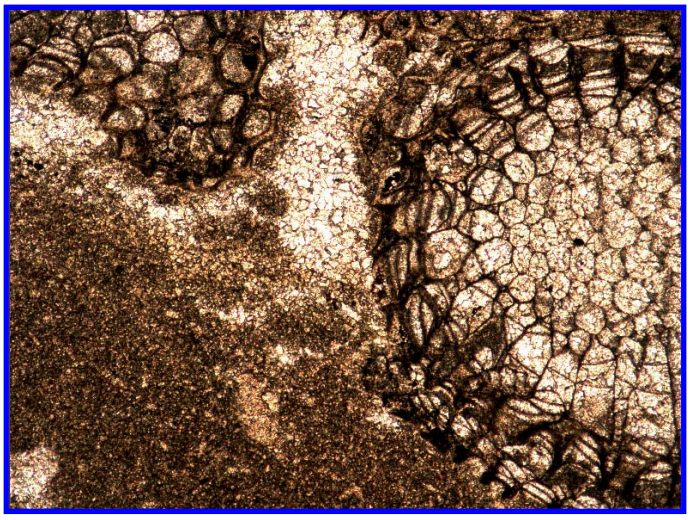

Bryozoan, Example #1, Trepostome
West Virginia, Wood County, Trenton Formation, 9560 ft

This is an example of a transverse section of a trepostome bryozoan colony. The numerous diaphrams (partions) within in the zooecia are characteristic of treptosomes. The zooecia are well preserved because they have been filled with sparry calcite cement.

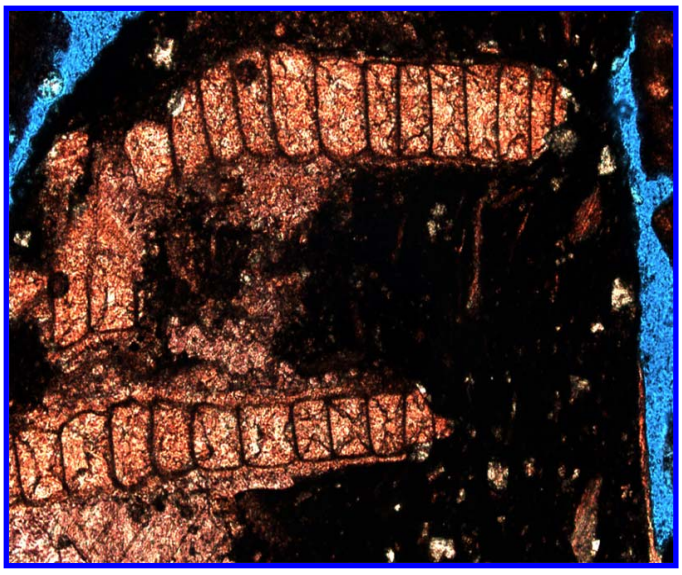

Bryozoan, Example #2, Treptosome
Pennsylvania, Bradford County
Bayles #1 Well, 12,350 ft

The majority of this thin section is occupied by a Fistuliporoid bryozoan grain. The majority of the intergranular material surrounding the bryozoan is dark micritic matrix, but there is a small amount of calcite cement adjacent to the bryozoan.

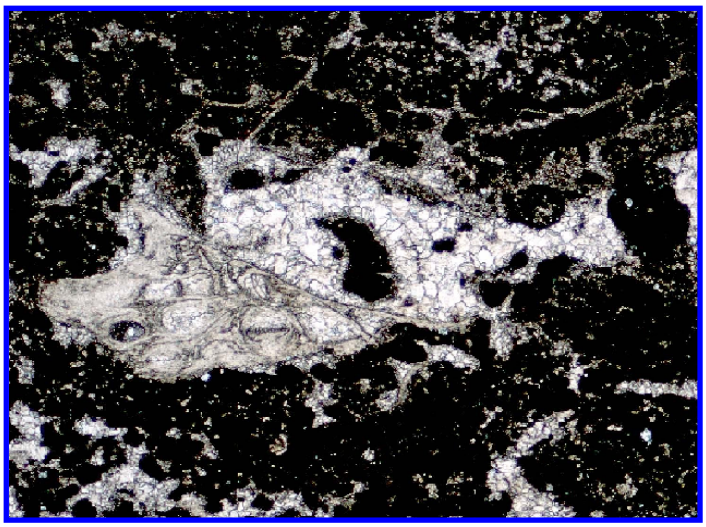

Bryozoan, Example #3, Fenestrate
West Virginia, Wood County, Trenton Formation, 9884 ft

Fenestrate bryozoan colonies, such as the one in this thin section, are frequently observed in Paleozoic limestones. The zooecia wall structure is preserved in this structure and has a fibrous microstructure. The zooecia have been filled with sparry calcite cement.

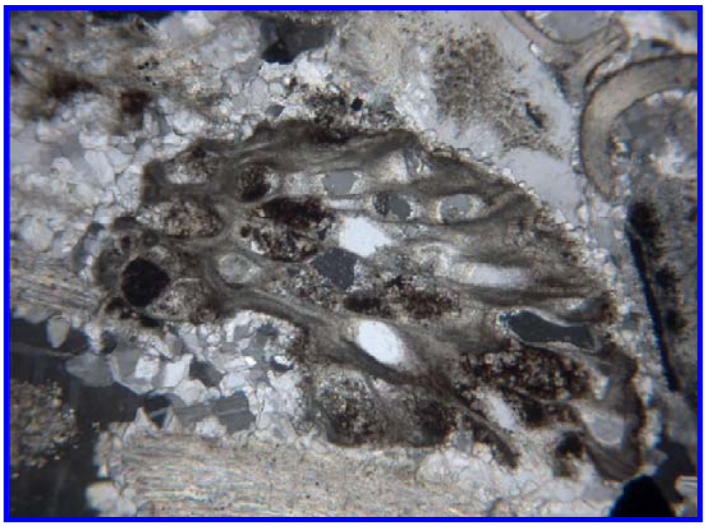

Bryozoan, Example #4, Fenestrate
Pennsylvania

The fibrous microstructure of the zooecia walls of this fenestrate brozoan colony is preserved. The zooecia have been filled with both sparry calcite cement and fine-grained dark micritic cement.

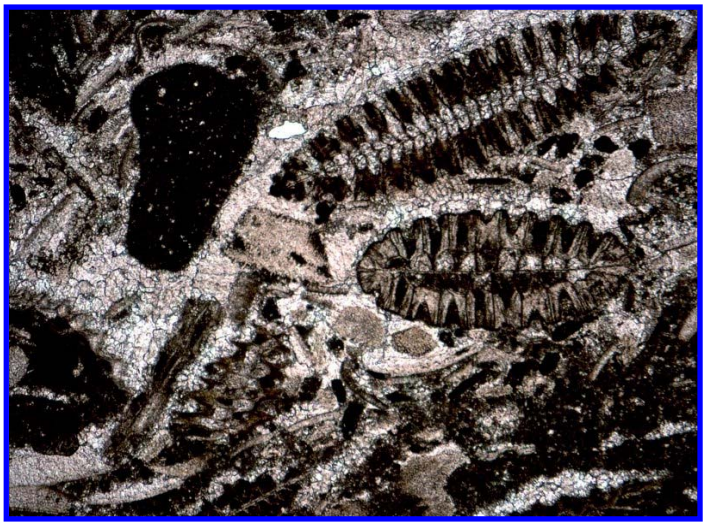

Bryozoan, Example #5, Cryptostomida, Ptilodictyina, *Stictopora fenestrata*
Pennsylvania

This is a transverse section through the bryozan, *Stictopora fenestrata*. These bryozoans have a bilateral symmetry and are often called bifoliates. The zooecial walls are laminated and flatten outward. These bryozoans typically occur as flattened branches.

Corals

Corals also contribute to the skeletal material observed in Trenton-Black River. In thin section corals are not as commonly observed as other skeletal grains, but they are common in the Pennsylvania, Union Furnace outcrop. The corals observed in the Trenton-Black River belong to the Order Tabulata and the Order Rugosa. Species determination of individual corals is dependent on the morphology of the coral skeleton. An outer wall and a series of internal vertical plates (septa), horizontal plates (tabula), and curved plates (dissepiments) characterized the coral skeleton. The original mineralogy of nearly all tabulate corals is calcite, but very few, including *Tetradium* corals may have been aragonitic (Scholle and Ulmer-Scholle, 2003, p.102).

In thin section corals tabulate corals are recognized by the presence of individual corallites arranged in colonies. Corallites can be round, oval, or polygonal in shape. Horizontal tabulae are prominent and the septa are often not well preserved. Tabulate corals are distinguished from bryozoans because they generally form large colonies and have larger individual chambers (Scholle and Ulmer-Scholle, 2003, p.102).

Rugose corals are solitary or colonial. Solitary forms have distinct horn shapes in longitudinal sections. The septa are better developed than tabulate coral septa and the rugose corals are bilaterally symmetrical. In thin section the wall structure of the rugose corals have a fuzzy appearance and are often filled with clear calcite crystals (Scholle and Ulmer-Scholle, 2003, p.105).

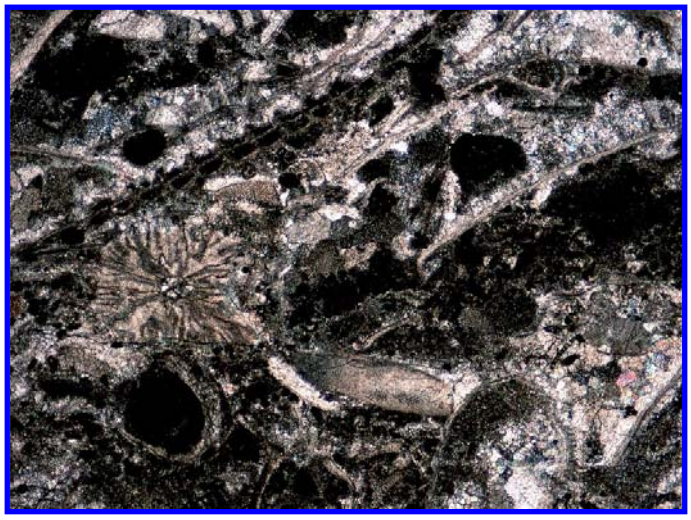

Coral, Example #1, Rugose
West Virginia, Wood County, Trenton Formation, 9828 ft

This is a transverse section through a solitary rugose coral. The grain is round in shape with a central columella and the individual septa are preserved. The internal area between the brownish septa has been filled with sparry calcite.

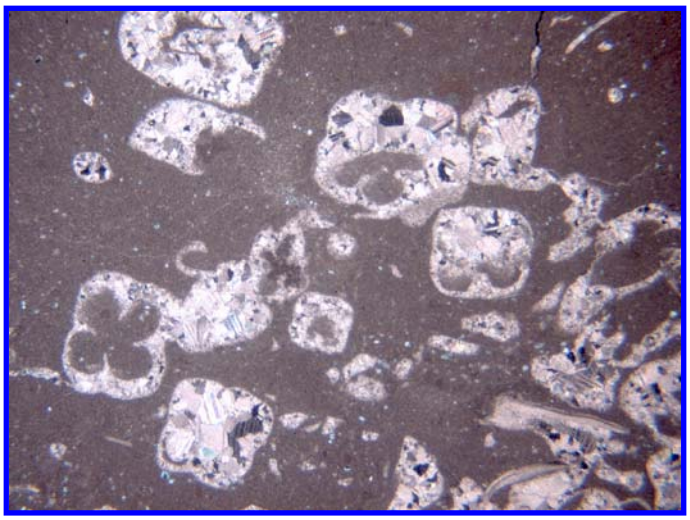

Coral, Example #2, Tetradium
Pennsylvania, Union Furnace Outcrop, UF8,

The *Tetradium* corals in this thin section dominate this skeletal wackestone. Notice the distinct polygonal shape of these Tetradium. This cloverleaf like morphology is observed in thin section and outcrop. The corallites have been completely replaced with sparry calcite and no internal structure is preserved indicating that they were originally aragonitic in composition.



Coral, Example #3, Tetradium
Pennsylvania, Union Furnace Outcrop

Tetradium corallites are common in this skeletal wackestone. The grains have been replaced with calcite and no internal structure is preserved.

Echinoderms

Crinoids (Class Crinoidea) are the echinoderms present in the Trenton-Black River rocks. They are very abundant in all of the subtidal environments observed in these rocks. Crinoids are composed of high-Mg calcite and have distinct pentameral symmetry. Although whole crinoids reached greater than 1 meter in size they normally disaggregate into mm or cm sized plates or ossicles (Scholle and Ulmer-Scolle, 2003, p. 184).

In thin section individual plates or columnals have circular, ovoid or pentagonal shapes and often have a central canal that is also circular or pentagonal. The single unit extinction of echinoderm fragments under crossed polars is the most distinct petrographic characteristic of these grains (Scholle and Ulmer-Scholle, 2003, p.184). This extinction pattern occurs because each individual skeletal component acts as a single crystal of calcite. The single crystal plates commonly have syntaxial overgrowths, which can form overgrowth cements (Tucker, 1991). Crinoid plates are often perforated with small pores

that are visible in thin section if they have been filled with some contrasting material (commonly micrite or organic material). These filled pores result in a distinctive dusty appearance of crinoid fragments in thin section (Scholle and Ulmer-Scholle, 2003, 1991).

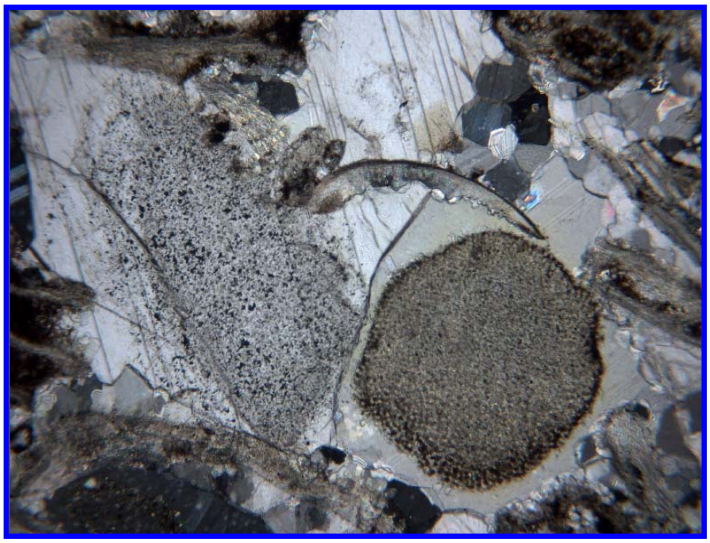

Echinoderm, Crinoid, Example #1
Pennsylvania

The crinoid present in this skeletal grainstone thin section is surrounded by clear calcite syntaxial overgrowth cement. The dusty appearance of the crinoid grain results from the filling of pores with micrite.



Echinoderm, Example #2
Pennsylvania, Mercer County, McKnight Well

There are several irregularly shaped crinoid fragments in this skeletal grainstone. The grains have a dusty appearance from the filling of pores with micritic carbonate material. Syntaxial overgrowth cements are not immediately obvious in this thin section, but are likely present.

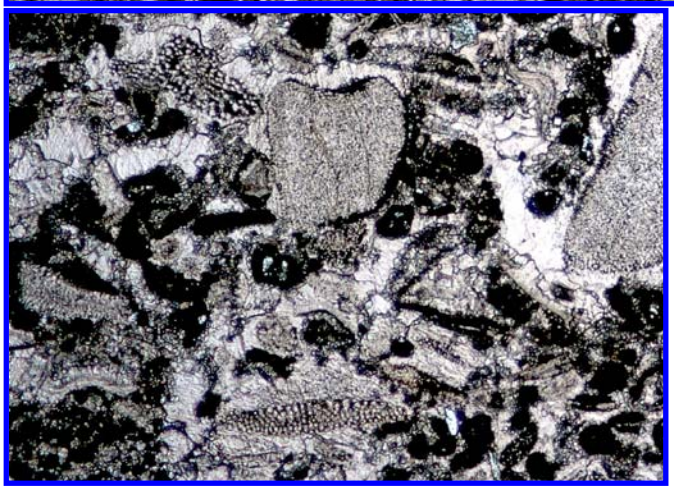

Echinoderm, Example #3
West Virginia, Wood County Well, Black River Group, 10,100 ft

The crinoids in this thin section are similar to those observed in the above photograph. The grains have pores filled with micritic carbonate giving them a dusty appearance. The grains are irregularly shaped.

Echinoderm, Example #4
West Virginia, Wood County, Trenton Formation, 9798 ft

This thin section of a skeletal/intraclastic grainstone contains a distinct “dumbbell” shaped crinoid grain. This discoidal crinoid plate is thickest at its margins and thinner in the interior. There are some small borings filled with micrite at the edges of the grain.

Echinoderm, Example #5
West Virginia, Wood County, Trenton Formation, 9554 ft

There are several rounded crinoid grains in this skeletal wackestone. The central canal or columnella is present in the round grain on the right side of the section.

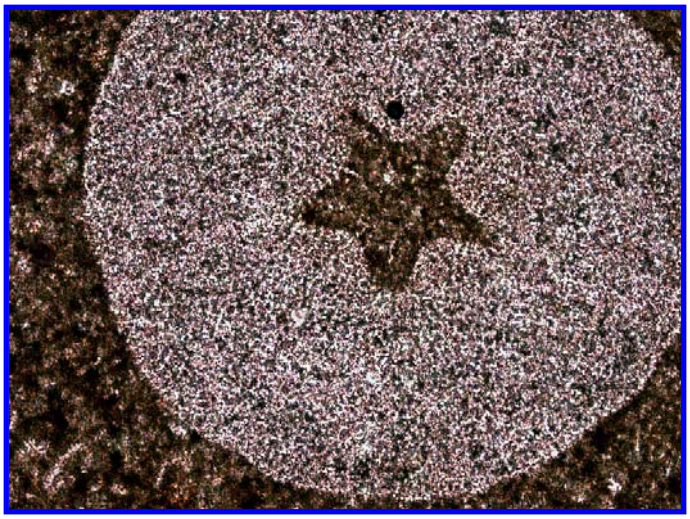

Echinoderm, Example #6
West Virginia, Wood County, Trenton Formation, 9532 ft

This star shaped canal in the center of this large rounded crinoid grain results from the pentameral symmetry of these skeletal grains.

Mollusks

Bivalves, gastropods, and cephalopods occur in the Middle Ordovician Trenton and Black River rocks. Bivalves and gastropods are the most common mollusks observed in thin section and examples are included in this discussion of the petrography of the Trenton-Black River in the Appalachian Basin.

Bivalves (pelecypods)

Bivalve species are found in marine, brackish, and freshwater environments (Tucker, 1991). Bivalves consist of two equal shells or valves whereas brachiopods valves are different shapes and sizes. The shell fragments observed in thin section are elongate, retangular to curved grains and are commonly disarticulated (Sholle and Ulmer-Scholle, 2003, p. 160).

Bivalves are aragonitic and consist of several layers of internal microstructure. The most common structure observed in bivalves is an inner layer composed of sheets of aragonite tablets and an outer layer of aragonite (or calcite) prisms. The aragonitic composition of bivalves often results in dissolution of the grains and repalcement by drusy calcite spar. Aragonitic shells may also be calcitized resulting in faint relics of the original microstructure. Bivalves with an original calcite mineralogy maintain their original microstructure and are often foliated and prismatic (Tucker, 1991).

Gastropods

Gastropods are abundant and diverse in normal marine conditions, but diversity decreases in hypersaline and brackish waters. Gastropod shells are primarily aragonitic with microstructure similar to the bivalve structure described above. This internal microstructure is not usually preserved and is typically replaced with drusy calcite spar. Gastropods are recognized in thin section by shell morphology which consist of distinctly curved shapes spiraled around a central axis (Tucker, 1991).

Mollusk micrsostructures *(Scholle and Ulmer-Scholle, 2003, p. 154)*:

Homogeneous—microstructure with no distinguishing characteristics; Wavy extinction-under crossed polars

Prismatic – certain layers of mollusk shells are composed of prismatic crystal shapes; Under crossed polars these prisms go to extinction at different times.

Granular – certain layers of mollusks are made up of small individual grains

Cross-lamellar – microstructure is composed of groups of little wedges, these wedges go to extinction at different times under crossed polars, mollusks are the only phylum to exhibit this type of microstructure.

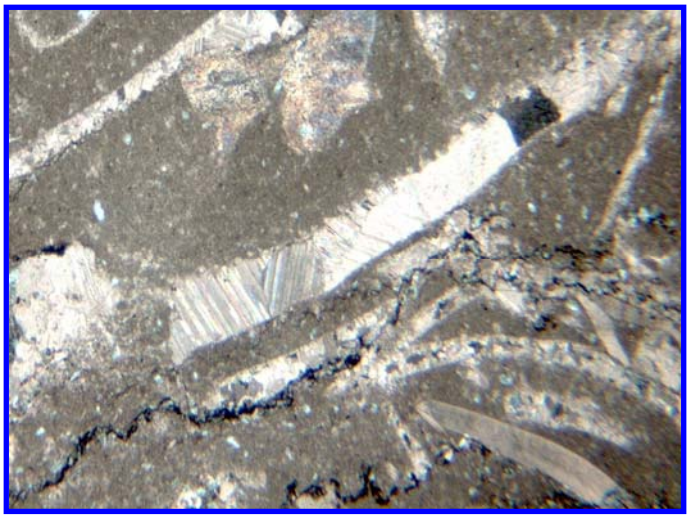

Mollusk, Example #1 Bivalve
Pennsylvania, Union Furnace Outcrop, Nealmont Formation

There are several bivalve shells present in this skeletal wackestone. The majority of the smaller elongage grains have been replaced with drusy calcite cement. This replacement is a common diagenetic process observed in mollusk grains. The large bivalve fragement in the center of the thin section has a coarse prismatic microstructure that is a distinctive petrographic characteristic of mollusks. The coarse nature of the prisms suggests that they may have been diagenetically altered.



Mollusk, Example #1 Bivalve
West Virginia, Wood County, Trenton Formation, 9636 ft

The bivalves in this thin setion are multilayered consisting of one fine, horizontally foliated layers, and coarser prismatic layers. This photograph was taken under crossed polars and the sweeping extinction pattern common in mollusks is evident.

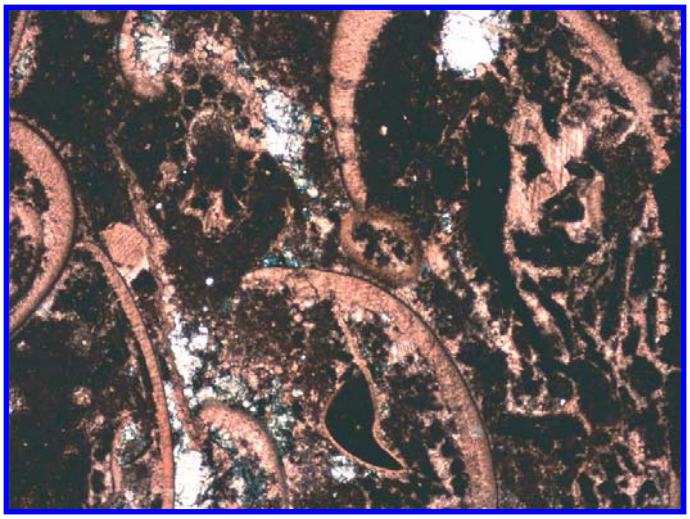

Mollusk, Example #2 Bivalve
Pennsylvania, Black River Group

Mollusk fragments, primarily bivalves, are the most common skeletal grains in this packstone. The bivalves have micritized rims and the inner portion has been replaced with sparry calcite.

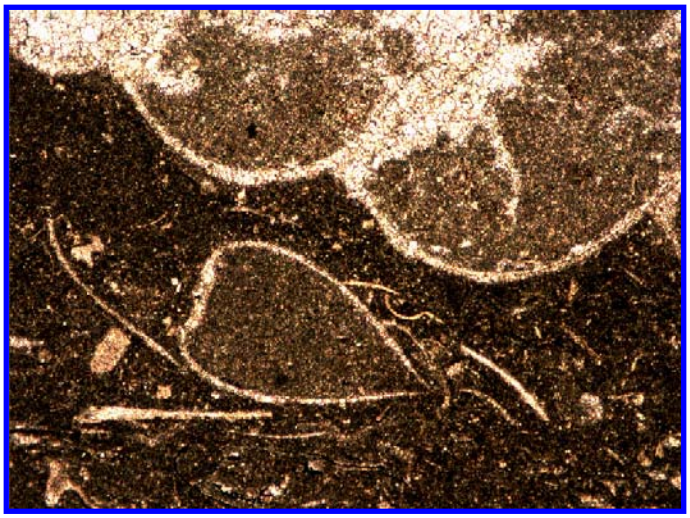

Mollusk, Example #1 Bivalve and Gastropod
West Virginia, Wood County, Trenton Formation, 9538 ft

This skeletal wackestone contains both a gastropod fragment (top) and a bivalve fragment (center). No original shell material is preserved in either of the grains. The outer shell of the gastropod has been replaced with sparry calcite and paritally filled with micrite and partially filled with sparry calcite intragranular cement. The outer shell of the bivalve has been replaced with fine sparry calcite and the central portion has been filled with micrite.

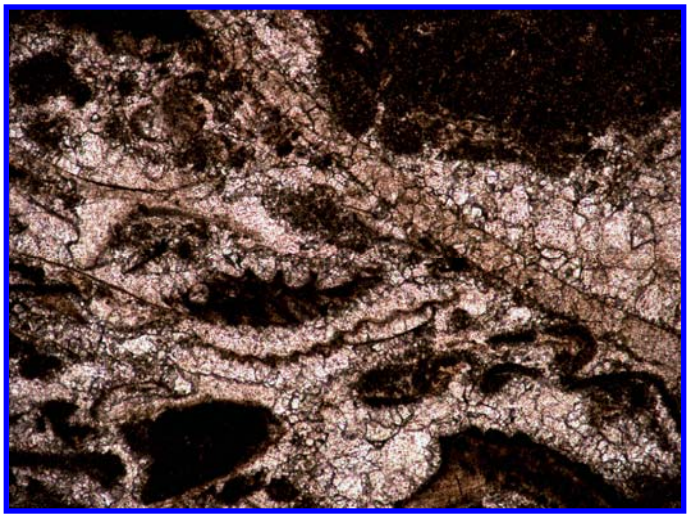

Mollusk, Example #1 Bivalve
West Virginia, Wood County, Trenton Formation, 9570 ft

There is no original microstructure maintained in the large bivalve fragment in this skeletal grainstone. The grain is identified by its shape. The shell has been completely replaced with sparry calcite cement.

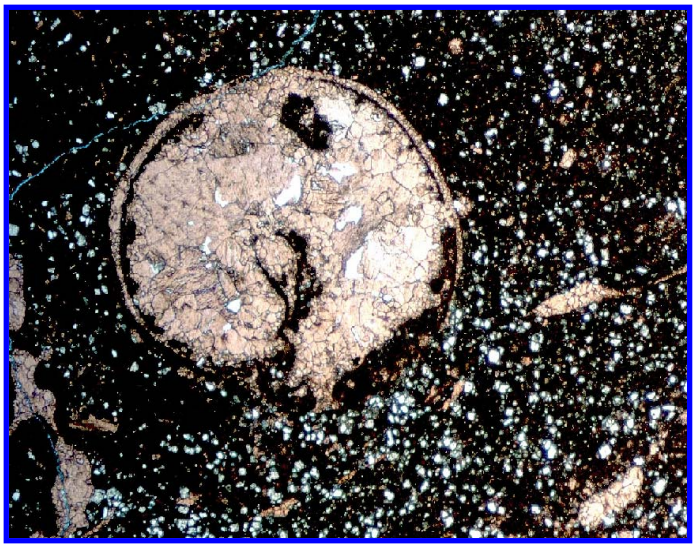

Mollusk, Example #1 Gastropod
West Virginia, Wood County, Trenton Formation, 10,431 ft

The gastropod in this thin section has a geometric shape that is often observed in gastropods of the Trenton-Black River. The outer shell of the gastropod has been replaced with fine calcite cement and the central portion has been replaced with coarser drusy calcite cement. There is a thin micritic rim surrounding the inner and outer portions of the gastropod shell.



Mollusk, Example #1 Bivalve
West Virginia, Wood County, Trenton Formation, 10,048 ft

A single valve of a bivalve shell is shown in this thin section. The shell has been replaced with fine calcite cement. The upper portion of the shell has been filled with coarser calcite cement. This calcite has been partially dolomitized.

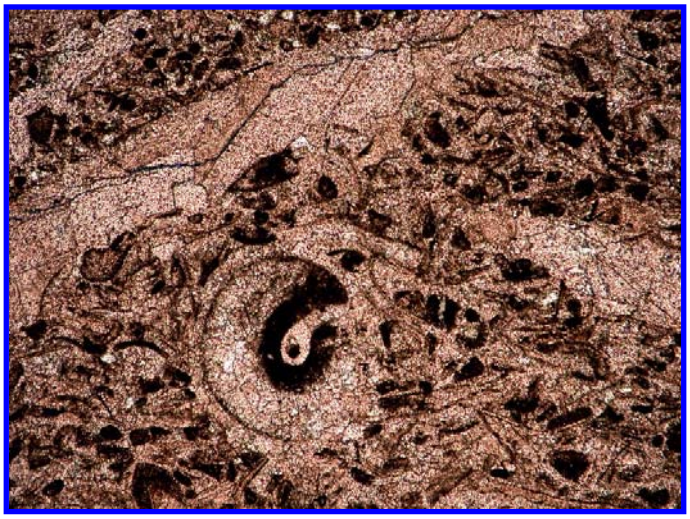

Mollusk, Example #1 Gastropod
West Virginia, Wood County, Trenton Formation, 9649 ft

The gastropod in this skeletal/peloidal grainstone has been completely replaced with calcite cement. The shape of the gastropod has been preserved because the outer layer of the shell has been micritized.

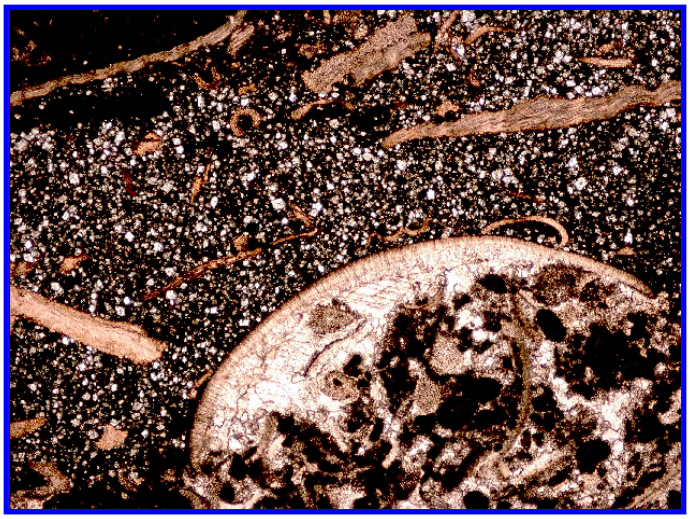

Mollusk, Example #1 Gastropod
West Virginia, Wood County, Trenton Formation, 9912 ft

This bivalve fragment has an outer micritized rim and a thin portion of the shell has the prismatic microstructure preserved. The central portion of the bivalve has been filled with coarse calcite spar.

Arthropods

Trenton-Black River skeletal debris belonging to the Phylum Arthropoda include fragments from both the Class Trilobita and the Class Ostracoda. Trilobites are more common than ostracodes in the rocks from the study area.

Trilobites

Although some of the individual trilobite grains observed in thin section are quite large they are composed of individual pieces that are less than 1 m in length and these small fragments are also observed. The large trilobite grains have a distinct morphology and are easily recognized. Trilobites are composed of calcite crystals oriented perpendicular to the wall of the shell. The crystals comprising the shell are very small and in thin section the microstructure appears homogenous, but under crossed polars it exhibits an undulose extinction pattern. Although trilobites usually have a smooth appearance they may have fine lamellar layers or be multilayered with organic rich, dark, outer layers (Scholle and Ulmer-Scholle, 2003, p.194).

The trilobite skeleton is composed calcite and variable amounts of calcium phosphate. The body of the trilobite is segmented often resulting in individual fragments present in thin section. The fragments have a characteristic "hook" or "shepard's crook" shape that is unique to trilobite grains (Scholle and Ulmer-Scholle, 2003, p.194).

Ostracodes

Ostracodes are smaller than trilobites and are comprised of two valves usually less than 1 mm in diameter. These valves are jointed along a hinge and overlap slightly resulting in assymetrical valves in thin section. The ostracode shell is thin and composed of calcite and chitin. The valves are commonly disarticulated resulting in fragments in thin section (Scholle and Ulmer-Scholle, 2003, p. 198).

Ostracodes have homogeneous primatic and finely prismatic microstructures with crystals oriented perpedicular to the valves. The structures are usually well preserved. Under crossed polars ostracodes exhibit a sweeping extinction pattern, which differentiates them from most bivalves (Scholle and Ulmer-Scholle, 2003, p.198).

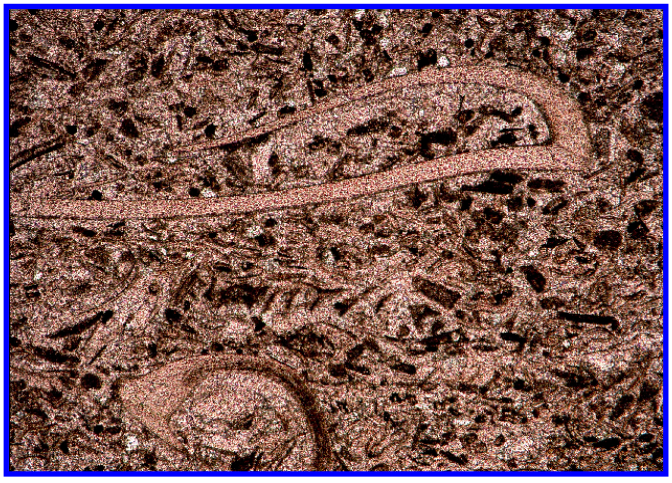

Trilobite, Example #1
West Virginia, Wood County, Trenton Formation, 9649 ft

The large trilobite grain in this skeletal grainstone has a distinct "shepard's crook" morphology that is characteristic of trilobites in thin section. The microstructure is homogeneous and there is slight micritization along the edges of the grain.



Trilobite, Example #2
West Virginia, Wood County, Trenton Formation, 9528 ft

There are several trilobite grains present in this skeletal packstone. They are easily distinguished from the other skeletal grains because of their "shepard's crook" structure.

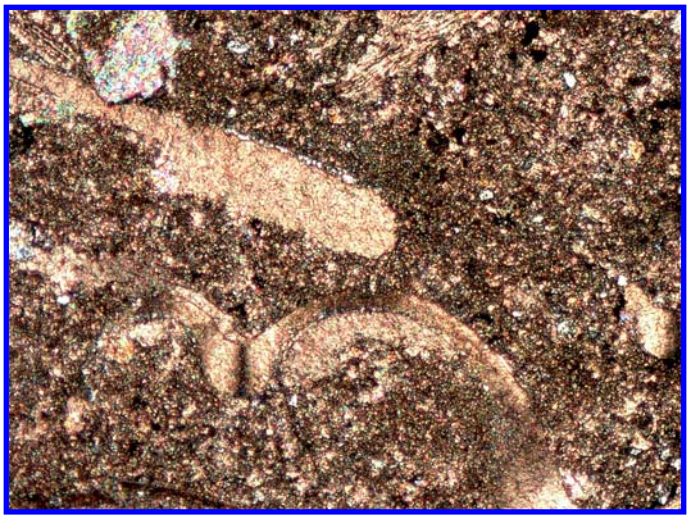

Trilobite, Example #3
West Virginia, Wood County, Trenton Formation, 9619 ft

The trilobite in this skeletal wackestone is a good example of the sweeping extinction pattern that is common in these skeletal grains. This photograph was taken under crossed polars and the extinction pattern is obvious by the alternating light and dark bands on the grain.

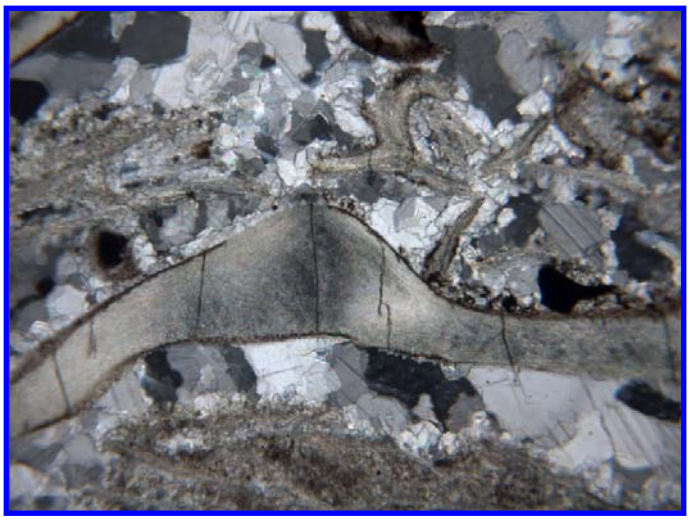

Trilobite, Example #4
Pennsylvania

This large trilobite has a convoluted shape that is common in these skeletal grains. The vertical lines on the grain are fine perforations (canaliculi) filled with micritic sediment.

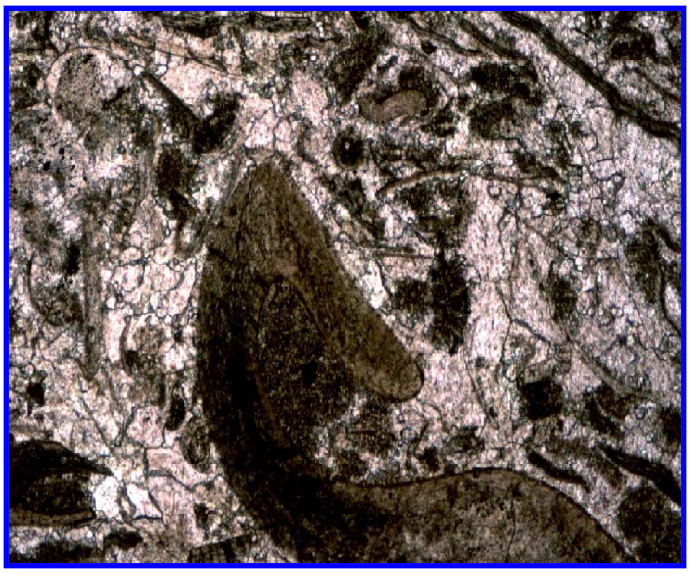

Trilobite, Example #5
West Virginia, Wood County, Trenton Formation, 9574 ft

This large convoluted trilobite grain is brownish in color due to the chitinous and organic constituents of the shell.

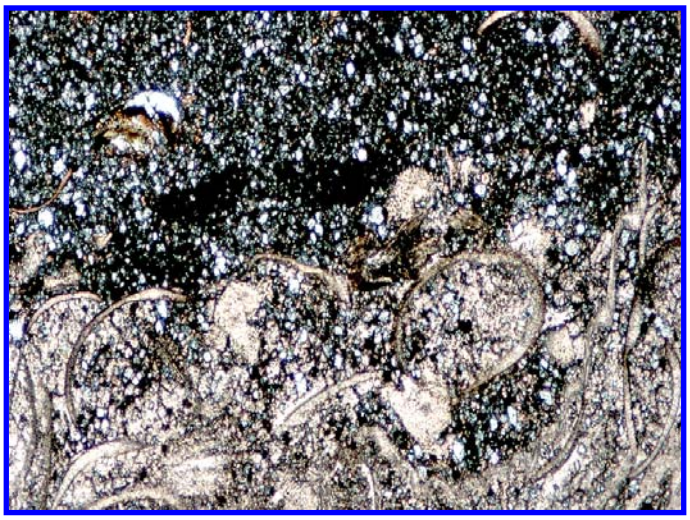

Ostracodes, Example #6
West Virginia, Wood County, Black River Group, 10,131 ft

The small size of the ostracode grains at the bottom of this thin section is typical of these skeletal grain types. Note the curved, disarticulated valves that thicken toward one end.

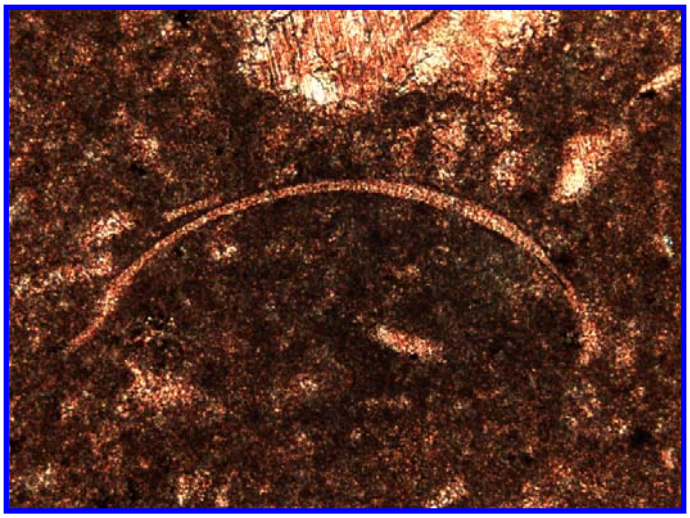

Ostracode, Example #7
Pennsylvania

The rounded shape and thin shell shown in this photograph are typical features of ostracode grains.

Appendix E-2 – Diagenesis

Cementation

Equant Calcite Spar



Equant Spar, Example #1
Pennsylvania, Mercer County, McKnight Well

The cement crystals filling the pore space of this skeletal grainstone are very "clean" and equal in size.

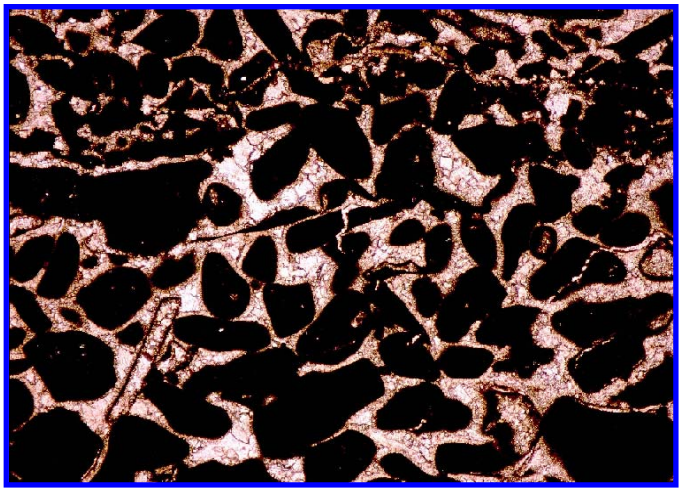

Equant Cement, Example #2
West Virginia, Wood County,
Black River Group, 9951 ft

In this intraclastic grainstone from the Black River Group in West Virginia the primary pore-filling cement is equant spar. Close observation of this thin section reveals two generations of cement an early prismatic fringe around the intraclasts and the later equant spar cement.

Peloidal Cement

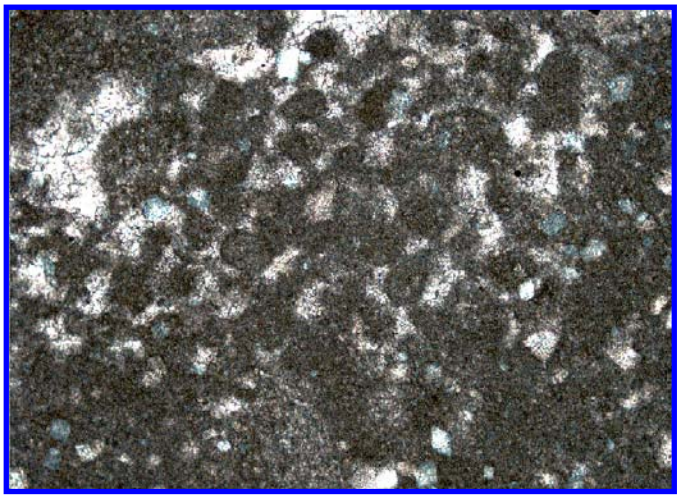

Peloidal Cement, Example #1
West Virginia, Wood County,
Black River Group, 10,018 ft

This is a typical example of a peloidal cement in the Black River Group in West Virginia. Notice that the neospar is not evenly distributed throughout the section, but the peloidal or clotted texture is evident throughout.

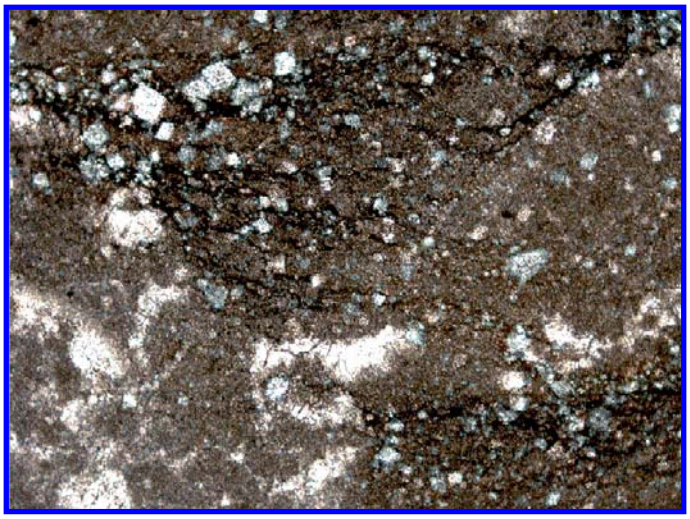

Peloidal Cement, Example #2
West Virginia, Wood County,
Black River Group, 10,034 ft

In this section the most distinct peloidal texture is evident in the lower left corner of the slide. In addition to the peloidal cement there are also wavy argillaceous laminations with associated dolomite crystals.

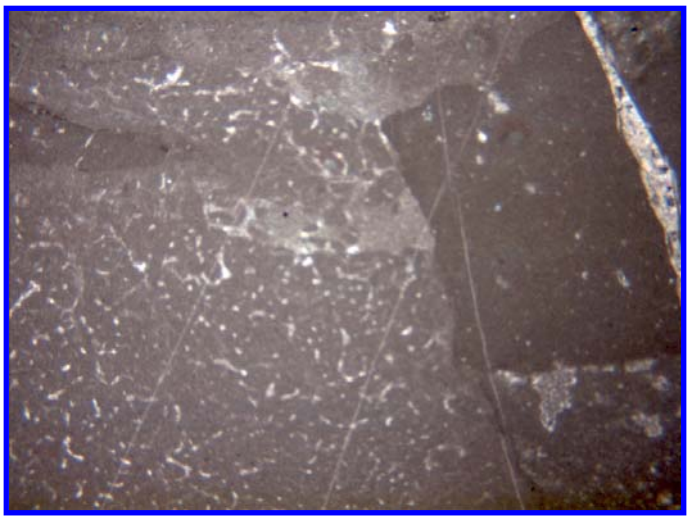

Peloidal Cement, Example #3
Pennsylvania, Union Furnace outcrop

The clotted texture of this mudstone shows the partial development of peloidal cement. Notice the somewhat rounded grains with sparry material in between. Further neomorphism will result in textures similar to those observed in the other peloidal cement slides.

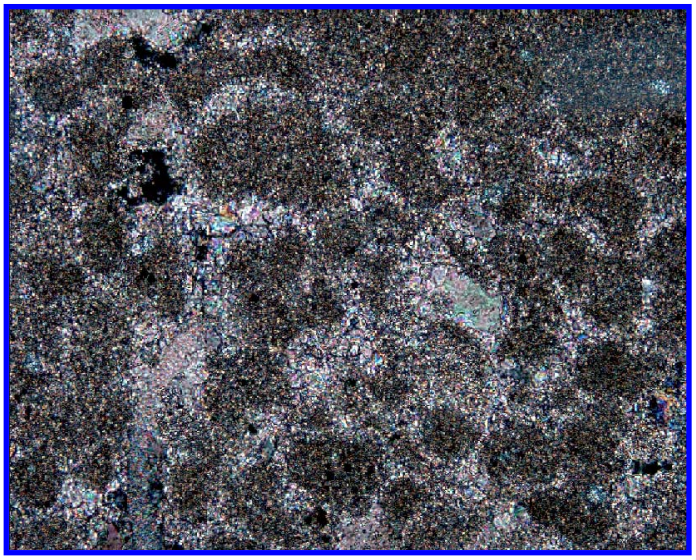

Peloidal Cement, Example #4
West Virginia, Wood County,
Black River Group, 10,054 ft

This peloidal cement was photographed under crossed polars. Notice the fuzzy grain boundaries between the peloids and the neospar.

Drusy Spar

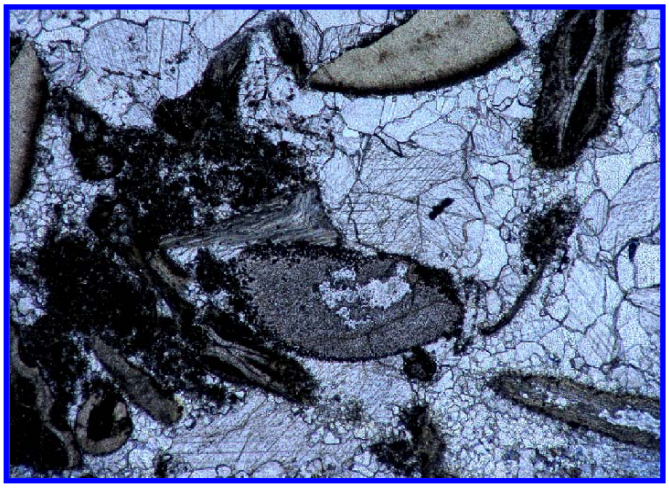

Drusy Spar, Example #1
West Virginia, Wood County,
Trenton Formation, 8495 ft

Notice the different crystal sizes in this drusy calcite spar cement. The smallest crystals occur close to grain boundaries and larger crystals are more common toward the center of the pore.

Drusy Spar, Example #2
West Virginia, Wood County,
Trenton Formation, 8530 ft

The primary intergranular material in this photo is drusy calcite spar. This cement type is recognized by increasing calcite crystals size toward the central portion of the pore.

Poikilotopic Spar

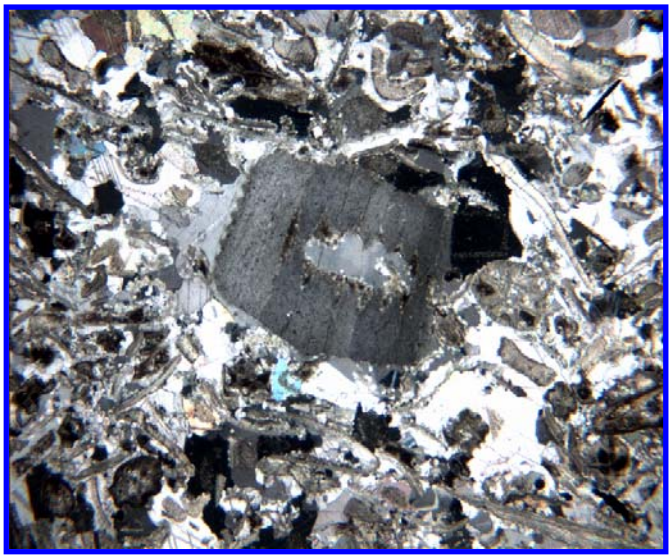

Poikilotopic Spar, Example #1
Pennsylvania

Poikilotopic textures are recognized in this crinoid rich grainstone. Notice the smaller echinoderm fragments that are encompassed by a single clean calcite crystal.



Poikilotopic Spar, Example #2
Pennsylvania

This skeletal grainstone is similar to above, also containing smaller grains encompassed by large calcite crystals.

Syntaxial Overgrowth

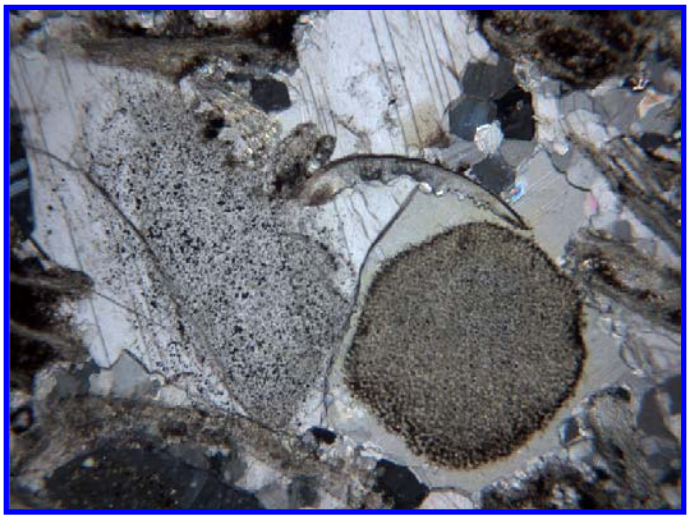

Syntaxial Overgrowth, Example #1
Pennsylvania

The syntaxial overgrowth on this crinoid grain is very clear in thin section. The calcite spar is very clear and clean.

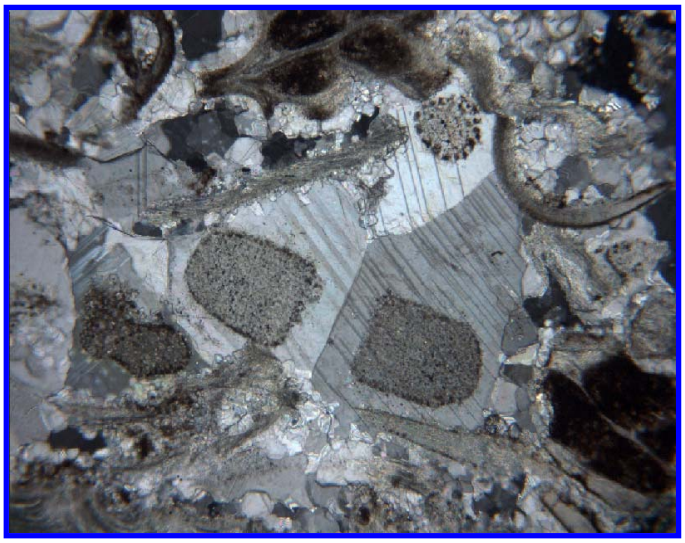

Syntaxial Overgrowth, Example #2
Pennsylvania

Two echinoderm fragments have large syntaxial overgrowths in this skeletal grainstone. Typical calcite cleavage patterns are very obvious on the overgrowths.



Prismatic fringe, Example #1
West Virginia, Wood County,
Trenton Formation, 9524 ft

Prismatic fringe cements are evident on both the large mollusk grain and the intraclast in this wackestone. The fine-grained material surrounding the fringe suggests that these cements were generated early in the diagenetic history of this rock.



Prismatic fringe, Example #2
West Virginia, Wood County,
Black River Group 9951 ft

Fringe cements are very common on the edges of the peloidal intraclasts and skeletal grains present in this grainstone. These fringes have been followed by another generation of coarser pore filling calcite spar.

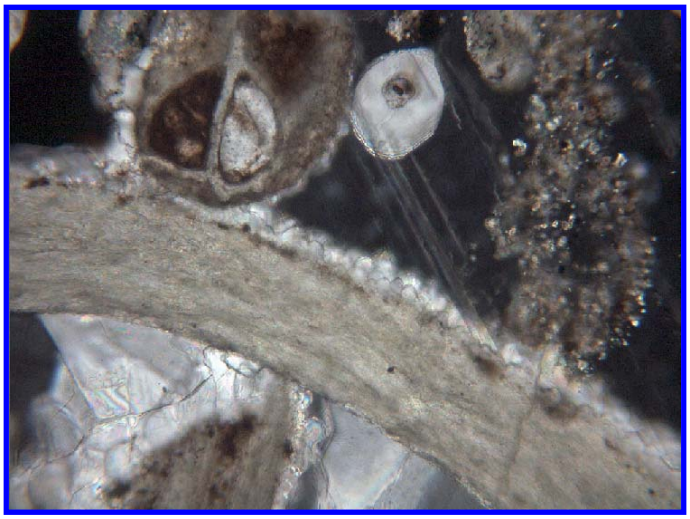

Prismatic fringe, Example #3
Pennsylvania

Prismatic fringe cement is very evident on this brachiopod grain under high magnification. Notice there is a second generation of coarse calcite spar filling the pores after the generation of the prismatic fringe.

Intragranular Spar

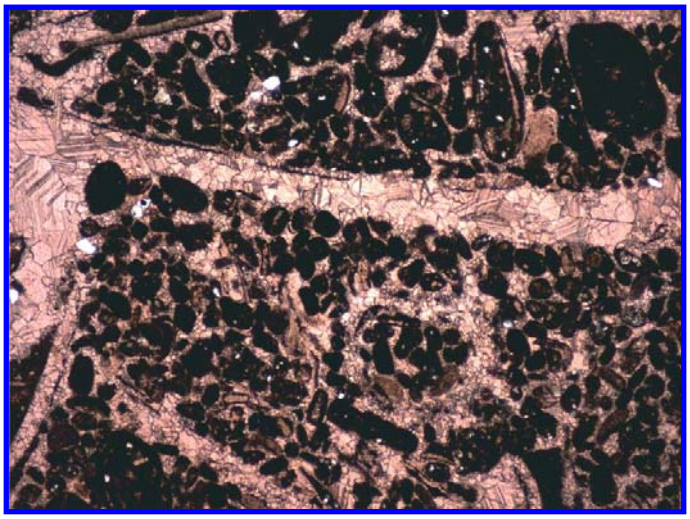

Intragranular Spar, Example #1
Pennsylvania
Trenton Formation

The central portion of this peloidal grainstone contains coarse calcite spar. The shape of the spar suggests that a skeletal grain, most likely a mollusk, was dissolved and replaced with coarser intragranular calcite. Notice the intergranular cement in this rock is much finer.

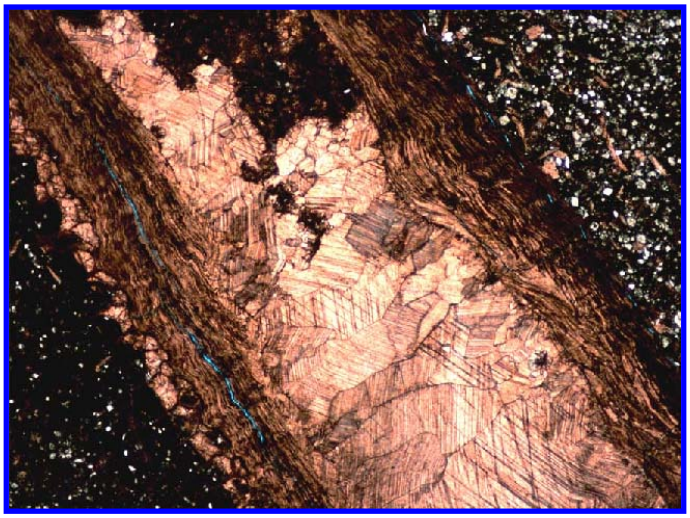

Intragranular Spar, Example #2
Pennsylvania
Trenton Formation

The microstructure of this large mollusk grain has been preserved on the outer edges of the grain, but the internal portion of the grain has been replaced with coarse calcite spar.

Micritization

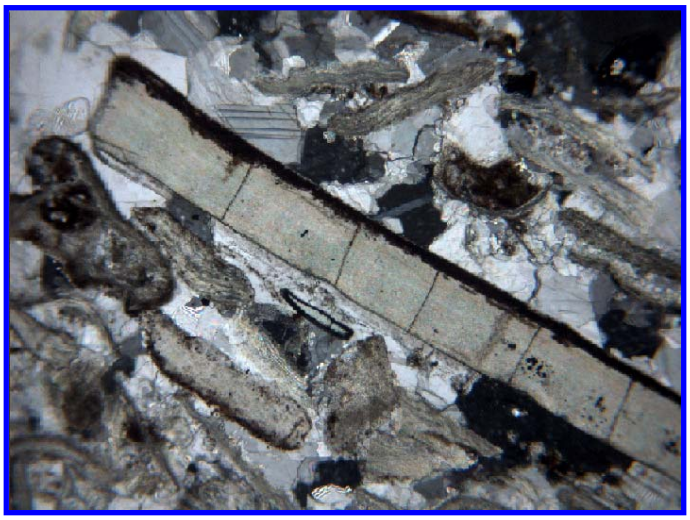

Micritization, Example #1
Pennsylvania
Trenton Formation

The upper edge of this brachiopod has been extensively micritized. The dark color results from the filling of these microscopic bores with micrite-sized cement.

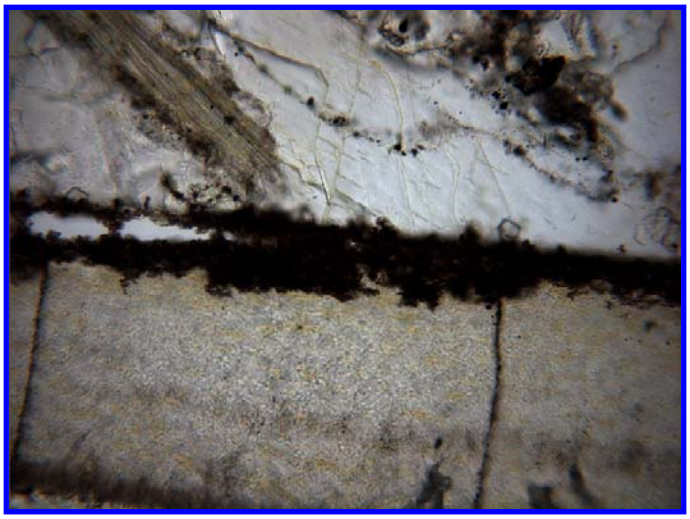

Micritization, Example #2
Pennsylvania
Trenton Formation

This is the same micritized brachiopod as shown above, but the photo was taken at higher magnification. Note the individual bores visible in the micritized grain.

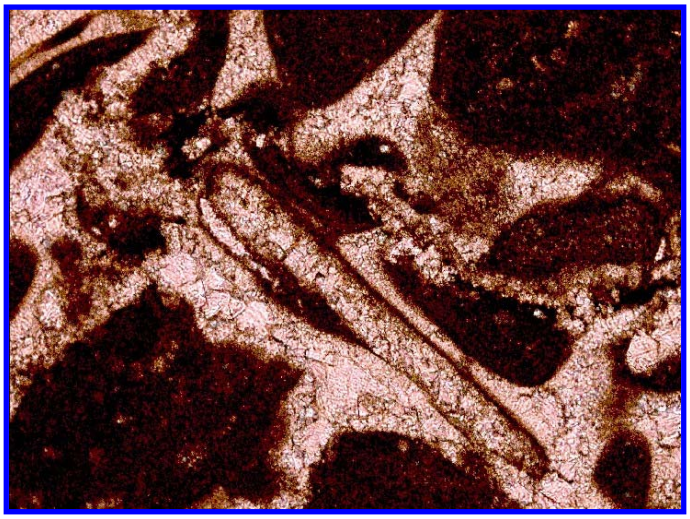

Micritization, Example #3
West Virginia, Wood County
Black River Group, 9951 ft

A micritic envelope is the only thing that remains of the elongate skeletal grain present in the center of this thin section. The original microstructure of the grain has been obliterated by diagenesis, but the micritic envelope maintains the original shape of the skeletal grain.



Micritization, Example #4
West Virginia, Wood County
Black River Group, 9655 ft

Micritization is clearly visible on the large mollusk grain in this thin section. Notice the individual borings that have been filled with micrite.

Fractures

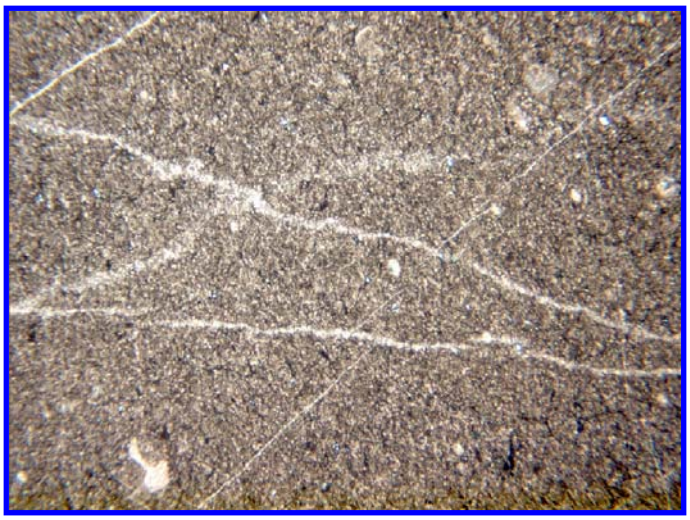

Fractures, Example #1
Pennsylvania, Union Furnace outcrop
Trenton Formation

There are several different fracture orientations in this wackestone. All of the fractures have been closed by calcite precipitation.

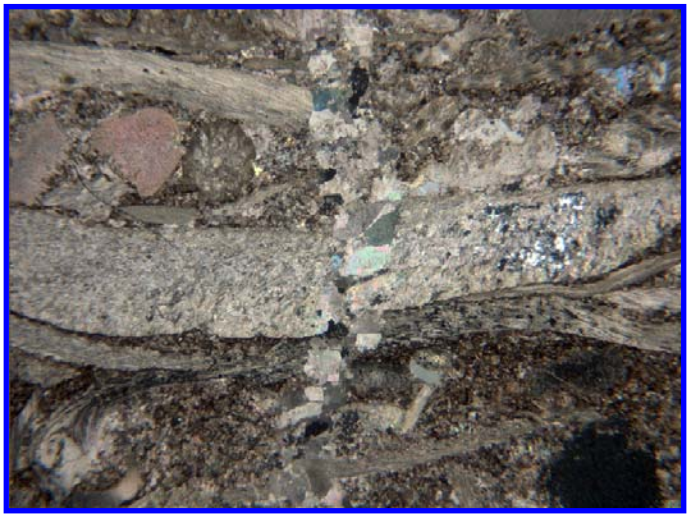

Fractures, Example #2
Pennsylvania, Union Furnace outcrop
Trenton Formation

There is one large fracture cutting across this slide vertically. There is slight offset of the large skeletal grains that the fracture cuts across. The fracture has been filled with sparry calcite.

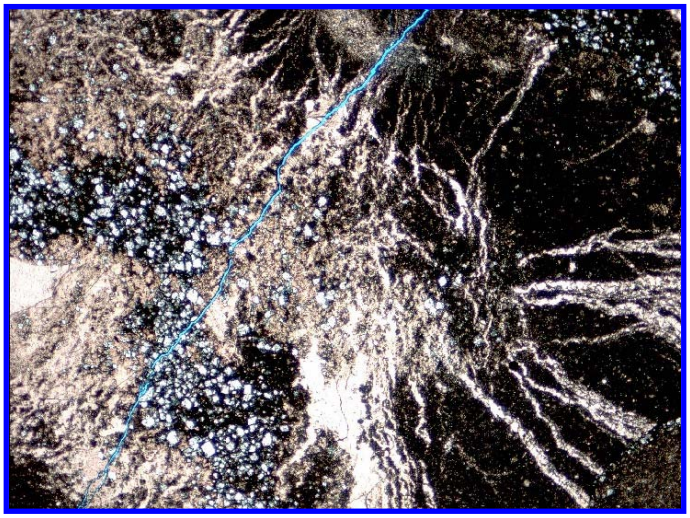

Fractures, Example #3
West Virginia, Wood County
Black River Group, 9880 ft

The majority of the fractures in this section are randomly oriented in a somewhat radial pattern. The radial fractures have been filled with sparry calcite. There is also a large open fracture cutting across the length of the slide.

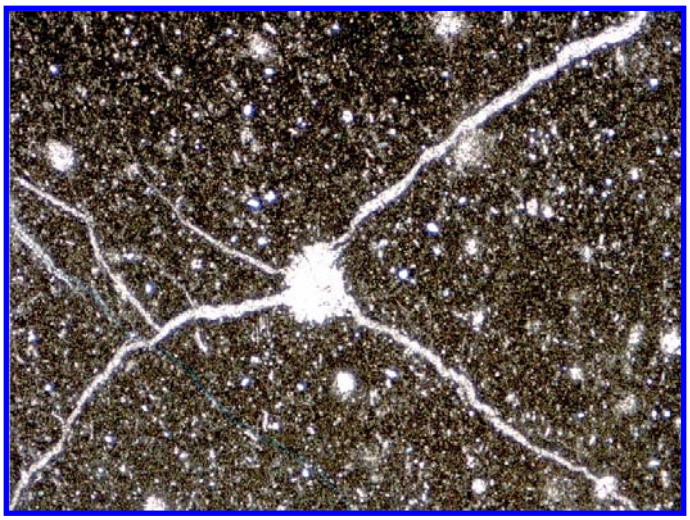

Fractures, Example #4
West Virginia, Wood County
Black River Group, 10,162 ft

The fractures in this mudstone/wackestone radiate out from the center of the section. All of the fractures have been closed with calcite.



Fractures, Example #5
Pennsylvania, Union Furnace outcrop
Trenton Formation
Black River Group, 9655 ft

There is a large open fracture in this skeletal packstone. There is some mineralization (white material) along the fracture, but not closing it.

Neomorphism



Neomorphism, Example #1
West Virginia, Wood County
Trenton Formation, 9538 ft

There is only neospar evident in this thin section. The lack of skeletal grains suggests that this rock was completely comprised of micrite prior to neomorphism.



Neomorphism, Example #2
West Virginia, Wood County
Trenton Formation, 9593 ft

This thin section is also dominated by microspar, although there are some remnants of skeletal grains. The skeletal remnants suggest that the rock was originally a wackestone. There is some micrite preserved between the neospar grain contacts.

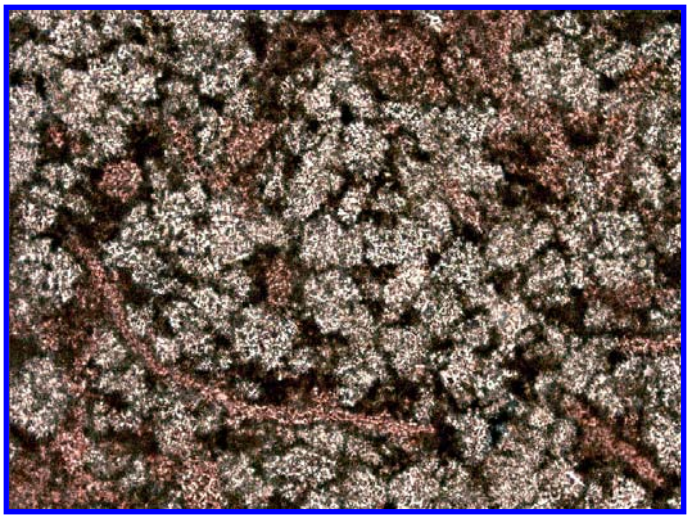

Neomorphism, Example #3
West Virginia, Wood County
Trenton Formation, 9795 ft

The neospar in this thin section is slightly coarser than that observed above. There are also more abundant skeletal remnants present.

Pyrite

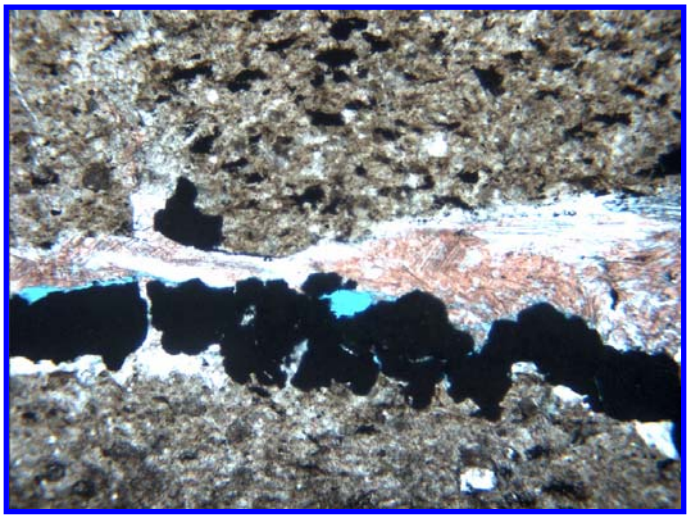

Pyrite, Example #1
Pennsylvania, Union Furnace outcrop
Black River Group

Pyrite is often concentrated along laminae or fractures such as in this photograph. Notice there is also calcite precipitating in the fracture.



Pyrite, Example #2
West Virginia, Wood County
Black River Group, 9819 ft

In this photomicrograph of a mudstone/wackestone the pyrite appears to be filling a vug or replacing a skeletal grain. The central portion of the grain/vug is filled with sparry calcite.

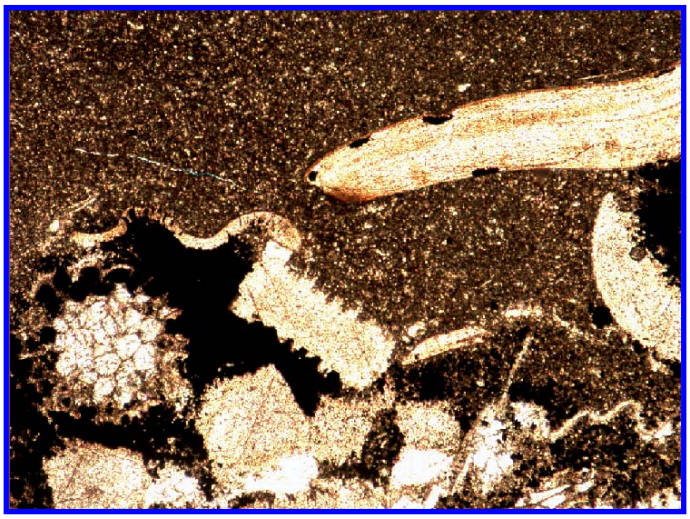

Pyrite, Example #3
West Virginia, Wood County
Trenton Formation, 9560 ft

In addition matrix pyrite and void filling pyrite, skeletal grains may also be pyritized. In this thin section mollusks, crinoids, and bryozoans are partially pyritized.

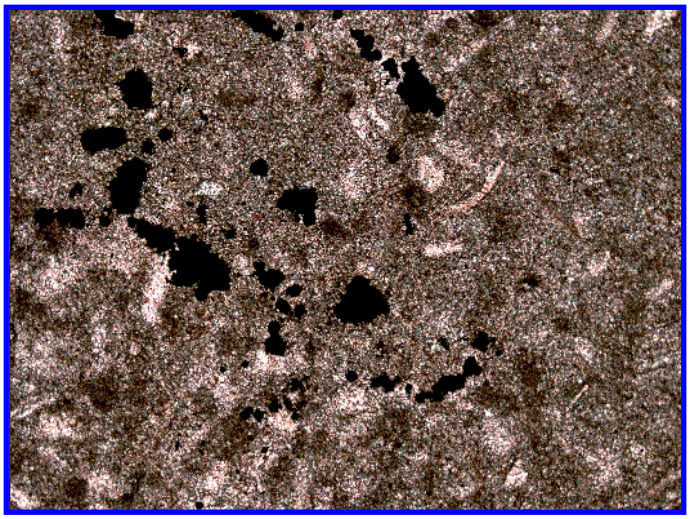

Pyrite, Example #4
West Virginia, Wood County
Trenton Formation, 9560 ft

In this thin section pyritization is not grain selective, pyrite grains are disseminated throughout the rock matrix. This matrix pyritization is common in the Trenton and Black River rocks.

Compaction

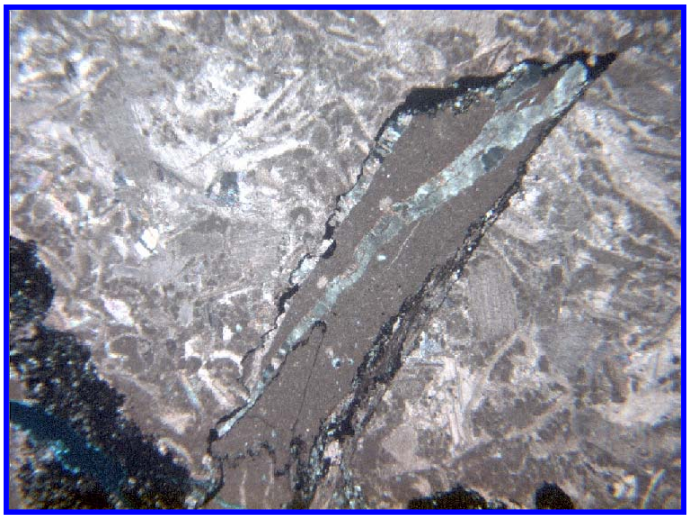

Compaction, Example #1, Stylolite
Pennsylvania, Union Furnace Outcrop
Black River Group

The stylolite in this photograph cuts into a skeletal packstone, but is filled with micrite-sized sediment. There is a large filled fracture in the muddy section underneath the stylolite. Insoluble residue is concentrated along the stylolite.

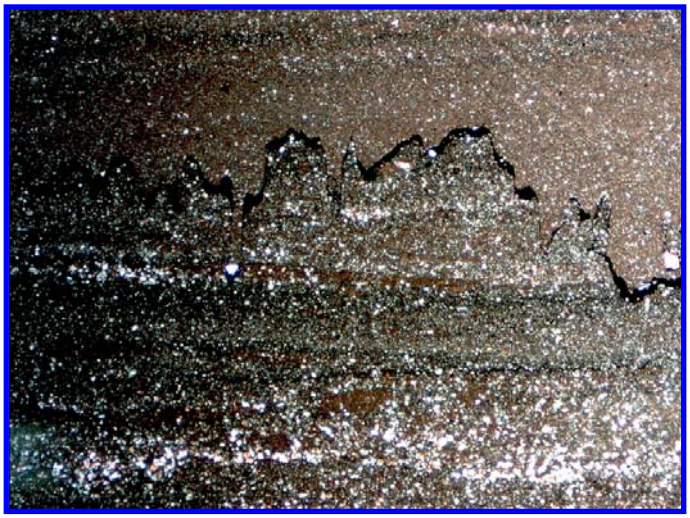

Compaction, Example #2, Stylolite
West Virginia, Wood County
Black River Group, 10,509 ft

Stylolites are common in this laminated mudstone of the Black River Group. The stylolite is dark in color because of the insoluble residue concentrated along it.



Compaction, Example #3, Stylolite
West Virginia, Wood County
Black River Group, 9978 ft

The stylolite in this mudstone of the Black River Group contains finely crystalline calcite spar.

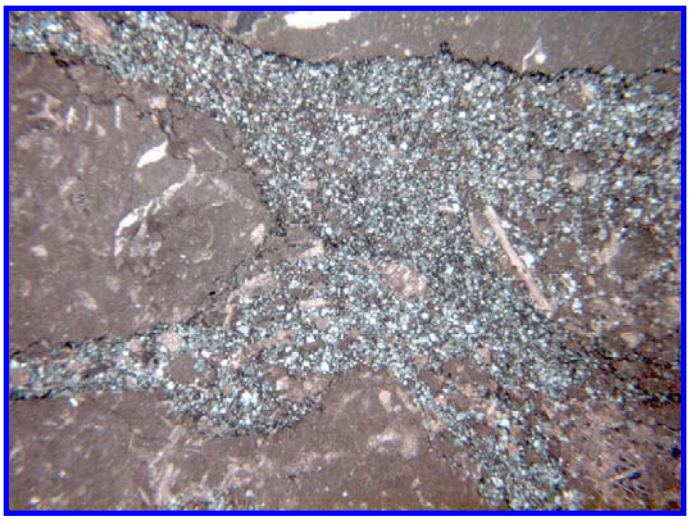

Compaction, Example #4
Pennsylvania, Union Furnace Outcrop
Black River Group

Throughout the Trenton Limestone and Black River Group compaction has distorted argillaceous laminations. One of these laminations is shown in this photograph. The laminations are easily recognizable because they are often preferentially dolomitized because of the argillaceous composition of the lamination.

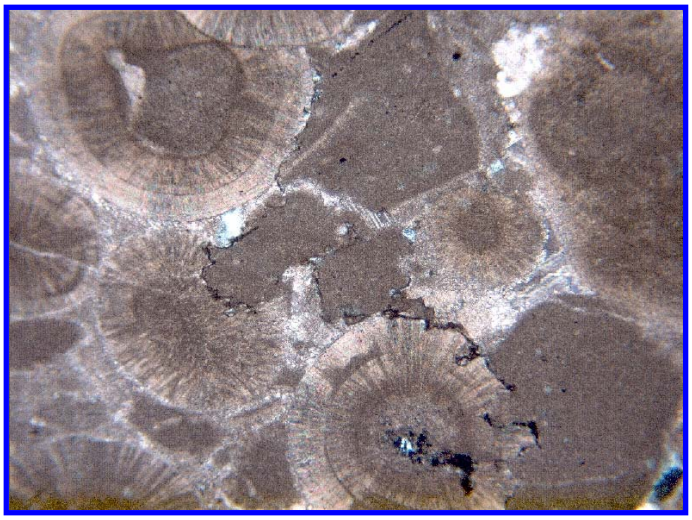

Compaction, Example #5
Pennsylvania, Union Furnace Outcrop
Black River Group

Pressure solution has partially obliterated the ooids in this photograph. Dissolution is evident by the jagged grain boundaries. Insoluble residue is concentrated along these dissolution seams.

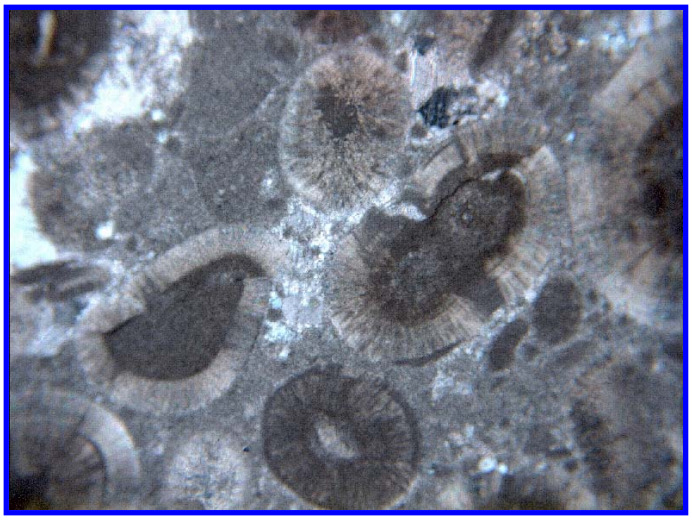

Compaction, Example #6
Pennsylvania, Union Furnace Outcrop
Black River Group

Compaction has offset the ooid laminae in this photograph. There is also partial dissolution of some of the ooid grains.

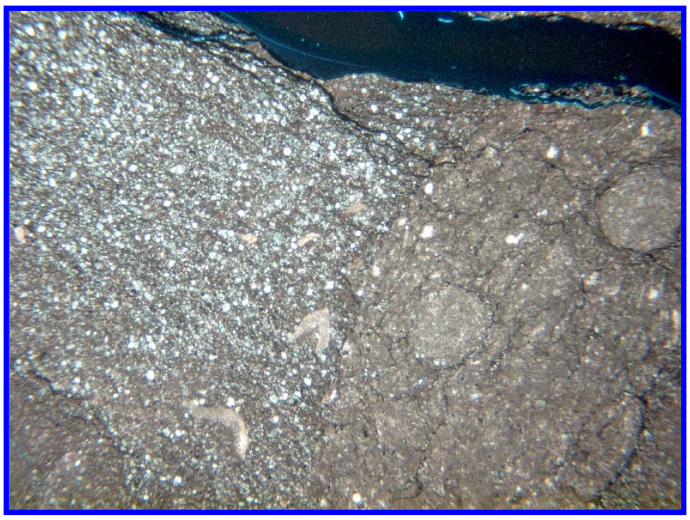

Compaction, Example #7
Pennsylvania, Union Furnace Outcrop
Black River Group

Compaction has resulted in wavy, discontinuous argillaceous lamination. The rock has also been partially dolomitized. Notice the nodular texture on the right side of the slide. This texture results from compaction of the muddy rock.

Silicification

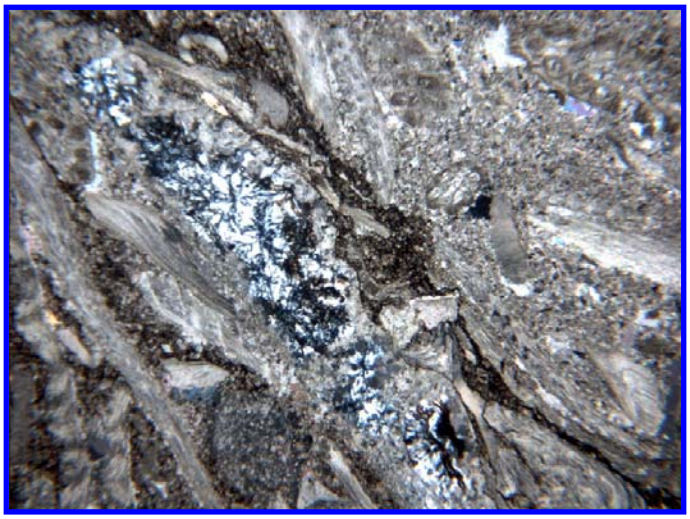

Silicification, Example #1
Pennsylvania, Union Furnace Outcrop
Black River Group

Silicification is common throughout the Trenton Limestone and Black River Group. In this skeletal floatstone chert is partially replacing the brachiopod grain. In these floatstones replacement by chert occurs only in the skeletal grains.

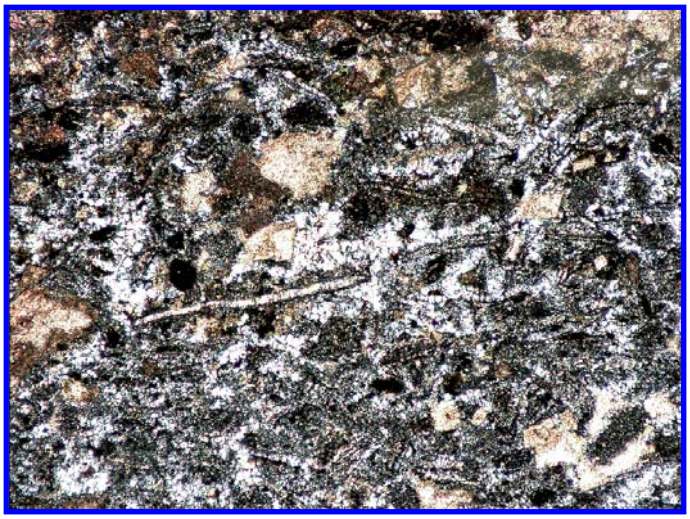

Silicification, Example #2
West Virginia, Wood County
Trenton Formation, 9656 ft

Silicification of this packstone/grainstone is not grain selective. The matrix and the grains in this rock have been silicified. This kind of pervasive silicification is not common in the Trenton and Black River.

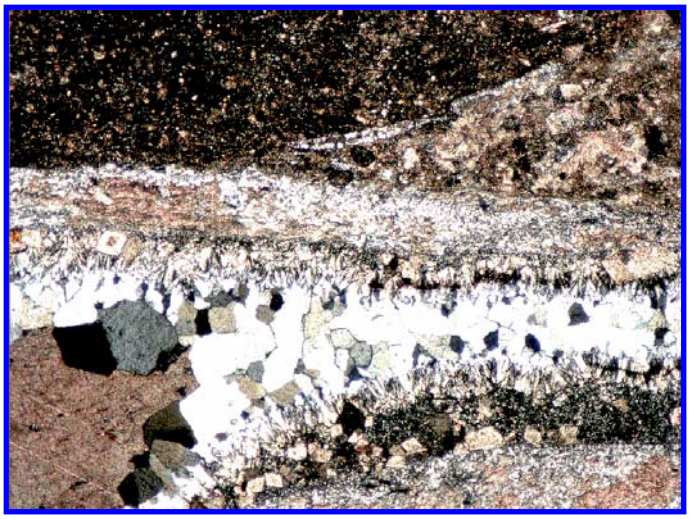

Silicification, Example #3
West Virginia, Wood County
Trenton Formation, 9618 ft

The outer portion and most of the central portion of this grain has been silicified. There is a small amount of calcite remaining in the lower left portion of the thin section.

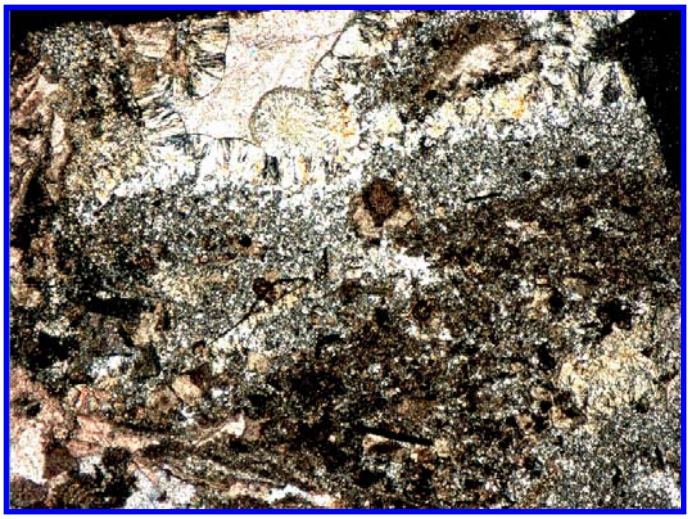

Silicification, Example #4
West Virginia, Wood County
Trenton Formation, 9618 ft

This photograph was taken at the same depth as the above thin section. Notice the pervasive silicification of the rock. The amount of silicification that has taken place makes it difficult to identify the rock type. Notice the botryoidal growth pattern of the chert in the upper portion of this slide.

Appendix E-3 – Dolomite textures in the Trenton Black River carbonate rocks of the Appalachian basin

Figure A3-1. Type I planar-p dolomite.

All of the illustrated dolomites are matrix-selective and occur in subtidal carbonate facies. These dolomites are not associated with fractures, faults, or rock alteration by hydrothermal basinal brine. They probably formed through burial dolomitization at a local scale via compaction-driven fluid flow.

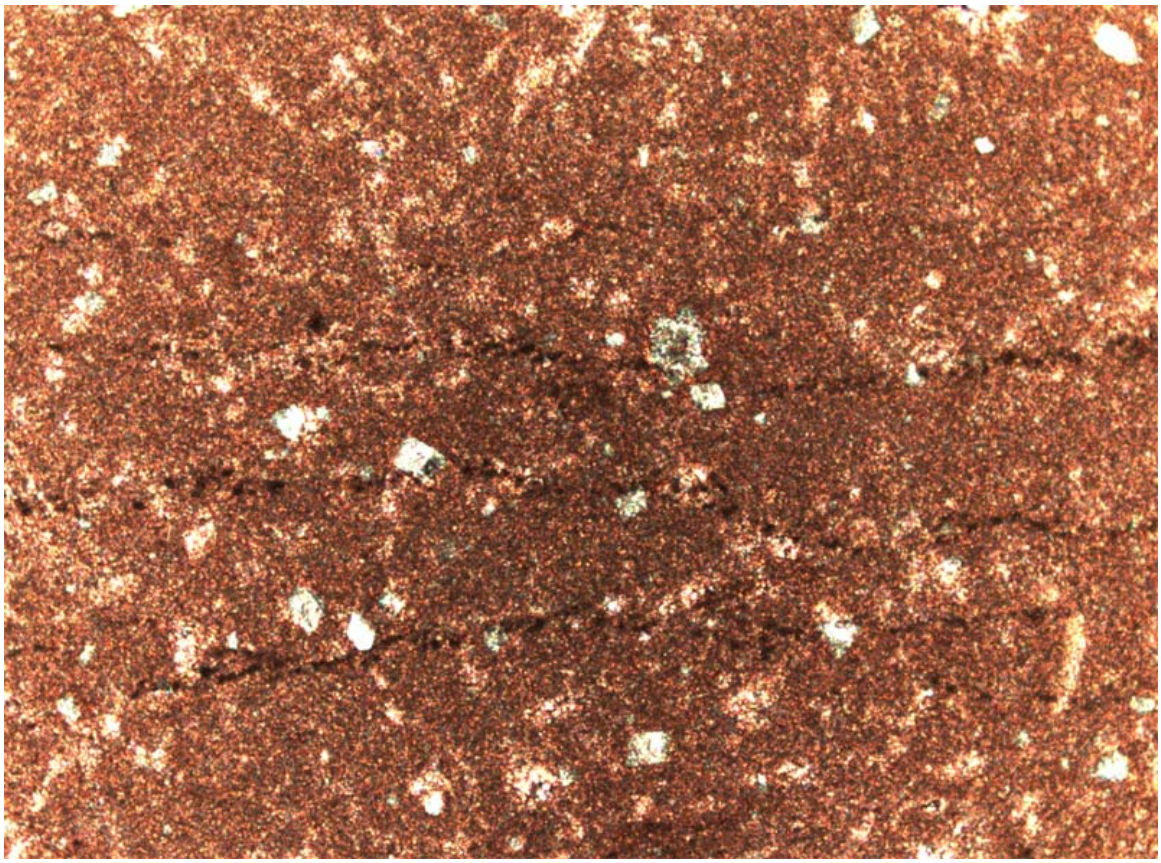

A3-1A. Planar-p dolomite replacing bioturbated, fossiliferous pelmicrite. The dolomite crystals are polymodal, ranging in size from 40 to 200 μm in diameter. The crystals have planar boundaries and are porphyrotopic, floating in the limestone matrix they replaced. Most dolomite crystals are cloudy due to inclusions, and some indistinct zoning is evident in most crystals. The matrix is peloidal micrite that we interpret as marine cement. Note the incipient solution seams, outlined by micron-size pyrite crystals, which impart a somewhat lenticular habit to the limestone. Some of the planar-p dolomite is partially dissolved along these seams indicating the dolomite formed before chemical compaction. Black River Group, Power Oil Company #9634 well (Sandhill well), Wood County, WV, 9906 ft.

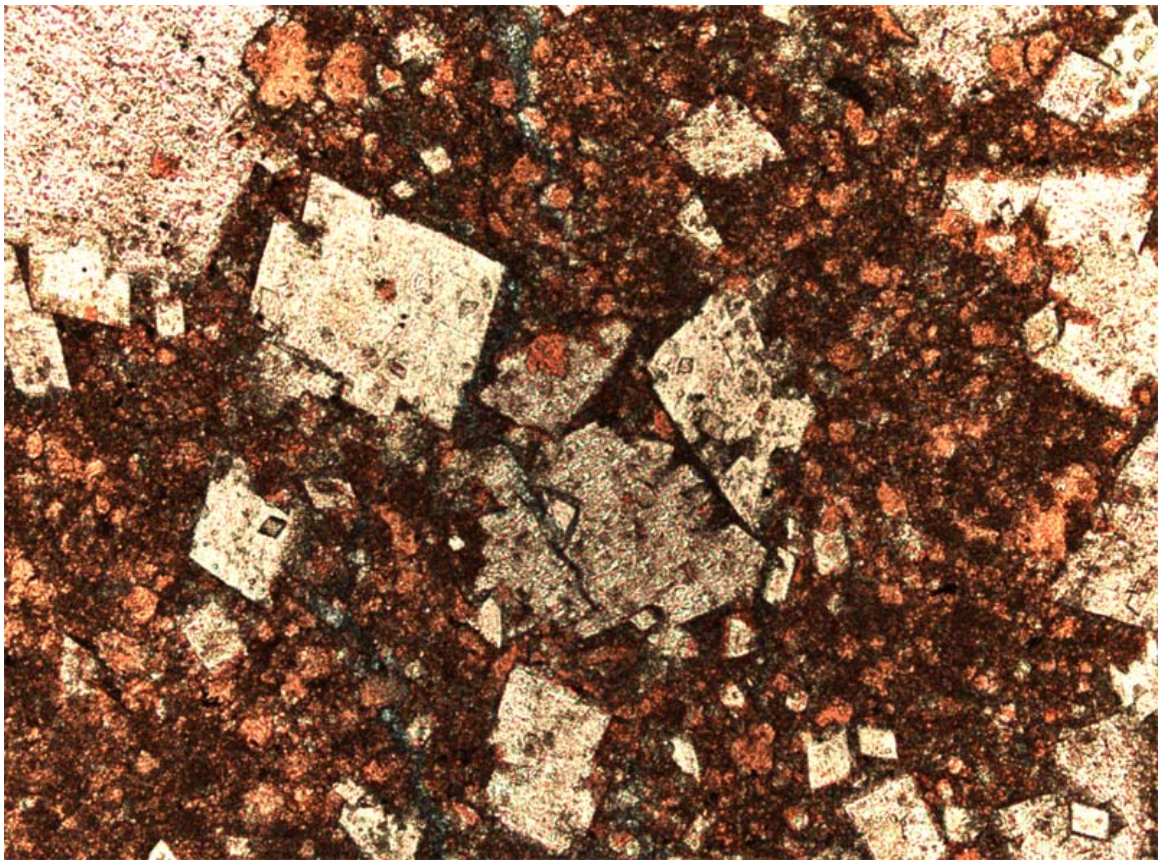

A3-1B. Finely to medium crystalline, polymodal, planar-p dolomite replacing decimicron-size neomorphic calcite crystals. The dolomite crystals are cloudy due to abundant inclusions, and predate fractures in the rock. . Black River Group, Power Oil Company #9634 well (Sandhill well), Wood County, WV, 10,162 ft.

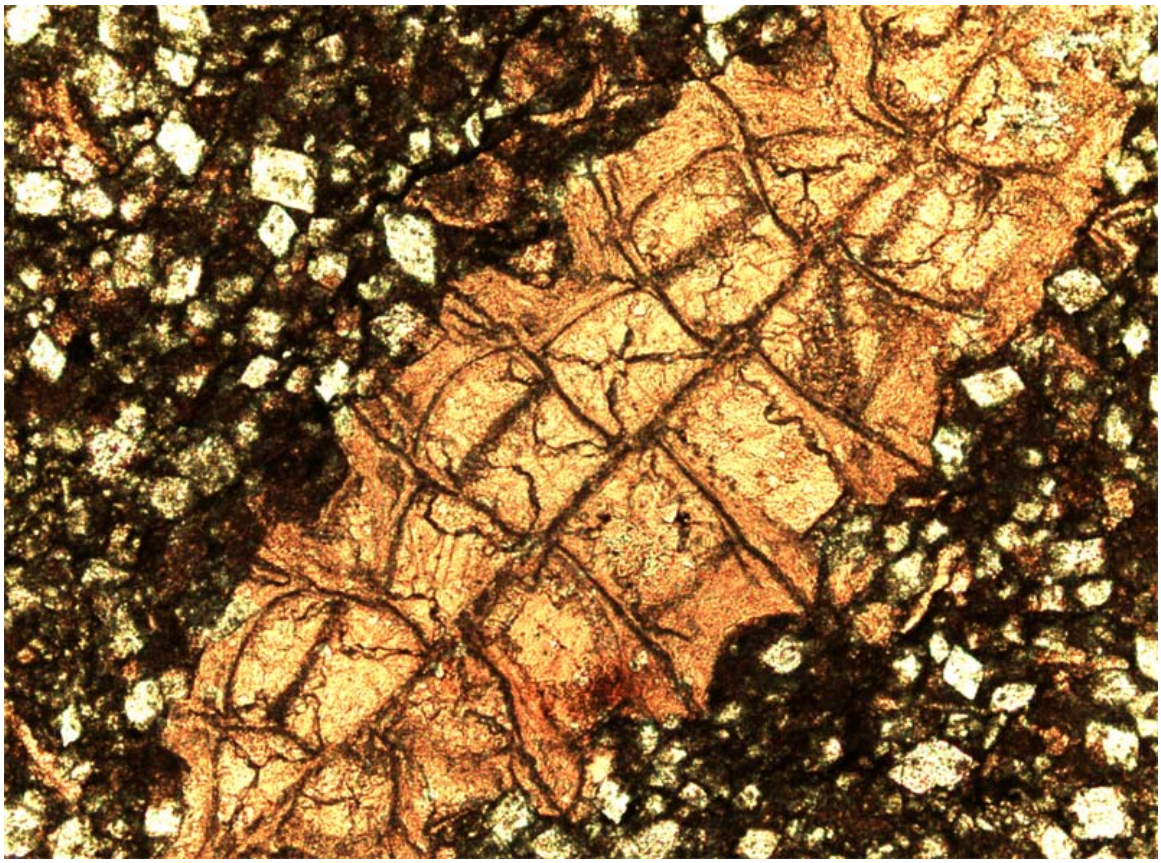

A3-1C. Polymodal, planar-p dolomite replacing matrix in a sparse biopelmicrite in the Black River Group. Outcrop sample from Union Furnace, Huntingdon County, PA.

Figure A3-2. Type I planar-p and planar-e dolomite.

All of the illustrated dolomites are matrix-selective and occur in subtidal carbonate facies. These dolomites are not associated with fractures, faults, or rock alteration by hydrothermal basinal brine. They probably formed through burial dolomitization at a local scale via compaction-driven fluid flow.

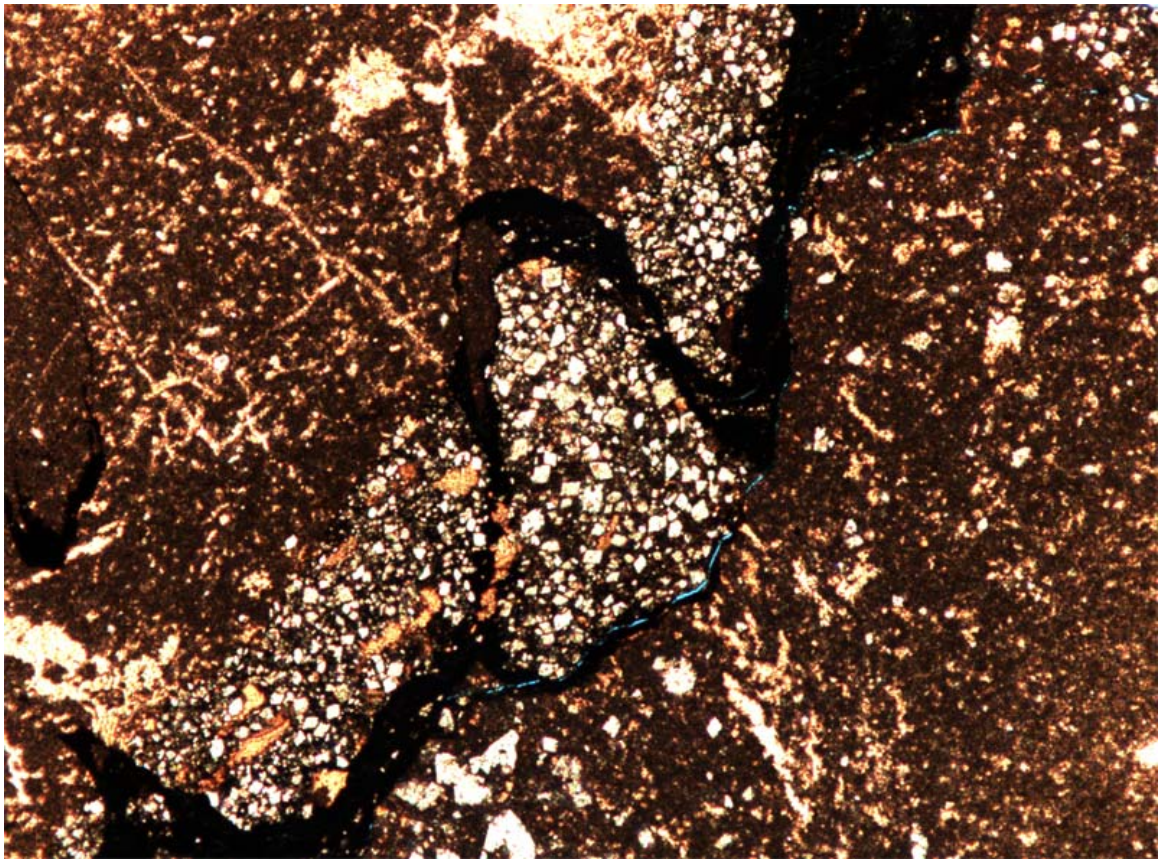

A3-2A. Polymodal planar-e dolomite replacing bioturbated, fossiliferous pelmicrite adjacent to stylolites. The dolomite crystals are 2 to 100 μm in diameter. Note the abundant inclusions in the dolomite crystals. This planar-e dolomite resembles the planar-p textures shown in the last three photomicrographs above, but the euhedral dolomite now forms a mosaic that almost entirely replaces limestone matrix. Note, however, the planar-p dolomite replacing limestone away from the solution seam. Chemical compaction might have concentrated the planar dolomite crystals along the solution seams. Black River Group, Power Oil Company #9634 well (Sandhill well), Wood County, WV, 10,162 ft.

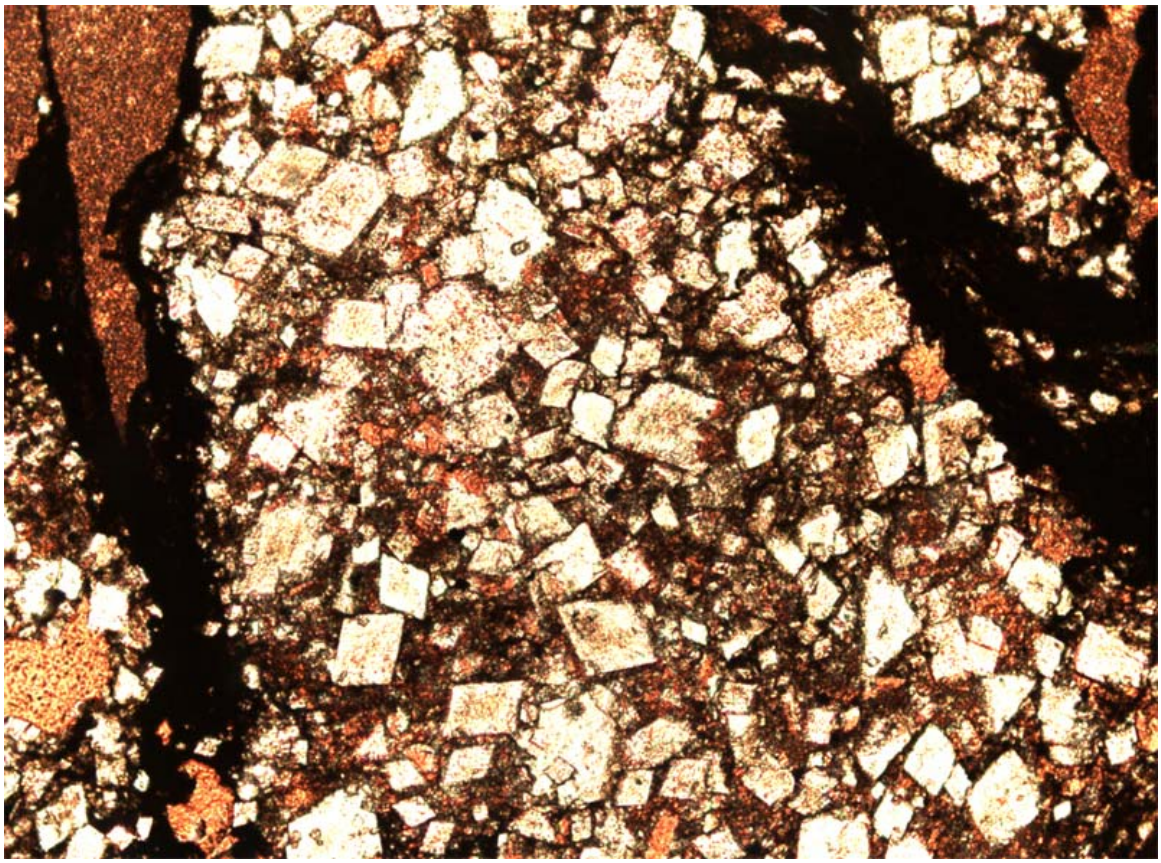

A3-2B. Higher magnification view of the planar-e dolomite in Figure A3-2 A. Note that some of the dolomite floats within the insoluble material of the seam, and is partially dissolved along it too. Dolomitization predates chemical compaction.



A3-2C. Laminae of brown planar-e dolomite interbedded with thicker beds of skeletal limestone (wackestone and packstone) in the Black River Group exposed at the Union Furnace outcrop in central PA.

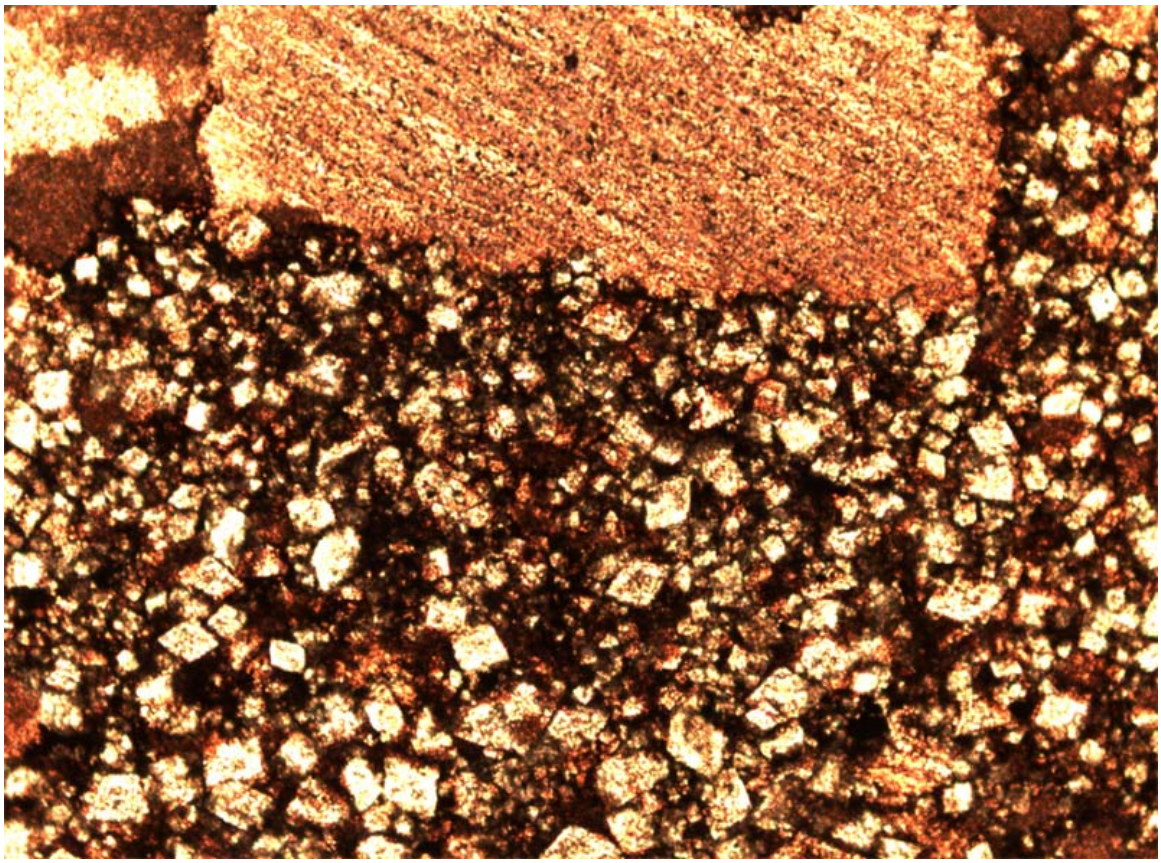

A3-2D. Thin section photomicrograph of matrix-selective, polymodal planar-e dolomite replacing micrite in one of the brown laminae shown previously in Figure A3-2C above.

Figure A3-3. Type I planar-e and planar-s dolomites.

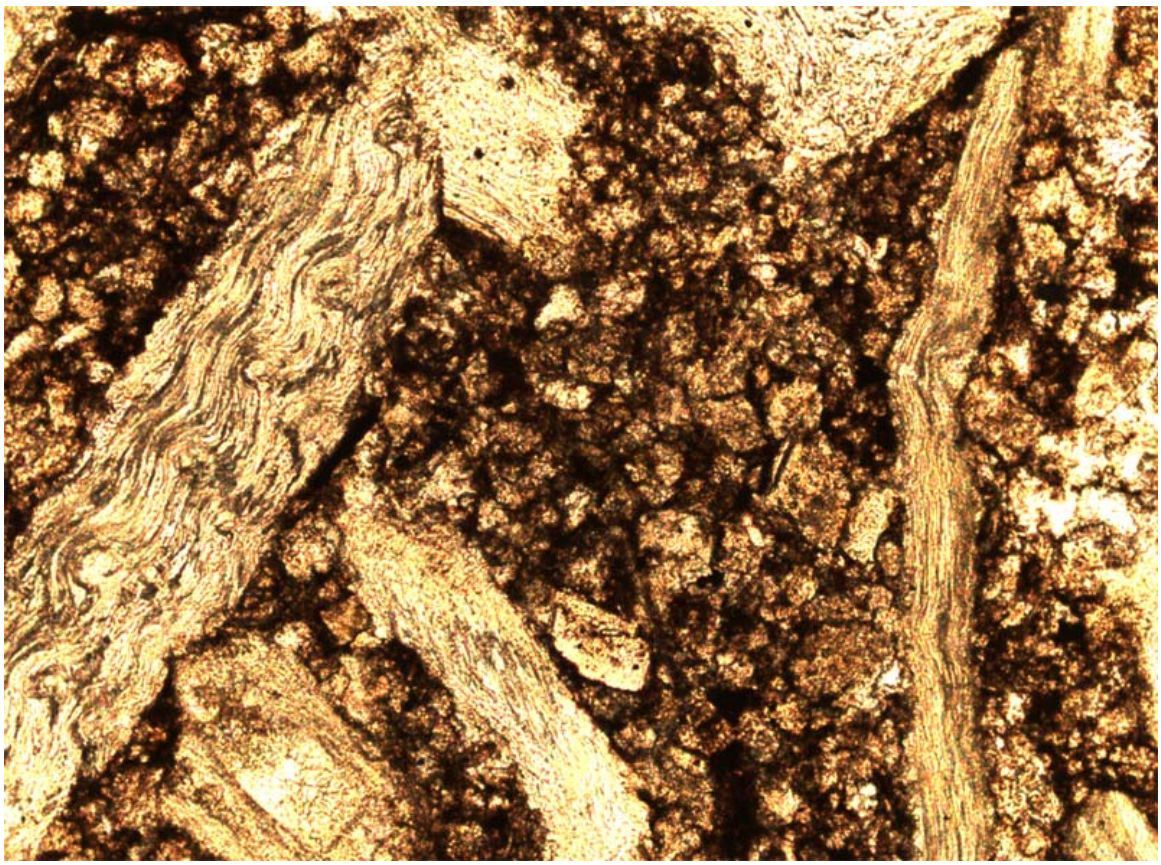

A3-3A. Thin section photomicrograph of decimicron- to centimicron-size polymodal, planar-e to planar-s dolomite replacing peloidal calcite cement in a grainstone. Trenton Formation, Melben Oil Company Emma McKnight #1 well, Mercer County, PA, 6845.2 ft. This dolomite is matrix-selective and occurs in a subtidal carbonate ramp facies. This dolomite is not associated with fractures, faults, or rock alteration by hydrothermal basinal brine.

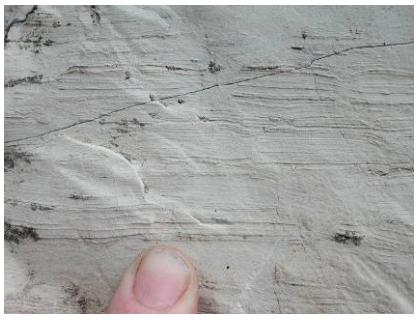

A3-3B1

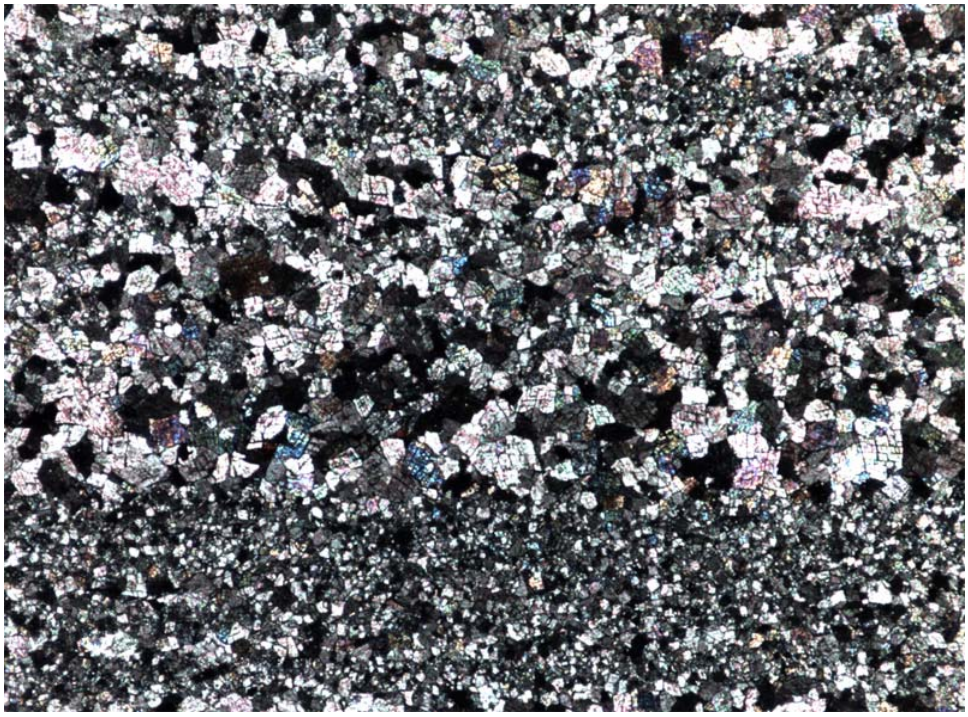

A3-3B2



A3-3B3

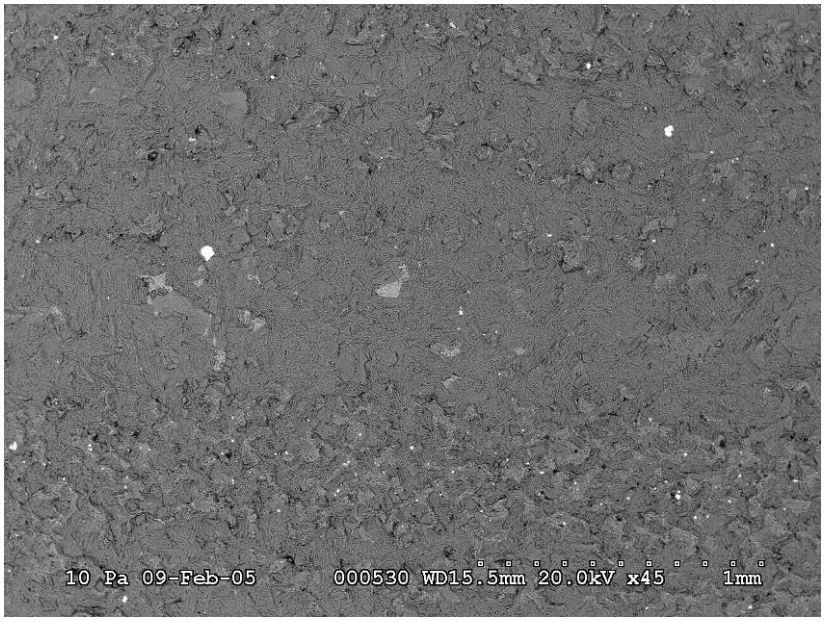

A3-3B4

B. Micron- and decimicron-size polymodal planar-e to planar-s dolomite in laminated peritidal carbonates. 1 and 2 are stromatolites exposed in the basal Black River Group at Union Furnace in Huntingdon County, PA in which the dolomite replaced the original limestone. 3 and 4 show respective core and backscattered electron SEM photographs of probable peritidal stromatolites in the Ohio #2854 well, Delaware County, Ohio (Trenton Formation, 2901 ft.). These planar dolomites probably formed through reflux and/or mixing zone dolomitization.

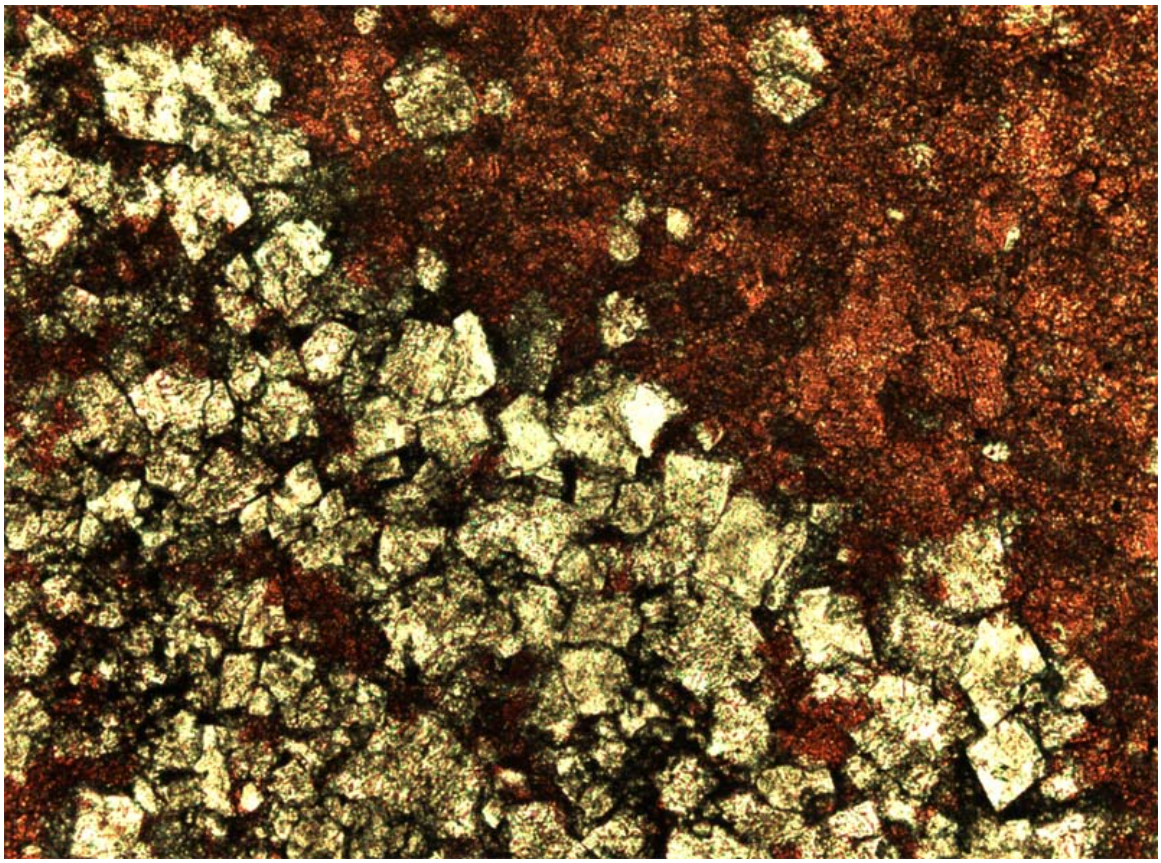

A3-3C. A hydrothermal dolomitization front in the Black River Group. Polymodal decimicron-size planar-e dolomite partially replaces pelmicrite. Intercrystalline porosity in the dolomite is filled by bitumen. This planar dolomite fabric occurs in a zone near the top of a faulted and fractured subsurface interval altered by hydrothermal dolomitization. The dolomite formed through rock alteration by saline basinal brines (the dolomite $\delta^{18}O$ = -9 permil, Smith, 2005, personal communication). Black River Group, Dominion Exploration and Production Company Bayles #1 well, Bradford County, PA, 12,425 ft.

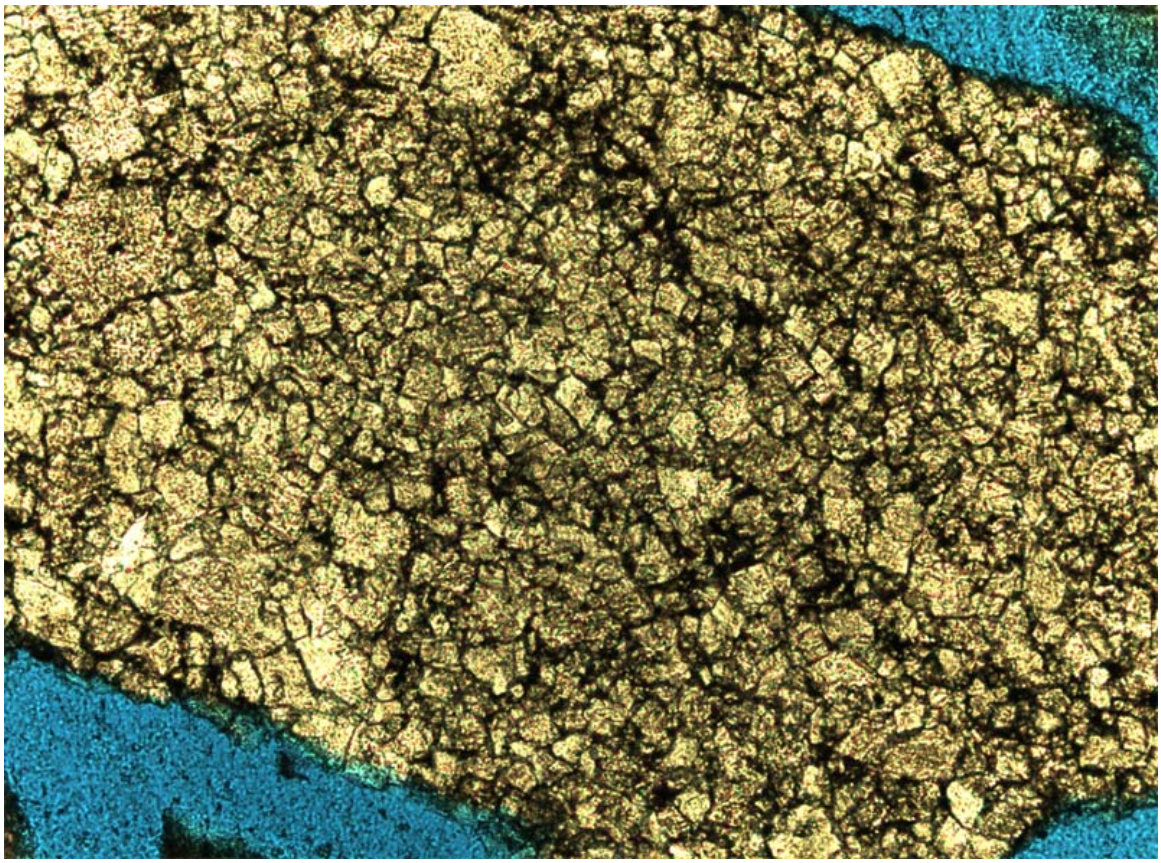

A3-3D. Polymodal decimicron- and centimicron-size planar-e to planar-s dolomite completely replacing pelmicrite. The apparent intercrystalline porosity is filled with bitumen. This planar fabric is associated with fracturing, faulting, and hydrothermal dolomitization. Black River Group, Dominion Exploration and Production Company Bayles #1 well, Bradford County, PA, 12,425 ft.

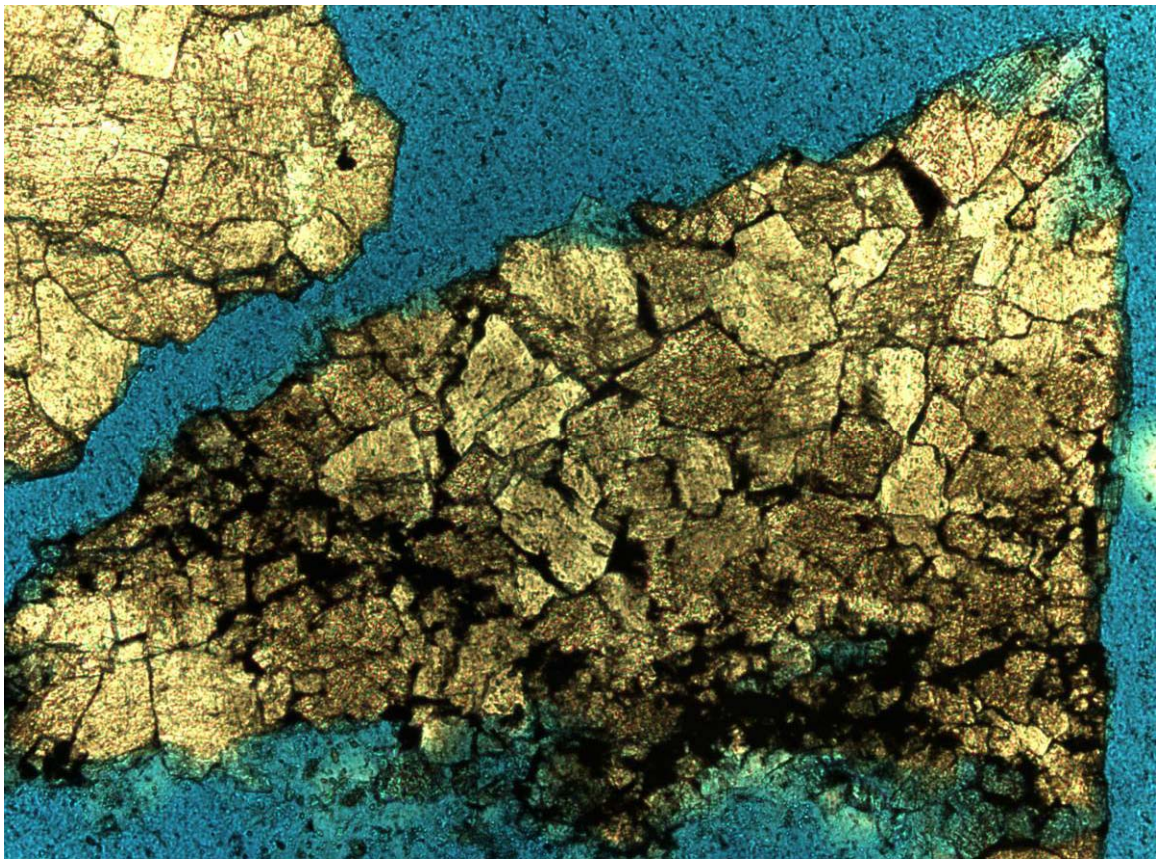

A3-3E. Hydrothermal decimicron- to centimicron-size polymodal planar-s dolomite. Bitumen fills intercrystalline void space. Also note the cutting composed of centimicron-size planar-s dolomite in the upper left corner of the photograph. Black River Group, Dominion Exploration and Production Company Bayles #1 well, Bradford County, PA, 12,425 ft.

Figure A3-4. Type I planar-c dolomite.



A3-4A. SEM photomicrograph of polymodal (60μm to 300μm crystals) planar-c dolomite lining and partially filling a small vug in the Trenton Limestone. Prudential 1A well, Marion County, OH, 2013.5 ft.

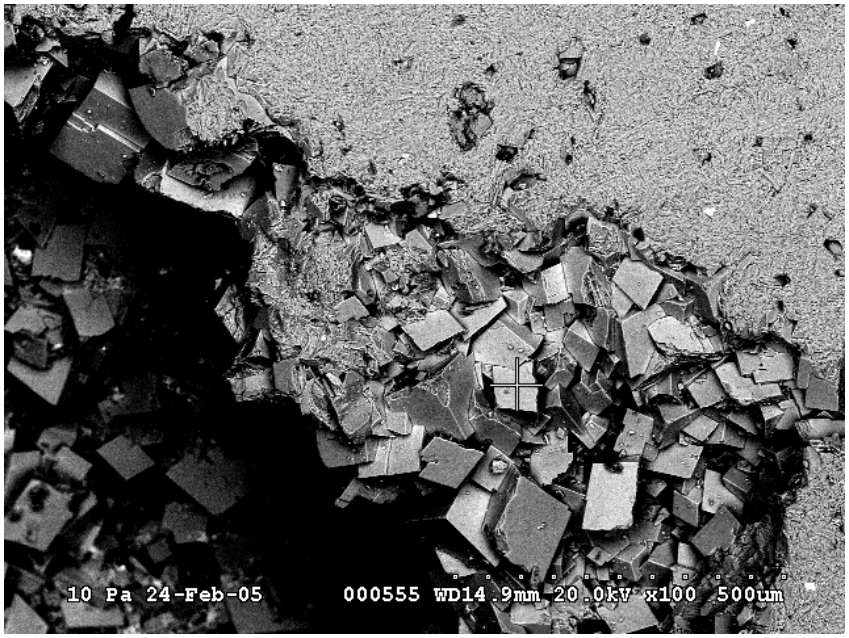

A3-4B. Higher magnification view of planar-c dolomite shown in Figure A3-4A. This dolomite is in the upper right corner of the vug. The cross on the crystal just right of the center of the SEM photo shows the spot of the EDS analysis presented next in Figure A3-4C.

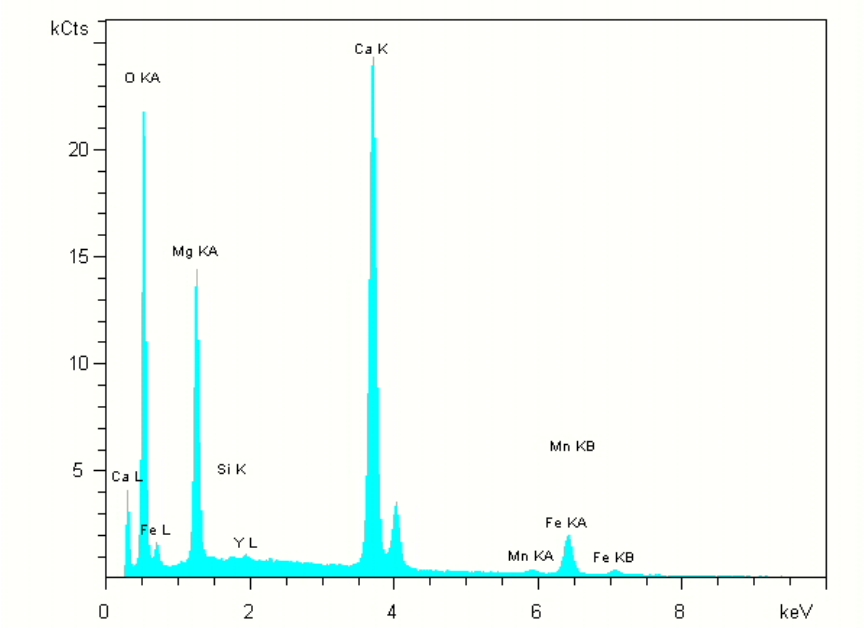

A3-4C. EDS spectra of the planar-c dolomite shown in Figure A3-4B. The dolomite is not stoichiometric, having an excess of Ca (Ca = 17.77%, Mg = 11.50 %), and it is ferroan (Fe = 3.53 wt.%), indicating formation from saline basinal fluid (see Allan and Wiggins, 1993).

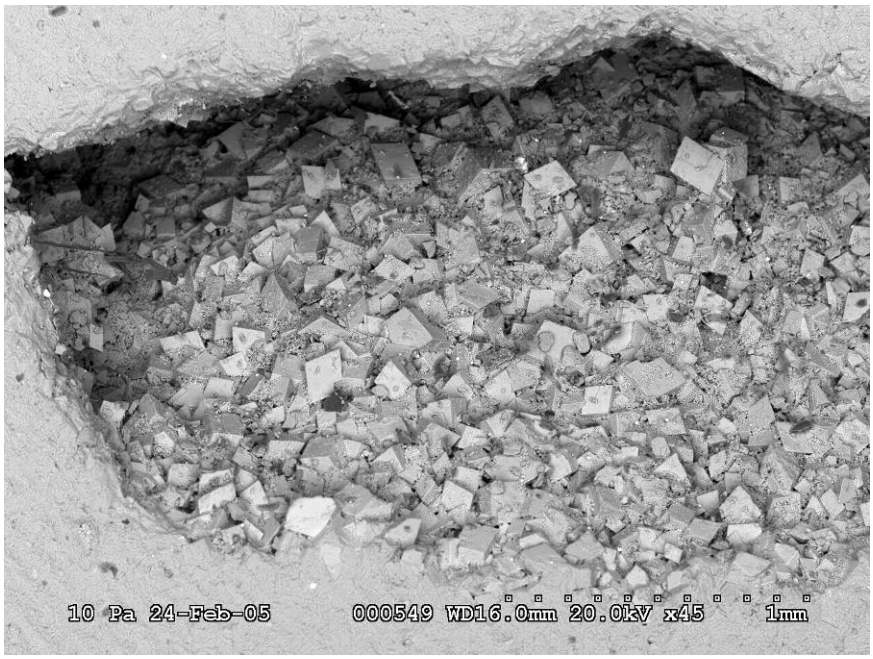

A3-4D. SEM photomicrograph of polymodal decimicron- to centimicron-size planar-c dolomite lining a medium vug in the Trenton Formation. The Fe concentration of this dolomite is 8.98 wt.%, indicating saline basinal brine as the dolomitizing fluid. Prudential 1A well, Marion County, OH, 1855 ft.

Figure A3-5. Type II planar-s to nonplanar (transitional) dolomites.

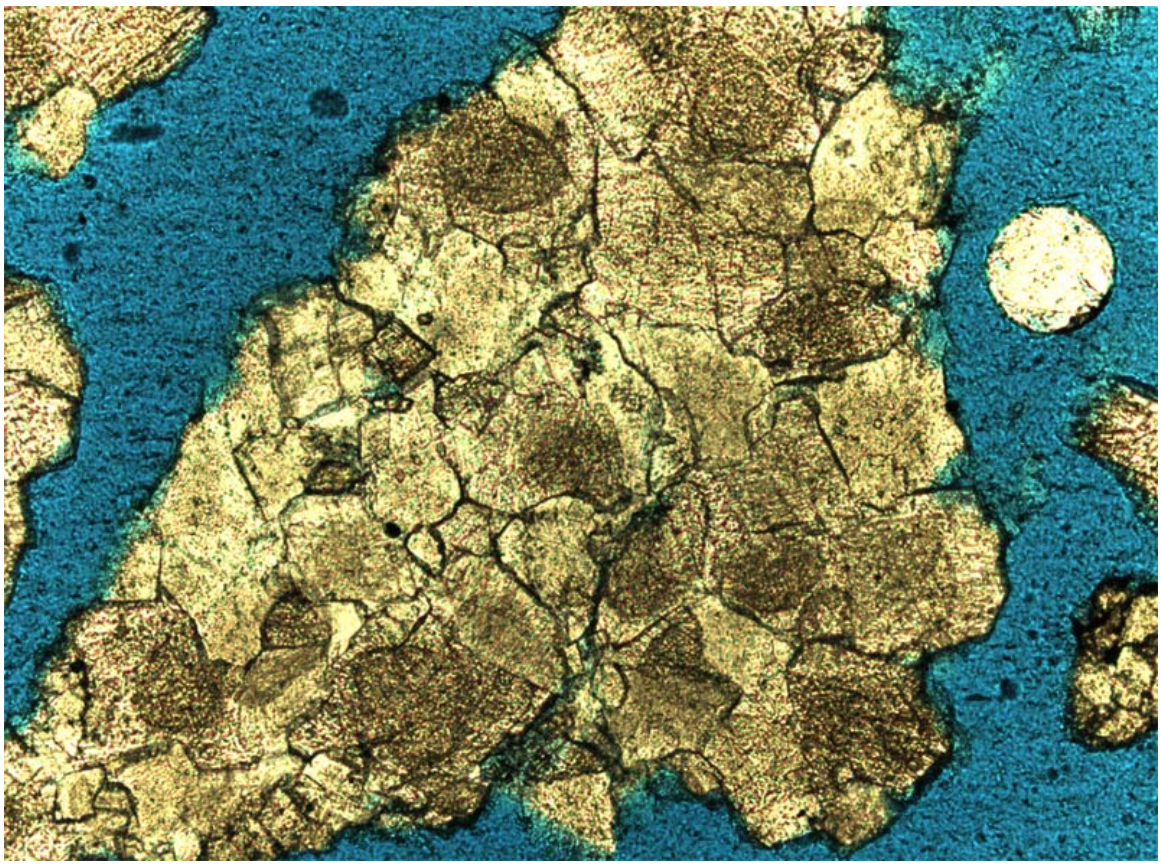

A3-5A. Planar-s to nonplanar (transitional) dolomite replacing a peloidal or oolitic limestone. Compare the ghosts of the peloids or ooids in this dolomite with the peloids (micritized ooids and grains) in the limestone cutting from the same sample shown in Figure A3-5B. Black River Group, Dominion Exploration and Production Company Bayles #1 well, Bradford County, PA, 12,425 ft.

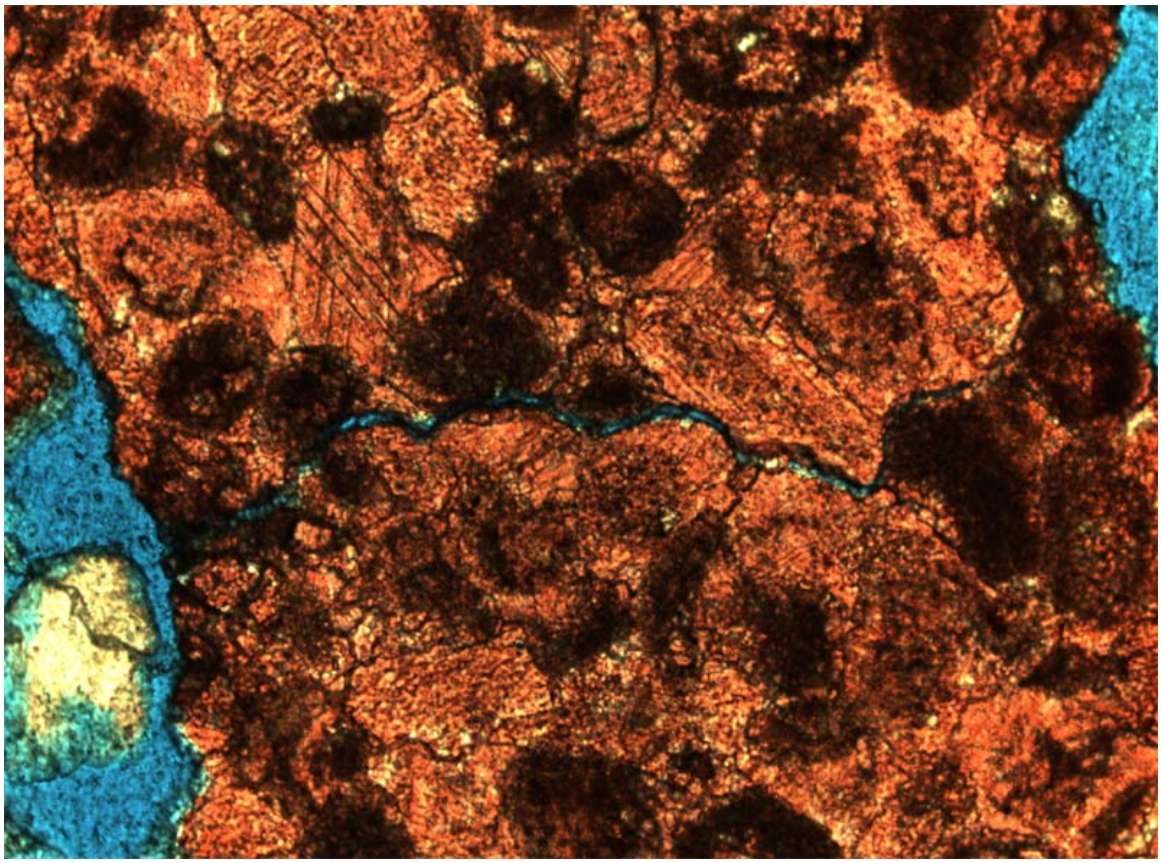

A3-5B. Peloidal limestone (pelsparite) cutting from 12,425 ft. in the Bayles #1 well, Bradford County, PA. The peloids, possibly micritized ooids, are cemented by calcite spar. Compare with the dolomite in Figure A3-5A.

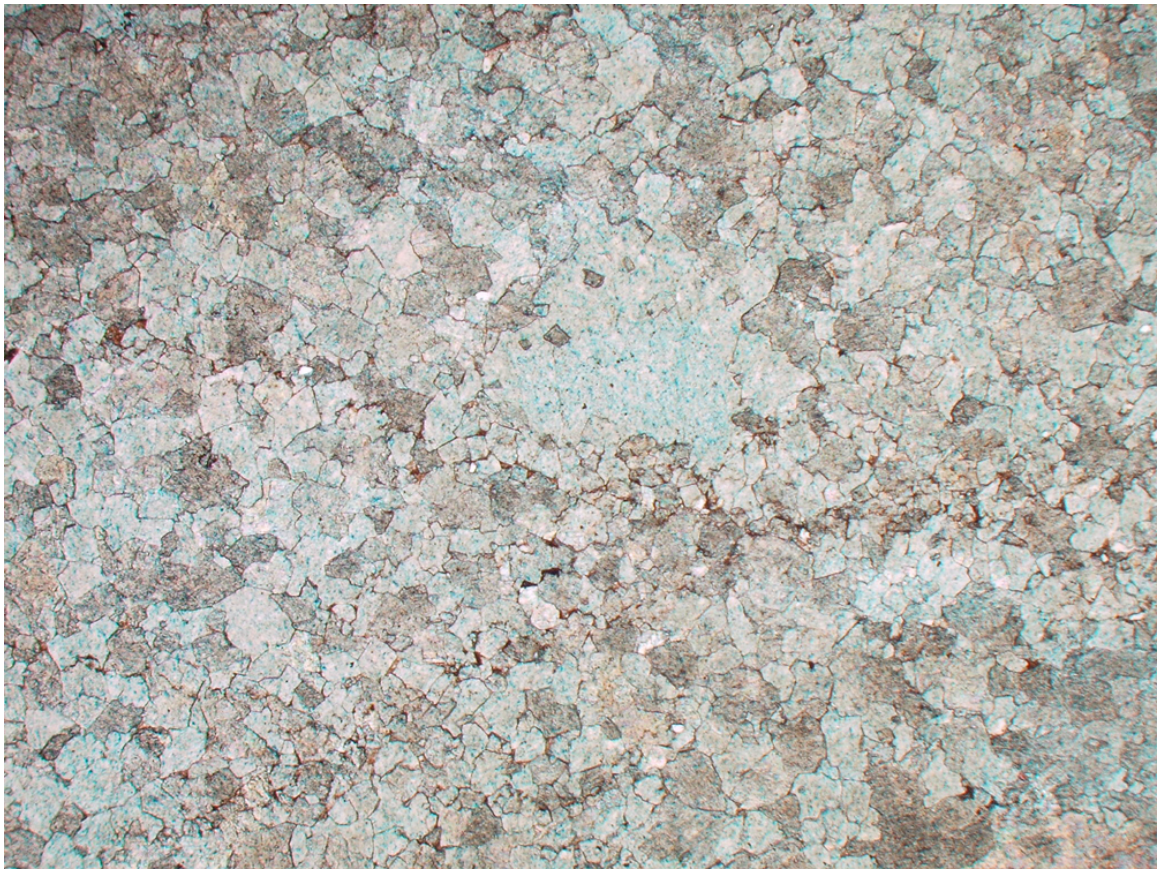

A3-5C. Polymodal decimicron- to centimicron-size planar-s to nonplanar-a (transitional) dolomite in the Black River Formation, CNR Gray #1 well, Steuben County, NY, 7793 ft.

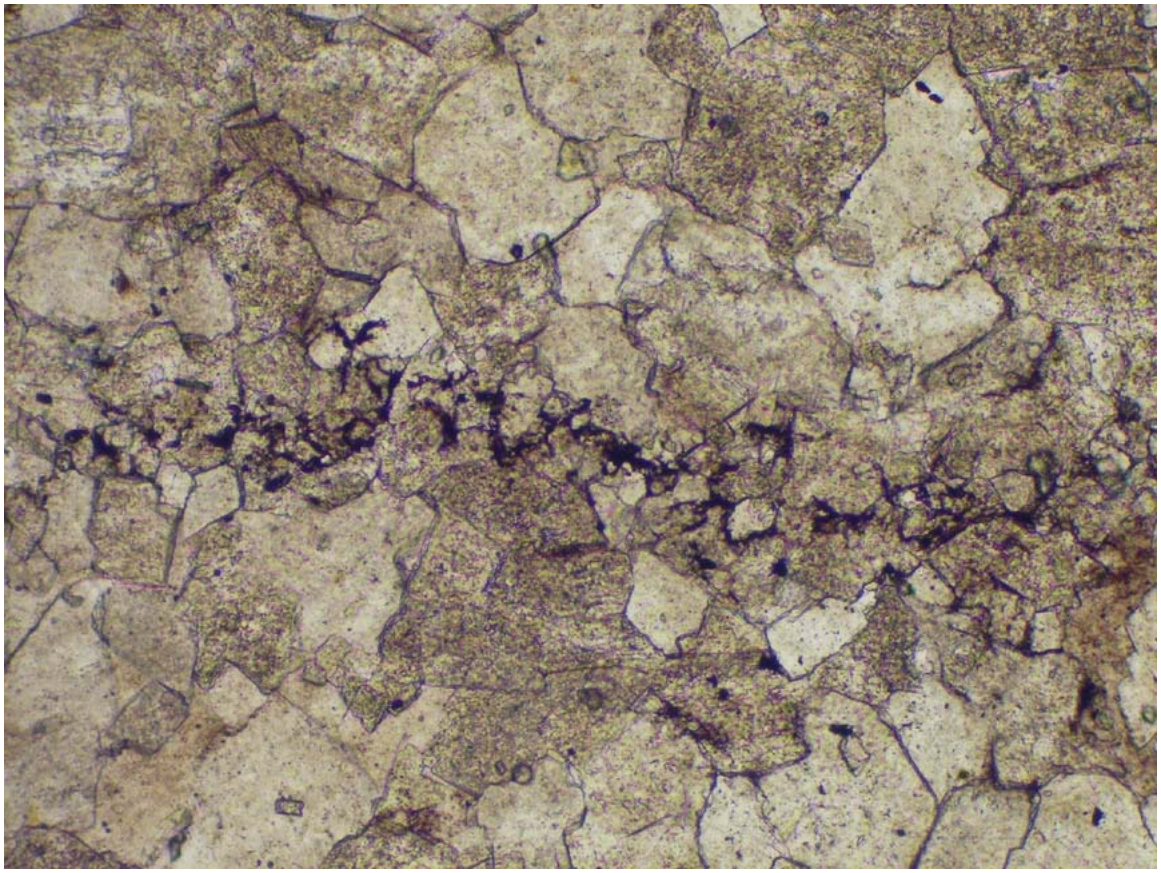

A3-5D. Polymodal decimicron- to centimicron-size planar-s to nonplanar-a (transitional) dolomite in the Black River Formation, CNR Gray #1 well, Steuben County, NY, 7793 ft.

Figure A3-6. Type II nonplanar-a dolomite textures.

All of the illustrated dolostones show fabric obliteration, and are fault and fracture-related, hydrothermal, nonplanar dolomites.

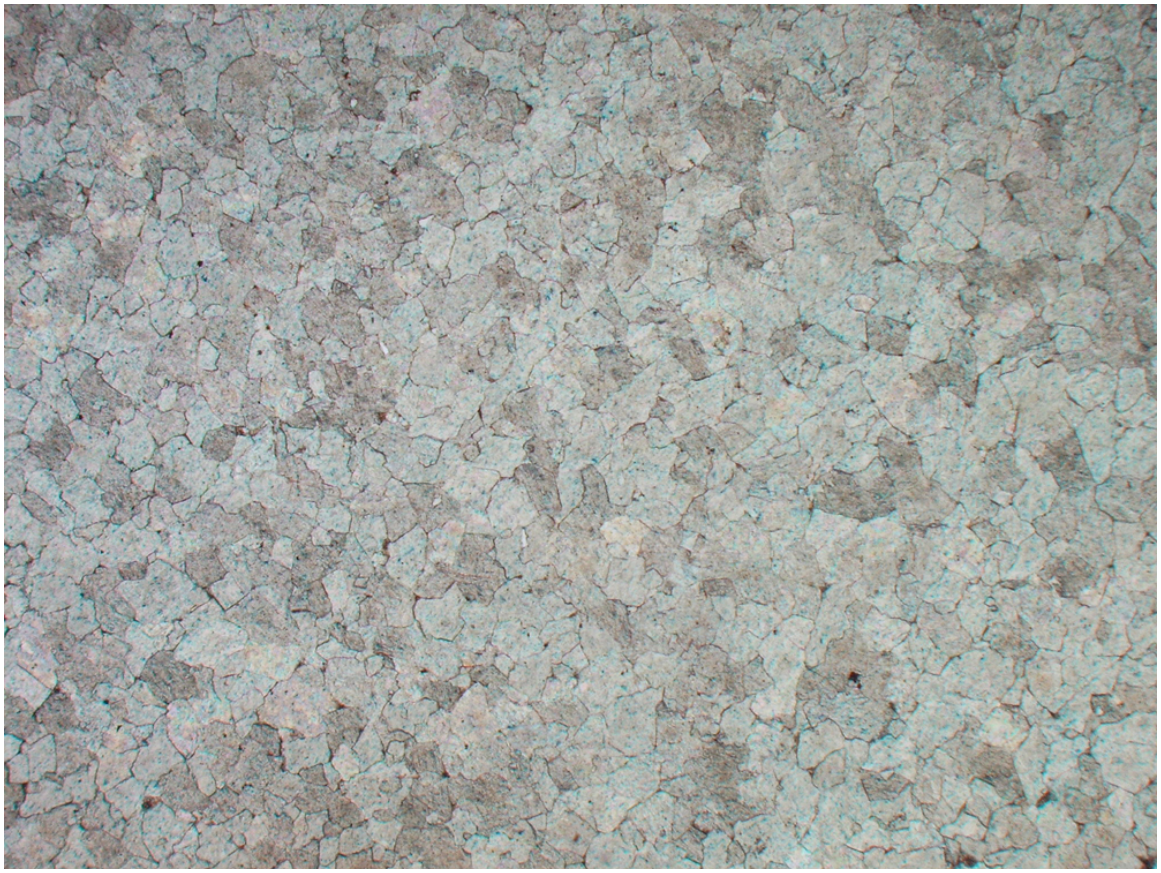

A3-6A. Unimodal, medium crystalline nonplanar-a dolomite (Black River Formation, Columbia Natural Resources Gray 24468 well, Steuben County, NY, 7796 ft.).

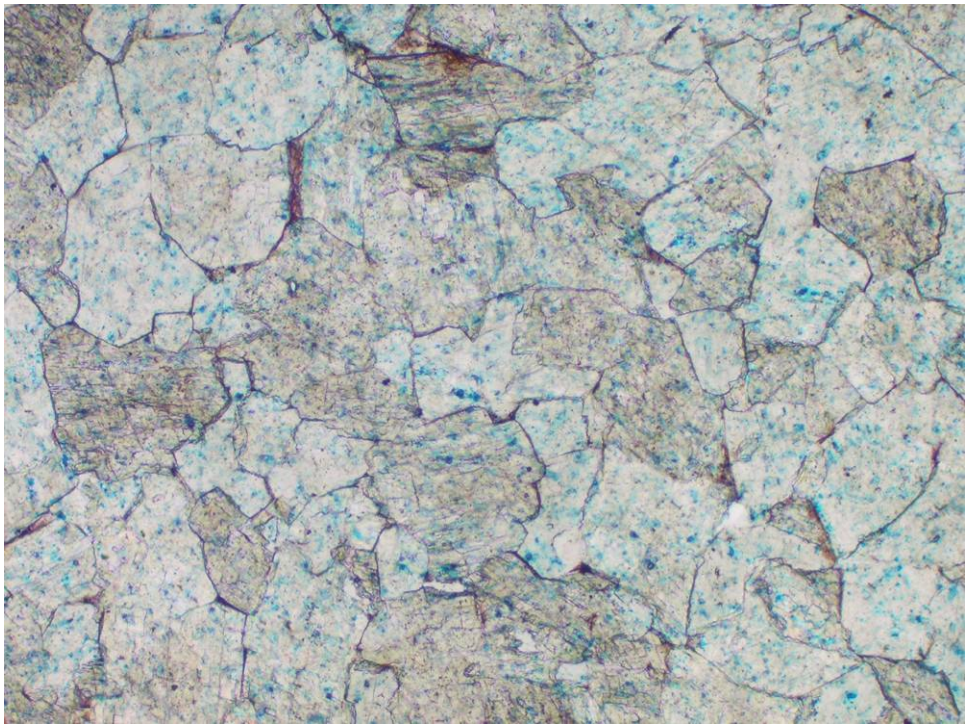

A3-6B. Higher magnification view of nonplanar-a dolomite shown in Figure A3-6A. Note the tightly interlocked crystal fabric and consequent lack of intercrystalline pore space.

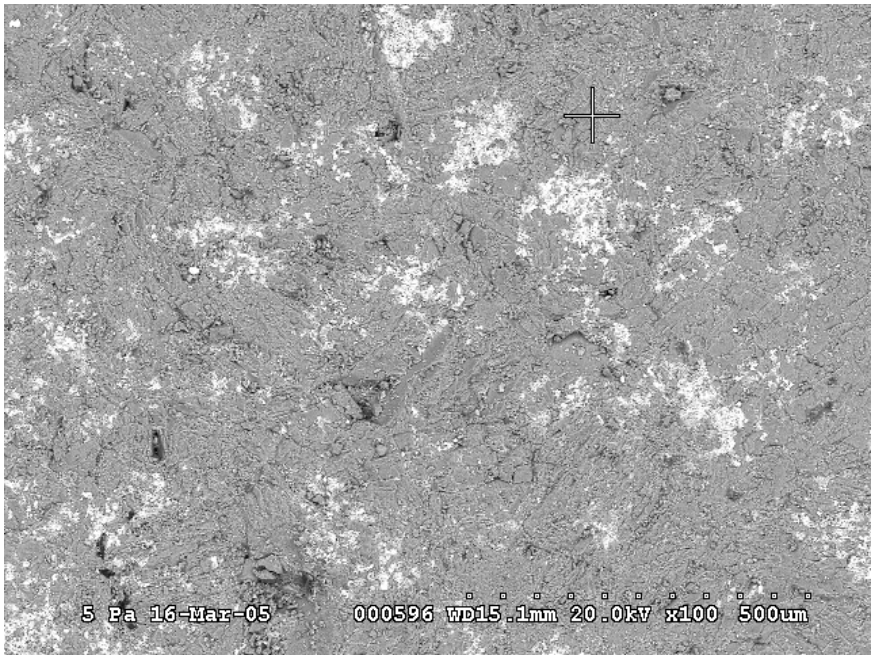

A3-6C. Backscattered SEM photomicrograph of nonplanar-a dolomite texture. This sample is from the same well core as those shown in Figure A3-6A and B, but is from a slightly deeper interval at 7799.9 ft. The predominant medium gray is nonplanar-a dolomite, which is not stoichiometric (Ca = 23.54 wt.%, Mg = 11.87 wt.%) and is ferroan (Fe = 2.17 wt.%). The white material is a chloride (Cl = 20.35 wt.%) with notable sodium and potassium (Na = 7.10 wt.%, K = 6.30 wt.%). The material does not appear in thin sections, probably due to high solubility in water and loss during preparation of the slide. It does appear as a dark, reddish, compact and granular mass in the hand samples of the core. The material might be an admixture of halite and sylvite, or a precipitate in the core that formed through evaporation of a residual K-Na-Cl brine.

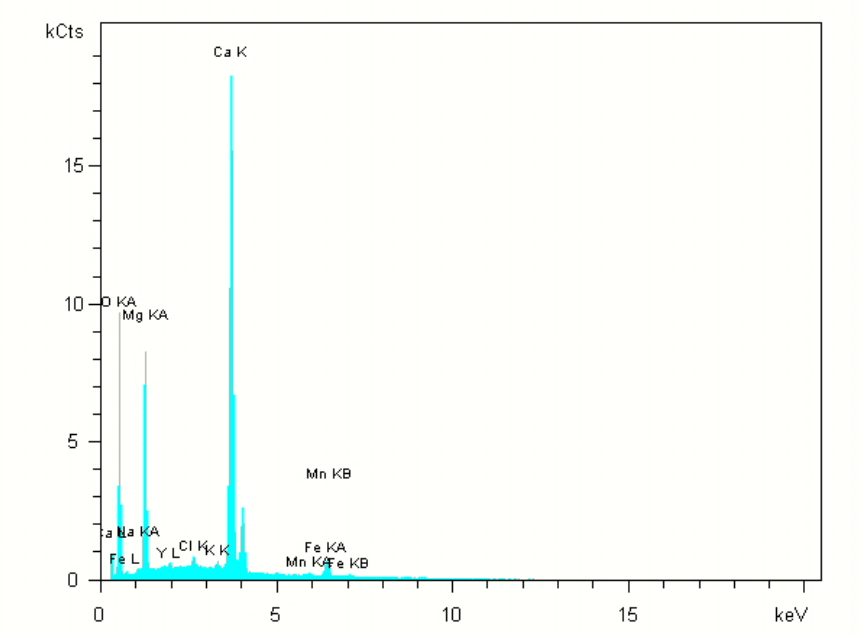

A3-6D. EDS spectra of the nonplanar-a dolomite in Figure A3-6C.

Figure A3-7. Nonplanar (saddle) dolomite textures.

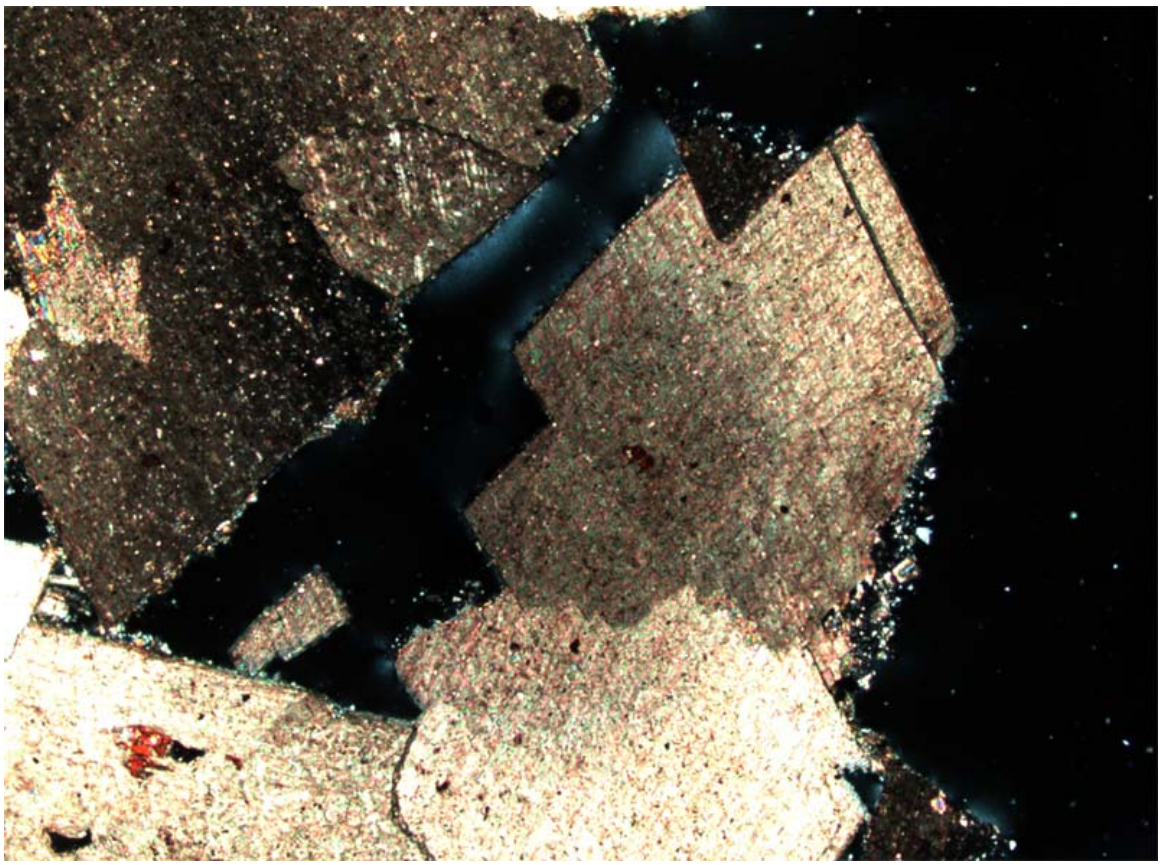

A3-7A. Nonplanar (saddle) dolomite cement partially filling a small vug in the Trenton Formation (OH 3479, Anderson well, Hancock Co., OH, 1337.8 ft.). Note the diagnostic spearhead crystal shape, mottled salt and pepper appearance (due to inclusions), and sweeping extinction under crossed polars.

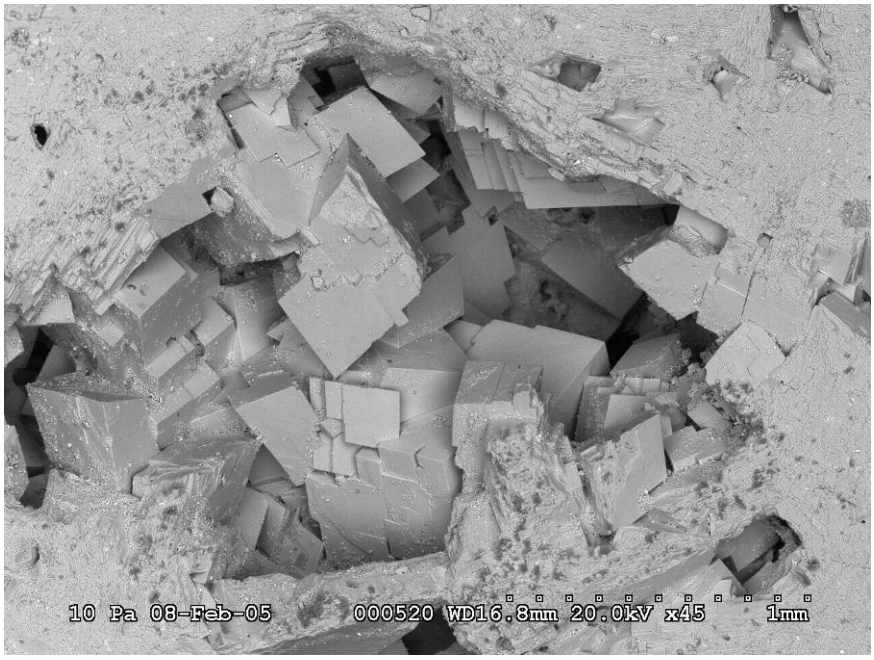

A3-7B. Backscattered SEM photomicrograph of nonplanar (saddle) dolomite cement filling a small vug in the Trenton Formation. This is the same sample shown in Figure A3-7A. The saddle dolomite crystals exhibit the same spearhead shape observed in thin section, and curved crystal faces are easier to see in this three dimensional view.



A3-7C. High magnification SEM view of nonplanar (saddle) dolomite filling a small vug in the same Ohio sample shown in Figure A3-7A and B. The cross on the crystal in the upper center of the photograph is the spot of the EDS analysis shown in Figure A3-7D. The saddle dolomite is not stoichiometric, with calcium excess (Ca = 17.05 wt.%, Mg = 12.68 wt.%), and it is nonferroan (Fe = 1.01 wt.%).

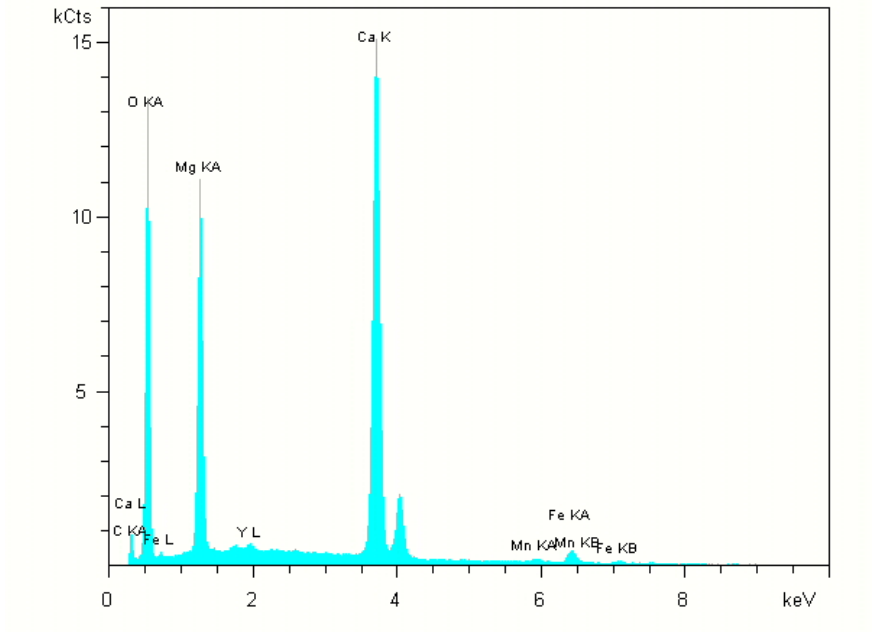

A3-7D. EDS spectra of nonplanar (saddle) dolomite shown in Figure A3-7C.



A3-7E. Pore-filling nonplanar (saddle) dolomite with oil staining in the Trenton Limestone. Note the curved crystal faces. (OH 2549 core, Wood Co., OH, 1168.25 ft.).

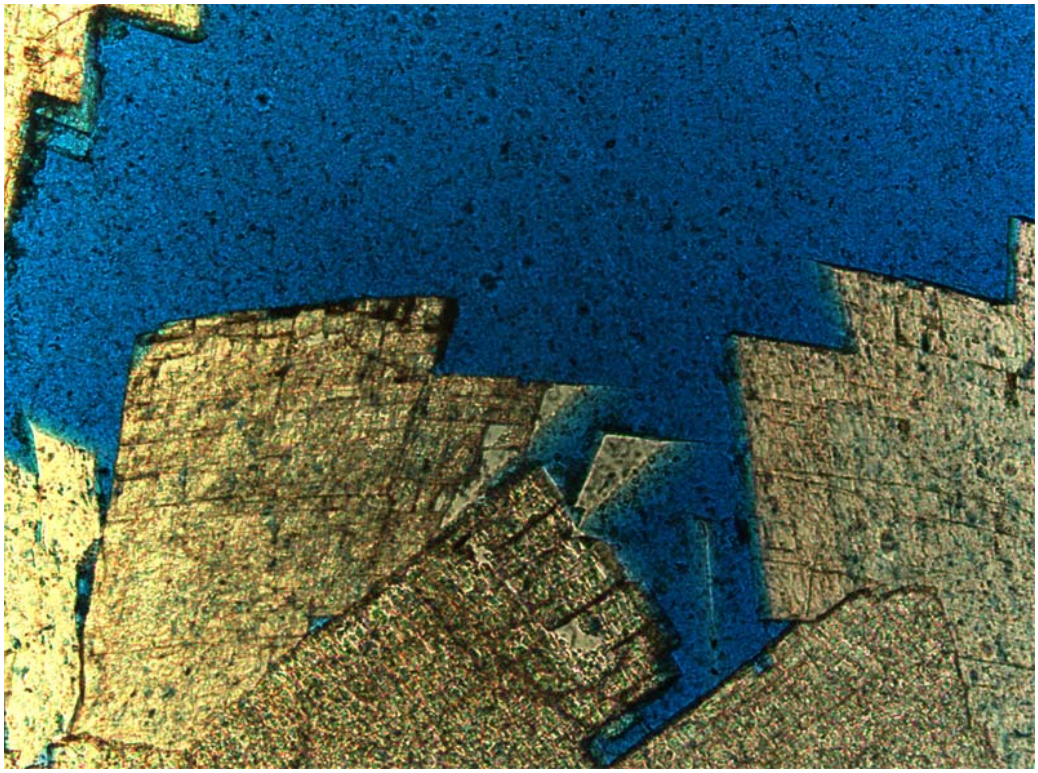

A3-7F. Nonplanar (saddle) dolomite lining a large vug in the Black River Formation. (Whiteman #1 well, Steuben Co., NY, 9531 ft.).



A3-7G. Backscattered SEM view of the same sample shown in Figure A3-7F. Nonplanar (saddle) dolomite cement lines a large vug. Note the bitumen coatings on some of the dolomite.

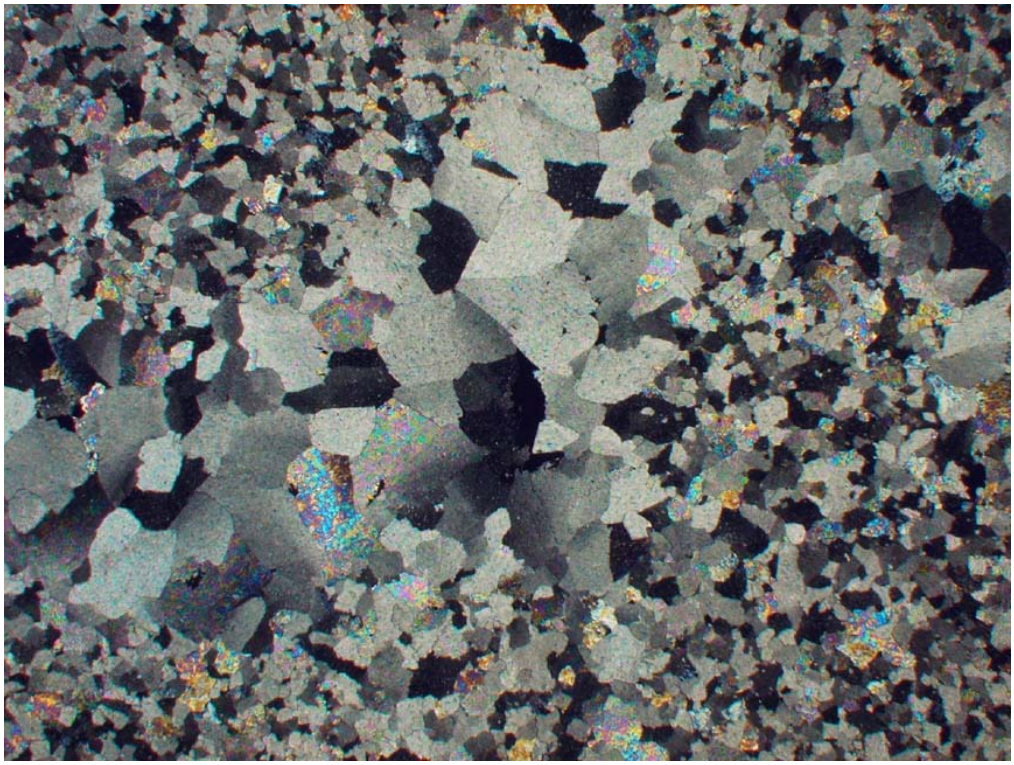

A3-7H. Nonplanar (saddle) dolomite cement completely fills a small vug in the same sample shown in Figures A3-7F and G.

Figure A3-8. Limestone replacement textures.

Mimetic and non-mimetic replacement of original crinoid bioclasts (originally composed of high-magnesium calcite) by planar-s to nonplanar-a dolomite. All examples from the Trenton Formation, OH 3479, Anderson well, Hancock Co., OH, 1337.8 ft.

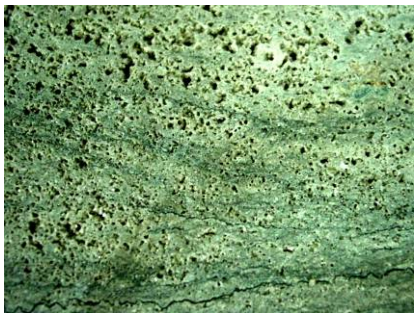

A3-8A. Core sample of vuggy crinoid/bryozoan dolograinstone with mimetically replaced crinoid visible near the top center of the photograph. A fabric selective intraparticle pore occurs in the crinoid's central lumen. Vague circular rinds and halos around some mesopores suggest they are non-mimetically replaced allochems.

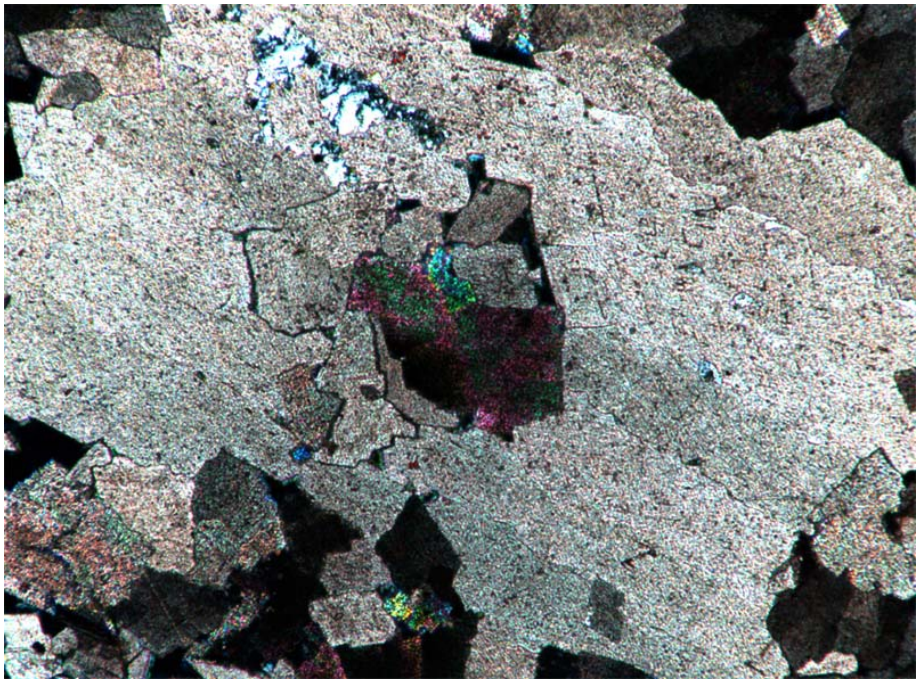

A3-8B. Thin section photomicrograph of a mimetically replaced crinoid in the same sample shown in (1). Planar-s to nonplanar-a dolomite replaced the original crinoid grain. Note chert replacing the dolomitized crinoid in the upper left corner of the fossil.

Figure A3-9. Hybrid dolomite fabrics.

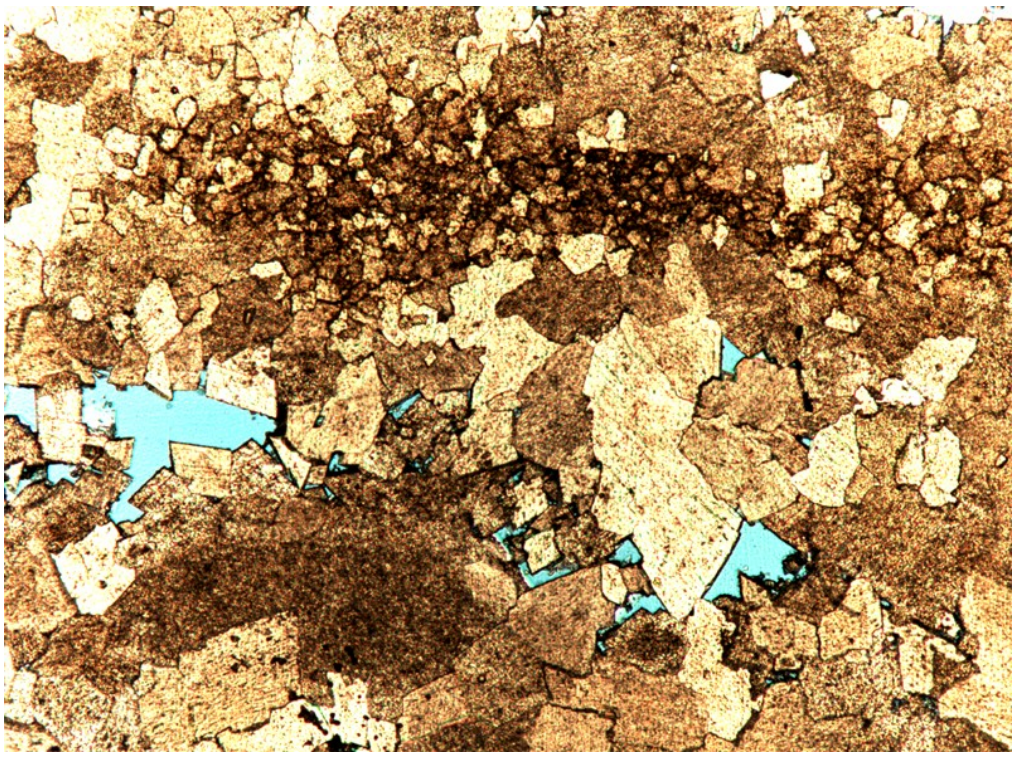

A3-9A. A small pocket of polymodal, decimicron-sized planar-s dolomite surrounded by coarser (centimicron- to millimeter-sized) planar and nonplanar dolomite. Centimicron-sized planar-s to nonplanar-a dolomite surrounds the finer crystalline planar-s dolomite. Centimicron-sized planar-e and centimicron- to millimeter-sized saddle dolomite both partially fill large mesopores and medium vugs. Nonplanar (saddle) dolomite also mimically replaces a large echinoderm fragment (lower left) in this former skeletal grainstone. Trenton Formation, Strayer #1 well, (OH 3478 core), Allen County, OH, 1211.25 ft.

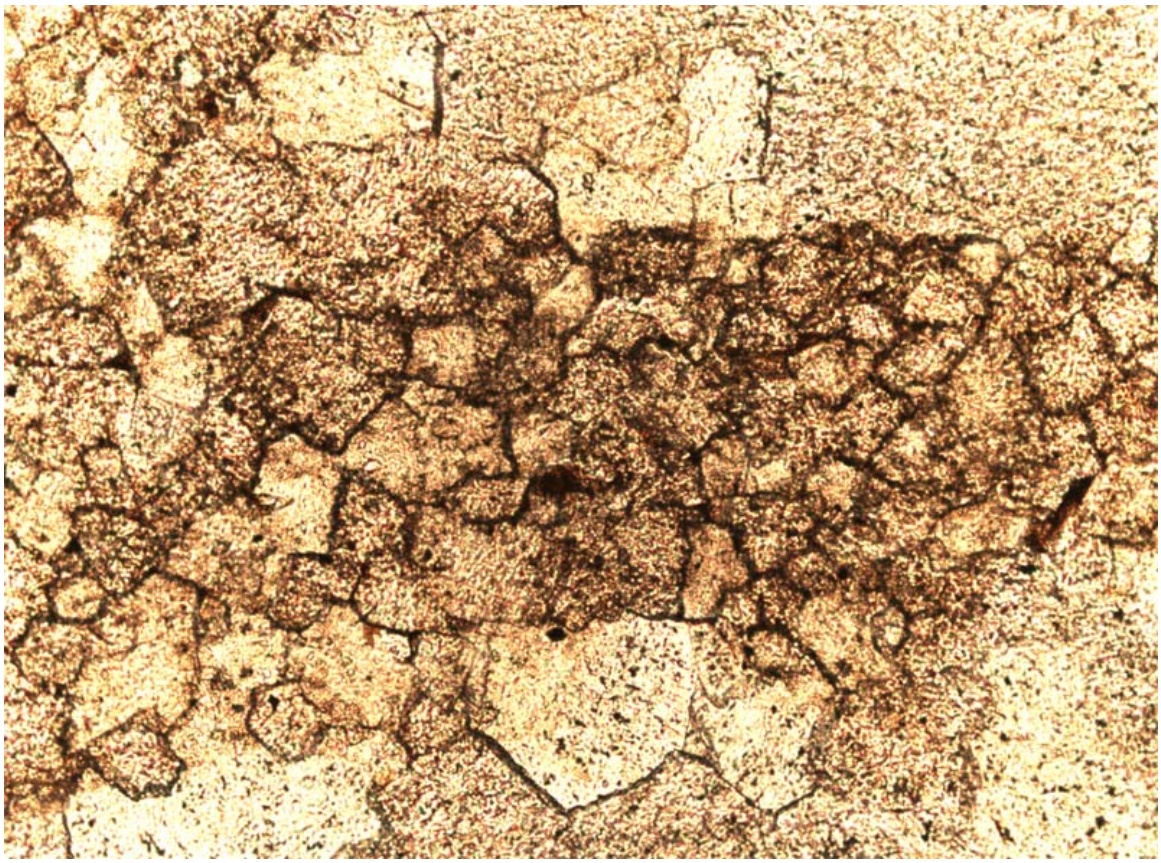

A3-9B. Higher magnification view of the pocket of decimicron-sized planar-s dolomite shown in Figure A3-9A.

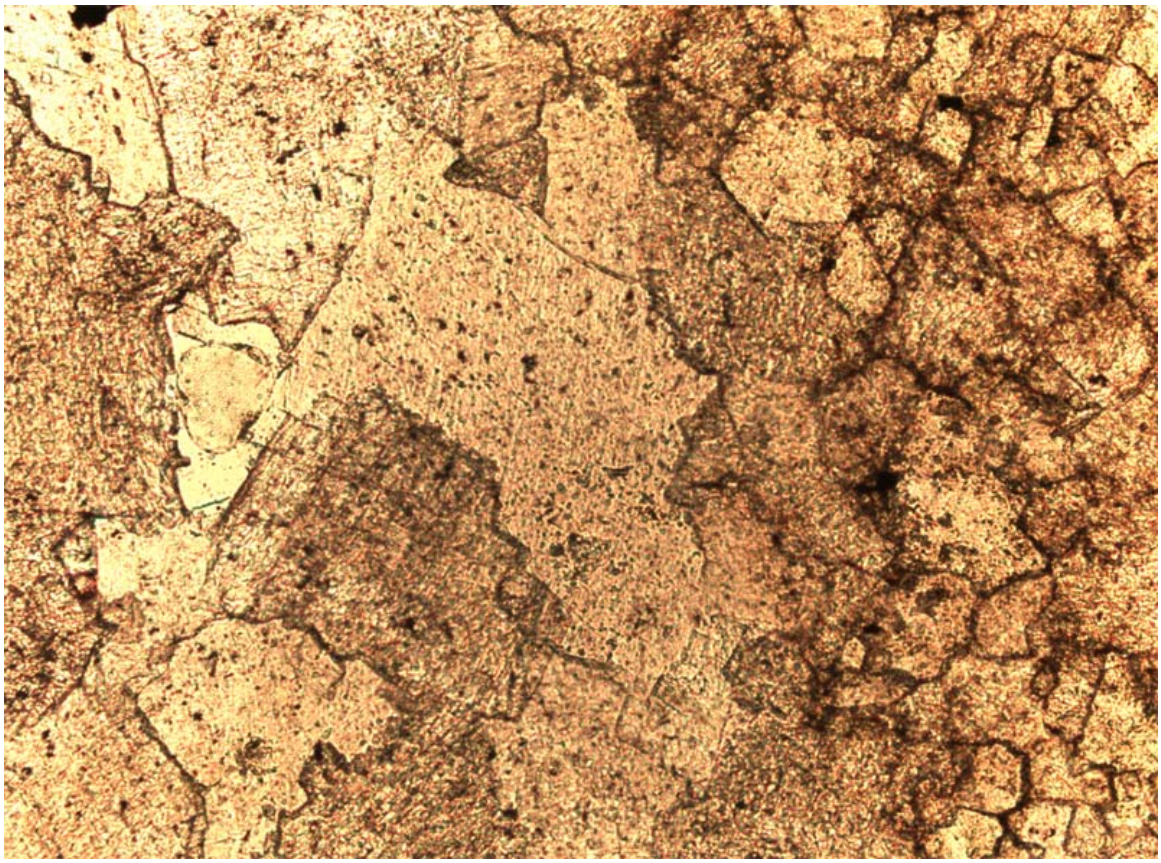

A3-9C. Contact between decimicron-sized planar-s dolomite (right) and centimicron-sized nonplanar (saddle) dolomite (left). Trenton Formation, Strayer #1 well, (OH 3478 core), Allen County, OH, 1211.25 ft.

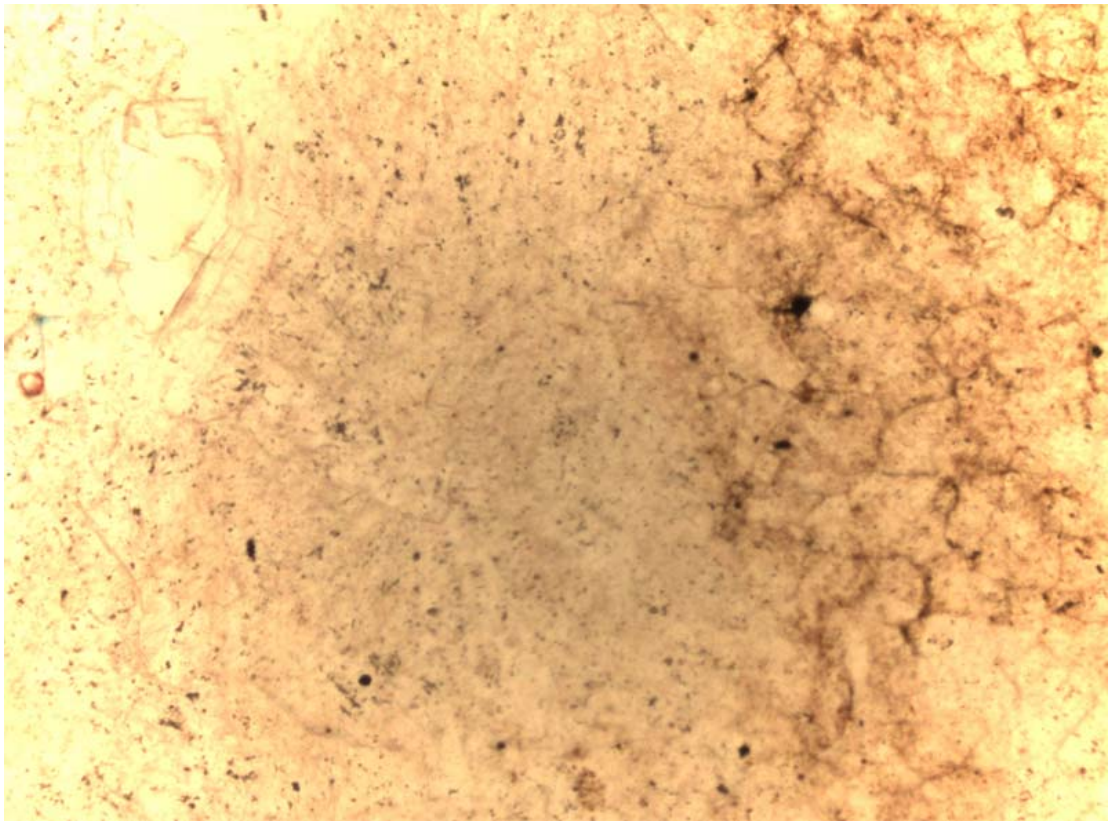

A3-9D. Same thin section photomicrograph as Figure A3-9C, but with white index card inserted beneath the thin section. Note the ghosts of the decimicron-sized planar-s dolomite (identical to the same dolomite texture on the right) within the saddle dolomite. This suggests that the saddle dolomite is a neomorphic recrystallization product of the earlier diagenetic planar-s dolomite.

Appendix E-4 - Base metal sulfide mineralization

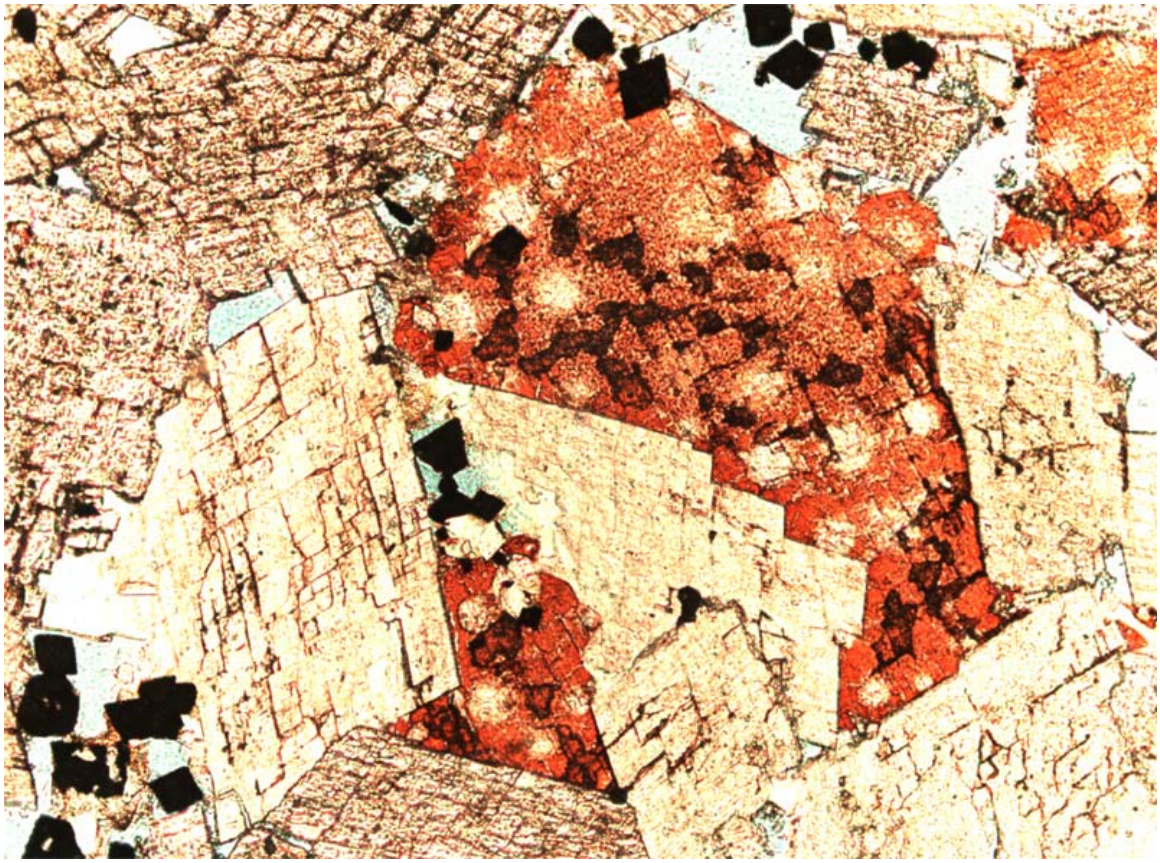

Figure A4-1.

Late-stage calcite replacing nonplanar (saddle) dolomite. Note the abundant pyrite associated with the calcite and dolomite. OH3267 core, Strayer #1 well, Allen County, OH, 1230.3 ft.



Figure A4-2.

A. Calcite replacing nonplanar (saddle) dolomite. Although the large, almost white crystal on the right side of the SEM photo exhibits the characteristic morphology of saddle dolomite, it's lighter color in the backscattered electron mode means that it's composition is different than the adjacent saddle dolomites in the picture. The EDS spectrum shown in B shows calcium excess in the crystal. Trenton Formation, OH 3479, Anderson well, Hancock Co., OH, 1337.8 ft.

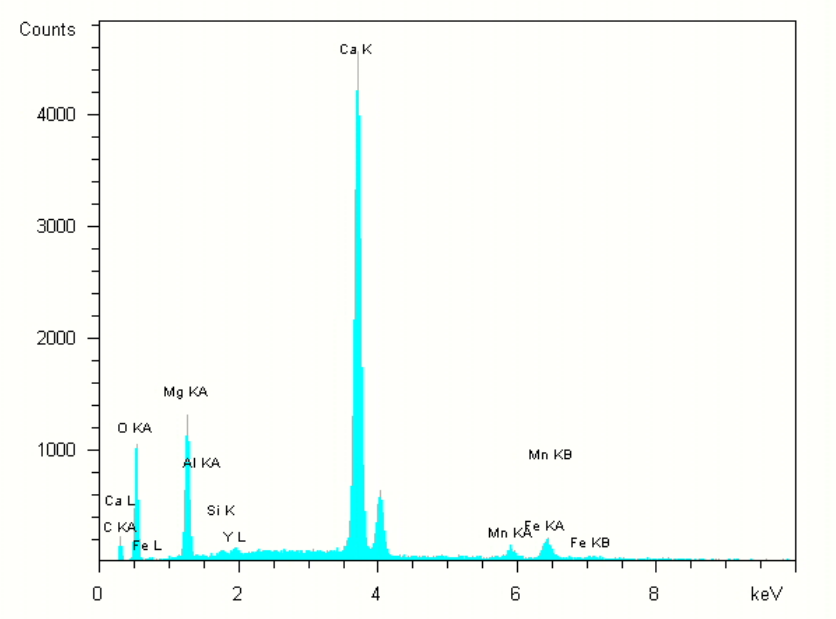

B. EDS spectra of the crystal shown in A.



Figure A4-3.
Authigenic quartz replacing anhydrite in the Trenton Formation, northwest Ohio.

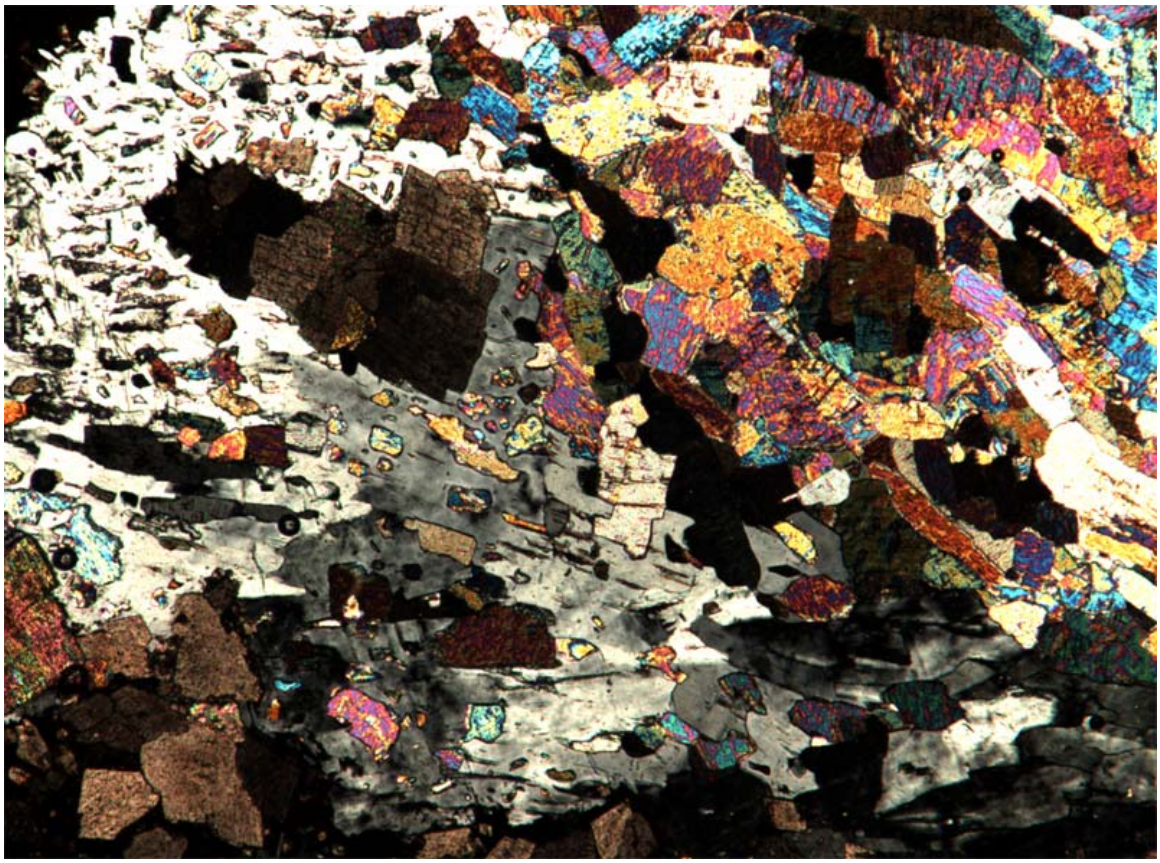

Figure A4-4.

Anhydrite and quartz replace nonplanar (saddle) dolomite and fill a large vug in the Trenton Formation in the subsurface of northwestern Ohio.

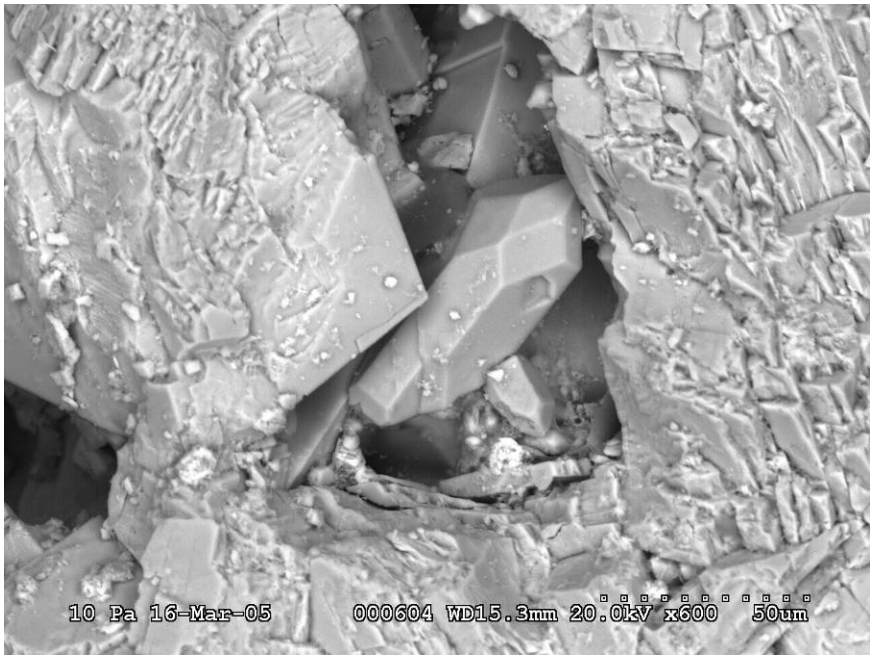

Figure A4-5.

Authigenic quartz partially filling a small vug in the Black River Group, Gray #1 well, Steuben County, NY, 7803 ft.



Figure A4-6A.

Supergene mineralization in the Black River Group in the subsurface of south-central NY. Gray #1 well, 7799.9 ft., Steuben County.

A. Bitumen coats a crystal of delafossite, a copper-iron oxide that commonly occurs as a secondary mineral near the base of the oxidized zone of copper deposits. Black crystals of delafossite fill many small vugs in the Grey well core (it appears white in this backscattered electron photomicrograph due to the high atomic number of the copper and iron).



B.

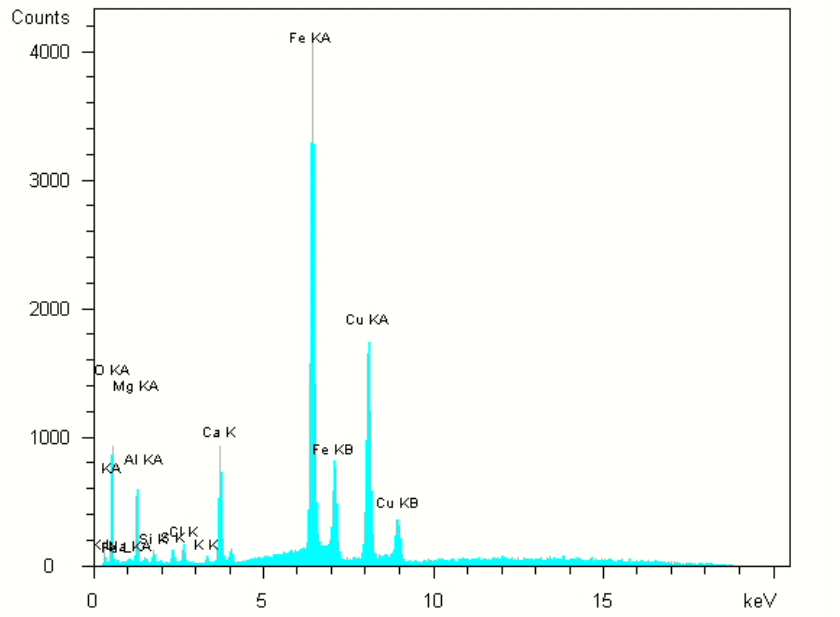

C. B. and C. show the location of EDS analysis in this sample and the EDS spectra for the white mineral.



Figure A4-7.

Nonplanar (saddle dolomite fills this small vug in the Black River Group (Gray #1 well, Steuben County, NY, 7803 ft.). White specks throughout the SEM photo are anhydrite.

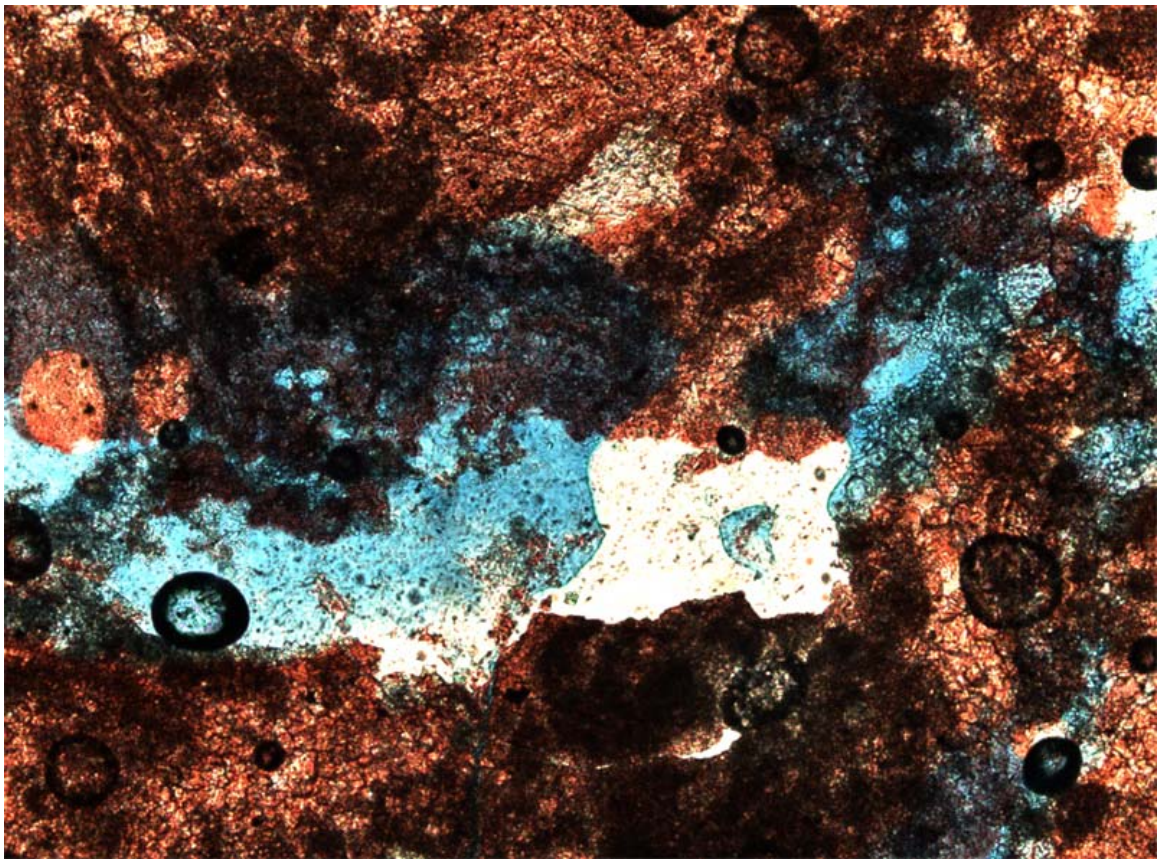

Figure A4-8.

Opal partially fills a small vug in peloidal limestone in the Black River Group in the subsurface of north central Pennsylvania. This sample is from a zone about 70 ft. above an extensively dolomitized section in the well. Identification of the white mineral as opal is based on its isotropic behavior under crossed polars and its index of refraction less than epoxy. Bayles #1 well, Bradford County, Pa, 12,300 ft.

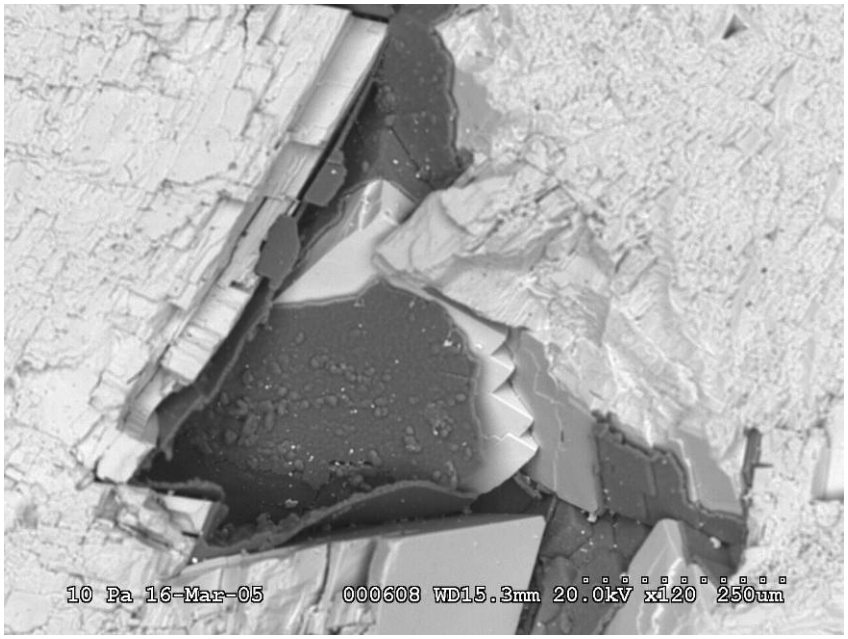

Figure A4-9.

Bitumen filling intercrystalline pore space in dolostone, Grey #1 well, Steuben County, NY, 7803 ft.

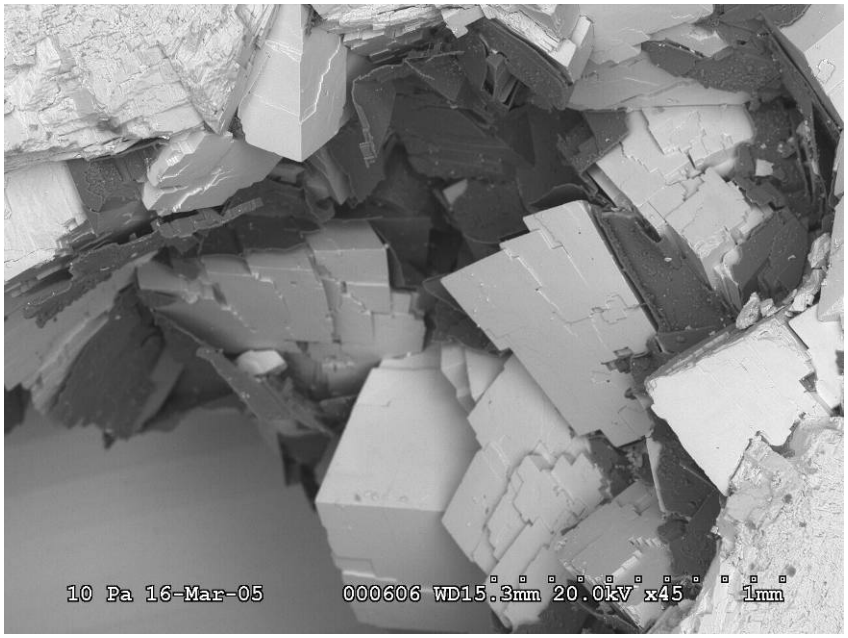

Figure A4-10.

Bitumen filling intercrystalline pore space in dolostone, Whiteman #1 well, Chemung County, NY, 9531 ft.

Appendix E-5 - Dolomite porosity in the Trenton Limestone and Black River Group



A **B**

Figure A5-1. Macroporosity in dolograinstone from northwestern Ohio.

A. Small and medium vugs in dolostone from the Trenton Formation. The rock's depositional texture is not recognizable, but its origin as a crinoidal grainstone can be inferred from adjacent core. OH3267 well core, Auglaize County, 1167.6 ft.

B. Small and medium vugs in crinoidal grainstone from the Trenton Formation. Much of this sample's original depositional texture was obliterated by dolomitization, but mimic relics of some crinoids can be discerned. Voids in the crinoid lumen (most likely moldic after calcite dissolution) provided the starting porosity for subsequent enlargement into vugs. OH 3479, Anderson well, Hancock Co., OH, 1337.8 ft.

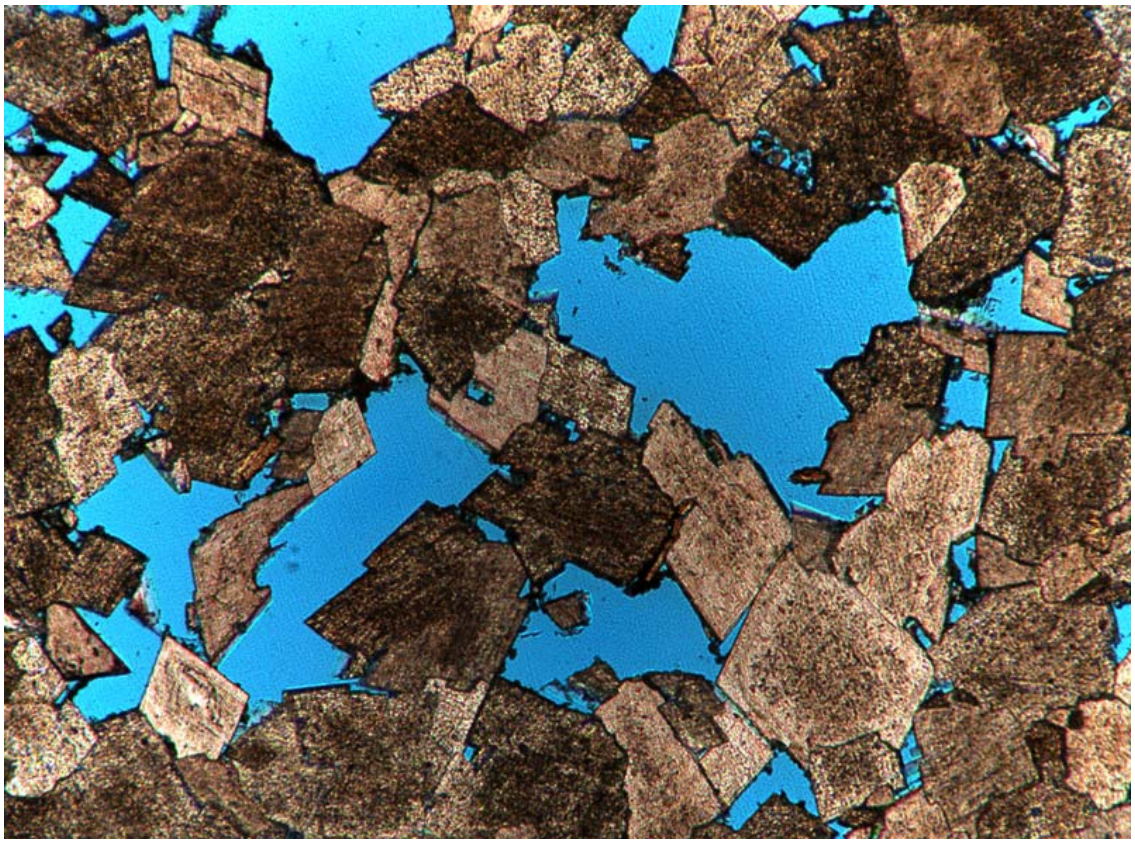

Figure A5-2.

Thin section photomicrograph of the same crinoidal dolograinstone shown in Figure A5-1B. Several types of pores are present in the rock – small to medium vugs, molds, intercrystalline pores, and intracrystalline voids. Several dolomite textures are evident, including nonplanar saddle dolomite cement, planar-s to nonplanar-a dolomite, and planar-c dolomite.

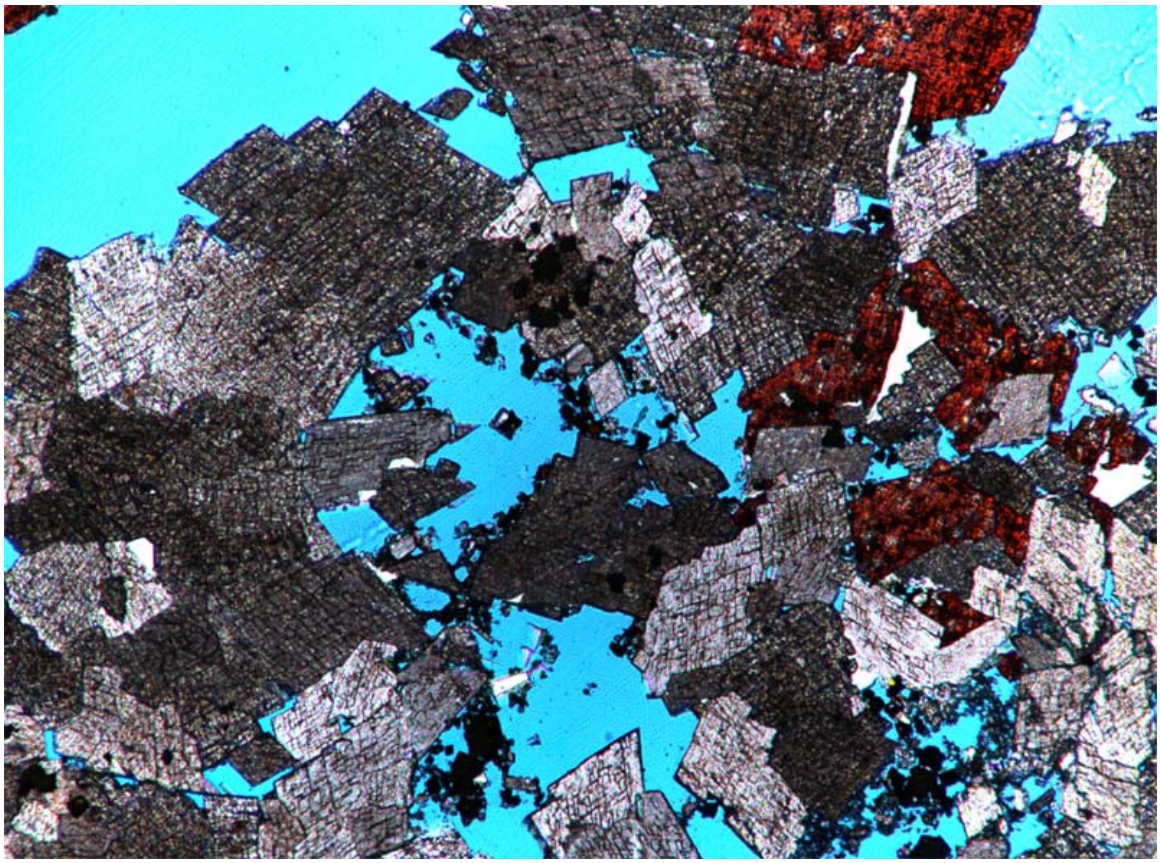

Figure A5-3.

Thin section photomicrograph of the same crinoidal dolograinstone shown in Figure A5-1B. Porosity developed through dissolution of dolomite and late-stage calcite cement.

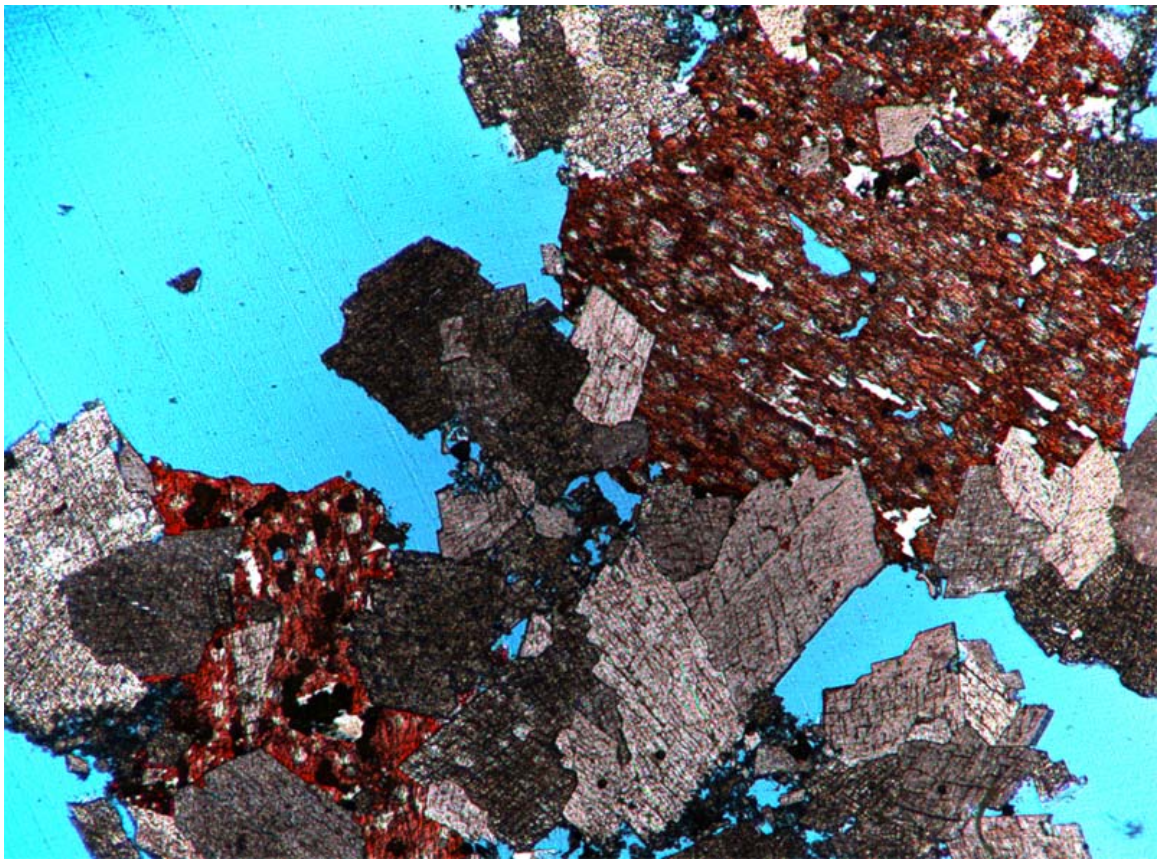

Figure A5-4.

Thin section photomicrograph of the same crinoidal dolograinstone shown in Figure A5-1B. Calcite is stained red, and some of the nonplanar (saddle) dolomite cement appears pink due to partial replacement by calcite. The vugs formed mostly through the dissolution of calcite, but dolomite dissolution also contributed to the development of void space.

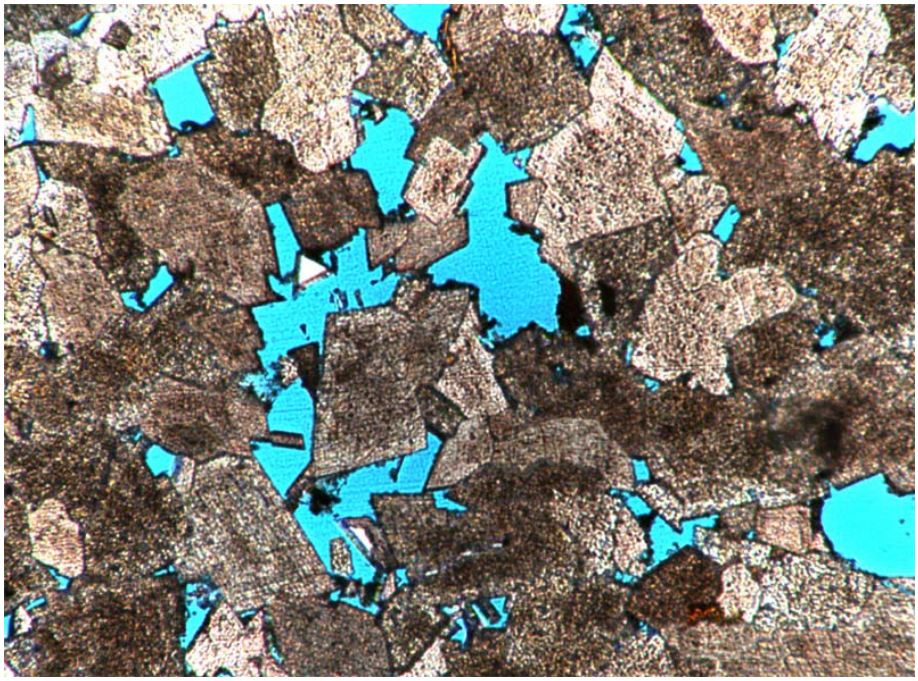

Figure A5-5.

A. Thin section photomicrograph of the same crinoidal dolograinstone shown in Figure A5-1B. Vugs and molds formed by dissolution of calcite and dolomite. The area outlined by the yellow box is shown in Figure A5-5B.

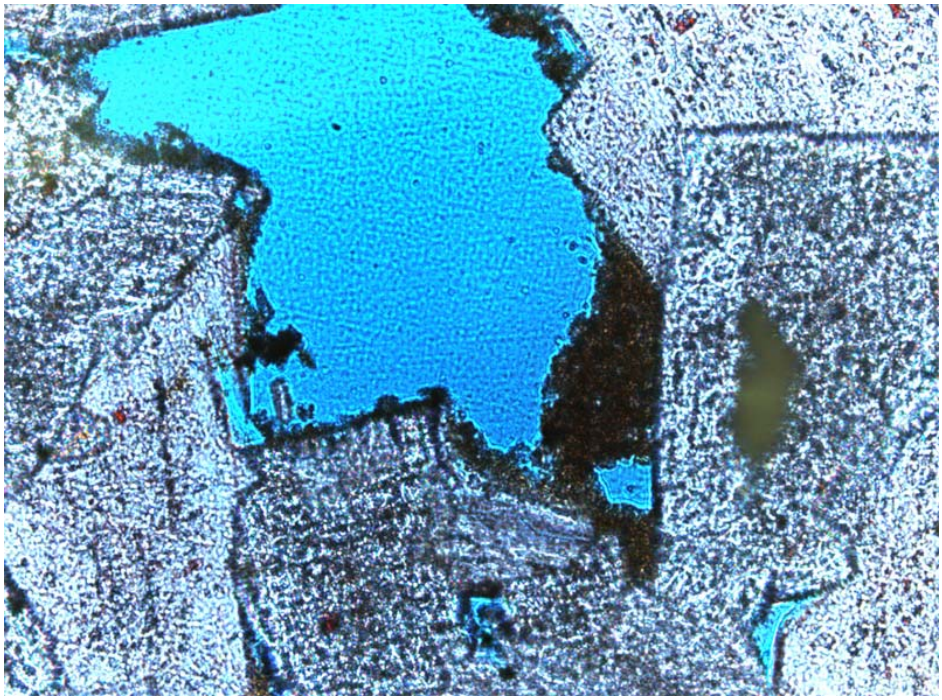

B. Residue of calcite remaining after dissolution created a small vug.

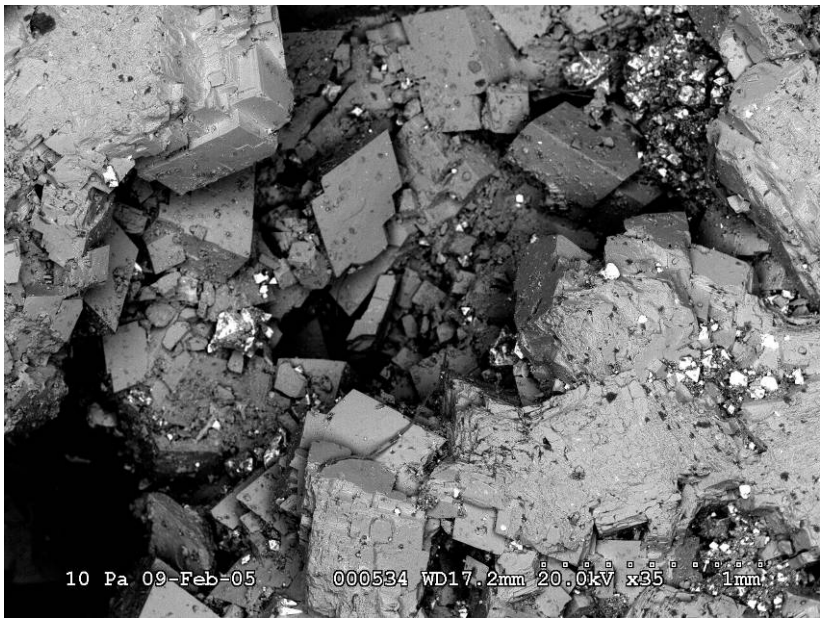

Figure A5-6.

Backscattered SEM image of vuggy pore space in the same crinoidal dolograinstone shown in Figure A5-1B. Planar-s to nonplanar-a dolomite and nonplanar (saddle) dolomite surround the void, which also contains pyrite left after calcite dissolution created the pore.



Figure A5-7.

SEM image of a small triangular intercrystalline pore space in the same crinoidal dolograinstone shown in Figure A5-1B.

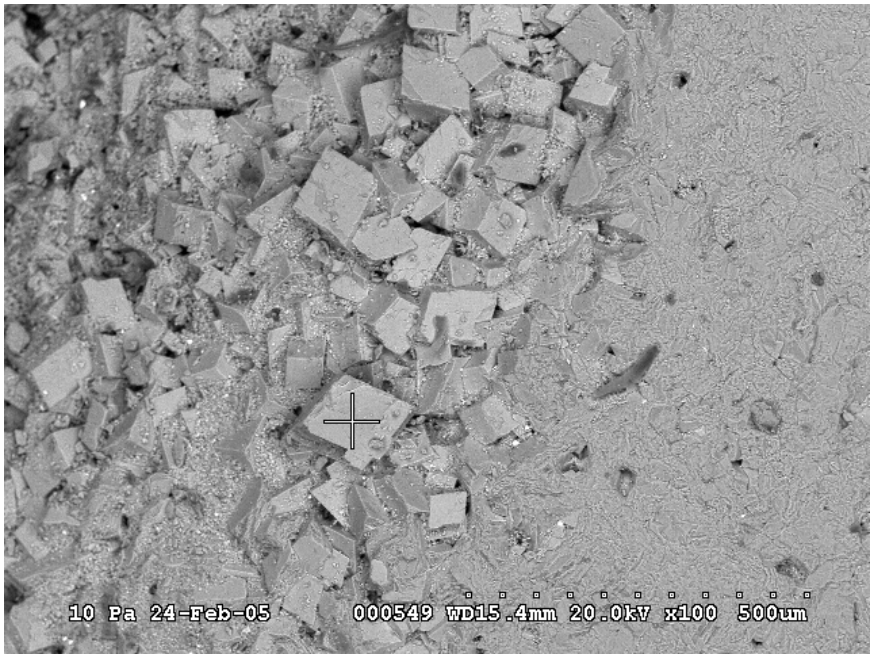

Figure A5-8.

SEM image of intercrystalline microporosity lining a small vug space in the same crinoidal dolograinstone shown in Figure A5-1B.



Figure A5-9.

Core sample of Black River dolomudstone with recognizable depositional fabric. The matrix is quite tight, but fracturing, brecciation, and dissolution created good reservoir porosity. Prudential #1A well (OH3372), Marion County, OH, 1840 ft.



Figure A5-10.

Core sample of Black River dolomudstone with recognizable subtidal depositional texture. The matrix is tight, but both vuggy and fracture porosity are evident. Nonplanar (saddle) dolomite and late-stage calcite reduce the porosity in these secondary voids. Gray # 1 well, Steuben County, NY, 7800 ft.

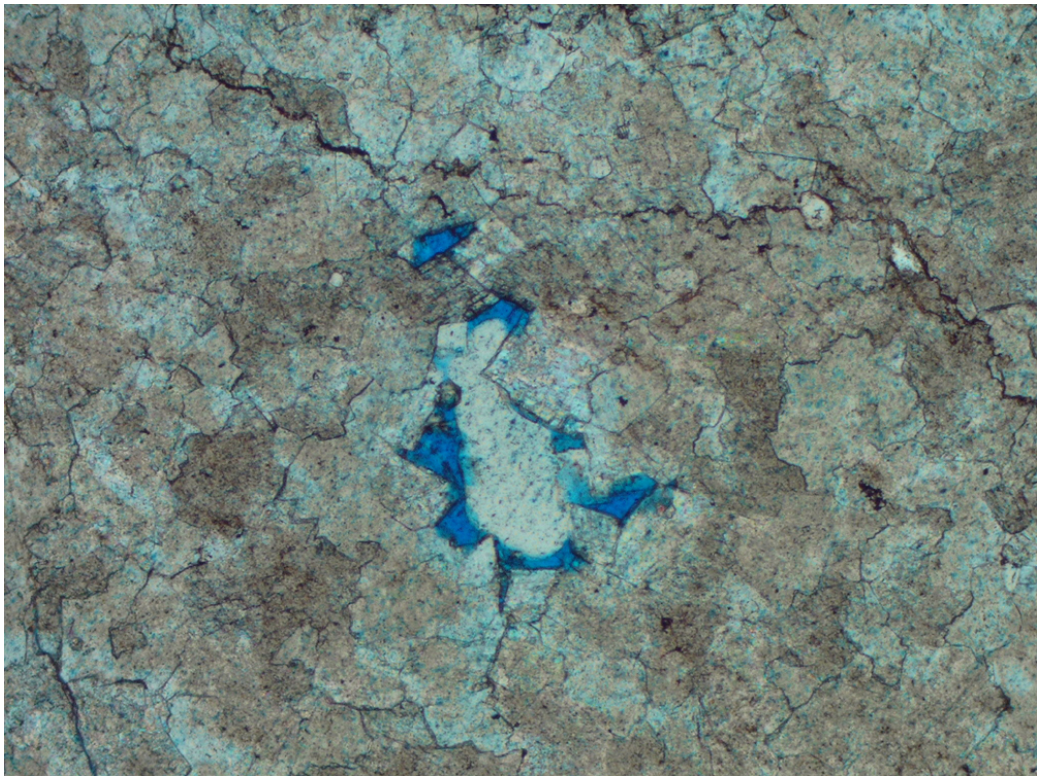

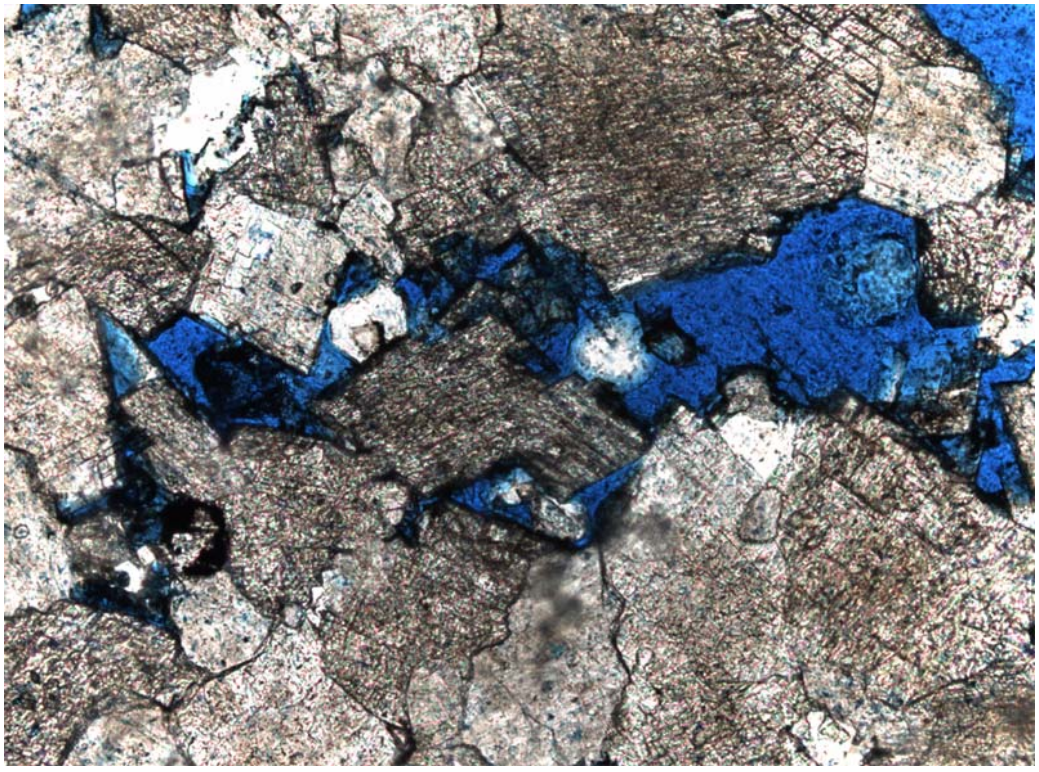

Figures A5-11 and A5-12.

Thin section photomicrographs of the dolomudstone shown in Figure A5-10.



Figure A5-13.

Backscattered SEM image of the dolomudstone shown in Figure A5-10. Vuggy porosity developed through dissolution of nonplanar-s to nonplanar-a dolomite groundmass, but nonplanar (saddle) dolomite later reduced this secondary mesoporosity.





Figure A5-14 and A5-15.

SEM views of nonplanar (saddle) dolomite reducing vuggy pore space dolomudstone shown in Figure A5-10. Bitumen stains the crystals in both photomicrographs.

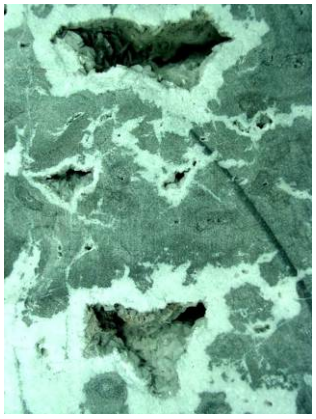

Figure A5-16.

Good mesoporosity and macroporosity development in bioturbated dolomudstone, Whiteman #1 well, Chemung County, NY, 9529.3 ft. The matrix is tight, but molds and small to medium vugs formed through dissolution. Nonplanar (saddle) dolomite partially fills the vugs and molds.



Figure A5-17.

Close up view of nonplanar (saddle) dolomite partially filling a medium vug in the same sample shown in Figure A5-16.

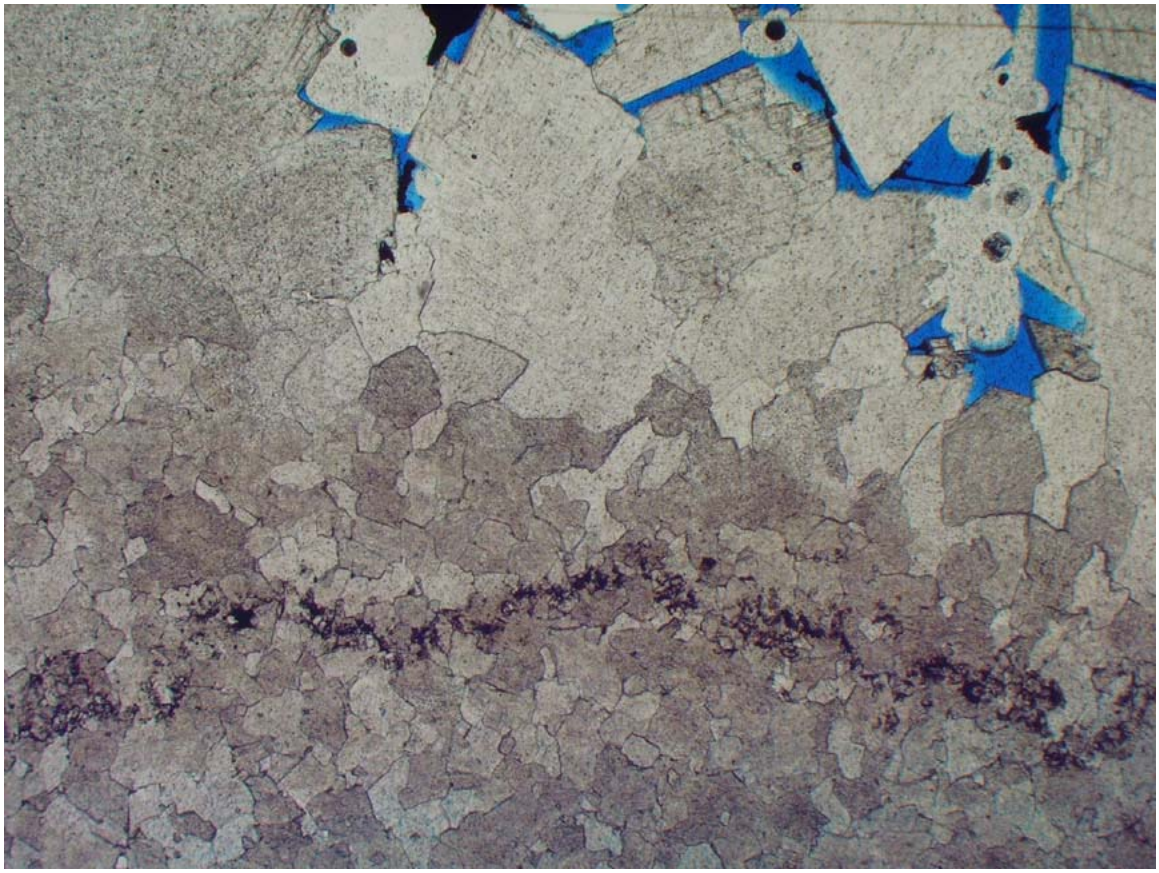

Figure A5-18.

Thin section photomicrograph of the nonplanar (saddle) dolomite partially filling vugs in the same sample shown in Figure A5-16.

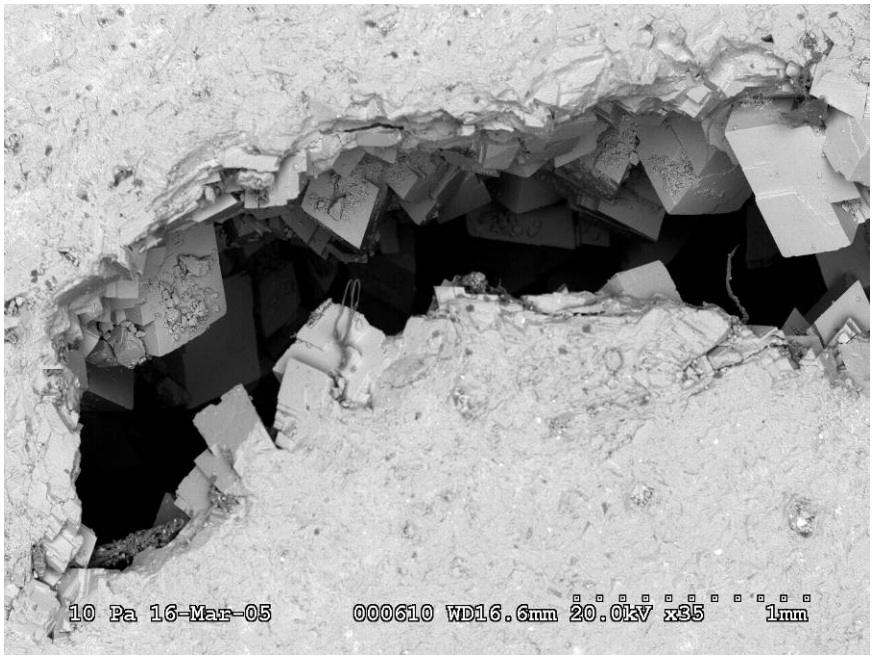



Figures A5-19 and A5-20.

SEM photographs of nonplanar (saddle) dolomite partially filling vugs in the same sample shown in Figure A5-16.

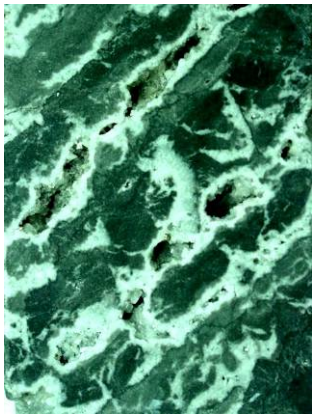

Figure A5-21.

Zebra and breccia fabric in dolomudstone in pay zone of the Whiteman #1well, Chemung County, NY, 9531 ft.

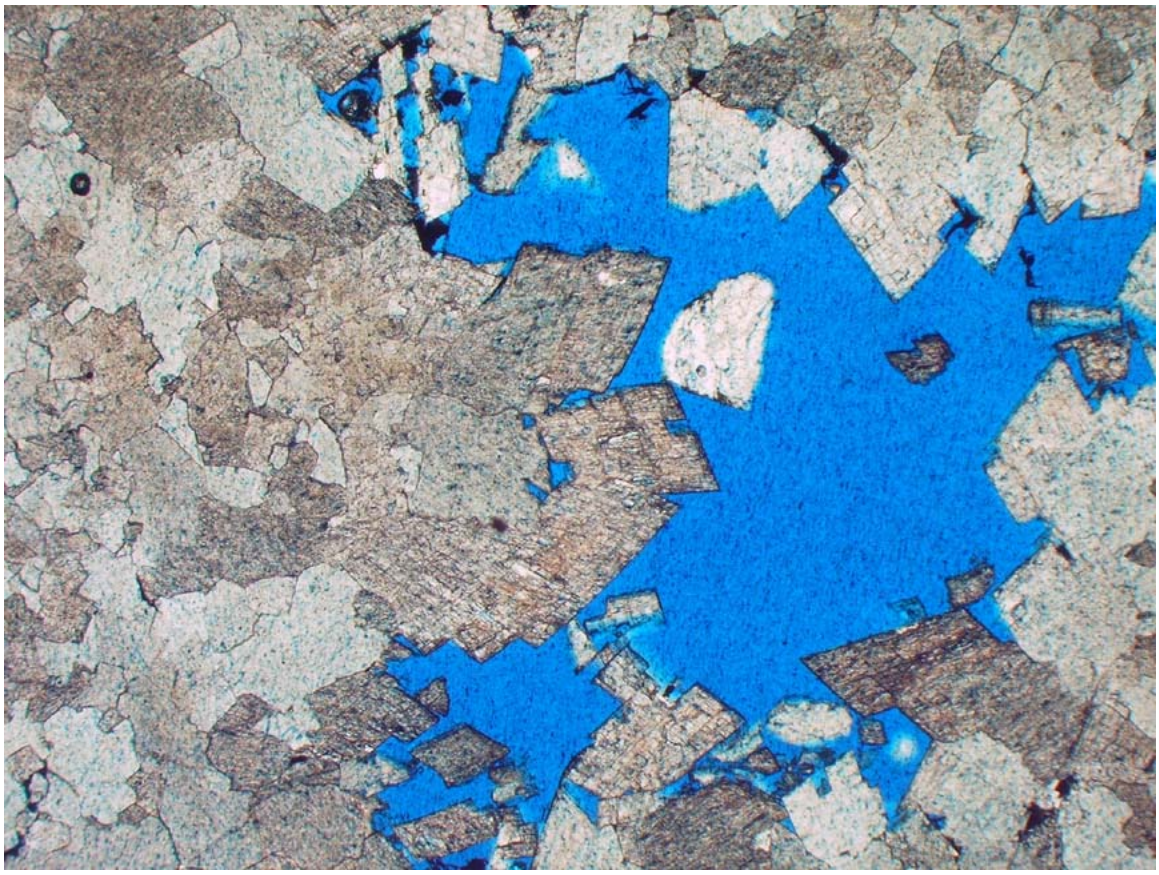

Figure A5-22.

Thin section photomicrograph of medium vug in the same core sample shown in Figure A5-21. Nonplanar (saddle) dolomite cement partially fills the void space.

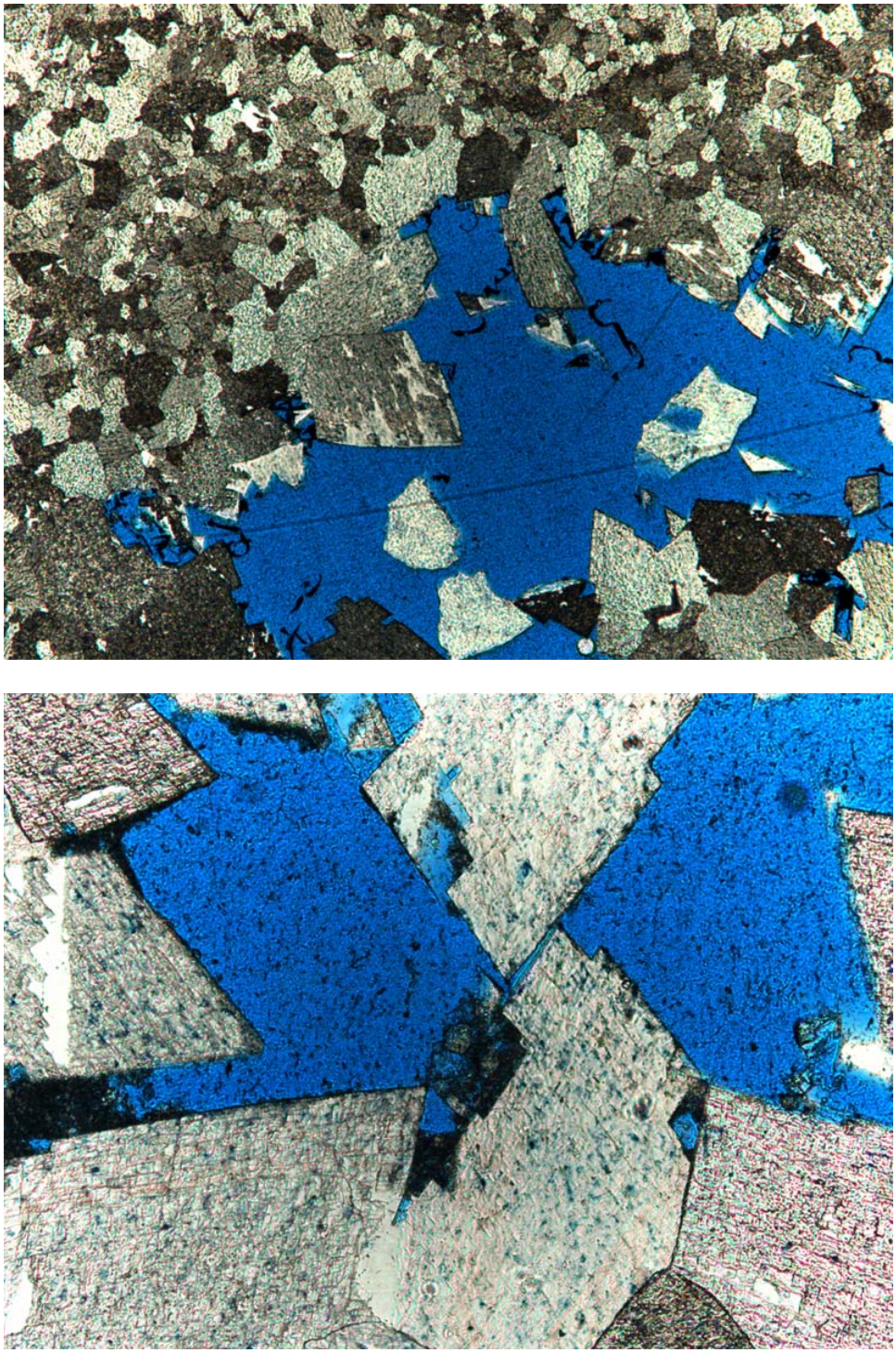

Figures A5-23 and A5-24.

Thin section photomicrographs of macroporosity in the same core sample shown in Figures A5-21 and A5-22. Note the partially dissolved late-stage calcite crystals (red), and their residue along corroded dolomite crystal boundaries and in intercrystalline void space.

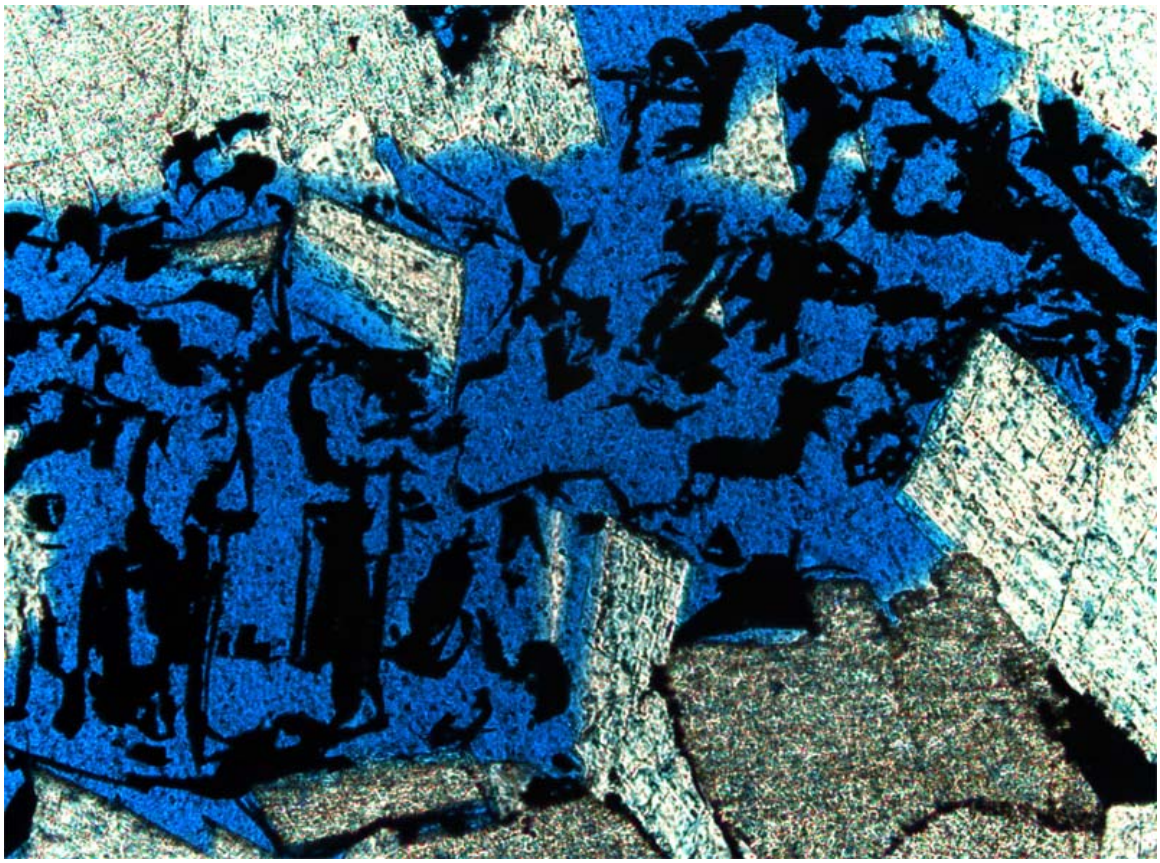

Figure A5-25.

This medium vug is in the same core sample shown in Figure A5-21. The bitumen residue in the vug once lined nonplanar (saddle) dolomite crystals (see Figure A5-26). It is not clear if the crystals were plucked during thin section preparation or actually dissolved to create the void space. Corroded remnants of the dolomite within the void suggest the latter might be true.

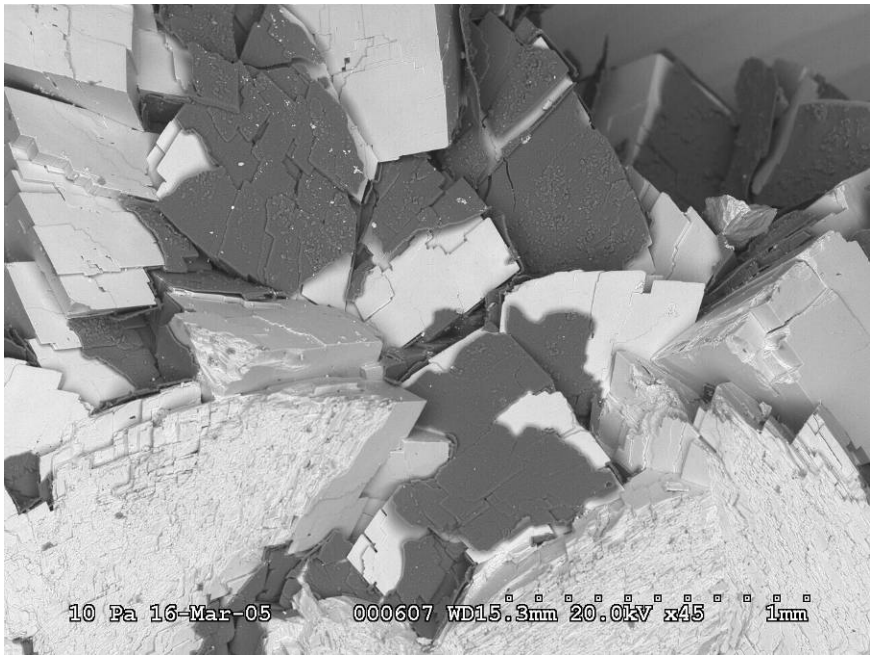

Figure A5-26.

Backscattered SEM photograph of bitumen coating nonplanar (saddle) dolomite that partially fills a medium vug in the Black River Group (Whiteman #1 well, Chemung County, NY, 9531 ft.).

APPENDIX F

Page size plates from Stratigraphy

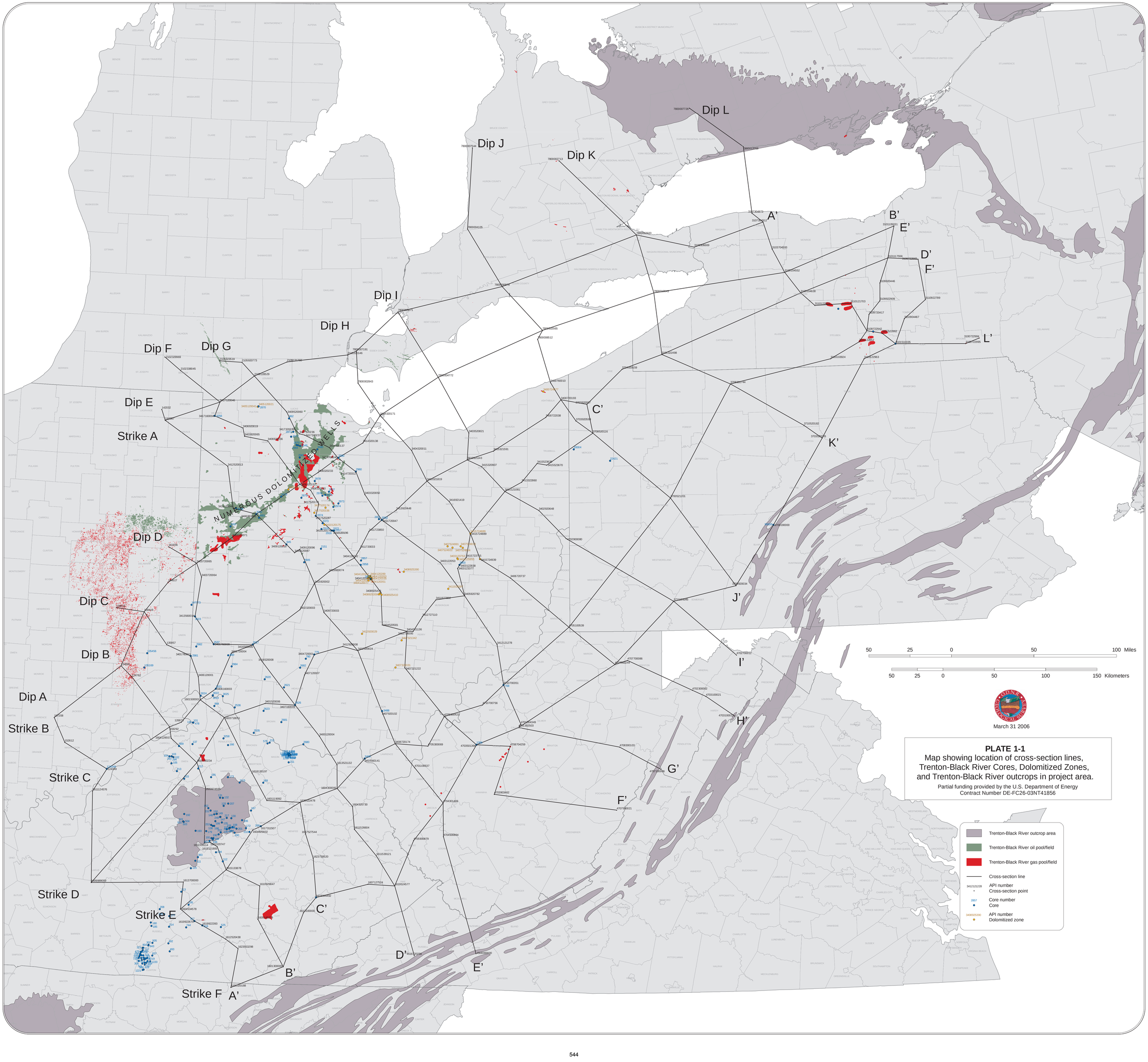
Dip L
Dip J
Dip K
Dip I
Dip H
Dip F
Dip G
Dip E
Dip D
Dip C
Dip B
Dip A
Strike A
Strike B
Strike C
Strike D
Strike E
Strike F
NUMEROUS DOLOMITIZED WELLS
A’
B’
C’
D’
E’
F’
G’
H’
I’
J’
K’
L’
50 25 0 50 100 Miles
50 25 0 50 100 150 Kilometers
March 31 2006
PLATE 1-1
Map showing location of cross-section lines, Trenton-Black River Cores, Dolomitized Zones, and Trenton-Black River outcrops in project area.
Partial funding provided by the U.S. Department of Energy
Contract Number DE-FC26-03NT41856
Trenton-Black River outcrop area
Trenton-Black River oil pool/field
Trenton-Black River gas pool/field
Cross-section line
API number
Cross-section point
Core number
Core
API number
Dolomitized zone

Dip A

107206 BROWN — 16.4 miles — 152612 MEDLOCK — 30.1 miles — 124349 ROSS — 16.0 miles — 1611134578 DUPONT DE NEMOURS & CO., INC. — 55.4 miles — 1609986059 BROOKS — 55.7 miles — 1613700000 SPEARS — 16.5 miles — 1604534578 GARNETT — 11.1 miles — 1618920870 DAULTON — 5.4 miles — 1619922393 EDWARDS — 16.3 miles — 1613520436 CUMBERLAND MINERALS — 9.6 miles — 1602555098 OHLER HEIRS "BIG LIME" — 23.9 miles — 4101320158 BEGLEY LUMBER

Dip A'

IN | KY | KY | TN

NW

SE

1000

0

-1000

Mapped Units

Informal units used for correlation purposes and mapping within the project. Stratigraphic names as used within each state are shown within log columns.

Tie well with strike line B-B'

Correlation: GR 0 GAPI 200 | Depth: MD 1100–2400 | Porosity: DT 120 µs/FT 40

Top of Ordovician
Facies relationships for all units in the uppermost portion of the Ordovician are not shown.
"Kope"
"Utica"
"Trenton/Lexington"
Datum
"Black River"
"Gull River"
"Wells Creek"
Top of Knox

TD=6806

Correlation: GR 0 GAPI 200 | Depth: MD 1300–2500 | Porosity: DPHI 30 PU -10; NPHI 30 PU -10

TD=2735

Tie well with strike line C-C'

Correlation: GR 0 GAPI 200 | Depth: MD 100–1600 | Porosity: NEUT 400 API 4000

Beekmantown Gp
Black River Gp
Ancell Gp
Knox Gp

TD=1608

Continuous core 10-1,608 ft

Correlation: GR 0 GAPI 200 | Depth: MD 200–1600 | Porosity: D 2 G/C3 3; SNP 30 PU -10

"Cincinnati Und"
Clays Ferry Fm
"Utica Shale"
Lexington Ls
Logana Mbr
Curdsville Mbr
High Bridge Gp
Wells Creek Dol
Knox Gp

TD=6011

Tie well with strike line D-D'

Correlation: GR 0 GAPI 200 | Depth: MD 500–2100 | Porosity: DT 120 µs/FT 40; PE 0 BARNELECT 10; RHOB 2 G/C3 3; NPHI 30 PU -10

TD=8257

Correlation: SP -200 MV 0 | Depth: MD 0–1300

TD=6117

Tie well with strike line E-E'

Correlation: GR 0 GAPI 200; GR 200 GAPI 400 | Depth: MD 200–1800 | Porosity: RHOB 2 G/C3 3; NPHI 30 PU -10; DT 120 µs/FT 40

TD=8251

Correlation: GR 0 GAPI 200 | Depth: MD 200–1900 | Porosity: RHOB 2 G/C3 3; NAPI 400 API 3000; DT 120 µs/FT 40

TD=6722

Correlation: GR 0 GAPI 200 | Depth: MD 500–2200 | Porosity: NAPI 400 API 3000; RHOB 2 G/C3 3; DT 120 µs/FT 40

TD=8868

Correlation: GR 0 GAPI 200 | Depth: MD 1400–3000 | Porosity: NAPI 400 NAPI 3000

TD=7343

Correlation: GR 0 GAPI 200 | Depth: MD 1700–3200 | Porosity: NPHI 30 PU -10; RHOB 2 G/C3 3

Martinsburg Fm
Clays Ferry Fm
Lexington Ls
Logana Mbr
High Bridge Gp
Wells Creek Dol

TD=5160

Tie well with strike line F-F'

Correlation: GR 0 GAPI 200 | Depth: MD 3100–5100 | Porosity: PEF 0 BARNELECT 10; RHOB 2 G/C3 3; NPHI 30 PU -10

Junista Fm
Trenton Ls
Black River Gp
Chickamauga Super Gp
Knox Gp

TD=8799

Mapped Units

Informal units used for correlation purposes and mapping within the project. Stratigraphic names as used within each state are shown within log columns.

Top of Ordovician
Facies relationships for all units in the uppermost portion of the Ordovician are not shown.
"Kope"
"Point Pleasant"
"Trenton/Lexington"
Datum
"Black River"
"Gull River"
"Wells Creek"
Top of Knox

Plate 1-2

Stratigraphic Cross Section Dip Line A-A'
based on Geophysical Well Logs

Trenton-Black River Appalachian Basin Research Consortium

Datum: top of Black River Group

Vertical scale shown in feet; well logs equally spaced with horizontal distance labeled in miles

Partial funding provided by the U.S. Department of Energy
Contract Number DE-FC26-03NT41856



APINO* 3703920593 HEAD — **Lease name** — **Well type**

Producing Formation MEDINA GP

*Indiana wells: Well identification numbers were provided by the Indiana Geological Survey and are not in the standard APINO format. Ontario wells: Well identification numbers were provided by the Ontario Geological Survey and the Ohio Geological Survey assigned pseudo APINO numbers.

WELL SYMBOL AND STATUS

- Dry hole
- Gas
- Oil
- Oil and gas
- Injection
- Storage
- Stratigraphic test
- Observation
- Unknown

March 31, 2006

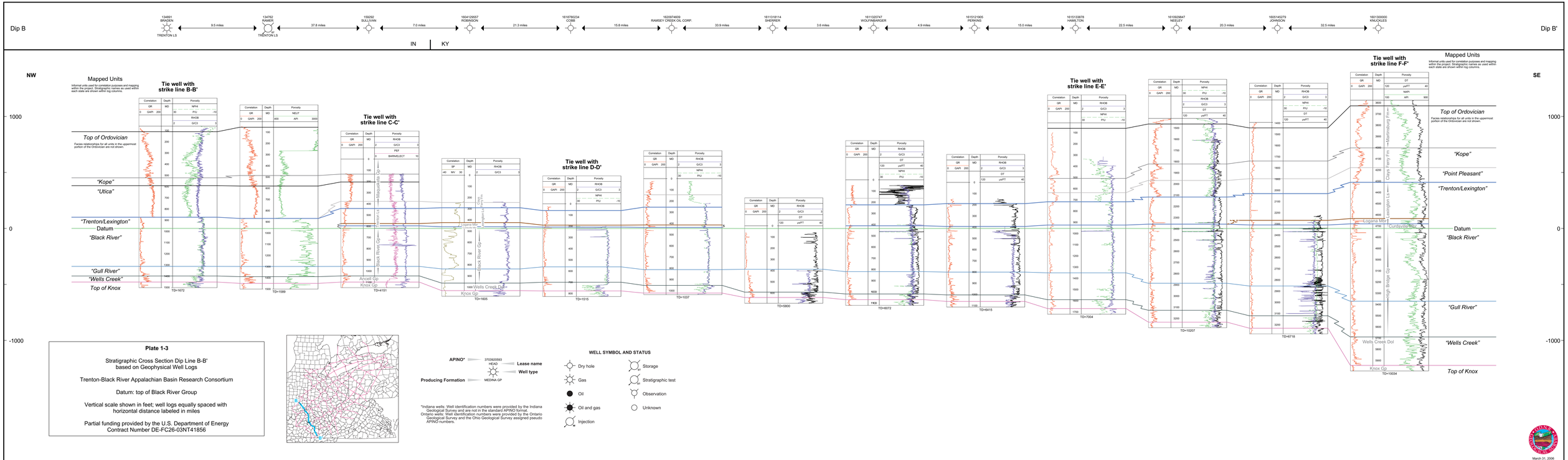

Dip B
Dip B'
134891 BRADEN TRENTON LS
9.5 miles
134762 RAMER TRENTON LS
37.8 miles
159292 SULLIVAN
7.0 miles
160412957 ROBINSON
21.3 miles
161878234 COBB
15.8 miles
162097469 RAMSEY CREEK OIL CORP.
33.9 miles
161131814 SHERRER
3.6 miles
161132047 WOLFINBARGER
4.9 miles
161512905 PERKINS
15.0 miles
161513878 HAMILTON
22.5 miles
161092847 NEELEY
20.3 miles
160514529 JOHNSON
32.5 miles
160130000 KNUCKLES
IN
KY
NW
SE
Mapped Units
Tie well with strike line B-B'
Tie well with strike line C-C'
Tie well with strike line D-D'
Tie well with strike line E-E'
Tie well with strike line F-F'
Top of Ordovician
"Kope"
"Utica"
"Trenton/Lexington"
Datum
"Black River"
"Gull River"
"Wells Creek"
Top of Knox
"Point Pleasant"
Logana Mbr
Curdsville Mbr
Wells Creek Dol
Knox Gp
Ancell Gp
Black River Gp
Trenton Ls
Maquoketa Gp
Clays Ferry Fm
Martinsburg Fm
Lexington Ls
High Bridge Gp
TD=1672
TD=1589
TD=4151
TD=1605
TD=1515
TD=1037
TD=5800
TD=6072
TD=6415
TD=7004
TD=10207
TD=6718
TD=10034
1000
0
-1000
Plate 1-3
Stratigraphic Cross Section Dip Line B-B' based on Geophysical Well Logs
Trenton-Black River Appalachian Basin Research Consortium
Datum: top of Black River Group
Vertical scale shown in feet; well logs equally spaced with horizontal distance labeled in miles
Partial funding provided by the U.S. Department of Energy Contract Number DE-FC26-03NT41856
APINO*
3703920593
HEAD
Lease name
Well type
Producing Formation
MEDINA GP
*Indiana wells: Well identification numbers were provided by the Indiana Geological Survey and are not in the standard APINO format.
Ontario wells: Well identification numbers were provided by the Ontario Geological Survey and the Ohio Geological Survey assigned pseudo APINO numbers.
WELL SYMBOL AND STATUS
Dry hole
Gas
Oil
Oil and gas
Injection
Storage
Stratigraphic test
Observation
Unknown
March 31, 2006

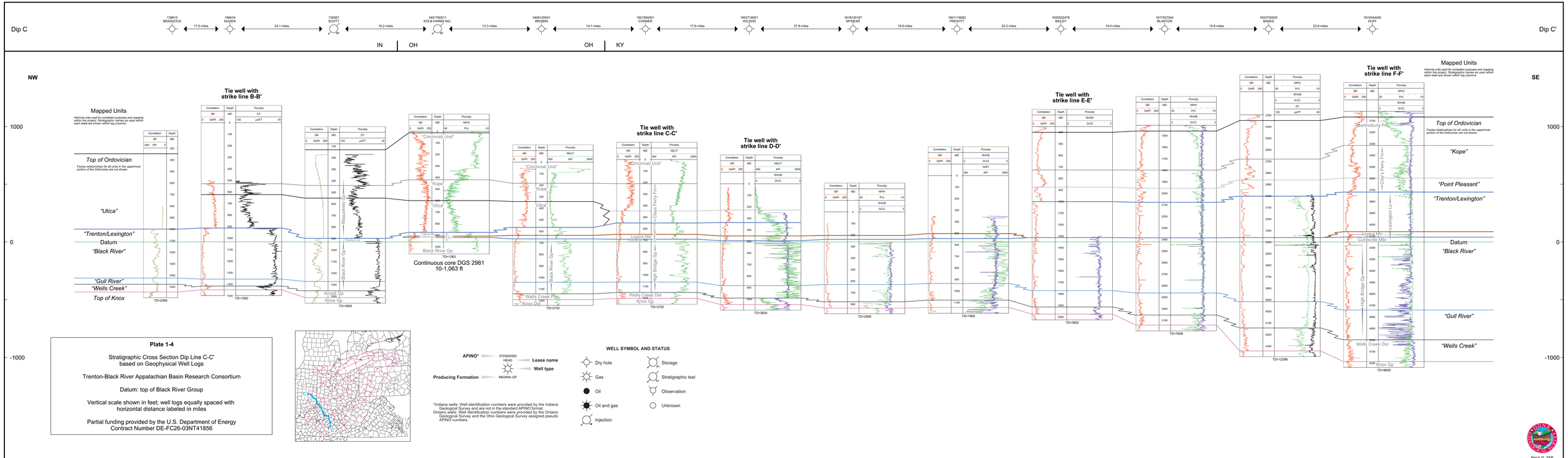

Dip C
Dip C'
IN
OH
OH
KY
NW
SE
Mapped Units
Top of Ordovician
"Utica"
"Trenton/Lexington"
Datum
"Black River"
"Gull River"
"Wells Creek"
Top of Knox
Tie well with strike line B-B'
Tie well with strike line C-C'
Tie well with strike line D-D'
Tie well with strike line E-E'
Tie well with strike line F-F'
Continuous core DGS 2981
10-1,063 ft
"Cincinnati Und"
"Kope"
"Point Pleasant"
Black River Gp
Knox Gp
Wells Creek Dol
Ancell Gp
Maquoketa Gp
Clays Ferry Fm
Logana Mbr
High Bridge Gp
Curdsville Mbr
Martinsburg Fm
Lexington Ls
Plate 1-4
Stratigraphic Cross Section Dip Line C-C'
based on Geophysical Well Logs
Trenton-Black River Appalachian Basin Research Consortium
Datum: top of Black River Group
Vertical scale shown in feet; well logs equally spaced with horizontal distance labeled in miles
Partial funding provided by the U.S. Department of Energy
Contract Number DE-FC26-03NT41856
APINO*
Lease name
Well type
Producing Formation
WELL SYMBOL AND STATUS
Dry hole
Gas
Oil
Oil and gas
Injection
Storage
Stratigraphic test
Observation
Unknown
*Indiana wells: Well identification numbers were provided by the Indiana Geological Survey and are not in the standard APINO format.
Ontario wells: Well identification numbers were provided by the Ontario Geological Survey and the Ohio Geological Survey assigned pseudo APINO numbers.
March 31, 2006

Dip D

161656
RB3LIR

19.7 miles

3403720065
BWEYMOR

6.9 miles

3403720064
MAMTAK

24.2 miles

3413560014
JORDAN

20.3 miles

3401750009
BEDER

23.7 miles

3416560000
AMERICAN AGGREGATES

11.5 miles

3416520008
KITTREDGE

33.0 miles

3407160009
GONG

23.9 miles

3405120004
BAILEY

20.3 miles

1615521132
WOLFE

14.4 miles

1604300000
STAMPER

14.3 miles

1604220730
MCZEAVEY

13.9 miles

1611526604
EVANS

20.8 miles

1611533121
KENTUCKY WEST VIRGINIA GAS CO.

21.4 miles

1618524077
STRATTON

43.8 miles

4516720256
PRICE

Dip D'

IN | OH | OH | KY | KY | VA

NW

SE

1000

0

-1000

Mapped Units

Informal units used for correlation purposes and mapping within the project. Stratigraphic names as used within each state are shown within log columns.

Top of Ordovician

Facies relationships for all units in the uppermost portion of the Ordovician are not shown.

"Kope"

"Utica"

"Trenton/Lexington"

Datum

"Black River"

"Gull River"

"Wells Creek"

Top of Knox

Cincinnati Grp
Cincinnati Und
Black River Gp
Utica
Kope
Trenton Ls
Knox Dol
Knox Gp
Maquoketa Shale
Point Pleasant
Lexington Ls
Curdsville Mbr
Logana Mbr
Wells Creek Fm
Maysville Grp
Clays Ferry Fm
Nicholas Fm
Lexington Ls
Tyrone Ls
High Bridge Gp
Wells Creek Dol
Knox Gp
Mascoutah Ls
Junista Fm
Mechanicsburg Fm
Trenton Ls
Black River Gp
Knox Dol
Knox Gp
Rockmuhr Member

Tie well with strike line B-B'

TD=3100 | TD=1800 | TD=1600

Continuous core DGS 3023

TD=1200 | TD=2940

Tie well with strike line C-C'

Continuous core DGS 2537

TD=1445

Continuous core DGS 2627

TD=1380 | TD=3790

Tie well with strike line D-D'

Continuous core DGS 2626
51-1,762 ft

TD=1792 | TD=5062

Tie well with strike line E-E'

TD=5085 | TD=9980 | TD=10000 | TD=10951 | TD=12450 | TD=16632

Tie well with strike line F-F'

Mapped Units

Informal units used for correlation purposes and mapping within the project. Stratigraphic names as used within each state are shown within log columns.

Top of Ordovician

Facies relationships for all units in the uppermost portion of the Ordovician are not shown.

"Kope"

"Point Pleasant"

"Trenton/Lexington"

Datum

"Black River"

"Gull River"

"Wells Creek"

Top of Knox

Plate 1-5

Stratigraphic Cross Section Dip Line D-D'
based on Geophysical Well Logs and continuous core

Trenton-Black River Appalachian Basin Research Consortium

Datum: top of Black River Group

Vertical scale shown in feet; well logs equally spaced with horizontal distance labeled in miles

Partial funding provided by the U.S. Department of Energy
Contract Number DE-FC26-03NT41856



APINo* 3703920593 — **Lease name**
HEAD — **Well type**
Producing Formation MEDINA GP

*Indiana wells: Well identification numbers were provided by the Indiana Geological Survey and are not in the standard APINO format. Ontario wells: Well identification numbers were provided by the Ontario Geological Survey and the Ohio Geological Survey assigned pseudo APINO numbers.

WELL SYMBOL AND STATUS

- Dry hole
- Gas
- Oil
- Oil and gas
- Injection
- Storage
- Stratigraphic test
- Observation
- Unknown

March 31, 2006

Dip E

142032 HELMER — 7.0 miles — 144367 BARKER — 47.0 miles — 34125200013 AREND — 25.5 miles — 34161250044 MILLER — 14.5 miles — 34065083691 BP CHEMICAL CORP — 25.8 miles — 34091230018 JONES ET AL UNIT — 7.1 miles — 34091130087 HEMLEBEN — 3.7 miles — 34091230096 PRIMKEY UNIT — 22.4 miles — 34155000502 ZENITH HOLDING & TRADING CORP. — 16.5 miles — 34087200003 HUME — 30.9 miles — 34123600024 KEITH — 39.8 miles — 34079200102 TREPANIER "BIEKMAN DOL" — 20.9 miles — 34085720174 PAYNE — 18.6 miles — 47511300537 KINSEY — 27.5 miles — 47543031469 MCCORMICK — 20.4 miles — 47545053864 CHAMBERS LOWER HURON MBR — 73.6 miles — 49200000000 UNKNOWN

Dip E'

IN | OH | OH | WV

NW

SE

1000

0

-1000

Mapped Units

Informal units used for correlation purposes and mapping within the project. Stratigraphic names as used within each state are shown within log columns.

Top of Ordovician

Facies relationships for all units in the uppermost portion of the Ordovician are not shown.

"Kope"

"Utica"

"Trenton/Lexington"

Datum

"Black River"

"Gull River"

"Wells Creek"

Top of Knox

Tie well with strike line A-A'

Tie well with strike line B-B'

Tie well with strike line C-C'

Tie well with strike line D-D'

Tie well with strike line E-E'

Tie well with strike line F-F'

Correlation | Depth | Porosity

GR | MD | RHOB

GAPI 200 | 0 | 2 GCI 3

NEUT | NPHI

API 3000 | 45 | 30 PU -15

DT | PU -15

120 µsFT 40 | PEF

RESI | BARNES,DCT 10

OHMM 3000 | RHOB

2 GCI 3

Mapped Units

Informal units used for correlation purposes and mapping within the project. Stratigraphic names as used within each state are shown within log columns.

Top of Ordovician

Facies relationships for all units in the uppermost portion of the Ordovician are not shown.

"Kope"

"Point Pleasant"

"Trenton/Lexington"

Datum

"Black River"

"Gull River"

"Wells Creek"

Top of Knox

"Cincinnati Unc"

Maysville Fm

Trenton Ls

Black River Gp

Knox Dol

Utica

Kope

Point Pleasant

Lexington Ls

Curdsville Mbr

Wells Creek Fm

Beekmantown Gp

Bellefonte Fm

Rochester Sh

Reedsville Sh

Core based on log curve; cliff not shown

Core interval 1,580-3,410 ft DGS 3952

Core interval 1,407-1,543 DGS 945

TD=3030 TD=3050 TD=3100 TD=3240 TD=3439 TD=3381 TD=3278 TD=3350 TD=3348 TD=3631 TD=4448 TD=6050 TD=7002 TD=6952 TD=19124 TD=7504

Continuous core 1440.1 from Ryder, and others (1997)

Plate 1-6

Stratigraphic Cross Section Dip Line E-E'
based on Geophysical Well Logs

Trenton-Black River Appalachian Basin Research Consortium

Datum: top of Black River Group

Vertical scale shown in feet; well logs equally spaced with horizontal distance labeled in miles

Partial funding provided by the U.S. Department of Energy
Contract Number DE-FC26-03NT41856



APINO* 3705900993 — Lease name

HEIO — Well type

Producing Formation MEDINA GP

*Indiana wells: Well identification numbers were provided by the Indiana Geological Survey and are not in the standard API#O format. Ontario well identification numbers were provided by the Ontario Geological Survey and the Ohio Geological Survey assigned pseudo API#O numbers.

WELL SYMBOL AND STATUS

- Dry hole
- Gas
- Oil
- Oil and gas
- Injection
- Storage
- Stratigraphic test
- Observation
- Unknown

March 31, 2006

Dip F

34103209990 CLARK — 12.7 miles — 34103209991 DARKE — 30.0 miles — 34171220046 LEWIS — 8.9 miles — 34171220024 STONE JR — 18.5 miles — 34083200219 FIRST — 9.1 miles — 34083200282 FLOYD SMITH — 14.3 miles — 34083200196 VOLL UNION — 32.7 miles — 34083201232 SHAMEL SMITH — 7.4 miles — 34083200140 CLARKE — 8.7 miles — 34117023173 FIRST — 7.4 miles — 34117023087 WASHINGTON — 13.2 miles — 34121201178 SHANDS 3 FARMS — 5.7 miles — 34121201136 CAMPBELL — 20.9 miles — 34024220024 ATLAS — 16.1 miles — 34024220019 CARTER — 10.3 miles — 34099200412 CHRISTOPHER JR — 19.8 miles — 34099200991 LEE — 15.4 miles — 34099201198 BOGGS — 22.5 miles — 34075231222 POLLOCK — 37.8 miles — 47000200423 APPALACHIAN POWER CO — 28.0 miles — 47000201969 MOSS — 23.4 miles — 47067242299 WHITE — 30.6 miles — 47000200442 FORD — 74.7 miles — 47072302021 VAN TRACT 357

Dip F

MI | OH — OH | WV

BLACK RIVER — COSHOCTON

NW — SE

3000 / 2000 / 1000 / 0 / -1000 / -2000

Mapped Units

Intervals are used for correlation purposes and mapping and may not be stratigraphically correct. Arrows mark tops and bases defining intervals.

Top of Ordovician
Picks redistributed for all wells in the supervised section of the Precise well set shown

"Utica"

"Trenton/Lexington"

Datum
"Black River"

"Gull River"
"Wells Creek"
Top of Knox

Tie well with strike line A-A'

Tie well with strike line B-B'

Tie well with strike line C-C'

Tie well with strike line D-D'

Tie well with strike line E-E'

Tie well with strike line F-F'

Mapped Units

Intervals are used for correlation purposes and mapping and may not be stratigraphically correct. Arrows mark tops and bases defining intervals.

Top of Ordovician
Picks redistributed for all wells in the supervised section of the Precise well set shown

"Kope"

"Utica"
"Point Pleasant"

"Trenton/Lexington"

Datum
"Black River"

"Gull River"

USA Trust 527 well along tie-line depths not corrected for structural considerations. Stratigraphic cross section Dip Line F-F' Geophysical Well Logs Trenton-Black River Appalachian Basin Research Consortium Datum: top of Black River Group Vertical scale shown in feet; well logs equally spaced with horizontal distance labeled in miles Partial funding provided by the U.S. Department of Energy Contract Number DE-FC26-03NT41856

March 31, 2006

Plate 1-7

Stratigraphic Cross Section Dip Line F-F' based on Geophysical Well Logs

Trenton-Black River Appalachian Basin Research Consortium

Datum: top of Black River Group

Vertical scale shown in feet; well logs equally spaced with horizontal distance labeled in miles

Partial funding provided by the U.S. Department of Energy Contract Number DE-FC26-03NT41856

APINO* ——— 3103209990 ——— Lease name
WAS ——— Well type
Producing Formation ——— MEDINA GP

*Indiana wells: Well identification numbers were provided by the Indiana Geological Survey and are not in the standard API#02 format. Kentucky wells: Well identification numbers were provided by the Kentucky Geological Survey and the Ohio Geological Survey assigned pseudo API#02 numbers.

WELL SYMBOL AND STATUS

Dry hole — Storage
Gas — Stratigraphic test
Oil — Observation
Oil and gas — Unknown
Injection

Dip G

2105803919 HAVENS — 13.5 miles — 2105805771 DOWICK — 11.3 miles — 2105812829 RUFFIT — 29.2 miles — 3405820990 KETTREDY UNIT — 12.2 miles — 3417202239 ANSELS — 3.4 miles — 3417202236 SMITH — 3.3 miles — 3417202027 CARTER — 16.8 miles — 3416200137 HAVENS — 8.1 miles — 34147R0960 W & B ASPHALT CO. — 13.8 miles — 3414735312 HICKEN UNIT — 14.9 miles — 3405300999 LEONHARDT — 18.5 miles — 3417170547 WINEBERGER — 43.8 miles — 3403122053 LEE — 24.8 miles — 3405800760 MOSHER L. — 35.4 miles — 3412121279 ULLMAN — 24.8 miles — 4701700301 POWER OIL CO. — 28.3 miles — 4701506340 JOHNSON — 2.5 miles — 4701503955 HUTSINPILLAR — 62.4 miles — 4708300103 WV BOUNDRY OF CONTROL — 28.3 miles — 4707100858 SPANGLER — Dip G'

OH | WV

NW

SE

Mapped Units

Altered white ash bed correlation pulsates and warping within 5 mile radius of well control are shown (within each state and shown without log controls.

Top of Ordovician

Facies relationships for all units in the uppermost portion of the Ordovician are not shown.

"Trenton/Lexington"

Datum

"Black River"

"Top of Knox"

Tie well with strike line A-A'

Tie well with strike line B-B'

Tie well with strike line C-C'

Tie well with strike line D-D'

Tie well with strike line E-E'

Tie well with strike line F-F'

"Cincinnati Lds"

"Kope"

"Utica"

Trenton Ls

Black River Gp

Wells Creek Fm

Knox Gp

Precambrian

Queenston Shale

Juniata Fm

Reedsville Sh

"Point Pleasant"

Curdsville Ls

Lexington Ls

Assuming section encountered in this an board of control well is equivalent to the Clark-Shelby Limestone Bed, the Thickness of Trenton & Black River Gp. is 1,180', 1,180', 1,180',

Dip H

7900007191 PEMBINA RESOURCES LIM. BASS ISLAND DOL	19.5 miles	7800002843 LAKE ERIE 359	23.7 miles	3404320171 KELLSTONE INC.	28.5 miles	3404320011 KRYSIK-WAKEFIELD KRYSIK SS	20.6 miles	3415521819 WANDEL	18.4 miles	3416921419 DRAKE COPPER RIDGE DOL	23.3 miles	3415724889 DINGERICH ROSE RUN SS	16.4 miles	3415724939 HERBERT UNIT BLACK RIVER GP	21.6 miles	3406720737 ZECHMAN UNIT ST. PETER SS	46.3 miles	4705100539 BURLEY	35.8 miles	4704900244 FINCH ORISKANY SS	8.0 miles	4707700696 WALLS ORISKANY SS	43.3 miles	4702300002 GREENLAND LODGE	9.0 miles	4703100021 BEAN	21.0 miles	4703100022 SNYDER

Dip H'

ON | OH | OH | WV

NW

SE

5000 4000 3000 2000 1000 0 -1000 -2000 -3000

Mapped Units

Informal units used for correlation purposes and mapping within the project. Stratigraphic names as used within each state are shown within log columns.

Tie well with strike line A-A'

Tie well with strike line B-B'

Tie well with strike line C-C'

Tie well with strike line D-D'

Tie well with strike line E-E'

Tie well with strike line F-F'

Top of Ordovician

Facies relationships for all units in the uppermost portion of the Ordovician are not shown.

"Kope"

"Utica"

"Trenton/Lexington"

Datum

"Black River"

"Gull River"

"Wells Creek"

Top of Knox

Correlation | Depth MD | Porosity NPHI PU RHOB GCI PEF BARNELECT

Correlation | Depth MD | Porosity NEUT API RHOB GCI

Correlation | Depth MD | Porosity NPHI PU RHOB GCI DT µsFT PEF BARNELECT

Correlation | Depth MD | Porosity NPHI PU RHOB GCI PEF BARNELECT

Correlation | Depth MD | Porosity NEUT API RHOB GCI

Correlation | Depth MD | Porosity NPHI PU RHOB GCI PEF BARNELECT

Correlation | Depth MD | Porosity NPHI PU RHOB GCI

Correlation | Depth MD | Porosity RHOB GCI NEUT API

Correlation | Depth MD | Porosity NEUT API RHOB GCI

Correlation | Depth MD | Porosity NPHI PU RHOB GCI

Correlation | Depth MD | Porosity NEUT API RHOB GCI

Correlation | Depth MD | Porosity NPHI PU RHOB GCI

Mapped Units

Informal units used for correlation purposes and mapping within the project. Stratigraphic names as used within each state are shown within log columns.

"Trenton/Lexington"

Datum

"Black River"

Top of Knox

Along hole depths for the Greenland Lodge well were not corrected for dip. Thrust faulting at 2710, 3000, 5000, and 6450 in Ryder, 1982.

TD=3670 TD=3070 TD=3436 TD=4463 TD=5667 TD=6897 TD=8650 TD=7120 TD=10625 TD=16512 TD=17111 TD=14094 TD=13000 TD=16075 TD=8977

Plate 1-9

Stratigraphic Cross Section Dip Line H-H'
based on Geophysical Well Logs

Trenton-Black River Appalachian Basin Research Consortium

Datum: top of Black River Group

Vertical scale shown in feet; well logs equally spaced with horizontal distance labeled in miles

Partial funding provided by the U.S. Department of Energy
Contract Number DE-FC26-03NT41856

APINO* 3709920593 HEAD **Lease name** **Well type**

Producing Formation MEDINA GP

*Indiana wells: Well identification numbers were provided by the Indiana Geological Survey and are not in the standard APINO format. Ontario wells: Well identification numbers were provided by the Ontario Geological Survey and the Ohio Geological Survey assigned pseudo APINO numbers.

WELL SYMBOL AND STATUS

Dry hole | Gas | Oil | Oil and gas | Injection | Storage | Stratigraphic test | Observation | Unknown

March 31, 2006

Dip I

7800003071 WALPOLE ISLAND	46.5 miles	7800004772 GOVERNMENT OF ONTARIO	38.5 miles	3403520821 JONES & LAUGHLIN STEEL CORP.	16.3 miles	3410321143 SMITH ESTATE "TREMPEALEAU DOL"	9.8 miles	3415320907 NORTHAMPTON BOARD OF TRUSTEES	20.5 miles	3415121081 WESTFALL COMM.	23.6 miles	3402920648 MURRAY "CLINTON" SS	23.7 miles	4702900080 MINESINGER	75.4 miles	3711120045 SVETZ	50.0 miles	4702700012 DUCKWORTH
ON		OH								OH		WV		WV		PA		PA		WV

Dip I'

NW

SE

3000

2000

1000

0

-1000

Mapped Units

Informal units used for correlation purposes and mapping within the project. Stratigraphic names as used within each state are shown within log columns.

Tie line with strike line A-A'

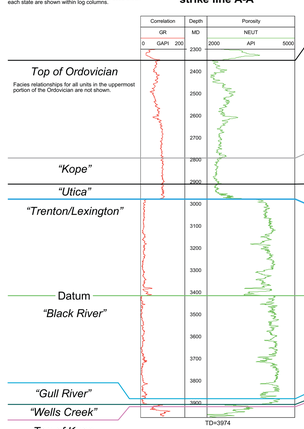

Tie line with strike line B-B'

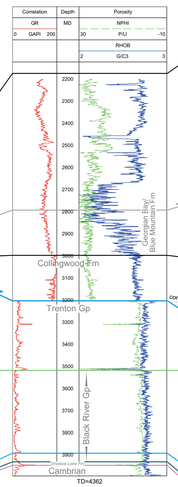

Tie line with strike line C-C'

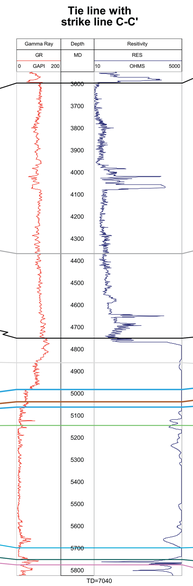

Tie line with strike line D-D'

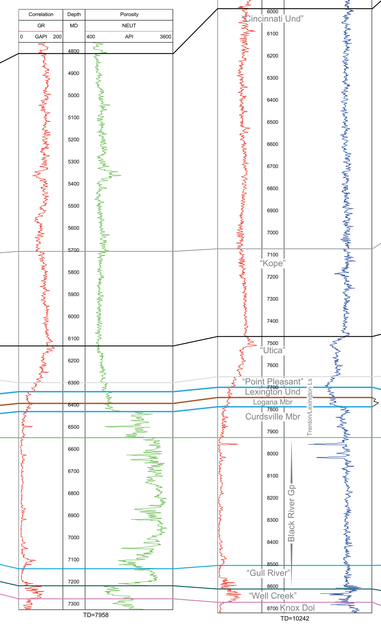

Tie line with strike line F-F'

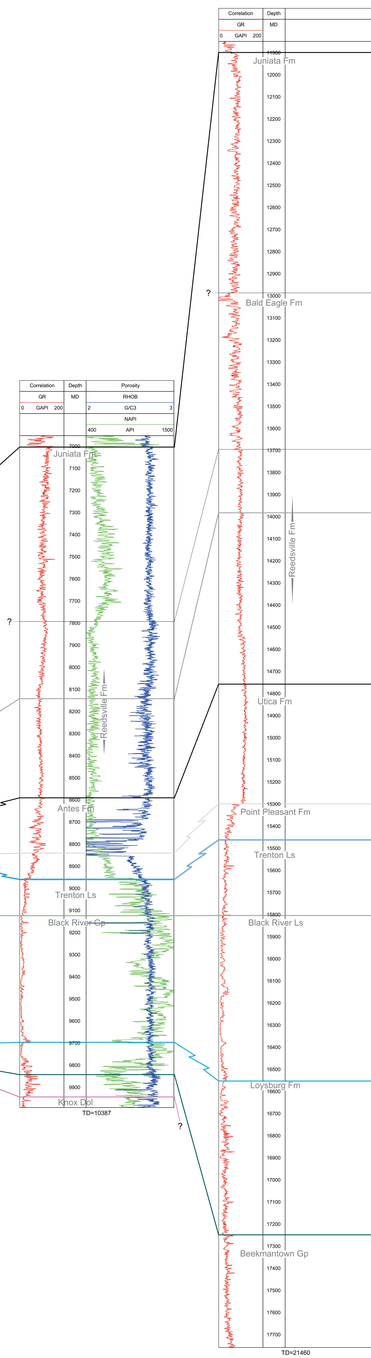

Mapped Units

Informal units used for correlation purposes and mapping within the project. Stratigraphic names as used within each state are shown within log columns.

Top of Ordovician

Facies relationships for all units in the uppermost portion of the Ordovician are not shown.

"Kope"

"Utica"

"Trenton/Lexington"

Datum

"Black River"

"Gull River"

"Wells Creek"

Top of Knox

Plate 1-10

Stratigraphic Cross Section Dip Line I-I'
based on Geophysical Well Logs

Trenton-Black River Appalachian Basin Research Consortium

Datum: top of Black River Group

Vertical scale shown in feet; well logs equally spaced with horizontal distance labeled in miles

Partial funding provided by the U.S. Department of Energy
Contract Number DE-FC26-03NT41856

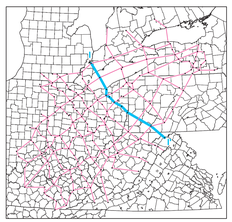

APINO* 3703920593 — Lease name

HEAD — Well type

Producing Formation MEDINA GP

*Indiana wells: Well identification numbers were provided by the Indiana Geological Survey and are not in the standard APINO format. Ontario wells: Well identification numbers were provided by the Ontario Geological Survey and the Ohio Geological Survey assigned pseudo APINO numbers.

WELL SYMBOL AND STATUS

- Dry hole
- Gas
- Oil
- Oil and gas
- Injection
- Storage
- Stratigraphic test
- Observation
- Unknown

March 31, 2006

Dip J

7800007544 — 49 miles — 7800004105 FIREBIRD — 41 miles — 7800006878 DENISON — 36 miles — 7800002565 CONSUMERS PAN AM (GRIMSBY FM) — 6 miles — 7800008512 PEMBINA CENTRAL (GRIMSBY FM) — 27 miles — 34007600010 RESERVE ENVIROMENTAL SERVICES — 12 miles — 34007201103 BRAYMAN — 16 miles — 3703920593 HEAD (MEDINA GP) — 13 miles — 3708520116 FLECK (MEDINA GP) — 61 miles — 3700521201 MARTIN (HUNTERSVILLE CHERT) — 66 miles — 3700920034 SCHELLSBURG

Dip J'

ON | OH | OH | PA

NW

SE

4000

3000

2000

1000

0

Tie well with strike line A-A'

Correlation: GR 0 GAPI 200 | Depth: MD | Porosity: RHOB 2 G/C3 3, PEF 0 BARN/ELECT 10

Top of Ordovician

Facies relationships for all units in the uppermost portion of the Ordovician are not shown.

"Kope"

"Utica"

"Trenton/Lexington"

Datum

"Black River"

"Gull River"

"Wells Creek"

Top of Knox

TD=3608

Tie well with strike line B-B'

Correlation: GR 0 GAPI 200 | Depth: MD | Porosity: NPHI 30 PU -10, RHOB 2 G/C3 3, PEF 0 BARN/ELECT 10

TD=3785

Tie well with strike line A-A'

Correlation: GR 0 GAPI 200 | Depth: MD | Porosity: NPHI 30 PU -10, DPHI 30 PU -10, PEF 0 BARN/ELECT 10

TD=3670

Tie well with strike line B-B'

Correlation: GR 0 GAPI 200 | Depth: MD | Porosity: NPHI 30 PU -10, RHOB 2 G/C3 3, NEUT 300 API 1300

TD=4525

Correlation: GR 0 GAPI 200 | Depth: MD | Porosity: NPHI 30 PU -10, RHOB 2 G/C3 3, PEF 0 BARN/ELECT 10

Rochester Sh / Brassfield Ls / Bois Blanc Fm / Bass Islands Dol / Salina Gp / Bertie Gp / Camillus Sh / Cobleskill Ls / Akron Dol / Williamsville Ls / Oriskany Ss / Helderberg Gp / Onondaga Ls / Onondaga Chert / Needmore Sh / Tioga Bentonite / Tioga Ash Bed / Huntersville Chert / Oriskany Ss / Keyser Ls / Corriganville Ls / New Creek Ls / Wills Creek Fm / Tonoloway Ls

Dip K

7800002713 ARTHUR	65 miles	7800002033 IMPERIAL OIL	37 miles	7800010043 TALISMAN EAST GRIMSBY FM	38 miles	3101322498 BUTTS	45 miles	3708331744 MINARD RUN GATESBURG FM	51 miles	3710502182 PA DEPT OF FOREST & WATER ST	14 miles	3703520276 PA STATE TRACT BALD EAGLE FM
ON		NY				NY		PA				

Dip K'

NW

SE

3000

2000

1000

0

Mapped Units

Informal units used for correlation purposes and mapping within the project. Stratigraphic names as used within each state are shown within log columns.

Top of Ordovician

Facies relationships for all units in the uppermost portion of the Ordovician are not shown.

"Kope"

"Utica"

"Trenton/Lexington"

Datum

"Black River"

"Wells Creek"

"Gull River"

"Top of Knox

Tie well with strike line A-A'

Tie well with strike line

Tie well with strike line E-E'

Tie well with strike line F-F'

Correlation: GR 0 GAPI 200

Depth: MD

Porosity: NEUT 1500 API 3000; RHOB 2 G/C3 3

Porosity: TT 400 µs/FT 100

Porosity: NPHI 30 P/U -10; RHOB 2 G/C3 3; PEFZ 0 BARN/ELECT 10

Porosity: RHOB 2 G/C3 3; NPHI 30 P/U -10

Queenston Fm

Georgian Bay/ Blue Mountain Fm

Collingwood Fm

Lorraine Gp

Utica Fm

Trenton Gp

Trenton Ls

Black River Gp

Shadow Lake Fm

Cambrian

Little Falls Fm

Juniata Fm

Bald Eagle Fm

Reedsville Fm

Point Pleasant Fm

Black River Ls

Wells Creek Fm

Beekmantown Fm

TD=2340

TD=2424

TD=4270

TD=7620

TD=10478

TD=18834

TD=19365

Plate 1-12

Stratigraphic Cross Section Dip Line K-K'
based on Geophysical Well Logs

Trenton-Black River Appalachian Basin Research Consortium

Datum: top of Black River Group

Vertical scale shown in feet; well logs equally spaced with horizontal distance labeled in miles

Partial funding provided by the U.S. Department of Energy
Contract Number DE-FC26-03NT41856

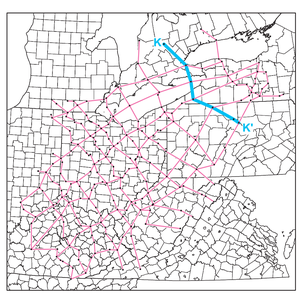

APINO* 3703920593

HEAD — **Lease name**

Well type

Producing Formation MEDINA GP

*Indiana wells: Well identification numbers were provided by the Indiana Geological Survey and are not in the standard APINO format. Ontario wells: Well identification numbers were provided by the Ontario Geological Survey and the Ohio Geological Survey assigned pseudo APINO numbers.

WELL SYMBOL AND STATUS

- Dry hole
- Gas
- Oil
- Oil and gas
- Injection
- Storage
- Stratigraphic test
- Observation
- Unknown

March 31, 2006

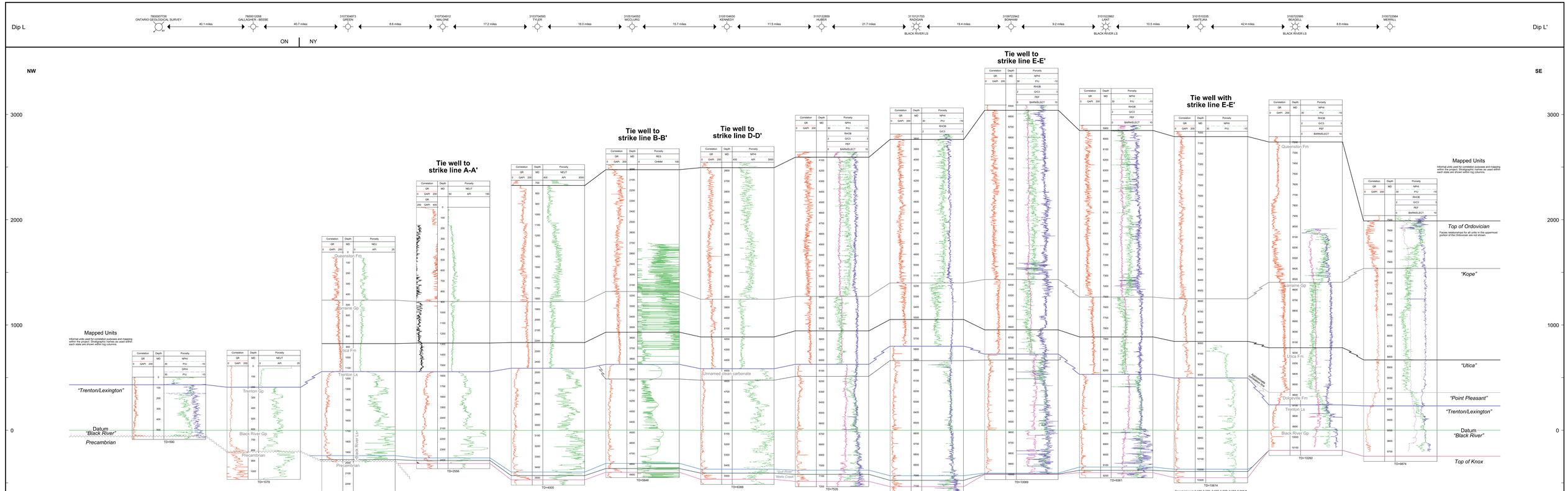

Plate 1-13

Stratigraphic Cross Section Dip Line L-L'
based on Geophysical Well Logs

Trenton-Black River Appalachian Basin Research Consortium

Datum: top of Black River Group

Vertical scale shown in feet; well logs equally spaced with horizontal distance labeled in miles

Partial funding provided by the U.S. Department of Energy
Contract Number DE-FC26-03NT41856



APINO* 3703920593 HEAD — Lease name
Well type
Producing Formation MEDINA GP

*Indiana wells: Well identification numbers were provided by the Indiana Geological Survey and are not in the standard APINO format. Ontario wells: Well identification numbers were provided by the Ontario Geological Survey and the Ohio Geological Survey assigned pseudo APINO numbers.

WELL SYMBOL AND STATUS

- Dry hole
- Gas
- Oil
- Oil and gas
- Injection
- Storage
- Stratigraphic test
- Observation
- Unknown

March 31, 2006

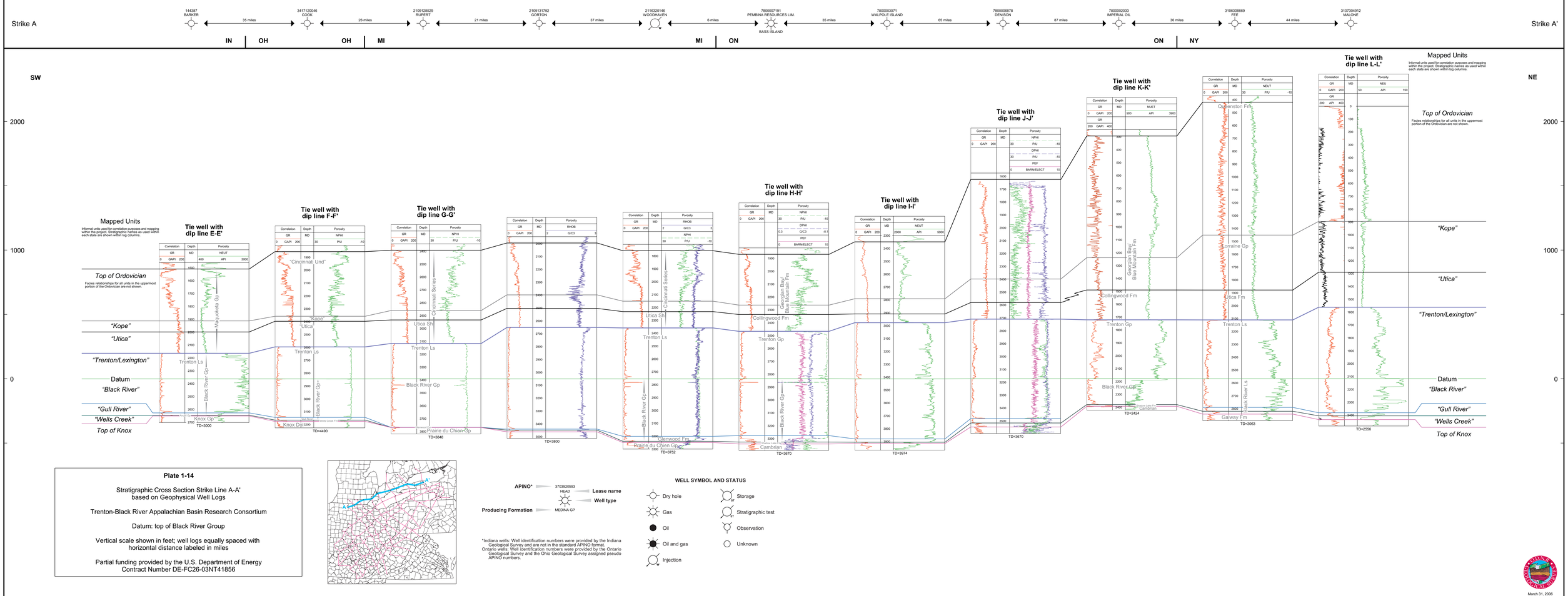
Strike A
Strike A'
144387 BARKER
35 miles
3417120046 COOK
26 miles
2109128529 RUPERT
21 miles
2109131792 GORTON
37 miles
2116320146 WOODHAVEN
6 miles
7800007191 PEMBINA RESOURCES LIM. BASS ISLAND
35 miles
7800003071 WALPOLE ISLAND
65 miles
7800006878 DENISON
87 miles
7800002033 IMPERIAL OIL
36 miles
3106306869 FEE
44 miles
3107304912 MALONE
IN
OH
OH
MI
MI
ON
ON
NY
SW
NE
2000
1000
0
Mapped Units
Informal units used for correlation purposes and mapping within the project. Stratigraphic names as used within each state are shown within log columns.
Tie well with dip line E-E'
Tie well with dip line F-F'
Tie well with dip line G-G'
Tie well with dip line H-H'
Tie well with dip line I-I'
Tie well with dip line J-J'
Tie well with dip line K-K'
Tie well with dip line L-L'
Top of Ordovician
Facies relationships for all units in the uppermost portion of the Ordovician are not shown.
"Kope"
"Utica"
"Trenton/Lexington"
Datum
"Black River"
"Gull River"
"Wells Creek"
Top of Knox
Maquoketa Gp
Black River Gp
Knox Gp
Cincinnati Und
Cincinnati Series
Utica Sh
Trenton Ls
Prairie du Chien Gp
Glenwood Fm
Cambrian
Knox Dol
Wells Creek Fm
Georgian Bay/ Blue Mountain Fm
Collingwood Fm
Trenton Gp
Black River Gp
Queenston Fm
Lorraine Gp
Utica Fm
Trenton Ls
Black River Ls
Galway Fm
TD=3000
TD=4490
TD=3848
TD=3800
TD=3752
TD=3670
TD=3974
TD=3670
TD=2424
TD=3063
TD=2556
Plate 1-14
Stratigraphic Cross Section Strike Line A-A'
based on Geophysical Well Logs
Trenton-Black River Appalachian Basin Research Consortium
Datum: top of Black River Group
Vertical scale shown in feet; well logs equally spaced with horizontal distance labeled in miles
Partial funding provided by the U.S. Department of Energy
Contract Number DE-FC26-03NT41856
APINO*
3703920593
HEAD
Lease name
Well type
Producing Formation
MEDINA GP
WELL SYMBOL AND STATUS
Dry hole
Gas
Oil
Oil and gas
Injection
Storage
Stratigraphic test
Observation
Unknown
*Indiana wells: Well identification numbers were provided by the Indiana Geological Survey and are not in the standard APINO format. Ontario wells: Well identification numbers were provided by the Ontario Geological Survey and the Ohio Geological Survey assigned pseudo APINO numbers.
March 31, 2006

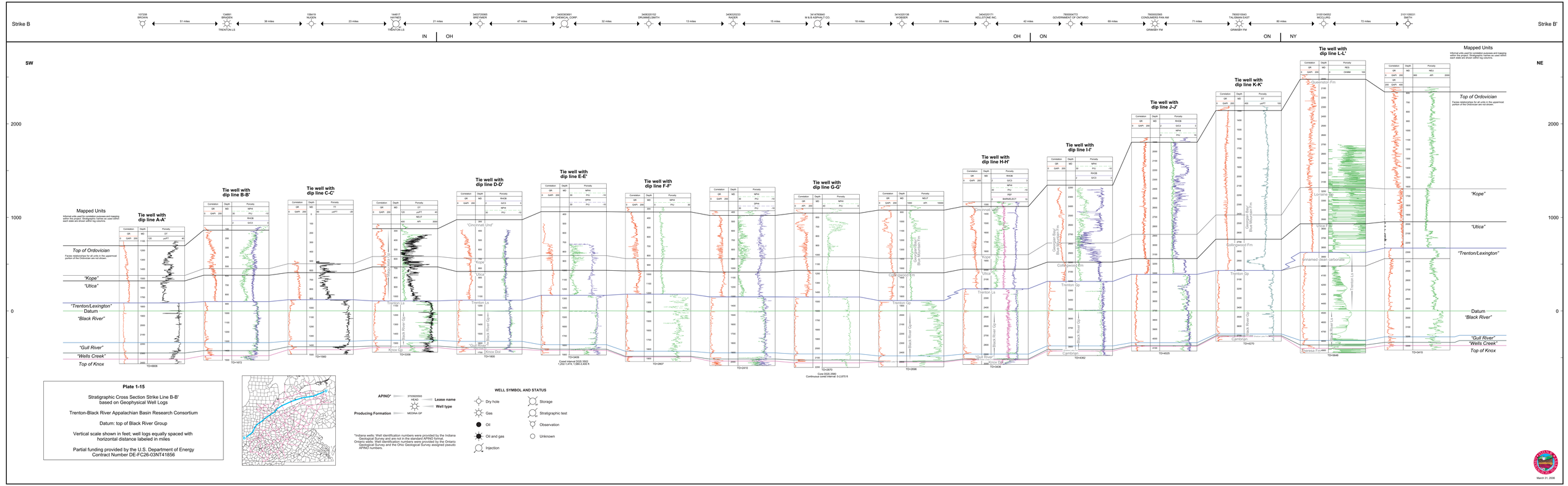
Strike B
Strike B'
SW
NE
IN
OH
OH
ON
ON
NY
102308
BROWN
51 miles
134891
BRADEN
TRENTON LS
36 miles
156419
NUGEN
23 miles
144617
HAYNES
TRENTON LS
21 miles
3403720065
SIBO'BAKER
47 miles
3403953691
BP CHEMICAL CORP.
32 miles
3406303152
ORLIMAR/J.SMITH
13 miles
3406303233
RADER
15 miles
3414760840
M & S ASPHALT CO.
18 miles
3414320138
HOBSER
20 miles
3404320779
KELLYSTONE INC.
42 miles
7800004772
GOVERNMENT OF ONTARIO
69 miles
7800002995
CONSUMERS PAN AM
GRIMSBY FM
71 miles
7800010043
TALISMAN EAST
GRIMSBY FM
80 miles
3105104502
MCCLUREO
72 miles
3101105231
SMITH
Mapped Units
Informal units used for correlation purposes and mapping within the project. Stratigraphic hiatses as used within each state are shown within log columns.
Tie well with dip line A-A'
Tie well with dip line B-B'
Tie well with dip line C-C'
Tie well with dip line D-D'
Tie well with dip line E-E'
Tie well with dip line F-F'
Tie well with dip line G-G'
Tie well with dip line H-H'
Tie well with dip line I-I'
Tie well with dip line J-J'
Tie well with dip line K-K'
Tie well with dip line L-L'
Top of Ordovician
Facies relationships for all units in the uppermost portion of the Ordovician are not shown.
"Kope"
"Utica"
"Trenton/Lexington"
"Black River"
"Gull River"
"Wells Creek"
Top of Knox
Datum
"Cincinnati Unit"
Queenston Fm
Lorraine Gp
Utica Sh
Ellenburg Fm
Black River Gp
Trenton Ls
Knox Dol
Cambrian
Precambrian
Eaton Sandstone
Grimsby Fm
Whirlpool Ss
Manitoulin Dol
Cabot Head Fm
Georgian Bay
Blue Mountain Fm
Collingwood Fm
Trenton Gp
Gull River
Wells Creek
Fairmount Mbr
Kope
Utica
Dolgeville
Coburg Ls
Sherman Fall Fm
Kirkfield
Coboconk Ls
Gull River Gp
Shadow Lake Fm
Gelasinous Ss
Theresa Fm
Potsdam Ss
Precambrian
Mapped Units
Informal units used for correlation purposes and mapping within the project. Stratigraphic hiatses as used within each state are shown within log columns.
Top of Ordovician
Facies relationships for all units in the uppermost portion of the Ordovician are not shown.
"Kope"
"Utica"
"Trenton/Lexington"
Datum
"Black River"
"Gull River"
"Wells Creek"
Top of Knox
2000
1000
0
TD=6606
TD=1872
TD=1960
TD=1056
TD=1800
TD=3409
Cored interval DOS 3002
1,202-1,474; 1,583-3,400 ft
TD=2907
TD=2410
TD=2870
Core DOS 2080
Continuous cored interval: 0-2,870 ft
TD=3996
TD=3438
TD=4362
TD=4525
TD=4270
TD=3648
TD=3415
Plate 1-15
Stratigraphic Cross Section Strike Line B-B' based on Geophysical Well Logs
Trenton-Black River Appalachian Basin Research Consortium
Datum: top of Black River Group
Vertical scale shown in feet; well logs equally spaced with horizontal distance labeled in miles
Partial funding provided by the U.S. Department of Energy Contract Number DE-FC26-03NT41856
APINo*
3703920093
HEAD
MEDINA GP
Lease name
Well type
Producing Formation
WELL SYMBOL AND STATUS
Dry hole
Gas
Oil
Oil and gas
Injection
Storage
Stratigraphic test
Observation
Unknown
*Indiana wells: Well identification numbers were provided by the Indiana Geological Survey and the Ohio Geological Survey assigned pseudo APINO numbers.
Ontario wells: Well identification numbers were provided by the Ontario Geological Survey and the Ohio Geological Survey assigned pseudo APINO numbers.
March 01, 2006

Strike C

| 15048 ROSE | 45.8 miles | 15092 SULLIVAN | 7.7 miles | 10873 COLLINS | 17.7 miles | 16015000? CONNER | 11.6 miles | 34061000? CITY OF CINCINNATI | 23.5 miles | 34077000? ARMCO STEEL CORP. | 14.8 miles | 34166000? AMERICAN AGGREGATES | 35.8 miles | 34022000? ELIZABETHTOWN INC. | 18.1 miles | 34156000? ZENITH HOLDINGS & TRADING CORP. | 11.2 miles | 34155000? LOH | 17.8 miles | 34041000? SMITH | 8.7 miles | 34111000? HENRY | 11.7 miles | 34117000? REFERMINE | 10.4 miles | 34111000? WHARDALE | 10.8 miles | 34112000? LOCKPORT OIL | 34125000? EMPIRE REFINED STEEL CO. | 29.7 miles | 34103? WARD | 27.5 miles | 34103? WARD | 34103?/1143 SMITH ESTATE "TRIMPHOLLEAU OIL" | 16.8 miles | 34103?/1361 A.S.T. OIL & GAS CO., INC. | 37.8 miles | 34053?/2036 PACKARD | 18.5 miles | 34053?/2183 MARTINS | 15.8 miles | 37050/0007 HARGUS |

IN | KY | KY | OH | OH | PA

Strike C'

SW

NE

2000

1000

0

Mapped Units

Informal units used to correlate cuttings and logged units in the study. Stratigraphic names as used within each state and shown within log columns.

Top of Ordovician
Packer Sandstone/top of unit only in the uppermost portion of the Ordovician was not shown.

"Kope"

"Utica"

"Trenton/Lexington"

Datum
"Black River"

"Gull River"

"Wells Creek"

Top of Knox

Tie well with dip line A-A'

TD=5008
Continuous cored interval: 10/1,508-5

Tie well with dip line B-B'

TD=4101

Tie well with dip line C-C'

TD=4125

Tie well with dip line D-D'

TD=5080
OGS 0507
Continuous cored interval: 0-5,380 ft

Tie well with dip line E-E'

TD=5048

Tie well with dip line F-F'

TD=4035

Tie well with dip line G-G'

TD=4988
OGS 2830
Continuous cored interval: 1,803-4,029 ft

Tie well with dip line H-H'

TD=5067

Tie well with dip line I-I'

TD=7040

Tie well with dip line J-J'

TD=7125

Tie well with strike line D-D'

TD=6800

Mapped Units

Informal units used to correlate cuttings and logged units in the study. Stratigraphic names as used within each state and shown within log columns.

Top of Ordovician
Packer Sandstone/top of unit only in the uppermost portion of the Ordovician was not shown.

"Kope"

"Utica"

"Point Pleasant"

"Trenton/Lexington"

Datum
"Black River"

"Gull River"

"Wells Creek"

Top of Knox

Plate 1-16

Stratigraphic Cross Section Strike Line C-C'
based on Geophysical Well Logs

Trenton-Black River Appalachian Basin Research Consortium

Datum: top of Black River Group

Vertical scale shown in feet; well logs equally spaced with horizontal distance labeled in miles

Partial funding provided by the U.S. Department of Energy
Contract Number DE-FC26-03NT41856



WELL SYMBOL AND STATUS

APINO* 3705900000 — Lease name — Well type

Producing Formation — MORA-4P

Dry hole
Gas
Oil
Oil and gas
Injection
Storage
Stratigraphic test
Observation
Unknown

*Indiana wells: Well identification numbers were provided by the Indiana Geological Survey and are not in the standard APINO format. Ontario wells: Well identification numbers were provided by the Ontario Division of Mines Survey and the Ohio Geological Survey assigned pseudo APINO numbers.

March 31, 2006

Strike D

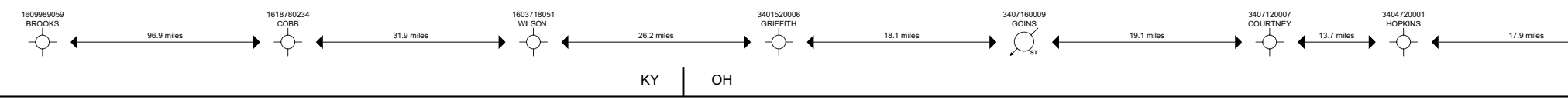
1609989059
BROOKS
96.9 miles
1618780234
COBB
31.9 miles
1603718051
WILSON
26.2 miles
3401520006
GRIFFITH
18.1 miles
3407160009
GOINS
ST
19.1 miles
3407120007
COURTNEY
13.7 miles
3404720001
HOPKINS
17.9 miles
KY
OH

SW

Plate 1-17

Stratigraphic Cross Section Strike Line D-D'
based on Geophysical Well Logs

Trenton-Black River Appalachian Basin Research Consortium

Datum: top of Black River Group

Vertical scale shown in feet; well logs equally spaced with
horizontal distance labeled in miles

Partial funding provided by the U.S. Department of Energy
Contract Number DE-FC26-03NT41856

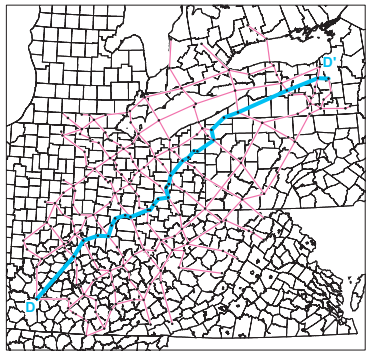

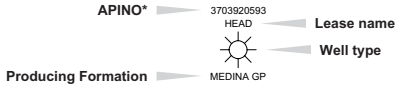
APINO*
3703920593
HEAD
Lease name
Well type
Producing Formation
MEDINA GP

*Indiana wells: Well identification numbers were provided by the Indiana Geological Survey and are not in the standard APINO format.
Ontario wells: Well identification numbers were provided by the Ontario Geological Survey and the Ohio Geological Survey assigned pseudo APINO numbers.

Mapped Units

Informal units used for correlation purposes and mapping within the project. Stratigraphic names as used within each state are shown within log columns.

Tie well with dip line A-A'

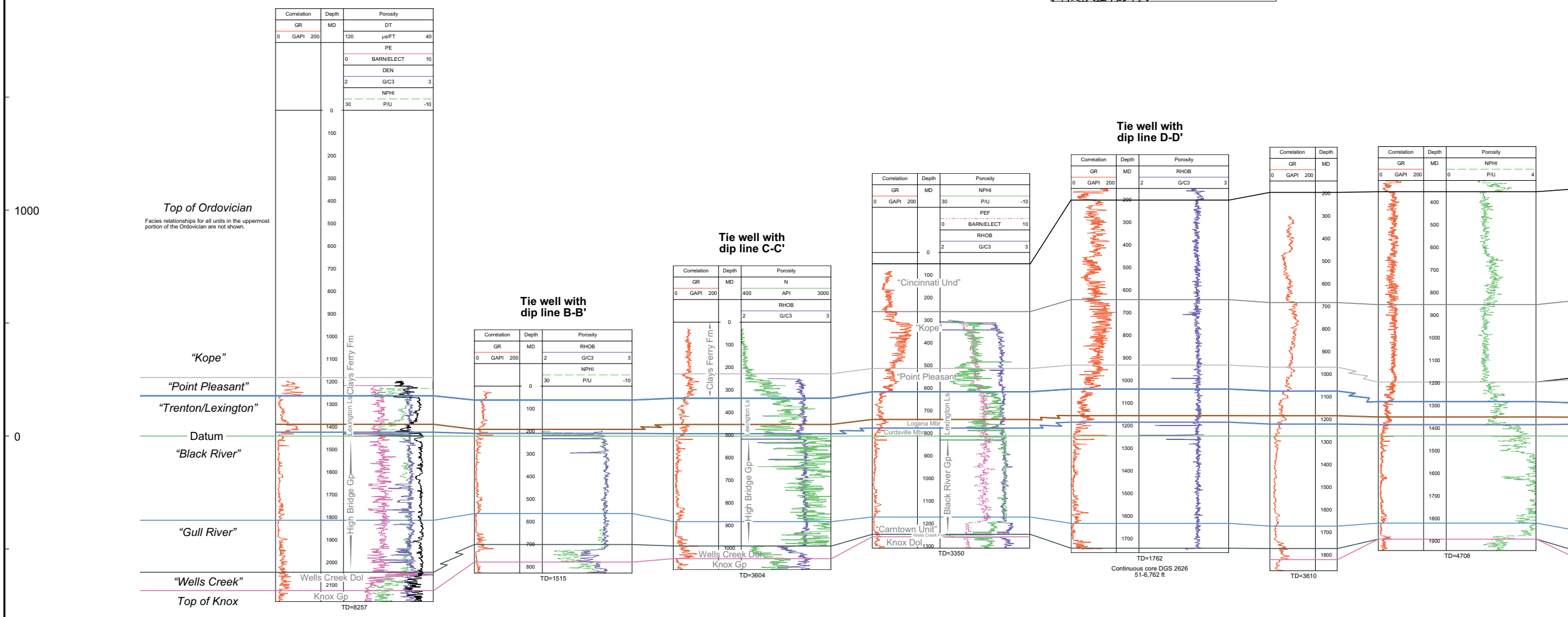

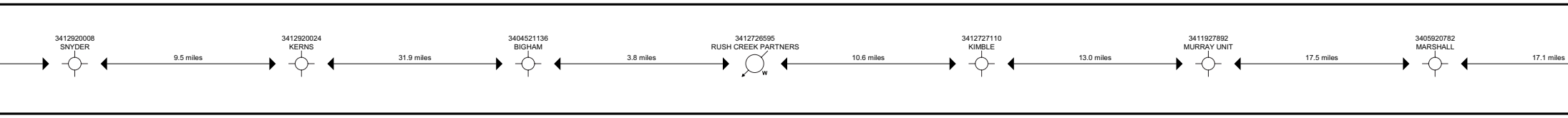
3412920008
SNYDER
9.5 miles
3412920024
KERNS
31.9 miles
3404521136
BIGHAM
3.8 miles
3412726595
RUSH CREEK PARTNERS
W
10.6 miles
3412727110
KIMBLE
13.0 miles
3411927892
MURRAY UNIT
17.5 miles
3405920782
MARSHALL
17.1 miles

WELL SYMBOL AND STATUS

⌖ Dry hole	○ Storage
✷ Gas	○ Stratigraphic test
● Oil	○ Observation
✷ Oil and gas	○ Unknown
○ Injection	

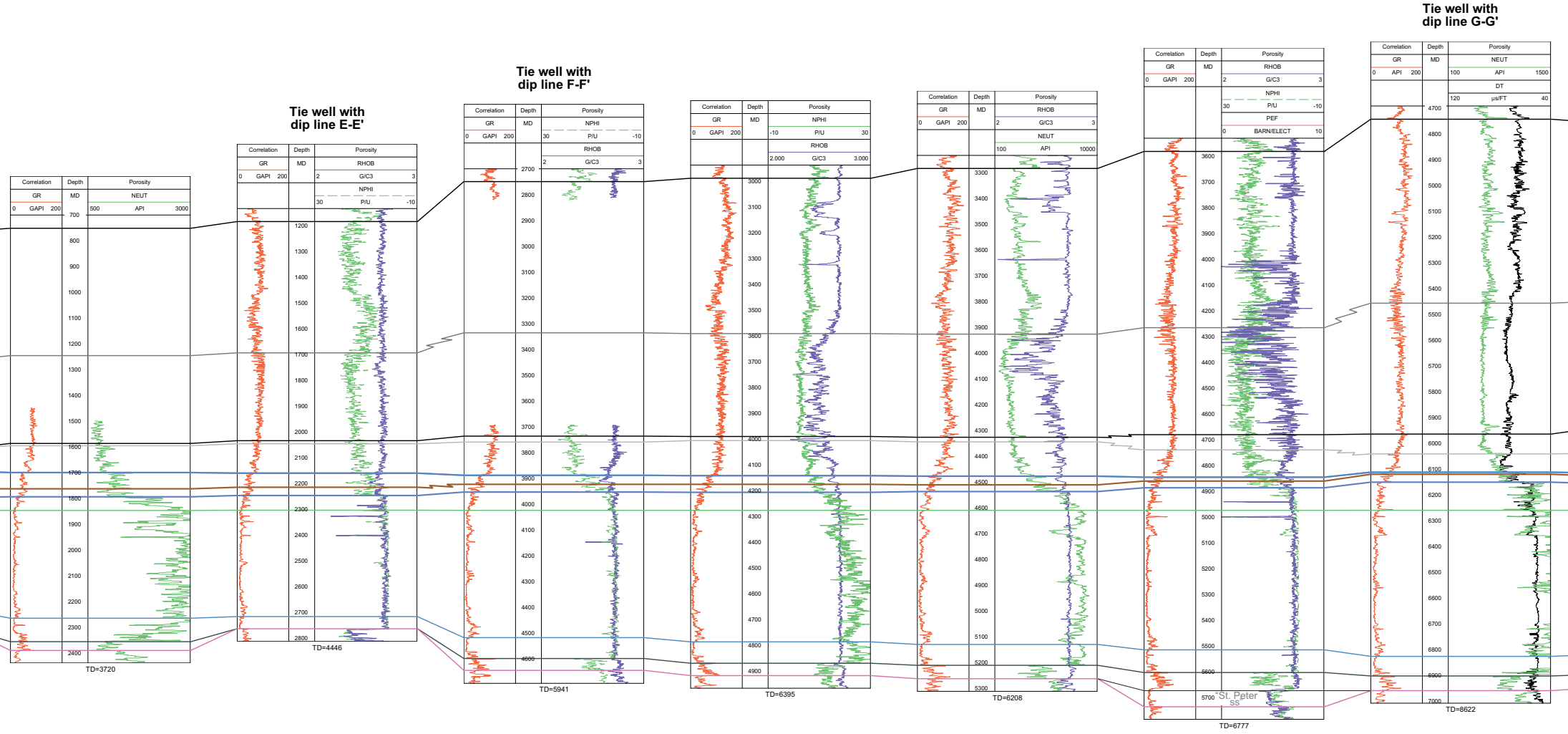

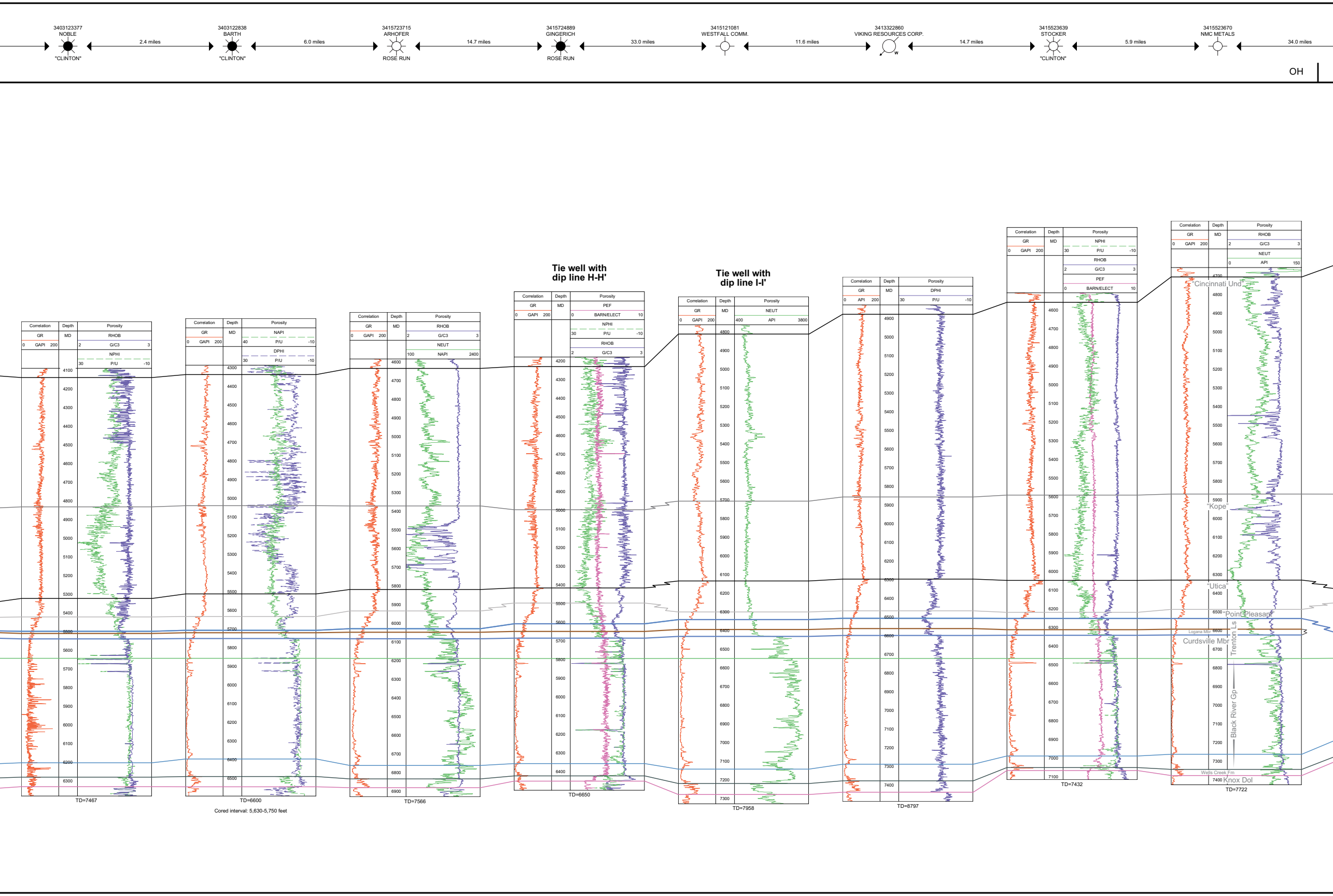
3403123377
NOBLE
"CLINTON"
2.4 miles
3403122838
BARTH
"CLINTON"
6.0 miles
3415723715
ARHOFER
ROSE RUN
14.7 miles
3415724889
GINGERICH
ROSE RUN
33.0 miles
3415121081
WESTFALL COMM.
11.6 miles
3413322860
VIKING RESOURCES CORP.
14.7 miles
3415523639
STOCKER
"CLINTON"
5.9 miles
3415523670
NMC METALS
34.0 miles
OH
Tie well with dip line H-H'
Tie well with dip line I-I'
Correlation
Depth
Porosity
GR
MD
GAPI
RHOB
G/C3
NPHI
P/U
NAPI
DPHI
NEUT
PEF
BARN/ELECT
API
"Cincinnati Und"
"Kope"
"Utica"
Point Pleasant
Logana Mbr
Curdsville Mbr
Trenton Ls
Black River Gp
Wells Creek Fm
Knox Dol
TD=7467
TD=6600
Cored interval: 5,630-5,750 feet
TD=7566
TD=6650
TD=7958
TD=8797
TD=7432
TD=7722

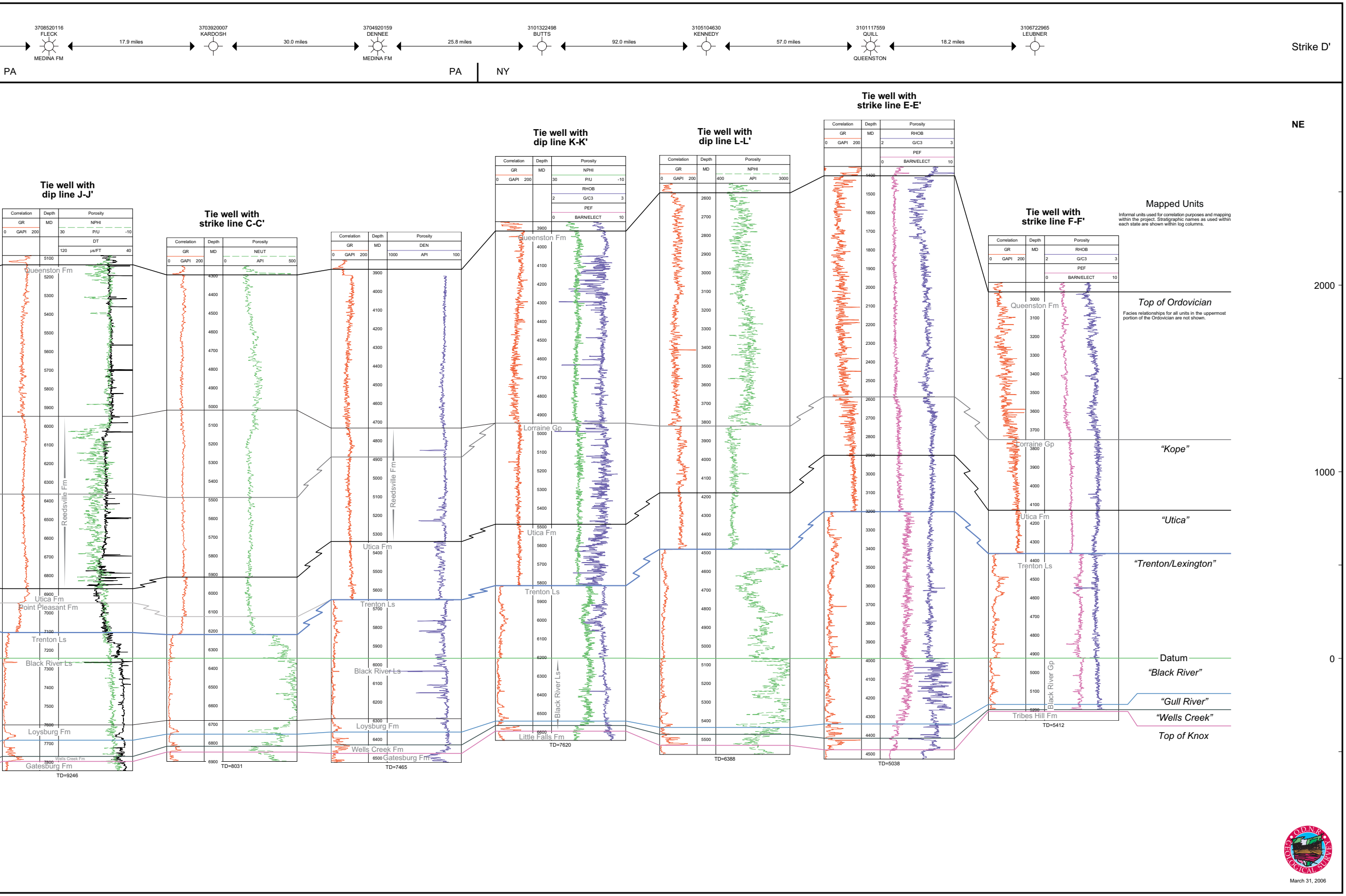
3708520116
FLECK
MEDINA FM
17.9 miles
3703920007
KARDOSH
30.0 miles
3704920159
DENNEE
MEDINA FM
25.8 miles
3101322498
BUTTS
92.0 miles
3105104630
KENNEDY
57.0 miles
3101117559
QUILL
QUEENSTON
18.2 miles
3106722965
LEUBNER
Strike D'
PA
PA
NY
NE
Tie well with dip line J-J'
Tie well with strike line C-C'
Tie well with dip line K-K'
Tie well with dip line L-L'
Tie well with strike line E-E'
Tie well with strike line F-F'
Correlation
Depth
Porosity
GR
MD
NPHI
0 GAPI 200
30 P/U -10
DT
120 µs/FT 40
NEUT
0 API 500
DEN
1000 API 100
RHOB
2 G/C3 3
PEF
0 BARN/ELECT 10
400 API 3000
Queenston Fm
Reedsville Fm
Utica Fm
Point Pleasant Fm
Trenton Ls
Black River Ls
Loysburg Fm
Wells Creek Fm
Gatesburg Fm
Lorraine Gp
Little Falls Fm
Black River Gp
Tribes Hill Fm
TD=9246
TD=8031
TD=7465
TD=7620
TD=6388
TD=5038
TD=5412
2000
1000
0
"Kope"
"Utica"
"Trenton/Lexington"
Datum
"Black River"
"Gull River"
"Wells Creek"
Top of Knox

Mapped Units

Informal units used for correlation purposes and mapping within the project. Stratigraphic names as used within each state are shown within log columns.

Top of Ordovician

Facies relationships for all units in the uppermost portion of the Ordovician are not shown.

March 31, 2006

Strike E

WASHINGTON MARRIOTT — 38.4 miles — WASHINGTON MAMA TOM — 29.7 miles — WASHINGTON OLIVER — 5.4 miles — WAYNE EAST WYOTECH — 27.9 miles — WASHINGTON BAILEY — 23.9 miles — WASHINGTON STAMPEDE — 24.8 miles — MORGAN HILL ANKATHON CHEMICAL CORP — 20.6 miles — MARKSMAN PATOC — 19.8 miles — ATHENS/MEIGS APPERSON — 20.6 miles — ATHENS/MEIGS APPALACHIAN POWER CO — 24.2 miles — WYANDOT DEER — 17.8 miles — WYANDOT PENNEC CO. CO — 22.6 miles — ATHENS/MEIGS BAILEY — 58.6 miles — STARK/OHIO MARTIN — 77.6 miles — STARK/OHIO FM HUNTSBURG FM — 62.8 miles — SNYDER/UNION GUTSHALL — 25.1 miles — SNYDER/UNION FAIR CLOTT — 8.2 miles — SNYDER/UNION BLOUGH — 9.9 miles — SNYDER/UNION STEVENS — 10.6 miles — SNYDER/UNION CAMPION — 16.8 miles — SNYDER/UNION QUEENSTOWN FM — 12.9 miles — SNYDER/UNION SCULL QUEENSTON — 19.7 miles — SYDER/UNION SMITH

KY | OH | OH | WV | WV | PA | PA | NY

Strike E'

SW

NE

3000 2000 1000 0 -1000

Plate 1-18

Stratigraphic Cross Section Strike Line E-E' based on Geophysical Well Logs

Trenton-Black River Appalachian Basin Research Consortium

Datum: top of Black River Group

Vertical scale shown in feet; well logs equally spaced with horizontal distance labeled in miles

Partial funding provided by the U.S. Department of Energy Contract Number DE-FC26-02NT41656



APINo* — 3705900000 — Lease name
HEAD — Well type
Producing Formation — MEDINA-UP

*Indiana wells: Well identification numbers were provided by the Indiana Geological Survey and are not in the standard APINO format.
Kentucky wells: Well identification numbers were provided by the Ontario Geological Survey and the Ohio Geological Survey assigned pseudo APINO numbers.

WELL SYMBOL AND STATUS

Dry hole	Storage
Gas	Stratigraphic test
Oil	Observation
Oil and gas	Unknown
Injection	

Mapped Units

Information for all the formation tops in the wells is listed in the appendix section of this cross section and not shown within the log columns.

Top of Ordovician

Faulty interpretations for all units in the upper section of the Ordovician are not shown.

"Kope"

"Point Pleasant"

"Trenton/Lexington"

Datum
"Black River"

"Gull River"

"Wells Creek"
Top of Knox

Tie well with dip line A-A'

Tie well with dip line B-B'

Tie well with dip line C-C'

Tie well with dip line D-D'

Tie well with dip line E-E'

Tie well with dip line F-F'

Tie well with dip line G-G'

Tie well with dip line H-H'

Tie well with dip line J-J'

Tie well with dip line K-K'

Tie well with dip line L-L'

Tie well with strike line D-D'

Tie well with strike line B-B'

Mapped Units

Information for all the formation tops in the wells is listed in the appendix section of this cross section and not shown within the log columns.

Top of Ordovician

Faulty interpretations for all units in the uppermost section of the Ordovician are not shown.

"Kope"

"Utica"

"Trenton/Lexington"

Datum
"Black River"

"Gull River"

"Wells Creek"
Top of Knox

March 01, 2006

Strike F

| 41073203188 BEGLEY LUMBER | 34 miles | 1601300000 KNUCKLES | 35 miles | 1601320000 FORBSON COAL CO. | 12 miles | 1601304492 DUFF | 32 miles | 1601727524 HALL | 18 miles | 1616524377 STRATTON | 30 miles | 4705900879 HUNTINGTON REALTY | 5 miles | 4705900805 COLUMBIA GAS TRANS. CORP. | 25 miles | 4704504485 MCCORMICK | 41 miles | 4702001396 MCCOY COMAGASA GP | 27 miles | 4701302503 HATHAWAY | 70 miles | 4714900244 FINCH ORDWAY SS | 52 miles | 3711120045 SVETZ | 39 miles | 3709302834 SCHELLSBURG | 43 miles | 3708190000 BALDAUF | 60 miles | 3705352078 PA STATE TRACT 597 BALD EAGLE FM | 58 miles | 3115122963 WAXWELL | 21 miles | 3101510225 MATEJKA | 16 miles | 3101094467 RICHARDSON | 17 miles | 3115022785 KEHEWEWACALI | 25 miles | 3106722965 LEUMBER |
|---|---|---

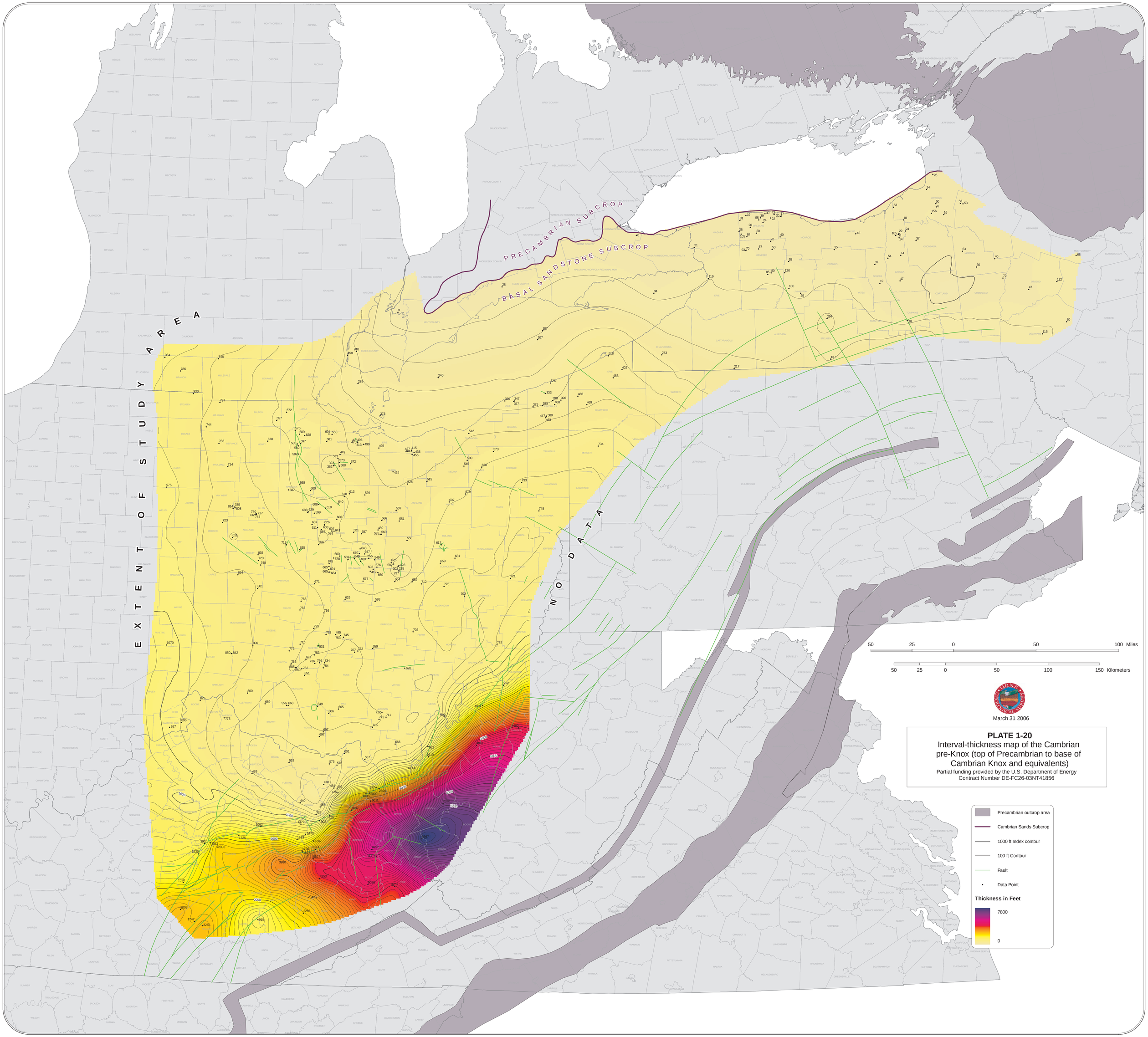
PRECAMBRIAN SUBCROP
BASAL SANDSTONE SUBCROP
EXTENT OF STUDY AREA
NO DATA
50 25 0 50 100 Miles
50 25 0 50 100 150 Kilometers
March 31 2006
PLATE 1-20
Interval-thickness map of the Cambrian pre-Knox (top of Precambrian to base of Cambrian Knox and equivalents)
Partial funding provided by the U.S. Department of Energy
Contract Number DE-FC26-03NT41856
Precambrian outcrop area
Cambrian Sands Subcrop
1000 ft Index contour
100 ft Contour
Fault
Data Point
Thickness in Feet
7800
0

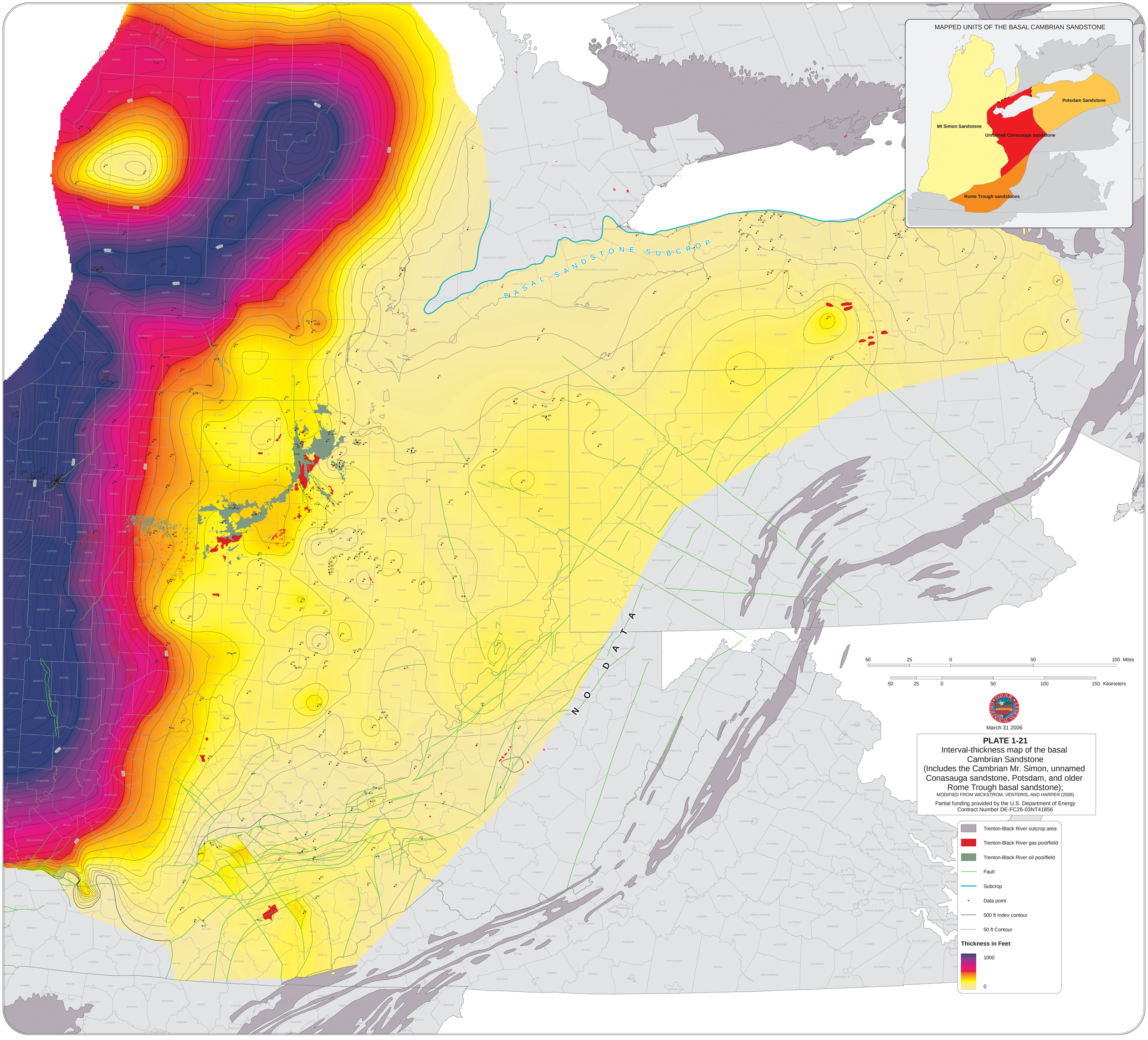
MAPPED UNITS OF THE BASAL CAMBRIAN SANDSTONE
Potsdam Sandstone
Mt Simon Sandstone
Unnamed Conasauga sandstone
Rome Trough sandstones
BASAL SANDSTONE SUBCROP
NO DATA
50 25 0 50 100 Miles
50 25 0 50 100 150 Kilometers
March 31 2006
PLATE 1-21
Interval-thickness map of the basal Cambrian Sandstone
(Includes the Cambrian Mr. Simon, unnamed Conasauga sandstone, Potsdam, and older Rome Trough basal sandstone);
MODIFIED FROM WICKSTROM, VENTERIS, AND HARPER (2005)
Partial funding provided by the U.S. Department of Energy
Contract Number DE-FC26-03NT41856
Trenton-Black River outcrop area
Trenton-Black River gas pool/field
Trenton-Black River oil pool/field
Fault
Subcrop
Data point
500 ft Index contour
50 ft Contour
Thickness in Feet
1000
0

STUDY AREA

EXTENT OF

NO DATA

50 25 0 50 100 Miles

50 25 0 50 100 150 Kilometers

March 31 2006

PLATE 1-22

Interval thickness map of the Cambrian-Ordovician Knox (base of Knox to top of Knox)

Partial funding provided by the U.S. Department of Energy
Contract Number DE-FC26-03NT41856

Data point

Fault

500 ft Index contour

50 ft Contour

Thickness in Feet

3350

0

NO DATA

NO DATA

50 25 0 50 100 Miles

50 25 0 50 100 150 Kilometers

March 31 2006

PLATE 1-23

Interval thickness map of the Cambrian Rose Run sandstone (top of the Copper Ridge to top of Rose Run; includes the Upper Sandy member of the Gatesburg Formation in Pennsylvania and the Theresa Formation sandstone equivalent in New York).

Partial funding provided by the U.S. Department of Energy
Contract Number DE-FC26-03NT41856

- Trenton-Black River gas pool/field
- Trenton-Black River oil pool/field
- Area of erosional remnants
- Rose Run Subcrop
- Fault
- Data point
- 125 ft Index contour
- 25 ft Contour

Thickness in Feet

800

0

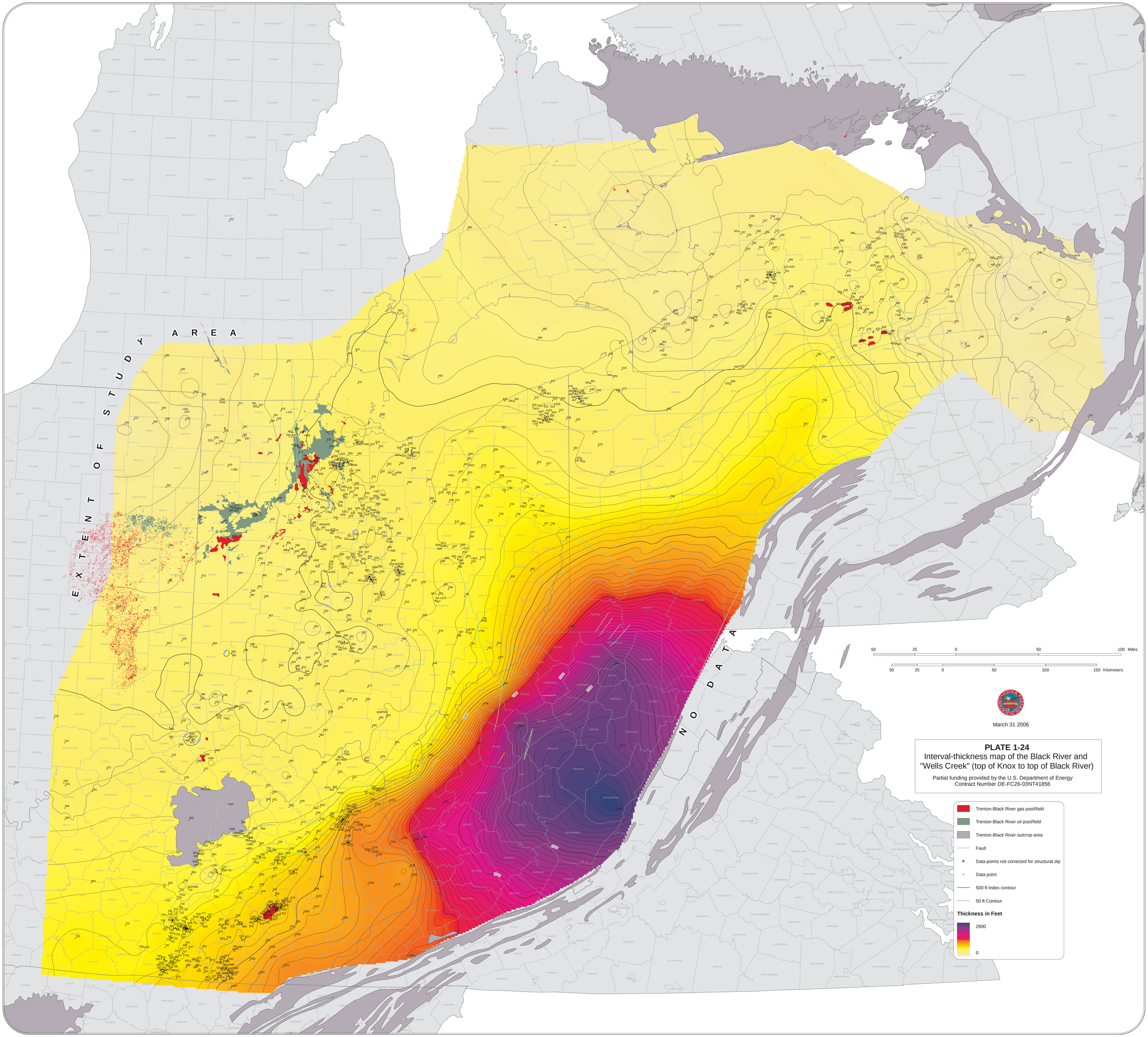
EXTENT OF STUDY AREA
NO DATA
50 25 0 50 100 Miles
50 25 0 50 100 150 Kilometers
March 31 2006
PLATE 1-24
Interval-thickness map of the Black River and "Wells Creek" (top of Knox to top of Black River)
Partial funding provided by the U.S. Department of Energy
Contract Number DE-FC26-03NT41856
Trenton-Black River gas pool/field
Trenton-Black River oil pool/field
Trenton-Black River outcrop area
Fault
Data points not corrected for structural dip
Data point
500 ft Index contour
50 ft Contour
Thickness in Feet
2900
0

EXTENT OF STUDY AREA

NO DATA

50 25 0 50 100 Miles

50 25 0 50 100 150 Kilometers

March 31 2006

PLATE 1-25

Interval-thickness map of the Black River
(top of "Wells Creek" to top of Black River)

Partial funding provided by the U.S. Department of Energy
Contract Number DE-FC26-03NT41856

- Trenton-Black River outcrop area
- Trenton-Black River gas pool/field
- Trenton-Black River oil pool/field
- Fault
- Data point
- Data points not corrected for structural dip
- 250 ft Index contour
- 50 ft Contour

Thickness in Feet

1550

0

EXTENT OF STUDY AREA

EXTENT OF LOGANA

EXTENT OF LOGANA

NO DATA

NO DATA

Union Furnace outcrop

50 25 0 50 100 Miles

50 25 0 50 100 150 Kilometers

March 31 2006

PLATE 1-26

Interval-thickness map of the Trenton/Curdsville (top of Black River to top of Trenton/Curdsville) The extent of the Logana is also shown

Partial funding provided by the U.S. Department of Energy
Contract Number DE-FC26-03NT41856

- Trenton-Black River outcrop area
- Trenton-Black River gas pool/field
- Trenton-Black River oil pool/field
- Logana border known
- Logana border inferred
- Fault
- Data point
- 250 ft Index contour
- 50 ft Contour

Thickness in Feet

- 850
- 0
- Data points not corrected for structural dip

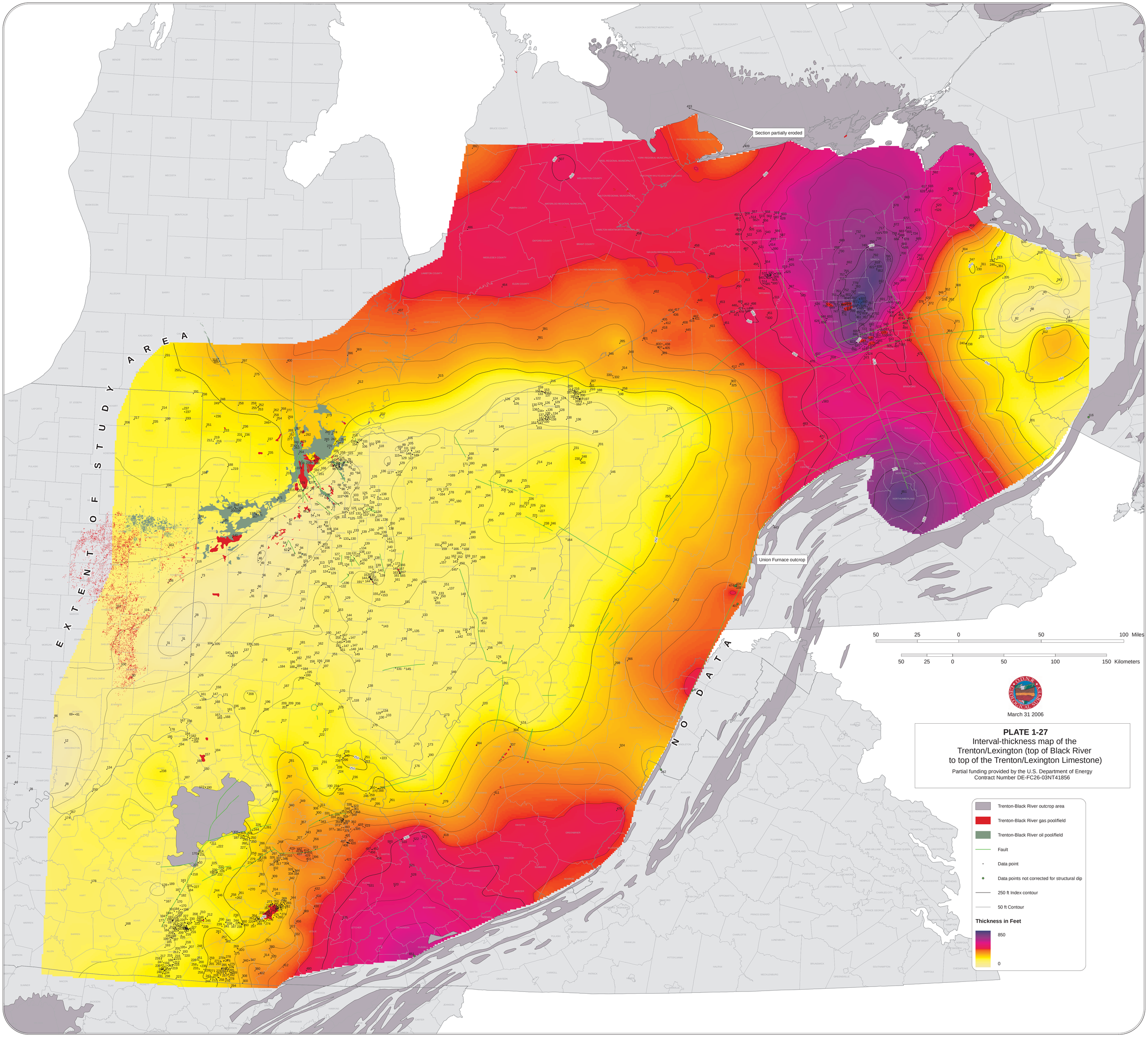
Section partially eroded
Union Furnace outcrop
EXTENT OF STUDY AREA
NO DATA
50 25 0 50 100 Miles
50 25 0 50 100 150 Kilometers
ODNR GEOLOGICAL SURVEY
March 31 2006
PLATE 1-27
Interval-thickness map of the
Trenton/Lexington (top of Black River
to top of the Trenton/Lexington Limestone)
Partial funding provided by the U.S. Department of Energy
Contract Number DE-FC26-03NT41856
Trenton-Black River outcrop area
Trenton-Black River gas pool/field
Trenton-Black River oil pool/field
Fault
Data point
Data points not corrected for structural dip
250 ft Index contour
50 ft Contour
Thickness in Feet
850
0

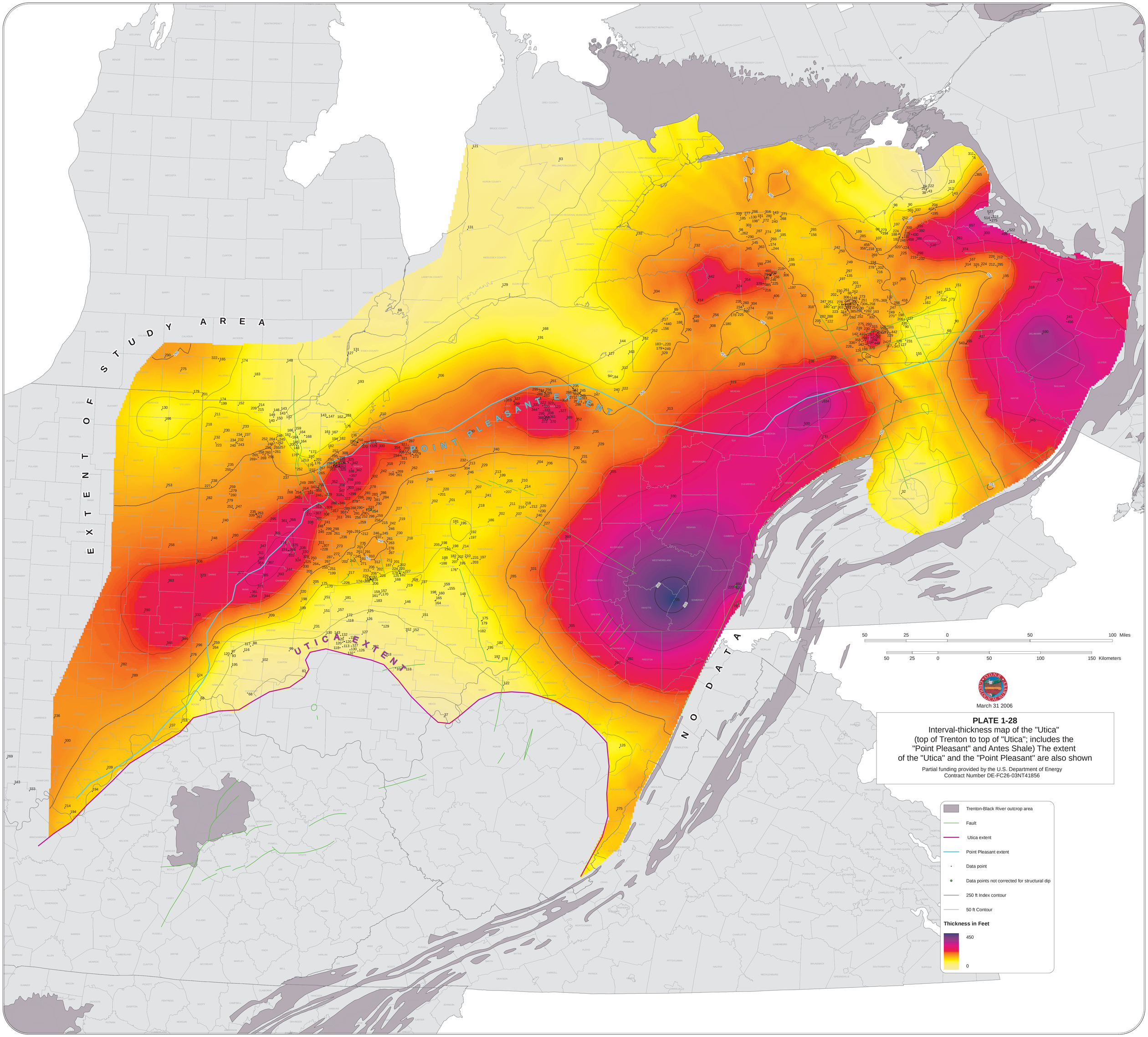
E X T E N T O F S T U D Y A R E A
POINT PLEASANT EXTENT
UTICA EXTENT
N O D A T A
50 25 0 50 100 Miles
50 25 0 50 100 150 Kilometers
March 31 2006
PLATE 1-28
Interval-thickness map of the "Utica"
(top of Trenton to top of "Utica"; includes the
"Point Pleasant" and Antes Shale) The extent
of the "Utica" and the "Point Pleasant" are also shown
Partial funding provided by the U.S. Department of Energy
Contract Number DE-FC26-03NT41856
Trenton-Black River outcrop area
Fault
Utica extent
Point Pleasant extent
Data point
Data points not corrected for structural dip
250 ft Index contour
50 ft Contour
Thickness in Feet
450
0

EXTENT OF STUDY AREA

"Kope" outcrop not shown

NO DATA

50 25 0 50 100 Miles

50 25 0 50 100 150 Kilometers

March 31 2006

PLATE 1-29

Interval-thickness map of the "Kope", (top of the Trenton/Lexington to the top of the "Kope", includes the partial equivalents of the Reedsville and Martinsburg in West Virginia, Pennsylvania, and New York, and the Blue Mountain/Georgian Bay in Ontario; also includes the "Utica" and "Point Pleasant")

Partial funding provided by the U.S. Department of Energy
Contract Number DE-FC26-03NT41856

Trenton-Black River outcrop area

Fault

Data point

Data points not corrected for structural dip

500 ft Index contour

50 ft Contour

Thickness in Feet

2650

0

EXTENT OF STUDY AREA

INCOMPLETE SECTION OF UPPER ORDOVICIAN

NO DATA

50 25 0 50 100 Miles

50 25 0 50 100 150 Kilometers

March 31 2006

PLATE 1-30

Interval thickness map of the upper Ordovician undifferentiated (top of the "Kope" and equivalents to the top of the Ordovician undifferentiated)

Partial funding provided by the U.S. Department of Energy
Contract Number DE-FC26-03NT41856

Fault

Data point

Data points not corrected for structural dip

Trenton-Black River outcrop area

Cincinnati Group

500 ft Index contour

50 ft Contour

Thickness in Feet

2300

0

APPENDIX G

Page size plates from Seismic and Structure

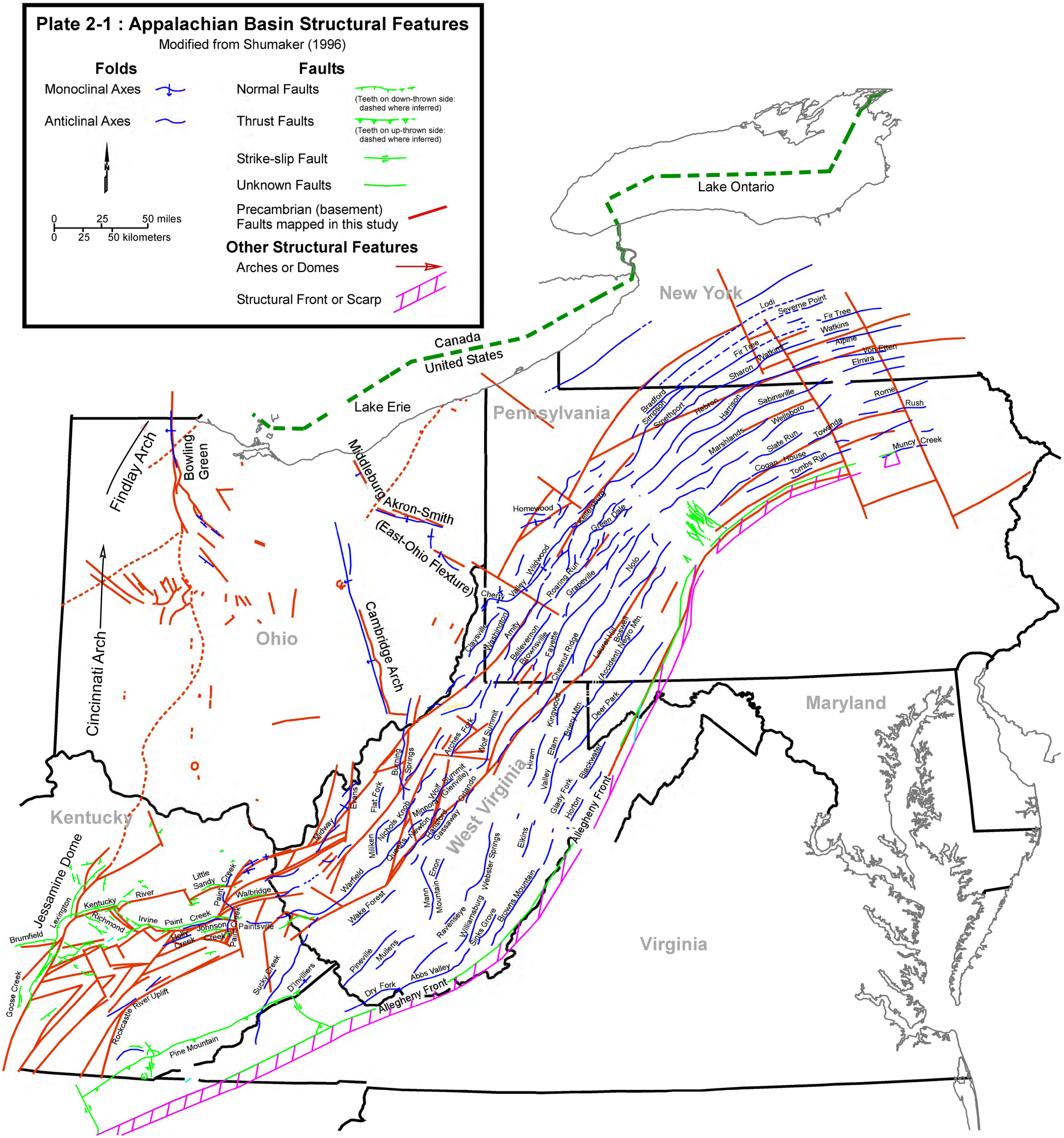
Plate 2-1 : Appalachian Basin Structural Features
Modified from Shumaker (1996)
Folds
Monoclinal Axes
Anticlinal Axes
Faults
Normal Faults
(Teeth on down-thrown side: dashed where inferred)
Thrust Faults
(Teeth on up-thrown side: dashed where inferred)
Strike-slip Fault
Unknown Faults
Precambrian (basement) Faults mapped in this study
Other Structural Features
Arches or Domes
Structural Front or Scarp
0 25 50 miles
0 25 50 kilometers
Lake Ontario
Lake Erie
Canada
United States
New York
Pennsylvania
Ohio
Maryland
Kentucky
West Virginia
Virginia
Findlay Arch
Bowling Green
Middleburg
Akron-Smith
(East-Ohio Flexture)
Cambridge Arch
Cincinnati Arch
Jessamine Dome
Allegheny Front
Lodi
Severne Point
Fir Tree
Watkins
Alpine
Von Etten
Elmira
Sharon
Bradford
Simpson
Smethport
Hebron
Harrison
Sabinsville
Wellsboro
Rome
Rush
Marshlands
Slate Run
Towanda
Muncy Creek
Cogan House
Tombs Run
Homewood
Kellersburg
Green Dale
Wildwood
Roaring Run
Grapeville
Nolo
Cherry Valley
Claysville
Washington
Amity
Bellevernon
Brownsville
Fayette
Chesnut Ridge
Laurel Hill
Boswell
(Accident) Negro Mtn.
Kingwood
Briery Mtn.
Deer Park
Arches Fork
Wolf Summit
Burning Springs
Evans
Flat Fork
Wolf Summit (Glenville)
Orlando
Minnora
Nichols Knob
Newton
Hansford
Gassaway
Milliken
Queens
Midway
Warfield
Wake Forest
Hiram
Etam
Valley
Glady Fork
Blackwater
Horton
Elkins
Webster Springs
Mann Mountain
Enon
Ravenseye
Williamsburg
Sinks Grove
Browns Mountain
Pineville
Mullens
Dry Fork
Abbs Valley
Little Sandy
Paint Creek
Walbridge
Kentucky River
Lexington
Richmond
Irvine
Paint Creek
Johnson Creek
Holly Creek
Paintsville
Brumfield
Goose Creek
Rockcastle River Uplift
Sucky Creek
D'Invilliers
Pine Mountain

Plate 2-2 : Structure of the Top of the Precambrian Unconformity

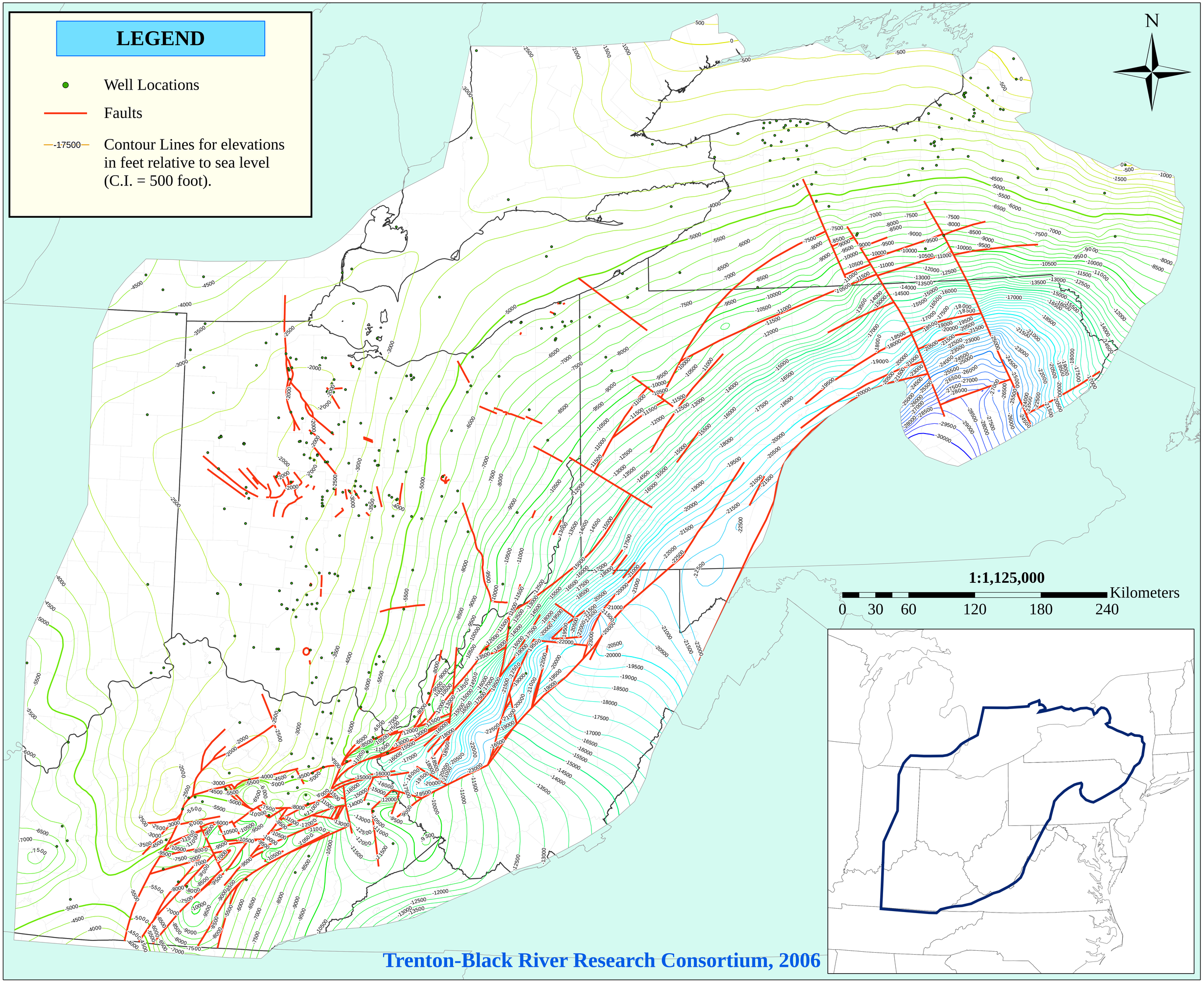

Plate 2-3 : Structure of the Base of the Knox Supergroup

LEGEND

- Well Locations
- Faults
- 2500 — Contour Lines for elevations in feet relative to sea level (C.I. = 500 foot).

N

1:1,125,000

0 30 60 120 180 240 Kilometers



Trenton-Black River Research Consortium, 2006

Plate 2-4 : Structure of the Top of the Knox Supergroup

LEGEND

- Well Locations
- Faults
- 2500 — Contour Lines for elevations in feet relative to sea level (C.I. = 500 foot).

N

1:1,125,000

0 30 60 120 180 240 Kilometers

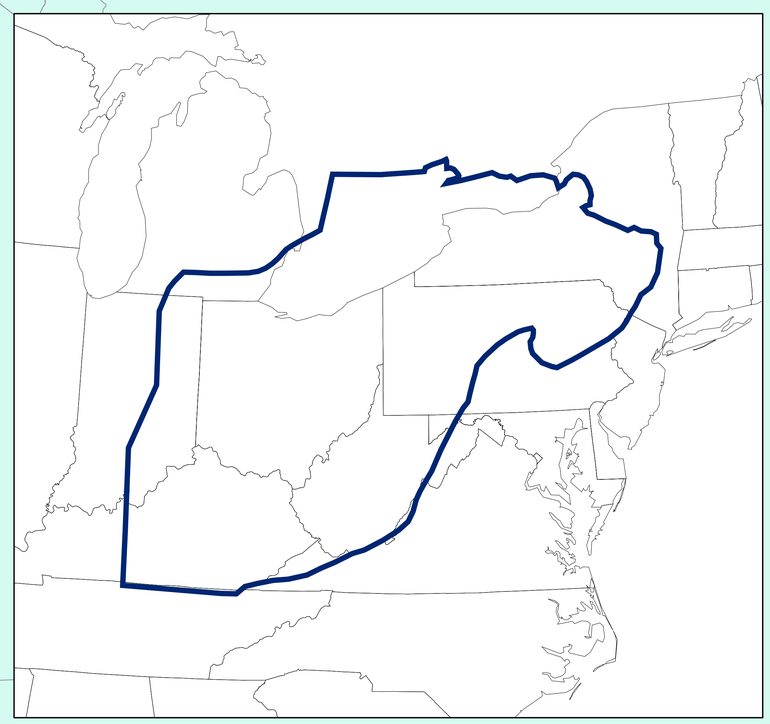

Trenton-Black River Research Consortium, 2006

Plate 2-5 : Structure of the Top of the Black River Limestone

LEGEND

- Well Locations
- Faults
- 2500 — Contour Lines for elevations in feet relative to sea level (C.I. = 500 foot).
- Trenton-Black River Oil Fields
- Trenton-Black River Gas Fields

N

1:1,125,000

0 30 60 120 180 240 Kilometers

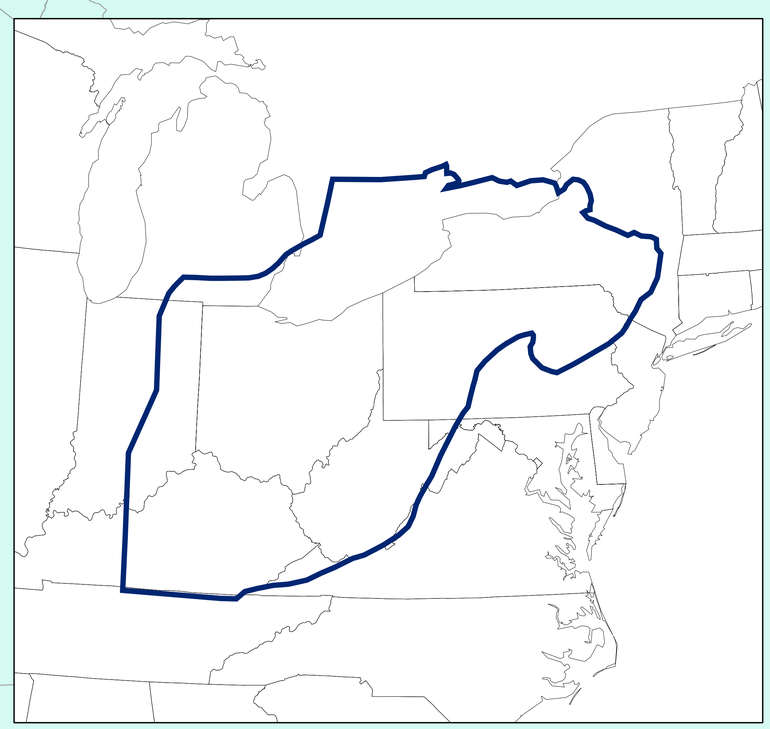

Trenton-Black River Research Consortium, 2006

Plate 2-6 : Structure of the Top of the Trenton Limestone

LEGEND

- Well Locations
- Faults
- 2500 — Contour Lines for elevations in feet relative to sea level (C.I. = 500 foot).
- Trenton Ls exposed/not present
- Trenton-Black River Oil Fields
- Trenton-Black River Gas Fields

N

1:1,125,000

0 30 60 120 180 240 Kilometers

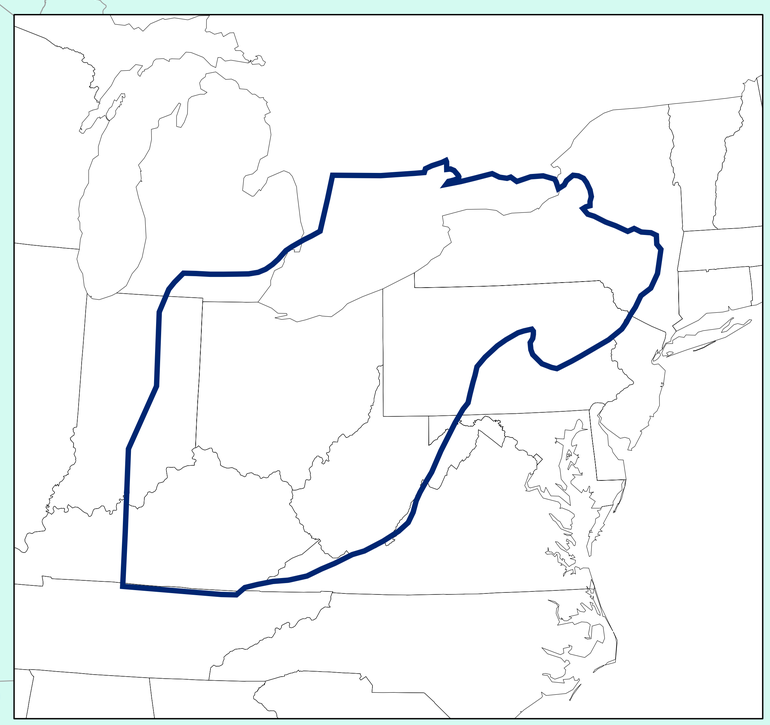

Trenton-Black River Research Consortium, 2006

Plate 2-7 : Structure of the Top of the Ordovician Section

LEGEND

- Well Locations
- Faults
- 2500 — Contour Lines for elevations in feet relative to sea level (C.I. = 500 foot).
- Top of Ordovician exposed/not present

N

1:1,125,000

0 30 60 120 180 240 Kilometers

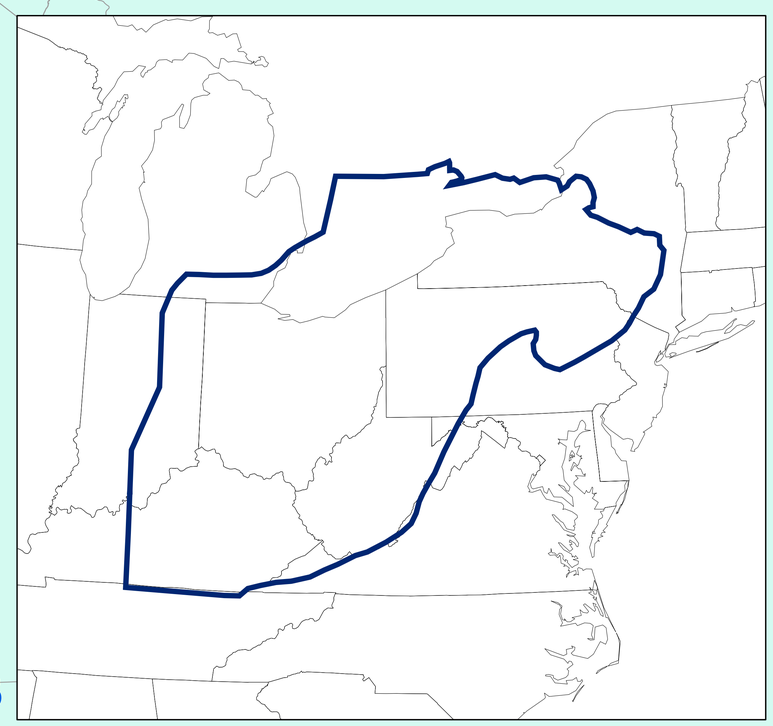

Trenton-Black River Research Consortium, 2006

Plate 2-8 : Structure of the Base of the Devonian Shale

LEGEND

- Well Locations
- Faults
- 2500 — Contour Lines for elevations in feet relative to sea level (C.I. = 500 foot).
- Base of Devonian Shale exposed or not present

N

1:1,125,000

0 30 60 120 180 240 Kilometers

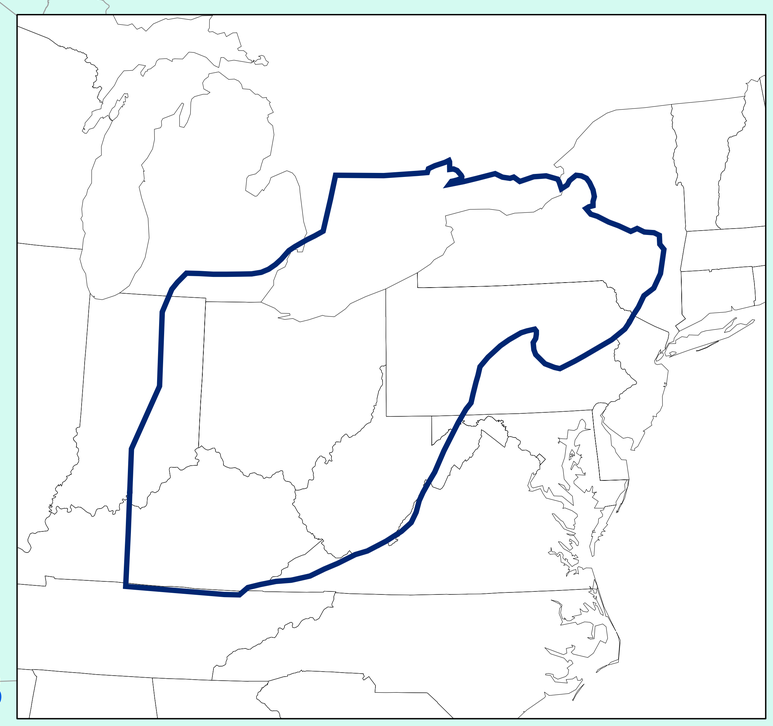

Trenton-Black River Research Consortium, 2006